Strategies for the Total Synthesis of Highly Oxidized Dibenzocyclooctadiene Lignan Natural Products

by

Madison Carroll

A thesis submitted to McGill University

In partial fulfillment of the requirements for the degree of

Doctor of Philosophy

Department of Chemistry

McGill University, Montreal

April 2024

Madison Carroll, 2024

Abstract

Dibenzocyclooctadiene lignan (DBCOD) natural products are isolated from plants of the *Schisandraceae* family, which includes the *Schisandra* and *Kadsura* species, the former of which has been used for thousands of years in Asia as traditional medicine to treat a plethora of ailments. More than 500 DBCODs have been isolated and have reported bioactivities including but not limited to: anti-cancer, hepatoprotective, antiviral, neuroprotective, cardioprotective, and antioxidant activity. These natural products are structurally intriguing in that they possess a conformationally stable chiral biaryl axis and an eight membered ring with a variable oxidation pattern. Studies on the more highly oxidized family members are scarce due to the meager supply available from natural sources and difficulty of synthesis. Our work aims to create a highly convergent synthetic route enabling access to diverse members of the DBCOD family of natural products. Our syntheses begin by coupling two pre-functionalized aryl fragments to furnish the alkyl chain, bearing several stereocenters, which will later become the 8-membered ring of the DBCOD. An intramolecular atroposelective Suzuki coupling is used to form the biaryl bond, establishing the axial chirality. Then, the oxidation pattern around the 8-membered ring can be modified via deoxygenation(s) and esterification(s) to access a variety of stage two DBCODs. Non-canonical oxidations such as photoredox-catalyzed spirocyclization or macrocyclization can be performed subsequently to access the elusive stage three DBCODs. This thesis focuses on work towards the total syntheses of the highly oxidized stage three DBCODs kadsuraol C and taiwanschirin B, reported to have potential hepatoprotective and anti-hepatitis B activity, respectively. In the kadsuraol C project, the linear substrate was successfully constructed, however it was recalcitrant to Suzuki coupling, which provided valuable insights into the substrate requirements for biaryl bond formation. The biaryl bond formation proceeded smoothly during the synthesis of taiwanschirin B. Following this step, *bis*-deoxygenation, acetylation, formation of the *ortho*-spirodienone, and oxidative cleavage of the C2-C3 bond were required to reach the target. These transformations have been successfully accomplished except for the final C6 deoxygenation where efforts are still ongoing.

Résumé

Les produits naturels du dibenzocyclooctadiène lignane (DBCOD) sont isolés de plantes de la famille des *Schisandraceae*, qui comprend les espèces de *Schisandra* et *Kadsura*, dont la première est utilisée depuis des milliers d'années en Asie comme médecine traditionnelle pour traiter une pléthore de maladies. Plus de 500 DBCODs ont été isolés et ont rapporté des bioactivités, notamment : une activité anticancéreuse, hépatoprotectrice, antivirale, neuroprotectrice, cardioprotectrice et antioxydante. Ces produits naturels sont structurellement intrigants dans la mesure où ils possèdent un axe biaryle chiral conformationnellement stable et un cycle à huit chaînons avec un modèle d'oxydation variable. Les études sur les membres de la famille les plus fortement oxydés sont rares en raison de la maigre offre disponible à partir de sources naturelles et de la difficulté de synthèse. Notre travail vise à créer une voie de synthèse hautement convergente permettant l'accès à divers membres de la famille de produits naturels DBCOD. Nos synthèses commencent par coupler deux fragments aryles pré-fonctionnalisés pour fournir la chaîne alkyle, portant plusieurs stéréocentres, qui deviendra plus tard le cycle à 8 chaînons du DBCOD. Un couplage Suzuki atroposélectif intramoléculaire est utilisé pour former la liaison biaryle, établissant la chiralité axiale. Ensuite, le modèle d'oxydation autour du cycle à 8 chaînons peut être modifié via une ou plusieurs désoxygénations et estérifications pour accéder à une variété de DBCODs de deuxième étape. Des oxydations non canoniques telles que la spirocyclisation ou la macrocyclisation catalysée par photorédox peuvent être effectuées ultérieurement pour accéder à l'insaisissable étape trois DBCOD. Cette thèse se concentre sur les travaux visant à la synthèse totale des DBCODs de stade trois hautement oxydés, le kadsuraol C et la taiwanschirine B, signalés comme ayant une activité hépatoprotectrice et anti-hépatite B potentielle, respectivement. Dans le projet kadsuraol C, le substrat linéaire a été construit avec succès, mais il était récalcitrant au couplage de Suzuki, ce qui a fourni des informations précieuses sur les exigences du substrat pour la formation de liaisons biaryles. La formation de la liaison biaryle s'est déroulée sans problème au cours de la synthèse de la taiwanschirine B. À la suite de cette étape, la bis-désoxygénation, l'acétylation, la formation de l'*ortho*-spirodiénone et le clivage oxydatif de la liaison C2-C3 ont été nécessaires pour atteindre la cible. Ces transformations ont été réalisées avec succès à l'exception de la désoxygénation finale C6 où les efforts sont toujours en cours.

Acknowledgments

Firstly, I would like to thank my supervisor Prof. Jean-Philip Lumb for his guidance and support. He has provided a tremendous learning environment for me and the other group members. He has been a great resource for troubleshooting synthetic challenges throughout the projects discussed in this thesis. His knowledge and passion for chemistry have motivated me to accomplish more than I thought I could throughout this work. Secondly, I would like to thank my committee members Prof. Gleason and Prof. Arndtsen for their insightful questions, advice, and discussions. I would also like to thank the professors with whom I took graduate classes, helping strengthen my chemistry background: Prof. Li, Prof. Lumb, Prof. Gleason, and Prof. Arndsten. I would like to thank Dr. Danielle Vlaho for being the best TA supervisor anyone could ask for.

A special thanks goes to the past and present members of the Lumb research group, whose thought-provoking discussions and support were invaluable throughout my degree: Ohhyeon Kwon, Luke Burke, Yalun Xu, Matt Halloran, Dr. Naresh Vermula, Wenyu Qian, Dr. Camilo Viasus, Dr. Tom Singleton, Xueqing Wang, En Zhao, Laura Jeliazkov, Darcy Burley, Yiming Zhang, Xiaobo Zhao, Glen Loo, Veronica Wu, Mathéo La Torre, Sean Elliott, William Bouthillier, and Béatrice Denis. I am especially grateful for Dr. Zheng Huang, a senior graduate student at the time I joined the group, for showing me the ropes, sharing his vast knowledge, and training me in the art of dibenzocyclooctadiene lignan synthesis. Thank you to Simon Edelmann, for keeping the lab running smoothly, being incredibly kind, and always being willing to assist group members in any way needed. I would like to thank Carlos Razziel Azpilcueta Nicolas for helpful discussions about both chemistry and non-chemistry alike and for bringing in the best snacks to share with the group. Thank you to Haiyan Huang for being both kind and knowledgeable and making the Lumb group feel more like a family. Thank you to Dr. Burhan Hussein for always boosting the group's morale with his positive attitude and fun nature. I would like to thank Dr. Eric Falk for sharing his extensive chemical knowledge as well as his friendship. I would like to thank Jackie Wu for showing me how to use the Légaré group's instruments for IR spectrometry and cyclic voltammetry. Thank you to Derek Meng for assisting in preparing starting materials for the synthesis of kadsuraol C.

Additionally, I would like to thank all the faculty members and graduate students in the department who allowed me to borrow chemicals and equipment. Thank you to my many friends and colleagues in the department who have both empathized with my struggles and celebrated my victories alongside me, making the journey that is grad school a more enjoyable experience. Although there are too many great members of our department to list, I'd like to make a quick mention of Juan Lasso for letting me talk his ear off every time he borrows a chemical from our lab as well as Leo Hall for always keeping me on my toes. I would also like to thank Kaleena Basran, Yiram Kim, and Spencer Petras for being so positive and friendly and always lending a listening ear. Thank you to Anne Labarre and Thershan Satkunarajah for training on the Moitessier group's polarimeter and ozonizer.

I am grateful for the technical support from Dr. Robin Stein and Kirill Levin at the NMR facility. A thank you also goes out to Dr. Nadim Saade and Dr. Alexander Wahba at the MS facility and Dr. Hatem Titi for the X-ray crystallography. I would like to thank Chantal Marotte, the chemistry graduate student coordinator as well as the other members of the department's administrative team and chemistry stores: Nikoo Taghavi, Chelsea Briand-Pitts, Ross Commodari, Rachel D'Ermo, Taleah Levesque, and Joyce Gyan. Thank you to Richard Rossi, Weihua Wang, and Jean-Philippe Guay for constructing and repairing equipment.

Finally, I would like to thank my family for always putting an emphasis on higher education. Thank you to my siblings for their encouragement, friendship, and interesting discussions. Thank you to Dr. Jan-Hendrik Carroll-Poehls for his unprecedented kindness and constant love and support.

Contribution of Authors

During my doctoral research, all work was performed by me unless otherwise stated in the text. All manuscripts are co-authored by Dr. Jean-Philip Lumb, who acted as research supervisor.

Chapter 1:

This chapter provides a review of the relevant literature about dibenzocyclooctadiene lignan natural products, including a background on lignin and lignans, structural features and classification, occurrence and biological activity, the proposed biosynthesis, and previous chemical syntheses.

Chapter 2:

This chapter describes work on a simplified model system devised to investigate the key steps to be used in the DBCOD syntheses: alkylation or aldol coupling, methyl addition, and benzylic deoxygenation. The work in the introduction (2.1.2) was conducted by Zheng Huang. The work in the rest of the chapter (2.2–2.6) was conducted by the author.

Chapter 3:

This chapter describes the efforts towards the synthesis of kadsuraol C, including key steps of aldol coupling, methyl addition, benzylic deoxygenation, functional group manipulations, and Suzuki coupling. The author developed the entire synthetic route. Derek Meng assisted in preparing more material up to the aldol coupling step.

Chapter 4:

This chapter describes the synthesis of 6-benzyloxy taiwanschirin B. The author performed all the studies described. The shortened route to 5-hydroxypiperonal (**4-14**) was previously described by Derek Meng. The route to **4-21** was previously described by Zheng Huang and the sample of heteroclitin J utilized was synthesized by Zheng Huang.

Table of Contents

Chapter 1. Introduction to dibenzocyclooctadiene lignan natural products

1.1. Introduction…….. 1

1.1.1. Synthetic dibenzocyclooctadiene targets of this thesis…….. 1

1.1.2. Background on lignin and lignan……... 1

1.2. General structural features and classification of DBCODs……. 3

1.3. Spectral data and conformational properties…… 5

1.3.1. Conformational analysis……... 5

1.3.2. Spectral data…….. 8

1.4. Occurrence and biological activity…….. 9

1.5. Biosynthesis……... 16

1.6. Previous syntheses……. 24

1.6.1. Overview of progress in DBCOD synthesis 1976–2021……. 24

1.6.2. Biaryl bond formation……. 27

1.6.2.1. Intermolecular biaryl bond formation…….. 29

1.6.2.2. Intramolecular biaryl bond formation…….. 33

1.6.2.3. Atroposelective biaryl bond formation methods…….. 43

1.6.3. Alkyl chain and 8-membered ring formation…….. 45

1.6.3.1. Intermolecular alkyl chain forming reactions…….. 46

1.6.3.2. Intramolecular 8-membered ring formation……. 51

1.6.4. Ring expansion strategies……... 55

1.6.5. Methods for introducing chirality……... 58

1.6.6. Distinctive synthetic steps: late-stage oxidation modification…… 62

1.6.7. Selected linear syntheses…… 68

1.6.8. Progress toward DBCODs…….. 82

1.9. Conclusions…… 86

1.10. References…… 87

Chapter 2. Aldol, methyl addition, and benzylic deoxygenation studies on model systems

2.1. Introduction…….. 101

2.1.1. Introduction to the synthetic strategy for DBCODs targeted in this thesis……101

2.1.2. Previous work on model aldol and methyl addition systems…… 104

2.2. Fragment coupling by alkylation or aldol reaction……..… 108

2.3. Methyl addition…… 115

2.4. Benzylic deoxygenation……... 119

2.5. Conclusions…….. 125

2.6. Experimental section…… 125

2.6.1 Materials and methodologies……. 125

2.6.2. Preparative procedures for compounds **2-7** to **2-37**……...127

2.7. References…… 140

Chapter 3. Efforts towards the synthesis of kadsuraol C

3.1. Introduction…….. 143

3.2. Retrosynthetic analysis…… 144

3.3. Strategy 1: brominated ketone + chlorinated aldehyde……... 146

3.3.1. Synthesis of the brominated ketone fragments……. 147

3.3.2. Synthesis of the chlorinated aldehyde fragment……..…... 149

3.3.3. Aldol addition…… 154

3.3.4. Chelate-controlled methyl addition……... 160

3.4. Strategy 2: non-brominated ketone + chlorinated aldehyde…… 164

3.4.1. Synthesis of the non-brominated ketone fragment……... 164
3.4.2. Aldol addition…… 165
3.4.3. Chelate-controlled methyl addition……... 169
3.4.4. Benzylic deoxygenation…… 173
3.4.5. Functional group manipulations to prepare for Suzuki coupling…….. 177
3.4.6. Suzuki coupling…… 187
3.5. Strategy 3: non-brominated ketone + non-chlorinated aldehyde……. 195
3.5.1. Aldol addition…… 196
3.5.2. Chelate-controlled methyl addition……... 198
3.5.3. Benzylic deoxygenation…… 199
3.5.4. Functional group manipulations to prepare for Suzuki coupling…….. 200
3.5.5. Suzuki coupling…… 203
3.6. Analysis of aldol addition results……. 205
3.7. Analysis of methyl addition results…….. 208
3.8. Conclusions and future directions…… 211
3.9. Experimental section…… 213
3.9.1 Materials and methodologies……. 208
3.9.2. Preparative procedures for compounds **3-11** to **3-112**…….. 215
3.9.3. X-ray crystallographic data…….. 273
3.10. References……. 274
Chapter 4. Synthesis of 6-benzyloxy-taiwanschirin B
4.1. Introduction…….. 279
4.2. Retrosynthetic analysis…… 282
4.3. Preparation of the known intermediate **4-21**…… 283
4.4. Benzylic deoxygenation on a cyclic system…… 286
4.5. Synthesis of 6-benzyloxy-taiwanschirin B…….. 300
4.6. Conclusions and future directions…… 307

4.7. Experimental section…… 308

4.7.1 Materials and methodologies…… 308

4.7.2. Preparative procedures for compounds **4-8** to **4-55**……. 309

4.9. References…… 345

Chapter 5. Summary and future directions

5.1. Summary of thesis…… 348

5.2. Future directions…….. 350

5.2.1. Synthesis of kadsuraol C…….. 350

5.2.2. Synthesis of taiwanschirin B……. 352

5.2.3. Selective deoxygenation to access other DBCODs…….. 354

5.3. References…… 355

Supplementary information (^{1}H and ^{13}C NMR spectra)……... 358

List of Figures

Chapter 1

Figure 1.1. Synthetic dibenzocyclooctadiene targets of this thesis: kadsuraol C and taiwanschirin B and a target of previous work in our group: heteroclitin J…….. 1

Figure 1.2. Lignans and lignin share monolignols as common precursors…… 2

Figure 1.3. A) Numbering and classification of DBCODs, B) steganacins, and C) gymnothelignans…… 4

Figure 1.4. A) Minimum energy conformations of the 8-membered ring; B) conformations of the biaryl axis…… 5

Figure 1.5. Conformational analysis of a DBCOD (kadsurin, **1-1**)…… 7

Figure 1.6. Characterization of DBCOD compounds……. 8

Figure 1.7. Antioxidant DBCODs and comparison to commercial antioxidants…….. 10

Figure 1.8. Antiviral DBCODs with A. anti-HIV activity; B. anti-HBV activity and antiviral drug tenofovir…… 11

Figure 1.9. Hepatoprotective DBCODs and positive control bicyclol (with cell survival rates)..12

Figure 1.10. DBCODs with anticancer activity…… 13

Figure 1.11. DBCODs with neuroprotective activity……... 15

Figure 1.12. DBCODs with cardiovascular protective activity…… 16

Figure 1.13. Syntheses of each stage of DBCOD……. 25

Figure 1.14. Timeline of key innovations in DBCOD synthesis…….. 26

Figure 1.15. Syntheses of each individual DBCOD……. 27

Figure 1.16. Techniques used for biaryl formation…….. 28

Figure 1.17. Atroposelective biaryl bond forming methods……. 44

Figure 1.18. Alkyl chain construction techniques……. 46

Figure 1.19. Techniques used in asymmetric syntheses…… 58

Chapter 2

Figure 2.1. Current and previous DBCOD targets in the Lumb group……... 101

Figure 2.2. A) Biosynthetic and synthetic approaches to controlling the oxidation pattern around the 8-membered ring and B) synthetic C6 deoxygenation strategy…… 102

Figure 2.3. Model system for investigating the key steps of DBCOD synthesis…… 103

Figure 2.4. Reactor setups for photoredox-catalyzed benzylic deoxygenation: A. vial; B. thermowell flask; C. Schlenk flask……. 124

Chapter 3

Figure 3.1. Kadsuraols A–C and positive control bicyclol…...…….. 143

Figure 3.2. Ketone and aldehyde fragments for use in strategy 1……... 147

Figure 3.3. X-ray crystal structure of aldol **3-36**……..... 168

Figure 3.4. Reactor setups for photoredox-catalyzed benzylic deoxygenation: A) vial; B) RBF; C) Schlenk flask; D) flow setup…….. 173

Figure 3.5. Importance of the tethered aryl borinic ester…… 177

Figure 3.6. Catalysts and ligands used in the Suzuki coupling……... 189

Chapter 4

Figure 4.1. Taiwanschirins A–C…….. 279

Figure 4.2. Challenges associated with the C6 deoxygenation of a cyclic system: A. sterics and B. electronics…….. 281

Figure 4.3. A) Synthetic target taiwanschirin B; B) Controlling the oxidation pattern of the DBCOD 8-membered ring……. 282

Chapter 5

Figure 5.1. Potential future DBCOD targets with deoxygenation at various ring positions….. 355

List of Schemes

Chapter 1

Scheme 1.1. Biosynthesis of monolignol building blocks……..... 17

Scheme 1.2. Aryltetralin biosynthetic pathway…… 18

Scheme 1.3. Biosynthetic hypotheses for DBCODs: A. origin of the *cis* methyl groups, B. cyclization……. 19

Scheme 1.4. Canonical and non-canonical oxidations in DBCOD biosynthesis…….. 20

Scheme 1.5. Biosynthetic hypotheses for spirocyclization: A. radical pathway; B. ionic pathway.. ……... 21

Scheme 1.6. Hypotheses for the biosynthesis of steganacin type DBCODs…… 22

Scheme 1.7. Proposal for the biosynthesis of gymnothelignan type DBCODs…… 24

Scheme 1.8. Three synthetic strategies for biaryl bond formation in DBCOD syntheses…… 28

Scheme 1.9. Comparison of different oxidants in the synthesis of (+)-schizandrin precursor…. 38

Scheme 1.10. Comparison of Tl and Ru oxidants in the synthesis of (±)-deoxyschisandrin precursors…….. 39

Scheme 1.11. Study of reagents for oxidative coupling of phenolic dibenzylbutanolides……... 40

Scheme 1.12. Possible byproducts of oxidative coupling: A. aryltetralins; B. spirodienones; and C. oxidative coupling to form a stage 2 DBCOD……. 41

Scheme 1.13. Synthetic strategies for A) intermolecular alkyl chain formation and B) intramolecular alkyl chain formation, that is, 8-membered ring formation…….. 45

Scheme 1.14. Ring expansion strategy……. 55

Scheme 1.15. Cyclopropanation/ ring-expansion strategy from Magnus's steganacin synthesis. 57

Scheme 1.16. Selective reductions of inequivalent ketones at C6 and C9 in the synthesis of kadsurin (Ghera 1977)…….. 63

Scheme 1.17. Bis-deoxygenation via tetrahydrofuran intermediate in the synthesis of (±)-deoxyschizandrin (Stevenson 1978)……. 64

Scheme 1.18. Methods for late-stage C(sp^3)-H oxidation in the syntheses of (+)- and (−)-steganacin (Koga 1984)…… 65

Scheme 1.19. Stereoselective epoxidation and Zn-mediated reduction in the synthesis of kadsurin (Wakamatsu 1995)…… 65

Scheme 1.20. Mukaiyama hydration in the synthesis of (+)-schizandrin and (+)-isoschizandrin from a common starting material (Wakamatsu 1995)……... 66

Scheme 1.21. A) Stereoselective olefin reduction to form the cycloctadiene ring with four contiguous stereocentres in the synthesis of bis-oxygenated DBCODs; B) formation of the C7 tertiary alcohol in the synthesis of tri-oxygenated DBCODs (RajanBabu 2013)……. 67

Scheme 1.22. Mimcry of non-canonical oxidations: A) spirocyclization to give heteroclitin J; B) oxidative cleavage / cyclization to give taiwankadsurins A and B; C) macrocyclization; D) Mukaiyama hydration to give kadsuphilin N (Lumb 2021)……. 68

Scheme 1.23. A short synthesis of (±)-isostegane (Schlessinger 1976)…… 69

Scheme 1.24. A synthesis of (±)-steganone featuring 6-π electrocyclization (Raphael 1976)…. 70

Scheme 1.25. The first asymmetric DBCOD synthesis: (−)-steganone (Robin 1980)…..…….. 71

Scheme 1.26. Synthesis of (−)-schizandrin and (−)-isoschizandrin featuring a chiral oxazoline to impart atropselectivity (Meyers 1990)…….. 72

Scheme 1.27. Synthesis of (−)-steganone featuring SmI_2-mediated ketyl-olefin cyclization (Molander 2000)……... 73

Scheme 1.28. Synthesis of interiotherin A and angeloylgomisin (Coleman 2005)…….. 75

Scheme 1.29. Synthesis of (±)-deoxyschisandrin featuring double organocuprate oxidation (Spring 2012)…… 76

Scheme 1.30. Synthesis of bis-oxygenated DBCODs (−)-interiotherin C and (−)-ananolignans B, C, D, and F (RajanBabu 2012–2013)…… 77

Scheme 1.31. Synthesis of tris-oxygenated DBCODs tiegusanin D, kadsuralignan B, and schizandrin F (RajanBabu 2013)…….. 79

Scheme 1.32. Synthesis of stage 3 DBCODs heteroclitin J and taiwankadsurins A/B (part 1) (Lumb 2021)……. 80

Scheme 1.33. Synthesis of stage 3 DBCODs heteroclitin J and taiwankadsurins A/B (part 2) (Lumb 2021)……. 81

Scheme 1.34. Synthesis of stage 3 DBCOD kadsulignan E (Lumb 2021)……... 82

Scheme 1.35. Synthesis of stage 3 DBCOD kadsuphilin N (Lumb 2021)……... 82

Scheme 1.36. Synthesis of (+)-5-detigloyloxy-steganolide C, a DBCOD derivative (Pelter and Ward 1992)…… 83

Scheme 1.37. Cobalt-mediated [2+2+2] cycloaddition for the synthesis of steganone analogues (Motherwell 1999)…… 84

Scheme 1.38. Lewis acid-mediated spirocyclization (Coleman 2000)……. 84

Scheme 1.39. Partial synthesis of schisandrene featuring ring-closing metathesis (Babu 2018). 85

Chapter 2

Scheme 2.1. Retrosynthetic analysis of kadsuraol C…….. 103

Scheme 2.2. Enolization studies on the model ketone **2-7**……. 105

Scheme 2.3. Aldol reaction using TMPMgBr on the ketone **2-7**; A) Potential diastereomers of aldol product; B) Intermediates and chair transition state leading to **2-11-TBS-b**……. 106

Scheme 2.4. A) Methyl addition on model substrates varying the α-siloxy group. B) Explanation of the stereochemical outcome of the chelate-controlled methyl addition……. 107

Scheme 2.5. Fragment coupling via A) aldol or B) alkylation reaction……. 109

Scheme 2.6. Synthesis of ketones A) (±)-**2-7** and B) (±)-**2-18**……... 109

Scheme 2.7. Alkylation attempts on ketone (±)-**2-7** using NaHMDS…… 112

Scheme 2.8. Aldol condensation attempt between (±)-**2-7** and **2-14** or **2-21**……...…….. 112

Scheme 2.9. Aldol addition giving the 1,2-*syn*-1,3-*syn* aldol **2-26**……. 113

Scheme 2.10. Aldol addition giving the 1,2-*anti*-1,3-*syn* aldol **2-15**…….. 114

Scheme 2.11 Synthesis of the TIPS-protected ketone **2-28**…… 115

Scheme 2.12. Aldol addition giving the 1,2-*anti*-1,3-*syn* aldol **2-29**…….. 115

Scheme 2.13. Methyl addition on the 1,2-*syn*-1,3-*syn* aldol **2-26**…….. 116

Scheme 2.14. A. Methyl addition on the 1,2-*anti*-1,3-*syn* aldol **2-29**; B. Confirmation of the diol stereochemistry via formation of the boronic ester and nOe…….. 118

Scheme 2.15. Attempt at preparing the imidazyl thiocarbamate Barton ester **2-33**…… 119

Scheme 2.16. Preparation of the phenyl thionocarbonate Barton ester and deoxygenation attempt ……. 120

Scheme 2.17. Preparation of the of the 3,5-(bistrifluoromethyl)benzoate **2-37**……. 121

Scheme 2.18. Proposed mechanism of visible light photoredox-catalyzed deoxygenation of **2-37** ……. 122

Scheme 2.19. Superior conditions for deoxygenation of 3,5-(bistrifluoromethyl)benzoate **2-37** ……. 125

Chapter 3

Scheme 3.1. Key steps towards kadsuraol C following the methyl addition…….. 144

Scheme 3.2. Retrosynthetic analysis of kadsuraol C…….. 145

Scheme 3.3. Comparison to the previous Suzuki coupling leading to heteroclitin J…….. 146

Scheme 3.4. Deoxygenation of a A) linear substrate or B) cyclic substrate……... 146

Scheme 3.5. Preparation of A. TBS-protected ketone **3-13** and B. TIPS-protected ketone **3-15** ……. 148

Scheme 3.6. Preparation of TBDPS-, TES-, and TMS- protected ketones **3-17**, **3-18**, and **3-19** ……. 149

Scheme 3.7. Preparation of intermediate **3-22**…… 149

Scheme 3.8. Preparation of the chlorinated aldehyde **3-25** from intermediate **3-22**…….. 153

Scheme 3.9. Partial preparation of the benzyl bromide **3-27**…….. 154

Scheme 3.10. Aldol addition of ketone **3-15** and aldehyde **3-25** using conditions developed on the model system for formation of a 1,2-*anti*-1,3-*syn* aldol……... 154

Scheme 3.11. Aldol addition of model ketone **2-28** and chlorinated aldehyde **3-25**…….. 160

Scheme 3.12. Confirmation of the diol stereochemistry of **3-34** via formation of the boronic ester and nOe……... 161

Scheme 3.13. Comparison to methyl addition on previous substrates……... 163

Scheme 3.14. A) Steric and B) electronic effect of the aryl bromide on chelation with $TiCl_4$... 163

Scheme 3.15. Synthesis of the non-brominated ketone **3-37** A) from brominated ketone **3-15** or B) from 5-hydroxypiperonal **4-14**…….. 164

Scheme 3.16. Synthesis of the non-brominated ketone **3-41**……. 165

Scheme 3.17. Aldol addition attempt from the (*E*)-silyl enol ether…… 166

Scheme 3.18. Aldol addition of TBS-protected ketone **3-41** with aldehyde **3-25**…….. 169

Scheme 3.19. Confirmation of the stereochemistry of the methyl addition products **3-44** and **3-45** ……. 170

Scheme 3.20. Preparation of the 3,5-bis-(trifluoromethyl)benzoyl ester **3-48**……... 173

Scheme 3.21. Benzylic deoxygenation of **3-48** in vial or RBF setup……. 174

Scheme 3.22. Functional group manipulation strategy 1: deprotection of the TIPS ether, formation of the boronic ester, *ortho*-lithiation…….. 178

Scheme 3.23. Functional group manipulation strategy 2: deprotection of the MOM ether, *ortho*-bromination, formation of the boronic ester, lithium-bromine exchange…….. 180

Scheme 3.24. Functional group manipulation strategy 3: *ortho*-bromination, formation of the boronic ester, lithium-bromine exchange…….. 181

Scheme 3.25. Boronic ester migration A) in the current work and B) in the previous synthesis of heteroclitin J…… 183

Scheme 3.26. Attempted formation of the Ar-Bpin **3-65** or **3-66** via Miyaura boration…… 187

Scheme 3.27. Comparison of **3-52** to the Suzuki coupling substrate from the synthesis of heteroclitin J…… 190

Scheme 3.28. Intermolecular Suzuki couplings…….. 190

Scheme 3.29. Deprotection of the phenolic benzyl ether……... 191

Scheme 3.30. Burgess dehydration of **3-52** and **3-71**……. 192

Scheme 3.31. Attempted biaryl formation via Sanford's photoredox catalyzed S_NAr conditions ……. 193

Scheme 3.32. Attempted formation of biaryl **3-78** via A) Denmark's anhydrous conditions or B) Jasti's oxidative coupling conditions…….. 194

Scheme 3.33. Attempted biaryl formation via Coleman's oxidative cuprate coupling conditions ……. 195

Scheme 3.34. Attempted preparation of aryl bromide **3-87** via dechlorination of **3-50**……. 196

Scheme 3.35. Synthesis of the non-chlorinated aldehyde **3-90**…….. 197

Scheme 3.36. Aldol addition of non-brominated ketone **3-37** and non-chlorinated aldehyde **3-90** ……. 197

Scheme 3.37. Aldol addition of brominated ketone **3-15** and non-chlorinated aldehyde **3-90**.. 198

Scheme 3.38. Confirmation of the diol stereochemistry of **3-92** via formation of the boronic ester and nOe……... 199

Scheme 3.39. Benzylic esterification of **3-92** and deoxygenation…….. 200

Scheme 3.40. Functional group manipulation strategy 1…… 200

Scheme 3.41. Functional group manipulation strategy 2…… 202

Scheme 3.42. Functional group manipulation strategy 3……...…. 203

Scheme 3.43. Attempted intramolecular Suzuki coupling of aryl bromide **3-101**…….. 204

Scheme 3.44. Effect of the C6 substituent on transmetallation A) in our group's previous synthesis of heteroclitin J and B) in the current work…… 205

Scheme 3.45. Plan for Suzuki coupling with C6 OTIPS in place and late stage deoxygenation ……. 212

Scheme 3.46. Testing C6 deoxygenation on a cyclic system…….. 213

Chapter 4

Scheme 4.1. Previously reported synthetic work towards the taiwanschirins…… 280

Scheme 4.2. Retrosynthetic analysis of taiwanschirin B…… 283

Scheme 4.3. Synthesis of the A) ketone fragment **4-12** and B) aldehyde fragment **4-15**…….. 284

Scheme 4.4. A) Transformations of the linear precursor and B) atroposelective Suzuki coupling ……. 286

Scheme 4.5. Functional group manipulations on the Suzuki coupling product **4-21**……. 287

Scheme 4.6. Preparation of other (C6 equatorial) substrates for C6 deoxygenation…….. 288

Scheme 4.7. Attempted C6 deoxygenation via the equatorial imidazyl thiocarbamate **4-24** … 288

Scheme 4.8. Attempted C6 deoxygenation via the equatorial benzoate **4-26** using Wickens' photoredox-catalyzed conditions…… 290

Scheme 4.9. Attempted C6 deoxygenation via the equatorial toluate **4-27**…… 290

Scheme 4.10. Attempted C6 deoxygenation via the iodide…… 291

Scheme 4.11. Attempted C6 deoxygenation directly from the equatorial alcohol **4-6** A. using Newman's Ni-catalyzed conditions and B. using Ph_2SiHCl / $InCl_3$ conditions……. 292

Scheme 4.12. Comparison of the orbital overlap of the C6-O bond to be cleaved and the allylic π-system in axial vs. equatorial substrates ……. 293

Scheme 4.13. Burgess dehydration of **4-6**…….. 294

Scheme 4.14. A. Epimerization of the C6 alcohol of **4-6**; B. Burgess dehydration of **4-31**….. 294

Schemes 4.15. Attempts at C6 deoxygenation of the ketone via A) Wolff-Kishner reduction; B) Myers' modified Wolff-Kishner reduction; C) Clemmensen reduction……. 295

Scheme 4.16. Preparation of C6 axial substrates for deoxygenation…….. 296

Scheme 4.17. Attempt at SmI_2-mediated deoxygenation of the axial toluate **4-33**…… 297

Scheme 4.18. Burgess dehydration of the C7 tertiary alcohol…… 298

Scheme 4.19. Attempts at C6 deoxygenation of C7-*exo*-methylene substrates using Reiser's photoredox-catalyzed conditions…… 298

Scheme 4.20. Attempts at C6 deoxygenation of C7 *exo*-methylene substrates using Wickens' photoredox-catalyzed conditions…… 299

Scheme 4.21. Attempts at C6 deoxygenation using Pd-catalyzed allylic deoxygenation conditions ……. 300

Scheme 4.22. Revised retrosynthetic analysis of taiwanschirin B…….. 301

Scheme 4.23. Transformations of benzoate **4-35**…… 302

Scheme 4.24. Transformations of acetate **4-34**……... 302

Scheme 4.25. Transformations of C7 *exo*-methylene acetate **4-41**……. 303

Scheme 4.26. Synthesis starting from heteroclitin J……...… 304

Scheme 4.27. Attempts at C6 allylic deoxygenation using Pd-catalysis…… 305

Scheme 4.28. Attempts at Zn-mediated C6 allylic reduction followed by alkene isomerization ……. 307

Scheme 4.29. Attempts at C6 allylic deoxygenation using triethylsilane and acid…… 307

Chapter 5

Scheme 5.1. Exploration of the key steps in DBCOD synthesis on a model system (Chapter 2) and in efforts towards kadsuraol C (Chapter 3)…….. 349

Scheme 5.2. A) C6 deoxygenation screening and B) synthesis of 6-benzyloxy taiwanschirin B (Chapter 4)…….. 350

Scheme 5.3. Synthetic plan for the preparation of kadsuraol C…….. 351

Scheme 5.4. C6 deoxygenation strategy for the synthesis of taiwanschirin B from **4-55**..…..... 353

Scheme 5.5. Additional C6 deoxygenation strategies from **4-6**, **4-31** or **4-30**…….. 354

List of Tables

Chapter 1

Table 1.1. Comprehensive table of DBCOD syntheses using intermolecular biaryl bond forming techniques……... 30–32

Table 1.2. Comparison of intermolecular biaryl bond forming techniques…….. 33

Table 1.3. Intramolecular biaryl bond forming techniques (excluding oxidative coupling)……. 34

Table 1.4. Comprehensive table of intramolecular oxidative coupling techniques (Ar-H to Ar-H coupling)……. 36–38

Table 1.5. Comparison of reagents for intramolecular oxidative coupling……... 40

Table 1.6. Other oxidative coupling reagents with potential to be used in DBCOD syntheses… 43

Table 1.7. Comprehensive list of intermolecular alkyl chain forming techniques……..... 48–51

Table 1.8. Intramolecular eight-membered ring forming techniques……. 53–55

Table 1.9. Ring expansion strategies proceeding through a phenanthrene intermediate…….. 56

Table 1.10. Examples of each technique utilized to incorporate chirality…….. 60–62

Chapter 2

Table 2.1. Alkylation attempts on ketones (±)-**2-7** and (±)-**2-18** with benzyl halides…… 110

Table 2.2. Alkylation attempts on ketone (±)-**2-7** via the potassium enoxytrialkylborate…….. 111

Table 2.3. Optimization of the synthesis of phenyl thionocarbonate **2-35**……. 120

Table 2.4. Screening deoxygenation conditions for the 3,5-(bistrifluoromethyl)benzoate **2-37** ……. 123

Chapter 3

Table 3.1. *Ortho*-chlorination using DCDMH and NH_2*i*PrCl catalyst……... 150

Table 3.2. *Ortho*-chlorination using SO_2Cl_2 and amine catalyst A) mechanistic proposal; B) optimization of conditions……..……. 152

Table 3.3. Enolization studies: trapping the silyl enol ethers of **3-15**……. 156

Table 3.4. Aldol addition using the various α-siloxy ketones……. 157

Table 3.5. Transmetallation studies……. 158

Table 3.6. Increasing the scale of the aldol addition (and increasing reaction time with aldehyde) ……. 159

Table 3.7. Studies on the chelation step of the methyl addition……..... 161

Table 3.8. Studies on the Lewis acid and nucleophile identities in the methyl addition…… 162

Table 3.9. Trapping the (*E*)-silyl enol ether of **3-37**……... 166

Table 3.10. Aldol addition of MOM-protected ketone **3-37** and aldehyde **3-25**……. 167

Table 3.11. Methyl addition on substrates **3-36** and **3-43**……... 170

Table 3.12. Optimization of the chelation and alkylation times in the methyl addition……. 171

Table 3.13. Increasing the scale of the methyl addition on **3-36**…… 172

Table 3.14. Optimization and scale-up of the benzylic deoxygenation in batch (Schlenk flask) ……. 175

Table 3.15. Optimization and further scale-up of the benzylic deoxygenation in flow…….. 176

Table 3.16. Screening *ortho*-lithiation conditions……... 179

Table 3.17. Screening conditions for deprotection of the MOM ether……... 180

Table 3.18. Screening *ortho*-bromination conditions……. 182

Table 3.19. Optimization of the lithium-bromine exchange / cyclization conditions……. 184

Table 3.20. Scale-up of the lithium-bromine exchange / cyclization……. 185

Table 3.21. Attempted formation of an aryl boronic ester **3-62** via the Ar-B$(OMe)_2$ intermediate ……. 186

Table 3.22. Screening Suzuki coupling conditions on **3-52**…… 188

Table 3.23. Screening Suzuki coupling conditions on **3-71**…… 191

Table 3.24. Suzuki coupling attempts on alkene substrates **3-75** and **3-76**……..... 193

Table 3.25. Chelate-controlled methyl addition on the non-halogenated aldol **3-91**…….. 199

Table 3.26. Summary of Lumb group aldol additions……..... 206–207

Table 3.27. Summary of Lumb group methyl additions……..…….. 210–211

Chapter 4

Table 4.1. Attempted C6 deoxygenation via the equatorial mesylate **4-25**…… 289

Table 4.2. Attempts at C6 allylic reduction using a $Pd(PPh_3)_4$ and a hydride source……. 306

List of Abbreviations

°C	degrees Celsius
Å	angstrom
$A_{1,3}$	allylic 1,3-strain
Ac	acetyl
acac	acetylacetonate
Ac_2O	acetic anhydride
AcOH	acetic acid
AIBN	azobis(isobutyronitrile)
APAP	acetaminophen
Ang	angelate
Ar	aryl
aq.	aqueous
BINAP	2,2'-bis(diphenylphosphino)-1,1'-binapthyl
Bn	benzyl
B_2pin_2	bis(pinacolato)diboron
Bpin	pinacol boronic ester
BPO	benzoyl peroxide
bpy	2,2'-bipyridine
br	broad
brsm	based on recovered starting material
Bu	butyl
Bz	benzoyl
calcd.	calculated
CBS	Corey-Bakshi-Shibata
CD	circular dichroism
COD	cyclooctadiene
COSY	correlation spectroscopy

Cp	cyclopentadienyl
CPME	cyclopentyl methyl ether
Cy_2BCl	chlorodicyclohexylborane
CYP450	cytochrome P450
d	doublet
Δδ	change in chemical shift
δ	chemical shift
dba	dibenzylideneacetone
DBCOD	dibenzocyclooctadiene
DBDMH	1,3-dibromo-5,5-dimethylhydantoin
DBU	1,8-diazabicyclo[5.4.0]undec-7-ene
DCDMH	1,3-dichloro-5,5-dimethylhydantoin
DCE	dichloroethane
dd	doublet of doublets
DDQ	2,3-dichloro-5,6-dicyano-1,4-benzoquinone
DIAD	diisopropyl azodicarboxylate
DIBAl / DIBALH	diisobutylaluminum hydride
DIC	*N,N'*-diisopropylcarbodiimide
DIP-Chloride™	B-chlorodiisopinocampheylborane
DIPEA	*N,N*-diisopropylethylamine
DMA	dimethylacetamide
DMAP	4-(dimethylamino)-pyridine
DME	dimethoxyethane
DMEDA	*N,N'*-dimethylethylenediamine
DMF	*N,N'*-dimethylformamide
DMP	Dess-Martin Periodinane
DMS	dimethyl sulfide
DMSO	dimethyl sulfoxide

dpm	dipivaloylmethanate or dogs per mile
dppf	1,1’-bis(diphenylphosphino)ferrocene
dq	2,2’-biquinoline
dr	diastereomeric ratio
dtb-bpy / dtbpy	4,4’-di-*tert*-butyl-2,2’-dipyridyl
EC_{50}	half maximal effective concentration
ee	enantiomeric excess
EtOAc	ethyl acetate
equiv. or eq	equivalent(s)
Et	ethyl
Et_2O	diethyl ether
EtOAc	ethyl acetate
EtOH	ethanol
FEP	fluorinated ethylene-propylene
FG	functional group
g	gram(s)
$\Delta G^{\ddagger}$	free energy barrier
h	hour(s)
HAT	hydrogen atom transfer
HMBC	heteronuclear multiple bond correlation
HMPA	hexamethylphosphoramide
HOMO	highest occupied molecular orbital
HRMS	high resolution mass spectrometry
HSQC	heteronuclear single quantum correlation
hν	light irradiation
Hz	Hertz
IBX	2-iodoxybenzoic acid
IC_{50}	half maximal inhibitory concentration

*i*Pr / ^{i}Pr	isopropyl
IR	infrared
J	coupling constant
KHMDS	potassium bis(trimethylsilyl)amide
LDA	lithium diisopropylamide
LED	light-emitting diode
LHMDS	lithium bis(trimethylsilyl)amide
LRMS	low resolution mass spectrometry
LUMO	lowest unoccupied molecular orbital
M	molar (mol/L)
m	multiplet or milli
m	meta
Me	methyl
MeCN	acetonitrile
MeOH	methanol
mesna	2-mercaptoethanesulfonate
MOM	methoxy methyl
MOMCl	chloromethyl methyl ether
min	minute(s)
mol	mole(s)
Ms	mesyl
MS	molecular sieves
m/z	mass to charge ratio
NaHMDS	sodium bis(trimethylsilyl)amide
*n*Bu	*n*-butyl
*n*BuLi	*n*-butyllithium
NMR	nuclear magnetic resonance
NBS	*N*-bromosuccinimide

NEt_3	triethylamine
NHPI	*N*-hydroxyphthalimide
NMO	*N*-methylmorpholin *N*-oxide
nOe	nuclear Overhauser effect
NOESY	nuclear Overhauser enhancement spectroscopy
Nu	nucleophile
o	ortho
OAc	acetate
OMe	methoxy
OTf	trifluoromethanesulfonate
p	para
PCC	pyridinium chlorochromate
PEPPSI-IPr	[1,3-bis(2,6-diisopropylphenyl)imidazol-2-ylidene](3-chloropyridyl)palladium(II) dichloride
PET	photoinduced electron transfer
Ph	phenyl
PhH	benzene
PIDA	(diacetoxyiodo)benzene
PIFA	(bis(trifluoroacetoxy)iodo)benzene
ppm	parts per million
PPTS	pyridinium *p*-toluenesulfonate
ppy	2-phenylpyridine
PTH	*N*-phenylphenothiazine
py	pyridine
q	quartet
Rf	retention factor
R_L	largest substituent
ROS	reactive oxygen species
rt	room temperature

RuPhos	2-dicyclohexylphosphino-2’,6’-diisopropoxybiphenyl
s	singlet
SAR	structure activity relationship
SCE	standard calomel electrode
s-BuLi	*sec*-butyllithium
SM	starting material
SPhos	2-dicyclohexylphosphino-2’,6’-dimethoxybiphenyl
SPhos Pd G2	chloro(2-dicyclohexylphosphino-2′,6′-dimethoxy-1,1′-biphenyl)[2-(2′-amino-1,1′-biphenyl)]palladium(II)
T	temperature
t	triplet
t	time
TB	twist boat
^{t}Bu	*tert*-butyl
TBC	twist boat chair
TBAF	tetra-*n*-butylammonium fluoride
TBAI	tetra-*n*-butylammonium iodide
TBDPS	*tert*-butyldiphenylsilyl
TBS	*tert*-butyldimethyl silyl
*t*Bu	*tert*-butyl
t-BuLi	*tert*-butyllithium
TES	triethylsilyl
TFA	trifluoroacetic acid or trifluoroacetate
TFAA	triluoroacetic anhydride
TFE	trifluoroethanol
TFP	tri(2-furyl)phosphine
THF	tetrahydrofuran
TIPS	triisopropylsilyl
TLC	thin layer chromatography

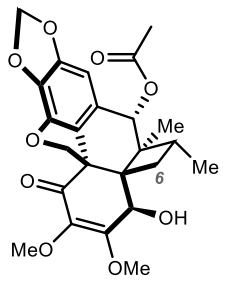
TMEDA	*N,N,N',N'*-tetramethylethylenediamine
TMDSO	tetramethyldisiloxane
TMP	2,2,6,6-tetramethylpiperidine
TMPMgBr	2,2,6,6-tetramethylpiperidine magnesium bromide
TMS	trimethylsilyl
Toluene	PhMe
TsOH / PTSA	*p*-toluenesulfonic acid
UV-Vis	ultraviolet-visible
V	Volt(s)
VT	variable temperature
XantPhos	4,5-bis(diphenylphosphino)-9,9-dimethylxanthene
XPhos	2-dicyclohexylphosphino-2',4',6'-triisopropylbiphenyl

Chapter 1. Introduction to Dibenzocyclooctadiene Lignan Natural Products

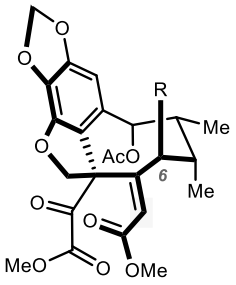
1.1. Introduction

1.1.1. Synthetic dibenzocyclooctadiene targets of this thesis

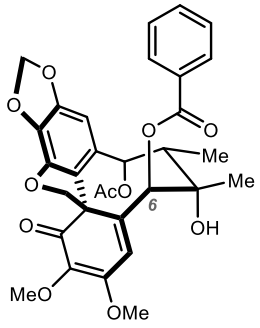
This thesis will focus on synthetic work towards two target dibenzocyclooctadiene (DBCOD) lignan natural products: kadsuraol C and taiwanschirin B (Figure 1.1). Chapter 1 provides a review of the relevant literature on DBCOD lignan natural products, including a background on lignin and lignans, structural features and classification, occurrence and biological activity, the proposed biosynthesis, and an emphasis on previous chemical syntheses. In Chapter 2, several of the key steps towards these targets were first investigated on a simplified model system. In Chapter 3, efforts towards the synthesis of kadsuraol C are described and in Chapter 4, the synthesis of 6-benzyloxy taiwanschirin B is reported. A deoxygenation strategy serves as a unifying approach to access both DBCODs, which unlike previously targeted DBCODs (eg. heteroclitin J, Figure 1.1),[1] do not possess oxygenation at C6. A bulky substituent at C6 proved to be crucial for biaryl bond formation, therefore this stereocenter had to be set in the linear system and removed post-cyclization. The development of selective deoxygenation strategies could also allow for the possibility of accessing DBCODs with various oxidation patterns around C6–C9.



kadsuraol C



R= OBz: 6-benzyloxy taiwanschirin B
R= H: taiwanschirin B



heteroclitin J

Figure 1.1. Synthetic dibenzocyclooctadiene targets of this thesis: kadsuraol C and taiwanschirin B and a target of previous work in our group: heteroclitin J

1.1.2. Background on Lignin and Lignan

DBCODs are members of the lignan family of natural products which are studied both for their intriguing structures and array of bioactivities.[2] Lignans and lignin share the same monomeric building blocks: phenylpropanoid radicals derived from coniferyl alcohol, sinapyl alcohol, and *p*-

coumaryl alcohol (Figure 1.2). However, lignans and lignin have appreciably different overall structures and functions, with lignin being a high molecular weight complex polymer with applications in the field of materials and lignans being small (usually dimeric) molecules, more commonly studied for their bioactive properties.[3–5] It is interesting to consider the relationship between these two types of molecules in the context of the valorization of lignin.[6,7] We expect that lignin, which is a readily available feedstock chemical, could potentially be depolymerized[7] to use for the synthesis of lignans from these same building blocks.

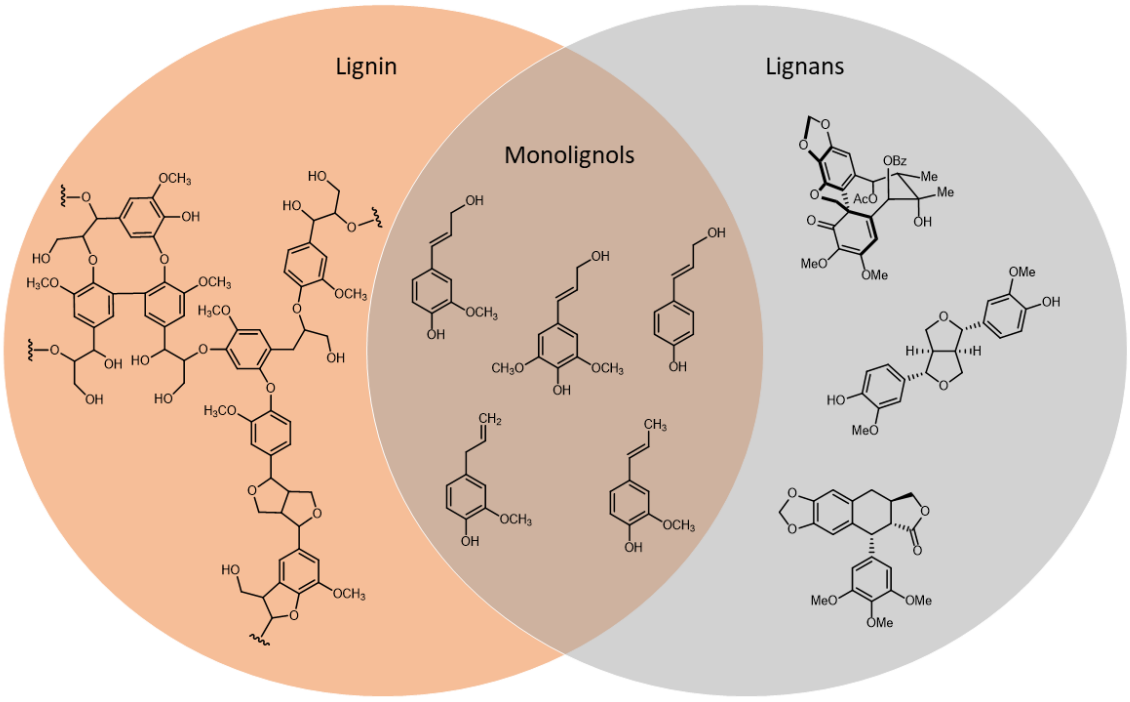


Figure 1.2. Lignans and lignin share monolignols as common precursors

Lignin is present in all woody (vascular) plants. The lignin's role in the cell wall is to act as a cross-linking agent that rigidifies the cell wall, whereas cellulose provides tensile strength.[3] It is made up of polymerized phenylpropanoid units in complex cross-linked networks, where several different C-O and C-C linkages are possible. Lignin polymerization begins at "lignin initiation sites" at the outermost of the cell wall and the polymer is built inward towards the plasma membrane.[8,9] After lignification is complete, the cell dies. Biosynthetic hypotheses for the polymerization of lignin include random coupling (with only chemical control) or enzymatic control provided by dirigent proteins (which are proteins that dictate the stereochemistry of a compound synthesized by other enzymes), similar to lignan biosynthesis (*vide infra*).[10,11]

Lignans are isolated from selected vascular plants, where they act as metabolites for plant defense (eg. antioxidants or biocides) and play a role in cell signaling pathways.[12–14] Lignans are made up of phenylpropanoid units which are coupled by a laccase or peroxidase with the help of a dirigent protein, usually as dimers. Types of lignans include: dibenzyl butanes, furofurans, furans, dibenzylbutyrolactones, dibenzylbutyrolactols, cyclobutanes, aryltetralins (e.g. aryltetrahydronaphthalenes), arylnapthalenes, dibenzocyclooctadienes, cyloheptenes, neolignans, norlignans, oxyneolignans, and norneolignans.[15] Several reviews on lignans have already been published,[15–19] so this chapter will focus on the dibenzocyclooctadiene lignans (DBCODs) which have not been reviewed since 2013[2,20,21] and are the targets of this synthetic work .

1.2. General Structural Features and Classification of DBCODs

DBCODs are lignans made from two monolignol building blocks. They possess several defining features: i) a biaryl bond with an axis of chirality, ii) an 8-membered ring with (usually *syn*) methyl groups, iii) a varied degree of oxidation around the 8-membered ring (can be highly oxygenated), and iv) varied aromatic substituents. The steganacins and gymnothelignans are similar in structure to the DBCODs but have different biosynthetic origins. Steganacins differ from the DBCODs in that they have a *trans* lactone instead of methyl groups. Gymnothelignans have an oxygen bridge across C6 and C9.

DBCODs are numbered according to the formalism depicted in Figure 1.3, beginning with the carbon that is *ortho* to the biaryl axis but not part of the 8-membered ring. Numbering continues in a clockwise manner around the core structure (Figure 1.3). The methyl groups on the cyclooctadiene are then sequentially numbered, and then the aryl substituents. Any esters on C6 or C9 are numbered as 1', 2', etc. starting from the end bound to the cyclooctadiene.

DBCODs from *Schisandraceae* can be classified by stage (Figure 1.3).[1] Stage 1 DBCODs have a non-oxidized carbon framework. That is, there is no oxidation along the cyclooctadiene, however, oxidations on the aromatic rings are allowed. Stage 2 DBCODs are those which have any oxygenation around the 8-membered ring (mono, di, and tri-oxidized are all included). Stage 3 DBCODs have undergone additional non-canonical oxidations, for example possessing a spirodienone or a macrocycle. Steganacins and gymnothelignans are classified separately. Steganacins can be either stage 1 or stage 2 using an analogous definition to that used for the DBCODs, whereas gymnothelignans are not classified by stages.

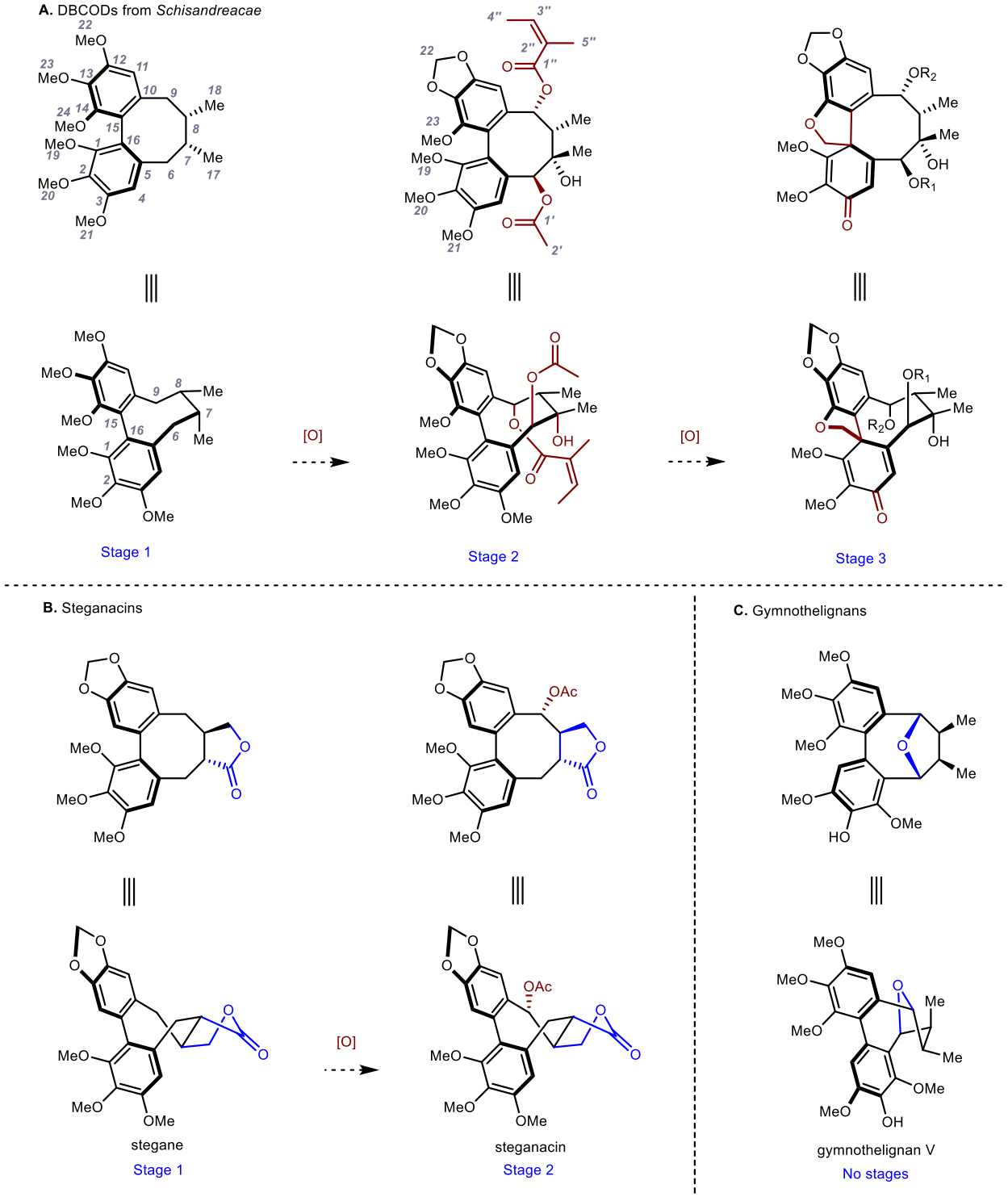


Figure 1.3. A) Numbering and classification of DBCODs, B) steganacins, and C) gymnothelignans

1.3. Spectral Data and Conformational Properties

1.3.1. Conformational Analysis

Medium sized rings (7–11 membered) are a prevalent motif in natural products but less common in medicinal chemistry due, in part, to the difficulty of their synthesis.[22] The synthesis of 8-membered rings is particularly difficult due to their relatively high strain energy, but also the entropic factors that complicate cyclization from a linear precursor. The strain energy is a combination of torsional strain, bond stretching, bond-angle bending, out of plane bending, and non-bonding interactions which have been investigated via NMR studies and computationally.[23] The 8-membered ring in DBCODs is often highly functionalized, possessing esters or hydroxyl groups at C6 and C9, as well as methyl groups at C7 and C8, which poses the challenge of setting stereocenters in a sterically congested environment.[24] There is plenty of room for future work in this area as there is currently a lack of synthetic methods for the concise and divergent synthesis of cyclooctanoid molecules.

Calculations on *cis*-*cis*-1,3-cyclooctadiene have found that the twist boat (TB) and twist boat chair (TBC) are the two minimum energy conformations.[23] For an unsubstituted *cis*-*cis*-1,3-cyclooctadiene, these two conformations have very similar strain energies of 7.12 and 7.66 kcal/mol for the TBC and TB, respectively. The TB is only slightly higher in energy due to stem-to-stern interactions (Figure 1.4A).

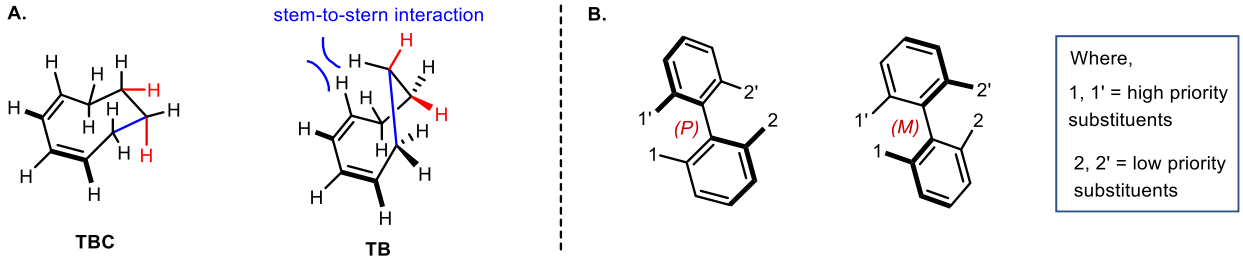


Figure 1.4. A) Minimum energy conformations of the 8-membered ring; B) conformations of the biaryl axis

Besides the 8-membered ring, the other key feature of the DBCOD skeleton is the chiral biaryl axis. Hindered rotation about the aryl-aryl single bond leads to optical activity, meaning each biaryl can exist as two possible atropisomers, (*M*) or (*P*) (Figure 1.4.B). Atropisomers are recognized as physically separable species when, at a given temperature, they have a half-life of

at least 1000 s (16.7 min).[25] Over a thousand biaryls having a configurationally stable axis (fixed as either *M* or *P*) have been isolated from nature, eg. vancomycin and DBCODs. Drastically differing bioactivity and pharmokinetics can be observed in the (*M*) vs. (*P*) atropisomer of the same biaryl compound, which gives chemists the crucial and challenging task of setting this axial chirality correctly during synthesis.[25,26] Although a biaryl species may be axially chiral at room temperature, it may be able to atropisomerize (physically rotate) at higher temperature, giving a thermodynamically controlled equilibrium of the two atropisomers.[26] This strategy is applied in several DBCOD syntheses where the unnatural atropisomer was initially synthesized.

DBCODs are considered conformationally stable as it is too sterically demanding for them to isomerize from the (*P*) to (*M*) conformation or vice-versa at room temperature. A DBCOD such as kadsurin (**1-6**) will undergo interconversion from the (*P*)-TBC to (*P*)-TB conformations at room temperature as this has an energy barrier no greater that 14 kcal/mol (Figure 1.5A). The (*P*)-TB to (*M*)-TB interconversion, however, has a higher energy barrier of at least 35 kcal/mol and can only occur at elevated temperatures.[27] Transitioning from (*P*)-TBC to (*P*)-TB does not incur much of an energetic penalty as the C7 and C8 methyl groups are staggered in both conformations, however, going to the boat conformation requires more energy as the methyl groups must eclipse (as depicted by Newman projections in Figure 1.5B). The boat transition state which occurs midway through the biaryl bond rotation of the (*P*)-TB to the (*M*)-TB conformation necessitates that the *ortho* methoxy substituents on each aromatic ring are in the same plane, incurring $A_{1,3}$ strain. This can be depicted by Newman projections, looking down the biaryl axis (C15–C16), where in the TB conformation the methoxy groups are staggered, but in the boat conformation they are eclipsed (Figure 1.5C).

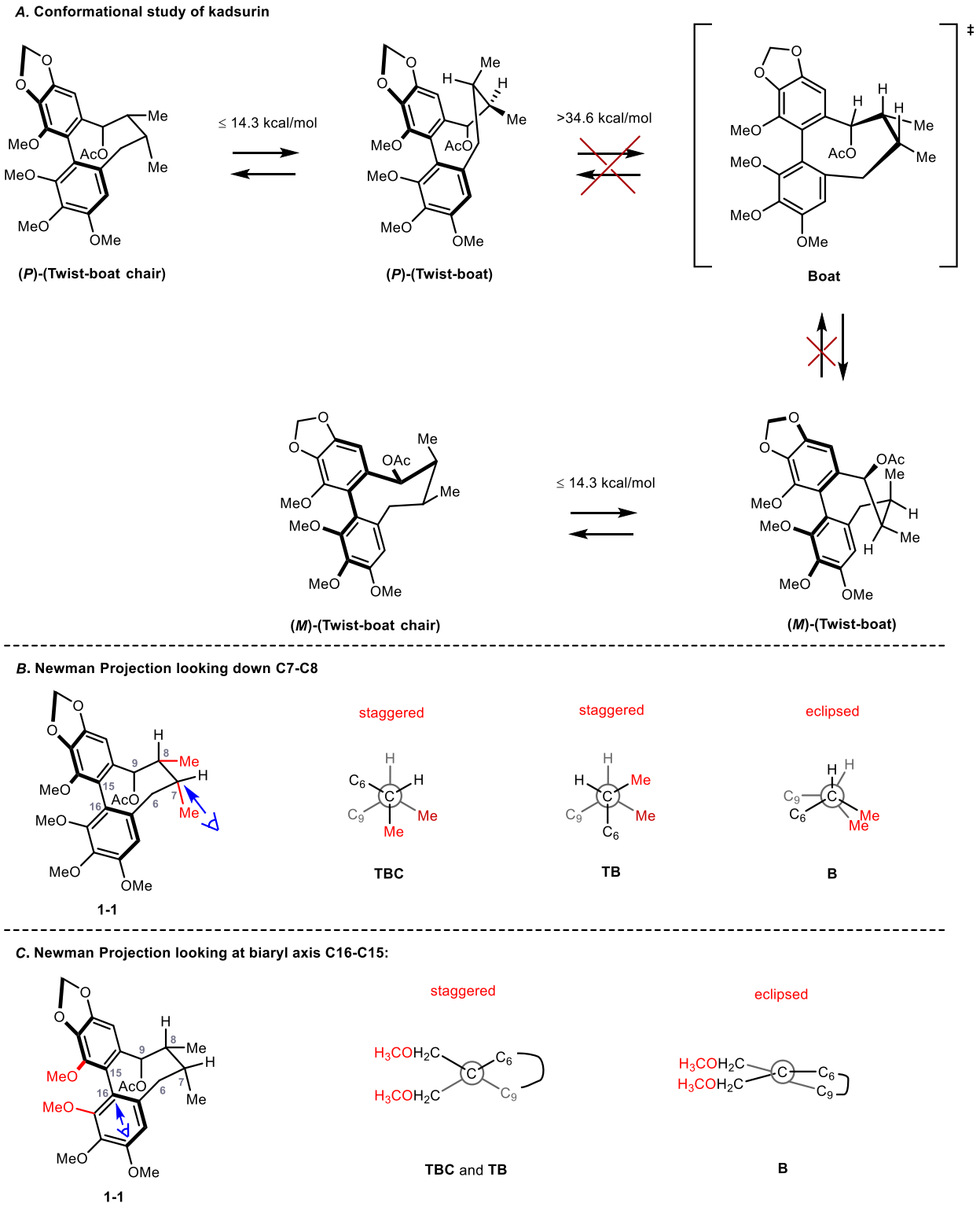


Figure 1.5. Conformational analysis of a DBCOD (kadsurin, **1-1**)

1.3.2. Spectral Data

Various spectroscopic techniques, including NMR, UV-Vis, and circular dichroism (CD), reveal key features about the degree of oxidation, connectivity, and conformational flexibility of DBCODs.[2] In the ^{1}H NMR spectrum, aromatic protons on the C4 and C11 positions of the electron-rich aromatic rings have typical chemical shift values (δ) between 6.4 – 7.0 ppm. The difference in chemical shift values between these two pseudo-symmetrical protons can vary as a function of the conformation of the biaryl linkage. Coleman and coworkers observed a Δδ value of 0.52 ppm for (*P*)-configured intermediate **1-19** during their synthesis of C6-monooxygenated DBCODs, while the Δδ value for the (*M*)-atropisomer was 0.11 ppm (Figure 1.6).[28,29] If the DBCOD is in a TBC conformation, the vicinal coupling between the axial hydrogen atom at C8 and the equatorial hydrogen at C9 is usually negligible (around 0 Hz), and the C9 proton appears as a singlet. Due to the shielding effect of the perpendicular aromatic rings, the axial benzylic esters at C6 and C9 experience an upfield shift (*e.g.* δ = 1.56 ppm for C9-OAc in heteroclitin Q **1-20**) relative to regular benzylic esters (δ = 2.10 ppm for benzyl acetate). For the same reason, the C1- and C14-OMe groups are shifted upfield (δ = 3.39 ppm for C14-OMe in **1-20**), whereas the chemical shift values for typical aromatic methoxy groups are greater than 3.70 ppm. Stage 3 DBCODs also exhibit enlightening spectral properties. For example, in the ^{1}H NMR spectrum of spirodienones such as **1-21**, the diastereotopic protons of the methylene at C19 exhibit a large geminal coupling constant ($^{2}J \approx 9.0$ Hz) and appear between 4.0–4.7 ppm. The *ortho*- and *para*-isomers of the spirodienone are distinguishable by their ^{13}C NMR spectra. For *ortho*-spirobenzofuranoids such as kadsulignan C (**1-21**),[30] a chemical shift of 194.9 ppm is observed for the carbonyl, whereas in the *para*-isomer as in kadsulignan E (**1-22**), the chemical shift appears at 182.5 ppm.[31]

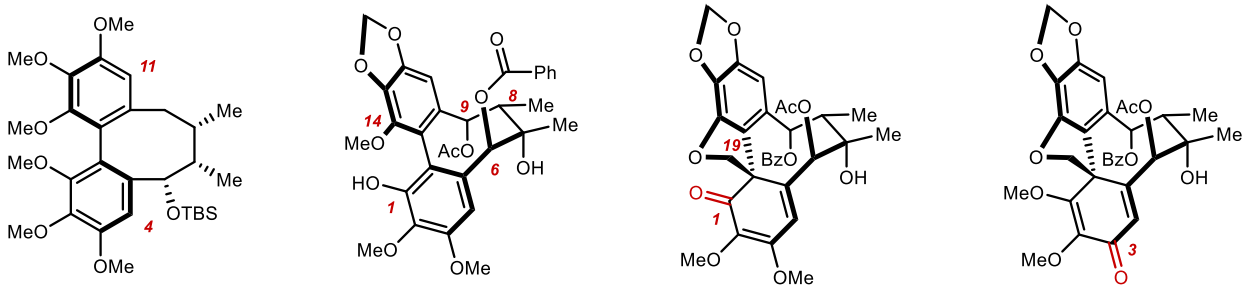


Figure 1.6. Characterization of DBCOD compounds.

DBCODs also have several characteristic signals that can be observed by UV-Vis spectroscopy. They display strong absorption signals at 220, 254 and 278 nm, due to the configurationally stable biaryl bond.[2] UV-Vis spectroscopy can also distinguish between *ortho*- and *para*-spirobenzofuranoids. The *ortho*-spirobenzofuranoid in kadsulignan C (**1-21**) exhibits a characteristic absorption at 325-335 nm that is consistent with its slightly yellow color,[30] whereas the colorless *para*-isomer's absorbance is blue shifted to 305–310 nm.[31] While X-ray crystallography is the most reliable way of determining the absolute stereochemistry of the chiral axis, CD spectroscopy can also serve as a powerful alternative when the compound is not crystalline. The *P* (or *S*) configuration of the biaryl axis usually shows a positive Cotton effect at 220 nm as well as a negative Cotton effect at 254 nm, while the *M* (or *R*) configured compounds exhibit equal, but opposite signs.[2]

1.4. Occurrence and Biological Activity

Since the first report in 1961,[32] more than 500 DBCOD natural products have been isolated. Most are isolated from plants within the *Schisandraceae* family, including *Schisandra chinensis*, *Kadsura coccinea*, and other species within these genera. Only the steganacins and gymnothelignans originate from different plant sources, ie. the *Steganotaenia* and *Gymnotheca* genera of the *Apiaceae* and *Saururaceae* families, respectively. *Schisandra chinensis* in particular is a well-known plant whose berries have been used for thousands of years in traditional Chinese medicine to treat ailments ranging from cough to cancer and hepatotoxicity. It still remains a part of the Chinese, Russian, Japanese, Korean, and American Pharmacopoeias today.[33–35] *Kadsura* is less popular, having mostly been utilized medicinally by some indigenous tribes and only more recently making its way into the Chinese Pharmacopeia. Although *S. chinensis* products (eg. herbal teas) are available for purchase, *Schisandra* and *Kadsura* grow exclusively in specific portions of Asia and only small quantities of DBCODs have been isolated from the plant material, often as complex mixtures. As a result, a few of the more naturally abundant DBCODs (such as deoxyschizandrin and gomisin N) have been thoroughly assayed for bioactivity but most remain underexplored to date. Many diverse bioactivities have been reported for DBCODs with the most prevalent being antioxidant, antiviral, hepatoprotective, anticancer, neuroprotective, and cardiovascular protective activity.

Antioxidant activity

Reactive oxygen species (ROS) and oxidative stress play a role in the progression of human degenerative diseases such as inflammation, aging, and cancer. In a 2006 study by Khan and coworkers, seven out of thirteen DBCODs screened were found to have antioxidant activity against H_2O_2-induced oxidative stress in HL-60 cells.[36] Gomisin K, angeloylgomisin, tigloylgomisin H, gomisin J, gomisin B, gomisin G and schisandrene were found to have IC_{50} values ranging from 2.8 to 160.9 μM, with the most potent being schisandrene (**1-23**, 2.8 μM) and gomisin G (**1-24**, 38.2 μM, Figure 1.7). The antioxidant activity of schisandrene is superior to that of the commercial antioxidant vitamin C (**1-25**, 10.2 μM) and comparable to that of Trolox (**1-26**, 3.6 μM). Study of the structure-antioxidant activity relationship found that the presence of an exocyclic methylene greatly increased activity and a benzoyl group provided a smaller increase. A potential mechanism of the DBCODs' antioxidant activity involves the *in vivo* oxidation of the aromatic methoxy groups to reveal free phenols, well known antioxidants.[37] DBCOD gomisin T (**1-27**) demonstrated inhibition of NOX2 (NADPH oxidase 2, which generates ROS) and was confirmed to be a superoxide scavenger.[38] Studies on gomisin J (**1-28**) have found that it has an anti-lipid peroxidation effect in liver mitochondria and that it is a scavenger of superoxide anion radicals as well as hydroxyl radicals.[39]

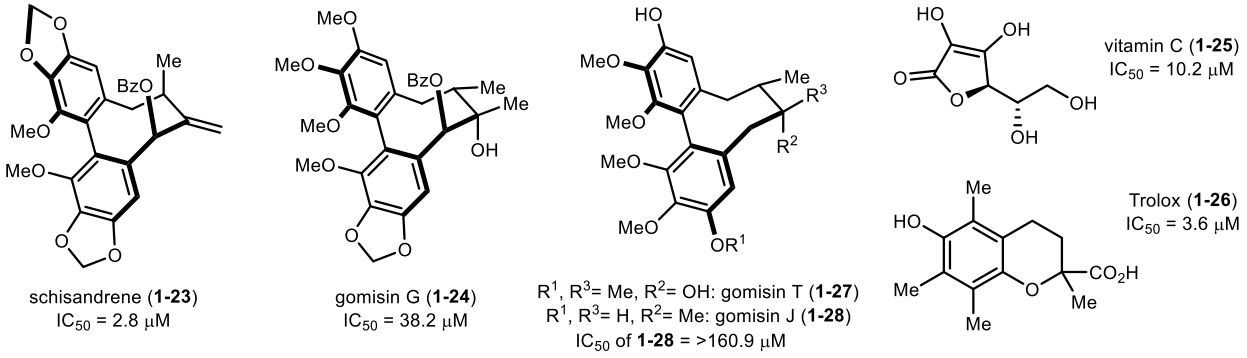


Figure 1.7. Antioxidant DBCODs and comparison to commercial antioxidants.

Antiviral activity

A number of DBCODs have demonstrated antiviral activity against HIV and/ or hepatitis B (HBV). In a study of 12 lignans, seven DBCODs were found to be active against HIV, with gomisin G (**1-29**), schisantherin D (**1-30**), kadsuranin (**1-31**), and schisandrin C (**1-32**) displaying the highest activities with EC_{50} values of 0.01, 1.0, 2.0, and 3.1 μM, respectively (Figure 1.8A).[40] These values

were superior to the antihepatic drug biphenyldicarboxylate (DDB, EC_{50} = 12.0 μM). Investigation of the SAR implied that 7-hydroxy and 6-benzoyl substituents improved anti-HIV activity. Additionally, it was found that compounds bearing at least one benzodioxolane moiety were more active than those solely bearing methoxy substituents on the aromatic rings. The mechanism of action was studied on gomisin M1 (**1-33**), a DBCOD which displayed anti-HIV activity against a wide variety of viral strains with EC_{50} values of 1-3 μM.[41] qPCR and *in vitro* enzyme assays were used to determine that gomisin M1 acted as a non-nucleoside reverse transcriptase inhibitor (NNRTI). Testing of DBCODs for anti-HBV activity has been performed by measuring the inhibition of the secretion of antigens HBsAg and HBeAg (Figure 1.8B). Kuo *et al.* found that schizarin B (**1-34**) displayed the highest anti-HBV activity out of six DBCODs screened, where it inhibited both antigens by > 40 % (at 10 μg/mL concentration).[42] Analysis of the SAR determined that the identity of the C6 substituent could be important for bioactivity. Work by Pu, Sun, and coworkers found that schinlignan G (**1-35**) demonstrated potent anti-HBV activity, with IC_{50} values of 9.73 and 11.21 μg/mL for inhibition of the secretion of HBsAg and HBeAg, respectively, comparable to those of the antiviral drug tenofovir (with IC_{50} values of 19.19 and 23.13 μg/mL,

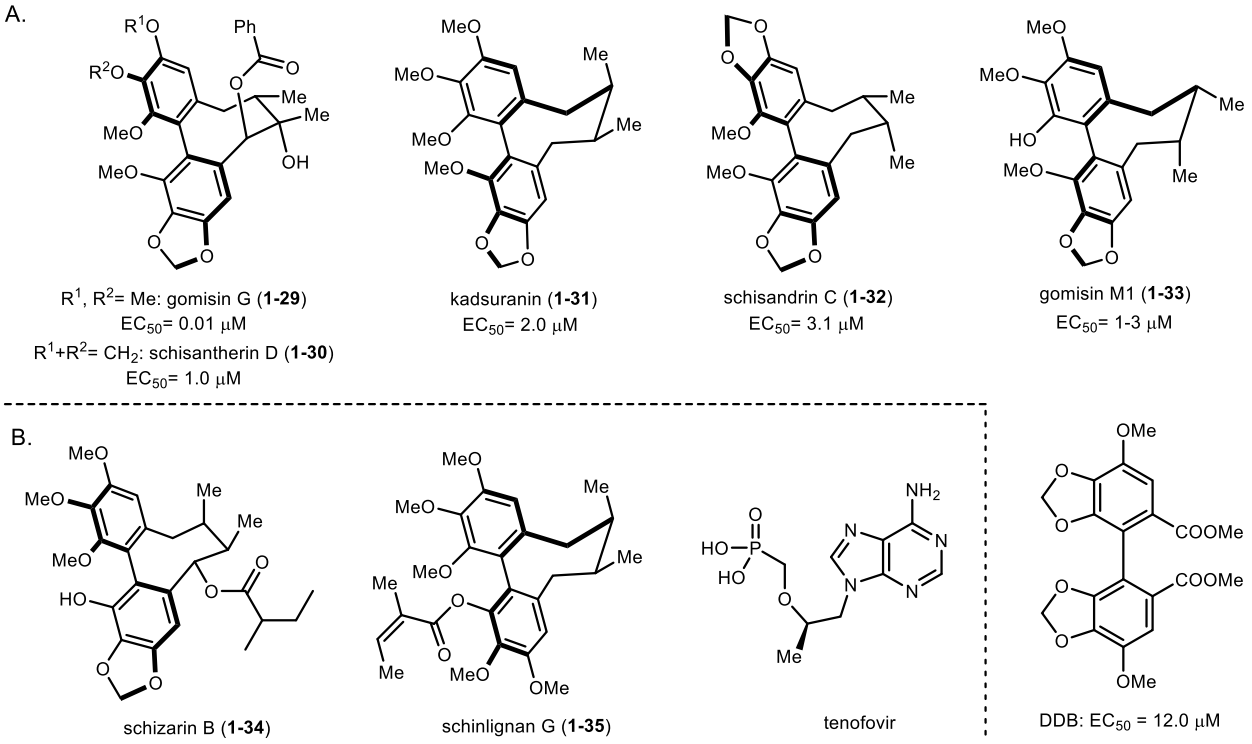


Figure 1.8. Antiviral DBCODs with A. anti-HIV activity; B. anti-HBV activity and antiviral drug tenofovir

respectively). **1-35** also showed potent inhibition against HBV DNA replication (IC_{50} = 5.13 μg/mL).[43]

Hepatoprotective activity

Several DBCODs have been reported to have hepatoprotective activities, which could be used to combat chemical liver injury, the second largest cause of liver disease.[44] In a study by Mu and coworkers, the DBCODs schizandrin (**1-17**), schizandrin B (**1-16**), and schisanhenol (**1-36**, Figure 1.9) all demonstrated stronger hepatoprotective effects against CCl_4-induced injury of liver cells (43.3-48.1 % cell survival rate) than the positive control DDB (cell survival rate of 40.3 ± 5.4 %).[45] The mechanism of hepatoprotection of **1-16** was studied using a proteomics approach, which found that Raf kinase inhibitor protein (RKIP) was most likely the key regulator involved in drug-induced liver cell damage.[46] The study established that **1-16** triggers the Raf/MEK/ERK signalling pathway, likely by downregulating RKIP, thus providing protection against CCl_4-induced liver

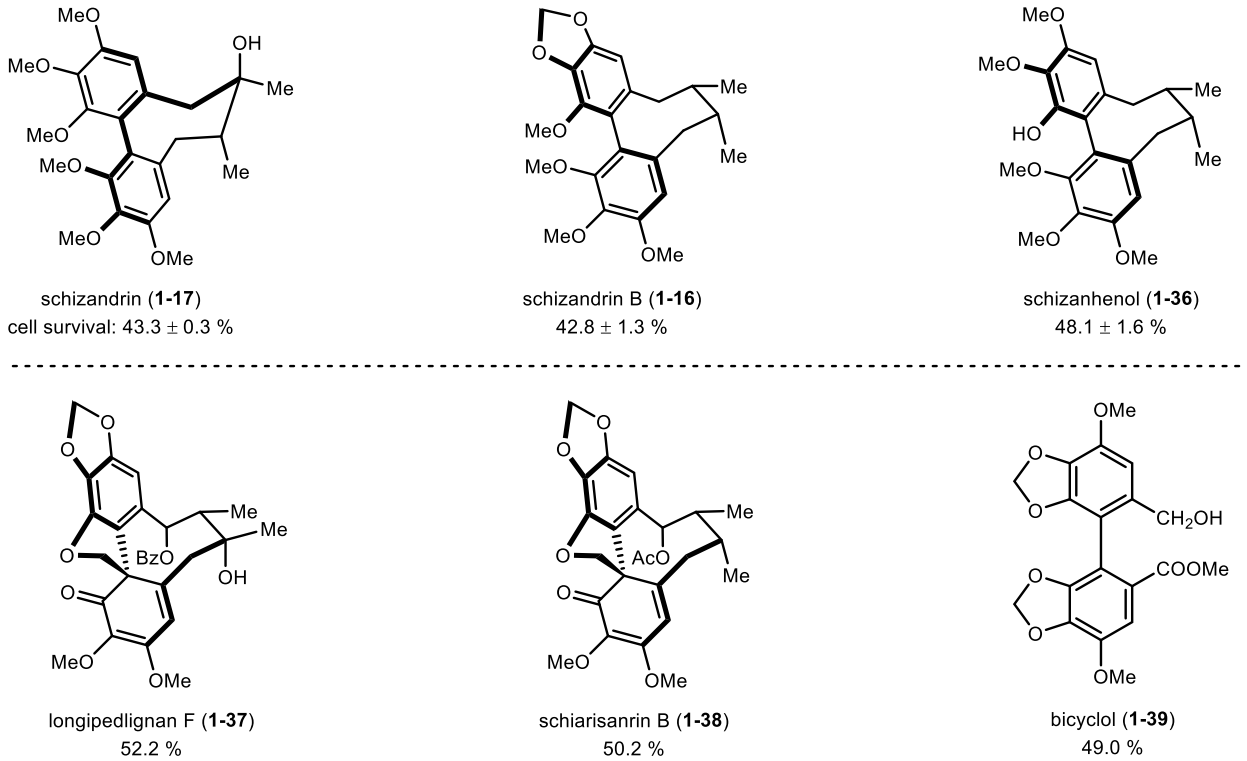


Figure 1.9. Hepatoprotective DBCODs and positive control bicyclol (with cell survival rates)

injury. Spirocyclic DBCODs schiarisanrin B (**1-38**) and longipedlignan F (**1-37**) have been reported to have hepatoprotective activity against APAP-induced toxicity in HepG2 cells, effecting cell survival rates of 50.2 and 52.2 %, which is comparable to that of the positive control bicyclol (**1-39**, 49.0 %).[47]

Anticancer activity

Cancer is one of the leading causes of morbidity and mortality, making the discovery of new anticancer drugs essential.[48] Kupchan and coworkers found that the steganacin-type lignans steganacin (**1-40**) and steganangin (**1-41**) exhibited high activity *in vitro* against human carcinoma nasopharynx cells (KB) at concentrations of 10^{-1}–10^{-3} μg/mL and *in vivo* against P-388 leukemia in mice (Figure 1.10).[49] Investigation into the mechanism of action determined that steganacin inhibits the polymerization of tubulin *in vitro* and causes a slow depolymerization of preformed microtubules.[50] It inhibits the binding of colchicine to tubulin in a similar manner to podophyllotoxin. A few stage 2 and 3 DBCODs have also demonstrated anticancer activity. In a study evaluating kadsufolins A–D for cytotoxicity against several human tumor cell lines, kadsufolin D (**1-42**) was found to be the most potent, with strong activities against lung carcinoma (A549) and ileocecal carcinoma (HCT-8) with GI_{50} values of 5.1 and 5.7 μg/mL, respectively.[51]

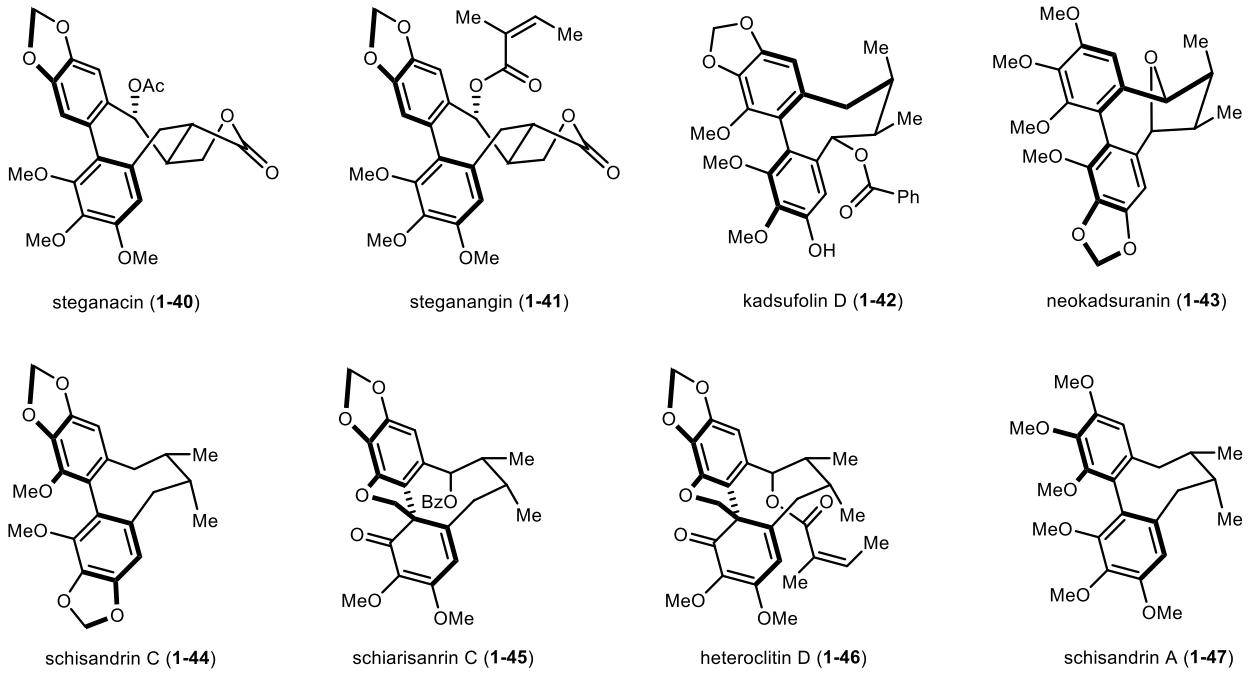


Figure 1.10. DBCODs with anticancer activity

In work by Chen *et al.*, 14 neolignans were screened for their ability to inhibit Epstein-Barr virus early antigen (EBV-EA) activation, which correlates to antitumor-promoting activity.[52] Neokadsurin (**1-43**) and schisandrin C (**1-44**) displayed potent inhibition of EBV-EA, indicating that they could serve as antitumor promoters. In a study by Kuo and coworkers, *ortho*-spirodienone schiarisanrin C (**1-45**) was found to exhibit cytotoxicity against KB, colon carcinoma (COLO-205), hepatoma (HEPA), and cervix (HELA) tumor cells, with ED_{50} values of 0.36, 7.1, 4.9, and 5.7 μg/mL respectively.[53] *Ortho*-spirodienone heteroclitin D (**1-46**) has shown the ability to promote apoptosis and inhibit the growth of gastric cancer cells.[39] Some DBCODs have even been able to reverse the effects of multidrug resistant (MDR) cancer. In a study of five schisandrins, schisandrin A (**1-47**) demonstrated the most potent MDR reversal activity, with reversal of vincristine resistance in KBv200 (human epidermal cancer) cells, MCF-7/Doxorubicin (human breast cancer) cells and Bel7402 (human liver cancer) cells by 309-, 38- and 84-fold, respectively.[54]

Neuroprotective activity

There are currently no drugs approved to prevent neuronal cell loss in the brains of patients afflicted by Parkinson's disease or Alzheimer's disease, thus making the discovery of neuroprotective drugs for these applications enticing.[55] In a study by Sun and coworkers, ananolignans A–N were screened for antineurodegenerative activity using SH-SY5Y neuroblastoma cells.[56] Ananolignans F and L (**1-48** and **1-49**) demonstrated the highest cell survival rates against H_2O_2-induced neurotoxicity (90.0 ± 2.1 % and 79.2 ± 3.7 %, respectively, with concentrations of 1 μM substrate and 100 μM H_2O_2), indicating that they exhibit significant neuroprotective activity (Figure 1.11). In another study, polysperlignans A, B, D, and E as well as tiegusanin I and kadsurin displayed neuroprotective effects against PC12 neuroblastoma cells, demonstrating promising cell survival rates against H_2O_2 or $A\beta_{25–35}$-induced neurotoxicity (Figure 1.11).[57] Schizandrin (**1-17**, Figure 1.9) has been found to improve $A\beta_{1–42}$-induced memory impairment in mice via antioxidative action, suggesting that it could serve as a potential cognitive enhancer against Alzheimer's disease.[58] **1-17** has also been observed to reduce neurological deficits and prevent cognitive impairment caused by ischemic brain injury in mice.[39] In a study by Wang and coworkers, gomisin N (also known as schizandrin B, **1-16**, Figure 1.9) displayed neuroprotective effects against Alzheimer's disease by selectively targeting glycogen synthase

kinase-3β (a key enzyme in the hyperphosporylation of tau proteins) in an orthosteric binding mode with an IC_{50} value of 70 nm.[59]

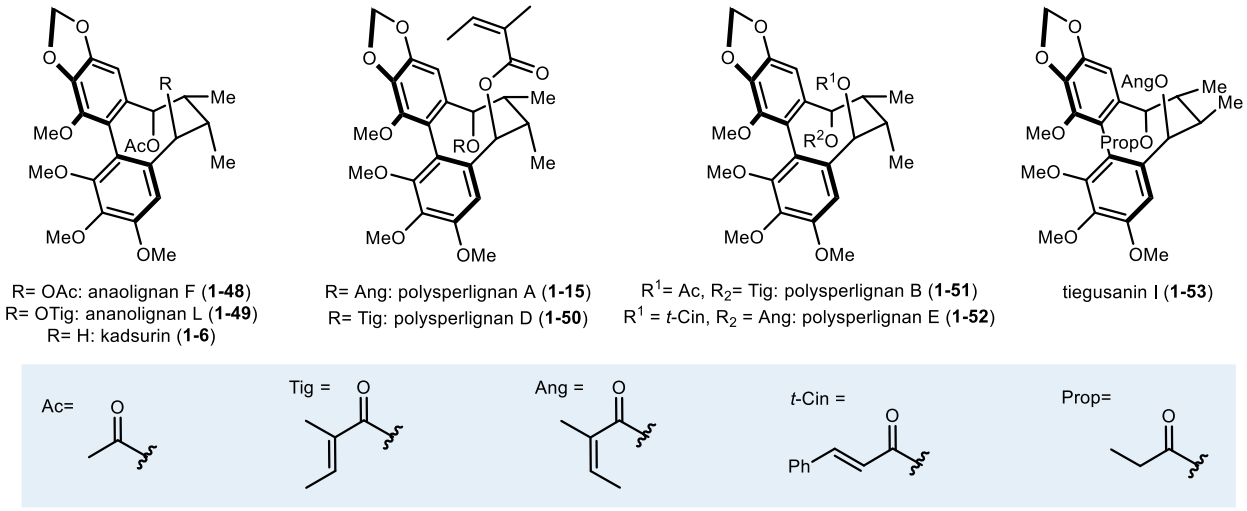


Figure 1.11. DBCODs with neuroprotective activity

Cardiovascular protective activity

Several DBCODs have been reported to exhibit cardiovascular protection effects. Schisandrin A (**1-47**, Figure 1.10) was able to suppress inflammation and oxidative stress *in vitro* and in rats, thus protecting against cerebral ischemia/ reperfusion injury.[60] This effect is the result of **1-47** activating the Nrf2 and the AMPK signaling pathways, where Nrf2 regulates the expression of various antioxidant and ROS detoxifying genes and AMPK induces apoptotic cell death in a neuronal context. Schisandrin C (**1-32**, Figure 1.8) was found to protect against angiotensin II (Ang II)-induced aorta oxidative stress and relaxation in mice.[61] Mechanistically, it alleviates oxidative stress by regulating the Keap/Nrf2 signaling pathway. These results support the potential use of **1-32** for the improvement of endothelial dysfunction and treatment of cardiovascular diseases (CVD). Isovaleroylbinankadsurin A (**1-54**) demonstrated a cardioprotective effect against myocardial ischemia/ reperfusion injury, making it a potential drug candidate for CVD (Figure 1.12).[62] It acts by inhibiting the generation of reactive oxygen species via activating the glucocorticoid receptor dependent reperfusion injury salvage kinase pathway. Gomisin J (**1-55**) has displayed vasodilatory and antihypertensive activity *in vitro* and in mice (Figure 1.12).[63] It is proposed that **1-55** decreases blood pressure in Ang II-induced hypertensive mice by inhibiting

ROS production, preserving vascular nitric oxide bioavailability, and preventing the impairment of eNOS (endothelial nitric oxide synthase) function.

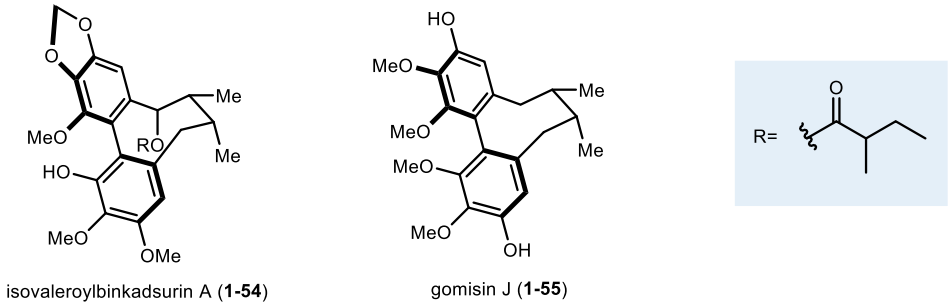


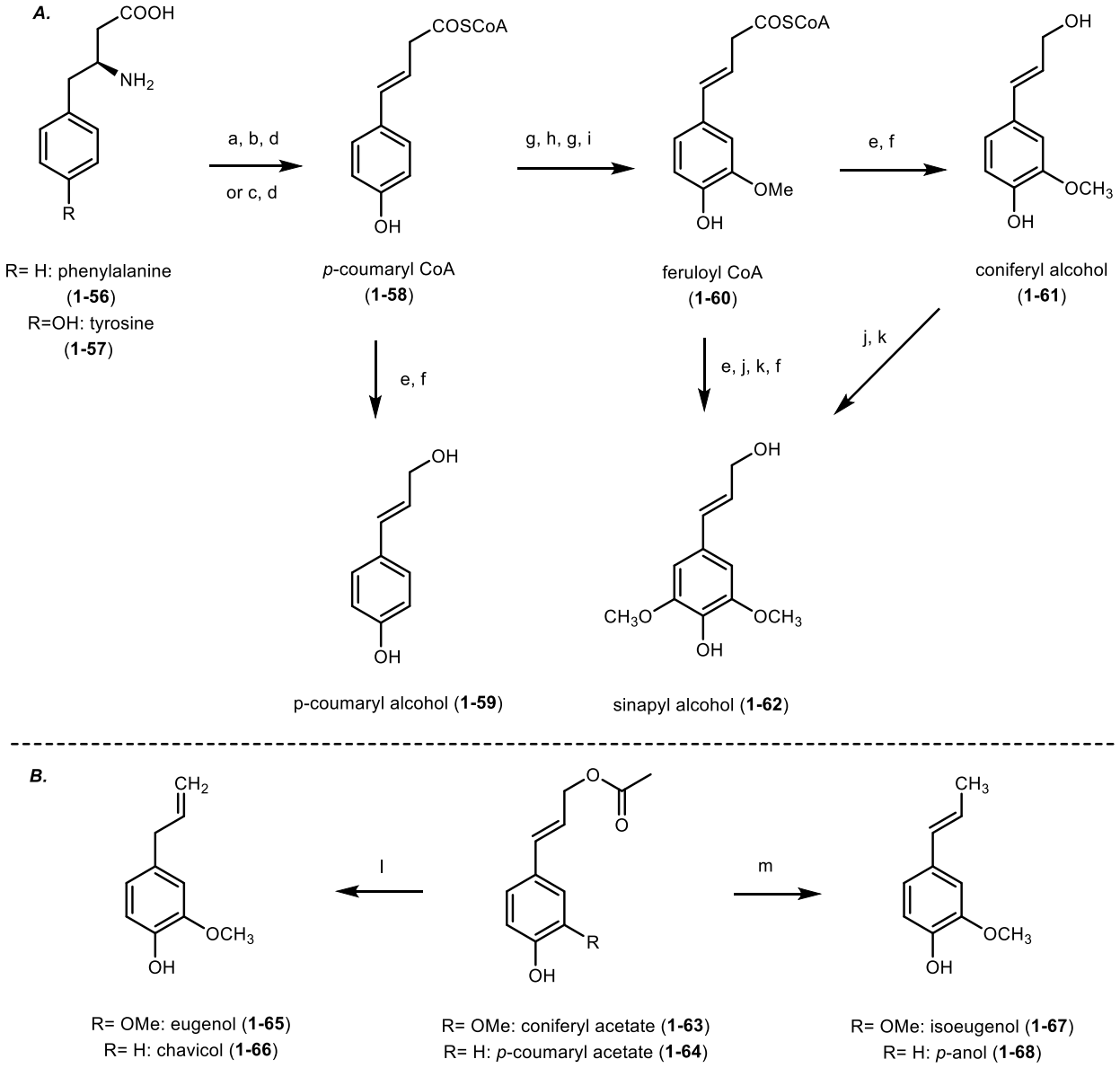
Figure 1.12. DBCODs with cardiovascular protective activity

1.5. Biosynthesis

All lignan natural products are biosynthesized by the coupling of monolignol building blocks: coniferyl alcohol, sinapyl alcohol, *p*-coumaryl alcohol, or analogous C9-deoxygenated phenylpropanoids. Monolignols, in turn, are derived from phenylalanine or tyrosine (Scheme 1.1A). These processes include 4–11 enzymatic steps which have been described in detail in a review by Davin *et al.*[10,64] The C9-deoxygenated phenylpropanoids eugenol, isoeugenol, chavicol, and *p*-anol are biosynthesized in one enzymatic step from coniferyl acetate or *p*-coumaryl acetate (Scheme 1.1B). The biosynthetic origin of dibenzocyclooctadiene lignans remains unknown, however it is putatively thought to follow a similar enzymatic sequence to that of the well-studied aryltetralin biosynthetic pathway.[2,65]

Aryltetralins are comprised of coniferyl alcohol building blocks (**1-61**) which are oxidatively coupled together by laccase or another oxidant, forming a dimer (Scheme 1.2).[15] A dirigent protein is involved in this step to direct the stereochemical outcome of the coupling, giving an asymmetric product (**1-70**). From the dimer, intramolecular cyclization of the alcohols onto the para-quinone methides gives furanolignan (+)-pinoresinol (**1-71**). This is then reduced to the diol (−)-secoisolariciresinol (**1-72**) by pinoresinol/lariciresinol reductase (PLR). The aliphatic alcohols are then oxidized by secoisolariciresinol dehydrogenase (SDH), providing the lactone (−)-matairesinol (**1-73**). Oxidation of the *o*-methoxy phenol to the benzodioxolane is catalyzed by cytochrome P450 CYP719A23, giving (−)-pluviatolide (**1-74**). Methylation of the phenol by *O*-methyltransferase OMT3, aromatic C-H oxidation by CYP71CU1, and a second methylation by OMT1 give (−)-

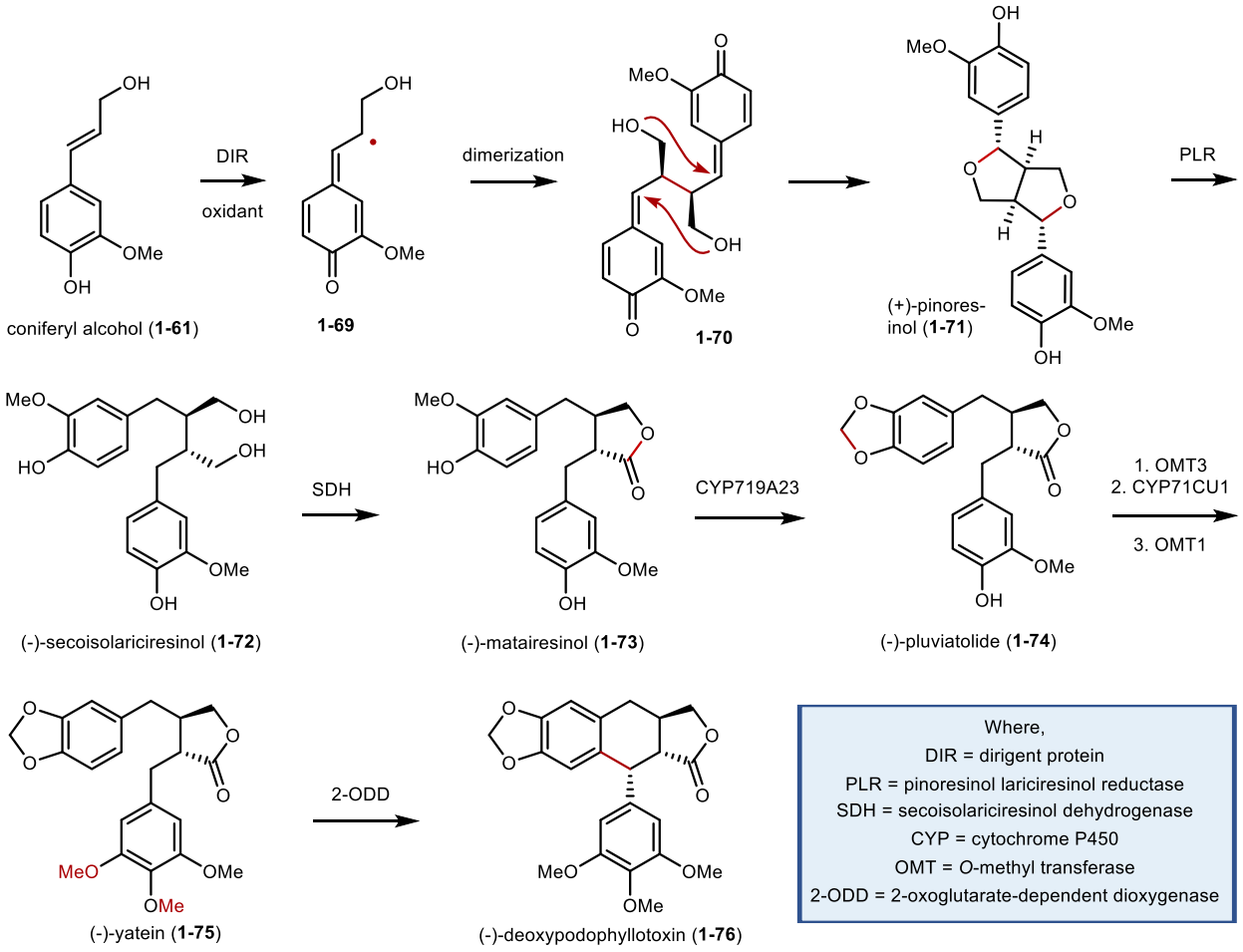
yatein (**1-75**). 2-oxo-glutarate-dependent dioxygenase (2-ODD) then catalyzes the stereoselective cyclization of (−)-yatein to (−)-deoxypodophyllotoxin (**1-76**).[65] It is possible that the steganacin-type dibenzocyclooctadiene lignans, also possessing a *trans* lactone, could arise from (−)-yatein as well, where a different enzyme catalyzes the cyclization to the eight-membered ring instead of



a = phenylalanine ammonia lyase (PAL), b= cinnamate 4-hydroxylase (C4H), c= tyrosine ammonia lyase (TAL), d= hydroxycinnamoyl CoA ligase (4CL), e= cinnamyl-CoA NADP oxidoreductase (CCR), f= cinnamyl alcohol dehydrogenase (CAD), g= hydroxycinnamoyl CoA shikamate hydroxycinnamyl transferase (HCT) or hydroxycinnamoyl CoA quinate hydroxycinnamyl transferase (HQT), h = *p*-coumarate 3-hydroxylasse (pC3H), i = hydroxycinnamoyl CoA *O*-methyltransferase (CCOMT), j= ferulate 5-hydroxylase (F5H), k= caffeic acid *O*-methyltransferase (COMT), l= eugenol synthase, m = isoeugenol synthase (l and m are NADPH-dependent reductases).

Scheme 1.1. Biosynthesis of monolignol building blocks

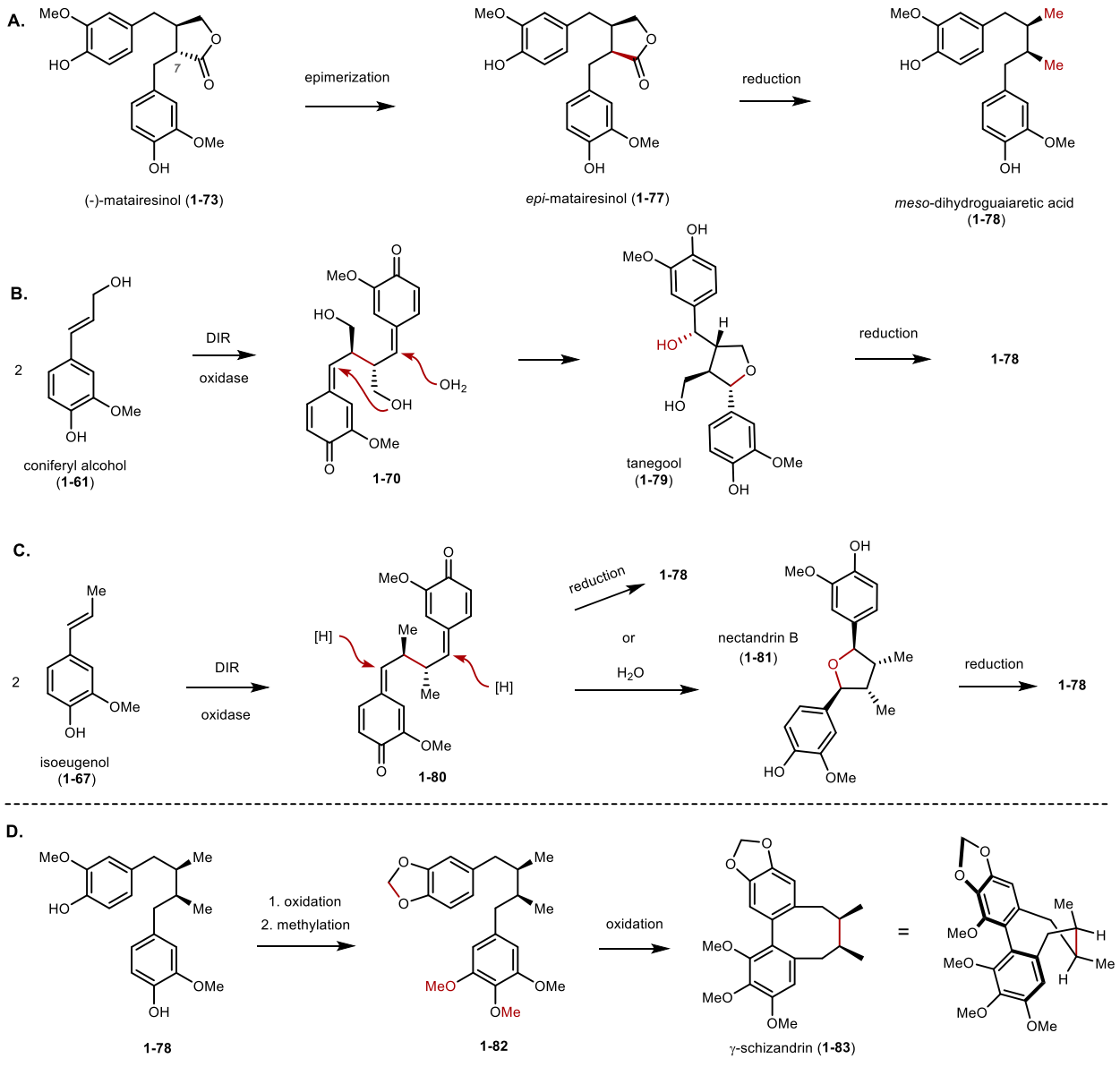
the six-membered ring (*vide infra*).



Scheme 1.2. Aryltetralin biosynthetic pathway

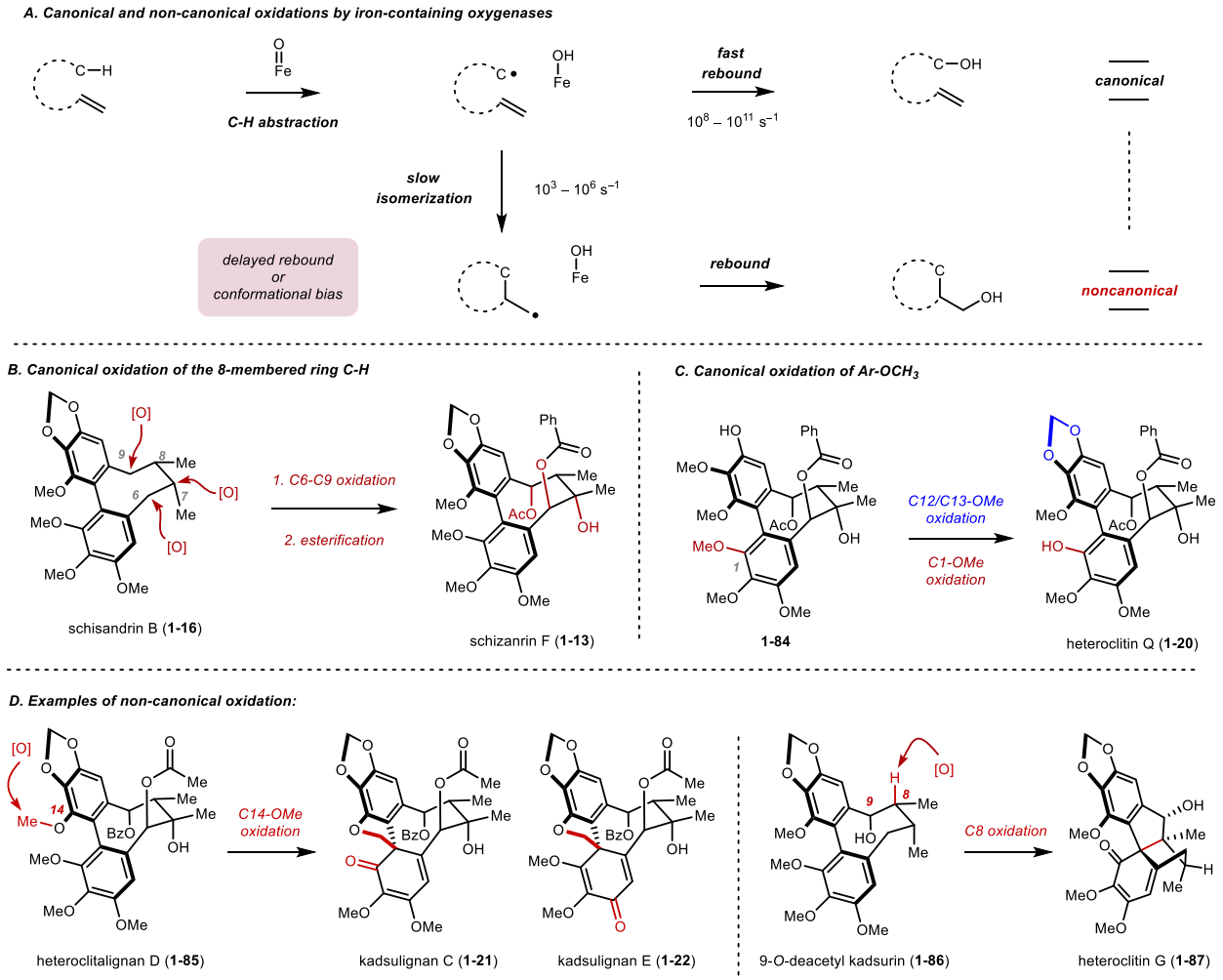
The dibenzocyclooctadiene lignans possessing *cis* methyl groups at C7 and C8, could potentially arise from one of three different biosynthetic pathways proposed in Scheme 1.3A–C. Pathway A diverges from the aryl tetralin biosynthetic pathway at the stage of (−)-maitairesinol (**1-73**), which undergoes epimerization at C7 to give *epi*-maitairesinol (**1-77**). This is then fully reduced to give *meso*-dihydroguairetic acid (**1-78**), bearing *cis* methyl groups at C7 and C8. **1-78** is the substrate which will undergo biaryl coupling to form the eight membered ring, however, the mechanism for this process is currently unknown. Pathway B involves homocoupling of **1-61** by an oxidase, with stereochemistry conferred by a dirigent protein. Nucleophilic attack by water onto one para-quinone methide and intramolecular cyclization of the alcohol onto the other would provide furanolignan tanegool (**1-79**), which can then be reduced to **1-78**. Pathway C begins with the

homocoupling of **1-67**, followed by reduction of the both *para*-quinone methides to the corresponding phenols, yielding **1-78**. Alternatively, water can attack at the stage of the *para*-quinone methide intermediate (**1-80**), resulting in the furofuran nectandrin B (**1-81**) as a byproduct. However, reduction of nectandrin B will also give **1-78**. **1-78** would then undergo oxidation and methyl transfer reactions about the aromatic ring to provide suitable functionality (Scheme 1.3D). Finally, cyclization to the 8-membered ring would be catalyzed by a CYP450 or another oxidant (eg. cyclization of **1-82** would give γ-schizandrin, a stage 1 DBCOD).



Scheme 1.3. Biosynthetic hypotheses for DBCODs: A. origin of the *cis* methyl groups, B. cyclization.

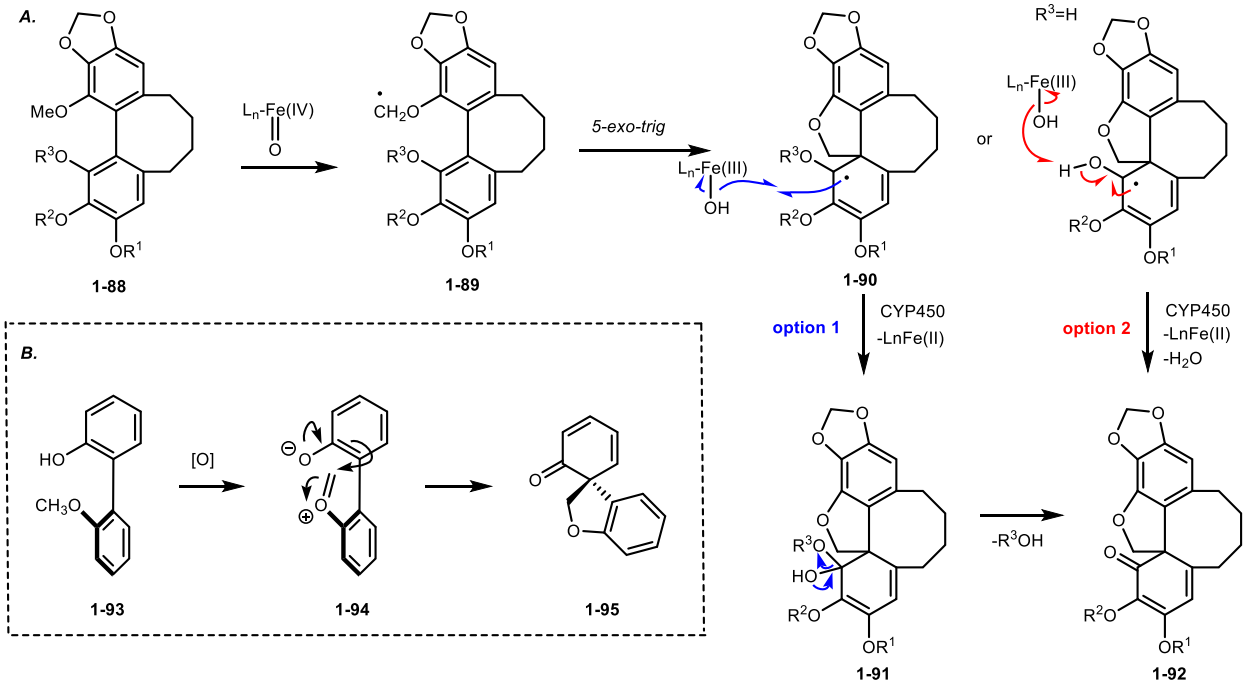
The biosynthesis of DBCODs contains both canonical and non-canonical oxidation steps, both of which contribute to constructing the highly oxidized natural products.[1] Both types of oxidation commence with C-H abstraction by a CYP450 or non-haem iron oxygenase (Scheme 1.4A). The most common fate of the resulting C-centered radical is to undergo rebound (canonical oxidation), where it is quickly hydroxylated by Fe(III)-OH (at a rate of 10^7–10^{11} s^{-1}).[66,67] Alternatively, in the non-canonical oxidation pathway, rebound is delayed, and the radical undergoes intramolecular cyclization prior to being hydroxylated. The occurrence of this second pathway is intriguing as radical cyclizations occur at a much slower rate (~10^5 s^{-1} for 5-*exo* or 11-*endo*-trig) than rebound (10^8-10^{11} s^{-1}), indicating that either cyclization is being accelerated (eg. by conformational bias) or rebound is being delayed.[68–70] In the biosynthesis of DBCODs, oxidation about the aliphatic ring (Scheme 1.4B) occurs via canonical oxidation to give stage 2 DBCODs. DBCODs with



Scheme 1.4. Canonical and non-canonical oxidations in DBCOD biosynthesis

hydroxyl groups at C7 or C8 are observed, whereas hydroxylation at C6 or C9 is followed by esterification. Canonical oxidation also occurs on the aryl rings to give hydroxy, methoxy, or dioxolane substituents (Scheme 1.4C). Stage 3 DBCODs are the result of non-canonical oxidation (Scheme 1.4D). For example, C-H abstraction at the C14 methoxy of heteroclitalignan D (**1-85**) is followed by radical cyclization onto C16 to give the spirodienone DBCODs kadsulignans C and E (**1-21** and **1-22**). C-H abstraction at C8 of 9-*O*-deacetylkadsurin (**1-86**) followed by cyclization onto C16 gives the 5-5 ring system of heteroclitin G (**1-87**). Non-canonical oxidation is responsible for the great structural diversity observed throughout the DBCOD family such as the 11-membered macrocycle of kadsuphilin N and the 6-4 ring system of kadsuraol A.[71,72]

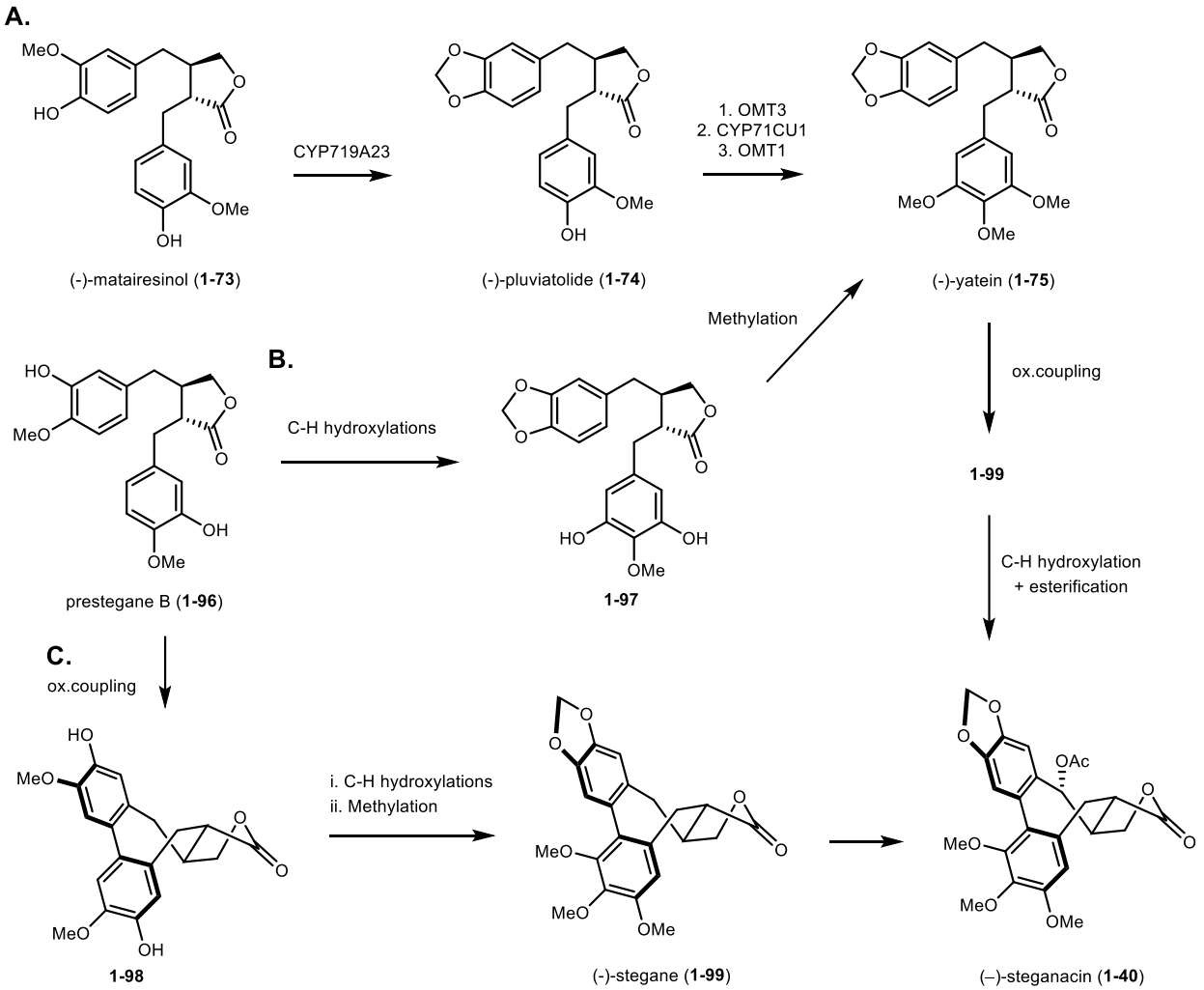
Two different biosynthetic pathways leading to spirocyclic stage 3 DBCODs have been proposed. Whiting *et al.* have suggested a radical pathway catalyzed by a CYP450 enzyme.[73] H-atom abstraction from the methoxy of **1-88** gives the phenoxymethyl radical (**1-89**) which attacks the lower aromatic ring in a 5-*exo*-trig cyclization (Scheme 1.5A). The resulting radical **1-90** either undergoes rebound, followed by loss of alcohol RO_3H (option 1) or when R^3=H, Fe(III)-OH abstracts another hydrogen atom (option 2), both of which give *ortho*-spirodienone **1-92**. Coleman *et al.* have put forward an alternative ionic mechanism for the spirocyclization (Scheme 1.5B).[74]



Scheme 1.5. Biosynthetic hypotheses for spirocyclization: A. radical pathway; B. ionic pathway

Oxidation ($2e^-$, $2H^+$) of the methyl ether **1-93** gives zwitterionic species **1-94**, possessing an electrophilic oxonium and nucleophilic phenolate. The phenolate then performs an intramolecular nucleophilic attack on the oxonium ion. This 5-*endo*-trig cyclization results in *ortho*-spirodienone **1-95**.

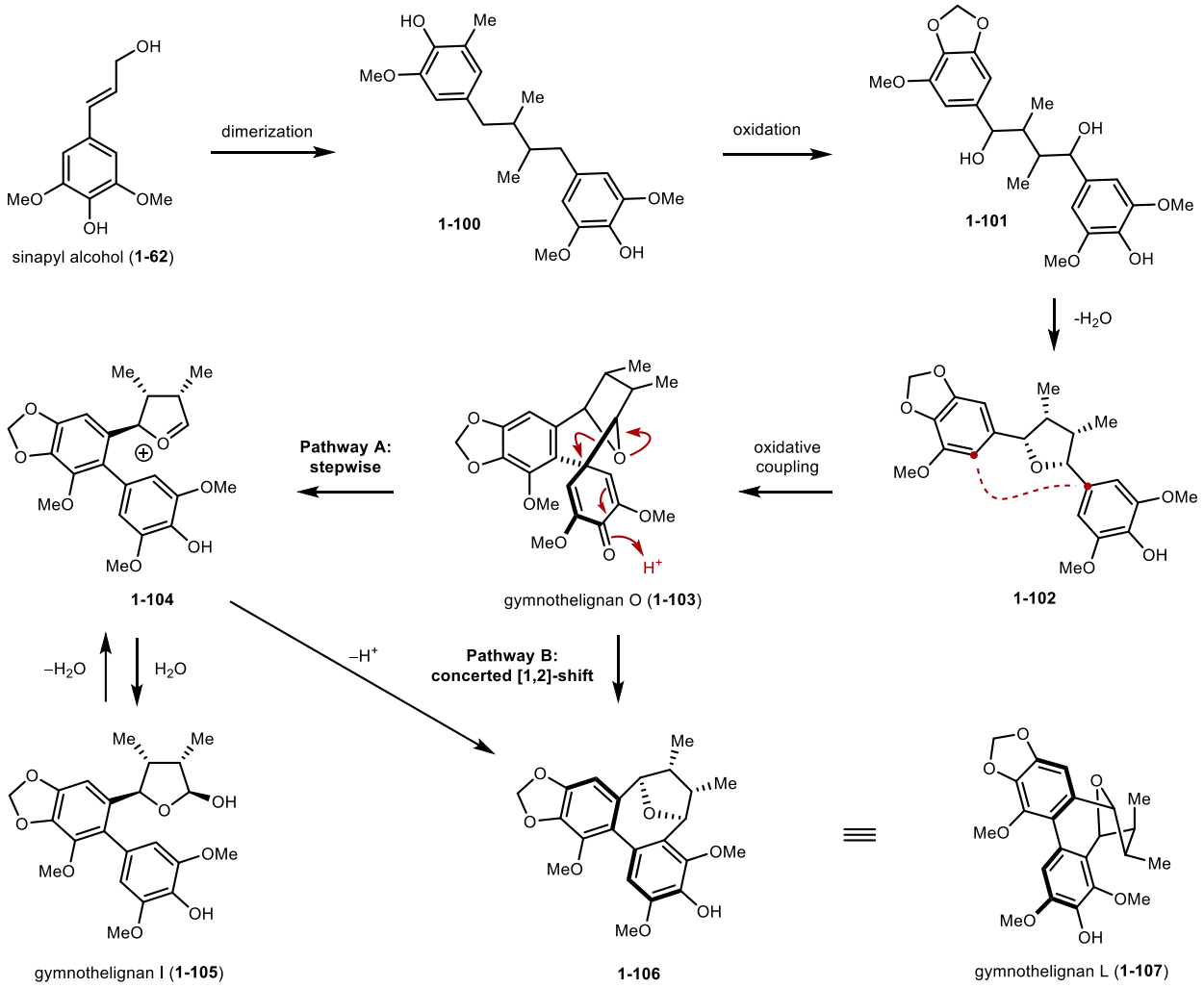
The steganacin type DBCODs possess a *trans* lactone at C7 and C8 rather than the *syn* methyl groups of traditional DBCODs and thus must arise from a different biosynthetic pathway. The *trans* lactone is identical to that of the aryl tetralin lignans, ergo it is possible the steganacins and aryl tetralins share a common biosynthetic precursor, such as (−)-yatein (**1-75**, Scheme 1.6A). The biosynthetic pathway would then diverge depending on whether **1-75** is in the presence of 2-ODD, which catalyzes cyclization to the 6-membered ring of (−)-deoxypodophyllotoxin, or another



Scheme 1.6. Hypotheses for the biosynthesis of steganacin type DBCODs

enzyme which catalyzes cyclization to the 8-membered ring of (−)-stegane (**1-99**). C-H hydroxylation of **1-99** at C9, followed by acetylation would then provide steganacin (**1-40**). The steganacins could also arise from the oxidative coupling of prestegane B (**1-96**), which has been isolated from the same plant as the steganacins, *Steganotaenia araliacea* (Scheme 1.6B).[75] Hydroxylation of the lower aromatic ring of **1-96** and oxidation of the *ortho*-methoxy phenol (of the upper aromatic ring) to the benzodioxolane would give **1-97,** which upon methylation would furnish **1-75**. Alternatively, **1-96** could first undergo oxidative coupling to give biaryl **1-98**, followed by hydroxylations on the aromatic rings, and then methylation to provide **1-99** (Scheme 1.6C).

Some gymnothelignans (natural products isolated from *Gymnotheca* species) resemble DBCODs with an oxygen bridging across C6 and C9. The DBCOD type gymnothelignans have been proposed to arise via two possible biosynthetic pathways, sharing a common spirohemiketal intermediate **1-103** (Scheme 1.7).[76,77] The biosynthesis of diaryl THF lignans such as **1-102** is known to occur in three steps.[78,79] First, sinapyl alcohol (**1-62**) is enzymatically oxidized and dimerized stereoselectively with the help of a dirigent protein to give dibenzylbutane lignan **1-100**. Second, **1-100** undergoes C-H oxidation at both aliphatic and aromatic positions to yield **1-101**. Third, dehydration of **1-101** gives 2,5-diaryltetrahydrofuran lignan **1-102**. It has been further proposed that **1-102** undergoes oxidative coupling to give spirodienone lignan **1-103** (gymnothelignan O).[78] Compound **1-103** can then proceed either via a concerted [1,2]-shift or a two step pathway (rearomatization / oxonium ion formation and then dehydration) to furnish gymnothelignan L (**1-107**)**.** This second pathway could also be a source of non-DBCOD type gymnothelignans such as gymnothelignan I (**1-105**).



Scheme 1.7. Proposal for the biosynthesis of gymnothelignan type DBCODs

1.6. Previous Syntheses

1.6.1. Overview of progress in DBCOD synthesis 1976–2021

Of the 529 DBCODs isolated thus far, only 44 have been synthesized. This is due to the challenges associated with their syntheses. Even to prepare the simplest (stage 1) DBCODs, the synthetic chemist must tackle the task of forming the biaryl bond atroposelectively. In stage 2 DBCODs, one must also set several contiguous stereocentres along the 8-membered ring and often perform chemoselective transformations to differentiate between various hydroxyl groups. Further oxidation is required for the synthesis of stage 3 DBCODs. Inventing novel methodologies that can mimic the non-canonical oxidative cyclizations in complex settings can be useful for the synthesis of stage 3 DBCODs. The majority of the DBCODs synthesized thus far are steganacin

type, stage 1, or stage 2 (Figure 1.13). Only 2 % of the reported syntheses target the gymnothelignan type and only one publication (7 % of reported syntheses) features stage 3 DBCODs.[1]

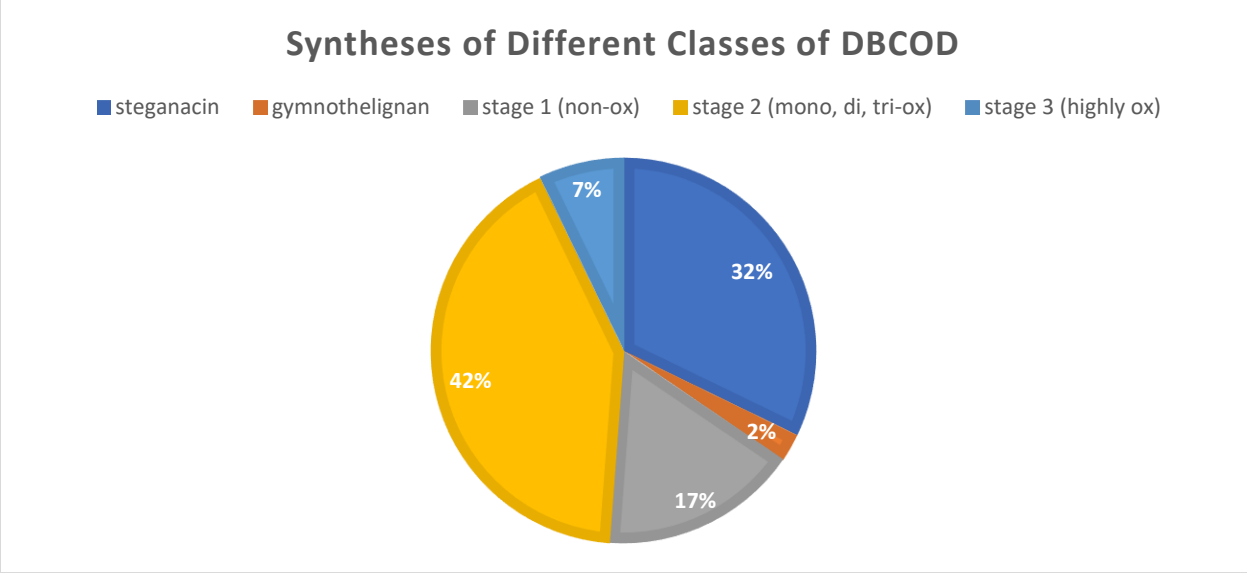


Figure 1.13. Syntheses of each stage of DBCOD

The first DBCOD syntheses of racemic steganacin were reported in 1976[80–82] and the first stage 1 and stage 2 DBCOD syntheses were reported the following year[83,84] (Figure 1.14). It was not until 1980, that Robin documented the first asymmetric DBCOD synthesis.[85] Chiral resolution is a popular method for obtaining a single DBCOD enantiomer, a practice which was initiated by Raphael in 1982.[86] The original intermolecular atroposelective biaryl formation was performed by Meyers in 1987 and a few years later, Uemura used a chiral chromium arene in a Suzuki coupling to impart atropselectivity.[87,88] Other unique steps developed for the synthesis of DBCODs include Molander's SmI_2-mediated reductive cyclization in 2000,[89] Coleman's oxidative cuprate coupling in 2005,[90] RajanBabu's Pd-catalyzed boryl-stannylation in 2008,[91] and Chang's asymmetric Ullmann coupling in 2009.[92] 2013 marks the initial synthesis of tri-oxygenated DBCODs by RajanBabu, which possess three hydroxyl groups or esters along the 8-membered ring (C6–C9).[93] The only two gymnothelignan syntheses were reported independently in 2018 by Soorukram and She.[78,94] In 2021, the pioneering work on stage 3 DBCOD synthesis was reported by Lumb.[1]

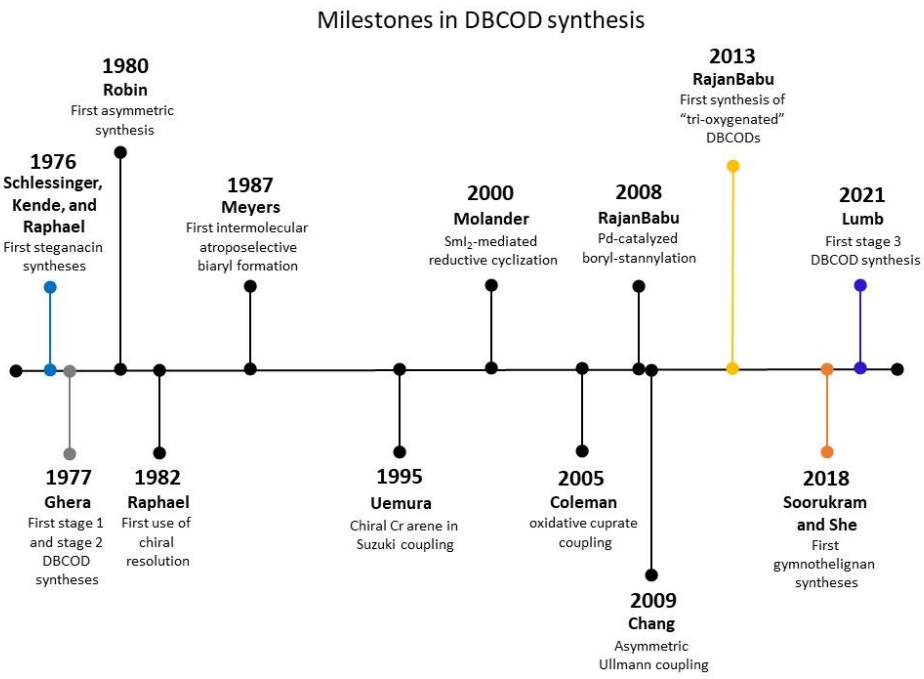


Figure 1.14. Timeline of key innovations in DBCOD synthesis

Overall, 83 DBCOD syntheses have been reported, with the most frequently synthesized being steganone (12 syntheses), deoxyschizandrin (seven times), and isoschizandrin (eight times, Figure 1.15). Steganone, isosteganone, schisandrin C, schizandrin, and gomisin A have also been prepared many times. Stage 2 and stage 3 DBCODs have been targeted far less, with only one or two reported syntheses each. Steganacins were synthesized in 3–13 steps with overall yields of 1–55 %. Gymnothelignans were synthesized in five steps with overall yields of 29–30 %. Stage 1 non-oxygenated DBCODs were synthesized 5–11 steps with overall yields of 10–30 %. Stage 1 mono-oxygenated DBCODs were synthesized in in 4–16 steps with overall yields of 5–36 %. Stage 2 bis-oxygenated DBCODs were synthesized in 16–19 steps with overall yields of 8–11 %. Stage 2 tris-oxygenated DBCODs were synthesized in 19–22 steps with overall yields of 5–6 %. Stage 3 DBCODs were synthesized in 20–21 steps with yields of 6–14 %.

The two key components of any DBCOD synthesis are the formation of the biaryl linkage and the construction of the alkyl chain. Section 1.6.2 of this chapter will focus on the former and section 1.6.3 on the latter. Section 1.6.4 will focus on syntheses using a ring expansion method to construct the 8-membered ring. In section 1.6.5, we survey the various methods used to create asymmetry in DBCOD syntheses. In 1.6.6, we look closely at some methods used for late-stage oxidation. In

1.6.7, we look at some completed DBCOD total syntheses and in 1.6.8, some incomplete DBCOD syntheses are discussed.

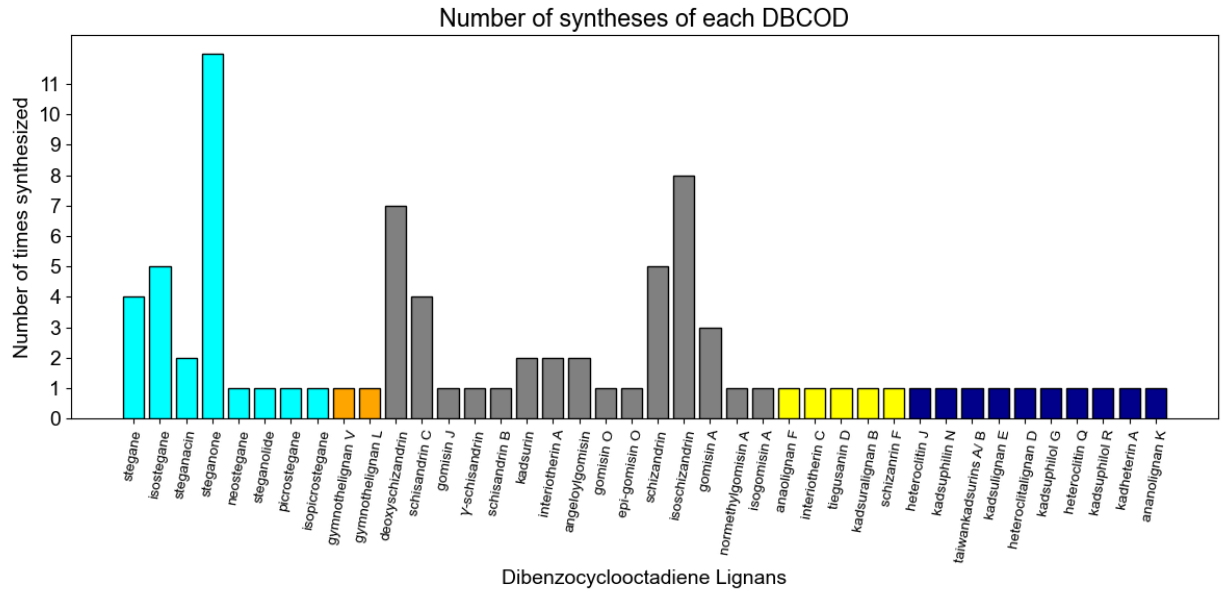
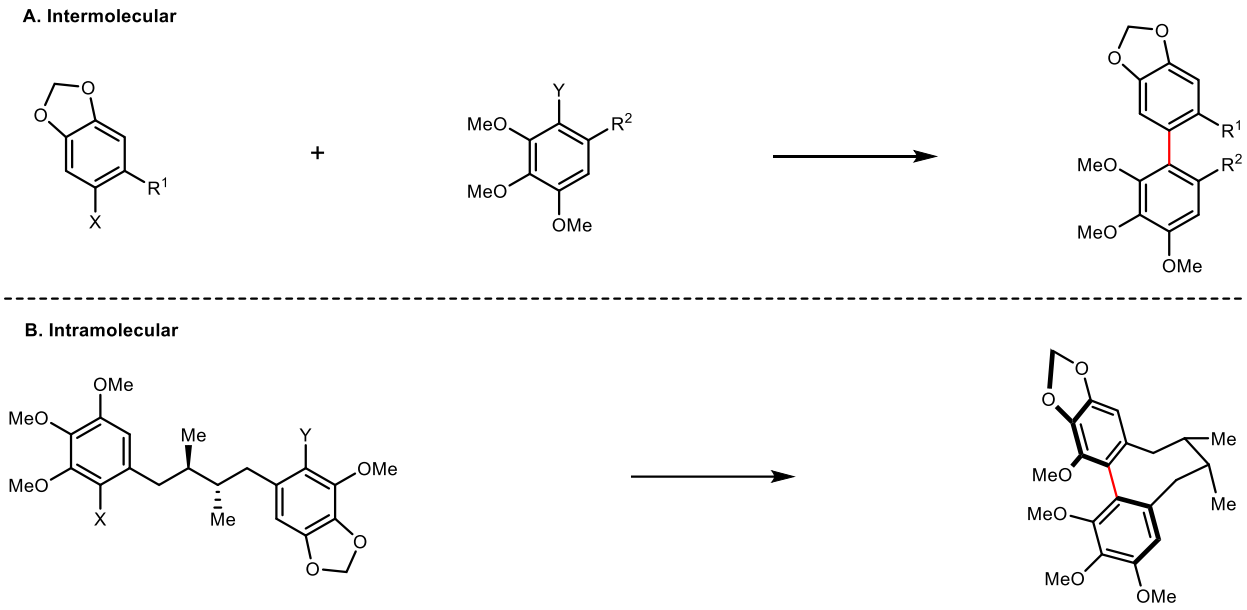


Figure 1.15. Syntheses of each individual DBCOD

1.6.2. Biaryl bond formation

This section will focus on the biaryl bond forming step of DBCOD synthesis and is organized based on the order of operations: section 1.6.2.1 focuses on intermolecular reactions and 1.6.2.2 on intramolecular reactions. In the intermolecular cases, the biaryl bond is formed early on from two fragments and the 8-membered ring is not formed until later in the synthesis (Scheme 1.8A). In the intramolecular cases, the alkyl chain connecting the two aromatic rings is formed first, and the biaryl linkage later (Scheme 1.8B). These two approaches are equally common, with 56 % of reported syntheses employing the former, and 44 % the latter. A total of 17 different sets of conditions have been reported for forming the biaryl linkages of DBCODs. The simplest approaches do not involve a biaryl bond forming step and instead start from preexisting biaryl compounds (three examples, Figure 1.16). The most prevalent method used (reported 13 times) is oxidative coupling, using oxidants such as $Fe(ClO_4)_3$, RuO_2, $Tl(TFA)_3$, or VOF_3. An oxidative cuprate coupling and several instances of photochemical oxidative coupling using iodine have also been documented. Cases where the biaryl bond formation step leads to the formation of a 6-membered ring which is then subjected to ring expansion will be discussed in section 1.6.4 instead.

Both Ullmann couplings and a Cu-mediated coupling have been utilized, as well as an asymmetric Nickel-catalyzed variation of the Ullmann coupling. One example each of electrocyclization and of Negishi coupling have been reported. Two cases of Pd catalyzed C-H activation as well as five instances of intermolecular Suzuki coupling have been documented, whereas intramolecular Suzuki coupling has only been used once.



Scheme 1.8. Two synthetic strategies for biaryl bond formation in DBCOD syntheses

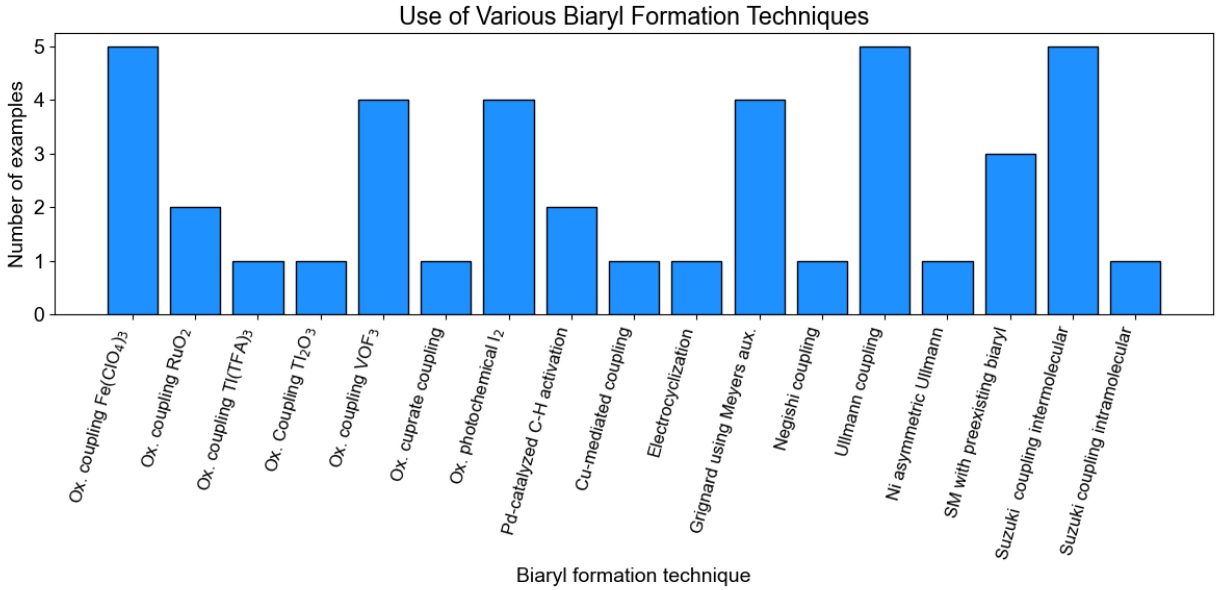
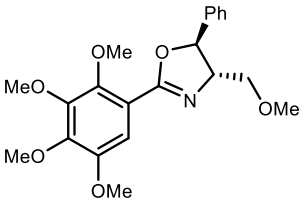
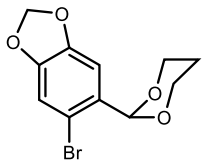
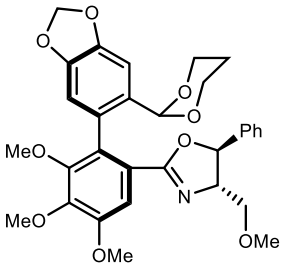
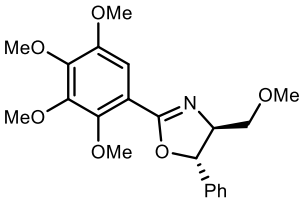
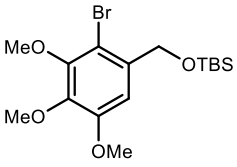
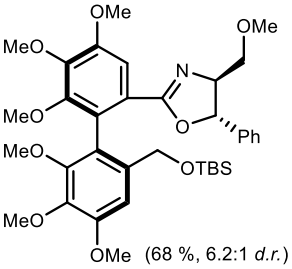
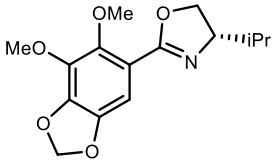
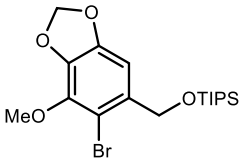
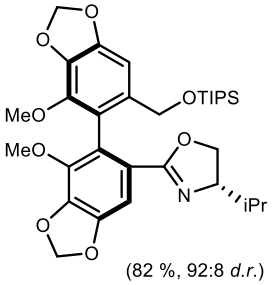
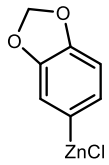
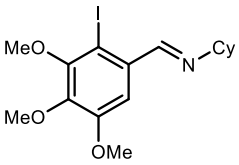
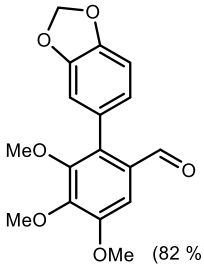
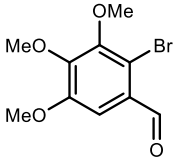
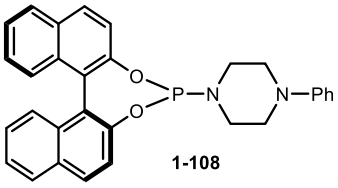
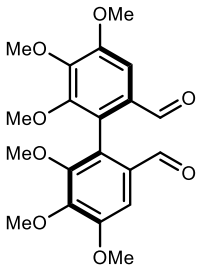
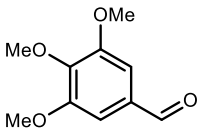
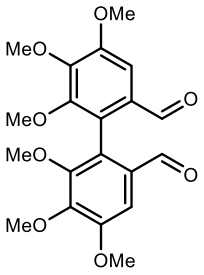
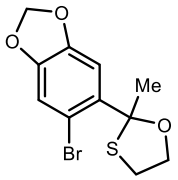
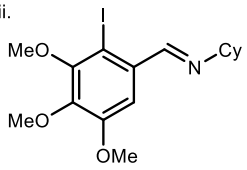
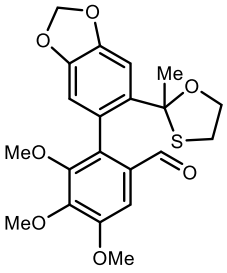
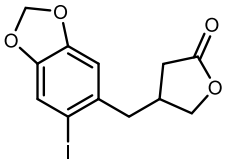
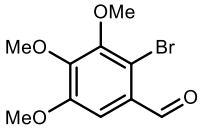
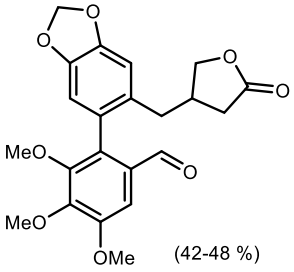
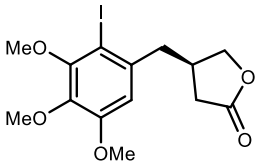
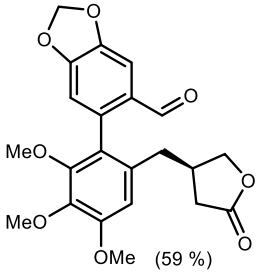
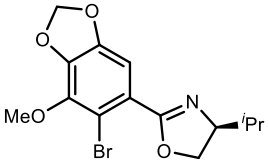
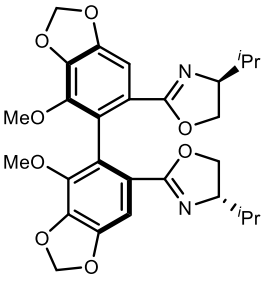


Figure 1.16. Techniques used for biaryl formation

1.6.2.1. Intermolecular biaryl bond formation

A comprehensive survey of intermolecular biaryl bond formations performed in DBCOD syntheses is presented in Table 1.1. Entries **1**–**3** employ an aryl species bearing a chiral oxazoline, known as Meyers' auxiliary, to act as the electrophile in a Grignard reaction. This coupling is believed to proceed through an addition-elimination mechanism. Stereoselective addition of the Grignard reagent leads to an azaenolate intermediate. The orientation of the *ortho* substituents of the Grignard reagent are translated to the axial chirality of the product.[95] RajanBabu observed an increased yield and diastereoselectivity in his Grignard reaction (entry **3**)[91] compared to the two previous works by Meyers (entries **1, 2**).[87,95] RajanBabu's electrophile bore a dioxolane in place of two methoxy groups, which improved reactivity. He also used a chiral oxazoline bearing a bulkier isopropyl rather than methylenemethoxy, which led to better *dr*. In entry **4**, Raphael demonstrated the Negishi coupling of an aryl zinc chloride with and aryl iodide with a very good yield of 82 %.[96] In entry **5**, Xu performed an asymmetric nickel-catalyzed homo-Ullmann coupling with an aryl bromide, obtaining a good yield of 67 % and *ee* of 68 %.[97] Entries **6**–**10** utilize Cu-catalyzed Ullmann coupling. Molander and Chang each performed homo-Ullmann couplings using aryl bromides and obtained comparable yields of 71 % and 68 % (entries **6, 10**).[92,98] Entries **7**–**9**, involving heterocoupling between an aryl bromide and an aryl iodide, exhibit variable yields ranging from 42–82 %.[85,99,100] Entries **11**–**13** employ a Suzuki coupling, with all three entries providing similar fair to good yields (49–67 %) and high *dr*.[88,94,101] She (entry **14**) demonstrated a Suzuki coupling with an excellent yield of 92 % (*dr* not reported) using a dioxolane-bearing aryl iodide substrate.[78] A breakdown of advantages and disadvantages for each biaryl bond forming technique can be found in Table 1.2.

Entry	Starting Material	Technique and Reagents	Product (Yield)
1.		*Grignard reaction*  Mg, THF, reflux	 (65 %, + 9 % atropisomer)
2.		*Grignard reaction*  Mg, THF, reflux	 (68 %, 6.2:1 *d.r.*)
3.		*Grignard reaction*  Mg, THF, reflux	 (82 %, 92:8 *d.r.*)
4.	 + 	*Negishi coupling* $Ni(acac)_2$ PPh_3, DIBAl then HCl	 (82 %)
5.		*Ni-catalyzed asymmetric Ullmann coupling* $NiCl_2(PPh_3)_2$, **1-108**, TBAI, Zn, 45°C  **1-108**	 (67 %, 68 % *ee*)

Entry	Starting Material	Technique and Reagents	Product (Yield)
6.		*Ullmann coupling* 1. NBS 2. Cu, DMF, reflux	 (71 % over 2 steps)
7.		*Ullmann coupling* i. ^{n}BuLi, ii. CuI-P(OEt)$_3$ iii.  iv. HOAc	 (82 %)
8.		*Ullmann coupling*  Cu, 195^{o}C	 (42-48 %)
9.		*Ullmann coupling*  Cu, 225 ^{o}C	 (59 %)
10.		*Ullmann coupling* Cu, DMF reflux	 (68 %, > 99 % *de)*

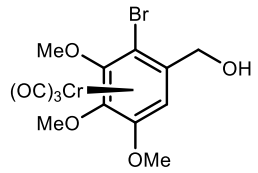
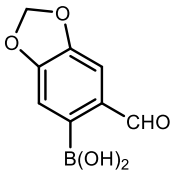
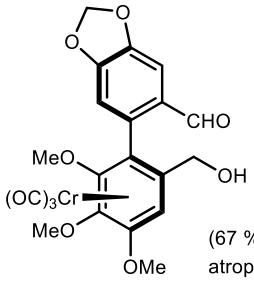
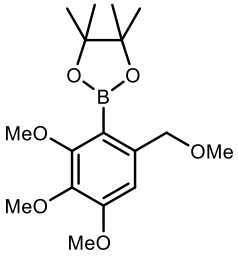
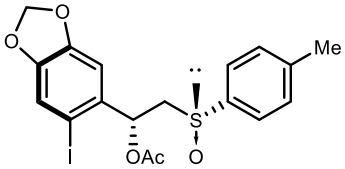
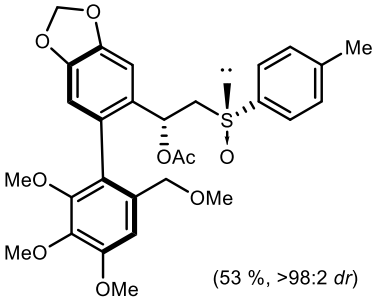
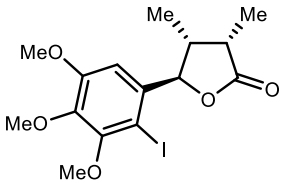
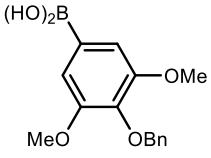
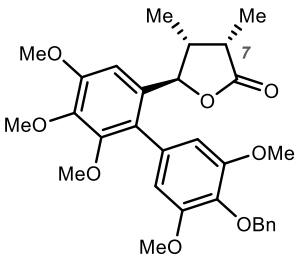
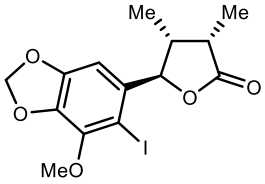
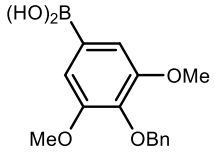
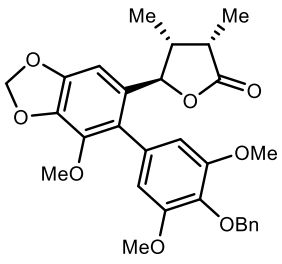
Entry	Starting Material	Technique and Reagents	Product (Yield)
11.	 (> 99% *e.e.)*	*Suzuki-Miyaura coupling*  $Pd(PPh_3)_4$, aq. Na_2CO_3, MeOH, reflux	 (67 %, single atropisomer)
12.		*Suzuki-Miyaura coupling*  $Pd(PPh_3)_4$, CsF, dioxane, 70°C	 (53 %, >98:2 *dr*)
13.		*Suzuki-Miyaura coupling*  $Pd(PPh_3)_4$, $NaHCO_3$ DME/H_2O, reflux	 (49 %, *9:1 d.r. at C7)*
14.		*Suzuki-Miyaura coupling*  $Pd(PPh_3)_4$, $NaHCO_3$ DME, reflux	 (92 %)

Table 1.1. Comprehensive table of DBCOD syntheses using intermolecular biaryl bond forming techniques

Technique	Advantages	Disadvantages
Grignard reaction	Good to very good yield and high atroposelectivity.	Chiral auxiliary needs to be added and removed. Some functional groups will not tolerate organomagnesium conditions.
Negishi Coupling	Very good yield.	Not atroposelective. Only one report.
Ni-Ullmann coupling	Good yield and moderate atroposelectivity.	Only one report.
Ullmann coupling	Moderate to very good yields. Cu is cheap and abundant.	Cu is inactivated if there is an OH in the starting material. Not atroposelective unless an auxiliary is used.
Suzuki–Miyaura coupling	High atroposelectivity and good to high yield can be obtained.	Pd catalysts are expensive.

Table 1.2. Comparison of intermolecular biaryl bond forming techniques

1.6.2.2. Intramolecular biaryl bond formation

Many DBCOD syntheses choose to build a functionalized linear molecule prior to performing the biaryl coupling in an intramolecular fashion. The various techniques used for this transformation are depicted in Table 1.3, with the exclusion of oxidative coupling techniques (coupling of Ar-H to Ar-H), which will be discussed later in this section. Entry **1** features Coleman's oxidative cuprate coupling methodology, which utilizes a diarylbromide as starting material.[28,90] Treatment with *tert*-butyllithium gives the diaryllithium which then undergoes addition with CuCN to give an $Ar_2Cu(I)CN^{2-}$ intermediate. This is oxidized by 1,3-dinitrobenzene to give $Ar_2Cu(III)CN$ which then undergoes reductive elimination, forming the biaryl bond (69 %, as a single atropisomer) as well as regenerating Cu(I)CN. Spring (entry **2**) used an analogous Cu-mediated coupling, where a diaryliodide is converted into the corresponding Grignard reagent rather than diarryllithium.[102] Transmetallation proceeds with $CuBr{\cdot}SMe_2$ and

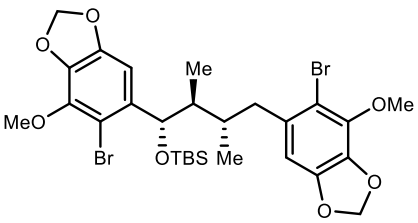
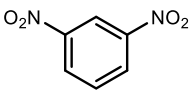
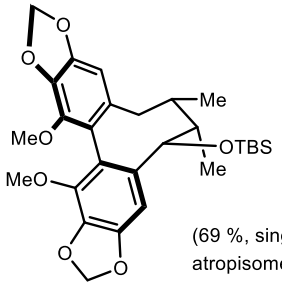
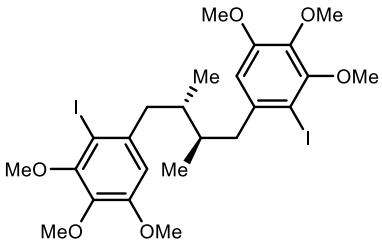
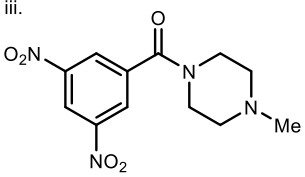
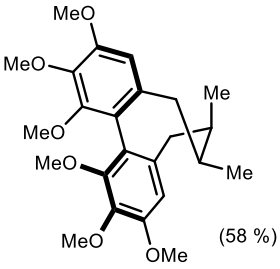
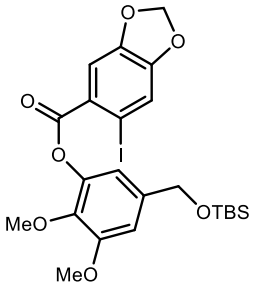
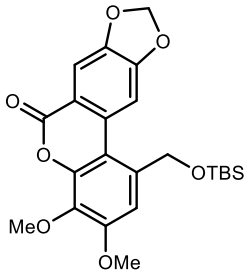
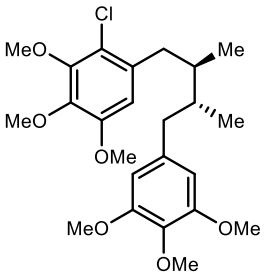
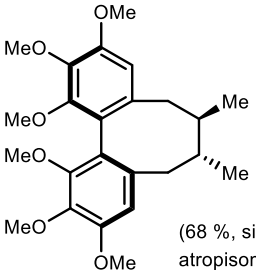
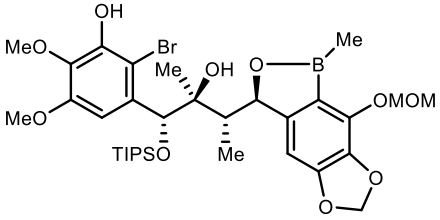
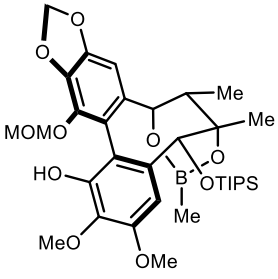
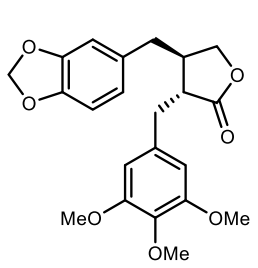
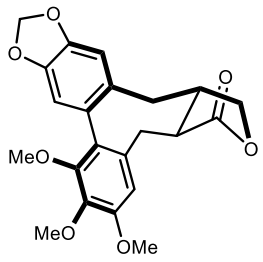
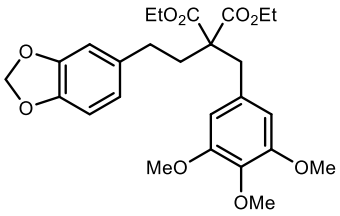
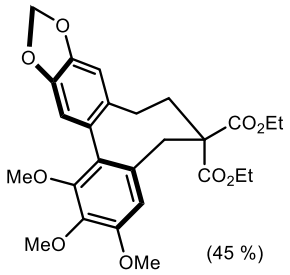
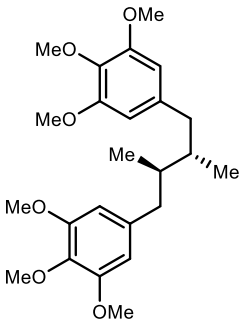
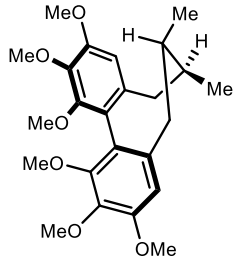
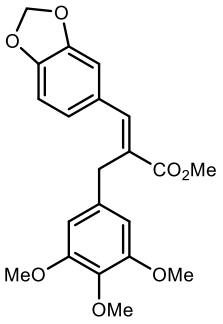
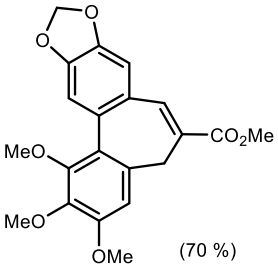
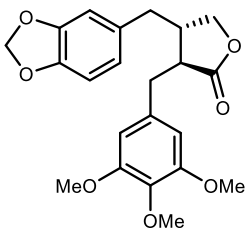
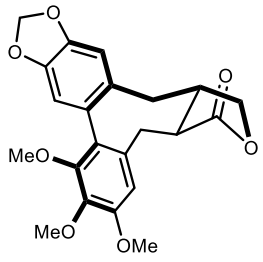
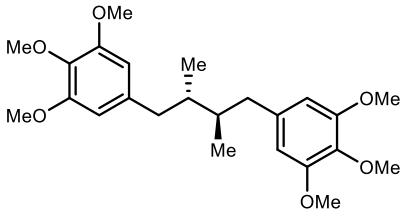
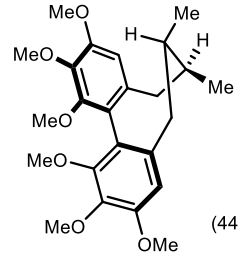
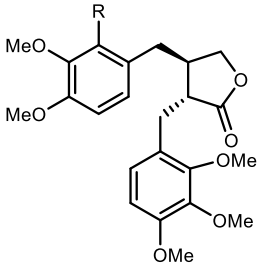
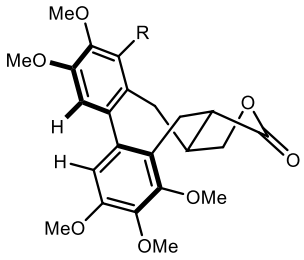
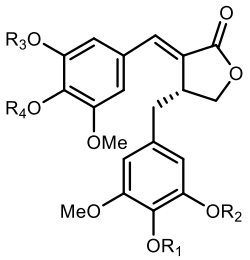
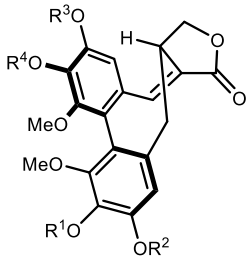
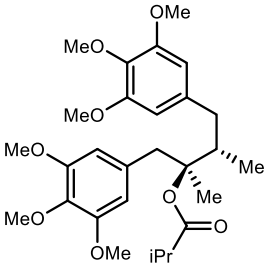
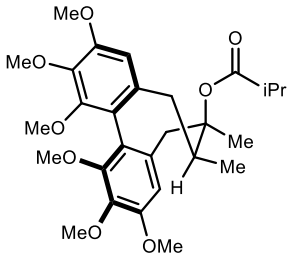
Entry	Starting Material	Technique and Reagents	Product (Yield)
1.		*Oxidative cuprate coupling* i. ^{t}BuLi ii. CuCN iii. 	 (69 %, single atropisomer)
2.		*Cu-mediated coupling* i. ^{i}PrMgCl•LiCl ii. CuBr•SMe$_2$ iii. 	 (58 %)
3.		*C-H activation* Pd(OAc)$_2$, *n*Bu$_3$P, K$_2$CO$_3$	 (63 %, interconverting atropisomers)
4.		*C-H activation* PEPPSI-IPr (1 mol%) K$_2$CO$_3$, DMA, 130 ^{o}C	 (68 %, single atropisomer)
5.		*Suzuki-Miyaura coupling (intramolecular)* SPhos Pd G2 / SPhos (cat.), K$_3$PO$_4$	 (87 %, single atropisomer)

Table 1.3. Intramolecular biaryl bond forming techniques (excluding oxidative coupling)

(3,5-dinitrophenyl)(4-methyl-1-piperazinyl)-methanone is used as the oxidant, furnishing the biaryl product in 58 % yield. Entries **3** and **4** feature Pd-catalyzed aryl-aryl couplings between a C-H bond and an aryl halide. In Abe's work (entry **3**) the alkyl chain has not yet been formed, with the aromatic rings being connected by an ester linkage instead.[103] This reaction used $Pd(OAc)_2$ as the catalyst and furnished the biaryl product as a mixture of interconverting atropisomers in a 63 % yield. Coy and Sefkow (entry **4**) utilized Organ's PEPPSI-IPr catalyst to atroposelectively form deoxyschizandrin from the linear aryl chloride in a 68 % yield.[104] The biaryl forming method developed by Lumb (entry **5**) is an intramolecular Suzuki coupling between an aryl bromide and an aryl borinic ester.[1] This reaction used Buchwald's SPhos Pd G2 catalyst and furnished the product as a single atropisomer in an 87 % yield. Entries **1** and **5** are particularly noteworthy in that they formed products bearing ethers around the 8-membered ring (stage 2 DBCODs).

Oxidative coupling of two aryl C-H bonds is the most prevalent intramolecular biaryl bond forming method reported in the literature (Table 1.4). Yields can vary from poor to excellent (36–98 %) depending on the substrate and reagent choice. Substrates bearing a lactone moiety at C7 and C8 tend to furnish higher yields compared to their methylated counterparts, indicating that hindered rotation within the aliphatic chain is beneficial for oxidative coupling. This torsional strain, leading to increased yield can be observed in entry **1**[81] using VOF_3 (compare to entry **2**[80]), **7**-**8**[105] using RuO_2 (compare to **6**[106]), and **9**–**12**[107–110] using $Fe(ClO_4)_3$ (compare to **13**–**15**[111,112]). Entry **5**, employing Tl_2O_3, also provides an example of oxidative coupling on a lactone substrate in good yield, however the analogous methylated substrate has not been subjected to the same conditions.[113] The substituent pattern along the aromatic rings also affects the yield, with the more electron rich tri-methoxy arenes often being more reactive than the benzodioxolanes. Comparing entries **2** and **3**[114], both using VOF_3, the substrate bearing two trimethoxy arenes is produced in a higher yield (54 %, entry **3**) compared to a substrate where one ring bears a dioxolane instead (45 %, entry **2**). Using $Fe(ClO_4)_3$ (entries **9**–**12**), this effect is even more pronounced, where substrates bearing one or two benzodioxolanes are produced in 58–62 % yield, whereas the hexamethoxy substrate is given in 90 % yield. Entry **4** demonstrates that oxidative coupling proceeds in good yield using $Tl(TFA)_3$ to provide the dibenzocycloheptadiene product, which was later subjected to ring expansion to furnish a DBCOD.[115]

Entry	Starting Material	Reagents	Product (Yield)
1.		VOF_3, TFA	 (±) -isostegane (65 - 70 %)
2.		VOF_3, TFAA	 (45 %)
3.		VOF_3, TFA	 deoxyschisandrin (54 %)
4.		$Tl(TFA)_3$	 (70 %)
5.		Tl_2O_3, TFA BF_3•OEt_2	 (-)-isostegane (77 %)

Entry	Starting Material	Reagents	Product (Yield)
6.		RuO_2, TFA, TFAA, $BF_3•Et_2O$	 (44 %)
7-8.		RuO_2, TFA, TFAA, $BF_3•Et_2O$	 **7.** (+/-)-neostegane, R= H, (98 %) **8.** (+/-)-steganolide A, R= OMe, (96 %)
9-12.		$Fe(ClO_4)_3$, TFA, CH_2Cl_2	 **9.** ($R^1 + R^2 = CH_2$, $R^3 + R^4 = CH_2$, 58 %) **10.** ($R^1 + R^2 = CH_2$, $R^3 = R^4$= Me, 66 %) **11.** ($R^1 = R^2$= Me, R^3, $R^4 = CH_2$, 62 % over 2 steps) **12.** ($R^1 = R^2 = R^3 = R^4$= Me, 90 %)
13.		$Fe(ClO_4)_3 \cdot 9H_2O$ CH_2Cl_2-MeCN	 (36 %, 7:3 *dr*)

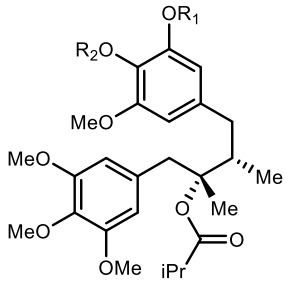
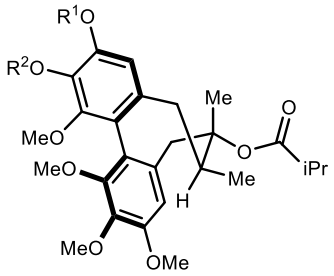
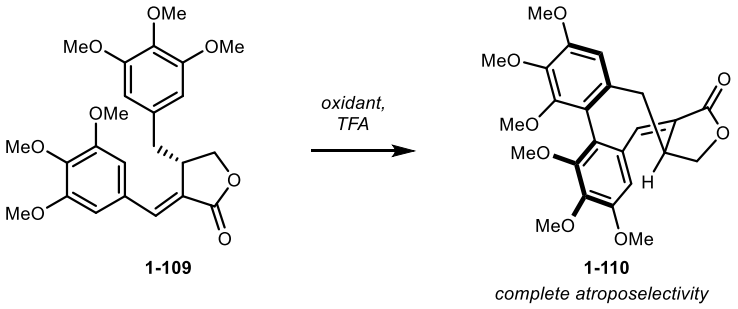
Entry	Starting Material	Reagents	Product (Yield)
14-15.		$Fe(ClO_4)_3 \cdot 9H_2O$ CH_2Cl_2-MeCN	 **14.** ($R^1 = R^2$= Me, 36 %, 4:1 *dr*) **15.** ($R^1 + R^2 = CH_2$, 41 %, 4:1 *dr*)

Table 1.4. Comprehensive table of intramolecular oxidative coupling techniques (Ar-H to Ar-H coupling)

The choice of reagents used in oxidative coupling is of equal import. Vanadium and thallium-based oxidants were the first used, however are less common nowadays due to the observance of unwanted side reactions and toxicity, respectively.[116] Tanaka and Wakamatsu screened several oxidants to convert intermediate **1-109** to cyclic **1-110** in their synthesis of (+)-schizandrin (Scheme 1.9).[109] $Ru(TFA)_4$ with $BF_3 \cdot Et_2O$ and $Fe(ClO_4)_3 \cdot 6H_2O$ provided the best yields of cyclized product at 91 %, with the latter reacting much faster. CoF_3 was not far behind at 81 % yield, whereas $FeCl_3$ and $Mn(acac)_3$ did not perform as well (35 % and 63 %, respectively). Robin observed that Ru(IV) species were also efficient oxidants for forming the biaryl linkage between two tri-methoxy substituted arenes in their synthesis of (±)-deoxyschisandrin.[105] They compared the use of $RuO_2 \cdot 2H_2O$ to the more traditional Tl_2O_3 and found the former more effective in mediating the transformation on two substrates (Scheme 1.10). Using Tl_2O_3 with TFA, TFAA, and

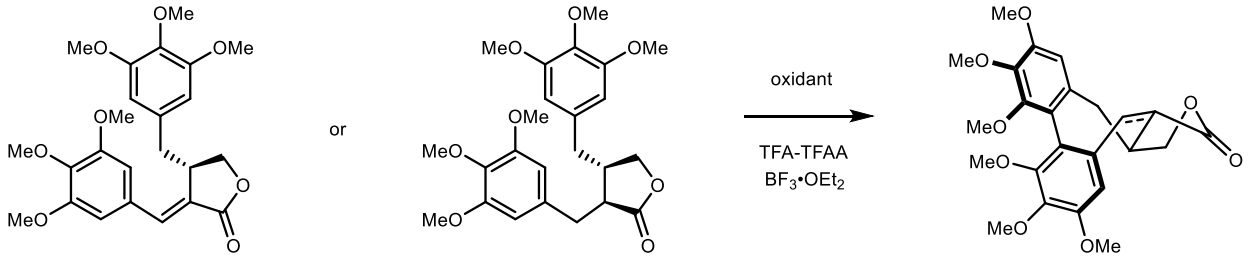


1-109 → **1-110**
complete atroposelectivity

oxidant	time (h)	yield (%)
$Ru(TFA)_4$, $BF_3 \cdot Et_2O$	26	91
$FeCl_3$	25	35
$Mn(acac)_3$	4.5	63
CoF_3	28	81
$Fe(ClO_4)_3 \cdot 6H_2O$	1	91

Scheme 1.9. Comparison of different oxidants in the synthesis of (+)-schizandrin precursor

$BF_3 \cdot Et_2O$, **1-112a** could be produced from **1-111a** in 83 % yield and **1-112b** from **1-111b** in 65 % yield. Replacing the Tl_2O_3 with milder $RuO_2 \cdot 2H_2O$ necessitated longer reaction time, yet ultimately offered improved yields of 90 % for both reactions.

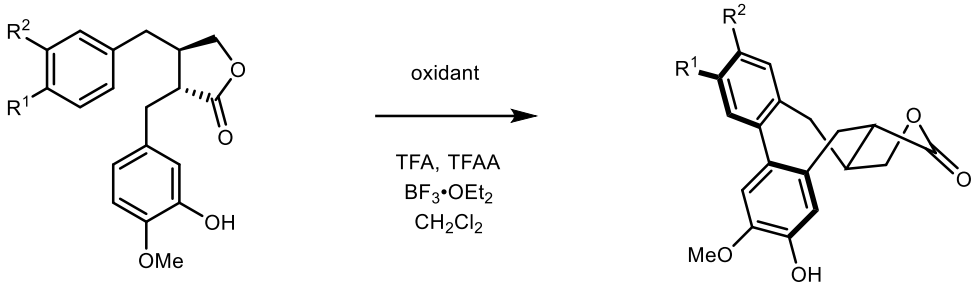


1-111a **1-111b** **1-112a** (with double bond) **1-112b** (saturated)

SM	Product	oxidant	time (h)	yield (%)
1-111a	**1-112a**	Tl_2O_3	1	83
1-111a	**1-112a**	RuO_2•$2H_2O$	24	90
1-111b	**1-112b**	Tl_2O_3	1	65
1-111b	**1-112b**	RuO_2•$2H_2O$	24	90

Scheme 1.10. Comparison of Tl and Ru oxidants in the synthesis of (±)-deoxyschisandrin precursors

Robin went on to further investigate the effect of various oxidants on the oxidative coupling of phenolic dibenzylbutanolides (Scheme 1.11).[117] The tris-methoxy substrate **1-113a** was subjected to eight separate oxidants which all provided some amount of the desired product **1-114a**. Re_2O_7 and $Cu(OAc)_2 \cdot 2H_2O$ provided excellent yields of 98 % and 90 %, respectively, whereas $Mn(OAc)_3 \cdot 2H_2O$ only gave 34 %. Consistent with previous reports, $RuO_2 \cdot 2H_2O$ performed well, furnishing the product in a 76 % yield. V_2O_5 (75 %), TeO_2 (70 %), and Co_3O_4 (72 %) provided comparable yields. Interestingly, $RuO_2 \cdot 2H_2O$ was the worst performing oxidant on the benzodioxolane substrate **1-113b**, providing only 18 % of the product **1-114b**, closely followed by $Mn(OAc)_3 \cdot 2H_2O$ (30 %). Tl_2O_3 was found to be the best oxidant for this substrate, effecting the coupling in a 64 % yield. These studies led us to the conclusion that when selecting a reagent for use in oxidative coupling, several advantages and disadvantages (summarized in Table 1.5) must be considered.



1-113a: R^1=R^2=OMe
1-113b: R^1+R^2=OCH_2O

1-114a: R^1=R^2=OMe
1-114b: R^1+R^2=OCH_2O

oxidant	1-114a		1-114b	
	time (h)	Yield (%)	time (min)	Yield (%)
Tl_2O_3	2	58	2	64
$Mn(OAc)_3•H_2O$	1	34	2	30
$RuO_2•2H_2O$	15	76	120	18
Re_2O_7	1	98		
V_2O_5	120[a]	75		
$Cu(OAc)_2•H_2O$	0.5	90		
TeO_2	40	70		
Co_3O_4	15	72		

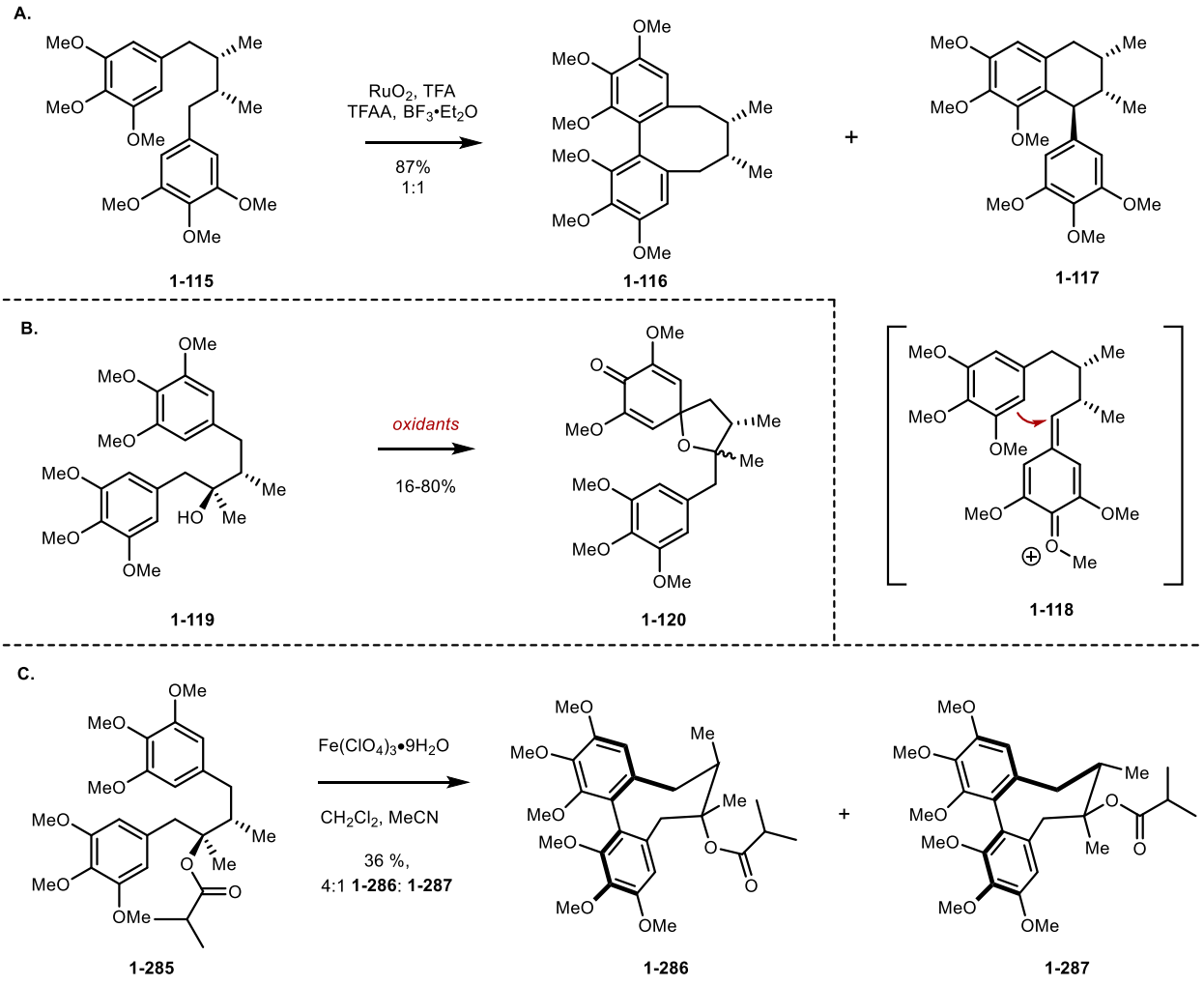
[a]= ultra-sound

Scheme 1.11. Study of reagents for oxidative coupling of phenolic dibenzylbutanolides

Reagent	Advantages	Disadvantages
VOF_3	Can be used to prepare simple DBCODs. Moderate to good yields.	Side reactions often occur.
$Tl(TFA)_3$ or Tl_2O_3	Fast reaction time. Good yield. Can be used on phenolic or non-phenolic substrates.	Toxic.
RuO_2 or $Ru(TFA)_4$	Can be used on phenolic or tri-OMe-Ar substrates. Low toxicity. Good to high yields.	Doesn't work on benzodioxolane substrates.
$Fe(ClO_4)_3$	Good to high yields. Fast reaction time.	Not used on phenolic substrates.

Table 1.5. Comparison of reagents for intramolecular oxidative coupling

In some instances, oxidative coupling has resulted in unexpected products along with or instead of dibenzocycloctadienes. Robin observed a 1:1 mixture of 8-membered ring and 6-membered ring formation upon the treatment of diarylbutane lignan **1-115** with RuO_2, TFA, TFAA, and $BF_3 \cdot Et_2O$ (Scheme 1.12A).[106] The aryl tetralin byproduct **1-117** is proposed to arise from the intermediate radical cation undergoing further oxidation to the cationic *p*-quinone methide (**1-118**), which then experiences intramolecular 1,6-conjugate addition. This byproduct was observed while using the substrate bearing methyl groups at C7 and C8 (**1-115**), but not when there is a lactone at these positions (**1-111b**), indicating that the lactone plays a role in locking the conformation in a manner that is favorable for 8-membered ring formation. Steric hinderance of the methoxy groups *ortho*



Scheme 1.12. Possible byproducts of oxidative coupling: A. aryltetralins; B. spirodienones; and C. oxidative coupling to form a stage 2 DBCOD

to the biaryl bond also contributes to the difficulty in forming **1-116** over **1-117**. Takeya observed a spirodienone product **1-120** in their attempt to oxidatively couple **1-119**, which bears a free alcohol on the alkyl chain (Scheme 1.12B).[118] It was not feasible to form the biaryl linkage as the alcohol attacked the phenyl radical cation more rapidly than the aromatic ring. This led to the realization of one of the limitations of oxidative coupling: that it cannot proceed with substrates bearing an aliphatic alcohol. The coupling was however successful after the alcohol was protected as the isobutyrate (**1-285**), providing a 4:1 mixture of stage 2 DBCODs **1-286** and **1-287** (Scheme 1.12C).

Some additional oxidative coupling techniques which have been used to synthesize unnatural DBCODs are reported in Table 1.6. Kramer has synthesized three DBCOD-like molecules bearing two to five aromatic methoxy groups and no substituents along the alkyl chain (entries **1**–**3**).[119,120] This was accomplished in 38–62 % yield using $MoCl_5$ with $TiCl_4$. The yield increased with the number of methoxy substituents, indicating that this could be a useful method to prepare hexa-methoxy DBCODs. Pelter and Ward reported the oxidative coupling of a phenolic dibenzylbutanolide using PIDA or PIFA in trifluorethanol to give a DBCOD-like product in 58 % yield (**4**).[121] They obtained a similar yield of 56 % using DDQ with TFA to couple the analogous tetramethoxy substrate (**5**).[122]

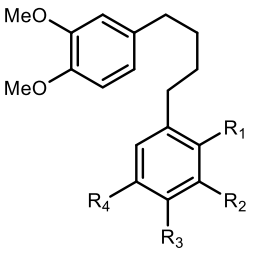
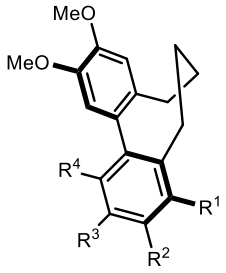
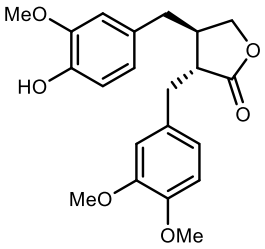
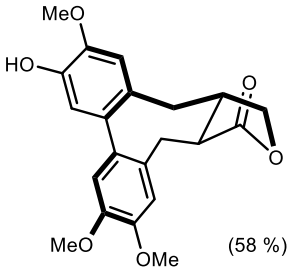
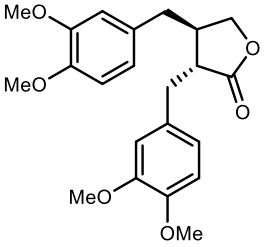
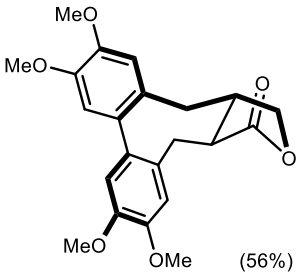
Entry	Starting Material	Reagents	Product (Yield)
1.-3.		$MoCl_5$, $TiCl_4$	 **1:** R^1-R^4=H, 38 % **2:** R^1=R^2=OMe, R^3=R^4=H, 41 % **3:** R^1=R^2=R^3=OMe, R^4= H, 62 % (*d.r.* not reported)
4.		$PhI(OAc)_2$/ $PhI(TFA)_2$ TFE	 (58 %)
5.		DDQ, TFA	 (56%)

Table 1.6. Other oxidative coupling reagents with potential to be used in DBCOD syntheses

1.6.2.3. Atroposelective biaryl bond formation methods

19 examples of biaryl bond forming reactions resulting in an atropisomerically pure product have been reported in DBCOD syntheses (Figure 1.17). Three of these reactions produced a mixture of atropisomers and then utilized kinetic resolution to isolate the desired atropisomer.[103,123] Oxidative coupling using $Fe(ClO_4)_3 \cdot 6H_2O$[107,108,110], Grignard reaction using Meyers' auxiliary[87,91,93,95], and Suzuki coupling employing a chiral substrate[1,88,101,124] are the most common atroposelective biaryl bond forming methods. One example each of oxidative cuprate coupling,[90] Pd-catalyzed C-H activation,[104] Ullman coupling,[92] and Ni-catalyzed Ullman

coupling[97] have been reported to proceed atroposelectively. An example of Ullman coupling followed by chiral resolution has also been used to obtain a single atropisomer.[98]

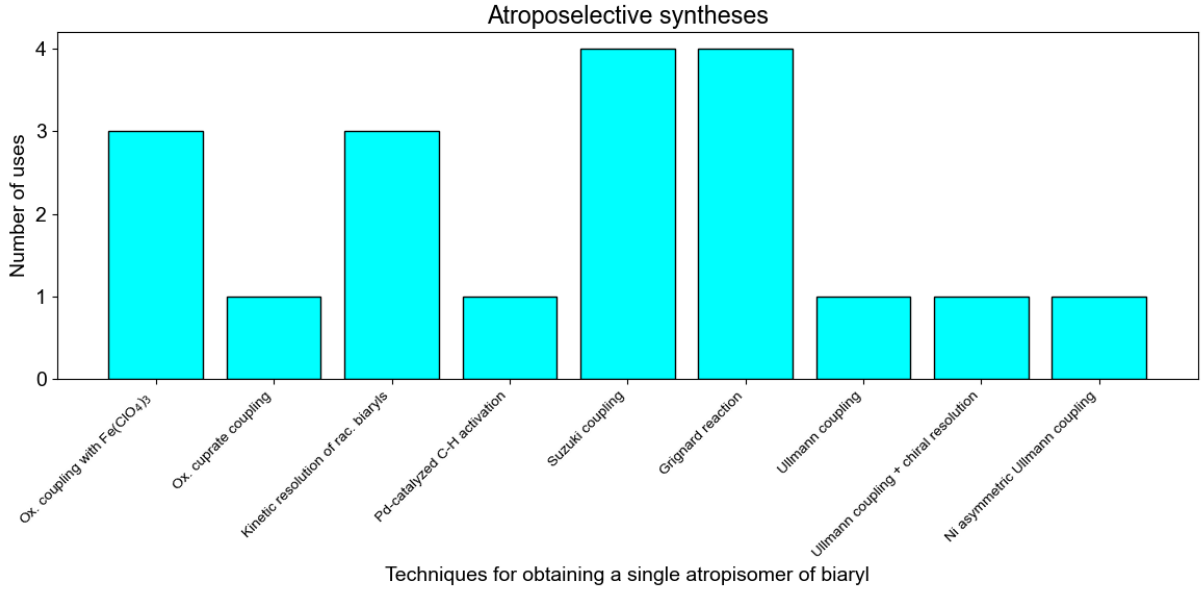


Figure 1.17. Atroposelective biaryl bond forming methods

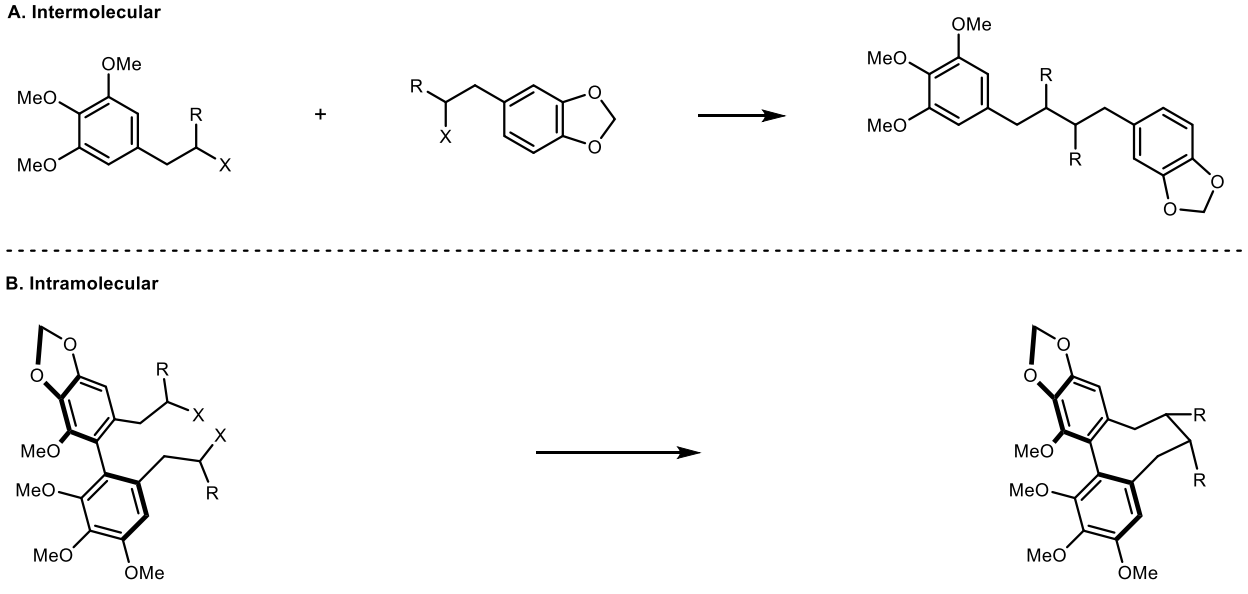
In the examples using kinetic resolution, a biaryl that is not stereochemically defined is first formed. This is followed by treatment with a chiral reagent to introduce stereochemical information at the axis. For example, CBS reduction of an (*M*)/(*P*)-lactone mixture giving a mixture of the (*P*)-lactol and unreacted (*M*)-lactone, which are separable by column chromatography (Table 1.10, entry **9**). Although effective, these methods often result in a large loss of material as the undesired atropisomer.

All other methods involve an atroposelective aryl-aryl coupling step, where the formation of the biaryl axis occurs concomitantly with asymmetric induction. Intermolecular Ni-catalyzed Ullman coupling is performed enantioselectively on an achiral aryl bromide, with chirality introduced by the ligand **1-108** (Table 1.1, entry **5**). Diastereoselective intermolecular Grignard reactions employ an aromatic ring bearing Meyers' chiral auxillary to transfer chirality to the axis during coupling with an achiral aryl bromide (eg. Table 1.1, entry **1**). Analogously, Ullman coupling of aryl bromides bearing a similar chiral oxazoline auxillary has been performed diastereoselectively (Table 1.1, entry **10**).

Intramolecular couplings involve the incorporation of a chiral bridge to prelink the two aromatic substrates. Stereochemical information from the alkyl linker is transferred to the biaryl axis during its formation. Examples of this type of reaction include oxidative coupling using $Fe(ClO_4)_3 \cdot 6H_2O$ (Table 1.4, entry **10**), Suzuki coupling (Table 1.3, entry **5**), oxidative cuprate coupling (Table 1.3, entry **1**), and Pd-catalyzed C-H activation (Table 1.3, entry **4**).

1.6.3. Alkyl chain and 8-membered ring formation

This section will focus on methods for the formation of the alkyl chain which constitutes the 8-membered ring of the DBCODs. The "alkyl chain formation" step highlighted in this section is defined as the step where two aromatic rings become connected by a linker other than the biaryl linkage. This section is divided into two subsections: 1.6.3.1 focuses on intermolecular alkyl chain forming reactions (Scheme 1.13A) and 1.6.3.2 on intramolecular alkyl chain formation (Scheme 1.13B). In the intermolecular case, the alkyl chain is formed early in the synthesis, giving a linear precursor which will later be cyclized to give the 8-membered ring. In the intramolecular methods, the biaryl linkage has previously been formed, thus equating the alkyl chain forming step to an 8-membered ring forming step. Cases where a 6-membered ring is formed first and then expanded to an 8-membered ring will be discussed in section 1.6.4 instead.



Scheme 1.13. Synthetic strategies for A) intermolecular alkyl chain formation and B) intramolecular alkyl chain formation, that is, 8-membered ring formation

A total of 15 different methods have been reported for alkyl chain formation in DBCOD syntheses. The most utilized technique for creating the 8-membered ring is via ring expansion (seven examples), closely followed by via SmI_2-mediated coupling (six examples) and intramolecular alkylation (five examples, Figure 1.18). Intermolecular alkylation, intermolecular aldol condensation, and conjugate addition followed by alkylation were each employed in three reports. Intramolecular aldol reaction, Pd-catalyzed boryl-stannylation, homocoupling of ketones, Stobbe-like alkylidenation, and intramolecular Friedel–Crafts reaction were each applied twice. Rarer techniques, reported only once each, include intermolecular aldol reaction, Suzuki coupling, Cu-mediated coupling, and Nicholas reaction.

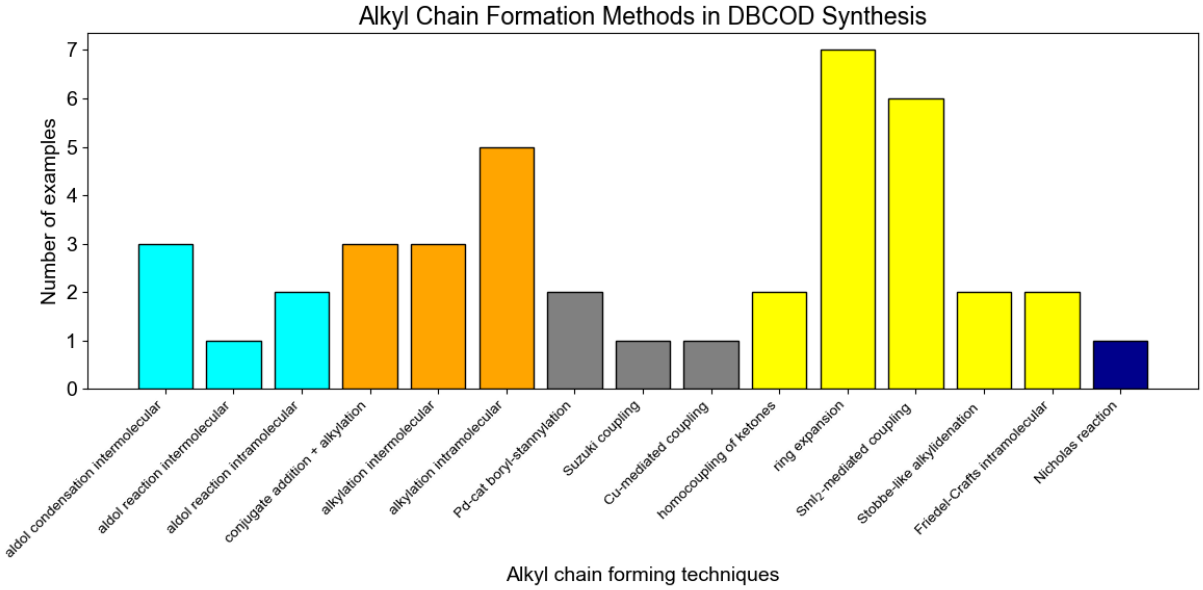
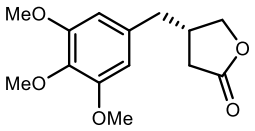
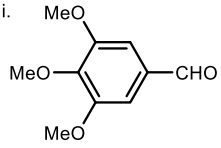
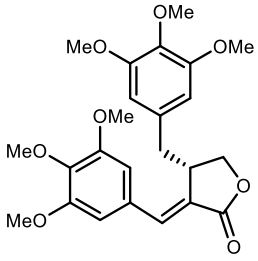
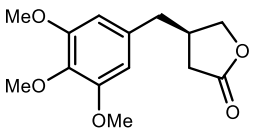
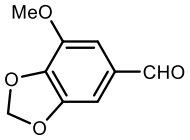
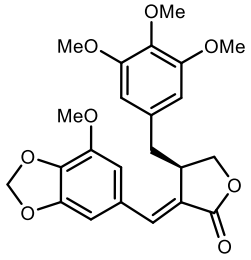
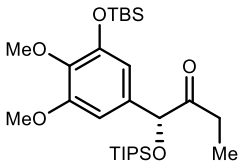
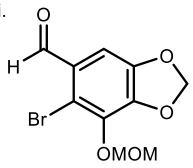
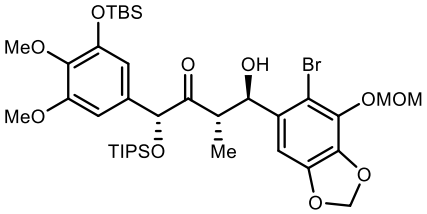
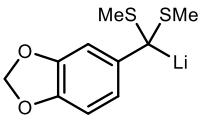
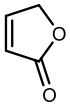
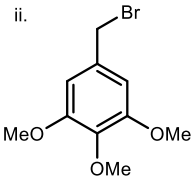
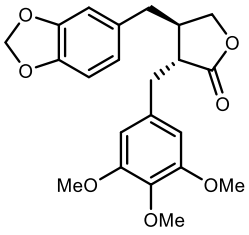
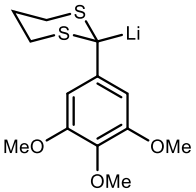
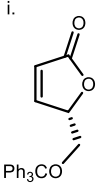
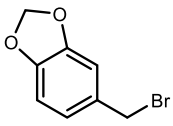
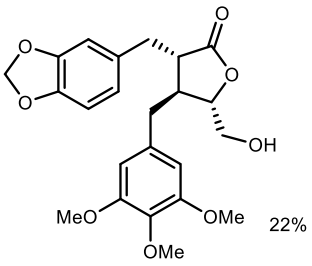


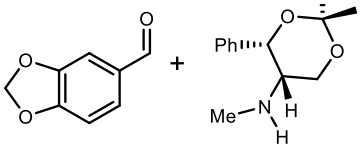
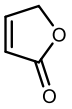
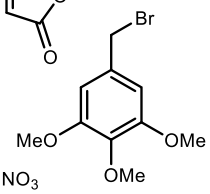
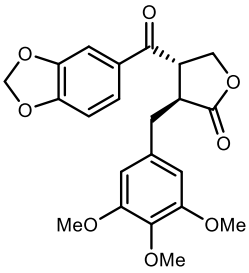
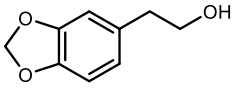
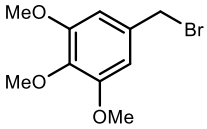
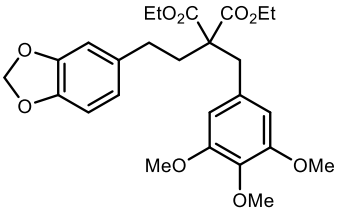
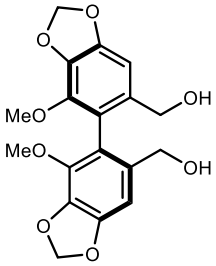
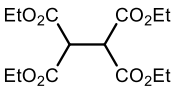
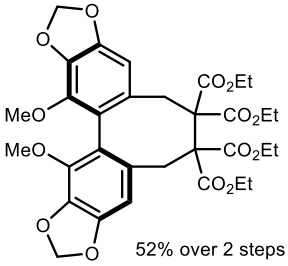
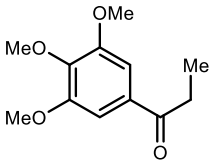
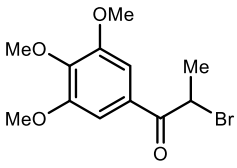
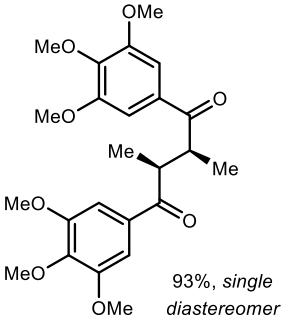
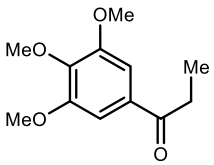
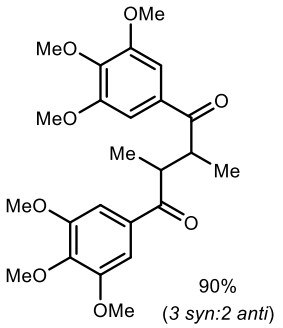
Figure 1.18. Alkyl chain construction techniques

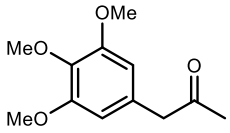
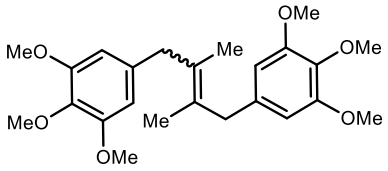
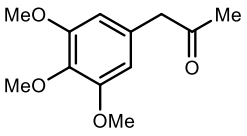
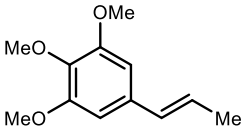
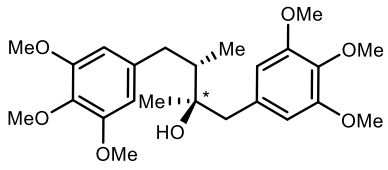
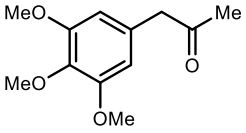
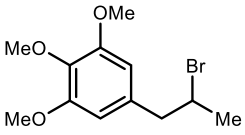
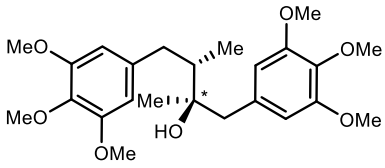
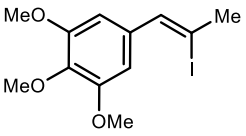
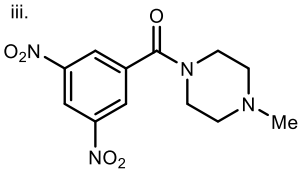
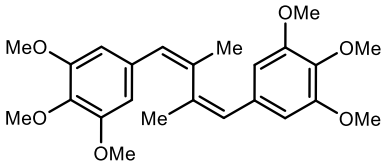
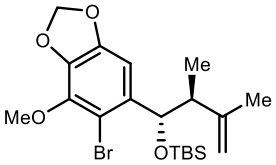
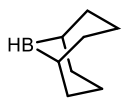
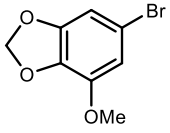
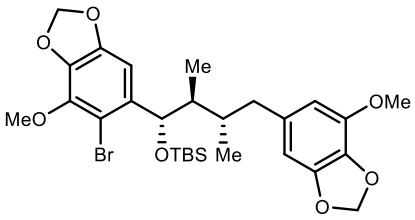
1.6.3.1. Intermolecular alkyl chain forming reactions

A compilation of reported reactions for the intermolecular formation of the alkyl chain in DBCOD syntheses is presented in Table 1.7. Entries **1** and **2** employ the same aldol condensation conditions proceeding through lithium enolates but use opposite enantiomers of the ketone and different aldehydes. Both reactions proceeded with complete (*E*)-selectivity, however the more electrophilic tris-methoxy benzaldehyde (entry **1**[110]) provided a higher yield (91 %) of aldol than the benzodioxolane-bearing aldehyde from entry **2**[108] (73 %). The aldol reaction in entry **3** initially gave an (*E*)-magnesium enolate which was then transmetallated to the (*E*)-boron enolate before

reacting with the aldehyde.[1] This reaction proceeded in good yield (79 %) and excellent *dr* (20:1), with excellent *ee* being obtained after recrystallization (66 % yield, > 99 % *ee*). Entries **4**–**6** each feature a three-component coupling involving a conjugate addition followed by an alkylation. Schlessinger's reaction (entry **4**) was the most effective of the three, providing the desired product in an 85 % yield.[81] A direct comparison can be drawn between entries **4** and **6**,[113] which use the same three coupling partners, although with an α-amino nitrile auxiliary appended to the aldehyde in entry **6** as opposed to dithiolation and lithiation of the aldehyde in entry **4**. The auxiliary provided high diastereo- and enantioselectivity, however the steric encumbrance decreased the yield of the conjugate addition / alkylation sequence (46 %). Entry **5** demonstrated the lowest yield (22 %) due to the use of a bulky Michael acceptor and a less electrophilic dioxolane-bearing benzyl bromide.[125] Entries **7**–**9** utilize alkylation reactions to form the alkyl chain. The homobenzylic alcohol in entry **7** was subjected to mesylation, then substitution to give the diethyl malonate, followed by deprotonation and alkylation, giving the product in 52 %, a good yield considering three steps are involved.[80] Entry **8** is an unusual case for this section, where the biaryl linkage has already been constructed.[92] The two benzylic alcohols were converted to the corresponding bromides and then bisalkylation was conducted using sodium ethoxide and tetrakis(ethoxycarbonyl)ethane, forming the 8-membered ring in a 52 % yield over two steps. Entry **9** features formation of the sodium enolate followed by alkylation, giving a single diastereomer in excellent yield (93 %).[114] The same ketone used in entry **9** was converted to the lithium enolate and homocoupled using $Cu(OTf)_2$ in entry **10**, which proceeded in excellent yield (90 %), giving a mixture of separable diastereomers (3 *syn*: 2 *anti*).[114] McMurry coupling was employed on a constitutionally isomeric ketone (entry **11**), giving the condensation product in good yield (86 %) but with poor *dr* (27 E: 73 Z).[112] Entries **12** and **13** make use of the same homobenzylic ketone in a Samarium-Barbier reaction with either a styrene or homobenzylic bromide.[111,118] A large discrepancy was observed between the two substrates, with the styrene reacting slowly (32 %) albeit with high *dr* (9:1) and the bromide providing higher yield (82 %) but low diastereoselectivity (42: 58). Entry **14** features the formation of a Grignard reagent from a vinyl iodide, followed by transmetallation to give the cuprate.[102] After oxidation to the neutral Cu(I) species, a second equivalent of starting material underwent oxidative addition to the copper center, followed by reductive elimination to give the dimeric product in fair yield (63 %). The linear DBCOD precursor in Coleman's asymmetric synthesis of interiotherin A (entry **15**) was

Entry	Starting Material	Technique and Reagents	Product, Yield
1.		*Aldol condensation* i.  LDA, THF ii. Ac_2O, NEt_3, DMAP then DBU	 91%, *complete E-selectivity*
2.		*Aldol condensation* i.  LDA, THF ii. Ac_2O, NEt_3, DMAP iii. DBU, toluene	 73%, *E-selective*
3.		*Aldol reaction* i. TMPMgBr, THF ii. Cy_2BCl, hexanes iii.  CH_2Cl_2-hexanes, –78 °C to –30 °C	 79% (20:1 *dr*) after recrystallization, 66% (>99% *ee*)
4.		*Conjugate addition + alkylation* i.  ii.  then TMEDA iii. Raney-Ni	 85%
5.		*Conjugate addition + alkylation* i.  ii. LDA,  iii. Raney-Ni iv. conc. HCl-MeOH (3:97)	 22%

Entry	Starting Material	Technique and Reagents	Product, Yield
6.		*Conjugate addition + alkylation* 1. KCN, HCl, pH= 4-5 2. LDA,  3. *t*BuLi,  then $AgNO_3$	 46% (>98% *dr*. 96% *ee*)
7.		*Alkylation* 1. MsCl, NEt_3, 2. $NaCH(CO_2Et)_2$ 3.  NaH, DMF	 52% over 3 steps
8.		*(Bis)alkylation* 1. PBr_3 2. NaOEt, 	 52% over 2 steps
9.		*Alkylation* $NaNH_2$, NH_3, 	 93%, *single diastereomer*
10.		*Enolate homocoupling* LDA, $Cu(OTf)_2$	 90% (*3 syn:2 anti*)

Entry	Starting Material	Technique and Reagents	Product, Yield
11.		*McMurry Coupling* 1. $TiCl_4$, Zn 2. PPTS, $HC(OEt)_3$ 3. Ac_2O	 23% *E,* 63% *Z*
12.		*SmI_2 Coupling*  SmI_2, HMPA	 32% (*9:1 dr*)
13.		*SmI_2 Coupling*  SmI_2, HMPA	 82% *(42:58 dr)*
14.		*Cu-mediated coupling* i. ^{i}PrMgCl•LiCl ii. CuBr•SMe_2 iii. 	 63%
15.		*Suzuki coupling* i.  ii. $Pd(PPh_3)_4$, PPh_3 NaOH, THF 	 77%, *single diastereomer*

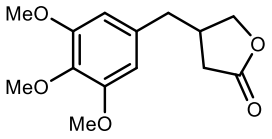
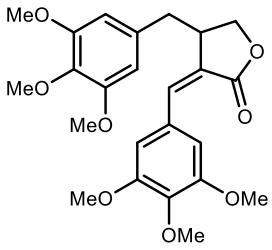
Entry	Starting Material	Technique and Reagents	Product, Yield
16.		*Stobbe-like alkylidenation* NaH toluene	 63 %

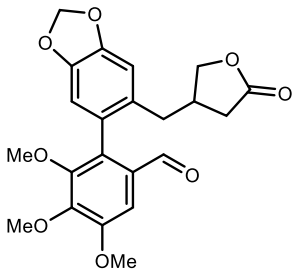
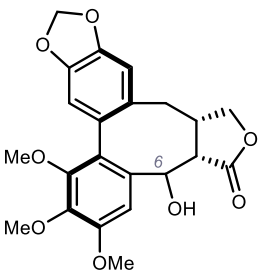
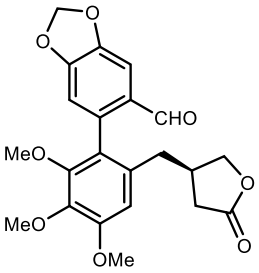
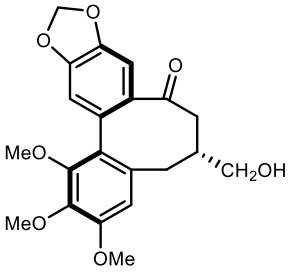
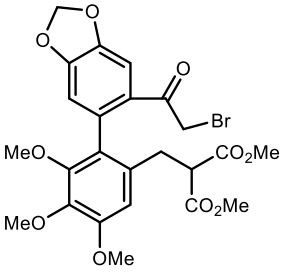
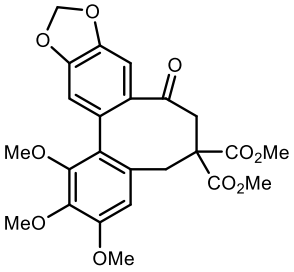
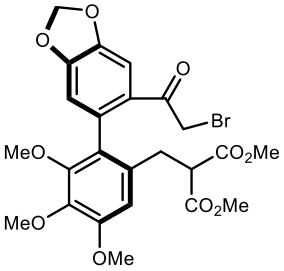
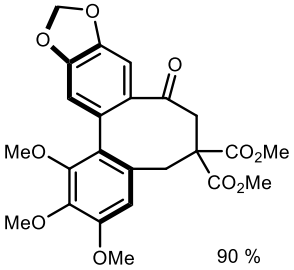
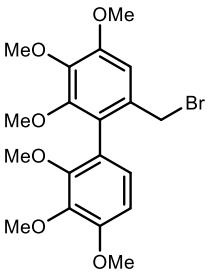
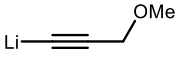
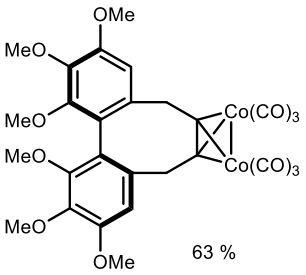
Table 1.7. Comprehensive list of intermolecular alkyl chain forming techniques

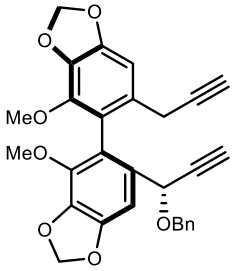
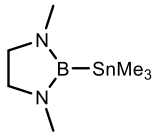
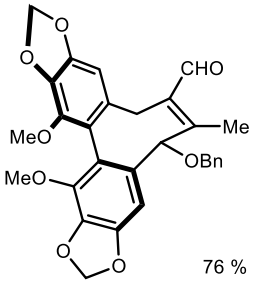
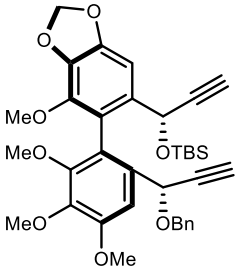
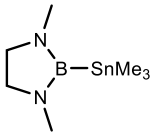
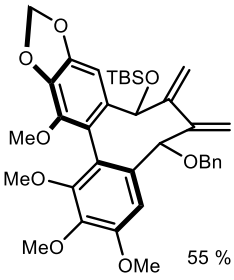
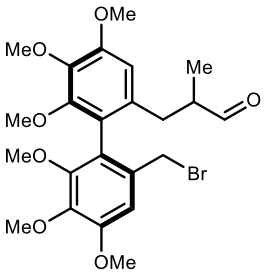
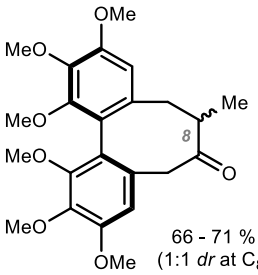
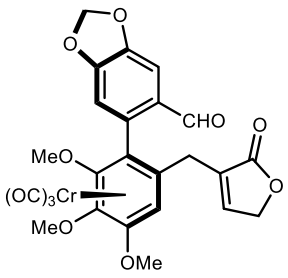
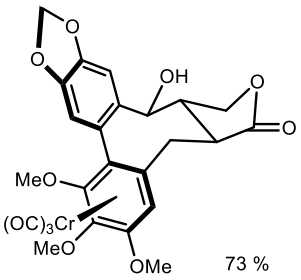
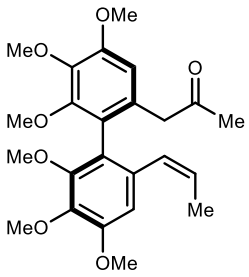
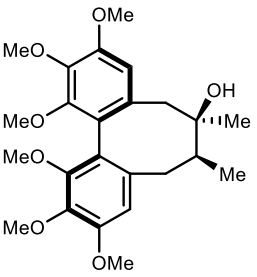
obtained as a single diastereomer in good yield (77 %) by hydroboration of an alkene fragment with 9-BBN, followed by Suzuki coupling to an aryl bromide fragment.[90] Robin *et al.* utilized Stobbe-like alkylidenation (sodium hydride and toluene) to convert 3,4,5-trimethoxybenzyl-4-butanolide to a linear DBCOD precursor in good yield (entry **16**, 63 %).[106,126]

1.6.3.2. Intramolecular 8-membered ring formation

Reported methods used to form the 8-membered ring of DBCODs via an intramolecular reaction are presented in Table 1.8. Robin has used intramolecular aldol reactions to produce two DBCOD scaffolds (entries **1**, **2**). In both cases, the lactone was converted to the lithium enolate by treatment with LHMDS, which then attacked the aldehyde, giving an 8-membered ring with a fused lactone. In entry **1**, the product is formed in an excellent yield of 99 % but with a mixture of C6 stereoisomers.[100] In entry **2**, the aldol product was further subjected to oxidation using CrO_3 and then lactone opening by $Ba(OH)_2$, followed by decarboxylation, giving the product in 67 % yield over 3 steps as a mixture of separable atropisomers.[85] Intramolecular alkylation as a ring closing strategy, using the α-bromo ketone substrate (entry **3**), was first performed by Ziegler in 1978 using potassium *tert*-butoxide, furnishing the product in 73 % yield as a mixture of atropisomers.[99] In 2018, Shi developed an improved alkylation procedure for the (*P*) atropisomer of the same substrate using DBU, which gave a 90 % yield (entry **4**).[123] Green employed a unique approach for alkyl chain construction in entry **5**, where a benzylic bromide is reacted with the lithium acetylide derived from propargyl methyl ether. $Co_2(CO)_8$ then coordinated to the resulting alkyne, and treatment with BF_3 etherate initiated a Nicholas reaction, where the distal arene acted as the nucleophile, giving the 8-membered ring product in 63 % yield.[127] RajanBabu has developed

the method of Pd-catalyzed borylstannylation which they have utilized in two reports of DBCOD syntheses (entries **6, 7**).[91,93] Treatment of a bisalkyne substrate with $Pd(PPh_3)_2Cl_2$ and a [BSn] reagent led to the formation of an axially chiral product possessing an 8-membered ring with vinyl trimethyl tin and vinyl diazoborolidine groups at C7 and C8, respectively. In entry **6**, this intermediate was treated with H_2O_2 and NaOH to give the α,β- unsaturated aldehyde product (in 76 % yield over 2 steps). In entry **7**, the analogous intermediate was treated with pinacol followed by acetic acid to afford the 1,3-diene product (in 55 % yield over 2 steps). SmI_2-mediated coupling, which we saw in section 1.6.3.1 as an intermolecular alkyl chain forming technique, has also been employed for intramolecular construction of the 8-membered ring (Table 1.8, entries **8-10**). Meyers performed a SmI_2-mediated coupling intramolecularly between a ketone and a benzyl bromide to form the 8-membered ring in their synthesis of (−)-isoschizandrin and (−)-schizandrin (entry **8**).[95] The coupling was followed by PCC oxidation of the resulting alcohol to the ketone, which resulted in yields of 66–71 % over two steps with a mixture of stereoisomers at C8. The Molander group has used intramolecular SmI_2-mediated coupling in both their synthesis of steganone (entry **9**)[89] and (+)-isoschizandrin (entry **10**)[98]. In entry **9**, a benzylic aldehyde was coupled to the 1,4-position of an α,β-unsaturated lactone in a 73 % yield. In entry **10**, a homobenzylic ketone was coupled to a benzylic alkene in 85 % yield. Notably, this intramolecular ketone to alkene coupling is considerably higher yielding than the analogous intermolecular reaction mentioned in Table 1.7, entry **12**. The two reported DBCOD-type gymnothelignan syntheses both utilize intramolecular Friedel–Crafts cyclizations to construct the 8-membered ring (Table 1.8, entries **11**, **12**). In entry **11**, catalytic tosic acid is used to form an oxocarbenium cation from the hemiacetal, which is then attacked by the arene in a Friedel-Crafts reaction, giving (−)-gymnothelignan V in an excellent yield of 90 %.[94] In entry **12**, BF_3-Et_2O is used to catalyze the oxocarbenium cation formation and the Friedel–Crafts cyclization is followed by benzyl deprotection of the phenol, providing (−)-gymnothelignan L in a 65 % yield over 2 steps.[78]

Entry	Starting Material	Technique and Reagents	Product, Yield
1.		*Intramolecular aldol reaction* LHMDS PhH/ hexanes, 1 min, rt then 30 % HCl	 99 % (*3S:2R at C6*)
2.		*Intramolecular aldol reaction* 1. LHMDS 2. CrO_3 3. $Ba(OH)_2$	 67 % *for mixture of atropisomers, then separated*
3.		*Alkylation* ^{t}BuOK	 73 % *(1:1 atropisomeric mixture)*
4.		*Alkylation* DBU	 90 %
5.		*Nicholas Reaction* 1. $Pd(dppf)Cl_2$, $InCl_3$  2. $Co_2(CO)_8$ 3. $BF_3{\bullet}Et_2O$	 63 %

Entry	Starting Material	Technique and Reagents	Product, Yield
6.		*Pd-catalyzed borylstannylation* 1. $Pd(PPh_3)_2Cl_2$  2. H_2O_2, NaOH	 76 %
7.		*Pd-catalyzed borylstannylation* 1. $Pd(PPh_3)_2Cl_2$,  2. Pinacol 3. HOAc, reflux	 55 %
8.		*SmI_2-mediated coupling* 1. SmI_2, HMPA 2. PCC, Al_2O_3	 66 - 71 % (1:1 *dr* at C_8)
9.		*SmI_2-mediated coupling* SmI_2 ^{t}BuOH THF/HMPA	 73 %
10.		*SmI_2-mediated coupling* SmI_2 (2.2 equiv) ^{t}BuOH,HMPA	 (+)-isoschizandrin 85 %

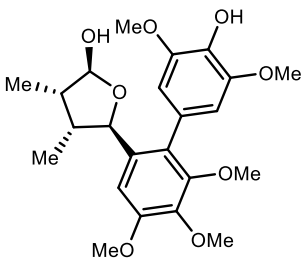
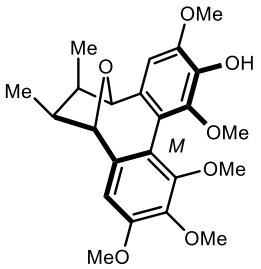
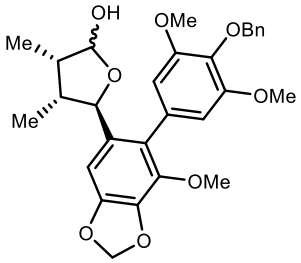
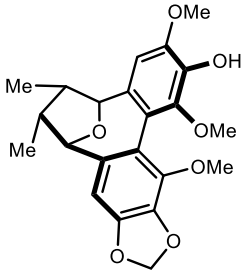
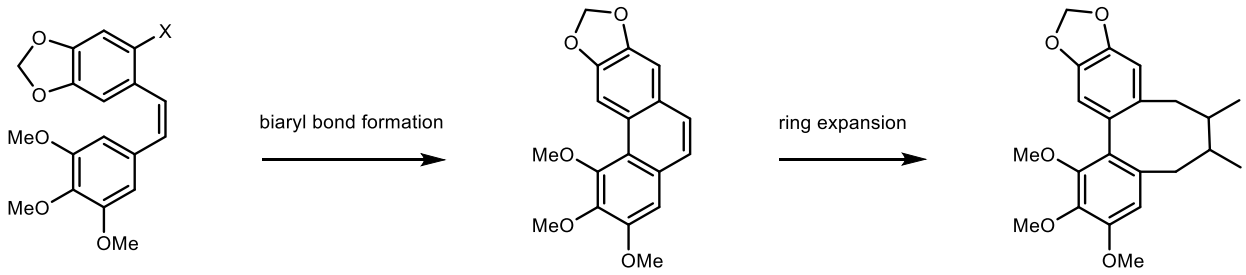
Entry	Starting Material	Technique and Reagents	Product, Yield
11.		*Friedel-Crafts* TsOH	 (-)-gymnothelignan V 90 %
12.		*Friedel-Crafts* 1. $BF_3 \cdot Et_2O$ 2. H_2, 10 % Pd/C	 (-)-gymnothelignan L 65 %

Table 1.8. Intramolecular eight-membered ring forming techniques

1.6.4. Ring expansion strategies

Ring expansion strategies involve first involve forming a < 8-membered ring during the biaryl bond forming step, followed by expansion of this ring to the desired 8-membered ring (Scheme 1.14).



Scheme 1.14. Ring expansion strategy

Six examples where the alkyl chain is constructed by first forming a 6-membered and then later expanded into an 8-membered ring are reported (Table 1.9). A highly functionalized stilbene is

used as the starting material. Entries **1** and **2** target similar intermediates in steganone syntheses, differing only by the choice of amine. In Raphael's syntheses (entry **1**), pyrrolidine was condensed onto the ketone **1-121**, which was followed by 6 π electrocyclization and elimination of HBr to give the intermediate phenanthrene **1-122**. Initially they used potassium *tert*-butoxide and light to initiate the electrocyclization[82] but later found that $POCl_3$ could incite the same transformation with improved yield.[96] The ring expansion product **1-123** was then generated when the cyclooctene ring underwent a formal 2+2 reaction with dimethyl acetylenedicarboxylate (presumably giving a bicyclo[4.2.0]oct-7-ene system) followed by ring opening. Krow's synthetic sequence (entry **2**), using I_2 and light to instigate the electrocyclization, followed by functional group manipulations to produce an analogous phenanthrene intermediate **1-125**, was lower yielding than both of

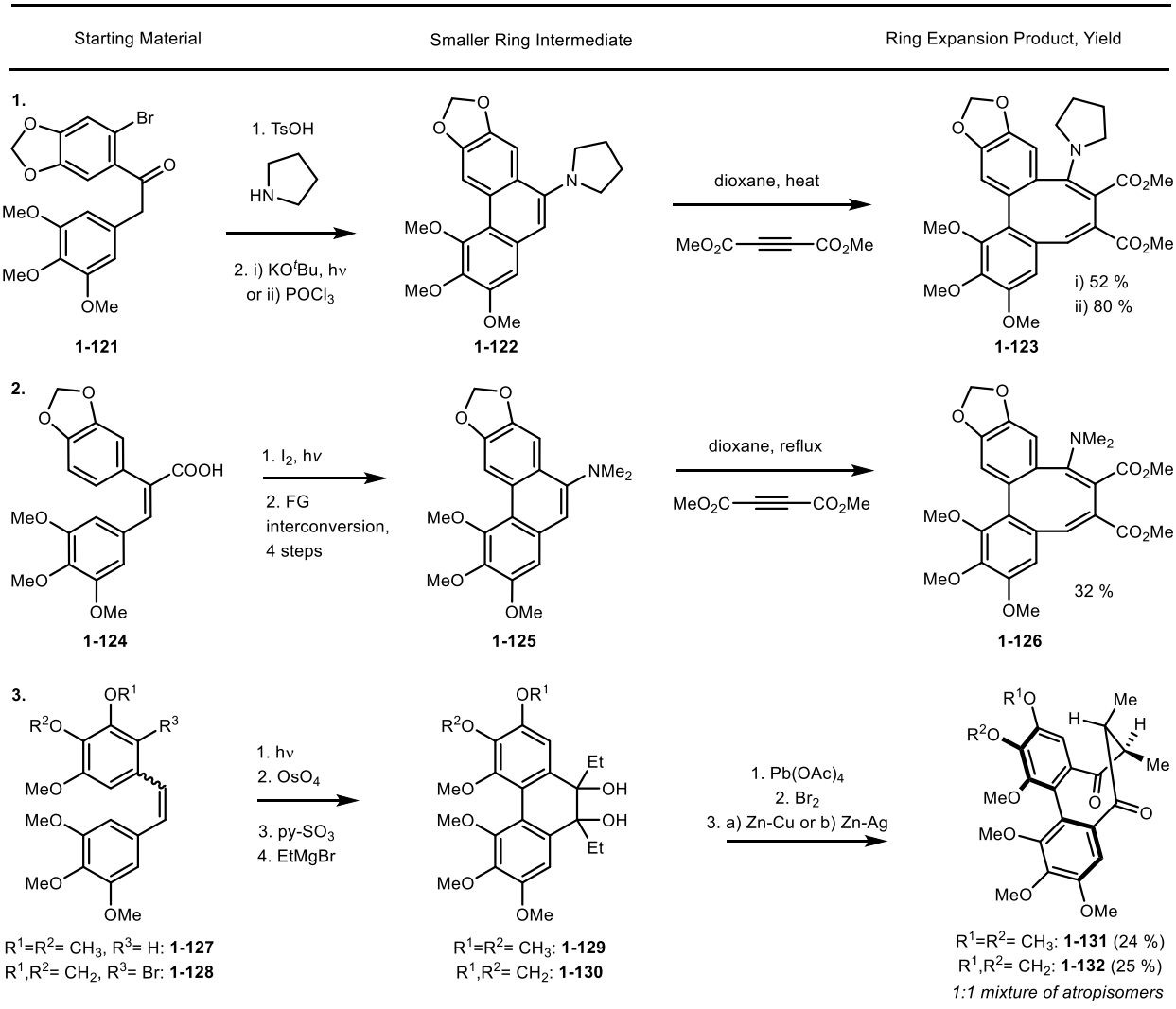
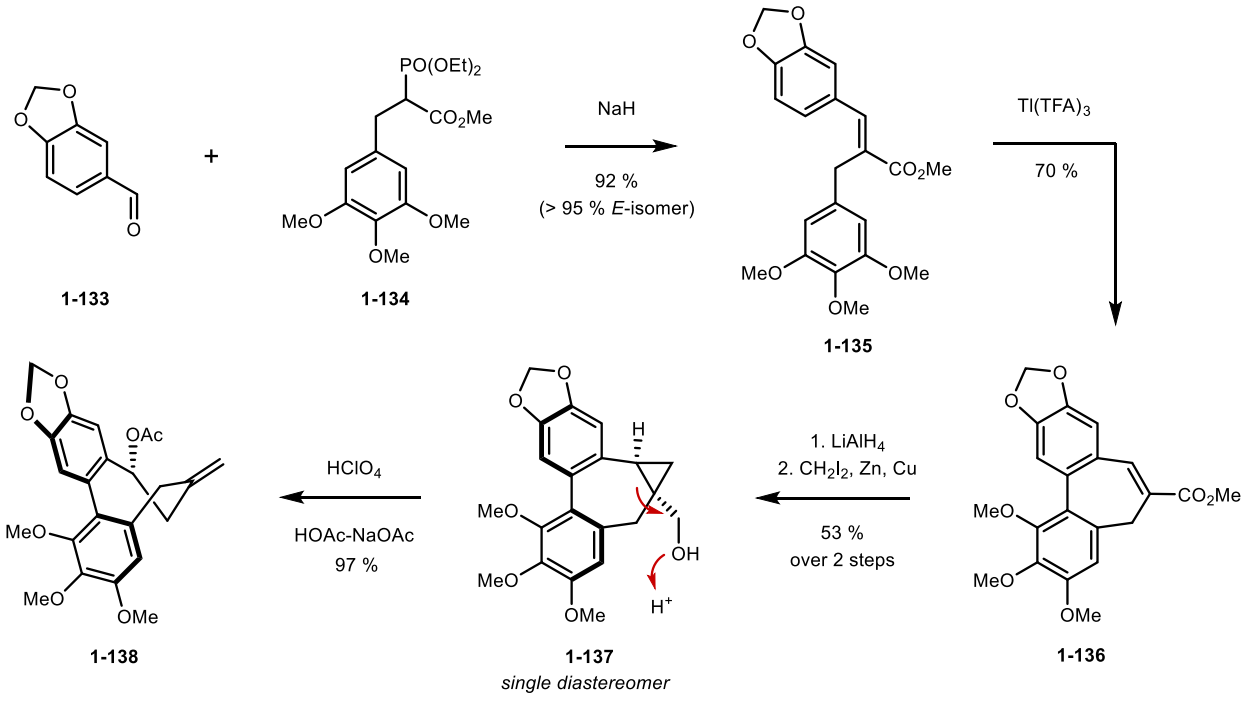


Table 1.9. Ring expansion strategies proceeding through a phenanthrene intermediate

Raphael's conditions.[128] Entry **3** includes a ring expansion strategy developed by Ghera *et al.* which they have used in three reported DBCOD syntheses.[83,84,129] Treatment of a functionalized stilbene (**1-127** or **1-128**) with light led to 6 π electrocyclization and loss of HBr. The resulting alkenes were oxidized to the corresponding diketones then converted to the diethyl diols by Grignard reaction, giving the pictured intermediates **1-129** and **1-130**, respectively. Subsequent oxidative cleavage using lead tetraacetate opened the rings. Dual α-brominations and reductive coupling using either Zn-Cu or Zn-Ag led to closure of the 8-membered rings. Compound **1-131** (obtained in 24 % yield from **1-127**) was used in the syntheses of both deoxyschizandrin and schizandrin, whereas substrate **1-132** (obtained in 25 % yield from **1-128**) was used to prepare kadsurin.

Another ring expansion strategy, proceeding via a seven-membered ring, was developed by Magnus in their synthesis of steganacin (Scheme 1.15).[115] The route commenced with a Wittig reaction between piperonal (**1-133**) and a benzylic ylide (**1-134**), generating **1-135** as primarily the *E*-isomer. Oxidative cyclization mediated by $Tl(TFA)_3$ gave the cycloheptene **1-136**, which was then subjected to Simmons-Smith cyclopropanation. The cyclopropane ring of **1-137** was opened under acidic conditions, yielding the 8-membered ring product, bearing an exocyclic alkene



Scheme 1.15. Cyclopropanation/ ring-expansion strategy from Magnus's steganacin synthesis

(**1-138**). This ring formation and ring expansion sequence was accomplished in five steps with an overall yield of 32 %.

1.6.5. Methods for introducing chirality

DBCOD natural products are isolated as a single enantiomer from the natural source, thus it is desirable to synthesize them asymmetrically to obtain material with identical bioactivity. Twenty two asymmetric DBCOD syntheses have been reported (Figure 1.19). This section will focus on the key step where chirality is introduced in those syntheses. Six of these reports begin their syntheses using previously reported chiral starting materials. Four of them append Meyers' chiral auxiliary to one of their aryl starting materials and subject this to a Grignard reaction, forming the biaryl axis atroposelectively. Another method (twice reported) involves the use of a chiral chromium auxiliary appended to one of the arene fragments. Kinetic resolution (via either asymmetric alkynylation or CBS reduction) has also been utilized several times to obtain optically pure biaryl material. Other techniques for introducing chirality, reported once each include: Rh-catalyzed asymmetric hydrogenation, Ni-catalyzed Ullmann coupling, asymmetric hydrocyanation, asymmetric crotylation, and chiral resolution. The use of chiral sulfoxide, oxazoline, and amine as auxillaries have each been reported once, for use in Suzuki coupling, Ullmann coupling, and 1,4-addition, respectively. One example of each of these techniques is

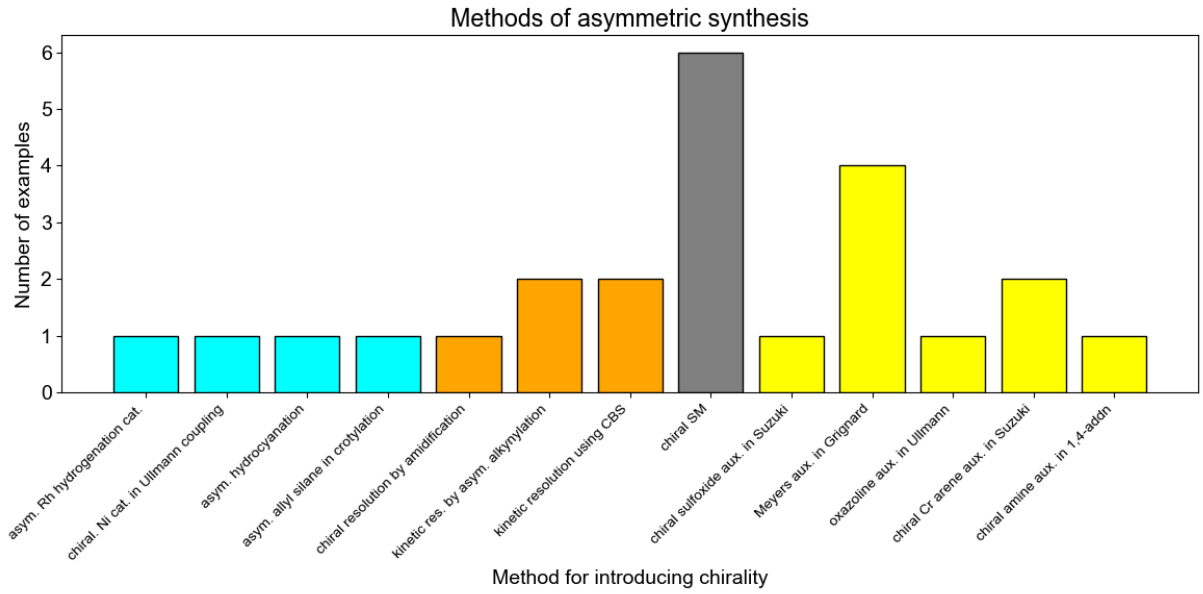
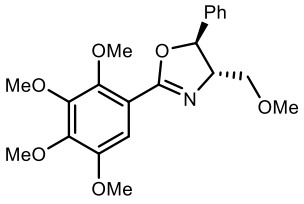
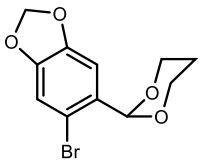
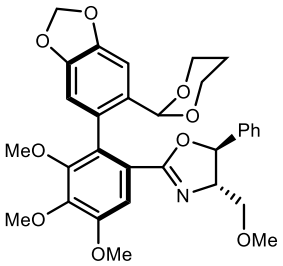
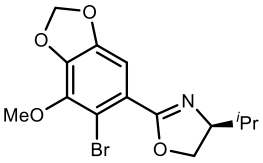
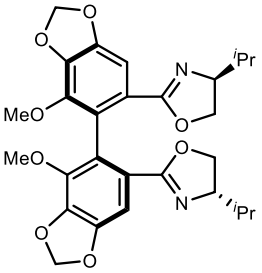
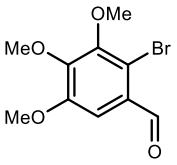
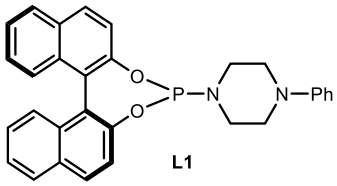
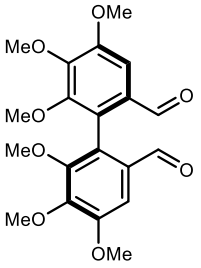
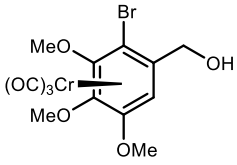
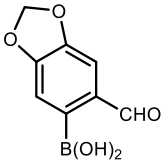
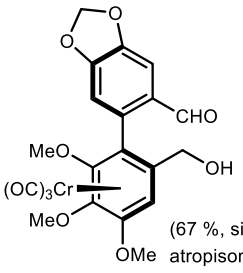
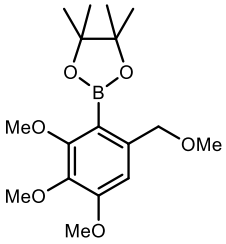
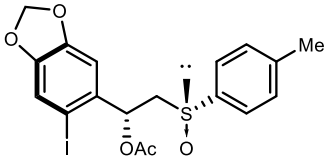
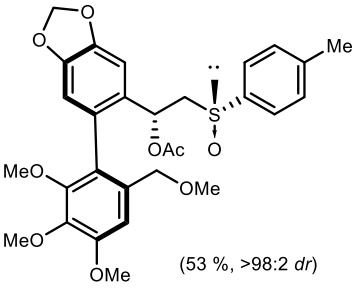
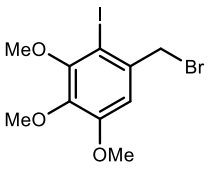
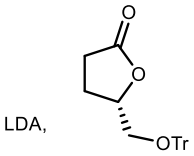
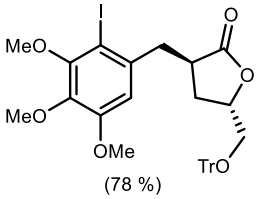
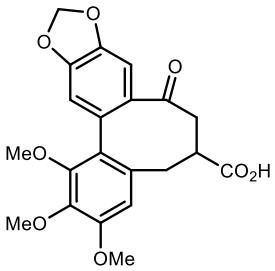
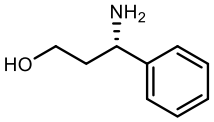
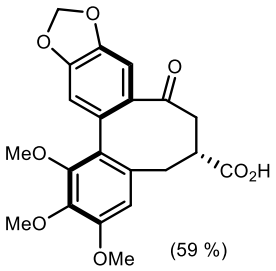
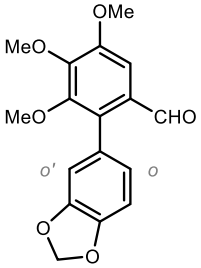
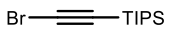
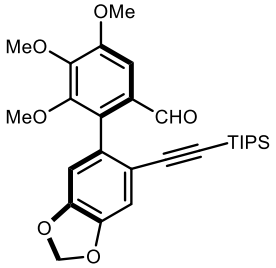
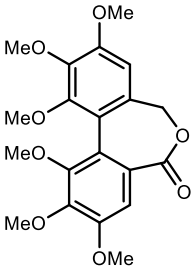
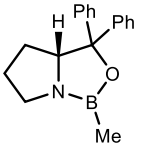
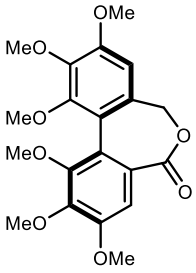
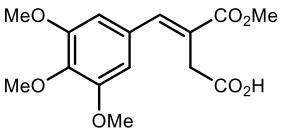
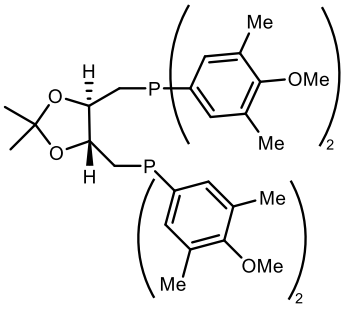
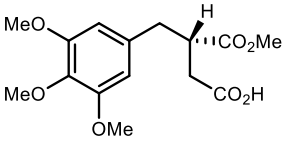


Figure 1.19. Techniques used in asymmetric syntheses

presented in Table 1.10.

Entries **1**–**5** of Table 1.10 were mentioned in section 1.6.2 on intermolecular biaryl bond formation (Table 1.1) and each involve the introduction of chirality either shortly before or during the biaryl bond formation step, providing the biaryl product atroposelectively. In entry **1**, the starting material bearing Meyers' chiral auxiliary could be prepared from the corresponding aryl carboxylic acid in two steps. This substrate was subjected to a reaction with an aryl Grignard reagent (generated *in situ*) to give the biaryl product with a preference for the *P* atropisomer (65 % *P* and 9 % *M* were isolated).[87] In entry **2**, a different chiral oxazoline auxiliary was appended to the *ortho* position of an aryl bromide for Cu-mediated Ullmann homocoupling, furnishing the biaryl product in good yield (68 %) and excellent *d.e.* (>99 %).[92] Entry **3** features a less traditional Ullmann coupling, where a nickel complex bearing a chiral BINOL-based monodentate phosporamidite ligand (**1-108**) catalyzed the homocoupling of an aryl bromide in a 67 % yield with moderate *ee* (68 %).[97] Entries **4** and **5** both involve the $Pd(PPh_3)_4$-catalyzed Suzuki coupling of an aryl halide fragment bearing a chiral auxiliary to an aryl boronic acid or ester. Entry **4** features a chiral chromium auxiliary on the arene which successfully transfered chirality to the product biaryl, giving a 67 % yield of a single atropisomer.[88,89] Entry **5** demonstrates the use of a chiral sulfoxide auxiliary appended to C8, which upon coupling gave the biaryl product in 53 % yield with >98:2 *dr*.[101] An example of using a chiral starting material is presented in entry **6**, where a chiral furanone was alkylated with a functionalized benzyl bromide to give a chiral aryl iodide product in 78 % yield.[85] This product is poised for biaryl bond formation, eg. via Ullmann or Suzuki coupling. In entry **7**, chiral resolution was used to obtain enantiomerically pure material from a racemic DBCOD precursor. Amidification of the racemic carboxylic acid with a chiral amine gave diastereomeric amides which were separable by preparative TLC. The desired diastereomer was then subjected to acidic hydrolysis at 35 ºC, giving the (+)-oxo-acid in a 59 % yield.[96] Entries **8** and **9** utilized kinetic resolution to obtain optically pure products from racemic precursors. In entry **8**, Pd-catalyzed C-H alkynylation of a biaryl substrate was accomplished with high *ee* (98 %) by using L-*tert*-leucine as a catalytic transient chiral auxiliary.[123] Mildly acidic conditions were used to facilitate recycling of the auxiliary and silver acetate was added to boost the reactivity of the alkynyl bromide, providing a good yield of 68 %. In entry **9**,[98] the racemic 7-membered lactone was subjected to Bringmann's kinetic resolution conditions.[130] Treatment of the configurationally labile lactone with CBS-oxazaborolidine led to selective reduction of the (*P*)-lactone to the corresponding diol,

Entry	Starting Material	Technique and Reagents	Product, Yield
1.		*Meyers' auxillary in Grignard reaction*  Mg, THF, reflux	 (65 %, + 9 % atropisomer)
2.		*Oxazoline auxillary in Ullmann coupling* Cu, DMF reflux	 (68 %, > 99 % *d.e.)*
3.		*Chiral ligand in Ni-Ullmann coupling* $NiCl_2(PPh_3)_2$, **L1**, TBAI, Zn, 45°C  **L1**	 (67 %, 68 % *e.e.*)
4.	 (> 99% *e.e.)*	*Suzuki-Miyaura coupling*  $Pd(PPh_3)_4$, aq. Na_2CO_3, MeOH, reflux	 (67 %, single atropisomer)
5.		*Suzuki-Miyaura coupling*  $Pd(PPh_3)_4$,CsF, dioxane, 70 °C	 (53 %, >98:2 *dr*)

Entry	Starting Material	Technique and Reagents	Product, Yield
6.		*Chiral furanone SM*  LDA,	 (78 %)
7.		1. *Amidification*  $SOCl_2$, NEt_3 2. *Separation of diastereomers* 3. H_2SO_4, DME, 35°C	 (59 %)
8.		*Asymmetric alkynylation* $Pd(OAc)_2$ L-*tert*-leucine AgTFA KH_2PO_4, HOAc 	 (68 %, 98 % *e.e., o:o'* = 5.9 :1)
9.		*CBS reduction*  BH_3, -20°C Then, H_2O, HCl	 (61 % yield after recycling, 98 % *e.e.*)
10.		*Asymmetric hydrogenation* H_2, Rh(COD)Cl 	 (85 %)

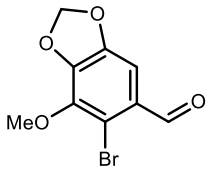
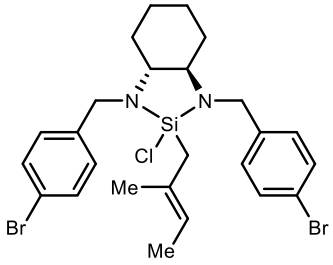
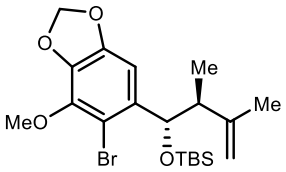
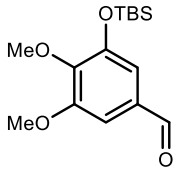
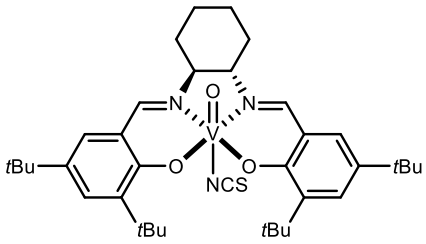
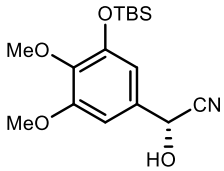
Entry	Starting Material	Technique and Reagents	Product, Yield
11.		1. *Asymmetric crotylation*  2. TBSCl	 (76 %, 96 % *e.e.)*
12.		*Asymmetric hydrocyanation*  TMSCN	 (>95 %, 92.7 % *e.e.*)

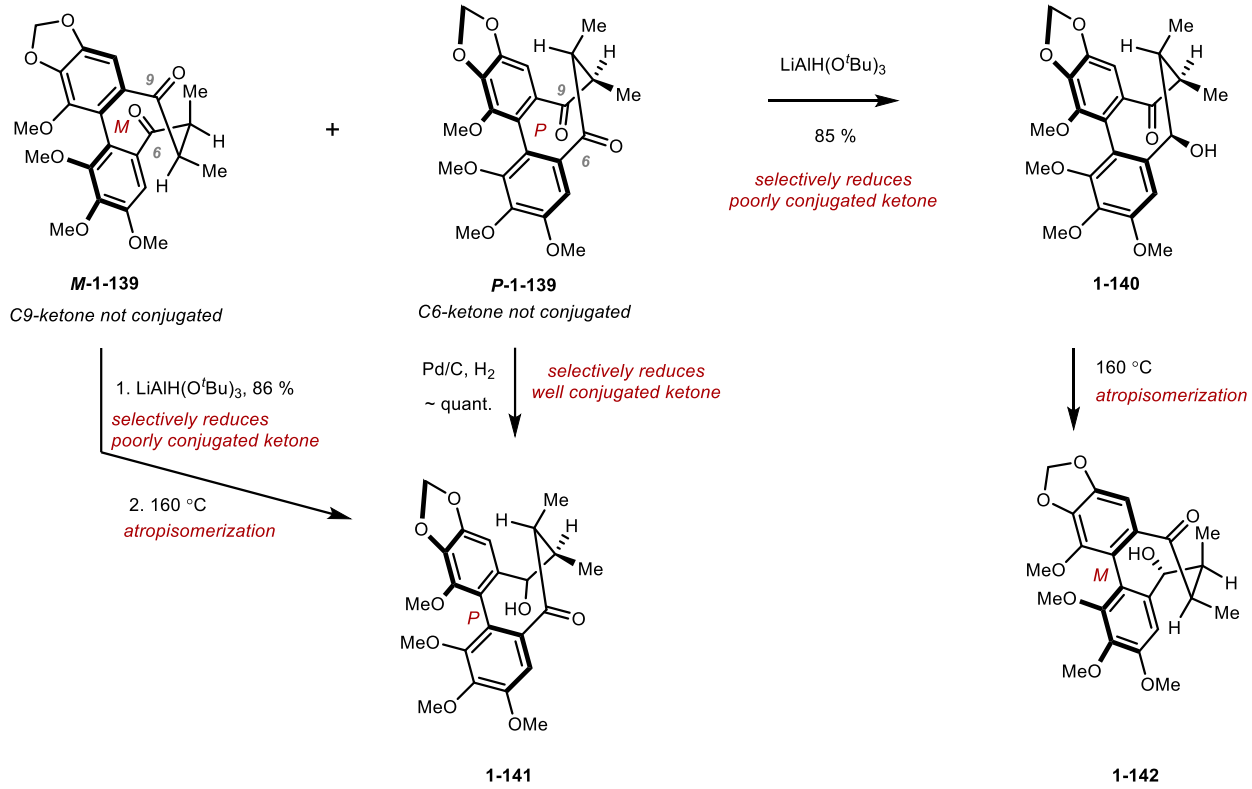
Table 1.10. Examples of each technique utilized to incorporate chirality

which was separable from the remaining (*M*)-lactone by chromatography. The (*P*)-diol could be recycled by oxidation to the dialdehyde, racemization by heating, and treatment with Canizarro conditions and DCC to give the racemic lactone. After recycling, a yield of 61 % of the (*M*)-lactone product was obtained in 98 % *ee*. Asymmetric hydrogenation of an achiral styrene derivative (entry **10**) was catalyzed by a (*R,R*)-MOD-DIOP rhodium complex, furnishing a half acid product as a single enantiomer in 85 % yield.[110] Coleman performed an asymmetric crotylation on an aryl aldehyde using a chiral tiglylsilane (entry **11**) to construct most of the alkyl chain (C6–C8) as well as setting two stereocentres with full diastereoselectivity and 96 % *ee*. The (6S,7S)-*anti* product was obtained in a good yield of 76 % after TBS protection.[29] Lumb performed an asymmetric hydrocyanation on a benzylic aldehyde (entry **12**) using TMSCN and a VO(salen) catalyst to impart chirality, giving the α-hydroxy nitrile product in an excellent yield of > 95 % with 92.7 % *ee*.[1]

1.6.6. Distinctive synthetic steps: late-stage oxidation modification

The reported syntheses of DBCODs contain many noteworthy steps beyond the alkyl chain formation, biaryl axis formation, or ring expansion steps mentioned in sections 1.6.2–1.6.5. This section will highlight some of the unique steps from DBCOD syntheses, most of which enable late-stage modification of the oxidation pattern around the 8-membered ring. Three instances of non-canonical oxidation will also be presented.

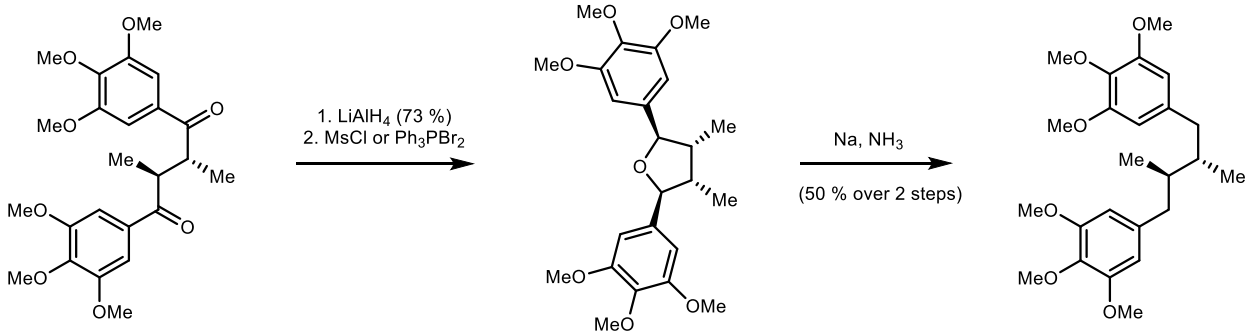
During Ghera's synthesis of kadsurin, the fascinating discovery was made that the C6 and C9 ketones of DBCODs can be differentiated.[84] Both atropisomers of **1-139** were examined, and it was found that in the (*M*)-atropisomer, the C6 ketone is conjugated to the neighbouring aromatic ring, however the C9 ketone experiences less effective orbital overlap with the aromatic ring (Scheme 1.16). The opposite is true for the (*P*)-atropisomer. This was evidenced by differences in the absorptions of the carbonyls in the IR spectra and the chemical shifts of the adjacent aromatic protons in the ^{1}H NMR spectra. Using this knowledge, Ghera *et al.* developed conditions to selectively reduce each of the ketones to the



Scheme 1.16. Selective reductions of inequivalent ketones at C6 and C9 in the synthesis of kadsurin (Ghera 1977)

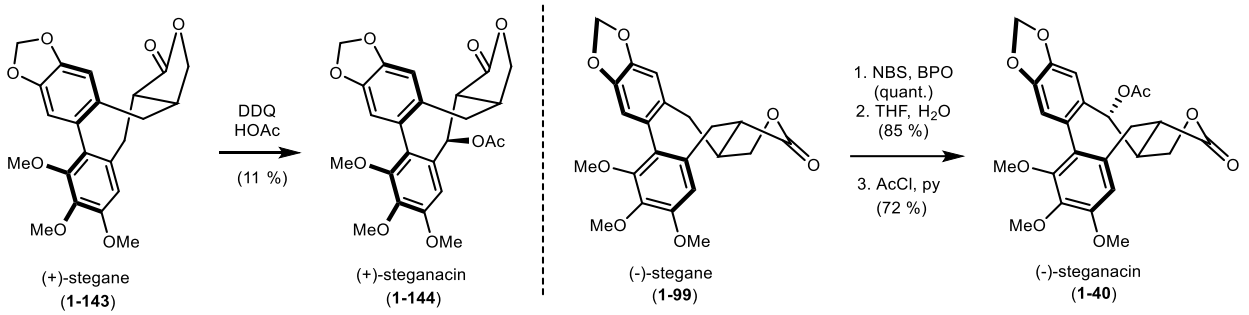
corresponding alcohols. They found that LiAlH(O*t*Bu)$_3$ could reduce the poorly conjugated ketones (C6 of ***M*-1-139** or C9 of ***P*-1-139**), without affecting the well conjugated ketones, in yields of 85–86 %. Hydrogenation with catalytic palladium on carbon was used to selectively reduce the well conjugated ketone (C6 of ***P*-1-139**) without affecting the poorly conjugated ketone in quantitative yield. LiAlH(O*t*Bu)$_3$ is sterically encumbered so it only reacts with the less hindered ketone, which is the non-conjugated ketone. Hydrogenation of ketones with palladium on carbon occurs more readily on benzylic ketones as the inductive withdrawing effect of the aromatic ring makes them more electrophilic as well as the fact that the metal surface can interact with the π-system. After reduction of the conjugated ketone, it was possible to fully atropisomerize the substrates by heating at 160 °C for 30 h (***M*-1-139** to **1-141** and **1-140** to **1-142**). Atropisomerization prior to reduction (***M*-1-139** to ***P*-1-139**) had proved slothful with only 25 % conversion after 30 h at 160 °C.

Stevenson's synthesis of (±)-deoxyschizandrin included the bis-deoxygenation of a diarylketone (**1-143**) in a three step process (Scheme 1.17).[114] **1-143** was subjected to lithium aluminum hydride, furnishing the diol in 73 % yield, followed by monosubstitution with either methanesulphonyl choride or triphenylphosphine dibromide. Intramolecular attack of the remaining alcohol onto the leaving group-bearing carbon provided the tetrahydrofuran intermediate **1-144**. Reduction of **1-144** with sodium in liquid ammonia, provided diarylbutane **1-145** (which is one step away from (±)-deoxyschizandrin) in 50 % yield over two steps.



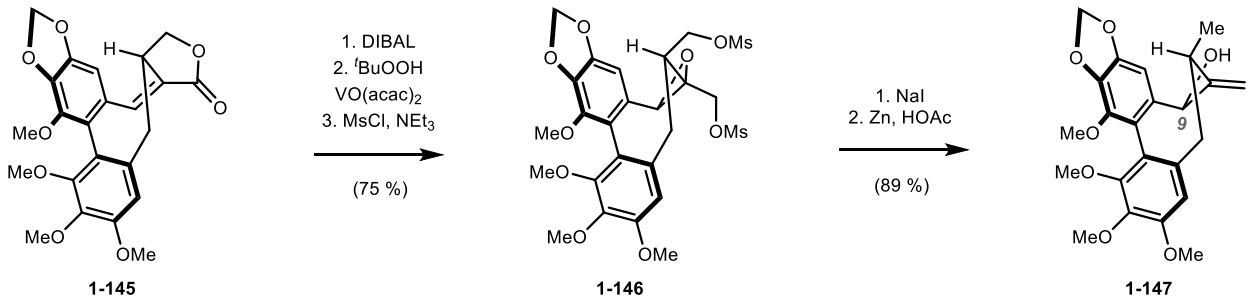
Scheme 1.17. Bis-deoxygenation via tetrahydrofuran intermediate in the synthesis of (±)-deoxyschizandrin (Stevenson 1978)

In Koga's syntheses of (+)- and (−)-steganacin, they developed two methods for late-stage C(sp^3)-H oxidation in order to introduce the C6 or C9 acetyl group (Scheme 1.18).[125] (+)-Steganacin could be prepared in 11 % yield by selective DDQ oxidation at C6 of (+)-stegane in acetic acid. (−)-Steganacin was prepared from (−)-stegane in 61 % yield over three steps by first brominating C9 using NBS-BPO, followed by substitution with H_2O to give the corresponding alcohol, then acetylation.



Scheme 1.18. Methods for late-stage C(sp^3)-H oxidation in the syntheses of (+)- and (−)-steganacin (Koga 1984)

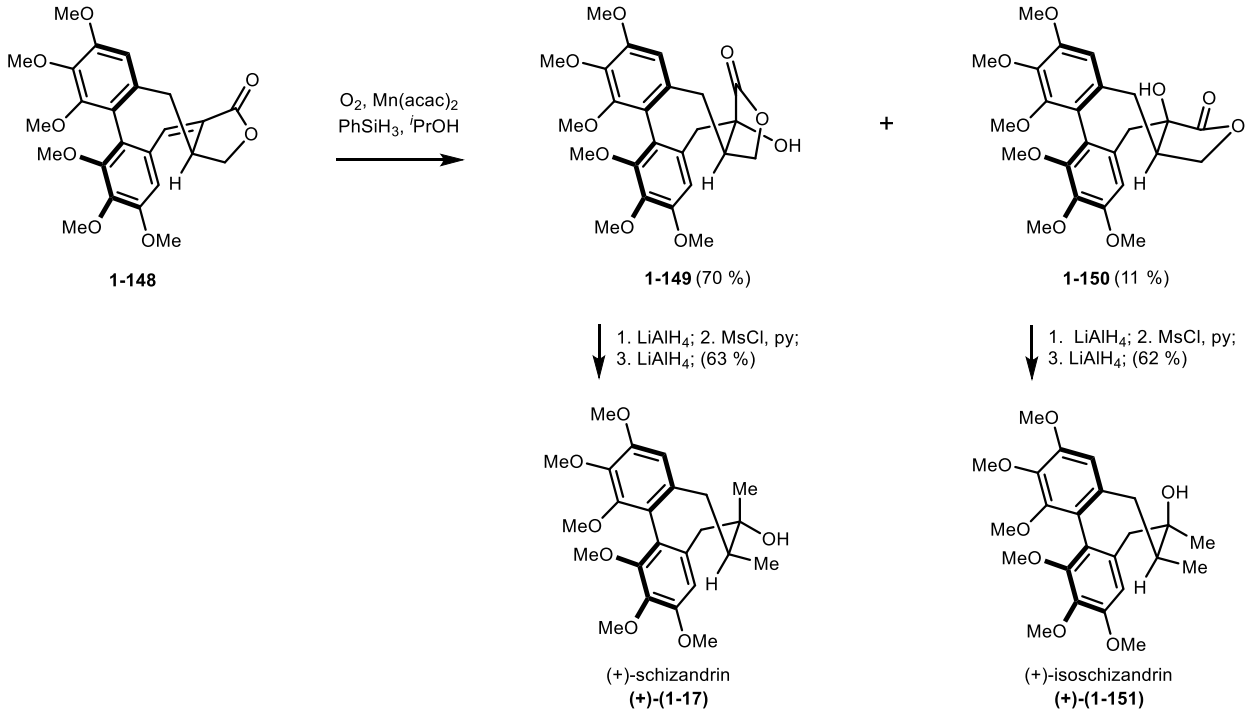
In 1995, Wakamatsu targeted kadsurin, which possesses an acetyl group at C9.[108] Desiring to utilize oxidative coupling mediated by $Fe(ClO_4)_3 \cdot 6H_2O$ to form the biaryl linkage, it was necessary to select a substrate not possessing free alcohols. Therefore, **1-145** was successfully formed via oxidative coupling by masking the alcohols as a lactone. Compound **1-145** was then subjected to DIBAL, reducing the lactone to the diol (Scheme 1.19). *Tert*-butyl peroxide and $VO(acac)_2$ were added, stereoselectively epoxidizing the alkene, followed by mesylation of the diol, providing **1-146** in a 75 % yield. Treatment with NaI gave a mixture of the diiodide and the oxirane ring opened



Scheme 1.19. Stereoselective epoxidation and Zn-mediated reduction in the synthesis of kadsurin (Wakamatsu 1995)

monoiodide. Reduction of the mixture with Zn in acetic acid gave a single product **1-147**, bearing a hydroxyl group at the desired position, in 89 % yield.

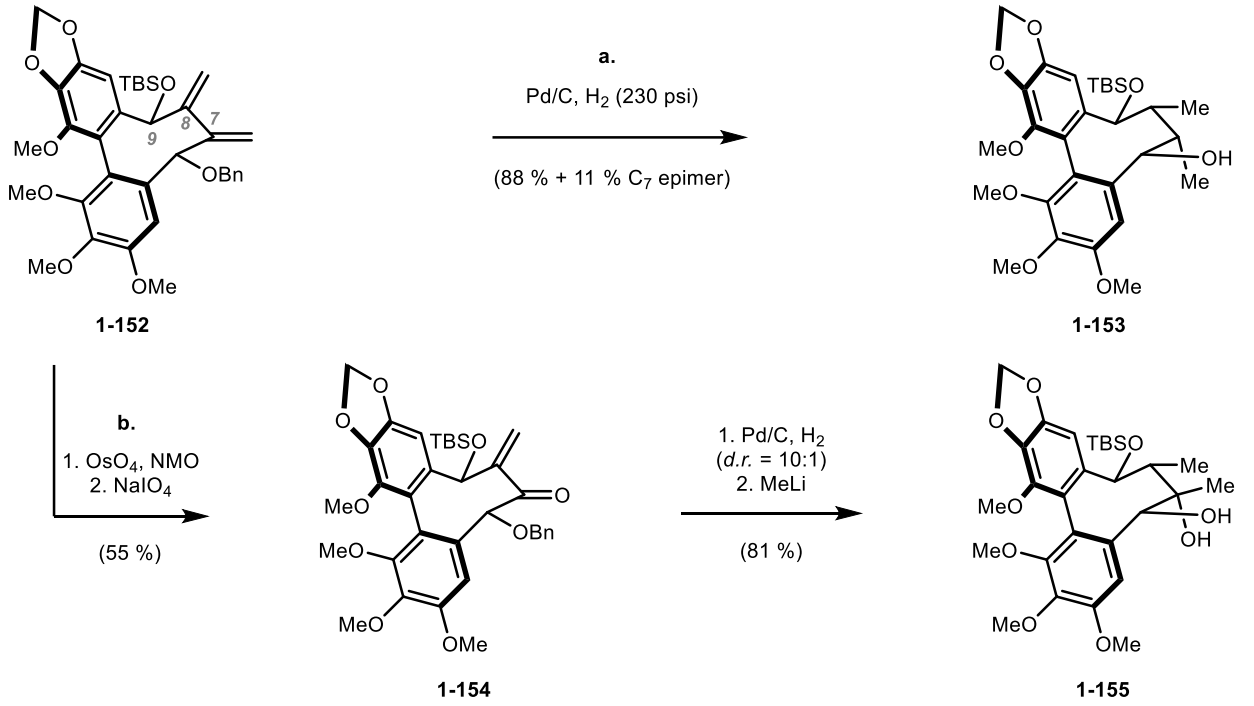
In a second synthesis from Wakamatsu's group, they synthesized both (+)-schizandrin and (+)-isoschizandrin from a common α-alkylidene butyrolactone precursor **1-148** (Scheme 1.20).[109] Mukaiyama hydration catalyzed by manganese(II) acetyl-acetonate was used to regioselectively hydrate the alkene of **1-148**, with partial stereoselectivity, providing a 70 % yield of **1-149** and 11 % of the minor diastereomer **1-150**. **1-149** was converted into (+)-schizandrin in 63 % yield by reduction of the lactone with $LiAlH_4$, mesylation of the resulting diol, and reduction of the mesylates by a second treatment with $LiAlH_4$. **1-150** was converted to (+)-isoschizandrin in a similar yield (62 %) using the same three step sequence.



Scheme 1.20. Mukaiyama hydration in the synthesis of (+)-schizandrin and (+)-isoschizandrin from a common starting material (Wakamatsu 1995)

After effecting the atroposelective biaryl bond formation described in Table 1.8, entry **7**, RajanBabu was able to stereoselectively reduce the diene **1-152** using hydrogen gas and Pd/C to give the *syn* product **1-153** (88 %, Scheme 1.21A).[93] It is proposed that the bulky siloxy group at C9 blocks the α-face of the C8 alkene, leading to hydrogenation of the β-face. The C7 alkene is

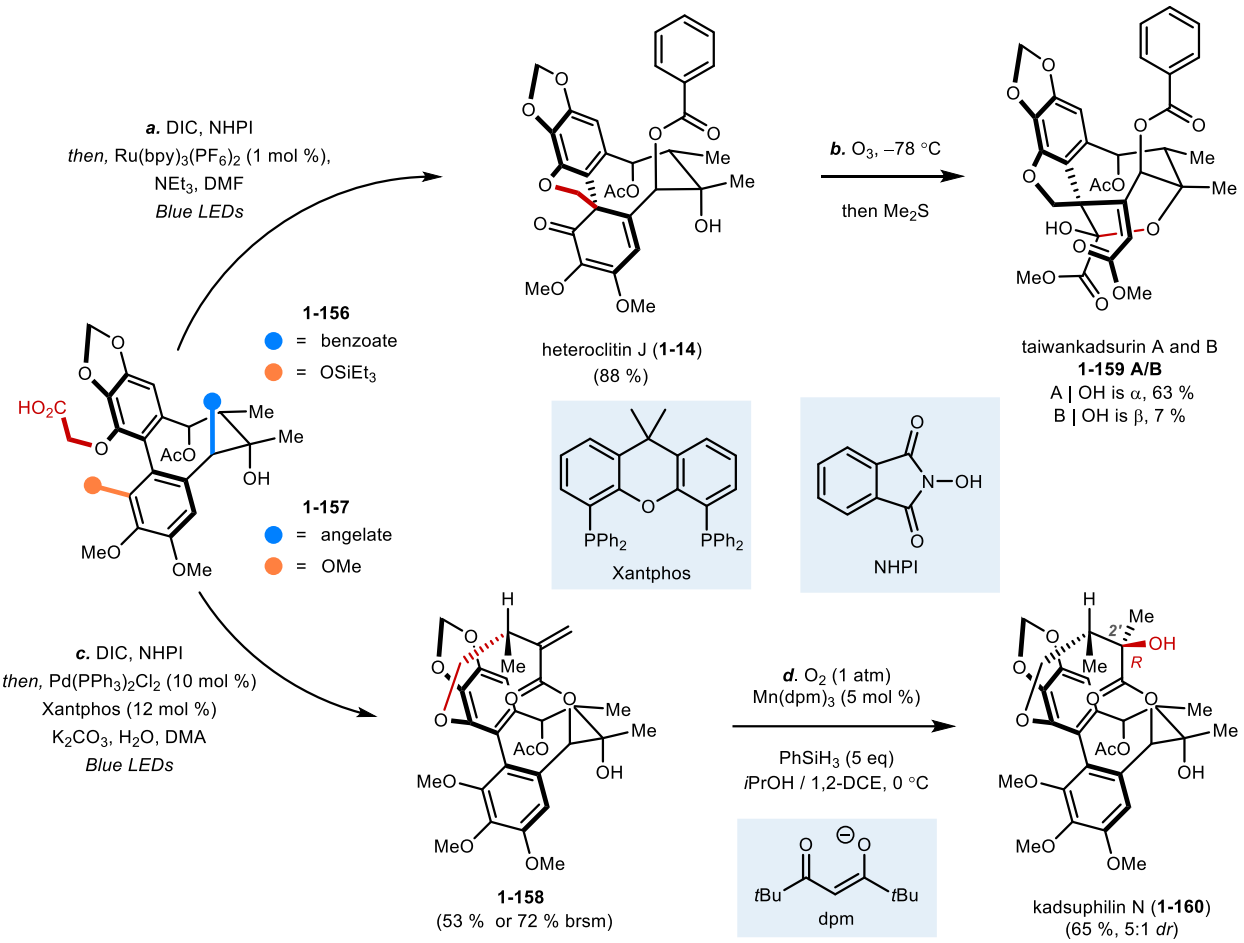
also preferentially hydrogenated on the more exposed β-face (with 8:1 *dr*). **1-153** contains four contiguous stereocentres and serves as an intermediate in the synthesis of bis-oxygenated DBCODs (−)-interiotherin C and (−)-ananolignans B, C, D, and F. Compound **1-152** was also used to prepare **1-155**, an intermediate in the syntheses of tri-oxygenated DBCODs kadsuralignan B, tiegusanin D, and schizanrin F (Scheme 1.21B). **1-152** was subjected to osmylation conditions, where reaction occurred at the more accessible C7 alkene, giving the diol. Exposure to $NaIO_4$ led to oxidation of the diol to ketone **1-154** (55 % over two steps), which was treated with catalytic hydrogenation conditions to stereoselectively reduce the C8 alkene (10:1 *dr*). Finally, addition of methyl lithium provided the desired tertiary alcohol at C7 (**1-155**, 81 % over two steps).



Scheme 1.21. A) Stereoselective olefin reduction to form the cycloctadiene ring with four contiguous stereocentres in the synthesis of bis-oxygenated DBCODs; B) formation of the C7 tertiary alcohol in the synthesis of tri-oxygenated DBCODs (RajanBabu 2013)

In the first reported synthesis of stage 3 DBCODs, Lumb prepared heteroclitin J and taiwanschirins A/B from the tri-oxygenated stage 2 DBCOD **1-156** and kadsuphilin N from **1-157** (Scheme 1.22).[1] In both cases, the first step was formation of the NHPI ester radical progenitor from the carboxylic acid. The NHPI ester of **1-156** was then treated with Overman's photocatalytic conditions using $Ru(bpy)_3(PF_6)_2$, triethylamine, and blue light, where a 5-*exo*-*trig* radical cyclization gives the

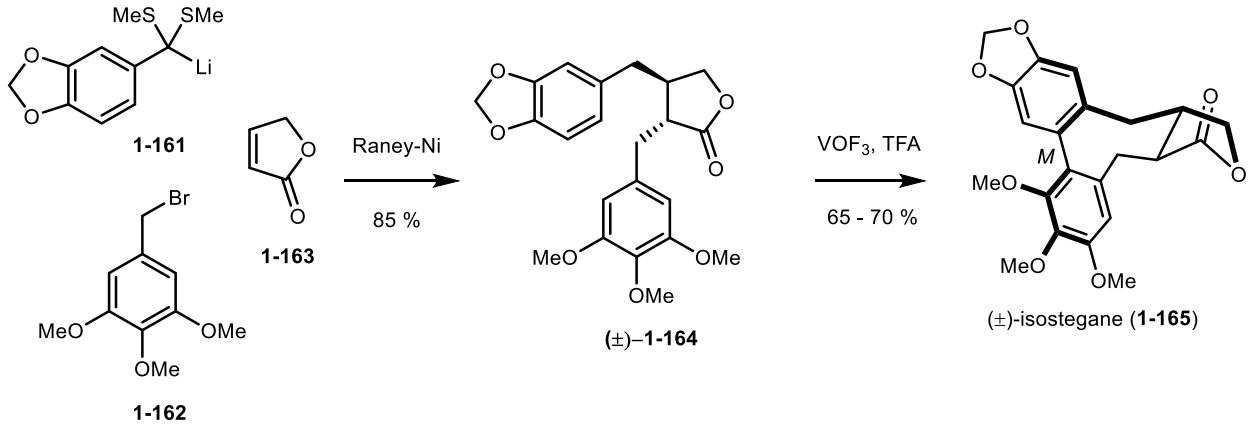
ortho-spirodienone heteroclitin J (**1-14**, 88 %). Compound **1-14** could be further converted into taiwanschirins A/B (63 % A, 7 % B) by ozonolysis of the C2-C3 bond, then intramolecular attack of the tertiary alcohol onto the C1 ketone. The NHPI ester of **1-157** was treated with Fu's photocatalytic conditions employing $Pd(PPh_3)_2Cl_2$, Xantphos and blue light, leading to radical cyclization onto the C6 angelate group, creating an 11-membered macrocycle **1-158** (53 % or 70 % brsm). $Mn(dpm)_3$-catalyzed Mukaiyama hydration was then used to convert the exocyclic alkene into the C2' tertiary alcohol, giving kadsuphilin N (65 %, 5:1 *dr*).



Scheme 1.22. Mimcry of non-canonical oxidations: **a.** spirocyclization to give heteroclitin J; **b.** oxidative cleavage / cyclization to give taiwankadsurins A and B; **c.** macrocyclization; **d.** Mukaiyama hydration to give kadsuphilin N (Lumb 2021)

1.6.7. Selected linear syntheses

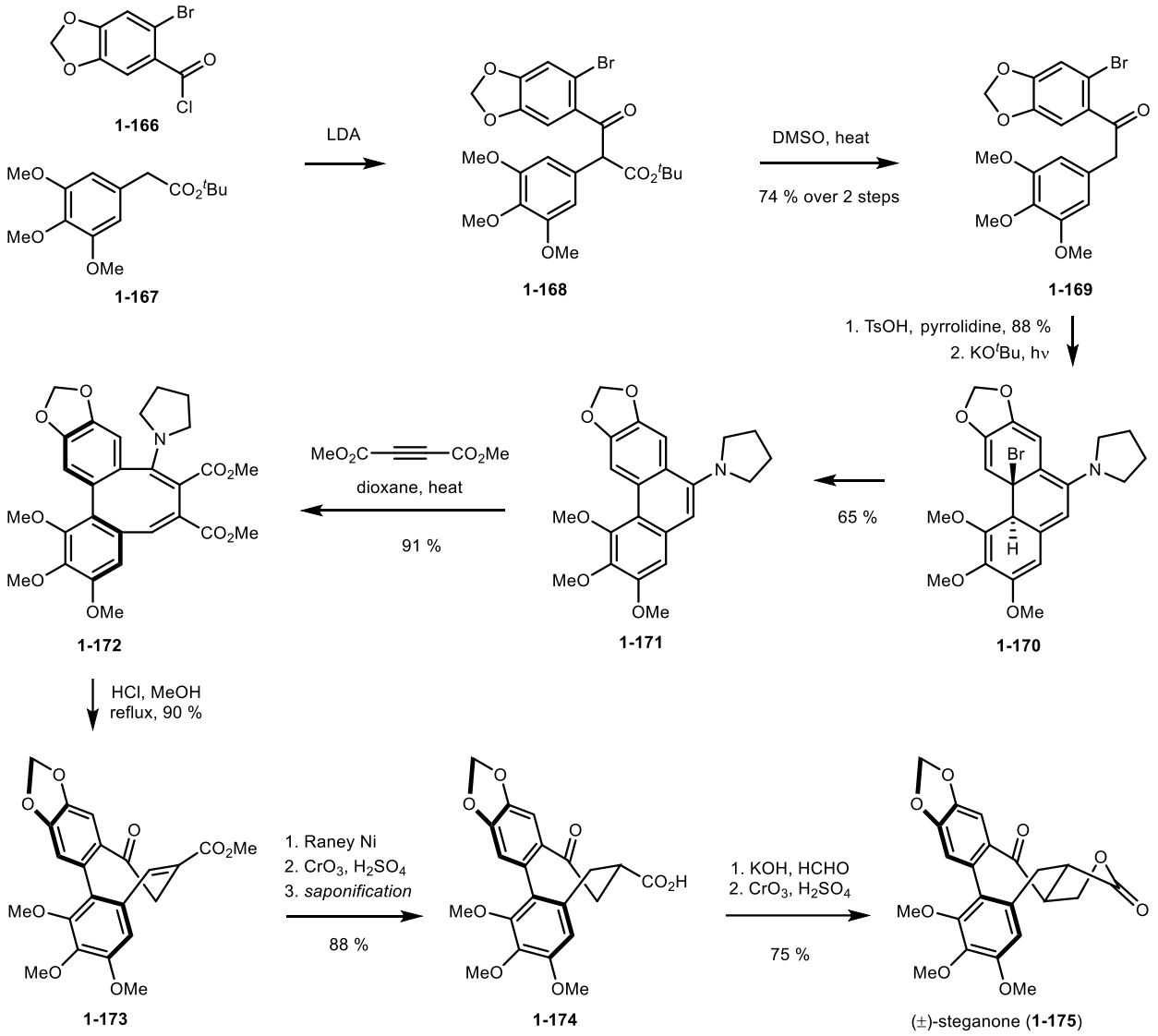
In this section, some distinguished DBCOD total syntheses have been selected for analysis in detail. One of the first three DBCOD syntheses reported in 1976, that of (±)-isostegane, was accomplished in just three steps by the Schlessinger group (Scheme 1.23).[81] The first step was a three component coupling, where alkyl lithium **1-161** underwent conjugate addition to α,β-unsaturated ketone **1-163** which then underwent alkylation with benzyl bromide **1-162**. In the second step, Raney Nickel was added to the crude reaction mixture to remove sulfur at C9, giving **(±)-1-164** in an 85 % yield. Oxidative coupling mediated by VOF_3 was used to form the biaryl linkage, resulting in (±)-isostegane (**1-165**) in yields of 65–70 %.



Scheme 1.23. A short synthesis of (±)-isostegane (Schlessinger 1976)

Raphael's 11-step synthesis of (±)-steganone, featuring a ring expansion strategy, was also published in 1976 (Scheme 1.24).[82] The initial two-carbon alkyl linkage was formed by enolization of *tert*-butyl 3,4,5-trimethoxyphenylacetate **1-167** using LDA and subsequent attack onto acyl chloride **1-166**, thus giving **1-168**. Heating **1-168** in DMSO led to hydrolysis of the ester, followed by decarboxylation, yielding **1-169** in 74 % over 2 steps. Condensation of ketone **1-169** with pyrrolidine gave the corresponding (*E*)-enamine, which was then combined with a suspension of potassium *tert*-butoxide in ammonia and subjected to irradiation from a mercury lamp. A conrotatory 6-π electrocyclization ensued, followed by elimination of HBr from the presumed intermediate **1-170** to give **1-171** in 65 % yield. Heating the 6-membered **1-171** with dimethyl acetylenedicarboxylate led to a formal 2+2 reaction, providing the ring-expanded product **1-172** in 91 % yield. Refluxing **1-172** in methanolic HCl led to cleavage of the pyrrolidine moiety as well as hydrolysis and decarboxylation of the C9 ester, yielding the unsaturated ketoester **1-173** in 90 %. Catalytic hydrogenation with Raney nickel, followed by Jones oxidation gave the saturated

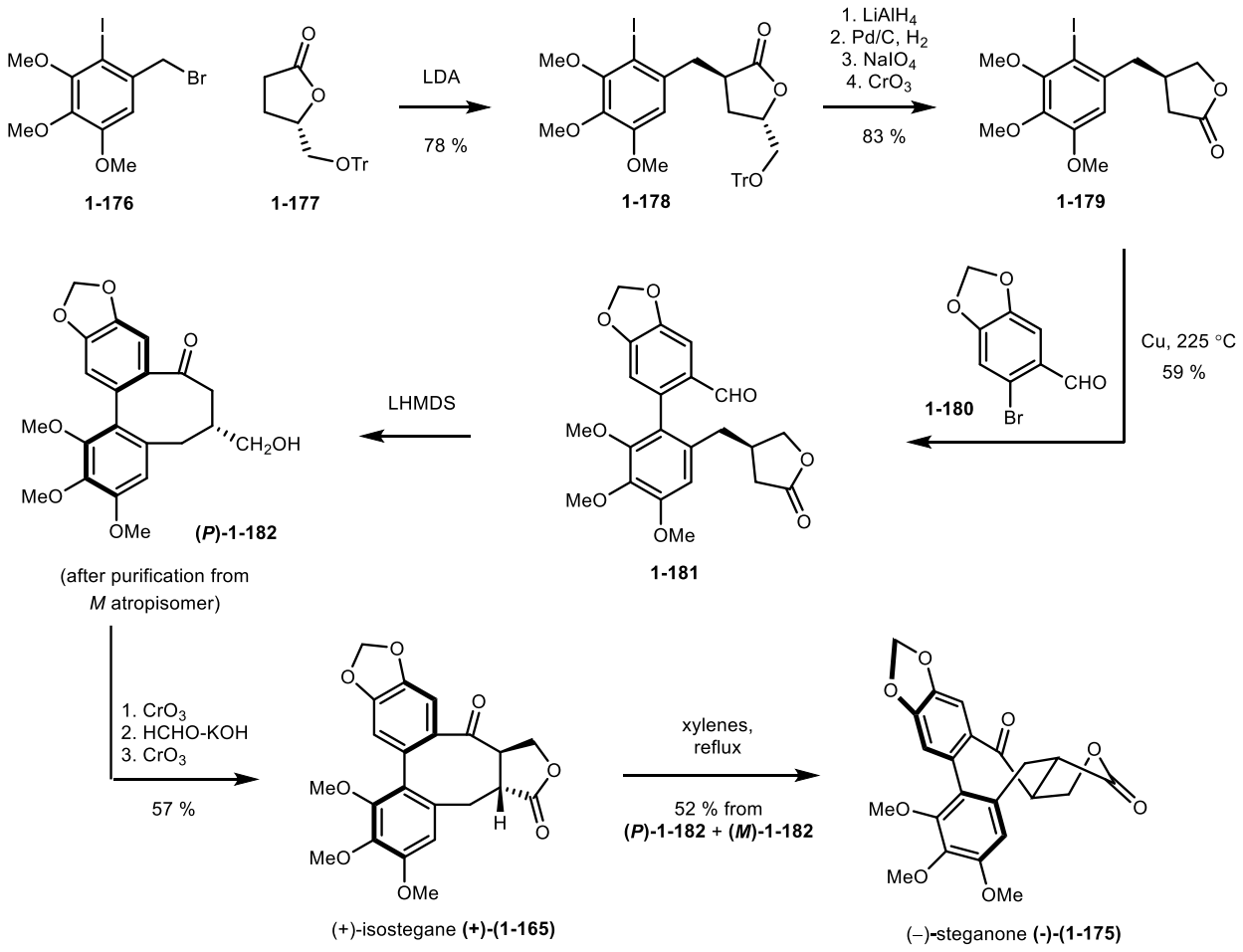
ketoester which was then treated with base to yield the ketoacid **1-174** (88 %). An aldol reaction between the potassium enolate of **1-174** and formaldehyde was followed by Jones oxidation and lactonization, providing (±)-steganone (**1-175**) in 75 % yield.



Scheme 1.24. A synthesis of (±)-steganone featuring 6-π electrocyclization (Raphael 1976)

The first asymmetric synthesis of a DBCOD was that of (−)-steganone, reported by Robin in 1980 (Scheme 1.25).[85] Optically active lactone **1-177** was converted to the lithium enolate which then participated in an alkylation reaction with benzyl bromide **1-176**, stereoselectively giving **1-178** in 78 % yield. The lactone of **1-178** was opened using $LiAlH_4$ and the trityl group deprotected using Pd-catalyzed hydrogenation to give a triol. Oxidative cleavage by $NaIO_4$ followed by lactonization

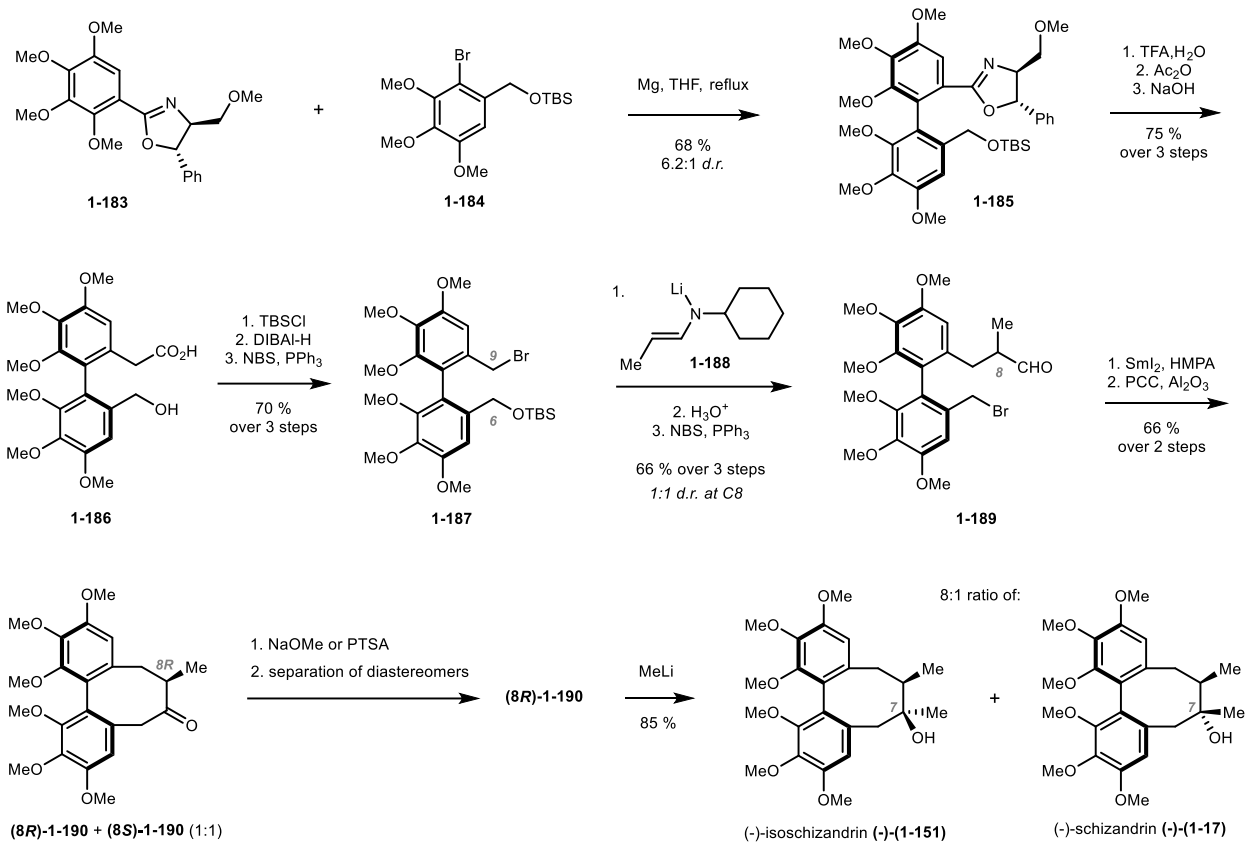
and Jones oxidation provided **1-179** in 83 % yield over four steps. Ullmann coupling of aryl iodide **1-179** with aryl bromide **1-180** generated the biaryl **1-181** in 59 % yield. An intramolecular aldol coupling proceeding via the lithium enolate was then implemented to close the 8-membered ring, giving two atropisomeric products, **(*M*)-1-182** and **(*P*)-1-182**. The desired atropisomer **(*P*)-1-182** was isolated by column chromatography and then subjected to Jones oxidation, giving the carboxylic acid at C7. This was followed by aldol reaction with formaldehyde, lactonization, and Jones oxidation to provide (+)-isostegane **(+)-1-165** in 57 % yield over three steps. Thermal isomerization of **(+)-1-165** could be accomplished by refluxing in xylenes to give (−)-steganone **(−)-1-175** (in 52 % yield over four steps).



Scheme 1.25. The first asymmetric DBCOD synthesis: (−)-steganone (Robin 1980)

Meyers' 1990 synthesis[95] of (−)-isoschizandrin and (−)-schizandrin includes the use of a chiral oxazoline auxiliary to impart atropselectivity during the biaryl bond formation step, a technique

which has been widely applied in DBCOD synthesis since Meyers' seminal report[87] in 1987 (Scheme 1.26). The biaryl coupling occured between the auxiliary-bearing tetramethoxybenzene **1-183** and the Grignard reagent formed from aryl bromide **1-184**. The reaction was proposed to proceed via an addition-elimination mechanism, where the chelate-controlled addition is

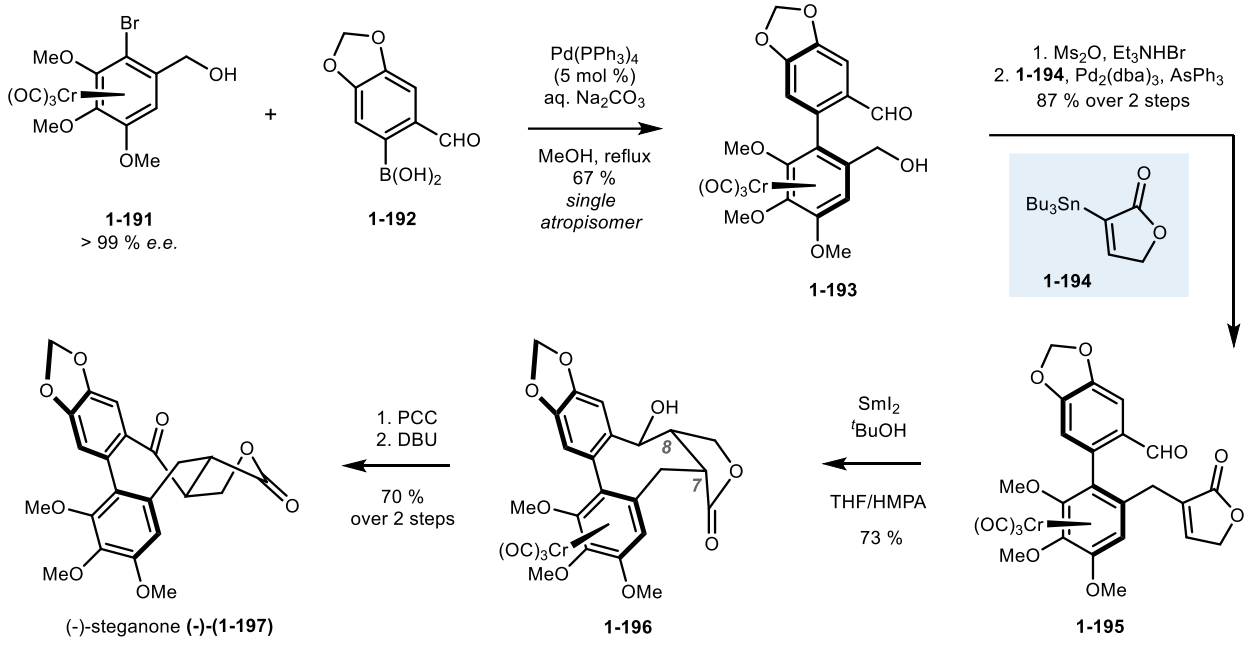


Scheme 1.26. Synthesis of (−)-schizandrin and (−)-isoschizandrin featuring a chiral oxazoline to impart atropselectivity (Meyers 1990)

stereoselective. The orientation of the *ortho* substituents conferred stereochemistry to the biaryl axis, giving **1-185** in 6.2:1 *dr* (68 %). Treatment with TFA opened the oxazoline to give the ester, however it also deprotected the silyl ether. The product was diacetylated and then both esters were saponified under basic conditions yielding **1-186** in 75 %. The C6 alcohol was reprotected using TBSCl and the carboxylic acid was reduced to the alcohol with DIBALH. Substitution using PPh_3 and NBS gave the primary bromide **1-187** in 70 % over three steps. The carbon chain was then extended via alkylation between the bromide **1-187** and lithium enamide **1-188**, which after aqueous acid workup gave the aldehyde. The TBS group was also deprotected upon exposure to

acid, giving the alcohol, which reacted with PPh_3 and NBS in the next step to provide the primary bromide **1-189** in 66 % with 1:1 *dr* at C8. Intramolecular cross-coupling between the acyl radical and the alkyl bromide was mediated by SmI_2 in THF/HMPA and followed by oxidation with PCC on alumina to give the cyclic ketone **1-190** in 66 % with 1:1 *dr* at C8. The ratio of diastereomers could be altered by treatment with acid or base where it reached an equilibrium at 7:3 **(8*S*)-1-190**: **(8*R*)- 1-190**. The diastereomers were then separated and each subjected to methyllithium to furnish the tertiary alcohol at C7. Surprisingly, (−)-isoschizandrin matching the natural sample (85 % yield, in an 8:1 ratio with (−)-schizandrin) was formed from **(8*R*)- 1-190** rather than **(8*S*)-1-190**, which led to structural reassignment of (−)-isoschizandrin.

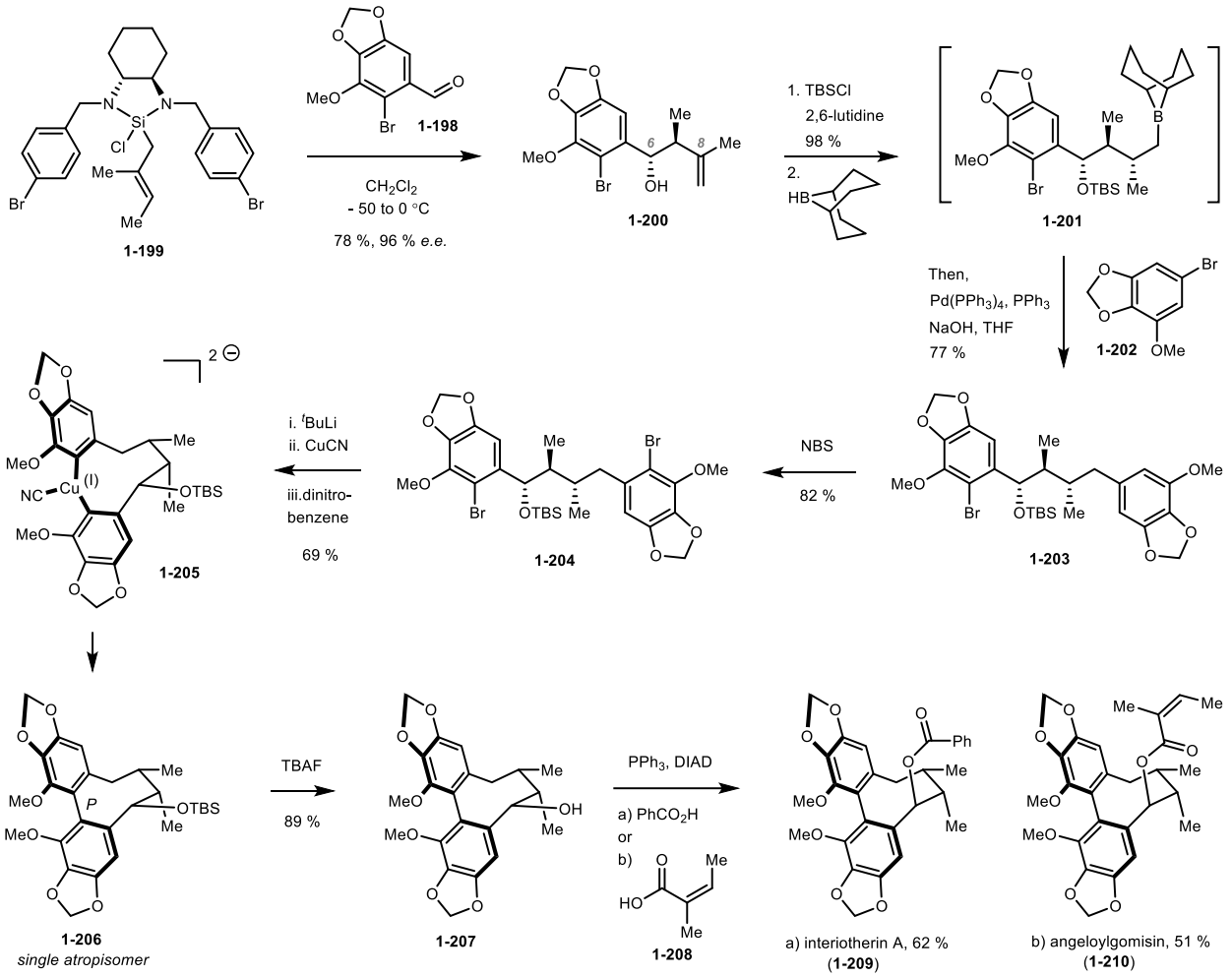
Molander's 2000 synthesis of (−)-steganone features several interesting steps, the first of which is an atroposelective Suzuki coupling between an aryl boronic acid **1-192** and an aryl bromide bearing a chiral chromium auxiliary **1-191** (Scheme 1.27).[89] The chirality from the chromium auxiliary was transferred to the biaryl axis during the coupling, forming **1-193** as a single atropisomer in 67 % yield. The alcohol was converted to the corresponding bromide by treatment with methanesulfonic anhydride followed by triethylamine hydrobromide. The bromide was then subjected to Stille coupling with vinylstannane **1-194** to give butanolide **1-195** in 87 % over two



Scheme 1.27. Synthesis of (−)-steganone featuring SmI_2-mediated ketyl-olefin cyclization (Molander 2000)

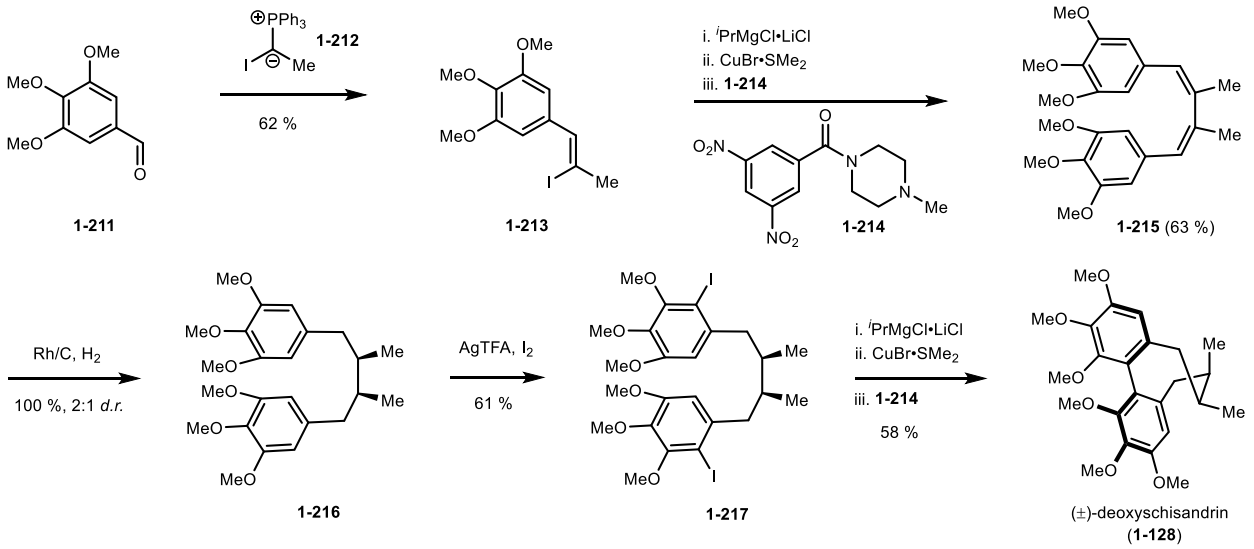
steps. They then implemented the unprecedented use of SmI_2-mediated ketyl-olefin coupling to form an 8-5 ring system. The oxygen of the reacting ketyl sits pseudoequatorially and the C8 stereocenter was set by attack on the α-face of the butenolide. The C7 stereocenter was set by protonation (by *t*BuOH) of the convex side (β-face) of the samarium enolate, yielding the tricarbonyl chromium complex of isopicrosteganol as a single diastereomer (**1-196**, 73 %). Treatment with PCC cleaved off the chromium auxiliary as well as oxidizing the secondary alcohol to the corresponding ketone. Next, the substrate was refluxed with DBU in THF to isomerize the lactone from *cis* to *trans*, giving (−)-steganone **(−)-(1-197)** in 70 % over two steps.

Coleman's 2005 total synthesis of interiotherin A and angeloylgomisin also features a variety of unique methodologies (Scheme 1.28).[28,90] It began with the asymmetric crotylation of aryl aldehyde **1-198** using a chiral tiglylsilane **1-199**. This step installed the alkyl chain from C6 to C8 as well as setting two stereocentres with full diastereoselectivity and 96 % *ee*. The (6S,7S)-*anti* product **1-200** was obtained in 76 % yield after TBS protection. Alkene **1-200** was then submitted to hydroboration with 9-BBN which proceeded with full diastereofacial selectivity. The resulting intermediate borane **1-201** was subjected to Suzuki coupling *in situ* with aryl bromide **1-202**, giving **1-203** in 77 % yield. **1-203** was regioselectively brominated at C15 using NBS, providing **1-204** in 82 % yield. Treating **1-204** with *tert*-butyllithium gave the diaryllithium which then underwent transmetallation with CuCN to give **1-205**. This underwent oxidation by 1,3-dinitrobenzene, followed by reductive elimination forming the biaryl **1-206** as a single atropisomer in 69 % yield. Silyl deprotection of the C6 alcohol provided the common intermediate for both natural products, **1-207**, in 89 % yield. Mitsunobu reactions with the appropriate carboxylic acids were then applied to append the desired esters while inverting the C6 stereochemistry. The use of benzoic acid furnished interiotherin A (**1-209**) in 62 % yield while angelic acid **1-208** was employed to give angeloylgomisin (**1-210**) in 51 % yield.



Scheme 1.28. Synthesis of interiotherin A and angeloylgomisin (Coleman 2005)

Spring's 2012 synthesis of (±)-deoxyschisandrin features an organocuprate coupling reminiscent of Coleman's work to form the biaryl axis, as well as an organocuprate coupling to form the 8-membered ring (Scheme 1.29).[102] This concise synthesis started with a Stork-Wittig reaction of trimethoxybenzaldehyde **1-211** with iodo-ylide **1-212**, providing **1-213** exclusively as the *Z* diastereomer (62 %). Metalation with *tert*-butyllithium proved unproductive, however isopropyl magnesium chloride HCl salt could cleanly effect the I/Mg exchange. The resulting organomagnesium species underwent transmetallation with $CuBr{\cdot}SMe_2$, giving an anionic Cu(I) species which was then oxidized by **1-214** to the neutral Cu(I). Oxidative addition of a second molecule of **1-213** onto Cu(I) occured and the resulting Cu(III) species underwent reductive elimination, regenerating Cu(I) and releasing the homocoupled product **1-215**. Reduction of the 1,3-diene was catalyzed by Rh/C, giving **1-216** in a 2:1 mixture of inseparable diastereomers

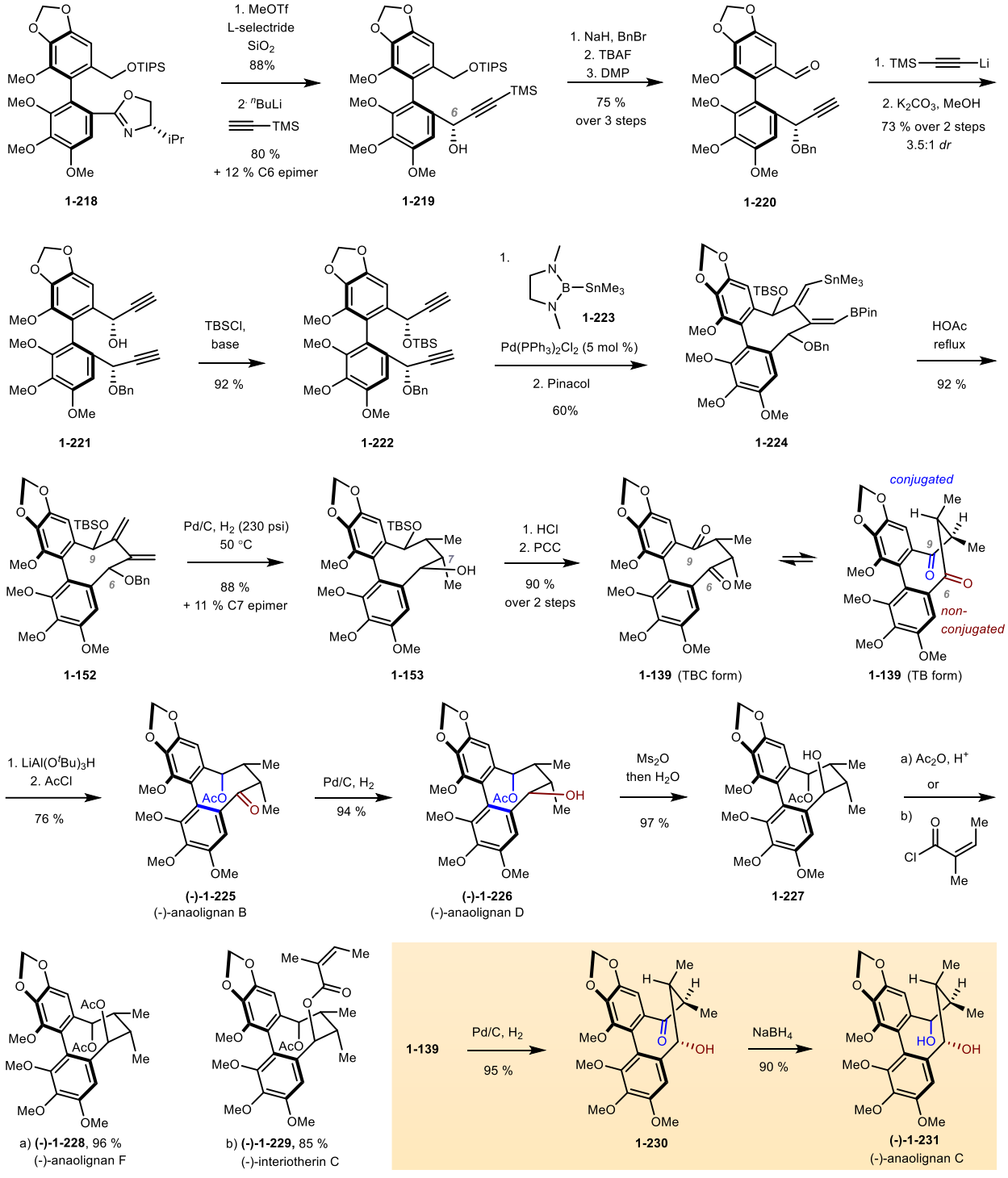


Scheme 1.29. Synthesis of (±)-deoxyschisandrin featuring double organocuprate oxidation (Spring 2012)

(100 %). Treatment with elemental iodine and silver triflate gave monoiodination of each aromatic ring. At this point, the diastereomers could be separated, yielding 61 % of the desired (*R, S*) diastereomer **1-217**. This diaryliodide was subjected to a second oxidative organocuprate coupling, using the same conditions as previously, to form the biaryl axis, giving (±)-deoxyschisandrin (**1-128**) in 58 %.

RajanBabu's preparation of (−)-interiotherin C, (−)-ananolignans B, C, D, and F, tiegusanin D, kadsuralignan B, and schizandrin F in 2013 represents the first report of polyoxygenated stage 2 DBCOD syntheses.[131,132] The oxygenation at C6 and C9 was installed early in the synthesis and these positions were manipulated later to give the desired stereochemistry and esterification pattern. This report includes the novel methodology of bis-metallative cyclization mediated by a [BSn] reagent to close the 8-membered ring. The synthesis began from **1-218** (Scheme 1.30) which was prepared using Meyers' fragment coupling between an chiral oxazoline auxiliary-bearing arene and an aryl Grignard reagent to give the chiral biaryl axis.[91] The oxazoline auxiliary was then deprotected to reveal the aldehyde (88 %), which was subjected to alkynylation by lithium (trimethylsilyl)acetylide (generated *in situ*) to give **1-219** in an 80 % yield along with 12 % of the C6 epimer. **1-219** was then subjected to removal of the TMS ether and benzyl protection of the free alcohol, followed by deprotection of the TIPS ether, and then oxidation of the primary alcohol to the aldehyde, providing **1-220** (75 % over 3 steps). A second alkynylation followed by removal

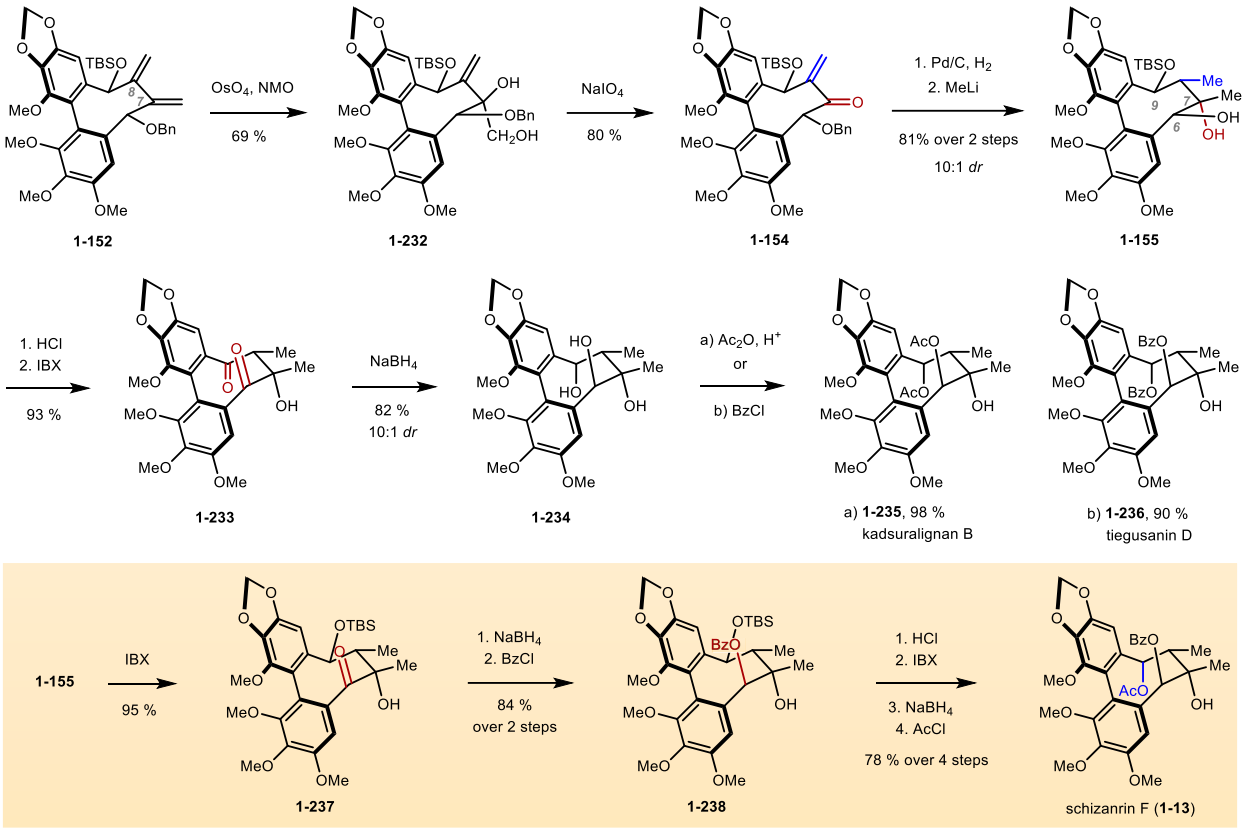
of TMS gave the di-propargyl **1-221** in 73 % yield with 3.5:1 *dr*.[131] The free alcohol was protected with a TBS group prior to subjecting to bis-metallative cyclization. The resulting **1-222** was



Scheme 1.30. Synthesis of bis-oxygenated DBCODs (−)-interiotherin C and (−)-ananolignans B, C, D, and F (RajanBabu 2012–2013)

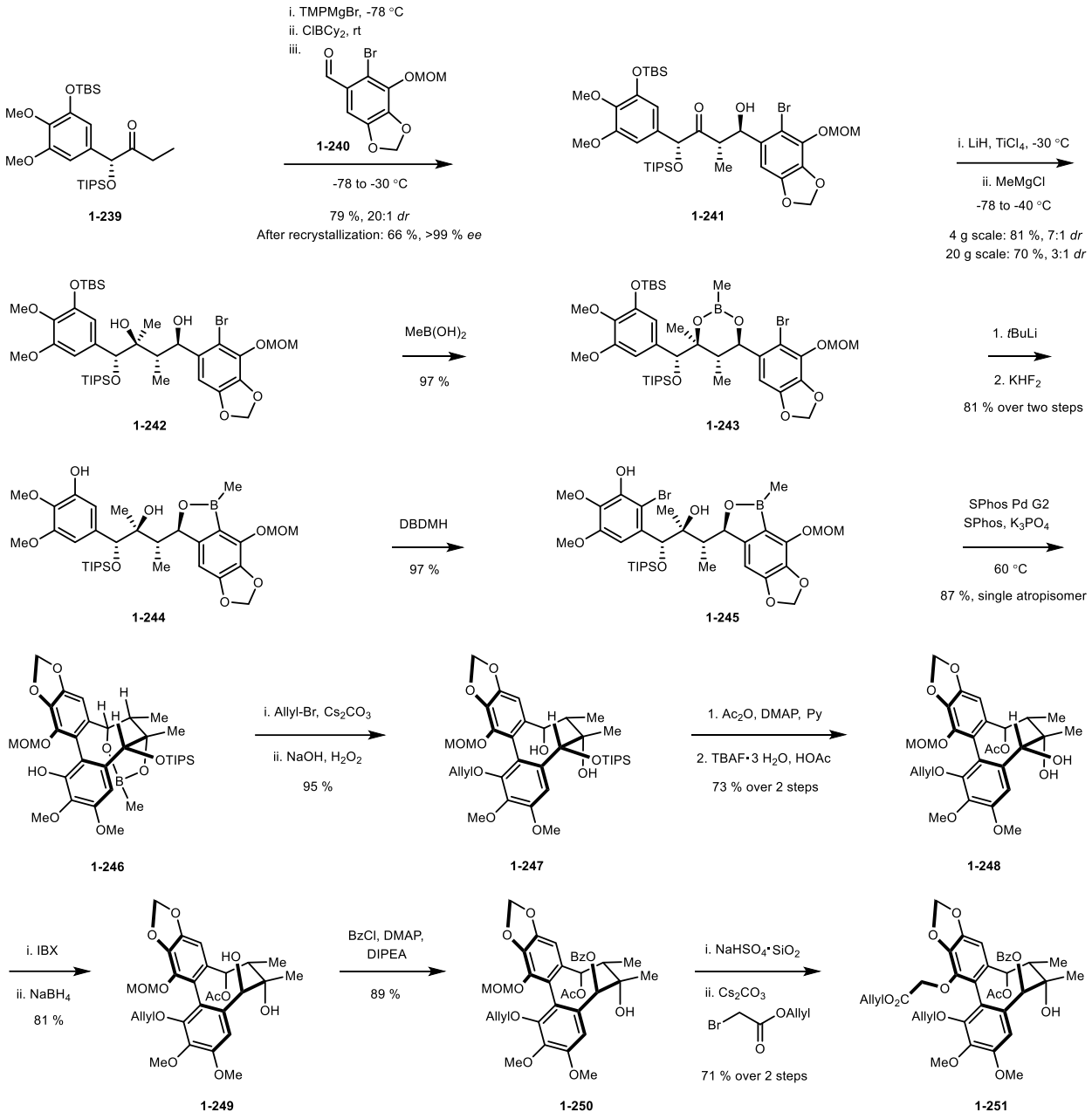
subjected to 1-trimethylstannyl-2,5-dimethyl-2,5-diazaborolidine (**1-223**) and catalytic $(Ph_3P)_2PdCl_2$ to give the boryl stannylation product, which was immediately converted to the BPin derivative for ease of isolation (**1-224**, 60 %). Treatment of **1-224** with refluxing acetic acid yielded the bis-methylene product **1-152** (92 %). To give the bis-oxygenated DBCODs, the C6 and C9 alcohols were deprotected and then oxidized to their respective ketones by treatment with Pd/C and H_2, followed by HCl, and then PCC, providing **1-139** (79 % over 3 steps).[131] **1-139** has been previously prepared by Ghera in his synthesis of kadsurin.[84] In this study, he developed conditions for the selective reduction of the ketone at C9 or C6 (using $LiAlH(OtBu)_3$ or Pd/C, H_2). RajanBabu reduced the C9 ketone of **1-139** using Ghera's methodology, followed by acetylation to give (−)-ananolignan B in a 76 % yield. A second reduction at C6 furnished (−)-ananolignan D **(−)-(1-226)** in a 94 % yield. **(−)-(1-226)** was then treated with methanesulfonic anhydride and water to epimerize the C6 alcohol, providing **1-227** (97 %). Treatment of **1-227** with acetic anhydride under acidic conditions gave (−)-ananolignan F (96 %) or with angelic chloride gave (−)-interiotherin C (85 %). Alternatively, the C6 ketone of intermediate **1-139** could be reduced using Ghera's conditions to give **1-230** (95 %), followed by reduction of C9 using $NaBH_4$ to give the diol (−)-ananolignan C (90 %).

For the synthesis of tris-oxygenated DBCODs, bis-methylene **1-152** was subjected to OsO_4, which reacted with the more accessible alkene at C7 to give diol **1-232** in 69 % yield (Scheme 1.31). Subsequent oxidation with $NaIO_4$ gave the C7 ketone **1-154** (80 %). The C8 methylene was then hydrogenated using catalytic Pd/C, proceeding with 10:1 *dr*, followed by methylation of the C7 ketone to give the tertiary alcohol in the desired stereochemistry (**1-155**, 81 % yield over 2 steps). Silyl deprotection under acidic conditions gave the C6, C9-diequatorial diol which was epimerized to the diaxial diol **1-234** by IBX oxidation followed by reduction with $NaBH_4$ (76 % yield over 3 steps, 10:1 *dr*). Treatment of **1-234** with acetic anhydride under acidic conditions provided kadsuralignan B (98 %), whereas treatment with benzoyl chloride gave tiegusanin D (90 %). Intermediate **1-155** was also used in the synthesis of schizandrin F (**1-13**), where C6 was epimerized by treatment with IBX followed by $NaBH_4$ and then benzoylated to give **1-238** in 80 % yield over 3 steps. The desired ester functionality at C9 was introduced to by silyl deprotection of the C9 alcohol, epimerization (via oxidation/ reduction sequence), and then acetylation to provide **1-13** in 78 % over 4 steps.[131]



Scheme 1.31. Synthesis of tris-oxygenated DBCODs tiegusanin D, kadsuralignan B, and schizandrin F (RajanBabu 2013)

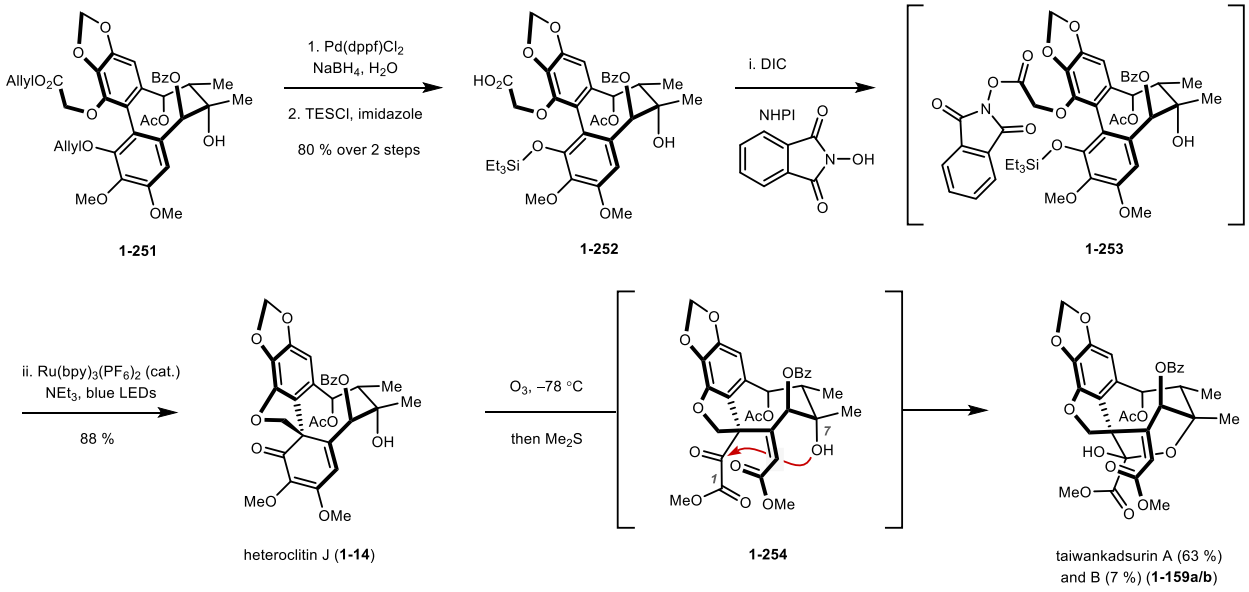
The first syntheses of stage 3 DBCODs (heteroclitin J, taiwanschirins A/B, kadsulignan E, and kadsuphilin N) was reported by our group in 2021.[1] These syntheses feature an unprecedented atroposelective intramolecular Suzuki coupling to form the biaryl bond. Redox neutral photocatalysis methodologies were used to mimic biosynthetic non-canonical oxidations, leading to the conversion of stage 2 to stage 3 DBCODs via cyclization reactions. The asymmetric synthesis of heteroclitin J began with the aldol addition of ketone **1-239** to aldehyde **1-240**, furnishing aldol **1-241**, containing three stereocenters, in a 79 % yield and 20:1 *dr* (Scheme 1.32). Upon recrystallization, an *ee* of > 99 % was obtained as determined by chiral HPLC, with the yield dropping to 66 %. Chelation of the ketone using LiH and $TiCl_4$ was followed by addition of MeMgCl to set the fourth stereocenter, providing **1-242** with an 81 % yield in 7:1 *dr* on a 4 g scale (or 70 % with 3:1 dr on a 20 g scale). Treatment of **1-242** with methylboronic acid converted the diol to the 6-membered boronic ester **1-243** in 97 % yield. Treatment of **1-243** with *tert*-butyllithium led to lithium-halogen exchange then intramolecular attack of the aryllithium onto



Scheme 1.32. Synthesis of stage 3 DBCODs heteroclitin J and taiwankadsurins A/B (part 1) (Lumb 2021)

the boronic ester, giving the 5-membered borinic ester. This was followed by silyl deprotection of the phenol using KHF_2 to provide **1-244** in 81 % yield over two steps. *Ortho*-bromination of the phenol using dibromodimethylhydantoin provided **1-245** as a single regioisomer in 97 % yield. Compound **1-245** was subjected to SPhos Pd G2, SPhos, and K_3PO_4 in an intramolecular Suzuki coupling to provide **1-246** as a single atropisomer in 87 % yield. **1-246** was treated with allyl

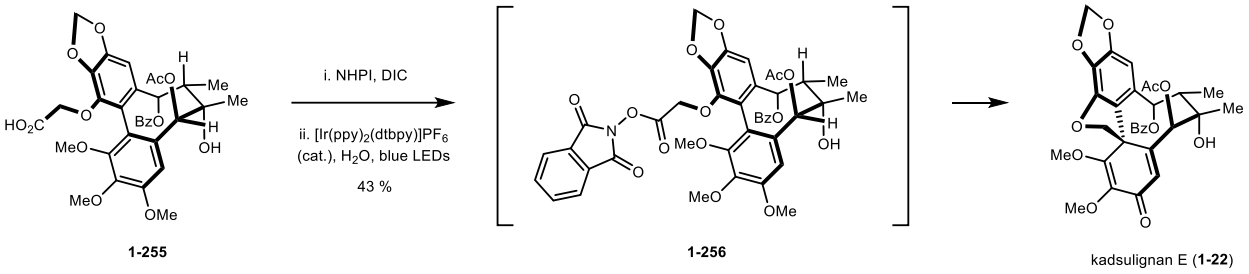
bromide and cesium carbonate followed by sodium hydroxide and hydrogen peroxide to install an allyl protecting group on the phenol and then hydrolyze the boronic ester, providing **1-247** in a 95 % yield over two steps. Acetylation of the C9 secondary alcohol was followed by silyl deprotection of the C6 alcohol, furnishing **1-248** in a 73 % yield. The equatorial C6 alcohol was epimerized to the axial position by IBX oxidation to the ketone, followed by regioselective reduction by $NaBH_4$ to give **1-249** in 81 % yield. The axial C6 alcohol was then benzoylated to provide **1-250** in an 89 % yield. Deprotection of the phenolic MOM group was followed by *O*-alkylation with allyl bromoacetate to furnish **1-251** in a 71 % yield. Dual allyl deprotection of **1-251** was accomplished using $Pd(dppf)Cl_2$ and $NaBH_4$, followed by triethylsilyl protection of the phenol to give **1-252** in an 80 % yield over two steps (Scheme 1.33). The *N*-hydroxyphthalimide (NHPI) redox-active ester of carboxylic acid **1-252** was generated *in situ* and treated with catalytic $Ru(bpy)_3(PF_6)_2$ and triethylamine under blue light irradiation to initiate cyclization to the *ortho*-spirodienone heteroclitin J (**1-14**) in 88 % yield. **1-14** could be further converted to another DBCOD product by ozonolysis, which cleaved the C2-C3 double bond to the keto-diester, followed by intramolecular attack of the C7 alcohol onto C1, giving macrocyclic taiwankadsurins A/B (63% A and 7% B).



Scheme 1.33. Synthesis of stage 3 DBCODs heteroclitin J and taiwankadsurins A/B (part 2) (Lumb 2021)

The *para*-spirodienone DBCOD kadsulignan E (**1-22**) was prepared divergently from the same route as **1-14**. **1-247** serves as a common intermediate, used to prepare **1-255** in an analogous

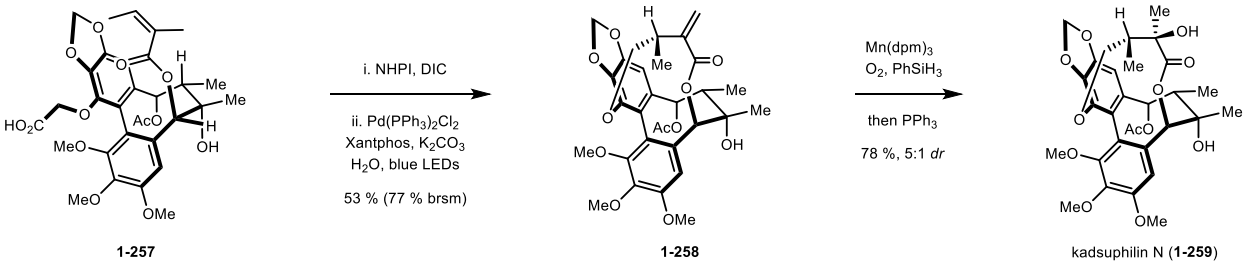
manner to the synthesis of **1-252**. In **1-255**, the positions of the acetate and benzoate have been swapped compared to **1-252** and C1 bears a methoxy group rather than $OSiEt_3$. The NHPI ester of **1-255** was generated *in situ* and then treated with catalytic $Ir(ppy)_2(dtbpy)PF_6$ and water under



Scheme 1.34. Synthesis of stage 3 DBCOD kadsulignan E (Lumb 2021)

blue light irradiation to provide the *para*-spirodienone **1-22** in 43 % yield (Scheme 1.34).

The macrocyclic DBCOD kadsuphilin N was also prepared from the intermediate **1-247**. In this case, an angelate was installed at C6, an acetate at C9, and a methoxy at C1 to provide **1-257**. The NHPI ester of **1-257** was generated *in situ*, followed by treatment with catalytic $Pd(PPh_3)Cl_2$, XantPhos, K_2CO_3 under blue light irradiation to give the 11-*exo-trig* product **1-258** (Scheme 1.35). Mukaiyama hydration of the exocyclic alkene using $Mn(dpm)_3$ and $PhSiH_3$ under O_2 followed by PPh_3 provided the natural product kadsuphilin N in 78 % yield and 5:1 *dr*.

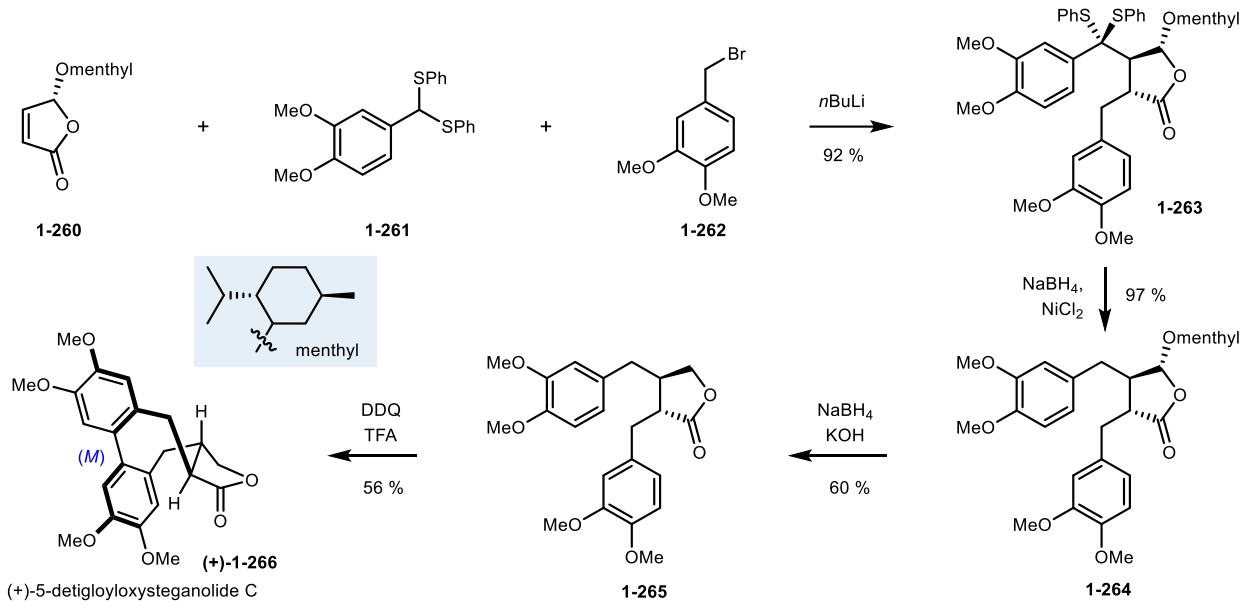


Scheme 1.35. Synthesis of stage 3 DBCOD kadsuphilin N (Lumb 2021)

1.6.8. Progress toward DBCODs

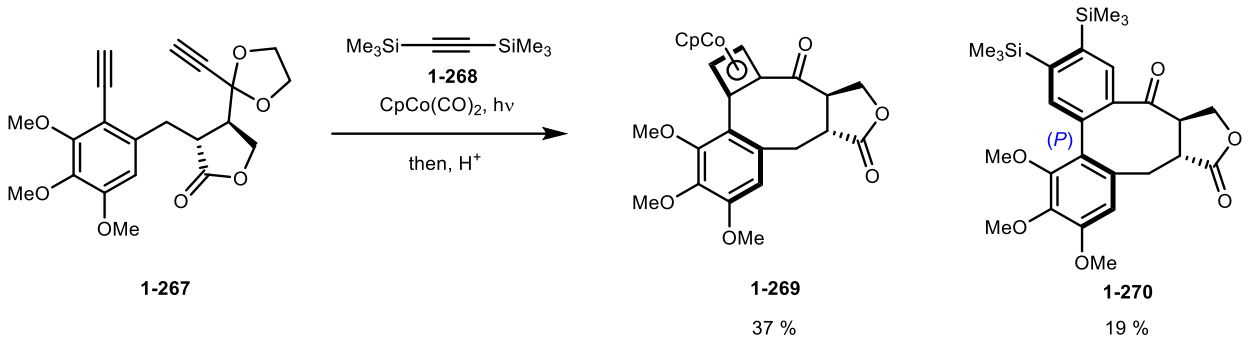
This section features the syntheses of non-natural DBCOD-like molecules as well as some partial syntheses of DBCODs. The methodologies within these syntheses have the potential to be utilized in the synthesis of natural DBCODs and analogues. Pelter and Ward prepared the DBCOD derivative (+)-5-detigloyloxy-steganolide C in four steps (Scheme 1.36).[133] The first step was a three-component coupling utilizing Schlessinger's conditions (see Scheme 1.23), which set two

stereocentres. Thioacetal **1-261** was treated with *n*BuLi to give the alkyl lithium, which underwent conjugate addition to chiral α,β-unsaturated ketone **1-260**, and then alkylation with benzyl bromide **1-262**, giving **1-263** in 92 % yield. Treatment with nickel boride (generated *in situ* from $NiCl_2$ and $NaBH_4$) led to the desulfurized product **1-264** in 97 % yield. The menthyloxy group was removed using sodium borohydride and potassium hydroxide to give **1-265** in 60 %. Oxidative cyclization to form the biaryl as the *M* atropisomer was then performed using DDQ and TFA, providing (+)-5-detigloyloxy-steganolide C in 56 %.



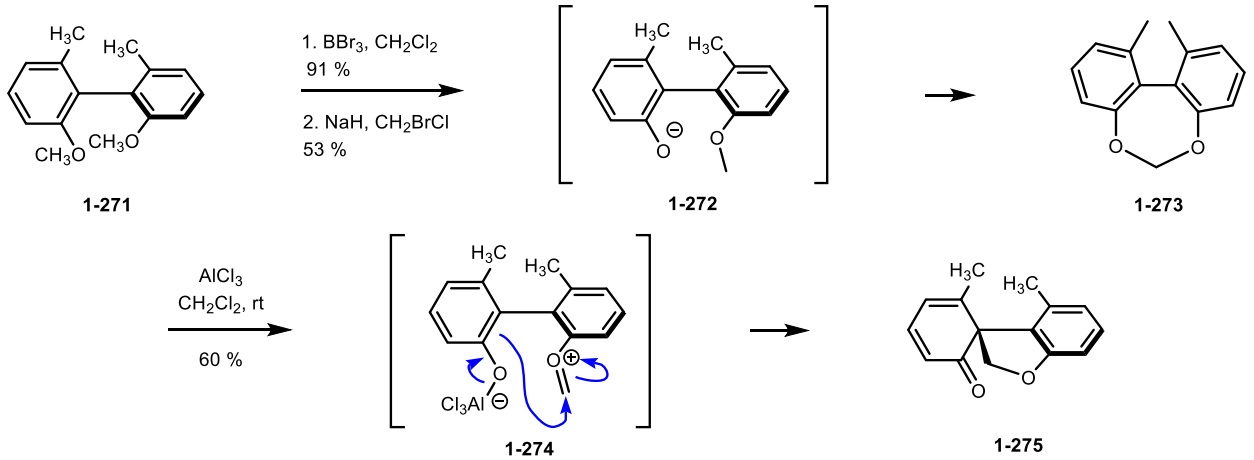
Scheme 1.36. Synthesis of (+)-5-detigloyloxy-steganolide C, a DBCOD derivative (Pelter and Ward 1992)

As the anticancer activity of steganone is well known, Motherwell was interested in a route to access analogues thereof for use in structure–activity relationship studies.[134] The tethered diyne **1-267** was convergently prepared in seven steps (four steps longest linear) from commercially available materials. Compound **1-267** was reacted in a light-induced [2+2+2] cobalt-mediated cycloaddition with acetylenic **1-268**, giving a mixture of two products after acidic workup: cobaltacyclobutadiene complex **1-269** (37 %) and the desired biaryl **1-270** (19 %) as the *P*-atropisomer (Scheme 1.37). Mono- or di-protodesilylation of **1-270** was feasible by treating with TFA. Although low–yielding, this methodology demonstrated the first instance of constructing a DBCOD core using [2+2+2] cycloaddition.



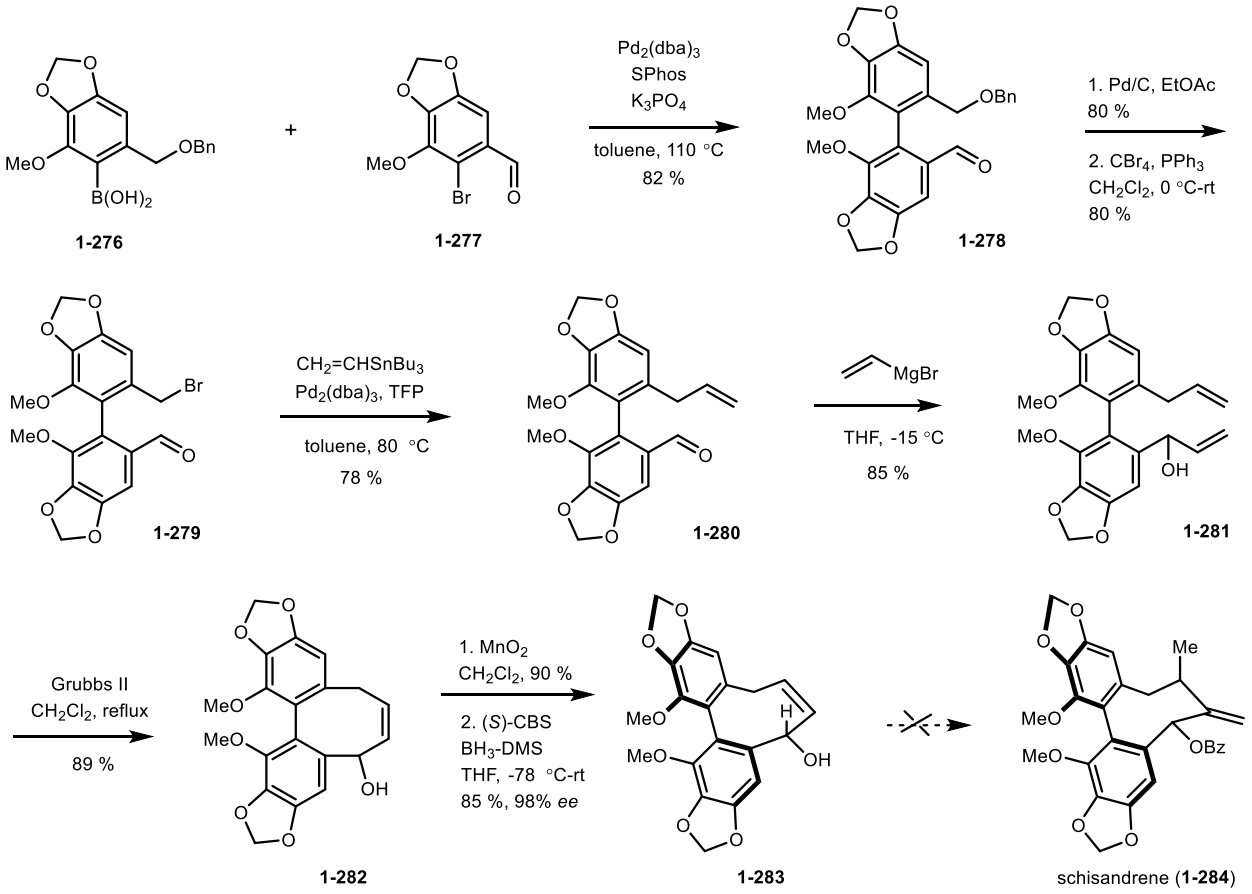
Scheme 1.37. Cobalt-mediated [2+2+2] cycloaddition for the synthesis of steganone analogues (Motherwell 1999)

Coleman has studied the spirocyclic cyclohexadienone motif which is present in many stage 3 DBCODs on a simplified system (Scheme 1.38).[74] They attempted to mimic the ionic mechanism which they proposed for the spirocyclization (see Scheme 1.5) and found the reaction did not proceed as straightforwardly as expected. Treatment of biaryl **1-271** with BBr_3 led to deprotection of one methoxy group, which was followed by deprotonation using NaH to give the phenolate **1-272** (48 %). Rather than undergoing 5-*endo* cyclization to give spirodienone **1-275** as anticipated, a 7-*endo* cyclization occurred yielding benzodioxepin **1-273**. However, due to the reversibility of the *O*-alkylation and the irreversibility of the *C*-alkylation, it was possible to convert **1-273** to **1-275** in a subsequent step. Treatment of **1-273** with a Lewis acid, such as $AlCl_3$, gave the ring opened oxonium ion **1-274** which readily underwent 5-*endo-trig* cyclization providing the desired spirodienone **1-275** in 60 % yield. This provides a complimentary ionic method of forming spirodienones to Lumb's radical method.[1]



Scheme 1.38. Lewis acid-mediated spirocyclization (Coleman 2000)

Babu's group targeted schisandrene in an ultimately unsuccessful synthesis which demonstrated the first instance of forming the 8-membered ring via ring-closing metathesis (Scheme 1.39).[135] An aryl boronic acid **1-276** and an aryl bromide **1-277** were subjected to Suzuki coupling, producing biaryl **1-278** in 82 % yield. Deprotection of the benzyl ether using Pd/C (in 80 % yield) followed by Appel reaction with CBr_4 (80 %) gave the bromide **1-279**, which was immediately subjected to Stille coupling with CH_2=$CHSnBu_3$, providing the terminal alkene **1-280** (78 %). Grignard reaction of the aldehyde with vinyl magnesium bromide gave diene **1-281** in 85 %. **1-281** was subjected to Grubbs ring closing metathesis using the second-generation catalyst, with successful formation of the 8-membered ring (**1-282**, 89 %). Oxidation of the racemic alcohol (90 %) followed by Corey-Bakshi-Shibata reduction furnished the enantioenriched alcohol **1-283** (85 %, 98 % *ee*). The planned endgame from **1-283** to schisandrene involved Sharpless epoxidation of the alkene, epoxide opening with a methyl Grignard at C8, Wittig olefination at C7, and



Scheme 1.39. Partial synthesis of schisandrene featuring ring-closing metathesis (Babu 2018)

Yamaguchi esterification of the C6 alcohol. However, both Sharpless epoxidation and Jacobsen-Katsuki epoxidation were unsuccessful and it was proposed that the substrate was too sterically hindered for the reaction to occur, thus halting the synthesis at the stage of **1-283**.

1.7. Conclusions

DBCODs possess unique structures and a wide array of bioactivities. They contain a conformationally stable biaryl axis as well as an 8-membered ring, a motif which is uncommon in medicinal chemistry due to the difficulty of their synthesis. The oxidation pattern around the 8-membered ring is variable, leading to diverse structures. DBCODs can interconvert between the TB and TBC conformations at room temperature. The conformation becomes more rigid when the DBCOD is more highly oxidized. Certain trends in IR and NMR spectra can be used to predict which conformation the DBCOD prefers without requiring analysis by X-ray crystallography.

DBCODs are isolated from plants within the *Schisandracae* family which have a long history of use in traditional Chinese medicine. Among the many reported bioactivities of DBCODs, the most prevalent are antioxidant, antiviral, hepatoprotective, anticancer, neuroprotective, and cardiovascular protective activity. Their biosynthesis remains unknown, however it is presumed to be similar to the well reported aryltetralin lignan biosynthesis, starting from monolignol building blocks such as coniferyl alcohol. The DBCODs, especially the highly oxidized stage 3 DBCODs, have only been isolated in small quantities from the natural source. Chemical synthesis could prove a valuable tool as a means of providing enough material for in-depth biological studies and could also be used to prepare derivatives for the study of SAR. Of the 529 DBCODs isolated thus far, 44 have been synthesized. The synthesis of DBCODs includes several challenges such as setting the biaryl bond atroposelectively and setting several contiguous stereocentres along the 8-membered ring. Of the reported DBCOD syntheses, only one paper (from our group) reports the synthesis of stage 3 DBCODs, thus leaving plenty of room for expansion in this area of study. This thesis will focus on work towards the synthesis of two stage 3 DBCODs: kadsuraol C and taiwanschirin B.

1.8. References

(1) Huang, Z.; Lumb, J. P. Mimicking Oxidative Radical Cyclizations of Lignan Biosynthesis Using Redox-Neutral Photocatalysis. *Nat. Chem.* **2021**, *13* (1), 24–32.

(2) Chang, J.; Reiner, J.; Xie, J. Progress on the Chemistry of Dibenzocyclooctadiene Lignans. *Chem. Rev.* **2005**, *105* (12), 4581–4609.

(3) Laskar, D. D.; Corea, O. R. A.; Patten, A. M.; Kang, C. H.; Davin, L. B.; Lewis, N. G. Vascular Plant Lignification: Biochemical/Structural Biology Considerations of Upstream Aromatic Amino Acid and Monolignol Pathways. In *Comprehensive Natural Products II: Chemistry and Biology*; 2010; Vol. 6, pp 541–604.

(4) Weng, J. K.; Chapple, C. The Origin and Evolution of Lignin Biosynthesis. *New Phytol.* **2010**, *187* (2), 273–285.

(5) Boerjan, W.; Ralph, J.; Baucher, M. Lignin Biosynthesis. *Annu. Rev. Plant Biol.* **2003**, *54*, 519–546.

(6) Kärkäs, M. D.; Matsuura, B. S.; Monos, T. M.; Magallanes, G.; Stephenson, C. R. J. Transition-Metal Catalyzed Valorization of Lignin: The Key to a Sustainable Carbon-Neutral Future. *Org. Biomol. Chem.* **2016**, *14* (6), 1853–1914.

(7) Sun, Z.; Fridrich, B.; De Santi, A.; Elangovan, S.; Barta, K. Bright Side of Lignin Depolymerization: Toward New Platform Chemicals. *Chem. Rev.* **2018**, *118* (2), 614–678.

(8) Liu, C. J. Deciphering the Enigma of Lignification: Precursor Transport, Oxidation, and the Topochemistry of Lignin Assembly. *Mol. Plant* **2012**, *5* (2), 304–317.

(9) Tobimatsu, Y.; Schuetz, M. Lignin Polymerization: How Do Plants Manage the Chemistry so Well? *Curr. Opin. Biotechnol.* **2019**, *56*, 75–81.

(10) Davin, L. B.; Patten, A. M.; Kim, K.; Vassão, D. G.; Lewis, N. G. Dissection of Lignin Macromolecular Configuration and Assembly : Comparison to Related Biochemical Processes in Allyl/ Propenyl Phenol and Lignan Biosynthesis. *Nat. Prod. Rep.* **2008**, *25*,

(11) Gang, D. R.; Costa, M. A.; Fujita, M.; Dinkova-Kostova, A. T.; Wang, H. Bin; Burlat, V.; Martin, W.; Sarkanen, S.; Davin, L. B.; Lewis, N. G. Regiochemical Control of

Monolignol Radical Coupling: A New Paradigm for Lignin and Lignan Biosynthesis. *Chem. Biol.* **1999**, *6* (3), 143–151.

(12) Lewis, N. G.; Davin, L. B. Evolution of Lignan and Neolignan Biochemical Pathways. In *Isopentenoids and Other Natural Products*; 1994; pp 202–246.

(13) Lewis, N. G.; Yamamoto, E. Lignin: Occurrence, Biogenesis and Biodegradation. *Annu. Rev. Plant Physiol. Plant Mol. Biol.* **1990**, *41*, 455–496.

(14) Zhu, Y.; Kawaguchi, K.; Kiyama, R. Differential and Directional Estrogenic Signaling Pathways Induced by Enterolignans and Their Precursors. *PLoS One* **2017**, *12* (2), 1–14.

(15) Umezawa, T. Diversity in Lignan Biosynthesis. *Phytochem. Rev.* **2003**, *2* (3), 371–390.

(16) Whiting, D. A. Lignans and Neolignans. *Nat. Prod. Rep.* **1985**, 191–211.

(17) Saleem, M.; Hyoung, J. K.; Ali, M. S.; Yong, S. L. An Update on Bioactive Plant Lignans. *Nat. Prod. Rep.* **2005**, *22* (6), 696–716.

(18) Vassão, D. G.; Kim, K. W.; Davin, L. B.; Lewis, N. G. Lignans (Neolignans) and Allyl/Propenyl Phenols: Biogenesis, Structural Biology, and Biological/Human Health Considerations. In *Comprehensive Natural Products II: Chemistry and Biology*; 2010; Vol. 1, pp 815–928.

(19) Albertson, A. K. F.; Lumb, J. A Bio-Inspired Total Synthesis of Tetrahydrofuran Lignans. *Angew. Chemie - Int. Ed.* **2015**, *54*, 2204–2208.

(20) Chang, J.; Song, C. *Progress in the Syntheses of Dibenzocyclooctadiene Lignans*, 1st ed.; Copyright © 2013 Elsevier B.V. All rights reserved., 2013; Vol. 40.

(21) Fazary, A. E.; Alfaifi, M. Y.; Saleh, K. A.; Alshehri, M. A.; Elbehairi, S. E. I. Bioactive Lignans: A Survey Report on Their Chemical Structures? *Nat. Prod. Chem. Res.* **2016**, *04* (04), 1000226.

(22) Bauer, R.; Wenderski, T.;Tan, D. Biomimetic Diversity-Oriented Synthesis of Benzannulated Medium Rings via Ring Expansion. *Nat Chem Biol.* **2013**, *9* (1), 21–29.

(23) Anet, F. A. L.; Yavari, I. Conformations of Cis,Cis- 1,3-Cyclooctadiene and Its Epoxides. Dynamic Nuclear Magnetic Resonance Spectroscopy and Iterative Force-Field

Calculations. *J. Am. Chem. Soc.* **1978**, *100* (25), 7814–7819.

(24) Hu, Y. J.; Li, L. X.; Han, J. C.; Min, L.; Li, C. C. Recent Advances in the Total Synthesis of Natural Products Containing Eight-Membered Carbocycles (2009-2019). *Chem. Rev.* **2020**, *120* (13), 5910–5953.

(25) Bringmann, G.; Mortimer, A. J. P.; Keller, P. A.; Gresser, M. J.; Garner, J.; Breuning, M. Atroposelective Synthesis of Axially Chiral Biaryl Compounds. *Angew. Chemie - Int. Ed.* **2005**, *44* (34), 5384–5427.

(26) Bringmann, G.; Gulder, T.; Gulder, T. A. M.; Breuning, M. Atroposelective Total Synthesis of Axially Chiral Biaryl Natural Products. *Chem. Rev.* **2011**, *111* (2), 563–639.

(27) Gottlieb, H. E.; Mervic, M.; Ghera, E. Conformational Study of Dibenzocyclo-Octadiene Systems Related to the Schizandrin-Type Lignans. *J. Chem Soc. Perkin Trans. 1* **1982**, 2353–2358.

(28) Coleman, R. S.; Gurrala, S. R. Asymmetric Synthesis of the Dibenzocyclooctadiene Lignans Interiotherin A and Gomisin R. *Org. Lett.* **2005**, *7* (9), 1849–1852.

(29) Coleman, R. S.; Gurrala, S. R.; Mitra, S.; Raao, A. Asymmetric Total Synthesis of Dibenzocyclooctadiene Lignan Natural Products. *J. Org. Chem.* **2005**, *70* (22), 8932–8941.

(30) Liu, J. S.; Huang, M. F.; Zhou, H. X. Kadsulignan C and D, Two Novel Lignans from Kadsura Longipedunculata. *Can. J. Chem.* **1991**, *69* (9), 1403–1407.

(31) Jia-Sen, L.; Mei-Fen, H. Kadsulignans E-G from Kadsura Longipedunculata. *Phytochemistry* **1992**, *31* (3), 957–960.

(32) Kochetkov, N. K.; Khorlin, A.; Chizhov, O. S.; Sheichenko, V. I. Schizandrin - Lignan of Unusual Structure. *Tetrahedron Lett.* **1961**, *2* (20), 730–734.

(33) Cunningham, A.; Brinckmann, J. “Cinderella” Schisandra: A Project Linking Conservation and Local Livelihoods in the Upper Yangtze Ecoregion of China. *J. Am. Bot. Counc.* **2010**, No. 85, 28–39.

(34) Panossian, A.; Wikman, G. Pharmacology of Schisandra Chinensis Bail.: An Overview of

Russian Research and Uses in Medicine. *J. Ethnopharmacol.* **2008**, *118* (2), 183–212.

(35) Zhou, Y.; Men, L.; Sun, Y.; Wei, M.; Fan, X. Pharmacodynamic Effects and Molecular Mechanisms of Lignans from Schisandra Chinensis Turcz. (Baill.), a Current Review. *Eur. J. Pharmacol.* **2021**, *892*, 173796.

(36) Choi, Y. W.; Takamatsu, S.; Khan, S. I.; Srinivas, P. V.; Ferreira, D.; Zhao, J.; Khan, I. A. Schisandrene, a Dibenzocyclooctadiene Lignan from Schisandra Chinensis: Structure-Antioxidant Activity Relationships of Dibenzocyclooctadiene Lignans. *J. Nat. Prod.* **2006**, *69* (3), 356–359. https://doi.org/10.1021/np0503707.

(37) Wu, J. J.; Cao, Y. F.; Feng, L.; He, Y. Q.; Hong, J. Y.; Dou, T. Y.; Wang, P.; Hao, D. C.; Ge, G. B.; Yang, L. A Naturally Occurring Isoform-Specific Probe for Highly Selective and Sensitive Detection of Human Cytochrome P450 3A5. *J. Med. Chem.* **2017**, *60* (9), 3804–3813.

(38) Park, J. M.; Pel, P.; Chin, Y. W.; Lee, M. Y. Lignans with NADPH Oxidase 2 (NOX2)-Inhibitory Activity from the Fruits of Schisandra Chinensis. *Nat. Prod. Sci.* **2018**, *24* (1), 59–65.

(39) Xu, H.; Wang, W.; Li, X.; Li, Y.; Deng, C.; Jiang, Y.; Song, X.; Zhang, D. Traditional Use, Pharmacology and Toxicology of the Lignans in Genus Kadsura: A Systematic Review. *Rec. Nat. Prod.* **2023**, *17* (5), 793–844.

(40) Chen, D. F.; Zhang, S. X.; Xie, L.; Xie, J. X.; Chen, K.; Kashiwada, Y.; Zhou, B. N.; Wang, P.; Cosentino, L. M.; Lee, K. H. Anti-AIDS Agents-XXVI. Structure-Activity Correlations of Gomisin-G-Related Anti-HIV Lignans from Kadsura Interior and of Related Synthetic Analogues. *Bioorganic Med. Chem.* **1997**, *5* (8), 1715–1723.

(41) Han, Y. S.; Xiao, W. L.; Xu, H.; Kramer, V. G.; Quan, Y.; Mesplède, T.; Oliveira, M.; Colby-Germinario, S. P.; Sun, H. D.; Wainberg, M. A. Identification of a Dibenzocyclooctadiene Lignan as a HIV-1 Non-Nucleoside Reverse Transcriptase Inhibitor. *Antivir. Chem. Chemother.* **2015**, *24* (1), 28–38.

(42) Kuo, Y. H.; Li, S. Y.; Huang, R. L.; Wu, M. Der; Huang, H. C.; Lee, K. H. Schizarin B, C, D, and E, Four New Lignans from Kadsura Matsudai and Their Antihepatitis

Activities. *J. Nat. Prod.* **2001**, *64* (4), 487–490. https://doi.org/10.1021/np000261m.

(43) Xue, Y.; Li, X.; Du, X.; Li, X.; Wang, W.; Yang, J.; Chen, J.; Pu, J.; Sun, H. Isolation and Anti-Hepatitis B Virus Activity of Dibenzocyclooctadiene Lignans from the Fruits of Schisandra Chinensis. *Phytochemistry* **2015**, *116* (1), 253–261.

(44) Larrey, D. Drug-Induced Liver Disease. *J. Hepatol.* **2000**, *32*, 77–88.

(45) He, T.; Wang, Q. Y.; Shi, J. Z.; Fan, T. Y.; Yan, C.; Huang, L. J.; Liu, S.; Hao, X. J.; Mu, S. Z. Synthesis and the Hepatoprotective Activity of Dibenzocyclooctadiene Lignan Derivatives. *Bioorganic Med. Chem. Lett.* **2014**, *24* (7), 1808–1811.

(46) Chen, Y.; Ip, S. P.; Ko, K. M.; Poon, T. C. W.; Ng, E. W. Y.; Lai, P. B. S.; Mao, Q. Q.; Xian, Y. F.; Che, C. T. A Proteomic Approach in Investigating the Hepatoprotective Mechanism of Schisandrin B: Role of Raf Kinase Inhibitor Protein. *J. Proteome Res.* **2011**, *10* (1), 299–304.

(47) Liu, J.; Pandey, P.; Wang, X.; Qi, X.; Chen, J.; Sun, H.; Zhang, P.; Ding, Y.; Ferreira, D.; Doerksen, R. J.; Hamann, M. T.; Li, S. Hepatoprotective Dibenzocyclooctadiene and Tetrahydrobenzocyclooctabenzofuranone Lignans from Kadsura Longipedunculata. *J. Nat. Prod.* **2018**, *81* (4), 846–857. https://doi.org/10.1021/acs.jnatprod.7b00934.

(48) Rayan, A.; Raiyn, J.; Falah, M. Nature Is the Best Source of Anticancer Drugs: Indexing Natural Products for Their Anticancer Bioactivity. *PLoS One* **2017**, *12* (11), 1–12.

(49) Kupchan, S. M.; Britton, R. W.; Ziegler, M. F.; Gilmore, C. J.; Restive, R. J.; Bryan, R. F. Steganacin and Steganangin, Novel Antileukemic Lignan Lactones from Steganotaenia Araliacea. *J. Am. Chem. Soc.* **1973**, *95* (4), 1335–1336.

(50) Wang, R. W. J.; Rebhun, L. I.; Kupchan, S. M. Antimitotic and Antitubulin Activity of the Tumor Inhibitor Steganacin. *J. Cell Biol.* **1976**, *70* (2 II), 3071–3079.

(51) Lu, Y.; Liu, Y.; Bastow, K. F.; Lee, K.; Chen, D. Kadsufolins A – D and Related Cytotoxic Lignans from Kadsura Oblongifolia. *Helv. Chim. Acta* **2011**, *94*, 519–527.

(52) Chen, D. F.; Zhang, S. X.; Kozuka, M.; Sun, Q. Z.; Feng, J.; Wang, Q.; Mukainaka, T.; Nobukuni, Y.; Tokuda, H.; Nishino, H.; Wang, H. K.; Morris-Natschke, S. L.; Lee, K. H.

Interiotherins C and D, Two New Lignans from Kadsura Interior and Antitumor-Promoting Effects of Related Neolignans on Epstein-Barr Virus Activation. *J. Nat. Prod.* **2002**, *65* (9), 1242–1245.

(53) Kuo, Y. H.; Kuo, L. M. Y.; Chen, C. F. Four New C19 Homolignans, Schiarisanrins A, B, and D and Cytotoxic Schiarisanrin C, from Schizandra Arisanensis. *J. Org. Chem.* **1997**, *62* (10), 3242–3245.

(54) Huang, M.; Jin, J.; Sun, H.; Liu, G. T. Reversal of P-Glycoprotein-Mediated Multidrug Resistance of Cancer Cells by Five Schizandrins Isolated from the Chinese Herb Fructus Schizandrae. *Cancer Chemother. Pharmacol.* **2008**, *62* (6), 1015–1026.

(55) Youdim, M. B. H. Why Do We Need Multifunctional Neuroprotective and Neurorestorative Drugs for Parkinson's and Alzheimer's Diseases as Disease Modifying Agents. *Exp. Neurobiol.* **2010**, *19* (1), 1–14.

(56) Yang, J. H.; Zhang, H. Y.; Wen, J.; Du, X.; Chen, J. H.; Zhang, H. B.; Xiao, W. L.; Pu, J. X.; Tang, X. C.; Sun, H. D. Dibenzocyclooctadiene Lignans with Antineurodegenerative Potential from Kadsura Ananosma. *J. Nat. Prod.* **2011**, *74* (5), 1028–1035.

(57) Dong, K.; Pu, J. X.; Zhang, H. Y.; Du, X.; Li, X. N.; Zou, J.; Yang, J. H.; Zhao, W.; Tang, X. C.; Sun, H. D. Dibenzocyclooctadiene Lignans from Kadsura Polysperma and Their Antineurodegenerative Activities. *J. Nat. Prod.* **2012**, *75* (2), 249–256.

(58) Hu, D.; Cao, Y.; He, R.; Han, N.; Liu, Z.; Miao, L.; Yin, J. Schizandrin, an Antioxidant Lignan from Schisandra Chinensis, Ameliorates Aβ 1-42-Induced Memory Impairment in Mice. *Oxid. Med. Cell. Longev.* **2012**, *2012*, 1–7.

(59) Hu, X.; Guo, C.; Hou, J. Q.; Feng, J. H.; Zhang, X. Q.; Xiong, F.; Ye, W. C.; Wang, H. Stereoisomers of Schisandrin B Are Potent ATP Competitive GSK-3β Inhibitors with Neuroprotective Effects against Alzheimer's Disease: Stereochemistry and Biological Activity. *ACS Chem. Neurosci.* **2018**, *10*, 996–1007.

(60) Zhou, F.; Wang, M.; Ju, J.; Wang, Y.; Liu, Z.; Zhao, X.; Yan, Y.; Yan, S.; Luo, X.; Fang, Y. Schizandrin A Protects against Cerebral Ischemia-Reperfusion Injury by Suppressing Inflammation and Oxidative Stress and Regulating the AMPK/Nrf2 Pathway Regulation.

Am. J. Transl. Res. **2019**, *11* (1), 199–209.

(61) Han, J.; Shi, X.; Du, Y.; Shi, F.; Zhang, B.; Zheng, Z.; Xu, J.; Jiang, L. Schisandrin C Targets Keap1 and Attenuates Oxidative Stress by Activating Nrf2 Pathway in Ang II-Challenged Vascular Endothelium. *Phyther. Res.* **2019**, *33* (3), 779–790.

(62) Zuo, Y. H.; Liu, Y. B.; Cheng, C. S.; Yang, Y. P.; Xie, Y.; Luo, P.; Wang, W.; Zhou, H. Isovaleroylbinankadsurin A Ameliorates Cardiac Ischemia/Reperfusion Injury through Activating GR Dependent RISK Signaling. *Pharmacol. Res.* **2020**, *158*, 104897.

(63) Ye, B. H.; Lee, S. J.; Choi, Y. W.; Park, S. Y.; Kim, C. D. Preventive Effect of Gomisin J from Schisandra Chinensis on Angiotensin II-Induced Hypertension via an Increased Nitric Oxide Bioavailability. *Hypertens. Res.* **2015**, *38* (3), 169–177.

(64) Lewis, N. G.; Davin, L. B.; Sarkanen, S. *Comprehensive Natural Products Chemistry*, vol. 3.; Elsevier: Oxford, 1999.

(65) Lau, W.; Sattely, E. S. Six Enzymes from Mayapple That Complete the Biosynthetic Pathway to the Etoposide Aglycone. *Science (80-.).* **2015**, *349* (6253), 1224–1228.

(66) Huang, X.; Groves, J. T. Oxygen Activation and Radical Transformations in Heme Proteins and Metalloporphyrins. *Chem. Rev.* **2018**, *118*, 2491–2553.

(67) White, M. C.; Zhao, J. Aliphatic C-H Oxidations for Late-Stage Functionalization. *J. Am. Chem. Soc.* **2018**, *140*, 13988–14009. https://doi.org/10.1021/jacs.8b05195.

(68) Tang, M.; Zou, Y.; Watanabe, K.; Walsh, C. T.; Tang, Y. Oxidative Cyclization in Natural Product Biosynthesis. *Chem. Rev.* **2017**, *117*, 5226–5333.

(69) Guengerich, F. P.; Yoshimoto, F. K. Formation and Cleavage of C-C Bonds by Enzymatic Oxidation-Reduction Reactions. *Chem. Rev.* **2018**, *118* (14), 6573–6655.

(70) Walsh, C. T.; Moore, B. S. Enzymatic Cascade Reactions in Biosynthesis. *Angew. Chemie - Int. Ed.* **2019**, *58*, 6846–6879.

(71) Lin, Y. C.; Cheng, Y. Bin; Liaw, C. C.; Lo, I. W.; Kuo, Y. H.; Chiang, M. Y.; Chou, C. H.; Shen, Y. C. New Lignans from the Leaves and Stems of Kadsura Philippinensis. *Molecules* **2013**, *18*, 6573–6583.

(72) Wang, X.; Liu, J.; Pandey, P.; Fronczek, F. R.; Doerksen, R. J.; Chen, J.; Qi, X.; Zhang, P.; Ferreira, D.; Valeriote, F. A.; Sun, H.; Li, S.; Hamann, M. T. Computationally Assisted Assignment of the Kadsuraols, a Class of Chemopreventive Agents for the Control of Liver Cancer. *Org. Lett.* **2018**, *20* (18), 5559–5563.

(73) Green, S. P.; Whiting, D. A. New Carbon Radical Chemistry as a Model for the Biogenesis of the Interiorin/Kadsulignan Type of Dibenzocyclooctadiene Lignan. *J. Chem Soc. Perkin Trans. 1* **1998**, 193–201.

(74) Coleman, R. S.; Guernon, J. M.; Roland, J. T. Synthesis of the Spirocyclic Cyclohexadienone Ring System of the Schiarisanrins. *Org. Lett.* **2000**, *2* (3), 277–280.

(75) Taafrout, M.; Rouessac, F.; Robin, J. P.; Davoust, D. Isolement Du Prestegane B à Partir de Steganotaenia Araliacea Hochst., Premier Lignane Bis-(Meta-Hydroxy-Benzyl)-Butanolide d'origine Végétale. - Isolement et Synthèse En Une Étape Du Diméthylmatairésinol-. *Tetrahedron Lett.* **1984**, *25* (37), 4127–4128.

(76) He, D.; Ding, L.; Xu, H.; Lei, X.; Xiao, H.; Zhou, Y. Gymnothelignans A-O: Conformation and Absolute Configuration Analyses of Lignans Bearing Tetrahydrofuran from Gymnotheca Chinensis. *J. Org. Chem.* **2012**, *77* (19), 8435–8443.

(77) Li, H.; Zhang, Y.; Xie, X.; Ma, H.; Zhao, C.; Zhao, G.; She, X. Bioinspired Total Synthesis of Gymnothelignan N. *Org. Lett.* **2014**, *16* (17), 4440–4443.

(78) Chen, P.; Huo, L.; Li, H.; Liu, L.; Yuan, Z.; Zhang, H.; Feng, S.; Xie, X.; Wang, X.; She, X. Bioinspired Total Synthesis of (-)-Gymnothelignan L. *Org. Chem. Front.* **2018**, *5* (7), 1124–1128.

(79) Davin, L. B.; Wang, H.; Crowell, A. L.; Bedgar, D. L.; Martin, D. M.; Sarkanen, S.; Lewis, N. G. Stereoselective Bimolecular Phenoxy Radical Coupling by an Auxiliary (Dirigent) Protein Without an Active Center. *Science.* **1997**, *275*, 362–366.

(80) Kende, A. S.; Liebeskind, L. S. Total Synthesis of (±)-Steganacin. *J. Am. Chem. Soc.* **1976**, *98* (1), 267–268.

(81) Damon, R. E.; Schlessinger, R. H.; Blount, J. F. A Short Synthesis of (±)-Isostegane. *J. Org. Chem.* **1976**, *41* (23), 3772–3773.

(82) Hughes, L. R.; Raphael, R. A. Synthesis of the Antileukaemic Lignan Precursor (±) Steganone. *Tetrahedron Lett.* **1976**, *17* (18), 1543–1546.

(83) Ghera, E.; Ben-David, Y.; Becker, D. Desoxyschizandrin, Stereochemistry and Total Synthesis. *Tetrahedron Lett.* **1977**, *18* (5), 463–466.

(84) Mervič, M.; Ghera, E. Total Synthesis of (±)-Kadsurin. *J. Am. Chem. Soc.* **1977**, *99* (23), 7673–7678.

(85) Robin, J. P.; Gringore, O.; Brown, E. Asymmetric Total Synthesis of the Antileukaemic Lignan Precursor (-)Steganone and Revision of Its Absolute Configuration. *Tetrahedron Lett.* **1980**, *21* (28), 2709–2712.

(86) Brown, E.; Robin, J.-P.; Dhal, R. Application de La Reaction d'Ullmann a La Synthese de Biaryles Precurseurs de Lignanes Bisbenzocylcooctadienes. *Tetrahedron* **1982**, *38* (16), 2569–2579.

(87) Meyers, A. I.; Flisak, J. R.; Aitken, R. A. An Asymmetric Synthesis of (-)-Steganone. Further Application of Chiral Biaryl Syntheses. *J. Am. Chem. Soc.* **1987**, *109* (18), 5446–5452.

(88) Uemura, M.; Daimon, A.; Hayashi, Y. An Asymmetric Synthesis of an Axially Chiral Biaryl via an (Arene)Chromium Complex: Formal Synthesis of (-)-Steganone. *J. Chem. Soc. Chem. Commun.* **1995**, 1943–1944.

(89) Monovich, L. G.; Le Huérou, Y.; Rönn, M.; Molander, G. A. Total Synthesis of (-)-Steganone Utilizing a Samarium(II) Iodide Promoted 8-Endo Ketyl-Olefin Cyclization. *J. Am. Chem. Soc.* **2000**, *122* (1), 52–57.

(90) Coleman, R. S.; Gurrala, S. R.; Mitra, S.; Raao, A. Asymmetric Total Synthesis of Dibenzocyclooctadiene Lignan Natural Products. *J. Org. Chem.* **2005**, *70*, 8932–8941.

(91) Singidi, R. R.; RajanBabu, T. V. Catalyzed Cyclizations Leading to Enrichment of Functionality and Chirality. A General Approach to Dibenzocyclooctadiene Lignans from α,ω-Diynes. *Org. Lett.* **2008**, *10* (15), 3351–3354.

(92) Li, Y.; Wang, Q.; Dong, L.; Guo, X.; Wang, W.; Xie, J.; Chang, J. Asymmetrie Synthesis

of (+)- and (-)-Wuweizisu C Stereoisomers and Their Chemosensitizing Effects on Multidrug-Resistant Cancer Cells. *Synthesis (Stuttg).* **2009**, No. 20, 3383–3390.

(93) Gong, W.; RajanBabu, T. V. Conformation and Reactivity in Dibenzocyclooctadienes (DBCOD). A General Approach to the Total Synthesis of Fully Substituted DBCOD Lignans via Borostannylative Cyclization of α,Ω-Diynes. *Chem. Sci.* **2013**, *4* (10), 3979–3985.

(94) Soorukram, D.; Pohmakotr, M.; Kuhakarn, C.; Reutrakul, V. Bioinspired Asymmetric Synthesis of (-)-Gymnothelignan V. *J. Org. Chem.* **2018**, *83* (7), 4173–4179.

(95) Warshawsky, A. M.; Meyers, A. I. Asymmetric Total Synthesis of Dibenzocyclooctadiene Lignans (-)-Schizandrin and (-)-Isoschizandrin. Structure Revision of (+)-Isoschizandrin. *J. Am. Chem. Soc.* **1990**, *112*, 8090–8099.

(96) Larson, E.; Raphael, R. Synthesis of (-)-Steganone. *J. Chem Soc. Perkin Trans. 1* **1982**, 521–525.

(97) Chen, W. W.; Zhao, Q.; Xu, M. H.; Lin, G. Q. Nickel-Catalyzed Asymmetric Ullmann Coupling for the Synthesis of Axially Chiral Tetra-Ortho-Substituted Biaryl Dials. *Org. Lett.* **2010**, *12* (5), 1072–1075.

(98) Molander, G. A.; George, K. M.; Monovich, L. G. Total Synthesis of (+)-Isoschizandrin Utilizing a Samarium(II) Iodide-Promoted 8-Endo Ketyl-Olefin Cyclization. *J. Org. Chem.* **2003**, *68* (25), 9533–9540.

(99) Ziegler, F. E.; Fowler, K. W.; Sinha, N. D. A Total Synthesis of (±) Steganacin via the Modified Ullmann Reaction. *Tetrahedron Lett.* **1978**, *19* (31), 2767–2770.

(100) Robin, J. P.; Brown, E. A New Route to the Bis-Benzocyclooctadiene Lignan Skeleton: Total Synthesis of (+/-)-Pictrostegane, (+/-)-Isopictrostegane and (+/-)-Isostegane. *Tetrahedron Lett.* **1978**, No. 38, 3613–3616.

(101) Yalcouye, B.; Choppin, S.; Panossian, A.; Leroux, F. R.; Colobert, F. A Concise Atroposelective Formal Synthesis of (-)-Steganone. *European J. Org. Chem.* **2014**, *2014* (28), 6285–6294.

(102) Zheng, S.; Aves, S. J.; Laraia, L.; Galloway, W. R. J. D.; Pike, K. G.; Wu, W.; Spring, D. R. A Concise Total Synthesis of Deoxyschizandrin and Exploration of Its Antiproliferative Effects and Those of Structurally Related Derivatives. *Chem. - A Eur. J.* **2012**, *18* (11), 3193–3198.

(103) Abe, H.; Takeda, S.; Fujita, T.; Nishioka, K.; Takeuchi, Y.; Harayama, T. Enantioselective Construction of Biaryl Part in the Synthesis of Stegane Related Compounds. *Tetrahedron Lett.* **2004**, *45* (11), 2327–2329.

(104) Coy, E. D.; Cuca, L. E.; Sefkow, M. Pd–NHC Catalyzed Biaryl Coupling by Direct C–H Activation— A Novel Strategy for the Synthesis of Dibenzocyclooctane Lignans. *Synth. Commun.* **2011**, *41*, 41–51. https://doi.org/10.1080/00397910903531755.

(105) Landais, Y.; Robin, J. P.; Lebrun, A. Ruthenium Dioxide in Fluoro Acid Medium: I. A New Agent in the Biaryl Oxidative Coupling. Application to the Synthesis of Non Phenolic Bisbenzocyclooctadiene Lignan Lactones. *Tetrahedron* **1991**, *47* (23), 3787–3804.

(106) Landais, Y.; Lebrun, A.; Lenain, V.; Robin, J. P. Synthesis of Diarylbutanes from Cordigerines and Reinvestigation of Their Oxidative Couplings in Deoxyschizandrins. — An Unusual Formation of Phenyltetralin Lignans —. *Tetrahedron Lett.* **1987**, *28* (43), 5161–5164.

(107) Tanaka, M.; Ikeya, Y.; Mitsuhashi, H.; Maruno, M.; Wakamatsu, T. Total Syntheses of the Metabolites of Schizandrin. *Tetrahedron* **1995**, *51* (43), 11703–11724.

(108) Ohshima, T.; Tanaka, M.; Mitsuhashi, H.; Maruno, M.; Wakamatsu, T. Total Synthesis of Homochiral Kadsurin Having the Natural Configuration. *Tetrahedron: Asymmetry* **1995**, *6* (1), 139–146.

(109) Tanaka, M.; Mukaiyama, C.; Mitsuhashi, H.; Maruno, M.; Wakamatsu, T. Synthesis of Optically Pure Gomisin Lignans : The Total Synthesis of (+)-Schizandrin, (+)-Gomisin A, and (+)-Isoschizandrin in Naturally Occurring Forms. *J. Org. Chem.* **1995**, *60*, 4339–4352.

(110) Tanaka, M.; Mukaiyama, C.; Mitsuhashi, H.; Wakamatsu, T. Synthesis of Optically Pure

Gomisin A and Schizandrin: The First Total Synthesis of Gomisin A and Schizandrin Having Naturally Occurring Configurations. *Tetrahedron Lett.* **1992**, *33* (29), 4165–4168.

(111) Takeya, T.; Ohguchi, A.; S., T. Synthesis of (+/-)-Dibenzocyclooctadiene Lignans, (+/-)-Isoschizandrin, and Their Stereoisomers, Utilizing the Samarium-Barbier Reaction. *Chem. Pharm. Bull.* **1994**, *42* (3), 438–442.

(112) Takeya, T.; Yamaki, S.; Itoh, T.; Hosogal, H.; Tobinaga, S. A General Synthesis of (+/-)-Dibenzocyclooctadiene Lignans. *Chem. Pharm. Bull.* **1996**, *44* (5), 909–918.

(113) Enders, D.; Lausberg, V.; Del Signore, G.; Berner, O. M. A General Approach to the Asymmetric Synthesis of Lignans: (-)-Methyl Piperitol, (-)-Sesamin, (-)-Aschantin, (+)-Yatein, (+)-Dihydroclusin, (+)-Burseran, and (-)-Isostegane. *Synthesis (Stuttg).* **2002**, No. 4, 515–522.

(114) Biftu, T.; Hazra, B. G.; Stevenson, R. Synthesis of the Lignan (±)-Deoxyschizandrin. *J. Chem. Soc. Chem. Commun.* **1978**, *7* (12), 491–492.

(115) Magnus, P.; Gallagher, T. A Short Synthesis of (±)-Steganone and (±)-Steganacin. *J. Chem. Soc. - Ser. Chem. Commun.* **1984**, No. 17, 1179–1180.

(116) Liu, Y.; Chang, J.; Xie, J. Progress of Aryl-Aryl Oxidative Coupling Reagents in the Synthetic Chemistry of Dibenzocyclooctadiene Lignans. *Chinese J. Org. Chem.* **2012**, *32* (11), 2040–2053.

(117) Planchenault, D.; Dhal, R.; Robin, J. P. New Agents of Biaryl Oxidative Coupling in Fluoro Acid Medium. VI. Application to the Synthesis of Phenolic Bisbenzocyclooctadiene Lignans. *Tetrahedron* **1995**, *51* (5), 1395–1404.

(118) Takeya, T.; Ohguchi, A.; Ara, Y.; Tobinaga, S. Synthesis of (+/-)-Dibenzocyclooctadiene Lignans, (+/-)-Schizandrin, (+/-)-Gomisin A and Their Stereoisomers, Utilizing the Samarium-Grignard Reaction. *Chem. Pharm. Bull.* **1994**, *42* (3), 430–437.

(119) Kramer, B.; Averhoff, A.; Waldvogel, S. R. Highly Selective Formation of Eight-Membered-Ring Systems by Oxidative Cyclization with Molybdenum Pentachloride – An Environmentally Friendly and Inexpensive Access to 2,2'-Cyclolignans. *Angew. Chemie - Int. Ed.* **2002**, *41* (16), 2981–2982.

(120) Kramer, B.; Fröhlich, R.; Waldvogel, S. R. Oxidative Coupling Reactions Mediated by MoCl5 Leading to 2,2′-Cyclolignans: The Specific Role of HCl. *European J. Org. Chem.* **2003**, No. 18, 3549–3554.

(121) Ward, R. S.; Pelter, A.; Abd-El-Ghani, A. Preparation of Tetrahydrodibenzocyclooctene Lignans and Spirodienones by Hypervalent Iodine Oxidation of Phenolic Dibenzylbutyrolactones. *Tetrahedron* **1996**, *52* (4), 1303–1336.

(122) Pelter, A.; Ward, R. S.; Jones, D. M.; Maddocks, P. Asymmetric Synthesis of Lignans of the Dibenzylbutanediol and Tetrahydrodibenzocyclooctene Series. *J. Chem Soc. Perkin Trans. 1* **1993**, 2631–2637.

(123) Liao, G.; Yao, Q. J.; Zhang, Z. Z.; Wu, Y. J.; Huang, D. Y.; Shi, B. F. Scalable, Stereocontrolled Formal Syntheses of (+)-Isoschizandrin and (+)-Steganone: Development and Applications of Palladium(II)-Catalyzed Atroposelective C−H Alkynylation. *Angew. Chemie - Int. Ed.* **2018**, *57* (14), 3661–3665.

(124) Molander, G. A.; George, K. M.; Monovich, L. G. Total Synthesis of (+)-Isoschizandrin Utilizing a Samarium(II) Iodide-Promoted 8-Endo Ketyl-Olefin Cyclization. *J. Org. Chem.* **2003**, *68* (25), 9533–9540. https://doi.org/10.1021/jo0347361.

(125) Tomioka, K.; Ishiguro, T.; Iitaka, Y.; Koga, K. Asymmetric Total Synthesis of Natural (-)- and Unnatural (+)-Steganacin. Determination of the Absolute Configuration of Natural Antitumor Steganacin. *Tetrahedron* **1984**, *40* (8), 1303–1312.

(126) Landais, Y.; Lebrun, A.; Robin, J. P. Ruthenium(IV) Tetrakis(Trifluoroacetate), a New Oxidizing Agent. II. A New Access to Schizandrins Skeleton Using Biaryl Oxidative Coupling of Cis-Substituted Butanolides. *Tetrahedron Lett.* **1986**, *27* (44), 5377–5380.

(127) Djurdjevic, S.; Green, J. R. Nicholas Reactions in the Synthesis of Dicobalt Dibenzocyclooctyne Complexes. *Org. Lett.* **2013**, *15* (21), 5468–5471.

(128) Krow, G. R.; Damodaran, K. M.; Michener, E.; Wolf, R.; Guare, J. Dibenzocyclooctadiene Antileukemic Lignan Synthesis. (±)-Steganone. *J. Org. Chem.* **1978**, *43* (20), 3950–3953.

(129) Ghera, E.; Ben-David, Y. Total Synthesis of the Lignan (±)-Schizandrin. *J. Chem. Soc.*

Chem. Commun. **1978**, *8* (11), 480–481.

(130) Bringmann, G.; Hinrichs, J. Efficient Kinetic Resolution of a Racemic 7-Membered Biaryl Lactone: Enantioselective Synthesis of 2,2'-Dihydroxymethyl-1,1'-Binaphthyl. *Tetrahedron Asymmetry* **1997**, *8* (24), 4121–4126.

(131) Gong, W.; RajanBabu, T. V. Conformation and Reactivity in Dibenzocyclooctadienes (DBCOD). A General Approach to the Total Synthesis of Fully Substituted DBCOD Lignans via Borostannylative Cyclization of α,ω-Diynes. *Chem. Sci.* **2013**, *4*, 3979–3985.

(132) Gong, W.; Singidi, R. R.; Gallucci, J. C.; Rajanbabu, T. V. On the Stereochemistry of Acetylide Additions to Highly Functionalized Biphenylcarbaldehydes and Multi-Component Cyclization of 1,n-Diynes. Syntheses of Dibenzocyclooctadiene Lignans. *Chem. Sci.* **2012**, *3*, 1221–1230.

(133) Pelter, A.; Ward, R. S.; Jones, D. M.; Maddocks, P. Asymmetric Syntheses of Lignans of the Dibenzylbutyrolactone, Dibenzylbutanediol, Aryltetraun and Dibenzocyclooctadiene Series. *Tetrahedron: Asymmetry* **1992**, *3* (2), 239–242.

(134) Bradley, A.; Motherwell, W. B.; Ujjainwalla, F. A Concise Approach towards the Synthesis of Steganone Analogues. *Chem. Commun.* **1999**, No. 10, 917–918.

(135) Venkanna, A.; Poornima, B.; Siva, B.; Babu, B. H.; Babu, K. S. Towards the Total Synthesis of Schisandrene : Stereoselective Synthesis of the Dibenzocyclooctadiene Lignan Core. *Synlett* **2018**, *29*, 908–911.

Chapter 2. Aldol, methyl addition, and benzylic deoxygenation studies on model systems

2.1. Introduction

2.1.1. Introduction to the synthetic strategy for DBCODs targeted in this thesis

Several stage 2 and 3 DBCODs have been previously synthesized in our group including kadsulignan E, heteroclitin J, kadsuphilol G, taiwankadsurin A, kadsuphilin N, and kadsuphilol R (Figure 2.1). The synthetic targets of the current work are stage 3 DBCODs: kadsuraol C and taiwanschirin B, which differ from our previous targets in that they do not possess an oxygen-containing substituent at C6. The syntheses of kadsuraol C and taiwanschirin B will be discussed in Chapters 3 and 4, respectively. Our synthetic strategy will involve preparing a substrate bearing a hydroxyl group at C6 via aldol addition and then removal of the C6 substituent later in the synthesis. It is proposed that the C6 oxygen-containing substituent could either be removed from a linear substrate (Scheme 2.1, conversion of **2-3** to **2-2**) or after cyclization has been performed (Figure 2.2B).

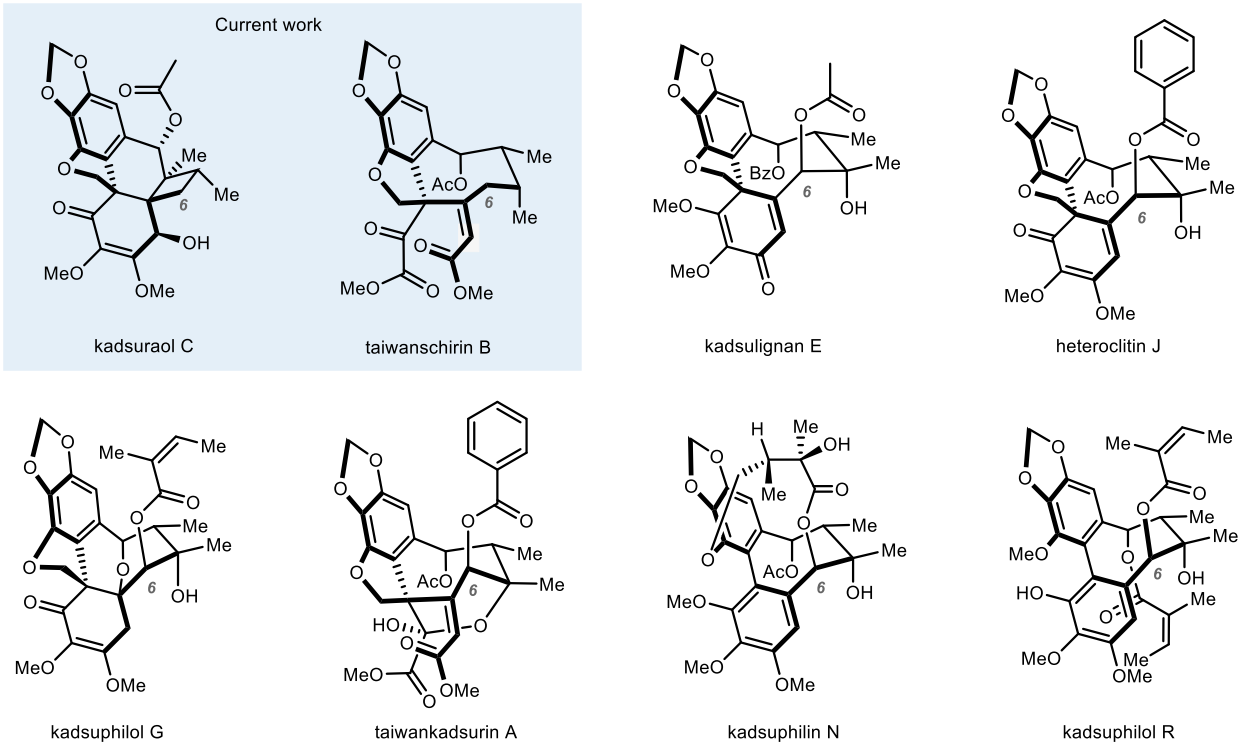


Figure 2.1. Current and previous DBCOD targets in the Lumb group

Biosynthetically, the DBCOD scaffold is synthesized in its non-oxygenated form and then selectively oxidized by CYP450s (Figure 2.2A). We plan to take the reverse approach of forming

the DBCOD scaffold with full oxygenation and then selectively reducing around the ring. This strategy was selected as it allows us to set the required stereocenters around the 8-membered ring early in the synthesis. This method should allow us to circumvent the challenges of late-stage selective oxidation, such as low yields and selectivity issues.[1] For the synthesis of kadsuraol C and taiwanschirin B, we plan to develop methodology for the selective reduction of the C6 alcohol to the methylene without affecting the other substituents around the 8-membered ring (Figure 2.2B).

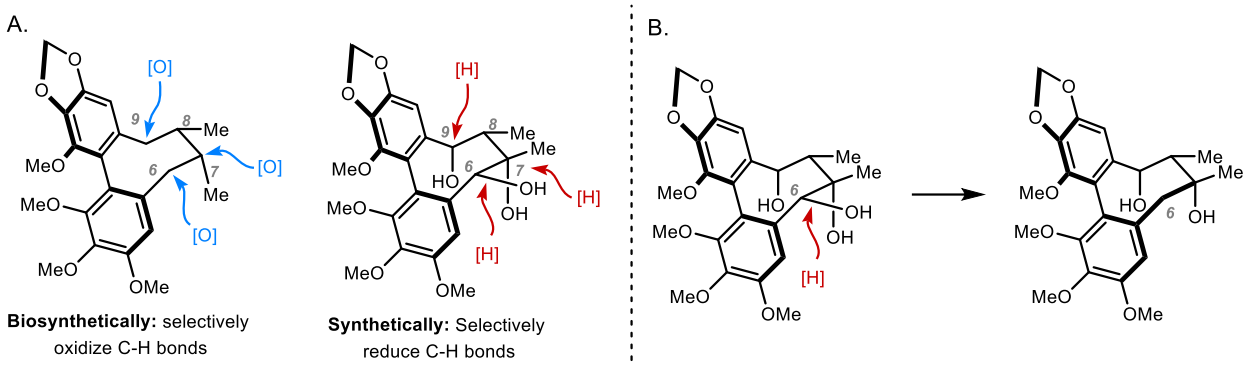
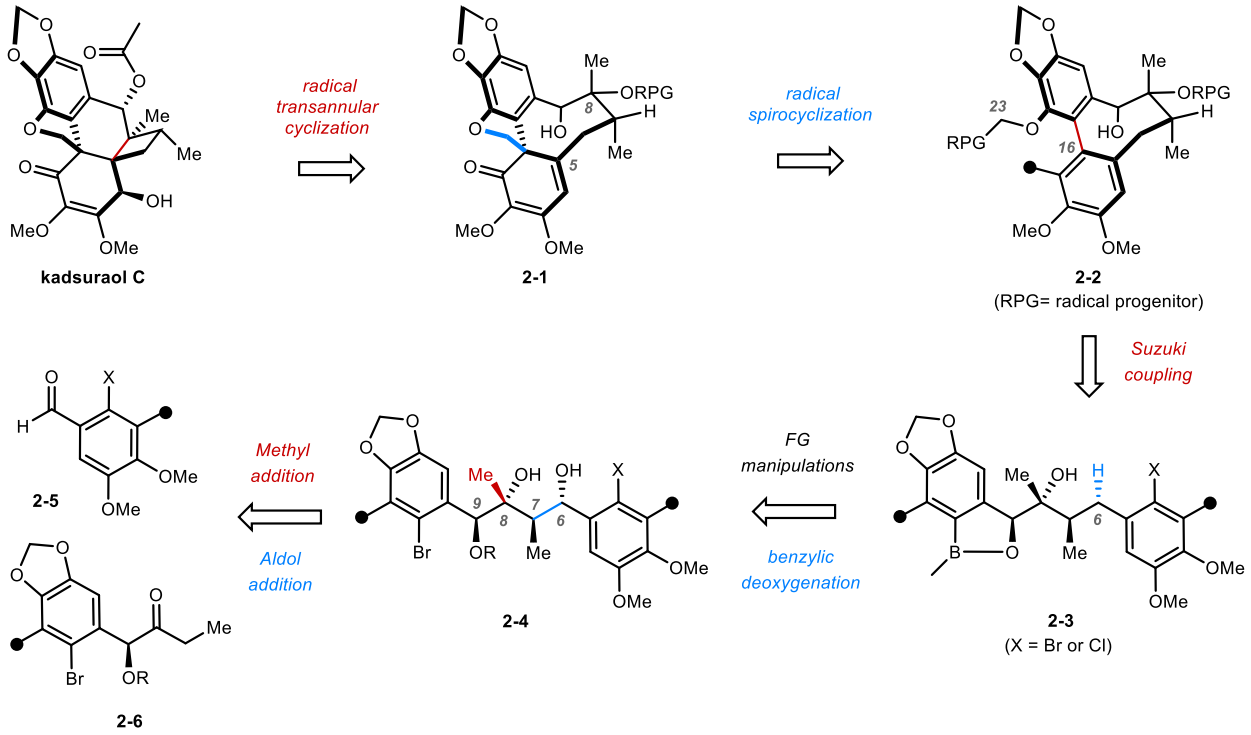


Figure 2.2. A) Biosynthetic and synthetic approaches to controlling the oxidation pattern around the 8-membered ring and B) synthetic C6 deoxygenation strategy

Analogous to lignan biosynthesis, where the coupling of two monolignol fragments occurs, we designed a convergent DBCOD synthesis where two prefunctionalized fragments are coupled together to give an alkyl chain which will later become the 8-membered ring of a DBCOD. We plan that a variety of DBCODs, including our targets kadsuraol C and taiwanschirin B, could be synthesized following a synthetic sequence comprising the same key steps. These are demonstrated in the retrosynthetic analysis of kadsuraol C (Scheme 2.1). Kadsuraol C is anticipated to originate from **2-1** undergoing a transannular radical cyclization of C8 onto C5. Compound **2-1** is expected to arise from a second radical cyclization: the spirocyclization of C23 onto C16 of **2-2**. Compound **2-2** is expected to come from the intramolecular Suzuki coupling of linear precursor **2-3**. Compound **2-3** can result from functionalization and C6 benzylic deoxygenation of compound **2-4**. Chelate-controlled methyl addition would be used to set the C8 stereocenter of **2-4**. The first linear substrate (not pictured) would be formed via aldol coupling of the prefunctionalized aromatic ketone and aldehyde fragments, **2-6** and **2-5**, setting the C6, C7, and C9 stereocenters. This strategy allows us to set all the stereocenters around the 8-membered ring at an early stage in the synthesis. After this, the biaryl bond is formed atroposelectively, thus introducing another



Scheme 2.1. Retrosynthetic analysis of kadsuraol C

stereochemical element. This step will likely be difficult due to 8-membered ring formation from a linear precursor being both enthalpically and entropically unfavorable due to transannular interactions and steric congestion. Previously reported DBCOD syntheses include examples of biaryl bond formation both before and after formation of the alkyl chain, however the latter more closely parallels the proposed biosynthetic pathway. Also taking inspiration from the biosynthetic pathway, after the formation of the stage 2 DBCOD, our strategy leaves the non-canonical oxidation steps leading to stage 3 DBCODs to the end of the synthesis. Despite this, leaving a radical novel cyclization as the final step poses a daunting challenge.

A racemic model system using simplified aromatic ketone and aldehyde fragments (**2-7** and **2-14**, Figure 2.3) was devised. Compound **2-7** was selected as a mimic for ketone **2-6** as it also bears a 3,4,5-ether-substituted aromatic ring, with the difference that two of the ethers are not tethered as a benzodioxolane. Additionally, it is easily accessible as its synthesis has been previously reported in our group in only 3 steps. Commercially available trimethoxybenzaldehyde (**2-14**) was selected as the mimic for aldehyde **2-5** as it also bears a 3,4,5-ether-substituted aromatic ring and should therefore be electronically similar. This model system was used to investigate the first three key

steps of the kadsuraol synthesis in this chapter: aldol addition, methyl addition, and benzylic deoxygenation.

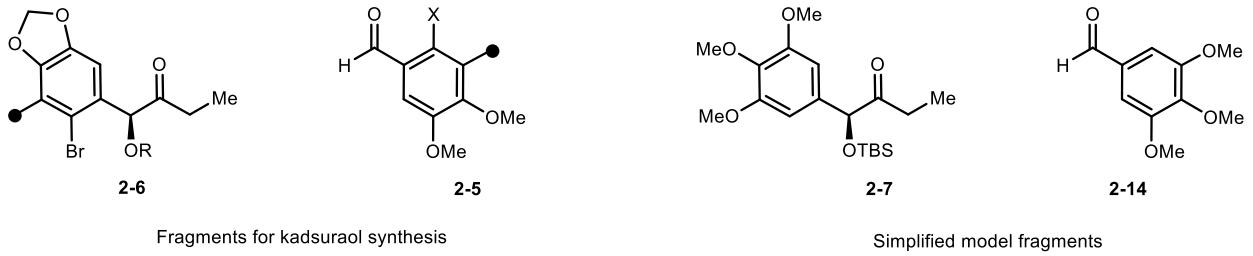


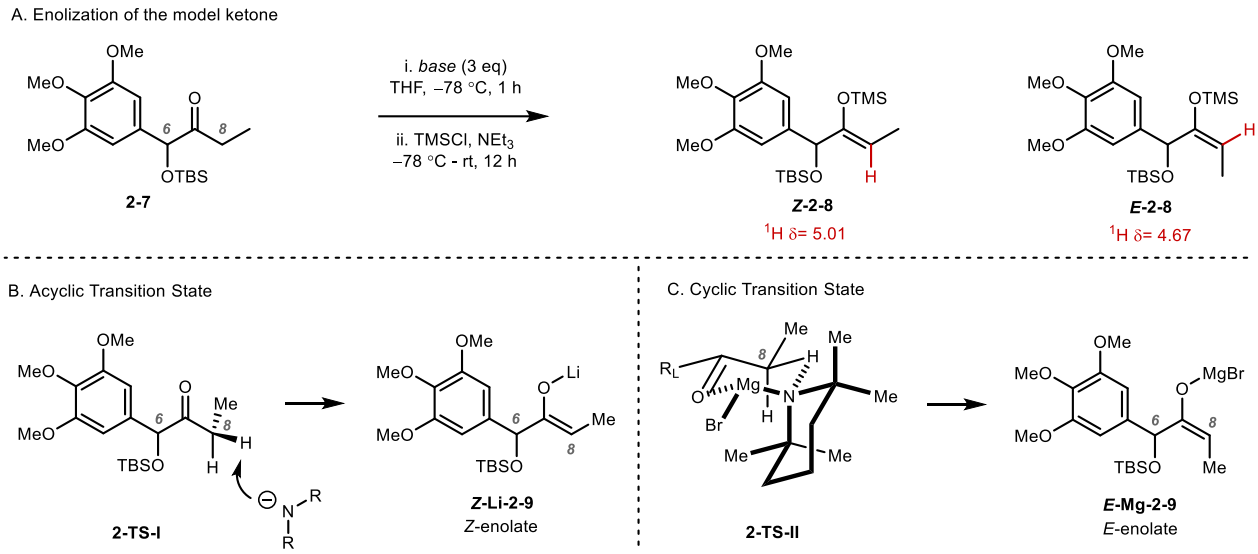
Figure 2.3. Model system for investigating the key steps of DBCOD synthesis

Aldol and methyl addition reactions have been used in our group's previous syntheses of DBCODs.[2] Section 2.1.2 describes work on a simplified racemic model system conducted by former graduate student Dr. Zheng Huang prior to his synthesis of these DBCODs. This system was used to investigate the stereochemical outcome of the key aldol and methyl addition steps. The rest of this chapter (2.2–2.6) describes another model system (**2-7** and **2-14**) devised to investigate the key steps to be used in the syntheses of kadsuraol C and taiwanschirin B: alkylation or aldol coupling, methyl addition, and benzylic deoxygenation.

2.1.2. Previous work on model aldol and methyl addition systems

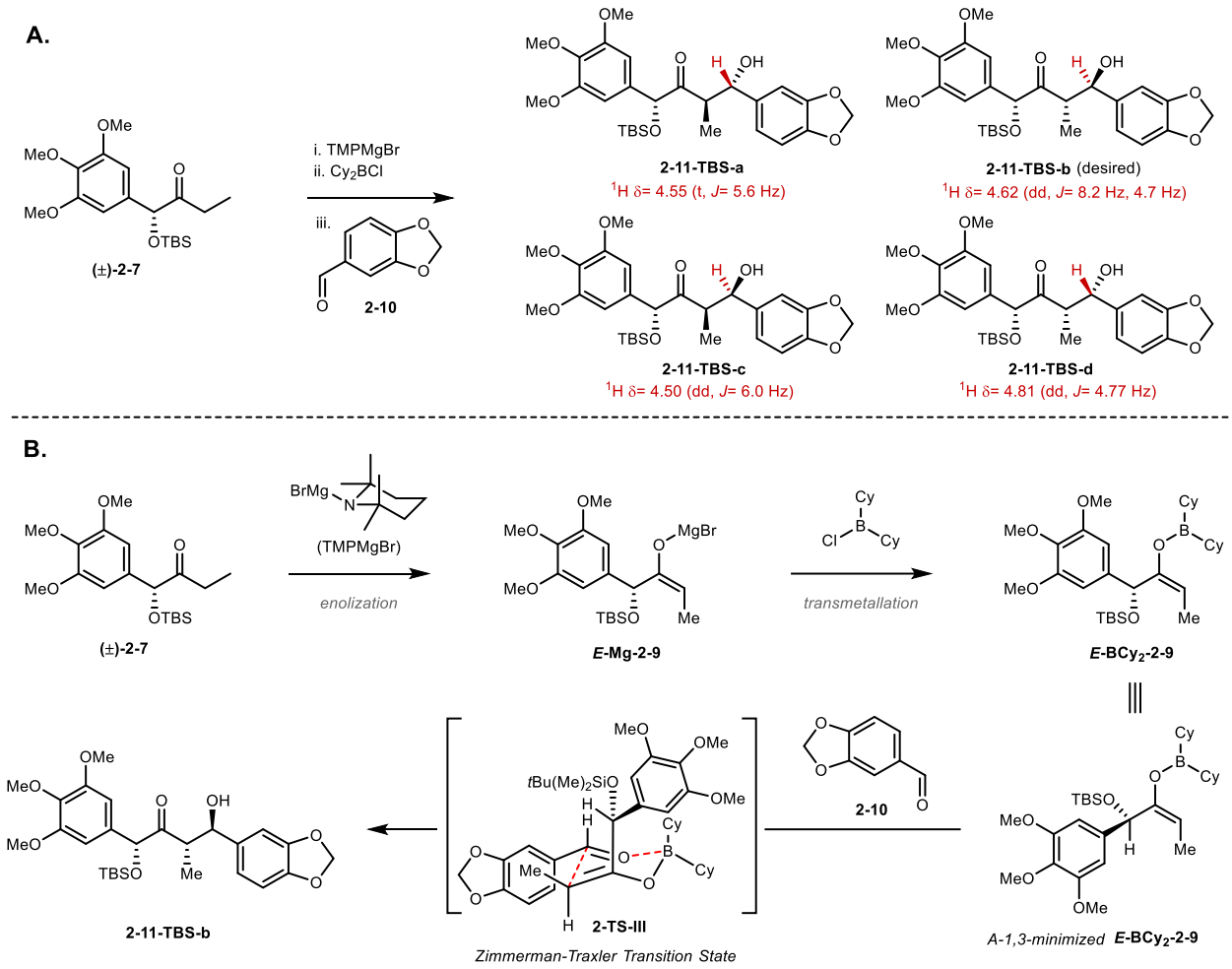
Before performing the aldol addition on functionalized coupling partners which take several steps to prepare, acyclic stereocontrol in the aldol addition was investigated by a previous PhD student in our group, Zheng Huang, using a model ketone **2-7** (prepared in 3 steps) and piperonal (commercially available). The aldol diastereomer required for our DBCOD syntheses is the 1,3-*syn*-1,2-*anti* product. To achieve this diastereoselectivity, the (*E*)-enolate of ketone **2-7** was needed to give the 1,2-*anti* relationship via simple diastereocontrol. Induced diastereocontrol would be used to give the 1,3-*syn* relationship, however, 1,3-induction in aldol reactions is a subject which had only been reported in two prior studies[3,4] which utilize ketones bearing α-alkyl groups (*tert*-butyl or methyl) rather than α-aryl groups . Firstly, the enolization of the model ketone was studied by treatment with various bases classically used for enolization[5–7] and trapping as the silyl enol ether (Scheme 2.2A).[3] The (*Z*)-silyl enol ether could be identified by the diagnostic vinyl ^{1}H NMR signal at 4.67 ppm (q, 1H) and the (*E*)-silyl enol ether by the vinyl proton signal at 5.01 ppm (q, 1H). Formation of the (*Z*)-enolate proceeded through an open transition state as steric

interactions between the C8 methyl group and the C6 stereocenter of the ketone led to **2-TS-I** being favored (Scheme 2.2B). The (*E*)-enolate was formed via a closed transition state (**2-TS-II**) where the bulky methyl substituents of 2,2,6,6-tetramethylpiperidine ensured an equatorial orientation for the C8 methyl group (Scheme 2.2C). LHMDS proved to be the superior base for producing the (*Z*)-enolate (99:1 *dr*) and TMPMgBr for obtaining the (*E*)-enolate (22:1 *dr*).



Scheme 2.2. Enolization studies on the model ketone **2-7**

The aldol reaction of the (*E*)-enolate with piperonal was then investigated. Treatment of racemic **2-7** with TMPMgBr followed by the addition of piperonal (**2-10**) gave a mixture of all four possible diastereomeric aldol products (yields of 17 % **2-11-TBS-a**, 13 % **b**, 8 % **c**, and 10 % **d**, Scheme 2.3A) as well as recovered **2-7** (14 %). The assignment of the relative stereochemistry of the different diastereomers was initially based on the ^{1}H NMR spectra and later confirmed by X-ray crystallography of **a** and **b**. The ^{1}H NMR signal used to distinguish each diastereomer was the C9 proton which had a distinctive chemical shift in the range of 4.5–4.8 ppm (Scheme 2.3A). The diverse mixture of products obtained implies that the aldol reaction using the Mg-enolate could be going through an open transition state with poor diastereocontrol and/ or that the aldol addition is reversible. The *dr* could be improved dramatically (5**b**: 1**a**) by incorporating a stereoretentive transmetallation of the (*E*)-Mg-enolate with Cy_2BCl to furnish the (*E*)-boron-enolate prior to the addition of piperonal. An (*E*)-B-enolate is expected to go through a tight 6-membered transition state, providing good diastereoselectivity in the aldol reaction.[3] After transmetallation, the faces of the boron enolate's π-plane are differentiated by allylic 1,3-strain between the α-stereocenter

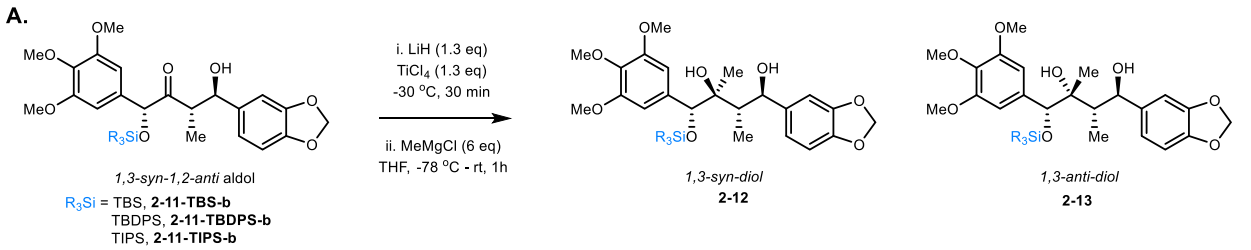


Scheme 2.3. Aldol reaction using TMPMgBr on the ketone **2-7**; A) Potential diastereomers of aldol product; B) Intermediates and chair transition state leading to **2-11-TBS-b**.

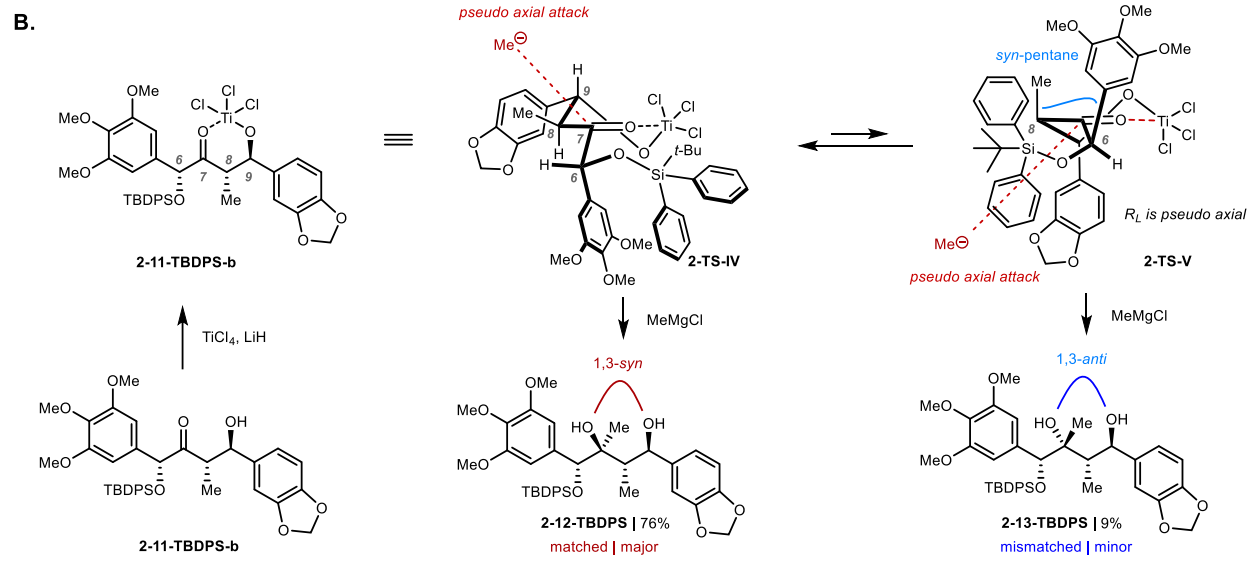
and the allylic methyl group, leading to a preferred conformation of the enolate, ***E*-BCy$_2$-2-9**. The aldehyde will favor approaching ***E*-BCy$_2$-2-9** from the face furthest away from the largest α-substituent (R_L, the aryl ring), when R_L is placed perpendicular to the plane (Scheme 2.3B). Of the α-substituents, the aryl group is larger than the OTBS group, leading to the closed Zimmerman-Traxler transition state **2-TS-III**. The stereochemistry of the (*E*)-enolate is translated to the 1,2-*anti*-stereochemistry of C8 and C9 in the desired product. The 1,3-*syn* stereochemistry of C6 and C8 results from the approach of the aldehyde to the Pro-*S* face of the enolate. The combination of these two factors result in the major stereoisomer produced being **2-11-TBS-b**. A screen of α-siloxy groups on the ketone found that TIPS offered even superior *dr* to TBS (20:1 **b**:**a**). The yield

of the desired aldol diastereomer also increased from 64 % using the TBS-protected substrate to 77 % using the TIPS-protected analogue.

Nucleophilic methyl addition to the ketone of the aldol was also optimized on this model system, using conditions developed by Bartoli,[8] which first involve chelation of $TiCl_4$ to the β-hydroxy ketone, followed by stereoselective addition of methyl magnesium chloride to the ketone. The observed diastereoselectivity is consistent with a larger silyl group disfavoring methyl addition from half-chair **2-TS-V** (giving the minor diastereomer) as this pathway would necessitate the methyl nucleophile eclipsing with the silyl group as it approached the carbonyl (Scheme 2.4B). The anticipated lowest energy Ti-chelate would adopt a half-chair conformation, placing the



Entry	Substrate	Conversion (%)	Yield (%) *1,3-syn-diol*	Yield (%) *1,3-anti-diol*	*dr*
1	**2-11-TBS-b**	100	70	22	3.2 :1
2	**2-11-TBDPS-b**	100	76	9	8.4 :1
3	**2-11-TIPS-b**	85	63	12	5.3: 1



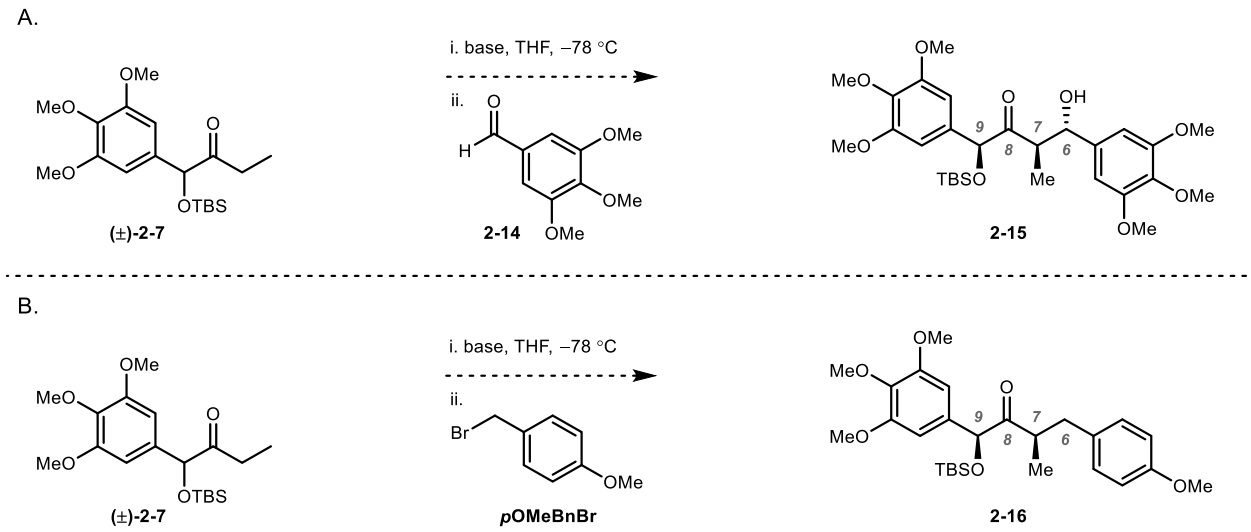
Scheme 2.4. A) Methyl addition on model substrates varying the α-siloxy group. B) Explanation of the stereochemical outcome of the chelate-controlled methyl addition.

aromatic and methyl substituents at C9 and C8 in equatorial positions as well as the α-stereocenter bearing the siloxy pointed away from the reactive center (**2-TS-IV**). This would permit an "allowed" Felkin-Ahn pseudo-axial attack of the methyl nucleophile along the Burgi-Dunitz trajectory to occur, resulting in product **2-12-TBDPS**, in 76 % yield, where a 1,3-*syn* relationship is observed between the newly formed alcohol and the existing benzylic alcohol. The disfavored transition state, a half-chair that places both aryl and methyl substituents into pseudo-axial positions at C8 and C9, incurring an unfavorable *syn*-pentane interaction, would give the minor product, the 1,3-*anti*-diol (**2-13-TDBPS,** 9 %).

Acyclic stereocontrol was then further investigated in the current work, using the model ketone **2-7** with a different model aldehyde (**2-14**, Figure 2.3) or benzyl halide in either an aldol coupling or alkylation reaction. The subsequent chelate-controlled methyl addition was performed on the model aldol products. Another key step in the syntheses of kadsuraol C and taiwanschirin B is a benzylic deoxygenation, performed to remove the additional C6 oxygenation introduced during the aldol coupling, which was also investigated on the model system.

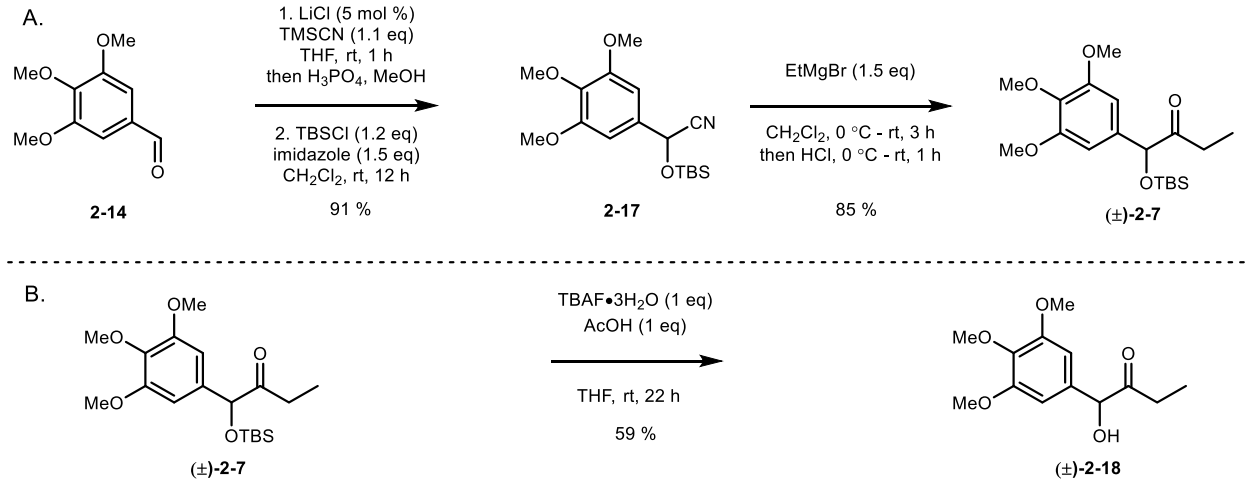
2.2. Fragment coupling by alkylation or aldol reaction

In the current work, it was expected that the fragment coupling step in our DBCOD syntheses could be accomplished by either an aldol addition or the alkylation of a ketone with a benzyl bromide. The aldol addition has the advantage that it has been previously studied in our group as the first step in the synthesis of DBCODs. However, our targets kadsuraol C and taiwanschirin B bear a methylene at C6, whereas the product of an aldol addition would bear a hydroxyl group at this position, necessitating deoxygenation at a later step. Alkylation could prove a more direct route to setting the desired stereocenters along the alkyl chain. Both methods were explored on a model system consisting of racemic ketone **2-7** and an aldehyde (**2-14**) or benzyl halide (eg. *p*OMeBnBr) coupling partner (Scheme 2.5).



Scheme 2.5. Fragment coupling via A) aldol addition or B) alkylation reaction

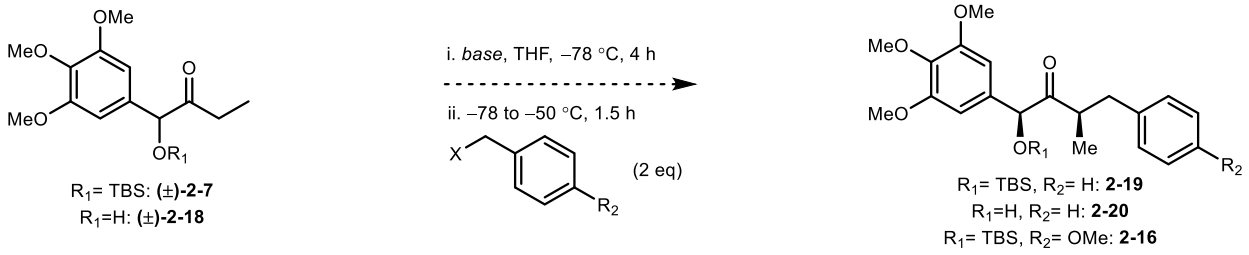
The ketone (±)**-2-7** was prepared following the reported procedure (Scheme 2.6). 3,4,5-Trimethoxybenzaldehyde (**2-14**) was subjected to hydrocyanation followed by protection of the resulting alcohol with TBS, providing silyl cyanohydrin **2-17** in 91 % yield over two steps (Scheme 2.6A). **2-17** was then treated with ethylmagnesium bromide to give the Grignard product (±)**-2-7**. The benzylic alcohol analogue (±)**-2-18** was also prepared (in 59 % yield) by deprotection of the silyl group of **2-7** using TBAF•3H_2O (Scheme 2.6B).

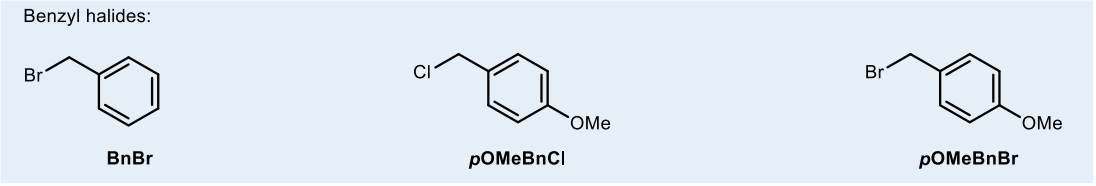


Scheme 2.6. Syntheses of ketones A) (±)**-2-7** and B) (±)**-2-18**

The alkylation strategy promised a shorter synthetic route, therefore this method was investigated first. This approach involved treatment of the ketone **2-7** with base to give the enolate, followed

by addition of a benzyl halide, with the expectation of forming a linear substrate bearing stereocenters at C9 and C7 (**2-19**, **2-20**, or **2-16**, Table 2.1). Benzyl bromide (BnBr), 4-methoxy benzyl chloride (*p*OMeBnCl), and 4-methoxy benzyl bromide (*p*OMeBnBr) were selected as the benzyl halides for use in this study as they could either be purchased or prepared in one step from commercially available starting materials. **2-7** was subjected to conditions developed by Palomo and coworkers for the alkylation of α-hydroxy ketones.[9] They found that LDA worked well for alkylation with alkyl iodides and that KHMDS was a more suitable base for alkylation with alkyl bromides. Therefore, the ketone was treated with KHMDS (2.3 eq) in THF at -78 °C for 4 h, followed by addition of the alkylating agent (2 equiv.), and warming to -50 °C for 1.5 h. Both (±)-**2-7** and its benzylic alcohol analogue (±)-**2-18** were subjected to these conditions, employing BnBr as the alkylating agent (Table 2.1, entries 1–2), however both reactions yielded a complex mixture of products, which could be the result of poor regioselectivity (enolate geometry) and/ or chemoselectivity (*O*- vs. *C*-alkylation). Next, the same alkylation procedure was applied to the coupling of (±)-**2-7** with either *p*OMeCl or *p*OMeBr (entries 3–4), once again yielding complex mixtures, with the former reaction not going to completion. In entries 5–8, the use of the Li-enolate instead of the K-enolate was investigated briefly, prepared using either LHMDS or LDA.



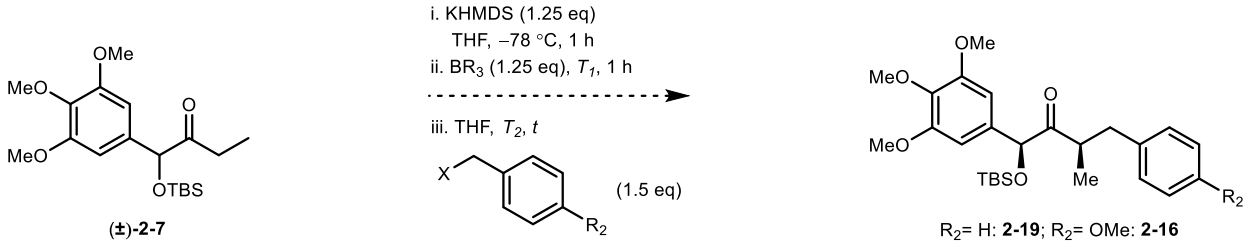


Entry	Ketone	Base (eq)	Benzyl halide	Result
1	(±)-**2-7**	KHMDS (2.3)	BnBr	complex mixture
2	(±)-**2-18**	KHMDS (2.3)	BnBr	complex mixture
3	(±)-**2-7**	KHMDS (2.3)	*p*OMeBnCl	complex mixture including SM
4	(±)-**2-7**	KHMDS (2.3)	*p*OMeBnBr	complex mixture
5	(±)-**2-7**	LHMDS (3)	*p*OMeBnBr	rec. SM
6	(±)-**2-7**	LDA (3)	*p*OMeBnBr	rec. SM
7	(±)-**2-7**	LHMDS (3)	*p*OMeBnCl	rec. SM
8	(±)-**2-7**	LDA (3)	*p*OMeBnCl	rec. SM

Table 2.1. Alkylation attempts on ketones (±)-**2-7** and (±)-**2-18** with benzyl halides

Alkylation of the Li-enolate was attempted with either *p*OMeCl or *p*OMeBr, however all four combinations of these conditions only returned starting materials under these conditions.

Negishi and coworkers have reported the α-alkylation of ketones by treatment of the potassium enolates with trialkylboranes, giving the potassium enoxytrialkylborates, which react with alkyl halides with high selectivity.[10] These conditions were applied to (±)-**2-7**, which was deprotonated by treatment with KHMDS (1.25 equiv.) at -78 °C for 1 h, then treated with BEt_3 (1.25 equiv.) and warmed to 0 °C for 1 h, followed by treatment with BnBr or *p*OMeBnBr (1.5 equiv.) for another 1 h (Table 2.2, entries 1–2). Neither displayed reactivity, thus the temperature was increased to rt

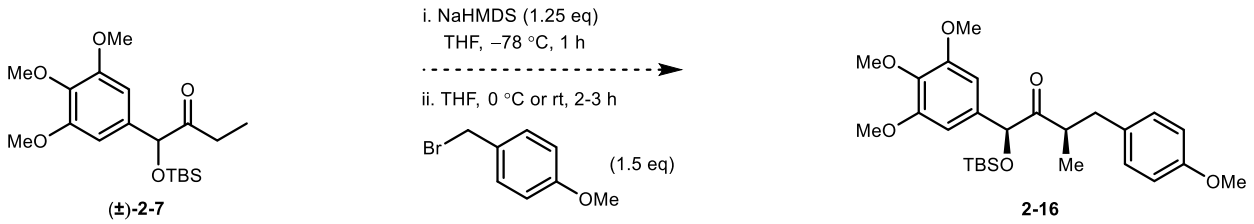


Entry	BR_3	T_1 (°C)	Benzyl halide	T_2, t	Result
1	BEt_3	0	BnBr	0 °C, 1 h	rec. SM
2	BEt_3	0	*p*OMeBnBr	0 °C, 1 h	rec. SM
3	BEt_3	rt	*p*OMeBnBr	rt, 1 h	rec. SM
4	BEt_3	rt	*p*OMeBnBr	0 °C, 1 h	rec. SM
5	BMe_3	0	*p*OMeBnBr	0 °C, 1 h + rt, 1 h	rec. SM

Table 2.2. Alkylation attempts on ketone (±)-**2-7** via the potassium enoxytrialkylborate

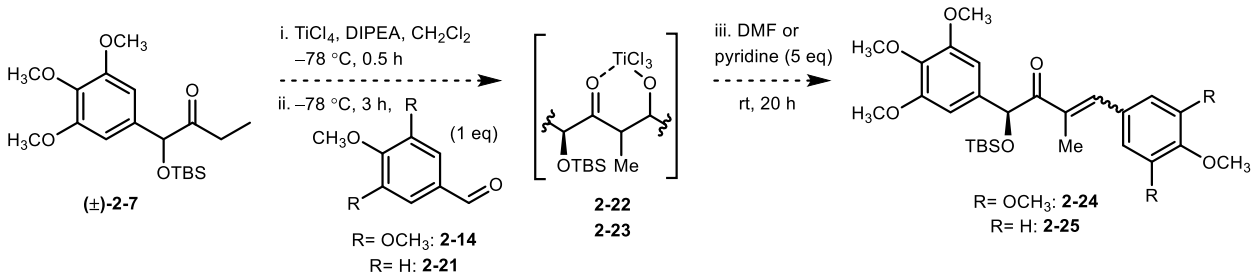
after the addition of BEt_3 and the *p*OMeBnBr addition step was run at either 0 °C or rt (entries 3–4). After increasing the temperature did not improve reactivity, the identity of the borane was modified instead, with BMe_3 being used in entry 5, giving only recovered starting material.

Considering the lack of selectivity in alkylation from the potassium enolate, and the dearth of reactivity of the lithium enolates or potassium enoxytrialkylborates, another base was selected for deprotonation. This time, treatment with NaHMDS (1.25 equiv.) at -78 °C for 1 h was utilized to prepare the Na-enolate of (±)-**2-7**, followed by the addition of *p*OMeBnBr with warming to either 0 °C or rt and reacting for 2–3 h at this temperature (Scheme 2.7). In both reactions, decomposition occurred.



Scheme 2.7. Alkylation attempts on ketone **(±)-2-7** using NaHMDS

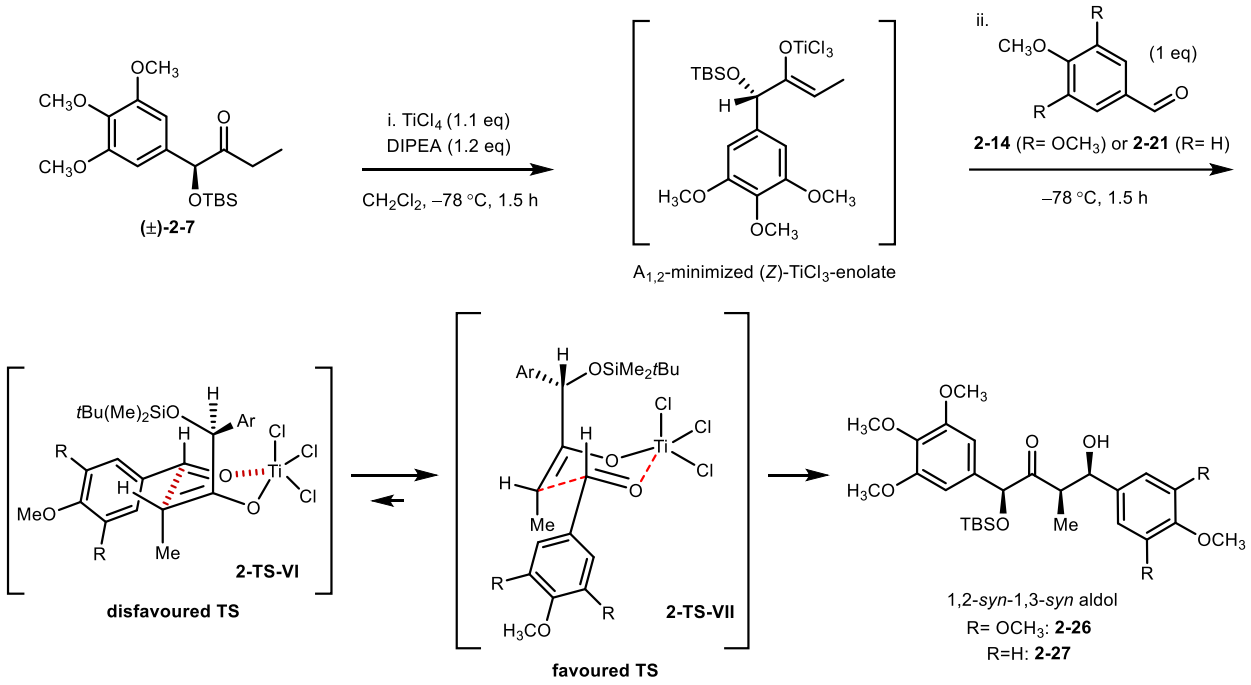
Due to the difficulty of alkylating ketone **(±)-2-7** selectively, the second fragment coupling strategy (via aldol reaction) was investigated. The first method explored was an aldol condensation, as this would alleviate the need to perform a benzylic deoxygenation as a later step (although an additional hydrogenation step would be required in lieu). Conditions reported by Sugiuara and coworkers were applied,[11] involving a $TiCl_4$-promoted aldol addition between ketone **(±)-2-7** and commercially available aldehydes **2-14** or **2-21**, followed by addition of an additive (DMF or pyridine) to facilitate the elimination of the titanoxy group from the Ti-aldolate **2-22** or **2-23**, providing the α,β-unsaturated ketone **2-24** or **2-25**. When **2-21** was employed as the aldehyde and DMF (5 equiv.) as the additive, the aldol addition appeared to have occurred, yielding a mixture of diastereomeric products, but the subsequent elimination did not proceed. When **2-14** was used as the aldehyde and pyridine (5 equiv.) as the additive, the condensation product **2-24** appeared to have formed based on the ^{1}H NMR spectrum, however it coeluted with residual **2-14** and was not pure. Considering the product yield would be less than 43 %, purification was not pursued, and a higher yielding aldol addition method was sought instead.



Scheme 2.8. Aldol condensation attempt between **(±)-2-7** and **2-14** or **2-21**

Next, aldol additions were explored. **(±)-2-7** was treated with Evans' conditions of $TiCl_4$ and DIPEA at -78 °C for 1.5 h to produce the (*Z*)-Ti-enolate, to which aldehyde **2-14** or **2-21** were added, stirring at -78 °C for another 1.5 h (Scheme 2.9).[12] The reaction with **2-21** did not go to completion (a mixture of starting materials and a new species were detected by ^{1}H NMR), whereas

the reaction with **2-14** did go to completion, providing the 1,2-*syn*-1,3-*syn* aldol **2-26** in 73 % yield and 10:1 *dr*. The 1,2-*syn* relationship is conferred from the enolate geometry, which is formed regioselectively as the (*Z*)-isomer. The 1,3-*syn* relationship is the result of the aldehyde approaching the face of the $A_{1,2}$-strain minimized Ti-enolate furthest away from the aryl ring (that is, the Pro-*R* face of the enolate), proceeding through the chair-like transition state **2-TS-VII**. The disfavored transition state, **2-TS-VI** would give the minor diastereomer, the 1,2-*syn*-1,3-*anti* aldol. The stereochemical outcome of the reaction was further confirmed by comparison to the ^{1}H NMR spectrum of 1,2-*syn*-1,3-*syn*-aldol **2-11-TBS-d** (see section 2.1.2), which had a distinctive C9 proton signal at 4.81 ppm (dd, *J*= 4.7 Hz). **2-26** had a C9 proton signal of 4.87 (d, J= 3.2 Hz) which compared favorably. As the aldehyde **2-14** reacted more rapidly than **2-21**, it was selected for use in the subsequent studies of aldol additions.

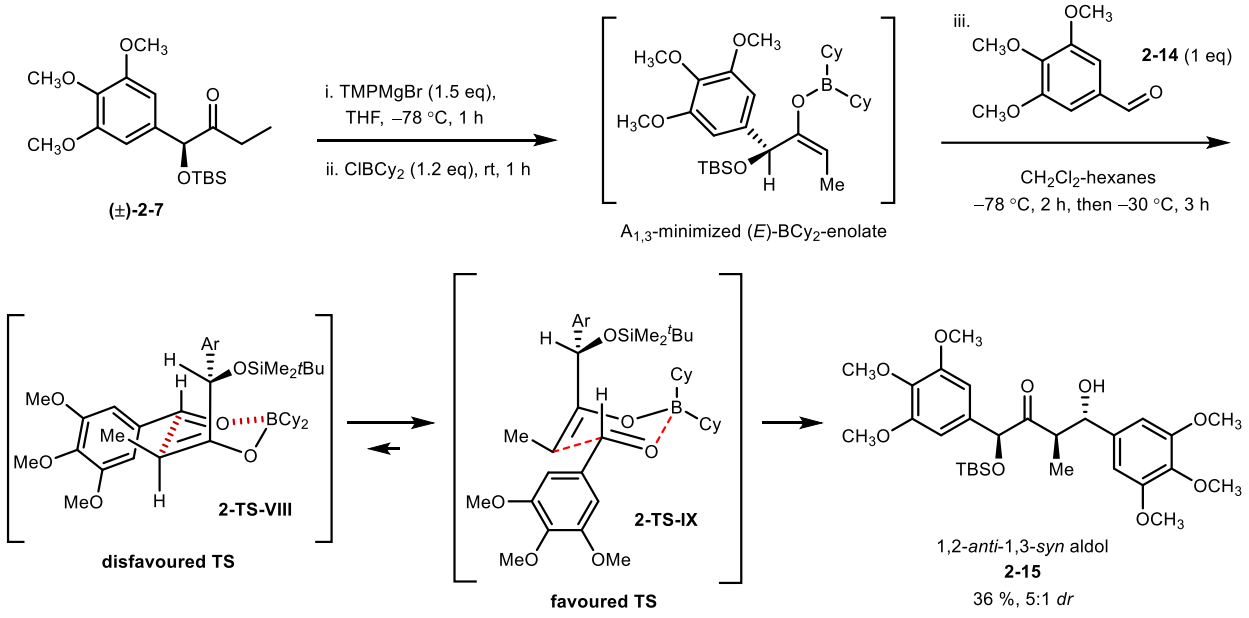


Scheme 2.9. Aldol addition giving the 1,2-*syn*-1,3-*syn* aldol **2-26**

The subsequent methyl addition step will preferentially give the 1,3-*syn* diol product (*vide infra*), therefore a 1,2-*syn*-1,3-*syn*-aldol (eg. **2-26**) and 1,2-*anti*-1,3-*syn* aldol would be expected to produce opposite stereocenters at C8. It would be valuable to have access to both C8 diastereomers later in the synthesis for a couple reasons: one diastereomer may undergo Suzuki coupling more readily than the other and one diastereomer may undergo transannular radical cyclization more

readily once the C8 alcohol is converted to a radical progenitor. For this reason, we also sought to prepare the 1,2-*anti*-1,3-*syn* aldol **2-15**.

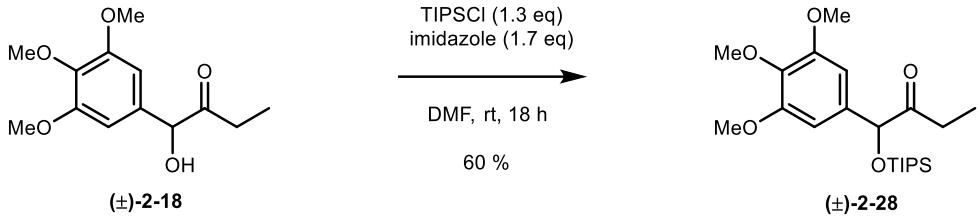
(±)-2-7 was treated with the conditions previously developed in our group for the synthesis of 1,2-*anti*-1,3-*syn* aldols (see Scheme 2.3). First, **(±)-2-7** was stirred with TMPMgBr at −78 °C for 1 h to provide the (*E*)-Mg-enolate, followed by the addition of Cy_2BCl with stirring at rt for 1 h to afford the (*E*)-B-enolate (Scheme 2.10). Aldehyde **2-14** was then added to the reaction mixture, stirring at −78 °C for 2 h and then warmed to −30 °C for 3 h, giving the 1,2-*anti*-1,3-*syn* aldol **2-15** in 36 % yield with 5:1 *dr*. The 1,2-*anti* relationship is conferred from the enolate geometry, which is formed regioselectively as the (*E*)-isomer. The 1,3-*syn* relationship is the result of the aldehyde approaching the Pro-*R* face of the boron-enolate, proceeding through the Zimmermann-Traxler transition state **2-TS-IX**. The disfavoured transition state **2-TS-VIII** leads to the minor diastereomer, the 1,2-*anti*-1,3-*anti* aldol. The stereochemical outcome of the reaction was further confirmed by comparison to the ^{1}H NMR spectrum of 1,2-*anti*-1,3-*syn*-aldol **2-11-TBS-b** (see section 2.1.2), which had a distinctive C9 proton signal at 4.62 ppm (dd, *J*= 8.2 Hz, 4.7 Hz). **2-15** had a C9 proton signal of 4.59 ppm (d, J= 8.6 Hz) which compared favorably.



Scheme 2.10. Aldol addition giving the 1,2-*anti*-1,3-*syn* aldol **2-15**

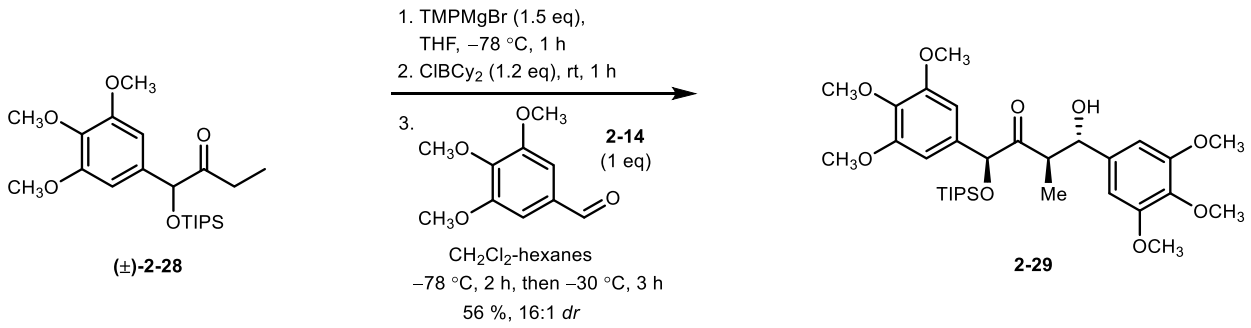
In our group's previous study of the aldol addition between **(±)-2-7** and piperonal, it was found that both the *dr* and the yield of the desired aldol diastereomer could be improved by replacing the

TBS protecting group of (±)-**2-7** with a TIPS group. Despite it not being entirely clear why a larger α-siloxy group lead to a superior result, we sought to employ this TIPS-protected ketone in our current model aldol system to see if any improvement could be offered. The TIPS-protected substrate, **2-28**, was prepared by first deprotecting the TBS group of (±)-**2-7** via treatment with TBAF•3H_2O to give the alcohol **2-18** (see Scheme 2.6B) and then stirring with triisopropylsilyl chloride and imidazole in DMF overnight to give **2-28** in 60 % yield (Scheme 2.11).



Scheme 2.11 Synthesis of the TIPS-protected ketone **2-28**

The TIPS-protected ketone **2-28** was subjected to our conditions for preparing a 1,2-*anti*-1,3-*syn* aldol, employing TMPMgBr, $ClBCy_2$, and aldehyde **2-14** (Scheme 2.12). This resulted in both better diastereoselectivity and higher yield of the desired aldol diastereomer **2-29** (56 % yield, 16:1 *dr*) than observed when using the TBS-protected ketone **2-7**. The ^{1}H NMR spectrum of **2-29** was consistent with 1,2-*anti*-1,3-*syn* stereochemistry, having a C9 proton signal at 4.65 ppm (d, *J*= 8.6 Hz) which compared favorably to previously characterized 1,2-*anti*-1,3-*syn* aldols **2-11-TBS-b** and **2-15**.



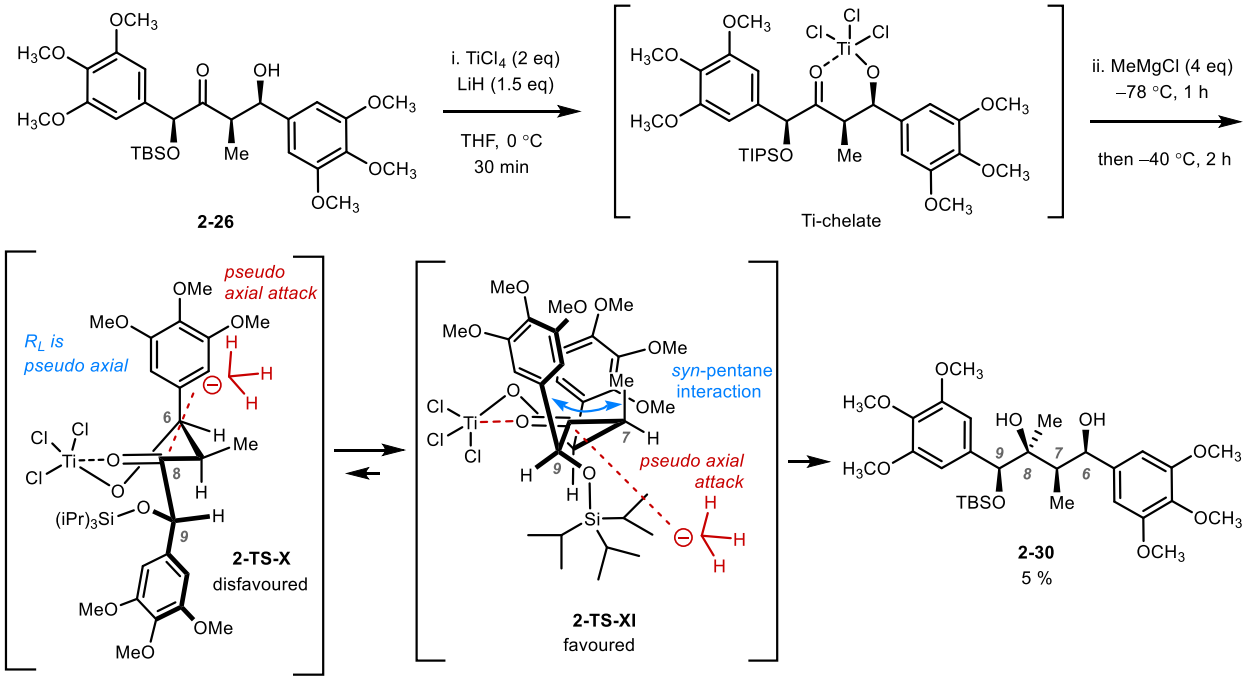
Scheme 2.12. Aldol addition giving the 1,2-*anti*-1,3-*syn* aldol **2-29**

2.3. Methyl addition

With a linear chain bearing three stereocenters (C6, C7, and C9) prepared during the aldol addition, the next transformation required was the stereoselective introduction of a methyl

nucleophile at C8, setting a fourth stereocenter. This would be done using the chelate-controlled methyl addition conditions developed by Bartoli,[8] which had been previously studied within our group. Although the C6 alcohol of our aldol substrate is not present in the DBCOD products taiwanschirin B or kadsuraol C, it turned out to be useful to have in place during the methyl addition step, as $TiCl_4$ formed a 6-membered chelate with this alcohol and the C8 carbonyl. In fact, a large difference in the reactivity of the aldol substrates was observed depending on the stereochemistry at C6. The 1,2-*syn*-1,3-*syn* aldol **2-26** and 1,2-*anti*-1,3-*syn* aldol **2-29** prepared in section 2.2 were both submitted to these conditions in order to obtain both C8 diastereomers.

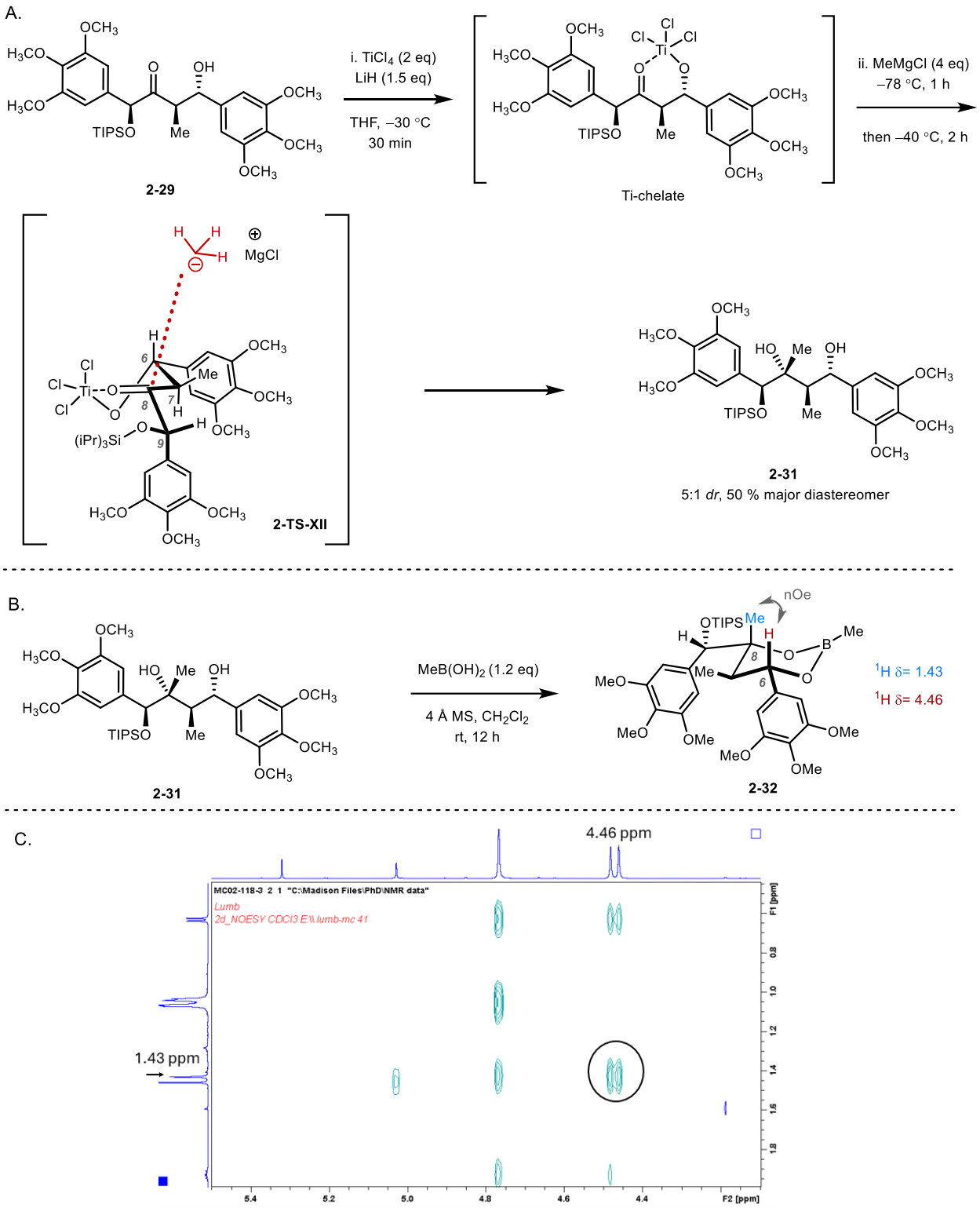
The 1,2-*syn*-1,3-*syn* aldol **2-26** was subjected to the chelate-controlled methyl addition conditions first (Scheme 2.13), returning a very poor yield of product (5 %) as well as recovered starting material (48 %). From analysis of the favored half-chair transition state (**2-TS-XI**), the expected product would be the 1,3-*syn* diol **2-30**, which bears the wrong stereochemistry at C8 from that which is desired in our DBCOD syntheses. The poor yield can be explained by looking at **2-TS-XI**, where the methyl substituent at C7 must be placed into a pseudo axial position, leading to a *syn*-pentane interaction and where the orientation of the silyl ether at C9 partly blocks the trajectory of nucleophilic attack. The alternative transition state (**2-TS-X**) would place the aryl substituent at



Scheme 2.13. Methyl addition on the 1,2-*syn*-1,3-*syn* aldol **2-26**

C6 into a *pseudo*-axial position, which would be even more disfavorable.

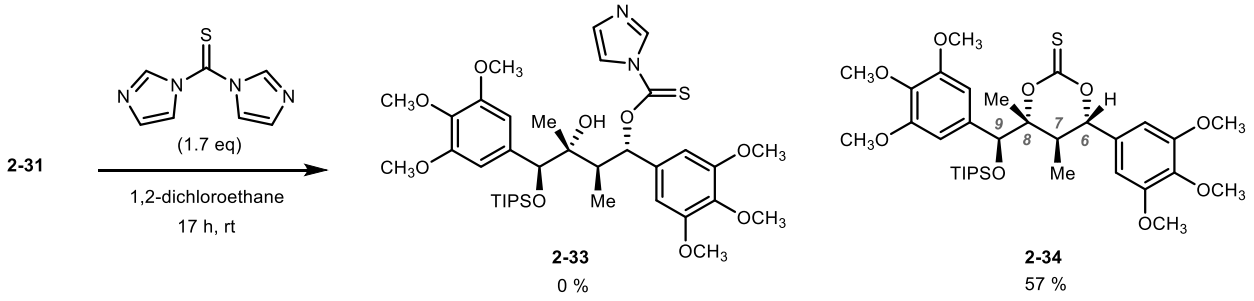
The 1,2-*anti*-1,3-*syn* aldol **2-29** was then subjected to the same chelate-controlled methyl addition conditions (Scheme 2.14A). The anticipated lowest energy Ti-chelate adopts a half-chair conformation, placing the aromatic and methyl substituents at C7 and C6 in equatorial positions as well as the α-stereocenter bearing the siloxy pointed away from the reactive center (**2-TS-XII**). This allows a Felkin-Ahn, pseudo-axial attack of the methyl nucleophile along the Burgi-Dunitz trajectory to occur unhindered, resulting in a product (**2-31**) where a 1,3-*syn* relationship is observed between the newly formed alcohol and the existing benzylic alcohol. Compound **2-31** bears the desired stereochemistry to carry forward in the synthetic route. The product was formed in 5:1 *dr*, where a 50 % yield of the major diastereomer could be isolated. The stereochemistry was confirmed by treating the diol of **2-31** with methyl boronic acid and running a NOESY experiment on the boronic ester product **2-32**, which showed a correlation between the C8 methyl group (1.43 ppm) and the C6 hydrogen (4.46 ppm), indicating that they are on the same side of the molecule (Scheme 2.14B,C).



Scheme 2.14. A. Methyl addition on the 1,2-*anti*-1,3-*syn* aldol **2-29**; B. Confirmation of the diol stereochemistry via formation of the boronic ester and nOe; C. NOESY spectrum of **2-32**

2.4. Benzylic deoxygenation

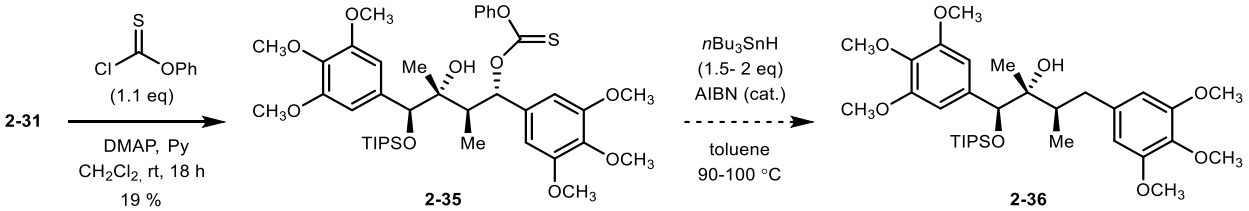
After serving its role to direct the stereochemical outcome of the chelate-controlled methyl addition, the unwanted C6 alcohol could be removed. It was expected that the secondary alcohol could be converted to the corresponding methylene using a Barton–McCombie deoxygenation. This method required first appending a Barton ester (eg. thionocarbonate or thiocarbamate), then treatment with tributyltin hydride, azobisisobutyronitrile (AIBN), and heat to homolytically cleave the C6-O bond. Conditions reported by Shibatomi and coworkers[13] were applied to the methyl addition product **2-31** in an attempt to form the imidazyl thiocarbamate **2-33**. **2-31** was treated with 1,1'-thiocarbonyldiimidazole (1.7 equiv.) in 1,2-dichloroethane at rt for 17 h and then analyzed by ^{1}H NMR. The starting material was fully consumed and the H6 and H7 signals had shifted downfield, however new signals corresponding to an imidazyl group were not observed. Based on analysis of the ^{1}H NMR and LRMS spectra, the product formed was most likely the cyclic carbonothioate **2-34** (57 % NMR yield), the result of both secondary and tertiary alcohols attacking the thione.



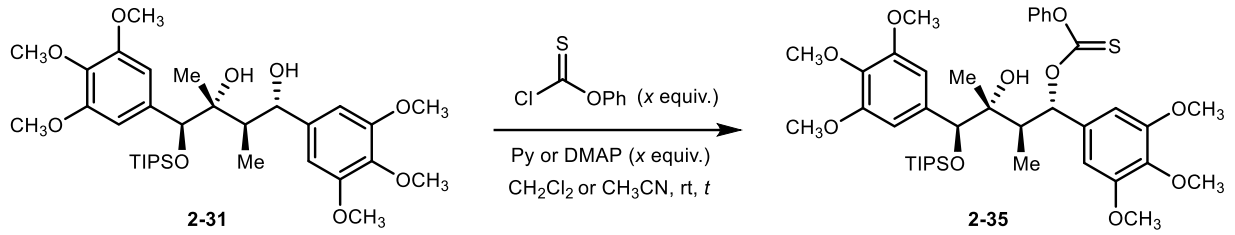
Scheme 2.15. Attempt at preparing the imidazyl thiocarbamate Barton ester **2-33**

Another Barton ester, the phenyl thionocarbonate **2-35**, was then targeted. **2-35** was prepared utilizing a procedure from Robins and coworkers,[14] which entailed treatment of the alcohol **2-31** with DMAP (0.5 equiv.), pyridine (3 equiv.), and phenylchlorothionoformate (1.1 equiv.) in CH_2Cl_2 (Scheme 2.16). The reaction proceeded slowly to provide a 19 % yield of the desired product after 18 h at rt, with recovery of starting material and a mixture of byproducts accounting for the mass balance. The reaction conditions (solvent, equivalents of phenylchlorothionoformate, equivalents of pyridine, and equivalents of DMAP) were screened (Table 2.3) and it was found that increasing the equivalents of phenylchlorothionoformate had the greatest impact, with 93–100 % consumption of starting material and NMR yields of 59–64 % observed when 5 equiv. of

phenylchlorothionoformate were used (along with either 3 equiv. Py in CH_2Cl_2 for 1 h or 5 equiv. DMAP in CH_3CN for 20 h, entries 6 and 9, respectively). The subsequent deoxygenation of **2-35** was attempted twice by treating it with tributyltin hydride (1.5 or 2 equiv.) and AIBN (catalytic) in toluene (0.03 or 0.06 M) at 90 or 100 °C for 20 h (Scheme 2.16), however these reactions yielded complex mixtures of products, in which the desired product **2-36** was not detected.



Scheme 2.16. Preparation of the phenyl thionocarbonate Barton ester and deoxygenation attempt



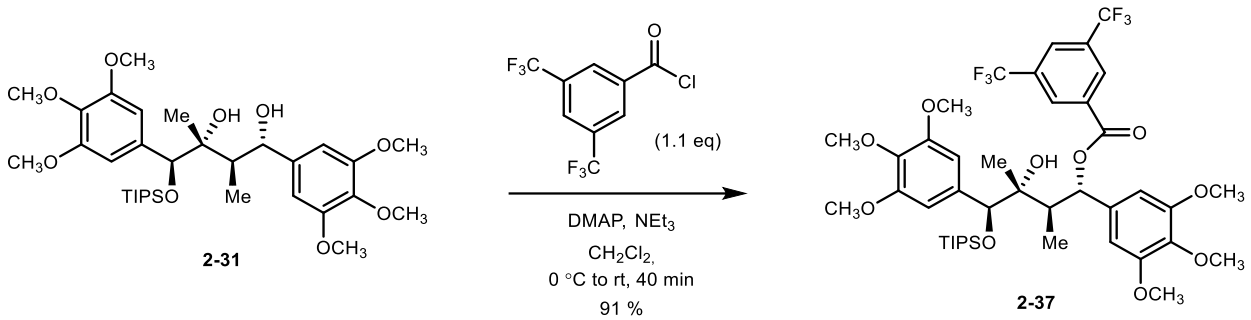
Entry	Time (h)	Equiv. ClC(S)OPh	Py or DMAP (equiv.)	Solvent	Consumption of **2-31** (%)[a]	Yield **2-35** (%)[a]
1	4.5	1	Py (3)	CH_2Cl_2	63	39
2	4.5	1	DMAP (2)	CH_3CN	51	35
3	4.5	1	Py (4)	CH_2Cl_2	63	33
4	4.5	1	DMAP (5)	CH_3CN	-	(1 **2-31**: 1 **2-35**)
5	1	2.5	Py (3)	CH_2Cl_2	100	44
6	1	5	Py (3)	CH_2Cl_2	100	59
7	4	2.5	DMAP (5)	CH_3CN	100	53
8	4	5	DMAP (5)	CH_3CN	61	42
9	20	5	DMAP (5)	CH_3CN	93	64

Reactions were performed on 0.05 mmol scale at room temperature, at a concentration 0.1 M (entries 2-9), under inert atmosphere.
a= as determined by ^1H NMR in $CDCl_3$, using hexamethylbenzene as internal standard.

Table 2.3. Optimization of the synthesis of phenyl thionocarbonate **2-35**

Considering the challenges with forming Barton esters in good yields and the failure of the Barton–McCombie deoxygenation of **2-35**, alternative deoxygenation conditions were sought. Reiser and coworkers have reported conditions for the visible light photoredox-catalyzed deoxygenation of benzylic alcohols via the 3,5-(bistrifluoromethyl)benzoate which avoid the use of toxic organotin reagents and elevated temperatures.[15] **2-31** was easily converted to the corresponding 3,5-

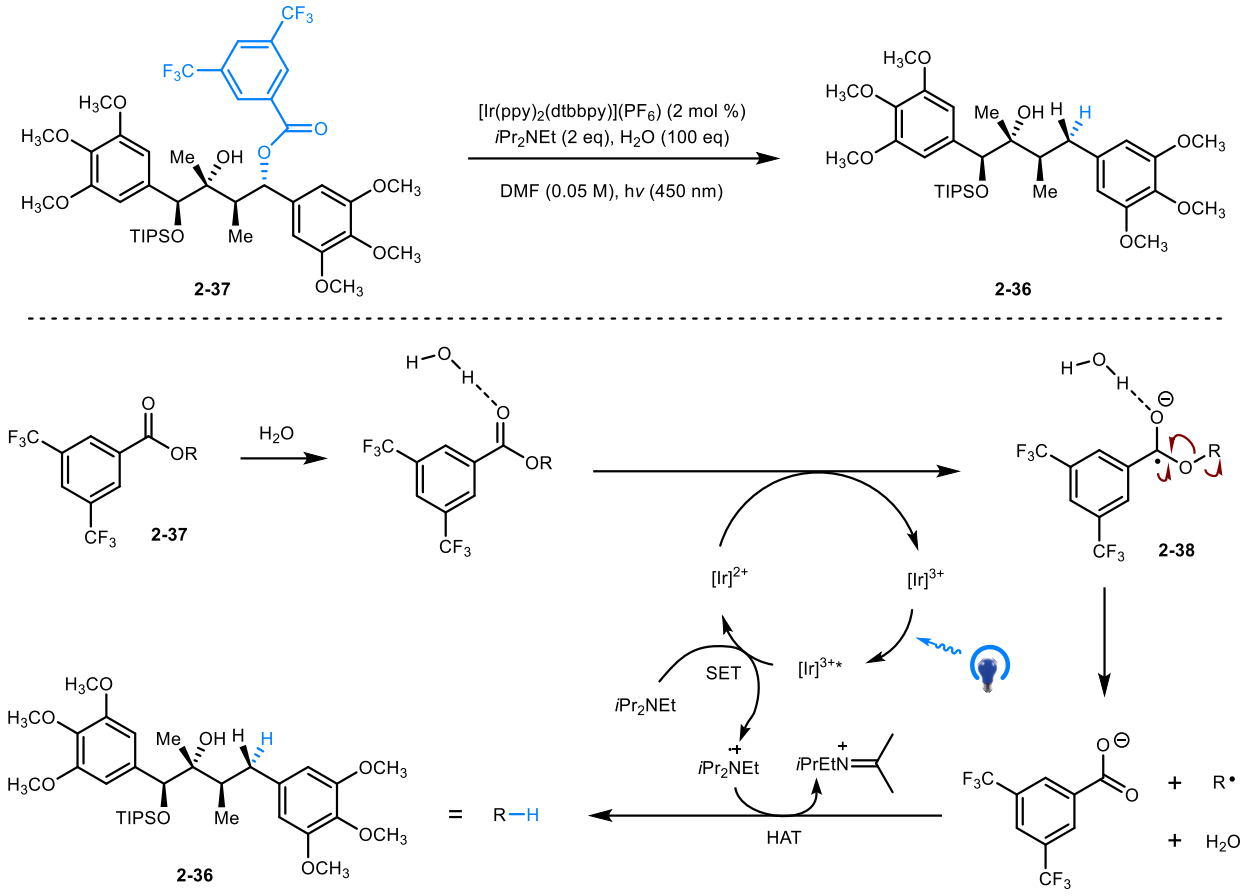
(bistrifluoromethyl)benzoate **2-37** in 91 % yield by treatment with 3,5-bis(trifluoromethylbenzoyl) chloride (1.1 equiv.), DMAP (5 mol %) and triethylamine (7 equiv.) in CH_2Cl_2 at rt for 40 minutes (Scheme 2.17).



Scheme 2.17. Preparation of the of the 3,5-(bistrifluoromethyl)benzoate **2-37**

The reported benzylic deoxygenation conditions employ $[Ir(ppy)_2(dtb\text{-}bpy)]PF_6$ (2 mol %) as photocatalyst, *i*Pr_2NEt (2 equiv.), and H_2O (100 equiv.) in acetonitrile (0.05 M) with irradiation by 455 nm LEDs at 40 °C for 1–16 h.[15] The anticipated mechanism of the deoxygenation of the active ester **2-37** to yield **2-36** is depicted in Scheme 2.18. Water likely plays a hydrogen bonding role, making the C6 ester a better electron acceptor for photoinduced electron transfer (PET), in an analogous manner to the activation of NHPI esters by water described by Glorius.[16] The Ir(III) photocatalyst is excited by blue light and the resulting Ir(III)* complex receives a single electron from DIPEA, resulting in an Ir(II) complex. This Ir(II) complex then donates an electron to the activated ester, giving a radical anion intermediate (**2-38**) and regenerating Ir(III). **2-38** undergoes fragmentation, to give 3,5-(bistrifluoromethyl)benzoate and the benzylic radical (R•). Hydrogen atom transfer (HAT) from the radical cation of DIPEA to R• results in the methylene-bearing product **2-36**.

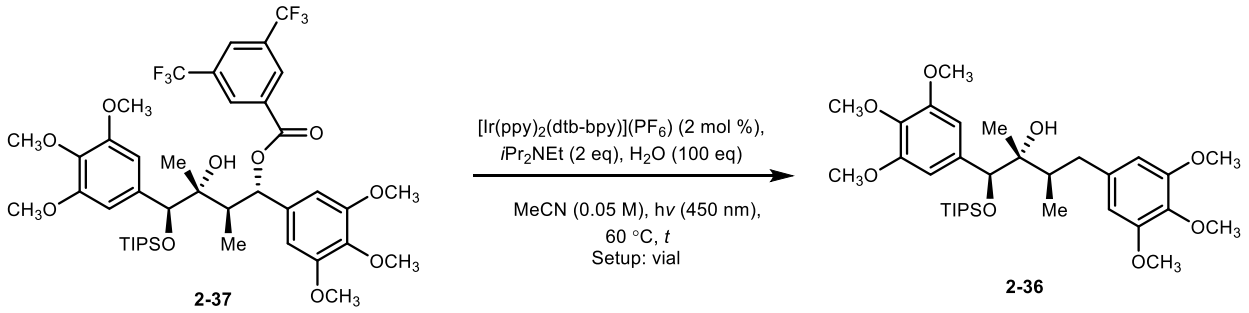
The reactions described in Table 2.4 were all run in a homemade photoreactor constructed from a 4-dram vial, capped with an upside-down 24/40 septum which had a hole cut in it to allow for the insertion of a 13×100 mm culture tube containing a 450 nm LED strip (Figure 2.4A). The gaps between parts were sealed with parafilm and electrical tape and nitrogen was introduced via a needle through the rubber septum. This setup allowed for irradiation from inside the reaction vessel with concomitant heating from outside via an oil bath. When subjected to the reported reaction conditions for 16 h, **2-37** displayed no reactivity (Table 2.4, entry 1). Increasing the reaction



Scheme 2.18. Proposed mechanism of visible light photoredox-catalyzed deoxygenation of **2-37**

temperature to 60 °C led to partial conversion of **2-37** (19 % recovered) to the desired product. Increasing the reaction time to 24 h did not offer any improvement in the consumption of **2-37**, giving worse results of 32 % recovered **2-37** and 37 % **2-36** (entry 3). It was found that the reaction time could be decreased to 4 h (entry 4), while providing a similar yield (51 %) to that observed after 16 h. Comparable % consumption of **2-37** and NMR yields were observed after 1 h (47 % consumption, 30 % yield) and 4 h (49 % consumption, 31 % yield), indicating that the reaction was mostly finished within the first hour, thus the following screening experiments were run for shorter periods of time (1–3 h). In addition to water's role of facilitating PET, Reiser *et al.* found that the addition of water to the reaction mixture greatly reduced the reaction time needed to reach full consumption, proposing that water protonates the intermediate radical anion, thus speeding up its fragmentation.[15] Therefore, in entry 5, twice as much water (200 equiv.) was added to the reaction mixture in attempts to improve consumption, however this did not have an effect, with 31 % **2-37** being recovered and 36 % **2-36** being isolated. Increasing the concentration of the reaction

mixture to 0.1 M or increasing the quantity of the sacrificial electron donor *i*Pr$_2$NEt to 3 equivalents did not improve reactivity either (entries 6–7). The addition of a hydrogen donor, Hantzsch ester, killed reactivity altogether with only **2-37** (45 %) being recovered (entry 8). Reiser *et al.* observed much higher yields when [Ir(ppy)$_2$(dtb-bpy)]PF$_6$ was employed as the photocatalyst rather than Ru(bpy)$_3$Cl$_2$•6H$_2$O, likely due to its higher reduction potential (E^0= -1.51 V vs E^0= -1.31 V vs. SCE), hence photocatalysts with even higher reduction potentials than [Ir(ppy)$_2$(dtb-bpy)]PF$_6$ were screened (entries 9–12). Ir(ppy)$_3$ (E^0= −1.73 V vs. SCE)[17] was utilized as the photocatalyst in entries 9–11, with either DMF or THF as the solvent, due to its poor solubility in acetonitrile. After 2 h reaction in DMF with Ir(ppy)$_3$, **2-37** was fully consumed although only a 45 % yield of **2-36** was isolated (entry 9). Decreasing the reaction time to 1 h led to incomplete consumption, with 9 % **2-37** being recovered and isolation of 35 % **2-36** (entry 10). No reactivity was observed with Ir(ppy)$_3$ in THF, with recovery of starting material (78 %, entry 11). A copper photocatalyst prepared by Collins and coworkers,[18] [Cu(BINAP)(dq)]BF$_4$ (E^0= −1.87 V vs. SCE), was also screened (entry 12), yielding quantitative recovery of **2-37**.



Entry	Time (h)	Variation from above conditions	Recovered **2-37** (%)	Isolated Yield **2-36** (%)
1	16	40 °C	quant.	0
2	16	-	19	56
3	24	-	32	37
4	4	-	35	51
5	2	200 eq. H_2O	31	36
6	2	0.1 M	36	28
7	2	3 eq *i*Pr$_2$NEt	57	37
8	3	added Hantzsch ester (1 eq)	45	0
9	3	Ir(ppy)$_3$, DMF	0	45
10	1	Ir(ppy)$_3$, DMF	9	35
11	1	Ir(ppy)$_3$, THF	78	0
12	2	[Cu(BINAP)(dq)]BF$_4$	quant.	0

Reactions were run on 0.5-0.8 mmol scale

Table 2.4. Screening deoxygenation conditions for the 3,5-(bistrifluoromethyl)benzoate **2-37**

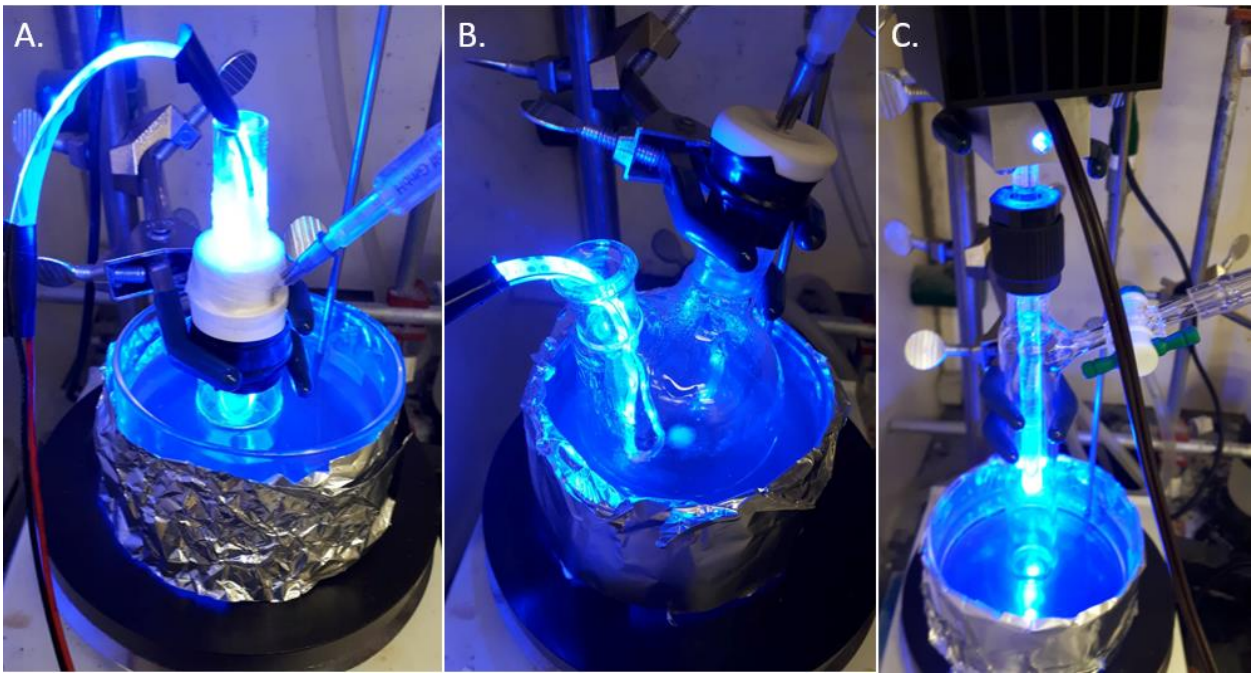
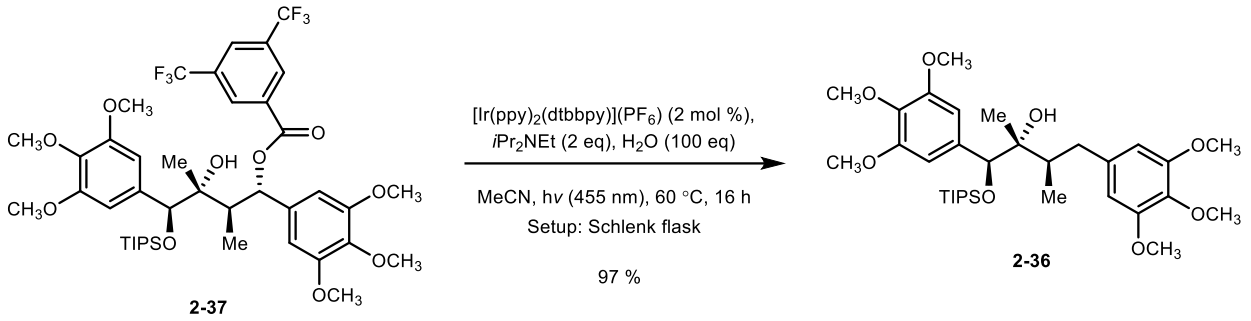


Figure 2.4. Reactor setups for photoredox-catalyzed benzylic deoxygenation: A. vial; B. thermowell flask; C. Schlenk flask

Incomplete consumption of starting material and inconsistent reproducibility were observed even under the best conditions (Table 2.4. entries 2, 4), which led us to suspect that the presence of O_2 played a role in reactivity. The homemade vial reactor (Figure 2.4A) was most likely not airtight, therefore alternative reactors were built to attain better oxygen exclusion. The second reactor was constructed from a 100 mL thermowell flask, with a 450 nm (12 V, 2 A) LED strip inserted into the internal side arm and the joint sealed with a rubber septum and electrical tape (Figure 2.4B). The reaction mixture was freeze-pump-thawed (x 5) before reacting in this flask under the best conditions overnight, returning only starting material (88 %), which indicated that this reactor was also insufficiently air-tight. The third reactor was constructed from a 50 mL screw cap Schlenk flask and a glass rod with a polished end inserted through the cap (see Figure 2.4C and Experimental section 2.6.2.). A 455 nm LED with a heat sink and constant current power supply (set to 410 mA) was placed on top of the glass rod to irradiate the reaction mixture from above. This third reactor proved to be sufficiently air-tight, as a reaction mixture which was freeze-pump thawed (x 5) and run in this setup using the best conditions furnished the desired deoxygenation product **2-36** in a superior isolated yield of 97 % (Scheme 2.19).



Scheme 2.19. Superior conditions for deoxygenation of 3,5-(bistrifluoromethyl)benzoate **2-37**

2.5. Conclusions

The three key steps in constructing the linear precursors of stage three DBCODs kadsuraol C and taiwanschirin B were modeled on a simplified system. These include fragment coupling (via aldol or alkylation reaction), methyl addition, and benzylic deoxygenation. Coupling of model ketone **2-7** with several benzyl halides via alkylation methods displayed poor selectivity and the desired product could not be cleanly obtained. Aldol addition proved to be a superior coupling strategy, able to produce either the 1,2-*syn*-1,3-*syn* aldol **2-26** or 1,2-*anti*-1,3-*syn* **2-29** in fair to good yields with high diastereoselectivity. Subsequent chelate-controlled methyl addition of **2-26** furnished a very low yield of **2-30** due to mismatched stereochemical elements in the favored transition state. The methyl addition of **2-29** proceeded smoothly with good *dr* and fair yield of the desired diastereomeric product **2-31** being isolated. **2-31** bore the correct C8 stereochemistry for the DBCOD linear precursor. The presence of a C6 oxygen was required to direct the stereochemistry of the methyl addition but is not present in the target molecules, therefore benzylic deoxygenation methodologies were investigated. It was found that the C6 hydroxyl group could be converted to the 3,5-(bistrifluoromethyl)benzoate and then to the methylene in very high yield using visible light photoredox-catalyzed conditions. These key methodologies will now be applied to the syntheses of kadsuraol C (Chapter 3) and taiwanschirin B (Chapter 4).

2.6. Experimental

2.6.1. Materials and methodologies

Chemicals and solvents were purchased from Sigma Aldrich, Strem Chemicals, Fisher Scientific, Combi-Blocks, or Oakwood Chemical, and used as received without further purification unless

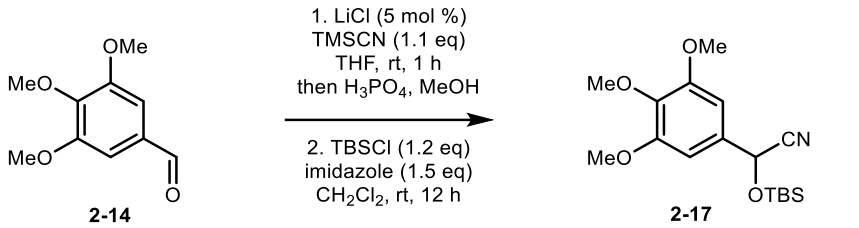
otherwise noted. Solvents were dried and purified using a PureSolv MD 7 (from Innovative Technology) or MB SPS 800 (from MBraun). Unless otherwise noted, solvent was degassed by sparging with N_2 for 5 min at rt prior to use. Amine bases were distilled over CaH_2 under N_2 (g).

Proton nuclear magnetic resonance (^{1}H NMR) spectra were acquired using Bruker AVIIIHD 500 MHz, Varian Inova QUANUC 500 MHz, Varian VNMRS 500 MHz, or Varian Mercury 400 MHz spectrometers. Chemical shifts (δ) are reported in parts per million (ppm) and are calibrated to the residual solvent peak. Coupling constants (*J*) are reported in Hz. Multiplicities are reported using the following abbreviations: s = singlet; d = doublet; t = triplet; q = quartet; dd = doublet of doublets; dt = doublet of triplets; dq = doublet of quartets; tt = triplet of triplets; qd = quartet of doublets; qq = quartet of quartets; ddd = doublet of doublet of doublets; ddt = doublet of doublet of triplets; dddd = doublet of doublet of doublet of doublets; ddq= doublet of doublet of quartets; br = broad; m = multiplet. Carbon nuclear magnetic resonance (^{13}C NMR) spectra were acquired using a Bruker AVIIIHD 126 MHz spectrometer.

High resolution mass spectra (HRMS) were recorded using a Bruker maXis Impact TOF mass spectrometer by electrospray ionization time of flight reflectron experiments. Fourier-transform infrared (FT-IR) spectra were recorded on a Bruker Alpha II FT-IR spectrometer. Optical rotations were recorded on a Jasco DIP-140 polarimeter (using the sodium D line; 589 nm). High performance liquid chromatography (HPLC) was measured on an Agilent 1100 HPLC system using a Chiralpak® IC analytical column (250 × 4.6 mm, 5 μm). Thin-layer chromatography was performed on pre-coated 250 mm layer thickness silica gel 60 F254 plates (EMD Chemicals Inc). Visualization was performed by ultraviolet light and/or by staining with potassium permanganate or *para*-anisaldehyde stain. Purifications by column chromatography were performed either using a Biotage Isolera™ One or standard column chromatography using silica gel (40-63 μm, 230-400 mesh). For the batch photoredox chemistry setup: 50 mL screw cap Schlenk flasks and a glass rod with a polished end were custom made by Cédric Ginart at Université de Montréal. A BOLA screw joint (no. D 590-16 or D 629-62) was used to attach the glass rod to the schlenk flask. A 455 nm LED was soldered onto a board, mounted on a heat sink (built by Richard Rossi and Weihua Wang at McGill University) and connected to a constant current power supply (Newark Electronics, Catalogue #: 82Y0614). This was placed on top of the glass rod to irradiate the reaction mixture from above.

2.6.2. Preparative procedures for compounds 2-7 to 2-37

Compound 2-17



2-14
Chemical Formula: $C_9H_{10}O_4$
Molecular Weight: 182.1750

91 %

2-17
Chemical Formula: $C_{17}H_{27}NO_4Si$
Molecular Weight: 337.4910

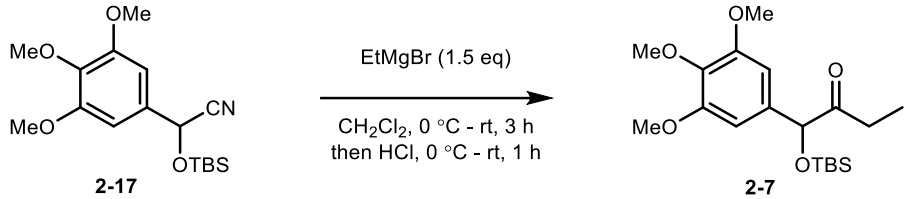
Procedure:

The reported procedure was followed.[19] A 250 mL flame-dried round bottom flask equipped with a Teflon-coated stir bar and a rubber septum was charged with 3,4,5-trimethoxybenzaldehyde (**2-14**, 20 mmol, 3.92 g, 1.0 equiv.) and lithium chloride (1.0 mmol, 42 mg, 5 mol %). The flask was evacuated and refilled with N_2 (repeated 3 times), prior to the addition of THF (20 mL). TMSCN (22 mmol, 2.75 mL, 1.1 equiv.) was then added via syringe and the reaction mixture was stirred at rt for 1 h. The reaction mixture was then diluted with hexanes (100 mL) and filtered through a silica plug, washing with 3:1 hexanes/EtOAc (200 mL). The filtrate was concentrated *in vacuo* and the resulting residue was dissolved in MeOH (40 mL). The resulting reaction mixture was then cooled to 0 °C and before adding aqueous H_3PO_4 (2 M, 10 mL). The reaction mixture was stirred at 0 °C for 10 min. before the addition of $NaHCO_3$ (sat. aq., 20 mL) and concentrated *in vacuo*. The reaction mixture was then extracted with EtOAc (3 × 50 mL). The combined organic layers were dried over $MgSO_4$, filtered and concentrated *in vacuo*. The crude product was dissolved in CH_2Cl_2 (40 mL). *Tert*-butyldimethylsilyl chloride (24 mmol, 3.62 g, 1.2 equiv.) and imidazole (30 mmol, 2.04 g, 1.5 equiv.) were added and the resulting reaction mixture was stirred at rt for 12 h. The reaction mixture was then poured onto HCl (1 M, 50 mL) and extracted with CH_2Cl_2 (3 × 50 mL). The combined organic layers were dried over $MgSO_4$, filtered and concentrated *in vacuo*. The crude product was then purified on silica gel (10:1 hexanes/EtOAc) to provide **2-17** (6.14 g, 18.2 mmol, 91 %) as a pale-yellow oil.

Characterization

^{1}H NMR (500 MHz, $CDCl_3$) δ 6.68 (s, 2H), 5.45 (s, 1H), 3.87 (s, 6H), 3.85 (s, 3H), 0.95 (s, 9H), 0.23 (s, 3H), 0.16 (s, 3H). The characterization data match the data reported previously.[19]

Compound 2-7



2-17
Chemical Formula: $C_{17}H_{27}NO_4Si$
Molecular Weight: 337.4910

85 %

2-7
Chemical Formula: $C_{19}H_{32}O_5Si$
Molecular Weight: 368.5450

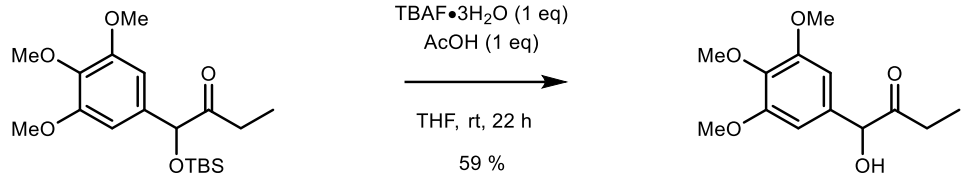
Procedure:

The reported procedure was followed.[19] A 100 mL flame-dried round bottom flask equipped with a Teflon-coated stir bar and a rubber septum was charged with **2-17** (18.1 mmol, 6.12 g, 1.0 equiv.). The flask was evacuated and refilled with N_2 (repeated 3 times), prior to the addition of CH_2Cl_2 (40 mL). The resulting solution was then cooled to 0 °C in an ice bath and EtMgBr (27.2 mmol, 3 M in Et_2O, 9.1 mL, 1.5 equiv.) was added dropwise via syringe. The solution was then warmed to rt and stirred for 3 h. The reaction mixture was then cooled to 0 °C in an ice bath, quenched by the addition of HCl (2 M, 50 mL), and stirred for another 1 h, allowing to warm to rt. The biphasic mixture was then extracted with CH_2Cl_2 (3 × 50 mL). The combined organic layers were dried over $MgSO_4$, filtered, and concentrated *in vacuo*. The crude product was then purified on silica gel (9:1 hexanes/EtOAc) to provide **2-7** (5.66 g, 15.3 mmol, 85 %) as a yellow oil.

Characterization:

^{1}H NMR (500 MHz, $CDCl_3$) δ 6.65 (s, 2H), 5.00 (s, 1H), 3.84 (s, 6H), 3.83 (s, 3H), 2.64 (dq, J = 18.6, 7.3 Hz, 1H), 2.47 (dq, J = 18.6, 7.3 Hz, 1H), 0.964 (s, 9H), 0.961 (t, J= 7.3 Hz, 3H), 0.09 (s, 3H), 0.02 (s, 3H). The characterization data match the data reported previously.[19]

Compound 2-18



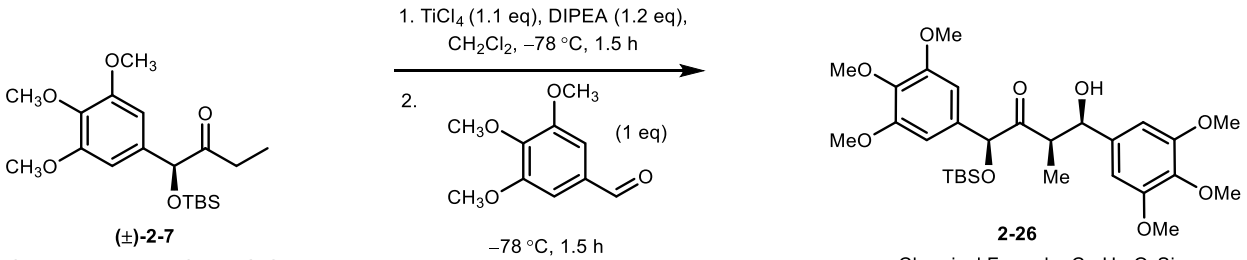
2-7
Chemical Formula: $C_{19}H_{32}O_5Si$
Molecular Weight: 368.5450

2-18
Chemical Formula: $C_{13}H_{18}O_5$
Molecular Weight: 254.2820

Procedure: A flame-dried 25 mL round bottom flask equipped with a Teflon-coated stir bar and a rubber septum was charged with **2-7** (1.00 mmol, 370 mg, 1.0 equiv.). The flask was evacuated and refilled with N_2 (repeated 3 times), prior to the addition of THF (1 mL). A solution of TBAF·3 H_2O (1.00 mmol, 281 mg, 3.0 equiv.) and acetic acid (1.00 mmol, 58 µL, 3.0 equiv.) in THF (1 mL) was then added via syringe, and the resulting mixture was stirred at rt for 14 h. The reaction mixture was then poured on $NaHCO_3$ (saturated aqueous, 3 mL) and extracted with CH_2Cl_2 (3 × 3 mL). The combined organic layers were dried over $MgSO_4$, filtered, and concentrated *in vacuo*. The crude product was purified on silica gel (25 % ethyl acetate in hexanes) to provide **2-18** (150 mg, 0.59 mmol, 59 %).

Characterization: $\mathbf{R_f}$ = (hexanes/EtOAc 3:1): 0.17; **^{1}H NMR** (500 MHz, $CDCl_3$) δ 6.48 (s, 2H), 4.97 (broad s, 1H), 3.81 (s, 3H), 3.79 (s, 3H), 2.37 (q, J= 7.4 Hz, 2 H), 0.99 (t, J= 7.3 Hz, 3 H). The characterization data match the data reported previously.

Compound 2-26



(±)-2-7
Chemical Formula: $C_{19}H_{32}O_5Si$
Molecular Weight: 368.5450

2-26
Chemical Formula: $C_{29}H_{44}O_9Si$
Molecular Weight: 564.7470

Procedure:

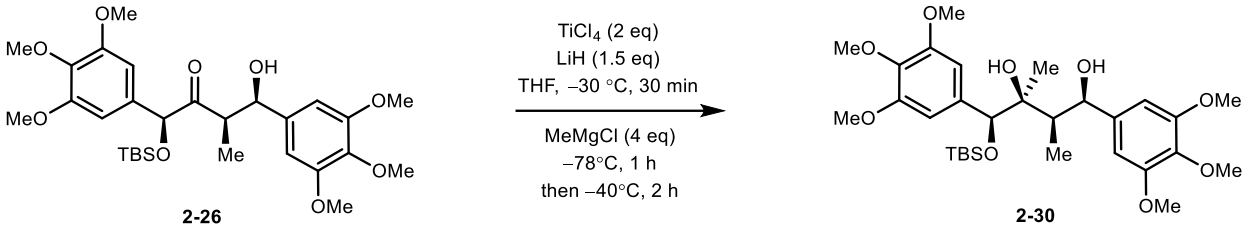
A flame-dried microwave vial equipped with a Teflon-coated stir bar and rubber septum was charged with **2-7** (0.2 mmol, 73.6 mg, 1.0 equiv.). The flask was evacuated and refilled with N_2

(repeated 3 times), prior to the addition of CH_2Cl_2 (1 mL). The mixture was cooled to –78 °C and $TiCl_4$ (0.22 mmol, 0.22 mL, 1 M in CH_2Cl_2, 1.1 equiv.) was added via syringe. After two minutes, *N,N*-diisopropylethylamine (DIPEA, 0.24 mmol, 42 µL, 1.2 equiv.) was added dropwise via syringe. The reaction mixture was stirred for 1.5 h at –78°C. Then, 3,4,5-trimethoxybenzaldehyde (0.2 mmol, 39 mg, 1.0 equiv.) was added as a solution in CH_2Cl_2 (0.5 mL) dropwise and the reaction mixture was stirred another 1.5 h at –78 °C. The reaction mixture was quenched by adding NH_4Cl (sat. aq., 1 mL) and extracted with CH_2Cl_2 (3 x 1 mL). The combined organic layers were dried over $MgSO_4$, filtered, and concentrated *in vacuo*. The crude product (10:1 *dr*) was then purified on silica gel (25 % to 35 % ethyl acetate in hexanes) to provide **2-26** (82 mg, 0.14 mmol, 73 %).

Characterization:

R_f = (hexanes/EtOAc 7:3): 0.20; **IR** (neat) v = 3507, 2995, 2934, 2856, 2838, 1720, 1591, 1505, 1459, 1418, 1327, 1125, 1006, 837, 779 cm^{-1}; **^{1}H NMR** (500 MHz, $CDCl_3$) δ 6.59 (s, 2H), 6.46 (s, 2H), 5.00 (s, 1H), 4.87 (d, *J*= 3.1 Hz) 1H), 3.81-3.80 (6 x s, 18H), 3.33 (dq, *J*= 3.3 Hz, 7.2 Hz, 1H), 0.95 (s, 9H), 0.82 (d, *J*= 7.2 Hz, 3H), 0.09 (s, 3H), 0.00 (s, 3H); **^{13}C NMR** (126 MHz, $CDCl_3$) δ 215.0, 153.3, 153.0, 137.8, 137.2, 136.9, 133.5, 103.0, 102.7, 80.5, 72.9, 60.9, 60.8, 56.1, 56.0, 46.1, 25.7, 18.2, 11.2, -4.8, -5.0; **HRMS**: Calcd. for $C_{29}H_{44}O_9Si$ $[M+Na]^+$ = 587.2652 m/z, found = 587.2659 m/z.

Compound 2-30



2-26
Chemical Formula: $C_{29}H_{44}O_9Si$
Molecular Weight: 564.7470

5 %

2-30
Chemical Formula: $C_{30}H_{48}O_9Si$
Molecular Weight: 580.7900

Procedure:

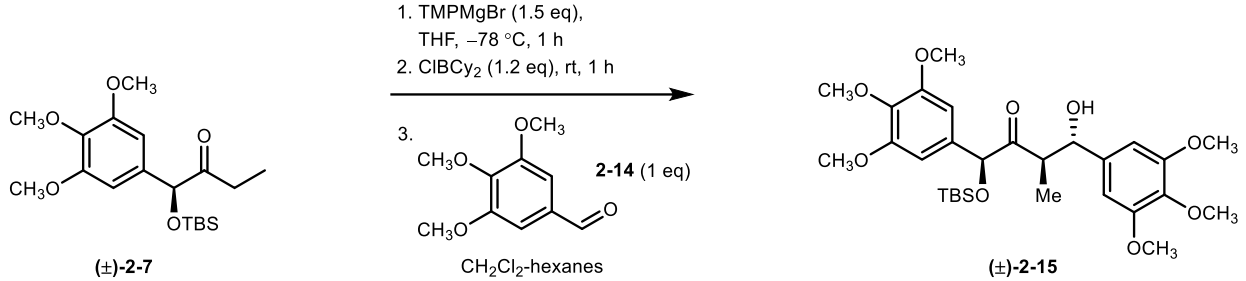
A 25 mL flame-dried round bottom flask equipped with a Teflon-coated stir bar and a rubber septum was charged with **2-26** (0.9 mmol, 509 mg, 1.0 equiv.) and LiH (1.35 mmol, 11 mg, 1.5 equiv.). The flask was evacuated and refilled with N_2 (repeated 3 times), prior to the addition of

THF (4.5 mL). The mixture was then cooled to –30 °C in a dry ice/ acetone bath, at which point $TiCl_4$ (1.8 mmol, 1 M in CH_2Cl_2, 1.8 mL, 2.0 equiv.) was added dropwise via syringe. The reaction mixture was stirred at this temperature for 30 min. The resulting red solution was then cooled to –78 °C, and a solution of MeMgCl (3.6 mmol, 1 M in THF, 3.6 mL, 4.0 equiv.) was added at a rate of 50 mL/h via syringe pump. The mixture was stirred at this temperature for 1 h, then warmed to –40 °C in a dry ice/ acetonitrile bath and stirred for another 2 h. It was then quenched by the addition of NH_4Cl (sat. aq., 2.4 mL) followed by NH_4OH (concentrated, 0.6 mL), and stirred for another 15 min at rt. The resulting mixture was filtered, and the filtrate was extracted with EtOAc (3 × 23 mL). The combined organic layers were dried over $MgSO_4$, filtered, and concentrated *in vacuo*. The crude product was then purified on silica gel (25 % to 45% ethyl acetate in hexanes) to provide 26 mg, 0.04 mmol, 5 % of **2-30**. Starting material **2-26** (249.3 mg, 0.44 mmol, 48 %) was also recovered.

Characterization:

R_f = (hexanes/EtOAc 7:3): 0.32; **IR** (neat) v = 3492, 2932, 2856, 1725, 1589, 1505, 1460, 1417, 1327, 1232, 1125, 1007, 836, 778 cm^{-1}; **^{1}H NMR** (500 MHz, $CDCl_3$) δ 6.54 (s, 2H), 6.46 (s, 2H), 5.15 (s, 1H), 4.77 (s, 1H), 4.10 (s, 1H), 3.84 (s, 3H), 3.81 (s, 3H), 3.79 (s, 12 H) 2.89 (s, 1H), 1.66 (m, 1H), 1.38 (s, 3H), 0.98 (d, *J*= 6.9 Hz, 3H), 0.96 (s, 9H) 0.07 (s, 3H), -0.15 (s, 3H); **^{13}C NMR** (126 MHz, $CDCl_3$) δ 152.9, 152.6, 139.3, 137.4, 136.3, 136.0, 104.3, 102.6, 78.7, 77.5, 72.8, 60.9, 60.8, 56.1, 43.3, 38.7, 25.8, 20.7, 18.2, 7.0, -4.4, -5.2; **HRMS**: Calcd. for $C_{30}H_{48}O_9Si$ $[M+Na]^+$ = 603.2965 m/z, found = 603.2966 m/z.

Compound 2-15



(±)-2-7
Chemical Formula: $C_{19}H_{32}O_5Si$
Molecular Weight: 368.5450

CH_2Cl_2-hexanes
–78 °C, 2 h, then –30 °C, 3 h
36 %, 5:1 *dr*

(±)-2-15
Chemical Formula: $C_{29}H_{44}O_9Si$
Molecular Weight: 564.7470

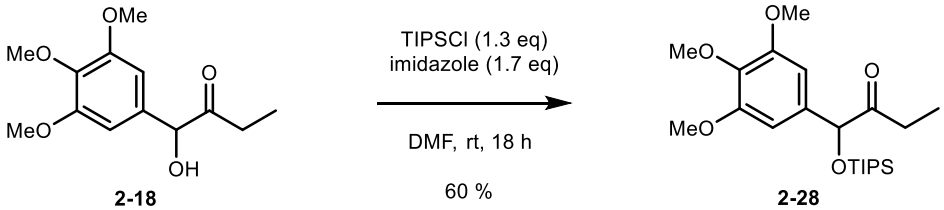
Procedure:

A 25 mL flame-dried round bottom flask equipped with a Teflon-coated stir bar and a rubber septum was charged with 2,2,6,6-tetramethylpiperidine (freshly distilled over CaH_2, 1.5 mmol, 255 µL, 1.68 equiv.) and THF (1.35 mL). EtMgBr (1.35 mmol, 0.45 mL of 3 M solution in Et_2O, 1.5 equiv.) was then added via syringe. The resulting solution was refluxed under N_2 for 12 h, then diluted with THF (1.35 mL), and cooled to –78 °C in a dry ice / acetone bath. A solution of **2-7** (0.90 mmol, 330 mg, 1.0 equiv.) in THF (1.8 mL) was slowly added dropwise. The reaction mixture was stirred for 1 h at –78 °C, then a solution of Cy_2BCl (1.17 mmol, 1.17 mL, 1 M in hexanes, 1.3 eq,) was added via syringe. The reaction mixture was warmed to rt and stirred for another 1 h. The reaction mixture was then cooled to –78 °C, and a solution of **2-14** (0.90 mmol, 176 mg, 1.0 equiv.) in hexanes and CH_2Cl_2 (1:1 mixture, 2.7 mL) was added dropwise. The resulting mixture was then stirred at –78 °C for 3 h followed by 2 h at –30 °C. It was quenched by the addition of $NaHCO_3$ (sat. aq., 6 mL) and diethanolamine (2.7 mmol, 477 mg, 3.0 equiv.), and stirred for another 30 min at rt. The mixture was then filtered, and the filtrate was extracted with EtOAc (3 × 12 mL). The combined organic layers were dried over $MgSO_4$, filtered, and concentrated *in vacuo*. The crude product was purified on silica gel (25 % to 35 % ethyl acetate in hexanes) to provide **2-15** (313 mg, 0.55 mmol, 36 %) as a 5:1 *d.r.* mixture.

Characterization:

R_f = (hexanes/EtOAc 7:3): 0.23 ; **IR** (neat) v = 3504, 2934, 2856, 1716, 1591, 1505, 1460, 1419, 1327, 1234, 1007, 838, 779 cm^{-1}; **^{1}H NMR** (500 MHz, $CDCl_3$) δ 6.59 (s, 2H), 6.48 (s, 2H), 4.97 (s, 1H) 4.58 (d, *J*= 8.5 Hz, 1H), 3.78 (6 x s, 18H), 3.51 (dq, *J*= 7.1 Hz, 1H), 0.94 (s, 9H), 0.70 (d, *J*= 7.2 Hz, 3H), 0.10 (s, 3H), -0.04 (s, 3H); **^{13}C NMR** (126 MHz, $CDCl_3$) δ 214, 153.17, 153.12, 138.1, 137.5, 137.3, 134.2, 80.6, 77.3, 77.0, 60.8, 60.7, 56.0, 55.9, 49.6, 25.7, 18.2, 15.6 -4.8, -5.1; **HRMS**: Calcd. for $C_{29}H_{44}O_9Si$ $[M+Na]^+$ = 587. 2652 m/z, found = 587.2645 m/z.

Compound 2-28



2-18
Chemical Formula: $C_{13}H_{18}O_5$
Molecular Weight: 254.2820

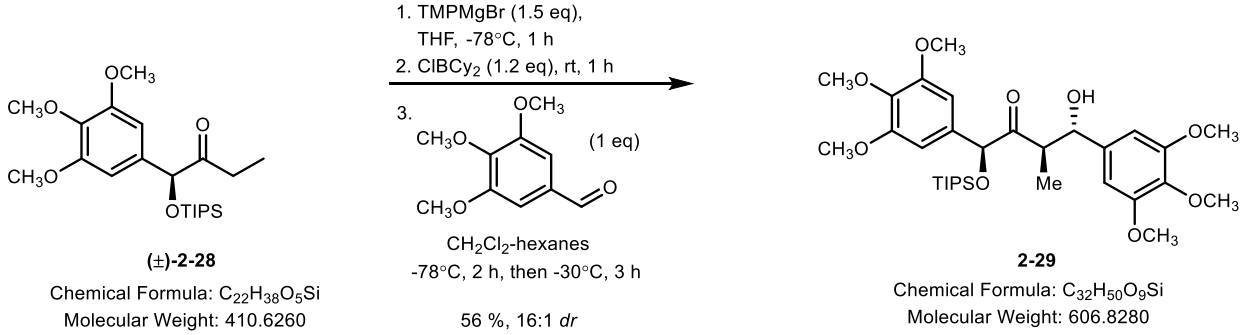
2-28
Chemical Formula: $C_{22}H_{38}O_5Si$
Molecular Weight: 410.6260

Procedure: The reported procedure was followed.[19] A 100 mL flame-dried round bottom flask equipped with a Teflon-coated stir bar and a rubber septum was charged with **2-18** (1.8 mmol, 461 mg, 1.0 equiv.) and imidazole (3.0 mmol, 204 mg, 1.7 equiv.). The flask was evacuated and refilled with N_2 (repeated 3 times), prior to the addition of DMF (2 mL). Triisopropylsilyl chloride (2.4 mmol, 514 µL, 1.3 equiv.) was then added to the reaction mixture via syringe. The resulting mixture was stirred at rt for 12 h. The reaction mixture was quenched by the addition of *N,N*-dimethylaminoethanol (0.8 mmol, 78 µL, 0.4 equiv.) and stirred another 1 h at rt. It was then diluted with EtOAc (10 mL), washed with HCl (1 M, 5 mL) and extracted with EtOAc (2 × 10 mL). The combined organic layers were washed sequentially with water (10 mL) and brine (10 mL), followed by drying over $MgSO_4$, filtration, and concentration *in vacuo*. The crude product was purified on silica gel (3 % to 10 % ethyl acetate in hexanes) to provide **2-28** (497 mg, 1.21 mmol, 60 %) as a pale yellow oil.

Characterization:

^{1}H NMR (500 MHz, $CDCl_3$) δ 6.69 (s, 2H), 5.10 (s, 1H), 3.84 (s, 6H), 3.83 (s, 3H), 2.73 (dq, *J* = 18.7, 7.3 Hz, 1H), 2.45 (dq, *J* = 18.7, 7.3 Hz, 1H), 1.14 (m, 3H), 1.04 (m, 18H), 0.95 (t, *J*= 7.3 Hz, 3H). The characterization data matches the data reported previously.[19]

Compound 2-29



Procedure:

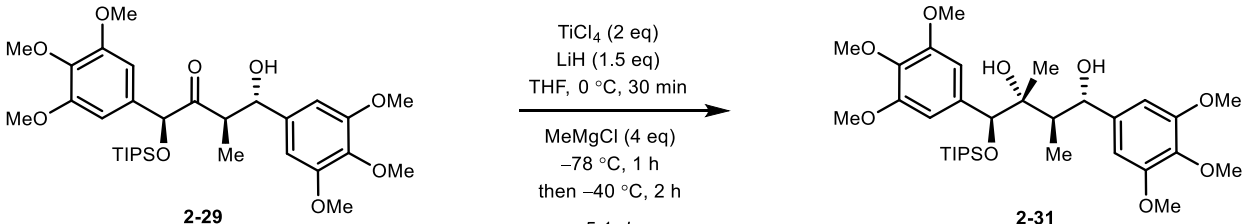
A 50 mL flame-dried round bottom flask equipped with a Teflon-coated stir bar and a rubber septum was charged with 2,2,6,6-tetramethylpiperidine (freshly distilled over CaH_2, 5.0 mmol, 0.84 mL, 1.68 equiv.) and THF (5 mL). EtMgBr (4.5 mmol, 1.5 mL of 3 M solution in Et_2O, 1.5 equiv.) was then added via syringe. The resulting solution was refluxed under N_2 for 12 h, then

diluted with THF (4.5 mL), and cooled to –78 °C in a dry ice / acetone bath. A solution of **(±)-2-28** (3.0 mmol, 1.23 g, 1.0 equiv.) in THF (6 mL) was added dropwise via syringe pump at a rate of 100 mL/h. The reaction mixture was stirred for 1 h at –78 °C, then a solution of Cy_2BCl (4.5 mmol, 1.5 equiv.) in hexane (6 mL) was added via syringe. The reaction mixture was warmed to rt and stirred for another 1 h. The reaction mixture was then cooled to –78 °C, and a solution of **2-14** (3.3 mmol, 647 mg, 1.1 equiv.) in hexanes and CH_2Cl_2 (1:1 mixture, 10 mL) was added dropwise via syringe pump at a rate of 150 mL/h. The resulting mixture was then stirred at –78 °C for 3 h followed by 2 h at –30 °C. It was quenched by the addition of $NaHCO_3$ (sat. aq., 15 mL) and diethanolamine (9.0 mmol, 945 mg, 3.0 equiv.), then stirred for another 30 min at rt. The mixture was filtered, and the filtrate was extracted with EtOAc (3 × 50 mL). The combined organic layers were dried over $MgSO_4$, filtered, and concentrated *in vacuo*. The crude product was purified on silica gel (25 % to 35 % ethyl acetate in hexanes) to provide **2-29** (1.02 g, 1.68 mmol, 56 %) as a 16:1 *d.r.* mixture.

Characterization:

R_f = (hexanes/EtOAc 7:3): 0.3; **IR** (neat) v = 3507, 2939, 2865, 1714, 1591, 1504, 1458, 1418, 1327, 1233, 1124, 1009, 882, 842, 683 cm^{-1}; **^{1}H NMR** (500 MHz, $CDCl_3$) δ 6.68 (s, 2H), 6.51 (s, 2H), 5.17 (s, 1H), 4.64 (d, *J*= 8.5 Hz, 1H), 3.83 (s, 15H), 3.82 (3H), 3.54 (dq, *J*= 7.3 Hz, 1H), 1.14 (m, 3H), 1.05 (m, 18H), 0.73 (d, *J*= 7.2 Hz, 3H); **^{13}C NMR** (126 MHz, $CDCl_3$) δ 214.3, 153.2, 153.1, 137.8, 137.7, 137.4, 134.5, 103.5, 103.1, 81.0, 60.9, 60.8, 56.1, 56.0, 47.3, 18.0, 17.9, 15.8, 12.3; **HRMS**: Calcd. for $C_{32}H_{50}O_9Si$ $[M+Na]^+$ = 629.3122 m/z, found = 629.3093 m/z.

Compound 2-30



2-29
Chemical Formula: $C_{32}H_{50}O_9Si$
Molecular Weight: 606.8280

2-31
Chemical Formula: $C_{33}H_{54}O_9Si$
Molecular Weight: 622.8710

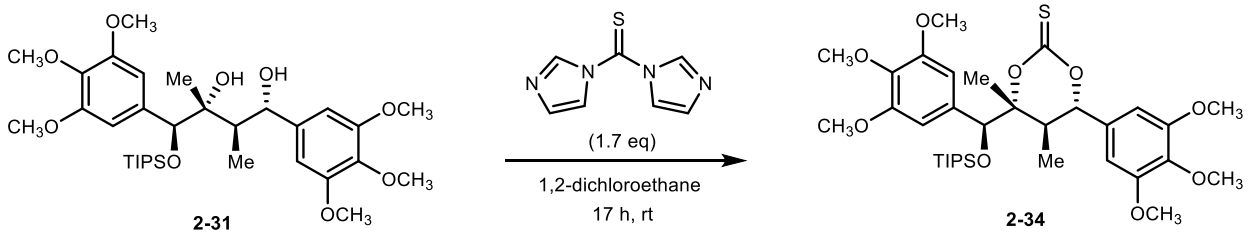
Procedure:

A 25 mL flame-dried round bottom flask equipped with a Teflon-coated stir bar and a rubber septum was charged with **2-29** (0.86 mmol, 520 mg, 1.0 equiv.) and LiH (1.29 mmol, 10 mg, 1.5 equiv.). The flask was evacuated and refilled with N_2 (repeated 3 times), prior to the addition of THF (4.3 mL). The mixture was then cooled to –30 °C in a dry ice/ acetone bath, at which point $TiCl_4$ (1.71 mmol, 1 M in CH_2Cl_2, 1.71 mL, 2.0 equiv.) was added dropwise via syringe. The reaction mixture was stirred at this temperature for 30 min. The resulting red solution was then cooled to –78 °C, and a solution of MeMgCl (3.43 mmol, 1 M in THF, 3.43 mL, 4.0 equiv.) was added dropwise at a rate of 50 mL/h via syringe pump. The mixture was stirred at this temperature for 1 h, then warmed to –40 °C and stirred for another 2 h. It was then quenched by the addition of NH_4Cl (sat. aq., 3.5 mL) and NH_4OH (concentrated, 1 mL), and stirred for another 15 min at rt. The resulting mixture was filtered, and the filtrate was extracted with EtOAc (3 × 12 mL). The combined organic layers were dried over $MgSO_4$, filtered, and concentrated *in vacuo*. The crude product (5:1 *dr*) was purified on silica gel (25 % to 45% ethyl acetate in hexanes) to provide 261 mg, 0.42 mmol, 50 % of the major diastereomer **2-31** as a puffy white solid.

Characterization:

R_f = (hexanes/EtOAc 7:3): 0.23; **^{1}H NMR** (500 MHz, $CDCl_3$) δ 6.85-6.49 (broad s, 2H), 6.40 (s, 2H), 4.60 (s, 1H), 4.55 (d, *J*= 9.3, 6.9 Hz, 1H), 3.83 (s, 3H), 3.82 (broad s, 6H), 3.78 (s, 3H), 3.77 (s, 6H), 1.56 (dq, J= 9.2 Hz, 1H), 1.50 (s, 3H), 1.03 (m, 12H), 0.94 (m, 9H), 0.40 (d, *J*= 7.0 Hz, 3H); **^{13}C NMR** (126 MHz, $CDCl_3$) δ 152.9, 138.9, 138.2, 137.2, 135.3, 106.2, 104.3, 80.4, 80.0, 77.9, 60.9, 60.8, 56.2, 56.0, 43.4, 21.0, 18.1, 18.0, 13.5, 12.6; **HRMS**: Calcd. for $C_{33}H_{54}O_9Si$ $[M+Na]^+$ = 645.3435 m/z, found = 645.3433 m/z.

Compound 2-34



2-31
Chemical Formula: $C_{33}H_{54}O_9Si$
Molecular Weight: 622.8710

2-34
Chemical Formula: $C_{34}H_{52}O_9SSi$
Molecular Weight: 664.9260

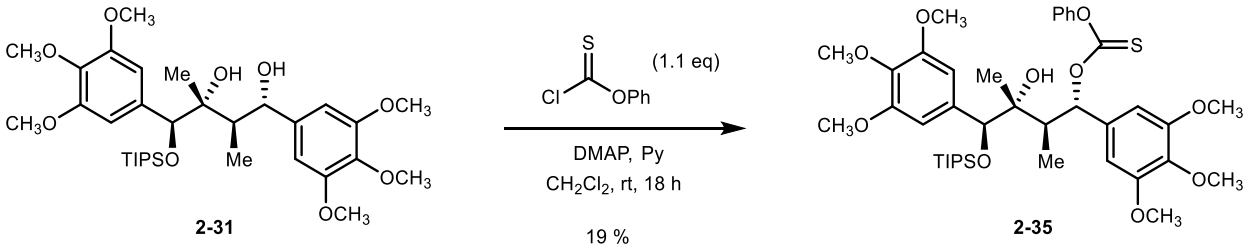
Procedure:

A flame-dried microwave vial equipped with a Teflon-coated stir bar and a rubber septum was charged with **2-31** (0.05 mmol, 31 mg, 1.0 equiv.) and hexamethylbenzene (2.7 mg, as an internal standard). 1,2-dichloroethane (0.33 mL) and then 1,1'-thiocarbonyldiimidazole (0.085 mmol, 15 mg, 1.7 equiv.) were added to the reaction mixture. The flask was evacuated and refilled with N_2, then the reaction mixture was stirred at rt for 17 h. The reaction mixture was quenched by adding $NaHCO_3$ (sat. aq., 1 mL) and extracted with CH_2Cl_2. The organic layer was dried over $MgSO_4$, filtered, and concentrated *in vacuo*. Analysis by crude ^{1}H NMR NMR (500 MHz, $CDCl_3$) indicated 100 % consumption of **2-31** and 57 % yield. **2-34** could be purified on silica gel (25 % to 35% ethyl acetate in hexanes).

Characterization:

^{1}H NMR (500 MHz, $CDCl_3$) δ 6.72 (broad s, 2H), 6.46 (s, 2H) 4.89 (s, 1H), 4.80 (d, J= 11.0Hz, 1H) 3.88 (s, 6 H), 3.85 (s, 3H), 3.845 (s, 3H), 3.844 (s, 6H), 2.66 (dq, *J*= 6.8 Hz, 1H), 1.49 (s, 3H), 1.08 (m, 3H), 1.05 (m, 18 H), 0.72 (d, *J*= 6.8 Hz, 3H); **LRMS**: Calcd. for $C_{34}H_{52}O_9Si$ $[M+Na]^+$ 687 m/z, found = 687 m/z.

Compound 2-35



Procedure:

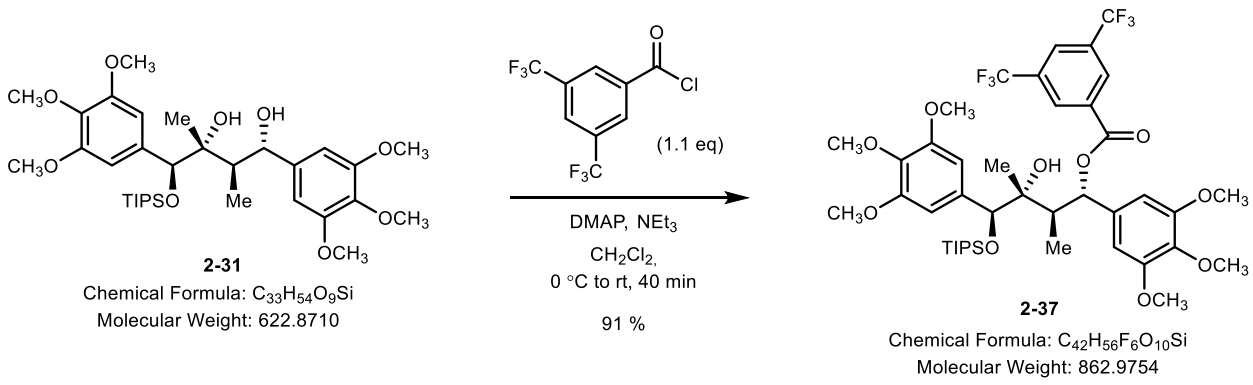
A flame-dried microwave vial equipped with a Teflon-coated stir bar and a rubber septum was charged with **2-31** (0.10 mmol, 65 mg, 1.0 equiv.) and DMAP (0.052 mmol, 6.4 mg, 0.5 equiv.). The vial was evacuated and refilled with N_2 (repeated 3 times), then CH_2Cl_2 (0.5 mL) and pyridine (0.31 mmol, 25 µL, 3 equiv.) were added sequentially, stirring to dissolve. Phenylchlorothionoformate (0.11 mmol, 16 µL, 1.1 equiv.) was added via syringe and then the reaction mixture was stirred for 18 h at rt. The reaction mixture was diluted with CH_2Cl_2 and

washed with brine. The combined organic layers were dried over $MgSO_4$, filtered, and concentrated *in vacuo*. The crude product was then purified on silica gel (10 % to 20% ethyl acetate in hexanes) to provide **2-35** (14.3 mg, 0.020 mmol, 19 %).

Characterization:

R_f = (hexanes/EtOAc 7:3): 0.50; **IR** (neat) v = 3535, 2940, 2866, 2838, 1726, 1588, 1505, 1457, 1420, 1324, 1237, 1186, 1092, 1004, 882, 823, 749, 686 cm^{-1}; **^{1}H NMR** (500 MHz, $CDCl_3$) δ 7.34 (dd, *J*= 7.8 Hz, 2 H) 7.20 (t, *J*= 7.5 Hz, 1H), 7.03 (d, *J*= 8.5 Hz, 2H), 6.86-6.44 (broad s, 2H), 6.61 (s, 1H), 5.17 (d, *J*= 3.8 Hz, 1H), 4.49 (s, 1H), 3.85 (s, 6H), 3.84 (s, 3H), 3.82 (s, 9H), 2.14 (m, 1H), 0.98 (m, 18H) 0.91 (m, 9H) ; **LRMS**: Calcd. for $C_{40}H_{58}O_{10}SSi$ $[M+Na]^+$ = 781 m/z, found = 781 m/z.

Compound 2-37



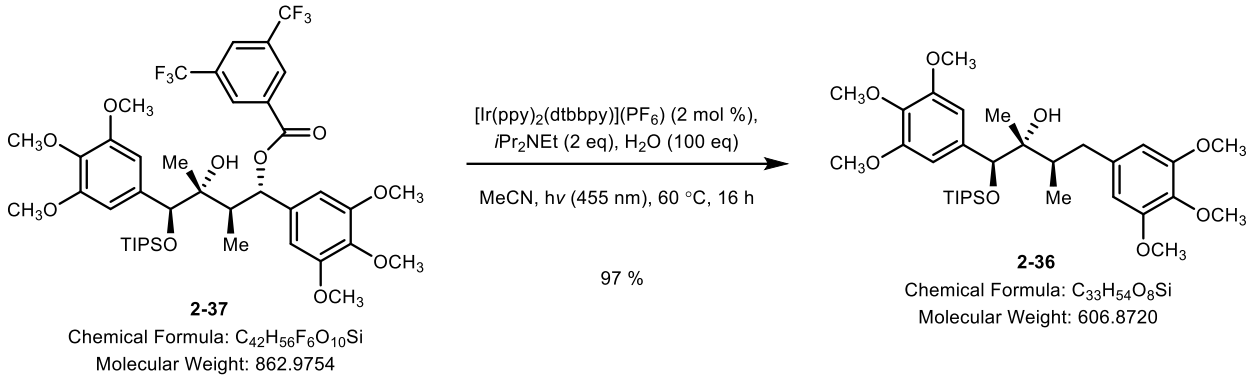
Procedure:

A flame-dried 50 mL round bottom flask equipped with a Teflon-coated stir bar and a rubber septum was charged with **2-31** (1.62 mmol, 1.01 g, 1.0 equiv.) and DMAP (0.075 mmol, 10 mg, 0.05 equiv.). The vial was evacuated and refilled with N_2 (repeated 3 times), before adding CH_2Cl_2 (15 mL) and triethylamine (10.5 mmol, 1.46 mL, 7.0 equiv.). The reaction mixture was cooled to 0 °C and then slowly added 3,5-bis(trifluoromethylbenzoyl) chloride (1.8 mmol, 322 µL, 1.1 equiv.). The resulting mixture was allowed to warm to rt and stirred for 40 minutes. The reaction mixture was concentrated *in vacuo* and then purified on silica gel (15 % to 25 % ethyl acetate in hexanes) to provide **2-37** (1.27 g, 1.47 mmol, 91 %).

Characterization:

R_f = (hexanes/EtOAc 7:3): 0.60; **IR** (neat) v = 3528, 2939, 2864, 1739, 1590, 1462, 1422, 1325, 1277, 1235, 1172, 1121, 1063, 1010, 960, 909, 828, 765, 680, 665, 442 cm^{-1}; **^{1}H NMR** (500 MHz, $CDCl_3$) δ 8.46 (s, 2H), 8.02 (s, 1H), 6.94-6.33 (broad s, 2H), 6.55 (s, 2H), 6.21 (d, *J*= 8.0 Hz, 1H), 4.60 (s, 1H), 3.85 (s, 3H), 3.82 (s, 6H), 3.80 (2 x s, 9H), 2.18 (dq, *J*= 7.1 Hz, 1H), 1.30 (s, 3H), 0.99 (m, 12H), 0.91 (m, 9H), 0.63 (d, *J*= 7.1 Hz, 3H); **^{13}C NMR** (126 MHz, $CDCl_3$) δ 162.9, 153.0, 138.0, 137.9, 135.7, 134.6, 133.4, 131.9 (q, *J*= 33.8 Hz), 129.7 (q, *J*= 4.0 Hz), 125.9 (m), 122.9 (d, *J*= 272.5 Hz), 105.1, 80.8, 78.4, 77.9, 60.9, 60.8, 56.1, 41.6, 21.4, 18.1, 17.9, 13.0, 12.6; **HRMS**: Calcd. for $C_{42}H_{56}O_{10}Si$ $[M+Na]^+$ = 885.3445 m/z, found = 885.3456 m/z.

Compound 2-36



2-37
Chemical Formula: $C_{42}H_{56}F_6O_{10}Si$
Molecular Weight: 862.9754

2-36
Chemical Formula: $C_{33}H_{54}O_8Si$
Molecular Weight: 606.8720

Procedure:

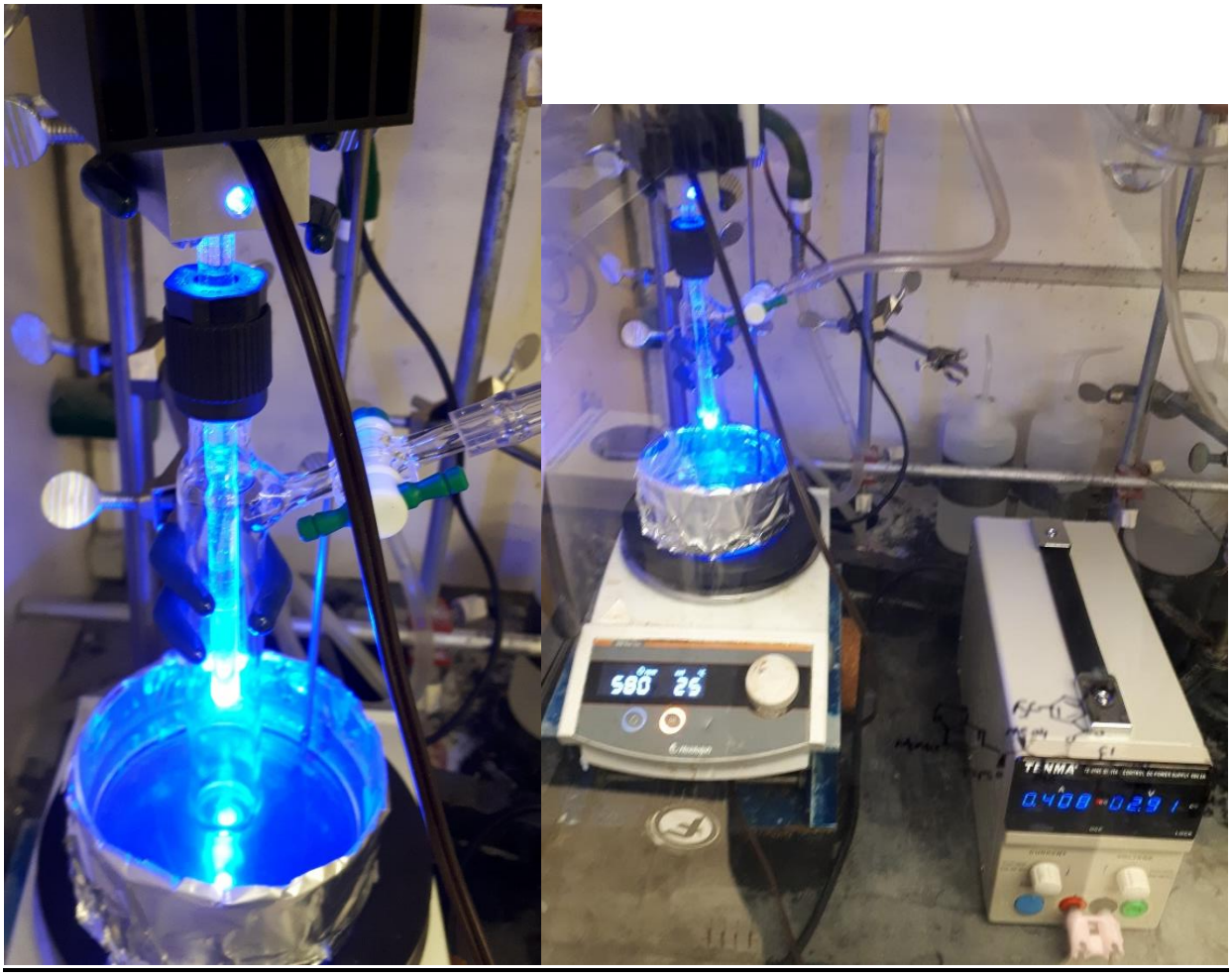
The acetonitrile and water were degassed by sparging with N_2 prior to use. A flame-dried 50 mL Schlenk flask equipped with a Teflon-coated stir bar and a screw cap was charged with **2-37** (0.050 mmol, 43 mg, 1.0 equiv.) and $[Ir(ppy)_2(dtbbpy)]PF_6$ (0.02 mmol, 100 µL of a 0.01 M solution in acetonitrile, 0.02 equiv.). The flask was evacuated and refilled with N_2 (repeated 3 times), before adding acetonitrile (1 mL), water (5.0 mmol, 90 µL, 100 equiv.), and DIPEA (0.10 mmol, 18 µL, 2 equiv.) sequentially. The reaction mixture was freeze-pump-thawed (x 5), backfilled with N_2, and the screw cap was replaced with a Teflon sealed inlet with a bevelled glass rod. The reaction mixture was stirred while irradiated from the top using a blue LED source (455 nm, 410 mA) connected to the glass rod while heating from below with an oil bath at 60ºC (see photo below) for 16 h. The reaction mixture was cooled to room temperature and then diluted with diethyl ether (8 mL). The mixture was washed sequentially with Na_2CO_3 (10 % aq., 4 mL), water (4 mL), and

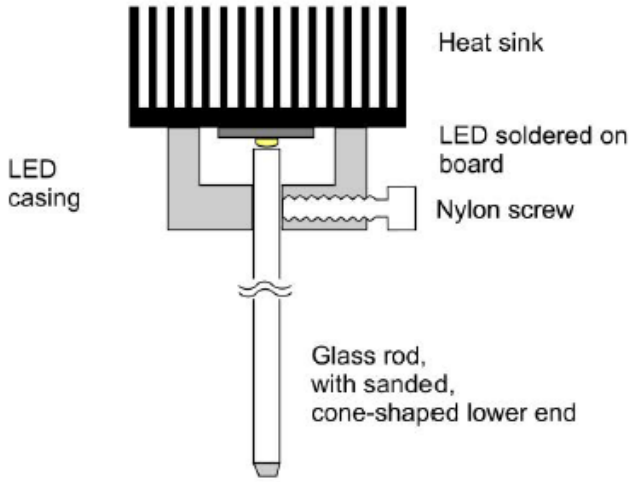
brine (4 mL). The combined organic layers were dried over $MgSO_4$, filtered, and concentrated *in vacuo*. Purified on silica gel (15 % to 25 % ethyl acetate in hexanes) to provide **2-36** (29 mg, 0.049 mmol, 97 %).

Characterization:

R_f = (hexanes/EtOAc 4:1): 0.23; **IR** (neat) v = 3548, 2939, 2866, 1587, 1505, 1458, 1419, 1326, 1236, 1125, 1011, 882, 843, 681 cm^{-1}; **^{1}H NMR** (500 MHz, $CDCl_3$) δ 6.85-6.47 (broad s, 2H), 6.27 (s, 2H), 4.65 (s, 1H) 3.81 (s, 9H), 3.78 (s, 3H), 3.75 (s, 6H) 3.23 (dd, *J*= 2.6 Hz, 13.1 Hz, 1H), 2.84 (broad s, 1H), 2.07 (dd, J= 2.2 Hz, 13.2 Hz, 1H), 1.54 (ddq, J= 2.8 Hz, 6.8 Hz, 1H), 1.32 (s, 3H), 1.02 (m, 12H), 0.96 (m, 9H), 0.69 (d, J= 6.8 Hz, 3H); **^{13}C NMR** (126 MHz, $CDCl_3$) δ 152.8, 137.8, 137.7, 136.1, 135.8, 106.1, 105.9, 80.8, 77.5, 60.9, 60.8, 56.2, 55.9, 40.3, 37.5, 21.2, 18.1, 18.0, 14.6, 12.7; **HRMS**: Calcd. for $C_{33}H_{54}O_8Si$ $[M+Na]^+$ = 629.3486 m/z, found = 629.3485 m/z.

Batch photoredox setup:





2.7. References

(1) Tomioka, K.; Ishiguro, T.; Iitaka, Y.; Koga, K. Asymmetric Total Synthesis of Natural (-)- and Unnatural (+)-Steganacin. Determination of the Absolute Configuration of Natural Antitumor Steganacin. *Tetrahedron* **1984**, *40* (8), 1303–1312.

(2) Huang, Z.; Lumb, J. P. Mimicking Oxidative Radical Cyclizations of Lignan Biosynthesis Using Redox-Neutral Photocatalysis. *Nat. Chem.* **2021**, *13* (1), 24–32.

(3) Draanen, N. A. Van; Arseniyadis, S.; Crimmins, M. T.; Heathcock, C. H. Protocols for the Preparation of Each of the Four Possible Stereoisomeric α-Alkyl-β-Hydroxy Carboxylic Acids from a Single Chiral Aldol Reagent. *J. Org. Chem.* **1991**, *56*, 2499–2506.

(4) Aullón, G.; Romea, P.; Urpí, F. Substrate-Controlled Aldol Reactions from Chiral α -Hydroxy Ketones. *Synthesis (Stuttg).* **2017**, *49*, 484–503.

(5) House, H. O.; Gall, M.; Olmstead, H. D. Chemistry of Carbanions. XIX. Alkylation of Enolates from Unsymmetrical Ketones. *J. Org. Chem.* **1971**, *36* (16), 2361–2371.

(6) Narula, A. S. An Analysis of the Diastereomeric Transition State Interactions for the Kinetic Deprotonation of Acyclic Carbonyl Derivatives with Lithium Diisopropylamide. *Tetrahedron Lett.* **1981**, *22* (41), 4119–4122.

(7) Ireland, R. E.; Mueller, R. H.; Willard, A. K. The Ester Enolate Claisen Rearrangement. Stereochemical Control through Stereoselective Enolate Formation. *J. Am. Chem. Soc.* **1976**, *98* (10), 2868–2877.

(8) Bartoli, G.; Bosco, M.; Martino, D.; Marcantoni, E.; Sambri, L. Highly Stereoselective and Efficient Addition of Organocerium Reagents to Syn- -Alkyl-β -Hydroxy-α-Methyl Ketones by Way of Their Titanium Alkoxides - Synthesis of Complex 1, 3-Diol Units with Three Stereodefined Centres. *European J. Org. Chem.* **2001**, 2901–2909.

(9) Palomo, C.; Oiarbide, M.; Mielgo, A.; Gonza, A.; Landa, C.; Lecumberri, A.; Linden, A. Alkylation of Chiral A-Hydroxy Ketones Derived from (1 R)-(+)-Camphor . An Asymmetric Variant of the Classical Acetylene Route to Carbonyl Compounds. *Org. Lett.* **2001**, *3* (21), 3249–3252.

(10) Negishi, E.; Idacavage, M. J. A Highly Selective Method for α-Alkylation of Ketones via Potassium Enoxytrialkylborates. *Tetrahedron Lett.* **1979**, No. 10, 845–848.

(11) Sugiura, M.; Ashikari, Y.; Nakajima, M. One-Pot Synthesis of β,β -Disubstituted α,β-Unsaturated Carbonyl Compounds. *J. Org. Chem.* **2015**, *80*, 8830–8835.

(12) Evans, D. A.; Rieger, D. L.; Bilodeau, M. T.; Urpí, F. Stereoselective Aldol Reactions of Chlorotitanium Enolates. An Efficient Method for the Assemblage of Polypropionate-Related Synthons. *J. Am. Chem. Soc.* **1991**, *113*, 1047–1049.

(13) Shibatomi, K.; Okimi, T.; Abe, Y.; Narayama, A.; Nakamura, N.; Iwasa, S. Organocatalytic Asymmetric Fluorination of α-Chloroaldehydes Involving Kinetic Resolution. *Beilstein J. Org. Chem.* **2014**, *10*, 323–331.

(14) Robins, M. J.; Wilson, J. S.; Hansske, F. Nucleic Acid Related Compounds. 42. A General Procedure for the Efficient Deoxygenation of Secondary Alcohols. Regiospecific and Stereoselective Conversion of Ribonucleosides to 2'-Deoxynucleosides. *J. Am. Chem. Soc.* **1983**, *105*, 4059–4065.

(15) Rackl, D.; Kais, V.; Kreitmeier, P.; Reiser, O. Visible Light Photoredox-Catalyzed Deoxygenation of Alcohols. *Beilstein J. Org. Chem.* **2014**, *10*, 2157–2165.

(16) Tlahuext-Aca, A.; Garza-Sanchez, R. A.; Glorius, F. Multicomponent Oxyalkylation of Styrenes Enabled by Hydrogen-Bond-Assisted Photoinduced Electron Transfer. *Angew. Chemie - Int. Ed.* **2017**, *56* (13), 3708–3711.

(17) Prier, C. K.; Rankic, D. A.; MacMillan, D. W. C. Visible Light Photoredox Catalysis with

Transition Metal Complexes: Applications in Organic Synthesis. *Chem. Rev.* **2013**, *113* (7), 5322–5363.

(18) Minozzi, C.; Caron, A.; Grenier-Petel, J. C.; Santandrea, J.; Collins, S. K. Heteroleptic Copper(I)-Based Complexes for Photocatalysis: Combinatorial Assembly, Discovery, and Optimization. *Angew. Chemie - Int. Ed.* **2018**, *57* (19), 5477–5481.

(19) Huang, Z. Biomimetic Aerobic Catalysis and Total Synthesis of Dibenzocyclooctadiene Lignans. *ProQuest Diss. Theses McGill Univ.* **2019**.

Chapter 3. Efforts towards the synthesis of kadsuraol C

3.1. Introduction

Kadsuraols A–C are Stage 3 DBCODs which were isolated from the *Kadsura longipedunculata* plant in 2018 (Figure 3.1).[1] They were evaluated *in vitro* for hepatoprotective activity against APAP-induced toxicity in HepG2 (human hepatocellular liver carcinoma) cells, with kadsuraol C (**3-3**) displaying a cell survival rate of 48.22 % at 10 μM, comparable to the clinical control bicyclol (48.77 %). The liver therapeutic bicyclol (**1-39**) was designed based off the DBCOD schizandrin C. In clinical trials, **1-39** was found to improve abnormal liver function, inhibit the replication of HBV in chronic hepatitis B patients, and induce differentiation of human hepatocarcinoma cells. These results indicate that DBCODs displaying hepatoprotectivity, such as kadsuraol C, could potentially serve as chemopreventive agents active in the control of liver carcinogenesis.[1] All three kadsuraols could presumably be synthesized using the same route while merely changing the identity of the ester introduced at C9. Compound **3-3** was selected as the first target of this synthetic work due to its reported bioactivity. **3-3** possesses a unique 6-4 ring system in place of the usual 8-membered ring. It bears a total of six stereocenters, three of which are vicinal quaternary stereocenters, posing a formidable synthetic challenge.

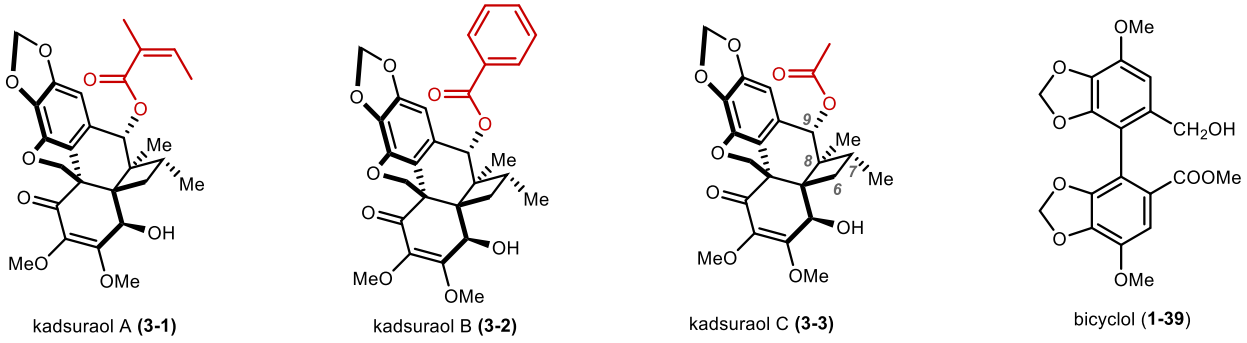
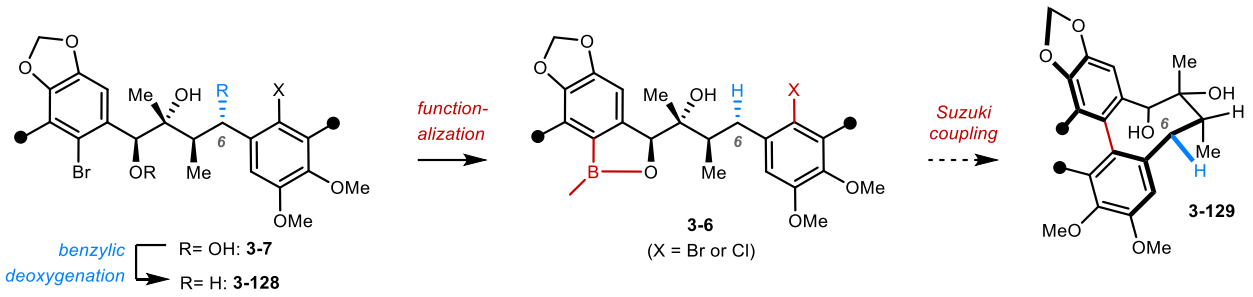


Figure 3.1. Kadsuraols A–C and positive control bicyclol

In this chapter, efforts towards the total synthesis of kadsuraol C are discussed. Several aromatic aldehyde and ketone fragments were prepared and reacted in aldol additions to provide linear DBCOD precursors bearing stereocenters at C6, C7, and C9. The C8 stereocenter was then set via chelate-controlled methyl addition. The effect of halides and phenolic protecting groups on the two fragments on the outcome of the aldol and methyl addition reactions was investigated. Benzylic deoxygenation conditions were developed to remove the superfluous C6 alcohol after it

had served its role in directing the stereochemical outcome of the methyl addition (Scheme 3.1). Functionalization to install tethered aryl borinic ester and aryl halide (either Cl or Br) handles for Suzuki coupling was performed. The substrate limitations of the Suzuki coupling to form the biaryl axis were explored, where the identity of the C6 substituent proved to play a key role.

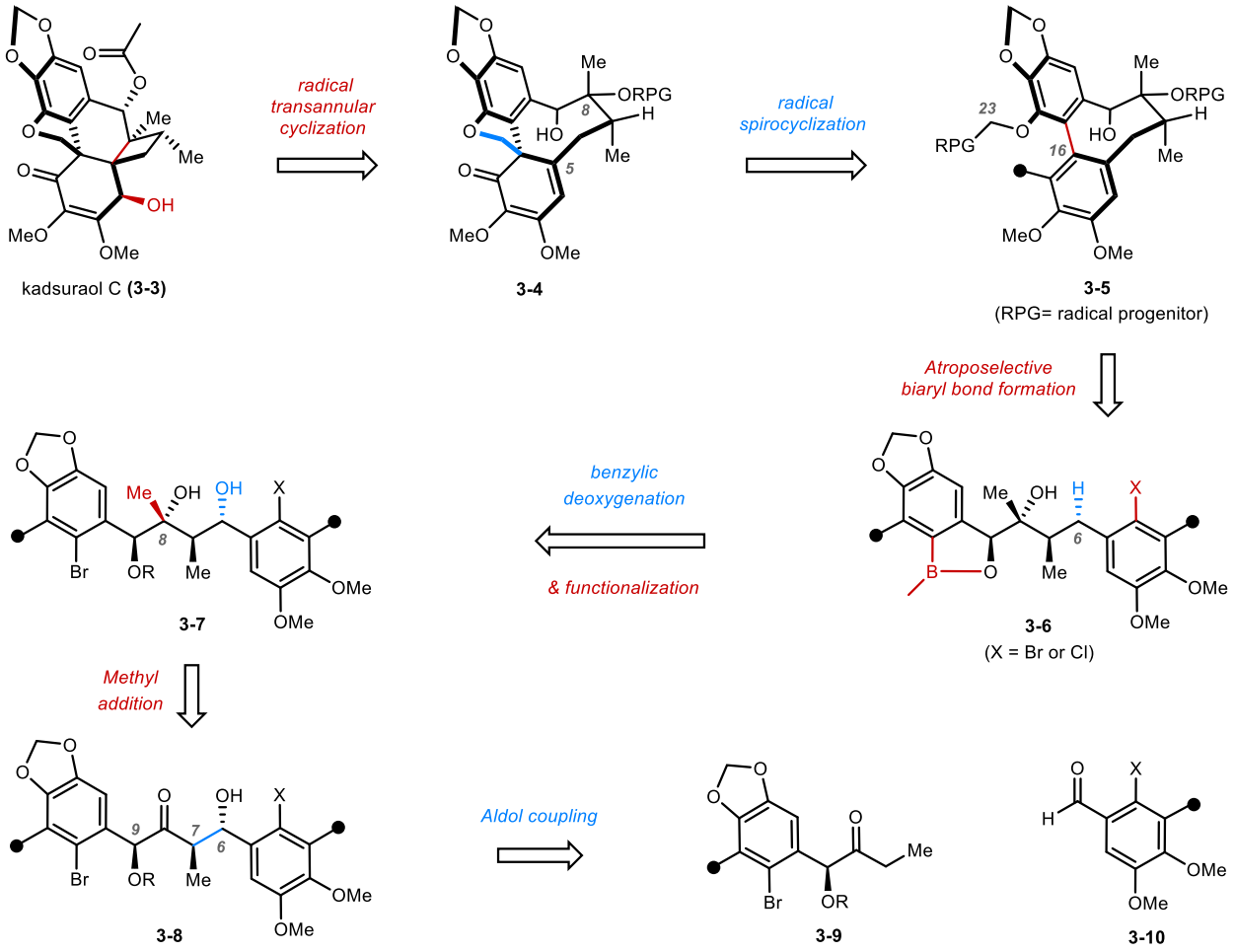


Scheme 3.1. Key steps towards kadsuraol C following the methyl addition

3.2. Retrosynthetic analysis

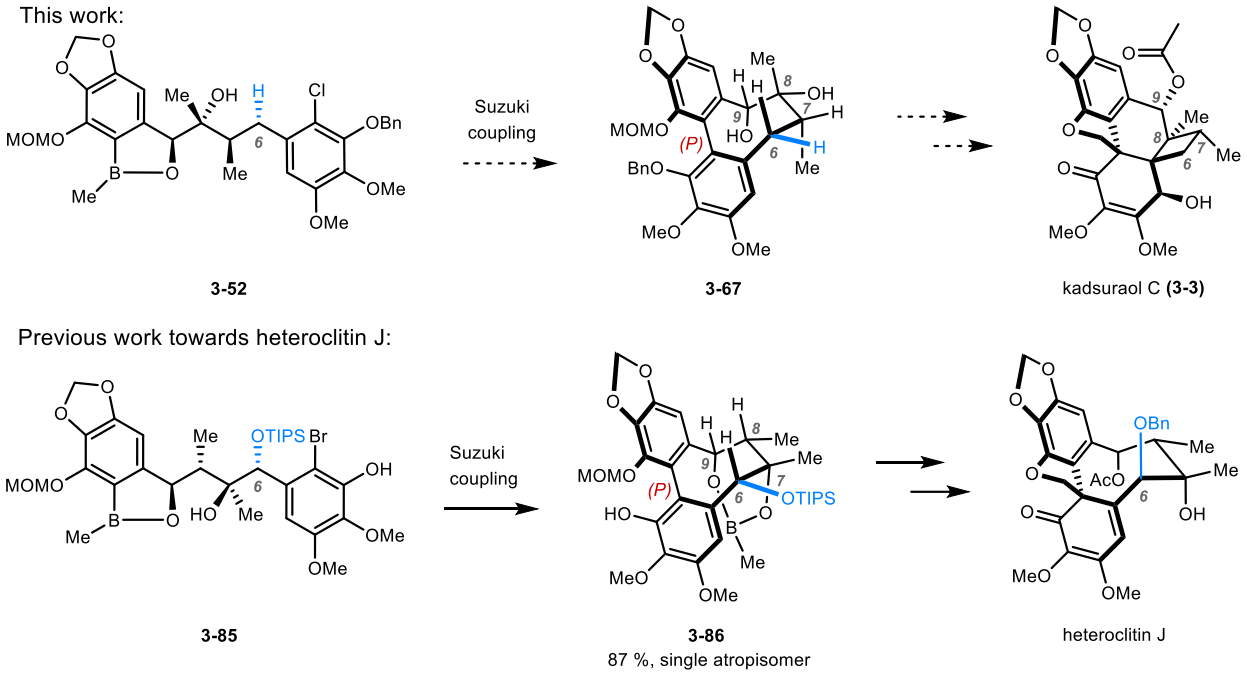
Retrosynthetically, it was expected that kadsuraol C (**3-3**) could result from spirodienone **3-4** via a transannular radical cyclization (Scheme 3.2). The radical progenitor at C8 would lead to the production of a tertiary radical which would undergo transannular attack onto C5, converting the 8-membered ring to a 6-4 ring system, bearing vicinal quaternary stereocenters. *Ortho*-spirodienone **3-4** could arise from dibenzocyclooctadiene **3-5** by regioselective photocatalyzed spirocyclization previously developed in our group. A radical would be generated from the radical progenitor at C23 (an *N*-hydroxyphthalimide redox-active ester) and would then undergo 5-*exo* cyclization, attacking C16, and yielding the *ortho*-spirodienone. The 8-membered ring of **3-5** could arise from atroposelective biaryl bond formation via intramolecular Suzuki coupling of **3-6**, which bears suitable handles for cross coupling, to selectively give the (*P*) atropisomer. Compound **3-6** can result from functionalization (to append the handles for Suzuki coupling) and C6 benzylic deoxygenation of compound **3-7**. Chelate-controlled methyl addition would be used to set the C8 stereocenter of **3-7** and the first linear substrate **3-8** would be formed via aldol addition of the prefunctionalized aromatic ketone and aldehyde fragments, **3-9** and **3-10**, setting the C6, C7, and C9 stereocenters along the linear chain.

In the previous DBCOD synthesis in our group, the deoxygenation of C6 was not required as the desired substrate heteroclitin J possessed an ester at C6 (Scheme 3.3). Therefore, the

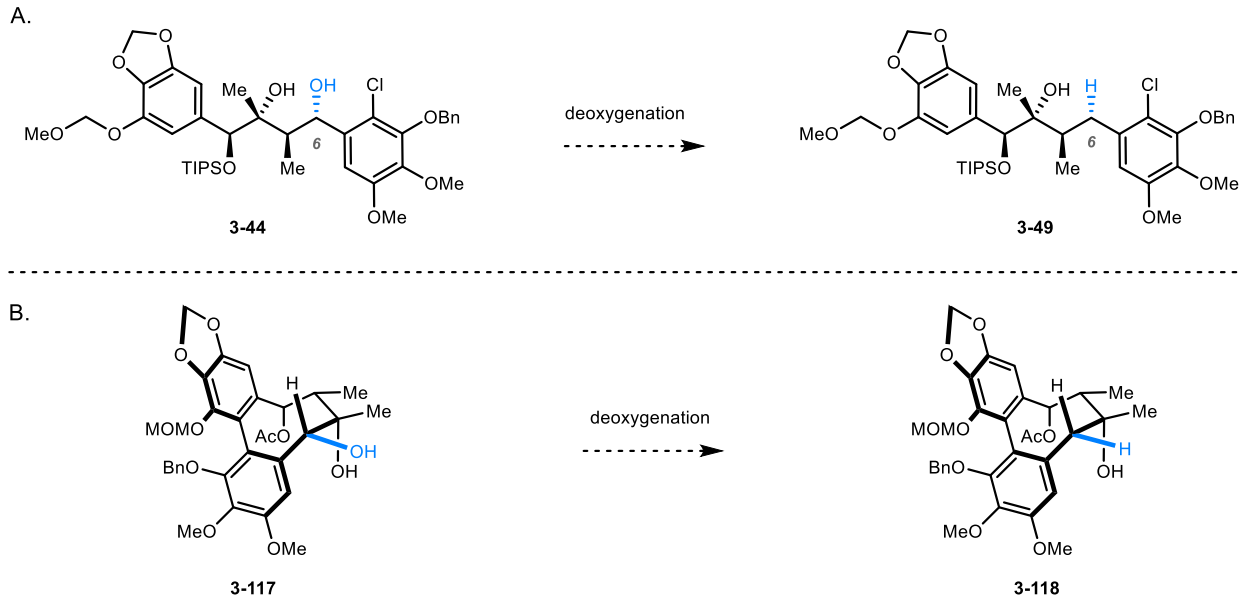


Scheme 3.2. Retrosynthetic analysis of kadsuraol C

deoxygenation of C6 poses a new challenge in the syntheses of kadsuraol C and taiwanschirin B. The two options for addressing this challenge are to either perform the deoxygenation on the linear substrate (ie. the methyl addition product **3-44**, Scheme 3.4A) or to perform the deoxygenation on a cyclic substrate (ie. the Suzuki coupling product **3-117**, Scheme 3.4B). The deoxygenation of the linear substrate could be performed using the methodology developed on our model system in section 2.4. This would then require that the Suzuki coupling be accomplished on a substrate bearing a methylene at C6 (**3-52**, Scheme 3.3). It is not known what effect this would have on biaryl bond formation as our previous Suzuki coupling substrate **3-85** bore an OTIPS group at C6. The second option, deoxygenation on a cyclic substrate, would require the development of new methodology and is likely more difficult than deoxygenation of a linear substrate due to increased steric encumbrance and worse overlap of the benzylic position with the neighboring π-system. Therefore, we chose to investigate deoxygenation on the linear system first.



Scheme 3.3. Comparison to the previous Suzuki coupling leading to heteroclitin J



Scheme 3.4. Deoxygenation of a A) linear substrate or B) cyclic substrate

3.3. Strategy 1: brominated ketone + chlorinated aldehyde

The ketone and aldehyde fragments initially selected as the starting materials for the synthesis of kadsuraol C were ketone **3-13** and aldehyde **3-24** (Figure 3.2). Different protecting groups (MOM and Bn) were selected for the protection of the ketone and aldehyde fragments to

allow for selective deprotection. A Br was placed at C16 of the ketone so that it could later be converted to the borinic ester handle for use in the Suzuki coupling to form the biaryl axis. A halide was required at C15 of the aldehyde to serve as the other handle for Suzuki coupling. A Cl was selected for this purpose so that it could be differentiated from the Br of the ketone fragment during lithium-halogen exchange. Several analogues of ketone **3-13** bearing different α-siloxy groups were prepared to test their effects on the yield and diastereoselectivity of the aldol addition. The ketones synthesized in this chapter were racemic, however future work includes the preparation of enantiopure kadsuraol C starting from the analogous enantiopure ketone, which we anticipate could be prepared using North's asymmetric hydrocyanation methodology.[2]

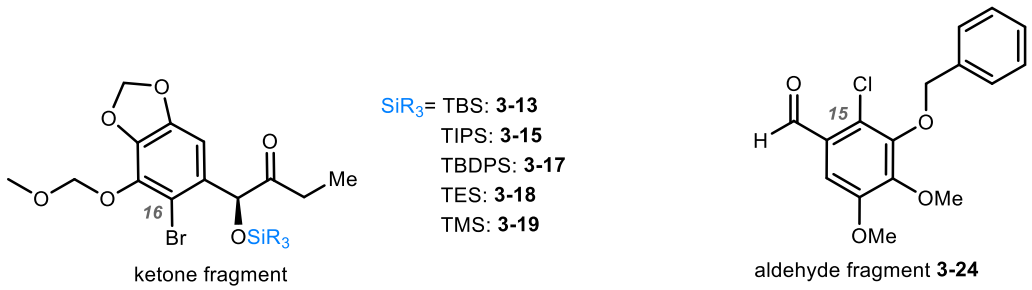
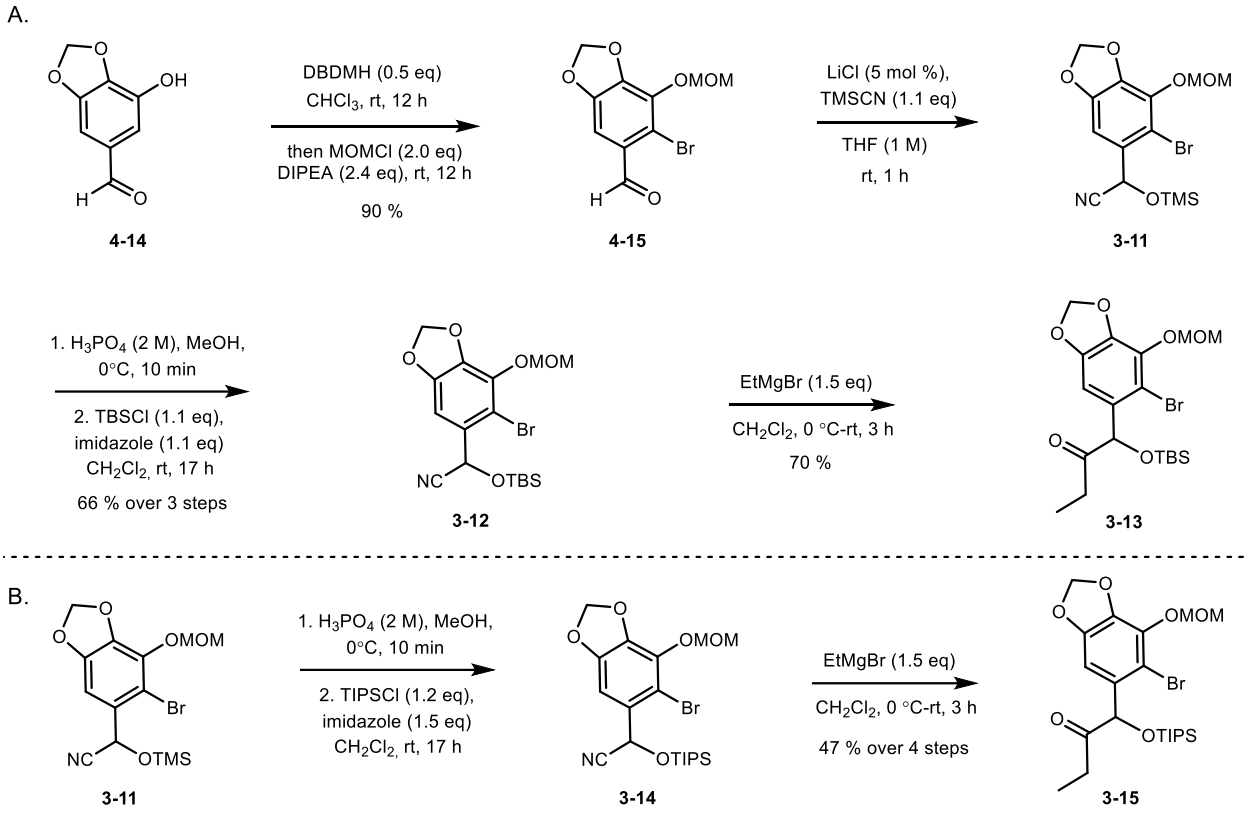


Figure 3.2. Ketone and aldehyde fragments for use in strategy 1

3.3.1. Synthesis of the brominated ketone fragments

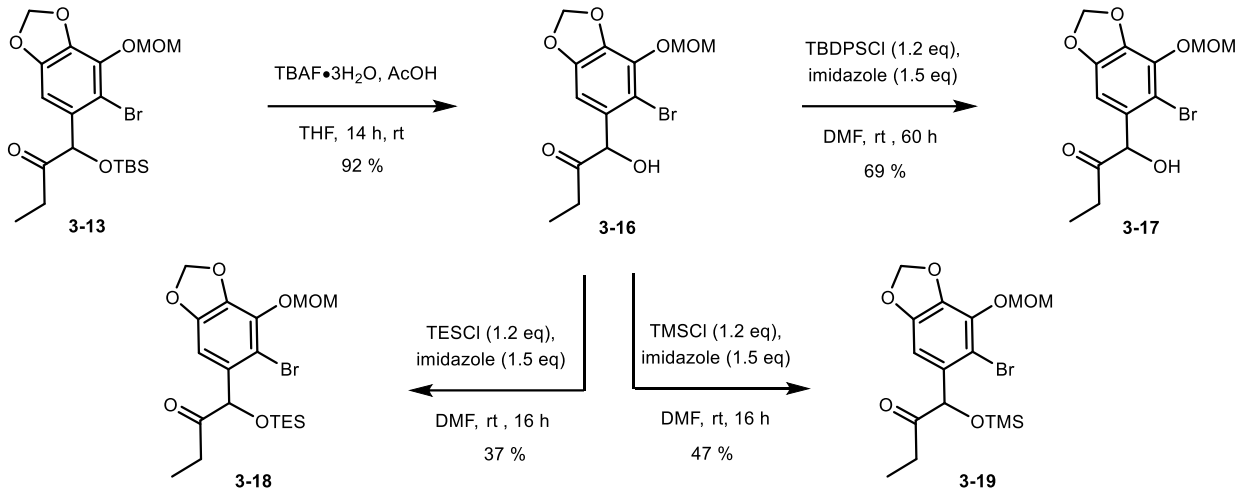
The ketone fragment **3-13** was prepared in five steps from 5-hydroxypiperonal (**4-14**). Compound **4-14** was subjected to phenol-directed *o*-bromination with dibromodimethylhydantoin (DBDMH) following RajanBabu's procedure, where hydrogen bonding between the carbonyl oxygen of DBDMH and the phenolic proton leads to high regioselectivity.[3] This was followed by protection of the phenol as the MOM ether in the same pot, providing **4-15** in 90 % yield. Aldehyde **4-15** was then converted to cyanohydrin **3-11** by hydrocyanation with LiCl (5 mol %) and trimethylsilyl cyanide (1.1 eq, Scheme 3.5A).[4] Deprotection of the TMS ether under acidic conditions and subsequent reprotection of the alcohol using *tert*-butyldimethylsilyl chloride (1.2 equiv.) and imidazole (1.1 equiv.) gave TBS-protected **3-12** in 66 % yield over three steps. The Grignard reaction of **3-12** with ethylmagnesium bromide (1.5 equiv.) furnished ketone **3-13** in 70 % yield. The analogous TIPS-protected ketone **3-15** was prepared in two steps from intermediate **3-11** (Scheme 3.5B). Compound **3-11** was subjected to deprotection of the TMS ether with acid, followed by treatment with triisopropylsilyl chloride (1.2 equiv.) and imidazole (1.5 equiv.) to

reprotect the alcohol as a TIPS ether, giving **3-14**. Then, **3-14** was treated with ethylmagnesium bromide (1.5 equiv.), providing **3-15** in 47 % yield over four steps.



Scheme 3.5. Preparation of A. TBS-protected ketone **3-13** and B. TIPS-protected ketone **3-15**

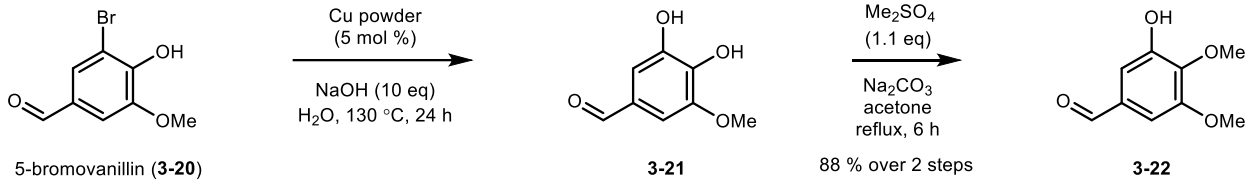
The TBDPS-, TES-, and TMS- protected derivates of the ketone fragment were prepared from **3-13** (Scheme 3.6). The TBS group of **3-13** was removed by treatment with TBAF•3H_2O buffered with acetic acid in THF, furnishing free alcohol **3-16** in 92 % yield. **3-16** could then be converted to the three derivatives by protection of the alcohol using the desired silyl chloride and imidazole in DMF. The TBDPS-protected ketone **3-17** was obtained in 69 % yield, the TES-protected ketone **3-18** in 37 % yield, and the TMS-protected ketone in 47 % yield.



Scheme 3.6. Preparation of TBDPS-, TES-, and TMS- protected ketones **3-17**, **3-18**, and **3-19**

3.3.2. Synthesis of the chlorinated aldehyde fragment

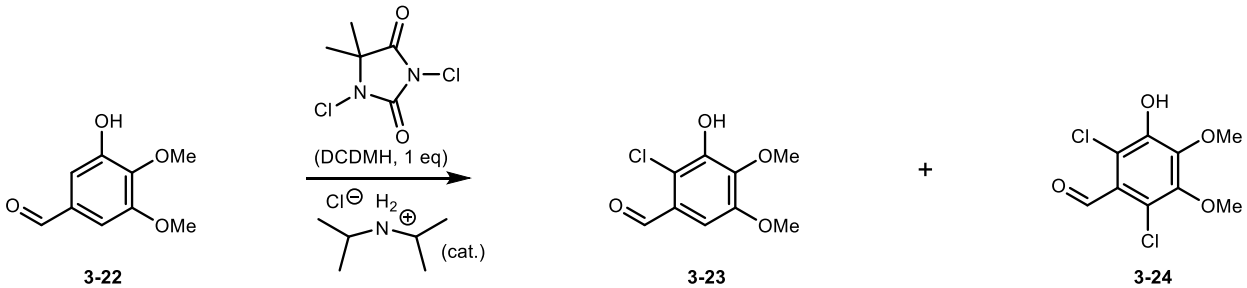
The first two steps in the synthesis of the aldehyde fragment **3-24** were accomplished using reported procedures[5] for the preparation of **3-22** from 5-bromovanillin (**3-20**, Scheme 3.7). **3-20** was treated with copper powder (5 mol %) and sodium hydroxide (10 equiv.) in water at 130 °C for 24 h, leading to nucleophilic aromatic substitution, where a hydroxyl group replaced the bromide, providing **3-21**. Subsequent methylation of catechol **3-21** with dimethyl sulfate and sodium bicarbonate in refluxing acetone for 6 h, provided the mono-methylated product **3-22** in 88 % yield over 2 steps on 50 mmol scale. Methylation occurs preferentially at the alcohol in the 4-position, which is more electron rich due to being positioned *ortho* to two activating substituents (OH and OMe).



Scheme 3.7. Preparation of intermediate **3-22**

It was expected that the regioselective mono-chlorination of **3-22** could be accomplished using 1,3-dichloro-5,5-dimethylhydantoin (DCDMH), which is known to hydrogen bond to phenols, directing *ortho*-chlorination. **3-22** (0.1 mmol) was subjected to conditions reported by Yeung and coworkers[6] for the *ortho*-chlorination of phenols involving DCDMH (1 equiv.) and catalytic

diisopropylamine hydrochloride (5 mol %) in PhMe (0.1 M) at 0 °C in the dark (Table 3.1, entry 1). The results were observed by ^{1}H NMR spectroscopy, which indicated that the starting material had been fully consumed and that 69 % yield of the desired mono-chlorinated product **3-23** had formed as well as 9 % of the dichlorinated byproduct **3-24**. Increasing the dilution of the reaction mixture to 0.05 M (entry 2) or increasing the catalyst loading to 10 mol % (entry 3), slightly increased the NMR yield of **3-23** to 75 or 73 %, respectively, however these conditions also increased the yield of the dichlorinated **3-24** to 11 %. To enable isolation, the reaction was scaled up to 1.1 mmol using the reported conditions, however separation of **3-23** and **3-24** proved challenging, with only 27 % yield of **3-23** being isolated cleanly after column chromatography followed by recrystallization (entry 4). Expecting that a higher yield might be obtained from recrystallization on a larger scale, the reaction was run on 3.3 mmol for either 4 or 6 h (entries 5, 6), however these resulted in only marginally higher yields of **3-23** (34 % and 39 %, respectively). Increasing the scale to 5 mmol offered a similar yield of **3-23** (36 %, entry 7). The low isolated yields of **3-23** were a result of the fact that it was difficult to separate from **3-24**. In attempts to avoid formation of any of the dichlorinated **3-24**, thus facilitating purification of the



Entry	Scale (mmol)	NH_2iPr_2Cl (mol %)	time (h)	% Consum.[c]	NMR Yield **3-23** (%)[c]	NMR Yield **3-24** (%)[c]	Isolated Yield **3-23** (%)
1	0.1	5	4	100	69	9	-
2[a]	0.1	5	4	100	75	11	-
3	0.1	10	4	100	73	11	-
4	1.1	5	4	100	-	-	27
5	3.3	5	4	100	-	-	34
6	3.3	5	6	100	-	-	39
7	5	5	6	100	-	-	36
8[b]	1.1	5	4	50	-	-	-

a= reaction concentration of 0.05 M rather than 0.1 M

b= using 0.5 eq DCDMH

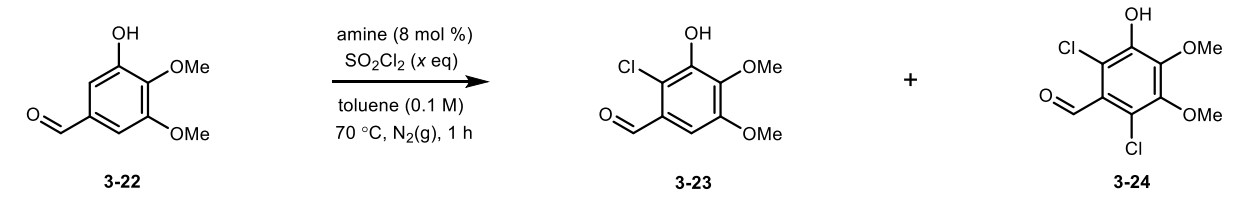
c= % Consum. = % consumption of **3-22**. Hexamethybenzene was used as an internal standard in $CDCl_3$

Table 3.1. *Ortho*-chlorination using DCDMH and NH_2iPr_2Cl catalyst

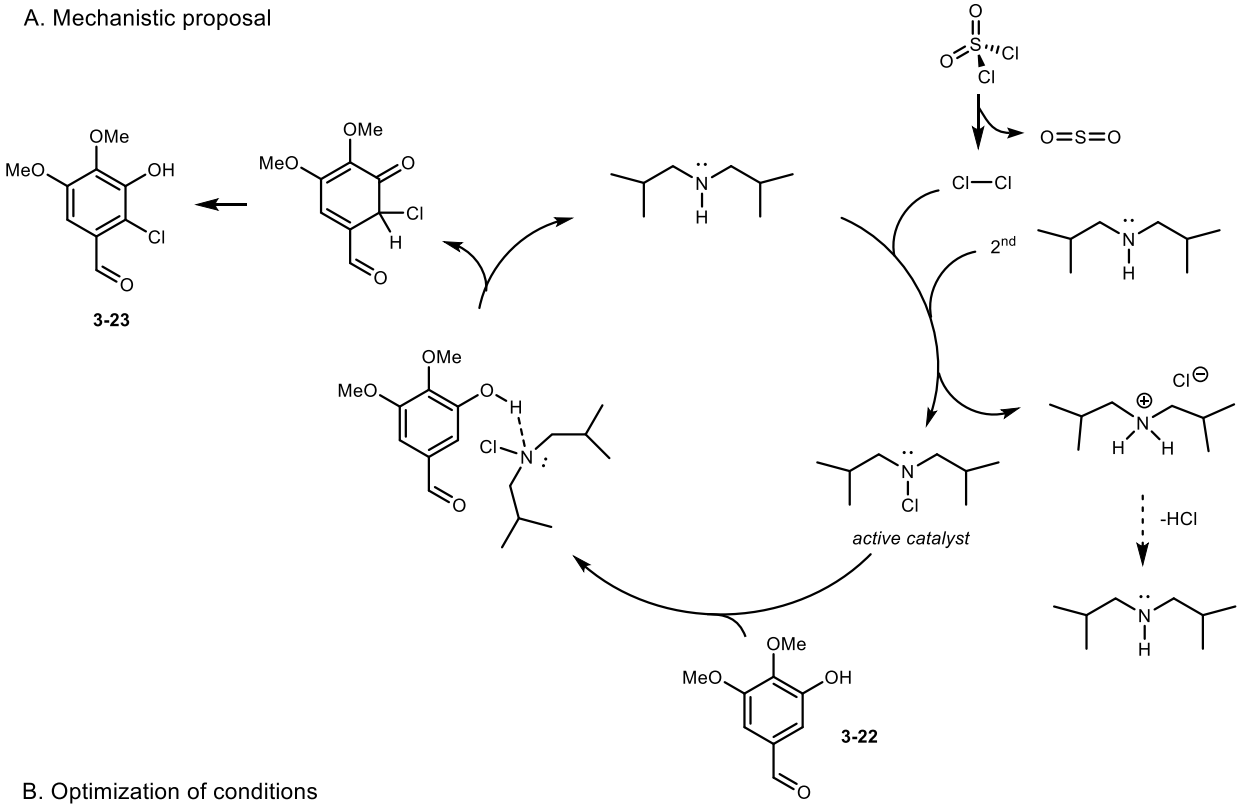
monochlorinated **3-23**, the equivalents of DCDMH were decreased to 0.5 (entry 8). However, this reaction only reached 50 % consumption of **3-22**, with a 1:1:0 ratio of **3-22**: **3-23**: **3-24** being observed by ^{1}H NMR, thus indicating that 1 equivalent of DCDMH is required for the reaction to proceed to completion.

Considering the poor yields of **3-23** obtained via chlorination with DCDMH and NH_2iPr_2Cl, alternative *ortho*-chlorination methods were pursued. Sheldon and coworkers reported the regioselective *ortho*-chlorination of phenol with sulfuryl chloride (1 equiv.) catalyzed by a variety of amines (8 mol %) in PhMe at 70 °C.[7] Their reaction was highly specific for monochlorination with only small amounts of polychlorophenols being produced, therefore, it was expected that these conditions could be suitable for our system. The expected mechanism is depicted in Table 3.2A. At 70°C, SO_2Cl_2 decomposes into SO_2 and Cl_2. Cl_2 reacts with the amine (in this case, diisobutylamine), yielding the active catalyst *N*-chloro-diisobutylamine as well as the HCl salt of diisobutylamine. *N*-chloro-diisobutylamine participates in hydrogen bonding with the phenol of **3-22**, directing chlorination via EArS to the *ortho* position, providing **3-23** as the product. Presumably the HCl salt of diisobutylamine undergoes loss of HCl to regenerate diisobutylamine and re-enter the catalystic cycle.

3-22 was subjected to these conditions on 0.1 mmol scale, utilizing three different amine catalysts (*tert*-butylamine, diisobutylamine, and *N*-benzylamine) which were described in the paper[7] (Table 3.2B, entries 1–3). All three entries displayed good to excellent consumption of **3-22** of 85 %, 99 %, and 90 %, respectively and only produced 8–9 % of the undesired dichlorinated **3-24**. The NMR yield using diisobutylamine (> 90 %) was superior to those using *tert*-butylamine (59 %) or *N*-benzylmethyl amine (83 %). 2,2,6,6-tetramethypiperidine (TMP) was also tried as the amine catalyst but provided poor consumption (30 %) and an NMR yield of merely 26 % **3-23** (entry 4). Due to the high consumption of **3-22** and yield observed in entry 2, diisobutylamine was selected as the amine of choice for the subsequent experiments. The reaction could be run at 0.2 mmol scale to provide **3-23** in 61 % isolated yield (entry 5), however attempts to run the reaction on larger scale (0.6 mmol, entry 6) led to a large amount of byproduct **3-24** (64 % yield by NMR) compared to the desired **3-23** (25 % yield by NMR). To avoid over-chlorination, the equivalents of SO_2Cl_2 were decreased in the subsequent experiments. Utilizing 0.5 equiv. SO_2Cl_2 led to incomplete consumption (60 %) and an isolated yield of only 21 % **3-23** (entry 7). The use of 0.8 equiv. SO_2Cl_2



A. Mechanistic proposal



B. Optimization of conditions

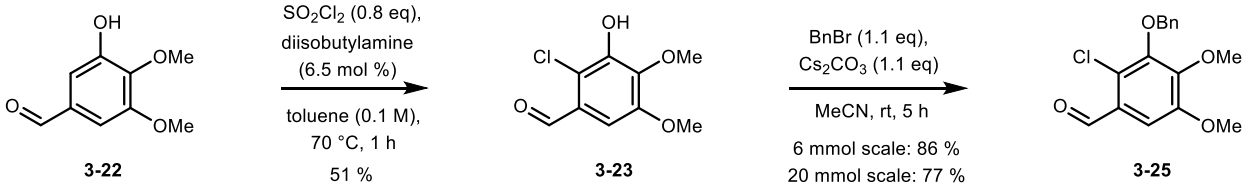
Entry	Scale (mmol)	amine	equivalents SO_2Cl_2	% Consum.[a]	NMR Yield **3-23** (%)[a]	NMR Yield **3-24** (%)[a]	Isolated Yield **3-23** (%)
1	01	*tert*-butylamine	1	85	59	9	-
2	0.1	diisobutylamine	1	99	>90	8	-
3	0.1	*N*-benzylmethylamine	1	90	83	8	-
4	0.1	TMP	1	31	26	0	-
5	0.2	diisobutylamine	1	100	-	-	61
6	0.6	diisobutylamine	1	90	25	64	-
7	0.3	diisobutylamine	0.5	60	-	-	21
8[b]	0.3	diisobutylamine	0.8	93	-	-	74
9[b]	1.8	diisobutylamine	0.8	91	-	-	59
10[b,c]	5.4	diisobutylamine	0.8	-	-	-	51
11[b]	7.0	diisobutylamine	0.8	-	-	-	43

a= % Consum. = % consumption of **3-22**. Hexamethybenzene was used as an internal standard in $CDCl_3$; b= using 6.5 mol % amine;
c= isolated yield is the average over 3 reactions

Table 3.2. *Ortho*-chlorination using SO_2Cl_2 and amine catalyst A) mechanistic proposal; B) optimization of conditions

along with 6.5 mol % diisobutylamine turned out to be the optimum quantities for near full consumption (93 %) without any production of the dichlorinated byproduct and a good isolated yield of **3-23** (74 %, entry 8). The reason for a sub-equimolar amount of SO_2Cl_2 performing best is likely due to the residual impurities in most of the samples of **3-22**. These impurities were challenging to remove at the stage of **3-22** but could be removed after the chlorination step via recrystallization. The reaction employing 0.8 equiv. SO_2Cl_2 was increased to 1.8, 5.4, and 7.0 mmol scale (entries 9–11), with % consumption remaining constant (~90 %) but with a drop in isolated yield observed upon increase in scale (59 %, 51 %, and 43 %, respectively). As a trade-off between material throughput and yield, reactions were typically run on 5 mmol scale (entry 10 conditions) with three reactions being set up concurrently.

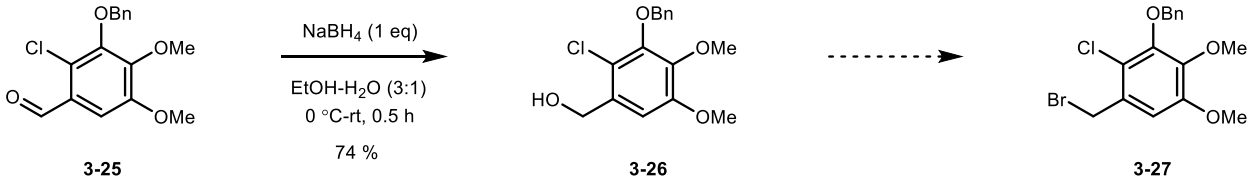
The conversion of intermediate **3-22** into aldehyde fragment **3-25** was performed in two steps (Scheme 3.8). After the chlorination, the phenol of **3-23** could be protected as the benzyl ether using either benzyl bromide, sodium hydride, and tetrabutylammonium iodide in THF overnight or benzyl bromide and cesium carbonate in acetonitrile for 5 h. Comparable yields were obtained using both methods so the latter was selected for increase in reaction scale due to the shorter reaction time. It was run on up to 20 mmol scale, providing a 77 % yield of **3-25**.



Scheme 3.8. Preparation of the chlorinated aldehyde **3-25** from intermediate **3-22**

As an alternative to aldol coupling, alkylation was briefly investigated as a coupling strategy to form the linear DBCOD precursor. While alkylation reactions between a ketone and a benzyl halide were being investigated on a model system (Section 2.2), an aryl bromide **3-27** was targeted which could potentially be coupled with one of the ketones prepared in section 3.3.1 for use in the kadsuraol C synthesis. It was expected that **3-27** could be formed in two steps from aldehyde **3-25**. The first step, reduction of the aldehyde to the alcohol, could be achieved by treatment with sodium borohydride, providing alcohol **3-26** in 74 % yield (Scheme 3.9). The second step, substitution of the hydroxyl with a bromide, was never performed as simultaneous studies on the merits of alkylation vs. aldol addition as a coupling method on the model system (section 2.2)

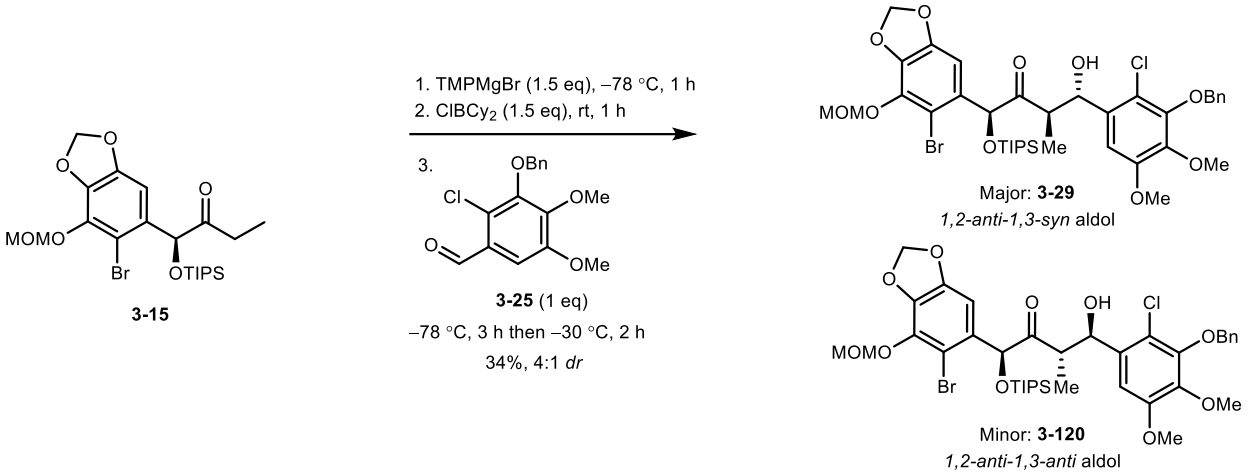
determined that the aldol addition was superior, therefore efforts to prepare **3-27** were abandoned at this stage.



Scheme 3.9. Partial preparation of the benzyl bromide **3-27**

3.3.3. Aldol addition

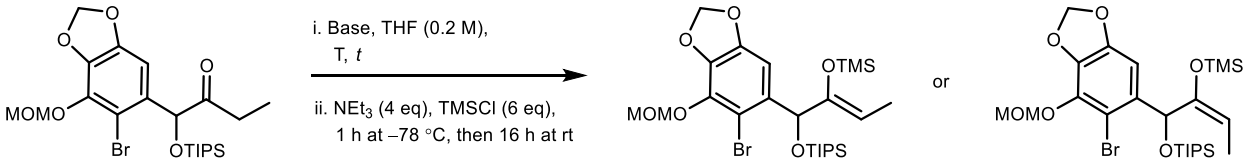
The ketone **3-15** and aldehyde **3-25** were subjected to the coupling conditions previously developed for the synthesis of 1,2-*anti*-1,3-*syn* aldols (see Section 2.2). First, the ketone **3-15** was treated with TMPMgBr (1.5 equiv.) at −78 °C for 1 h to provide the (*E*)-Mg-enolate, followed by the addition of Cy_2BCl (1.5 equiv.) and let stir at rt for 1 h to afford the (*E*)-B-enolate. Aldehyde **3-25** was then added to the reaction mixture at −78 °C and then, after 3 h, the reaction mixture was warmed to −30 °C and let stir another 2 h. Aliquots were periodically taken and analyzed by ^{1}H NMR (Scheme 3.10), revealing that aldehyde **3-25** was consumed after 3 h. Therefore, the reaction time was decreased accordingly for future experiments. The reaction proceeded with a 34 % yield of aldol being isolated in 4:1 *dr*. The major diastereomer was assigned as the desired 1,2-*anti*-1,3-*syn* aldol **3-29** and the minor diastereomer as the 1,2-*anti*-1,3-*anti* aldol **3-120**, which would also arise from the (*E*)-B-enolate.



Scheme 3.10. Aldol addition of ketone **3-15** and aldehyde **3-25** using conditions developed on the model system for formation of a 1,2-*anti*-1,3-*syn* aldol

Optimization of each step of the aldol addition was then performed to achieve the best possible diastereoselectivity and yield of the 1,2-*anti*-1,3-*syn* aldol **3-29**. The enolization step was investigated first by deprotonation of the ketone **3-15** with base and then trapping it as the silyl enol ether via treatment with trimethysilyl chloride and triethylamine (Table 3.3). Treatment of **3-15** with LHMDS or LDA was expected to provide the (*Z*)-silyl enol ether (***Z*-3-33**) as the major species (entries 1, 2). A small amount of ***Z*-3-33** (18 % yield by NMR) was observed using LHMDS, however LDA gave poor *E/Z* regioselectivity. ***Z*-3-33** isolated from entry 1 was characterized by ^{1}H NMR and could be distinguished from its isomer by the distinctive signals at δ = 5.18 (q, 1H) and 1.57 (d, 3H), corresponding to the vinyl proton and methyl protons, respectively. In previous work in our group, TMPMgBr was found to be a good base for the selective formation of (*E*)-enolates from α-siloxy ketones (see section 2.1.2). Therefore, the (*E*)-silyl enol ether (***E*-3-33**) was formed by employing TMPMgBr as the base and was distinguished by its ^{1}H NMR signals at δ = 4.65 (q, 1H) and 1.86 (d, 3H), corresponding to the vinyl proton and methyl protons, respectively. As the TMPMgBr solution utilized was homemade (prepared *in situ*), a minimum of 1.5 equiv. was used in each reaction to ensure that at least 1 equiv. was available to react with the ketone. **3-15** was deprotonated with 1.5 equiv. TMPMgBr for 1 or 2 h at −78 °C, followed by trapping as the silyl enol ether, where a slight drop in yield was observed with increased reaction time (51 % vs 43 %, entries 3, 4). Increasing the reaction temperature to −50 °C with a 1 h reaction time led to a significant drop in yield (23 %, entry 5). Increasing the quantity of TMPMgBr to 3 equivalents offered an increase in yield (entries 6–8). Deprotonations run at −50 °C or −30 °C for 3 h gave yields of 57 % and 50 % ***E*-3-33**, respectively (entries 6, 7). Decreasing the temperature to −78 °C and deprotonation time to 1 h gave an improved yield of 70 % (entry 8). The (*E*)-Mg-enolate had to be transmetallated to the corresponding (*E*)-B-enolate during the second step of the aldol reaction due to the poor diastereoselectivity observed using (*E*)-Mg-enolates (see section 2.1.2). We expected that it would be desirable to minimize Mg salts present in the reaction mixture to avoid the possibility of any (*E*)-Mg-enolate remaining and to prevent any unwanted Mg^{2+} coordination to our substrates, therefore the quantity of TMPMgBr was decreased to 2 equivalents in entries 10–12. Deprotonation times of 0.5, 1, or 2 h resulted in yields of 12 %, 65 %, and 35 % ***E*-3-33** respectively. These results indicate that conversion to the enolate is incomplete after 0.5 h and decomposition starts to occur after 2 h, making 1 h the ideal time for deprotonation. The yields using 3 or 2 equivalents of TMPMgBr (70 % and 65 %, entries 8 and

11) were close enough that 2 equiv. was selected as the standard condition to avoid potential issues during the subsequent transmetallation step.



3-15 ***Z*-3-33** ***E*-3-33**

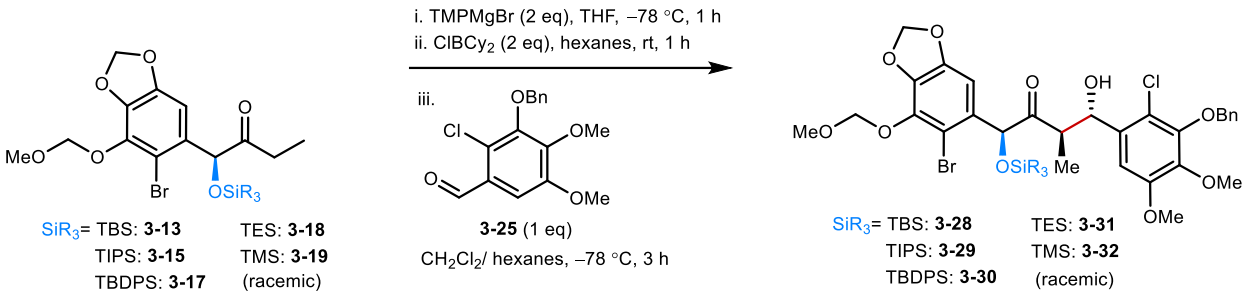
Entry	Base (eq)	T (°C)	t (h)	Stereochemistry[a]	Conv. (%)[b]	NMR Yield of **3-33** (%)[b]
1	LHMDS (3)	–78	3	*Z*	96	18
2	LDA (3)	–78	3	mixture	100	N/A
3	TMPMgBr (1.5)	–78	2	*E*	64	43
4	TMPMgBr (1.5)	–78	1	*E*	94	51
5	TMPMgBr (1.5)	–50	1	*E*	82	23
6	TMPMgBr (3)	–50	3	*E*	100	57
7	TMPMgBr (3)	–30	3	*E*	100	50
8	TMPMgBr (3)	–78	1	*E*	100	70
9	TMPMgBr (3)	–50	1	*E*	95	63
10	TMPMgBr (2)	–78	0.5	*E*	66	12
11	TMPMgBr (2)	–78	1	*E*	100	65
12	TMPMgBr (2)	–78	2	*E*	100	35

All experiments were performed on 0.2 mmol scale. a= (*Z*) silyl enol ether was identified by an vinyl δ of 5.18 (q) and methyl δ of 1.57 (d); (*E*) silyl enol ether was identified by an vinyl δ of 4.65 (q) and methyl δ of 1.86 (d).
b= hexamethybenzene was used as internal standard in $CDCl_3$.

Table 3.3. Enolization studies: trapping the silyl enol ethers of **3-15**

The identity of the α-siloxy group of the ketone fragment has been shown to affect diastereoselectivity of the aldol addition in the model system, hence five ketones bearing different α-siloxy groups (**3-13**, **3-15**, **3-17**, **3-18**, and **3-19**) were evaluated as substrates for aldol addition with aldehyde **3-25** (Table 3.4). The ketones and aldols are all racemic, with only the desired enantiomer depicted in the table for clarity. Each ketone was subjected to TMPMgBr (2 equiv.) at –78 °C for 1 h, followed by Cy_2BCl (2 equiv.) at rt for 1 h, and then aldehyde **3-25** at –78 °C for 3 h. The TIPS-protected ketone **3-15** displayed good consumption of starting material (78 %) under these conditions with 43 % yield of product **3-29** being isolated in 4:1 *dr* (entry 1). The TBS-protected ketone **3-13** (entry 2) produced a mixture of multiple diastereomeric aldols, surprisingly with the desired 1,2-*anti*-1,3-*syn* aldol only being a minor constituent (1:5 *dr*). No product was obtained from the TMS-protected ketone **3-19** which decomposed (entry 3). The TES-protected ketone **3-18** provided a comparable yield of aldol (46 %) to that obtained from **3-15** but with low diastereoselectivity (2:1 *dr*, entry 4). The TBDPS-protected ketone **3-17** furnished aldol product

in comparable *dr* to **3-15** (4:1) but proceeded slowly, with only 50 % consumption and 16 % isolated yield (entry 5). In general, bulkier α-siloxy substituents led to higher diastereoselectivity. This trend could possibly be attributed to dispersive interactions, which would increase with bulk of the α-siloxy substituent. It may be worth repeating entry 2 which appears anomalous, as we would expect the TBS-bearing substrate to provide a *dr* somewhere between 2:1 and 4:1 based on its size being between that of a TES group and a TIPS group. Since TIPS-protected **3-15** provided the best combination of yield and diastereoselectivity, it was selected for use in the subsequent experiments.



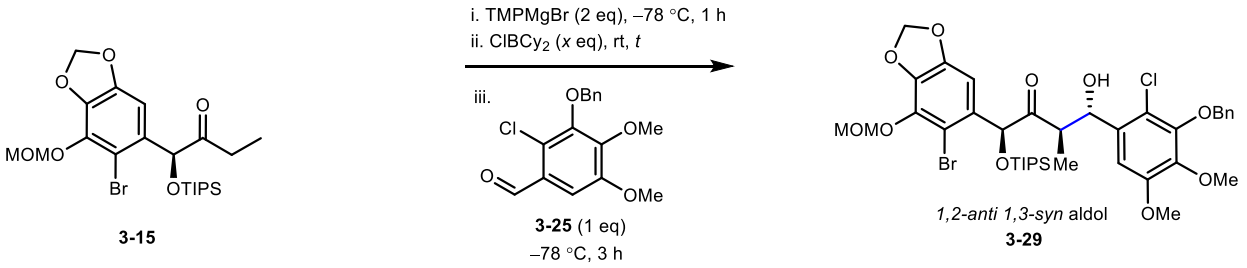
Entry	SiR_3	Consum. (%)[a]	Isolated yield (%)	*dr* of isolated
1	TIPS	78	43	4:1
2	TBS	-	38	1:5
3	TMS	-	decomp	decomp
4	TES	49	46	2:1
5	TBDPS	50	16	4:1

All reactions were run on 0.1 mmol scale.
a= Consum. = consumption of starting material. Hexamethylbenzene was used as an internal standard in $CDCl_3$

Table 3.4. Aldol addition using the various α-siloxy ketones

With the optimal enolization conditions for **3-15** (2 equiv. TMPMgBr at –78 °C for 1 h) in hand, the subsequent transmetallation step was then optimized (Table 3.5). Using less $ClBCy_2$ (1.5 equiv.) than TMPMgBr provided full consumption of starting material and an isolated yield of 47 % but as a mixture of 4 diastereostereomeric aldol products with low diastereoselectivity (2:1) for the desired 1,2-*anti*-1,3-*syn* aldol **3-29** (entry 1). Using equimolar amounts of $ClBCy_2$ and TMPMgBr (2 equiv.) led to the formation of only two diastereomeric aldol products with improved *dr* (entries 2–5). A transmetallation time of 1 h (entry 2) provided better yield and *dr* (43 %, 4:1) compared to a transmetallation time of 2 h (entry 3, 16 % yield, 3:1 *dr*). Entries 4 and 5 examine the use of homemade $ClBCy_2$ compared to the commercially available reagent which was employed in entries 1–3. Decreasing the transmetallation time to 0.5 h (entry 4) led to a drop in

yield (27 %) with comparable *dr* (3:1). 1 h of transmetallation with 2 equiv. homemade $ClBCy_2$ (entry 5) provided a slightly higher yield of **3-29** (50 %) than the commercial reagent and slightly worse *dr* (3:1). Entries 2 and 5 were deemed comparably good, thus future experiments employed the reaction of 2 equiv. of either homemade or commercially available $ClBCy_2$ for 1 h. Additionally, the use of other boranes such as Bu_2BOTf, (+)-DIP-Chloride™, and (−)-DIP-Chloride™ instead of $ClBCy_2$ in the transmetallation step was briefly explored but these led to inferior diastereoselectivity and yield.



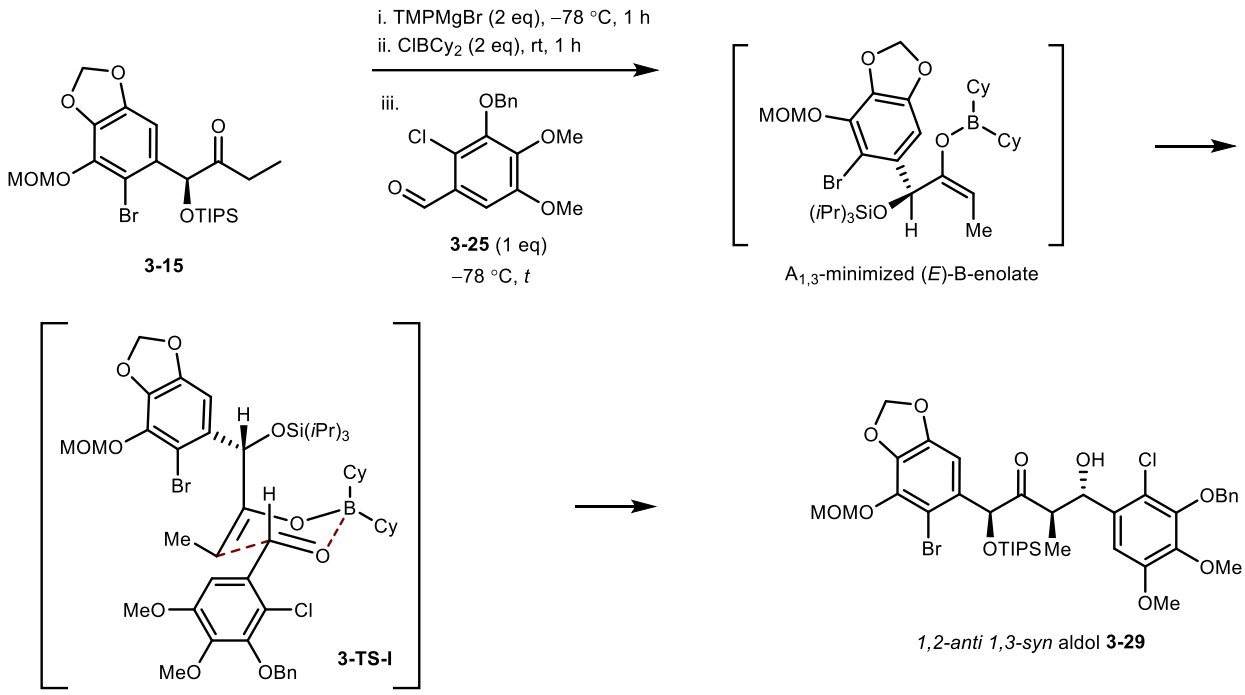
Entry	eq. $ClBCy_2$	time (h)	Conv. (%)[a]	NMR Yield (%)[a]	Isolated Yield (%)	*dr* of isolated	number of diastereomers
1	1.5	1	100	59	47	2:1	4
2	2.0	1	78	37	43	4:1	2
3	2.0	2	22	20	16	3:1	2
4[b]	2.0	0.5	58	45	27	3:1	2
5[b]	2.0	1	54	58	50	3:1	2

All experiments were run on a 0.2 mmol scale. a = hexamethylbenzene was used as internal standard in $CDCl_3$.
b = Commercially available $ClBCy_2$ was used (whereas all other entries used homemade $ClBCy_2$).

Table 3.5. Transmetallation studies

With the enolization and transmetallation steps of the aldol addition optimized, it was time to investigate the reaction of the (*E*)-B-enolate with the aldehyde. To obtain the desired 1,2-*anti*-1,3 *syn* aldol product, the 1,2-*anti* relationship is conferred from the enolate geometry. The 1,3-*syn* relationship is the result of the aldehyde approaching the face of the $A_{1,3}$-strain minimized boron-enolate furthest away from the large alpha substituent (R_L, the aryl ring), proceeding through the Zimmermann-Traxler transition state **3-TS-I** (Table 3.6). Reacting the (*E*)-B-enolate (formed *in situ* on 0.2 mmol scale) with aldehyde **3-25** for 3 h at –78 °C resulted in an isolated yield of 50 % **3-29** in 3:1 *dr* (entry 1). In attempts to improve this yield, the reaction time with **3-25** was increased concurrently with scale. In entry 2, the reaction was run on 1.0 mmol scale for 5 h at –78 °C with **3-25**, providing an increased yield of 57 % **3-29** in 4:1 *dr*. Increasing the scale to 8.0 mmol (entry 3), the reaction time with **3-25** was increased to 8 h, resulting in a yield of 74 % **3-29** in 3.5:1 *dr*.

This 8 h reaction time of the *in situ* generated (*E*)-B-enolate with **3-25** was selected as the best condition for the aldol addition. The slight fluctuation in *dr* between the three reactions was attributed to the use of homemade vs. commercially available $ClBCy_2$.

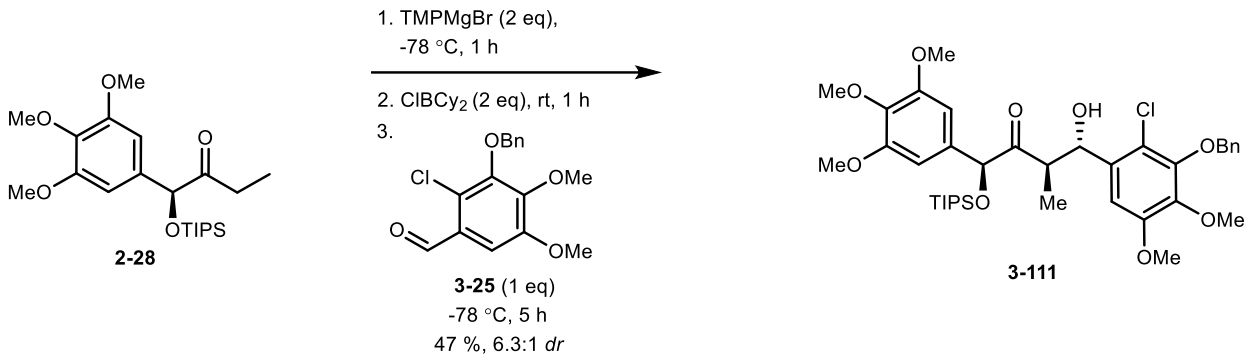


Entry	scale (mmol)	*t* (h)	yield (%)	*dr*
1	0.2	3	50	3:1
2	1.0	5	57	4:1
3	3.0	8	74	3.5:1

Table 3.6. Increasing the scale of the aldol addition (and increasing reaction time with aldehyde)

For comparison, the chlorinated aldehyde **3-25** was also reacted with the model ketone **2-28** from Chapter 2 (Scheme 3.11). **2-28** (0.2 mmol) was deprotonated with TMPMgBr (2 equiv.) at –78 °C for 1 h followed by the addition of $ClBCy_2$ which was let stir at rt for 1 h and then treated with **3-25** (1 equiv.) at –78 °C for 5 h, providing the 1,2-*anti*-1,3-*syn* aldol **3-111** in 47 % yield and 6.3:1 *dr*. Recalling that the reaction of model ketone **2-28** with model aldehyde **2-14** furnished the 1,2-*anti*-1,3-*syn* aldol **2-29** in 56 % yield and 16:1 *dr* (see Section 2.2), this points to a trend that better diastereoselectivity is achieved with the use of a tri-methoxy aryl-bearing ketone as opposed to a benzodioxolane-bearing ketone. The benzodioxolane of **3-15** is more inductively withdrawing than the tri-methoxy arene of **2-28**, leading to a less electron-rich enolate, which could lead to a

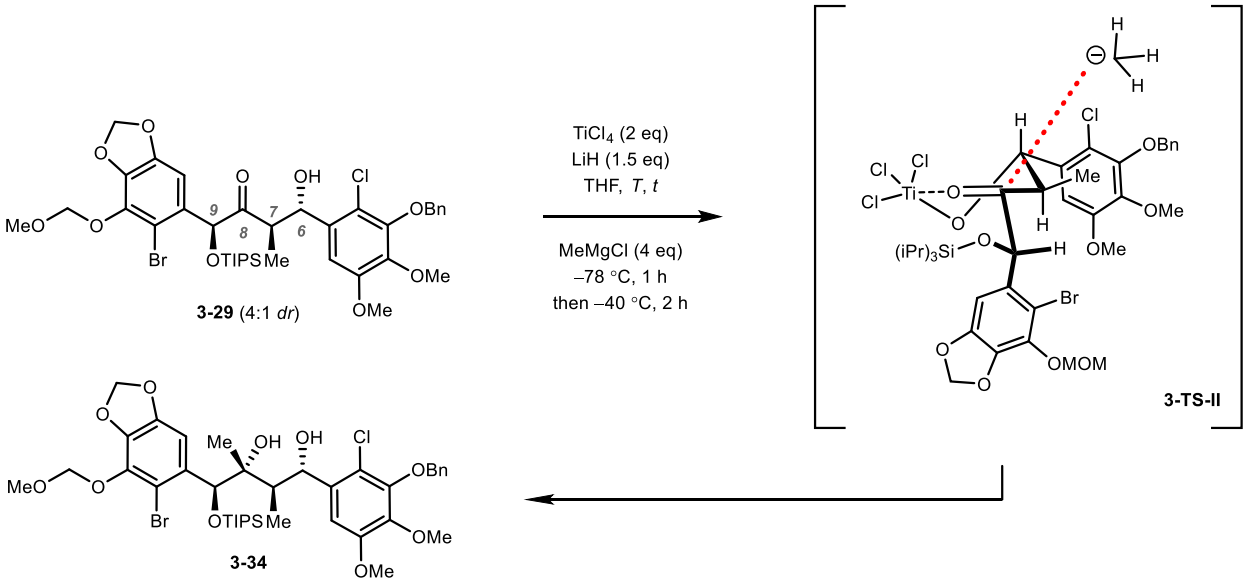
less tight 6-membered transition state, and therefore lower diastereoselectivity due to the presence of some open transition state. Another possible cause of the increased diastereoselectivity using **2-28**, is the ability of the methoxy groups to chelate and retain Mg^{2+} salts.



Scheme 3.11. Aldol addition of model ketone **2-28** and chlorinated aldehyde **3-25**

3.3.4. Chelate-controlled methyl addition

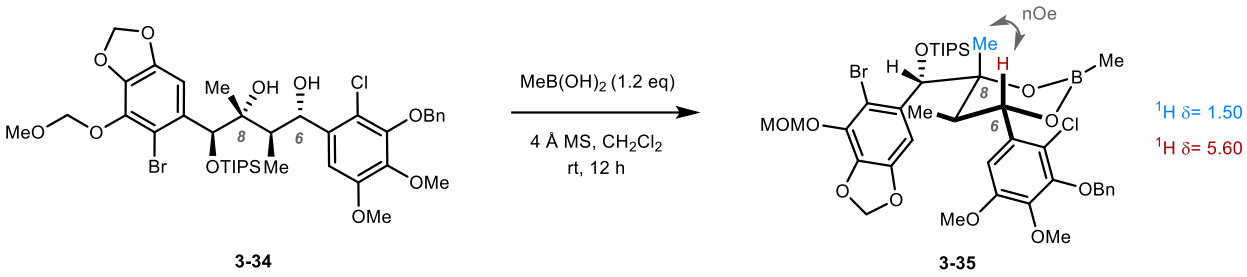
The 1,2-*anti* 1,3-*syn* aldol **3-29** was subjected to Bartoli's chelate controlled methyl addition[8] which had been successfully employed to install the C8 stereocenter of our model 1,2-*anti* 1,3-*syn* aldol (**2-29**) with high diastereoselectivity (see Section 2.3). These conditions involve two steps: first, formation of the Ti-(IV) chelate by deprotonation with LiH (1.5 equiv.) and $TiCl_4$ (2.0 equiv.) in THF at –30 °C for 0.5 h and second, alkylation with MeMgCl (4 equiv.) at –78 °C for 1 h followed by –40 °C for 2 h. This reaction produced a low 2 % yield of a mixture of methyl addition products along with recovered **3-29** (45 %, Table 3.7, entry 1). Optimization of both the chelation and alkylation steps was then conducted to obtain a better yield and diastereoselectivity for the desired methyl addition product, 1,3-*syn* diol **3-34** (Tables 3.7 and 3.8). Modifications to the chelation step were investigated first. Setting the reaction temperature to –15 °C during the chelation step led to the isolation of a 16 % yield of a single diastereomer of product **3-34** and recovery of 41 % **3-29** (Table 3.7, entry 2). As incomplete conversion was observed after 0.5 h chelation, followed by the standard alkylation time, the time for the chelation step was then increased to 1 h in entries 3 and 4. Chelation at 0 °C for 1 h (entry 3) or at –30 °C for 1 h (entry 4) yielded comparable amounts of the desired *syn* diol **3-34** (24 % and 28 %, respectively) and minor diastereomers (16 % and 12 %, respectively). A chelation temperature of –30 °C (entry 4) led to better mass balance than warmer temperatures, with 43 % **3-29** being recovered (vs. 20 % in entry 3) therefore these chelation conditions were selected for future experiments.



Entry	T (°C)	t (h)	Rec. SM **3-29** (%)	Isolated yield, minor diastereomers (%)	Isolated yield, desired diastereomer **3-34** (%)
1	-30	0.5	45	2	-
2	-15	0.5	41	-	16
3	0	1	20	16	24
4	-30	1	43	12	28

Table 3.7. Studies on the chelation step of the methyl addition

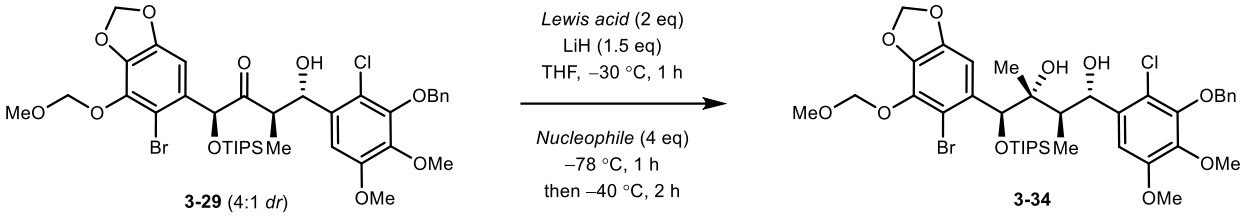
The 1,3-*syn* diol stereochemistry of the desired diastereomer **3-34** was confirmed by condensation of the diol with methyl boronic acid. An nOe experiment on the corresponding boronic ester **3-35** (Scheme 3.12) revealed correlations between the C8 methyl group (1.50 ppm) and the C6 hydrogen (5.60 ppm), confirming their *syn* relationship in the cyclic structure.



Scheme 3.12. Confirmation of the diol stereochemistry of **3-34** via preparation of the boronic ester and nOe

To improve upon the yield of **3-34** (28 %), further optimization was conducted by modifying the source and identity of the Lewis acid used in the chelation step as well as the methyl nucleophile

used in the alkylation step (Table 3.8). It was found that the use of a commercially available 1 M solution of $TiCl_4$ in CH_2Cl_2 led to higher consumption of **3-29** and yield than a homemade 1 M solution prepared from concentrated $TiCl_4$ when 2 equiv. of each were used for the chelation step (12 % and 4 % isolated yields of **3-24**, entries 1 and 2). A comparable yield of **3-24** (13 %) was only isolated using the homemade solution when the equivalents of $TiCl_4$ were doubled to 4 (entry 3), therefore the subsequent experiments used the solution from Sigma. The addition of (+)-sparteine (2 equiv.) along with $TiCl_4$ during the chelation step provided mostly the undesired diastereomer (10 %) and only 1 % yield of **3-24** (entry 4). Entries 5 and 6 employed diethylmethoxyborane as the Lewis acid instead of $TiCl_4$, with chelation at either –30 °C or –78 °C for 1 h, both resulting in extremely poor consumption (with 91 % **3-29** recovered in entry 6) and 0–6 % yield of **3-24**. $TiCl_4$ was utilized for chelation in entries 7–8, with different methyl nucleophiles: MeMgCl-$CeCl_3$ and MeLi. With MeMgCl-$CeCl_3$, decomposition was an issue as only 2 % **3-24** and 3 % of the undesired diastereomer of product were formed as well as 32 % **3-29** being recovered. With MeLi, none of the desired diastereomer was formed, with 5 % of the undesired diastereomer and 62 % **3-29** being isolated.



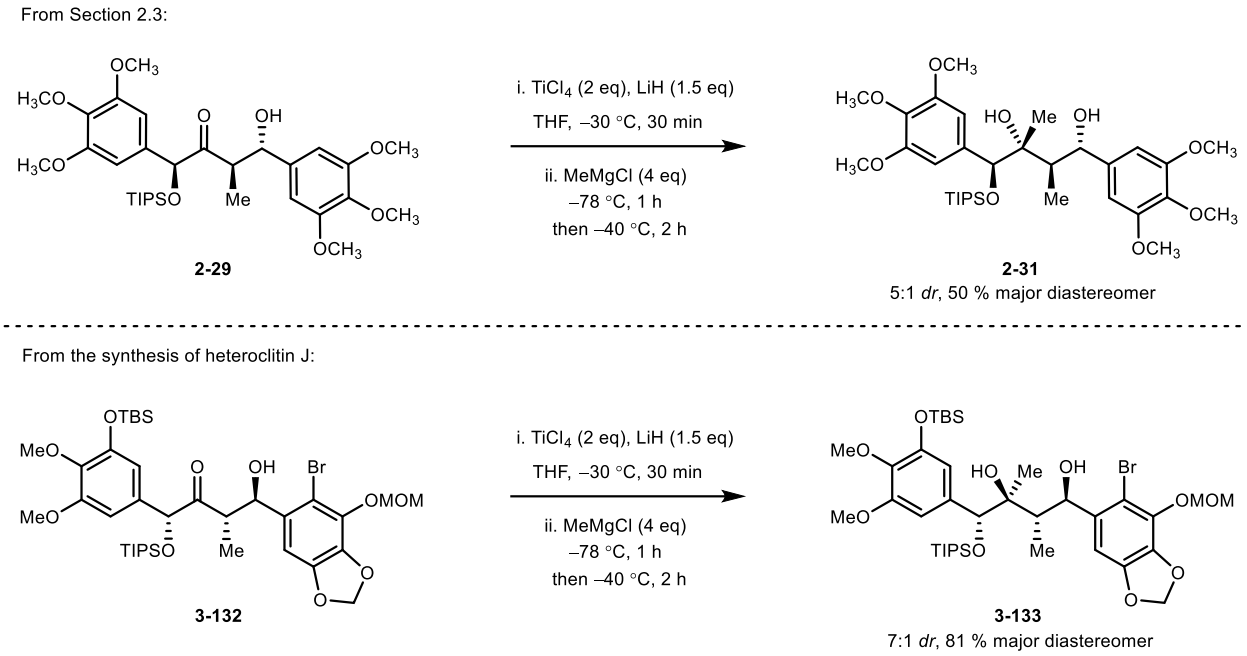
Entry	Lewis acid	Nucleophile	Rec. SM **3-29** (%)	Isolated yield, minor diastereomers (%)	Isolated yield, desired diastereomer **3-24** (%)
1	$TiCl_4$ (Sigma)	MeMgCl	29	8	12
2	$TiCl_4$ (from conc.)	MeMgCl	41	2	4
3[a]	$TiCl_4$ (from conc.)	MeMgCl	41	8	13
4	$TiCl_4$ (Sigma) + (-)-sparteine (2 eq)	MeMgCl	47	10	1
5	Et_2BOMe	MeMgCl	-[c]	4	6
6[b]	Et_2BOMe	MeMgCl	91	0	0
7	$TiCl_4$ (Sigma)	MeMgCl-$CeCl_3$	32	3	2
8	$TiCl_4$ (Sigma)	MeLi	62	5	0

$TiCl_4$ was added as a 1 M solution in CH_2Cl_2, either purchased from Sigma or prepared from conc. $TiCl_4$.
a= used 4 eq $TiCl_4$; b= chelation at –78 °C; c= the majority of the crude was recovered SM, not quantified.

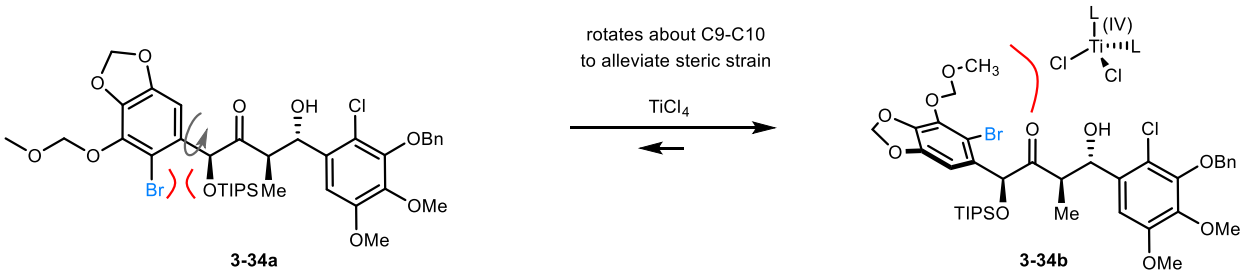
Table 3.8. Studies on the Lewis acid and nucleophile identities in the methyl addition

As screening the chelate-controlled methyl addition conditions did not result in a useful yield of **3-34**, modifying the starting material **3-29** was explored next. Methyl addition to previous substrates, the hexamethoxy model system **2-29** (Section 2.3, 5:1 *dr*, 50 % yield of desired

diastereomer of product) and **3-132** from our group's previous work on the synthesis of heteroclitin J (7:1 *dr*, 81 % yield of desired diastereomer of product),[9] worked well (Scheme 3.13). Therefore, it was surmised that the presence of the bromide at C15 in the current system may be impeding the chelation step, hence leading to poor yield and diastereoselectivity. The presence of a Br instead of an H on C15 will cause greater $A_{1,3}$ strain with the bulky OTIPS group on C9 (Scheme 3.14, **3-34a**), leading to rotation about the C9-C10 bond to alleviate this strain. In its strain-minimized conformation (Scheme 3.14, **3-34b**), the Br and OMOM substituents may sterically impede the approach of $TiCl_4$ for chelation to the ketone. The non-brominated aldol **3-36** was targeted as a substrate to use in the chelate-controlled methyl addition. It was expected that **3-36** could be prepared by aldol addition between aldehyde **3-25** and a non-brominated analogue of ketone **3-15**.



Scheme 3.13. Comparison to methyl addition on previous substrates

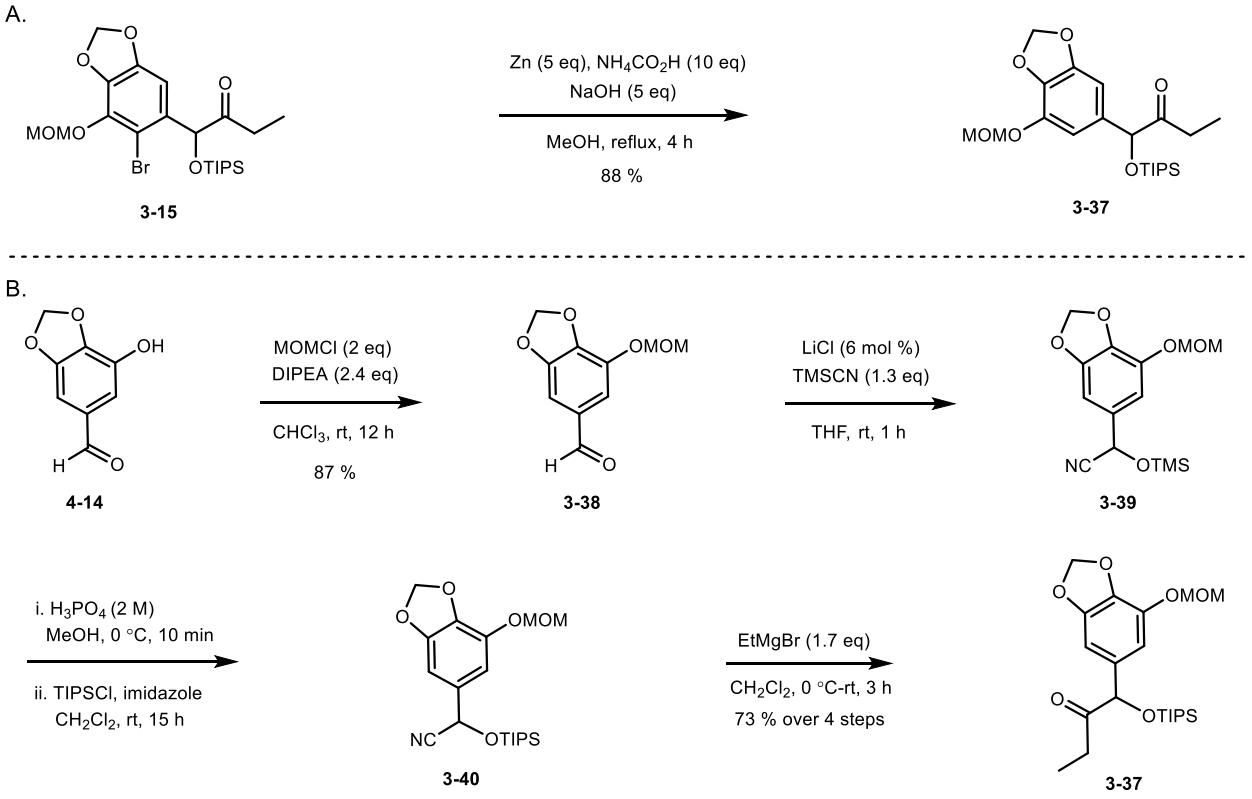


Scheme 3.14. Steric effect of the aryl bromide on chelation with $TiCl_4$

3.4. Strategy 2: non-brominated ketone + chlorinated aldehyde

3.4.1. Synthesis of the non-brominated ketone fragment

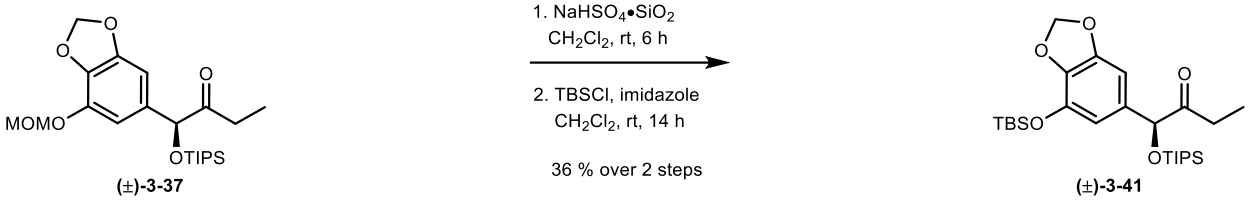
The non-brominated ketone fragment **3-37**, for use in the aldol addition with aldehyde **3-25** to provide aldol **3-36**, could be prepared via two methods. The first method involved the hydrodebromination of ketone **3-15** using zinc dust (5 equiv.), ammonium formate (10 equiv.), and sodium hydroxide (5 equiv.) in refluxing methanol[10] to provide **3-37** in 88 % yield on a 3 mmol scale (Scheme 3.15A). In the second method, **3-37** could be prepared in five steps from 5-hydroxypiperonal (**4-14**, Scheme 3.15B), where the preparation of **4-14** from piperonal is described in Experimental section 4.7. Protection of the phenol of **4-14** as the MOM ether employing chloromethyl methyl ether (2 equiv.) and DIPEA (2.4 equiv.) in chloroform at rt for 12 h provided **3-38** in 87 % yield on a 28 mmol scale. Aldehyde **3-38** was then subjected to hydrocyanation using catalytic LiCl (6 mol %) and trimethysilyl cyanide (1.3 equiv.) to give



Scheme 3.15. Synthesis of the non-brominated ketone **3-37** A) from brominated ketone **3-15** or B) from 5-hydroxypiperonal **4-14**

cyanohydrin **3-39**. Compound **3-39** was then subjected to deprotection of the TMS ether under acidic conditions, followed by protection of the resulting alcohol as the TIPS ether in one pot, furnishing **3-40**. The Grignard reaction of **3-40** with ethylmagnesium bromide (1.7 equiv.) in CH_2Cl_2 provided the ketone **3-37** in 73 % yield over 4 steps on a 24 mmol scale.

Additionally, to determine the effect of the phenolic protecting group of the ketone fragment on its reactivity in the aldol addition and methyl addition, a non-brominated ketone fragment bearing a TBS protecting group on the phenol instead of MOM was also prepared (**3-41**, Scheme 3.16). **3-41** was synthesized in 36 % yield over two steps from **3-37** by treatment with $NaHSO_4$-SiO_2 in CH_2Cl_2 for 6 h to deprotect the MOM group, followed by protection of the resulting phenol as a silyl ether using TBSCl and imidazole.

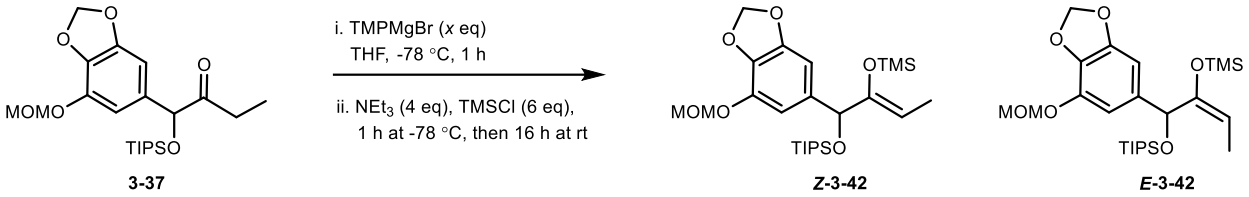


Scheme 3.16. Synthesis of the non-brominated ketone **3-41**

3.4.2. Aldol addition

The non-brominated ketone **3-37** was trapped as its silyl enol ether to ensure the desired (*E*) geometry of the enolate was formed selectively. Enolization of **3-37** was performed using TMPMgBr (1.5–3.0 equiv.) in THF at −78 °C for 1 h and the resulting enolate was trapped as the silyl enol ether by treatment with triethylamine (4 equiv.) and trimethylsilyl chloride (6 equiv.) (Table 3.9). The two isomeric silyl enol ether products could be differentiated by the ^{1}H NMR signal corresponding to their vinyl proton (δ= 5.22 for *Z* and 4.60 for *E*). The use of 1.5 equiv. TMPMgBr resulted in incomplete consumption of **3-37** (78 %) with the (*Z*)-silyl enol ether ***Z*-343** being produced as the major product (49 % yield) and the (*E*)-silyl enol ether ***E*-3-42** as the minor product (19 %, entry 1). This result seems to indicate that the concentration of our homemade TMPMgBr solution is lower than expected. If less than 1 equiv. TMPMgBr was present, some of the remaining ketone could have been deprotonated by the (*E*)-Mg-enolate in a non-stereoselective manner, leading to a mixture of *Z*/*E* enolates. Increasing the equivalents of TMPMgBr to 2.0 or 3.0 (entries 2, 3) gave full consumption of **3-37** and yields of 56 % and 93 % ***E*-3-42,** respectively,

as the sole product. The crude products from entries 2 & 3 were combined for purification and characterization, providing an average yield of 58 % ***E*-3-42** over the two reactions.



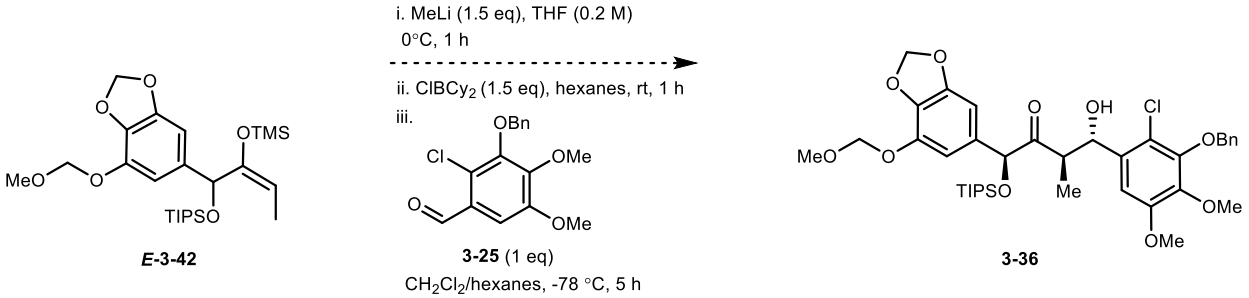
3-37 ***Z*-3-42** ***E*-3-42**

Entry	eq TMPMgBr	% consumption	NMR yield of ***Z*-3-43** (%)	NMR yield of ***E*-3-42** (%)
1	1.5	78	49	19
2	2.0	100	-	56
3	3.0	100	-	93

All experiments were performed on 0.1 mmol scale. Hexamethybenzene was used as internal standard in $CDCl_3$.
(*Z*) silyl enol ether was identified by a vinyl δ of 5.22 (q, 1H); (*E*) silyl enol ether was identified by a vinyl δ of 4.60 (q, 1H).

Table 3.9. Trapping the (*E*)-silyl enol ether of **3-37**

It was then investigated whether the desired aldol **3-36** could be obtained from the isolated (*E*)-silyl enol ether. ***E*-3-42** was subjected to MeLi to form the (*E*)-Li-enolate, followed by treatment with $ClBCy_2$ to give the (*E*)-B-enolate, and then addition of the aldehyde **3-25** (Scheme 3.17).[11,12] This method was unsuccessful, returning only starting material. Therefore, subsequent attempts at the synthesis of aldol **3-36** were performed starting from ketone **3-37**.

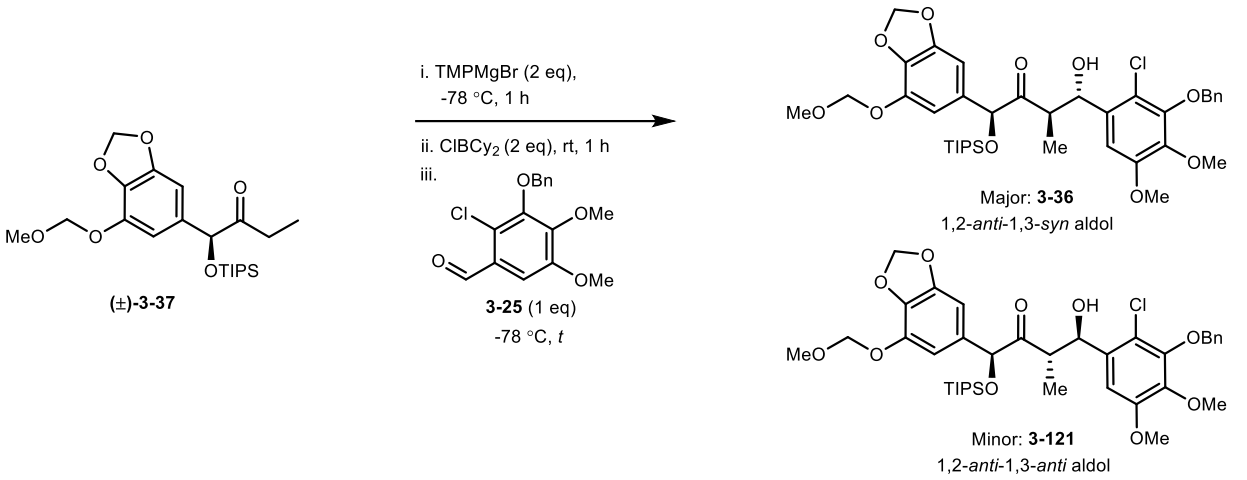


***E*-3-42** **3-25** (1 eq) CH_2Cl_2/hexanes, -78 °C, 5 h **3-36**

Scheme 3.17. Aldol addition attempt from the (*E*)-silyl enol ether

As the enolization of **3-37** using 2 or 3 equiv. TMPMgBr produced the (*E*)-enolate selectively, both enolization conditions were applied in the aldol addition with aldehyde **3-25** to give 1,2-*anti*-1,3-*syn* aldol **3-36**. In section 3.3.3, it was determined that the amount of $ClBCy_2$ employed in the transmetallation step should be equimolar to the amount of TMPMgBr employed in the enolization step to obtain the best diastereoselectivity. In Table 3.10, entry 1, the aldol addition of **3-37** and **3-25** was run on 0.2 mmol scale utilizing 3 equiv. each TMPMgBr and $ClBCy_2$, with 5 h reaction

time at –78 °C after the addition of the aldehyde, resulting in the isolation of a 59 % yield of **3-36** in 2.7:1 *dr*. The major diastereomer was assigned as the desired 1,2-*anti*-1,3-*syn* aldol **3-36** and the minor diastereomer as the 1,2-*anti*-1,3-*anti* aldol, which would also arise from the (*E*)-B-enolate. In entry 2, the reaction was run under the same conditions albeit with only 2 equiv. each TMPMgBr and $ClBCy_2$, resulting in 56 % yield of **3-36** with 4.3:1 *dr*. As the yields of entries 1 and 2 were comparable but the *dr* of entry 2 was superior, 2 equiv. each TMPMgBr and $ClBCy_2$ were employed in the subsequent experiments. In entry 3, the reaction scale was increased to 2.6 mmol and the reaction time after the addition of **3-25** to 8 h, leading to a higher yield of **3-36** (66 %) being isolated in 4.4:1 *dr*. The reaction scale was increased further to 8.0 mmol (entry 4), with a comparable yield of **3-36** (65 %) being obtained in 6.5:1 *dr*. This product could be recrystallized to further improve the *dr* to 16:1 (in 49 % yield) and the structure was confirmed by X-ray crystallography (Figure 3.3). Increasing the reaction time after the addition of **3-25** from 8 h to 17 h on 8.0 mmol scale led to an increase in yield (76 %) but a drop in diastereoselectivity (3:1, Table 3.10, entry 5). The *dr* of this product could be improved to 7:1 by recrystallization affording



Entry	Scale (mmol)	*t* (h)	Isolated yield after column (%)	*dr* after column	Isolated yield after recrystallization (%)	*dr* after recystallization
1[a]	0.2	5	59	2.7:1	-	-
2	0.2	5	56	4.3:1	-	-
3	2.6	8	66	4.4:1	-	-
4	8.0	8	65	6.4:1	49	16:1
5	8.0	17	76	3:1	50	7:1
6	11	8	53	4:1	37	17.5:1
7	16	24	62	2.9:1 to 5:1	41	13:1 to 20:1

a= used 3 eq each TMPMgBr and $ClBCy_2$

Table 3.10. Aldol addition of MOM-protected ketone **3-37** and aldehyde **3-25**

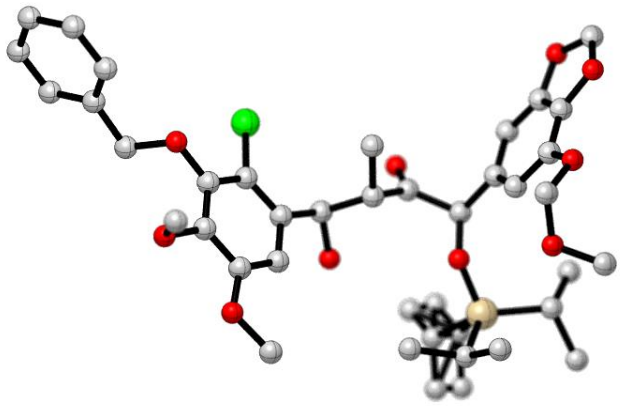
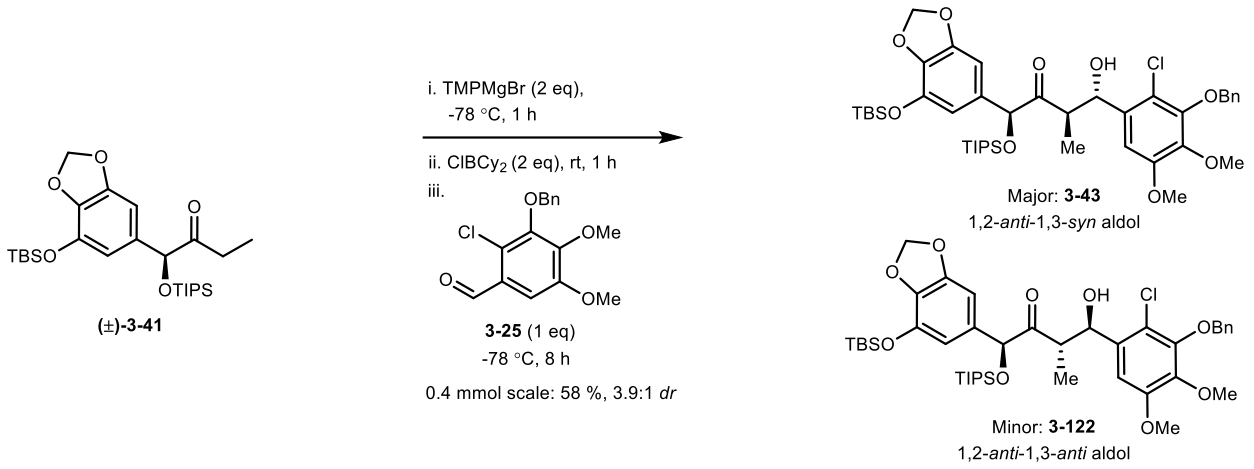


Figure 3.3. X-ray crystal structure of aldol **3-36**

3-36 in 50 % yield. It would appear that 8 h reaction time was sufficient on this scale considering the yields of aldol obtained after recrystallization were comparable. In entry 6, the reaction was run on 11.0 mmol scale with 8 h reaction time after the addition of **3-25**, with a drop in yield to 53 % observed (4:1 *dr*) or 37 % (17.5:1 *dr*) after recrystallization. Since the reaction appeared to require more time on larger scale, the 16 mmol reaction (entry 7) was stirred for 24 h after the addition of **3-25**, providing column fractions of **3-36** with *dr* ranging from 2.9:1 to 5.0:1 in a combined yield of 62 %. After recrystallization, the *dr* could be improved to 13:1 to 20:1, with a combined yield of 41 %.

The second non-brominated ketone fragment **3-41**, bearing a phenolic TBS group, was also subjected to aldol addition with aldehyde **3-25** using the standard conditions of TMPMgBr (2 equiv.), $ClBCy_2$ (2 equiv.), and reacted for 8 h with **3-25** (Scheme 3.18). A 58 % yield of the corresponding TBS-protected 1,2-*anti*-1,3-*syn* aldol **3-43** could be obtained in 3.9:1 *dr* on 0.4 mmol scale. The major diastereomer was assigned as the desired 1,2-*anti*-1,3-*syn* aldol **3-43** and the minor diastereomer as the 1,2-*anti*-1,3-*anti* aldol **3-122**, which would also arise from the (*E*)-B-enolate.

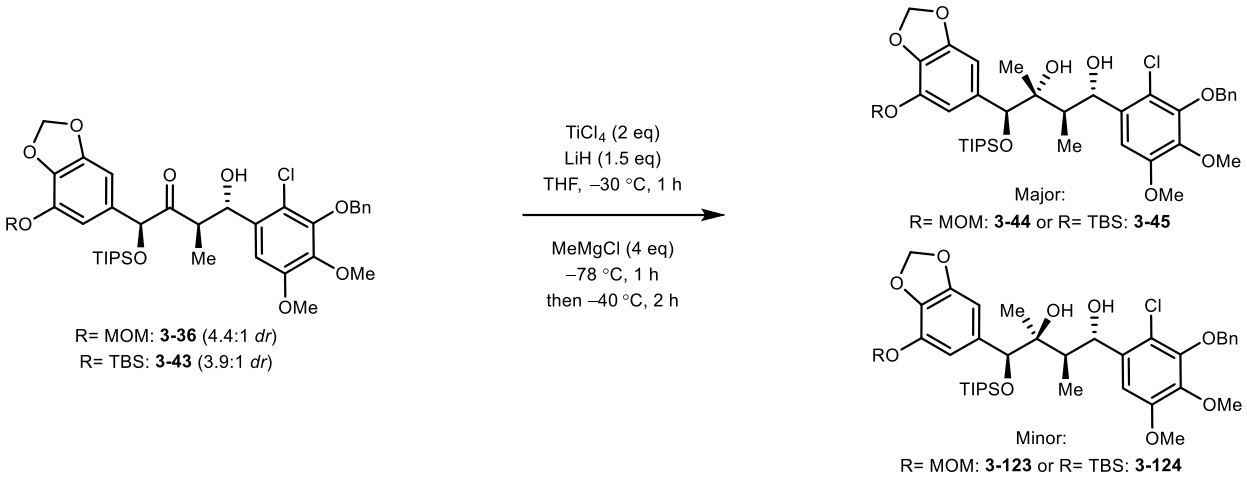


Scheme 3.18. Aldol addition of TBS-protected ketone **3-41** with aldehyde **3-25**

3.4.3. Chelate-controlled methyl addition

The aldol products synthesized in section 3.4.2., MOM-protected **3-36** and TBS-protected **3-43**, were subjected to chelate-controlled methyl addition conditions to set the C8 stereocenter. These consisted of chelation at −30 °C with $TiCl_4$ (2 equiv.) and LiH (1.5 equiv.) for 1 h, followed by alkylation at −78 °C with MeMgCl (4 equiv.) for 1 h and then −40 °C for 2 h. Gratifyingly, both substrates provided much higher yields of methyl addition product than brominated aldol **3-29** had. TBS-bearing **3-43** (which consisted of a 3.9:1 ratio of diastereomers **3-43** and **3-122**) gave product with 3:1 *dr* (as determined by integration of the crude ^{1}H NMR), with a 43 % yield of the major diastereomer **3-45** being isolated (Table 3.11, entry 1). A mixture of recovered **3-43** and the minor methyl addition diastereomer **3-124** was also obtained, accounting for some of the mass balance. MOM-bearing **3-36** (which consisted of a 4.4:1 ratio of 1,2-*anti*-1,3-*syn* aldol and 1,2-*anti*-1,3-*anti* aldol diastereomers) gave product with 12:1 *dr*, with a 56 % yield of the major diastereomer **3-44** being isolated, as well as some recovered **3-36** and minor diastereomer **3-123**. Considering the *dr* of the aldol starting material, the maximum yield of the desired product that could potentially be obtained would be 81 %. It was not immediately clear why the diastereoselectivity of the chelate-controlled methyl addition was significantly higher in entry 2 compared to entry 1, although it may be related to the purity of the aldol. Aldol **3-43** was an oil which could easily contain residual $ClBCy_2$ impurities (which would hinder chelation), whereas **3-36** was a solid. The stereochemistry of each of the major products was determined by condensation of the diol with methyl boronic acid and then running an nOe experiment on the resulting boronic

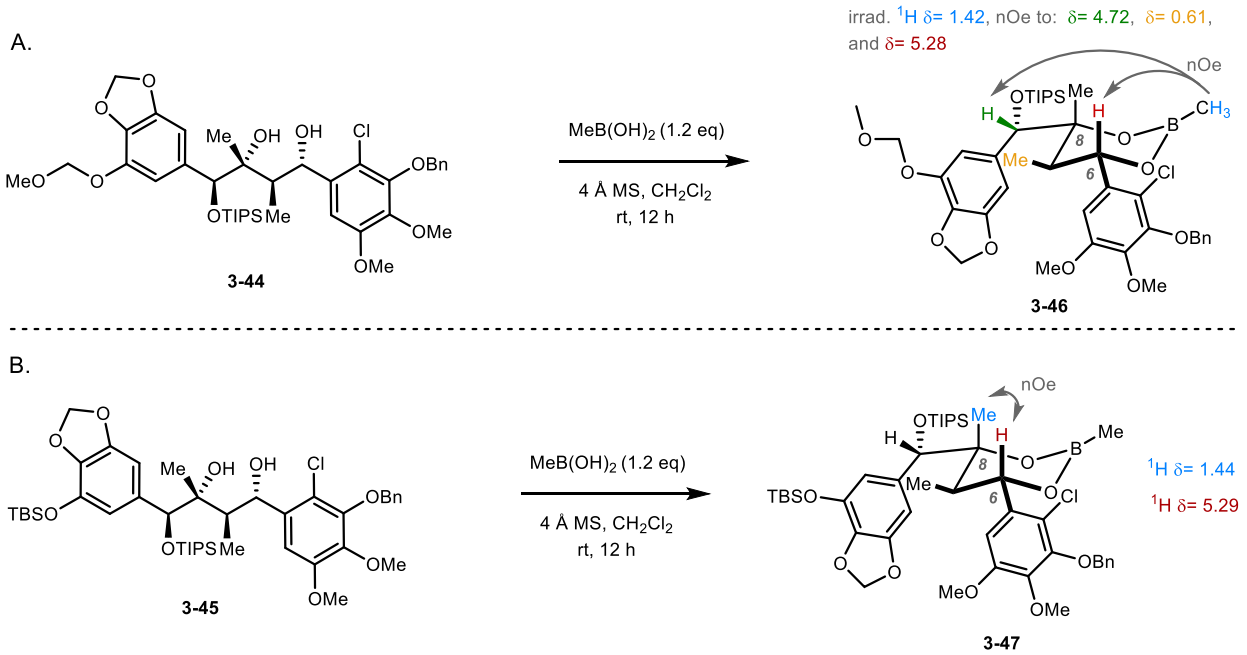
esters **3-46** and **3-47** (Scheme 3.19). For **3-46**, the boronic ester prepared from **3-44**, irradiation of the methyl group bound to boron (1.42 ppm), displayed nOes to the C9 H (4.72 ppm), the C7 CH_3 (0.61 ppm), and the C6 H (5.28 ppm), indicating that the boron-bound methyl group is on the same



Entry	R	Scale (mmol)	*dr* of product (from crude NMR)	Yield of major diastereomer (%)
1	TBS	0.2	3:1	43
2	MOM	0.1	12:1	56

Yields are isolated yields.

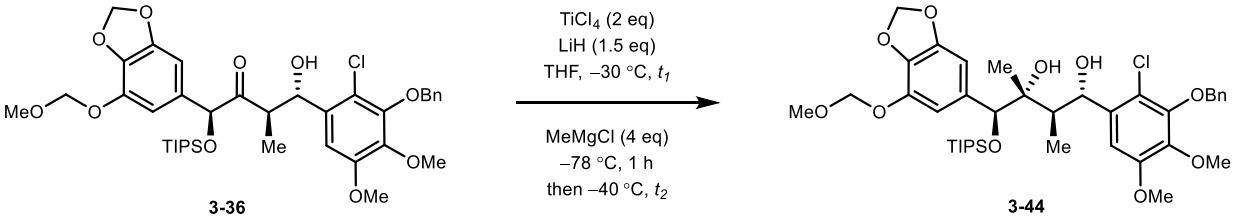
Table 3.11. Methyl addition on substrates **3-36** and **3-43**



Scheme 3.19. Confirmation of the stereochemistry of the methyl addition products **3-44** and **3-45**

side of the molecule as these hydrogens (Scheme 3.19A). For **3-47**, the boronic ester prepared from **3-45**, an nOe was observed between the C8 methyl group (1.44 ppm) and the C6 H (5.29 ppm), indicating that they are on the same side of the molecule (Scheme 3.19B). As **3-44** could be synthesized with higher *dr* and yield than **3-45**, it was selected for use in the linear synthesis.

The methyl addition onto **3-36** (16:1 *dr*) to give **3-44** was then optimized, varying the chelation and alkylation reaction times (Table 3.12). In entries 1–4, reactions were run on 0.1 mmol scale with formation of the Ti(IV) chelate for 0.5–1.5 h and alkylation at −78 °C for 1 h, followed by –40 °C for 2–3 h. Entries 1, 2, and 4 yielded similar results, with product being formed in 20:1 *dr,* The higher diastereoselectivity observed here (compared to 12:1 *dr* in Table 3.11) may be due to the use of aldol **3-36** with higher *dr* (16:1 vs. 4.4:1). 12–24 % of recovered **3-36** being isolated, and 73–86 % yield of the desired product diastereomer **3-44**. Entry 3, which employed alkylation at –40 °C for 2 h, proceeded with lower consumption of starting material, with 46 % recovery of **3-36** and 51 % yield of **3-44**, therefore the subsequent experiments were run for longer times at the –40 °C step to ensure good consumption of starting material. Varying the time allowed for chelation with Ti(IV) did not affect the results, thus it was concluded that 0.5 h was sufficient for this step. The reaction scale was then increased to 0.5 mmol (entries 5–6), with chelation for 0.5 h and alkylation at −78 °C for 1 h, followed by –40 °C for either 3 or 4 h. The yields of the desired diastereomer (59 % and 57 %) were comparable in entries 5 and 6 (with some **3-36** and minor diastereomer **3-123** being obtained as well), so −78 °C for 1 h followed by –40 °C for 3 h was



3-36 **3-44**

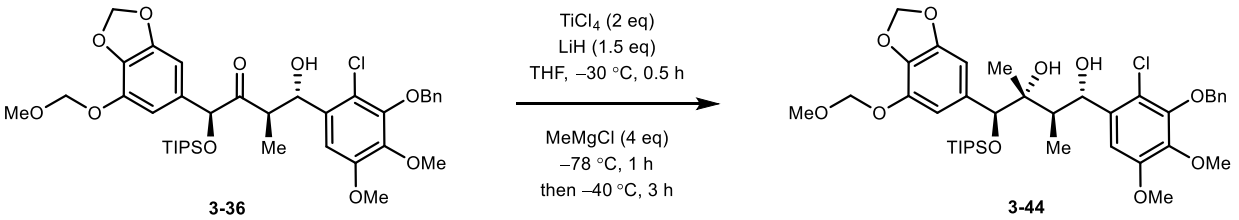
Entry	Scale (mmol)	t_1 (h)	t_2 (h)	*dr* of product (from crude NMR)	Yield of rec. **3-36**	Yield of major diastereomer (%)
1	0.1	1.5	2	20:1	12 % (2: 1 *dr*)	86
2	0.1	0.5	2	20:1	14 % (3: 1 *dr*)	86
3	0.1	1	2	20:1	46 % (6.5: 1 *dr*)	51
4	0.1	1	3	20:1	24 % (4.4: 1 *dr*)	73
5	0.5	0.5	3	9.7:1	-	59
6	0.5	0.5	4	20:1	-	57

3-36 used had a *dr* of 16:1. Yields are isolated yields.

Table 3.12. Optimization of the chelation and alkylation times in the methyl addition

deemed adequate time for alkylation to occur.

The scale of the chelate-controlled methyl addition to provide **3-44** was gradually increased utilizing the optimized conditions (Table 3.13). Although the conditions had been optimized on aldol with a high *dr* of 16:1, the methyl addition also worked well on aldol samples with lower *dr* and the desired methyl addition product was separable from the unreacted minor aldol diastereomer. Very high diastereoselectivity (20:1) and yield of **3-44** (96 %) were obtained on 0.92 mmol scale (entry 1). Reactions on 1.5 and 3.4 mmol scale proceeded with 20:1 *dr* and 73 % yield of **3-44** (entries 2, 3). In entry 4, the reaction was run on 6.6 mmol, yielding 80 % **3-44**. (The *dr* could not be determined from the crude ^{1}H NMR due to the overlapping of signals.) Reactions run on 14.5 and 18.0 mmol scale proceeded with lower *dr* (13:1 and 9:1, respectively), both provided a 55 % yield of **3-44** (entries 5, 6). The drop in yield in the last two entries could be caused by a few factors. These two reactions employed **3-36** which was prepared by another graduate student in the group, using a different purification procedure than for the **3-36** which was prepared by me; therefore the purity of the starting material may have affected the *dr* and yield of the product. If there was residual Cy_2BCl or its hydrolyzed form Cy_2BOH present, this would interfere with the chelation of the β-hydroxy ketone to $TiCl_4$, leading to lower *dr* and yield. Additionally, these samples of aldol had lower *dr* to begin with (3.8:1 and 4.2:1) compared to the aldol samples used in entries 1–4 (7:1 to 13:1 *dr*), so it stands to reason that the methyl addition product would also be formed in lower *dr*.



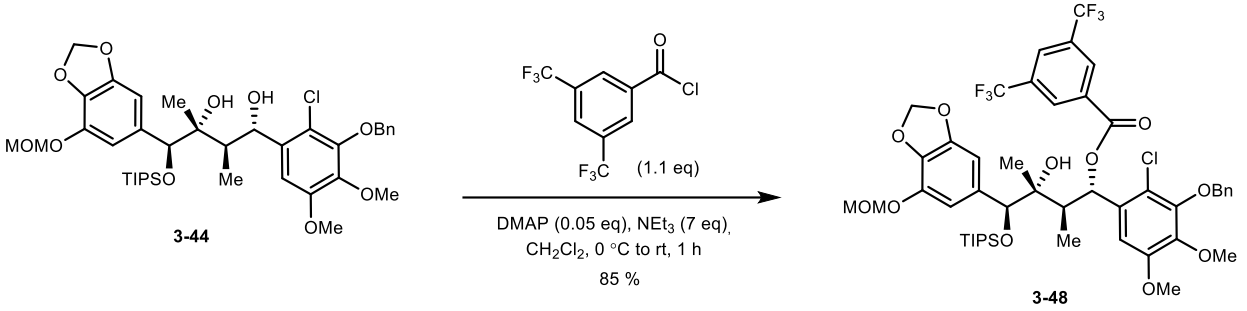
Entry	Scale (mmol)	*dr* of product (from crude NMR)	Yield of major diastereomer (%)
1	0.92	20:1	96
2	1.5	20:1	73
3	3.4	20:1	73
4	6.6	-	80
5	14.5	13:1	55
6	18.0	9:1	55

3-36 used in entries 1-2 had a *dr* of 11.6:1; **3-36** used in entry 3 had a *dr* of 7:1; **3-36** used in entry 4 had a *dr* of 13:1 to 20:1; **3-36** used in entry 5 had a *dr* of 4.2:1 to 8:1; **3-36** used in entry 6 had a *dr* of 3.8:1 to 4.6:1. Yields are isolated yields.

Table 3.13. Increasing the scale of the methyl addition on **3-36**

3.4.4. Benzylic deoxygenation

The C6 benzylic deoxygenation of **3-44** would be performed utilizing the deoxygenation conditions which have been successfully applied to our model system (see section 2.4). The conversion of the benzylic alcohol **3-44** to the corresponding 3,5-bis-(trifluoromethyl)benzoyl ester **3-48** in 85 % yield was performed on up to 9.9 mmol by treatment with benzoyl chloride (1.1 equiv.), catalytic DMAP, and triethylamine (7 equiv.) in CH_2Cl_2 at rt for 1 h (Scheme 3.20).



Scheme 3.20. Preparation of the 3,5-bis-(trifluoromethyl)benzoyl ester **3-48**

In our model system, the exclusion of oxygen from the reaction mixture proved crucial for obtaining reproducibly high yields of the deoxygenation product (see section 2.4). This also proved to be an important factor in the deoxygenation of **3-48**. When subjected to Reiser's modified benzylic deoxygenation conditions of $[Ir(ppy)_2(dtb\text{-}bpy)]PF_6$ (2 mol %), *i*Pr_2NEt (2 equiv.), and H_2O (100 equiv.) in acetonitrile (0.05 M) with irradiation by 455 nm LEDs at 60 °C for 15–16 h

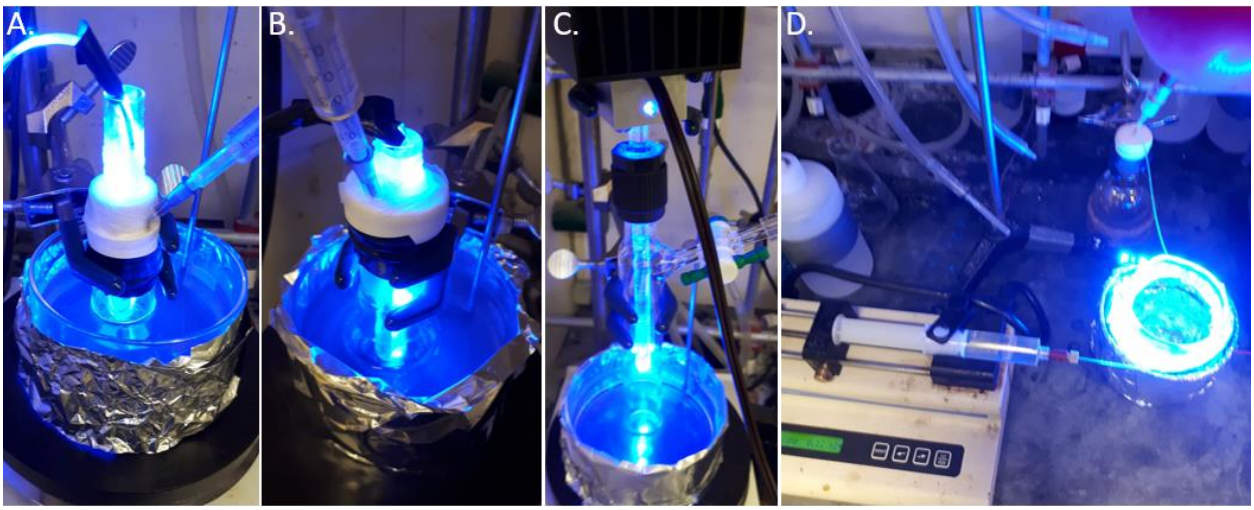
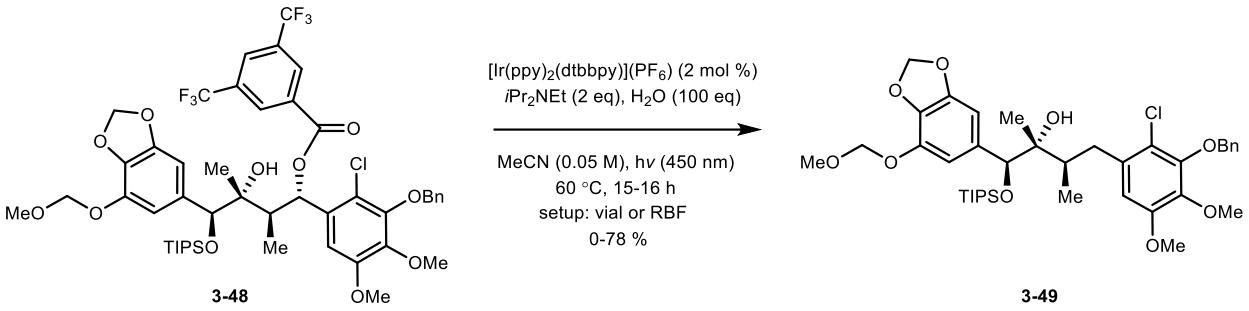


Figure 3.4. Reactor setups for photoredox-catalyzed benzylic deoxygenation: A) vial; B) RBF; C) Schlenk flask; D) flow setup

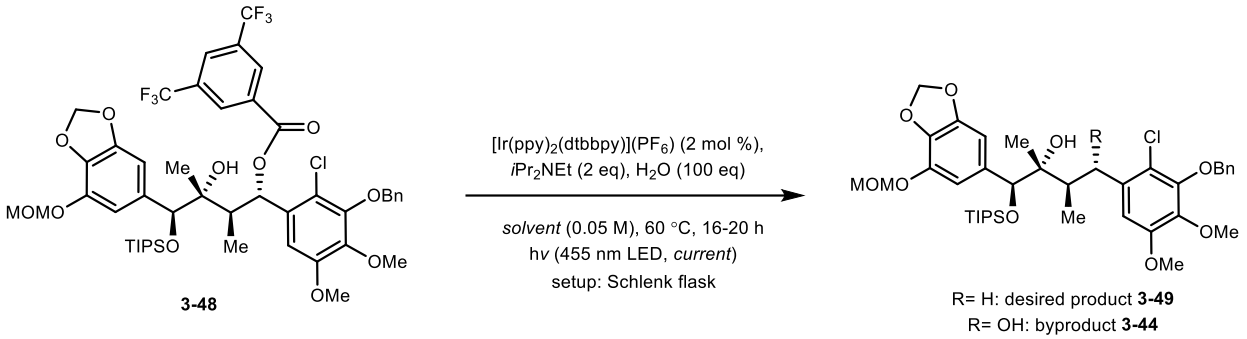
in either our homemade vial or RBF photoreactors (Figure 3.4A, B), the yields of **3-49** fluctuated greatly (0–78 %) due to the inconsistent exclusion of oxygen (Scheme 3.21).



Scheme 3.21. Benzylic deoxygenation of **3-48** in vial or RBF setup

The subsequent experiments were run in the Schlenk flask reactor developed in section 2.4 (Figure 3.4C), which had proved to be air-tight, providing reproducibly high yields of the model deoxygenation product. The conversion of **3-48** to **3-49** in the Schlenk flask reactor was performed using the conditions which had been optimized on the model system, consisting of $[Ir(ppy)_2(dtb\text{-}bpy)]PF_6$ (2 mol %), *i*Pr_2NEt (2 equiv.), and H_2O (100 equiv.) in acetonitrile (0.05 M) with irradiation by 455 nm LEDs at 60 °C for 16 h (Table 3.14, entry 1). Unexpectedly, only a 9 % yield of the desired deoxygenation product **3-49** was formed, with 52 % recovered starting material **3-48** and 29 % of the ester hydrolysis byproduct **3-44** being isolated as well. Experiments were run on 0.025 mmol scale omitting or substituting different components of the reaction mixture to determine the cause of ester hydrolysis, with characterization of the crude reaction mixtures by ^1H NMR. It was found that substituting DMF for MeCN resulted in the formation of **3-49** without the hydrolysis of **3-48** after 19 h at 60 °C. Therefore, DMF was used as the solvent in the subsequent experiments. In entry 2, the reaction of **3-48** on 0.1 mmol scale in DMF provided a 45 % yield of the desired **3-49**, with 26 % recovered **3-48**, and no hydrolysis byproduct. To push the reaction to further completion, the current was increased from 410 to 850 mA (entry 3), resulting in the isolation of 93 % **3-40** and recovery of 7 % **3-48**. The reaction scale could be increased to 0.6 and 1.0 mmol while maintaining high yields of 97 % and 83 % **3-49** (entries 4 and 5, respectively).

Two 50 mL Schlenk flask reactors which could each hold a 1 mmol reaction had been constructed, therefore a maximum of 2 mmol **3-48** could be reacted at once. As photon efficiency decreases when increasing scale in batch, further scale increase would be conducted in flow. A flow setup was constructed by coiling FEP tubing around a beaker and placing this inside a loop blue LED



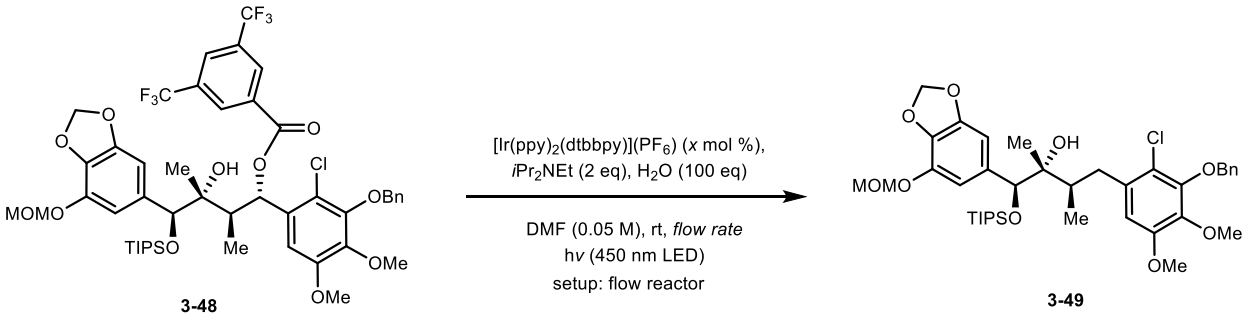
Entry	Scale (mmol)	solvent	current (mA)	Yield of rec. SM **3-48** (%)	Yield of byproduct **3-44** (%)	Yield of product **3-49** (%)
1	0.05	MeCN	410	52	29	9
2	0.1	DMF	410	26	-	45
3	0.1	DMF	850	7	-	93
4	0.6	DMF	850	-	-	97
5	1.0	DMF	850	-	-	83

Yield are isolated yields.

Table 3.14. Optimization and increasing the scale of the benzylic deoxygenation in batch (Schlenk flask)

photoreactor (Figure 3.4D). The reaction mixture was introduced to the system via syringe pump and dispensed into a receiving flask after passing through the irradiated tubing, with the entire system under inert atmosphere. Reiser *et al*. had reported that they could reduce their photocatalyst loading from 2 mol % to 0.1 mol % when taking their reactions from batch to flow.[13] Compound **3-48** was combined with $[Ir(ppy)_2(dtb\text{-}bpy)]PF_6$ (0.1 mol %), iPr$_2$NEt (2 equiv.), and H_2O (100 equiv.) in DMF (0.05 M) in a round-bottom flask, the reaction mixture was freeze-pump-thawed (x 5), and then passed through the flow setup at a rate of 10 mL/h (Table 3.15, entry 1). The reaction did not proceed to completion and poor mass balance was recovered, with the isolation of 16 % **3-49** and 33 % recovered **3-48**. At a flow rate of 10 mL/h, the residence time was 50 minutes. As the reaction was not complete, the flow rate was decreased to 2 mL/h to increase the residence time to 4 h 10 min in expectation of achieving greater conversion. The yield of product barely increased (to 22 %) and consumption of starting material was still poor, with 37 % recovery of **3-48** (entry 2). As increasing the residence time had little effect, the flow rate was returned to 10 mL/h and the photocatalyst loading increased to 2 mol %, which led to complete consumption of **3-48** and isolation of 94 % **3-49** (entry 3). Due to the expensive cost of $[Ir(ppy)_2(dtb\text{-}bpy)]PF_6$, experiments were then run with catalyst loadings greater than 0.1 mol % but lower than 2 mol % to see if full consumption of **3-48** could be obtained with a lower amount (entries 4–8). The use of

0.3 mol % photocatalyst led to only an 11 % yield of **3-49** and 69 % recovered **3-48** (entry 4), whereas the use of 1 mol % provided a 74 % yield of **3-49** and 13 % **3-48** (entry 5). The result of entry 5 looked promising as good albeit incomplete consumption had been attained, therefore in entry 6, 1 mol % photocatalyst was again employed, with the flow rate decreased slightly to 7 mL/h, aiming for full consumption. A very good yield of **3-49** (91 %) was obtained, however some starting material remained (9 %). Employing an even slower flow rate of 5 mL/h under the same conditions was detrimental to the reaction, giving only a 66 % yield **3-49**, with recovery of 19 % **3-48** (entry 7). A catalyst loading of 1.5 mol % with a flow rate of 7 mL/h also led to not quite complete consumption, where 60 % **3-49** was isolated and 4 % **3-48** recovered (entry 8). Considering decreasing flow rate did not improve reactivity much, it was questioned whether the flow rate could be increased to greater than 10 mL/h to expediate the reaction time. In entry 9, the reaction was run with 2 mol % photocatalyst and a flow rate of 20 mL/h, with 71 % **3-49** being isolated and 13 % **3-48** recovered. Upon analysis of the results, it was determined that the conditions in entry 3, employing a flow rate of 10 mL/h and a photocatalyst loading of 2 mol %, provided the best consumption of **3-48** and yield of **3-39** and would hence be ideal for increasing the reaction scale. In entry 10, these conditions were increased to 2.0 mmol scale, where full



3-48 **3-49**

Entry	Scale (mmol)	flow rate (mL/h)	photocatalyst loading (mol %)	Yield of rec. SM **3-48** (%)	Yield of product **3-49** (%)
1	0.84	10	0.1	33	16
2	0.28	2	0.1	37	22
3	0.15	10	2	-	94
4	0.11	10	0.3	69	11
5	0.12	10	1	13	74
6	0.16	7	1	9	91
7	0.15	5	1	19	66
8	0.17	7	1.5	4	60
9	0.16	20	2	13	71
10	2.0	10	2	-	90
11	3.9	10	2	-	84
12	8.4	10	2	3	79

Yields are isolated yields.

Table 3.15. Optimization and further increasing the scale of the benzylic deoxygenation in flow

conversion was observed and 90 % **3-49** obtained. The reaction also proceeded to full consumption of **3-48** on 3.9 mmol scale, producing an 84 % yield of **3-49** (entry 11). The largest scale reaction run to date was 8.4 mmol, which yielded 79 % **3-49** along with 3 % recovered **3-48** (entry 12).

3.4.5. Functional group manipulations to prepare for Suzuki coupling

The next key step in the synthesis of kadsuraol C was the atroposelective Suzuki coupling to form the biaryl axis. To perform this reaction, **3-49** first had to be functionalized with the appropriate aryl borinic ester and aryl chloride functional handles for Suzuki coupling. It was necessary that the aryl borinic ester be tethered to the C9 benzylic alcohol to prevent rotation about C9-C10. The C9 C-O bond of **3-125a** is nearly *syn* coplanar with the B-aryl bond, incurring $A_{1,3}$ strain (Figure 3.5). When C9 is untethered in the form of either a silyl ether or alcohol, rotation about C9-C10 occurs to alleviate this strain (**3-125a** to **3-125b**). This places the aryl-boron bond in a position which is misaligned for transmetallation. Tethering the C9 C-O bond to the aryl-boron (as in **3-52**) makes it unfeasible to rotate about C9-C10, thus retaining the proper orientation for transmetallation.

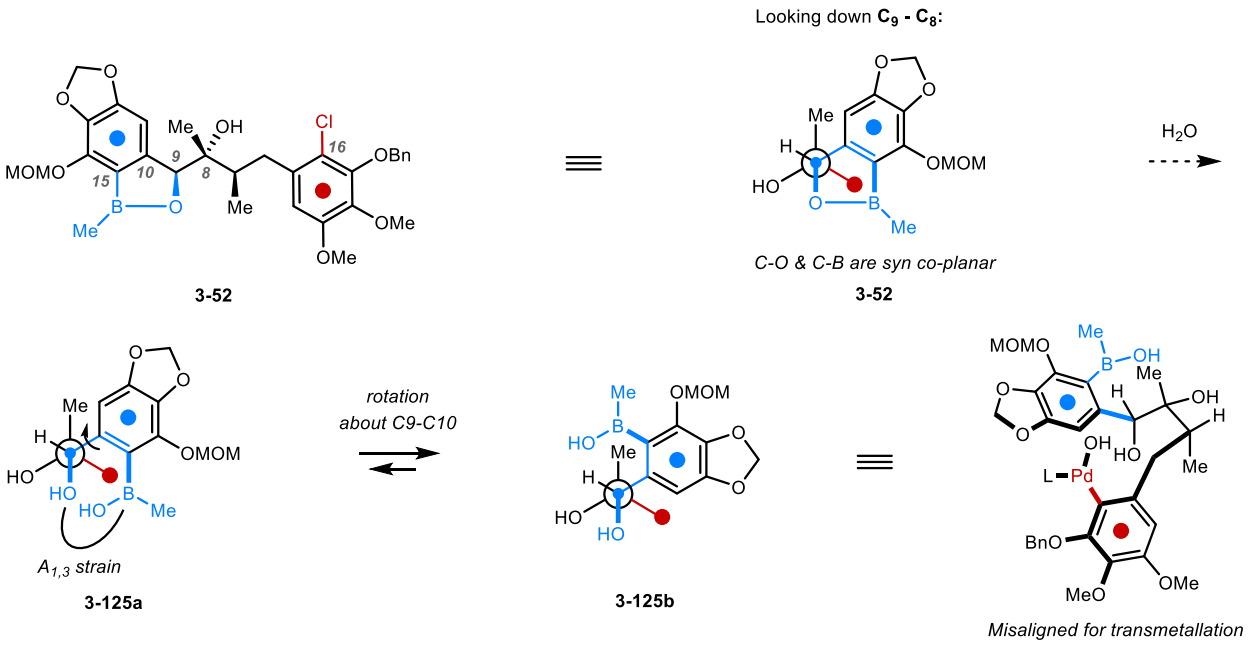
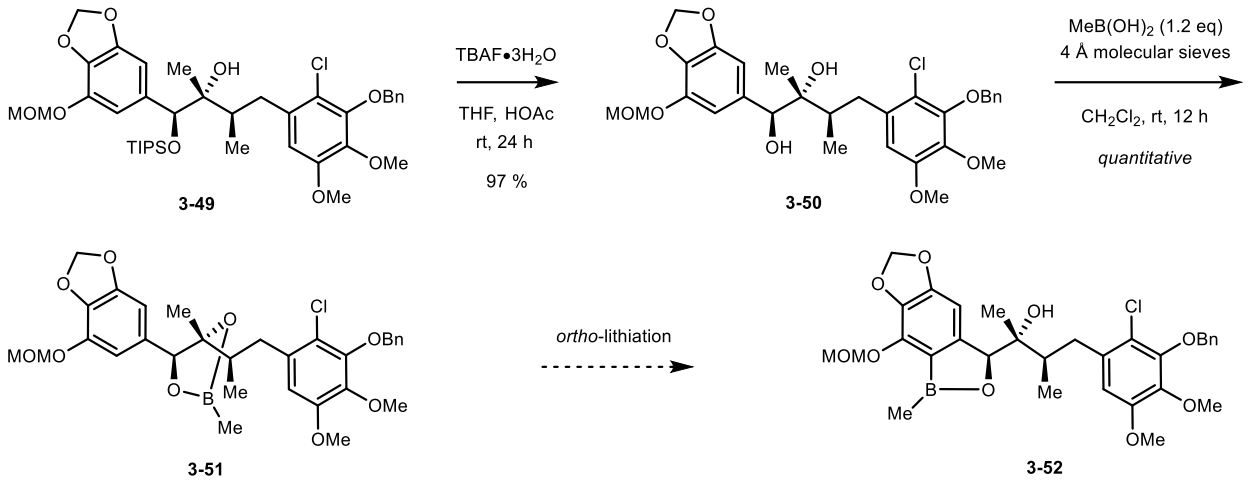


Figure 3.5. Importance of the tethered aryl borinic ester

It was proposed that this functionalization of **3-49** could be performed in a series of three steps: deprotection of the TIPS ether, conversion of the diol to the boronic ester, and *ortho*-lithiation to elicit migration (Scheme 3.22). The benzylic TIPS group of **3-49** was deprotected via treatment

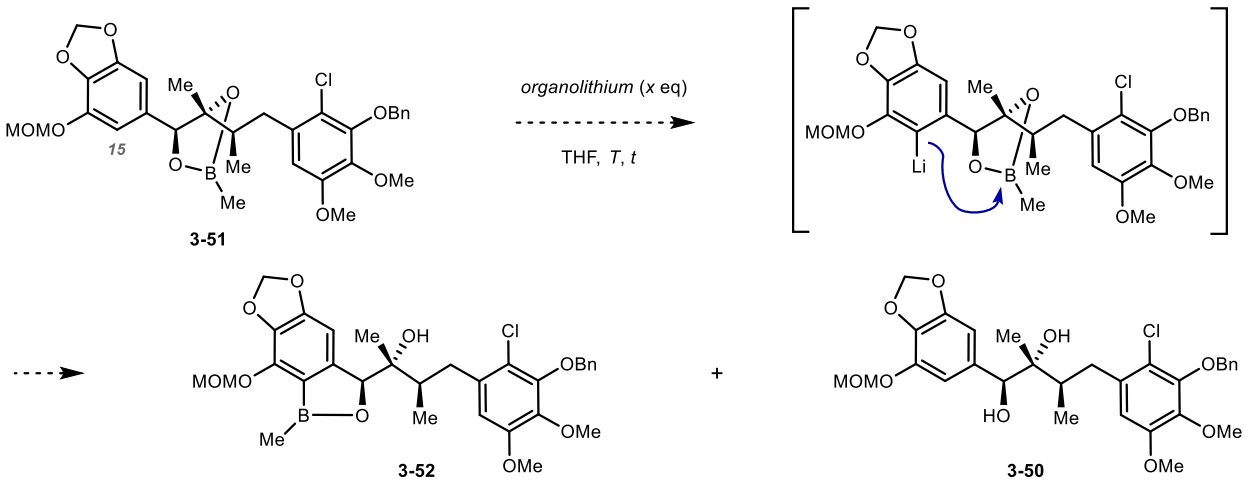
with TBAF•3H_2O buffered with acetic acid in THF, providing a 97 % yield of **3-50** on a 6.7 mmol scale. The conversion of the diol to the boronic ester was effected via treatment with methylboronic acid and 4 Å molecular sieves in CH_2Cl_2, giving **3-51** in quantitative yield on a 0.54 mmol scale. Then, *ortho*-lithiation of **3-51** with organolithium reagents was attempted, where the aryl lithium formed *ortho* to the MOM group was expected to attack the boronic ester intramolecularly, giving the corresponding aryl borinic ester (**3-52**).



Scheme 3.22. Functional group manipulation strategy 1: deprotection of the TIPS ether, formation of the boronic ester, *ortho*-lithiation

The *ortho*-lithiation of MOM-protected phenols followed by nucleophilic attack to give *ortho*-substituted phenols has been previously reported.[14,15] Several organolithium reagents were applied to **3-51** in attempts to convert it to **3-52**. Conditions utilizing *n*-butyllithium (1.0 equiv.) in THF from 0 °C to rt were tried first, leading to the recovery of 42 % starting material **3-51**, 39 % of the product of hydrolysis of the boronic ester **3-50**, and none of the desired **3-52** (Table 3.16, entry 1). Entry 2 employed similar conditions to entry 1 with the addition of TMEDA (1.1 equiv.) to decrease the degree of aggregation of the *n*BuLi, however the reaction once again yielded a mixture of **3-51** (63 %) and **3-50** (15 %). Treatment with the stronger base *tert*-butyllithium (1.1 equiv.) in THF at −78 °C for 1 h followed by warming to rt for 2 h led to a complex mixture of products which could not be identified (entry 3). Considering the high reactivity of *t*-BuLi, it likely reacted with other parts of the molecule such as hydrolyzing the boronic ester or undergoing lithium-halogen exchange with the aryl chloride. Running the reaction with *t*-BuLi at −78 °C for just 1 h gave a cleaner crude reaction mixture, however only **3-51** (13 %) and **3-50** (75 %) were isolated

(entry 4). Using *sec*-butyllithium (1.1 equiv.) was also ineffective at producing **3-52**, giving 29 % **3-51** and 65 % **3-50**. As MOM-directed *ortho*-lithiation had failed in all attempts, a different strategy for forming the aryl borinic ester **3-52**, starting from an *ortho*-brominated analogue of **3-51** was then explored.



Entry	organolithium (eq)	T, t	Yield of rec. SM **3-51** (%)	Yield of byproduct **3-50** (%)	Yield of product **3-52** (%)
1	*n*BuLi (1.0)	1.5 h at 0 °C + 3 h at rt	39	42	-
2	*n*BuLi, TMEDA (1.1 each)	1 h at 0 °C + 3 h at rt	65	15	-
3	*t*BuLi (1.1)	1 h at –78 °C + 2 h at rt	?	?	?
4	*t*BuLi (1.1)	1 h at –78 °C	13	75	-
5	*s*BuLi (1.1)	1 h at –78 °C	29	65	-

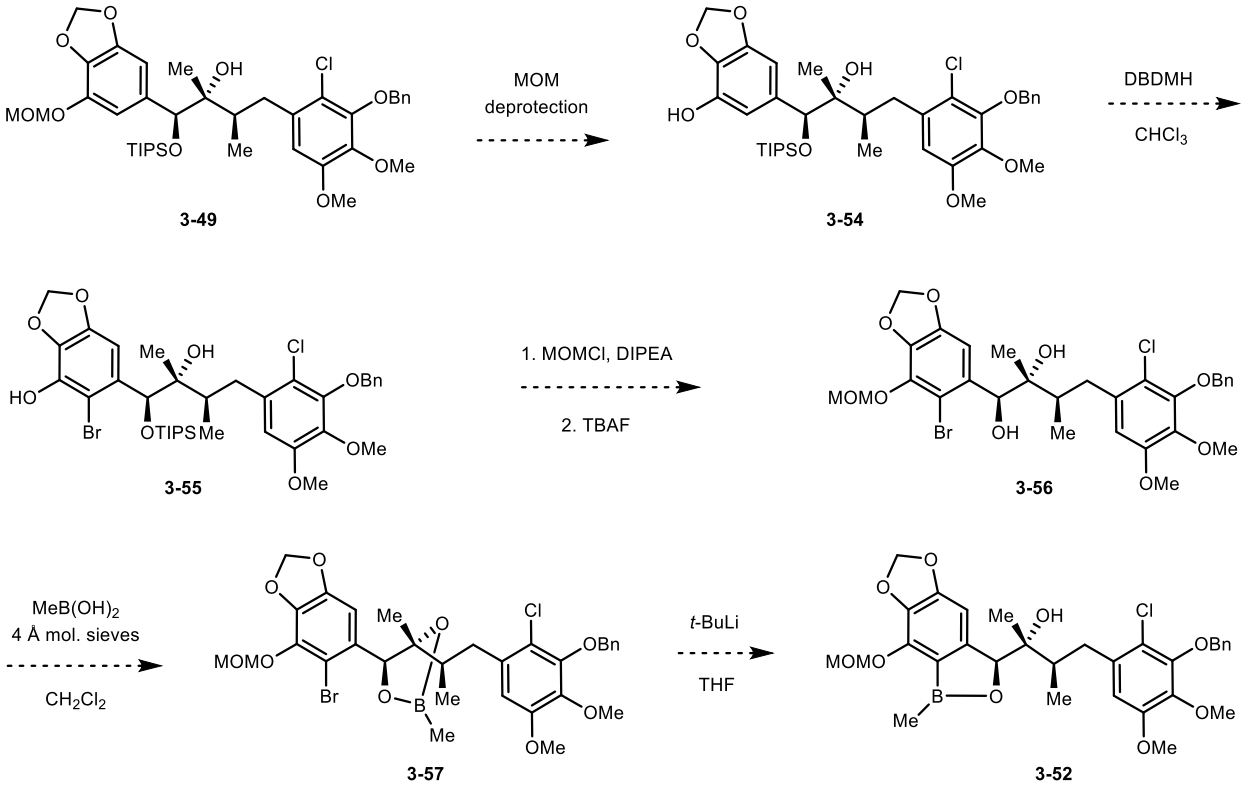
Reactions were run on 0.04-0.05 mmol scale.

Table 3.16. Screening *ortho*-lithiation conditions

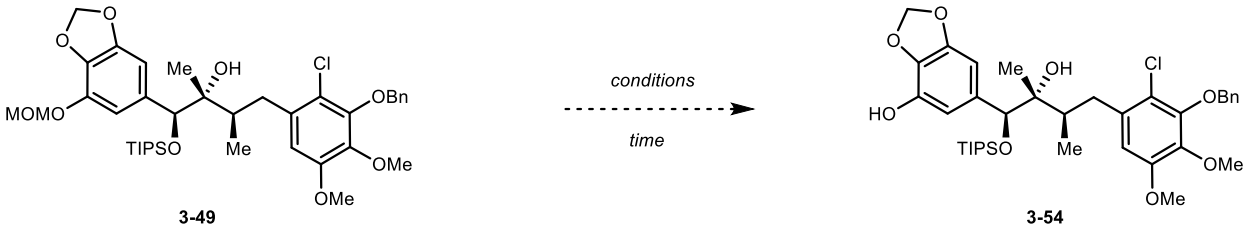
The new strategy, detailed in Scheme 3.23, began with deprotection of the MOM ether of **3-49** to reveal a free phenol (**3-54**) which could be used to direct *ortho*-bromination, providing **3-55**. The phenol could be reprotected using MOMCl and DIPEA, followed by deprotection of the benzylic OTIPS with TBAF to provide **3-56**. Treatment with methylboronic acid would give the boronic ester **3-57**. *t*-BuLi would then be added so that **3-57** would undergo lithium-bromine exchange to provide the aryl lithium which would attack the boronic ester intramolecularly to give the borinic ester **3-52**.

The deprotection of the MOM ether of **3-49** was attempted using four different sets of conditions which were reported as mild, functional group tolerant methods (Table 3.17). Compound **3-49** was first subjected to heterogenous catalysis with $NaHSO_4$-SiO_2 in CH_2Cl_2,[16] where the reaction was stopped after 2.5 h once the starting material was consumed as determined by TLC, however upon

analysis of the ^{1}H NMR spectrum, the desired product was not formed cleanly (entry 1). In entry 2, **3-49** was treated with TMSBr and 4 Å molecular sieves in CH_2Cl_2[17] at –30 °C for 1 h, followed by 0 °C for 1 h, resulting in the formation of several species as observed by ^{1}H NMR and the presence of 6 spots in the TLC. In entry 3, **3-49** was subjected to CBr_4 (20 mol %) and PPh_3 (20



Scheme 3.23. Functional group manipulation strategy 2: deprotection of the MOM ether, *ortho*-bromination, formation of the boronic ester, lithium-bromine exchange



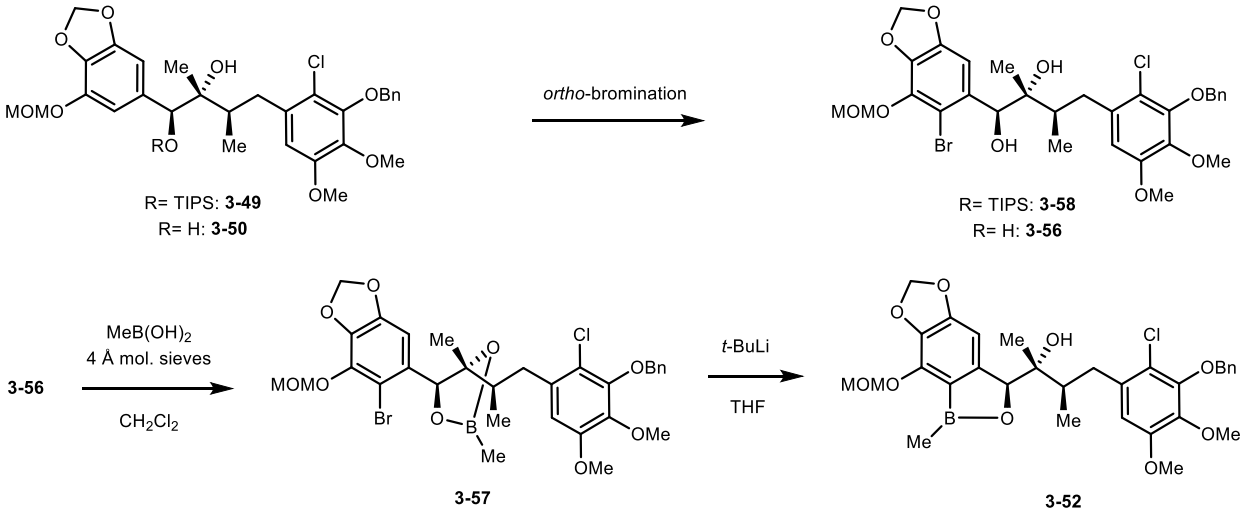
Entry	Scale (mmol)	Conditions	Time (h)	TLC result
1	0.05	$NaHSO_4$-SiO_2 (1g/mmol SM), CH_2Cl_2 (0.05 M), rt	2.5	1 spot
2	0.02	TMSBr (4 eq), 4 Å mol. sieves, CH_2Cl_2, –30 to 0 °C	2	6 spots
3	0.02	CBr_4 (0.2 eq), PPh_3 (0.2 eq), $ClCH_2CH_2Cl$, 40 °C	3.5	3 spots
4	0.02	Montmorillonite clay, CH_2Cl_2, 50 °C	6	2 spots

Table 3.17. Screening conditions for deprotection of the MOM ether

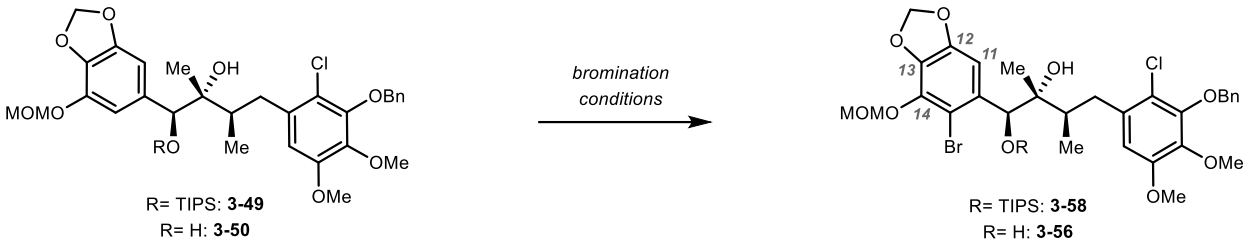
mol %) in dichloroethane at 40 °C for 3.5 h,[18] after which mostly starting material remained and two minor species were observed by TLC. Treatment with Montmorillonite K 10 clay in CH_2Cl_2[19] at 50 °C for 6 h gave two spots by TLC, which upon purification by column chromatography did not yield clean products (entry 4).

The deprotection of the MOM ether of **3-49** proved challenging, likely due to the presence of other reactive functional groups such as the acetal and the alcohol, therefore a strategy circumventing this step was devised. The direct *ortho*-bromination of **3-49** or free alcohol **3-50** was proposed (Scheme 3.24). This reaction would result in the formation of **3-58** or **3-56**, where **3-58** could be converted to **3-56** by treatment with TBAF. Next, diol **3-56** would be converted to the boronic ester using methylboronic acid. The resulting **3-57** would then be converted to the borinic ester **3-52** by lithium-bromine exchange with *t*-BuLi followed by intramolecular cyclization.

Compound **3-49** and its TIPS-deprotected analogue **3-50** were each subjected to three different sets of bromination conditions on 0.03 mmol scale. The use of elemental Br_2 (1.2 equiv.) in acetic acid (0.06 M) at rt for 1 h led to the decomposition of both substrates (Table 3.18, entries 1–2). Treatment with NBS (1.1 equiv.) in acetonitrile (0.06 M) at rt for 1 h in the dark led to the formation of three species in the case of **3-49** and a single major species in the case of **3-50**, as observed by the crude ^{1}H NMR (entries 3, 4). Bromination with DBDMH (0.5 equiv.) in chloroform (0.06 M) for 0.5 h at 0 °C, produced three species in the case of **3-49** and two species (where one was major)



Scheme 3.24. Functional group manipulation strategy 3: *ortho*-bromination, formation of the boronic ester, lithium-bromine exchange



R= TIPS: **3-49**
R= H: **3-50**

R= TIPS: **3-58**
R= H: **3-56**

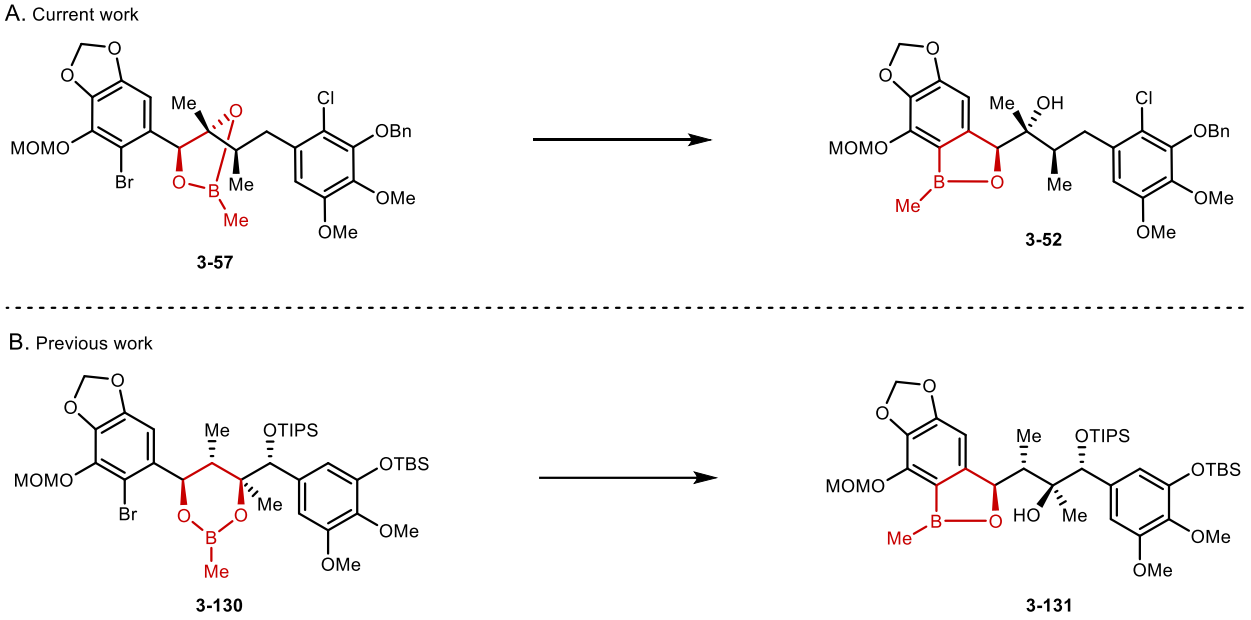
Entry	R	scale (mmol)	Conditions	Crude ^{1}H NMR	Isolated yield of **3-58** or **3-56** (%)
1	TIPS	0.03	Br_2 (1.2 eq), acetic acid (0.06 M), 1 h, rt	decomposition	-
2	H	0.03	Br_2 (1.2 eq), acetic acid (0.06 M), 1 h, rt	decomposition	-
3	TIPS	0.03	NBS (1.1 eq), MeCN (0.06 M), 1 h, rt, dark	3 species	-
4	H	0.03	NBS (1.1 eq), MeCN (0.06 M), 1 h, rt, dark	1 major species	-
5	TIPS	0.03	DBDMH (0.5 eq), $CHCl_3$ (0.06 M), 0.5 h, 0 °C	3 species	-
6	H	0.03	DBDMH (0.5 eq), $CHCl_3$ (0.06 M), 0.5 h, 0 °C	2 species, 1 is major	-
7	H	0.09	NBS (1.1 eq), MeCN (0.06 M), 1 h, rt, dark	3 species	29
8	H	0.30	NBS (1.1 eq), MeCN (0.1 M), 1 h, rt, dark	3 species	40
9	H	0.08	DBDMH (0.5 eq), $CHCl_3$ (0.08 M), 0.5 h, 0 °C	2 species, **3-56** is major	52
10	H	0.40	DBDMH (0.5 eq), $CHCl_3$ (0.08 M), 0.5 h, 0 °C	2 species, **3-56** is major	85
11	H	5.98	DBDMH (0.5 eq), $CHCl_3$ (0.1 M), 40 min, 0 °C	-	88

Table 3.18. Screening *ortho*-bromination conditions

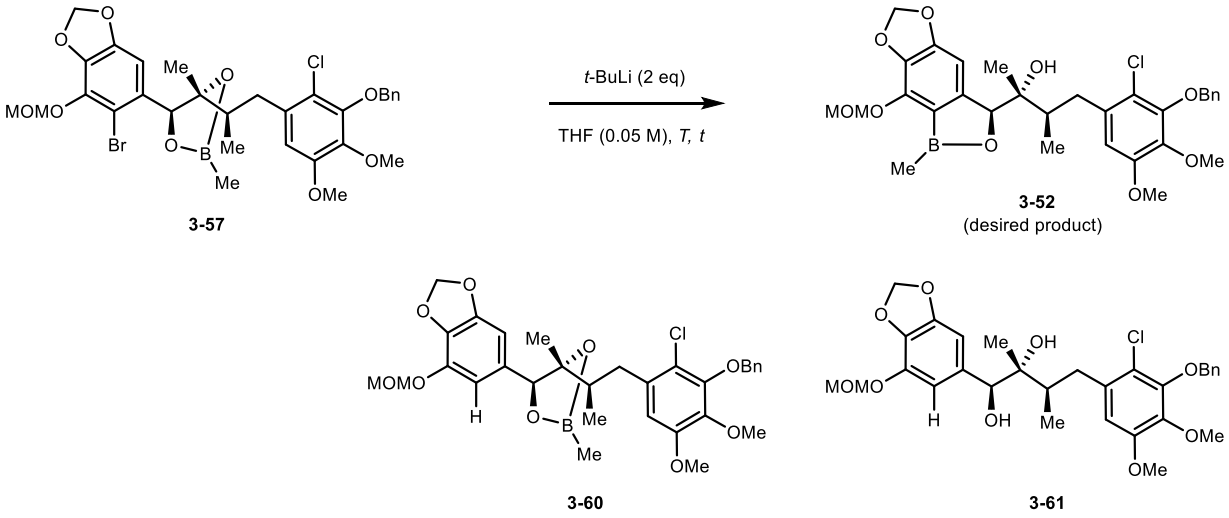
in the case of **3-50** (entries 5, 6). As substrate **3-50** reacted more selectively (producing fewer species) than **3-49**, it was selected for further experiments with either NBS or DBDMH. The major species from entries 4 and 6 appeared identical by ^{1}H NMR therefore these crude reaction mixtures were combined for purification. The desired regioisomer of product (**3-56**) was isolated and fully characterized, where regiochemistry was determined by the HMBC correlation from the C11 proton to C12 and C13 and a lack of correlation to C14. Increasing the scale of the reaction of **3-50** with NBS to 0.09 or 0.3 mmol led to decreased selectivity, with three species observed in the crude ^{1}H NMR spectra and isolated yields of merely 29 % and 40 % **3-56**, respectively being obtained (entries 7–8). Selectivity increased with increased reaction scale under the DBDMH conditions, with a 52 % yield of **3-56** being isolated on 0.08 mmol scale and an 85 % yield on 0.40 mmol scale (entries 9, 10). The scale of the regioselective *ortho*-bromination of **3-50** to produce **3-56** using DBDMH was eventually increased to 5.98 mmol, providing 88 % yield (entry 11).

Compound **3-56** was subjected to methylboronic acid (1.2 equiv.) and 4 Å molecular sieves in CH_2Cl_2 for 12 h at rt, furnishing **3-57** in quantitative yield on up to 4.4 mmol scale. To convert the 5-membered boronic ester **3-57** to the 5-membered borinic ester **3-52**, it was subjected to conditions which had been previously used in the synthesis of heteroclitin J for the transformation of a 6-membered boronic ester **3-130** to a 5-membered borinic ester **3-131** (Scheme 3.25).[9] These

consisted of treatment of **3-57** with *t*-BuLi in THF (0.05 M) at –78 °C for 1 h followed warming to rt for 3 h (Table 3.19, entry 1). A 37 % yield of the desired product **3-52** was formed along with the product of protodebromination and hydrolysis of the boronic ester (**3-61**). The structure of **3-52** was confirmed via X-ray crystallography (see section 3.7.3). In attempts to increase the yield of **3-52**, the reaction time at rt was increased to either 5 h or overnight (entries 2, 3), however only 29 % and 31 % yields of **3-52** were obtained, respectively. The byproduct **3-61** and a new protodebromination byproduct **3-60** were formed as well. In entry 4, the reaction was run at –78 °C for 1 h followed by heating to 60 °C for 3 h, yielding 33 % **3-52** as well as **3-61** and **3-60**. Entries 5 and 6 employed the standard conditions but with additives HMPA or TMEDA (5 equiv.), which strongly coordinate Li^+, with the former leading to the isolation of 36 % **3-52** as well as the production of byproducts **3-61** and **3-60** and the latter leading to decomposition. In entry 7, **3-57** was reacted under the standard conditions and then TMSCl (6 equiv.) and NEt_3 (4 equiv.) were added and reacted overnight in attempts to trap the tertiary alkoxide as the TMS ether. The tertiary alkoxide was not converted to the silyl ether under these conditions and unprotected **3-52** (in 46 % yield) was isolated instead. The byproducts **3-60** and the mono-TMS-protected version of **3-61** were isolated as well. Diluting the reaction mixture to 0.01 M (entry 8) did not affect the yield of **3-52** (31 %). An improvement in yield was finally observed when the reaction was run strictly at



Scheme 3.25. Boronic ester migration A) in the current work and B) in the previous synthesis of heteroclitin J



Entry	T, t	Changes to conditions	Rec. SM **3-57** (%)	**3-60** (%)	**3-61** (%)	Product **3-52** (%)
1	1 h at -78 °C + 3 h at rt	-	-	-	not quantified	37
2	1 h at -78 °C + 5 h at rt	-	28[a]	-	22	29
3	1 h at -78 °C + overnight at rt	-	-	18	49	31
4	1 h at -78 °C + 3 h at 60 °C	-	-	23	47	33
5	1 h at -78 °C + 3 h at rt	added HMPA (5 eq)	-	12	22	36
6	1 h at -78 °C + 3 h at rt	added TMEDA (5 eq)	-	-	-	-
7	1 h at -78 °C + 3 h at rt	added TMSCl, NEt_3[b]	-	46	14[c]	46
8	1 h at -78 °C + 3 h at rt	0.01 M	-	19	53	31
9	1 h at -78 °C	-	-	-	45	45
10	30 min at -78 °C	-	-	-	41	48
11	20 min at -78 °C	-	-	19	54	21
12	10 min at -78 °C	-	20	-	48	29
13	5 min at -78 °C	-	50	-	-	-
14	1 h at -78 °C	solvent: 2-MeTHF	-	11	42	35
15	1 h at -78 °C	solvent: Et_2O	-	16	16	38
16	1 h at -78 °C	solvent: CPME	-	15	27	42
17	30 min at -78 °C	added 12-crown-4 (2 eq)	-	19	12	34

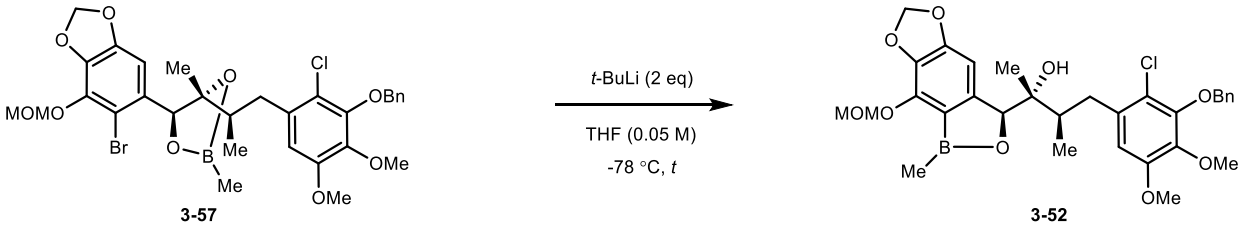
Reactions were run on 0.04-0.05 mmol scale. Yields are isolated yields. a= mixture of **3-57** and **3-60**;
b= added TMSCl (6 eq) and NEt_3 (4 eq) at the end of the reaction and then stirred overnight; c= **3-61** bearing a TMS group

Table 3.19. Optimization of the lithium-bromine exchange / cyclization conditions

–78 °C for 1 h, where a 45 % yield of **3-52** and 45 % **3-61** were obtained (entry 9). The reaction time was gradually decreased over entries 10–13 to determine the minimum reaction time required to obtain this result. A comparable yield of 48 % **3-52** and 41 % **3-61** was observed when the reaction was run at –78 °C for 30 minutes (entry 10). Yields of **3-52** decreased to 21–29 % when the reaction was only run for 10–20 minutes (entries 11-12). A reaction time of 5 minutes did not give any product, with only starting material **3-57** being recovered (entry 13). As reaction at –78 °C for 30 minutes or 1 h gave similar results, these reaction times were used interchangeably in the subsequent experiments. Alternative solvents, 2-MeTHF, Et_2O, and CPME, were employed in reactions at –78 °C for 1 h, however none offered a higher yield of **3-52** than THF (entries 14–16).

The addition of 12-crown-4 (2 equiv.) to sequester Li^+ did not improve the yield either, with 34 % **3-52** being isolated after reaction at −78 °C for 30 minutes.

The lithium-bromine exchange / cyclization was gradually increased in scale, using the optimized conditions of *t*BuLi (2 equiv.) in THF (0.05 M) at −78 °C for 30 minutes (Table 3.20). Reactions on 0.2, 0.5, and 0.9 mmol scale under these conditions provided comparable yields to the 0.05 mmol scale reaction (45–49 %, entries 1–3). Increasing the reaction time to 1 h on 1.0 mmol scale provided essentially the same result as the 30 minute reaction (51 % yield of **3-52**, entry 4). A drop in yield was observed upon increasing the scale beyond 1.0 mmol, with 41 % **3-52** being isolated from a 1.3 mmol reaction (entry 5) and 21 % yield of **3-52** from a 3.0 mmol reaction (entry 6). As 1.0 mmol appeared to be the largest scale where the yield was maintained, future experiments were conducted on this scale.



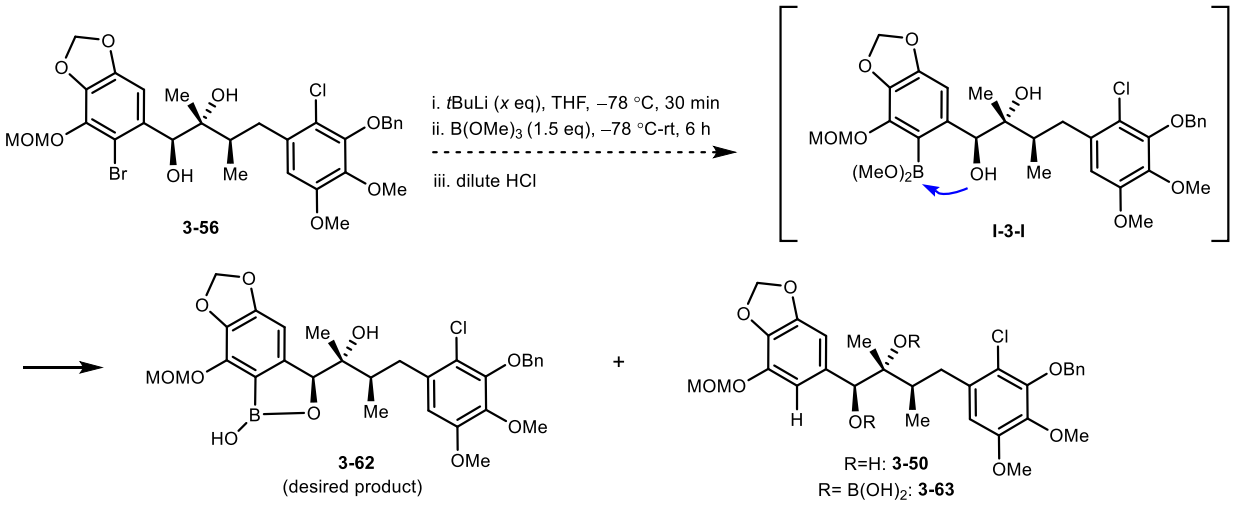
Entry	scale (mmol)	t (min)	Product **3-52** (%)
1	0.2	30	48
2	0.5	30	45
3	0.9	30	49
4	1.0	60	51
5	1.3	60	41
6	3.0	30	21

Yields are isolated yields.

Table 3.20. Increasing the scale of the lithium-bromine exchange / cyclization

Considering the maximum yield of **3-52** that was obtained after extensive optimization studies was only 51 %, other targets which could serve as the starting material for an intramolecular Suzuki coupling were briefly investigated (**3-62**, **3-65**, and **3-66**). The conversion of **3-56** to **3-62** was attempted using a modified version of Nicolaou's conditions,[20] involving treatment with *t*-BuLi to give the aryl lithium, followed by the addition of $B(OMe)_3$ to convert this to the aryl boronic ester **I-3-I**. The benzylic alcohol would then attack the aryl boronic ester, giving a 5-membered boronic ester which would be hydrolyzed to the boronic acid **3-62** upon acidic workup (Table 3.21). The use of two equivalents of *t*-BuLi led solely to a protodebrominated byproduct **3-50** (34 %, entry

1). Using 4 equivalents of *t*-BuLi led to the formation of a different byproduct, diborate **3-63** (63 %, entry 2), which was characterized by NMR and HRMS. The desired **3-62** was not detected in either reaction mixture.

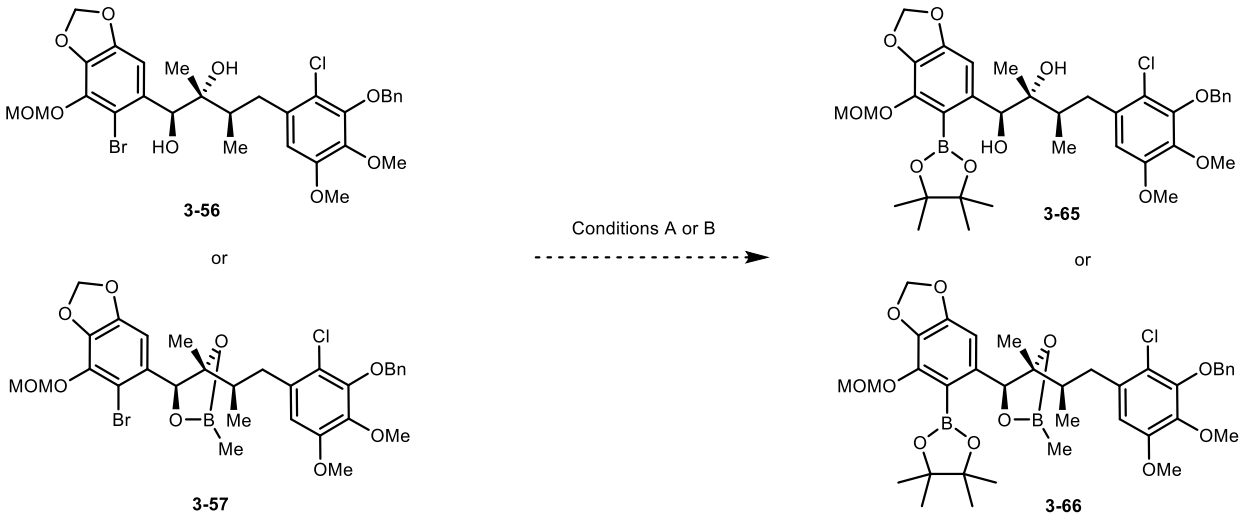


Entry	Eq. *t*-BuLi	**3-50** (%)	**3-63** (%)	Desired product **3-62** (%)
1	2	34	0	-
2	4	-	63	-

Reactions were run on 0.05 mmol scale

Table 3.21. Attempted formation of an aryl boronic ester **3-62** via the Ar-B(OMe)$_2$ intermediate

The synthesis of aryl boronic acids **3-65** and **3-66** were attempted utilizing Miyaura borylation (Scheme 3.26). Diol **3-56** and boronic ester **3-57** were each treated with two sets of borylation conditions: A) $Pd(PPh_3)Cl_2$ (4 mol %), B_2Pin_2 (1.2 equiv.), and KOAc (3 equiv.) in 1,4-dioxane (0.2 M) at 95 °C for 16 h[21] or B) $PdCl_2(dppf)$ (3 mol %), B_2Pin_2 (1.1 equiv.), and KOAc (3 equiv.) in DMSO (0.2 M) at 80 °C for 10 h.[22] Both substrates led mostly to the recovery of starting material when subjected to conditions A. A small amount of decomposition was observed in the reaction involving **3-56** and some hydrolysis of the boronic ester was observed in the case of **3-57**. Under conditions B, starting material was recovered in both cases as well as byproducts where the ^{1}H NMR spectra did not match the desired products **3-65** or **3-66**. After these failed attempts, substrate **3-52**, which could be formed in 51 % yield from **3-57**, was advanced in the synthesis of kadsuraol C.



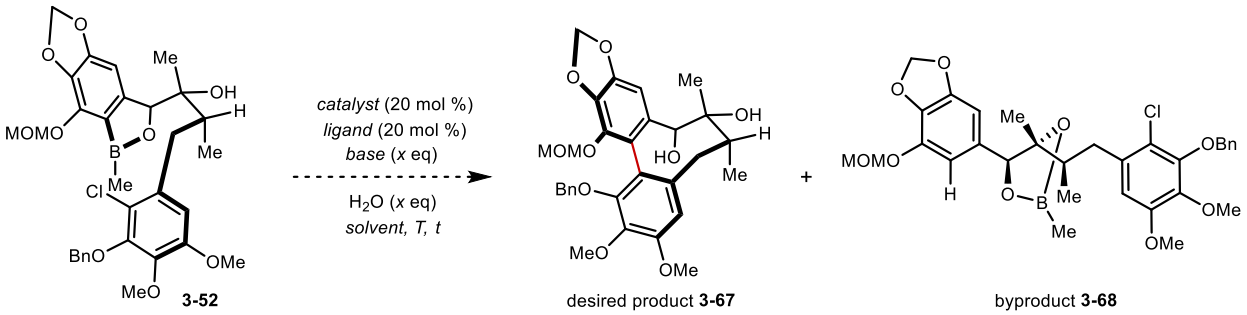
Conditions A: $Pd(PPh_3)Cl_2$ (4 mol %), B_2Pin_2 (1.2 eq), KOAc (3 eq), 1,4-dioxane (0.2 M), 95 °C, 16 h
Conditions B: $PdCl_2(dppf)$ (3 mol %), B_2Pin_2 (1.1 eq), KOAc (3 eq), DMSO (0.2 M), 80 °C, 10 h

Scheme 3.26. Attempted formation of the Ar-Bpin **3-65** or **3-66** via Miyaura boration

3.4.6. Suzuki coupling

This section will focus on the key atroposelective Suzuki coupling step to form the biaryl axis. Compound **3-52** was first subjected to the conditions which had been used to form the biaryl axis atroposelectively in 87 % yield in our group's previous synthesis of heteroclitin J.[9] These conditions consisted of placing **3-52** in a Schlenk flask under inert atmosphere and treatment with Buchwald's SPhos Pd G2 precatalyst (20 mol %), additional SPhos ligand (20 mol %), K_3PO_4 (5 equiv.), and H_2O (0.5 equiv.) in PhMe (0.05 M) at 60 °C for 16 h (Table 3.22, entry 1). The structures of the ligands and precatalysts screened for Suzuki coupling are shown in Figure 3.6. The desired biaryl product **3-67** was not observed and instead a byproduct of protodeborylation (**3-68**) was isolated as the major product. The effect of temperature was investigated by running reactions at either 30 °C or 100 °C for 2 h (entries 2, 3), resulting in the recovery of starting material (**3-52**) and decomposition, respectively. As 30 °C was too mild to effect any reactivity and 100 °C was too harsh, most of the subsequent experiments were run at 60 °C. A variety of catalysts and ligands, especially those which have been reported for Suzuki couplings involving aryl chlorides, were then screened. Entries 4 and 5 employ the use of different Pd(II) catalysts, $Pd(OAc)_2$ and $Pd_2(dba)_3$, along with SPhos ligand, with the former returning byproduct **3-68** and the latter a mixture of **3-52** and decomposition products. Other Buchwald precatalysts were then screened as these have been successfully used in the literature for the synthesis of extremely hindered biaryls

from aryl chlorides.[23] The use of Buchwald's XPhosPd G2 precatalyst[24] with additional XPhos ligand also gave a mixture of **3-52** and decomposition (entry 6), while RuPhos Pd G3 / RuPhos returned only **3-52** (Table 3.22, entry 7). The reactions of **3-52** with $Pd(OAc)_2$ and Buchwald ligand **3-69**[23] in either THF or PhMe provided a mixture of starting material and protodeborylation byproduct (entries 8–9). Four BI-DIME ligands, which have been reported in intermolecular asymmetric Suzuki couplings,[25] were screened with $Pd(OAc)_2$, none of which gave any reactivity, returning solely **3-52** (Table 3.22, entry 10). Next, sterically hindered adamantyl-bearing monophosphine ligands were investigated. The combination of $Pd(OAc)_2$ with CataCXium A® provided mainly **3-68** (entry 11).[26,27] Reaction with $[Pd(cinnamyl)Cl]_2$ and MeDalPhos in dioxane under anhydrous conditions at 65 °C resulted in protodeborylation (entry 12).[28] Organ's Pd-PEPPSI-IPent catalyst, which has been reported in the preparation of tetra-*ortho*-substituted biaryls from aryl chlorides,[29] was utilized with several sets of conditions, with increased reaction time and temperature (100 °C, 24 h), including with K_3PO_4 (5 equiv.) and 0.5 or 0 eq H_2O in PhMe



Entry	Catalyst	Ligand	Base (eq)	Solvent (0.05 M)	eq H_2O	T (°C)	time (h)	Result
1	SPhos Pd G2	SPhos	K_3PO_4 (5)	toluene	0.5	60	16	**3-68**
2	SPhos Pd G2	SPhos	K_3PO_4 (5)	toluene	0.5	30	2	SM
3	SPhos Pd G2	SPhos	K_3PO_4 (5)	toluene	0.5	100	2	decomp.
4	$Pd(OAc)_2$	SPhos	K_3PO_4 (5)	toluene	0.5	60	4	**3-68**
5	$Pd_2(dba)_3$	SPhos	K_3PO_4 (5)	toluene	0.5	60	4	SM + decomp.
6	XPhos Pd G2	XPhos	K_3PO_4 (5)	toluene	0.5	60	4	SM + decomp.
7	RuPhos Pd G3	RuPhos	K_3PO_4 (5)	toluene	0.5	60	4	SM
8	$Pd(OAc)_2$	**3-69**	K_3PO_4 (5)	toluene	0.5	60	4	SM + **3-68**
9	$Pd(OAc)_2$	**3-69**	K_3PO_4 (5)	THF	0.5	60	4	SM + **3-68**
10	$Pd(OAc)_2$	BI-DIME L	K_3PO_4 (5)	toluene	0.5	60	4	SM
11	$Pd(OAc)_2$	CataCXium $A^{(R)}$	K_3PO_4 (5)	toluene	0.5	60	4	**3-68**
12	$[Pd(cinnamyl)Cl]_2$	MeDalPhos	K_3PO_4 (5)	dioxane	0	65	4	**3-68**
13	Pd-PEPPSI-IPent	-	K_3PO_4 (5)	toluene	0.5	100	24	decomp.
14	Pd-PEPPSI-IPent	-	K_3PO_4 (5)	toluene	0	100	24	**3-68**
15	Pd-PEPPSI-IPent	-	KOH (3)	dioxane	0	65	24	decomp.
16	Pd-PEPPSI-IPent	-	KO*t*Bu (3)	*t*BuOH	0	65	24	several species

Reactions were run on 0.04-0.05 mmol scale. In addition to the reported result, some protodeborylation byproduct was observed in most reactions. BI-DIME L= Four BI-DIME ligands were screened, all producing similar results.

Table 3.22. Screening Suzuki coupling conditions on **3-52**

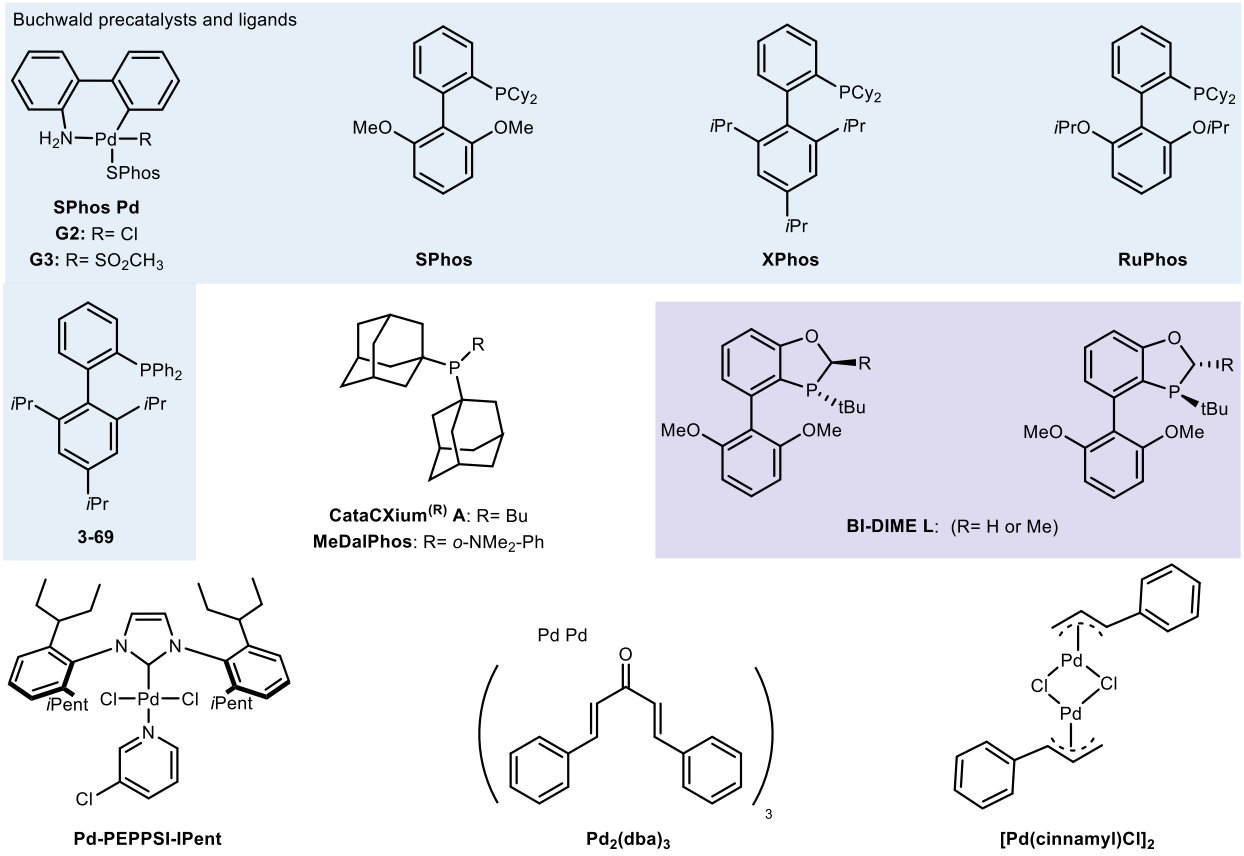
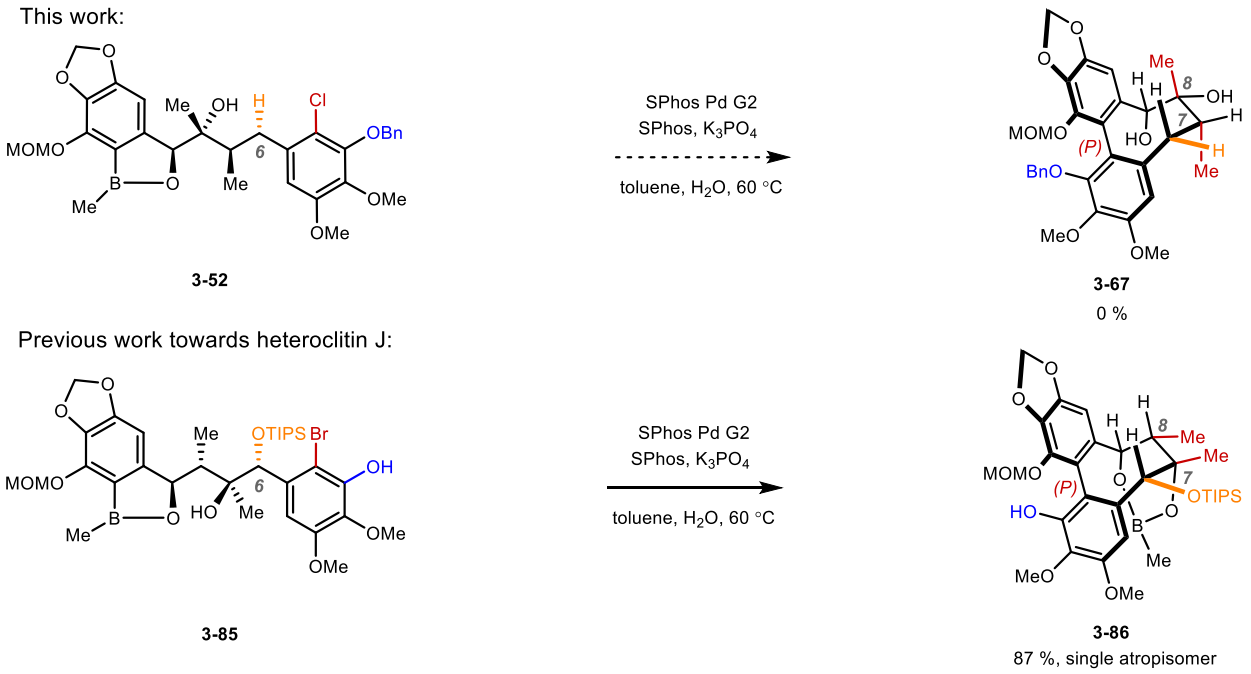


Figure 3.6. Catalysts and ligands used in the Suzuki coupling

(entries 13 and 14), leading to decomposition and protodeborylation, respectively. Entries 15 and 16 employ Pd-PEPPSI-IPent with either KOH (3 equiv.) in dioxane or KO*t*Bu (3 equiv.) in *t*BuOH under anhydrous conditions at 65 °C for 24 h, yielding decomposition and a complex mixture of species, respectively. As the intensive screening of reaction conditions did not result in even a trace amount of **3-67** being formed, it was postulated that reactivity could be an issue inherent to the substrate itself.

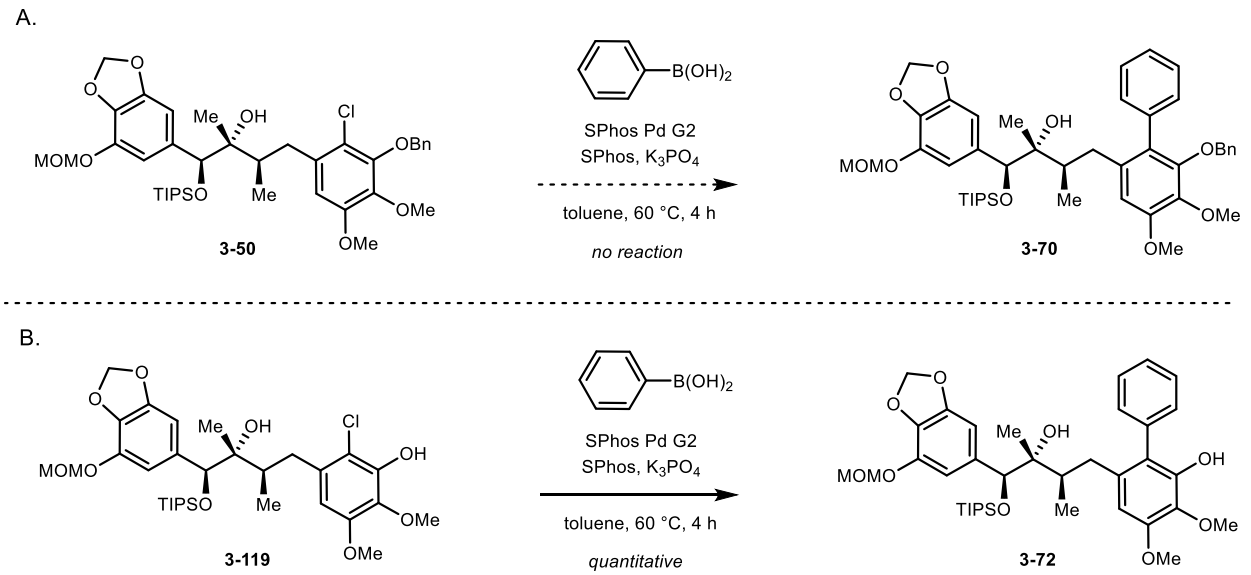
Comparing substrate **3-52** to the substrate which had successfully undergone Suzuki coupling in our synthesis of heteroclitin J, several differences can be noted (Scheme 3.27). Compound **3-52** bears a methylene at C6 whereas the previous substrate **3-85** bore an OTIPS group at this position. Additionally, **3-52** has an aryl chloride instead of an aryl bromide and the phenol is protected with a benzyl group. Finally, and perhaps most notably, the relative stereochemistry of the C7 and C8 methyl groups is different. In the previous product **3-86**, the methyl groups were both equatorial, whereas in **3-67**, they are both axial. Each one of these differences was investigated to determine

which led to the discrepancy in reactivity, starting with the effects of the aryl chloride and the benzyl protecting group on the phenol.



Scheme 3.27. Comparison of **3-52** to the Suzuki coupling substrate from the synthesis of heteroclitin J

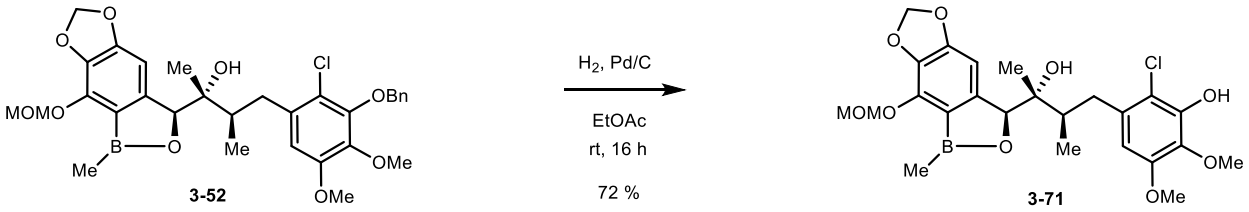
Substrate **3-50**, lacking the borinic ester, was subjected to intermolecular Suzuki coupling with phenylboronic acid to test the reactivity of the benzyl ether-bearing aryl chloride (Scheme 3.28A).



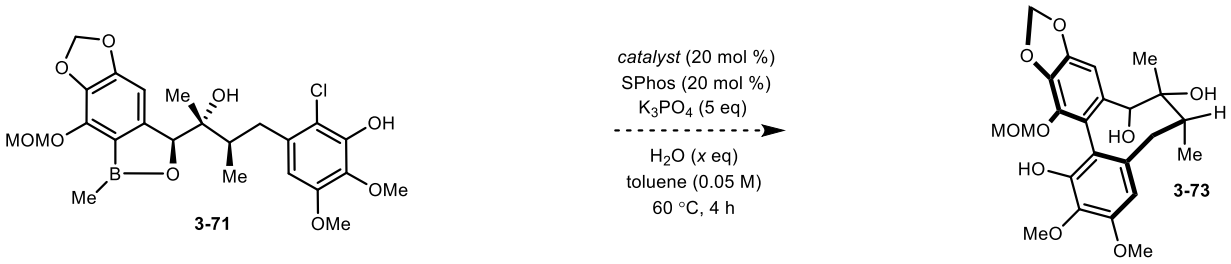
Scheme 3.28. Intermolecular Suzuki couplings

No reaction occurred, likely due to steric encumbrance. The corresponding free phenol **3-119** successfully partook in the intermolecular Suzuki coupling (Scheme 3.28B), hence confirming that oxidative addition of the aryl chloride into the active catalyst generated from SPhos Pd G2 is feasible and that a free phenol is a more suitable substrate than the benzyl-protected analogue.

Substrate **3-52** was then subjected to hydrogenation with catalytic Pd/C in EtOAc to deprotect the benzyl group, providing the free phenol **3-71** (in 72 % yield, Scheme 3.29) which would be expected to undergo oxidative addition more readily than its bulky counterpart **3-52**. Compound **3-71** was then treated to the standard Suzuki coupling conditions using SPhos Pd G2 and SPhos (Table 3.23, entry 1), which resulted in the production of multiple species. The use of $Pd(OAc)_2$ with SPhos in the Suzuki coupling led only to protodeborylation (entry 2).



Scheme 3.29. Deprotection of the phenolic benzyl ether



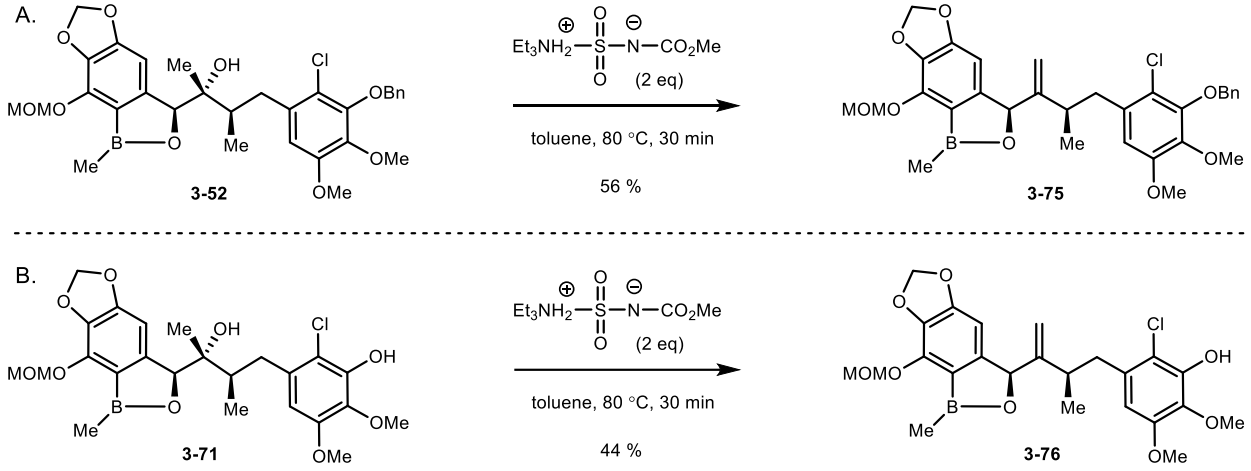
Entry	Catalyst	eq H_2O	Result
1	SPhos Pd G2	0.5	multiple species
2	$Pd(OAc)_2$	0	prodeborylation

Reactions were run on 0.04 mmol scale.

Table 3.23. Screening Suzuki coupling conditions on **3-71**

Next, the steric effect of the axial C8 methyl group in the desired product **3-67** was explored. This product is expected to be higher in energy than **3-86** due to the unfavorable transannular interactions between the axial methyl and other axial substituents such as the C6 hydrogen and the upper aromatic ring of the biaryl. To alleviate this steric repulsion, the tertiary alcohol of the

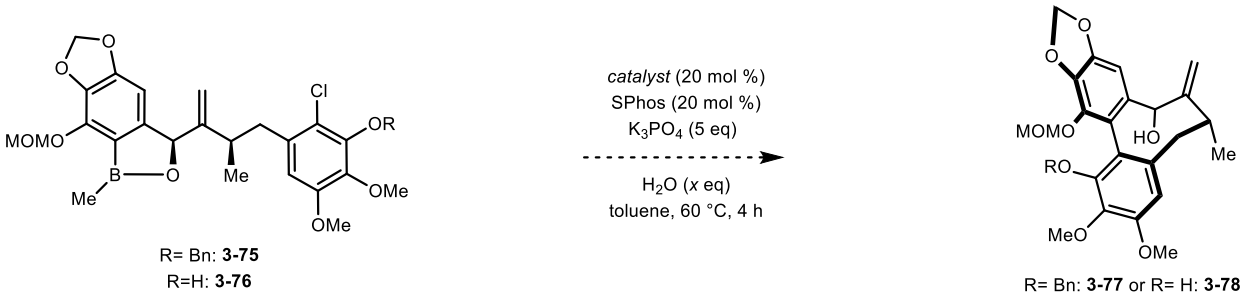
substrate was eliminated to the terminal alkene. Two terminal alkene substrates for use in the Suzuki coupling were prepared from either the benzyl ether-bearing **3-52** or the free phenol **3-71** via Burgess dehydration using Burgess reagent (2 equiv.) in PhMe at 80 °C for 30 minutes, providing **3-75** in 56 % yield and **3-76** in 44 % yield (Scheme 3.30).



Scheme 3.30. Burgess dehydration of **3-52** and **3-71**

The alkene substrates **3-75** and **3-76** were subjected to Suzuki coupling in attempts to form either biaryl **3-77** or **3-78**, which are expected to have less steric repulsions than **3-67** due to the lack of an axial substituent at C8. The standard Suzuki coupling conditions consisting of SPhos Pd G2, SPhos, K_3PO_4, and water in PhMe at 60 °C for 4 h were employed, leading to protodeborylation in both cases (Table 3.24, entries 1, 3). Compound **3-75** was also treated with $Pd(OAc)_2$ and SPhos, returning only starting material (entry 2). In entry 4, water was omitted in the reaction of **3-76**, with SPhos Pd G2 as catalyst, in attempts to alleviate protodeborylation, however a mixture of **3-76** and protodeborylation byproduct was returned.

Several alternative methods were then investigated for forming the biaryl axis (Schemes 3.31–3.33). **3-52** was subjected to photocatalyzed S_NAr conditions developed by Sanford and coworkers employing 9-mesityl-3,6-di-*tert*-butyl-10-phenylacridinium tetrafluoroborate (5 mol %) as photocatalyst and $LiPF_6$ (3 equiv.) in DCE: TFE (1:1, 0.1 M) under irradiation by blue LEDs.[30] The proposed mechanism is illustrated in Scheme 3.31. The reaction was run twice on 0.05 mmol scale, for either 1 h or 24 h, but the desired biaryl **3-79** was not observed in either case as both reactions resulted in decomposition.



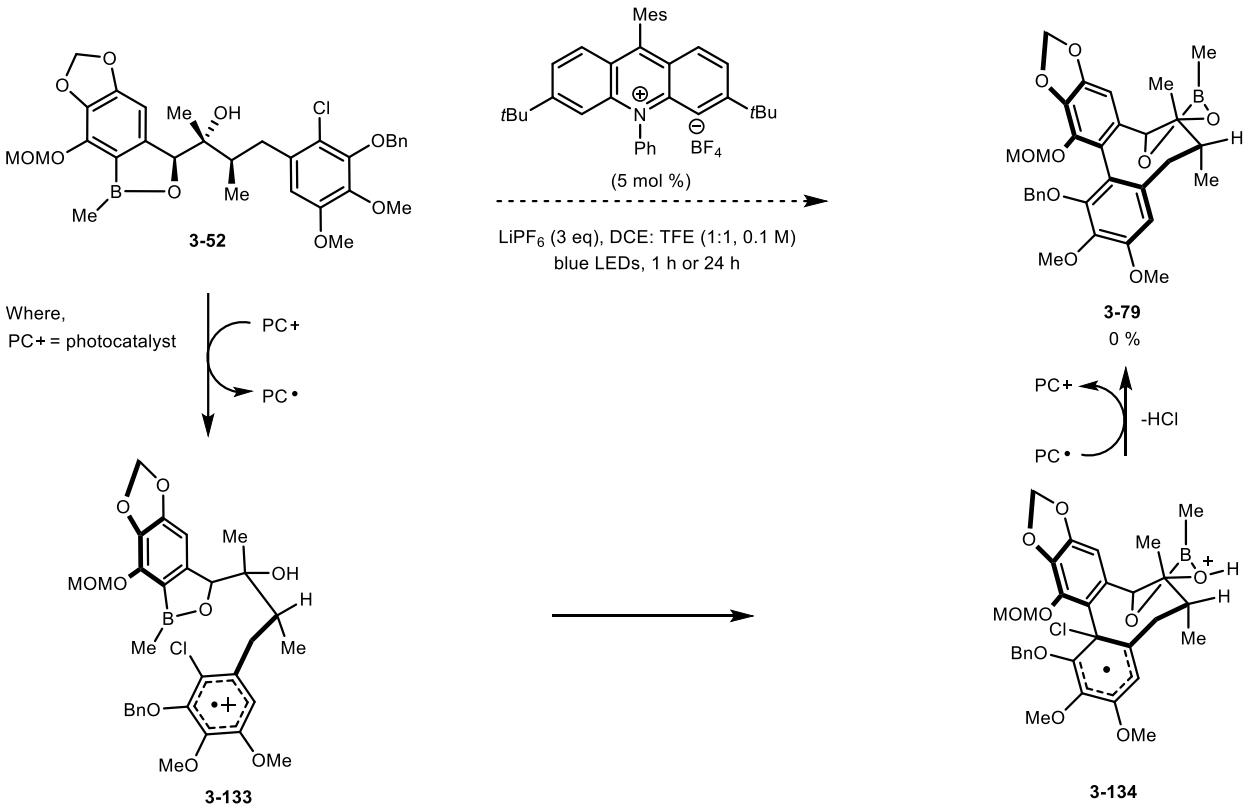
R= Bn: **3-75**
R=H: **3-76**

R= Bn: **3-77** or R= H: **3-78**

Entry	substrate	Catalyst	eq H_2O	Result
1	**3-75**	SPhos Pd G2	0.5	protodeborylation
2	**3-75**	$Pd(OAc)_2$	0.5	SM
3	**3-76**	SPhos Pd G2	0.5	protodeborylation
4	**3-76**	SPhos Pd G2	0	SM & protodeborylation

Reactions were run on 0.03 mmol-0.05 scale.

Table 3.24. Suzuki coupling attempts on alkene substrates **3-75** and **3-76**

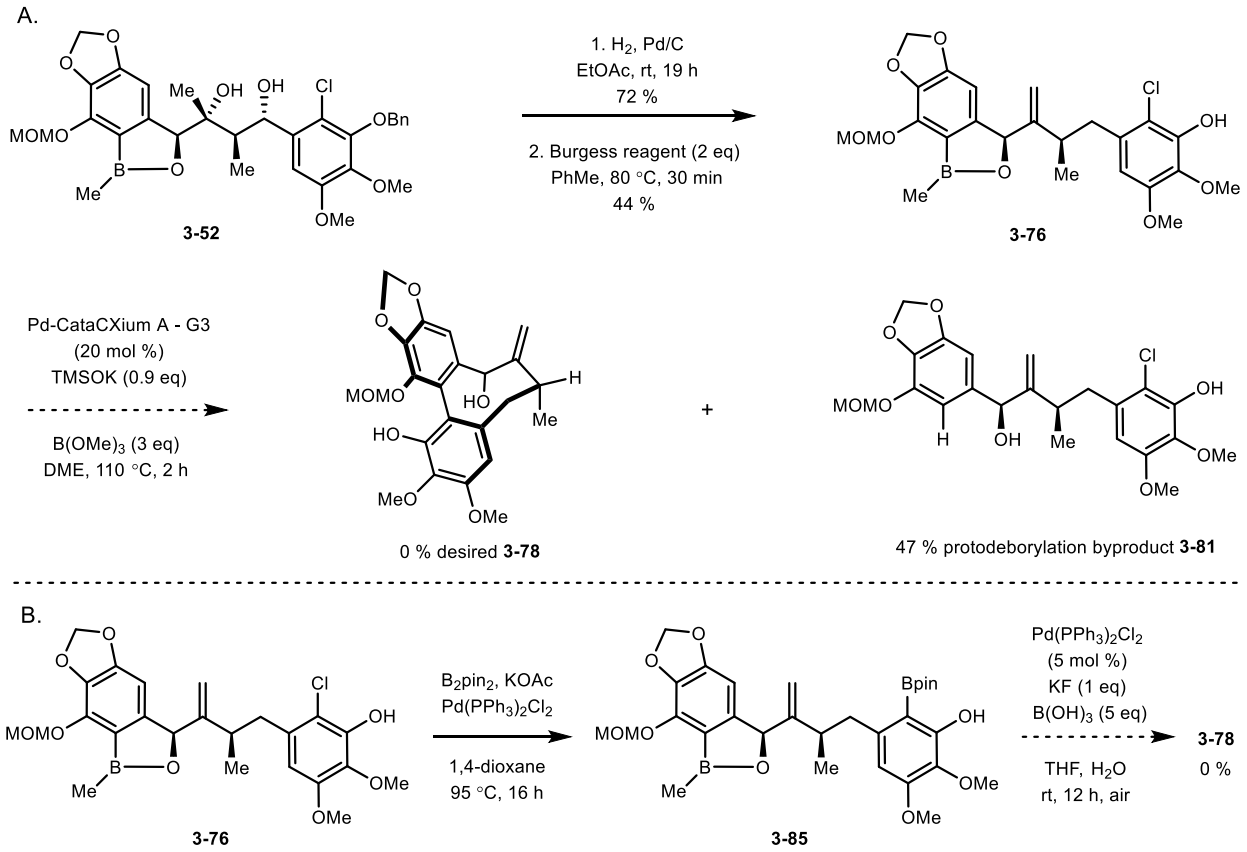


Scheme 3.31. Attempted biaryl formation via Sanford's photoredox catalyzed S_NAr conditions

Next, anhydrous Suzuki coupling conditions developed by Denmark and coworkers, designed to attenuate protodeborylation were explored (Scheme 3.32A).[31] The substrate **3-76** was prepared from **3-52** by hydrogenation with catalytic Pd/C in EtOAc (72 % yield), followed by Burgess

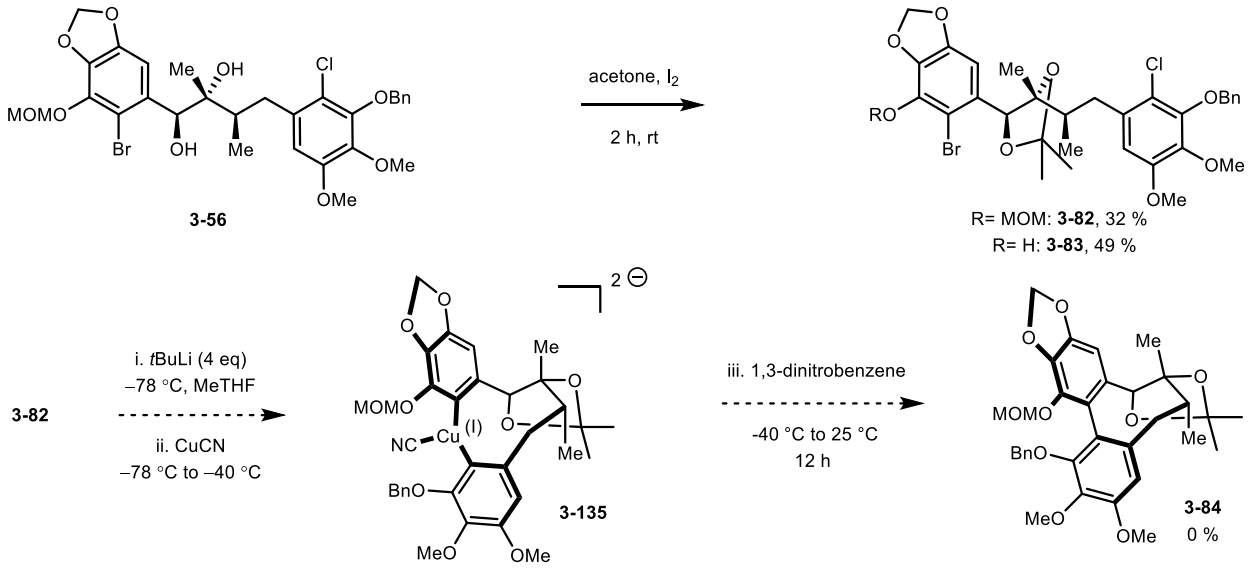
dehydration (44 % yield). **3-76** was subjected to the conditions consisting of the catalyst Pd-CataCXium A G3 (20 mol %), potassium trimethylsilanolate (TMSOK, 0.9 equiv.) and $B(OMe)_3$ (3 equiv.) in DME at 110 °C for 2 h. The reaction failed to produce biaryl **3-78** and instead gave the protodeborylation byproduct **3-81** in 47 % yield.

Methodology for the Pd-catalyzed intramolecular oxidative coupling of aryl boronic esters developed by Jasti and coworkers was studied next.[32] The boronic ester / borinic ester substrate **3-85** was prepared by Miyaura borylation of aryl chloride **3-76** using $Pd(PPh_3)_2Cl_2$ (10 mol%), bis(pinacolato)diboron (1.2 equiv.), and potassium acetate (4.3 equiv.) in 1,4-dioxane for 16 h at 95 °C (Scheme 3.32B). Upon subjecting **3-85** to the oxidative coupling conditions of $Pd(PPh_3)_2Cl_2$ (5 mol %), KF (1 equiv.) and $B(OH)_3$ (5 equiv.) in THF: water (10:1, 0.001 M) for 12 h at rt under air, the desired product **3-78** was not observed and starting material was recovered.



Scheme 3.32. Attempted formation of biaryl **3-78** via A) Denmark's anhydrous conditions or B) Jasti's oxidative coupling conditions

Coleman and coworkers' oxidative cuprate biaryl coupling methodology utilized in their syntheses of stage 2 DBCODs such as interiotherin A was explored next.[33] **3-56**, bearing aryl halides at C15 and C16, was selected as the starting material. The free alcohols of **3-56** had to be protected to be compatible with the oxidative coupling conditions, and this was done by tethering them together as an acetal. The acetalation was performed by treatment of **3-56** with acetone and iodine at rt for 2 h, resulting in 32 % yield of the desired **3-82** as well as 49 % of free phenol **3-83**, resulting from competitive deprotection of the MOM ether (Scheme 3.33). **3-82** was then subjected to Coleman's conditions of *t*-BuLi to give the diaryllithium, followed by transmetallation with CuCN to give an $Ar_2Cu(I)CN^{2-}$ (**3-135**), and then oxidation by 1,3-dinitrobenzene to give $Ar_2Cu(III)CN$ which would undergo reductive elimination, forming the biaryl bond as well as regenerating Cu(I)CN. Alas, decomposition occurred, with the desired biaryl product **3-84** not being formed.

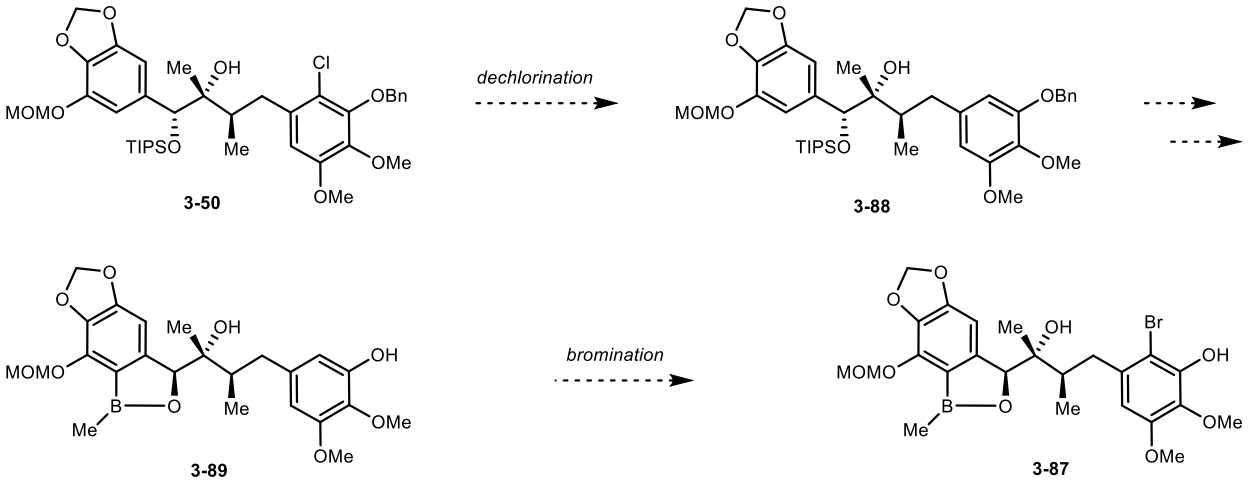


Scheme 3.33. Attempted biaryl formation via Coleman's oxidative cuprate coupling conditions

3.5. Strategy 3: non-brominated ketone + non-chlorinated aldehyde

The next modification to the Suzuki coupling was to employ an aryl bromide instead of an aryl chloride. Oxidative addition of Pd(0) into an aryl C-Cl bond was successful on substrates **3-76** and **3-119** (in Miyaura borylation and intermolecular Suzuki coupling, respectively), however the intramolecular Suzuki coupling poses a new challenge. The oxidative addition of Pd(0) into an aryl C-Br bond is faster than oxidative addition into an aryl C-Cl bond, therefore an aryl bromide substrate may stand a better chance of outcompeting hydrolysis of the borinic ester and reacting in

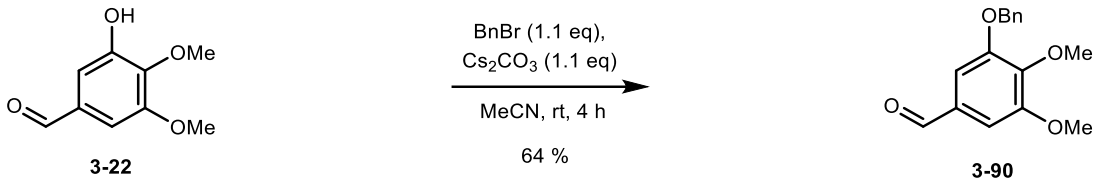
the intramolecular Suzuki coupling. To rapidly prepare the proposed aryl bromide substrate **3-87**, we sought to dechlorinate one of our existing intermediates **3-50** and brominate later at this same position (Scheme 3.34). The bromination would be performed after the formation of the borinic ester to avoid regioselectivity issues in the lithium-halogen exchange step. Three sets of dechlorination conditions were unsuccessfully applied to **3-50**. The first method, involving the use of zinc dust (5 equiv.), ammonium formate (10 equiv.), and sodium hydroxide (5 equiv.) in refluxing methanol,[10] returned only starting material. The second method employed the photocatalyst $[Ir(ppy)_2(dtbbpy)]PF_6$ (1 mol %), sodium 2-mercaptoethanesulfonate (mesna, 20 mol %), and sodium formate (5 equiv.) under blue light irradiation for 16 h at rt and also returned **3-50**.[34] The third method, utilizing Pd/C (20 mol %) and ammonium formate (30 equiv.) in H_2O/*i*PrOH/THF for 2 h at rt, led only to deprotection of the phenolic benzyl ether.[35] With the dechlorination of **3-50** unfeasible, the synthesis of **3-87** was instead started from scratch, using a non-chlorinated aldehyde in the initial aldol coupling.



Scheme 3.34. Attempted preparation of aryl bromide **3-87** via dechlorination of **3-50**

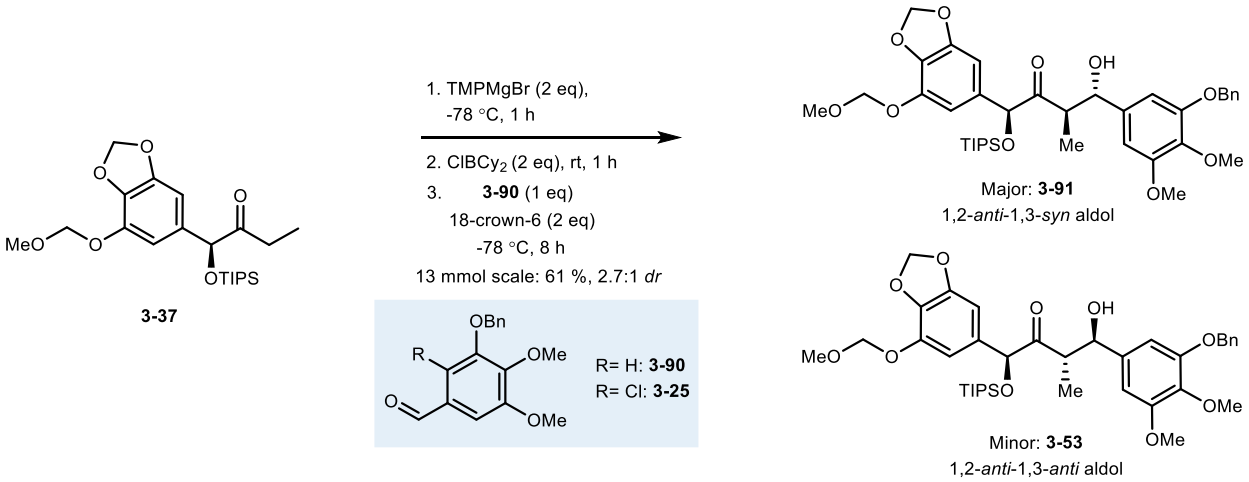
3.5.1. Aldol addition

The synthesis of the non-chlorinated aldehyde **3-90** was accomplished in one step from **3-22** (which was prepared from 5-bromovanillin in section 3.3.2). Treatment of phenol **3-22** with benzyl bromide (1.1 equiv.) and cesium carbonate (1.1 equiv.) in acetonitrile for 4 h at rt gave the benzyl ether-bearing product **3-90** in 64 % yield (Scheme 3.35).



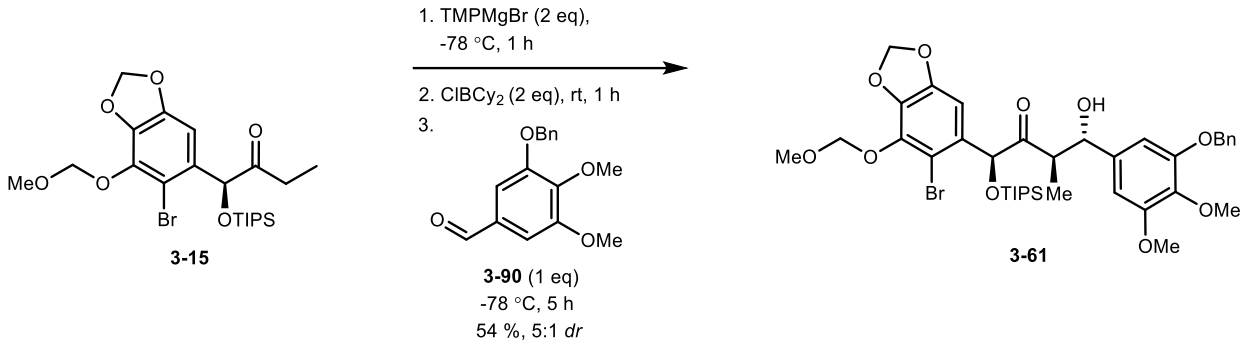
Scheme 3.35. Synthesis of the non-chlorinated aldehyde **3-90**

The aldehyde **3-90** was coupled to ketone **3-37** to provide aldol **3-91** (Scheme 3.36). At this point in the project, another graduate student, Derek Meng, was assisting with bringing more material through. He expected that the addition of 18-crown-6 to the standard aldol conditions developed in section 3.4.2. would be beneficial as it could bind the Mg^{2+} which was released into the reaction mixture during the transmetallation step. The chelation and retention of Mg^{2+} salts by 18-crown-6 could lead to better diastereoselectivity. In reality, the aldol reaction between **3-37** and **3-90** provided similar *dr* both with and without 18-crown-6 (~ 3:1 *dr* in both cases). The aldol addition of **3-37** and **3-90** was run on up to 13 mmol scale, employing treatment with TMPMgBr (2 equiv.) at −78 °C for 1 h, followed by the addition of $ClBCy_2$ (2 equiv.) which was let stir at rt for 1 h, followed by cooling to −78 °C, and then addition of 18-crown-6 (2 equiv.) and **3-90** (1 equiv.), which were let stir for at this temperature for 8 h to provide a 61 % yield of **3-91** in 2.7:1 *dr*. The major diastereomer was assigned as the desired 1,2-*anti*-1,3-*syn* aldol **3-91** and the minor diastereomer as the 1,2-*anti*-1,3-*anti* aldol **3-53**, which would also arise from the (*E*)-B-enolate. The yield of this reaction was slightly higher and the *dr* slightly lower than that observed using the analogous chlorinated aldehyde (**3-25**) on a similar scale (11 mmol, 53 % yield, 4:1 *dr*).



Scheme 3.36. Aldol addition of non-brominated ketone **3-37** and non-chlorinated aldehyde **3-90**

For comparison, the aldol addition of the brominated ketone **3-15** with the non-chlorinated aldehyde **3-90** proceeded with 54 % yield in 5:1 *dr* (Scheme 3.37). From the various combinations of aldol coupling partners employed in sections 3.3.3., 3.4.2., and here, it can be concluded that the presence or absence of halogen(s) on the aromatic ring(s) does not have a large impact on the yield and diastereoselectivity of the aldol reaction.

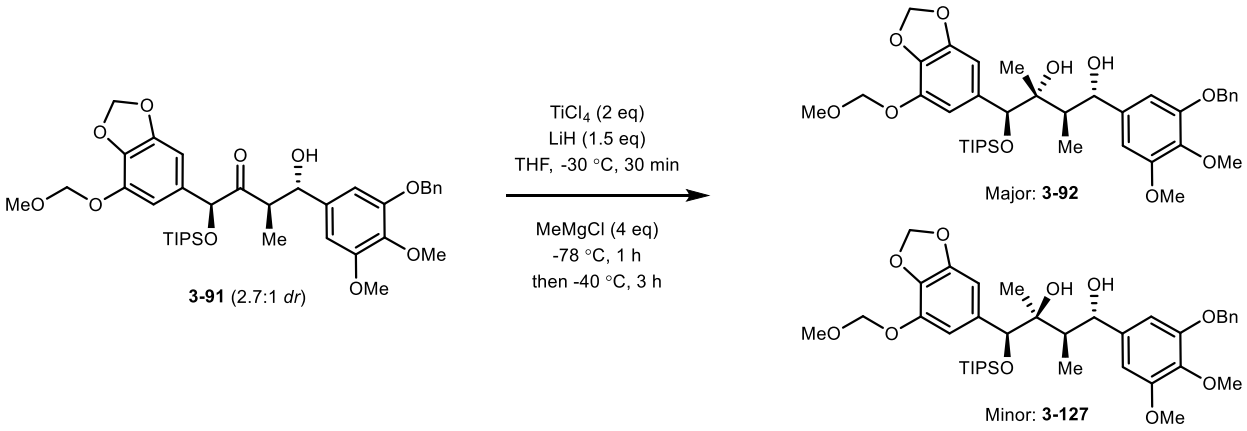


Scheme 3.37. Aldol addition of brominated ketone **3-15** and non-chlorinated aldehyde **3-90**

3.5.2. Chelate-controlled methyl addition

The chelate-controlled methyl addition on **3-91** was run using the conditions optimized in section 3.4.3., comprising of formation of the chelate with $TiCl_4$ (2 equiv.) and LiH (1.5 equiv.) at –30 °C for 30 minutes, followed by alkylation with MeMgCl (4 equiv.), keeping the temperature at –78 °C for 1 h before warming to –40 °C and allowing the reaction to continue for an additional 3 h. On 1.0 mmol scale, a *dr* of 1.7:1 was observed by ^{1}H NMR of the crude reaction mixture, from which **3-92** was isolated in 48 % yield, with a mixture of recovered **3-91** and the minor diastereomer **3-127** accounting for the mass balance (Table 3.25, entry 1). On 3.0 mmol scale, a similar diastereomeric ratio of 1.9:1 *dr* was observed, from which a 44 % yield of **3-92** was isolated (entry 2). Interestingly, better results were obtained with the largest reaction, on 9.0 mmol scale, which gave 2.5:1 *dr*, with isolation of a 64 % yield of **3-92** (entry 3). The yields and diastereoselectivities observed were lower than those observed using the chlorinated derivative **3-36** (see section 3.4.3). This is probably because aldol **3-91** was an oil which refused to undergo crystallization, therefore it likely contained more impurities than the crystalline aldol **3-36**. The $ClBCy_2$ impurities likely interfered with chelation of the β-hydroxy ketone to Ti(IV), thus decreasing the diastereoselectivity of the methyl addition. The stereochemistry of the desired diastereomer **3-92** was confirmed by treating the diol with methyl boronic acid to give the boronic

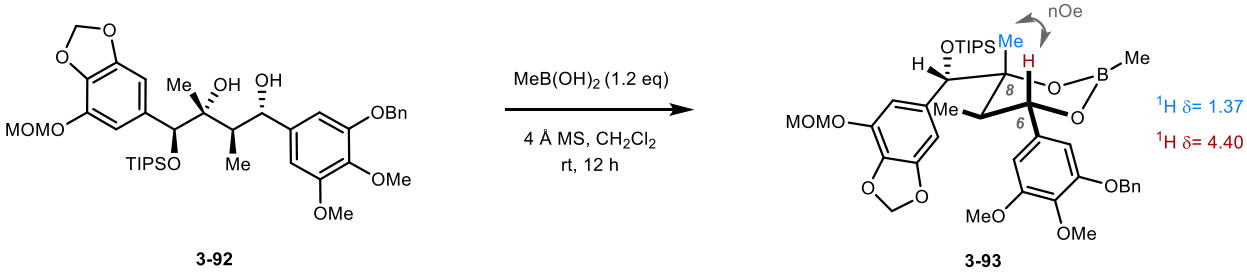
ester, on which an nOe experiment was run (Scheme 3.38). An nOe correlation was observed between the C8 methyl group (1.37 ppm) and the C6 hydrogen (4.40 ppm), indicating that they are on the same side of the molecule.



Entry	Scale (mmol)	*dr* of product (from crude NMR)	Yield of major diastereomer (%)
1	1.0	1.7:1	48
2	3.0	1.9:1	44
3	9.0	2.5:1	64

Yields are isolated yields.

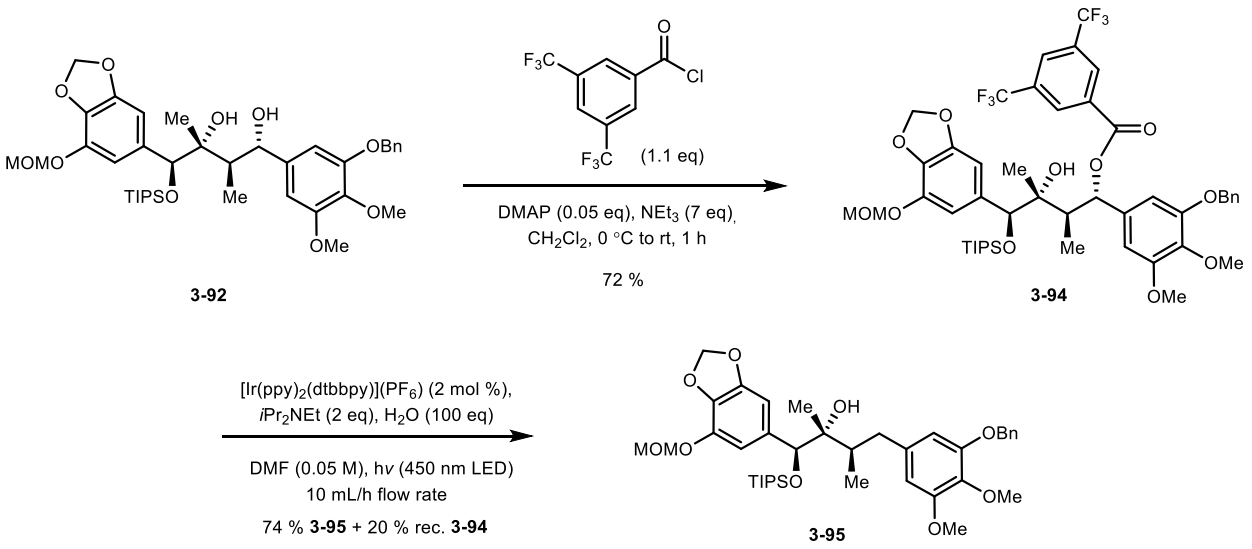
Table 3.25. Chelate-controlled methyl addition on the non-halogenated aldol **3-91**



Scheme 3.38. Confirmation of the diol stereochemistry of **3-92** via formation of the boronic ester and nOe

3.5.3. Benzylic deoxygenation

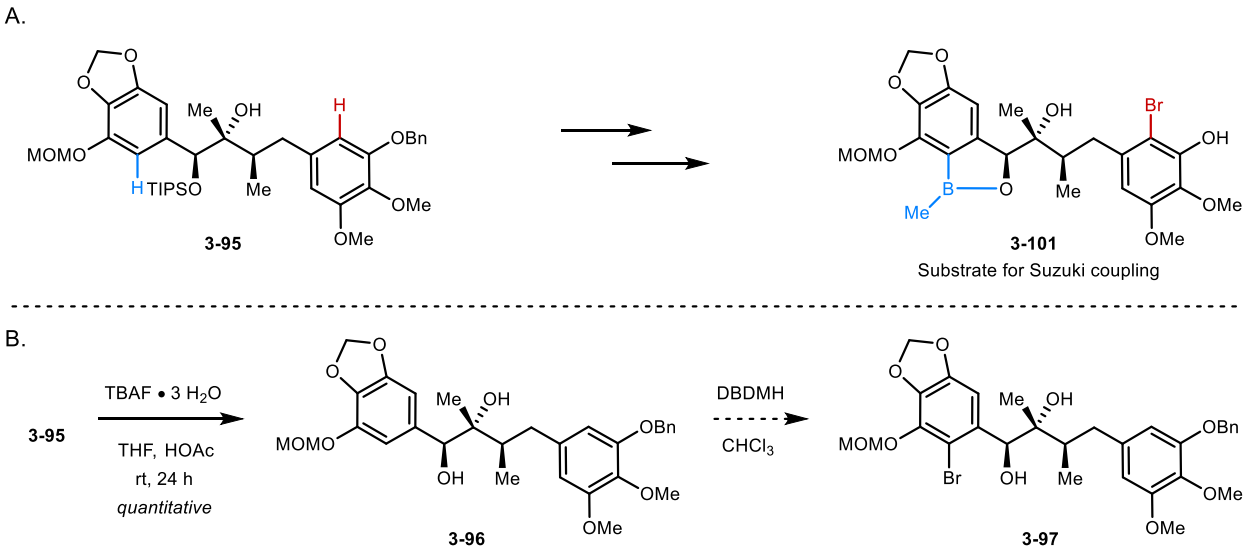
Diol **3-92** was esterified with 3,5-bis(trifluoromethyl)benzoyl chloride (1.1 equiv.), catalytic DMAP, and triethylamine (7 equiv.) in CH_2Cl_2 at rt for 1 h on 7.5 mmol scale to provide **3-94** in 72 % yield (Scheme 3.39). Ester **3-94** (5.4 mmol) was then subjected to the previously optimized deoxygenation conditions in flow from section 3.4.4, which led to the formation a 74 % yield of the deoxygenation product **3-95** as well as 20 % recovery of **3-94**.



Scheme 3.39. Benzylic esterification of **3-92** and deoxygenation

3.5.4. Functional group manipulations to prepare for Suzuki coupling

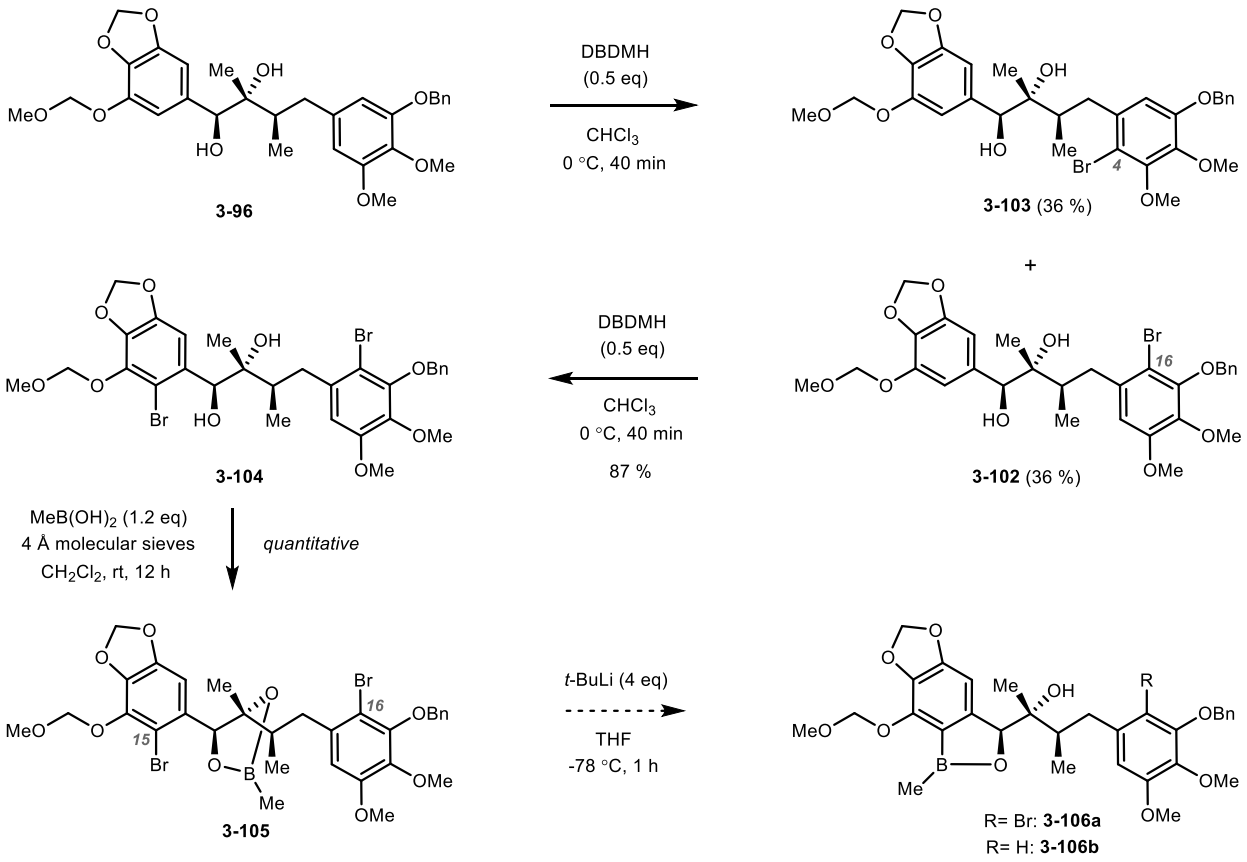
For the biaryl linkage to be formed via atroposelective Suzuki coupling, **3-95** needed to be functionalized with the appropriate aryl borinic ester and aryl bromide functional handles at C15 and C16 (Scheme 3.40A). In section 3.4.5, we showed that the bromination of **3-50**, possessing a phenolic MOM ether at C14, with DBDMH (0.5 equiv.) occurred with higher regioselectivity when the oxygen substituent at C9 was an alcohol rather than a silyl ether (substrate **3-50** vs.



Scheme 3.40. Functional group manipulation strategy 1

3-49). Therefore, we targeted benzylic alcohol **3-96** as a key intermediate in the transformation of **3-95** into **3-101**. The first step in preparing the substrate for Suzuki coupling from **3-95** was the deprotection of the silyl ether at C9 to provide free alcohol **3-96**, which was followed by bromination *ortho* to the phenolic MOM ether of **3-96** by treatment with DBDMH to provide **3-97** (Scheme 3.40B).

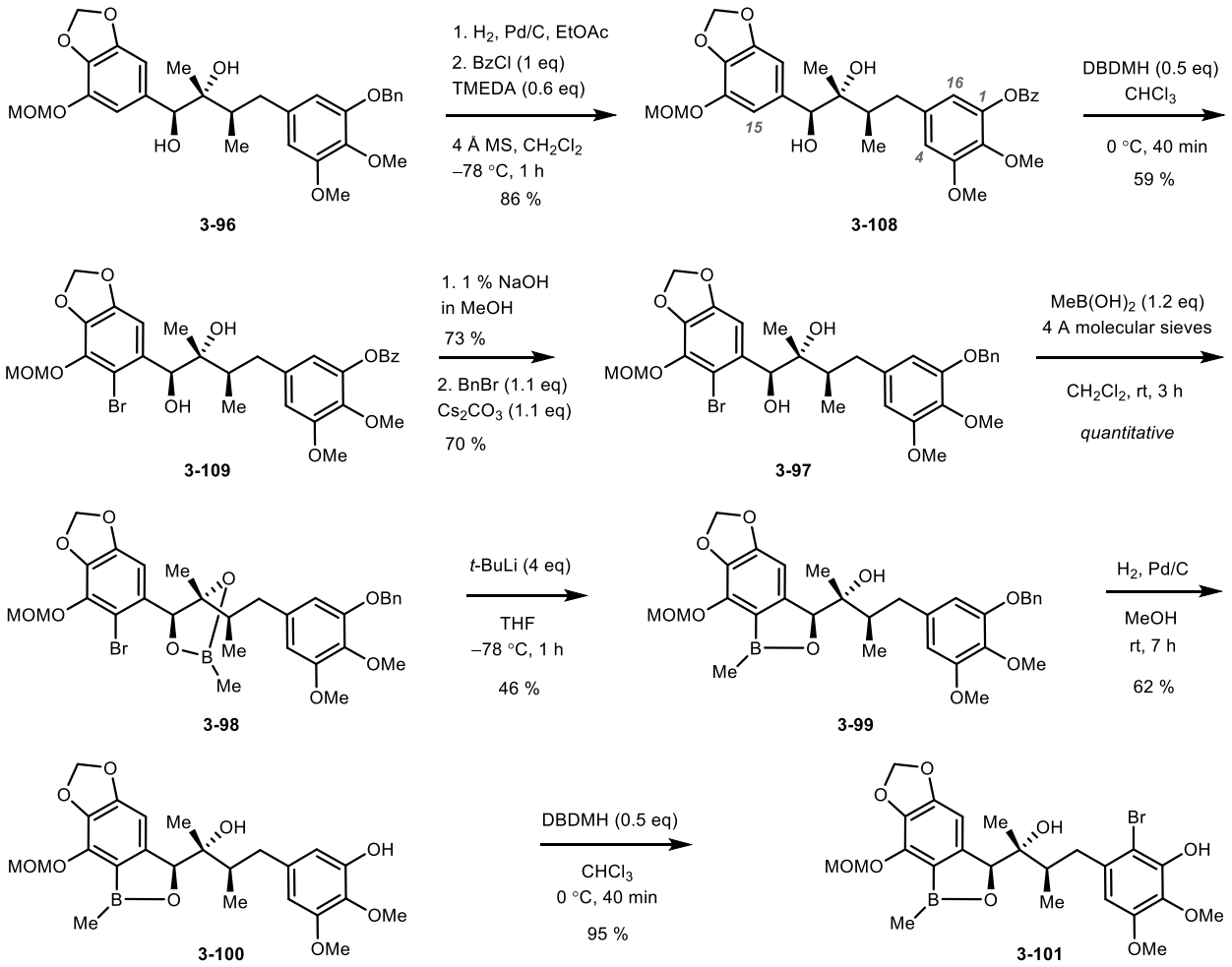
The silyl ether of **3-95** was deprotected on 4 mmol scale by treatment with TBAF•$3H_2O$ buffered with acetic acid in THF in quantitative yield, providing benzylic alcohol **3-96** (Scheme 3.40B). The bromination of **3-96** by treatment with DBDMH (0.5 equiv.) in $CHCl_3$ for 40 minutes at 0 °C did not proceed with the anticipated regioselectivity to give **3-97** (Scheme 3.40B), instead providing a mixture of two products where bromination had occurred on the ring bearing the OBn group in 36 % yield each (**3-103** and **3-102**, Scheme 3.41). As Br is required at C16 anyways later in the synthesis to serve as a handle for Suzuki coupling, an alternate strategy utilizing **3-102** was devised (Scheme 3.41). **3-102** was subjected to a second bromination with DBDMH (0.5 equiv.) to provide the dibrominated species **3-104** in 87 % yield. Conversion of the diol **3-104** to the boronic ester **3-105** proceeded in quantitative yield. **3-105** was then treated with *t*-BuLi (4 equiv.), anticipating higher regioselectivity for the formation of the desired 5-membered borinic ester **3-106a/b** arising from the attack of the C15 aryl lithium onto the boronic ester (as opposed to the 6-membered borinic ester that would be formed from the C16 aryl lithium). Upon subjecting **3-105** to these conditions, a complex mixture of products was formed. It appeared that both aryl-bromides were converted to the corresponding aryl-lithiums, as doubly protodebrominated starting material (13 %) as well as a doubly protodebrominated and deborylated species (28 %) were isolated. Neither of the expected products was obtained cleanly, although the mass of **3-106b** was detected by mass spectrometry in a small and impure column fraction (< 24 %). Considering the poor yield in the conversion of **3-96** to **3-102** along with the unselective and low yielding lithium-bromine exchange / cyclization step, this route did not seem suitable for providing sufficient material throughput for the total synthesis of kadsuraol C.



Scheme 3.41. Functional group manipulation strategy 2

A new plan for the preparation of the Suzuki coupling substrate **3-101** starting from **3-96** was then developed (Scheme 3.42). This plan hinged upon directing the bromination regioselectively to the desired C15 position by installing an electron withdrawing group (benzoyl) at the C1 phenol to disfavor bromination at C4 or C16. The benzoyl group was installed onto the phenol at C1 by first deprotecting the benzyl group of **3-96** via Pd-catalyzed hydrogenation in EtOAc, followed by treatment of the resulting free phenol with benzoyl chloride (1 equiv.), TMEDA (0.6 equiv.), and 4 Å molecular sieves in CH_2Cl_2 at −78 °C for 1 h to provide **3-108** in an 86 % yield over two steps. With the benzoyl group in place, the bromination of **3-108** with DBDMH (0.5 equiv.) proceeded regioselectively, providing the C15-brominated **3-109** in a 59 % yield. As the benzoyl ester would likely not be stable to treatment with *t*-BuLi, it was removed by treatment with NaOH (1% in MeOH) and the resulting phenol (73 % yield) was reprotected as the benzyl ether by treatment with benzyl chloride (1.1 equiv.) and cesium carbonate (1.1 equiv.), providing **3-97** in 70 % yield. Treatment of **3-97** with methylboronic acid gave boronic ester **3-98** quantitatively. Treatment of

3-98 with 2 equiv. *t*-BuLi was ineffective, but upon increasing to 4 equiv. *t*-BuLi, the borinic ester **3-99** could be obtained in up to 46 % yield. The benzyl ether of **3-99** was then removed via Pd-catalyzed hydrogenation in methanol to provide the free phenol **3-100** in 62 % yield. Treatment of **3-100** with DBDMH (0.5 equiv.) led to regioselective bromination *ortho* to the phenol, providing **3-101** in a 95 % yield.

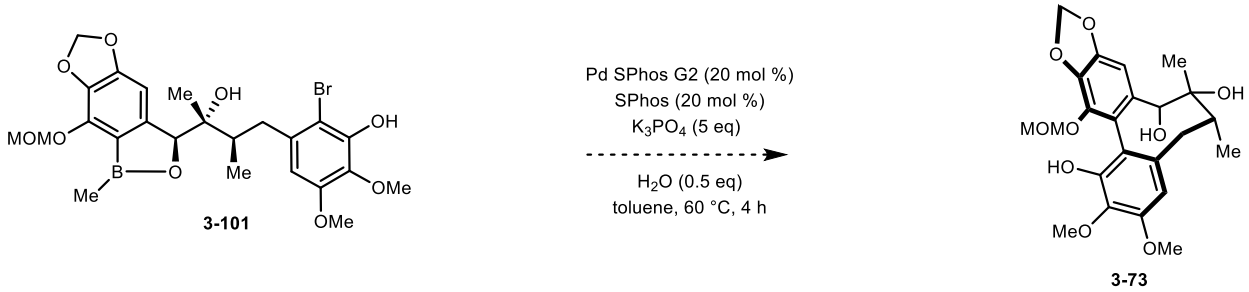


Scheme 3.42. Functional group manipulation strategy 3

3.5.5. Suzuki coupling

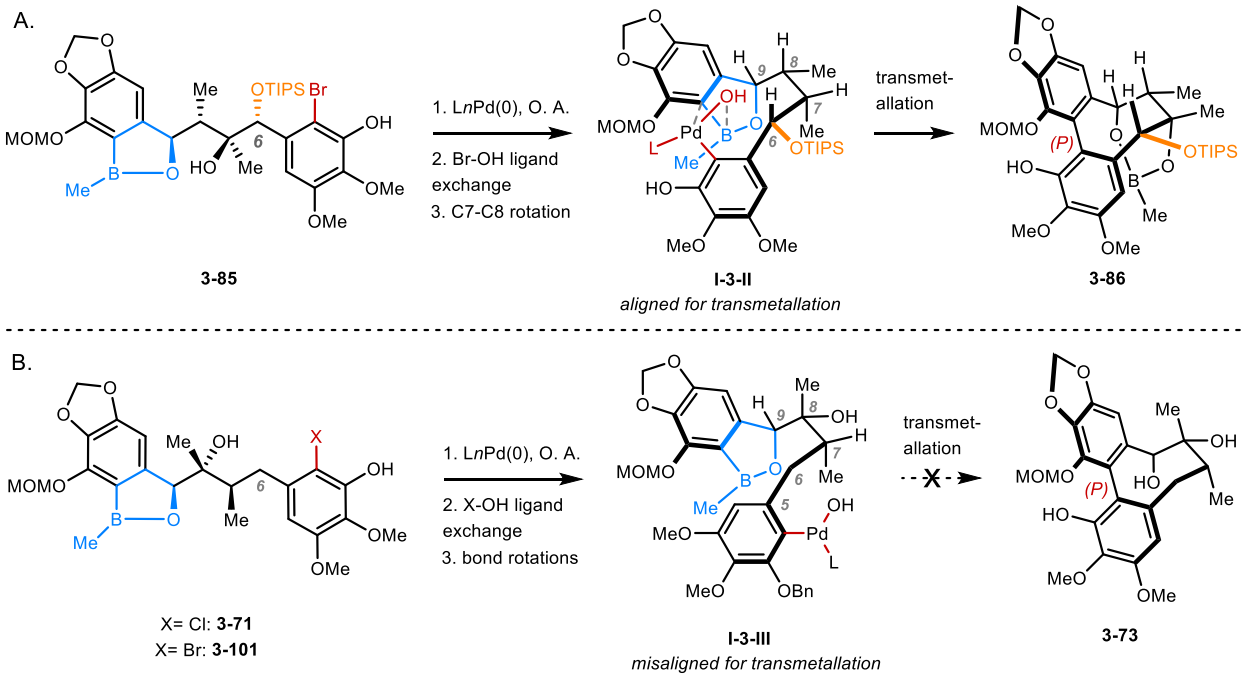
Substrate **3-101**, bearing a borinic ester at C15 and an aryl bromide at C16 was then subjected to our standard conditions for intramolecular Suzuki coupling, consisting of Pd SPhos G2 (20 mol %), SPhos (20 mol %), K_3PO_4 (5 equiv.), and H_2O (0.5 equiv.) in PhMe at 60 °C for 4 h (Scheme 3.43). The reaction yielded a complex mixture of products. Analysis by mass

spectrometry determined that the desired product **3-73** was not formed and that the major species still contained a Br atom (based on the significant M+2 peak). This result indicates that the aryl-bromide **3-101** was no better in Suzuki coupling than the analogous aryl-chloride substrate **3-71**.



Scheme 3.43. Attempted intramolecular Suzuki coupling of aryl bromide **3-101**

In section 3.4.6. and herein, the differences between a substrate which successfully underwent atroposelective Suzuki coupling in our group's previous synthesis of heteroclitin J (**3-85**, Scheme 3.44A) and the substrates used in the current work (**3-52**, **3-71**, **3-101**, **3-75**, and **3-76**), which did not undergo Suzuki coupling, were investigated. A free phenol at C1 allowed for oxidative addition to occur at the neighbouring C15, whereas a benzyl ether was found to block oxidative addition. The identity of the halide as a bromide or chloride had no effect on the reaction outcome nor did the elimination of the tertiary alcohol to a terminal alkene. We expect that the axial stereochemistry of the C7 and C8 methyl groups in the product is likely a factor contributing to the lack of reactivity. The main difference left unexplored between **3-85** and the current substrates was the identity of the C6 substituent. This is likely a contributing factor to why the Suzuki coupling has failed in the present case. Compound **3-85** bears a bulky OTIPS group at C6 which the aryl-Pd bond rotates away from in intermediate **I-3-II**, aligning it properly for transmetallation with the aryl-boron (Scheme 3.44A). The current substrate (**3-71** or **3-101**) bears a methylene at C6, which does not impose a rotational preference, and therefore, the aryl-Pd will preferentially point away from the bulky aryl-boron, making it misaligned for transmetallation (Scheme 3.44B). Therefore, it is proposed that the current Suzuki coupling is failing (at least in part) due to transmetallation not occurring.

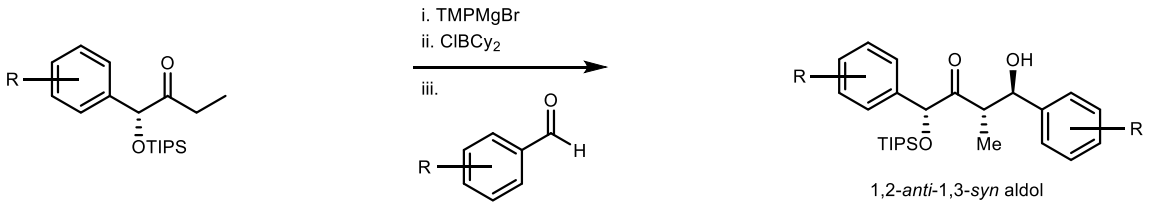


Scheme 3.44. Effect of the C6 substituent on transmetallation A) in our group's previous synthesis of heteroclitin J and B) in the current work

3.6. Analysis of aldol addition results

This section will take a closer look at the results of the aldol additions from sections 2.1.2, 2.2, 3.3.3, 3.4.2, and 3.5.1. During optimization studies, it was found that factors such the quantity of base (TMPMgBr) and lewis acid ($ClBCy_2$), as well as the reaction time with the aldehyde affected the yield and *dr* of the aldol additions. In general, equimolar quantities (1.2–2.0 equiv.) of TMPMgBr and $ClBCy_2$ led to the best diastereoselectivity. For reactions which gave low yields after 3 h reaction time with the aldehyde, the yield could be improved by increasing the reaction time to up to 8 h while maintaining comparable *dr*. Increasing the reaction time beyond 8 h led to higher yields but with some erosion of diasteroselectivity. The substrates also affected the outcome of the reaction, where a benzylic OTIPS group on the ketone fragment consistently led to better yield and *dr* than other α-siloxy groups. In Table 3.26, our aldol additions on various substrates are compiled for the elucidation of additional substrate effects. All the reactions were run using racemic ketones with the exception of entry 3, which utilized a chiral ketone (with 92.7% *ee*).

The best aldol addition results (77–79 % yield and 20:1 *dr*) were obtained in entries 1 and 3 with the use of a ketone bearing a 3,4,5-ether-substituted aromatic ring (**2-28** or **4-12**) and an aldehyde containing a benzodioxolane moiety (**2-10** or **4-15**). These two results were obtained by Dr. Zheng



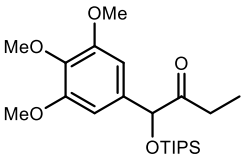
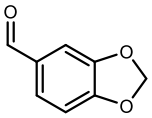
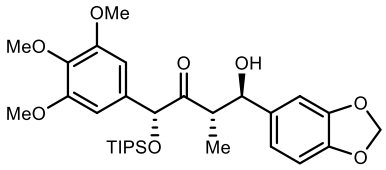
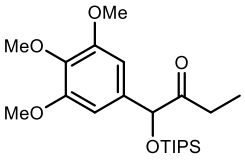
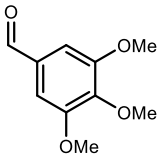
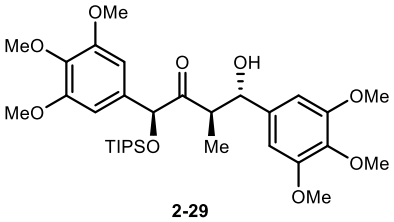
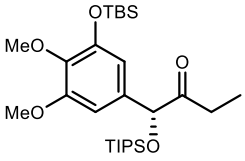
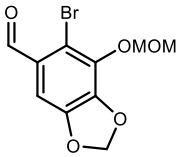
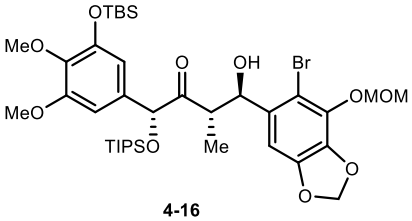
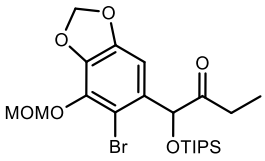
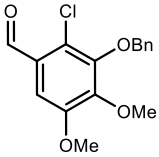
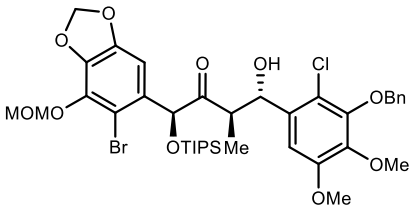
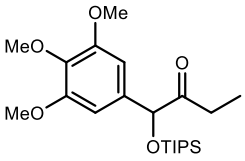
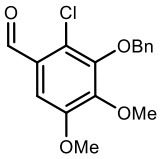
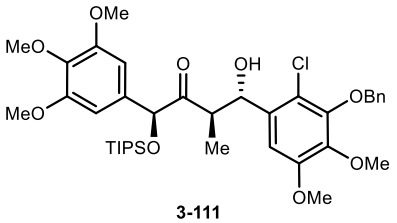
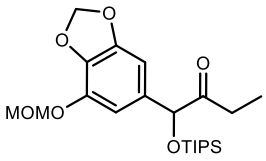
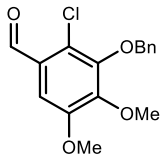
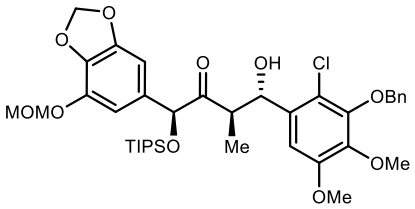
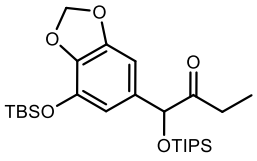
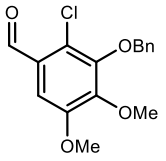
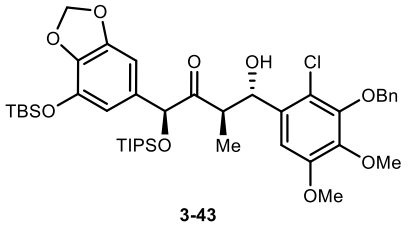
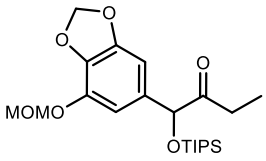
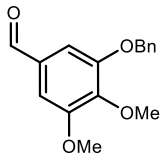
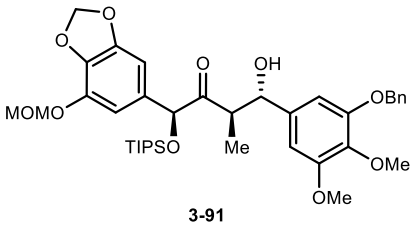
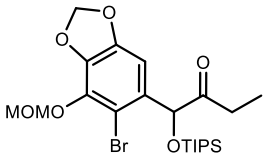
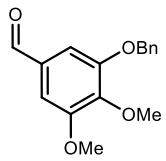
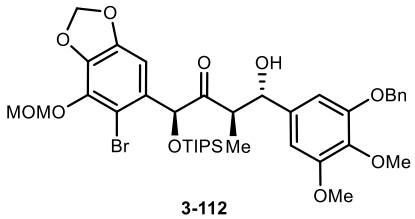
Entry	ketone	aldehyde	aldol	yield, *dr*
1*	 (±)-2-28	 2-10	 2-11-TIPS-b	77 % 20:1 *dr*
2	 (±)-2-28	 2-14	 2-29	56 % 16:1 *dr*
3*	 4-12	 4-15	 4-16	79 %, 20:1 *dr* (66 %, >99 % *ee* after recryst.)
4	 (±)-3-15	 3-25	 3-29	74 % 3.5:1 *dr*
5	 (±)-2-28	 3-25	 3-111	47 % 6.3:1 *dr*

Table 3.26. Summary of Lumb group aldol additions

Entry	ketone	aldehyde	aldol	yield, *dr*
6	 (±)-3-37	 3-25	 3-36	65 %, 3:1 dr (49 %, 16:1 *dr* after recryst.)
7	 (±)-3-41	 3-25	 3-43	58 % 3.9:1 *dr*
8	 (±)-3-37	 3-90	 3-91	61 % 2.7:1 *dr*
9	 (±)-3-15	 3-90	 3-112	54 % 5:1 *dr*

*= Entries 1 and 3 are results from the work of Dr. Zheng Huang. The remaining entries are my own results.

Table 3.26. Summary of Lumb group aldol additions (continued)

Huang, where I have reproduced entry 3 to give a 90 % yield of **4-16** in 20:1 *dr* (or 56 % yield after recrystallization). In entry 2, the use of trimethoxy aldehyde **2-14** instead of piperonal (**2-10**) in the aldol reaction with trimethoxy aryl ketone **2-28** led to a ~20 % drop in yield and a slight drop in diastereoselectivity (56 % yield, 16:1 *dr*). Effectively reversing the fragments, so that the ketone bears a benzodioxolane moiety (**3-15**) and the aldehyde bears a 3,4,5-ether-substituted aromatic ring (**3-25**, entry 4), gave aldol **3-29** in good yield (74 %) but with a significant decrease in diastereoselectivity (3.5:1 *dr*) compared to previous entries. Entry 5, employing the same aldehyde as in entry 4 (**3-25**) but with the trimethoxy aryl ketone **2-28** provided aldol in higher *dr*

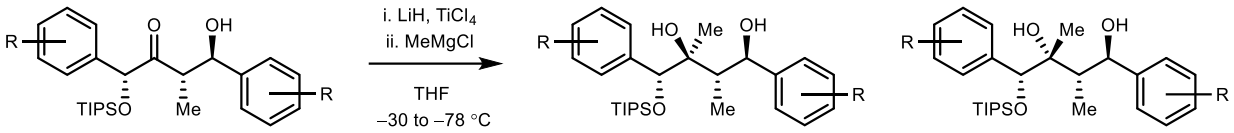
albeit lower yield (47 % yield of **3-111** in 6.3:1 *dr*). Entries 6 and 7 demonstrate that the identity of the phenolic protecting group on the ketone fragment (as either MOM or TBS) is inconsequential as these produced very similar results of 65 % yield, 3:1 *dr* and 58 % yield, 3.9:1 *dr*. The presence or absence of halides on either aromatic ring did not have a significant effect on the outcome of the aldol additions, where non-, mono-, and di-halogenated aldols could be produced in yields of 54–74 % and 2.7:1–5:1 *dr* (entries 4, 6, 8, 9). Analyzing the results of these reactions, diastereoselectivity typically decreases when a 3,4,5-ether-substituted aryl aldehyde is used rather than a benzodioxolane-bearing aldehyde, possibly due to the higher LUMO of the 3,4,5-ether-substituted aryl aldehyde leading to slightly poorer overlap well with the HOMO of the enolate and thus providing a less tight 6-membered transition state, leading to some competition from the open transition state. Ketones bearing a benzodioxolane provided aldol in lower *dr* than 3,4,5-ether-substituted aryl ketones, possibly due to the more inductively withdrawing nature of the benzodioxolane. This would lead to the corresponding enolate being less electron rich, and thus forming a less tight 6-membered transition state. Additionally, methoxy groups are better chelators of Mg^{2+} salts compared to a methylenedioxy group, which could increase the diastereoselectivity in the former case.

The benzodioxolane of **3-15** is more inductively withdrawing than the tri-methoxy arene of **2-28**, leading to a less electron-rich enolate, which could lead to a less tight 6-membered transition state, and therefore lower diastereoselectivity due to the presence of some open transition state.

3.7. Analysis of methyl addition results

This section will take a closer look at the results of the chelate-controlled methyl additions from sections 2.1.2, 2.3, 3.3.4, 3.4.3, and 3.5.2. All substrates were subjected to formation of the Ti(IV) chelate with $TiCl_4$ and LiH for 0.5–1 h followed by alkylation with MeMgCl at –78 °C, then warming to –40 °C for 2–3 h. In section 2.1.2, it was found by Dr. Zheng Huang that the identity of the α-siloxy group of the aldol influenced the outcome of the methyl addition. The order OTBDPS > OTIPS > OTBS was established, where OTBDPS-bearing aldols gave both higher yield and *dr* of methyl addition products. Despite this, OTIPS-bearing ketones performed better in the aldol addition, therefore these were selected for use in our total syntheses. In Table 3.27, our methyl additions on various α-OTIPS aldols are compiled to elucidate substrate effects.

Entries 1 and 3 are results that were obtained by Dr. Zheng Huang, where the remaining entries are my own results. Model systems **2-11-TIPS-b** and **2-29**, both originating from the trimethoxy aryl ketone **2-28**, gave comparable results, proceeding in ~5:1 *dr* with isolation of 50–63 % of the major diastereomer (entries 1 and 2). Substrate **4-16** underwent methyl addition with higher yield and diastereoselectivity than the model systems: 7:1 *dr*, 81 % yield of the major diastereomer **4-17** (entry 3). The result in entry 3 obtained by Dr. Zheng Huang was reproduced by me, with 9:1 *dr* being observed and isolation of 80 % **4-17**. The dihalogenated substrate **3-29** performed poorly in the methyl addition, giving 1:2 *dr* in favor of the 1,3-*anti* diol, with isolation of only 24 % of the desired 1,3-*syn* diol **3-34** (entry 4). The nonbrominated monochlorinated substrate **3-36** led to superior yield and diastereoselectivity (20:1 *dr*, 73 % yield of major diastereomer, entry 5). Replacement of the phenolic MOM ether with a TBS ether led to a drop in both yield and *dr* (3:1 *dr*, 43 % yield of major diastereomer, entry 6). The nonhalogenated substrate **3-91** gave the major methyl addition product **3-92** in fair yield albeit low *dr* (2.5:1 *dr*, 64 % yield). Analyzing the results of these reactions, aldols originating from sterically bulky ketones (eg. Br-bearing **3-29** and OTBS-bearing **3-43**) performed worse in the methyl addition, as the bulky substituents likely blocked the approach of $TiCl_4$ during the chelation step, leading to decreased yield and diastereoselectivity. Additionally, the purity of the aldol starting material appears to have affected the *dr* and yield of the product. If there was residual Cy_2BCl or its hydrolyzed form Cy_2BOH present, this would interfere with the chelation of the β-hydroxy ketone to $TiCl_4$, leading to lower *dr* and yield. Methyl addition to the purer crystalline aldol substrate **3-36** gave higher yield and *dr* than methyl additions to aldols which were oils (**3-43** and **3-91**).



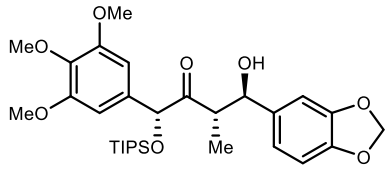
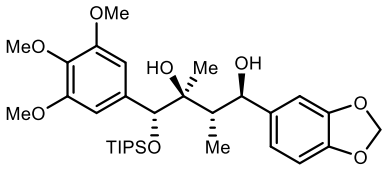
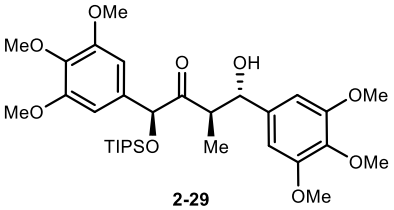
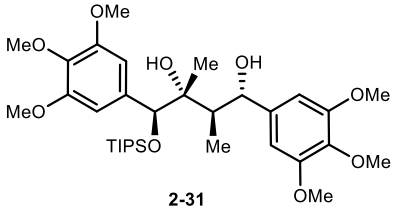
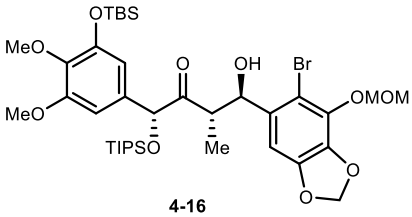
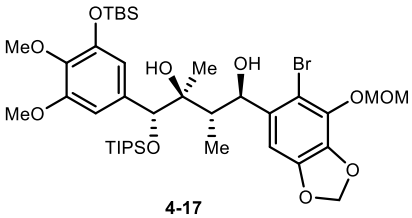
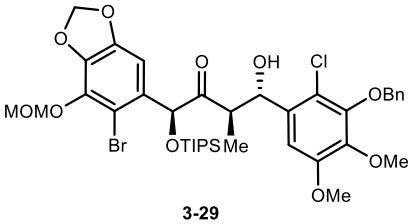
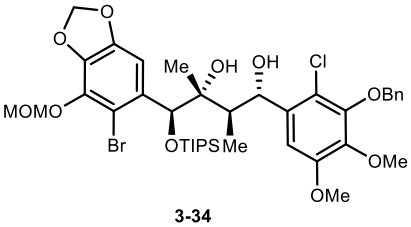
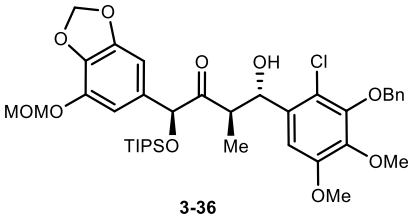
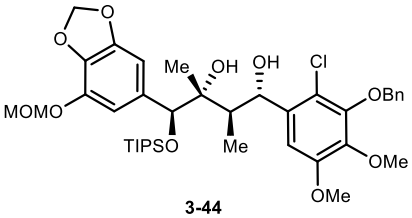
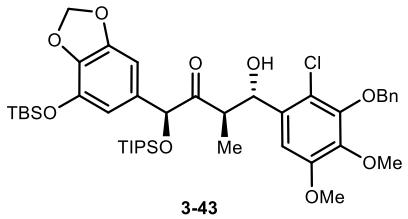
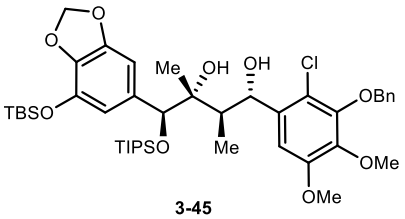
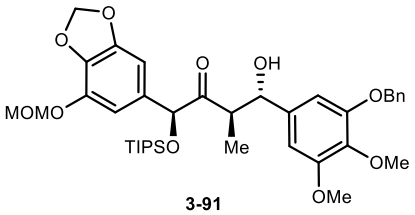
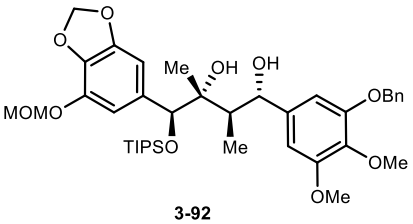
Entry	aldol (appearance)	product major diastereomer	*dr*	yield of major diastereomer
1*	 **2-11-TIPS-b** (appearance not reported)	 **2-12**	5.3:1	63 %
2	 **2-29** (oil)	 **2-31**	5:1	50 %
3*	 **4-16** (solid)	 **4-17**	7:1	81 %
4	 **3-29** (oil)	 **3-34**	1:2	24 %
5	 **3-36** (solid)	 **3-44**	20:1	73 %

Table 3.27. Summary of Lumb group methyl additions

Entry	aldol (appearance)	product major diastereomer	*dr*	yield of major diastereomer
6	 **3-43** (oil)	 **3-45**	3:1	43 %
7	 **3-91** (oil)	 **3-92**	2.5:1	64 %

*= Entries 1 and 3 are results from the work of Dr. Zheng Huang. The remaining entries are my own results.

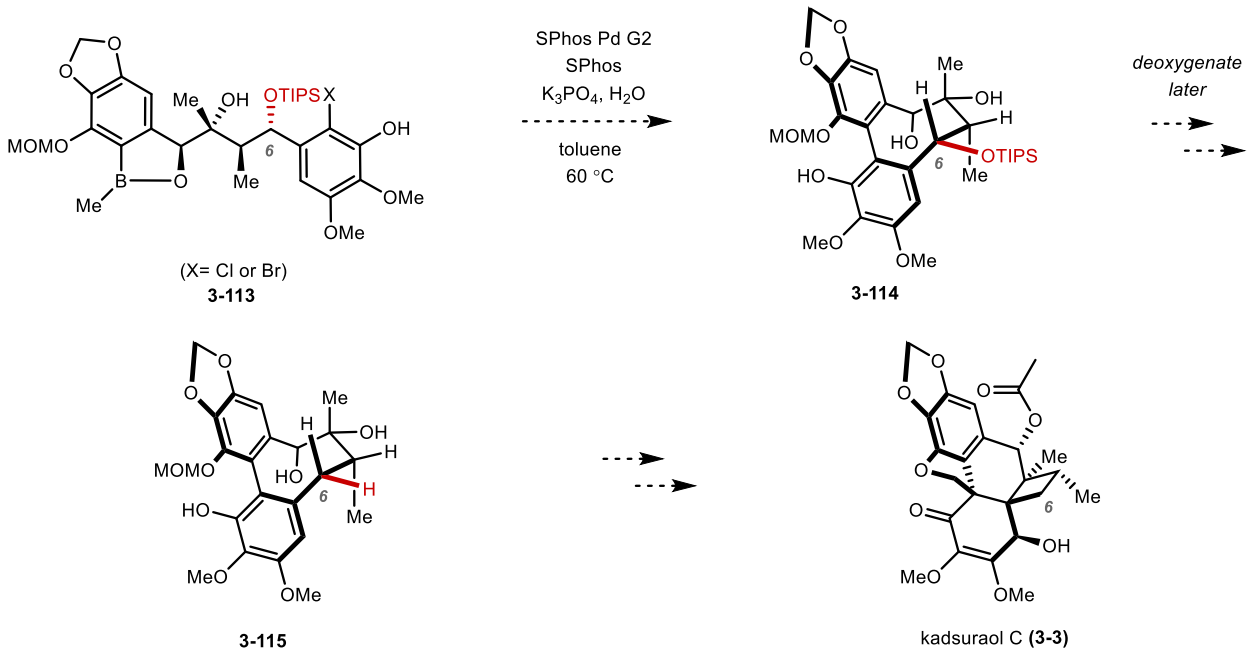
Table 3.27. Summary of Lumb group methyl additions (continued)

3.8. Conclusions and future directions

Linear precursors to kadsuraol C bearing stereocenters at C6–C9 were synthesized via the aldol addition of prefunctionalized aromatic ketone and aldehyde fragments. A benzylic OTIPS group on the ketone fragment provided the best yield and diastereoselectivity for the desired aldol product compared to other α-siloxy groups. The presence or absence of halides on either the ketone or aldehyde fragment did not have a significant impact on the aldol reaction outcome. The identity of the phenolic protecting group as MOM or TBS had little impact on the aldol addition, but MOM provided superior *dr* in the following methyl addition step. The chelate-controlled methyl addition was employed to set the fourth stereocenter of the linear precursor. This reaction worked best with aldol substrates derived from the non-brominated ketone fragment, providing yields between 48 and 96 % of the desired diastereomer of methyl addition product **3-92** or **3-44**, which were isolatable from the minor diastereomer and aldol starting material. The C6 hydroxyl group was necessary to direct the stereochemistry of the methyl addition step, but is not present in the final product, therefore a deoxygenation was performed at C6 in the next step. This benzylic deoxygenation was accomplished in high yield in batch (1 mmol, 83 %) and the reaction scale was increased in flow (6.7 mmol, 79 %). Subsequent functional group manipulations to append the required aryl halide and aryl borinic ester functional handles for Suzuki coupling were

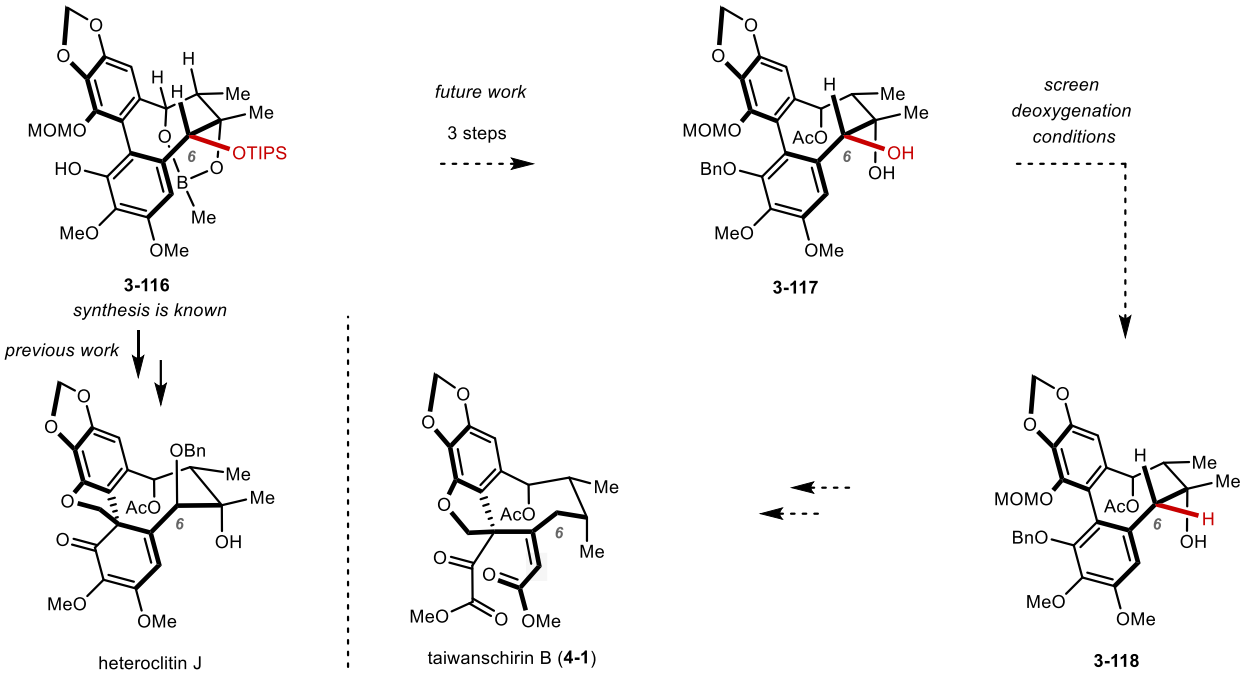
accomplished, including the development of a novel *ortho*-MOM / benzylic alcohol-directed bromination using DBDMH. Formation of the biaryl axis via atroposelective Suzuki coupling was attempted unsuccessfully. The substrate limitations of the Suzuki coupling were explored, and it was determined that the identity of the aryl halide (as either chloride or bromide) had little impact on reactivity. The effect of the stereochemistry of the C7 and C8 methyl groups was briefly investigated yet remains unclear. A determining factor for reactivity in the Suzuki coupling was found to be the presence of a bulky substituent at C6, such as OTIPS, which enables the intermediate to adopt a conformation which is properly aligned for transmetallation to occur. Without a bulky C6 substituent, the Suzuki coupling failed.

Therefore, the plan moving forward was to forgo the C6 deoxygenation after the methyl addition and to instead protect the C6 alcohol. This substrate would then be functionalized with the appropriate aryl halide and borinic ester handles to give **3-113**, which is expected to undergo Suzuki coupling more readily with a bulky C6 substituent in place, providing **3-114** (Scheme 3.45). The deprotection of the C6 silyl ether and deoxygenation would then be conducted at a later stage to afford **3-115**. We plan to utilize methodology for the C6 deoxygenation of a cyclic substrate in both the syntheses of kadsuraol C and taiwanschirin B. The methodology for the deoxygenation of the C6 position on a cyclic system would be developed on a substrate (**3-117**) as this could be



Scheme 3.45. Plan for Suzuki coupling with C6 OTIPS in place and late stage deoxygenation

prepared in 3 steps from an existing intermediate (**3-116**) in our lab from our group's previous synthesis of the DBCOD heteroclitin J[9] (Scheme 3.46). The product of the deoxygenation of **3-117** (**3-118**) would also serve as an intermediate in the synthesis of taiwanschirin B (which will be discussed in Chapter 4). Once the methodology for the C6 deoxygenation of a cyclic substrate was developed, this would also be applied to the synthesis of kadsuraol C.



Scheme 3.46. Testing C6 deoxygenation on a cyclic system

3.9. Experimental

3.9.1. Materials and methodologies

Chemicals and solvents were purchased from Sigma Aldrich, Strem Chemicals, Fisher Scientific, Combi-Blocks, or Oakwood Chemical, and used as received without further purification unless otherwise noted. Solvents were dried and purified using a PureSolv MD 7 (from Innovative Technology) or MB SPS 800 (from MBraun). Unless otherwise noted, solvent was degassed by sparging with N_2 for 5 min at rt prior to use. Amine bases were distilled over CaH_2 under N_2 (g).

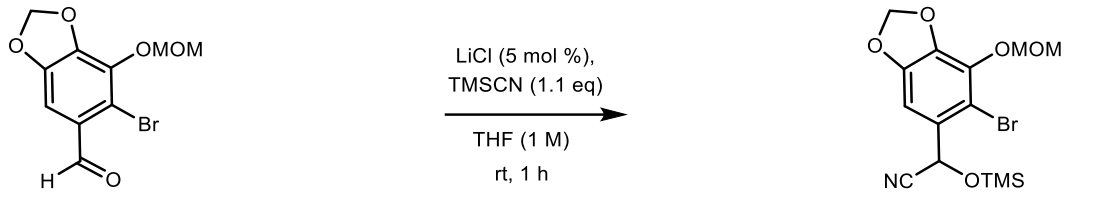
Proton nuclear magnetic resonance (^{1}H NMR) spectra were acquired using Bruker AVIIIHD 500 MHz, Varian Inova QUANUC 500 MHz, Varian VNMRS 500 MHz, or Varian Mercury 400 MHz spectrometers. Chemical shifts (δ) are reported in parts per million (ppm) and are calibrated to the

residual solvent peak. Coupling constants (*J*) are reported in Hz. Multiplicities are reported using the following abbreviations: s = singlet; d = doublet; t = triplet; q = quartet; dd = doublet of doublets; dt = doublet of triplets; dq = doublet of quartets; tt = triplet of triplets; qd = quartet of doublets; qq = quartet of quartets; ddd = doublet of doublet of doublets; ddt = doublet of doublet of triplets; dddd = doublet of doublet of doublet of doublets; ddq= doublet of doublet of quartets; br = broad; m = multiplet. Carbon nuclear magnetic resonance (^{13}C NMR) spectra were acquired using a Bruker AVIIIHD 126 MHz spectrometer.

High resolution mass spectra (HRMS) were recorded using a Bruker maXis Impact TOF mass spectrometer by electrospray ionization time of flight reflectron experiments. Fourier-transform infrared (FT-IR) spectra were recorded on a Bruker Alpha II FT-IR spectrometer. Optical rotations were recorded on a Jasco DIP-140 polarimeter (using the sodium D line; 589 nm). High performance liquid chromatography (HPLC) was measured on an Agilent 1100 HPLC system using a Chiralpak® IC analytical column (250 × 4.6 mm, 5 μm). Thin-layer chromatography was performed on pre-coated 250 mm layer thickness silica gel 60 F254 plates (EMD Chemicals Inc). Visualization was performed by ultraviolet light and/or by staining with potassium permanganate or *para*-anisaldehyde stain. Purifications by column chromatography were performed either using a Biotage Isolera™ One or standard column chromatography using silica gel (40-63 μm, 230-400 mesh). For the batch photoredox chemistry setup: 50 mL screw cap Schlenk flasks and a glass rod with a polished end were custom made my Cédric Ginart at Université de Montréal. A BOLA screw joint (no. D 590-16 or D 629-62) was used to attach the glass rod to the schlenk flask. A 455 nm LED was soldered onto a board, mounted on a heat sink (built by Richard Rossi and Weihua Wang at McGill University) and connected to a constant current power supply (Newark Electronics, Catalogue #: 82Y0614). This was placed on top of the glass rod to irradiate the reaction mixture from above. For the flow photoredox chemistry setup: the blue LED light strip (Product Code: CL-FRS5050WPDD-5M-12V-BL) and the 12V, 25W power supply (Product Code: CL-PS94670-25W) were purchased from Creative Lighting Solutions. The LED strip was cut into 2 meters pieces and coiled inside of a 125 × 65 crystallization dish wrapped with aluminum foil. 1/32” ID FEP tubing (approximately 2-3 m in length) was coiled around a 400 mL beaker and placed inside the crystallization dish. One end of the tubing was inserted through a septum into a receiving flask and the other end was connected to a syringe pump.

3.9.2. Preparative procedures for compounds 3-11 to 3-112

Compound 3-11



4-15
Chemical Formula: $C_{10}H_9BrO_5$
Molecular Weight: 289.0810

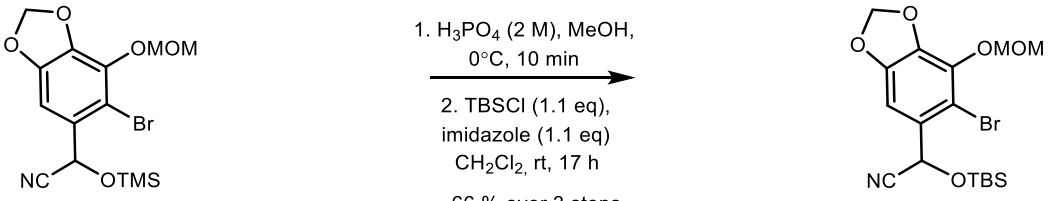
3-11
Chemical Formula: $C_{14}H_{18}BrNO_5Si$
Molecular Weight: 388.2890

Procedure:

The preparation of **4-15** from 5-hydroxypiperonal is described in Experimental Section 4.7.2. A flame-dried 25 mL round-bottom flask equipped with Teflon-coated stir bar and a rubber septum was charged with **4-15** (2.61 mmol, 753 mg, 1.0 equiv.) and LiCl (0.13 mmol, 5.5 mg, 0.05 equiv.). The flask was evacuated and refilled with N_2 (repeated 3 times), prior to the addition of THF (3.7 mL). Then, trimethylsilyl cyanide (2.87 mmol, 0.36 mL, 1.1 equiv.) was added via syringe. The reaction mixture was stirred at room temperature for 1 hour. Hexanes (13 mL) was added to the mixture, which was then filtered through silica, washing with hexanes/ethyl acetate (3:1, 26 mL). The filtrate was collected and concentrated *in vacuo*. The crude **3-11** was subjected directly to the next step.

Characterization: $\mathbf{R_f}$ = (hexanes/EtOAc 5:1): 0.30; **IR** (neat) v = 3395, 2909, 1681, 1606, 1474, 1388, 1283, 1158, 1025, 921 cm^{-1}; **^{1}H NMR** (500 MHz, $CDCl_3$) δ 7.00 (s, 1H), 6.02 (2 x d, *J*= 1.5 Hz, 2H), 5.73 (s, 1H), 5.31 (d, *J*= 0.7 Hz, 2H), 3.58 (s, 3H), 0.24 (s, 9H); **^{13}C NMR** (126 MHz, $CDCl_3$) δ 149.1, 138.9, 136.9, 129.9, 118.4, 107.9, 103.5, 102.2, 97.1, 63.4, 57.7, 0.0.

Compound 3-12



3-11
Chemical Formula: $C_{14}H_{18}BrNO_5Si$
Molecular Weight: 388.2890

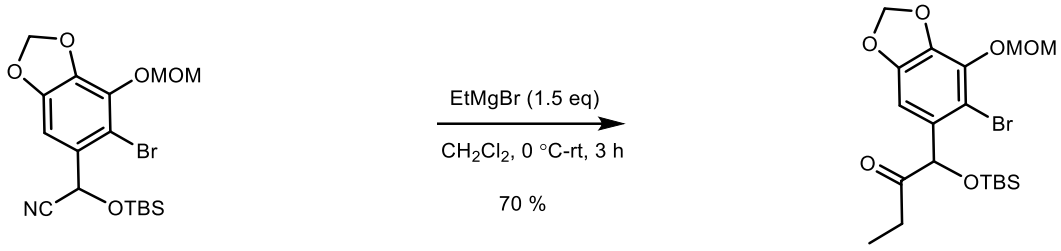
3-12
Chemical Formula: $C_{17}H_{24}BrNO_5Si$
Molecular Weight: 430.3700

Procedure:

A 25 mL round bottom flask equipped with a Teflon-coated stir bar and a rubber septum was charged with crude **3-11** (2.61 mmol, 1.0 equiv.). Methanol (5.2 mL) was added, and the crude **3-11** was dissolved. The resulting solution was cooled to 0 °C and then H_3PO_4 (2.61 mmol, 2 M aq., 1.3 mL, 1.0 equiv.) was added. The reaction mixture was stirred at room temperature for 10 minutes and then concentrated *in vacuo*. Water (6.5 mL) and CH_2Cl_2 (6.5 mL) were added and extracted. The aqueous layer was washed with CH_2Cl_2 (2 x 6.5 mL). The combined organic layers were dried, filtered, and concentrated *in vacuo*. The resulting residue was taken up in CH_2Cl_2 (5.2 mL), along with *tert*-butyldimethylsilyl chloride (2.87 mmol, 433 mg, 1.1 equiv.) and imidazole (2.87 mmol, 198 mg, 1.1 equiv.), then let stir at room temperature for 17 h. HCl (1 M aq., 5.2 mL), water (7.8 mL), and CH_2Cl_2 (8 mL) were added to the reaction mixture. The layers were separated, and the aqueous layer was extracted with CH_2Cl_2 (3 x 4 mL). The combined organic layers were dried, filtered, and concentrated *in vacuo*. The crude product was purified on silica gel (in 1:5 ethyl acetate: hexanes) to provide **3-12** (379 mg, 0.88 mmol, 66 % over 3 steps).

Characterization: $\mathbf{R_f}$ = (hexanes/EtOAc 5:1): 0.27; **^{1}H NMR** (500 MHz, $CDCl_3$) δ 6.97 (s, 1H), 6.00 (d, *J*= 6.4 Hz, 2H), 5.72 (s, 1H), 5.29 (s, 2H), 3.55 (s, 3H), 0.93 (s, 9H), 0.24 (s, 3H), 0.15 (s, 3H).

Compound 3-13



3-12
Chemical Formula: $C_{17}H_{24}BrNO_5Si$
Molecular Weight: 430.3700

3-13
Chemical Formula: $C_{19}H_{29}BrO_6Si$
Molecular Weight: 461.4240

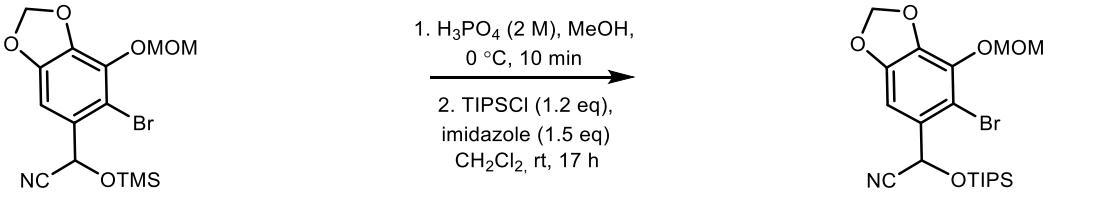
Procedure:

A flame-dried 25 mL round-bottom flask equipped with a Teflon-coated stir bar and a rubber septum was charged with **3-12** (0.90 mmol, 388 mg, 1.0 equiv.). The flask was evacuated and refilled with N_2 (repeated 3 times), prior to the addition of CH_2Cl_2 (2 mL). The solution was cooled

to 0 °C and ethyl magnesium bromide (1.35 mmol, 3 M in diethyl ether, 0.45 mL, 1.5 equiv.) was slowly added via syringe. The reaction mixture was stirred at room temperature for 3 h. It was then cooled to 0 °C, followed by the addition of water (3 mL) and HCl (1 M aq., 3 mL), and let stir an additional 30 minutes. The reaction mixture was extracted with CH_2Cl_2 (3 x 5 mL). The combined organic layers were dried over Na_2SO_4, filtered, and concentrated *in vacuo*. The crude product was purified on silica gel (in 2 % to 22 % ethyl acetate in hexanes) to provide **3-13** (292 mg, 0.63 mmol, 70 %).

Characterization: $\mathbf{R_f}$ = (hexanes/EtOAc 8:1): 0.28; **IR** (neat) v = 2954, 2930, 2897, 2857, 1722, 1608, 1470, 1387, 1257, 1160, 1099, 1059, 1028, 919, 838, 779 cm^{-1}; **^{1}H NMR** (500 MHz, $CDCl_3$) δ 6.77 (s, 1H), 6.00 (d, *J*= 1.4 Hz, 1H), 5.97 (d, *J*= 1.5 Hz, 1H), 5.47 (s, 1H), 5.30 (d, *J*= 6.0 Hz, 1H), 5.28 (d, *J*= 6.0 Hz, 1H), 3.58 (s, 3H), 2.50 (dq, *J*= 2.8 Hz, 7.3 Hz, 2H), 0.91 (s, 9H), 0.10 (s, 3H), -0.03 (s, 3H); **^{13}C NMR** (126 MHz, $CDCl_3$) δ 208.5, 148.7, 138.1, 136.6, 133.6, 108.8, 103.4, 101.9, 97.0, 79.0, 57.4, 30.8, 25.7, 22.6, 18.1, 14.1, 7.5, -4.8, -5.0; **HRMS**: Calcd. for $C_{19}H_{29}BO_6Si$ $[M+Na]^+$ = 483.0809 m/z, found $[M+Na]^+$ = 483.0792 m/z.

Compound 3-14



3-11
Chemical Formula: $C_{14}H_{18}BrNO_5Si$
Molecular Weight: 388.2890

3-14
Chemical Formula: $C_{20}H_{30}BrNO_5Si$
Molecular Weight: 472.4510

Procedure: A 250 mL round bottom flask equipped with a Teflon-coated stir bar and a rubber septum was charged with crude **3-11** (20 mmol, 7.76 g, 1.0 equiv.). Methanol (40 mL) was added and the crude **3-11** was dissolved. The resulting solution was cooled to 0 °C and then H_3PO_4 (20 mmol, 2 M aq., 10 mL, 1.0 equiv.) was added. The reaction mixture was stirred at room temperature for 10 minutes and then concentrated *in vacuo*. Water (50 mL) and CH_2Cl_2 (50 mL) were added and then extracted. The aqueous layer was washed with CH_2Cl_2 (2 x 50 mL). The combined organic layers were dried, filtered, and concentrated *in vacuo*. The resulting residue was taken up in CH_2Cl_2 (40 mL), along with triisopropylsilyl chloride (24 mmol, 5.14 mL, 1.2 equiv.) and imidazole (30 mmol, 2.04 g, 1.5 equiv.) and let stir at room temperature for 17 h. *N,N*-

dimethylaminoethanol (8 mmol, 0.8 mL, 0.4 equiv.) was added and let stir another 1 h. HCl (1 M aq., 40 mL), water (60 mL), and CH_2Cl_2 (60 mL) were then added. The layers were separated and the aqueous layer was extracted with CH_2Cl_2 (3 x 30 mL). The combined organic layers were dried, filtered, and concentrated *in vacuo*. The crude product was purified on silica gel (in 5 % to 15 % ethyl acetate in hexanes) to provide **3-14** (7.47 g, 15.8 mmol, 79 % over 3 steps) as a yellow solid.

Characterization: $\mathbf{R_f}$ = (hexanes/EtOAc 10:1): 0.37; **^{1}H NMR** (500 MHz, $CDCl_3$) δ 7.02 (s, 1H), 6.04 (d, *J*= 1.3 Hz, 1H), 6.02 (d, *J*= 1.3 Hz, 1H), 5.83 (s, 1H), 5.33 (d, *J*= 6.0 Hz, 1H), 5.31 (d, *J*= 6.0 Hz, 1H), 3.57 (s, 3H), 1.27-1.04 (m, 21H).

Compound 3-15



3-14
Chemical Formula: $C_{20}H_{30}BrNO_5Si$
Molecular Weight: 472.4510

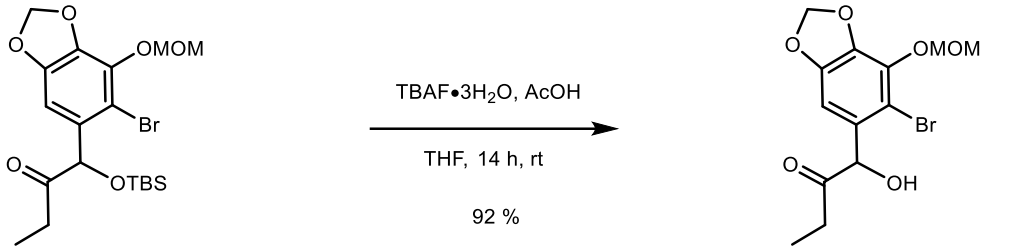
3-15
Chemical Formula: $C_{22}H_{35}BrO_6Si$
Molecular Weight: 503.5050

Procedure: A flame-dried 100 mL round-bottom flask equipped with a Teflon-coated stir bar and a rubber septum was charged with **3-14** (20 mmol, 1.0 equiv.). The flask was evacuated and refilled with N_2 (repeated 3 times), prior to the addition of CH_2Cl_2 (40 mL). The resulting solution was cooled to 0 °C and ethyl magnesium bromide (30 mmol, 3 M in diethyl ether, 10 mL, 1.5 equiv.) was slowly added via syringe. The reaction mixture was let stir at room temperature for 3 h. The reaction mixture was then cooled to 0 °C, added HCl (2 M aq., 90 mL), and let stir at rt for an additional 30 minutes. It was then extracted with CH_2Cl_2 (3 x 60 mL). The combined organic layers were dried over Na_2SO_4, filtered, and concentrated *in vacuo*. The crude product was purified on silica gel (in 9:1 hexanes: ethyl acetate) to provide **3-15** (3.86 g, 7.66 mmol, 47 % over 4 steps).

Characterization: $\mathbf{R_f}$ = (hexanes/EtOAc 9:1): 0.35 ; **IR** (neat) v = 2942, 2866, 1720, 1608, 1468, 1385, 1275, 1159, 1099, 1059, 1027, 918, 881, 854, 683 cm^{-1}; **^{1}H NMR** (500 MHz, $CDCl_3$) δ 6.89 (s, 1H), 6.01 (d, *J*= 1.5 Hz, 1H), 5.98 (d, *J*= 1.4 Hz, 1H), 5.61 (s, 1H), 5.30 (d, *J*= 6.0 Hz, 1H), 5.28 (d, *J*= 6.0 Hz, 1H), 3.57 (s, 3H), 2.58 (dq, *J*= 7.3 Hz, 18.4 Hz, 1H), 2.44 (dq, *J*= 7.4, 18.4 Hz,

1H), 1.11 (m, 3H), 1.00 (m, 21H) ; **^{13}C NMR** (126 MHz, $CDCl_3$) δ 208.2, 148.9, 138.4, 136.7, 134.0, 109.2, 103.4, 102.2, 97.0, 79.3, 57.9, 29.9, 17.8, 17.7, 12.1, 7.7; **HRMS**: Calcd. for $C_{22}H_{35}BrO_6Si$ $[M+Na]^+$ = 525.1284 m/z, found $[M+Na]^+$ = 525.1279 m/z.

Compound 3-16



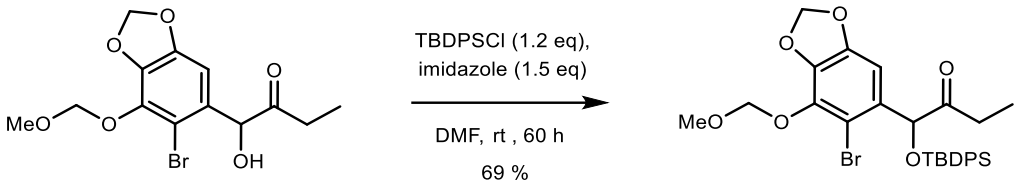
3-13
Chemical Formula: $C_{19}H_{29}BrO_6Si$
Molecular Weight: 461.4240

3-16
Chemical Formula: $C_{13}H_{15}BrO_6$
Molecular Weight: 347.1610

Procedure: A flame-dried 25 mL round bottom flask equipped with a Teflon-coated stir bar and a rubber septum was charged with **3-13** (1.11 mmol, 515 mg, 1.0 equiv.). The flask was evacuated and refilled with N_2 (repeated 3 times), prior to the addition of THF (1 mL). A solution of TBAF·3 H_2O (3.35 mmol, 936 mg, 3.0 equiv.) and acetic acid (3.35 mmol, 192 µL, 3.0 equiv.) in THF (1.2 mL) was then added via syringe, and the resulting mixture was stirred at rt for 14 h. It was then poured on $NaHCO_3$ (saturated aqueous, 5 mL) and extracted with CH_2Cl_2 (3 × 5 mL). The combined organic layers were dried over $MgSO_4$, filtered, and concentrated *in vacuo*. The crude product was purified on silica gel (20 % to 30 % ethyl acetate in hexanes) to provide **3-16** (356 mg, 1.02 mmol, 92 %).

Characterization: $\mathbf{R_f}$ = (hexanes/EtOAc 7:3): 0.56; **IR** (neat) v = 3453, 2922, 1716, 1608, 1472, 1387, 1274, 1219, 1160, 1058, 1026, 916, 772 cm^{-1}; **^{1}H NMR** (500 MHz, $CDCl_3$) δ 6.42 (s, 1H), 5.94 (d, *J*= 1.4 Hz, 1H), 5.93 (d, *J*= 1.4 Hz, 1H), 5.54 (s, 1H), 5.28 (d, *J*= 6.0 Hz, 1H), 5.24 (d, *J*= 6.0 Hz, 1H), 4.35 (broad s, 1H), 3.53 (s, 3H), 2.44 (dq, *J*= 7.3, 18.0 Hz, 1H), 2.30 (dq, *J*= 7.3, 18.0 Hz, 1H), 0.97 (t, *J*= 7.3 Hz, 3H).

Compound 3-17



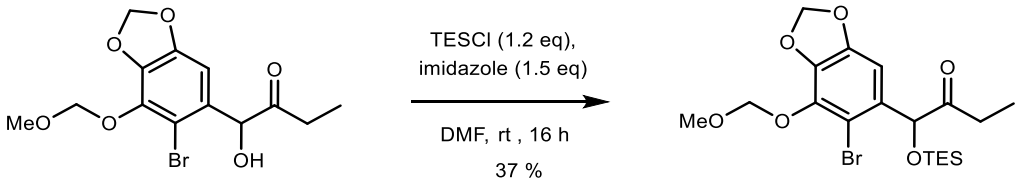
3-16
Chemical Formula: $C_{13}H_{15}BrO_6$
Molecular Weight: 347.1610

3-17
Chemical Formula: $C_{29}H_{33}BrO_6Si$
Molecular Weight: 585.5660

Procedure: A flame-dried microwave vial equipped with a Teflon-coated stir bar and a rubber septum was charged with **3-16** (0.38 mmol, 131 mg, 1.0 equiv.) and imidazole (0.56 mmol, 38 mg, 1.5 equiv.). DMF (0.5 mL) and then *tert*-butyl(chloro)diphenylsilane (0.45 mmol, 117 µL, 1.2 equiv.) were added. The resulting mixture was let stir at rt for 60 h. It was then diluted with ethyl acetate and washed with HCl (1M aq.). The mixture was extracted with ethyl acetate and then washed sequentially with water and brine. The combined organic layers were dried with Na_2SO_4, filtered, and concentrated *in vacuo*. The crude product was purified on silica gel (5 % to 15 % ethyl acetate in hexanes) to provide **3-17** (152 mg, 0.26 mmol, 69 %).

Characterization: $\mathbf{R_f}$ = (hexanes/EtOAc 7:3): 0.69; **IR** (neat) v = 3071, 2958, 2932, 2895, 2858, 1732, 1608, 1471, 1427, 1275, 1160, 1102, 1060, 1028, 919, 821, 772, 741, 702, 610, 505 cm^{-1}; **^{1}H NMR** (500 MHz, $CDCl_3$) δ 7.68 (d, *J*= 7.3 Hz, 2H), 7.49 (d, *J*= 7.5 Hz, 2H), 7.43 (t, *J*= 7.3 Hz, 1H), 7.37 (t, *J*= 7.7 Hz, 3H), 7.29 (d, *J*= 7.5 Hz, 3H), 6.89 (s, 1H), 6.01 (d, *J*= 1.4 Hz, 1H), 5.97 (d, *J*= 1.4 Hz, 1H), 5.58 (s, 1H), 5.28 (d, *J*= 6.0 Hz, 1H), 5.23 (d, *J*= 6.0 Hz, 1H), 3.57 (s, 3H), 2.33 (dq, *J*= 7.2 Hz, 18.0 Hz, 1H), 2.24 (dq, *J*= 7.2 Hz, 18.0 Hz, 1H), 1.10 (s, 9H), 0.85 (t, J= 7.3 Hz, 3H).

Compound 3-18



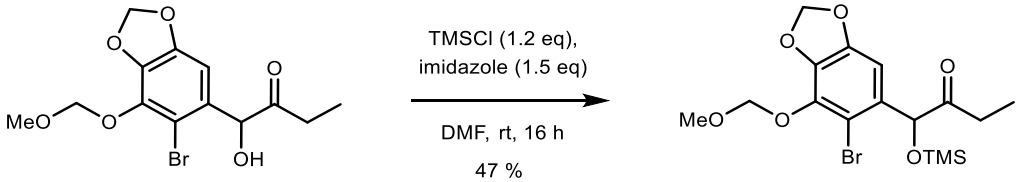
3-16
Chemical Formula: $C_{13}H_{15}BrO_6$
Molecular Weight: 347.1610

3-18
Chemical Formula: $C_{19}H_{29}BrO_6Si$
Molecular Weight: 461.4240

Procedure: A flame-dried microwave vial equipped with a Teflon-coated stir bar and a rubber septum was charged with **3-16** (0.32 mmol, 110 mg, 1.0 equiv.) and imidazole (0.48 mmol, 33 mg, 1.5 equiv.). DMF (0.5 mL) and then chlorotriethylsilane (0.38 mmol, 64 µL, 1.2 equiv.) were added. The resulting mixture was stirred rt for 16 h and then diluted with ethyl acetate and washed with HCl (1M aq.). The resulting mixture was extracted with ethyl acetate and then washed sequentially with water and brine. The combined organic layers were dried with Na_2SO_4, filtered, and concentrated *in vacuo*. The crude product was purified on silica gel (5 % to 15 % ethyl acetate in hexanes) to provide **3-18** (54 mg, 0.12 mmol, 37 %).

Characterization: $\mathbf{R_f}$ = (hexanes/EtOAc 7:3): 0.78; **^{1}H NMR** (500 MHz, $CDCl_3$) δ 6.80 (s, 1H), 6.00 (d, *J*= 1.4 Hz, 1H), 5.97 (d, *J*= 1.4 Hz, 1H), 5.49 (s, 1H), 5.30 (d, *J*= 6.0 Hz, 1H), 5.28 (d, *J*= 6.0 Hz, 1H), 3.57 (s, 3H), 2.49 (2 x dq, *J*= 7.3, 18.3 Hz, 2H), 0.97 (t, *J*= 7.5 Hz, 3H), 0.90 (t, *J*= 8.0 Hz, 9H), 0.59 (dq, *J*= 1.7, 7.5 Hz, 6H).

Compound 3-19



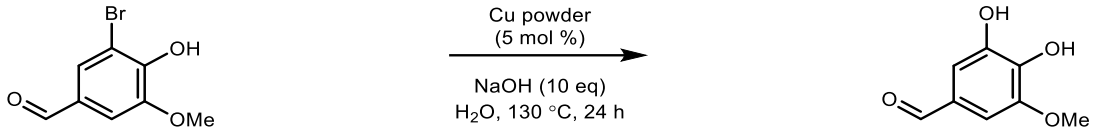
3-16
Chemical Formula: $C_{13}H_{15}BrO_6$
Molecular Weight: 347.1610

3-19
Chemical Formula: $C_{16}H_{23}BrO_6Si$
Molecular Weight: 419.3430

Procedure: A flame-dried microwave vial equipped with a Teflon-coated stir bar and a rubber septum was charged with **3-16** (0.28 mmol, 97 mg, 1.0 equiv.) and imidazole (0.50 mmol, 34 mg, 1.5 equiv.). DMF (0.5 mL) and then chlorotrimethylsilane (0.34 mmol, 43 µL, 1.2 equiv.) were added. The reaction mixture was stirred at rt for 16 h and then diluted with ethyl acetate and washed with HCl (1M aq.). The mixture was extracted with ethyl acetate and then washed sequentially with water and brine. The combined organic layers were dried with Na_2SO_4, filtered, and concentrated *in vacuo*. The crude product was purified on silica gel (5 % to 15 % ethyl acetate in hexanes) to provide **3-19** (55 mg, 0.13 mmol, 47 %).

Characterization: $\mathbf{R_f}$ = (hexanes/EtOAc 7:3): 0.76; **^{1}H NMR** (500 MHz, $CDCl_3$) δ 6.74 (s, 1H), 5.99 (d, *J*= 1.4 Hz, 1H), 5.96 (d, *J*= 1.4 Hz, 1H), 5.50 (s, 1H), 5.30 (d, *J*= 6.0 Hz, 1H), 5.28 (d, *J*= 6.0 Hz, 1H), 3.57 (s, 3H), 2.46 (q, *J*= 7.3 Hz, 2H), 0.99 (t, *J*= 7.3 Hz, 3H), 0.10 (s, 9H).

Compound 3-21



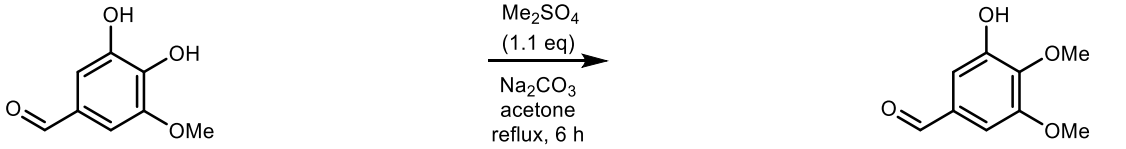
5-bromovanillin (**3-20**)
Chemical Formula: $C_8H_7BrO_3$
Molecular Weight: 231.0450

3-21
Chemical Formula: $C_8H_8O_4$
Molecular Weight: 168.1480

Procedure: The literature procedure was followed with slight modifications.[5] A 1 L round bottom flask equipped with Teflon-coated stir bar was charged with 5-bromovanillin (**3-20**, 50.1 mmol, 11.57 g, 1.0 equiv.), copper powder (2.50 mmol, 159 mg, 0.05 equiv.) and sodium hydroxide (500 mmol, 20.02 g, 10 equiv.). Water (250 mL) was added and the reaction mixture was let stir at 130 °C for 23 h. At this point, disodium phosphate (1.75 mmol, 248 mg, 0.035 equiv.) was added and let stir another 1 h. The reaction mixture was cooled to room temperature and then solids were filtered off. The filtrate was collected and HCl was added until pH = 3. The mixture was extracted with ethyl acetate (4 x 250 mL). The combined organic layers were washed with brine, dried over Na_2SO_4, filtered, and concentrated *in vacuo*. The resulting residue was subjected directly to the next reaction.

Characterization: **^{1}H NMR** (500 MHz, $CDCl_3$) δ 9.79 (s, 1H), 7.14 (d, *J*= 1.6 Hz, 1H), 7.08 (d, *J*= 1.6 Hz, 1H), 5.92 (s, 1H), 5.39 (s, 1H), 3.96 (s, 3H). The characterization data match the data reported previously.[5]

Compound 3-22



3-21
Chemical Formula: $C_8H_8O_4$
Molecular Weight: 168.1480

88 % over 2 steps

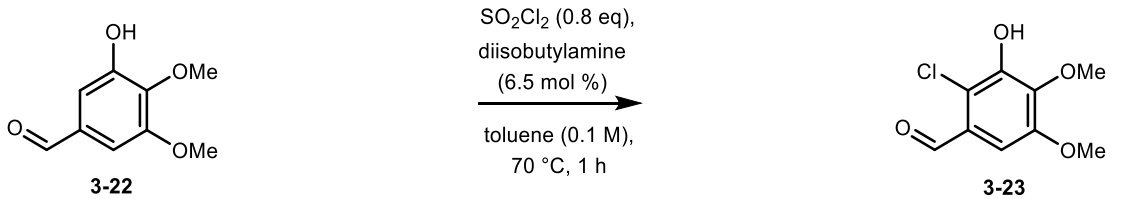
3-22
Chemical Formula: $C_9H_{10}O_4$
Molecular Weight: 182.1750

Procedure: The literature procedure was followed with slight modifications.[5] A 500 mL round bottom flask equipped with Teflon-coated stir bar was charged with **3-21** (8.42 g, 50.1 mmol, 1.0 equiv.), sodium carbonate (55.1 mmol, 6.82 g, 1.1 equiv.), dimethyl sulfate (55.1 mmol, 5.21 mL, 1.1 equiv.), and acetone (200 mL). The resulting slurry was refluxed (at 65 °C) for 6 h. The reaction

mixture was cooled to room temperature and solids were filtered off. The filtrate was collected and concentrated *in vacuo*. The crude product was purified via silica gel plug (1:1 ethyl acetate: hexanes) to provide **3-22** (7.98 g, 43.8 mmol, 88 % over two steps).

Characterization: **^{1}H NMR** (500 MHz, $CDCl_3$) δ 9.79 (s, 1H), 7.09 (d, *J*= 1.8 Hz, 1H), 7.02 (d, *J*= 1.8 Hz, 1H), 3.95 (s, 3H), 3.88 (s, 3H). The characterization data match the data reported previously.[5]

Compound 3-23



3-22
Chemical Formula: $C_9H_{10}O_4$
Molecular Weight: 182.1750

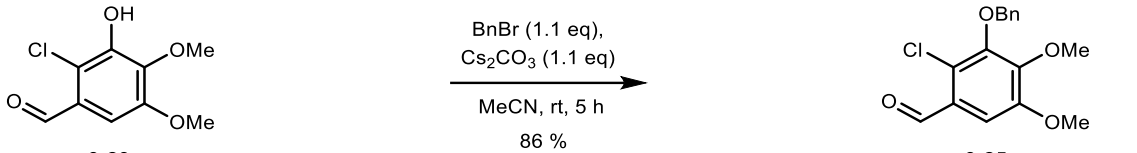
51 %

3-23
Chemical Formula: $C_9H_9ClO_4$
Molecular Weight: 216.6170

Procedure: A flame-dried 100 mL round-bottom flask equipped with a Teflon-coated stir bar and a rubber septum was charged with **3-22** (5.40 mmol, 984 mg, 1.0 equiv.). The flask was evacuated and refilled with N_2 (repeated 3 times), prior to the addition of toluene (54 mL) and then diisobutylamine (0.35 mmol, 61 µL, 0.065 equiv.). The reaction mixture was heated to 70 °C, sulfuryl chloride (4.32 mmol, 350 µL, 0.8 equiv.) was added, and let stir at 70 °C for 1 h. The reaction mixture was then let cool to room temperature and concentrated *in vacuo*. The crude product was purified on silica gel (30 % to 50 % ethyl acetate in hexanes). It was purified further via recrystallization from hexanes/ethyl acetate (5:1, 30 mL) to give **3-23** (602 mg, 2.78 mmol, 51 %) as a white solid.

Characterization: **R_f** = (hexanes/EtOAc 3:1): 0.43; **IR** (neat) v = 3358, 3105, 2995, 2948, 2876, 2843, 1675, 1580, 1496, 1429, 1343, 1259, 1200, 1149, 1031, 841, 735, 606 cm^{-1}; **^{1}H NMR** (500 MHz, $CDCl_3$) δ 10.38 (s, 1H), 7.11 (s, 1H) 6.18 (s, 1H), 4.02 (s, 3H), 3.91 (s, 3H); **^{13}C NMR** (126 MHz, $CDCl_3$) δ 188.8, 150.8, 146.0, 141.1, 127.5, 117.5, 103.6, 61.5, 56.2; **HRMS**: Calcd. for $C_9H_9ClO_4$ $[M-H]^-$ = 215.0189 m/z, found $[M-H]^-$ = 215.0117 m/z.

Compound 3-25



3-23
Chemical Formula: $C_9H_9ClO_4$
Molecular Weight: 216.6170

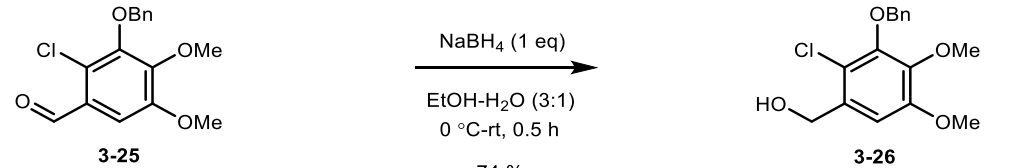
3-25
Chemical Formula: $C_{16}H_{15}ClO_4$
Molecular Weight: 306.7420

Procedure:

A flame-dried 250 mL round-bottom flask equipped with a Teflon-coated stir bar and a rubber septum was charged with **3-23** (6.0 mmol, 1.30 g, 1.0 equiv.) and cesium carbonate (6.6 mmol, 2.15 g, 1.1 equiv.). The flask was evacuated and refilled with N_2 (repeated 3 times), prior to the addition of benzyl bromide (6.6 mmol, 714 µL, 1.1 equiv.) and then acetonitrile (60 mL). The reaction mixture was stirred for 5 h at rt, followed by dilution with CH_2Cl_2 (150 mL) and sequential washing with water (42 mL) and brine (42 mL). the combined organic layers were dried with Na_2SO_4, filtered, and concentrated *in vacuo*. The crude product was purified on silica gel (5 % to 10 % ethyl acetate in hexanes) to provide **3-25** (1.58 g, 5.15 mmol, 86 %) as a pale yellow powder.

Characterization: $\mathbf{R_f}$ = (hexanes/EtOAc 10:1): 0.34; **IR** (neat) v = 3349, 3066, 3028, 3006, 2946, 2863, 1686, 1578, 1481, 1426, 1389, 1373, 1331, 1287, 1200, 1171, 1035, 1000, 946, 901, 859, 749, 694, 608 cm^{-1}; **^{1}H NMR** (500 MHz, $CDCl_3$) δ 10.3 (s, 1H), 7.53 (d, *J*= 7.7 Hz, 2H), 7.42-7.33 (m, 3H), 7.29 (s, 1H), 5.07 (s, 1H), 3.97 (s, 3H), 3.91 (s, 1H); **^{13}C NMR** (126 MHz, $CDCl_3$) δ 188.9, 152.4, 149.1, 148.7, 136.5, 128.5, 128.4, 127.8, 126.1, 106.7, 75.7, 61.4, 56.2; **HRMS**: Calcd. for $C_{16}H_{15}ClO_4$ $[M+Na]^+$ = 307.0737 m/z, found $[M+Na]^+$ = 307.0734 m/z.

Compound 3-26



3-25
Chemical Formula: $C_{16}H_{15}ClO_4$
Molecular Weight: 306.7420

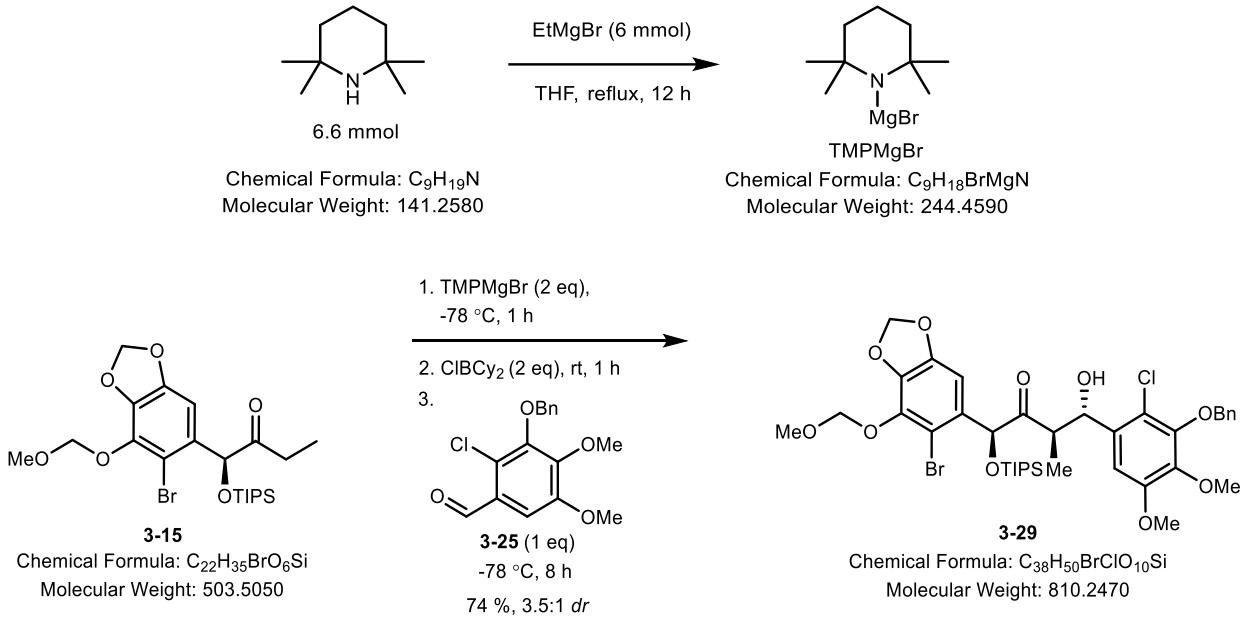
3-26
Chemical Formula: $C_{16}H_{17}ClO_4$
Molecular Weight: 308.7580

Procedure: A 25 mL round bottom flask equipped with Teflon-coated stir bar was charged with **3-25** (0.52 mmol, 160 mg, 1.0 equiv.). Ethanol/water (3:1, 5 mL) were added and the resulting

solution was cooled to 0 °C. Sodium borohydride (0.52 mmol, 20 mg, 1.0 equiv.) was slowly added. The reaction mixture was then warmed to room temperature and let stir 1 h, prior to the addition of NH_4Cl (sat. aq., 5 mL) and extraction with ethyl acetate (3 x 5 mL). The combined organic layers were dried over Na_2SO_4, filtered, and concentrated *in vacuo*. The crude product was purified on silica gel (3:1 hexanes: ethyl acetate) to provide **3-26** (120 mg, 0.39 mmol, 74 %).

Characterization: $\mathbf{R_f}$ = (hexanes/EtOAc 3:1): 0.18; **^{1}H NMR** (500 MHz, $CDCl_3$) δ 7.54 (d, *J* = 8.0 Hz, 2H), 7.41-7.31 (m, 3H), 6.87 (s, 1H), 5.05 (s, 2H), 4.70 (broad s, 1H), 3.87 (s, 3H), 3.85 (s, 3H), 2.50 (broad s, 1H); **^{13}C NMR** (126 MHz, $CDCl_3$) δ 152.4, 148.8, 142.8, 137.1, 134.0, 128.4, 128.2, 118.5, 107.2, 75.5, 62.8, 61.2, 56.0; **HRMS**: Calcd. for $C_{16}H_{17}ClO_4$ $[M+Na]^+$ = 331.0713 m/z, found $[M+Na]^+$ = 331.0703 m/z.

Compound 3-29

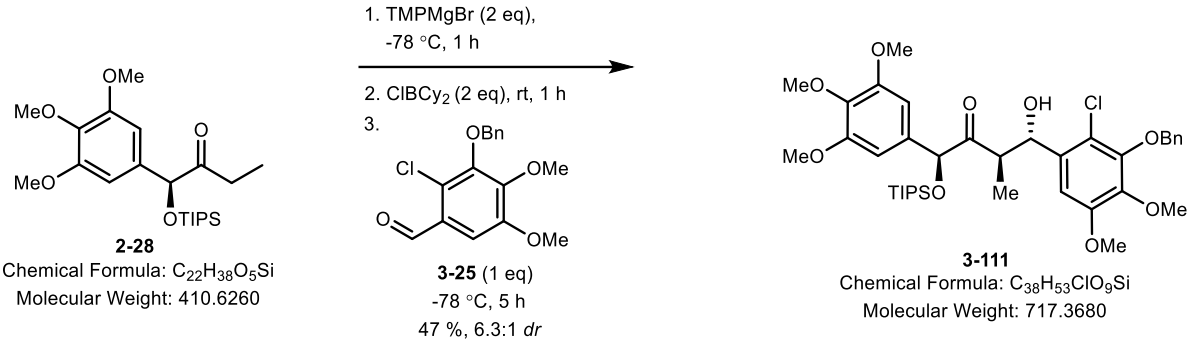


Procedure: A 100 mL flame-dried round bottom flask equipped with a Teflon-coated stir bar and a rubber septum was charged with 2,2,6,6-tetramethylpiperidine (freshly distilled over CaH_2, 7.2 mmol, 1.2 mL, 2.4 equiv.) and THF (6 mL). EtMgBr (6 mmol, 2 mL of 3 M solution in Et_2O, 2.0 equiv.) was added via syringe. The resulting solution was refluxed under N_2 for 12 h, diluted with additional THF (4 mL), and then cooled to –78 °C in a dry ice / acetone bath. A solution of **3-15** (3 mmol, 1.51 g, 1.0 equiv.) in THF (6 mL) was added at a rate of 100 mL/h via syringe pump. The reaction mixture was stirred for 1 h at –78 °C, then a solution of Cy_2BCl (6 mmol, 1.31 mL,

2.0 equiv.) in hexanes (6 mL) was added via syringe. The reaction mixture was warmed to rt and stirred for another 1 h. It was then cooled to –78 °C and a solution of **3-25** (3 mmol, 920 mg, 1.0 equiv.) in hexanes/CH_2Cl_2 (1:1 mixture, 12 mL) was added at a rate of 150 mL/h via syringe pump. The resulting mixture was stirred at –78 °C for 8 h. The reaction mixture was quenched by the addition of $NaHCO_3$ (sat. aq., 15 mL) and diethanolamine (9 mmol, 0.86 mL, 3.0 equiv.), and was stirred at rt for another 30 min. The mixture was filtered, and the filtrate was extracted with EtOAc (3 x 50 mL). The combined organic layers were dried over $MgSO_4$, filtered, and concentrated *in vacuo*. The crude product was purified on silica gel (7 % to 18 % ethyl acetate in hexanes) to provide **3-29** (1.80 g, 2.23 mmol, 74 %) as a 3.5:1 *d.r.* mixture.

Characterization: $\mathbf{R_f}$ = (hexanes/EtOAc 7:3): 0.59; **IR** (neat) v = 3487, 2937, 2865, 1732, 1608, 1572, 1468, 1418, 1370, 1161, 1110, 1060, 1026, 920, 848, 750, 696cm^{-1}; **^{1}H NMR** (500 MHz, $CDCl_3$, signals of major diastereomer) δ 7.53 (m, 2H), 7.41-7.31 (m, 3H), 6.60 (s, 2H), 5.94 (s, 1H), 5.92 (s, 1H), 5.59 (s, 1H), 5.35 (d, *J*= 5.9 Hz, 1H), 5.13 (d, *J*= 5.8 Hz, 1H), 5.13-4.98 (overlapping signals, 3H), 3.85 (s, 3H), 3.79 (s, 3H), 3.52 (s, 3H), 3.46 (m, 1H), 1.16 (d, *J*= 7.0 Hz, 3H), 1.06 (m, 3H), 1.00-0.92 (m, 18H); **^{13}C NMR** (126 MHz, $CDCl_3$, signals of major diastereomer) δ 212.8, 152.0, 148.7, 148.0, 142.3, 138.2, 137.1, 135.6, 128.4, 128.3, 128.1, 117.9, 105.8, 102.2, 97.0, 80.0, 75.3, 74.1, 70.3, 61.0, 57.3, 56.1, 55.88. 44.0, 35.5, 25.4, 21.0, 17.8, 17.7, 12.0; **HRMS**: Calcd. for $C_{38}H_{50}BrClO_{10}Si$ $[M+Na]^+$ = 831.1943 m/z, found $[M+Na]^+$ = 831.1960 m/z.

Compound 3-111

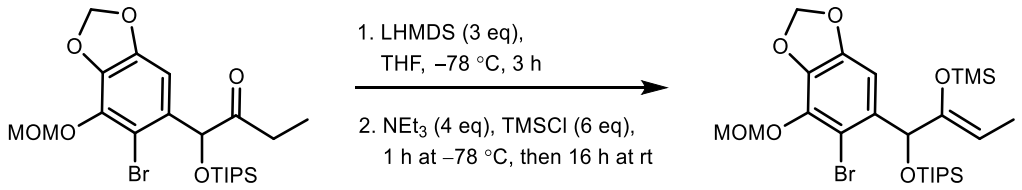


Procedure: A flame-dried microwave vial equipped with a Teflon-coated stir bar and a rubber septum was charged with 2,2,6,6-tetramethylpiperidine (freshly distilled over CaH_2, 0.48 mmol, 81 µL, 2.4 equiv.) and THF (0.3 mL). EtMgBr (0.40 mmol, 130 µL of 3 M solution in Et_2O, 2.0

equiv.) was then added via syringe. The resulting solution was refluxed under N_2 for 12 h, diluted with additional THF (0.37 mL), and cooled to –78 °C in a dry ice / acetone bath. A solution of **2-28** (0.20 mmol, 85 mg, 1.0 equiv.) in THF (0.4 mL) was then added dropwise via syringe. The reaction mixture was stirred for 1 h at –78 °C, then a solution of Cy_2BCl (0.40 mmol, 88 µL, 2.0 equiv.) in hexanes (0.4 mL) was added via syringe. The resulting mixture was warmed to rt and stirred for another 1 h. It was then cooled to –78 °C, and a solution of **3-25** (0.20 mmol, 61 mg, 1.0 equiv.) in hexanes and CH_2Cl_2 (1:1 mixture, 0.9 mL) was added dropwise via syringe. The reaction mixture was then stirred at –78 °C for 5 h. It was quenched by the addition of $NaHCO_3$ (sat. aq., 0.8 mL) and diethanolamine (0.6 mmol, 63 mg, 3 equiv.), and stirred for another 30 min at rt. The mixture was then filtered, and the filtrate was extracted with EtOAc (4 x 3 mL). The combined organic layers were dried over $MgSO_4$, filtered, and concentrated *in vacuo*. The crude product was purified on silica gel (15 % to 20 % ethyl acetate in hexanes) to provide **3-111** (67 mg, 0.094 mmol, 47%) as a 6.3:1 *d.r.* mixture.

Characterization: $\mathbf{R_f}$ = (hexanes/EtOAc 7:3): 0.63; **IR** (neat) v = 3487, 2937, 2866, 1715, 1591, 1461, 1418, 1327, 1237, 1112, 1012, 882, 843, 771, 684 cm^{-1}; **^{1}H NMR** (500 MHz, $CDCl_3$, signals of major diastereomer) δ 7.51 (m, 2H), 7.37 (m, 2H), 7.32 (m, 1H), 6.78 (s, 1H), 6.63 (s, 2H), 5.15 (broad s, 1H), 5.11 (s, 1H), 5.00 (d, *J*= 4.4 Hz, 2H), 3.86 (2 x s, 6H), 3.82 (s, 9H), 3.62 (m, 1H), 1.08 (m, 3H), 1.01 (m, 18H), 0.95 (d, *J*= 7.4 Hz, 3H); **^{13}C NMR** (126 MHz, $CDCl_3$) δ 214.7, 153.1, 152.2, 148.3, 142.6, 137.8, 137.1, 135.5, 134.0, 128.3, 128.2, 128.1, 118.8, 106.3, 103.3, 80.8, 75.2, 73.0, 70.1, 61.1, 60.9, 56.1, 56.0, 45.9, 17.9, 15.7, 12.1; **HRMS**: Calcd. for $C_{38}H_{53}ClO_9Si$ $[M+Na]^+$ = 739.3045 m/z, found $[M+Na]^+$ = 739.3026 m/z.

Compound *Z*-3-33 (*Z*-silyl enol ether)



3-15
Chemical Formula: $C_{22}H_{35}BrO_6Si$
Molecular Weight: 503.5050

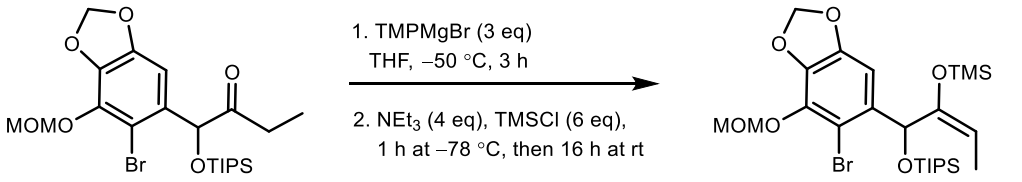
***Z*-3-33**
Chemical Formula: $C_{25}H_{43}BrO_6Si_2$
Molecular Weight: 575.6870

Procedure: A flame-dried microwave vial equipped with a Teflon-coated stir bar and a rubber septum was evacuated and refilled with N_2 (repeated 3 times), prior to the addition of LHMDS

(0.3 mmol, 1 M in THF, 0.3 mL, 3 equiv.). The solution was cooled to −78 °C and then added **3-15** (0.1 mmol, mg, 50 mg, 1.0 equiv.) dropwise as a solution in THF (0.2 mL). Stirred at −78 °C for 3 h and then diluted with THF (0.5 mL), followed by the addition of triethylamine (0.4 mmol, 55 µL, 4 equiv.) and chlorotrimethylsilane (0.6 mmol, 75 µL, 6 equiv.). The reaction mixture was let stir at −78 °C for an additional 1 h and then at rt for 16 h. It was then quenched by the addition of $NaHCO_3$ (sat. aq., 2 mL) and extracted with CH_2Cl_2 (4 x 2 mL). The combined organic layers were dried over Na_2SO_4, filtered, and concentrated *in vacuo*. ^{1}H NMR (500 MHz, $CDCl_3$) with hexamethylbenzene as the internal standard revealed an NMR yield of 18 % and consumption of **3-15** of 96 %. The crude product was purified on silica gel (3 % to 10 % ethyl acetate in hexanes) to provide ***Z*-3-33** (9 mg, 0.015 mmol, 15 %).

Characterization: $\mathbf{R}_f$ = (hexanes/EtOAc 19:1): 0.21; **^{1}H NMR** (500 MHz, $CDCl_3$) δ 6.90 (s, 1H), 5.99 (d, *J*= 1.4 Hz, 1H), 5.94 (d, *J*= 1.4 Hz, 1H), 5.44 (s, 1H), 5.28 (d, *J*= 5.9 Hz, 1H), 5.25(d, *J*= 5.9 Hz, 1H), 5.15 (q, *J*= 6.9 Hz, 1H), 3.55 (s, 3H), 1.54 (d, *J*= 6.7 Hz, 3H), 1.08 (m, 1H), 1.03-0.93 (m, 18H), 0.14 (s, 9H).

Compound *E*-3-33 (*E*-silyl enol ether)



3-15
Chemical Formula: $C_{22}H_{35}BrO_6Si$
Molecular Weight: 503.5050

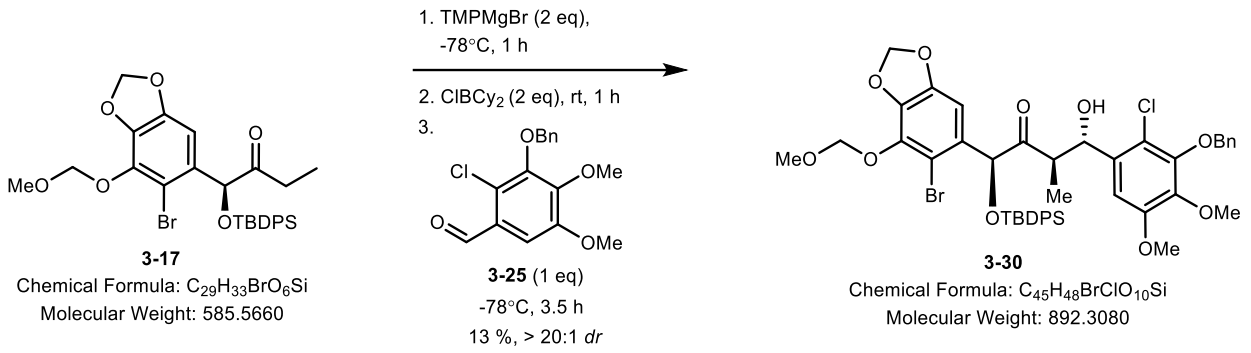
***E*-3-33**
Chemical Formula: $C_{25}H_{43}BrO_6Si_2$
Molecular Weight: 575.6870

Procedure: A flame-dried microwave vial equipped with a Teflon-coated stir bar and a rubber septum was evacuated and refilled with N_2 (repeated 3 times), prior to the addition of TMPMgBr (0.3 mmol, 0.91 M in THF, 0.33 mL, 3 equiv.). The solution was cooled to −78 °C and then added **3-15** (0.1 mmol, 50 mg, 1.0 equiv.) dropwise as a solution in THF (0.2 mL). The reaction mixture was let stir at −78 ºC for 3 h and then added THF (0.5 mL), followed by triethylamine (0.4 mmol, 55 µL, 4 equiv.) and chlorotrimethylsilane (0.6 mmol, 75 uL, 6 equiv.). It was let stir an at −78 ºC for an additional 1 h and then at rt for 16 h. The reaction mixture was quenched by addition of $NaHCO_3$ (sat. aq., 2 mL), prior to being extracted with CH_2Cl_2 (4 x 2 mL). The combined organic layers were dried over Na_2SO_4, filtered, and concentrated *in vacuo*. ^{1}H NMR (500 MHz, $CDCl_3$)

with hexamethylbenzene as the internal standard revealed an NMR yield of 57 % and > 99% consumption of **3-15**. The crude product was purified on silica gel (3 % to 10 % ethyl acetate in hexanes) to provide ***E*-3-33** (14 mg, 0.024 mmol, 24 %, average over two reactions).

Characterization: $\mathbf{R_f}$ = (hexanes/EtOAc 9:1): 0.52; **IR** (neat) v = 2944, 2866, 1665, 1610, 1468, 1251, 1220, 1160, 1060, 1030, 940, 844, 771, 683 cm^{-1}; **^{1}H NMR** (500 MHz, $CDCl_3$) δ 7.07 (s, 1H), 5.98 (d, *J*= 1.4 Hz, 1H), 5.99 (d, *J*= 1.4 Hz, 1H), 5.83 (s, 1H), 5.26 (2 x d, *J*= 5.7 Hz, 2H), 4.64 (q, *J*= 7.1 Hz, 1H), 3.55 (s, 3H), 1.84 (d, *J*= 7.3 Hz, 3H), 1.09 (m, 3H), 1.04-0.97 (m, 18 H), 0.05 (s, 9H); **^{13}C NMR** (126 MHz, $CDCl_3$) δ 149.6, 147.9, 137.3, 136.5, 107.2, 106.1, 104.7, 103.5, 101.6, 97.0, 74.9, 69.6, 57.3, 17.9, 12.2, 0.2.

Compound 3-30

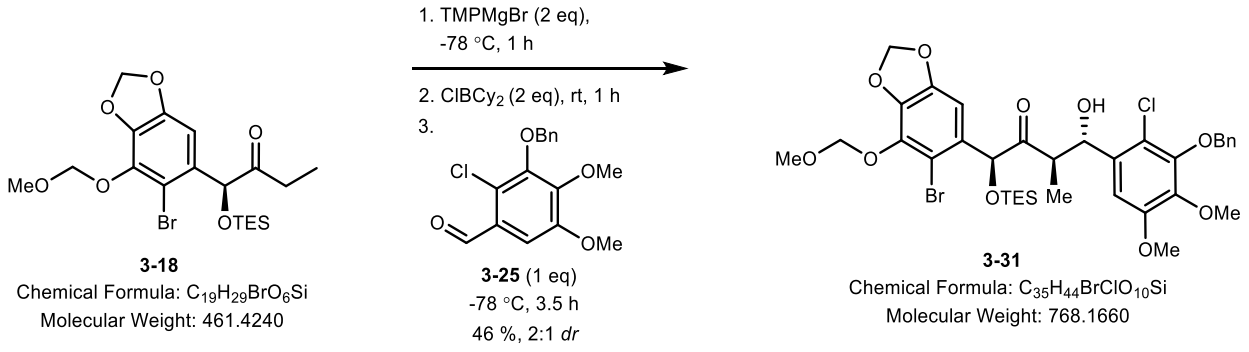


Procedure: A flame-dried microwave vial equipped with a Teflon-coated stir bar and a rubber septum was charged with 2,2,6,6-tetramethylpiperidine (freshly distilled over CaH_2, 0.29 mmol, 49 µL, 2.2 equiv.) and THF (0.3 mL). EtMgBr (0.26 mmol, 0.9 mL of 3 M solution in Et_2O, 2.0 equiv.) was added via syringe. The resulting solution was refluxed under N_2 for 12 h, diluted with additional THF (0.14 mL), and then cooled to –78 ºC in a dry ice / acetone bath. A solution of **3-17** (0.13 mmol, 76 mg, 1.0 equiv.) in THF (0.33 mL) was added dropwise via syringe. The reaction mixture was let stir at –78 °C for 1 h, then a solution of Cy_2BCl (0.26 mmol, 57 µL, 2.0 equiv.) in hexanes (0.2 mL) was added via syringe. It was warmed to rt and stirred for another 1 h. The reaction mixture was cooled to –78 °C, and a solution of **3-25** (0.13 mmol, 40 mg, 1.0 equiv.) in hexanes/CH_2Cl_2 (1:1 mixture, 0.52 mL) was added dropwise via syringe. It was stirred at –78 °C for 3.5 h, and then quenched by the addition of $NaHCO_3$ (sat. aq., 1 mL) and diethanolamine (0.39 mmol, 37 µL, 3.0 equiv.), and stirred at rt for another 30 min. The mixture was filtered, and the filtrate was extracted with EtOAc (3 × 1 mL). The combined organic layers were dried over

$MgSO_4$, filtered, and concentrated *in vacuo*. The crude product was purified on silica gel (10 % to 25 % ethyl acetate in hexanes) to provide **3-30** as a 4:1 *d.r.* mixture. Further purification on silica gel (0 % to 5 % methanol in CH_2Cl_2) gave **3-30** (15 mg, 0.016 mmol, 13 %) as a > 20:1 *d.r.* mixture.

Characterization: $\mathbf{R_f}$ = (hexanes/EtOAc 7:3): 0.50; **IR** (neat) v = 2927, 2855, 2361, 1732, 1608, 1574, 1470, 1371, 1219, 1111, 1026, 921, 772, 701 cm^{-1}; **^{1}H NMR** (500 MHz, $CDCl_3$) δ 7.66 (d, *J*= 7.6 Hz, 2H), 7.51 (d, *J*= 7.2 Hz, 2H), 7.44 (d, *J*= 7.3 Hz, 2H), 7.41-7.30 (m, 8H), 7.23 (d, *J*= 7.2 Hz, 1H), 6.66 (broad s, 1H), 6.58 (s, 1H), 5.96 (d, *J*= 1.5 Hz, 1H), 5.93 (d, *J*= 1.5 Hz, 1H), 5.69 (broad s), 5.27 (d, *J*= 6.0 Hz, 1H), 5.11 (d, *J*= 6.0 Hz, 1H), 4.99-4.95 (3 x d, overlapping, 3H), 3.83 (s, 3H), 3.71 (s, 3H), 3.52 (s, 3H), 3.22 (dq, *J*= 6.8 Hz, 1H), 2.86 (broad s, 1H), 1.07 (s, 9H), 0.86 (d, *J*= 7.4 Hz, overlapping with grease, should be 3H); **HRMS**: Calcd. for $C_{45}H_{48}ClBrO_{10}Si$ $[M+Na]^+$ = 913.1786 m/z, found $[M+Na]^+$ = 915.1761 m/z.

Compound 3-31

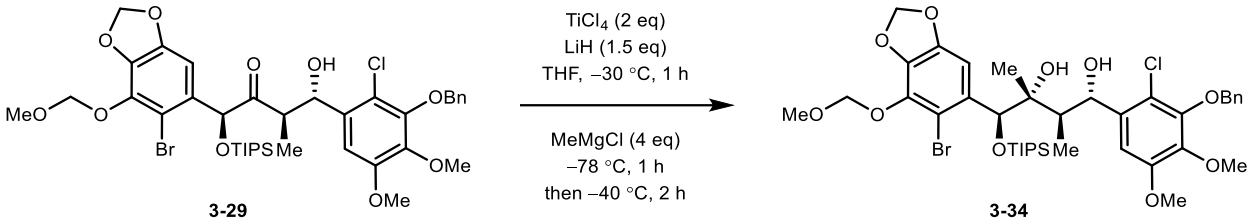


Procedure: A flame-dried microwave vial equipped with a Teflon-coated stir bar and a rubber septum was charged with 2,2,6,6-tetramethylpiperidine (freshly distilled over CaH_2, 0.29 mmol, 49 µL, 2.4 equiv.) and THF (0.3 mL). EtMgBr (0.26 mmol, 0.9 mL of 3 M solution in Et_2O, 2.1 equiv.) was added via syringe. The resulting solution was refluxed under N_2 for 12 h, then diluted with additional THF (0.14 mL), and cooled to –78 °C in a dry ice / acetone bath. A solution of **3-18** (0.12 mmol, 54 mg, 1.0 equiv.) in THF (0.53 mL) was added dropwise via syringe. The reaction mixture was stirred at –78 °C for 1 h, then a solution of Cy_2BCl (0.26 mmol, 57 µL, 2.1 equiv.) in hexanes (0.2 mL) was added via syringe. It was warmed to rt and stirred for another 1 h. The reaction mixture was then cooled to –78 °C, and a solution of **3-25** (0.13 mmol, 40 mg, 1.1 equiv.) in hexanes/CH_2Cl_2 (1:1 mixture, 0.52 mL) was added dropwise via syringe. The resulting mixture

was stirred at –78 °C for 3.5 h and then quenched by the addition of $NaHCO_3$ (sat. aq., 1 mL) and diethanolamine (0.36 mmol, 35 µL, 3.0 equiv.), and stirred at rt for another 30 minutes. The mixture was filtered, and the filtrate was extracted with EtOAc (3 × 1 mL). The combined organic layers were dried over $MgSO_4$, filtered, and concentrated *in vacuo*. The crude product was purified on silica gel (10 % to 25 % ethyl acetate in hexanes) to provide **3-31** (42 mg, 0.055 mmol, 46 %) as a 2:1 *d.r.* mixture.

Characterization: $\mathbf{R_f}$ = (hexanes/EtOAc 7:3): 0.54; **IR** (neat) v = 3486, 2930, 1730, 1608, 1572, 1469, 1417, 1369, 1196, 1109, 1059, 1014, 919, 844, 745, 697 cm^{-1}; **^{1}H NMR** (500 MHz, $CDCl_3$, signals of major diastereomer) δ 7.55-7.30 (2 x m, 5H), 6.69 (s, 1H), 6.29 (s, 1H), 6.00 (d, *J*= 1.7 Hz, 1H), 5.95 (d, *J*= 1.7 Hz, 1H), 5.61 (s, 1H), 5.29 (d, *J*= 5.9 Hz, 1H), 5.10 (d, *J*= 5.9 Hz, 1H), 5.02 (s, 1H), 4.95 (d and s, overlapping, 2H), 4.43 (d, *J*= 8.7 Hz, 1H), 3.86 (s, 3H), 3.84 (s, 3H), 3.50 (s, 3H), 3.39 (m, 1H), 1.36 (d, J= 7.4 Hz, 3H), 0.86 (m, 9H), 0.54 (m, 6H); **^{13}C NMR** (126 MHz, $CDCl_3$, signals of major diastereomer) δ; 213.0, 152.0, 148.6, 138.4, 135.5, 128.3, 128.1, 128.0, 106.1, 103.3, 102.3, 97.2, 77.8, 75.3, 75.1, 73.7, 61.1, 57.3, 56.1, 44.7, 35.5, 25.4, 24.1, 16.1, -6.5, -4.5.

Compound 3-34

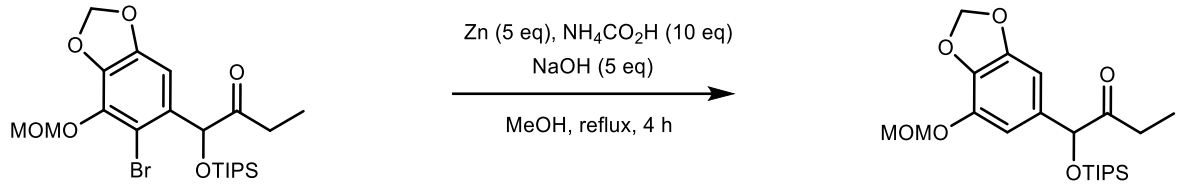


Procedure: A flame-dried microwave vial equipped with a Teflon-coated stir bar and a rubber septum was charged with **3-29** (0.20 mmol, 165 mg, 1.0 equiv.) and LiH (0.31 mmol, 2.4 mg, 1.5 equiv.). The flask was evacuated and refilled with N_2 (repeated 3 times), prior to the addition of THF (1 mL). The mixture was cooled to –30 °C, at which point $TiCl_4$ (0.41 mmol, 1 M in CH_2Cl_2, 0.41 mL, 2.0 equiv.) was added dropwise via syringe, after which the reaction mixture was let stir at this temperature for 1 h. The resulting red solution was then cooled to –78 °C, and a solution of MeMgCl (0.81 mmol, 1 M in THF, 0.81 mL, 4.0 equiv.) was added dropwise via syringe. The mixture was stirred at this temperature for 1 h, then warmed to –40 °C and stirred for another 2 h.

The reaction mixture was quenched by the addition of NH_4Cl (sat. aq., 1.9 mL) followed by NH_4OH (concentrated, 0.5 mL), and stirred for another 15 min at rt. The resulting mixture was filtered, and the filtrate was extracted with EtOAc (3 × 6 mL). The combined organic layers were dried over $MgSO_4$, filtered, and concentrated *in vacuo*. The crude product (1:2 *dr*) was purified on silica gel (7 % to 28 % hexanes/EtOAc) to provide 40 mg, 0.048 mmol, 24 % of the major diastereomer (**3-34**).

Characterization: $\mathbf{R_f}$ = (hexanes/EtOAc 7:3): 0.25; **IR** (neat) v = 3421, 2942, 2364, 1609, 1572, 1472, 1417, 1369, 1218, 1160, 1109, 1059, 1027, 924, 882, 771, 680 cm^{-1}; **^{1}H NMR** (500 MHz, $CDCl_3$) δ 7.50 (d, *J*= 7.4 Hz, 2H), 7.38-7.29 (m, 3H), 7.21 (s, 1H), 6.82 (s, 1H), 6.02 (d, *J*= 1.4 Hz, 1H), 5.96 (d, *J*= 1.4 Hz, 1H), 5.47 (s, 1H), 5.40 (d, *J*= 5.8 Hz, 1H), 5.21 (d, *J*= 5.8 Hz, 1H), 4.99 (2 x d, *J*= 10.7 Hz, 2H), 4.77 (d, *J*= 9.6 Hz, 1H), 4.39 (broad s, 1H), 3.84 (s, 3H), 3.83 (s, 3H), 3.57 (s, 3H), 2.09 (dq, *J*= 7.3 Hz, 9.6 Hz, 1H), 1.49 (s, 3H), 1.09 (m, 3H), 1.03 (d, *J*= 7.0 Hz, 9H), 0.93 (d, *J*= 7.1 Hz, 9H), 0.77 (d, J= 7.4 Hz, 3H); **^{13}C NMR** (126 MHz, $CDCl_3$) δ 152.4, 148.5, 147.9, 142.6, 138.2, 137.6, 137.1, 136.2, 134.9, 128.4, 128.3, 128.0, 119.5, 110.9, 106.6, 105.7, 101.9, 97.0, 81.1, 76.5, 75.3, 72.6, 61.1, 57.4, 56.1, 48.4, 27.6, 26.9, 18.1, 17.9, 12.8; **HRMS**: Calcd. for $C_{39}H_{54}BrClO_{10}Si$ $[M+Na]^+$ = 847.2256 m/z, found $[M+Na]^+$ = 847.2241 m/z.

Compound 3-37



3-15
Chemical Formula: $C_{22}H_{35}BrO_6Si$
Molecular Weight: 503.5050

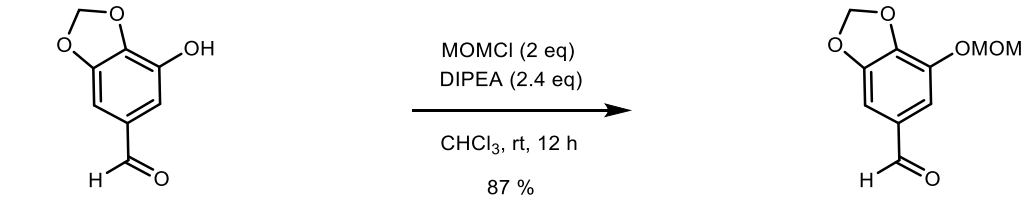
3-37
Chemical Formula: $C_{22}H_{36}O_6Si$
Molecular Weight: 424.6090

Procedure: A 100 mL flame-dried round bottom flask equipped with a Teflon-coated stir bar and a rubber septum was charged with **3-15** (3.0 mmol, 1.51 g, 1.0 equiv.), zinc (15 mmol, 981 mg, 5.0 equiv.), and ammonium formate (30 mmol, 1.89 g, 10 equiv.). Methanol (37.5 mL) and then sodium hydroxide (15 mmol, 600 mg, 5.0 equiv.) were added to the flask. The reaction mixture was stirred while refluxing at 65 °C for 4 h. It was cooled to room temperature and then filtered through celite. The filtrate was concentrated *in vacuo*. Water (37.5 mL) was added to the residue, followed by HCl until neutral pH was reached. The mixture was then extracted with ethyl acetate

(3 x 12 mL). The combined organic layers were dried with Na_2SO_4, filtered, and concentrated *in vacuo*. The crude product was purified on silica gel (3 % to 10 % ethyl acetate in hexanes) to provide **3-37** (1.12 g, 2.65 mmol, 88 %).

Characterization: $\mathbf{R_f}$ = (hexanes/EtOAc 19:1): 0.28; **^{1}H NMR** (500 MHz, $CDCl_3$) δ 6.85 (dd, *J*= 0.7 Hz, 1.4 Hz, 1H), 6.66 (dd, *J*= 0.6 Hz, 1.5 Hz, 1H), 5.96 (2 x d, *J*= 1.5 Hz, 2H), 5.21 (d, *J*= 6.5 Hz, 1H), 5.19 (d, *J*= 6.5 Hz, 1H), 5.03 (s, 1H), 3.49 (s, 3H), 2.70 (dq, *J*= 7.3 Hz, 18.7 Hz, 1H), 2.47 (dq, *J*= 7.3 Hz, 18.6 Hz, 1H), 1.13 (m, 3H), 1.02 (m, 18H), 0.94 (t, *J*= 7.4 Hz, 3H); **^{13}C NMR** (126 MHz, $CDCl_3$) δ 211.5, 149.2, 140.6, 136.1, 133.9, 109.4, 101.6, 101.0, 95.8, 81.3, 56.0, 28.6, 17.8, 12.3, 12.0, 7.41 ; **HRMS**: Calcd. for $C_{22}H_{36}O_6Si$ $[M+Na]^+$ = 447.2179 m/z, found $[M+Na]^+$ = 447.2174 m/z.

Compound 3-38



4-14
Chemical Formula: $C_8H_6O_4$
Molecular Weight: 166.1320

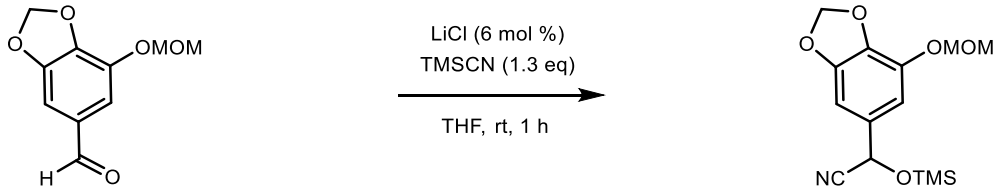
3-38
Chemical Formula: $C_{10}H_{10}O_5$
Molecular Weight: 210.1850

Procedure: A 500 mL flame-dried round bottom flask equipped with a Teflon-coated stir bar and a rubber septum was charged with 5-hydroxypiperonal (**4-14**, 27.7 mmol, 4.60 g, 1.0 equiv.) and $CHCl_3$ (277 mL). *N,N*-diisopropylethylamine (DIPEA, 66.4 mmol, 11.6 mL, 2.4 equiv.) and chloromethyl methyl ether (MOMCl, 55.4 mmol, 4.2 mL, 2.0 equiv.) were then added via syringe, and the mixture was stirred for 12 h at rt. The reaction mixture was then poured on HCl (1M, 110 mL), and extracted with CH_2Cl_2 (3 × 110 mL). The combined organic layers were dried over $MgSO_4$, filtered, and concentrated *in vacuo*. The crude product was purified on silica gel (15 % to 25 % ethyl acetate in hexanes) to provide **3-38** (5.04 g, 24.0 mmol, 87 %).

Characterization: $\mathbf{R_f}$ = (hexanes/EtOAc 5:1): 0.19; **IR** (neat) v = 2996, 2957, 2907, 2829, 2784, 2731, 1687, 1629, 1601, 1504, 1435, 1366, 1293, 1155, 1115, 1061, 1032, 972, 919, 753 cm^{-1}; **^{1}H NMR** (500 MHz, $CDCl_3$) δ 9.77 (s, 1H), 7.29 (d, *J*= 1.4 Hz, 1H), 7.10 (d, *J*= 1.4 Hz, 1H), 6.10 (s, 2H), 5.27 (s, 2H), 3.53 (s, 3H); **^{13}C NMR** (126 MHz, $CDCl_3$) δ 190.1, 149.7, 141.9, 140.8, 131.9,

116.1, 103.0, 102.6, 95.5, 56.5; **HRMS**: Calcd. for $C_{10}H_{10}O_5$ $[M+Na]^+$ = 233.0426 m/z, found $[M+Na]^+$ = 233.0420 m/z.

Compound 3-39



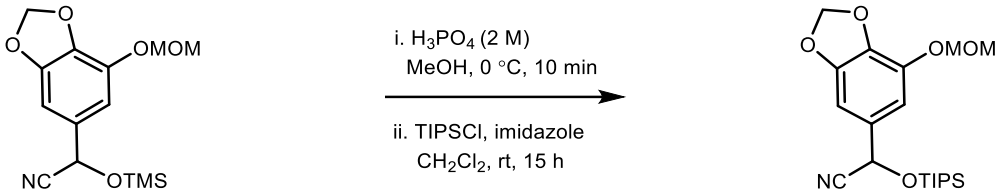
3-38
Chemical Formula: $C_{10}H_{10}O_5$
Molecular Weight: 210.1850

3-39
Chemical Formula: $C_{14}H_{19}NO_5Si$
Molecular Weight: 309.3930

Procedure: A flame-dried 100 mL round-bottom flask equipped with a Teflon-coated stir bar and a rubber septum was charged with **3-38** (24.0 mmol, 5.04 g, 1.0 equiv.) and LiCl (1.38 mmol, 59 mg, 0.06 equiv.). The flask was evacuated and refilled with N_2 (repeated 3 times), prior to the addition of THF (30 mL). Then, trimethylsilyl cyanide (30.5 mmol, 3.8 mL, 1.3 equiv.) was added via syringe, prior to stirring at rt for 1 h. Hexanes (140 mL) was added to the reaction mixture, which was then filtered through silica, washing with hexanes/ethyl acetate (3:1, 280 mL). The filtrate was collected and concentrated *in vacuo*. The crude product was subjected directly to the next step.

Characterization: $\mathbf{R_f}$ = (hexanes/EtOAc 5:1): 0.42.

Compound 3-40



3-39
Chemical Formula: $C_{14}H_{19}NO_5Si$
Molecular Weight: 309.3930

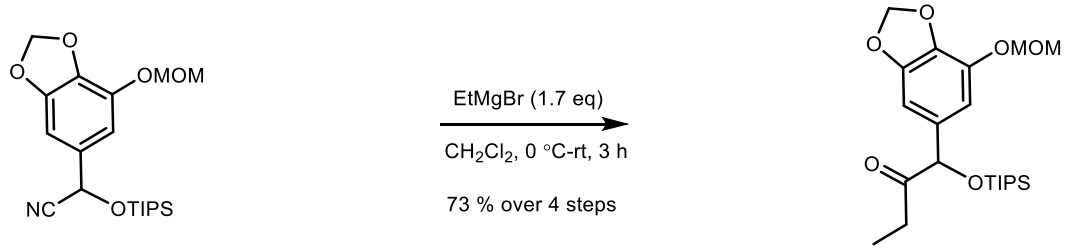
3-40
Chemical Formula: $C_{20}H_{31}NO_5Si$
Molecular Weight: 393.5550

Procedure: A 250 mL round bottom flask equipped with Teflon-coated stir bar was charged with crude **3-39** (24.0 mmol, 1.0 equiv.). Methanol (55 mL) was added and the crude was dissolved. The resulting solution was cooled to 0 °C and then added H_3PO_4 (27.7 mmol, 2 M aq., 13.8 mL, 1.1 equiv.). The reaction mixture was stirred 10 minutes at room temperature and then concentrated

in vacuo. Water (70 mL) and CH_2Cl_2 (3 x 70 mL) were added and then extracted. The combined organic layers were concentrated *in vacuo*. The resulting residue was taken up in CH_2Cl_2 (55 mL), along with triisopropylsilyl chloride (33.2 mmol, 7.1 mL, 1.4 equiv.) and imidazole (41.5 mmol, 2.83 g, 1.7 equiv.) and let stir at room temperature for 17 h. *N,N*-dimethylaminoethanol (11.07 mmol, 1.1 mL, 0.5 equiv.) was added and let stir an additional 1 h at rt. HCl (1 M aq., 55 mL), water (83 mL), and CH_2Cl_2 (83 mL) were then added. The layers were then separated and the aqueous layer was extracted with CH_2Cl_2 (3 x 42 mL). The combined organic layers were dried and concentrated *in vacuo*. The crude product was purified on silica gel (5 % to 10 % ethyl acetate in hexanes) to provide **3-40**, which was subjected to the next reaction.

Characterization: $\mathbf{R_f}$ = (hexanes/EtOAc 10:1): 0.35; **^{1}H NMR** (500 MHz, $CDCl_3$) δ 6.84 (dd, *J*= 0.5, 1.6 Hz, 1H), 6.72 (dd, *J*= 0.3 Hz, 1.6 Hz, 1H), 6.01 (s, 2H), 5.44 (s, 1H), 5.22 (s, 2H), 3.50 (s, 3H), 1.19 (m, 3H), 1.12-1.03 (m, 18H).

Compound 3-37



3-40
Chemical Formula: $C_{20}H_{31}NO_5Si$
Molecular Weight: 393.5550

3-37
Chemical Formula: $C_{22}H_{36}O_6Si$
Molecular Weight: 424.6090

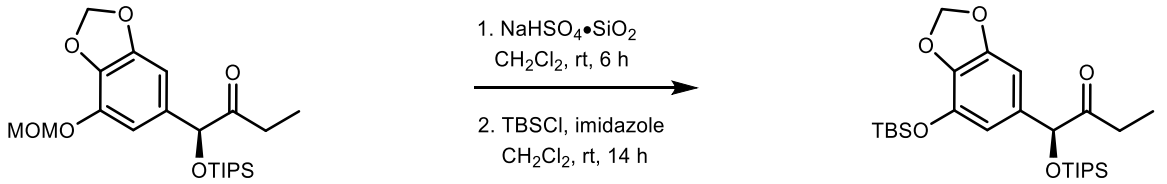
Procedure:

A flame-dried 250 mL round-bottom flask equipped with a Teflon-coated stir bar and a rubber septum was charged with **3-40** (24.0 mmol, 1.0 equiv.). The flask was evacuated and refilled with N_2 (repeated 3 times), prior to the addition of CH_2Cl_2 (55 mL). The solution was cooled to 0 °C and slowly added ethyl magnesium bromide (41.5 mmol, 3 M in diethyl ether, 13.8 mL, 1.7 equiv.) via syringe. The reaction mixture was stirred at room temperature for 3 h. It was then cooled to 0 °C, followed by the addition of HCl (2 M aq., 125 mL) and let stir at rt for an additional 30 minutes. The reaction mixture was extracted with CH_2Cl_2 (3 x 83 mL). The combined organic layers were dried over Na_2SO_4, filtered, and concentrated *in vacuo*. The crude product was purified on silica

gel (in 5 % to 10 % ethyl acetate in hexanes) to provide **3-37** (8.56 g, 20.2 mmol, 73 % over 4 steps).

Characterization: ^{1}H NMR matched the characterization of the previously synthesized product (see page 228).

Compound 3-41



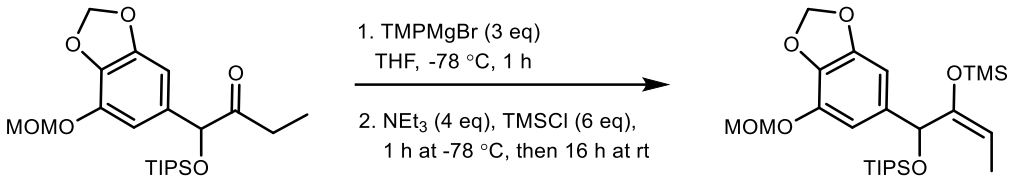
3-37
Chemical Formula: $C_{22}H_{36}O_6Si$
Molecular Weight: 424.6090

3-41
Chemical Formula: $C_{26}H_{46}O_5Si_2$
Molecular Weight: 494.8190

Procedure: $NaHSO_4 \cdot SiO_2$ was prepared following the literature procedure.[36] A 25 mL flame-dried round bottom flask equipped with a Teflon-coated stir bar was charged with **3-37** (458 mg, 1.08 mmol, 1.0 equiv.). CH_2Cl_2 (10.8 mL) was added and the substrate was dissolved. $NaHSO_4 \cdot SiO_2$ (440 mg) was added while still hot from the oven. The reaction mixture was stirred at rt for 6 h, followed by filtration, washing with CH_2Cl_2 (2 x 6 mL). The filtrate was collected and concentrated *in vacuo*. *Tert*-butyldimethylsilyl chloride (2.37 mmol, 357 mg, 2.2 equiv.), imidazole (1.62 mmol, 110 mg, 1.5 equiv.), and CH_2Cl_2 (4.4 mL) were added to the residue. The reaction mixture was let stir at rt for 14 h, prior to dilution with ethyl acetate (6 mL) and the addition HCl (1M aq., 8 mL). The mixture was extracted with ethyl acetate (3 x 6 mL) and washed with water (6 mL), followed by brine (6 mL). The combined organic layers were dried over Na_2SO_4 and concentrated *in vacuo*. The crude product was purified on silica gel (4 % to 10 % ethyl acetate in hexanes) to provide **3-41** (192 mg, 0.39 mmol, 36 %).

Characterization: $\mathbf{R_f}$ = (hexanes/EtOAc 19:1): 0.54; **^{1}H NMR** (500 MHz, $CDCl_3$) δ 6.58 (m 1H), 6.57 (m 1H), 5.90 (s, 2H), 5.00 (s, 1H), 2.66 (dq, *J*= 7.3 Hz, 18.5 Hz, 1H), 2.44 (dq, *J*= 7.2 Hz, 18.5 Hz, 1H), 1.11 (m, 1H), 1.01 (m, 18H), 0.96 (s, 9H), 0.92 (t, *J*= 7.3 Hz, 3H) ; **^{13}C NMR** (126 MHz, $CDCl_3$) δ 211.2, 149.2, 139.2, 137.4, 133.4, 112.9, 101.3, 100.3, 81.1, 28.4, 25.6, 18.3, 17.9, 12.1, 7.4, -4.6; **HRMS**: Calcd. for $C_{26}H_{46}O_5Si_2$ $[M+Na]^+$ = 517.2781 m/z, found $[M+Na]^+$ = 517.2776 m/z.

Compound *E*-3-42



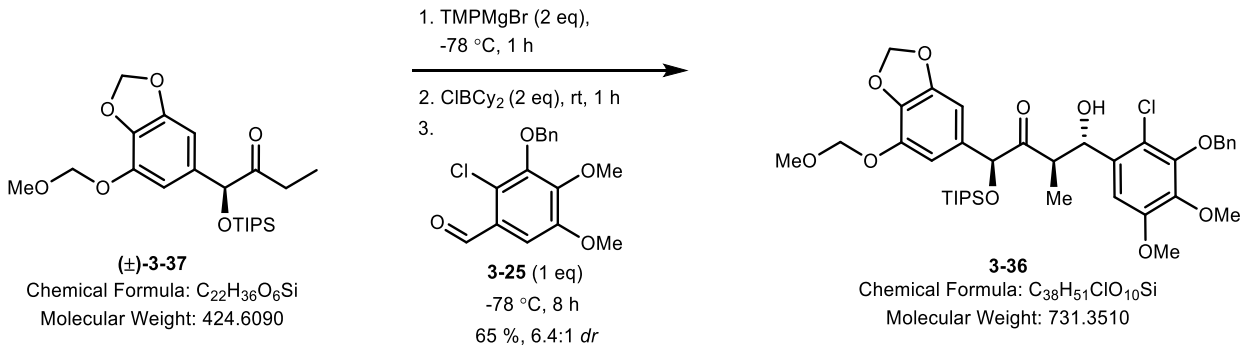
3-37
Chemical Formula: $C_{22}H_{36}O_6Si$
Molecular Weight: 424.6090

***E*-3-42**
Chemical Formula: $C_{25}H_{44}O_6Si_2$
Molecular Weight: 496.7910

Procedure: A flame-dried microwave vial equipped with a Teflon-coated stir bar and a rubber septum was evacuated and refilled with N_2 (repeated 3 times), prior to the addition of TMPMgBr (0.15 mmol, 0.77 M in THF, 0.39 mL, 3 equiv.) and THF (0.11 mL). The solution was cooled to −78 °C and then added **3-37** (0.1 mmol, 50 mg, 1.0 equiv.) dropwise as a solution in THF (0.2 mL). The reaction mixture was stirred 1 h at -78 °C and then added THF (0.5 mL), followed by triethylamine (0.4 mmol, 55 µL, 4 equiv.) and chlorotrimethylsilane (0.6 mmol, 75 uL, 6 equiv.). The reaction mixture was stirred at −78 °C for an additional 1 h, followed by at rt for 17 h. It was then quenched by addition of $NaHCO_3$ (sat. aq., 1 mL) and extracted with CH_2Cl_2 (3 x 1 mL). The combined organic layers were dried over Na_2SO_4, filtered, and concentrated *in vacuo*. ^{1}H NMR (500 MHz, $CDCl_3$) with hexamethylbenzene as the internal standard revealed an NMR yield of 93 % and 100 % consumption of **3-37**. The crude product was purified on silica gel (3 % to 10 % ethyl acetate in hexanes) to provide ***E*-3-42** (29 mg, 0.058 mmol, 58 %, average over two reactions) as a clear oil.

Characterization: $\mathbf{R_f}$ = (hexanes/EtOAc 19:1): 0.42; **IR** (neat) v = 2943, 2893, 2866, 1663, 1634, 1432, 1229, 1156, 1057, 939, 749, 681 cm^{-1}; **^{1}H NMR** (500 MHz, $CDCl_3$) δ 6.82 (d, *J*= 1.2 Hz, 1H), 6.61 (d, *J*= 1.2 Hz, 1H), 5.94 (d, *J*= 1.5 Hz, 1H), 5.93 (d, *J*= 1.5 Hz, 1H), 5.44 (s, 1H), 5.19 (m, 2H), 4.57 (q, *J*= 7.1 Hz, 1H), 3.48 (s, 3H), 1.74 (d, *J*= 7.1 Hz, 3H), 1.13-0.99 (m, 21H), 0.06 (s, 9H); **^{13}C NMR** (126 MHz, $CDCl_3$) δ 152.9, 148.3, 140.0, 138.2, 134.8, 109.8, 101.5, 101.2, 101.0, 95.5, 70.4, 56.1, 17.9, 12.2, 11.7, 0.28; **HRMS**: Calcd. for $C_{25}H_{44}O_6Si_2$ $[M+Na]^+$ = 519.2574 m/z, found $[M+Na]^+$ = 519.2581 m/z.

Compound 3-36

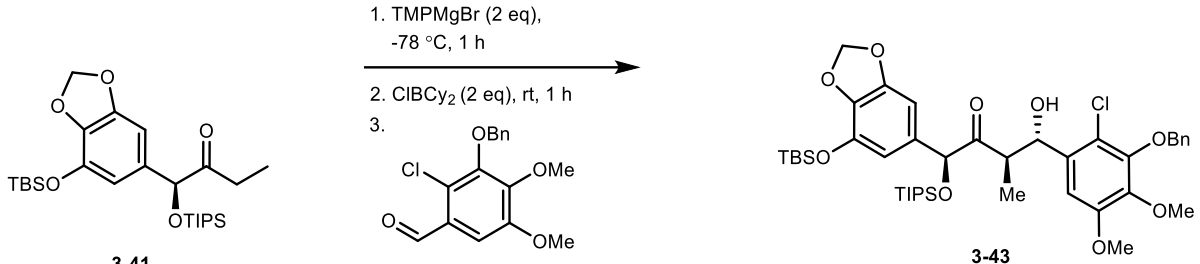


Procedure: A 250 mL flame-dried round bottom flask equipped with a Teflon-coated stir bar and a rubber septum was charged with 2,2,6,6-tetramethylpiperidine (freshly distilled over CaH_2, 19 mmol, 3.2 mL, 2.4 equiv.) and dissolved in THF (16 mL). EtMgBr (16 mmol, 5.3 mL of 3 M solution in Et_2O, 1.5 equiv.) was then added via syringe. The resulting solution was refluxed under N_2 for 12 h, then diluted with additional THF (16 mL), and cooled to –78 °C in a dry ice / acetone bath. A solution of **(±)-3-37** (8 mmol, 3.40 g, 1.0 equiv.) in THF (16 mL) was added dropwise via syringe pump at a rate of 100 mL/h. The reaction mixture was stirred at –78 °C for 1 h, then a solution of Cy_2BCl (16 mmol, 3.5 mL, 1.2 equiv.) in hexanes (16 mL) was added via syringe. The reaction mixture was warmed to rt and stirred for another 1 h, then cooled to –78 °C, at which point a solution of **3-25** (8 mmol, 2.41 g, 1.0 equiv.) in hexanes and CH_2Cl_2 (1:1 mixture, 24 mL) was added via syringe pump at a rate of 150 mL/h. The resulting mixture was stirred at –78 °C for 3 h followed by 2 h at –30 °C. It was quenched by the addition of $NaHCO_3$ (sat. aq., 27 mL) and diethanolamine (24 mmol, 2 mL, 3.0 equiv.), and stirred for another 30 min at rt. The mixture was filtered, and the filtrate was extracted with EtOAc (3 × 100 mL). The combined organic layers were dried over $MgSO_4$, filtered, and concentrated *in vacuo*. The crude product was purified on silica gel (7 % to 18 % ethyl acetate in hexanes) to provide **3-36** (3.83 g, 4.85 mmol, 65 %) as a 6.4:1 *d.r.* mixture.

Characterization: $\mathbf{R_f}$ = (hexanes/EtOAc 7:3): 0.57; **IR** (neat) v = 3487, 2941, 2866, 1712, 1634, 1572, 1484, 1430, 1370, 1111, 1061, 1030, 924, 882, 845, 751, 686 cm^{-1}; **^{1}H NMR** (500 MHz, $CDCl_3$) δ 7.52 (d, *J*= 8.0 Hz, 2H), 7.40-7.30 (m, 3H), 6.72 (s, 1H), 6.71 (d, *J*= 1.3 Hz, 1H), 6.48 (d, *J*= 1.3 Hz, 1H), 5.96 (d, *J*= 1.6 Hz, 1H), 5.93 (d, *J*= 1.6 Hz, 1H), 5.15 (d, *J*= 6.5 Hz, 1H), 5.10 (d, *J*= 6.5 Hz, 1H), 5.06 (d, *J*= 5.3 Hz, 1H), 5.04 (s, 1H), 5.01 (d, *J*= 10.6 Hz, 1H), 4.97 (d, *J*= 10.6

Hz, 1H), 3.86 (s, 3H), 3.85 (s, 3H), 3.50 (m, 1H), 3.43 (s, 3H), 1.10 (d, *J*= 7.4 Hz, 3H), 1.06 (m, 3H), 0.99 (m, 21H); **^{13}C NMR** (126 MHz, $CDCl_3$) δ 214.2, 152.2, 149.0, 148.2, 142.4, 140.2, 137.2, 135.9, 135.6, 132.3, 128.3, 128.0, 118.2, 110.1, 106.0, 101.7, 101.6, 95.4, 80.3, 75.1, 73.4, 61.1, 56.2, 56.0, 45.3, 17.9, 15.9, 12.1; **HRMS**: Calcd. for $C_{38}H_{51}ClO_{10}Si$ $[M+Na]^+$ = 753.2838 m/z, found $[M+Na]^+$ = 753.2806 m/z.

Compound 3-43



3-41
Chemical Formula: $C_{26}H_{46}O_5Si_2$
Molecular Weight: 494.8190

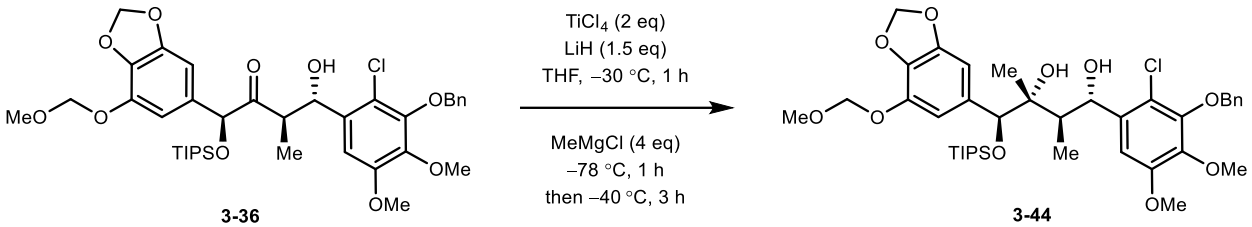
3-25 (1 eq)
-78 °C, 8 h
58 %, 3.9:1 *dr*

3-43
Chemical Formula: $C_{42}H_{61}ClO_9Si_2$
Molecular Weight: 801.5610

Procedure: A 25 mL flame-dried round bottom flask equipped with a Teflon-coated stir bar and a rubber septum was charged with 2,2,6,6-tetramethylpiperidine (freshly distilled over CaH_2, 0.94 mmol, 158 µL, 2.4 equiv.) and THF (0.9 mL). EtMgBr (0.78 mmol, 0.26 mL of 3 M solution in Et_2O, 1.5 equiv.) was added via syringe. The resulting solution was refluxed under N_2 for 12 h, then diluted with additional THF (0.7 mL), and cooled to –78 °C in a dry ice / acetone bath. A solution of **3-41** (0.39 mmol, 192 mg, 1.0 equiv.) in THF (0.8 mL) was added dropwise by syringe. The reaction mixture was stirred for 1 h at –78 °C, then a solution of Cy_2BCl (0.78 mmol, 171 µL, 1.2 equiv.) in hexanes (0.8 mL) was added via syringe. The reaction mixture was warmed to rt and let stir another 1 h, then cooled to –78 °C, at which point a solution of **3-25** (0.39 mmol, 120 mg, 1.0 equiv.) in hexanes and CH_2Cl_2 (1:1 mixture, 1.8 mL) was added via syringe. The resulting mixture was stirred at –78 °C for 3 h, followed by 2 h at –30 °C. The reaction mixture was quenched by the addition of $NaHCO_3$ (sat. aq., 1.6 mL) and diethanolamine (1.17 mmol, 120 µL, 3.0 equiv.), and stirred at rt for another 30 min. The mixture was then filtered, and the filtrate was extracted with EtOAc (3 × 6 mL). The combined organic layers were dried over $MgSO_4$, filtered, and concentrated *in vacuo*. The crude product was purified on silica gel (7 % to 18 % ethyl acetate in hexanes) to provide **3-43** (180 mg, 0.22 mmol, 58 %) as a 3.9:1 *d.r.* mixture.

Characterization: $\mathbf{R}_f$ = (hexanes/EtOAc 9:1): 0.24; **IR** (neat) v = 3477, 2933, 2864, 1713, 1630, 1572, 1426, 1370, 1110, 1013, 838, 784, 753, 683 cm^{-1}; **^{1}H NMR** (500 MHz, $CDCl_3$, major diastereomer signals) δ 7.51 (m, 2H), 7.40-7.24 (m, 3H), 6.74 (s, 1H), 6.43 (s, 2H), 5.88 (m, 2H), 5.07 (m, 1H), 5.01 (s, 1H), 4.98 (m, 2H), 3.84 (s, 6H), 3.49 (m, 1H), 1.11-0.94 (m, 24H), 0.93 (s, 9H), 0.12 (s, 6H); **^{13}C NMR** (126 MHz, $CDCl_3$, major diastereomer signals) δ 214.2, 152.3, 149.1, 148.3, 142.5, 138.7, 137.2, 135.6, 132.0, 128.8, 128.3, 118.4, 114.1, 106.1, 101.3, 100.8, 80.3, 75.2, 61.2, 56.0, 45.5, 25.6, 17.9, 12.1, -4.4; **HRMS**: Calcd. for $C_{42}H_{61}ClO_9Si_2$ $[M+Na]^+$ = 823.3440 m/z, found $[M+Na]^+$ = 823.3424 m/z.

Compound 3-44



3-36
Chemical Formula: $C_{38}H_{51}ClO_{10}Si$
Molecular Weight: 731.3510

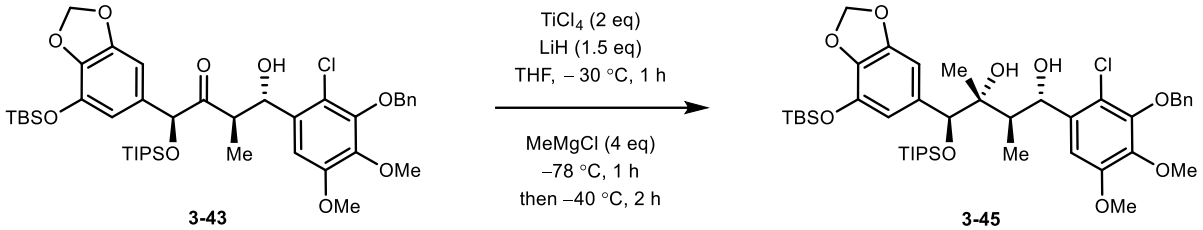
3.4 mmol scale: 20:1 *dr*, 73 % major diastereomer.
18 mmol scale: 10:1 *dr*, 55 % major diastereomer.

3-44
Chemical Formula: $C_{39}H_{55}ClO_{10}Si$
Molecular Weight: 747.3940

Procedure: A 500 mL flame-dried round bottom flask equipped with a Teflon-coated stir bar and a rubber septum was charged with **3-36** (17.9 mmol, 13.12 g, 1.0 equiv.) and LiH (26.9 mmol, 214 mg, 1.5 equiv.). The flask was evacuated and refilled with N_2 (repeated 3 times), prior to the addition of THF (90 mL). The mixture was cooled to –30 °C in a dry ice/ acetone bath, at which point $TiCl_4$ (35.9 mmol, 1 M in CH_2Cl_2, 35.9 mL, 2.0 equiv.) was added dropwise via syringe, followed by stirring at this temperature for 30 min. The resulting red solution was then cooled to –78 °C, and a solution of MeMgCl (71.8 mmol, 1 M in THF, 71.8 mL, 4.0 equiv.) was added via syringe pump at a rate of 40 mL/h. The mixture was stirred at this temperature for 1 h, then warmed to –40 °C and stirred for another 3 h. The reaction mixture was quenched by the addition of NH_4Cl (sat. aq., 72 mL) followed by NH_4OH (concentrated, 18 mL), and stirred at rt for another 15 min. The resulting mixture was filtered, and the filtrate was extracted with EtOAc (3 × 180 mL). The combined organic layers were dried over $MgSO_4$, filtered, and concentrated *in vacuo*. The crude product (10:1 *dr*) was purified on silica gel (7 % to 28 % ethyl acetate in hexanes) to provide 7.42 g, 9.93 mmol, 55 % of the major diastereomer **3-44**.

Characterization: $\mathbf{R}_f$ = (hexanes/EtOAc 7:3): 0.48; **IR** (neat) v = 3444, 2942, 2866, 1634, 1572, 1485, 1572, 1485, 1371, 1195, 1156, 1109, 1055, 923, 881, 838, 751, 680 cm^{-1}; **^{1}H NMR** (500 MHz, $CDCl_3$) δ 7.50 (d, *J*= 7.5 Hz, 2 H), 7.38-7.29 (m, 3H), 7.00-6.39 (broad s, 2H), 6.71 (s, 1H), 5.98 (s, 2H), 5.34 (d, *J*= 9.0 Hz, 1H), 5.18 (m, 2H), 5.01 (m, 2H), 4.54 (s, 1H), 3.84 (s, 3H), 3.79 (s, 3H), 3.45 (s, 3H), 1.53 (s, 3H), 1.05-0.92 (m, 21H), 0.40 (d, *J*= 7.2 Hz, 3H); **^{13}C NMR** (126 MHz, $CDCl_3$) δ 152.5, 148.0, 142.7, 137.1, 136.6, 135.9, 134.2, 128.5, 128.3, 128.1, 119.8, 116.3, 112.9, 106.8, 104.0, 101.5, 95.7, 80.7, 79.7, 75.4, 61.1, 56.1, 21.4, 18.2, 18.0, 12.6, 11.8 ; **HRMS**: Calcd. for $C_{39}H_{55}ClO_{10}Si$ $[M+Na]^+$ = 769.3151 m/z, found $[M+Na]^+$ = 769.3126 m/z.

Compound 3-45



3-43
Chemical Formula: $C_{42}H_{61}ClO_9Si_2$
Molecular Weight: 801.5610

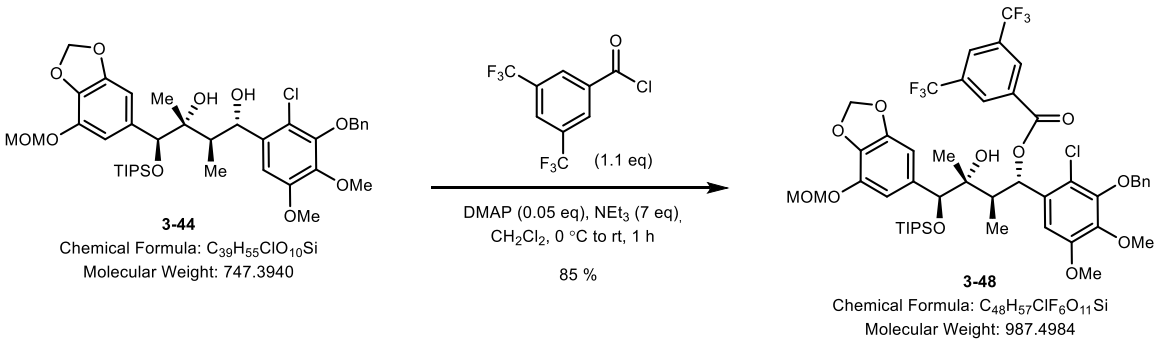
3:1 *dr*
43 % major diastereomer

3-45
Chemical Formula: $C_{43}H_{65}ClO_9Si_2$
Molecular Weight: 817.6040

Procedure: A flame-dried microwave vial equipped with a Teflon-coated stir bar and a rubber septum was charged with **3-43** (0.22 mmol, 180 mg, 1.0 equiv.) and LiH (0.34 mmol, 3 mg, 1.5 equiv.). The flask was evacuated and refilled with N_2 (repeated 3 times), prior to the addition of THF (1.1 mL). The mixture was then cooled to –30 °C in a dry ice/ acetone bath, at which point $TiCl_4$ (0.45 mmol, 1 M in CH_2Cl_2, 0.45 mL, 2.0 equiv.) was added dropwise via syringe, followed by stirring at this temperature for 30 min. The resulting red solution was then cooled to –78 °C, and a solution of MeMgCl (0.90 mmol, 1 M in THF, 0.90 mL, 4.0 equiv.) was added dropwise via syringe pump at a rate of 40 mL/h. The mixture was stirred at this temperature for 1 h, then warmed to –40 °C and stirred for another 3 h. The reaction mixture was quenched by the addition of NH_4Cl (sat. aq., 2.2 mL) followed by NH_4OH (concentrated, 0.24 mL), and stirred at rt for another 15 min. The resulting mixture was then filtered, and the filtrate was extracted with EtOAc (3 × 11 mL). The combined organic layers were dried over $MgSO_4$, filtered, and concentrated *in vacuo*. The crude product (3:1 *dr*) was purified on silica gel (10 % to 20 % ethyl acetate in hexanes) to provide 79 mg, 0.10 mmol, 43 % of the major diastereomer **3-45**.

Characterization: $\mathbf{R}_f$ = (hexanes/EtOAc 9:1): 0.12; **IR** (neat) v = 3462, 2942, 2866, 2355, 1635, 1572, 1486, 1371, 1327, 1157, 1110, 1059, 924, 882, 772, 682 cm^{-1}; **^{1}H NMR** (500 MHz, $CDCl_3$) δ 7.51 (d, *J*= 7.6 Hz, 2H), 7.39-7.28 (m, 3H), 7.05-6.08 (broad s, 2H), 6.70 (s, 1H), 5.93 (s, 1H), 5.35 (s, *J*= 8.8 Hz, 1H), 5.02 (2 x d, *J*= 10.8 Hz, 2H), 4.51 (s, 1H), 3.84 (s, 3H), 3.79 (s, 3H), 1.52 (s, 3H), 1.07-0.91 (m, 30H), 0.40 (d, *J*= 7.0 Hz, 3H), 0.17 (broad s, 6H); **^{13}C NMR** (126 MHz, $CDCl_3$) δ 152.5, 148.8, 147.8, 142.6, 137.3, 137.0, 136.6, 134.0, 128.6, 128.3, 128.1, 119.7, 116.3, 106.7, 103.3, 101.1, 80.5, 79.6, 75.3, 71.8, 61.1, 56.0, 45.1, 25.5, 21.3, 18.3, 18.2, 18.0, 12.6, 11.8, -4.6; **HRMS**: Calcd. for $C_{43}H_{65}ClO_9Si_2$ $[M+Na]^+$ = 839.3753 m/z, found $[M+Na]^+$ = 839.3730 m/z.

Compound 3-48

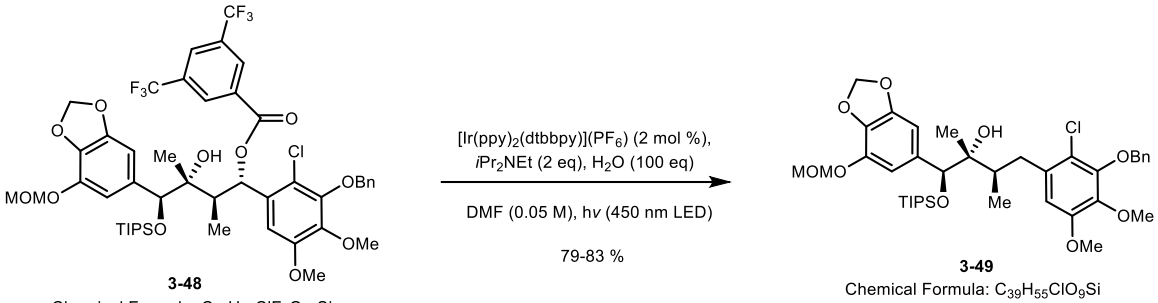


Procedure: A flame-dried 250 mL round bottom flask equipped with a Teflon-coated stir bar and a rubber septum was charged with **3-44** (9.93 mmol, 7.42 g, 1.0 equiv.) and DMAP (0.50 mmol, 61 mg, 0.05 equiv.). The flask was evacuated and refilled with N_2 (repeated 3 times), prior to the addition of CH_2Cl_2 (99 mL), and then triethylamine (69.5 mmol, 9.7 mL, 7.0 equiv.). The reaction mixture was cooled to 0 °C and 3,5-bis-(trifluoromethyl)benzoylchloride (10.9 mmol, 2.0 mL, 1.1 equiv.) was added dropwise. The reaction mixture was stirred at room temperature for 1 h and then concentrated *in vacuo*. The crude product was purified on silica gel (5 % to 15 % ethyl acetate in hexanes) to provide **3-48** (8.28 g, 8.38 mmol, 85 %).

Characterization: $\mathbf{R}_f$ = (hexanes/EtOAc 7:3): 0.71; **IR** (neat) v = 3534, 2943, 2868, 1732, 1636, 1487, 1278, 1138, 1059, 845, 681 cm^{-1}; **^{1}H NMR** (500 MHz, $CDCl_3$) δ 8.49 (s, 2H), 8.04 (s, 1H), 7.50 (d, *J*= 7.2 Hz, 2H), 7.38-7.29 (m, 3H), 6.96-6.44 (broad m, 4H), 6.62 (s, 1H), 6.01 (d, *J*= 1.4 Hz, 1H), 6.00 (d, *J*= 1.4 Hz, 1H), 5.20 (d, *J*= 6.6 Hz, 1H), 5.17 (d, *J*= 6.6 Hz, 1H), 5.04 (s, 2H), 4.56 (s, 1H), 3.85 (s, 3H), 3.80 (s, 3H), 3.45 (s, 3H), 2.23 (m, 1H), 1.45 (s, 3H), 0.99 (m, 12H),

0.92 (m, 9H), 0.46 (d, *J*= 7.2 Hz, 3H); **^{13}C NMR** (126 MHz, $CDCl_3$) δ 163.1, 152.4, 148.8, 148.5, 143.3, 139.6, 136.8, 135.9, 134.9, 133.3, 133.1, 131.9 (q, *J*= 33.6 Hz), 129.9 (m), 129.0, 128.5, 128.3, 128.1, 126.2, 125.9 (m), 122.9 (d, *J*= 272 Hz), 120.4, 119.7, 112.8, 107.0, 103.8, 101.5, 95.5, 80.2, 78.5, 75.3, 61.1, 56.3, 56.0, 53.4, 21.6, 18.1, 17.9, 12.6; **HRMS**: Calcd. for $C_{48}H_{57}ClF_6O_{11}Si$ $[M+Na]^+$ = 1009.3161 m/z, found $[M+Na]^+$ = 1009.3142 m/z.

Compound 3-49



3-48
Chemical Formula: $C_{48}H_{57}ClF_6O_{11}Si$
Molecular Weight: 987.4984

3-49
Chemical Formula: $C_{39}H_{55}ClO_9Si$
Molecular Weight: 731.3950

Procedure in batch: The dimethylformamide (DMF) and water were degassed by sparging with N_2 prior to use. A flame-dried 50 mL Schlenk flask equipped with a Teflon-coated stir bar and a screw cap was charged with **3-48** (1.0 mmol, 987 mg, 1.0 equiv.) and $[Ir(ppy)_2(dtbbpy)]PF_6$ (0.02 mmol, 2 mL of a 0.01 M solution in DMF, 0.02 equiv.). The flask was evacuated and refilled with N_2 (repeated 3 times), before sequentially adding DMF (18 mL), water (2.0 mmol, 1.8 mL, 100 equiv.), and DIPEA (2.0 mmol, 348 µL, 2 equiv.). The reaction mixture was freeze-pump-thawed (x 5), backfilled with N_2, and the screw cap was replaced with a Teflon sealed inlet with a bevelled glass rod. The reaction mixture was stirred while irradiated from the top using a blue LED source (455 nm, 850 mA) connected to the glass rod, while heating from below with an oil bath at 60 °C for 16 h (see photo of setup in Chapter 2.5). The reaction mixture was cooled to room temperature and then diluted with diethyl ether (100 mL). The mixture was washed sequentially with Na_2CO_3 (10 % aq., 50 mL), water (50 mL), and brine (50 mL). The combined organic layers were dried over $MgSO_4$, filtered, and concentrated *in vacuo*. Purified on silica gel (10 % to 25 % ethyl acetate in hexanes) to provide **3-49** (607 mg, 0.83 mmol, 83 %, average over 2 reactions).

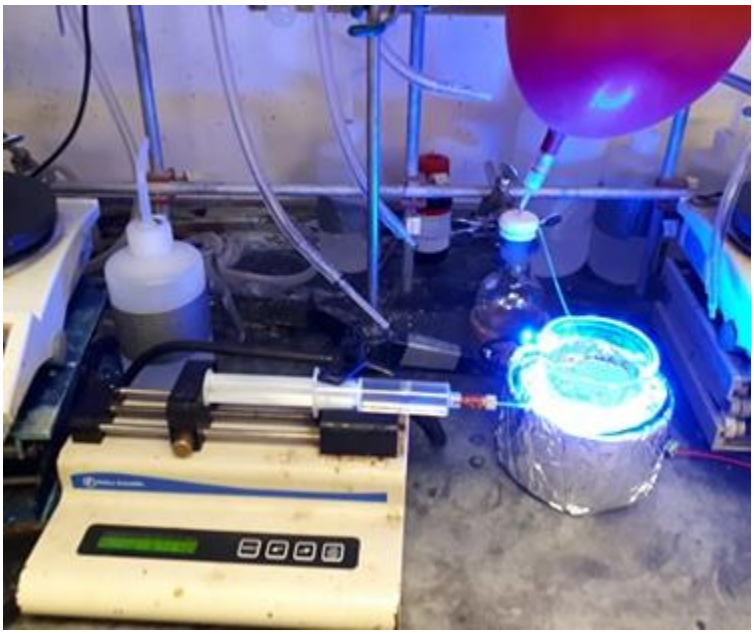
Procedure in flow:

The DMF and water were degassed by sparging with N_2 prior to use. Two flame-dried 250 mL round-bottom flasks* equipped with Teflon-coated stir bars were charged with **3-48** (8.39 mmol,

8.28 g, 1.0 equiv.) and $[Ir(ppy)_2(dtbbpy)]PF_6$ (0.17 mmol, 16.8 mL of a 0.01 M solution in DMF, 0.02 equiv.), distributed equally between the two flasks. The flasks were evacuated and refilled with N_2 (repeated 3 times), before adding DMF (151 mL), water (839 mmol, 15.1 mL, 100 equiv.), and DIPEA (16.8 mmol, 2.9 mL, 2 equiv.), distributed equally between the two flasks. The reaction mixtures were freeze-pump-thawed (x 5), then backfilled with N_2. A syringe pump was used to pump the reaction mixtures through the blue LED photochemical flow setup (see photo below) at a rate of 10 mL/h. After all the reaction mixture had gone through (17 h later), DMF (5 mL), followed by ethyl acetate (50mL) was pumped through the tubing, rinsing into the receiving flask. The contents of the receiving flask were poured into a separatory funnel and diluted with ethyl acetate (150 mL), followed by the addition of water (1.2 L) and separation of the layers. The aqueous layer was washed with ethyl acetate (4 x 200 mL). The combined organic layers were washed with brine, dried over Na_2SO_4, filtered, and concentrated *in vacuo*. Purified on silica gel (10 % to 25 % ethyl acetate in hexanes) to provide **3-49** (4.87g, 6.66 mmol, 79 %).

*Note: Distributing the reaction mixture between two flasks made freeze-pump-thawing much easier.

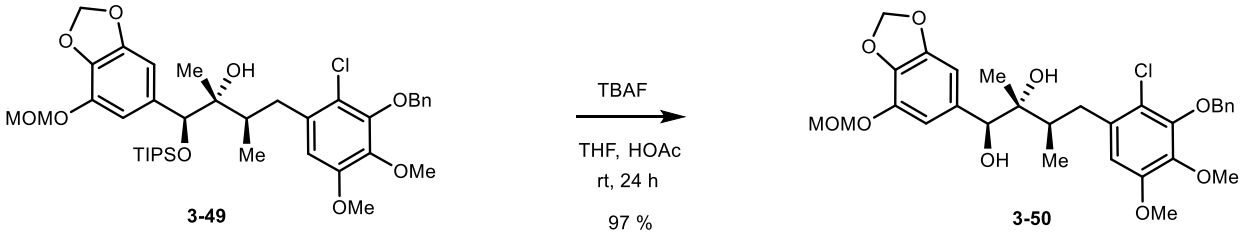
Flow photoredox setup:



Characterization: $\mathbf{R_f}$ = (hexanes/EtOAc 4:1): 0.36; **IR** (neat) v = 3550, 2941, 2866, 1634, 1570, 1486, 1370, 1157, 1117, 1057, 925, 882, 844, 681 cm^{-1}; **^{1}H NMR** (500 MHz, $CDCl_3$) δ 7.51 (d,

J= 7.6 Hz, 2H), 7.39-7.29 (m, 3H), 6.77 (broad s, 2H), 6.42 (s, 1H), 5.95 (d, *J*= 1.2 Hz, 2H), 5.92 (d, *J*= 1.1 Hz, 2H), 5.17 (2 x d, *J*= 6.5 Hz, 2H), 5.00 (s, 2H), 4.57 (s, 1H), 3.83 (s, 3H), 3.78 (s, 3H), 3.43 (s, 3H), 3.20 (dd, *J*= 2.7 Hz, 13.2 Hz, 1H), 2.91 (broad s, 1H), 2.45 (dd, *J*= 11.3 Hz, 13.1 Hz, 1H), 1.63 (ddq, *J*= 3.0 Hz, 6.7 Hz, 1H), 1.33 (s, 3H), 1.06-0.90 (m, 21H), 0.64 (d, *J*= 6.8 Hz, 3H); **^{13}C NMR** (126 MHz, $CDCl_3$) δ 151.5, 148.5, 141.4, 139.6, 137.2, 135.6, 135.3, 135.1, 128.4, 128.3, 128.0, 120.7, 112.8, 109.8, 103.9, 101.3, 95.5, 80.2, 77.8, 75.1, 61.1, 56.1, 56.0, 39.3, 34.5, 20.9, 18.2, 18.0, 14.2, 12.6; **HRMS**: Calcd. for $C_{39}H_{55}ClO_9Si$ $[M+Na]^+$ = 753. 3202 m/z, found $[M+Na]^+$ = 753.3173 m/z.

Compound 3-50



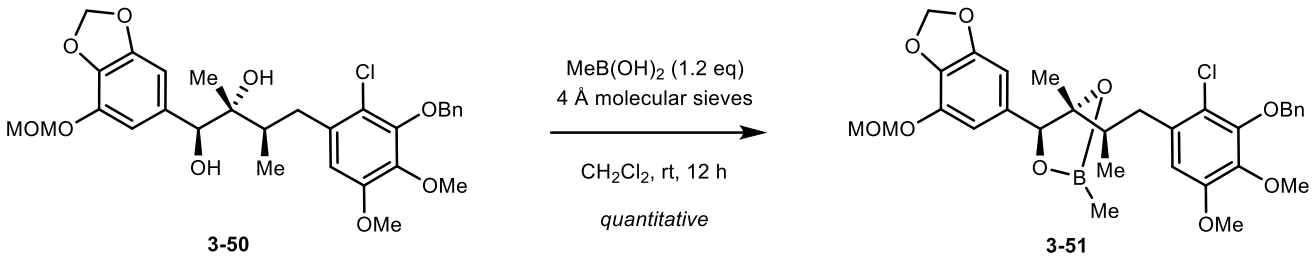
3-49
Chemical Formula: $C_{39}H_{55}ClO_9Si$
Molecular Weight: 731.3950

3-50
Chemical Formula: $C_{30}H_{35}ClO_9$
Molecular Weight: 575.0510

Procedure: A flame-dried 100 mL round bottom flask equipped with a Teflon-coated stir bar and a rubber septum was charged with **3-49** (6.66 mmol, 4.87 g, 1.0 equiv.). The flask was evacuated and refilled with N_2 (repeated 3 times), prior to the addition of THF (13.3 mL). A solution of TBAF·3 H_2O (20.0 mmol, 6.31 g, 3.0 equiv.) and acetic acid (7.99 mmol, 458 µL, 3.0 equiv.) in THF (20 mL) was added, and the resulting mixture was stirred at rt for 24 h. It was then poured on $NaHCO_3$ (saturated aqueous, 72 mL) and extracted with ethyl acetate (3 × 72 mL). The combined organic layers were dried over $MgSO_4$, filtered, and concentrated *in vacuo*. The crude product was purified on silica gel (20 % to 100 % ethyl acetate in hexanes) to provide **3-50** (3.44 g, 6.46 mmol, 97 %).

Characterization: **R_f** = (hexanes/EtOAc 1:1): 0.44; **^{1}H NMR** (500 MHz, $CDCl_3$) δ 7.50 (d, *J*= 7.5 Hz, 2H), 7.37-7.28 (m, 3H), 6.76 (d, 6.3 Hz, 2H), 6.46 (s, 1H), 5.92 (s, 1H), 5.17 (2 x d, *J*= 6.5 Hz, 2H), 5.00 (s, 1H), 4.53 (s, 1H), 3.83 (s, 3H), 3.79 (s, 3H), 3.45 (s, 3H), 3.20 (dd, *J*= 2.8 Hz, 13.3 Hz, 1H), 2.42 (dd, *J*= 11.1 Hz, 13.1 Hz, 1H), 1.79 (ddq, *J*= 3.0 Hz, 6.8 Hz, 1H), 1.28 (s, 3H), 0.74 (d, *J*= 6.9 Hz, 3H).

Compound 3-51



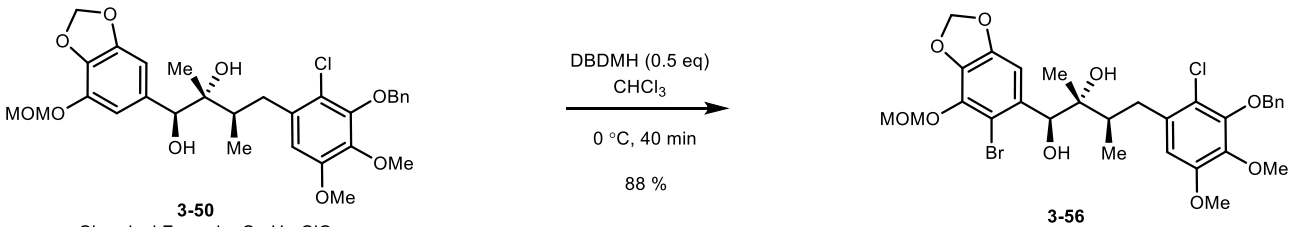
3-50
Chemical Formula: $C_{30}H_{35}ClO_9$
Molecular Weight: 575.0510

3-51
Chemical Formula: $C_{31}H_{36}BClO_9$
Molecular Weight: 598.8800

Procedure: A flame-dried 4-dram vial equipped with a Teflon-coated stir bar and a septum cap was charged with **3-50** (0.54 mmol, 353 mg, 1.0 equiv.), methylboronic acid (0.65 mmol, 39 mg, 1.0 equiv.), and 4 Å molecular sieves (270 mg). The flask was evacuated and refilled with N_2 (repeated 3 times), prior to the addition of CH_2Cl_2 (2.7 mL). The reaction mixture was stirred at room temperature for 12 h, followed by filtration to remove solids and then concentration of the filtrate *in vacuo*. The crude product was purified on silica gel (in 20 % to 50 % ethyl acetate in hexanes) to provide **3-51** (323 mg, 0.54 mmol, quantitative).

Characterization: $\mathbf{R_f}$ = (hexanes/EtOAc 1:1): 0.77; **^{1}H NMR** (500 MHz, $CDCl_3$) δ 7.51 (d, *J*= 7.5 Hz, 2H), 7.38-7.29 (m, 3H), 6.69 (s, 1H), 6.55 (s, 1H), 6.15 (s, 1H), 5.94 (d, *J*= 1.3 Hz, 2H), 5.18 (2 x d, *J*= 6.6 Hz, 2H), 5.01 (s, 2H), 4.99 (s, 1H), 3.82 (s, 3H), 3.76 (s, 3H), 3.41 (s, 3H), 3.09 (dd, *J*= 2.5 Hz, 13.1 Hz, 1H), 2.36 (dd, *J*= 11.2 Hz, 12.8 Hz, 1H), 1.91 (ddq, *J*= 2.9 Hz, 6.8 Hz, 1H), 1.49 (s, 3H), 0.44 (d, *J*= 6.8 Hz, 3H), 0.43 (s, 3H); **^{13}C NMR** (126 MHz, $CDCl_3$) δ 151.6, 149.1, 148.7, 141.7, 140.3, 137.2, 135.8, 134.7, 132.7, 128.5, 128.4, 128.1, 120.7, 110.8, 109.7, 102.0, 101.6, 95.5, 88.1, 87.1, 75.3, 61.2, 56.3, 56.0, 38.8, 34.9, 24.2, 14.3, -5.7; **HRMS**: Calcd. for $C_{31}H_{36}BClO_9$ $[M+Na]^+$ = 621.2039 m/z, found $[M+Na]^+$ = 621.2043 m/z.

Compound 3-56



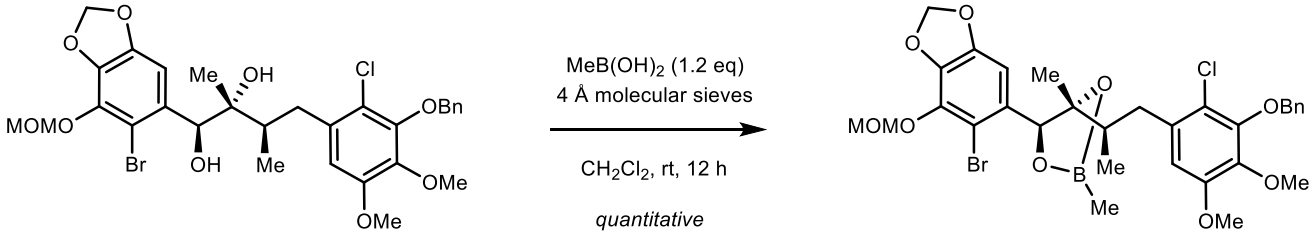
3-50
Chemical Formula: $C_{30}H_{35}ClO_9$
Molecular Weight: 575.0510

3-56
Chemical Formula: $C_{30}H_{34}BrClO_9$
Molecular Weight: 653.9470

Procedure: A 250 mL flame-dried round bottom flask equipped with a Teflon-coated stir bar and a rubber septum was charged with **3-50** (5.98 mmol, 3.44 g, 1.0 equiv.), which was then dissolved in $CHCl_3$ (60 mL). The mixture was cooled to 0 °C in an ice bath, at which point 1,3-dibromo-5,5-dimethylhydantoin (DBDMH, 2.99 mmol, 855 mg, 0.5 equiv.) was added as a solid in portions. (An orange color appeared when the first portion of DBDMH was added, and the next portion was added after the orange color faded). The resulting solution was stirred at 0 °C for 40 min and then concentrated *in vacuo*. The crude product was purified on silica gel (22 % to 32 % ethyl acetate in hexanes) to provide **3-56** (3.44 g, 5.27 mmol, 88 %).

Characterization: $\mathbf{R_f}$ = (hexanes/EtOAc 1:1): 0.44; **^{1}H NMR** (500 MHz, $CDCl_3$) δ 7.52 (d, *J*= 7.5 Hz, 2H), 7.39-7.29 (m, 3H), 7.38 (s, 1H), 6.51 (s, 1H), 5.96 (2 x d, *J*= 1.4 Hz, 2H), 5.29 (d, *J*= 6.0 Hz, 1H), 5.24 (d, *J*= 6.0 Hz, 1H), 5.19 (d, *J*= 4.5 Hz, 1H), 5.03 (s, 2H), 3.85 (s, 3H), 3.82 (s, 3H), 3.56 (s, 3H), 3.27 (dd, *J*= 2.9 Hz, 13.1 Hz, 1H), 2.43 (dd, *J*= 11.1 Hz, 13.1 Hz, 1H), 2.29 (d, J= 4.9 Hz, 1H), 1.97 (ddq, *J*= 3.0 Hz, 6.8 Hz, 1H), 1.36 (s, 3H), 0.72 (d, *J*= 6.9 Hz, 3H); **^{13}C NMR** (126 MHz, $CDCl_3$) δ 151.5, 148.7, 148.5, 141.7, 138.1, 137.2, 136.4, 134.8, 134.2, 128.4, 128.3, 128.0, 120.5, 111.0, 110.1, 104.8, 101.9, 97.1, 78.2, 75.8, 75.3, 61.1, 57.5, 56.1, 40.2, 35.1, 21.0, 20.5, 13.9; **HRMS**: Calcd. for $C_{30}H_{34}BrClO_9$ $[M+Na]^+$ = 675. 0972 m/z, found $[M+Na]^+$ = 675.0969 m/z.

Compound 3-57



3-56
Chemical Formula: $C_{30}H_{34}BrClO_9$
Molecular Weight: 653.9470

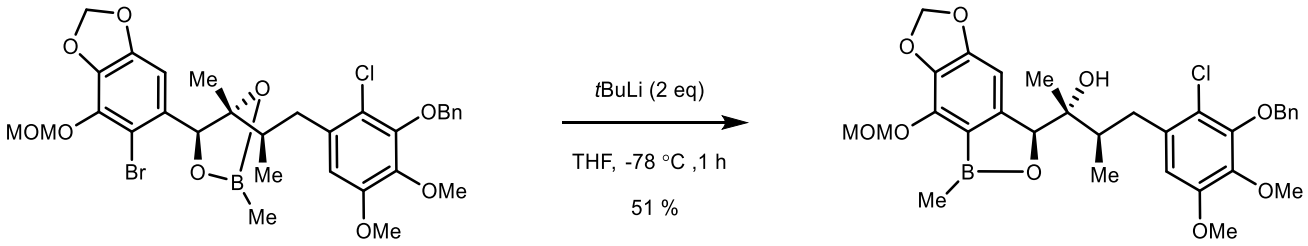
3-57
Chemical Formula: $C_{31}H_{35}BBrClO_9$
Molecular Weight: 677.7760

Procedure: A flame-dried 50 mL round bottom flask equipped with a Teflon-coated stir bar and a septum cap was charged with **3-56** (4.42 mmol, 2.89 g, 1.0 equiv.), methylboronic acid (5.30 mmol, 318 mg, 1.0 equiv.), and 4 Å molecular sieves (2.21 g). The flask was evacuated and refilled with N_2 (repeated 3 times), prior to the addition of CH_2Cl_2 (22.1 mL). The reaction mixture was stirred at room temperature for 12 h. The solids were filtered off and the filtrate was concentrated

in vacuo. The crude product was purified via silica gel plug (in 20% to 50% ethyl acetate in petroleum ether) to provide **3-57** (3.00 g, 4.42 mmol, quantitative).

Characterization: $\mathbf{R_f}$ = (hexanes/EtOAc 7:3): 0.49; **IR** (neat) v = 2933, 1738, 1609, 1570, 1474, 1416, 1363, 1270, 1160, 1112, 1060, 1017, 924, 838, 749, 698 cm^{-1}; **^{1}H NMR** (500 MHz, $CDCl_3$) δ 7.53 (d, J= 8.0 Hz, 2H), 7.38 (m, 2H), 7.33 (m, 1H), 6.67 (s, 1H), 6.33 (s, 1H), 5.96 (s, 2H), 5.58 (s, 1H), 5.26 (d, J= Hz, 2H), 5.24 (d, J= 6.0 Hz, 2H), 5.03 (s, 1H), 3.85 (s, 3H), 3.80 (s, 3H), 3.53 (s, 3H), 3.23 (dd, *J*= 2.9 Hz, 13.2 Hz, 1H), 2.32 (dd, J= 11.0 Hz, 13.2 Hz, 1H), 1.99 (ddq, *J*= 2.9 Hz, 6.5 Hz, 1H), 1.58 (s, 3H), 0.42 (s, 3H), 0.40 (d, *J*= 6.7 Hz, 3H); **^{13}C NMR** (126 MHz, $CDCl_3$) δ 151.5, 148.7, 148.6, 141.7, 138.0, 137.2, 136.3, 134.6, 132.4, 128.4, 128.3, 128.1, 120.6, 110.0, 109.9, 103.8, 102.0, 97.0, 87.6, 86.5, 75.2, 61.1, 57.4, 56.1, 38.5, 35.7, 23.9, 14.3, -5.9; **HRMS**: Calcd. for $C_{31}H_{35}BBrClO_9$ $[M+Na]^+$ = 699.1144 m/z, found $[M+Na]^+$ = 699.1138 m/z.

Compound 3-52



3-57
Chemical Formula: $C_{31}H_{35}BBrClO_9$
Molecular Weight: 677.7760

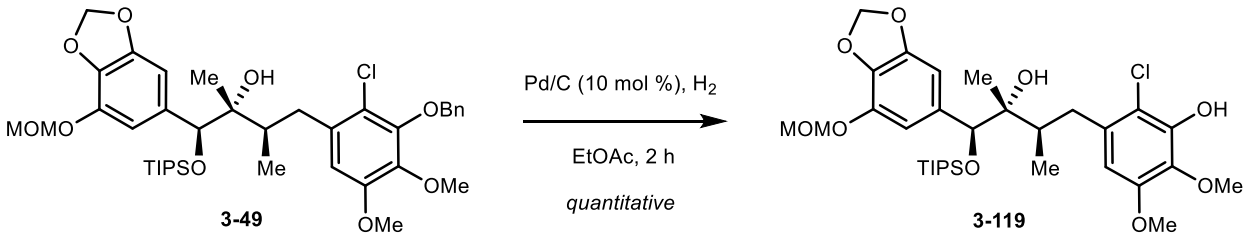
3-52
Chemical Formula: $C_{31}H_{36}BClO_9$
Molecular Weight: 598.8800

Procedure: A flame-dried 25 mL round bottom flask equipped with a Teflon-coated stir bar and a septum cap was charged with **3-57** (1.02 mmol, 693 mg, 1.0 equiv.). The flask was evacuated and refilled with N_2 (repeated 3 times), prior to the addition of THF (10.2 mL). The reaction mixture was cooled to −78 °C in a dry ice/ acetone bath and then *tert*-butyllithium (2.04 mmol, 4.01 mL of 0.50 M solution in pentanes, 2.0 equiv.) was slowly added via syringe. The reaction mixture was stirred for 1 h at −78 °C. It was quenched with NH_4Cl (sat. aq., 1.25 mL) and water (6.25 mL), then extracted with ethyl acetate (3 x 6 mL). The combined organic layers were dried over Na_2SO_4, filtered, and concentrated *in vacuo*. The crude product was purified via silica gel (25 % to 35 % ethyl acetate in hexanes) to provide **3-52** (315 mg, 0.57 mmol, 51 %).

Characterization: $\mathbf{R_f}$ = (hexanes/EtOAc 7:3): 0.38; **IR** (neat) v = 3503, 2965, 2936, 2906, 1730, 1603, 1571, 1465, 1323, 1248, 1158, 1105, 1014, 928, 837, 752, 698 cm^{-1}; **^{1}H NMR** (500 MHz,

$CDCl_3$) δ 7.54 (d, 2H), 7.40-7.30 (m, 3H), 6.80 (s, 1H), 6.60 (s, 1H), 5.98 (s, 2H), 5.39 (d, *J*= 6.0 Hz, 1H), 5.33 (broad s, 1H), 5.31 (d, *J*= 6.0 Hz, 1H), 5.06 (s, 2H), 3.88 (s, 3H), 3.86 (s, 3H), 3.54 (s, 3H), 3.23 (dd, *J*= 3.0 Hz, 13.2 Hz, 1H), 2.66 (dd, *J*= 11.3 Hz, 13.1 Hz, 1H), 2.23 (ddq, *J*= 3.1 Hz, 6.8 Hz, 1H), 1.01 (s, 3H), 0.88 (d, *J*= 6.9 Hz, 3H), 0.84 (s, 3H); **^{13}C NMR** (126 MHz, $CDCl_3$) δ 153.1, 151.6, 150.8, 148.7, 141.69, 141.67, 137.2, 135.6, 135.1, 128.4, 128.3, 128.0, 125.1, 120.7, 110.0, 101.4, 99.4, 96.4, 88.1, 76.5, 75.3, 61.2, 56.8, 56.1, 41.3, 34.9, 19.5, 13.5, 0,98; **HRMS**: Calcd. for $C_{31}H_{36}BClO_9$ $[M+Na]^+$ = 621.2039 m/z, found $[M+Na]^+$ = 621.2021 m/z.

Compound 3-119



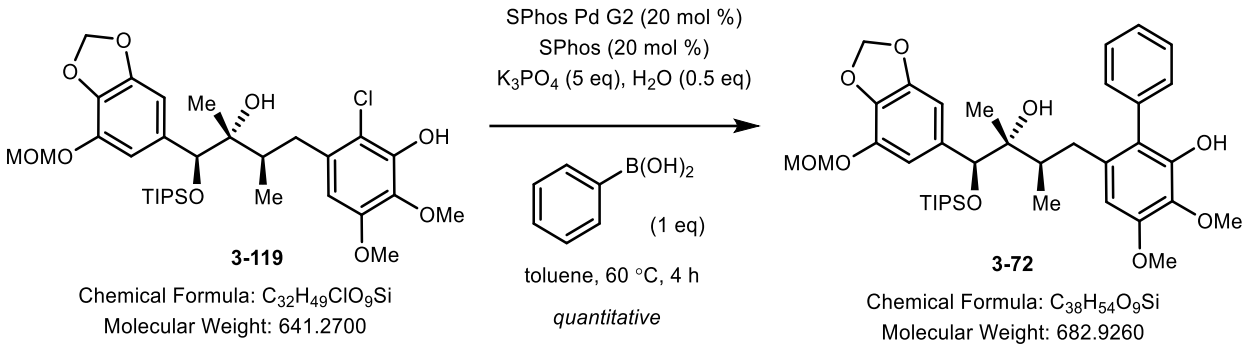
Chemical Formula: $C_{39}H_{55}ClO_9Si$
Molecular Weight: 731.3950

Chemical Formula: $C_{32}H_{49}ClO_9Si$
Molecular Weight: 641.2700

Procedure: A flame-dried microwave vial equipped with Teflon-coated stir bar was charged with **3-49** (0.10 mmol, 73.5 mg, 1.0 equiv.) and palladium on carbon (10 wt %, 0.01 mmol, 7.4 mg, 0.1 equiv.). The flask was evacuated and refilled with N_2 (repeated 3 times), prior to the addition of ethyl acetate (0.5 mL). The N_2 atmosphere was exchanged for H_2. The reaction mixture was stirred at rt under H_2 for 2 h. It was then filtered through celite and the filtrate was concentrated *in vacuo*. The crude product was purified via silica gel (15 % to 50 % ethyl acetate in hexanes) to provide **3-119** (64 mg, 0.10 mmol, *quantitative*).

Characterization: $\mathbf{R_f}$ = (hexanes/EtOAc 4:1): 0.20; **^{1}H NMR** (500 MHz, $CDCl_3$) δ 6.77 (broad s, 2H), 6.21 (s, 1H), 5.93 (m, 3H), 5.15 (2 x d, *J*= 6.4 Hz, 2H), 4.55 (s, 1H), 3.84 (s, 3H), 3.76 (s, 3H), 3.42 (s, 3H), 3.21 (dd, *J*= 2.3 Hz, 13.2 Hz, 1H), 2.92 (s, 1H), 2.36 (dd, J= 11.3 Hz, 12.8 Hz, 1H), 1.63 (m, 1H), 1.32 (s, 3H), 1.02-0.93 (m, 21H), 0.63 (d, *J*= 6.7 Hz, 3H); **^{13}C NMR** (126 MHz, $CDCl_3$) δ 150.5, 148.4, 145.4, 139.5, 135.6, 135.2, 135.0, 134.3, 112.9, 112.7, 106.0, 103.9, 101.3, 95.4, 80.2, 77.7, 60.9, 56.1, 55.8, 38.9, 34.4, 20.8, 18.1, 17.9, 12.6; **HRMS**: Calcd. for $C_{39}H_{55}ClO_9Si$ $[M+Na]^+$ = 663.2732 m/z, found $[M+Na]^+$ = 663.2730 m/z.

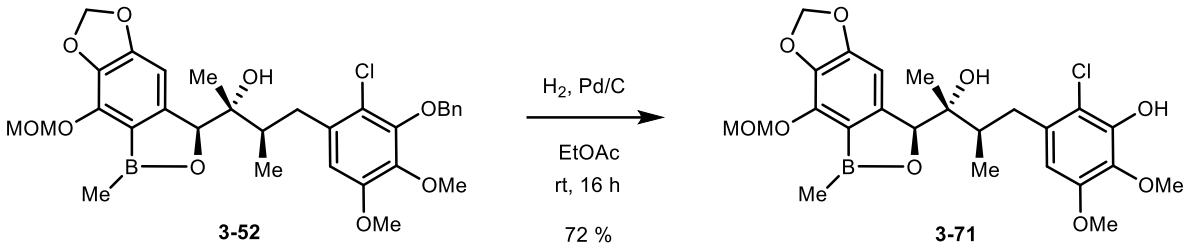
Compound 3-72



Procedure: A 10 mL flame-dried Schlenk flask equipped with a Teflon-coated stir bar and a glass stopper was charged with **3-119** (0.05 mmol, 32 mg, 1.0 equiv.), phenylboronic acid (0.05 mmol, 6.1 mg, 1.0 equiv.), SPhos Pd G2 (0.01 mmol, 7.2 mg, 20 mol%), SPhos (0.01 mmol, 4.1 mg, 20 mol%) and K_3PO_4 (0.25 mmol, 53.1 mg, 5.0 equiv.). The flask was evacuated and refilled with N_2 (repeated 3 times), prior to the addition of a stock solution of H_2O (0.5 mmol, 0.5 μL, 0.5 equiv.) in toluene (1 mL). The mixture was warmed to 60 °C in a pre-heated oil bath for 4 h. It was then poured on a solution consisting of H_3PO_4 (2 M, 0.5 mL) and brine (0.5 mL), and extracted with EtOAc (3 × 1 mL). The combined organic layers were dried over $MgSO_4$, filtered, and concentrated *in vacuo*. The crude product was purified on silica gel (15 % to 50 % ethyl acetate in hexanes) to provide **3-72** (34 mg, 0.05 mmol, quantitative).

Characterization: $\mathbf{R_f}$ = (hexanes/EtOAc 4:1): 0.32; **IR** (neat) v = 3522, 2942, 2360, 1635, 1614, 1580, 1490, 1458, 1338, 1135, 1058, 925, 882, 771, 681 cm^{-1}; **^{1}H NMR** (500 MHz, $CDCl_3$) δ 7.35 (m, 2H), 7.30 (m, 1H), 7.23-6.88 (m, 2H), 6.60 (broad s, 2H), 6.26 (s, 1H), 6.00 (d, *J*= 1.3 Hz, 1H), 5.99 (d, *J*= 1.3 Hz, 1H), 5.51 (s, 1H), 5.18 (s, 2H), 4.48 (s, 1H), 3.88 (s, 3H), 3.83 (s, 3H), 3.45 (s, 3H), 3.04 (dd, *J*= 2.4 Hz, 13.2 Hz, 1H), 1.98 (dd, *J*= 10.9 Hz, 13.2 Hz, 1H), 1.58 (broad s, 1H), 1.26 (m, 1H), 1.09 (s, 3H), 0.97 (m, 12H), 0.90 (m, 9H), 0.58 (dd, *J*= 6.7 Hz, 3H); **^{13}C NMR** (126 MHz, $CDCl_3$) δ 150.8, 146.6, 139.4, 136.0, 135.9, 135.5, 135.2, 133.3, 130.6, 128.1, 126.9, 122.2, 112.6, 105.6, 103.9, 101.4, 95.5, 79.6, 77.5, 60.9, 56.1, 55.7, 39.9, 34.0, 19.9, 18.1, 18.0, 14.5, 12.6; **HRMS**: Calcd. for $C_{38}H_{54}O_9Si$ $[M+Na]^+$ = 705.3435 m/z, found $[M+Na]^+$ = 705.34207 m/z.

Compound 3-71



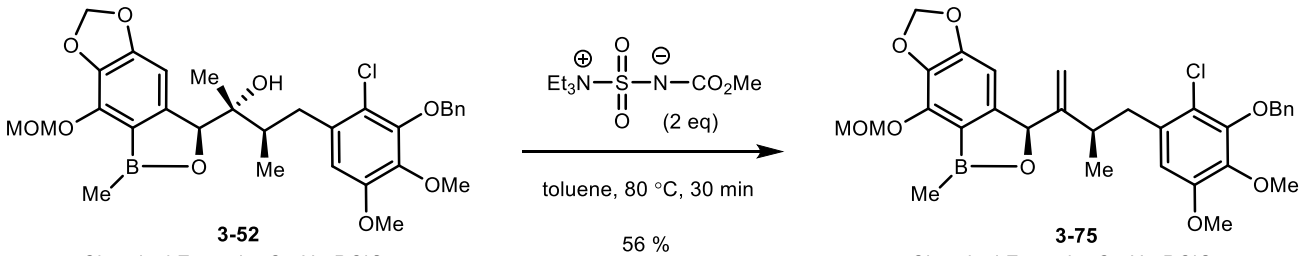
3-52
Chemical Formula: $C_{31}H_{36}BClO_9$
Molecular Weight: 598.8800

3-71
Chemical Formula: $C_{24}H_{30}BClO_9$
Molecular Weight: 508.7550

Procedure: A flame-dried 25 mL round bottom flask equipped with Teflon-coated stir bar was charged with **3-52** (0.59 mmol, 353 mg, 1.0 equiv.) and palladium on carbon (10 wt %, 0.059 mmol, 62.7 mg, 0.1 equiv.). The flask was evacuated and refilled with N_2 (repeated 3 times), prior to the addition of ethyl acetate (6 mL). The N_2 atmosphere was exchanged for H_2. The reaction mixture was stirred at rt under H_2 for 16 h. It was then filtered through celite and the filtrate was concentrated *in vacuo*. The crude product was purified via silica gel (25 % to 35 % ethyl acetate in hexanes) to provide **3-71** (215 mg, 0.42 mmol, 72 %).

Characterization: $\mathbf{R_f}$ = (hexanes/EtOAc 3:1): 0.52; **IR** (neat) v = 3537, 3321, 2961, 2934, 2895, 1732, 1603, 1579, 1467, 1315, 1247, 1153, 1104, 1043, 1017, 969, 915, 823 cm^{-1}; **^{1}H NMR** (500 MHz, $CDCl_3$) δ 6.79 (s, 1H), 6.39 (s, 1H), 5.98 (s, 2H), 5.38 (d, *J*= 6.0 Hz, 1H), 5.32 (s, 1H), 5.31 (d, *J*= 6.1 Hz, 1H), 3.89 (s, 3H), 3.85 (s, 3H), 3.53 (s, 3H), 3.22 (dd, *J*= 2.8 Hz, 13.2 Hz, 1H), 2.61 (dd, J= 11.4 Hz, 13.0 Hz, 1H), 2.23 (ddq J= 3.2 Hz, 7.1 Hz, 1H), 1.03 (s, 3H), 0.88 (d, *J*= 7.0 Hz, 3H), 0.84 (s, 3H); **^{13}C NMR** (126 MHz, $CDCl_3$) δ 153.1, 150.7, 150.6, 145.6, 141.6, 135.6, 135.1, 134.5, 112.9, 106.2, 101.4, 99.3, 96.3, 88.2, 76.6, 61.0, 56.8, 56.0, 41.1, 34.8, 19.5, 13.5; **HRMS**: Calcd. for $C_{24}H_{30}BClO_9$ $[M+Na]^+$ = 531.1569 m/z, found $[M+Na]^+$ = 531.15708 m/z.

Compound 3-75



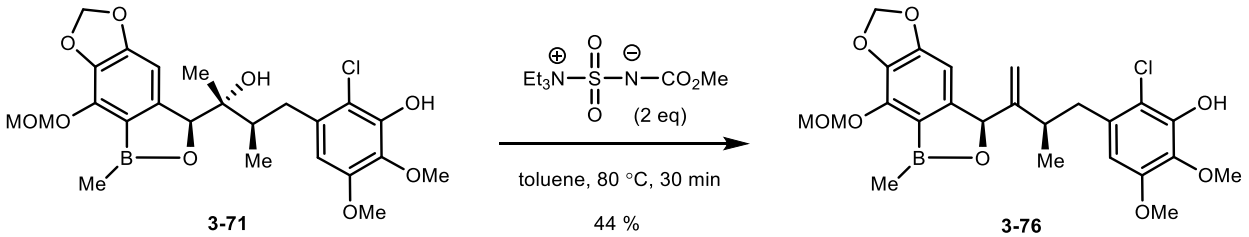
3-52
Chemical Formula: $C_{31}H_{36}BClO_9$
Molecular Weight: 598.8800

3-75
Chemical Formula: $C_{31}H_{34}BClO_8$
Molecular Weight: 580.8650

Procedure: A flame-dried 25 mL round bottom flask equipped with a Teflon-coated stir bar and a rubber septum was charged with **3-52** (0.060 mmol, 36 mg, 1.0 equiv.) and Burgess reagent (0.12 mmol, 29 mg, 2.0 equiv.). The flask was evacuated and refilled with N_2 (repeated 3 times), prior to the addition of toluene (3 mL). The reaction mixture was stirred at 80 °C for 30 minutes and then allowed to cool to room temperature. It was then concentrated *in vacuo* and the residue was taken up in ethyl acetate and water. The layers were separated and the organic layer was washed with brine. The organic layer was dried over Na_2SO_4, filtered, and concentrated *in vacuo*. The crude product was purified via silica gel (15 % to 30 % ethyl acetate in hexanes) to provide **3-75** (20 mg, 0.034 mmol, 56 %).

Characterization: $\mathbf{R_f}$ = (hexanes/EtOAc 7:3): 0.40; **IR** (neat) v = 2959, 2930, 1735, 1605, 1570, 1465, 1368, 1313, 1247, 1217, 1159, 1112, 1055, 1018, 932 cm^{-1}; **^{1}H NMR** (500 MHz, $CDCl_3$) δ 7.52 (d, *J*= 7.8 Hz, 2H), 7.39-7.29 (m, 3H), 6.49 (s, 1H), 6.43 (d, *J*= 0.7 Hz, 1H), 5.97 (2 x d, *J*= 1.3 Hz, 2H), 5.59 (s, 1H), 5.38 (d, *J*= 6.0 Hz, 1H), 5.32 (d, *J*= 6.0 Hz, 1H), 5.28 (s, 1H), 5.19 (s, 1H), 5.02 (2 x d, *J*= 10.6 Hz, 2H), 3.84 (s, 3H), 3.83 (s, 3H), 3.54 (s, 3H), 3.02 (dd, *J*= 5.3 Hz, 13.4 Hz, 1H), 2.58 (dd, *J*= 9.7, 13.6 Hz, 1H), 2.12 (m, 1H), 0.87 (s, 3H), 0.80 (d, *J*= 6.9 Hz, 3H); **^{13}C NMR** (126 MHz, $CDCl_3$) δ 153.3, 152.9, 152.0, 151.4, 148.6, 141.7, 141.5, 137.2, 135.6, 134.3, 128.38, 128.34, 128.0, 125.4, 120.3, 113.9, 110.1, 101.5, 97.9, 96.4, 90.1, 75.2, 61.1, 56.9, 56.1, 41.9, 33.1, 20.7; **HRMS**: Calcd. for $C_{31}H_{34}BClO_8$ $[M+Na]^+$ = 603.1933 m/z, found $[M+Na]^+$ = 603.1937 m/z.

Compound 3-76



3-71
Chemical Formula: $C_{24}H_{30}BClO_9$
Molecular Weight: 508.7550

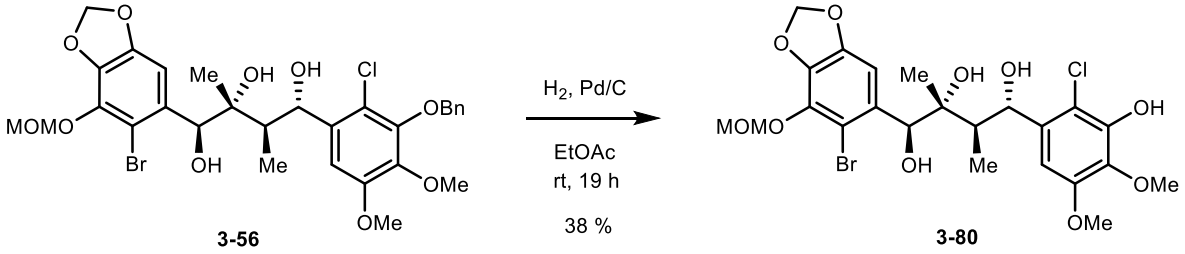
3-76
Chemical Formula: $C_{24}H_{28}BClO_8$
Molecular Weight: 490.7400

Procedure: A flame-dried 25 mL round bottom flask equipped with Teflon-coated stir bar and a rubber septum was charged with **3-71** (0.42 mmol, 215 mg, 1.0 equiv.) and Burgess reagent (0.84 mmol, 201 mg, 2.0 equiv.). The flask was evacuated and refilled with N_2 (repeated 3 times), prior to the addition of toluene (21 mL). The reaction mixture was stirred at 80 °C for 30 minutes and

then allowed to cool to room temperature. It was then oncentrated *in vacuo* and the residue was taken up in ethyl acetate (50 mL) and water (50 mL). The layers were separated and the aqueous layer was washed with ethyl acetate (2 x 50 mL). The combined organic layers were washedwith brine, dried over Na_2SO_4, filtered, and concentrated *in vacuo*. The crude product was purified via silica gel (20 % to 50 % ethyl acetate in hexanes) to provide **3-76** (90 mg, 0.18 mmol, 44 %).

Characterization: $\mathbf{R_f}$ = (hexanes/EtOAc 3:1): 0.38; **^{1}H NMR** (500 MHz, $CDCl_3$) δ 6.42 (s, 1H), 6.28 (s, 1H), 5.96 (2 x d, J= 1.2 Hz, 2H), 5.93 (s, 1H), 5.58 (s, 1H), 5.38 (d, *J*= 6.0 Hz, 1H), 5.31 (d, *J*= 6.0 Hz, 1H), 5.29 (s, 1H), 5.20 (s, 1H), 3.85 (s, 3H), 3.81 (s, 3H), 3.54 (s, 3H), 2.99 (dd, *J*= 5.3 Hz, 13.4 Hz, 1H), 2.54 (dd, *J*= 9.5 Hz, 13.5 Hz, 1H), 2.10 (m, 1H), 0.86 (s, 3H), 0.80 (d, *J*= 6.9 Hz, 3H); **^{13}C NMR** (126 MHz, $CDCl_3$) δ 153.3, 152.9, 152.0, 150.4 145.5, 141.5, 135.6, 134.5, 134.2, 113.9, 112.5, 106.3, 101.4, 97.8, 96.4, 90.1, 61.0, 56.8, 55.9, 41.8, 32.9, 20.8, 14.2, 1.1; **HRMS**: Calcd. for $C_{24}H_{28}BClO_8$ $[M+Na]^+$ = 513.1463 m/z, found $[M+Na]^+$ = 513.1455 m/z.

Compound 3-80



3-56
Chemical Formula: $C_{30}H_{34}BrClO_{10}$
Molecular Weight: 669.9460

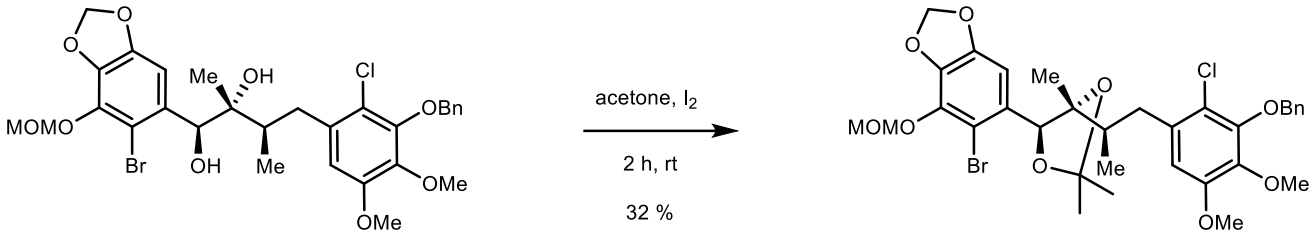
3-80
Chemical Formula: $C_{23}H_{28}BrClO_{10}$
Molecular Weight: 579.8210

Procedure: A flame-dried 50 mL round bottom flask equipped with Teflon-coated stir bar was charged with **3-56** (1.3 mmol, 856 mg, 1.0 equiv.) and palladium on carbon (10 wt %, 0.13 mmol, 139 mg, 0.1 equiv.). The flask was evacuated and refilled with N_2 (repeated 3 times), prior to the addition of ethyl acetate (13 mL). The N_2 atmosphere was exchanged for H_2. The reaction mixture was stirred for 16 h at rt under H_2. It was then filtered through celite and the filtrate was concentrated *in vacuo*. The crude product was purified via silica gel (40 % ethyl acetate in hexanes) to provide **3-80** (280 mg, 0.50 mmol, 38 %).

Characterization: $\mathbf{R_f}$ = (hexanes/EtOAc 3:2): 0.03; **IR** (neat) v = 3464, 3376, 2969, 2938, 2903, 2832, 1604, 1582, 1463, 1341, 1220, 1160, 1098, 1058, 1005, 983, 924, 813, 736, 513, 478 cm^{-1}; **^{1}H NMR** (500 MHz, $CDCl_3$) δ 7.39 (s, 1H), 6.30 (s, 1H), 5.97 (m, 2H), 5.92 (s, 1H), 5.29 (d, *J*=

6.0 Hz, 1H), 5.24 (d, *J*= 6.0 Hz, 1H), 5.18 (s, 1H), 3.87 (s, 3H), 3.81 (s, 3H), 3.56 (s, 3H), 3.28 (dd, *J*= 2.6 Hz, 13.0 Hz, 1H), 2.37 (dd, *J*= 11.2 Hz, 12.8 Hz, 1H), 1.97 (ddq, *J*= 3.1, 7.0 Hz, 1H), 1.36 (s, 3H), 0.71 (d, *J*= 6.9 Hz, 3H); **^{13}C NMR** (126 MHz, $CDCl_3$) δ 150.5, 148.5, 145.6, 138.1, 136.4, 134.8, 134.5, 134.1, 112.6, 111.0, 106.3, 104.8, 101.9, 97.1, 78.2, 75.8, 61.0, 57.5, 56.0, 39.9, 35.0, 20.4, 13.9; **HRMS**: Calcd. for $C_{23}H_{28}BrClO_{10}$ $[M+Na]^+$ = 585.0503 m/z, found $[M+Na]^+$ = 585.0505 m/z.

Compound 3-82



3-56
Chemical Formula: $C_{30}H_{34}BrClO_9$
Molecular Weight: 653.9470

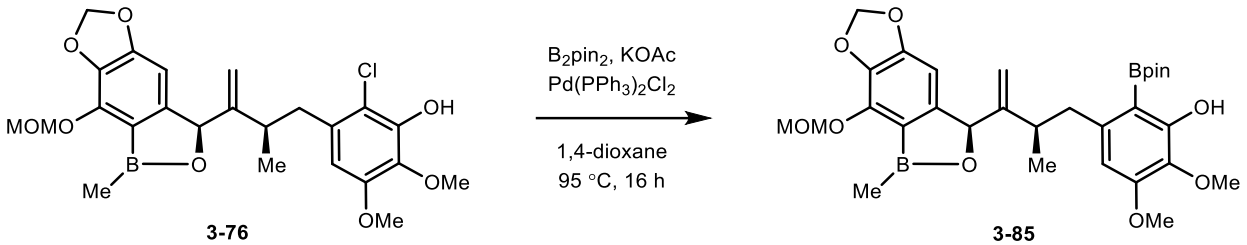
3-82
Chemical Formula: $C_{33}H_{38}BrClO_9$
Molecular Weight: 694.0120

Procedure: A flame-dried 25 mL two-necked flask equipped with Teflon-coated stir bar was charged with **3-56** (0.23 mmol, 150 mg, 1.0 equiv.). The flask was evacuated and refilled with N_2 (repeated 3 times), prior to the addition of acetone (7.5 mL). Then, iodine (45 mg) was added and the reaction mixture was let stir at rt for 2 h. The reaction mixture was quenched by the addition of $Na_2S_2O_3$ (aq., 10 mL) and extracted with CH_2Cl_2 (3 x 10 mL). The combined organic layers were washed with water, dried over Na_2SO_4, filtered, and concentrated *in vacuo*. The crude product was purified via silica gel (25 % to 35 % ethyl acetate in hexanes) to provide **3-82** (51 mg, 0.074 mmol, 32 %).

Characterization: $\mathbf{R_f}$ = (hexanes/EtOAc 3:2): 0.52; **IR** (neat) v = 2931, 2856, 1734, 1608, 1570, 1473, 1417, 1379, 1247, 1216, 1113, 1061, 1027, 926, 772 cm^{-1}; **^{1}H NMR** (500 MHz, $CDCl_3$) δ 7.54 (d, *J*= 7.4 Hz, 2H), 7.41-7.29 (m, 3H), 6.98 (s, 1H), 6.43 (s, 1H), 5.96 (d, *J*= 1.4 Hz, 1H), 5.95 (d, *J*= 1.4 Hz, 1H), 5.41 (s, 1H), 5.28 (d, *J*= 6.0 Hz, 1H), 5.24 (d, *J*= 6.0 Hz, 1H), 5.06 (d, *J*= 10.5 Hz, 1H), 5.02 (d, *J*= 10.6 Hz, 1H), 3.85 (s, 3H), 3.81 (s, 3H), 3.53 (s, 3H), 3.30 (dd, *J*= 3.6 Hz, 13.2 Hz, 1H), 2.33 (dd, *J*= 11.3 Hz, 13.1 Hz, 1H), 2.16 (ddq, *J*= 3.7 Hz, 6.6 Hz, 1H), 1.65 (s, 3H), 1.58 (s, 3H), 1.51 (s, 3H), 0.05 (d, *J*= 6.7 Hz, 3H); **^{13}C NMR** (126 MHz, $CDCl_3$) δ 151.4, 148.67, 148.66, 141.6, 138.0, 137.2, 136.4, 134.9, 130.9, 128.4, 128.3, 128.0, 120.6, 110.3, 109.4, 106.7,

104.1, 101.9, 97.0, 86.3, 83.8, 75.2, 61.1, 57.4, 56.1, 37.3, 35.5, 28.3, 26.6, 21.9, 14.6; **HRMS**: Calcd. for $C_{33}H_{38}BrClO_9$ $[M+Na]^+$ = 715.1285 m/z, found $[M+Na]^+$ = 715.12740 m/z.

Compound 3-85



3-76
Chemical Formula: $C_{24}H_{28}BClO_8$
Molecular Weight: 490.7400

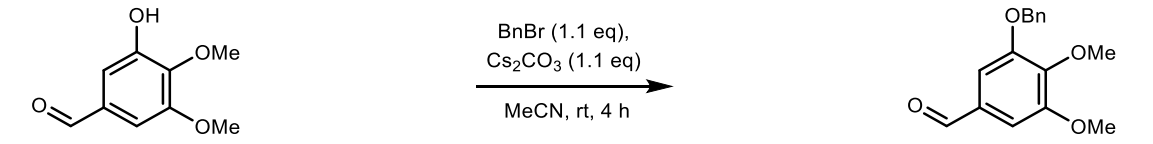
3-85
Chemical Formula: $C_{24}H_{28}BO_8$
Molecular Weight: 455.2900

Procedure: A flame-dried 10 mL Schlenk flask equipped with a Teflon-coated stir bar and a glass stopper was charged with **3-76** (0.15 mmol, 75 mg, 1.0 equiv.), potassium acetate (0.65 mmol, 64 mg, 4.3 equiv.), $Pd(PPh_3)_2Cl_2$ (0.015 mmol, 11 mg, 0.1 equiv.), and bis(pinacolato)diboron (0.18 mmol, 46 mg, 1.2 equiv.). The flask was evacuated and refilled with N_2 (repeated 3 times), prior to the addition of 1,4-dioxane (0.76 mL). The reaction mixture was let stir at 95 °C for 16 h. It was cooled to rt, filtered, and the filtrate was concentrated *in vacuo*. The crude product was purified on silica gel (in 13 % to 23 % ethyl acetate in hexanes) to provide a mixture containing **3-85** and an impurity (3:1 ratio of **3-85** : impurity, 17 mg).*

*Note: Some of the product was spilled prior to weighing, therefore the actual yield may be higher.

Characterization: $\mathbf{R_f}$ = (hexanes/EtOAc 3:1): 0.12; **IR** (neat) v = 3432, 2957, 2926, 1733, 1634, 1579, 1494, 1435, 1348, 1157, 1117, 1058, 922, 694, 541 cm^{-1}; **^{1}H NMR** (500 MHz, $CDCl_3$, major species) δ 6.43 (s, 1H), 6.28 (s, 1H), 5.97 (2 x d, *J*= 1.2 Hz, 2H), 5.89 (s, 1H), 5.58 (s, 1H), 5.39 (d, *J*= 6.1 Hz, 1H), 5.31 (m, 2H), 5.21 (s, 1H), 3.86 (s, 3H), 3.82 (s, 3H), 3.55 (s, 3H), 3.00 (dd, *J*= 5.3 Hz, 13.4 Hz, 1H), 2.54 (m, 1H), 2.09 (m, 1H), 1.25 (s, 9H), 1.23 (s, 3H), 0.86 (s, 3H), 0.80 (d, *J*= 6.9 Hz, 3H).

Compound 3-90



3-22
Chemical Formula: $C_9H_{10}O_4$
Molecular Weight: 182.1750

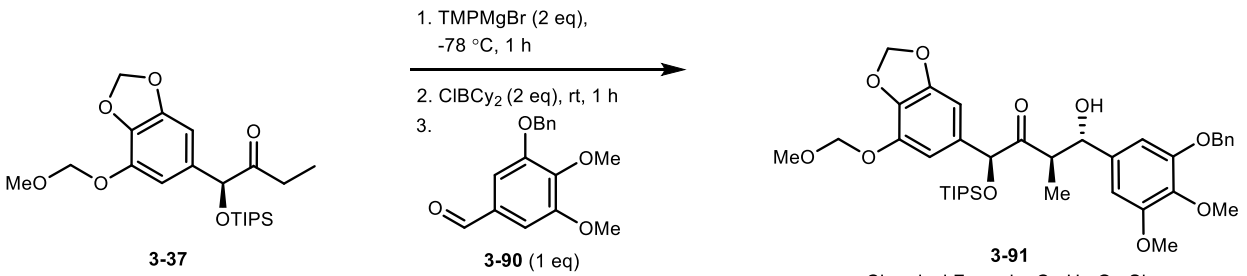
3-90
Chemical Formula: $C_{16}H_{16}O_4$
Molecular Weight: 272.3000

Procedure:

A flame-dried 50 mL round-bottom flask equipped with a Teflon-coated stir bar and a rubber septum was charged with **3-22** (2.6 mmol, 483 mg, 1.0 equiv.) and cesium carbonate (2.86 mmol, 932 mg, 1.1 equiv.). The flask was evacuated and refilled with N_2 (repeated 3 times), prior to the addition of benzyl bromide (2.86 mmol, 340 µL, 1.1 equiv.) and then acetonitrile (26 mL). The reaction mixture was stirred for 4 h at rt. It was then diluted with CH_2Cl_2 (75 mL) and washed sequentially with water (21 mL) and brine (21 mL). The aqueous layers were washed with CH_2Cl_2 (3 x 75 mL). The combined organic layers were dried with Na_2SO_4 and concentrated *in vacuo*. The crude product was purified on silica gel (15 % to 25 % ethyl acetate in hexanes) to provide **3-90** (456 mg, 1.67 mmol, 64 %).

Characterization: $\mathbf{R_f}$ = (hexanes/EtOAc 3:1): 0.45; **IR** (neat) v = 3064, 3031, 3003, 2940, 2833, 2733, 1688, 1584, 1498, 1454, 1426, 1384, 1323, 1231, 1112, 999, 834, 729, 697 cm^{-1}; **^{1}H NMR** (500 MHz, $CDCl_3$) δ 9.82 (s, 1H), 7.45 (d, *J*= 7.8 Hz, 2H), 7.39 (m, 2H), 7.33 (m, 1H), 7.17 (d, *J*= 1.7 Hz, 1H), 7.13 (d, *J*= 1.7 Hz, 1H), 5.19 (s, 2H), 3.96 (s, 3H), 3.93 (s, 3H); **^{13}C NMR** (126 MHz, $CDCl_3$) δ 190.9, 153.9, 152.6, 144.3, 136.4, 131.6, 128.7, 128.2, 127.3, 109.2, 106.7, 71.2, 61.0, 56.5; **HRMS**: Calcd. for $C_{16}H_{16}O_4$ $[M+Na]^+$ = 295.0946 m/z, found $[M+Na]^+$ = 295.09450 m/z.

Compound 3-91



3-37
Chemical Formula: $C_{22}H_{36}O_6Si$
Molecular Weight: 424.6090

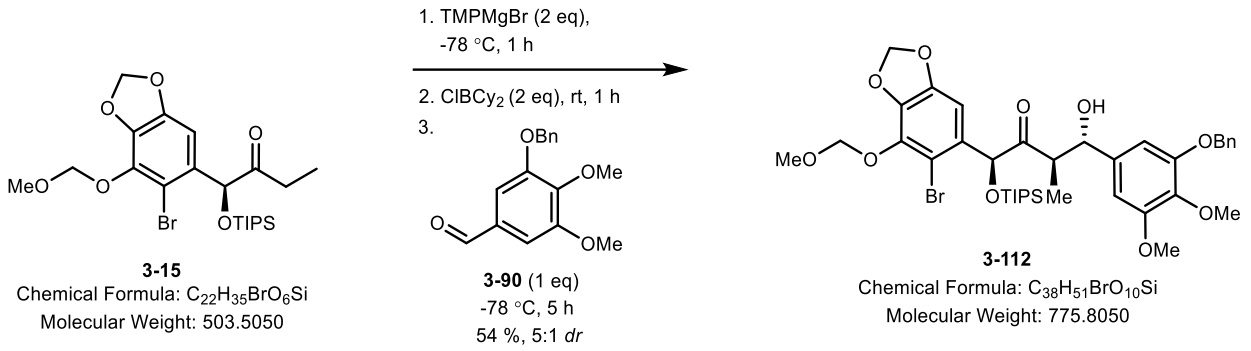
3-90 (1 eq)
18-crown-6 (2 eq)
-78 °C, 8 h
61 %, 2.7:1 *dr*

3-91
Chemical Formula: $C_{38}H_{52}O_{10}Si$
Molecular Weight: 696.9090

Procedure: A 500 mL flame-dried round bottom flask equipped with a Teflon-coated stir bar and a rubber septum was charged with 2,2,6,6-tetramethylpiperidine (freshly distilled over CaH_2, 30.9 mmol, 5.22 mL, 2.4 equiv.) and THF (26 mL). EtMgBr (25.8 mmol, 8.6 mL of 3 M solution in Et_2O, 2.0 equiv.) was added via syringe. The resulting solution was refluxed under N_2 for 12 h, then diluted with additional THF (26 mL), and cooled to –78 °C in a dry ice / acetone bath. A solution of **3-37** (12.9 mmol, 5.47 g, 1.0 equiv.) in THF (26 mL) was added at a rate of 100 mL/h via syringe pump. The reaction mixture was stirred for –78 °C for 1 h, then a solution of Cy_2BCl (26 mmol, 1 M solution in hexanes, 26 mL, 2.0 equiv.) was added via syringe. The reaction mixture was warmed to rt and let stir for another 1 h. It was then cooled to –78 °C, and a solution of **3-90** (12.9 mmol, 3.51 g, 1.0 equiv.) and 18-crown-6 (25.8 mmol, 5.5 mL, 2.0 equiv.) in hexanes/CH_2Cl_2 (1:1 mixture, 39 mL) was added at a rate of 150 mL/h via syringe pump. The resulting mixture was stirred at –78 °C for 8 h. The reaction mixture was quenched by the addition of $NaHCO_3$ (sat. aq., 43 mL) and diethanolamine (3.2 mL), and stirred for another 30 min at rt. The mixture was filtered, and the filtrate was extracted with EtOAc (3 x 160 mL). The combined organic layers were dried over $MgSO_4$, filtered, and concentrated *in vacuo*. The crude product was purified on silica gel (7 % to 18 % ethyl acetate in hexanes) to provide **3-91** (5.44 g, 7.81 mmol, 61 %) as a 2.7:1 *d.r.* mixture.

Characterization: $\mathbf{R_f}$ = (hexanes/EtOAc 7:3): 0.57; **IR** (neat) v = 3496, 2941, 2866, 1716, 1634, 1592, 1504, 1432, 1327, 1236, 1119, 1060, 1031, 924, 882, 845, 771, 683 cm^{-1}; **^{1}H NMR** (500 MHz, $CDCl_3$, signals of major diastereomer) δ 7.42 (m, 2H), 7.35 (m, 2H), 7.29 (m, 1H), 6.80 (d, *J*= 1.2 Hz, 1H), 6.56 (d, *J*= 1.2 Hz, 1H), 6.49 (s, 2H), 5.97 (d, *J*= 1.5 Hz, 1H), 5.96 (d, *J*= 1.5 Hz, 1H), 5.18 (d, J= 6.5 Hz, 1H), 5.16 (d, J= 6.5 Hz, 1H), 5.09 (s, 1H), 5.08 (s, 2H), 4.57 (d, *J*= 8.0 Hz, 1H), 3.839 (s, 3H), 3.830 (s, 3H), 3.45 (s, 3H), 1.11 (m, 3H), 1.05-0.97 (m, 18H), 0.73 (d, *J*= 7.2 Hz, 3H); **^{13}C NMR** (126 MHz, $CDCl_3$, signals of major diastereomer) δ 213.6, 153.4, 152.1, 149.2, 140.3, 138.2, 137.7, 137.0, 136.0, 133.3, 128.5, 127.9, 127.3, 110.2, 105.9, 103.6, 101.7, 101.6, 95.5, 80.7, 76.7, 70.9, 60.9, 56.2, 55.9, 47.1, 17.93, 17.90, 15.8, 12.1; **HRMS**: Calcd. for $C_{38}H_{52}O_{10}Si$ $[M+Na]^+$ = 719.3227 m/z, found $[M+Na]^+$ = 719.3241 m/z.

Compound 3-112

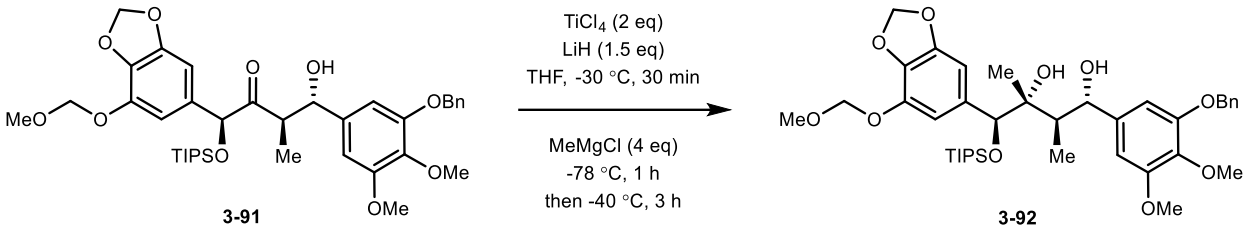


Procedure: A flame-dried microwave vial equipped with a Teflon-coated stir bar and a rubber septum was charged with 2,2,6,6-tetramethylpiperidine (freshly distilled over CaH_2, 0.48 mmol, 81 µL, 2.4 equiv.) and THF (0.4 mL). EtMgBr (0.40 mmol, 130 µL of 3 M solution in Et_2O, 2.0 equiv.) was added via syringe. The resulting solution was refluxed under N_2 for 12 h, then diluted with additional THF (0.22 mL), and cooled to –78 °C in a dry ice / acetone bath. A solution of **3-15** (0.20 mmol, 101 mg, 1.0 equiv.) in THF (0.4 mL) was then added dropwise via syringe. The reaction mixture was stirred for 1 h at –78 °C, then added a solution of Cy_2BCl (0.40 mmol, 88 µL, 2.0 equiv.) in hexanes (0.4 mL) via syringe. The reaction mixture was warmed to rt and stirred for another 1 h, then cooled to –78 °C, and a solution of **3-90** (0.20 mmol, 55 mg, 1.0 equiv.) in hexanes/CH_2Cl_2 (1:1 mixture, 0.9 mL) was added dropwise via syringe. The resulting mixture was then stirred at –78 °C for 5 h. The reaction mixture was quenched by the addition of $NaHCO_3$ (sat. aq., 0.8 mL) and diethanolamine (0.6 mmol, 63 mg, 3 equiv.), and stirred for another 30 min at rt. The mixture was then filtered, and the filtrate was extracted with EtOAc (4 x 3 mL). The combined organic layers were dried over $MgSO_4$, filtered, and concentrated *in vacuo*. The crude product was purified on silica gel (7 % to 18 % ethyl acetate in hexanes) to provide **3-112** (84 mg, 0.11 mmol, 54 %) as a 5:1 *d.r.* mixture.

Characterization: $\mathbf{R_f}$ = (hexanes/EtOAc 7:3): 0.60; **IR** (neat) v = 3497, 2939, 2865, 1729, 1592, 1503, 1467, 1426, 1371, 1236, 1115, 1058, 1026, 917, 882, 842, 736, 682 cm^{-1}; **^{1}H NMR** (500 MHz, $CDCl_3$, signals of major diastereomer) δ 7.48-7.29 (m, 5H), 6.66 (s, 1H), 6.50 (s, 2H), 6.00 (d, *J*= 1.4 Hz, 1H), 5.98 (d, *J*= 1.4 Hz, 1H), 5.81 (s, 1H), 5.39 (d, *J*= 6.0 Hz, 1H), 5.20 (d, *J*= 6.0 Hz, 1H), 5.10 (m, 2H), 5.02 (d, *J*= 3.4 Hz, 1H), 4.54 (d, *J*= 7.0 Hz, 1H), 3.84 (s, 6H) 3.55 (s, 3H), 3.14 (dq, *J*= 6.7 Hz, 1H), 2.93 (broad s, 1H), 1.10 (m, 3H), 1.05-0.95 (m, 18H), 0.77 (d, *J*= 7.0 Hz, 3H); **^{13}C NMR** (126 MHz, $CDCl_3$) δ 211.5, 153.2, 152.0, 148.8, 138.2, 138.1, 137.9, 137.0, 136.4, 132.3, 128.4, 127.8, 127.3, 109.4, 105.3, 103.2, 102.6, 102.1. 97.0, 80.2, 77.9, 70.8, 60.7, 57.3,

55.9, 47.4, 17.8, 15.6, 12.1; **HRMS**: Calcd. for $C_{38}H_{51}BrO_{10}Si$ $[M+Na]^+$ = 797.2333 m/z, found $[M+Na]^+$ = 797.2310 m/z.

Compound 3-92



3-91
Chemical Formula: $C_{38}H_{52}O_{10}Si$
Molecular Weight: 696.9090

2.5 : 1 *dr*
64 % major diastereomer

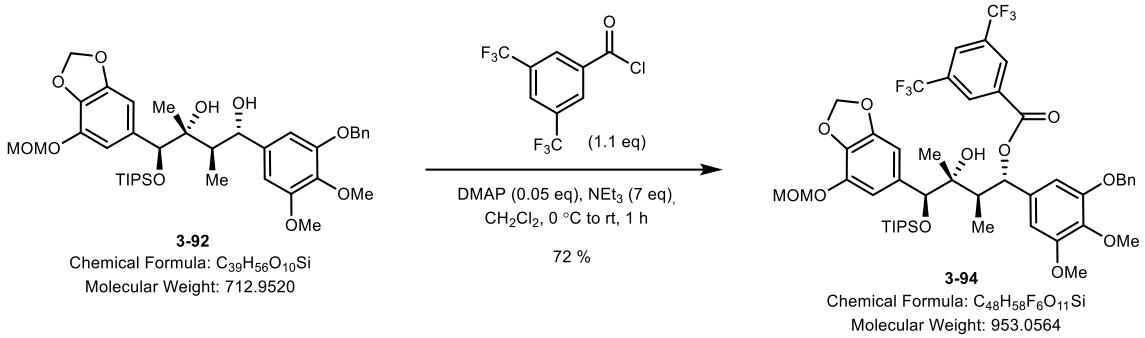
3-92
Chemical Formula: $C_{39}H_{56}O_{10}Si$
Molecular Weight: 712.9520

Procedure: A 250 mL flame-dried round bottom flask equipped with a Teflon-coated stir bar and a rubber septum was charged with **3-91** (8.85 mmol, 6.17 g, 1.0 equiv.) and LiH (13.2 mmol, 106 mg, 1.5 equiv.). The flask was evacuated and refilled with N_2 (repeated 3 times), prior to the addition of THF (44 mL). The mixture was then cooled to –30 °C, at which point $TiCl_4$ (17.7 mmol, 1 M in CH_2Cl_2, 17.7 mL, 2.0 equiv.) was added dropwise via syringe, followed by stirring at this temperature for 1 h. The resulting red solution was then cooled to –78 °C, and a solution of MeMgCl (35.4 mmol, 1 M in THF, 35.4 mL, 4.0 equiv.) was added dropwise via syringe pump (40 mL/h). The mixture was stirred at this temperature for 1 h, then warmed to –40 °C and stirred for another 3 h. The reaction mixture was quenched by the addition of NH_4Cl (sat. aq., 37 mL) followed by NH_4OH (concentrated, 3.3 mL), and stirred for another 15 min at rt. The resulting mixture was filtered, and the filtrate was extracted with EtOAc (3 × 90 mL). The combined organic layers were dried over $MgSO_4$, filtered, and concentrated *in vacuo*. The crude product (2.5:1 *dr*) was purified on silica gel (7 % to 28 % hexanes/EtOAc) to provide 4.06 g, 5.69 mmol, 64 % of the major diastereomer (**3-92**).

Characterization: $\mathbf{R_f}$ = (hexanes/EtOAc 7:3): ; **IR** (neat) v = 3444, 2942, 2866, 1634, 1592, 1503, 1432, 1380, 1323, 1231, 1116, 1055, 922, 882, 833, 751, 679 cm^{-1}; **^{1}H NMR** (500 MHz, $CDCl_3$) δ 7.40 (d, *J*= 7.4 Hz, 2H), 7.34 (m, 2H), 7.28 (m, 1H), 7.07-6.54 (broad s, 2H), 6.50 (d, *J*= 1.5 Hz, 1H), 6.48 (d, *J*= 1.5 Hz, 1H), 5.98 (s, 2H), 5.44 (s, 1H), 5.19 (m, 2H), 5.07 (m, 2H), 4.55 (s, 2H), 4.53 (d, *J*= 9.3 Hz, 1H) 3.82 (s, 3H), 3.81 (broad s, 1H), 3.62 (s, 3H), 3.45 (s, 3H), 1.56 (dq, *J*= 6.9 Hz , 9.2 Hz, 1H), 1.47 (s, 3H), 1.08-0.93 (m, 21H), 0.32 (d, *J*= 6.9 Hz, 3H); **^{13}C NMR** (126 MHz, $CDCl_3$) δ 153.1, 151.8, 148.6, 139.7, 138.8, 138.1, 137.2, 135.9, 134.2, 128.4, 127.7, 127.4,

113.0, 107.1, 104.9, 104.0, 101.4, 95.5, 80.3, 79.6, 77.7, 71.1, 60.7, 56.1, 56.0, 53.4, 43.5, 18.1, 17.9, 13.1, 12.5; **HRMS**: Calcd. for $C_{39}H_{56}O_{10}Si$ $[M+Na]^+$ = 735.3540 m/z, found $[M+Na]^+$ = 735.3532 m/z.

Compound 3-94



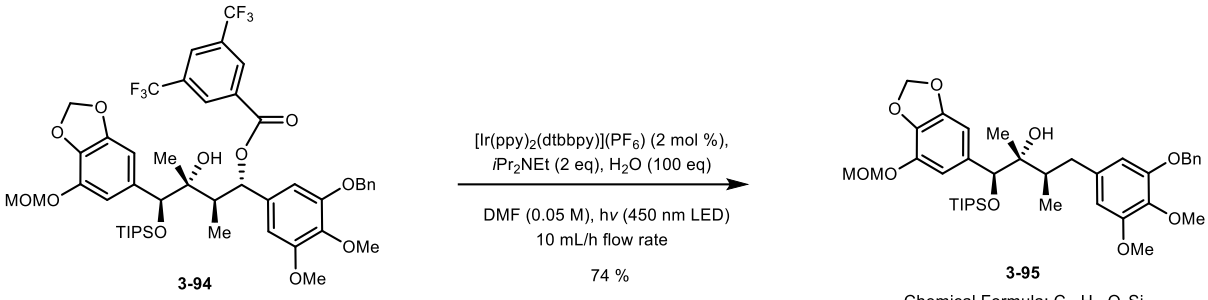
3-92
Chemical Formula: $C_{39}H_{56}O_{10}Si$
Molecular Weight: 712.9520

3-94
Chemical Formula: $C_{48}H_{58}F_6O_{11}Si$
Molecular Weight: 953.0564

Procedure: A flame-dried 250 mL round bottom flask equipped with a Teflon-coated stir bar and a rubber septum was charged with **3-92** (7.51 mmol, 5.36 g, 1.0 equiv.) and DMAP (0.38 mmol, 46 mg, 0.05 equiv.). The flask was evacuated and refilled with N_2 (repeated 3 times), prior to the addition of CH_2Cl_2 (75 mL), and then triethylamine (52.6 mmol, 7.3 mL, 7.0 equiv.). The reaction mixture was cooled to 0 °C and added 3,5-bis-(trifluoromethyl)benzoylchloride (8.27 mmol, 1.5 mL, 1.1 equiv.) dropwise. The reaction mixture was let at rt for 1 h and then concentrated *in vacuo*. The crude product was purified on silica gel (5 % to 15 % ethyl acetate in hexanes) to provide **3-94** (5.14 g, 5.39 mmol, 72 %).

Characterization: $\mathbf{R_f}$ = (hexanes/EtOAc 17:3): 0.32; **^{1}H NMR** (500 MHz, $CDCl_3$) δ 8.45 (s, 2H), 8.05 (s, 1H), 7.38 (d, *J*= 7.3 Hz, 2H), 7.30 (m, 2H), 7.23 (m, 1H) 7.00-6.50 (broad s, 2H), 6.60 (d, *J*= 1.4 Hz, 1H), 6.58 (d, *J*= 1.4 Hz, 1H), 6.16 (d, *J*= 7.5 Hz, 1H), 6.02 (d, *J*= 1.4 Hz, 1H), 6.01 (d, *J*= 1.4 Hz, 1H), 5.21 (s, 2H), 5.16 (d, *J*= 12.3 Hz, 1H), 5.10 (d, *J*= 12.3 Hz, 1H), 4.54 (s, 1H), 3.866 (s, 3H), 3.861 (s, 3H), 3.47 (s, 3H), 2.73 (broad s, 1H), 2.14 (m, 1H), 1.18 (s, 3H), 1.01 (m, 12H), 0.95 (m, 9H), 0.59 (d, *J*= 7.2 Hz, 3H); **^{13}C NMR** (126 MHz, $CDCl_3$) δ 162.9, 153.1, 152.0, 148.7, 139.6, 138.7, 137.0, 136.0, 134.9, 134.4, 133.3, 131.9, 129.8, 128.4, 127.7, 127.2, 125.9, 122.9, 119.7, 112.7, 107.7, 105.7, 103.8, 101.5, 80.4, 78.2, 77.7, 71.1, 60.8, 56.2, 56.1, 41.5, 21.3, 18.1, 17.9, 14.2, 12.6; **HRMS**: Calcd. for $C_{48}H_{58}F_6O_{11}Si$ $[M+Na]^+$ = 975.3550 m/z, found $[M+Na]^+$ = 975.35582 m/z.

Compound 3-95



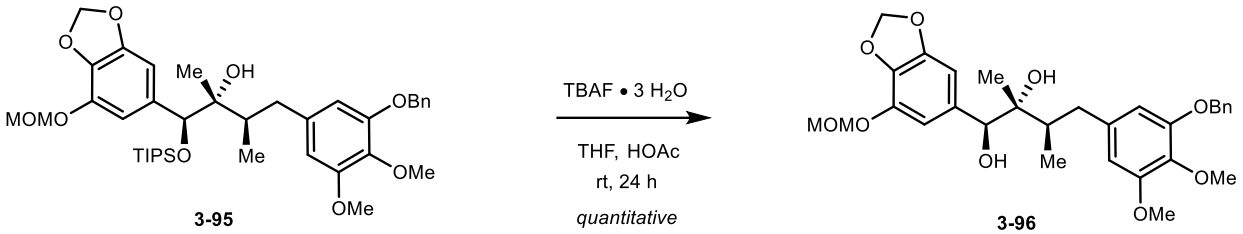
3-94
Chemical Formula: $C_{48}H_{58}F_6O_{11}Si$
Molecular Weight: 953.0564

3-95
Chemical Formula: $C_{39}H_{56}O_9Si$
Molecular Weight: 696.9530

Procedure: The DMF and water were degassed by sparging with N_2 prior to use. A flame-dried 250 mL round-bottom flask equipped with Teflon-coated stir bar was charged with **3-94** (5.39 mmol, 5.14 g, 1.0 equiv.) and [Ir(ppy$_2$)dtbbpy]PF_6 (0.11 mmol, 10.8 mL of a 0.01 M solution in DMF, 0.02 equiv.). The flask was evacuated and refilled with N_2 (repeated 3 times), before adding DMF (97 mL), water (539 mmol, 9.72 mL, 100 equiv.), and DIPEA (10.8 mmol, 1.88 mL, 2 equiv.). The reaction mixture was freeze-pump-thawed (x 5), then backfilled with N_2. A syringe pump was used to pump the reaction mixture through the blue LED photochemical flow setup at a rate of 10 mL/h. After all the reaction mixture had gone through (12 h later), pumped DMF (5 mL), followed by ethyl acetate (50 mL) through the tubing, rinsing into the receiving flask. The contents of the receiving flask were poured into a separatory funnel and diluted with ethyl acetate (80 mL). Water (780 mL) was added and the mixture was extracted. The aqueous layer was washed with ethyl acetate (4 x 130 mL). The combined organic layers were washed with brine (130 mL), dried over Na_2SO_4, filtered, and concentrated *in vacuo*. Purified on silica gel (10 % to 25 % ethyl acetate in hexanes) to provide **3-95** (2.77 g, 3.98 mmol, 74 %) as well as recovered starting material **3-94** (1.04 g, 1.09 mmol, 20 %).

Characterization: $\mathbf{R_f}$ = (hexanes/EtOAc 17:3): 0.22; **^{1}H NMR** (500 MHz, $CDCl_3$) δ 7.41 (d, J= Hz, *J*= 7.30 Hz, 2H), 7.35 (m, 2H), 7.28 (m, 1H), 6.96-6.59 (broad s, 2H), 6.33 (d, *J*=1.7 Hz, 1H), 6.28 (d, *J*=1.7 Hz, 1H), 5.93 (d, *J*= 1.5 Hz, 1H), 5.90 (d, *J*= 1.3 Hz, 1H), 5.17 (s, 2H), 5.04 (s, 2H), 4.59 (s, 1H), 3.81 (s, 3H), 3.78 (s, 3H), 3.43 (s, 3H), 3.18 (dd, *J*= 2.4 Hz, 13.2 Hz, 1H), 2.86 (s, 1H), 2.01 (dd, *J*= 11.1 Hz, 13.2 Hz, 1H), 1.49 (ddq, 2.8 Hz, 6.8 Hz, 1H), 1.28 (s, 3H), 1.02 (m, 12H), 0.95 (m, 9H), 0.61 (d, *J*= 6.8 Hz, 3H); **^{13}C NMR** (126 MHz, $CDCl_3$) δ 152.9, 151.8, 148.5, 139.5, 137.6, 137.3, 136.6, 135.6, 135.1, 128.4, 127.7, 127.3, 112.8, 108.5, 106.5, 103.8, 101.3, 95.5, 80.4, 77.5, 71.0, 60.8, 56.1, 56.0, 40.3, 37.5, 21.1, 18.1, 18.0, 14.3, 12.6; **HRMS**: Calcd. for $C_{39}H_{56}O_9Si$ $[M+Na]^+$ = 719.3591 m/z, found $[M+Na]^+$ = 719.3564 m/z.

Compound 3-96



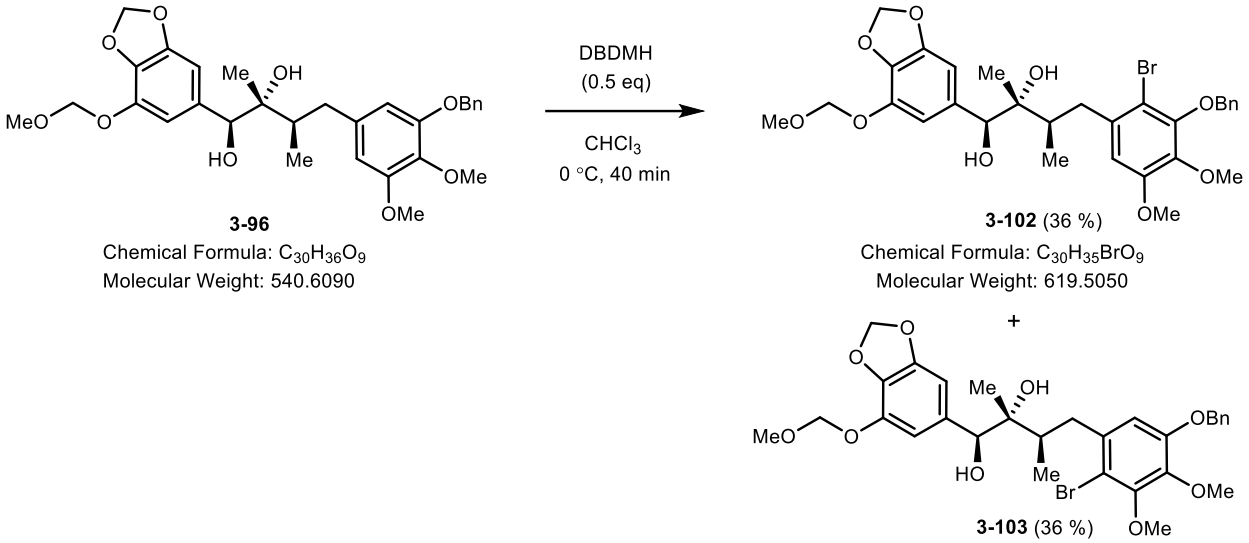
3-95
Chemical Formula: $C_{39}H_{56}O_9Si$
Molecular Weight: 696.9530

3-96
Chemical Formula: $C_{30}H_{36}O_9$
Molecular Weight: 540.6090

Procedure: A flame-dried 50 mL round bottom flask equipped with a Teflon-coated stir bar and a rubber septum was charged with **3-95** (3.95 mmol, 2.75 g, 1.0 equiv.). The flask was evacuated and refilled with N_2 (repeated 3 times), prior to the addition of THF (8 mL). A solution of TBAF·3 H_2O (11.86 mmol, 3.74 g, 3.0 equiv.) and acetic acid (4.74 mmol, 272 µL, 3.0 equiv.) in THF (12 mL) was then added, and the resulting mixture was stirred at rt for 24 h. The reaction mixture was poured on $NaHCO_3$ (saturated aqueous, 42 mL), separated the layers, and washed with brine (42 mL). The combined aqueous layers were extracted with ethyl acetate (3 × 42 mL). The combined organic layers were dried over $MgSO_4$, filtered, and concentrated *in vacuo*. The crude product was purified on silica gel (20 % to 100 % ethyl acetate in hexanes) to provide **3-96** (2.14 g, 3.95 mmol, quantitative).

Characterization: $\mathbf{R_f}$ = (hexanes/EtOAc 4:1): 0.0; **^{1}H NMR** (500 MHz, $CDCl_3$) δ 7.42 (d, *J*= 8.0 Hz, 2H), 7.36 (m, 2H), 7.30 (m, 1H), 6.81 (d, *J*= 1.3 Hz, 1H), 6.77 (d, *J*= 1.3 Hz, 1H), 6.37 (d, *J*= 1.6 Hz, 1H), 6.33 (d, *J*= 1.6 Hz, 1H), 5.95 (d, *J*= 1.4 Hz, 1H), 5.93 (d, *J*= 1.4 Hz, 1H), 5.19 2 x d, *J*= 6.5 Hz, 2H), 5.07 (s, 2H), 4.52 (s, 1H), 3.83 (s, 3H), 3.81 (s, 3H), 3.47 (s, 3H), 3.14 (dd, *J*= 2.9 Hz, 13.3 Hz, 1H), 2.20 (broad s, 1H), 2.10 (dd, *J*= 10.8 Hz, 13.2 Hz, 1H), 1.68 (ddq, J= 3.1 Hz, 6.8 Hz, 1H), 1.27 (s, 3H), 0.70 (d, J= 6.8 Hz, 3H); **^{13}C NMR** (126 MHz, $CDCl_3$) δ 153.0, 151.9, 148.9, 139.9, 137.4, 137.3, 136.7, 135.8, 135.4, 128.4, 127.7, 127.3, 112.0, 108.5, 106.5, 103.1, 101.4, 95.5, 78.1, 77.0, 71.0, 60.8, 56.3, 56.0, 41.0, 37.4, 20.2, 14.3; **HRMS**: Calcd. for $C_{30}H_{36}O_9$ $[M+Na]^+$ = 563.2257 m/z, found $[M+Na]^+$ = 563.22403 m/z.

Compounds 3-102 and 3-103



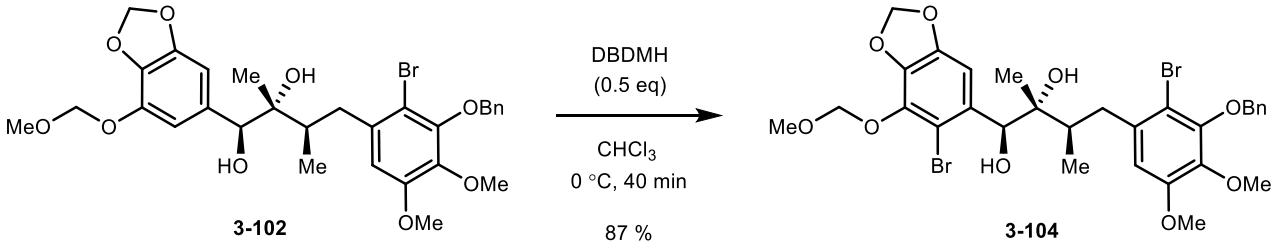
Procedure: A flame-dried microwave vial equipped with a Teflon-coated stir bar and a rubber septum was charged with **3-96** (0.14 mmol, 77 mg, 1.0 equiv.), which was dissolved in $CHCl_3$ (1.4 mL). The mixture was cooled to 0 °C in an ice bath, at which point 1,3-dibromo-5,5-dimethylhydantoin (DBDMH, 0.071 mmol, 20.4 mg, 0.5 equiv.) was added as a solid in portions. The resulting solution was stirred at 0 °C for 40 min and then quenched by the addition of water (6 mL). The mixture was extracted with CH_2Cl_2 (3 x 6 mL). The combined organic layers were dried over Na_2SO_4, filtered, and concentrated *in vacuo*. The crude products were purified on silica gel (20 % to 40 % ethyl acetate in hexanes) to provide **3-102** (36 %) and **3-103** (36 %).

Characterization of 3-102: $\mathbf{R_f}$ = (hexanes/EtOAc 2:3): 0.18; **^{1}H NMR** (500 MHz, $CDCl_3$) δ 7.55 (d, *J*= 8.0 Hz, 2H), 7.41-7.32 (m, 3H), 6.78 (2 x d, *J*= 1.1 Hz, 2H), 6.53 (s, 1H), 5.97 (2 x d, *J*= 1.5 Hz, 2H), 5.21 (2 x d, *J*= 6.6 Hz, 2H), 5.03 (s, 2H), 4.57 (s, 1H), 3.86 (s, 3H), 3.84 (s, 3H), 3.48 (s, 3H), 3.27 (dd, *J*= 2.7 Hz, 13.2 Hz, 1H), 2.48 (dd, *J*= 11.0 Hz, 13.1 Hz, 1H), 1.83 (m, 1H), 1.33 (s, 3H), 0.80 (d, *J*= 6.8 Hz, 3H); **^{13}C NMR** (126 MHz, $CDCl_3$) δ 152.2, 149.6, 149.0, 141.5, 140.0, 137.1, 136.4, 135.8, 135.2, 128.5, 128.3, 128.0, 111.7, 111.6, 110.5, 103.0, 101.4, 95.5, 77.9, 77.3, 75.1, 61.1, 56.3, 56.1, 39.6, 37.3, 19.6, 14.1.

Characterization of 3-103: $\mathbf{R_f}$ = (hexanes/EtOAc 2:3): 0.30; **^{1}H NMR** (500 MHz, $CDCl_3$) δ 7.44-7.31 (m, 5H), 6.78 (2 x d, *J*= 1.4 Hz, 2H), 6.55 (s, 1H), 5.96 (d, *J*= 1.4 Hz, 1H), 5.95 (d, *J*= 1.4 Hz, 1H), 5.21 (2 x d, *J*= 6.5 Hz, 2H), 5.07 (2 x d, *J*= 11.9 Hz, 2H), 4.56 (d, *J*= 5.1 Hz, 1H), 3.89 (s, 3H), 3.88 (s, 3H), 3.49 (s, 3H), 3.25 (dd, *J*= 2.7 Hz, 13.3 Hz, 1H), 2.46 (d, *J*= 5.4 Hz, 1H), 2.37 (dd, *J*= 11.2 Hz, 13.2 Hz, 1H), 2.02 (s, 1H), 1.79 (m, 1H), 1.31 (s, 3H), 0.71 (d, J= 6.8 Hz, 3H);

^{13}C NMR (126 MHz, $CDCl_3$) δ 151.1, 150.9, 149.0, 141.9, 140.0, 136.7, 136.1, 135.8, 135.1, 128.5, 128.0, 127.3, 112.7, 111.7, 111.6, 103.0, 101.4, 95.5, 77.9, 77.3, 71.1, 61.1, 60.9, 56.3, 39.3, 37.3, 19.6, 14.0.

Compound 3-104



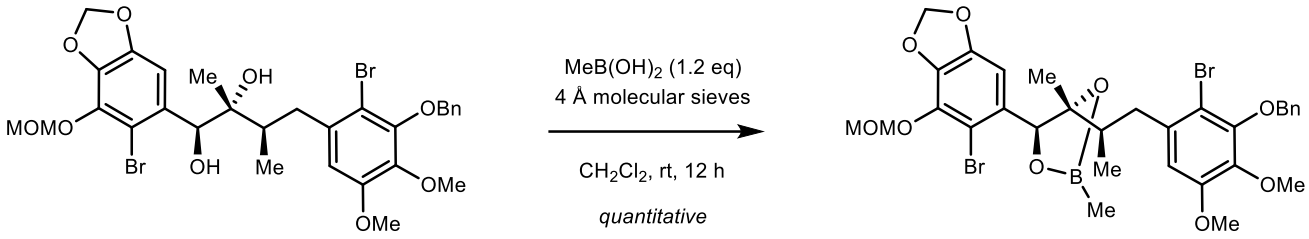
3-102
Chemical Formula: $C_{30}H_{35}BrO_9$
Molecular Weight: 619.5050

3-104
Chemical Formula: $C_{30}H_{34}Br_2O_9$
Molecular Weight: 698.4010

Procedure: A flame-dried microwave vial equipped with a Teflon-coated stir bar and a rubber septum was charged with **3-102** (0.052 mmol, 32 mg, 1.0 equiv.), which was dissolved in $CHCl_3$ (0.5 mL). The mixture was cooled to 0 °C in an ice bath, at which point 1,3-dibromo-5,5-dimethylhydantoin (DBDMH, 0.026 mmol, 7.4 mg, 0.5 equiv.) was added as a solid in portions. The resulting solution was stirred at 0 °C for 40 min and then quenched by the addition of water (2 mL). The mixture was extracted with CH_2Cl_2 (3 x 2 mL). The combined organic layers were dried over Na_2SO_4, filtered, and concentrated *in vacuo*. The crude product was purified on silica gel (20 % to 40 % ethyl acetate in hexanes) to provide **3-104** (31.4 mg, 0.044 mmol, 87 %).

Characterization: $\mathbf{R_f}$ = (hexanes/EtOAc 1:1): 0.58; **^{1}H NMR** (500 MHz, $CDCl_3$) δ 7.54 (m, 2H), 7.40-7.30 (m, 3H), 7.39 (s, 1H), 6.54 (s, 1H), 5.96 (s, 2H), 5.29 (d, *J*= 6.0 Hz, 1H), 5.24 (d, *J*= 6.0 Hz, 1H), 5.19 (m, 1H), 5.02 (s, 2H), 3.85 (s, 3H), 3.83 (s, 3H), 3.56 (s, 3H), 3.31 (dd, *J*= 2.8 Hz, 13.1 Hz, 1H), 2.46 (dd, *J*= 11.1 Hz, 13.1 Hz, 1H), 2.36 (m, 1H), 2.31 (s, 1H), 2.00 (ddq, *J*= 2.8 Hz, 6.9 Hz, 1H), 1.36 (s, 3H), 0.73 (d, *J*= 6.9 Hz, 3H); **^{13}C NMR** (126 MHz, $CDCl_3$) δ 152.2, 149.6, 148.5, 141.5, 138.1, 137.1, 136.49, 136.43, 134.2, 128.5, 128.3, 128.0, 111.6, 111.0, 110.6, 104.8, 101.9, 97.1, 78.2, 75.8, 75.1, 61.1, 57.5, 56.1, 40.0, 37.5, 20.4, 13.9; **HRMS**: Calcd. for $C_{39}H_{54}Br_2O_9Si$ $[M+Na]^+$ = 719.0467 m/z, found $[M+Na]^+$ = 719.04470 m/z.

Compound 3-105



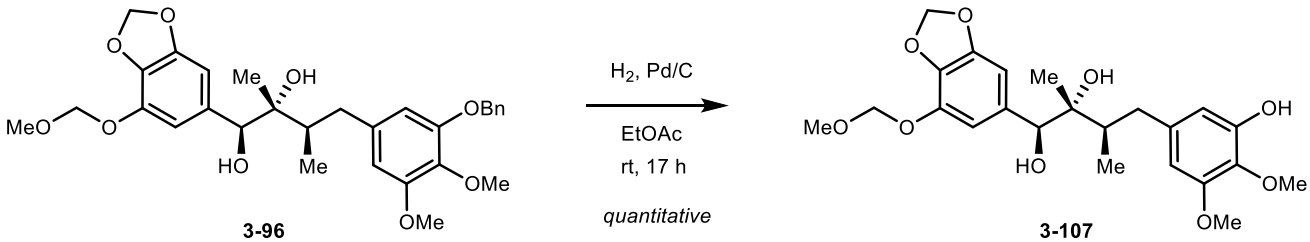
3-104
Chemical Formula: $C_{30}H_{34}Br_2O_9$
Molecular Weight: 698.4010

3-105
Chemical Formula: $C_{31}H_{35}BBr_2O_9$
Molecular Weight: 722.2300

Procedure: A flame-dried microwave vial equipped with a Teflon-coated stir bar and a septum was charged with **3-104** (0.038 mmol, 27 mg, 1.0 equiv.), methylboronic acid (0.045 mmol, 2.7 mg, 1.2 equiv.), and 4 Å molecular sieves (19 mg). The vial was evacuated and refilled with N_2 (repeated 3 times), prior to the addition of CH_2Cl_2 (1 mL). The reaction mixture was stirred at room temperature for 12 h. The solids were filtered off and the filtrate was concentrated *in vacuo*. The crude product was purified via silica gel plug (in 20 % to 50 % ethyl acetate in hexanes) to provide **3-105** (25 mg, 0.038 mmol, quantitative).

Characterization: $\mathbf{R_f}$ = (hexanes/EtOAc 4:1): 0.22; **IR** (neat) ν = 2965, 2928, 2909, 2355, 1474, 1363, 1219, 1109, 1061, 1018, 772 cm^{-1}; **^{1}H NMR** (500 MHz, $CDCl_3$) δ 7.56 (m, 2H), 7.38 (m, 2H), 7.33 (m, 1H), 6.69 (s, 1H), 6.38 (s, 1H), 5.96 (s, 2H), 5.59 (s, 1H), 5.26 (d, *J*= 6.0 Hz, 1H), 5.24 (d, *J*= 6.0 Hz, 1H), 5.02 (s, 2H), 3.85 (s, 3H), 3.80 (s, 3H), 3.53 (s, 3H), 3.28 (dd, *J*= 3.0, 13.2 Hz, 1H), 2.35 (dd, *J*= 11.0 Hz, 13.2 Hz, 1H), 2.05 (m, 1H), 1.58 (s, 3H), 0.42 (s, 3H), 0.40 (d, *J*= 6.8 Hz, 3H); **^{13}C NMR** (126 MHz, $CDCl_3$) δ 152.1, 149.7, 148.6, 141.5, 138.1, 137.1, 136.3, 132.4, 128.5, 128.3, 128.1, 111.6, 110.5, 109.9, 103.9, 102.0, 97.0, 87.6, 86.5, 75.1, 61.1, 57.4, 56.1, 38.3, 38.1, 29.7, 23.9, 14.3; **HRMS**: Calcd. for $C_{31}H_{35}BBr_2O_9$ $[M+Na]^+$ = 743.0639 m/z, found $[M+Na]^+$ = 743.0606 m/z.

Compound 3-107



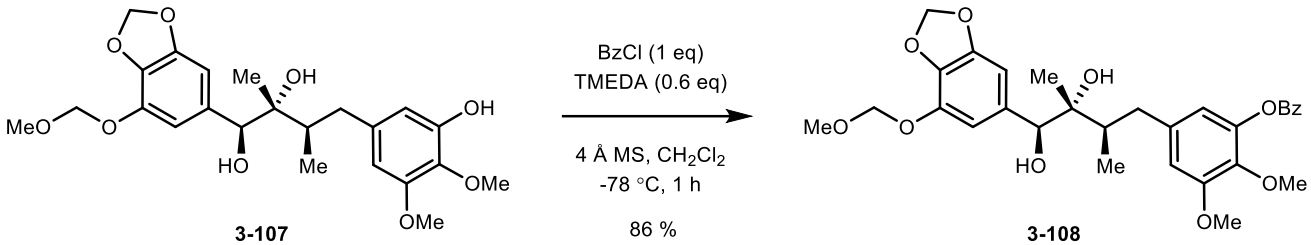
3-96
Chemical Formula: $C_{30}H_{36}O_9$
Molecular Weight: 540.6090

3-107
Chemical Formula: $C_{23}H_{30}O_9$
Molecular Weight: 450.4840

Procedure: A flame-dried 50 mL round bottom flask equipped with a Teflon-coated stir bar and a rubber septum was charged with **3-96** (2.27 mmol, 1.23 g, 1.0 equiv.) and palladium on carbon (10 wt %, 0.27 mmol, 241 mg, 0.1 equiv.). The flask was evacuated and refilled with N_2 (repeated 3 times), prior to the addition of ethyl acetate (23 mL). The N_2 atmosphere was exchanged for H_2. The reaction mixture was stirred for 16 h at rt under H_2 and then filtered through celite. The filtrate was concentrated *in vacuo*. The crude product was purified via silica gel (40 % ethyl acetate in hexanes) to provide **3-107** (1.02 g, 2.27 mmol, quantitative).

Characterization: $\mathbf{R_f}$ = (hexanes/EtOAc 1:1): 0.30; **^{1}H NMR** (500 MHz, $CDCl_3$) δ 6.74 (s, 2H), 6.30 (d, *J*= 1.8 Hz, 1H), 6.16 (d, *J*= 1.8 Hz, 1H), 5.91 (s, 2H), 5.16 (d, *J*= 6.5 Hz, 1H), 5.14 (d, *J*= 6.5 Hz, 1H), 4.46 (s, 1H), 3.78 (s, 3H), 3.75 (s, 3H), 3.43 (s, 3H), 3.07 (dd, *J*= 2.7 Hz, 13.2 Hz, 1H), 2.85 (broad s, 1H), 2.29 (broad s, 1H), 2.04 (dd, *J*= 11.1 Hz, 13.2 Hz, 1H), 1.65 (ddq, *J*= 3.1 Hz, 6.7 Hz, 1H), 1.23 (s, 3H), 0.70 (d, *J*= 6.8 Hz, 3H); **^{13}C NMR** (126 MHz, $CDCl_3$) δ 152.0, 148.9, 148.8, 139.8, 138.0, 135.8, 135.4, 133.5, 111.9, 108.7, 105.0, 103.2, 101.4, 95.4, 78.1, 77.0, 60.8, 56.2, 55.7, 40.8, 37.2, 20.0, 14.3; **HRMS**: Calcd. for $C_{23}H_{30}O_9$ $[M+Na]^+$ = 473.1788 m/z, found $[M+Na]^+$ = 473.17728 m/z.

Compound 3-108

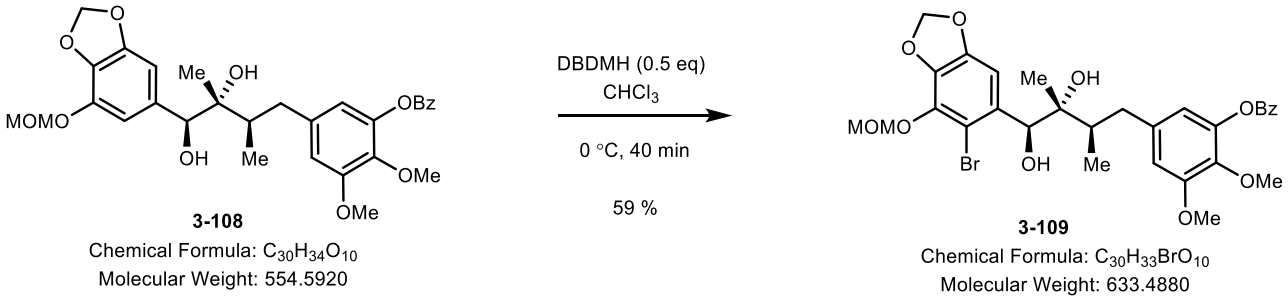


Procedure: A 50 mL flame-dried round bottom flask equipped with a Teflon-coated stir bar and a rubber septum was charged with **3-107** (2.27 mmol, 1.02 g, 1.0 equiv.) and 4 Å molecular sieves (227 mg). The flask was evacuated and refilled with N_2 (repeated 3 times), prior to the addition of CH_2Cl_2 (15.1 mL), followed by tetramethylethylenediamine (TMEDA, 1.36 mmol, 203 µL, 0.6 equiv.). The reaction mixture was cooled to −78 °C and then added benzoyl chloride (2.27 mmol, 0.67 M in CH_2Cl_2, 263 µL, 1.0 equiv.) and let stir for 1 h. The reaction mixture was quenched by adding phosphate buffer (20 mL) and then extracted with CH_2Cl_2 (3 x 25 mL). The combined organic layers were dried over Na_2SO_4, filtered, and concentrated *in vacuo*. The crude product was

purified on silica gel (35 % to 45 % ethyl acetate in hexanes) to provide **3-108** (1.08 g, 1.95 mmol, 86 %).

Characterization: $\mathbf{R_f}$ = (hexanes/EtOAc 1:1): 0.39; **^{1}H NMR** (500 MHz, $CDCl_3$) δ 8.17 (d, J= 7.8 Hz, 2H), 7.60 (t, *J*= 7.4 Hz, 1H), 7.48 (t, *J*= 7.7 Hz, 2H), 6.76 (s, 2H), 6.56 (s, 1H), 6.53 (s, 1H), 5.91 (2 x s, 2H), 5.15 (2 x d, *J*= 6.8 Hz, 2H), 4.49 (s, 1H), 3.81 (s, 3H), 3.76 (s, 3H), 3.43 (s, 3H), 3.17 (dd, *J*= 2.1 Hz, 13.3 Hz, 1H), 2.70 (broad s, 1H), 2.23 (broad s, 1H), 2.14 (dd, *J*= 11.2 Hz, 13.1 Hz, 1H), 1.71 (ddq, *J*= 2.8 Hz, 6.7 Hz, 1H), 1.24 (s, 3H), 0.76 (d, J= 6.8 Hz, 1H); **^{13}C NMR** (126 MHz, $CDCl_3$) δ 164.9, 153.2, 148.9, 143.8, 139.9, 139.0, 137.6, 135.8, 135.3, 133.4, 130.2, 129.4, 128.5, 115.7, 111.9, 111.2, 103.2, 101.4, 95.5, 78.0, 76.9, 60.8, 56.3, 56.0, 40.9, 37.1, 20.1, 14.4; **HRMS**: Calcd. for $C_{30}H_{34}O_{10}$ $[M+Na]^+$ = 577.2050 m/z, found $[M+Na]^+$ = 557.20281 m/z.

Compound 3-109



3-108
Chemical Formula: $C_{30}H_{34}O_{10}$
Molecular Weight: 554.5920

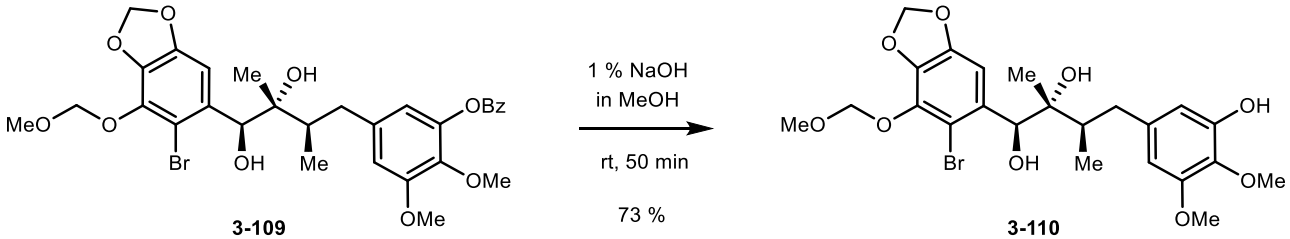
3-109
Chemical Formula: $C_{30}H_{33}BrO_{10}$
Molecular Weight: 633.4880

Procedure: A 50 mL flame-dried round bottom flask equipped with a Teflon-coated stir bar and a rubber septum was charged with **3-108** (1.95 mmol, 1.08 g, 1.0 equiv.) and dissolved in $CHCl_3$ (20 mL). The mixture was then cooled to 0 °C in an ice bath, at which point 1,3-dibromo-5,5-dimethylhydantoin (DBDMH, 0.98 mmol, 279 mg, 0.5 equiv.) was added as a solid in portions. (An orange color appeared when the first portion of DBDMH was added, the next portion was added after the orange color faded.) The resulting solution was stirred at 0 °C for 40 min and then concentrated *in vacuo*. The crude product was purified on silica gel (35 % to 45 % ethyl acetate in hexanes) to provide **3-109** (731 mg, 1.15 mmol, 59 %).

Characterization: $\mathbf{R_f}$ = (hexanes/EtOAc 3:2): 0.21; **^{1}H NMR** (500 MHz, $CDCl_3$) δ 8.19 (d, *J*= 8.0 Hz, 2H), 7.62 (m, 1H), 7.49 (m, 2H), 7.35 (s, 1H), 6.62 (d, *J*= 1.7 Hz, 1H), 6.58 (d, *J*= 1.7 Hz, 1H), 5.94 (s, 2H), 5.29 (d, *J*= 6.0 Hz, 1H), 5.23 (d, *J*= 6.0 Hz, 1H), 5.13 (d, *J*= 4.2 Hz, 1H), 3.85 (s, 3H), 3.78 (s, 3H), 3.55 (s, 3H), 3.19 (dd, *J*= 2.7, 13.2 Hz, 1H), 2.46 (d, *J*= 4.6 Hz, 1H), 2.36 (s,

1H), 2.18 (dd, *J*= 10.6 Hz, 13.3 Hz, 1H), 1.87 (ddq, *J*= 2.9 Hz, 6.7 Hz, 1H), 1.32 (s, 3H), 0.74 (d, *J*= 6.7 Hz, 3H); **^{13}C NMR** (126 MHz, $CDCl_3$) δ 164.9, 153.3, 148.5, 143.8, 139.1, 138.1, 137.5, 136.4, 134.2, 133.4, 130.2, 129.4, 128.5, 115.7, 111.2, 111.0, 104.8, 101.9, 97.1, 78.0, 75.7, 60.8, 57.5, 56.1, 41.5, 37.4, 20.6, 14.2; **HRMS**: Calcd. for $C_{30}H_{33}BrO_{10}$ $[M+Na]^+$ = 655.1155 m/z, found $[M+Na]^+$ = 655.1138 m/z.

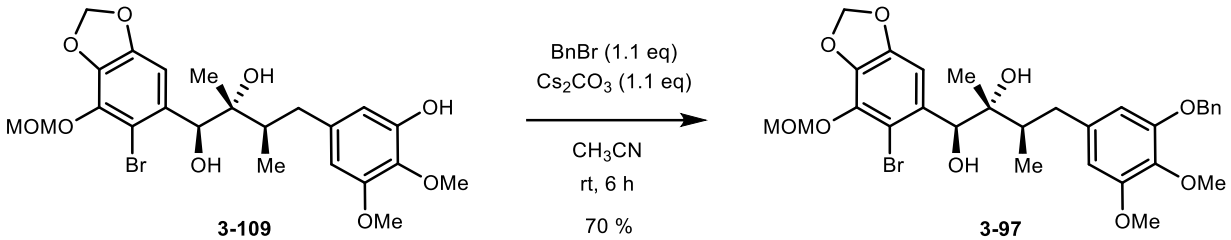
Compound 3-110



Procedure: A 100 mL round bottom flask equipped with Teflon-coated stir bar was charged with **3-109** (1.16 mmol, 731 mg, 1.0 equiv.). A solution of NaOH in MeOH (7.97 mmol, 1 % by weight, 45 mL, 6.9 equiv.) was added to and the reaction mixture was let stir at rt for 2 h. It was then concentrated *in vacuo* and the residue was taken up in water (35 mL) and ethyl acetate (35 mL). The layers were separated and the aqueous layer was washed with ethyl acetate (3 x 35 mL). The combined organic layers were dried over Na_2SO_4, filtered, and concentrated *in vacuo*. The crude product was purified on silica gel (35 % to 45 % ethyl acetate in hexanes) to provide **3-110** (443 mg, 0.838 mmol, 73 %).

Characterization: **R_f** = (hexanes/EtOAc 1:1): 0.34; **^{1}H NMR** (500 MHz, $CDCl_3$) δ 7.37 (s, 1H), 6.37 (d, *J*= 1.7 Hz, 1H), 6.24 (d, *J*= 1.7 Hz, 1H), 5.98 (d, *J*= 1.4 Hz, 1H), 5.97 (d, *J*= 1.4 Hz, 1H), 5.71 (s, 1H), 5.29 (d, *J*= 6.0 Hz, 1H), 5.25 (d, *J*= 6.0 Hz, 1H), 5.13 (d, *J*= 4.6 Hz, 1H), 3.84 (s, 3H), 3.82 (s, 3H), 3.56 (s, 3H), 3.12 (dd, *J*= 2.9 Hz, 13.2 Hz, 1H), 2.29 (s, 1H), 2.10 (dd, *J*= 10.7 Hz, 13.2 Hz, 1H), 1.84 (ddq, *J*= 3.0, 6.7 Hz, 1H), 1.33 (s, 3H), 0.71 (d, J= 6.8 Hz, 3H); **^{13}C NMR** (126 MHz, $CDCl_3$) δ 152.0, 148.8, 148.5, 138.1, 138.0, 136.4, 133.5, 111.1, 108.6, 105.1, 104.8, 101.9, 97.1, 78.1, 75.8, 60.9, 57.5, 55.8, 41.4, 37.5, 20.6, 14.2; **HRMS**: Calcd. for $C_{23}H_{29}BrO_9$ $[M+Na]^+$ = 551.0893 m/z, found $[M+Na]^+$ = 551.08785 m/z.

Compound 3-97



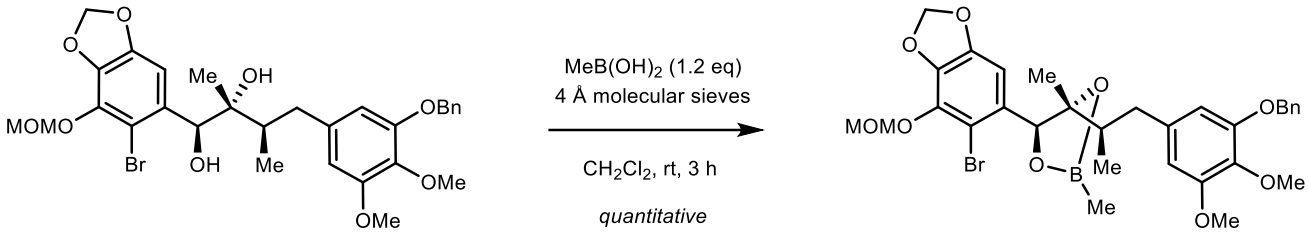
3-109
Chemical Formula: $C_{23}H_{29}BrO_9$
Molecular Weight: 529.3800

3-97
Chemical Formula: $C_{30}H_{35}BrO_9$
Molecular Weight: 619.5050

Procedure: A flame-dried 25 mL round-bottom flask equipped with a Teflon-coated stir bar and a rubber septum was charged with **3-109** (0.838 mmol, 443 mg, 1.0 equiv.) and cesium carbonate (0.92 mmol, 300 mg, 1.1 equiv.). The flask was evacuated and refilled with N_2 (repeated 3 times), prior to the addition of benzyl bromide (0.92 mmol, 110 µL, 1.1 equiv.) and then acetonitrile (8.4 mL). The reaction mixture was stirred for 6 h at rt. It was then diluted with CH_2Cl_2 (30 mL) and washed sequentially with water (30 mL) and brine (30 mL). The aqueous layers were washed with CH_2Cl_2 (3 x 30 mL). The combined organic layers were dried with Na_2SO_4 and concentrated *in vacuo*. The crude product was purified on silica gel (35 % to 45 % ethyl acetate in hexanes) to provide **3-97** (365 mg, 0.589 mmol, 70 %).

Characterization: $\mathbf{R_f}$ = (hexanes/EtOAc 13:7): 0.20; **IR** (neat) v = 3485, 2926, 1738, 1589, 1472, 1380, 1239, 1159, 1119, 1059, 1020, 923, 772 cm^{-1}; **^{1}H NMR** (500 MHz, $CDCl_3$) δ 7.42 (d, *J*= 7.7 Hz, 2H), 7.39 (s, 1H), 7.35 (m, 2H), 7.29 (m, 1H), 6.40 (d, *J*= 1.7 Hz, 1H), 6.36 (d, *J*= 1.6 Hz, 1H), 5.96 (d, *J*= 1.3 Hz, 1H), 5.93 (d, *J*= 1.3 Hz, 1H), 5.30 (d, *J*= 6.0 Hz, 1H), 5.23 (d, *J*= 6.0 Hz, 1H), 5.13 (d, *J*= 4.3 Hz, 1H), 5.08 (s, 2H), 3.83 (s, 1H), 3.82 (s, 3H), 3.56 (s, 3H), 3.13 (dd, *J*= 3.0 Hz, 13.2 Hz, 1H), 2.27 (s, 1H), 2.17 (d, *J*= 4.8 Hz, 1H), 2.11 (dd, *J*= 10.5, 13.1 Hz, 1H), 1.84 (ddq, *J*= 3.2 Hz, 6.8 Hz, 1H), 1.33 (s, 3H), 0.67 (d, *J*= 6.8 Hz, 3H); **^{13}C NMR** (126 MHz, $CDCl_3$) δ 153.1, 152.0, 148.5, 138.1, 137.38, 137.33, 136.8, 136.4, 134.1, 128.4, 127.7, 127.3, 111.1, 108.5, 106.5, 104.7, 101.9, 97.1, 78.0, 75.8, 71.0, 60.9, 57.5, 56.1, 41.7, 37.8, 20.7, 14.2; **HRMS**: Calcd. for $C_{30}H_{35}BrO_9$ $[M+Na]^+$ = 641. 1362 m/z, found $[M+Na]^+$ = 641.1357 m/z.

Compound 3-98



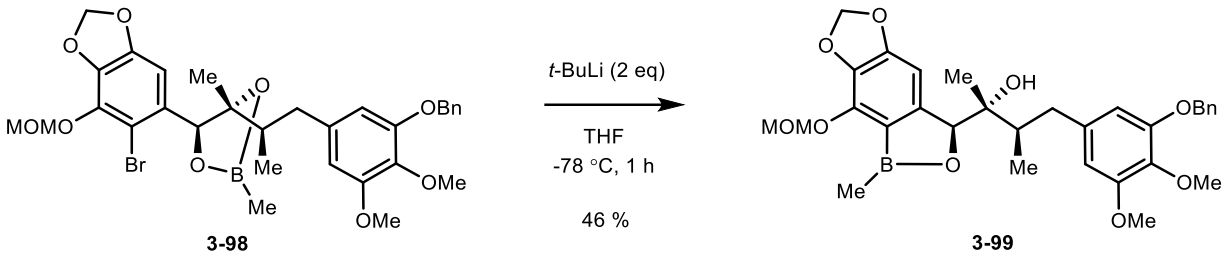
3-97
Chemical Formula: $C_{30}H_{35}BrO_9$
Molecular Weight: 619.5050

3-98
Chemical Formula: $C_{31}H_{36}BBrO_9$
Molecular Weight: 643.3340

Procedure: A flame-dried 20 mL vial equipped with a Teflon-coated stir bar and a septum cap was charged with **3-97** (0.37 mmol, 232 mg, 1.0 equiv.), methylboronic acid (0.45 mmol, 27 mg, 1.0 equiv.), and 4 Å molecular sieves (187 mg). The vial was evacuated and refilled with N_2 (repeated 3 times), prior to the addition of CH_2Cl_2 (3 mL). The reaction mixture was stirred at room temperature for 3 h. The solids were filtered off and the filtrate was concentrated *in vacuo*. The crude product was purified via silica gel plug (35 % ethyl acetate in hexanes) to provide **3-98** (241 mg, 0.37 mmol, quantitative).

Characterization: $\mathbf{R_f}$ = (hexanes/EtOAc 13:7): 0.54; **^{1}H NMR** (500 MHz, $CDCl_3$) δ 7.42, 7.35, 7.29 (d, J= 7.9 Hz, 2H), 7.35 (m, 2H), 7.29 (m, 1H), 6.69 (s, 1H), 6.16 (d, *J*= 1.6 Hz, 1H), 6.11 (d, *J*= 1.6 Hz, 1H), 5.96 (d, *J*= 1.3 Hz, 1H), 5.93 (d, *J*= 1.3 Hz, 1H), 5.54 (s, 1H), 5.30 (d, *J*= 6.0 Hz, 1H), 5.21 (d, *J*= 6.0 Hz, 1H), 5.05 (s, 2H), 3.82 (s, 3H), 3.79 (s, 3H), 3.53 (s, 3H), 2.93 (dd, *J*= 2.1 Hz, 13.3 Hz, 1H), 2.00 (dd, *J*= 11.0 Hz, 13.3 Hz, 1H), 1.76 (ddq, *J*= 2.4 Hz, 6.6 Hz, 1H), 1.56 (s, 3H), 0.47 (d, J= 6.7 Hz, 3H), 0.43 (s, 3H); **^{13}C NMR** (126 MHz, $CDCl_3$) δ 153.0, 151.9, 148.5, 137.9, 137.3, 136.8, 136.4, 132.8, 128.4, 127.8, 127.3, 109.9, 108.3, 106.4, 103.9, 102.0, 97.0, 87.6, 86.9, 71.0, 60.8, 57.4, 56.0, 40.3, 38.3, 25.5, 14.5, -6.0; **HRMS**: Calcd. for $C_{31}H_{36}BBrO_9$ $[M+Na]^+$ = 665.1533 m/z, found $[M+Na]^+$ = 665.15336 m/z.

Compound 3-99



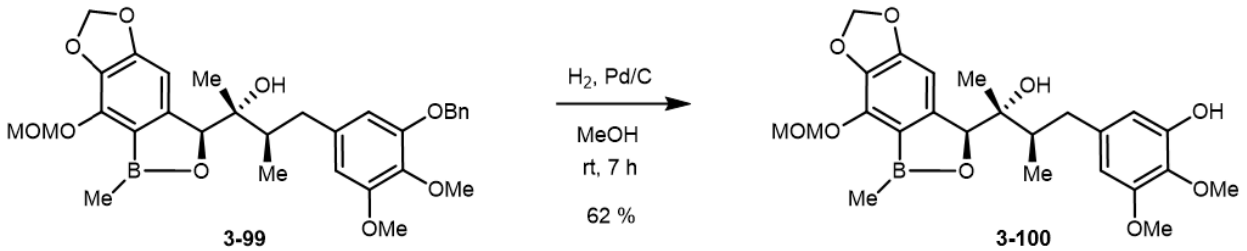
3-98
Chemical Formula: $C_{31}H_{36}BBrO_9$
Molecular Weight: 643.3340

3-99
Chemical Formula: $C_{31}H_{37}BO_9$
Molecular Weight: 564.4380

Procedure: A flame-dried microwave vial equipped with a Teflon-coated stir bar and a rubber septum was charged with **3-98** (0.039 mmol, 25 mg, 1.0 equiv.). The vial was evacuated and refilled with N_2 (repeated 3 times), prior to the addition of THF (0.4 mL). The resulting solution was cooled to −78 °C in a dry ice/ acetone bath and then slowly added *tert*-butyllithium (0.15 mmol, 80 µL of 1.9 M solution in pentanes, 4.0 equiv.) via syringe. The reaction mixture was stirred at −78 °C for 1 h. The reaction mixture was quenched with a solution of NH_4Cl (sat. aq.) and water (1:5, 1 mL), then extracted with ethyl acetate (3 x 1 mL). The combined organic layers were dried over Na_2SO_4, filtered, and concentrated *in vacuo*. The crude product was purified via silica gel (25 % to 35 % ethyl acetate in hexanes) to provide **3-99** (10 mg, 0.018 mmol, 46 %).

Characterization: $\mathbf{R_f}$ = (hexanes/EtOAc 13:7): 0.32; **^{1}H NMR** (500 MHz, $CDCl_3$) δ 7.45 (d, J= 7.5 Hz, 2H), 7.36 (m, 2H), 7.29 (m, 1H), 6.77 (s, 1H), 6.46 (d, *J*= 1.5 Hz, 1H), 6.43 (d, *J*= 1.5 Hz, 1H), 5.99 (m, 2H), 5.39 (d, *J*= 5.3 Hz, 1H), 5.32 (m, 2H), 5.12 (s, 2H), 3.86 (s, 3H), 3.85 (s, 3H), 3.54 (s, 3H), 3.18 (dd, *J*= 2.4 Hz, 13.2 Hz, 1H), 2.21 (m, 1H), 2.09 (ddq, *J*= 3.0, 7.1 Hz, 1H), 0.98 (s, 3H), 0.84 (m, 6H); **^{13}C NMR** (126 MHz, $CDCl_3$) δ 153.1, 152.0, 150.8, 141.7, 137.4, 137.3, 136.8, 135.5, 128.4, 127.7, 127.4, 108.7, 106.6, 101.4, 99.3, 96.3, 88.1, 76.4, 71.0, 60.9, 60.4, 56.8, 56.1, 42.2, 37.6, 21.0, 19.7, 14.2, 13.7.

Compound 3-100



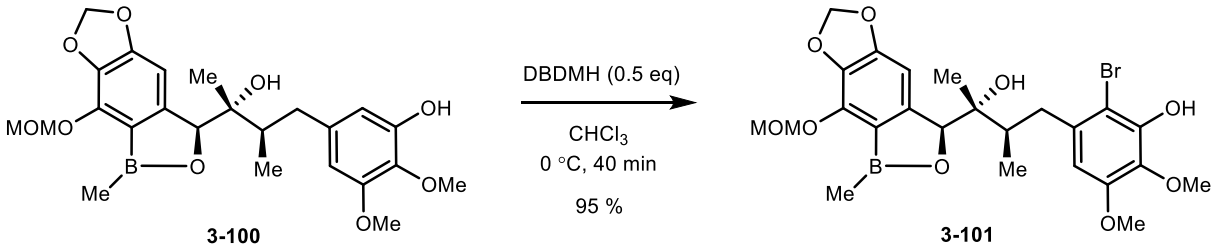
3-99
Chemical Formula: $C_{31}H_{37}BO_9$
Molecular Weight: 564.4380

3-100
Chemical Formula: $C_{24}H_{31}BO_9$
Molecular Weight: 474.3130

Procedure: A flame-dried microwave vial equipped with a Teflon-coated stir bar and a rubber septum was charged with **3-99** (0.074 mmol, 42 mg, 1.0 equiv.) and palladium on carbon (10 wt %, 7.9 mg, 0.1 equiv.). The vial was evacuated and refilled with N_2 (repeated 3 times), prior to the addition of methanol (1 mL). The N_2 atmosphere was exchanged for H_2. The reaction mixture was stirred for 7 h at rt under H_2. It was then filtered through celite and the filrate was concentrated *in vacuo*. The crude product was purified via silica gel (40 % ethyl acetate in hexanes) to provide **3-100** (22 mg, 0.046 mmol, 62 %).

Characterization: $\mathbf{R_f}$ = (hexanes/EtOAc 13:7): 0.27; **^{1}H NMR** (500 MHz, $CDCl_3$) δ 6.78 (s, 1H), 6.46 (d, *J*= 1.6 Hz, 1H), 6.32 (d, *J*= 1.6 Hz, 1H), 5.99 (s, 2H), 5.73 (s, 1H), 5.38 (d, J= 6.1 Hz, 1H), 5.32 (m, 2H), 3.87 (s, 3H), 3.85 (s, 3H), 3.54 (s, 3H), 3.18 (dd, *J*= 1.8, 12.9 Hz, 1H), 2.22 (dd, J= 11.3, 12.6 Hz, 1H), 2.12 (ddq, *J*= 2.6, 6.6 Hz, 1H), 0.98 (s, 3H), 0.89 (d, *J*= 6.8 Hz, 3H), 0.84 (s, 3H); **^{13}C NMR** (126 MHz, $CDCl_3$) δ 153.1, 152.1, 150.8, 148.8, 141.6, 138.2, 135.6, 133.5, 108.8, 105.1, 101.4, 99.4, 96.4, 88.1, 76.4, 60.9, 56.8, 55.8, 42.1, 37.4, 19.7, 13.7, 1.0; **HRMS**: Calcd. for $C_{24}H_{31}BO_9$ $[M+Na]^+$ = 497.1959 m/z, found $[M+Na]^+$ = 497.19431 m/z.

Compound 3-101



3-100
Chemical Formula: $C_{24}H_{31}BO_9$
Molecular Weight: 474.3130

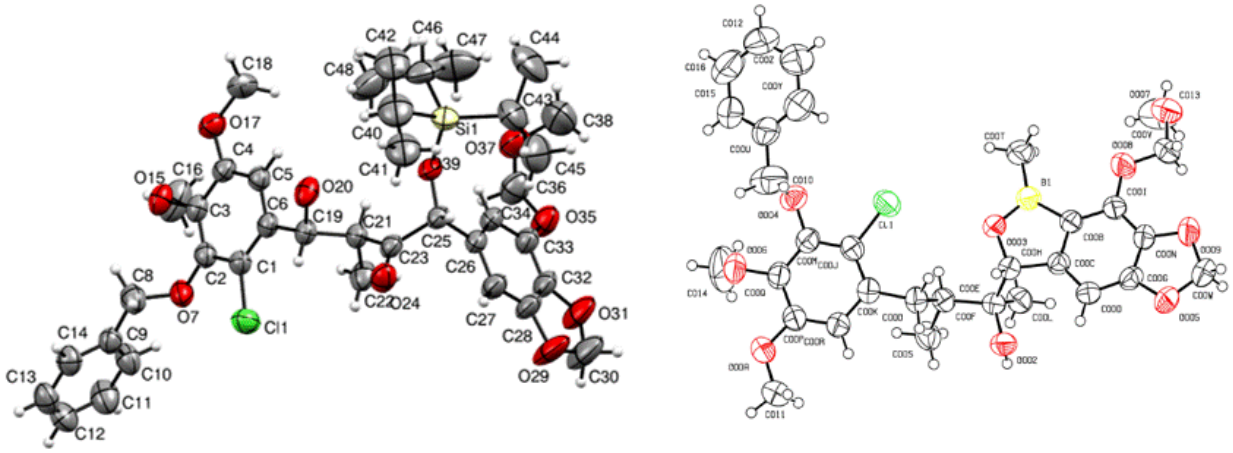
3-101
Chemical Formula: $C_{24}H_{30}BBrO_9$
Molecular Weight: 553.2090

Procedure: A flame-dried microwave vial equipped with a Teflon-coated stir bar and a rubber septum was charged with **3-100** (0.046 mmol, 22 mg, 1.0 equiv.), which was dissolved in $CHCl_3$ (1 mL). The mixture was then cooled to 0 °C in an ice bath, at which point 1,3-dibromo-5,5-dimethylhydantoin (DBDMH, 0.023 mmol, 6.5 mg, 0.5 equiv.) was added as a solid in portions. (An orange color appeared when the first portion of DBDMH was added, the next portion was added after the orange color faded.) The resulting solution was stirred at 0 °C for 40 min and then concentrated *in vacuo*. The crude product was purified on silica gel (25 % to 35 % ethyl acetate in hexanes) to provide **3-101** (24 mg, 0.044 mmol, 95 %).

Characterization: $\mathbf{R_f}$ = (hexanes/EtOAc 3:2): 0.44; **^{1}H NMR** (500 MHz, $CDCl_3$) δ 6.79 (s, 1H), 6.43 (s, 1H), 6.05 (s, 1H), 5.99 (s, 2H), 5.38 (d, *J*= 6.0 Hz, 1H), 5.31 (m, 2H), 3.89 (s, 3H), 3.85 (s, 3H), 3.53 (s, 3H), 3.25 (dd, *J*= 3.0 Hz , 13.2 Hz, 1H), 2.64 (dd, *J*= 11.4 Hz, 13.1 Hz, 1H), 2.26 (ddq, *J*= 3.2 Hz, 6.9 Hz, 1H), 1.04 (s, 3H), 0.88 (d, *J*= 7.0 Hz, 3H), 0.84 (s, 3H); **^{13}C NMR** (126 MHz, $CDCl_3$) δ 153.1, 151.1, 150.7, 146.5, 141.6, 136.7, 135.6, 134.2, 106.6, 103.4, 101.4, 99.4, 96.3, 88.2, 76.6, 61.1, 56.8, 55.9, 41.1, 37.1, 19.5, 13.5, 1.00; **HRMS**: Calcd. for $C_{24}H_{30}BBrO_9$ $[M+Na]^+$ = 575.1064 m/z, found $[M+Na]^+$ = 575.10576 m/z.

3.9.3. X-ray crystallographic data

General Procedure: A suitable crystal was selected and mounted on a Cryoloop on a Bruker Venture Metaljet diffractometer. The crystal was kept at 150 K during data collection. Using Olex2,[37] the structure was solved with the XT[38] structure solution program using Intrinsic Phasing and refined with the XL[39] refinement package using Least Squares minimization.



ORTEP representations of aldol **3-36** and cyclic borinic ester **3-52**

Crystal data and structure refinement for aldol **3-36** and cyclic borinic ester **3-52**:

Identification code	**3-36**	**3-52**
Empirical formula	$C_{38}H_{50}ClO_{10}Si$	$C_{31}H_{36}BClO_9$
Formula weight	730.32	598.903
Temperature/K	298(2)	296.15
Crystal system	monoclinic	triclinic
Space group	C2/c	P-1
a/Å	18.726(4)	10.4090(2)
b/Å	9.842(2)	12.3115(3)
c/Å	42.584(9)	12.3631(3)
α/°	90	99.951(1)
β/°	97.882(9)	97.270(1)
γ/°	90	100.165(1)
Volume/Å^3	7774(3)	1515.72(6)
Z	8	2
ρ_{calc}g/cm^3	1.248	1.312
μ/mm^{-1}	1.616	1.561
F(000)	3112.0	634.9
Crystal size/mm^3	0.370 × 0.230 × 0.110	0.187 × 0.060 × 0.052
Radiation	CuKα (λ = 1.54178)	Cu Kα (λ = 1.54178)
2Θ range for data collection/°	10.256 to 145.308	7.36 to 144.4
Index ranges	-23 ≤ h ≤ 20, -12 ≤ k ≤ 12, -52 ≤ l ≤ 52	-12 ≤ h ≤ 12, -15 ≤ k ≤ 15, -15 ≤ l ≤ 15
Reflections collected	74001	46868
Independent reflections	7648 [R_{int} = 0.0467, R_{sigma} = 0.0219]	5957 [R_{int} = 0.0554, R_{sigma} = 0.0279]
Data/restraints/parameters	7648/12/467	5957/0/382
Goodness-of-fit on F^2	1.036	1.149
Final R indexes [I>=2σ (I)]	R_1 = 0.0475, wR_2 = 0.1283	R_1 = 0.0587, wR_2 = 0.1581
Final R indexes [all data]	R_1 = 0.0569, wR_2 = 0.1401	R_1 = 0.0794, wR_2 = 0.1901
Largest diff. peak/hole / e Å^{-3}	0.49/-0.46	0.34/-0.33

3.10. References

(1) Wang, X.; Liu, J.; Pandey, P.; Fronczek, F. R.; Doerksen, R. J.; Chen, J.; Qi, X.; Zhang, P.; Ferreira, D.; Valeriote, F. A.; Sun, H.; Li, S.; Hamann, M. T. Computationally Assisted Assignment of the Kadsuraols, a Class of Chemopreventive Agents for the Control of Liver Cancer. *Org. Lett.* **2018**, *20* (18), 5559–5563.

(2) Belokon, Y. N.; North, M.; Parsons, T. Vanadium-Catalyzed Asymmetric Cyanohydrin

Synthesis. *Org. Lett.* **2000**, *2* (11), 1617–1619.

(3) Gong, W.; Singidi, R. R.; Gallucci, J. C.; Rajanbabu, T. V. On the Stereochemistry of Acetylide Additions to Highly Functionalized Biphenylcarbaldehydes and Multi-Component Cyclization of 1,n-Diynes. Syntheses of Dibenzocyclooctadiene Lignans. *Chem. Sci.* **2012**, *3*, 1221–1230.

(4) Kurono, N.; Yamaguchi, M.; Suzuki, K.; Ohkuma, T. Lithium Chloride : An Active and Simple Catalyst for Cyanosilylation of Aldehydes and Ketones. *J. Org. Chem.* **2005**, *70*, 6530–6532.

(5) Cervi, A.; Aillard, P.; Hazeri, N.; Petit, L.; Chai, C. L. L.; Willis, A. C.; Banwell, M. G. Total Syntheses of the Coumarin-Containing Natural Products Pimpinellin and Fraxetin Using Au(I)-Catalyzed Intramolecular Hydroarylation (IMHA) Chemistry. *J. Org. Chem.* **2013**, *78*, 9876–9882.

(6) Xiong, X.; Yeung, Y. Ammonium Salt-Catalyzed Highly Practical Ortho -Selective Monohalogenation and Phenylselenation of Phenols : Scope and Applications. *ACS Catal.* **2018**, *8*, 4033–4043.

(7) Gnaim, J.; Sheldon, R. A. Highly Regioselective Ortho-Chlorination of Phenol With Sulfuryl Chloride in the Presence of Amines. *Tetrahedron Lett.* **1995**, *36* (22), 3893–3896.

(8) Bartoli, G.; Bosco, M.; Martino, D.; Marcantoni, E.; Sambri, L. Highly Stereoselective and Efficient Addition of Organocerium Reagents to Syn- -Alkyl-β -Hydroxy-α-Methyl Ketones by Way of Their Titanium Alkoxides - Synthesis of Complex 1, 3-Diol Units with Three Stereodefined Centres. *European J. Org. Chem.* **2001**, 2901–2909.

(9) Huang, Z.; Lumb, J. P. Mimicking Oxidative Radical Cyclizations of Lignan Biosynthesis Using Redox-Neutral Photocatalysis. *Nat. Chem.* **2021**, *13* (1), 24–32.

(10) Liu, G. Bin; Zhao, H. Y.; Yang, B.; Thiemann, T. Zinc Dust-Mediated Reductive Degradation of Decabromodiphenyl Ether. *Green Chem. Lett. Rev.* **2010**, *3* (1), 1–6.

(11) Crimmins, M. T.; Heathcock, C. H.; Van Draanen, N. A.; Arseniyadis, S. Protocols for the Preparation of Each of the Four Possible Stereoisomeric α-Alkyl-β-Hydroxy Carboxylic Acids from a Single Chiral Aldol Reagent. *J. Org. Chem.* **1991**, *56* (7), 2499–2506.

(12) Evans, D. A.; Nelson, J. V.; Vogel, E.; Taber, T. R. Stereoselective Condensations via Boron Enolates. *Jounal Am. Chem. Soc.* **1981**, *103*, 3099–3111.

(13) Rackl, D.; Kais, V.; Kreitmeier, P.; Reiser, O. Visible Light Photoredox-Catalyzed Deoxygenation of Alcohols. *Beilstein J. Org. Chem.* **2014**, *10*, 2157–2165.

(14) Lau, S. Y. W.; Keay, B. A. A Highly Efficient Strategy for the Synthesis of 3-Substituted Salicylic Acids by Either Directed Ortho-Lithiation or Halogen-Metal Exchange of Substituted Mom Protected Phenols Followed by Carboxylation. *Can. J. Chem.* **2001**, *79* (11), 1541–1545.

(15) Winkle, M. R.; Ronald, R. C. Regioselective Metalation Reactions of Some Substituted (Methoxymethoxy)Arenes. *J. Org. Chem.* **1982**, *47* (11), 2101–2108.

(16) Ramesh, C.; Ravindranath, N.; Das, B. Simple, Efficient, and Selective Deprotection of Phenolic Methoxymethyl Ethers Using Silica-Supported Sodium Hydrogen Sulfate as a Heterogeneous Catalyst. *J. Org. Chem.* **2003**, *68*, 7101–7103.

(17) Hanessian, Stephen; Delorme, Daniel; Dufresne, Y. Mild Cleavage of Methoxymethyl (MOM) Ethers with Trimethylsilyl Bromide. *Tetrahedron Lett.* **1984**, *25* (24), 2515–2518.

(18) Peng, Y.; Ji, C.; Chen, Y.; Huang, C.; Jiang, Y. An Efficient and Selective Deprotecting Method for Methoxymethyl Ethers. *Synth. Commun.* **2004**, *34* (23), 4325–4330.

(19) Deville, J. P.; Behar, V. Chelation-Controlled Selectivity in the Clay-Catalyzed Deprotection of Phenolic Methoxy Methyl Ethers. *J. Org. Chem.* **2001**, *66*, 4097–4098.

(20) Nicolaou, K. C.; Natarajan, S.; Li, H.; Jain, N. F.; Hughes, R.; Solomon, M. E.; Ramanjulu, J. M.; Boddy, C. N. C.; Takayanagi, M. Total Synthesis of Vancomycin Aglycon - Part I: Synthesis of Amino Acids 4-7 and Construction of the AB-COD Ring Skeleton. *Angew. Chemie - Int. Ed.* **1998**, *37* (19), 2708–2714.

(21) Zhang, Y. K.; Plattner, J. J.; Freund, Y. R.; Easom, E. E.; Zhou, Y.; Ye, L.; Zhou, H.; Waterson, D.; Gamo, F. J.; Sanz, L. M.; Ge, M.; Li, Z.; Li, L.; Wang, H.; Cui, H. Benzoxaborole Antimalarial Agents. Part 2: Discovery of Fluoro-Substituted 7-(2-Carboxyethyl)-1,3-Dihydro-1-Hydroxy-2,1-Benzoxaboroles. *Bioorganic Med. Chem. Lett.* **2012**, *22* (3), 1299–1307.

(22) Ishiyama, T.; Murata, M.; Miyaura, N. Palladium(0)-Catalyzed Cross-Coupling Reaction of Alkoxydiboron with Haloarenes: A Direct Procedure for Arylboronic Esters. *J. Org. Chem.* **1995**, *60* (23), 7508–7510.

(23) Barder, T. E.; Walker, S. D.; Martinelli, J. R.; Buchwald, S. L. Catalysts for Suzuki-Miyaura Coupling Processes: Scope and Studies of the Effect of Ligand Structure. *J. Am. Chem. Soc.* **2005**, *127* (13), 4685–4696.

(24) Kinzel, T.; Zhang, Y.; Buchwald, S. L. A New Palladium Precatalyst Allows for the Fast Suzuki-Miyaura Coupling Reactions of Unstable Polyfluorophenyl and 2-Heteroaryl Boronic Acids. *J. Am. Chem. Soc.* **2010**, *132*, 14073–14075.

(25) Patel, N. D.; Rivalti, D.; Buono, F. G.; Chatterjee, A.; Qu, B.; Braith, S.; Desrosiers, J. N.; Rodriguez, S.; Sieber, J. D.; Haddad, N.; Fandrick, K. R.; Lee, H.; Yee, N. K.; Busacca, C. A.; Senanayake, C. H. Effective BI-DIME Ligand for Suzuki–Miyaura Cross-Coupling Reactions in Water with 500 Ppm Palladium Loading and Triton X. *Asian J. Org. Chem.* **2017**, *6* (9), 1285–1291.

(26) Zhang, S.; Neumann, H.; Beller, M. Pd-Catalyzed Synthesis of α,β-Unsaturated Ketones by Carbonylation of Vinyl Triflates and Nonaflates. *Chem. Commun.* **2019**, *55* (42), 5938–5941.

(27) Li, H.; Zhong, Y. L.; Chen, C. Y.; Ferraro, A. E.; Wang, D. A Concise and Atom-Economical Suzuki-Miyaura Coupling Reaction Using Unactivated Trialkyl- and Triarylboranes with Aryl Halides. *Org. Lett.* **2015**, *17* (14), 3616–3619.

(28) Hesp, K. D.; Lundgren, R. J.; Stradiotto, M. Palladium-Catalyzed Mono-α-Arylation of Acetone with Aryl Halides and Tosylates. *J. Am. Chem. Soc.* **2011**, *133* (14), 5194–5197.

(29) Organ, M. G.; Çalimsiz, S.; Sayah, M.; Hoi, K. H.; Lough, A. J. Pd-PEPPSI-IPent: An Active, Sterically Demanding Cross-Coupling Catalystand Its Application in the Synthesis of Tetra-Ortho-Substituted Biaryls. *Angew. Chemie - Int. Ed.* **2009**, *48* (13), 2383–2387.

(30) Mantell, M. A.; Lasky, M. R.; Lee, M.; Remy, M.; Sanford, M. S. SNAr and C-H Amination of Electron Rich Arenes with Pyridine as a Nucleophile Using Photoredox Catalysis. *Org. Lett.* **2021**, *23* (13), 5213–5217.

https://doi.org/10.1021/acs.orglett.1c01749.

(31) Kassel, V. M.; Hanneman, C. M.; Delaney, C. P.; Denmark, S. E. Heteroaryl-Heteroaryl, Suzuki-Miyaura, Anhydrous Cross-Coupling Reactions Enabled by Trimethyl Borate. *J. Am. Chem. Soc.* **2021**, *143* (34), 13845–13853.

(32) Darzi, E. R.; White, B. M.; Loventhal, L. K.; Zakharov, L. N.; Jasti, R. An Operationally Simple and Mild Oxidative Homocoupling of Aryl Boronic Esters To Access Conformationally Constrained Macrocycles. *J. Am. Chem. Soc.* **2017**, *139* (8), 3106–3114.

(33) Coleman, R. S.; Gurrala, S. R.; Mitra, S.; Raao, A. Asymmetric Total Synthesis of Dibenzocyclooctadiene Lignan Natural Products. *J. Org. Chem.* **2005**, *70*, 8932–8941.

(34) Hendy, C. M.; Smith, G. C.; Xu, Z.; Lian, T.; Jui, N. T. Radical Chain Reduction via Carbon Dioxide Radical Anion (CO2•-). *J. Am. Chem. Soc.* **2021**, *143* (24), 8987–8992.

(35) Chen, J.; Chen, C.; Ji, C.; Lu, Z. Cobalt-Catalyzed Asymmetric Hydrogenation of 1,1-Diarylethenes. *Org. Lett.* **2016**, *18* (7), 1594–1597.

(36) Breton, G. W. Selective Monoacetylation of Unsymmetrical Diols Catalyzed by Silica Gel-Supported Sodium Hydrogen Sulfate. *J. Org. Chem.* **1997**, *62* (25), 8952–8954.

(37) Dolomanov, O. V; Bourhis, L. J.; Gildea, R. J.; Howard, J. A. K.; Puschmann, H. OLEX2: A Complete Structure Solution, Refinement and Analysis Program. *J. Appl. Crystallogr.* **2009**, *42* (2), 339–341.

(38) Sheldrick, G. M. SHELXT - Integrated Space-Group and Crystal-Structure Determination. *Acta Crystallogr. Sect. A* **2015**, *71* (1), 3–8.

(39) Sheldrick, G. M. Crystal Structure Refinement with SHELXL. *Acta Crystallogr. Sect. C* **2015**, *71* (1), 3–8.

Chapter 4. Synthesis of 6-benzyloxy-taiwanschirin B

4.1. Introduction

Taiwanschirins A–C (Figure 4.1) were isolated from *Schisandra arisanensis* in 1999 and assayed for *in vitro* cytotoxicity against hepatoma, displaying promising activity (Hepa-3B, ED_{50} = 2.2 μg/mL for taiwanschirin C).[1] Progress towards the chemical synthesis of the taiwanschirins has been reported once before by Donohoe and coworkers, who constructed an [8,6,5] core lacking functionalization around the 8-membered and aromatic rings (**4-65**) in 11 steps (Scheme 4.1).[2] Their synthesis started with the 6-membered ring in place, from 3-bromophenol (**4-57**). The five membered ring was constructed via formylation followed by condensation with ethyl diazoacetate (**4-57** to **4-59**). An alkynylation followed by a Heck coupling were used to construct the 8-membered ring (**4-61** to **4-64**). Oxidative cleavage was then used to convert **4-64** to **4-65**.

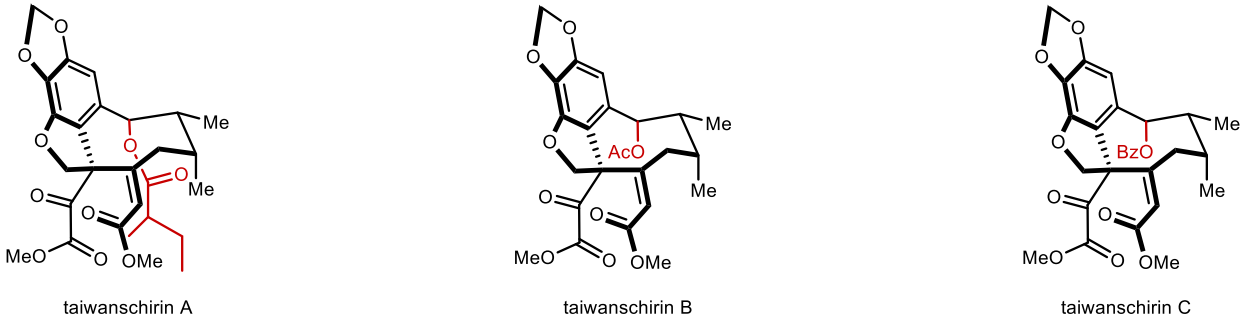
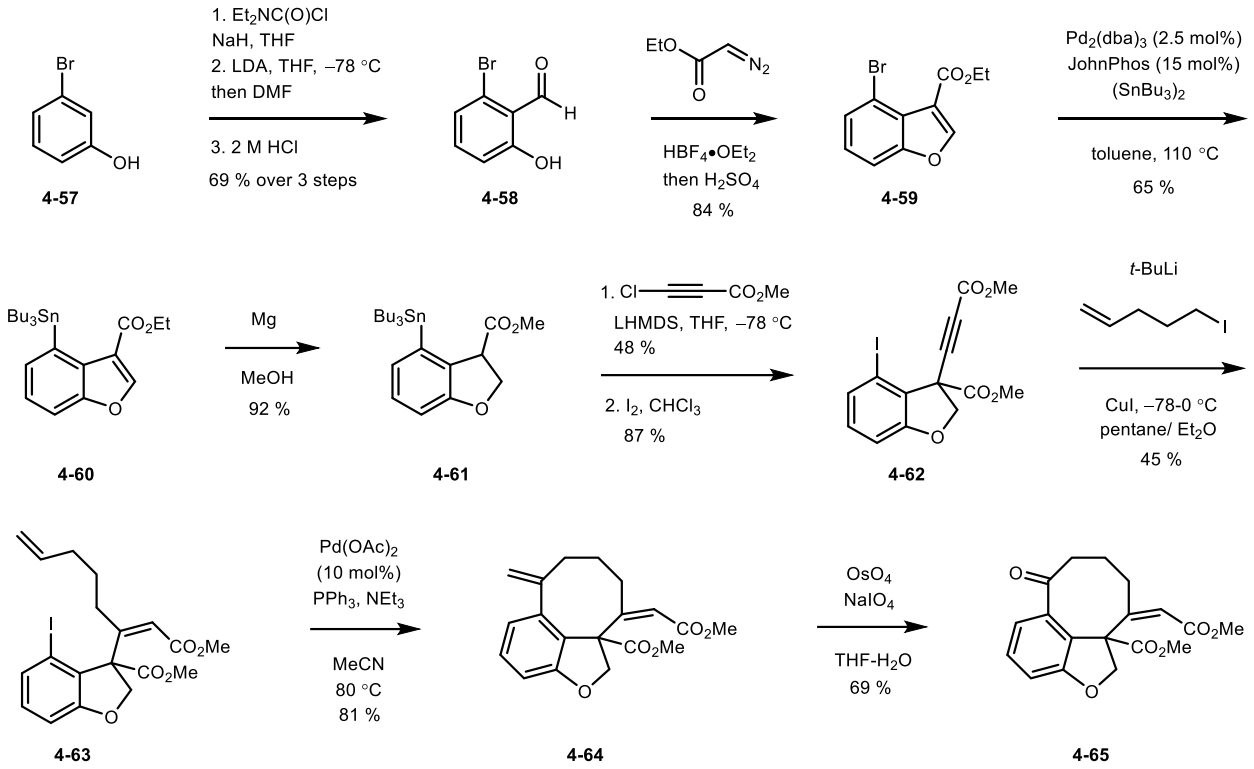


Figure 4.1. Taiwanschirins A–C

The synthetic targets of the current work, kadsuraol C and taiwanschirin B, differ from previous targets in our group in that they do not possess an oxygen-containing substituent at C6. We have selected a deoxygenation approach to access these targets, where a C6 stereocenter is installed during an aldol addition and used to direct the stereochemical outcome of the subsequent methyl addition to the C8 ketone. In Chapter 3, we performed deoxygenation of the C6 alcohol at this stage, however this led to the inability to form the biaryl bond via Suzuki coupling later. In this chapter, the C6 substituent will be kept in place until after the biaryl bond has been formed, at which point we attempt to perform the C6 deoxygenation on the cyclic substrate.

The total synthesis of the taiwanschirins involves setting four stereocenters along the 8-membered ring, including a quaternary spirocenter. Additionally, the lower aromatic ring must be dearomatized and oxidatively cleaved to the keto-diester. The taiwanschirins lack oxygenation



Scheme 4.1. Previously reported synthetic work towards the taiwanschirins

at C6 and C7 therefore we will perform two deoxygenation steps. The three taiwanschirins differ only by the identity of the C9 ester (2-methylbutanoate for taiwanschirin A, acetate for B, and benzoate for C). Taiwanschirin B was selected as the synthetic target for this project as the C9 acetate makes it most structurally similar to our other target kadsuraol C.

A strategy for the deoxygenation of the C6 alcohol on a cyclic substrate will be developed and applied to both the syntheses of taiwanschirin B and kadsuraol C. Deoxygenation of the cyclic substrate is expected to be more challenging than deoxygenation of a linear substrate (such as the one seen in Chapter 3) due to both steric and electronic effects. Appending an ester or other activating group onto the C6 alcohol of the cyclic substrate proceeds more slowly due to the sterically congested nature of the cyclic system (Figure 4.2A). Due to the twisted nature of the biaryl bond in DBCODs, the C6 and C9 positions are inequivalent. It was found that in kadsurin, bearing carbonyls at C6 and C9, that the C9 carbonyl was conjugated with the neighbouring aromatic ring whereas the C6 carbonyl experienced less efficient orbital overlap with the aromatic ring.[3] This electronic effect is also applicable to our C6 alcohol (**4-6**), which does not behave like

a traditional benzylic alcohol due to the twisted biaryl linkage leading to poor orbital overlap with the π system of the aromatic ring (Figure 4.2B).

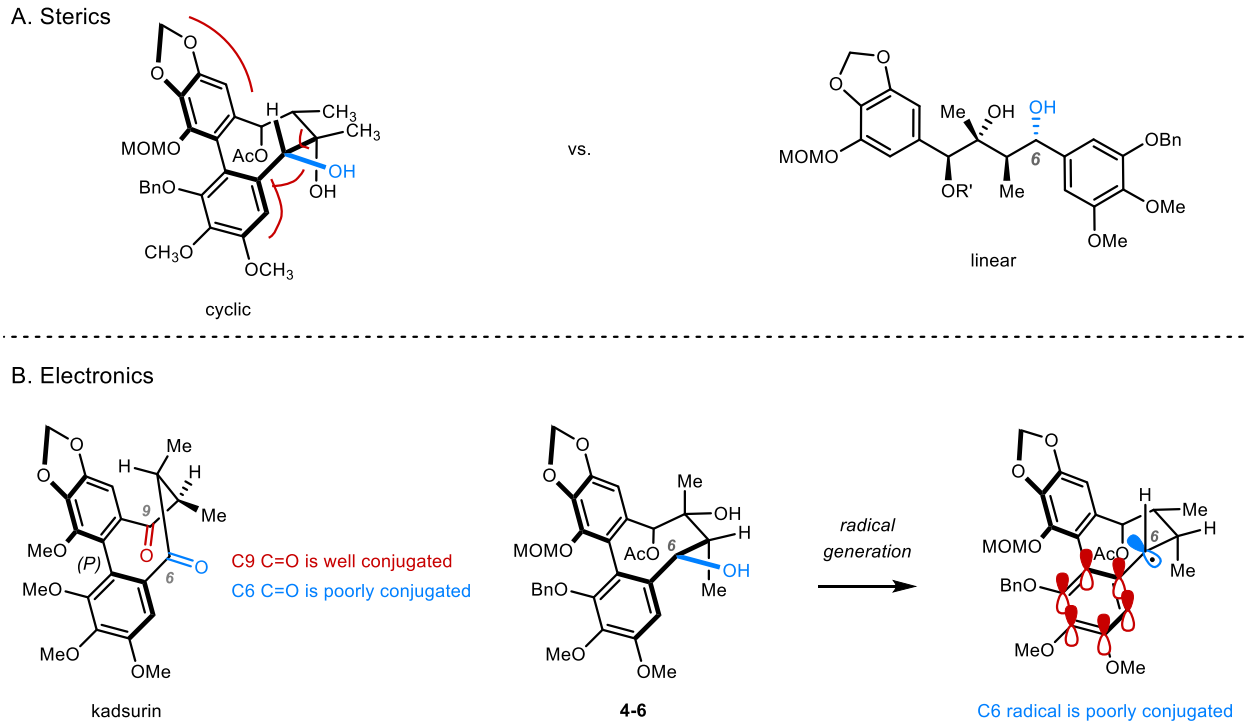


Figure 4.2. Challenges associated with the C6 deoxygenation of a cyclic system: A. sterics and B. electronics

As a broader goal we would like to develop methodology for the selective deoxygenation of each position of the 8-membered ring, allowing us to access a greater diversity of DBCODs. Biosynthetically, the DBCOD scaffold is synthesized in its non-oxygenated form and then selectively oxidized by CYP450s. We will take the reverse approach of forming the DBCOD scaffold with full oxygenation and then selectively reducing around the ring (Figure 4.3B). Different methodologies for the selective reduction of the C6, C7, or C9 position would allow for the synthesis of diverse stage 2 DBCODs, for example longipedlignan E, kadhetrin A, and gomisin C (Figure 4.3B).

In this chapter, efforts towards the synthesis of taiwanschirin B are discussed. The known intermediate **4-21** was prepared and converted to **4-6** in 3 steps, a cyclic substrate on which C6 deoxygenation conditions were screened. Changing strategies, 6-benzyloxy taiwanschirin B was

prepared in 3 steps from heteroclitin J. Deoxygenation conditions for the conversion of 6-benzyloxy taiwanschirin B to taiwanschirin B were screened.

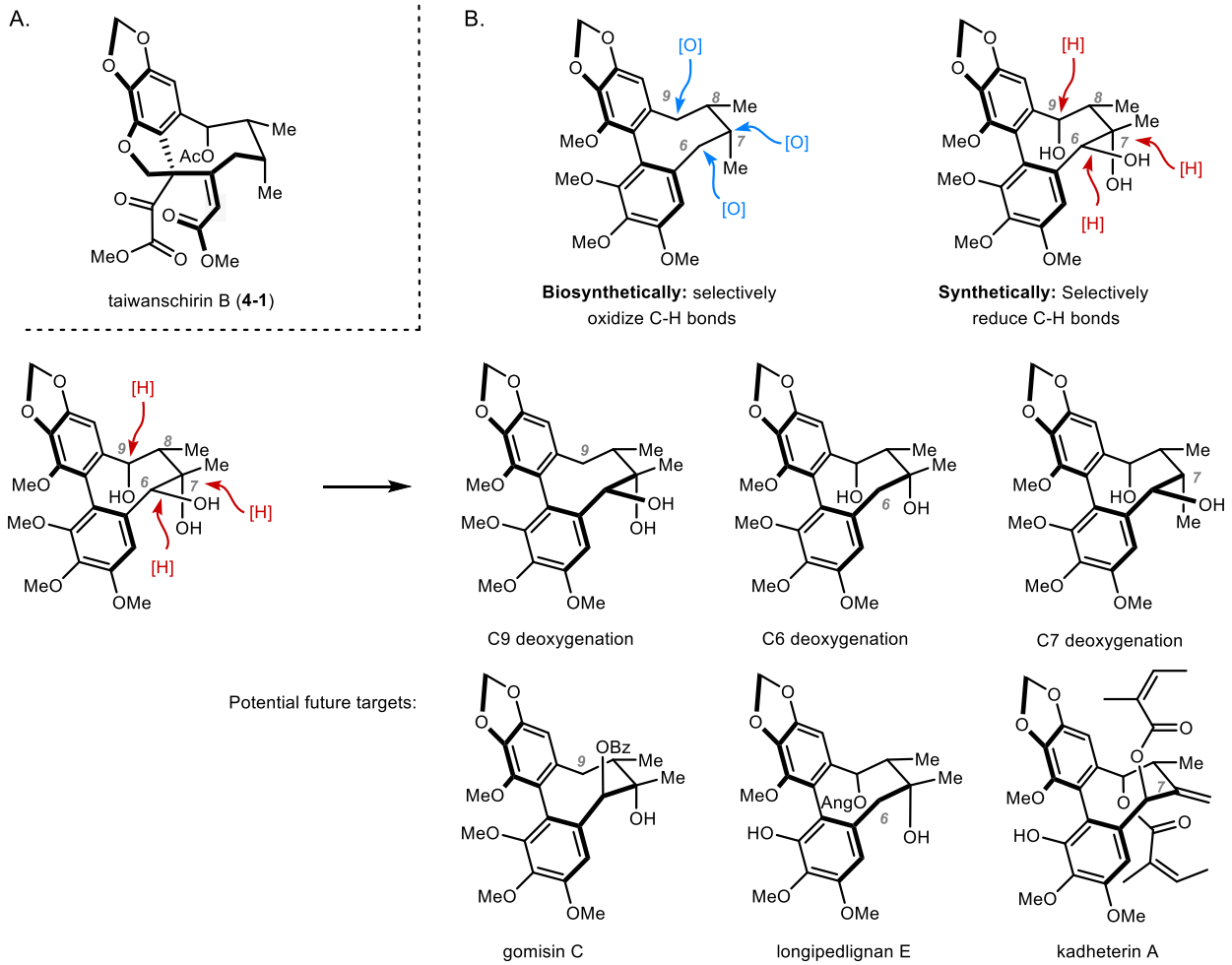
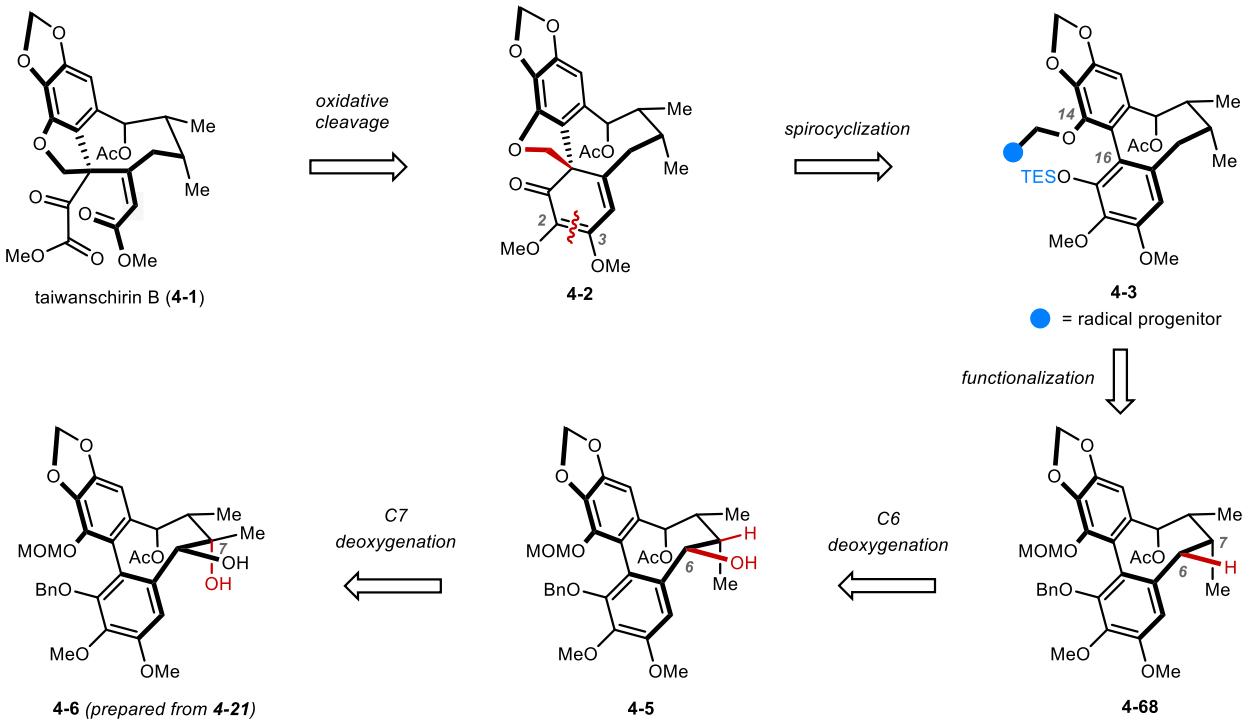


Figure 4.3. A) Synthetic target taiwanschirin B; B) Controlling the oxidation pattern of the DBCOD 8-membered ring

4.2. Retrosynthetic analysis

Retrosynthetically, it was anticipated that taiwanschirin B (**4-1**) could arise from the oxidative cleavage of the C2-C3 bond of the *ortho*-spirodienone **4-2** (Scheme 4.2). Compound **4-2** can be formed from **4-3**, which bears an *N*-hydroxyphthalimide (NHPI) redox-active ester at C14 to serve as a radical progenitor, using the regioselective photocatalyzed spirocyclization methodology previously developed in our group.[4] Compound **4-3** in turn comes from manipulating the phenolic substituents *ortho* to the biaryl of **4-68** to append suitable handles for the

spirocyclization reaction. Compound **4-68** is the product of C6 deoxygenation of compound **4-5**, which can arise from a two-step C7 deoxygenation (Burgess dehydration followed by hydrogenation) of intermediate **4-6**. Compound **4-6** was expected to be prepared in two steps from **4-21**, an intermediate reported in our group's previous synthesis of another DBCOD, heteroclitin J.[5]

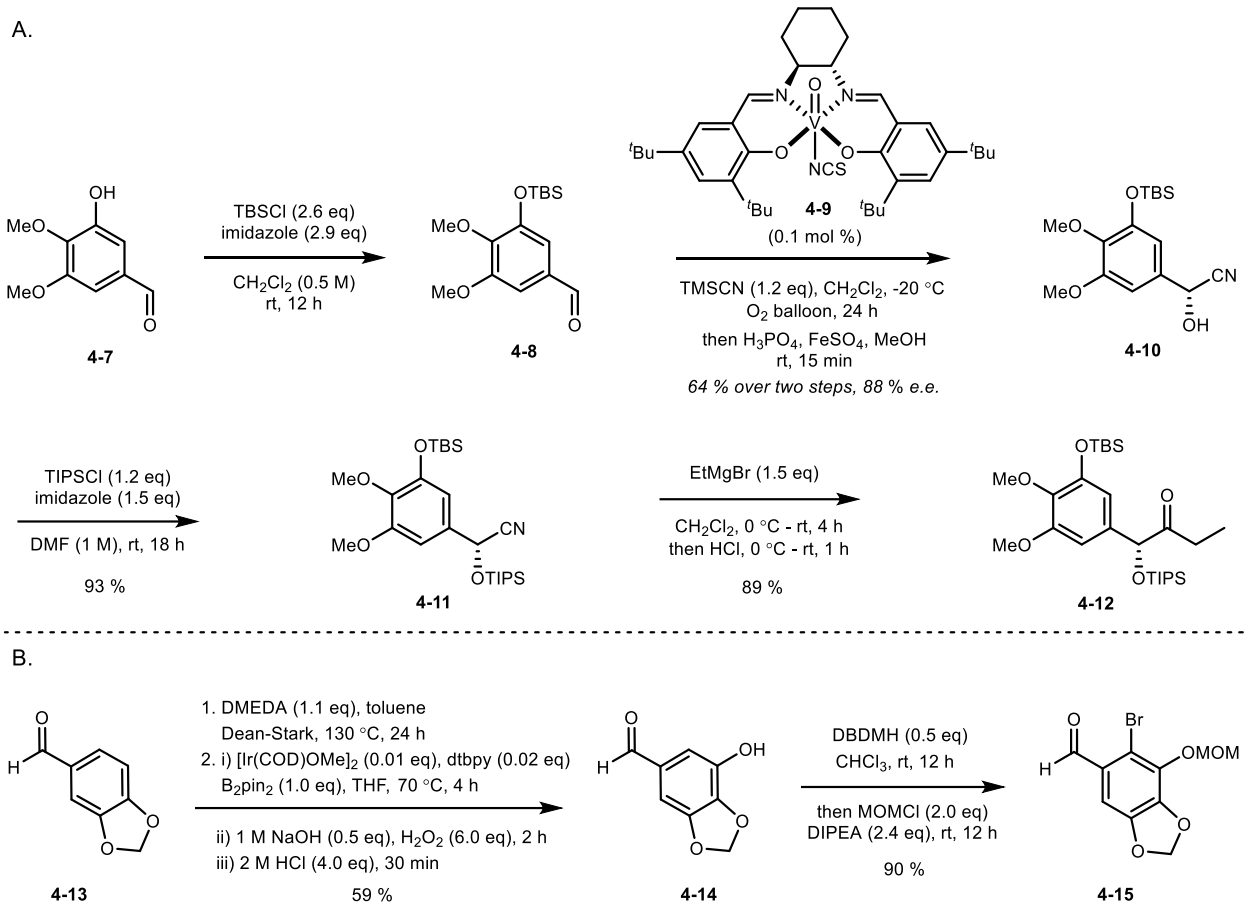


Scheme 4.2. Retrosynthetic analysis of taiwanschirin B

4.3. Preparation of the known intermediate 4-21

Compound **4-21** (Scheme 4.4B) serves as a common intermediate in our group's previous synthesis of heteroclitin J and the current work towards taiwanschirin B. Compound **4-21** was prepared following the reported procedure.[5] This convergent route first involved the separate syntheses of aromatic ketone and aldehyde fragments which would then be coupled to form the alkyl chain of the DBCOD. The synthesis of the chiral ketone **4-12** began by silyl protection of the phenol of 3,4-dimethoxy-5-hydroxybenzaldehyde (**4-7**, Scheme 4.3A). *Tert*-butyldimethylsilyl-protected **4-8** was subjected directly to North and coworkers' (*S,S*)-VO(salen)NCS-catalyzed asymmetric hydrocyanation conditions,[6] providing cyanohydrin **4-10** in 64 % yield over two steps with an enantiomeric excess of 88 %. (It appeared that some degradation of the catalyst occurred

during storage for several years, as this transformation has previously been accomplished using the same catalyst in quantitative yield with an enantiomeric excess of 92.7%.[5]) The secondary alcohol of **4-10** was protected with triisopropylsilyl chloride, yielding **4-11** in 93 %. The TIPS ether **4-11** was then subjected to a Grignard reaction with ethylmagnesium bromide to provide ketone **4-12** in 89 % yield.

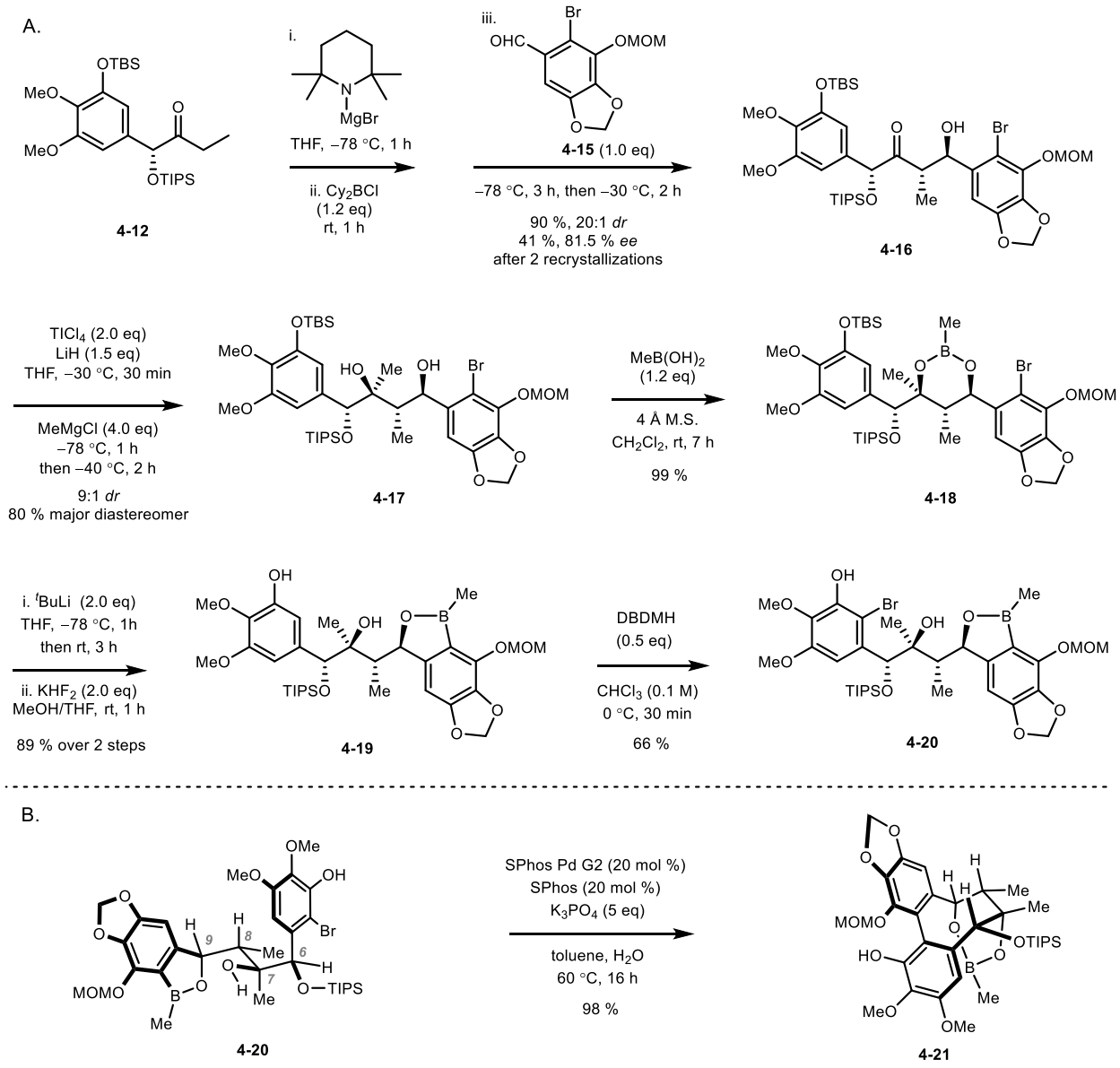


Scheme 4.3. Synthesis of the A) ketone fragment **4-12** and B) aldehyde fragment **4-15**

In our original synthesis, the aldehyde fragment **4-15** was prepared in six steps from vanillin. As a result of a shorter synthesis of intermediate **4-14** (5-hydroxypiperonal) developed by a graduate student in our group, Derek Meng, **4-15** can now be prepared in three steps from piperonal (**4-13**, Scheme 4.3B). First, **4-13** was treated with DMEDA to protect the aldehyde as the aminal. The crude product was then subjected to Ir-catalyzed borylation which occurred regioselectively at the 5-position. The resulting Bpin group was oxidized by treatment with sodium hydroxide / hydrogen peroxide and the aminal was deprotected under acidic conditions to reveal the aldehyde, giving **4-**

14 in 59 % yield over two steps. **4-14** was then converted to the aldehyde **4-15** (in 90 % yield) by phenol-directed *o*-bromination with dibromodimethylhydantoin (DBDMH) followed by protection of the phenol as the MOM ether.

With the ketone and aldehyde fragments in hand, these could be coupled via an aldol addition to form the linear chain which would later become the 8-membered ring of the DBCOD. Compound **4-12** was treated with 2,2,6,6-tetramethypiperidine magnesium bromide (TMPMgBr) at –78 °C to give the (*E*)-magnesium enolate which was then transmetallated to the (*E*)-boron enolate by treatment with chlorodicyclohexylborane. Aldehyde **4-15** was added subsequently, leading to the formation of the 1,3-*syn*-1,2-*anti* aldol **4-16**, possessing a stereotriad, in 90 % yield with 20:1 *dr* (Scheme 4.4A). An enantiomeric excess of 81.5 % could be obtained after two rounds of recrystallization, however, this caused the yield to drop to 41 %. The drop in *ee* of **4-16** compared to cyanohydrin **4-10** is possibly due to some epimerization of the α-stereocenter of **4-12**. (In our previous report, starting from ketone with higher *ee*, the aldol could be obtained in 66 % yield with >99 % *ee*.[5]) Chelate-controlled methyl addition employing titanium (IV) chloride and methylmagnesium chloride was used to install the fourth stereocenter at C7. The methylated product **4-17** was formed with 9:1 *dr*, where the major diastereomer (the 1,3-*syn* diol) could be isolated in 80 % yield. Subjecting the diol **4-17** to methylboronic acid furnished the 6-membered boronic ester **4-18** in 99 % yield. Treatment with 2 equivalents of *tert*-butyllithium led to lithium-bromine exchange, where the resulting aryl lithium then attacked the boron of the boronic ester to give the 5-membered borinic ester. In the same pot, the phenolic TBS group was removed without affecting the TIPS-protected secondary alcohol, by treatment with potassium bifluoride, furnishing **4-19** in 89 % yield over two steps. Phenol-directed *o*-bromination using DBDMH provided **4-20** in 66 % yield. **4-20** was subjected to intramolecular Suzuki coupling conditions using Buchwald's SPhos Pd G2 precatalyst (20 mol %), additional SPhos ligand (20 mol %), K_3PO_4 (5 equiv.), and H_2O (0.5 equiv.) in PhMe at 60 °C, to give **4-21** in 98 % yield as a single atropisomer (Scheme 4.4B).

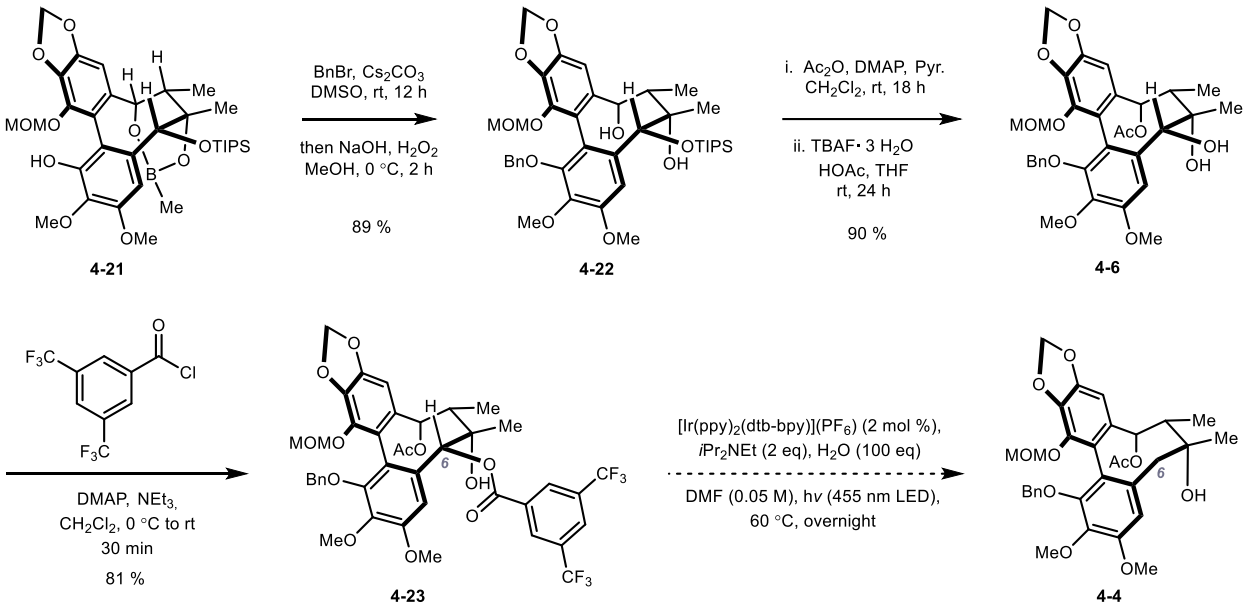


Scheme 4.4. A) Transformations of the linear precursor and B) atroposelective Suzuki coupling

4.4. Benzylic deoxygenation on a cyclic system

Compound **4-6**, bearing an equatorial alcohol at C6, was selected as the substrate to use in a proof-of-concept study for the C6 deoxygenation of cyclic DBCOD systems, as well as serving as an intermediate in the synthesis of taiwanschrin B. Once developed, the C6 deoxygenation methodology could be applied to other DBCOD syntheses, such as that of kadsuraol C. Compound **4-6** was prepared in three steps from the Suzuki coupling product **4-21**. First, the phenol was protected using benzyl bromide and the boronic ester was hydrolyzed by treatment with sodium

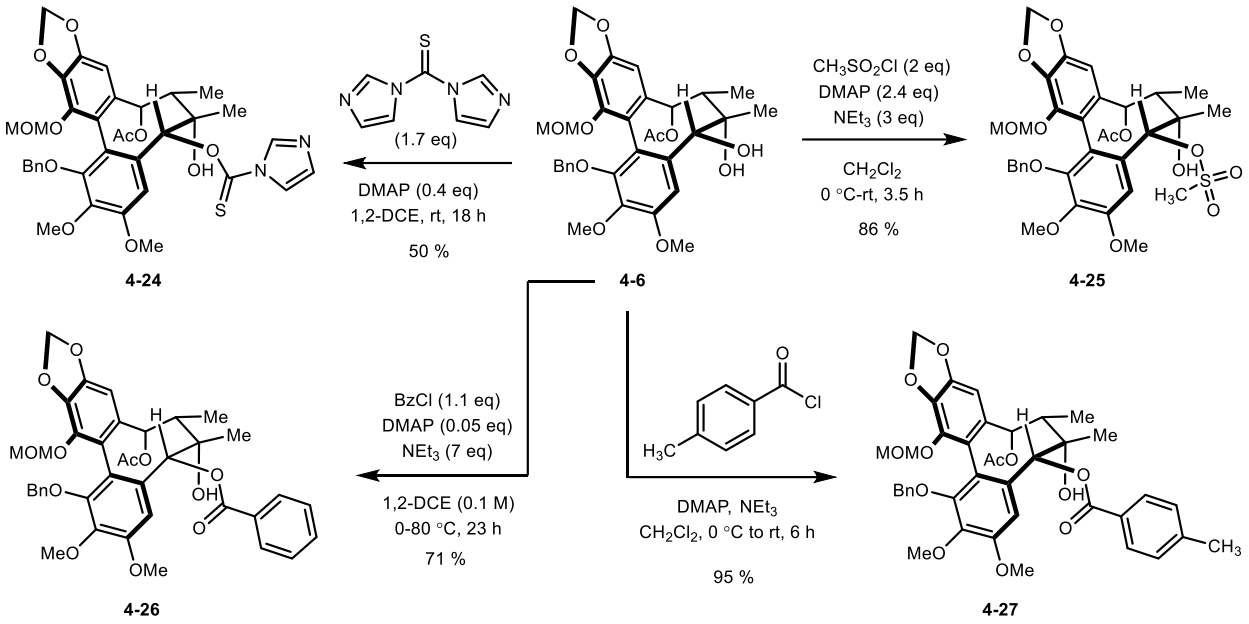
hydroxide / hydrogen peroxide, yielding the diol **4-22** in 89 % (Scheme 4.5). Next, the C9 alcohol was protected with an acetyl group, followed by deprotection of the C6 silyl ether using TBAF, providing **4-6** in 90 % yield. As Reiser's photoredox-catalyzed deoxygenation conditions for benzylic alcohols[7] had been successfully applied to a linear substrate in the kadsuraol C project (Chapter 3), these were the first conditions attempted for the C6 deoxygenation of cyclic **4-6**. A photoactive ester, 3,5-bis(trifluoromethyl)benzoate, was appended to the C6 alcohol, providing **4-23** in 81 % yield. Subjecting **4-23** to Reiser's conditions of $[Ir(ppy)_2(dtb\text{-}bpy)](PF_6)$ (2 mol %), triethylamine (2 equiv.) and water (100 equiv.) in DMF (0.05 M) under blue light irradiation at 60 °C for 20 h, resulted solely in recovered starting material **4-23**. Variations to these conditions including dilution (0.001 M in DMF), changing the solvent to acetonitrile, increasing the temperature to 90 °C, and the addition of HFIP (100 equiv.) did not improve reactivity.



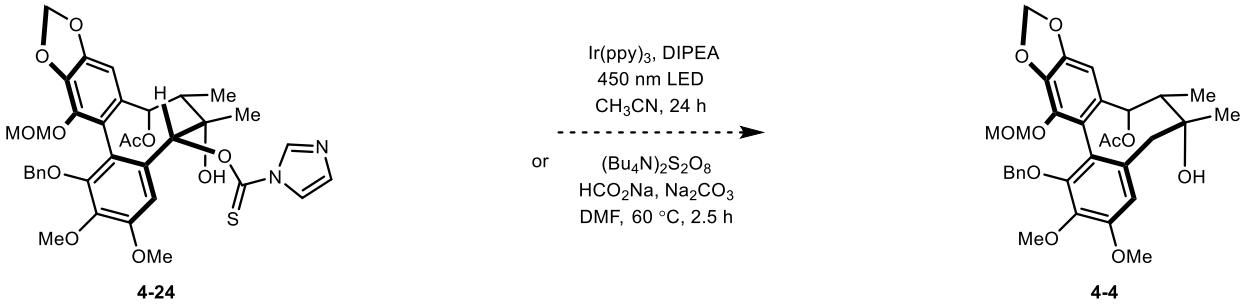
Scheme 4.5. Functional group manipulations on the Suzuki coupling product **4-21**

Alternative conditions for the C6 deoxygenation of **4-6** were then investigated. Various handles could be appended to the C6 alcohol to provide species which were activated for deoxygenation, such as the imidazyl thiocarbamate **4-24**, mesylate **4-25**, benzoate **4-26**, and toluate **4-27** (Scheme 4.6). The preparation of another Barton ester, the C6 *S*-methyldithiocarbonate (OC(S)SMe), from **4-6** was unsuccessful, leading only to deprotection of the C9 acetate. The reaction of the sterically encumbered C6 alcohol of **4-6** with the bulky 1,1'-thiocarbonyldiimidazole proceeded sluggishly and incompletely, providing a maximum yield of 50 % **4-24**. Nevertheless, the thiocarbamate **4-**

24 was then subjected to two sets of tin-free Barton–McCombie conditions (Scheme 4.7). The first, developed by Ollivier and coworkers for the deoxygenation of secondary alcohols,[8] involved $Ir(ppy)_3$ (5 mol %) as a photocatalyst and DIPEA (5 equiv.) in acetonitrile (0.07 M) under irradiation by blue LEDs and provided a complex mixture of products which were not easily separable. The second, from Kim and coworkers, employed tetrabutylammonium peroxydisulfate ($(Bu4N)_2S_2O_8$), a one electron oxidant which converts sodium formate to a carbon dioxide radical anion ($CO_2^{\bullet -}$), which transfers an electron to the thiocarbamate, which then undergoes cleavage.[9] When applied to **4-24**, these conditions gave a mixture of products which did not include the desired deoxygenation species **4-4**.

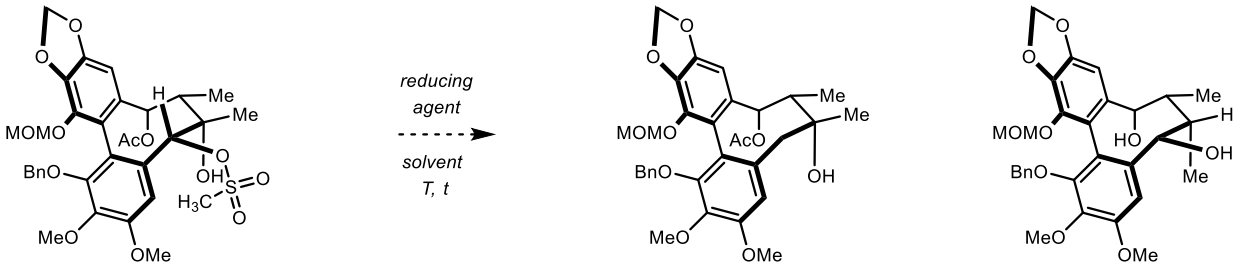


Scheme 4.6. Preparation of other (C6 equatorial) substrates for C6 deoxygenation



Scheme 4.7. Attempted C6 deoxygenation via the equatorial imidazyl thiocarbamate **4-24**

The mesylate **4-25**, formed in 86 % yield, was subjected to several sets of conditions reported in the literature for the reduction of benzylic mesylates, however none successfully furnished the desired product **4-4** (Table 4.1). Pd/C catalyzed hydrogenation[10] (entry 1) and reduction using sodium borohydride (entry 2) returned starting material **4-25** as the major species (49–56 %). A minor species detected in the reaction mixture of entry 2 was assigned as a product of elimination based on its molecular weight of 96 less than **4-25** (equivalent to the loss of methanesulfonic acid), as determined by mass spectrometry. In entry 3, lithium triethylborohydride was employed as a reducing agent, which apparently led to hydrolysis of the C9 acetate and migration of the mesylate to the C7 alcohol, followed by reduction at C7, furnishing unwanted byproduct **4-28** (in 71 % yield). **4-28** was characterized by HRMS and NMR spectroscopy, where the HSQC spectrum indicated the presence of two C<u>H</u>CH$_3$ signals (δ= 2.68 and 2.38, multiplets integrating to 1H each) on different carbons rather than diastereotopic protons on the same <u>C</u>H$_2$. Additionally, the ^{1}H NMR spectrum displayed two C<u>H</u>OH signals (a multiplet at 4.28 ppm and a doublet at 4.34 ppm, integrating to 1H each). The stereochemistry at C7 could not be determined by NMR so it is also possible we have the epimer at this position. **4-28** (in 35 % yield) was also observed when lithium aluminum hydride[11] (entry 4) was utilized as the reducing agent, as well as another byproduct (in 49 % yield) where **4-25** had undergone deprotection of the benzyl ether. The sterically encumbered nature of the C6 position may have been detrimental in methods proceeding via SN2 reaction, making hydride delivery to the backside of the C6 mesylate unfeasible.

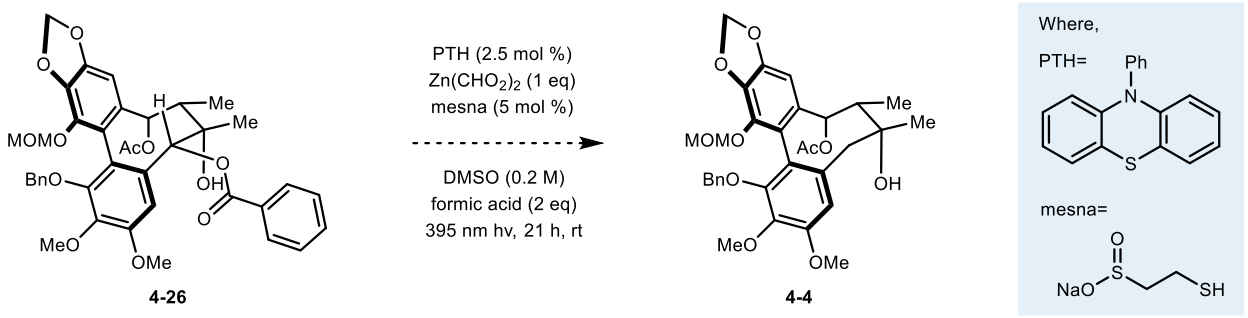


4-25 **4-4** **4-28**

Entry	reducing agent	solvent	T (^{o}C)	t (h)	**4-25** (%)	**4-4** (%)	**4-28** (%)	**other** (%)
1	Pd/C (0.1 eq), H_2	EtOAc/MeOH	rt	16	49	-	-	-
2	$NaBH_4$ (5 eq)	EtOH	0-rt	5	56	-	-	24
3	$Li(BHEt_3)$ (1.2 eq)	THF	0-rt	2	-	-	71	-
4	$LiAlH_4$	THF	0-rt	4	-	-	35	49

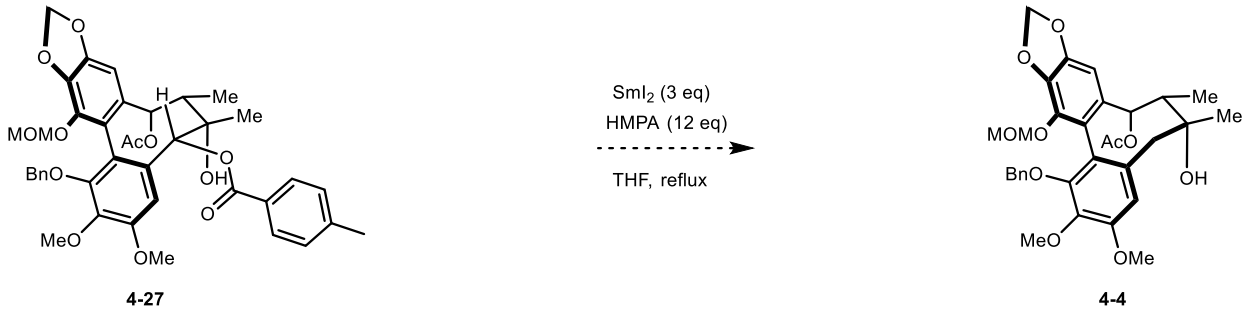
Table 4.1. Attempted C6 deoxygenation via the equatorial mesylate **4-25**

The benzoylation of **4-6** was low yielding at rt (36 % after 70 h), however **4-26** could be formed in a good yield of 71 % when heated to 80 °C for 23 h. The resulting **4-26** was subjected to photoredox-catalyzed conditions recently reported by Wickens and coworkers for the reductive cleavage of benzoate esters (Scheme 4.8).[12] These conditions employ the organic photocatalyst *N*-phenylphenothiazine (PTH, 2.5 mol %), zinc formate (1 equiv.) as a terminal reductant, 2-mercaptoethanesulfonate (mesna, 5 mol %) as an HAT co-catalyst, and formic acid (2 equiv.) in DMSO under violet light irradiation (395 nm). Only recovered starting material **4-26** was obtained after a 21 h reaction time. It is worth noting that our experimental setup utilized an LED loop reactor instead of Kessil lamps as reported by Wickens *et al.*, which may have caused the reaction to fail due to their lower light intensity.



Scheme 4.8. Attempted C6 deoxygenation via the equatorial benzoate **4-26** using Wickens' photoredox-catalyzed conditions

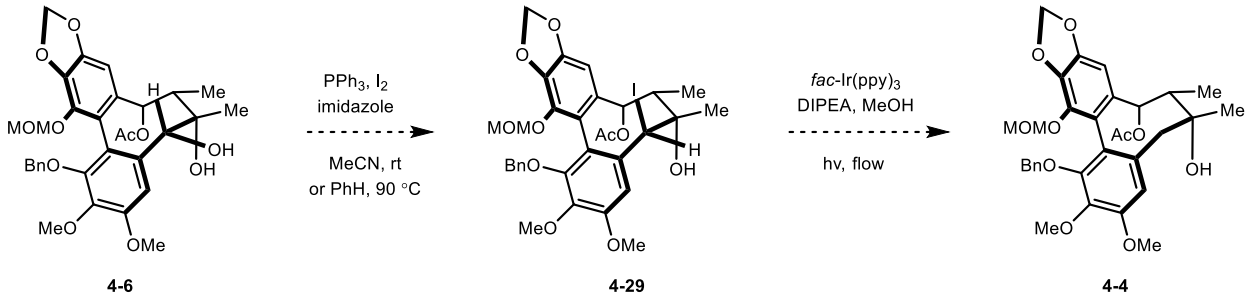
Toluate **4-27** could be prepared from **4-6** in a high yield of 95 % after a reaction time of 6 h at rt. It was subjected to benzoate reduction conditions from Markó and coworkers,[13] using SmI_2 (3 equiv.) as the reductant with HMPA (12 equiv.) in refluxing THF (Scheme 4.9). Markó *et al.* reported the deoxygenation of secondary alcohols within 10 seconds to 5 minutes under these



Scheme 4.9. Attempted C6 deoxygenation via the equatorial toluate **4-27**

conditions, however in this case, only starting material **4-27** was recovered after 5 minutes. Increasing the reaction time to 4 hours did not improve reactivity.

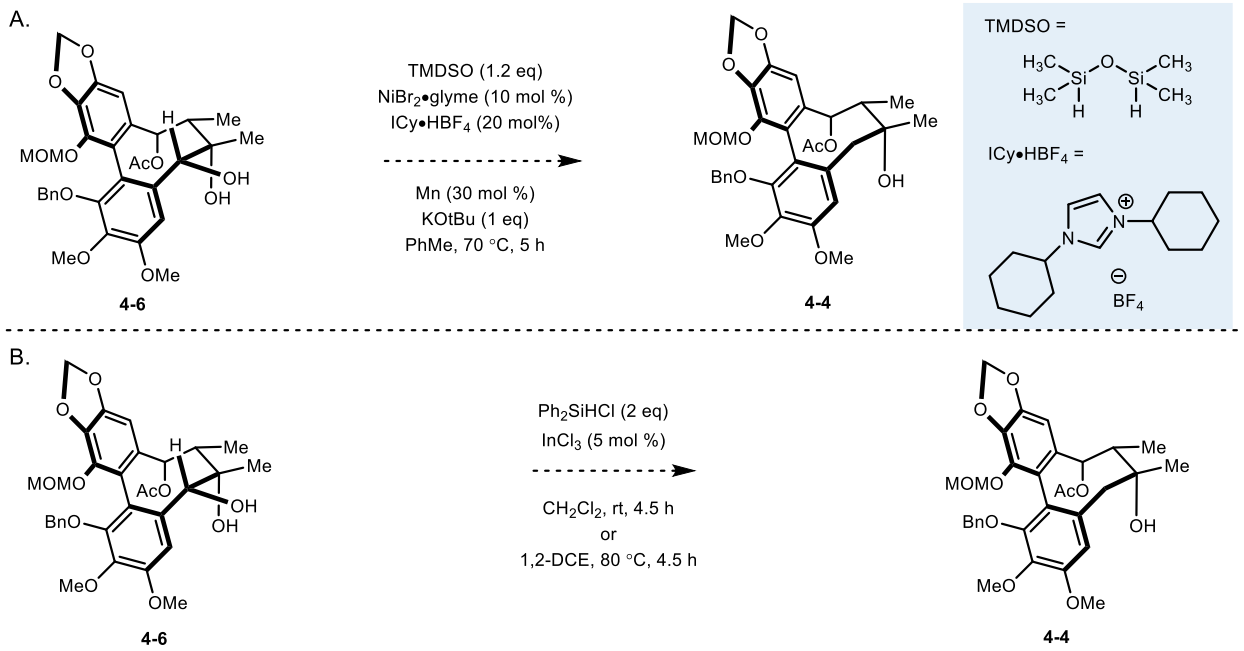
An alternative method to activate the alcohol for deoxygenation involves substituting the hydroxyl group with an iodide. Hydrodeiodination of secondary iodides has been reported using visible light photoredox catalysis[14] and copper catalysis.[15] Alcohol **4-6** was subjected to the Garegg-Samuelsson reaction, involving triphenylphosphine, imidazole, and iodine (1.2 equiv.) in acetonitrile at rt in an attempt to form the corresponding iodide **4-29** (Scheme 4.10). Even upon addition of another 1 equiv. iodine, **4-29** was not formed and instead deprotection of the MOM ether of the phenol occurred. Increasing the reaction temperature to 90 °C and changing the solvent to benzene only led to decomposition. Preparation of **4-29** was also attempted in a two-step sequence from **4-6** by first treating with trifluoromethanesulfonyl chloride to form the C6 triflate, followed by NaI (3 equiv.) in acetone at 50 °C, which also failed to provide the desired iodide. Due to the inability to prepare **4-29**, the subsequent hydrodeiodination reaction could not be attempted.



Scheme 4.10. Attempted C6 deoxygenation via the iodide

Although less common, a few papers report conditions for the deoxygenation of unactivated alcohols, hence these were investigated as well, using **4-6** as the substrate. In Scheme 4.11A, conditions developed by Newman and coworkers,[16] involving a $NiBr_2$•glyme (10 mol %), ICy•HBF_4 (20 mol %), tetramethyldisiloxane (TMDSO, 1.2 equiv.), manganese (0.3 equiv.), and potassium *tert*-butoxide (1 equiv.) in PhMe at 70 °C were applied, failing to return anything other than recovered **4-6**. $NiBr_2$•glyme serves as the Ni(II) pre-catalyst, potassium *tert*-butoxide deprotonates ICy•HBF_4 which serves as ligand, manganese reduces Ni(II) to Ni(0), and tetramethyldisiloxane (TMDSO) plays the role of hydride source. Newman *et al.* found that these conditions worked well on substrates which included a nearby π-system (including allylic,

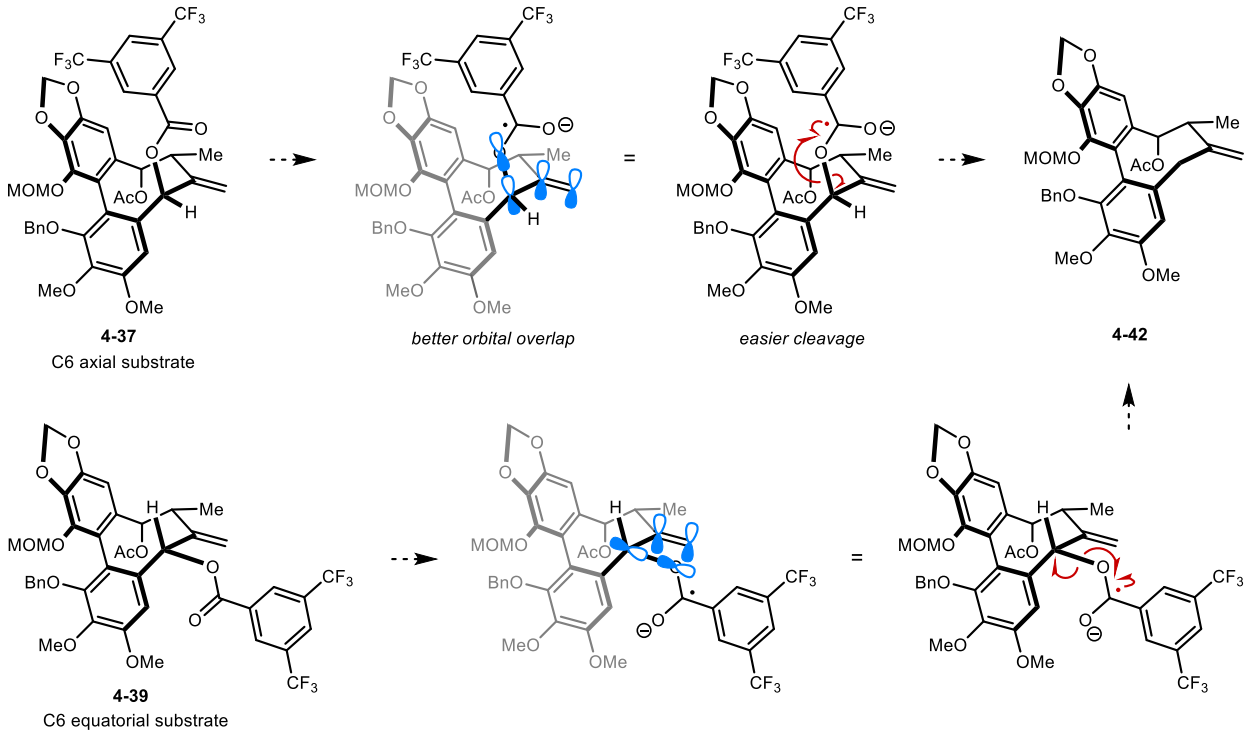
benzylic, and homobenzylic alcohols) but were ineffective on aliphatic systems, which led us to question the nature of our "benzylic" alcohol. In Scheme 4.11B, chlorodiphenylsilane was employed as a hydride source in the presence of catalytic indium trichloride, a chemoselective method described by Baba and coworkers for the reduction of benzylic, secondary, and tertiary alcohols which can be performed in the presence of esters.[17] Compound **4-6** was subjected to two variations of these conditions, as most substrates were reported to undergo deoxygenation at room temperature in CH_2Cl_2 whereas others required heating to 80 °C in dichloroethane, however both sets of conditions led to a complex mixture of decomposition products.



Scheme 4.11. Attempted C6 deoxygenation directly from the equatorial alcohol **4-6** A. using Newman's Ni-catalyzed conditions and B. using Ph_2SiHCl / $InCl_3$ conditions

The lack of reactivity towards deoxygenation of the alcohol **4-6** and its derivatives, **4-24** to **4-27**, is likely the result of the substrate's electronics. It was found by Ghera in his study of kadsurin, which bears both C6 and C9 carbonyls, that the C6 carbonyl was poorly conjugated with the neighbouring aromatic ring, due to the twisted nature of the biaryl linkage.[3] Many conditions for benzylic deoxygenation proceed via the homolytic cleavage of the C-O bond, generating a radical intermediate. The radical generated would be poorly conjugated with the neighbouring aromatic ring and would therefore not be as stable as a traditional benzylic radical. If the C6 radical could be in better conjugation with another π-system instead, this could provide some added stabilization.

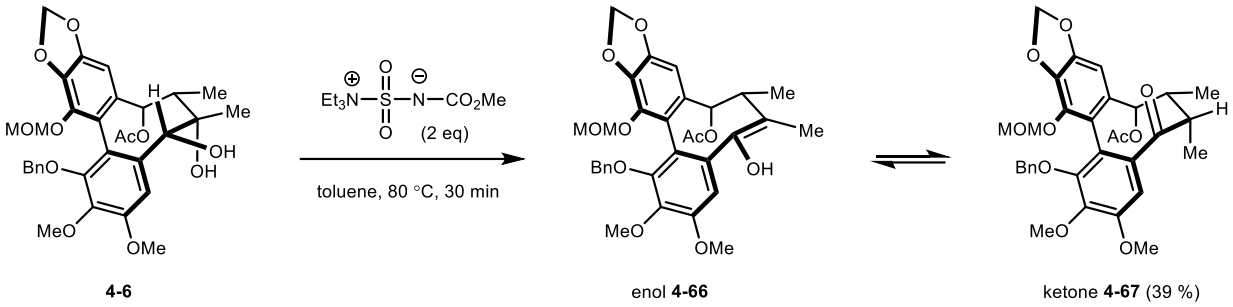
For example, the introduction of an exocyclic alkene at C7 by dehydration of the tertiary alcohol would make the C6 alcohol allylic. Dehydration of the tertiary alcohol would also serve to advance the synthesis, as when followed by hydrogenation of the resulting alkene, this accomplishes the C7 deoxygenation. Considering starting material was recovered in most of the reactions, it appeared that the generation of the C6 radical did not occur. We surmised that the generation of this radical may be easier starting from a substrate where the C6 position has been epimerized in addition to bearing a C7 methylene, as the C-O bond to be cleaved should be better aligned with the π-system of the alkene (see example substrates in Scheme 4.12).



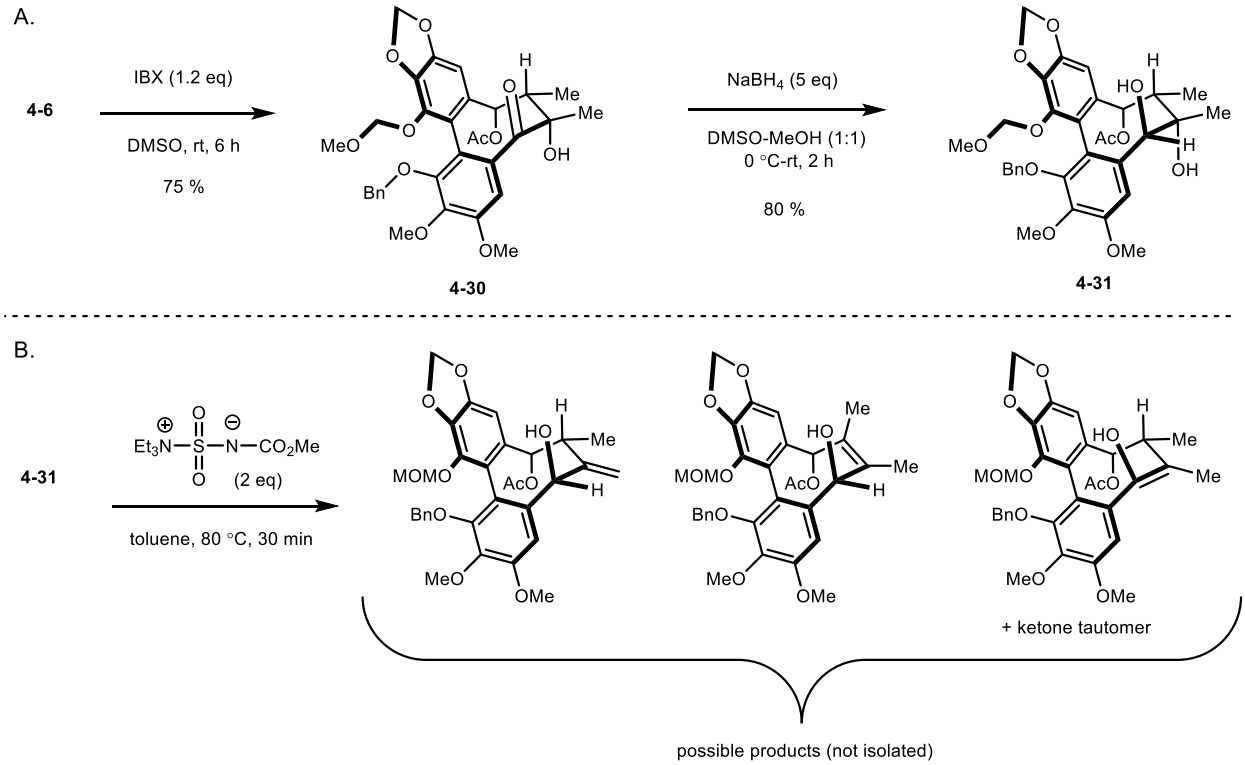
Scheme 4.12. Comparison of the orbital overlap of the C6-O bond to be cleaved and the allylic π-system in axial vs. equatorial substrates

In terms of order of operations, it was necessary to perform the epimerization and esterification of the C6 alcohol prior to the dehydration of the C7 alcohol to impart regioselectivity during the Burgess dehydration. Subjecting the free alcohol **4-6** to Burgess conditions led to a mixture of products, with the major constituent being the C6 ketone (**4-67**, isolated in 39 % yield), which would have arisen from tautomerization of enol **4-66** (Scheme 4.13). Therefore, **4-31**, bearing the epimeric C6 alcohol was prepared in two steps from **4-6** (Scheme 4.14A). First, the secondary

alcohol of **4-6** was oxidized by treatment with iodoxybenzoic acid (IBX), providing **4-30** in 75 % yield, then the resulting ketone was selectively reduced to the axial alcohol using sodium borohydride, providing **4-31** in 80 % yield. Treating **4-31** with Burgess dehydration conditions was not regioselective, yielding a complex mixture of alkenes (Scheme 4.14B), confirming that the esterification step should precede the dehydration step.



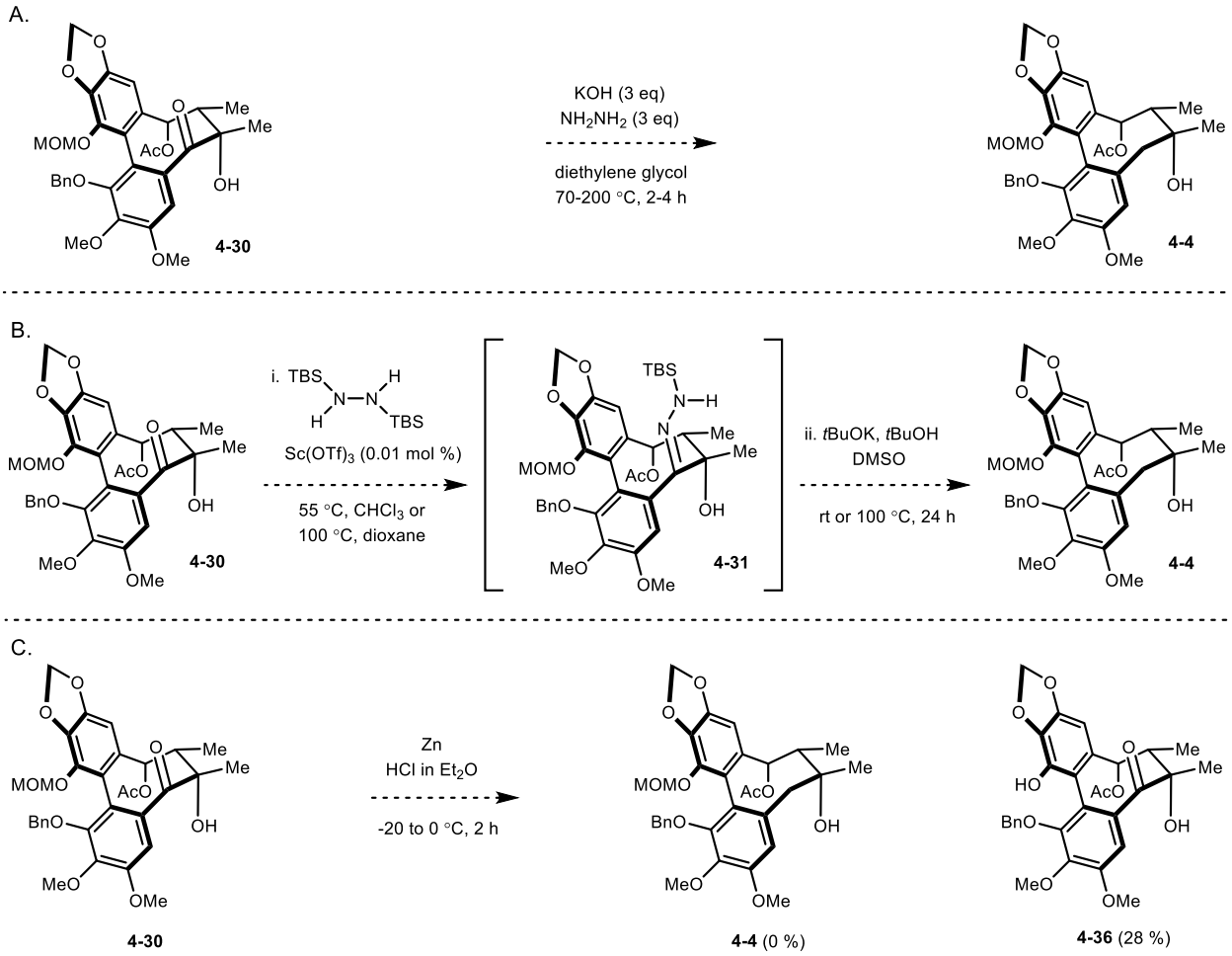
Scheme 4.13. Burgess dehydration of **4-6**



Scheme 4.14. A. Epimerization of the C6 alcohol of **4-6**; B. Burgess dehydration of **4-31**

Prior to exploring the esterification and subsequent deoxygenation of **4-31**, deoxygenation directly from the ketone **4-30** was investigated. Ketone **4-30** was subjected to classic Wolff-Kishner

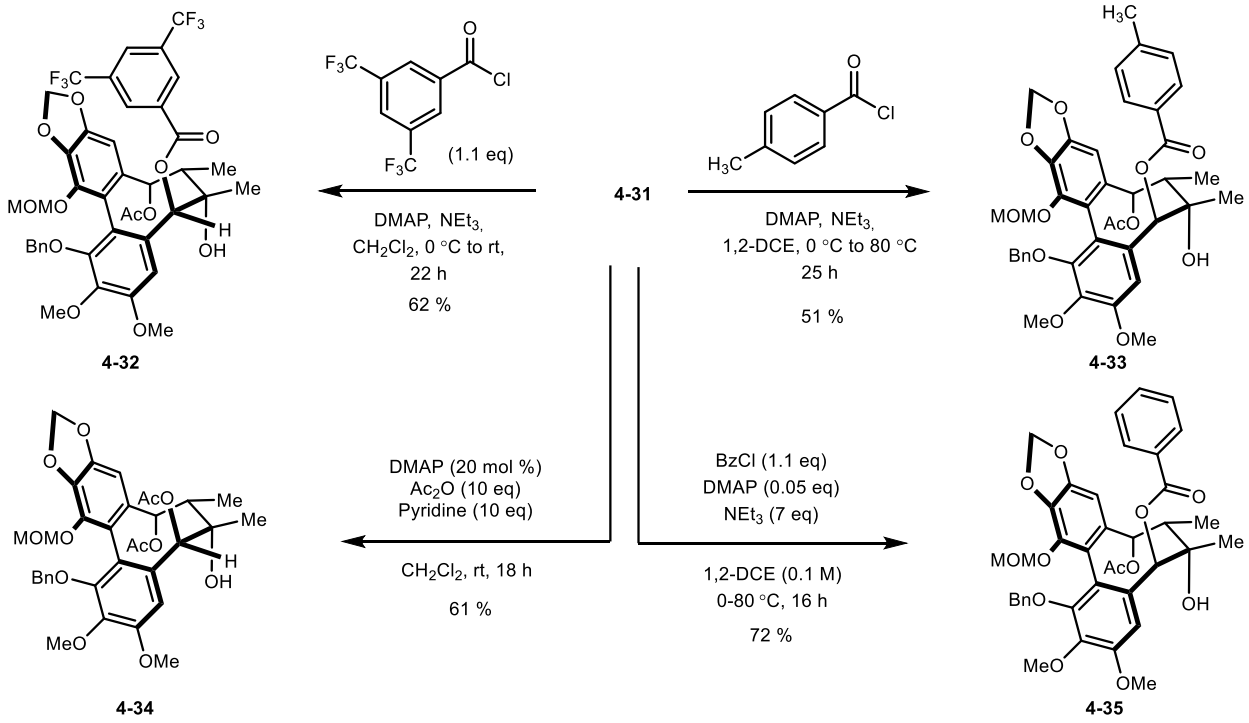
reduction conditions[18] involving potassium hydroxide (3 equiv.) and hydrazine (3 equiv.) in diethylene glycol with heating (Scheme 4.15A). The typical conditions using high heat (200 °C), led to decomposition of the substrate. Implementing the same conditions but at lower temperatures of 70 °C or 150 °C alleviated the decomposition issue but did not lead to formation of the desired product. In these cases, a mixture of starting material **4-30** and deacetylated **4-30** was obtained (in a 2.6:1 ratio). Next, milder modified Wolff-Kishner conditions developed by Myers and coworkers[19] were attempted (Scheme 4.15B). This two-step procedure involves the preparation of the *N*-*tert*-butyldimethylsilylhydrazone (TBSH) derivative of the ketone, followed by treatment with potassium *tert*-butoxide and *tert*-butanol in DMSO to yield the methylene, neither of which step requires temperatures exceeding 100 °C. Treatment of **4-30** with TBSH and catalytic



Schemes 4.15. Attempts at C6 deoxygenation of the ketone via A) Wolff-Kishner reduction; B) Myers' modified Wolff-Kishner reduction; C) Clemmensen reduction

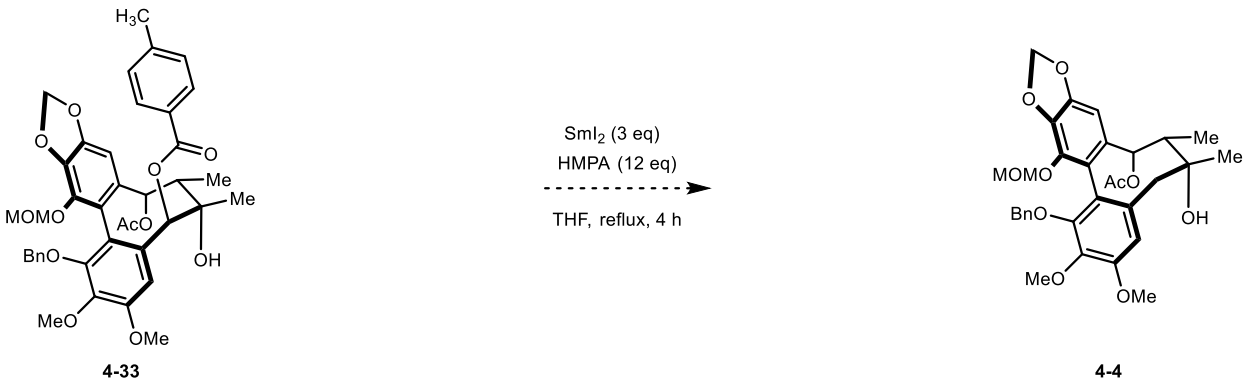
scandium triflate at 55 °C in chloroform solely returned starting material. Increasing the temperature to 100 °C and changing the solvent to dioxane did not improve the reactivity. It would appear that TBSH is too bulky to condense onto the sterically encumbered C6 ketone of **4-30**, therefore the intermediate **4-31** could not be formed. Another reported method for the reduction of ketones to the corresponding methylene is the Clemmensen reduction. The classic procedure is quite harsh, employing 40 %aqueous hydrochloric acid and amalgamated zinc (Zn/Hg), however more recent procedures have been developed which are compatible with acid-sensitive functional groups and avoid the use of toxic mercury. Our ketone **4-30** was subjected to one of these milder Clemmensen reduction protocols (Scheme 4.15C), utilizing zinc dust, and ethereal HCl (2 M).[20] Unfortunately, even these conditions were too acidic as the only product observed was **4-30** which had undergone deprotection of the MOM ether (**4-36**, 28 % yield).

Returning to the C6 axial alcohol **4-31**, this could be converted into several activated esters for use in deoxygenation reactions (Scheme 4.16). The esterification of **4-31** to the 3,5-bis(trifluoromethyl)benzoate **4-32**, toluate **4-33**, acetate **4-34**, and benzoate **4-35** proceeded with fair to good yields (51–72 %). The syntheses of the C6 axial mesylate and C6 axial imidazyl



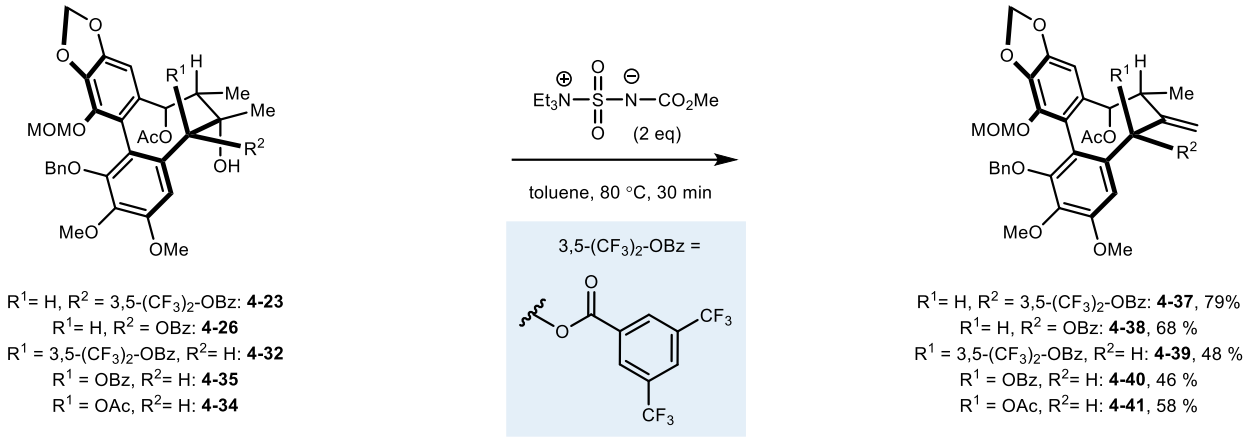
Scheme 4.16. Preparation of C6 axial substrates for deoxygenation

thiocarbamate from **4-31** were also attempted but only returned starting material. The formation of the axial toluate **4-33** was noticeably more challenging than the corresponding equatorial toluate **4-27**, requiring heating to 80 °C for 25 h (vs. 6 h at rt) and yet still yielding 44 % less product (with recovered starting material accounting for the mass balance). Axial toluate **4-33** was then subjected to SmI_2-mediated reduction conditions (Scheme 4.17) which failed at yielding the desired **4-4**, only returning starting material (54 %).



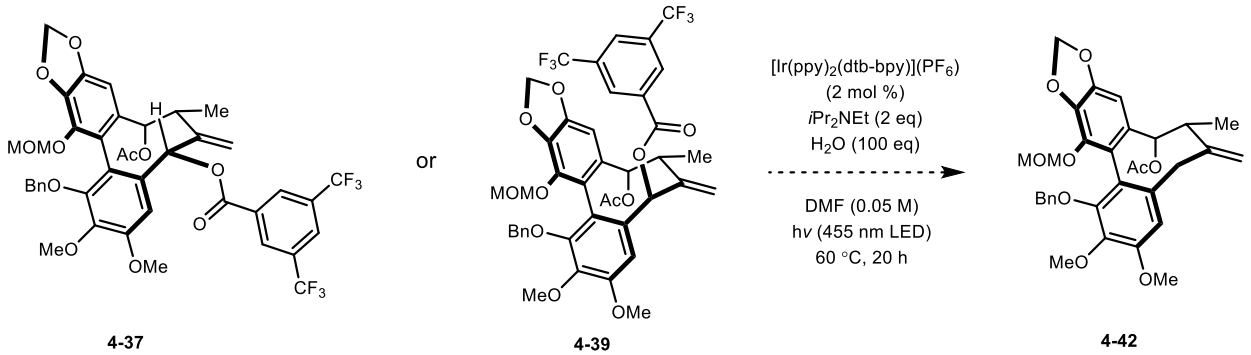
Scheme 4.17. Attempt at SmI_2-mediated deoxygenation of the axial toluate **4-33**

The Burgess dehydration of substrates bearing an ester at C6 (**4-23**, **4-26**, **4-32**, **4-35**, and **4-34**) proceeded with better regioselectivity than the free alcohols **4-6** and **4-31**, as the electron withdrawing esters destabilized the formation of the C6-C7 internal alkene, favoring the formation of the exocyclic alkene at C7. Standard conditions of heating at 80 °C for 30 minutes with Burgess reagent (2 equiv.) were used to prepare five *exo*-methylene products (Scheme 4.18). The equatorial C6 esters **4-23** and **4-26** could be converted into the corresponding alkenes **4-37** and **4-38** in 79 % and 68 % yield, respectively. The axial C6 esters **4-32**, **4-35**, and **4-34** were transformed into the analogous alkenes **4-39**, **4-40**, and **4-41** in 48 %, 46 %, and 58 % yield, respectively. The lower yields of *exo*-cyclic methylene products from the C6 axial esters are likely due to poorer regioselectivity in these substrates, as the mechanism of Burgess reagent involves *syn*-elimination and the C6 H is *syn* to the C7 OH in these substrates, making the formation of the C6-C7 alkene more favorable (compared to the *anti* elimination that would be required from a C6 equatorial substrate). The C6 equatorial imidazyl thiocarbamate **4-24** (see Scheme 4.6) displayed poor regioselectivity in the Burgess dehydration, therefore this substrate was not pursued.



Scheme 4.18. Burgess dehydration of the C7 tertiary alcohol

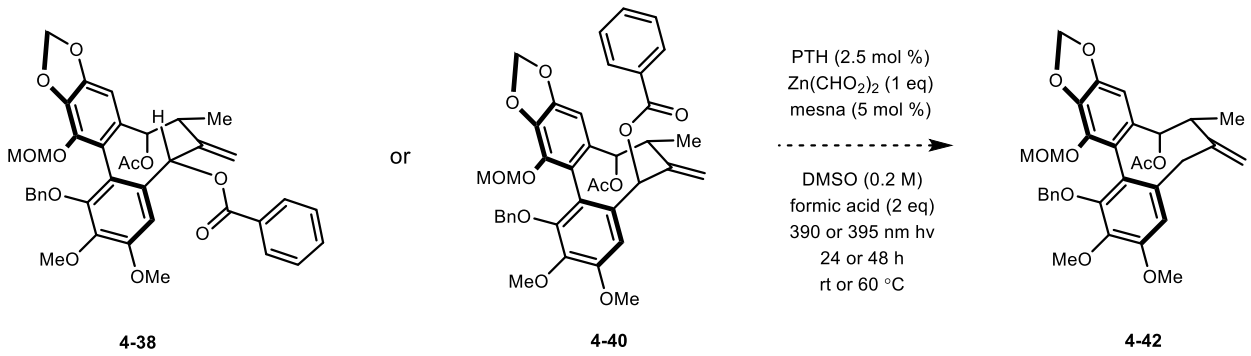
To test the theory on improving the orbital overlap of C6-O with the allylic π-system, both equatorial and axial 3,5-bis(trifluoromethyl)benzoates **4-37** and **4-39** were independently subjected to Reiser's photoredox-catalyzed deoxygenation conditions (Scheme 4.19). These conditions have only been reported for the deoxygenation of benzylic alcohols. Both reactions solely returned starting materials, indicating that stabilization from the C7 alkene was not sufficient to compensate for the lack of conjugation with the neighbouring aromatic ring and to enable the C6 radical to form. Subsequent deoxygenation efforts were then focused on more general deoxygenation conditions which did not require the activated alcohol to be benzylic.



Scheme 4.19. Attempts at C6 deoxygenation of C7-*exo*-methylene substrates using Reiser's photoredox-catalyzed conditions

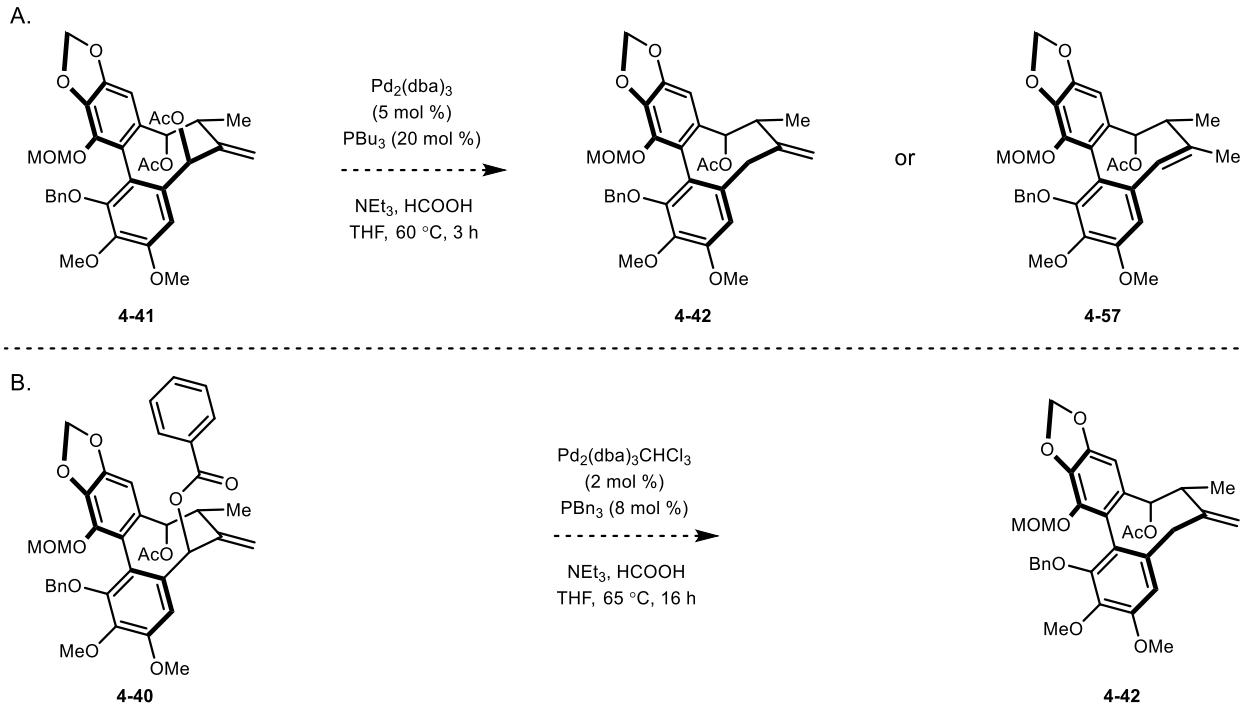
Benzoates **4-38** and **4-40** were each subjected to Wickens' photoredox-catalyzed deoxygenation conditions (Scheme 4.20). The equatorial **4-38** was either irradiated with a 395 nm LED loop reactor for 24 h at rt or with 390 nm Kessil lamps for 48 h at 60 °C under the standard conditions.

The former led to recovery of starting material and the latter led to decomposition. Since the combination of extended heating and irradiation from the high powered Kessil lamps was excessively harsh, the axial **4-40** was irradiated with 390 nm Kessil lamps at rt for 24 h. However, these conditions proved too harsh as well, resulting only in decomposition.



Scheme 4.20. Attempts at C6 deoxygenation of C7 *exo*-methylene substrates using Wickens' photoredox-catalyzed conditions

As our C7 *exo*-methylene substrates bear an activated allylic alcohol, conditions specifically designed for the deoxygenation of this type of system were investigated next. Acetate **4-41** was subjected to Tsuji Pd-catalyzed allylic alcohol reduction conditions employing $Pd(dba)_3$ (5 mol %), PBu_3 (20 mol %), triethylamine (11 equiv.), and formic acid (10 equiv.) in THF at 60 °C for 3 h under inert atmosphere (Scheme 4.21A).[21] The expected product of this reaction is either **4-42**, that of reduction at C6, or **4-57**, where the olefin has undergone isomerization after the hydride delivery. Neither of the expected products were observed under these conditions, with only starting material **4-41** being recovered. Wipf and coworkers reported an improved version of these conditions which use PBn_3 as the Pd ligand instead of the highly oxygen-sensitive PBu_3, allowing the reaction to be set up outside of the glovebox. These conditions, reported for the reduction of allylic benzoates, were applied to our substrate **4-40** (Scheme 4.21B), but solely returned starting material after reacting at 65 °C for 16 h.



Scheme 4.21. Attempts at C6 deoxygenation using Pd-catalyzed allylic deoxygenation conditions

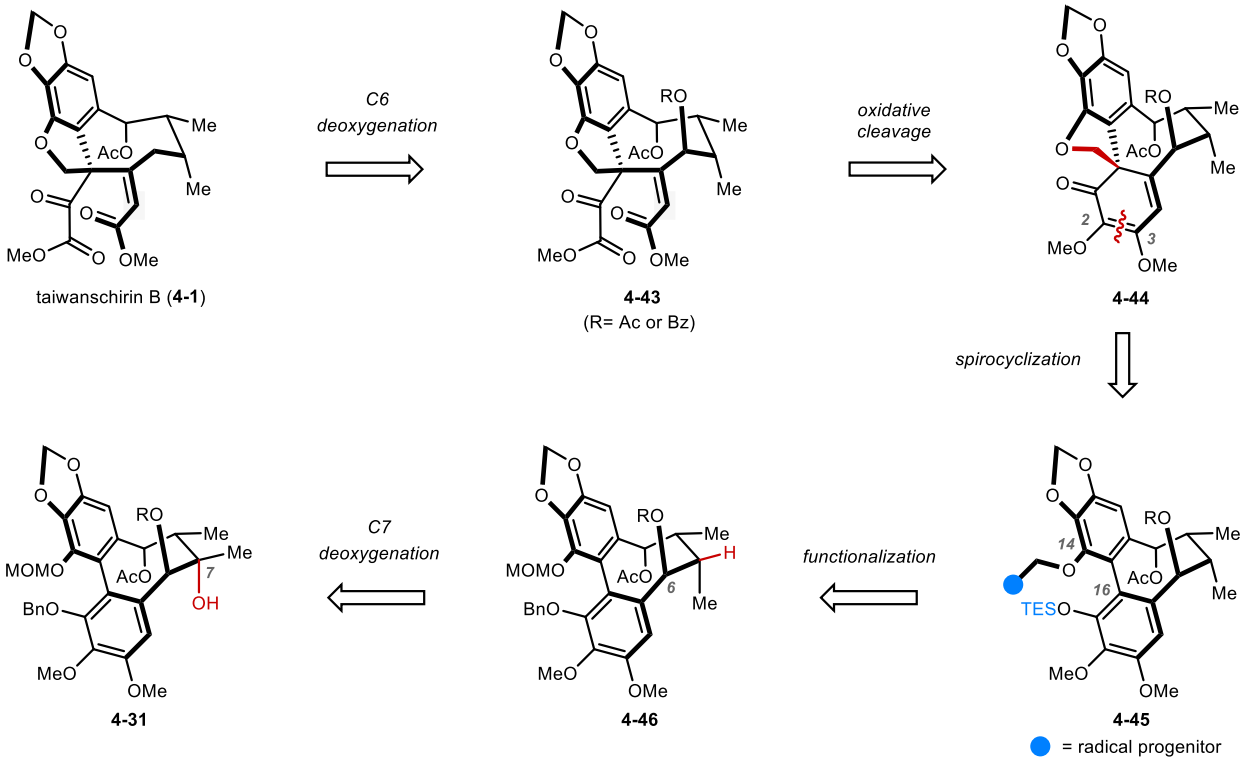
4.5. Synthesis of 6-benzyloxy-taiwanschirin B

Where many deoxygenation methodologies employing alcohol **4-6** (or its derivatives) as the substrate failed, the C6 deoxygenation step was pushed to a later stage in the total synthesis of taiwanschirin B. Considering the radical generated at C6 during a deoxygenation reaction would be poorly conjugated with the neighbouring aromatic ring due to the twisted nature of the biaryl linkage and the presence of a C7 *exo*-cyclic methylene did not provide enough stabilization to compensate for this, we sought to include a π-system elsewhere in our system which could better conjugate with the C6 position. Therefore, the C6 deoxygenation step was moved to after the oxidative cleavage of the cyclohexadienone, with the expectation that the π-system of the resulting acyclic α,β-unsaturated ester would provide better orbital overlap with the C6 position.

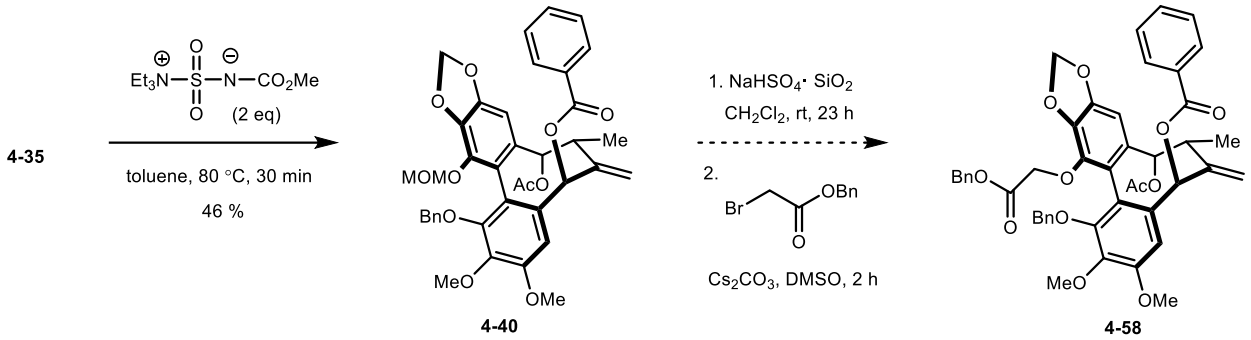
The revised retrosynthetic analysis of taiwanschirin B (**4-1**) is depicted in Scheme 4.22. Compound **4-1** is expected to arise from the C6 deoxygenation of **4-43**, which bears an activated alcohol (either an acetate or a benzoate) at C6. Ketodiester **4-43** is the product of oxidative cleavage of the C2-C3 double bond of cyclohexadienone **4-44**. *Ortho*-spirodienone **4-44** can result from the photoredox-mediated spirocyclization of NHPI ester **4-45**. Compound **4-45** arises from

manipulating the phenolic substituents *ortho* to the biaryl of **4-46** and **4-46** comes from the C7 deoxygenation of intermediate **4-31.**

For the C6 substituent (R in Scheme 4.22), it was expected that an activated alcohol in the pseudo-axial position would provide the best chance of good C-O orbital overlap with the π-system, enabling deoxygenation. Literature reports exist for allylic deoxygenation conditions using either acetate or benzoate as alcohol activating groups. Both potential starting materials **4-34** (**4-31** where R= OAc) and **4-35** (**4-31** where R= OBz) had been prepared earlier (see Scheme 4.16). The first step in the C7 deoxygenation (the Burgess dehydration) of **4-35** has already been accomplished (Schemes 4.18, 4.23), giving the C7 *exo*-methylene **4-40**. The second step of the C7 deoxygenation (hydrogenation of the alkene) can be postponed to the same time as the deprotection of the benzyl groups (also via hydrogenation) to decrease the step count of the synthesis. Compound **4-40** was subjected to deprotection of the MOM ether using $NaHSO_4$•SiO_2, immediately followed by alkylation of the resulting phenol using benzylbromoacetate and cesium carbonate (Scheme 4.23). The desired product **4-58** was formed under these conditions but could not be fully purified.

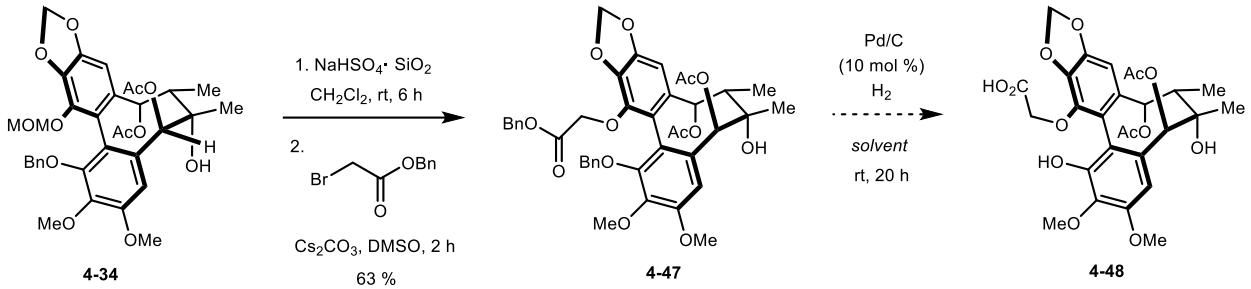


Scheme 4.22. Revised retrosynthetic analysis of taiwanschirin B



Scheme 4.23. Transformations of benzoate **4-35**

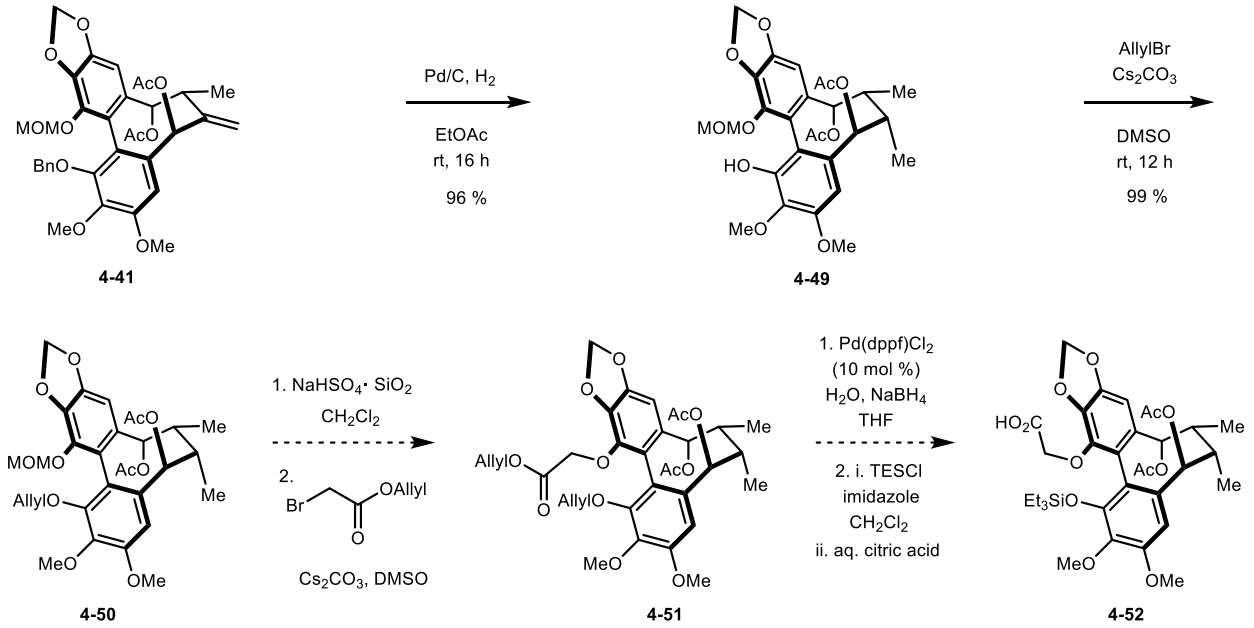
Due to the challenges associated with purifying the alkylated benzoate product **4-58**, the other potential starting material, acetate **4-34** was studied instead. In this instance, the functional group manipulations in preparation for spirocyclization were conducted prior to the C7 deoxygenation step. Deprotection of the MOM ether of **4-34** followed by *O*-alkylation with benzyl bromoacetate was successful, with the product **4-47** being obtained cleanly in 63 % yield (Scheme 4.24). The next required transformation was the dual deprotection of the phenolic and aliphatic benzyl ethers. **4-47** was submitted to Pd-catalyzed hydrogenation in several solvents (EtOAc, THF, and MeOH) for 20 h at rt. The reactions in EtOAc and THF merely returned starting material. The reaction in MeOH gave a mixture of species, none of which were the desired **4-48** and included two mono-benzylated products as well as a fully benzyl deprotected species bearing a methyl ester (resulting from the reaction of the carboxylic acid with the solvent).



Scheme 4.24. Transformations of acetate **4-34**

To avoid the difficult dual benzyl deprotection step, allyl protecting groups were deployed instead. In this case, the C7 deoxygenation was completed prior to the functional group manipulations in preparation for spirocyclization to avoid regioselectivity issues between the C7 *exo*-cyclic alkene and the allyl groups. This route started from **4-34**, which was converted to **4-41** via Burgess

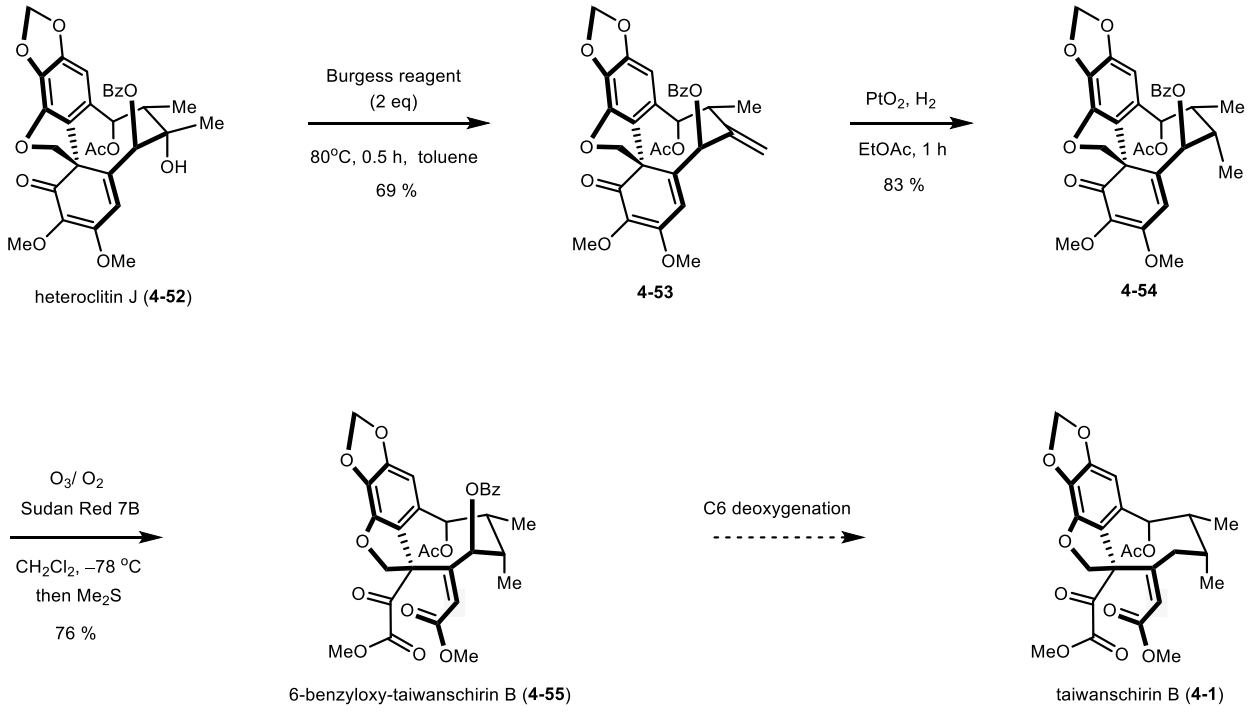
dehydration (see Scheme 4.18) and then subjected to Pd-catalyzed hydrogenation in EtOAc, accomplishing the C7 deoxygenation, providing **4-49** as a single diastereomer in 96 % yield (Scheme 4.25). This hydrogenation is highly stereoselective due to the preference for reduction of the more accessible *exo*-face of the alkene. Next, allylation of the phenol utilizing allyl bromide and cesium carbonate in DMSO gave **4-50** in 99 % yield. **4-50** was then subjected to deprotection of the MOM ether, followed by *O*-alkylation with allyl bromoacetate. This reaction sequence was performed five times, always yielding impure product. The ^{1}H NMR spectrum and HRMS indicated a species that looked like the desired product **4-51**, however the ^{13}C NMR spectrum could not be fully assigned due to impurities. Efforts to purify the material further by column chromatography or recrystallization have thus far been unsuccessful. An attempt to telescope the impure **4-51** was performed by subjecting it to the subsequent deprotection of the allyl ethers and protection of the C1 phenol as the TES ether. Treatment of the impure **4-51** with Pd(dppf)Cl_2 (10 mol %), sodium borohydride, and water in THF followed by triethysilyl chloride and imidazole in CH_2Cl_2 and then aqueous citric acid resulted in decomposition.



Scheme 4.25. Transformations of C7 *exo*-methylene acetate **4-41**

Due to scarcity of material and the inability to cleanly prepare either **4-58**, **4-48**, or **4-51**, an alternate route to taiwanschirin B (**4-1**) was sought. At this point, it was realized that our group's previous synthesis of heteroclitin J (**4-52**)[5] could intersect with the synthesis of **4-1**. It was

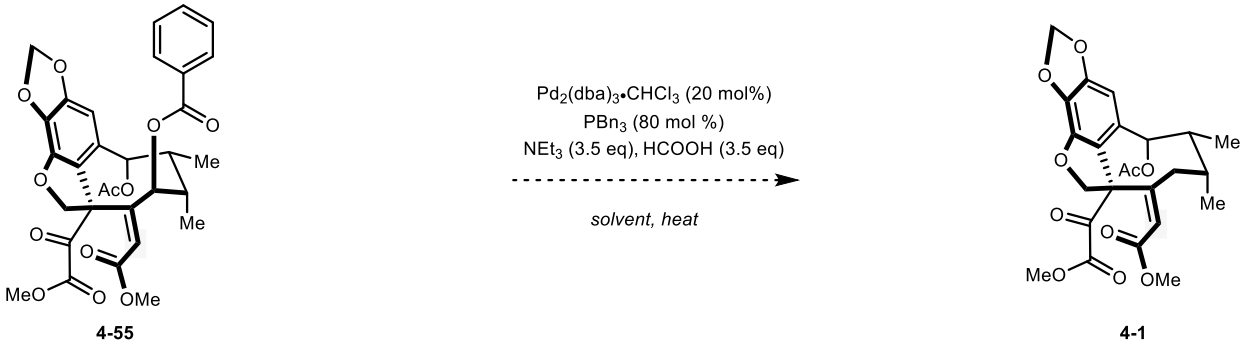
proposed that taiwanschirin B could be prepared by the C7 deoxygenation of heteroclitin J, followed by oxidative cleavage, and then C6 deoxygenation. The tertiary alcohol of **4-52** was dehydrated under Burgess conditions with good regioselectivity and 69 % yield, providing **4-53** (Scheme 4.26). The regio- and stereo- selective hydrogenation of the C7 *exo*-cyclic alkene of **4-53** to give **4-54** proved challenging. Attempts at hydrogenating **4-53** using Pd/C and H_2 in EtOAc or MeOH returned only starting material even when increased catalyst loading, temperature, and pressure were employed. Hydrogenations employing Pt/C, $Pd(OH)_2$, or $RhCl(PPh)_3$ as the catalyst were also ineffective. Reactivity was finally observed upon overnight hydrogenation with PtO_2 (1 equiv.) at rt in MeOH, where both the *exo*-cyclic alkene and the C6 benzoate were hydrogenated. High regioselectivity for the desired reduction product **4-54** (obtained in 83 % yield) could be obtained by decreasing the catalyst loading to 30 mol %, using EtOAc as the solvent, and stopping the reaction promptly after one hour. Compound **4-53** was less reactive towards hydrogenation than that the previous *exo*-cyclic alkene substrate **4-41** due to the greater steric bulk of the C6 benzoate (compared to a C6 acetate), making the alkene less accessible. The C6 benzoate and the diene of **4-53** act as potential sites for hydrogenation, making regioselectivity more challenging with this substrate as well. Compound **4-54** was then oxidatively cleaved by ozonolysis, utilizing



Scheme 4.26. Synthesis starting from heteroclitin J

a stream of O_3/O_2 and Sudan Red 7B as a colour indicator in CH_2Cl_2 at −78 °C, providing 6-benzyloxy-taiwanschirin B **4-55** in 76 % yield. Investigation into the final step of C6 deoxygenation to convert **4-55** to **4-1** has been commenced but is yet to be accomplished.

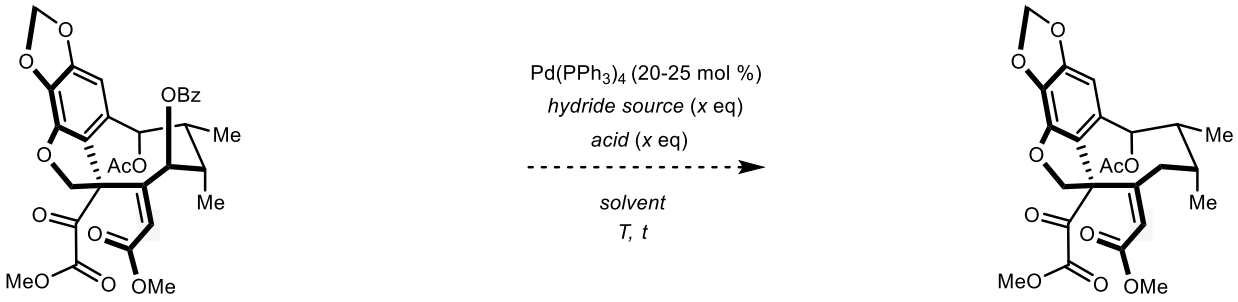
With the allylic benzoate **4-55** in hand, Wipf's conditions for Pd-catalyzed allylic deoxygenation were employed (Scheme 4.27). The reactions were run on 2 mg (0.004 mmol) scale and the catalyst and ligand loading were increased by ten-fold compared to the literature (to 20 and 80 mol %, respectively). Only starting material was recovered after 16 h reaction time at 70 °C in THF, therefore the temperature was increased to 100 °C in dioxane and then 150 °C or 180 °C in DMSO. No reactivity was observed until 180 °C was reached, at which point some of the substrate had decomposed into multiple species.



Scheme 4.27. Attempts at C6 allylic deoxygenation using Wipf's Pd-catalyzed conditions

Compound **4-55** was then submitted to allylic reduction conditions from Keinan and coworkers,[22] utilizing a reducing system consisting of $Pd(PPh_3)_4$ and diphenylsilane (Table 4.2, entry 1). They reported that the addition of a Lewis acid, $ZnCl_2$, had a rate-accelerating effect on the allylic reduction so a Lewis acid (either $ZnCl_2$ or $Sc(OTf)_3$) was included in the subsequent reactions (entries 2–5) after no reactivity was observed in entry 1. Additionally, the temperature of the reactions were increased to promote reactivity, including reactions at 70 °C, 150 °C, and 180 °C. Higher boiling point solvents such as DMF and DMSO were used for the higher temperature reactions. The allylic reduction of **4-55** was not accomplished with any of these variations, returning starting material each time. Similar conditions, employing borane dimethylamine complex instead of diphenylsilane as the hydride source, were then investigated. In entry 6, **4-55** was treated with conditions from the literature[23] using $(CH_3)_2NH•BH_3$ and acetic acid at rt, where it failed to react. Adding $ZnCl_2$ and increasing the reaction temperature to 150 °C in DMF (entry

7) did not improve reactivity. It is possible that the Pd-catalyzed allylic deoxygenation methods failed due to the approach of Pd from the *endo* face of the alkene being blocked by the axial C9 acetate and C7 methyl groups.



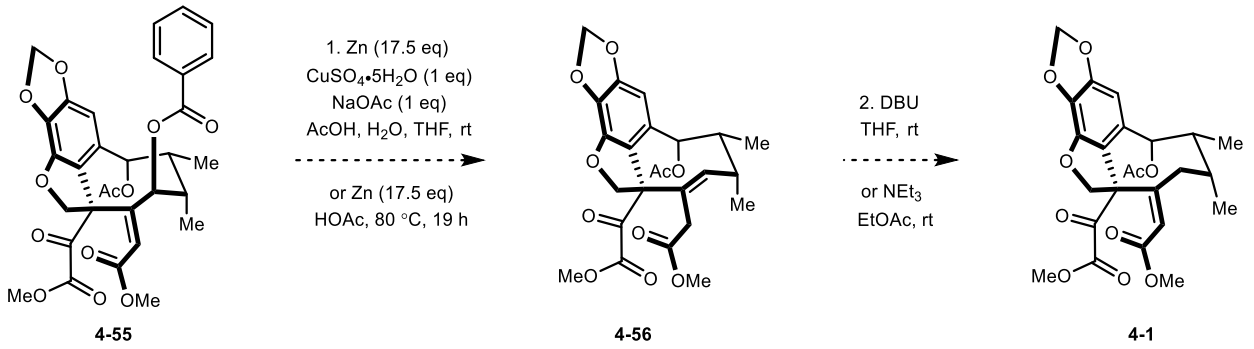
4-55 **4-1**

Entry	hydride source (eq)	acid (eq)	solvent	T (°C)	t (h)	Result
1	$Ph_2Si_2H_2$ (2)	none	THF	rt	2.5	rec. SM
2	$Ph_2Si_2H_2$ (3)	$ZnCl_2$ (3)	THF	70	17	rec. SM
3	$Ph_2Si_2H_2$ (3)	$Sc(OTf)_3$ (3)	THF	70	17	rec. SM
4	$Ph_2Si_2H_2$ (3)	$ZnCl_2$ (3)	DMF	150	19	rec. SM
5	$Ph_2Si_2H_2$ (3)	$ZnCl_2$ (3)	DMSO	180	2	rec. SM
6	$(CH_3)_2NH{\bullet}BH_3$ (2.2)	AcOH (2.8)	CH_2Cl_2	rt	2.5	rec. SM
7	$(CH_3)_2NH{\bullet}BH_3$ (2.2)	$ZnCl_2$ (3)	DMF	150	21	rec. SM

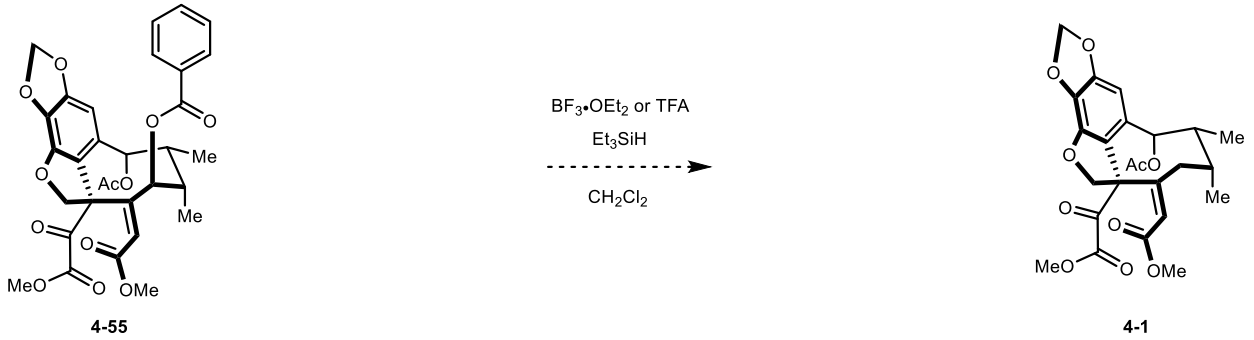
Table 4.2. Attempts at C6 allylic reduction using catalytic $Pd(PPh_3)_4$ and a hydride source

Considering the lack of reactivity observed under several Pd-catalyzed conditions for allylic reduction, catalysts composed of other metals were then explored, with the expectation that one of these may coordinate in a more suitable manner to the alkene to allow for hydride delivery at C6. Treatment of **4-55** with allylic deoxygenation conditions using $RuH_2(PPh_3)_4$ (0.5 equiv.)[24] in PhMe at either rt or 100 °C returned starting material. A two-step method[25,26] involving Zn-mediated reduction of the allylic benzoate followed by base-catalyzed alkene isomerization to reestablish conjugation was then investigated. Two variations of these conditions were applied to **4-55,** however the first step failed in both instances, returning only **4-55** (Scheme 4.28).

SmI_2 (3 equiv.)-mediated reduction conditions in HMPA (12 equiv.) and THF at 70 °C were applied to **4-55** but returned starting material. Next, allylic reduction conditions using a combination of triethylsilane and an acid were implemented (Scheme 4.29). The use of triethylsilane (2.1 equiv.) with trifluoracetic acid (3.5 equiv.) was reported by Khachik and coworkers for the deoxygenation of a free secondary allylic alcohol during a hydroxycarotenoid



Scheme 4.28. Attempts at Zn-mediated C6 allylic reduction followed by alkene isomerization



Scheme 4.29. Attempts at C6 allylic deoxygenation using triethylsilane and acid

synthesis,[27] however it did nothing to our allylic benzoate. A combination of BF_3•OEt_2 and triethylsilane was reported to carry out chemoselective deoxygenation of a primary allylic alcohol (leaving a primary homoallylic alcohol intact), by Beeler and coworkers in the synthesis of a dihydronaphthalene lignan.[28] These conditions, however, only returned starting material when applied to our DBCOD substrate **4-55**.

4.6. Conclusions and future directions

The total synthesis of taiwanschirin B involves two key deoxygenation steps. The C7 deoxygenation could be accomplished in two steps by dehydration of the C7 tertiary alcohol, yielding the *exo*-cyclic methylene, followed by hydrogenation of the alkene. The C6 deoxygenation proved to be more challenging. It was determined that the C6 alcohol of **4-6** and its activated alcohol derivatives do not behave like traditional benzylic alcohols. To compensate for this lack of stabilization from the neighbouring aromatic ring, the C6 deoxygenation step was then

attempted on substrates where this alcohol is allylic (either bearing an *exo*-methylene at C7 or an α,β-unsaturated ester at C5).

The synthesis of taiwanschirin B starting from heteroclitin J, including C7 deoxygenation and oxidative cleavage of the cyclohexadienone, has been nearly completed, with one step remaining to convert 6-benzyloxy-taiwanschirin B (**4-55**) into taiwanschirin B. Compound **4-55** has proved uncooperative towards this final C6 deoxygenation step, therefore harsher methods including elevated temperatures will be applied in future efforts. Additionally, the substrate could be modified to provide a more active substrate for deoxygenation. For example, the C6 benzoate could be deprotected and replaced with other activating groups such as an acetate. Once methodology for the C6 deoxygenation of the cyclic system **4-55** has been developed, this could be applied to the synthesis of other DBCODs such as kadsuraol C and longipedlignans A, C, and E. As a longer term goal, we would also like to develop a method for selective deoxygenation of the C9 position to allow access to an even greater diversity of DBCODs.

4.7. Experimental

4.7.1. Materials and methodologies

Chemicals and solvents were purchased from Sigma Aldrich, Strem Chemicals, Fisher Scientific, Combi-Blocks, or Oakwood Chemical, and used as received without further purification unless otherwise noted. Solvents were dried and purified using a PureSolv MD 7 (from Innovative Technology) or MB SPS 800 (from MBraun). Unless otherwise noted, solvent was degassed by sparging with N_2 for 5 min at rt prior to use. Amine bases were distilled over CaH_2 under N_2 (g).

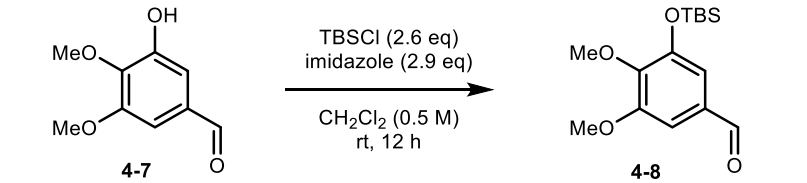
Proton nuclear magnetic resonance (^{1}H NMR) spectra were acquired using Bruker AVIIIHD 500 MHz, Varian Inova QUANUC 500 MHz, Varian VNMRS 500 MHz, or Varian Mercury 400 MHz spectrometers. Chemical shifts (δ) are reported in parts per million (ppm) and are calibrated to the residual solvent peak. Coupling constants (*J*) are reported in Hz. Multiplicities are reported using the following abbreviations: s = singlet; d = doublet; t = triplet; q = quartet; dd = doublet of doublets; dt = doublet of triplets; dq = doublet of quartets; tt = triplet of triplets; qd = quartet of doublets; qq = quartet of quartets; ddd = doublet of doublet of doublets; ddt = doublet of doublet of triplets; dddd = doublet of doublet of doublet of doublets; ddq= doublet of doublet of quartets;

br = broad; m = multiplet. Carbon nuclear magnetic resonance (^{13}C NMR) spectra were acquired using a Bruker AVIIIHD 126 MHz spectrometer.

High resolution mass spectra (HRMS) were recorded using a Bruker maXis Impact TOF mass spectrometer by electrospray ionization time of flight reflectron experiments. Fourier-transform infrared (FT-IR) spectra were recorded on a Bruker Alpha II FT-IR spectrometer. Optical rotations were recorded on a Jasco DIP-140 polarimeter (using the sodium D line; 589 nm). High performance liquid chromatography (HPLC) was measured on an Agilent 1100 HPLC system using a Chiralpak® IC analytical column (250 × 4.6 mm, 5 μm). Thin-layer chromatography was performed on pre-coated 250 mm layer thickness silica gel 60 F254 plates (EMD Chemicals Inc). Visualization was performed by ultraviolet light and/or by staining with potassium permanganate or *para*-anisaldehyde stain. Purifications by column chromatography were performed either using a Biotage Isolera^{TM} One or standard column chromatography using silica gel (40-63 μm, 230-400 mesh).

4.7.2. Preparative procedures for compounds 4-8 to 4-55

Compound 4-8



4-7
Chemical Formula: $C_9H_{10}O_4$
Molecular Weight: 182.1750

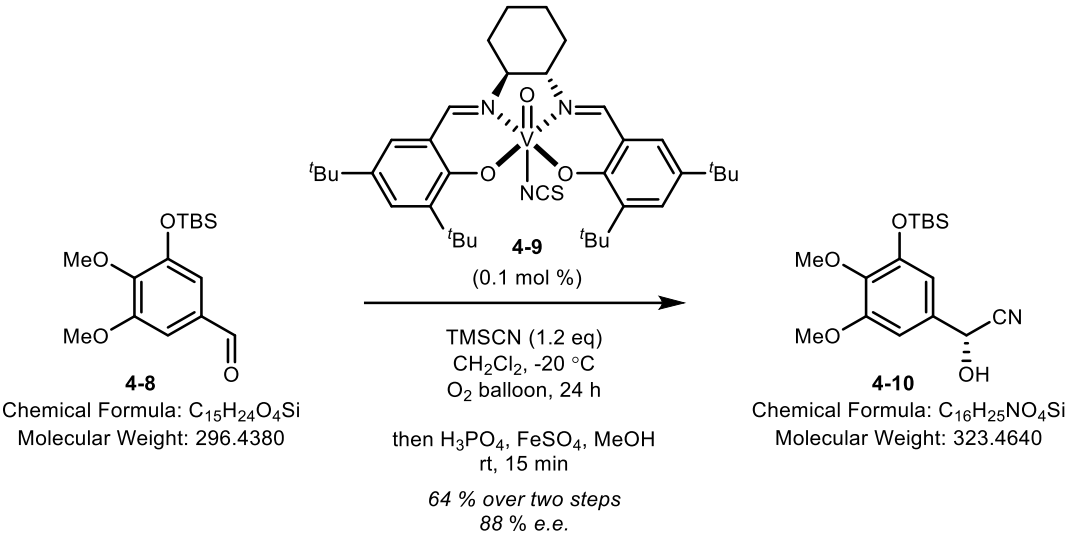
4-8
Chemical Formula: $C_{15}H_{24}O_4Si$
Molecular Weight: 296.4380

Procedure: A 1 L flame-dried round bottom flask equipped with a Teflon-coated stir bar and a rubber septum was charged with 3,4-dimethoxy-5-hydroxybenzaldehyde (**4-7**, 155 mmol, 28.2 g, 1.0 equiv.). CH_2Cl_2 (100 mL), *tert*-butyldimethylsilyl chloride (407 mmol, 61.3 g, 2.6 equiv.), and imidazole (444 mmol, 30.2 g, 2.9 equiv.) were added sequentially to the reaction mixture. The reaction mixture was stirred at rt for 12 h. *N*,*N*-Dimethylaminoethanol (24.2 mL, 240 mmol, 1.3 equiv.) was added and the reaction mixture was allowed to stir an additional 1 hour at rt. The reaction mixture was then poured on HCl (1 M in H_2O, 370 mL), and extracted with CH_2Cl_2 (3 × 370 mL). The combined organic layers were dried over $MgSO_4$, filtered, and concentrated *in vacuo*. The crude product was purified on silica gel (20:1 hexanes/EtOAc) to provide a cleaner

sample of **4-8** (39.2 g) as a yellow-orange oil which was carried into the next reaction before fully purifying.

Characterization: **^{1}H NMR** (500 MHz, $CDCl_3$) δ 9.82 (s, 1H), 7.11 (d, J= 1.8 Hz, 1H), 7.02 (d, J= 1.8 Hz, 1H), 3.92 (s, 3H), 3.87 (s, 3H), 1.02 (s, 9H), 0.21 (s, 6H). The characterization data match the data reported previously.[5]

Compound 4-10

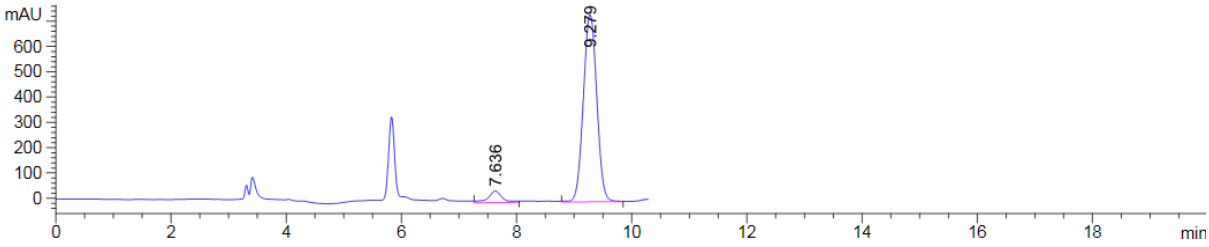


Procedure: A 250 mL flame-dried round bottom flask equipped with a Teflon-coated stir bar and a rubber septum was charged with (*S,S*)-VO(salen)NCS (**4-9**, 0.062 mmol, 41.2 mg, 0.1 mol %) and **4-8** (61.5 mmol, 18.23 g, 1.0 equiv.). It was then evacuated and refilled with O_2 three times and then left under a balloon of O_2. CH_2Cl_2 (62 mL), which had been sparged with O_2 for 10 min, was then added give a homogeneous dark green solution. The mixture was cooled to –20 °C and TMSCN (73.8 mmol, 9.2 mL, 1.2 equiv.) was added dropwise via syringe. The reaction mixture was then placed in a –20 °C freezer for 24 h. The reaction mixture was quenched at this temperature by adding a solution consisting of $FeSO_4 \cdot 7H_2O$ (6.15 mmol, 1.71 g, 0.1 equiv.) and H_3PO_4 (24.6 mmol, 85 wt% aq., 1.7 mL, 0.4 equiv.) in MeOH (12.3 mL), and stirred for 15 min while the reaction mixture gradually warmed to rt. It was then poured on brine (100 mL) and extracted with CH_2Cl_2 (3 × 100 mL). The combined organic layers were dried over $MgSO_4$, filtered, and concentrated *in vacuo*. The crude product was then purified on silica gel (3:1 hexanes/EtOAc) to

provide **4-10** (12.73 g, 39.4 mmol, 64% over two steps) as a pale-green oil with an *e.e.* of 88 % as determined by chiral HPLC.

Characterization: **^{1}H NMR** (500 MHz, $CDCl_3$) δ 6.71 (d, *J* = 2.1 Hz, 1H), 6.67 (d, *J* = 2.1 Hz, 1H), 5.43 (broad s, 1H), 3.88 (s, 3H), 3.79 (s, 3H), 1.00 (s, 9H), 0.20 (s, 6H). The characterization data match the data reported previously.[5] **HPLC** (Chiralpak® IC analytical column, eluent 5:95 ^{i}PrOH:hexanes, 1 mL/min) t_R 9.3 min (major), 7.61 min (minor), 88 % *e.e.*

HPLC chromatogram of the chiral product:

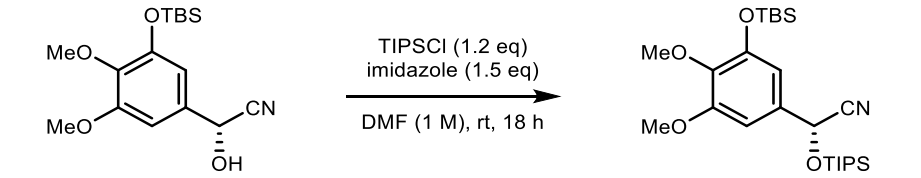



```
Signal 3: DAD1 D, Sig=209,16 Ref=360,100

Peak RetTime Type  Width     Area      Height     Area
  #   [min]       [min]   [mAU*s]     [mAU]       %
----|-------|----|-------|----------|----------|--------|
   1   7.636 BV    0.2440  760.13159   45.23864   5.9837
   2   9.279 BB    0.2544 1.19433e4   739.74384  94.0163

Totals :                  1.27035e4   784.98248
```

Compound 4-11



4-10
Chemical Formula: $C_{16}H_{25}NO_4Si$
Molecular Weight: 323.4640

93 %

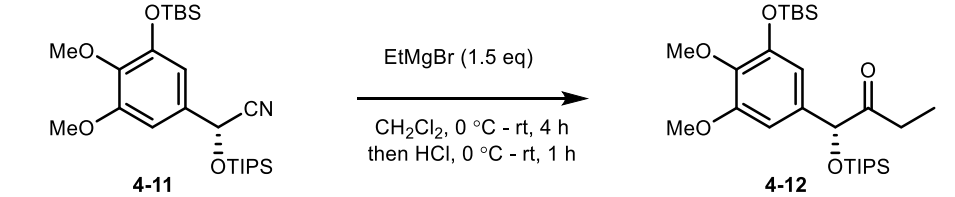
4-11
Chemical Formula: $C_{25}H_{45}NO_4Si_2$
Molecular Weight: 479.8080

Procedure: A 250 mL flame-dried round bottom flask equipped with a Teflon-coated stir bar and a rubber septum was charged with **4-10** (70.9 mmol, 22.9 g, 1.0 equiv.) and DMF (71 mL). TIPSCl (85 mmol, 18.2 mL, 1.2 equiv.) was then added via syringe, followed by the addition of imidazole (106 mmol, 7.24 g, 1.5 equiv.). The resulting solution was stirred at rt for 18 h. Quenched by the addition of *N*,*N*-dimethylaminoethanol (2.83 mL) and stirred for another 1 h. It was then diluted with EtOAc (240 mL) and washed with HCl (1 M in H_2O, 120 mL). The aqueous layer was further

extracted with EtOAc (2 × 240 mL). The combined organic layers were washed with water (240 mL) and brine (240 mL), dried over $MgSO_4$, filtered, and concentrated *in vacuo*. The crude product was purified on silica gel (20:1 hexanes/EtOAc) to provide **4-11** (31.7 g, 66.1 mmol, 93 %) as a colorless oil.

Characterization: **^{1}H NMR** (500 MHz, $CDCl_3$) δ 6.69 (d, *J* = 2.0 Hz, 1H), 6.62 (d, *J* = 2.0 Hz, 1H), 5.47 (s, 1H), 3.86 (s, 3H), 3.79 (s, 3H), 1.26 – 1.16 (m, 3H), 1.11 (d, *J* = 7.3 Hz, 9H), 1.07 (d, *J* = 7.3 Hz, 9H), 1.00 (s, 9H), 0.17 (s, 6H). The characterization data match the data reported previously.[5]

Compound 4-12



4-11
Chemical Formula: $C_{25}H_{45}NO_4Si_2$
Molecular Weight: 479.8080

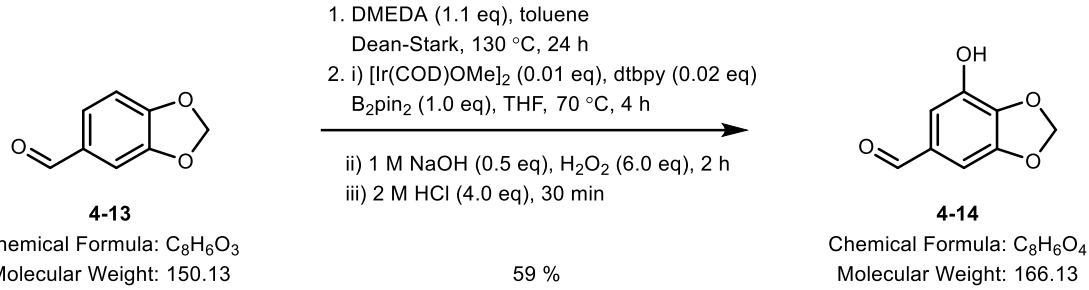
89 %

4-12
Chemical Formula: $C_{27}H_{50}O_5Si_2$
Molecular Weight: 510.8620

Procedure: A 500 mL flame-dried round bottom flask equipped with a Teflon-coated stir bar and a rubber septum was charged with **4-11** (66.2 mmol, 31.74 g, 1.0 equiv.). The flask was evacuated and refilled with N_2 (repeated 3 times), prior to the addition of CH_2Cl_2 (276 mL). The resulting solution was then cooled to 0 °C in an ice bath, at which point EtMgBr (99.2 mmol, 3 M in Et_2O, 33.1 mL, 1.5 equiv.) was added dropwise via syringe. The solution was warmed to rt and stirred for 4 h, then poured into a 1 L Erlenmeyer flask and cooled to 0 °C in an ice bath. The reaction mixture was quenched by the addition of HCl (2 M in H_2O, 280 mL), and stirred for an additional 1 h at rt. The biphasic mixture was extracted with CH_2Cl_2 (3 × 200 mL). The combined organic layers were dried over $MgSO_4$, filtered, and concentrated *in vacuo*. The crude product was purified on silica gel (20:1 hexanes/EtOAc) to provide **4-12** (29.91 g, 58.5 mmol, 89 %) as a pale-yellow oil.

Characterization: **^{1}H NMR** (500 MHz, $CDCl_3$) δ 6.66 (d, *J* = 2.0 Hz, 1H), 6.61 (d, *J* = 1.9 Hz, 1H), 5.05 (s, 1H), 3.82 (s, 3H), 3.77 (s, 3H), 2.70 (dq, *J* = 18.6, 7.3 Hz, 1H), 2.46 (dq, *J* = 18.6, 7.3 Hz, 1H), 1.17 – 1.07 (m, 3H), 1.06 – 1.01 (m, 18H), 1.00 (s, 9H), 0.94 (t, *J* = 7.3 Hz, 3H), 0.16 (s, 3H), 0.16 (d, J= 5.4 Hz, 3H). The characterization data match the data reported previously.[5]

5-Hydroxypiperonal (compound 4-14)



4-13
Chemical Formula: $C_8H_6O_3$
Molecular Weight: 150.13

59 %

4-14
Chemical Formula: $C_8H_6O_4$
Molecular Weight: 166.13

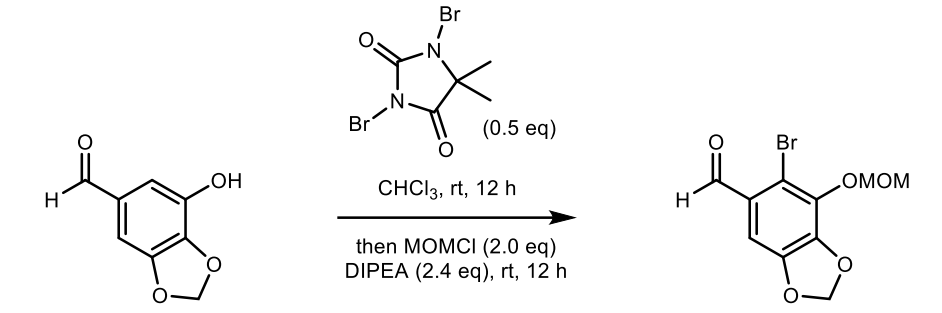
Procedure:

A 500 mL RBF equipped with a Teflon-coated stir bar and rubber septum was charged with piperonal (**4-13**, 15 g, 100 mmol), followed by toluene (250 mL, 0.4 M). The reaction mixture was stirred until solids were completely dissolved, then DMEDA (12 mL, 110 mmol, 1.1 equiv.) was added. The reaction flask was then fitted with a Dean-Stark Apparatus and stirred at 130 °C for 24 hours. Then, the mixture was cooled to room temperature and concentrated *in vacuo* to obtain a brown-yellow residue which was left under high vacuum overnight (to remove residual toluene). A flame-dried 250 mL Schlenk tube equipped with a Teflon-coated stir bar and a glass stopper was charged with bis(pinacolato)diboron (25.4 g, 100 mmol, 1.0 equiv.), 4,4-di-*tert*-butyl-2,2-dipyridyl (537 mg, 2 mmol, 0.02 equiv.), and $[Ir(COD)OMe]_2$ (700 mg, 1 mmol, 0.01 equiv.). The flask was evacuated and refilled with N_2 (repeated 3 times). The residue from the previous step was dissolved in THF (100 mL, 1.0 M) under N_2 atmosphere and added to the Schlenk tube via cannula addition. The reaction mixture was stirred at 70 °C for 4 hours and then allowed to cool to room temperature. The mixture was poured into a 2 L Erlenmeyer flask equipped with a Teflon-coated stir bar and then cooled to 0°C in an ice bath. In a separate Erlenmeyer flask, NaOH (1 M in H_2O, 50 mL) and H_2O_2 (30 % aq. solution, 50 mL) were combined and then slowly added to the reaction mixture. The reaction mixture was stirred at room temperature for 2 hours. HCl (2 M in H_2O, 200 mL) was added and the pH was confirmed to be acidic using pH paper. The reaction mixture was stirred for an additional 30 minutes at room temperature and then extracted with EtOAc (4 x 250 mL). The combined organic layers were dried over Na_2SO_4, filtered, and concentrated *in vacuo* to obtain a black oil. The crude product was purified on silica gel (15 % to 20 % EtOAc in hexanes). The resulting product was washed with chloroform while concentrating *in vacuo*, yielding a brown solid. Recrystallization from hexanes/ ethyl acetate (5:1) yielded a tan

solid. The filtrate was subjected to purification on silica gel (15 % to 20 % EtOAc in hexanes) and the isolated product was combined with the solid isolated during recrystallization for a total of 9.74 g, 58.6 mmol, 59 % 5-hydroxypiperonal (**4-14**).

Characterization: **^{1}H NMR** (500 MHz, $CDCl_3$) δ 9.76 (s, 1H), 7.09 (s, 1H), 7.02 (d, J= 1.3 Hz, 1H), 6.10 (s, 2H), 5.23 (broad s, 1H). The characterization data match the data reported previously.[29]

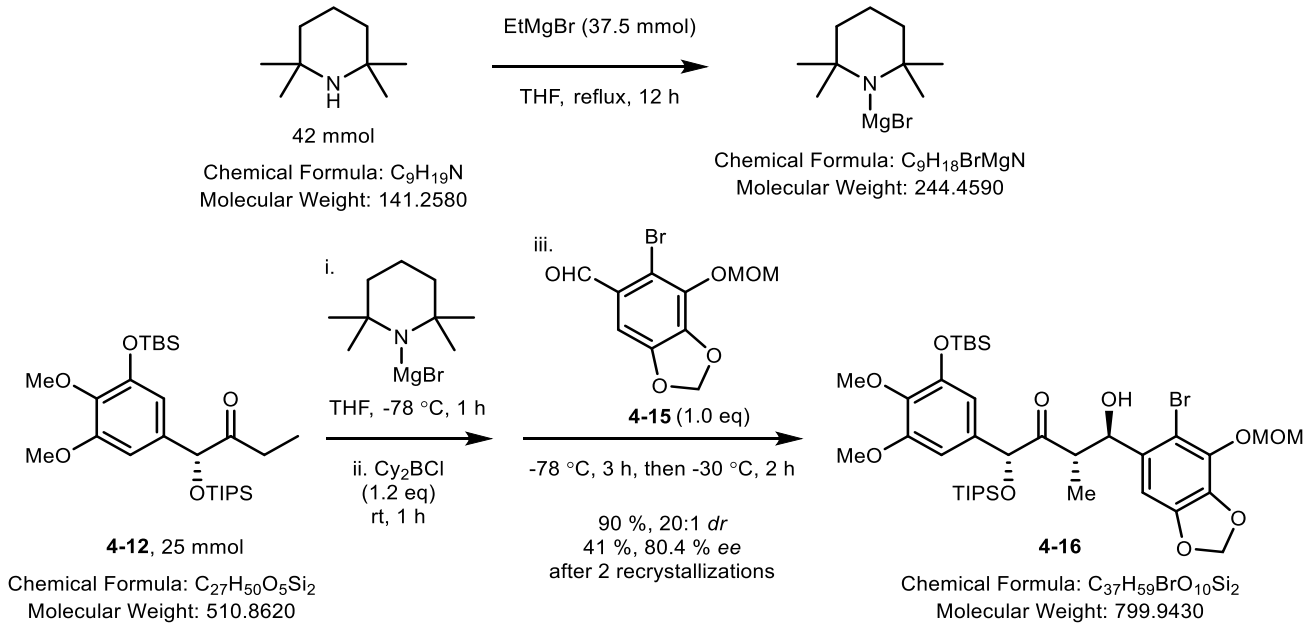
Compound 4-15



Procedure: A 1 L flame-dried round bottom flask equipped with a Teflon-coated stir bar and a rubber septum was charged with 5-hydroxypiperonal (**4-14**, 30 mmol, 4.98 g, 1.0 equiv.) and $CHCl_3$ (300 mL). 1,3-Dibromo-5,5-dimethylhydantoin (DBDMH, 15 mmol, 4.29 g, 0.5 equiv.) was added as a solid in small portions (an orange color appeared when the first portion of DBDMH was added, and the next portion was added after the orange color had faded to yellow). The reaction mixture was stirred at rt for 12 h. *N,N*-Diisopropylethylamine (DIPEA, 72 mmol, 12.54 mL, 2.4 equiv.) and MOMCl (60 mmol, 4.56 mL, 2.0 equiv.) were added via syringe and the mixture was stirred for another 12 h at rt. It was then poured on HCl (1M in H_2O, 120 mL), and extracted with CH_2Cl_2 (4 × 120 mL). The combined organic layers were dried over $MgSO_4$, filtered, and concentrated *in vacuo*. The crude product was purified on silica gel (10:1 to 5:1 hexanes/EtOAc), followed by recrystallization from CH_2Cl_2-hexanes (1:5, 180 mL) to provide **4-15** (5.51 g, 19.2 mmol, 64 %) as a white solid.

Characterization: **^{1}H NMR** (500 MHz, $CDCl_3$) δ 10.27 (s, 1H), 7.21 (s, 1H), 6.10 (s, 2H), 5.33 (s, 2H), 3.61 (s, 3H). The characterization data match the data reported previously.[5]

Compound 4-16

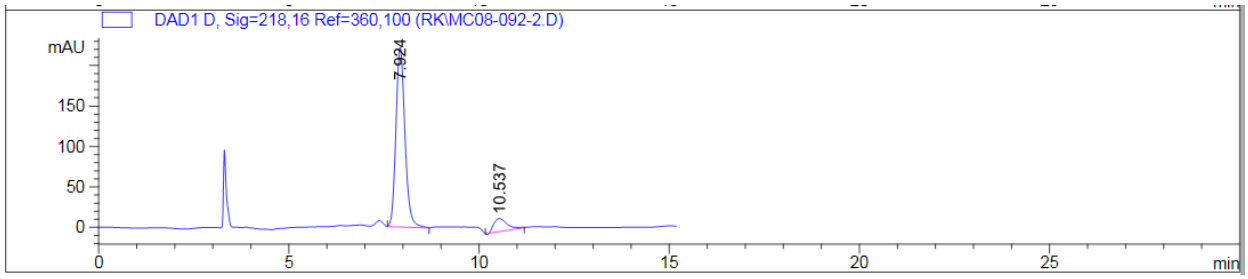


Procedure: A 500 mL flame-dried round bottom flask equipped with a Teflon-coated stir bar and a rubber septum was charged with 2,2,6,6-tetramethylpiperidine (freshly distilled over CaH_2, 42 mmol, 7.15 mL, 1.68 equiv.) and THF (37.5 mL). EtMgBr (37.5 mmol, 12.5 mL of 3 M solution in Et_2O, 1.5 equiv.) was added via syringe. The resulting solution was refluxed under N_2 for 12 h, then diluted with THF (37.5 mL), and cooled to –78 °C in a dry ice / acetone bath. A solution of ketone **4-12** (25 mmol, 12.77 g, 1.0 equiv.) in THF (50 mL) was added via syringe pump at a rate of 100 mL/h. Stirred at –78 °C for 1 h, then a solution of Cy_2BCl (30 mmol, 6.6 mL, 1.2 equiv.) in hexanes (30 mL) was added via syringe. Warmed to rt and stirred for another 1 h. Then, cooled to –78 °C, and a solution of aldehyde **4-15** (25 mmol, 7.23 g, 1.0 equiv.) in hexanes/CH_2Cl_2 (1:1 mixture, 75 mL) was added via syringe pump at a rate of 150 mL/h. The resulting mixture was stirred at –78 °C for 3 h, followed by –30 °C for 2 h. Quenched by the addition of $NaHCO_3$ (sat. aq., 100 mL) and diethanolamine (75 mmol, 7.89 g, 3.0 equiv.), and stirred for another 30 min at rt. The mixture was then filtered, and the filtrate was extracted with EtOAc (3 × 200 mL). The combined organic layers were dried over $MgSO_4$, filtered, and concentrated *in vacuo*. The crude product was then purified on silica gel (10:1 to 5:1 hexanes/EtOAc) to provide **4-16** (18.00 g, 22.50 mmol, 90 %) as a ≥ 20:1 *d.r.* mixture. To further purify the product via recrystallization, it was dissolved in hexanes (60 mL) with gentle heat, cooled to rt, and left in a –20 °C freezer for 12 h. The resulting white solid was collected by filtration. The recrystallization process was repeated a

second time, giving 8.16 g, 10.3 mmol, 41 % (average over 3 reactions) of **4-16** as a white solid with 80.4 % *e.e.* as determined by chiral HPLC.

Characterization: **^{1}H NMR** (500 MHz, $CDCl_3$) δ 6.67 (s, 1H), 6.55 (d, *J* = 1.9 Hz, 1H), 6.53 (d, *J* = 1.8 Hz,1H), 5.96 (2 x d, *J* = 1.5 Hz, 2 H), 5.31 (d, *J* = 5.9 Hz, 1H), 5.17 (d, *J* = 6.0 Hz, 1H), 5.09 (d, J = 5.8 Hz ,1H), 5.03 (s, 1H), 3.90 (d, 11.5 Hz, 1H), 3.81 (s, 3H), 3.77 (s, 3H), 3.55 (s, 3H), 3.52 (m, 1H), 1.11 – 1.02 (m, 3H), 1.01 – 0.97 (m, 30H), 0.14 (s, 6H). The characterization data match the data reported previously.[5] **HPLC** (Chiralpak® IC analytical column, eluent 10:90 ^{i}PrOH:hexanes, 1 mL/min) t_R 7.9 min (major), 10.5 min (minor), 81.5 % *e.e.*

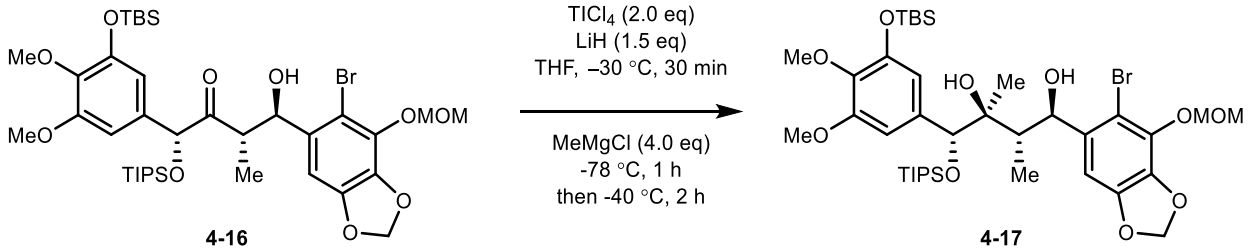
HPLC trace of the chiral product:




```
Signal 4: DAD1 D, Sig=218,16 Ref=360,100

Peak RetTime Type  Width     Area      Height     Area
  #   [min]        [min]    [mAU*s]     [mAU]       %
----|-------|----|-------|----------|----------|--------|
   1   7.924 VV    0.2554 3679.23291  221.91628  90.7530
   2  10.537 BB    0.3732  374.88477   15.89228   9.2470
```

Compound 4-17



Chemical Formula: $C_{37}H_{59}BrO_{10}Si_2$
Molecular Weight: 799.9430

9:1 *dr*
80 % major diastereomer

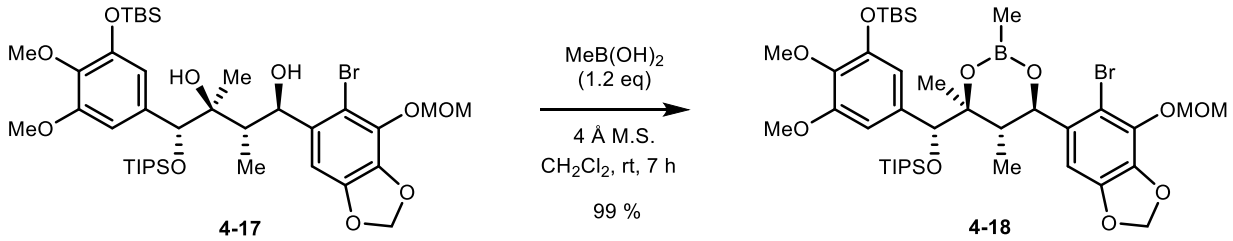
Chemical Formula: $C_{38}H_{63}BrO_{10}Si_2$
Molecular Weight: 815.9860

Procedure: A 250 mL flame-dried round bottom flask equipped with a Teflon-coated stir bar and a rubber septum was charged with **4-16** (9.0 mmol, 7.21 g, 1.0 equiv.) and LiH (13.8 mmol, 109 mg, 1.5 equiv.). The flask was evacuated and refilled with N_2 (repeated 3 times), prior to the

addition of THF (46 mL). The reaction mixture was cooled to –30 °C in a dry ice/ acetone bath, at which point $TiCl_4$ (18.4 mmol, 1 M in CH_2Cl_2, 18.4 mL, 2.0 equiv.) was added dropwise via syringe. The reaction mixture was stirred at this temperature for 30 min, then cooled the resulting red solution to –78 °C. A solution of MeMgCl (36.7 mmol, 1 M in THF, 36.7 mL, 4.0 equiv.) was added via syringe pump at a rate of 50 mL/h. The mixture was stirred at this temperature for 1 h, then warmed to –40 °C and stirred for another 2 h. The reaction mixture was quenched by the addition of NH_4Cl (sat. aq., 37 mL) followed by NH_4OH (concentrated, 9.2 mL), and stirred for another 15 min at rt. The resulting mixture was filtered, and the filtrate was extracted with EtOAc (3 × 90 mL). The combined organic layers were dried over Na_2SO_4, filtered, and concentrated *in vacuo*. The crude product (9:1 *dr*) was purified on silica gel (5:1 to 3:1 hexanes/EtOAc) to provide 5.88 g, 7.2 mmol, 80 % (average over 3 reactions) of the major diastereomer (**4-17**) as a pale-yellow oil.

Characterization: ***Major diastereomer:*** **^{1}H NMR** (500 MHz, $CDCl_3$) δ 7.01-6.20 (br s, 1H), 6.55 (s, 1H), 6.43 (br s, 1H), 5.92 (d, J = 1.4 Hz, 1H), 5.91 (d, J = 1.4 Hz, 1H), 5.35 (d, J = 9.0 Hz, 1H), 5.27 (d, J = 6.0 Hz, 1H), 5.22 (d, J = 6.0 Hz, 1H), 4.52 (s, 1H), 3.82 (broad s, 3H), 3.80 (s, 3H), 3.55 (s, 3H), 1.54 (s, 3H), 1.53 – 1.46 (m, 1H), 1.06 – 0.91 (m, 30H), 0.46 (d, J = 7.0 Hz, 3H), 0.16 (br s, 6H). The characterization data match the data reported previously.[5]

Compound 4-18



4-17
Chemical Formula: $C_{38}H_{63}BrO_{10}Si_2$
Molecular Weight: 815.9860

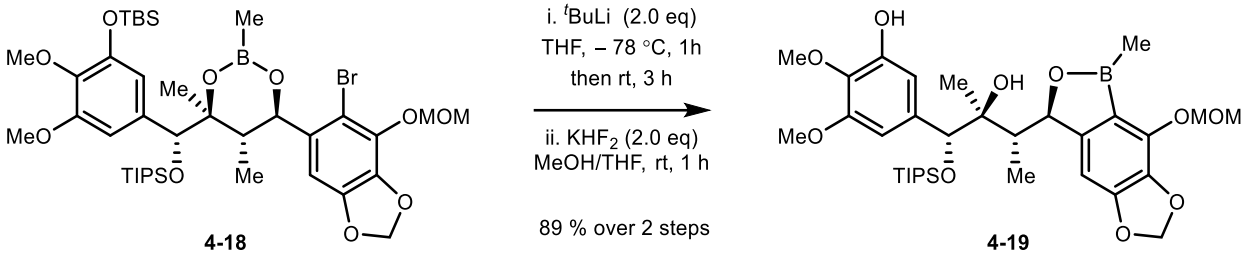
4-18
Chemical Formula: $C_{39}H_{64}BBrO_{10}Si_2$
Molecular Weight: 839.8150

Procedure: A 250 mL flame-dried round bottom flask equipped with a Teflon-coated stir bar and a rubber septum was charged with **4-17** (20.5 mmol, 16.75 g, 1.0 equiv.), $MeB(OH)_2$ (24.6 mmol, 1.47 g, 1.2 equiv.) and 4 Å molecular sieves (10.26 g). The flask was evacuated and refilled with N_2 (repeated 3 times), prior to the addition of CH_2Cl_2 (103 mL). The resulting mixture was stirred at rt for 7 h. It was then filtered, and the filtrate concentrated *in vacuo*. The crude product was

purified on silica gel (10:1 hexanes/EtOAc) to provide **4-18** (17.02 g, 19.8 mmol, 99 %) as a pale-yellow oil.

Characterization: **^{1}H NMR** (500 MHz, $CDCl_3$) δ 6.82 (br s, 1H), 6.37 (br s, 1H), 6.32 (s, 1H), 5.94 (s, 2H), 5.32 (d, *J* = 10.8 Hz, 1H), 5.29 (d, *J* = 6.1 Hz, 1H), 5.23 (d, *J* = 5.9 Hz, 1H), 4.64 (s, 1H), 3.83 (s, 3H), 3.79 (s, 3H), 3.55 (s, 3H), 1.62 – 1.52 (m, 1H), 1.48 (s, 3H), 1.04– 0.94 (m, 30H), 0.70 (d, *J* = 6.9 Hz, 3H), 0.22 (s, 3H), 0.13 (s, 3H), 0.11 (s, 3H). The characterization data match the data reported previously.[5]

Compound 4-19



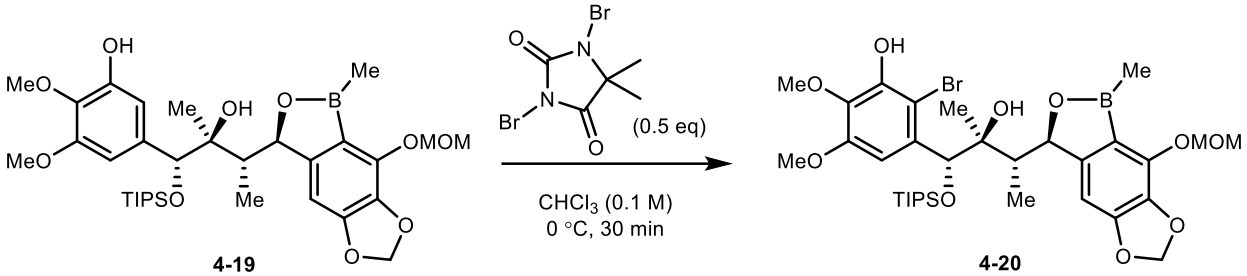
4-18
Chemical Formula: $C_{39}H_{64}BBrO_{10}Si_2$
Molecular Weight: 839.8150

4-19
Chemical Formula: $C_{33}H_{51}BO_{10}Si$
Molecular Weight: 646.6560

Procedure: A 250 mL flame-dried round bottom flask equipped with a Teflon-coated stir bar and a rubber septum was charged with **4-18** (6.13 mmol, 5.14 g, 1.0 equiv.). The flask was evacuated and refilled with N_2 (repeated 3 times), prior to the addition of THF (61 mL). The mixture was cooled to −78 °C in a dry ice / acetone bath, at which point *tert*-butyllithium (12.25 mmol, 1.390 M in pentane, 8.8 mL, 2.0 equiv.) was added via syringe pump at a rate of 30 mL/h. Stirred at −78 °C for 1 h, and at rt for another 3 h. The reaction mixture was quenched by the addition of saturated aqueous NH_4Cl solution and H_2O (1:5, 50 mL), and extracted with EtOAc (3 × 42 mL). The combined organic layers were dried over $MgSO_4$, filtered, and concentrated *in vacuo*. The crude product was dissolved in MeOH/THF (1:1, 61 mL). KHF_2 (12.25 mmol, 956.7 mg, 2.0 equiv.) was then added. The resulting solution was stirred at rt for 1 h, then diluted with toluene (21 mL), and concentrated *in vacuo* to ~ 20 mL. H_2O (21 mL) and brine (21 mL) were added, and the resulting mixture was extracted with EtOAc (3 × 42 mL). The combined organic layers were dried over $MgSO_4$, filtered, and concentrated *in vacuo*. The crude product was purified on silica gel (5:1 to 3:1 hexanes/EtOAc) to provide **4-19** (3.52 g, 5.45 mmol, 89 %) as a white foam.

Characterization: **^{1}H NMR** (500 MHz, $CDCl_3$) δ 6.72 (s, 1H), 6.69 (br s, 1H), 6.58 (br s, 1H), 5.97 (d, J= 1.5 Hz, 1H), 5.95 (d, J= 1.4 Hz, 1H), 5.70 (s, 1H), 5.46 (d, *J* = 3.5 Hz, 1H), 5.37 (d, *J* = 6.0 Hz, 1H), 5.29 (d, *J* = 6.0 Hz, 1H), 4.63 (s, 1H), 3.90 (s, 3H), 3.85 (s, 3H), 3.53 (s, 3H), 2.81 (s, 1H), 2.31 (m, 1H), 1.28 (s, 3H), 1.07 – 0.94 (m, 21H), 0.79 (s, 3H), 0.63 (d, *J* = 7.3 Hz, 3H). The characterization data match the data reported previously.[5]

Compound 4-20



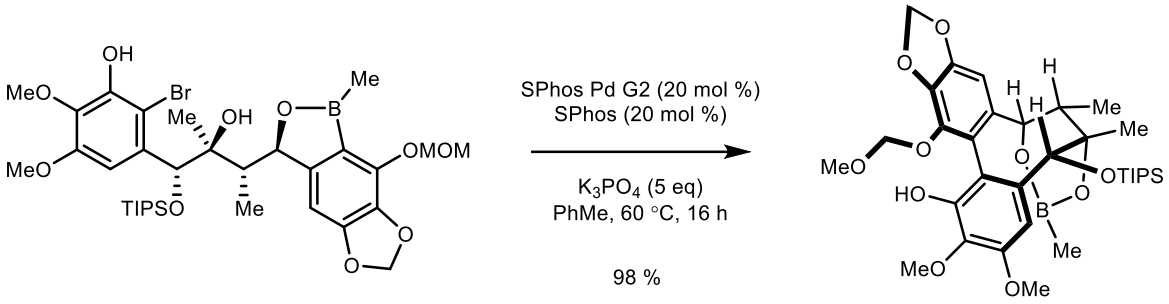
4-19
Chemical Formula: $C_{33}H_{51}BO_{10}Si$
Molecular Weight: 646.6560

4-20
Chemical Formula: $C_{33}H_{50}BBrO_{10}Si$
Molecular Weight: 725.5520

Procedure: A 250 mL flame-dried round bottom flask equipped with a Teflon-coated stir bar and a rubber septum was charged with **4-19** (5.44 mmol, 3.52 g, 1.0 equiv.). $CHCl_3$ (54 mL) was added and stirred until all solids were dissolved. The mixture was then cooled to 0 °C in an ice bath, at which point 1,3-dibromo-5,5-dimethylhydantoin (DBDMH, 2.72 mmol, 778 mg, 0.5 equiv.) was added as a solid in portions. (An orange color appeared when the first portion of DBDMH was added, and the next portion was added after the orange color faded.) The resulting solution was stirred at 0 °C for 30 min and then concentrated *in vacuo*. The crude product was purified on silica gel (3:1 hexanes/EtOAc) and then recrystallized from CH_2Cl_2-hexanes (1:5) to provide **4-20** (2.60 g, 3.59 mmol, 66 %) as an off-white solid.

Characterization: **^{1}H NMR** (500 MHz, $CDCl_3$) δ 7.00 (s, 1H), 6.66 (s, 1H), 6.08 (s, 1H), 5.96 (s, 2H), 5.49 (d, *J* = 3.6 Hz, 1H), 5.38 (d, *J* = 6.0 Hz, 1H), 5.32 (s, 1H), 5.28 (d, *J* = 6.0 Hz, 1H), 3.94 (s, 3H), 3.84 (s, 3H), 3.53 (s, 3H), 2.72 (s, 1H), 2.24 (qd, *J* = 7.2, 3.8 Hz, 1H), 1.35 (s, 3H), 1.11 – 1.03 (m, 3H), 1.01 (d, *J* = 6.2 Hz, 9H), 0.91 (d, *J* = 6.9 Hz, 9H), 0.80 (d, *J* = 7.2 Hz, 3H), 0.77 (s, 3H). The characterization data match the data reported previously.[5]

Compound 4-21



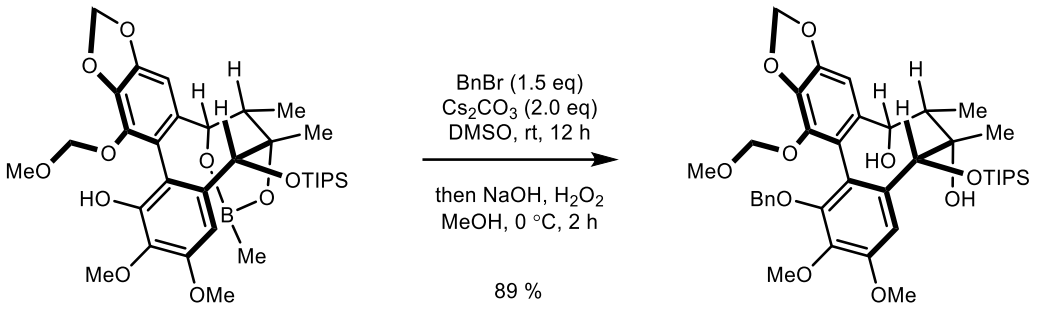
4-20
Chemical Formula: $C_{33}H_{50}BBrO_{10}Si$
Molecular Weight: 725.5520

4-21
Chemical Formula: $C_{33}H_{49}BO_{10}Si$
Molecular Weight: 644.6400

Procedure: A 250 mL flame-dried Schlenk flask equipped with a Teflon-coated stir bar and a glass stopper was charged with **4-20** (2.70 mmol, 1.96 g, 1.0 equiv.), SPhos Pd G2 (0.54 mmol, 389 mg, 20 mol %), SPhos (0.54 mmol, 222 mg, 20 mol %) and K_3PO_4 (13.5 mmol, 2.87 g, 5.0 equiv.). The flask was evacuated and refill with N_2 (repeated 3 times), prior to the addition of a stock solution of H_2O (1.35 mmol, 24.3 μL, 0.5 equiv.) in toluene (54 mL). The resulting mixture was stirred at 60 °C in a pre-heated oil bath for 16 h. It was then poured on a mixture consisting of H_3PO_4 (2 M in H_2O, 13 mL) and brine (13 mL), and extracted with EtOAc (4 × 26 mL). The combined organic layers were dried over $MgSO_4$, filtered, and concentrated *in vacuo*. The crude product was purified on silica gel (3:1 hexanes/EtOAc) to provide **4-21** (1.70 g, 2.65 mmol, 98 %) as a pale-yellow foam.

Characterization: **^{1}H NMR** (500 MHz, $CDCl_3$) δ 6.78 (s, 1H), 6.38 (s, 1H), 5.95 (2 x d, J = 1.3 Hz, 2H), 5.75 (s, 1H), 5.19 (d, J = 5.1 Hz, 1H), 5.14 (d, J = 5.2 Hz, 1H), 4.80 (s, 1H), 4.78 (s, 1H), 3.91 (s, 3H), 3.89 (s, 3H), 3.38 (s, 3H), 1.96 (q, J = 7.2 Hz, 1H), 1.40 (s, 3H), 1.22 (d, J = 7.2 Hz, 3H), 0.89 (s, 21H), -0.38 (s, 3H). The characterization data match the data reported previously.[5]

Compound 4-22



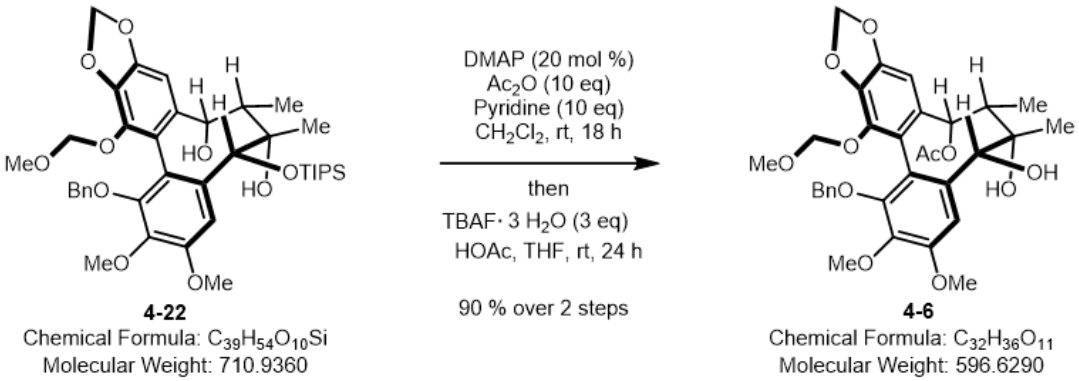
4-21
Chemical Formula: $C_{33}H_{49}BO_{10}Si$
Molecular Weight: 644.6400

4-22
Chemical Formula: $C_{39}H_{54}O_{10}Si$
Molecular Weight: 710.9360

Procedure: A 250 mL flame-dried round bottom flask equipped with a Teflon-coated stir bar and a rubber septum was charged with **4-21** (2.96 mmol, 1.91 g, 1.0 equiv.) and Cs_2CO_3 (5.91 mmol, 1.93 g, 2.0 equiv.). The flask was evacuated and refilled with N_2 (repeated 3 times), prior to the addition of DMSO (15 mL) and benzyl bromide (4.43 mmol, 0.50 mL, 1.5 equiv.). The resulting mixture was stirred at rt for 17 h. MeOH (75 mL) was then added, and the mixture was cooled to 0 °C. NaOH (1 M in H_2O, 9.5 mL) and 30 % H_2O_2 (4.43 mmol, 450 µL, 1.5 equiv.) were added, and the resulting mixture was stirred for 2 h. The reaction mixture was quenched by the addition of $NaHCO_3$ (saturated aqueous, 15 mL) and $Na_2S_2O_3$ (saturated aqueous, 15 mL), then concentrated *in vacuo*. The mixture was extracted with EtOAc (3 × 75 mL). The combined organic layers were washed with sequentially with H_2O (75 mL) and brine (75 mL). They were then dried over $MgSO_4$, filtered, and concentrated *in vacuo*. The crude product was purified on silica gel (15 % to 35 % ethyl acetate in hexanes) to provide **4-22** (1.87 g, 2.63 mmol, 89 %) as a tan oil.

Characterization: $\mathbf{R_f}$ = (hexanes/EtOAc 3:1): 0.28; **IR** (neat) v = 3421, 2994, 2939, 2891, 2865, 1618, 1599, 1461, 1372, 1104, 1045, 933, 882, 828, 751, 677 cm^{-1}; **^{1}H NMR** (500 MHz, $CDCl_3$) δ 7.17 (m, 3H), 7.07 (s, 1H), 6.97 (dd, J= 6.3, 1.6 Hz, 2H), 6.23 (s, 1H), 5.98 (d, J= 1.3 Hz, 1H), 5.93 (d, J= 1.3 Hz, 1H), 5.20 (d, J= 5.4 Hz, 1H), 5.07 (d, J= 5.4 Hz, 1H), 4.96 (d, J= 11.5 Hz, 1H), 4.83 (d, J= 11.5 Hz, 1H), 4.60 (s, 1H), 4.46 (d, J= 5.0 Hz, 1H), 3.90 (s, 3H), 3.89 (s, 3H), 3.41 (s, 3H), 2.07 (br s, 1H), 1.68 (q, J= 7.0 Hz, 1H), 1.34 (s, 3H), 1.26 (d, J= 7.1 Hz, 3H), 0.86 (m, 12 H), 0.82 (d, J= 5.3 Hz, 9H), 0.69 (d, J= 5.1 Hz, 1H); **^{13}C NMR** (126 MHz, $CDCl_3$) δ 152.3, 148.8, 148.5, 141.3, 138.4, 138.32, 138.30, 136.5, 135.0, 128.5, 128.2, 127.8, 122.1, 119.2, 109.4, 101.9, 101.1, 96.9, 83.5, 78.0, 76.0, 74.1, 61.1, 57.0, 56.0, 47.7, 25.4, 18.2, 18.0, 17.7, 12.6; **$[\alpha]^{23}_D$** –108.4 °, (c = 1.0, $CHCl_3$); **HRMS**: Calcd. for $C_{39}H_{54}O_{10}$ $[M+Na]^+$ = 733.3384 m/z, found = 733.3383 m/z.

Compound 4-6



4-22
Chemical Formula: $C_{39}H_{54}O_{10}Si$
Molecular Weight: 710.9360

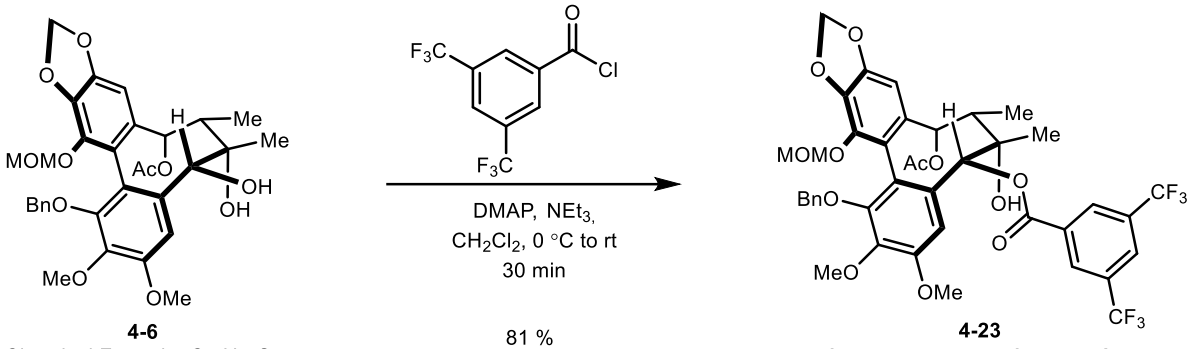
4-6
Chemical Formula: $C_{32}H_{36}O_{11}$
Molecular Weight: 596.6290

Procedure: A 250 mL flame-dried round bottom flask equipped with a Teflon-coated stir bar and a rubber septum was charged with **4-22** (2.54 mmol, 1.81 g, 1.0 equiv.) and 4-(*N,N*-dimethylamino)pyridine (DMAP, 0.51 mmol, 62 mg, 20 mol %). The flask was evacuated and refilled with N_2 (repeated 3 times), prior to the addition of CH_2Cl_2 (13 mL). Pyridine (25.4 mmol, 2.1 mL, 10 equiv.) and acetic anhydride (25.4 mmol, 2.4 mL, 10 equiv.) were then added via syringe, and the resulting mixture was stirred at rt for 18 h. The reaction mixture was cooled to 0 °C in an ice bath, and quenched by the dropwise addition of MeOH (25.4 mmol, 1.0 mL, 10 equiv.). The mixture was warmed to rt and stirred for another 30 min. Then, it was poured onto HCl (1 M, 43 mL) and extracted with CH_2Cl_2 (3 × 30 mL). The combined organic layers were washed with sequentially with $NaHCO_3$ (saturated aqueous, 30 mL) and brine (30 mL), dried over $MgSO_4$, filtered, and concentrated *in vacuo*. The round bottom flask containing the crude product was evacuated and refilled with N_2 (repeated 3 times), prior to the addition of THF (5.1 mL). A solution of TBAF·3 H_2O (7.63 mmol, 2.41 g, 3.0 equiv.) and acetic acid (3.05 mmol, 175 µL, 1.2 equiv.) in THF (7.6 mL) was prepared in a separate flask, then added via syringe to the reaction mixture and stirred at rt for 24 h. The reaction mixture was poured on $NaHCO_3$ (saturated aqueous, 15 mL) and brine (15 mL), and extracted with EtOAc (3 × 30 mL). The combined organic layers were dried over $MgSO_4$, filtered, and concentrated *in vacuo*. The crude product was purified on silica gel (1:2 hexanes/EtOAc) to provide **4-6** (1.36 g, 2.28 mmol, 90 %) as an off-white foam.

Characterization: $\mathbf{R_f}$ = (hexanes/EtOAc 1:2): 0.33; **IR** (neat) ν = 3571, 3466, 2924, 1743, 1622, 1596, 1460, 1373, 1227, 1148, 1109, 1035, 930, 754 cm^{-1}; **^{1}H NMR** (500 MHz, $CDCl_3$) δ 7.23 (m, 3H), 7.13 (s, 1H), 7.09 (dd, 2H, J= 7.7, 1.8 Hz), 6.52 (s, 1H), 5.99 (d, J= 1.4 Hz, 1H), 5.92 (d, J=

1.3 Hz, 1H), 5.66 (s, 1H), 5.06 (d, J= 6.0 Hz, 1H), 4.99 (d, J= 10.6 Hz, 1H), 4.75 (d, J= 6.0 Hz, 1H), 4.61 (s, 1H), 4.56 (d, J= 10.6 Hz, 1H), 3.95 (s, 3H), 3.87 (s, 3H), 3.07 (s, 3H), 1.94 (q, J= 6.8 Hz, 1H), 1.68 (broad s, 1H), 1.58 (s, 3H), 1.39 (s, 3H), 1.21 (d, J=7.0 Hz, 3H), 0.87 (broad, 1H); **^{13}C NMR** (126 MHz, $CDCl_3$) δ 169.0, 153.0, 149.6, 149.0, 141.2, 138.0, 137.9, 137.2, 135.4, 134.1, 128.0, 127.6, 127.4, 122.9, 120.5, 106.9, 103.4, 101.5, 97.3, 82.1, 76.4, 75.2, 74.3, 60.8, 56.7, 56.3, 47.1, 24.4, 20.4, 16.8; **[α]^{23}D** –27.0 °, (c = 1.0, $CHCl_3$); **HRMS**: Calcd. for $C_{39}H_{36}O_{11}$ $[M+Na]^+$ = 619.2155 m/z, found = 619.2153 m/z.

Compound 4-23



4-6
Chemical Formula: $C_{32}H_{36}O_{11}$
Molecular Weight: 596.6290

4-23
Chemical Formula: $C_{41}H_{38}F_6O_{12}$
Molecular Weight: 836.7334

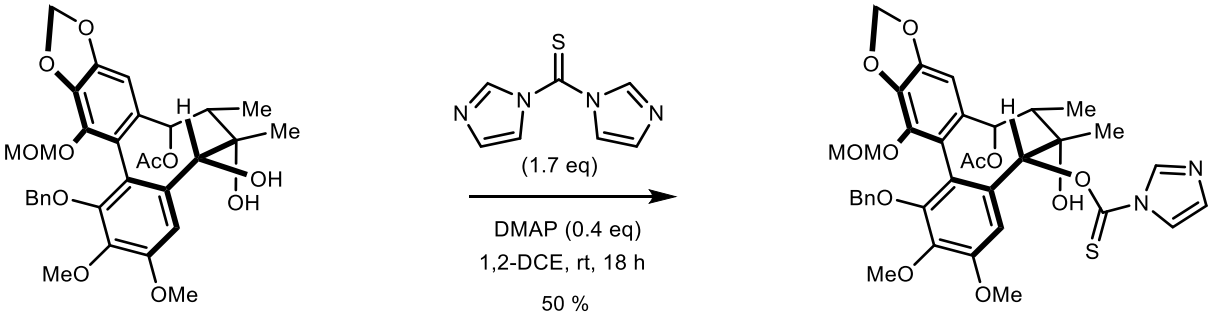
Procedure:

A flame-dried vial equipped with a Teflon-coated stir bar and a septum cap was charged with **4-6** (0.17 mmol, 101 mg, 1.0 equiv.) and DMAP (0.0085 mmol, 1.0 mg, 0.05 equiv.). The vial was evacuated and refilled with N_2 (repeated 3 times), prior to the addition of CH_2Cl_2 (1.7 mL). The reaction mixture was cooled to 0 °C, then slowly added 3,5-bis-(trifluoromethyl)benzoyl chloride (0.19 mmol, 34 μL, 1.1 equiv.) via microsyringe. It was allowed to warm to room temperature and stirred for 3 h. The resulting mixture was concentrated *in vacuo*. The crude product was purified on silica gel (25 % to 35 % ethyl acetate in hexanes) to provide **4-23** (115 mg, 0.137 mmol, 81 %) as a white foam.

Characterization: **R_f** = (hexanes/EtOAc 3:1): 0.20; **IR** (neat) v = 3571, 3000, 2939, 2850, 1734, 1623, 1596, 1462, 1374, 1278, 1247, 1138, 1055, 930, 845, 756, 699, 681 cm^{-1}; **^{1}H NMR** (500 MHz, $CDCl_3$) δ 8.54 (s, 2H), 8.10 (s, 1H), 7.27 (m, 3H), 7.16 (s, 1H), 7.15 (m, 2H), 6.58 (s, 1H), 6.12 (s, 1H), 6.05 (d, J= 1.2 Hz, 1H), 5.97 (d, J= 1.3 Hz, 1H), 5.78 (s, 1H), 5.05 (d, J= 10.8 Hz,

1H), 4.95 (d, J= 6.0 Hz, 1H), 4.91(d, J= 5.9 Hz, 1H), 4.74 (d, J= 10.9 Hz, 1H), 3.96 (s, 3H), 3.88 (s, 3H), 3.11 (s, 3H), 2.13 (q, J= 7.0 Hz, 1H), 2.05 (s, 1H), 1.65 (s, 3H), 1.36 (s, 3H), 1.30 (d, J= 7.0 Hz, 3H); **^{13}C NMR** (126 MHz, $CDCl_3$) δ 168.7, 162.3, 153.0, 149.9, 149.4, 141.7, 138.1, 137.9, 137.6, 133.7, 132.5, 132.4 (q, J= 34 Hz), 130.7, 129.7 (q, J= 3 Hz), 128.0, 127.4, 126.5 (m), 123.5, 122.8 (q, J= 272 Hz), 119.7, 107.1, 103.4, 101.6, 97.5, 82.2, 78.6, 75.7, 74.3, 60.7, 56.6, 55.9, 46.9, 24.2, 20.4, 16.7; **[α]^{23}D** 41.2 °, (c = 1.0, $CHCl_3$); **HRMS**: Calcd. for $C_{41}H_{38}F_6O_{12}$ $[M+Na]^+$ = 859.2165 m/z and $[M+NH_4]^+$ = 854.2611, found $[M+Na]^+$ = 859.2159 m/z and $[M+NH_4]^+$ = 854.2617 m/z.

Compound 4-24



4-6
Chemical Formula: $C_{32}H_{36}O_{11}$
Molecular Weight: 596.6290

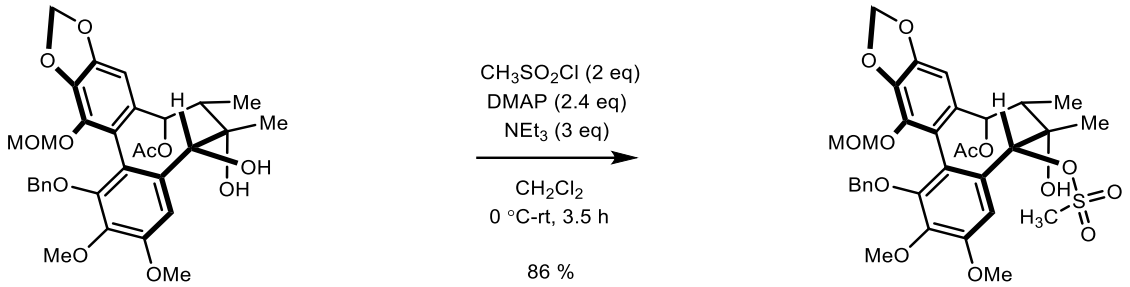
4-24
Chemical Formula: $C_{36}H_{38}N_2O_{11}S$
Molecular Weight: 706.7630

Procedure: A flame-dried 10 mL round bottom flask equipped with Teflon-coated stir bar was charged with **4-6** (0.17 mmol, 103 mg, 1.0 equiv.), DMAP (0.07 mmol, 8 mg, 0.4 equiv.), and 1,1'-thiocarbonyldiimidazole (0.29 mmol, 52 mg, 1.7 equiv.). The flask was evacuated and refilled with N_2 (repeated 3 times), prior to the addition of 1,2-dichloroethane (1 mL). The reaction mixture was stirred at room temperature for 18 h and then quenched by the addition of $NaHCO_3$ (sat. aq.), followed by extraction with CH_2Cl_2 (x 3). The combined organic layers were dried and concentrated *in vacuo.* The crude product was purified on silica gel (60 % to 90 % ethyl acetate in hexanes) to provide **4-24** (61 mg, 0.086 mmol, 50 %).

Characterization: **R_f** = (hexanes/EtOAc 1:4): 0.21; **IR** (neat) v = 2927, 1745, 1462, 1376, 1333, 1283, 1225, 1109, 976, 750 cm^{-1}; **^{1}H NMR** (500 MHz, $CDCl_3$) δ 8.44 (s, 1H), 7.72 (s, 1H), 7.23 (m, 3H), 7.09 (m, 2H), 7.06 (broad s, 1H), 6.93 (s, 1H), 6.52 (s, 1H), 6.51 (s, 1H), 6.02 (d, *J*= 1.2 Hz, 1H), 5.92 (d, *J*= 1.2 Hz, 1H), 5.74 (s, 1H), 4.99 (d, *J*= 10.7 Hz, 1H), 4.93 (d, *J*= 5.5 Hz, 1H), 4.89 (d, *J*= 5.5 Hz, 1H), 4.61 (d, *J*= 10.7 Hz, 1H), 3.90 (s, 3H), 3.86 (s, 3H), 3.17 (s, 3H), 2.10 (q,

J= 6.9 Hz, 1H), 2.03 (broad s, 1H), 1.61 (s, 3H), 1.34 (s, 3H), 1.25 (d, *J*= 7.0 Hz, 3H); **^{13}C NMR** (126 MHz, $CDCl_3$) δ 182.3, 168.7, 153.0, 149.8, 149.5, 142.0, 138.3, 137.8, 136.7, 136.2, 133.8, 130.9, 129.3, 128.0, 127.5, 127.4, 124.2, 118.7, 117.9, 107.0, 102.6, 101.4, 97.0, 86.3, 82.1, 75.8, 74.3, 60.8, 56.8, 56.1, 47.0, 24.2, 20.4, 16.5; **[α]$^{23}_D$** 38.4 °, (c = 1.0, $CHCl_3$); **HRMS**: Calcd. for $C_{36}H_{38}N_2O_{11}S$ $[M+Na]^+$ = 729.2094 m/z, found = 729.2111 m/z.

Compound 4-25



4-6
Chemical Formula: $C_{32}H_{36}O_{11}$
Molecular Weight: 596.6290

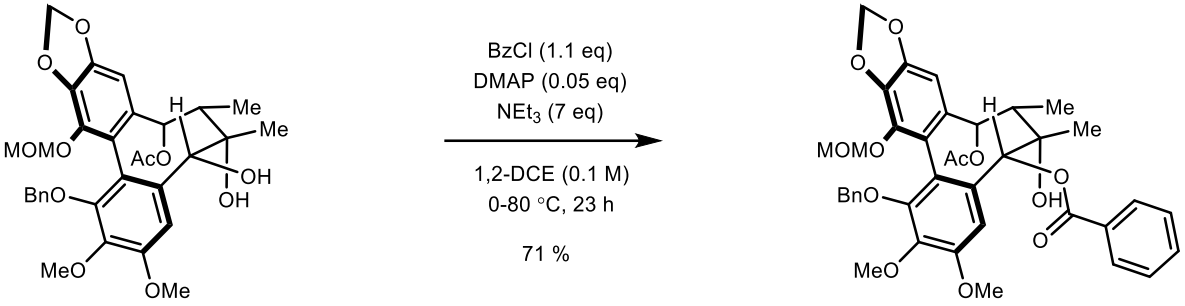
4-25
Chemical Formula: $C_{33}H_{38}O_{13}S$
Molecular Weight: 674.7140

Procedure: A flame-dried flask equipped with a Teflon-coated stir bar and a rubber septum was charged with **4-6** (0.42 mmol, 249 mg, 1.0 equiv.) and DMAP (1.00 mmol, 122 mg, 2.4 equiv.). The flask was evacuated and refilled with N_2 (repeated 3 times), prior to the addition of CH_2Cl_2 (16.7 mL). The reaction mixture was chilled in an ice bath and then added triethylamine (1.25 mmol, 175 µL, 3.0 equiv.), followed by methanesulfonyl chloride (0.84 mmol, 65 µL, 2.0 equiv.). The reaction mixture was allowed to warm to room temperature and stirred for 3 hours. Then, it was poured into ice water (44 mL) and stirred for 30 min. The mixture was then diluted with CH_2Cl_2 (44 mL). The organic layer was washed sequentially with water (44 mL) and brine (44 mL), dried over $MgSO_4$, filtered, and concentrated *in vacuo*. The crude product was purified on silica gel (40 % to 50 % ethyl acetate in hexanes) to provide **4-25** (244 mg, 0.36 mmol, 86 %) as a white solid.

Characterization: **R_f** = (hexanes/EtOAc 1:2): 0.56; **IR** (neat) v = 2969, 2939, 2901, 1746, 1622, 1596, 1457, 1373, 1224, 1172, 1111, 1072, 926, 878, 749, 530; **^{1}H NMR** (500 MHz, $CDCl_3$) δ 7.26 (m, 3H), 7.08 (m, 3H), 6.51 (s, 1H), 6.00 (s, 1H), 5.92 (s, 1H), 5.68 (s, 1H), 5.42 (s, 1H), 4.98 (m, 2H), 4.90 (d, J= 5.1 Hz, 1H), 4.52 (d, J= 10.5 Hz, 1H), 3.96 (s, 3H), 3.90 (s, 3H), 3.24 (s, 3H), 2.62 (s, 3H), 2.02 (q, J= 6.8 Hz, 1H), 1.90 (s, 1H), 1.59 (s, 3H), 1.45 (s, 3H), 1.24 (d, J= 7.0 Hz,

3H); **^{13}C NMR** (126 MHz, $CDCl_3$) δ 168.6, 153.2, 149.7, 149.6, 142.1, 137.68, 137.61, 136.3, 133.9, 129.6, 128.1, 127.6, 127.5, 123.5, 117.9, 107.5, 103.0, 101.5, 97.1, 85.1, 82.0, 75.8, 74.3, 60.9, 56.9, 56.4, 46.9, 38.4, 25.0, 20.3, 16.8; **[α]$^{23}_D$** –17.8 °, (c = 1.0, $CHCl_3$); **HRMS**: Calcd. for $C_{33}H_{38}NaO_{13}S$ $[M+Na]^+$ = 697.1931 m/z, found $[M+Na]^+$ = 697.1912 m/z.

Compound 4-26



4-6
Chemical Formula: $C_{32}H_{36}O_{11}$
Molecular Weight: 596.6290

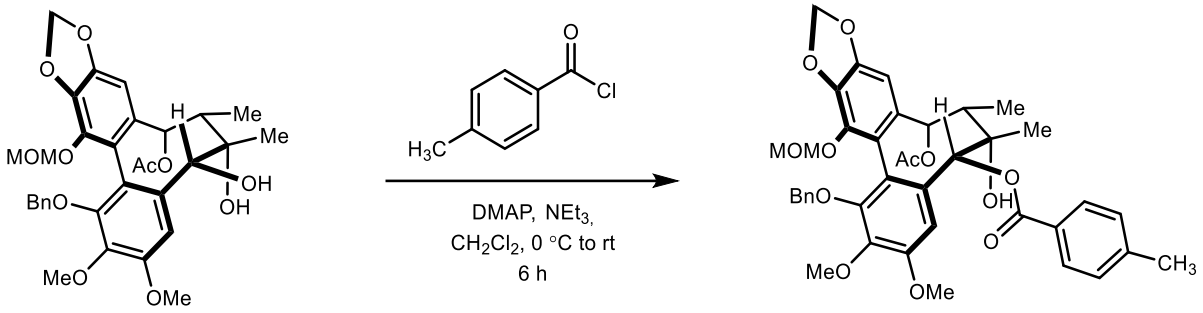
4-26
Chemical Formula: $C_{39}H_{40}O_{12}$
Molecular Weight: 700.7370

Procedure: A flame-dried microwave vial equipped with a Teflon-coated stir bar and a rubber septum was charged with **4-6** (0.09 mmol, 56 mg, 1.0 equiv.) and DMAP (0.005 mmol, 0.6 mg, 0.1 equiv.). The flask was evacuated and refilled with N_2 (repeated 3 times), prior to the addition of 1,2-dichloroethane (1 mL) followed by triethylamine (0.65 mmol, 91 µL, 7.0 equiv.). The reaction mixture was cooled to 0 °C and benzoyl chloride (0.10 mmol, 12 µL, 1.1 equiv.) was added dropwise. The reaction mixture was allowed to warm to room temperature and then stirred at 80 °C for 23 h. It was quenched by the addition of $NaHCO_3$ (sat. aq.) and then extracted with ethyl acetate (x 3). The combined organic layers were washed with brine, dried, and concentrated *in vacuo.* The crude product was purified on silica gel (33 % to 66 % ethyl acetate in hexanes) to provide **4-26** (46 mg, 0.66 mmol, 71 %).

Characterization: **R_f** = (hexanes/EtOAc 2:1): 0.67; **IR** (neat) v = 3567, 2999, 2937, 2901, 1745, 1717, 1623, 1596, 1453, 1373, 1268, 1221, 1150, 1107, 1024, 928, 751, 711 cm^{-1}; **^{1}H NMR** (500 MHz, $CDCl_3$) δ 8.11 (m, 2H), 7.57 (m, 1H), 7.45 (t, *J*= 7.7 Hz, 2H), 7.25-7.19 (m, 3H), 7.15 (s, 1H), 7.13 (m, 2H), 6.53 (s, 1H), 6.04 (s, 1H), 6.02 (d, *J*= 1.2 Hz, 1H), 5.95 (d, *J*= 1.2 Hz, 1H), 5.75 (s, 1H), 5.02 (d, *J*= 11.0 Hz, 1H), 4.94 (d, *J*= 5.5 Hz, 1H), 4.90 (d, *J*= 5.5 Hz, 1H), 4.74 (d, *J*= 11.0 Hz, 1H), 3.92 (s, 3H), 3.83 (s, 3H), 3.09 (s, 3H), 2.07 (q, *J*= 6.9 Hz, 1H), 1.93 (broad s, 1H), 1.61 (s, 3H), 1.33 (s, 3H), 1.25 (d, *J*= 6.9 Hz, 3H); **^{13}C NMR** (126 MHz, $CDCl_3$) δ 168.8, 164.7, 152.8,

149.8, 149.2, 141.5, 138.1, 138.0, 137.8, 133.7, 133.0, 131.5, 130.2, 129.6, 128.5, 128.0, 127.3, 127.2, 123.4, 120.0, 107.4, 103.3, 101.5, 97.5, 82.2, 77.2, 75.8, 74.2, 60.7, 56.6, 56.1, 46.9, 24.2, 20.4, 16.8; **[α]^{23}D** 146.8 °, (c = 1.0, $CHCl_3$); **HRMS**: Calcd. for $C_{39}H_{40}O_{12}$ $[M+Na]^+$ = 723.2417 m/z, found = 723.2427 m/z.

Compound 4-27



4-6
Chemical Formula: $C_{32}H_{36}O_{11}$
Molecular Weight: 596.6290

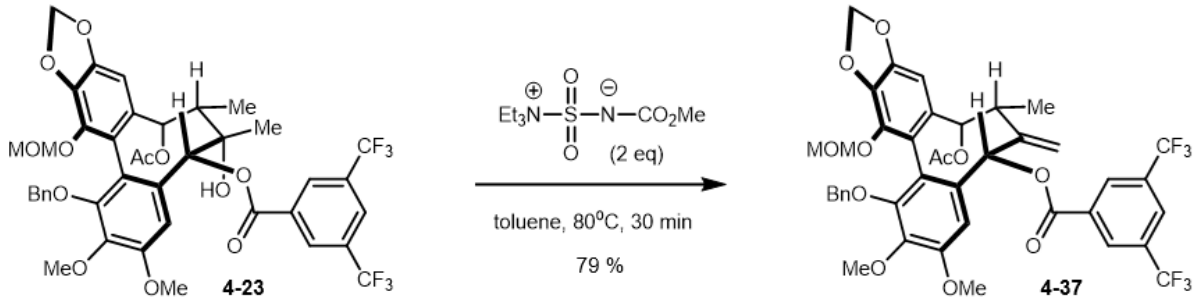
4-27
Chemical Formula: $C_{40}H_{42}O_{12}$
Molecular Weight: 714.7640

A flame-dried vial equipped with a Teflon-coated stir bar and a septum cap was charged with **4-6** (0.087 mmol, 52 mg, 1.0 equiv.) and DMAP (0.004 mmol, 0.5 mg, 0.05 equiv.). The vial was evacuated and refilled with N_2 (repeated 3 times), prior to the addition of CH_2Cl_2 (0.9 mL). The reaction mixture was cooled to 0 °C, then *p*-toluoyl chloride (0.096 mmol, 13 μL, 1.1 equiv.) was slowly added via microsyringe. The reaction mixture was allowed to warm to room temperature and stirred for 6 h prior to concentration *in vacuo*. The crude product was purified on silica gel (33 % to 66 % ethyl acetate in hexanes) to provide **4-27** (59 mg, 0.083 mmol, 95 %) as a white foam.

Characterization: **R$_f$** = (hexanes/EtOAc 1:2): 0.33; **IR** (neat) v = 3571, 2925, 1746, 1717, 1611, 1478, 1374, 1271, 1224, 1151, 1106, 930, 753; **^{1}H NMR** (500 MHz, $CDCl_3$) δ 7.99 (d, J= 8.1 Hz, 2H), 7.29-7.19 (m, 5H), 7.15 (s, 1H), 7.13 (d, J= 7.4 Hz, 2H), 6.53 (s, 1H), 6.02 (s, 1H), 6.01 (d, J= 1.0 Hz, 1H), 5.94 (d, J= 1.1 Hz, 1H), 5.74 (s, 1H), 5.02 (d, J= 10.9 Hz, 1H), 4.95 (d, J= 5.5 Hz, 1H), 4.89 (d, J= 5.5 Hz, 1H), 4.75 (d, J= 10.9 Hz, 1H), 3.92 (s, 3H), 3.83 (s, 3H), 3.08 (s, 3H), 2.40 (s, 3H), 2.07 (q, J= 6.8 Hz, 1H), 1.94 (broad s, 1H), 1.62 (s, 3H), 1.33 (s, 3H), 1.25 (d, J= 6.8 Hz, 3H); **^{13}C NMR** (126 MHz, $CDCl_3$) δ 168.8, 164.7, 152.8, 149.8, 149.2, 143.8, 141.4, 138.2, 138.0, 137.8, 133.7, 131.6, 130.1, 129.6, 129.2, 128.0, 127.6, 127.4, 127.3, 123.3, 120.1, 107.4, 103.3, 101.5, 97.5, 82.2, 76.8, 75.9, 74.2, 60.7, 56.6, 56.1, 46. 9, 24.2, 21.6, 20.4, 16.8; **[α]^{23}D** 61.6 °, (c =

1.0, $CHCl_3$); **HRMS**: Calcd. for $C_{40}H_{42}O_{12}$ $[M+Na]^+$ = 737.2574 m/z, found $[M+Na]^+$ = 737.2572 m/z.

Compound 4-37



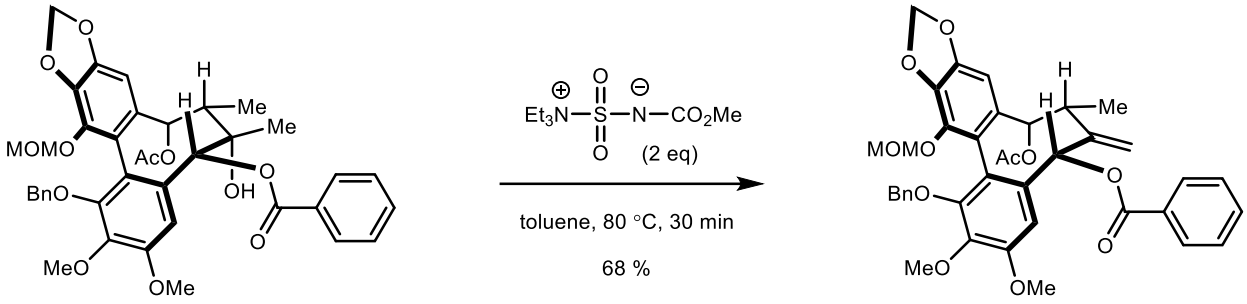
Chemical Formula: $C_{41}H_{38}F_6O_{12}$
Molecular Weight: 836.7334

Chemical Formula: $C_{41}H_{36}F_6O_{11}$
Molecular Weight: 818.7184

Procedure: A flame-dried 10 mL round bottom flask equipped with Teflon-coated stir bar was charged with **4-23** (0.022 mmol, 18 mg, 1.0 equiv.) and Burgess reagent (0.044 mmol, 10 mg, 2.0 equiv.). Th flask was evacuated and refilled with N_2 (repeated 3 times), prior to the addition of toluene (1.1 mL). The reaction mixture was stirred at 80 °C for 30 minutes and then allowed to cool to room temperature. It was concentrated *in vacuo* and then the residue was taken up in ethyl acetate and water. The layers were separated and the organic layer was washed with brine. The organic layer was dried over Na_2SO_4, filtered, and concentrated *in vacuo*. The crude product was purified via silica gel (15 % to 50 % ethyl acetate in hexanes) to provide **4-37** (14 mg, 0.017 mmol, 79 %).

Characterization: $\mathbf{R_f}$ = (hexanes/EtOAc 2:1): 0.67; **IR** (neat) v = 2925, 2854, 1737, 1622, 1599, 1456, 1371, 1039, 931, 844, 754, 698, 681 cm^{-1}; **^{1}H NMR** (500 MHz, $CDCl_3$) δ 8.52 (s, 2H), 8.09 (s, 1H), 7.23 (m, 3H), 7.08 (m, 3H), 6.67 (s, 1H), 6.05 (s, 1H), 6.02 (d, *J*= 1.1 Hz, 1H), 5.95 (d, *J*= 1.1 Hz, 1H), 5.80 (s, 1H), 5.53 (s, 1H), 5.00 (d, *J*= 10.9 Hz, 1H), 4.97 (m, 2H), 4.79 (d, *J*= 5.9 Hz, 1H), 4.72 (d, *J*= 10.9 Hz, 1H), 3.98 (s, 3H), 3.85 (s, 3H), 3.04 (s, 3H), 2.86 (q, *J*= 7.1 Hz, 1H), 1.57 (s, 3H), 1.26 (d, *J*= 7.0 Hz, 3H); **^{13}C NMR** (126 MHz, $CDCl_3$) δ 169.8, 162.3, 153.7, 150.0, 149.2, 149.1, 141.2, 138.4, 137.9, 137.5, 134.7, 133.7, 132.4 (q, *J*= 33 Hz), 132.3, 129.5 (m), 128.2, 128.0, 127.43, 127.41, 126.5 (m), 123.8, 122.7 (q *J*= 272 Hz), 121.7, 119.7, 110.3, 103.9, 102.4, 101.6, 97.3, 79.6, 75.7, 74.3, 60.8, 56.6, 55.9, 43.0, 20.5, 18.3; **$[\alpha]^{23}_D$** –24.2 °, (c = 0.9, $CHCl_3$); **HRMS**: Calcd. for $C_{41}H_{36}F_6O_{11}$ $[M+Na]^+$ = 841.2068 m/z, found = 841.2060 m/z.

Compound 4-38



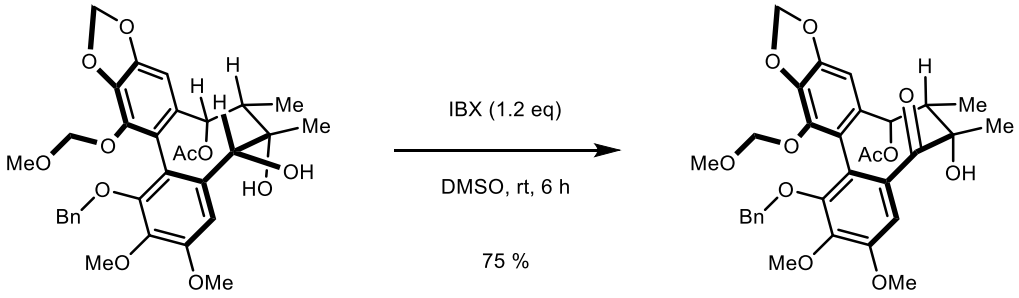
4-26
Chemical Formula: $C_{39}H_{40}O_{12}$
Molecular Weight: 700.7370

4-38
Chemical Formula: $C_{39}H_{38}O_{11}$
Molecular Weight: 682.7220

Procedure: A flame-dried 10 mL round bottom flask equipped with Teflon-coated stir bar was charged with **4-26** (0.07 mmol, 46 mg, 1.0 equiv.) and Burgess reagent (0.13 mmol, 31 mg, 2.0 equiv.). The flask was evacuated and refilled with N_2 (repeated 3 times), prior to the addition of toluene (3.3 mL). The reaction mixture was stirred at 80 °C for 30 minutes and then allowed to cool to room temperature. The mixture was concentrated *in vacuo* and then the residue was taken up in ethyl acetate and water. The layers were separated and the organic layer was washed with brine. The organic layer was dried over Na_2SO_4, filtered, and concentrated *in vacuo*. The crude product was purified via silica gel (20 % to 35 % ethyl acetate in hexanes) to provide **4-38** (30.4 mg, 0.04 mmol, 68 %).

Characterization: $\mathbf{R_f}$ = (hexanes/EtOAc 2:1): 0.45; **^{1}H NMR** (500 MHz, $CDCl_3$) δ 8.09 (m, 2H), 7.58 (m, 1H), 7.47 (m, 2H), 7.23 (m, 2H), 7.14 (s, 1H), 7.10 (m, 2H), 6.65 (s, 1H), 6.03 (s, 1H), 6.01 (d, *J*= 1.3 Hz, 1H), 5.94 (d, *J*= 1.3 Hz, 1H), 5.79 (s, 1H), 5.58 (broad s, 1H), 4.99 (2 x d, *J*= 11.3 and 6.0 Hz, 2H), 4.94 (d, *J*= 1.7 Hz, 1H), 4.79 (d, *J*= 5.9 Hz, 1H), 4.76 (d, *J*= 11.0 Hz, 1H), 3.99 (s, 3H), 3.84 (s, 3H), 3.01 (s, 3H), 2.87 (q, *J*= 6.7 Hz, 1H), 1.58 (s, 3H), 1.26 (d, *J*= 7.0 Hz, 3H); **^{13}C NMR** (126 MHz, $CDCl_3$) δ 169.9, 165.0, 153.5, 149.9, 149.7, 149.1, 140.9, 138.3, 138.1, 137.6, 134.7, 134.6, 133.1, 130.2, 129.5, 128.5, 128.0, 127.3, 121.6, 120.1, 110.1, 103.9, 102.9, 101.5, 97.2, 79.7, 74.4, 74.3, 60.8, 56.5, 56.1, 43.0, 20.5, 18.4; **HRMS**: Calcd. for $C_{39}H_{38}O_{11}$ $[M+Na]^+$ = 705.2312 m/z, found = 705.2310 m/z.

Compound 4-30



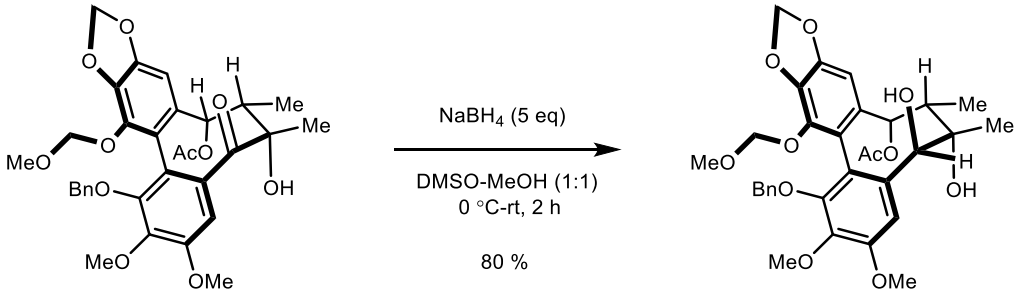
4-6
Chemical Formula: $C_{32}H_{36}O_{11}$
Molecular Weight: 596.6290

4-30
Chemical Formula: $C_{32}H_{34}O_{11}$
Molecular Weight: 594.6130

Procedure: A 25 mL flame-dried round bottom flask equipped with a Teflon-coated stir bar and a rubber septum was charged with **4-6** (0.45 mmol, 268 mg, 1.0 equiv.) and iodoxybenzoic acid (IBX, 0.54 mmol, 151 mg, 1.2 equiv.). The flask was evacuated and refilled with N_2 (repeated 3 times), prior to the addition of DMSO (2.2 mL). The resulting mixture was stirred at rt for 6 h. Added water (6.6 mL) and extracted with ethyl acetate (3 x 6.6 mL). The combined organic layers were washed sequentially with $NaHCO_3$ (sat. aq., 6.6 mL, with vigorous shaking), water (6.6 mL), and brine (6.6 mL). The organic layer was dried over Na_2SO_4, filtered, and concentrated *in vacuo*. The crude product was purified on silica gel (35 % to 45 % ethyl acetate in hexanes) to provide **4-30** (199 mg, 0.34 mmol, 75 %) as an off-white/ beige solid.

Characterization: $\mathbf{R_f}$ = (hexanes/EtOAc 3:2): 0.32; **IR** (neat) v = 3568, 2936, 1750, 1702, 1590, 1478, 1372, 1327, 1215, 1159, 1108, 1030, 927, 836, 750, 698 cm^{-1}; **^{1}H NMR** (500 MHz, $CDCl_3$) δ 7.24 (m, 3H), 7.15 (d, J= 7.3 Hz, 2H), 6.76 (s, 1H), 6.42(s, 1H), 5.95 (d, J= 1.1 Hz, 1H), 5.90 (d, J= 1.1 Hz, 1H), 5.74 (s, 1H), 5.04 (d, J= 11.2 Hz, 1H), 4.94 (d, J= 5.7 Hz, 1H), 4.86 (d, J= 5.4 Hz, 1H), 4.85 (d, J= 12 Hz, 1H), 3.92 (s, 3H), 3.84 (s, 3H), 3.19 (s, 3H), 2.73 (broad s, 1H), 1.99 (q, J= 7.0 Hz, 1H), 1.67 (s, 3H), 1.42 (s, 3H), 1.26 (d, J= 7.2 Hz, 3H); **^{13}C NMR** (126 MHz, $CDCl_3$) δ 210.7, 168.3, 152.4, 150.9, 149.2, 142.2, 138.1, 138.0, 137.8, 135.3, 131.6, 128.0, 127.3, 127.2, 120.8, 119.9, 105.0, 103.8, 101.6, 97.1, 82.9, 80.6, 74.6, 60.8, 56.8, 56.3, 46.4, 23.7, 20.5, 14.9; **$[\alpha]^{23}_D$** 1.7 °, (c = 1.0, $CHCl_3$); **HRMS**: Calcd. for $C_{32}H_{34}O_{11}$ $[M+Na]^+$ = 617.1999 m/z, found $[M+Na]^+$ = 617.19826 m/z.

Compound 4-31



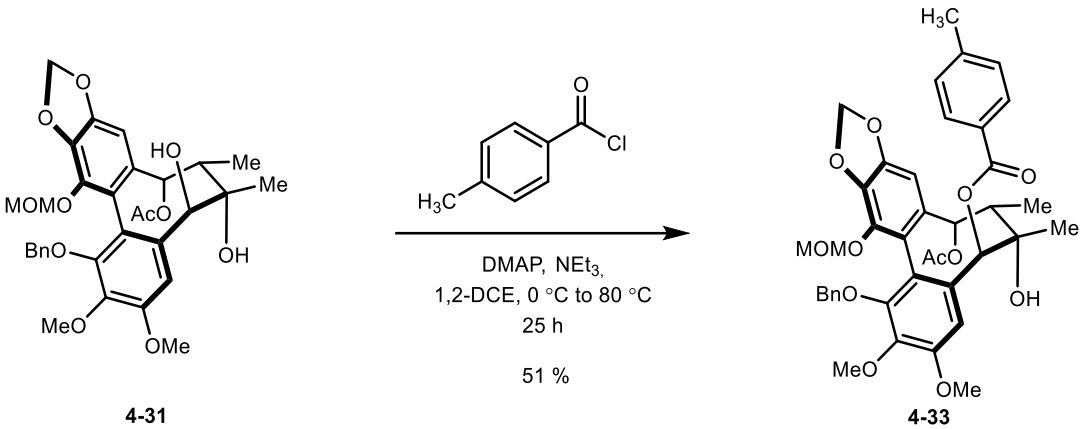
4-30
Chemical Formula: $C_{32}H_{34}O_{11}$
Molecular Weight: 594.6130

4-31
Chemical Formula: $C_{32}H_{36}O_{11}$
Molecular Weight: 596.6290

Procedure: A 25 mL flame-dried round bottom flask equipped with a Teflon-coated stir bar and a rubber septum was charged with **4-30** (0.18 mmol, 104 mg, 1.0 equiv.). MeOH (2 mL) and DMSO (2 mL) were added under air and the reaction mixture was cooled to 0 °C using an ice bath. $NaBH_4$ (0.88 mmol, 33 mg, 5.0 equiv.) was then added as a solid in one portion. The reaction mixture was stirred for 2 h, allowing the ice bath to melt. The reaction mixture was quenched by the addition of NH_4Cl (sat. aq., 5 mL). It was then concentrated *in vacuo* and extracted with EtOAc (3 × 5 mL). The combined organic layers were washed with $NaHCO_3$ (sat. aq., 5 mL), water (5 mL) and brine (2.5 mL), then dried over Na_2SO_4, filtered, and concentrated *in vacuo*. The crude product was purified on silica gel (40 % to 50 % ethyl acetate in hexanes) to provide **4-31** (76 mg, 0.14 mmol, 80 %) as a beige-yellow oil.

Characterization: $\mathbf{R_f}$ = (hexanes/EtOAc 1:2): 0.62; **IR** (neat) v = 3550, 3450, 3005, 2925, 2854, 1745, 1627, 1595, 1455, 1371, 1220, 1149, 1109, 1049, 930, 749, 698, 665 cm^{-1}; **^{1}H NMR** (500 MHz, $CDCl_3$) δ 7.22 (m, 3H), 7.05 (m, 2H), 6.75 (s, 1H), 6.58 (s, 1H), 5.99 (d, *J*= 1.4 Hz, 1H), 5.92 (d, *J*= 1.4 Hz, 1H), 5.70 (s, 1H), 5.01 (d, *J*= 6.9 Hz, 1H), 4.95 (d, *J*= 10.5 Hz, 1H), 4.80 (d, *J*= 1.6 Hz, 1H), 4.75 (d, *J*= 6.8 Hz, 1H), 4.82 (d, *J*= 10.5 Hz, 1H), 3.92 (s, 3H), 3.87 (s, 3H), 3.16 (d, *J*= 1.9 Hz, 1H), 2.86 (s, 3H), 2.14 (q, J= 7.3 Hz, 1H), 2.07 (broad s, 1H), 1.58 (s, 3H), 1.45 (s, 3H), 1.26 (d, *J*= 7.2 Hz, 3H); **^{13}C NMR** (126 MHz, $CDCl_3$) δ 168.7, 151.9, 150.8, 148.8, 141.5, 138.5, 138.0, 137.7, 134.4, 132.9, 128.0, 127.6, 127.4, 122.9, 122.5, 110.6, 104.5, 101.8, 98.5, 85.8, 83.5, 75.1, 74.4, 61.0, 56.4, 56.3, 41.9, 29.0, 20.5, 17.2; **$[\alpha]^{23}_D$** –45.6 °, (c = 1.0, $CHCl_3$); **HRMS**: Calcd. for $C_{39}H_{36}O_{11}$ $[M+Na]^+$ = 619.2155 m/z, found = 619.2152 m/z.

Compound 4-33



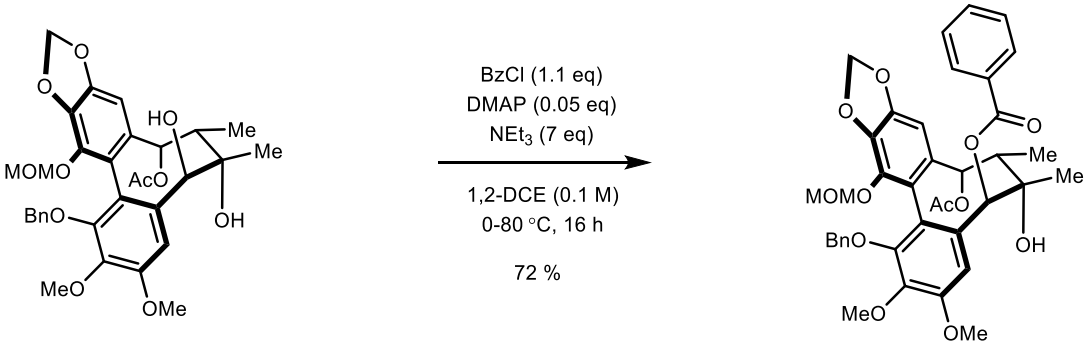
4-31
Chemical Formula: $C_{32}H_{36}O_{11}$
Molecular Weight: 596.6290

4-33
Chemical Formula: $C_{40}H_{42}O_{12}$
Molecular Weight: 714.7640

Procedure: A flame-dried microwave vial equipped with a Teflon-coated stir bar and a rubber septum was charged with **4-31** (0.096 mmol, 57 mg, 1.0 equiv.) and DMAP (0.096 mmol, 12 mg, 1.0 equiv.). The vial was evacuated and refilled with N_2 (repeated 3 times), prior to the addition of 1,2-dichloroethane (1 mL). The reaction mixture was cooled to 0 °C, then *p*-toluoyl chloride (0.105 mmol, 14 μL, 1.1 equiv.) was slowly added via microsyringe. The reaction mixture was allowed to warm to room temperature and then stirred at 80 °C for 25 h. The mixture was then cooled to rt and concentrated *in vacuo*. The crude product was purified on silica gel (33 % to 66 % ethyl acetate in hexanes) to provide **4-33** (35 mg, 0.049 mmol, 51 %) as well as recovered starting material **4-31** (21 mg, 0.036 mmol, 37 %).

Characterization: $\mathbf{R_f}$ = (hexanes/EtOAc 1:2): 0.61; **IR** (neat) v = 3567, 2927, 1747, 1718, 1612, 1456, 1371, 1254, 1159, 1107, 932, 753 cm^{-1}; **^{1}H NMR** (500 MHz, $CDCl_3$) δ 7.28 (d, *J*= 8.2 Hz, 2H), 7.18 (m, 3H), 7.08 (d, *J*= 8.0 Hz, 2H), 7.02 (m, 2H), 6.89 (s, 1H), 6.62 (s, 1H), 6.01 (s, 1H), 5.83 (s, 1H), 5.77 (d, *J*= 1.4 Hz, 1H), 5.72 (d, *J*= 1.4 Hz, 1H), 4.92 (d, *J*= 10.6 Hz, 1H), 4.51 (d, *J*= 10.6 Hz, 1H), 4.43 (d, *J*= 5.9 Hz, 1H), 4.24 (d, *J*= 5.9 Hz, 1H), 3.96 (s, 3H), 3.82 (s, 3H), 2.82 (s, 3H), 2.36 (s, 3H), 2.30 (q, *J*= 7.2 Hz, 1H), 2.20 (s, 1H), 1.63 (s, 3H), 1.37 (s, 3H), 1.32 (d, *J*= 7.2 Hz, 3H); **^{13}C NMR** (126 MHz, $CDCl_3$) δ 168.7, 164.8, 151.9, 150.7, 148.6, 143.5, 141.5, 138.1, 137.9, 136.0, 132.7, 130.2, 129.4, 128.4, 127.9, 127.4, 127.3, 126.8, 122.7, 121.5, 110.6, 102.5, 100.9, 96.1, 84.2, 83.4, 74.2, 74.1, 60.7, 56.1, 56.0, 43.1, 28.7, 21.7, 20.6, 27.1; **$[\alpha]^{23}_D$** –82.2 °, (c = 1.0, $CHCl_3$); **HRMS**: Calcd. for $C_{40}H_{42}O_{12}$ $[M+Na]^+$ = 737.2574 m/z, found = 737.2587 m/z.

Compound 4-35



4-31
Chemical Formula: $C_{32}H_{36}O_{11}$
Molecular Weight: 596.6290

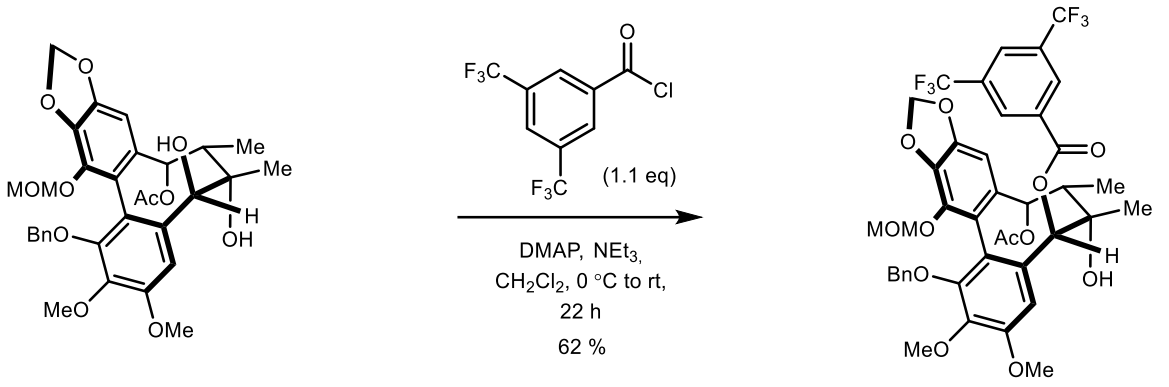
4-35
Chemical Formula: $C_{39}H_{40}O_{12}$
Molecular Weight: 700.7370

Procedure: A flame-dried microwave vial with a Teflon-coated stir bar and a rubber septum was charged with **4-31** (0.14 mmol, 81 mg, 1.0 equiv.) and DMAP (0.007 mmol, 0.8 mg, 0.1 equiv.). The vial was evacuated and refilled with N_2 (repeated 3 times), prior to the addition of 1,2-dichloroethane (1 mL) followed by triethylamine (0.95 mmol, 133 µL, 7.0 equiv.). The reaction mixture was cooled to 0 °C and benzoyl chloride (0.15 mmol, 17 µL, 1.1 equiv.) was added dropwise. It was then allowed to warm to room temperature, followed by stirring at 80 °C for 16 h. The reaction mixture was cooled to rt and quenched by addition of $NaHCO_3$ (sat. aq.), followed by extraction with ethyl acetate (x 3). The combined organic layers were washed with brine, dried, and concentrated *in vacuo.* The crude product was purified on silica gel (25 % to 38 % ethyl acetate in hexanes) to provide **4-35** (69 mg, 0.098 mmol, 72 %).

Characterization: $\mathbf{R_f}$ = (hexanes/EtOAc 2:1): 0.28; **IR** (neat) v = 3567, 2976, 2935, 2854, 1746, 1720, 1622, 1598, 1450, 1370, 1220, 1149, 1108, 1024, 930, 751, 709 cm^{-1}; **^{1}H NMR** (500 MHz, $CDCl_3$) δ 7.47 (m, 1H), 7.40 (m, 1H), 7.28 (m, 1H), 7.18 (m, 1H), 7.01 (m, 1H), 6.90 (s, 1H), 6.62 (s, 1H), 6.03 (s, 1H), 5.83 (s, 1H), 5.75 (d, *J*= 1.3 Hz, 1H), 5.73 (d, *J*= 1.3 Hz, 1H), 4.92 (d, *J*= 10.6 Hz, 1H), 4.51 (d, *J*= 10.6 Hz, 1H), 4.41 (d, *J*= 5.9 Hz, 1H), 4.22 (d, *J*= 5.9 Hz, 1H), 3.96 (s, 3H), 3.83 (s, 3H), 2.81 (s, 3H), 2.31 (q, *J*= 7.1 Hz, 1H), 2.22 (broad s, 1H), 1.63 (s, 3H), 1.38 (s, 3H), 1.32 (d, *J*= 7.2 Hz, 3H); **^{13}C NMR** (126 MHz, $CDCl_3$) δ 168.7, 164.7, 151.9, 150.7, 148.6, 141.6, 138.1, 137.9, 136.0, 132.8, 132.7, 130.2, 129.5, 129.4, 127.9, 127.7, 127.4, 127.3, 122.7, 121.5, 110.6, 102.6, 101.0, 96.1, 84.4, 83.4, 74.2, 74.1, 60.7, 56.1, 56.0, 43.1, 28.7, 20.6, 17.1;

[α]^{23}D –48.8 °, (c = 1.0, $CHCl_3$); **HRMS**: Calcd. for $C_{39}H_{40}O_{12}$ $[M+Na]^+$ = 723.2417 m/z, found = 723.23989 m/z.

Compound 4-33



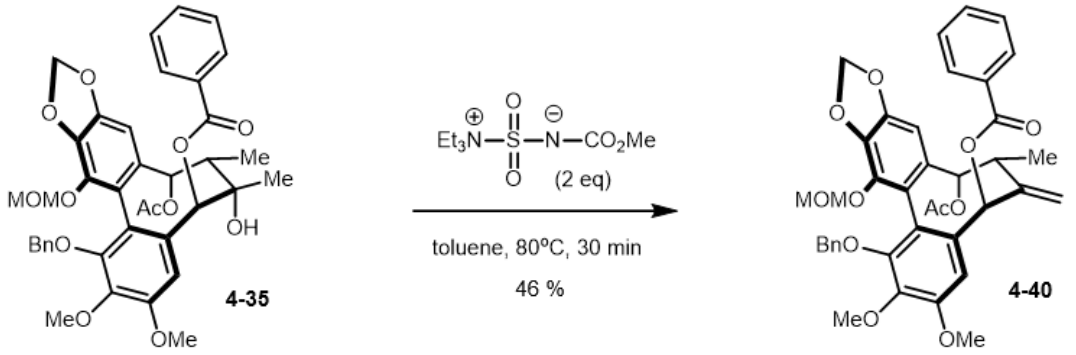
4-31
Chemical Formula: $C_{32}H_{36}O_{11}$
Molecular Weight: 596.6290

4-33
Chemical Formula: $C_{41}H_{38}F_6O_{12}$
Molecular Weight: 836.7334

Procedure: A flame-dried vial equipped with a Teflon-coated stir bar and a rubber septum was charged with **4-31** (0.24 mmol, 144 mg, 1.0 equiv.) and DMAP (0.024 mmol, 3 mg, 0.1 equiv.). The vial was evacuated and refilled with N_2 (repeated 3 times), prior to the addition of CH_2Cl_2 (2.4 mL). The reaction mixture was cooled to 0 °C, then 3,5-bis-(trifluoromethyl)benzoyl chloride (0.27 mmol, 48 μL, 1.1 equiv.) was slowly added via microsyringe. The reaction mixture was allowed to warm to room temperature and stirred for 3 h, prior to concentration *in vacuo*. The crude product was purified on silica gel (20 % to 35 % ethyl acetate in hexanes) to provide **4-33** (126 mg, 0.15 mmol, 62 %).

Characterization: R_f = (hexanes/EtOAc 2:1): 0.41; **^{1}H NMR** (500 MHz, $CDCl_3$) δ 7.98 (s, 1H), 7.88 (s, 2H), 7.18 (m, 3H), 6.97 (m, 2H), 6.92 (s, 1H), 6.62 (s, 1H), 6.03 (s, 1H), 5.82 (s, 1H), 5.71 (d, *J*= 1.3 Hz, 1H), 5.66 (d, *J*= 1.3 Hz, 1H), 4.91 (d, *J*= 10.4 Hz, 1H), 4.38 (m, 2H), 4.33 (d, *J*= 6.1 Hz, 1H), 3.98 (s, 3H), 3.85 (s, 3H), 2.80 (s, 3H), 2.31 (broad s, 1H), 2.26 (q, *J*= 7.1 Hz, 1H), 1.62 (s, 3H), 1.39 (s, 3H), 1.35 (d, *J*= 7.2 Hz, 3H); **^{13}C NMR** (126 MHz, $CDCl_3$) δ 168.6, 162.4, 152.1, 150.5, 148.7, 141.9, 138.1, 137.6, 136.4, 132.6, 132.0, 131.7 (q, *J*= 34.0 Hz), 129.4, 129.0 (q, *J*= 3.5 Hz), 127.9, 127.6, 127.4, 126.1 (m), 122.7 (q, *J*= 273 Hz), 122.5, 121.1, 110.7, 103.0, 101.2, 96.6, 85.9, 83.4, 74.3, 73.9, 60.8, 56.2, 56.0, 43.2, 28.4, 20.5, 17.2; **[α]^{23}D** –82.2 °, (c = 1.0, $CHCl_3$); **HRMS**: Calcd. for $C_{41}H_{38}F_6O_{12}$ $[M+Na]^+$ = 859.2165 m/z, found = 859.21508 m/z.

Compound 4-40



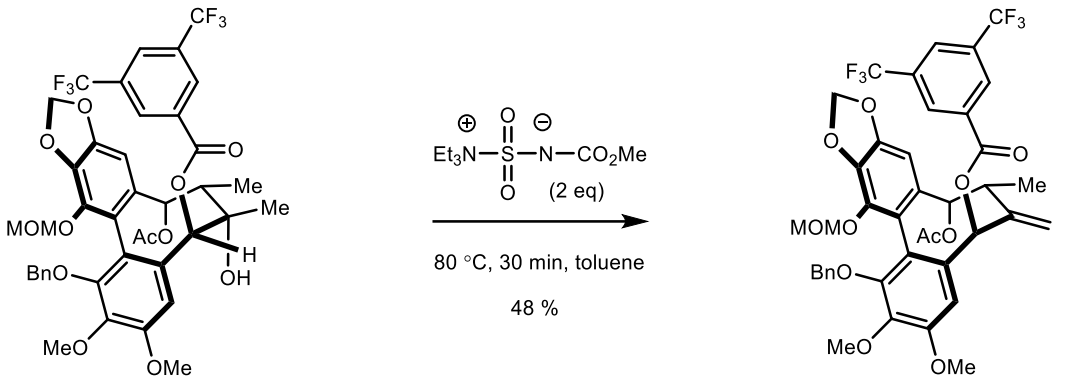
Chemical Formula: $C_{39}H_{40}O_{12}$
Molecular Weight: 700.7370

Chemical Formula: $C_{39}H_{38}O_{11}$
Molecular Weight: 682.7220

Procedure: A flame-dried 25 mL round bottom flask equipped with Teflon-coated stir bar was charged with **4-35** (0.098 mmol, 69 mg, 1.0 equiv.) and Burgess reagent (0.20 mmol, 47 mg, 2.0 equiv.). The flask was evacuated and refilled with N_2 (repeated 3 times), prior to the addition of toluene (4.9 mL). The reaction mixture was stirred at 80 °C for 30 minutes and then allowed to cool to room temperature. It was then concentrated *in vacuo* and the residue taken up in ethyl acetate and water. The layers were separated and the organic layer was washed with brine. The organic layer was dried over Na_2SO_4, filtered, and concentrated *in vacuo*. The crude product was purified via silica gel (15 % to 25 % ethyl acetate in hexanes) to provide **4-40** (31 mg, 0.045 mmol, 46 %).

Characterization: $\mathbf{R_f}$ = (hexanes/EtOAc 4:1): 0.27; **IR** (neat) v = 3008, 2967, 2933, 2900, 1715, 1597, 1451, 1368, 1236, 1148, 1109, 1038, 931, 751, 710 cm^{-1}; **^{1}H NMR** (500 MHz, $CDCl_3$) δ 7.48 (m, 3H), 7.29 (m, 2H), 7.19 (m, 3H), 7.00 (m, 2H), 6.83 (s, 1H), 6.68 (s, 1H), 6.66 (s, 1H), 5.83 (m, 3H), 5.42 (s, 1H), 4.94 (s, 1H), 4.90 (d, *J*= 13.4 Hz, 1H), 4.58 (d, *J*= 7.2 Hz, 1H), 4.54 (d, *J*= 13.4 Hz, 1H), 4.47 (d, *J*= 7.2 Hz, 1H), 3.95 (s, 3H), 3.83 (s, 3H), 2.97 (q, *J*= 8.7 Hz, 1H), 2.91 (s, 3H), 1.58 (s, 3H), 1.30 (d, *J*= 8.8 Hz, 3H); **^{13}C NMR** (126 MHz, $CDCl_3$) δ 170.1, 164.9, 152.7, 150.8, 148.4, 146.2, 141.4, 138.7, 137.9, 136.6, 134.0, 133.2, 132.8, 129.8, 129.5, 127.9, 127.8, 127.4, 127.3, 122.1, 121.8, 115.3, 107.4, 102.9, 101.1, 96.4, 81.5, 79.5, 74.2, 60.8, 56.1, 40.5, 20.5, 18.7; **$[\alpha]^{23}_D$** 0.5 °, (c = 1.0, $CHCl_3$); **HRMS**: Calcd. for $C_{39}H_{38}O_{11}$ $[M+Na]^+$ = 705.2312 m/z, found = 705.2328 m/z.

Compound 4-39



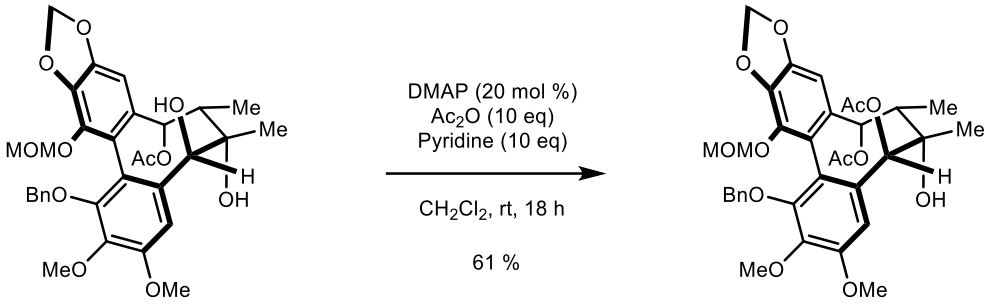
4-32
Chemical Formula: $C_{41}H_{38}F_6O_{12}$
Molecular Weight: 836.7334

4-39
Chemical Formula: $C_{41}H_{36}F_6O_{11}$
Molecular Weight: 818.7184

Procedure: A flame-dried 25 mL round bottom flask equipped with Teflon-coated stir bar was charged with **4-32** (0.15 mmol, 126 mg, 1.0 equiv.) and Burgess reagent (0.30 mmol, 72 mg, 2.0 equiv.). The flask was evacuated and refilled with N_2 (repeated 3 times), prior to the addition of toluene (7.6 mL). The reaction mixture was stirred at 80 °C for 30 minutes and then allowed to cool to room temperature. The reaction mixture was concentrated *in vacuo* and then the residue was taken up in ethyl acetate and water. The layers were separated and the organic layer was washed with brine. The organic layer was dried over Na_2SO_4, filtered, and concentrated *in vacuo*. The crude product was purified via silica gel (10 % to 25 % ethyl acetate in hexanes) to provide **4-39** (59 mg, 0.073 mmol, 48 %).

Characterization: $\mathbf{R_f}$ = (hexanes/EtOAc 2:1): 0.61; **IR** (neat) v = 3019, 2969, 2931, 1732, 1500, 1477, 1456, 1419, 1371, 1333, 1279, 1215, 1142, 745, 667 cm^{-1}; **^{1}H NMR** (500 MHz, $CDCl_3$) δ 8.00 (s, 2H), 7.97 (s, 1H), 7.19 (m, 3H), 6.95 (m, 2H), 6.84 (s, 1H), 6.71 (s, 1H), 6.65 (s, 1H), 5.83 (d, *J*= 1.1 Hz, 1H), 5.81 (d, *J*= 1.3 Hz, 1H), 5.74 (d, *J*= 1.3 Hz, 1H), 5.41 (s, 1H), 4.97 (m, 1H), 4.89 (d, *J*= 10.5 Hz, 1H), 4.54 (d, *J*= 6.2 Hz, 1H), 4.50 (d, *J*= 6.2 Hz, 1H), 4.42 (d, *J*= 10.5 Hz, 1H), 3.96 (s, 3H), 3.84 (s, 3H), 2.98 (q, *J*= 6.8 Hz, 1H), 2.88 (s, 3H), 1.56 (s, 3H), 1.33 (d, *J*= 7.1 Hz, 3H); **^{13}C NMR** (126 MHz, $CDCl_3$) δ 169.9, 162.5, 152.8, 150.7, 148.6, 145.5, 141.8, 138.7, 137.7, 137.0, 132.3, 131.7 (q, *J*= 34 Hz), 129.3 (q, *J*= 3.3 Hz), 127.9, 127.6, 127.4, 126.1, 122.8 (q, *J*= 273 Hz), 122.2, 121.3, 115.9, 107.6, 103.1, 101.3, 96.7, 82.8, 79.3, 74.2, 60.8, 56.17, 56.15, 40.8, 20.5, 18.6; **$[\alpha]^{23}_D$** –72.6 °, (c = 1.0, $CHCl_3$); **HRMS**: Calcd. for $C_{41}H_{36}F_6O_{11}$ $[M+Na]^+$ = 841.2060 m/z, found = 841.20355 m/z.

Compound 4-34



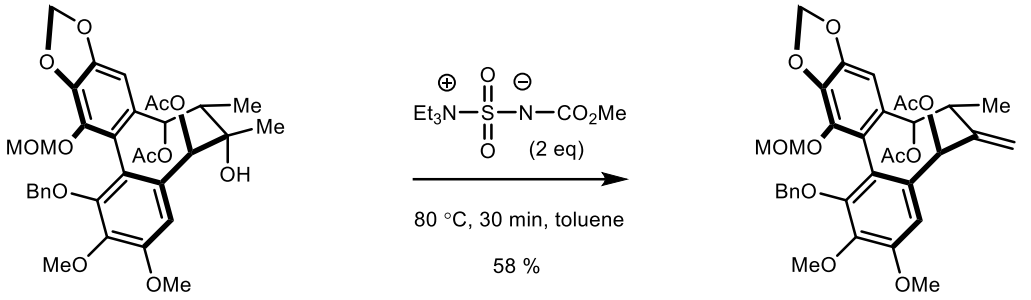
4-31
Chemical Formula: $C_{32}H_{36}O_{11}$
Molecular Weight: 596.6290

4-34
Chemical Formula: $C_{34}H_{38}O_{12}$
Molecular Weight: 638.6660

Procedure: A flame-dried vial equipped with a Teflon-coated stir bar and a rubber septum was charged with **4-31** (0.085 mmol, 50 mg, 1.0 equiv.) and 4-(*N,N*-dimethylamino)pyridine (DMAP, 0.017 mmol, 2 mg, 20 mol %). The vial was evacuated and refilled with N_2 (repeated 3 times), prior to the addition of CH_2Cl_2 (1 mL). Pyridine (0.85 mmol, 68 µL, 10 equiv.) and acetic anhydride (0.85 mmol, 80 µL, 10 equiv.) were then added via syringe, and the resulting mixture was stirred at rt for 18 h. The reaction mixture was cooled to 0 °C in an ice bath and quenched by the dropwise addition of MeOH (0.85 mmol, 33 µL, 10 equiv.). The mixture was warmed to rt and stirred for another 30 min. Then, it was poured onto HCl (1 M, 1.4 mL) and extracted with CH_2Cl_2 (3 × 1 mL). The combined organic layers were washed sequentially with $Na_2S_2O_3$ (sat. aq., 1 mL) and brine (1 mL), dried over $MgSO_4$, filtered, and concentrated *in vacuo*. The crude product was purified on silica gel (28 % to 38 % ethyl acetate in hexanes) to provide **4-34** (33 mg, 0.052 mmol, 61 %).

Characterization: $\mathbf{R_f}$ = (hexanes/EtOAc 2:1): 0.22; **IR** (neat) ν = 2977, 2936, 2898, 1731, 1475, 1455, 1372, 1330, 1226, 1155, 1110, 1028, 922, 839, 738, 697, 486 cm^{-1}; **^{1}H NMR** (500 MHz, $CDCl_3$) δ 7.22 (m, 3H), 7.05 (m, 2H), 6.80 (s, 1H), 6.54 (s, 1H), 5.94 (s, 1H), 5.86 (s, 1H), 5.81 (s, 1H), 5.75 (s, 1H), 4.99 (d, 1H), 4.96 (d, 1H), 4.69 (d, 1H), 4.56 (d, 1H), 3.93 (s, 3H), 3.84 (s, 3H), 3.02 (s, 3H), 2.12 (q, 1H), 2.07 (broad s, 1H), 1.63 (s, 3H), 1.61 (s, 3H), 1.30 (s, 3H), 1.25 (d, 3H); **^{13}C NMR** (126 MHz, $CDCl_3$) δ; $\mathbf{[\alpha]^{23}_D}$ 10.4 °, (c = 1.0, $CHCl_3$); **HRMS**: Calcd. for $C_{34}H_{38}O_{12}$ $[M+Na]^+$ = 661.2261 m/z, found = 661.22427 m/z.

Compound 4-41



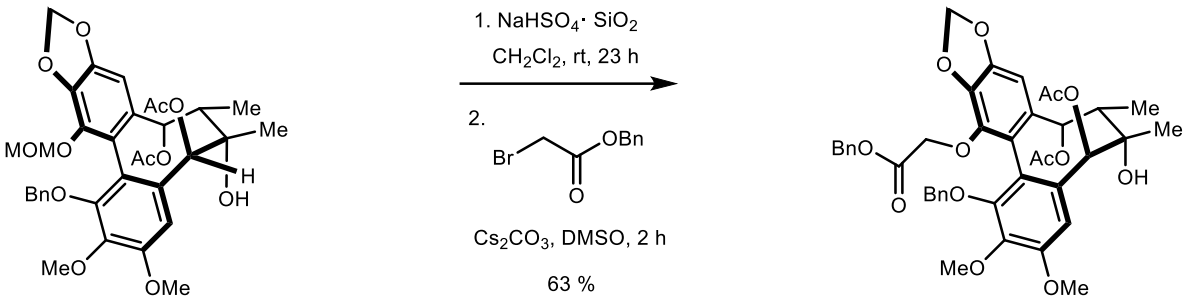
4-34
Chemical Formula: $C_{34}H_{38}O_{12}$
Molecular Weight: 638.6660

4-41
Chemical Formula: $C_{34}H_{36}O_{11}$
Molecular Weight: 620.6510

Procedure: A flame-dried 25 mL round bottom flask equipped with Teflon-coated stir bar was charged with **4-34** (0.086 mmol, 55 mg, 1.0 equiv.) and Burgess reagent (0.17 mmol, 41 mg, 2.0 equiv.). The flask was evacuated and refilled with N_2 (repeated 3 times), prior to the addition of toluene (4.3 mL). The reaction mixture was stirred at 80 °C for 30 minutes and then allowed to cool to room temperature. The reaction mixture was concentrated *in vacuo* and then the residue was taken up in ethyl acetate and water. The layers were separated and the organic layer was washed with brine. The organic layer was dried over Na_2SO_4, filtered, and concentrated *in vacuo*. The crude product was purified via silica gel (20 % to 35 % ethyl acetate in hexanes) to provide **4-41** (31 mg, 0.050 mmol, 58 %).

Characterization: $\mathbf{R_f}$ = (hexanes/EtOAc 2:1): 0.38; **IR** (neat) v = 3017, 2930, 1731, 1596, 1477, 1369, 1228, 1148, 1112, 1037, 934, 752, 667 cm^{-1}; **^{1}H NMR** (500 MHz, $CDCl_3$) δ 7.21 (m, 3H), 7.01 (m, 2H), 6.73 (s, 1H), 6.57 (s, 1H), 6.42 (s, 1H), 5.96 (s, 1H), 5.87 (s, 1H), 5.77 (d, *J*= 2.1 Hz, 1H), 5.24 (s, 1H), 4.96 (d, *J*= 7.6 Hz, 1H) 4.92 (d, *J*= 13.4 Hz, 1H), 4.82 (s, 1H), 4.76 (d, *J*= 7.6 Hz, 1H), 4.56 (d, *J*= 13.4 Hz, 1H), 3.92 (s, 3H), 3.84 (s, 3H), 3.11 (s, 3H), 2.81 (q, *J*= 8.7 Hz, 1H), 1.74 (s, 3H), 1.56 (s, 3H), 1.24 (d, *J*= 8.7 Hz, 3H); **^{13}C NMR** (126 MHz, $CDCl_3$) δ 170.0, 169.6, 152.6, 150.7, 148.2, 146.2, 141.5, 138.6, 137.9, 136.9, 133.6, 133.1, 127.9, 127.5, 127.3, 122.4, 122.1, 114.7, 107.6, 103.0, 101.2, 96.8, 80.1, 79.2, 74.2, 60.8, 56.5, 56.1, 41.1, 20.59, 20.54, 17.9; **$[\alpha]^{23}_D$** 31.6 °, (c = 1.0, $CHCl_3$); **HRMS**: Calcd. for $C_{34}H_{36}O_{11}$ $[M+Na]^+$ = 643.2155 m/z, found = 643.21436 m/z.

Compound 4-47



4-34
Chemical Formula: $C_{34}H_{38}O_{12}$
Molecular Weight: 638.6660

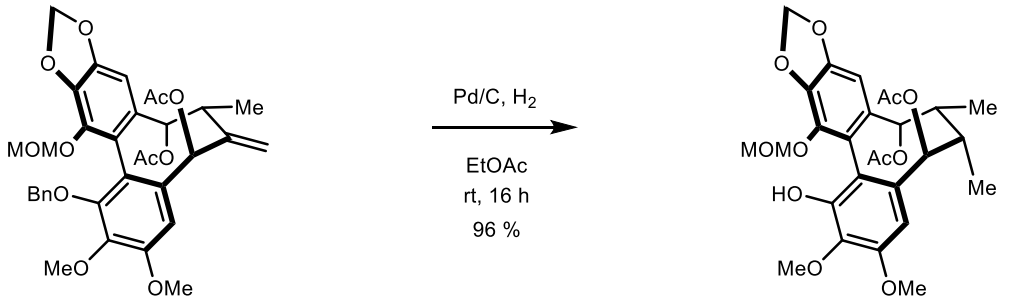
4-47
Chemical Formula: $C_{41}H_{42}O_{13}$
Molecular Weight: 742.7740

Procedure: A flame-dried microwave vial equipped with Teflon-coated stir bar was charged with **4-34** (0.047 mmol, 30 mg, 1.0 equiv.), followed by hot (stored in 120 °C oven) $NaHSO_4$-SiO_2 (50 mg). The flask was evacuated and refilled with N_2 (repeated 3 times), prior to the addition of CH_2Cl_2 (1 mL). The reaction mixture was stirred vigorously at room temperature for 23 h, followed by filtration through celite and concentration *in vacuo*. To the crude, cesium carbonate (0.095 mmol, 31 mg, 2 equiv.) was added. The flask was evacuated and refilled with N_2 (repeated 3 times), then DMSO (1 mL) was added, followed by benzyl bromoacetate (0.071 mmol, 11.2 µL, 1.5 equiv.). The reaction mixture was stirred at room temperature for 2 h. It was then diluted with H_2O (10 mL) and extracted with ethyl acetate (3 x 10 mL). The combined organic layers were washed sequentially with H_2O (20 mL) and brine (10 mL). The combined aqueous layers were washed with additional ethyl acetate (3 x 13 mL). The combined organic layers were dried and concentrated *in vacuo.* The crude product was purified on silica gel (30 % to 40 % ethyl acetate in hexanes) to provide **4-47** (22 mg, 0.030 mmol, 63 %).

Characterization: $\mathbf{R_f}$ = (hexanes/EtOAc 3:2): 0.30; **IR** (neat) v = 3567, 2923, 2852, 1735, 1624, 1597, 1499, 1456, 1370, 1333, 1222, 1106, 1048, 751, 698 cm^{-1}; **^{1}H NMR** (500 MHz, $CDCl_3$) δ 7.34-7.28 (m, 3H), 7.25-7.19 (m, 5H), 6.96 (m, 2H), 6.81 (s, 1H), 6.52 (s, 1H), 5.72 (m, 2H), 5.68 (m, 2H), 5.11 (d, J= 12.4 Hz, 1H), 5.03 (d, J= 12.4 Hz, 1H), 4.95 (d, J= 10.0 Hz, 1H), 4.29 (d, J= 16.6 Hz, 1H), 4.25 (d, J= 16.6 Hz, 1H), 4.19 (d, J= 10.0 Hz, 1H), 3.91 (s, 3H), 3.82 (s, 3H), 2.21 (broad s, 1H), 2.10 (q, J= 6.9 Hz, 1H), 1.63 (s, 3H), 1.58 (s, 3H), 1.32 (s, 3H), 1.26 (d, 3H, overlaps with t from EtOAc); **^{13}C NMR** (126 MHz, $CDCl_3$) δ 169.6, 169.2, 168.9, 152.0, 150.3, 148.4, 141.6, 139.7, 137.6, 135.5, 135.1, 132.8, 130.9, 128.4, 128.3, 128.2, 128.07, 128.03, 127.7, 121.8,

120.5, 110.7, 102.8, 101.1, 83.9, 83.7, 74.4, 73.6, 68.8, 66.2, 60.7, 56.0, 42.5, 28.5, 20.5, 20.1, 17.0; **[α]^{23}D** 15.1 °, (c = 0.7, $CHCl_3$); **HRMS**: Calcd. for $C_{41}H_{42}O_{13}$ $[M+Na]^+$ = 765.2523 m/z, found = 765.25055 m/z.

Compound 4-49



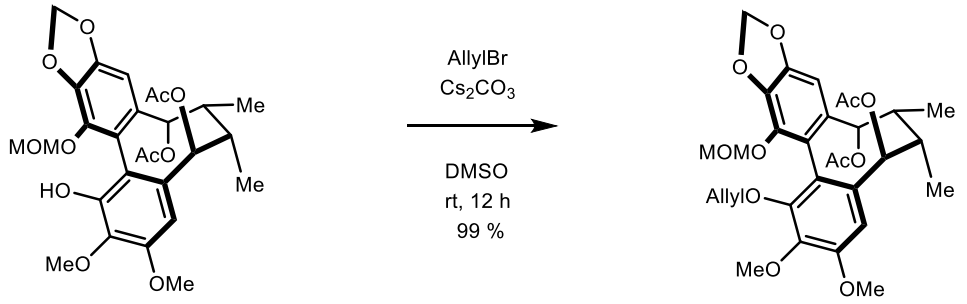
4-41
Chemical Formula: $C_{34}H_{36}O_{11}$
Molecular Weight: 620.6510

4-49
Chemical Formula: $C_{27}H_{32}O_{11}$
Molecular Weight: 532.5420

Procedure: A flame-dried 4-dram vial equipped with a Teflon-coated stir bar and a septum cap was charged with **4-41** (0.22 mmol, 137 mg, 1.0 equiv.) and palladium on carbon (10 wt %, 0.022 mmol, 23 mg, 0.1 equiv.). The vial was evacuated and refilled with N_2 (repeated 3 times), prior to the addition of ethyl acetate (6.7 mL). The reaction mixture was sparged with H_2 for 10 minutes and then stirred at rt for 16 h under H_2. It was then filtered through celite and the filtrate was concentrated *in vacuo*. The crude product was purified via silica gel (35 % to 45 % ethyl acetate in hexanes) to provide **4-49** (112 mg, 0.21 mmol, 96 %) as a single diastereomer.

Characterization: $\mathbf{R_f}$ = (hexanes/EtOAc 3:2): 0.22; **IR** (neat) v = 3431, 3014, 2967, 2935, 2883, 2845, 1729, 1612, 1515, 1456, 1426, 1367, 1335, 1230, 1108, 929, 666 cm^{-1}; **^{1}H NMR** (500 MHz, $CDCl_3$) δ 6.54 (s, 1H), 6.51 (broad s, 1H), 6.01 (d, J= 1.4 Hz, 1H), 5.97 (d, J= 1.4 Hz, 1H), 5.75 (d, J= 8.3 Hz, 1H), 5.66 (d, J= 4.3 Hz, 1H), 5.64 (broad s, 1H), 5.00 (d, J= 5.9 Hz, 1H), 4.94 (d, J= 5.8 Hz, 1H), 3.91 (s, 3H), 3.89 (s, 3H), 3.23 (broad s, 3H), 2.18 (m, 1H), 2.09 (m, 1H), 1.77 (s, 3H), 1.55 (s, 3H), 1.00 (d, J= 7.3 Hz, 3H), 0.90 (d, J= 7.1 Hz, 3H); **^{13}C NMR** (126 MHz, $CDCl_3$) δ 170.2, 170.0, 150.6, 148.7, 147.3, 138.3, 137.8, 134.8, 134.1, 131.6, 121.0, 116.6, 107.3, 103.8, 101.5, 97.2, 80.6, 80.2, 60.8, 56.6, 55.9, 41.0, 38.3, 20.8, 20.3, 14.2, 14.1; **[α]^{23}D** 67.2 °, (c = 1.0, $CHCl_3$); **HRMS**: Calcd. for $C_{27}H_{32}O_{11}$ $[M+Na]^+$ = 555.1842 m/z, found = 555.1850 m/z.

Compound 4-50



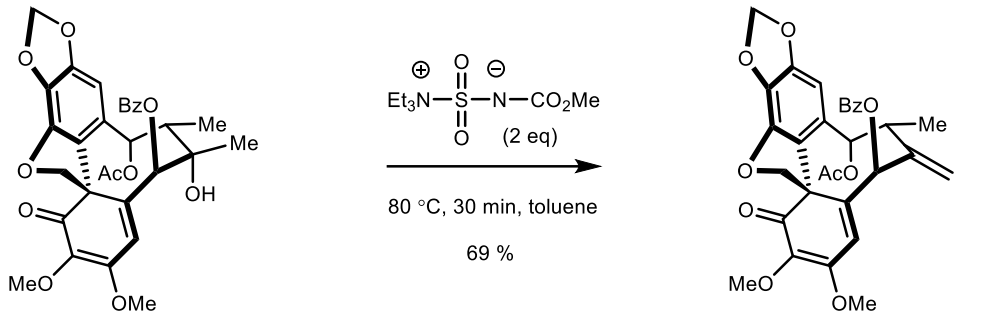
4-49
Chemical Formula: $C_{27}H_{32}O_{11}$
Molecular Weight: 532.5420

4-50
Chemical Formula: $C_{30}H_{36}O_{11}$
Molecular Weight: 572.6070

Procedure: A flame-dried 4-dram vial equipped with a Teflon-coated stir bar and a septum cap was charged with **4-49** (0.44 mmol, 234 mg, 1.0 equiv.) and Cs_2CO_3 (0.88 mmol, 286 mg, 2.0 equiv.). The vial was evacuated and refilled with N_2 (repeated 3 times), prior to the addition of DMSO (2 mL). Allyl bromide (0.66 mmol, 57 µL, 1.5 equiv.) was added via microsyringe. The reaction mixture was stirred for 12 h at room temperature. The reaction mixture was quenched by the addition of $NaHCO_3$ (sat. aq., 30 mL) and H_2O (30 mL), followed by extraction with ethyl acetate (3 x 30 mL). The combined organic layers were washed sequentially with H_2O (60 mL) and brine (30 mL). The aqueous layer was then washed with additional ethyl acetate (3 x 30 mL) until all the product went into the organic layer. The combined organic layers were dried with Na_2SO_4, filtered, and concentrated *in vacuo*. The crude product was purified via silica gel (15 % to 30 % ethyl acetate in hexanes) to provide **4-50** (249 mg, 0.44 mmol, 99 %) as a white solid.

Characterization: $\mathbf{R_f}$ = (hexanes/EtOAc 4:1): 0.27; **IR** (neat) v = 3016, 2966, 2934, 2882, 2845, 1729, 1595, 1500, 1477, 1369, 1232, 1153, 1108, 1034, 933, 752, 667 cm^{-1}; **^{1}H NMR** (500 MHz, $CDCl_3$) δ 6.68 (br s, 1H), 6.48 (s, 1H), 5.99 (d, J= 1.3 Hz, 1H), 5.96 (d, J= 1.3 Hz, 1H), 5.80-5.70 (m, 3H), 5.05-4.97 (m, 3H), 4.92 (m, 1H), 4.37 (ddt, J= 1.4, 5.3, 12.1 Hz, 1H), 4.14 (m, 1H), 3.88 (s, 3H), 3.85 (s, 3H), 3.23 (br s, 3H), 2.15 (m, 1H), 2.07 (m, 1H), 1.78 (br s, 3H), 1.56 (s, 3H), 0.97 (d, J= 6.5 Hz, 3H), 0.89 (d, J= 7.0 Hz, 3H); **^{13}C NMR** (126 MHz, $CDCl_3$) δ 170.1, 169.9, 151.9, 151.1, 148.2, 141.5, 138.6, 137.5, 134.5, 132.9, 131.3, 123.4, 122.7, 116.1, 110.5, 103.3, 101.3, 97.1, 80.4, 79.7, 73.5, 60.6, 56.5, 56.0, 39.5, 38.0, 20.8, 20.6, 15.7, 14.1; **$[\alpha]^{23}_D$** 101.8 °, (c = 1.0, $CHCl_3$); **HRMS**: Calcd. for $C_{30}H_{36}O_{11}$ $[M+Na]^+$ = 595.2155 m/z, found = 595.2124 m/z.

Compound 4-53



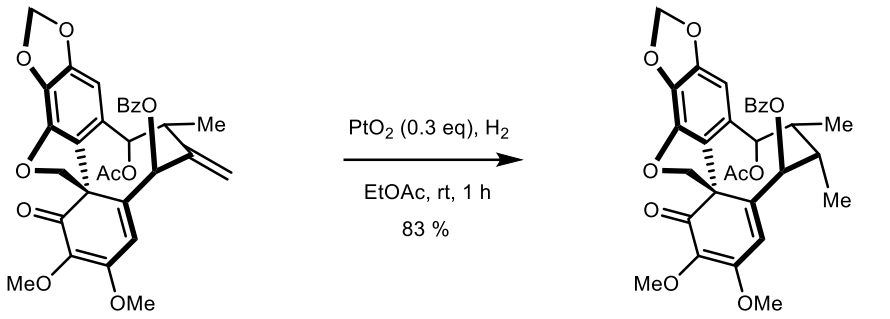
4-52
Chemical Formula: $C_{31}H_{30}O_{11}$
Molecular Weight: 578.5700

4-53
Chemical Formula: $C_{31}H_{28}O_{10}$
Molecular Weight: 560.5550

Procedure: A flame-dried 50 mL round bottom flask equipped with a Teflon-coated stir bar and a rubber septum was charged with heteroclitin J (**4-52**, 0.34 mmol, 197 mg, 1.0 equiv.) and Burgess reagent (0.68 mmol, 162 mg, 2.0 equiv.). The flask was evacuated and refilled with N_2 (repeated 3 times), prior to the addition of toluene (17 mL). The reaction mixture stirred at 80 °C for 30 minutes and then allowed to cool to room temperature. The reaction mixture was concentrated *in vacuo* and then the residue was taken up in ethyl acetate and water. The layers were separated and the organic layer was washed with brine. The organic layer was dried over Na_2SO_4, filtered, and concentrated *in vacuo*. The crude product was purified via silica gel (35 % to 45 % ethyl acetate in hexanes) to provide **4-53** (132 mg, 0.24 mmol, 69 %) as a yellow waxy solid.

Characterization: $\mathbf{R_f}$ = (hexanes/EtOAc 1:1): 0.50; **IR** (neat) v = 3013, 2933, 1718, 1649, 1585, 1374, 1222, 1092, 1060, 1024, 932, 748, 710 cm^{-1}; **^{1}H NMR** (500 MHz, $CDCl_3$) δ 7.88 (d, J= 7.6 Hz, 2H), 7.57 (t, J= 7.2 Hz, 1H), 7.43 (t, J= 7.6 Hz, 2H), 6.63 (s, 1H), 6.46 (s, 1H), 6.33 (s, 1H), 6.02 (s, 1H), 5.95 (m, 2H), 4.94 (s, 1H), 4.69 (d, J= 8.6 Hz, 2H), 4.61 (m, 2H), 4.06 (s, 3H), 3.75 (s, 3H), 2.94 (m, 1H), 1.82 (s, 3H), 1.21 (d, J= 7.3 Hz, 3H); **^{13}C NMR** (126 MHz, $CDCl_3$) δ 195.2, 169.7, 164.6, 155.5, 150.1, 145.2, 144.3, 141.9, 133.6, 133.1, 130.1, 129.6, 129.2, 129.0, 128.7, 126.6, 121.2, 114.6, 102.0, 100.7, 78.4, 77.3, 76.5, 64.1, 59.2, 59.0, 46.1, 20.4, 15.1; **$[\alpha]^{23}_D$** 210.8 °, (c = 1.0, $CHCl_3$); **HRMS**: Calcd. for $C_{31}H_{28}O_{10}$ $[M+Na]^+$ = 583.1580 m/z, found = 583.1565 m/z.

Compound 4-54



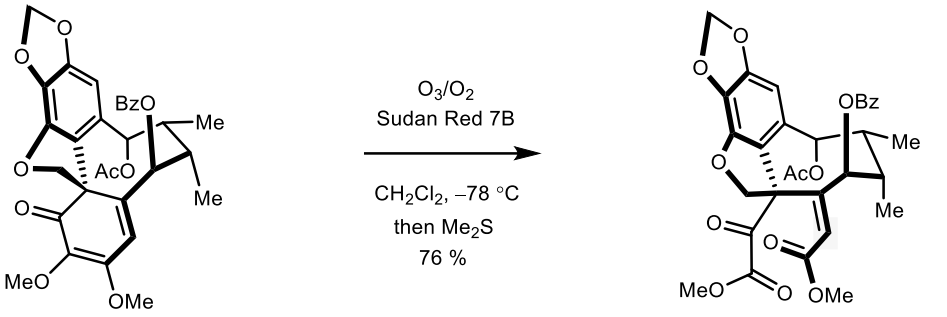
4-53
Chemical Formula: $C_{31}H_{28}O_{10}$
Molecular Weight: 560.5550

4-54
Chemical Formula: $C_{31}H_{30}O_{10}$
Molecular Weight: 562.5710

Procedure: A flame-dried 25 mL round bottom flask equipped with a Teflon-coated stir bar and a septum cap was charged with **4-53** (0.24 mmol, 132 mg, 1.0 equiv.) and PtO_2 (0.07 mmol, 16 mg, 0.3 equiv.). The flask was evacuated and refilled with N_2 (repeated 3 times), prior to the addition of ethyl acetate (7.9 mL). The reaction mixture was sparged with H_2 for 5 minutes and then stirred for 1 h at rt under H_2. The mixture was filtered through celite and the filtrate was concentrated *in vacuo*. The crude product was purified via silica gel (25 % to 35 % ethyl acetate in hexanes) to provide **4-54** (110 mg, 0.20 mmol, 83 %) as a yellow fluffy solid.

Characterization: $\mathbf{R_f}$ = (hexanes/EtOAc 2:1): 0.31; **IR** (neat) ν = 2966, 2926, 1739, 1716, 1650, 1588, 1451, 1374, 1227, 1105, 1065, 1023, 934, 752, 714 cm^{-1}; **^{1}H NMR** (500 MHz, $CDCl_3$) δ 7.95 (d, J= 7.6 Hz, 2H), 7.57 (t, J= 7.3 Hz, 1H), 7.44 (t, J= 7.7 Hz, 2H), 6.62 (s, 1H), 6.36 (s, 1H), 6.08 (s, 1H), 6.00 (m, 2H), 5.67 (d, J= 11.0 Hz, 1H), 4.71 (d, J= 8.6 Hz, 1H), 4.56 (d, J= 8.6 Hz, 1H), 4.05 (s, 3H), 3.74 (s, 3H), 2.14 (m, 1H), 2.08 (m, 1H), 1.80 (s, 3H), 0.99 (d, J= 7.3 Hz, 3H), 0.91 (d, J= 6.6 Hz, 3H); **^{13}C NMR** (126 MHz, $CDCl_3$) δ 195.3, 169.9, 165.2, 155.5, 150.4, 144.4, 141.1, 133.4, 133.0, 130.4, 129.6, 129.4, 128.7, 127.7, 127.6, 121.9, 102.1, 101.2, 82.0, 78.5, 76.3, 63.8, 59.2, 58.9, 41.9, 36.2, 20.3, 18.6, 9.0; **$[\alpha]^{23}_D$** 204.4 °, (c = 1.0, $CHCl_3$); **HRMS**: Calcd. for $C_{31}H_{30}O_{10}$ $[M+Na]^+$ = 585.1737 m/z, found = 585.1733 m/z.

Compound 4-55



4-54
Chemical Formula: $C_{31}H_{30}O_{10}$
Molecular Weight: 562.5710

4-55
Chemical Formula: $C_{31}H_{30}O_{12}$
Molecular Weight: 594.5690

Procedure: A flame-dried 100 mL round bottom flask equipped with a Teflon-coated stir bar was charged with **4-54** (0.11 mmol, 60 mg, 1.0 equiv.). CH_2Cl_2 (21 mL) was added and the reaction mixture was stirred until **4-54** had dissolved. A solution of Sudan red 7B (20 µL, 1 mg/mL in CH_2Cl_2) was added as a color indicator and the reaction mixture turned red. The reaction mixture was cooled to −78 °C and sparged with N_2 for 5 minutes. The N_2 stream was then replaced with a stream of O_3/O_2 until the reaction mixture turned from red to clear and colorless (approximately 5 seconds). The O_3/O_2 stream was then promptly replaced by the N_2 stream. The reaction mixture was bubbled with N_2 for 5 minutes prior to capping with a rubber septum equipped with an N_2 balloon. Me_2S (2 mL) was added via syringe and the reaction mixture was allowed to warm to room temperature. The reaction mixture was stirred for 1 h under N_2 at room temperature and then concentrated *in vacuo*. The crude product was purified on silica gel (20 % to 30 % ethyl acetate in hexanes) to provide **4-55** (48 mg, 0.081 mmol, 76 %) as a white solid.

Characterization: $\mathbf{R_f}$ = (hexanes/EtOAc 3:1): 0.34; **IR** (neat) v = 3329, 2972, 2923, 1710, 1435, 1388, 1269, 1215, 1047, 933, 880, 711 cm^{-1}; **^{1}H NMR** (500 MHz, $CDCl_3$) δ 7.53 (m, 1H), 7.48 (m, 2H), 7.34 (t, J=7.7 Hz, 2H), 6.41 (s, 1H), 6.37 (s, 1H), 5.98 (d, J= 10.2 Hz, 1H), 5.92 (s, 1H), 5.89 (s, 1H), 5.74 (m, 2H), 4.70 (d, J= 10.4 Hz), 3.74 (s, 3H), 3.58 (s, 3H), 2.40 (m, 2H), 2.07 (s, 3H), 1.17 (m, 6H); **^{13}C NMR** (126 MHz, $CDCl_3$) δ 185.0, 170.8, 165.8, 165.1, 161.8, 150.6, 149.7, 145.3, 133.1, 132.5, 130.5, 129.5, 129.1, 128.0, 127.8, 117.6, 102.1, 85.1, 83.9, 80.5, 62.4, 52.5, 51.8, 40.1, 38.2, 20.8, 20.4, 12.7; **$[\alpha]^{23}_D$** 149.8 °, (c = 1.0, $CHCl_3$); **HRMS**: Calcd. for $C_{31}H_{30}O_{12}$ $[M+Na]^+$ = 617.1635 m/z, found = 617.1620 m/z.

4.8. References

(1) Kuo, Y. H.; Huang, H. C.; Kuo, L. M. Y.; Chen, C. F. Novel C19 Homolignans, Taiwanschirin A, B, and Cytotoxic Taiwanschirin C, and a New C18 Lignan, Schizanrin A, from Schizandra Arisanensis. *J. Org. Chem.* **1999**, *64* (19), 7023–7027.

(2) Haughey, M. B.; Christensen, K. E.; Poole, D. L.; Donohoe, T. J. Development of an Enolate Alkynylation Approach towards the Synthesis of the Taiwanschirin Natural Products. *Chem. Sci.* **2021**, *12*, 13392–13397.

(3) Mervič, M.; Ghera, E. Total Synthesis of (±)-Kadsurin. *J. Am. Chem. Soc.* **1977**, *99* (23), 7673–7678.

(4) Azpilcueta-Nicolas, C. R.; Meng, D.; Edelmann, S.; Lumb, J. Dearomatization of Biaryls through Polarity Mismatched Radical Spirocyclization. **2023**, *62*, e202214422.

(5) Huang, Z.; Lumb, J. P. Mimicking Oxidative Radical Cyclizations of Lignan Biosynthesis Using Redox-Neutral Photocatalysis. *Nat. Chem.* **2021**, *13* (1), 24–32.

(6) Belokon, Y. N.; North, M.; Parsons, T. Vanadium-Catalyzed Asymmetric Cyanohydrin Synthesis. *Org. Lett.* **2000**, *2* (11), 1617–1619.

(7) Rackl, D.; Kais, V.; Kreitmeier, P.; Reiser, O. Visible Light Photoredox-Catalyzed Deoxygenation of Alcohols. *Beilstein J. Org. Chem.* **2014**, *10*, 2157–2165.

(8) Chenneberg, L.; Baralle, A.; Daniel, M.; Fensterbank, L.; Goddard, J.; Ollivier, C. Visible Light Photocatalytic Reduction of O-Thiocarbamates : Development of a Tin-Free Barton – McCombie Deoxygenation Reaction. *Adv. Synth. Catal.* **2014**, *356*, 2756–2762.

(9) Hee, S. P.; Hee, Y. L.; Yong, H. K. Facile Barton-McCombie Deoxygenation of Alcohols with Tetrabutylammonium Peroxydisulfate and Formate Ion. *Org. Lett.* **2005**, *7* (15), 3187–3190.

(10) Morita, S.; Yoshimura, T.; Matsuo, J. I. Catalytic Intermolecular Aldol Reactions of Transient Amide Enolates in Domino Michael/Aldol Reactions of Nitroalkanes, Acrylamides, and Aldehydes. *Green Chem.* **2021**, *23* (3), 1160–1164.

(11) Muñoz-Molina, J. M.; Bafaluy, D.; Funes-Ardoiz, I.; de Aguirre, A.; Maseras, F.;

Belderrain, T. R.; Perez, P. J.; Muñiz, K. Mechanistic Studies on the Synthesis of Pyrrolidines and Piperidines via Copper-Catalyzed Intramolecular C.H Amination. *Organometallics* **2022**, *41* (9), 1099–1105.

(12) Williams, A. O. P.; Chmiel, A. F.; Mikhael, M.; Bates, F.; Yeung, C. S.; Wickens, Z. K. Practical and General Alcohol Deoxygenation Protocol. *Angew. Chemie - Int. Ed.* **2023**,

(13) Lam, K.; Marko, I. Using Toluates as Simple and Versatile Radical Precursors. *Org. Lett.* **2008**, *10* (13), 2773–2776.

(14) Nguyen, J. D.; Reiß, B.; Dai, C.; Stephenson, C. R. J. Batch to Flow Deoxygenation Using Visible Light Photoredox Catalysis. *Chem. Commun.* **2013**, *49*, 4352–4354.

(15) Dang, H.; Cox, N.; Lalic, G. Copper-Catalyzed Reduction of Alkyl Triflates and Iodides : An Efficient Method for the Deoxygenation of Primary and Secondary Alcohols. *Angew. Chemie - Int. Ed.* **2014**, *53*, 752–756.

(16) Cook, A.; Maclean, H.; Onge, P. S.; Newman, S. G. Nickel-Catalyzed Reductive Deoxygenation of Diverse C–O Bond-Bearing Functional Groups. *ACS Catal.* **2021**, *11*, 13337–13347.

(17) Yasuda, M.; Onishi, Y.; Ueba, M.; Miyai, T.; Baba, A. Direct Reduction of Alcohols : Highly Chemoselective Reducing System for Secondary or Tertiary Alcohols Using Chlorodiphenylsilane with a Catalytic Amount of Indium Trichloride. *J. Org. Chem.* **2001**, *66*, 7741–7744.

(18) Miyaoka, H.; Kajiwara, Y.; Hara, Y.; Yamada, Y. Total Synthesis of Natural Dysidiolide. *J. Org. Chem.* **2001**, *66* (4), 1429–1435.

(19) Furrow, M. E.; Myers, A. G. Practical Procedures for the Preparation of N-Tert-Butyldimethylsilylhydrazones and Their Use in Modified Wolff-Kishner Reductions and in the Synthesis of Vinyl Halides and Gem-Dihalides. *J. Am. Chem. Soc.* **2004**, *126* (17), 5436–5445.

(20) LeNaruse, M.; Aoyagi, S.; Kibayashi, C. Stereoselective Total Synthesis of (-)-Pumiliotoxin C by an Aqueous Intramolecular Acylnitroso Diels-Alder Approach. *J. Chem Soc. Perkin Trans. 1* **1996**, 1113–1124.

(21) Hanessian, S.; Maianti, J. P.; Matias, R. D.; Feeney, L. A.; Armstrong, E. S. Hybrid Aminoglycoside Antibiotics via Tsuji Palladium-Catalyzed Allylic Deoxygenation. *Org. Lett.* **2011**, *13* (24), 6476–6479.

(22) Keinan, E.; Greenspoon, N. Highly Chemoselective Allylic Reductions with Silicon Hydrides and Palladium Catalyst. *Isr. J. Chem.* **1984**, *24*, 82–87.

(23) Posner, G. H.; Lee, S. H. T.; Kim, J.; Peleg, S.; Dolan, P.; Kensler, T. W. Novel A-Ring Analogs of the Hormone 1a,25-Dihydroxyvitamin D 3: Synthesis and Preliminary Biological Evaluation. *Bioorg. Med. Chem.* **2005**, *13*, 2959–2966.

(24) Hayashi, Y.; Komiya, S.; Yamamoto, T.; Yamamoto, A. Regioselective C-O Bond Cleavage of Allylic Phenyl Carbonates Promoted by Group 8 Transition Metal Hydrido Complexes. *Chem. Lett.* **1984**, 977–980.

(25) Tsubuki, M.; Kanai, K.; Nagase, H.; Honda, T. Stereocontrolled Syntheses of Novel Styryl Lactones, (+)-Goniodiol, (+)-Goniotriol, (+)-8-Acetylgoniotriol, (+)-Goniopypyrone, and (+)-Altholactone from Common Intermediates and Cytotoxicity of Their Congeners. *Tetrahedron* **1999**, *55*, 2493–2514.

(26) Roth, B.; Roark, W. H. Synthesis of a Chiral Synthon for the Lactone Portion of Compactin and Mevinolin. *Tetrahedron Lett.* **1988**, *29* (11), 1255–1258.

(27) Khachik, F.; Chang, A.-N.; Gana, A.; Mazzola, E. Partial Synthesis of (3 R,6 ′R)- a-Cryptoxanthin and (3 R)-b-Cryptoxanthin from (3R,3'R,6'R)-Lutein. *J. Nat. Prod.* **2007**, *70*, 220–226.

(28) Alfonzo, E.; Millimaci, A. M.; Beeler, A. B. Photoredox Generated Carbonyl Ylides Enable a Modular Approach to Aryltetralin, Dihydronaphthalene, and Arylnaphthalene Lignans. *Org. Lett.* **2020**, *22*, 6489–6493.

(29) Gong, W.; Singidi, R. R.; Gallucci, J. C.; Rajanbabu, T. V. On the Stereochemistry of Acetylide Additions to Highly Functionalized Biphenylcarbaldehydes and Multi-Component Cyclization of 1,n-Diynes. Syntheses of Dibenzocyclooctadiene Lignans. *Chem. Sci.* **2012**, *3*, 1221–1230.

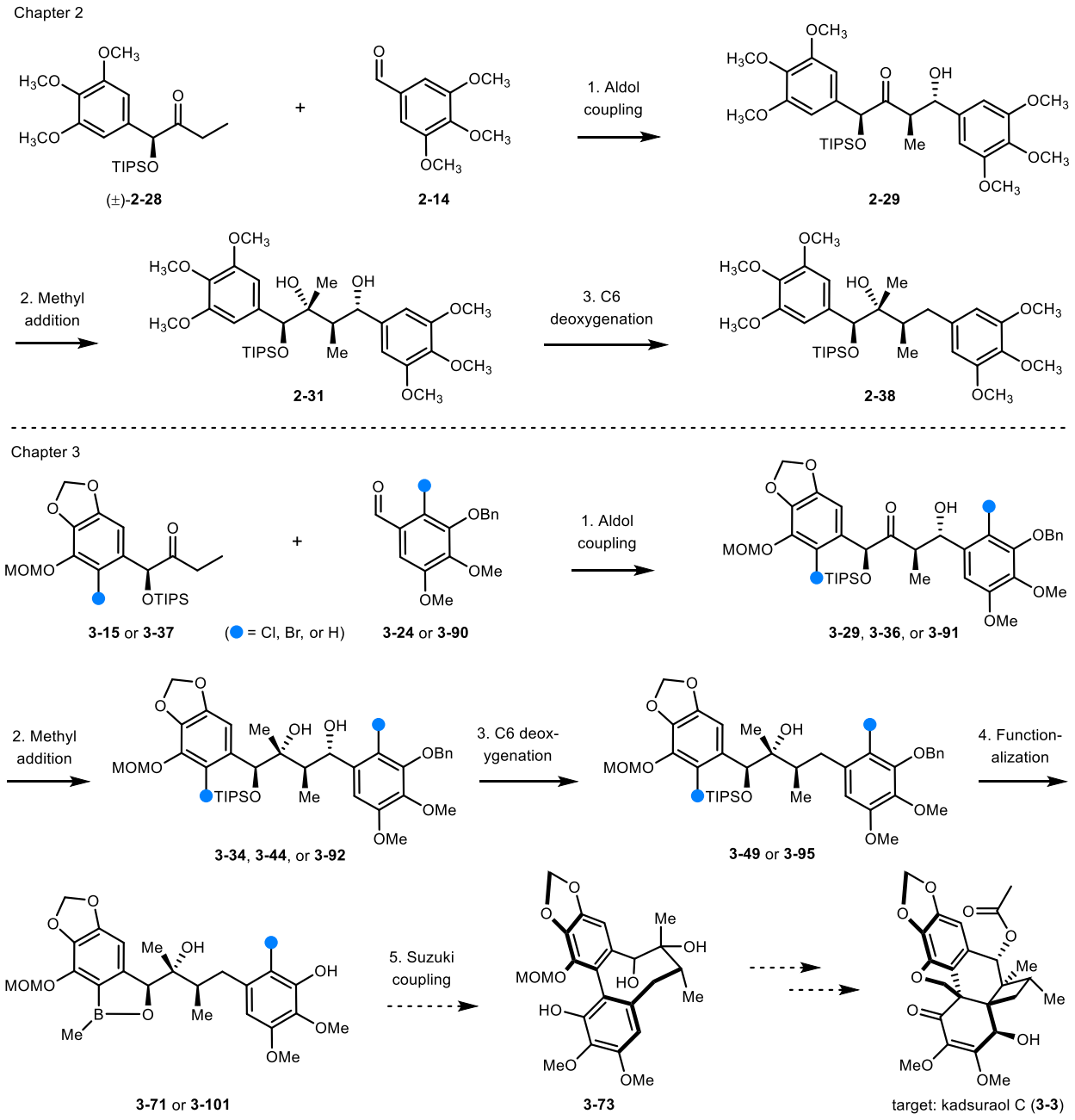
Chapter 5. Summary and future directions

5.1. Summary of thesis

Dibenzocyclooctadiene lignan natural products (DBCODs) are the major bioactive constituents of plants of the *Schisandraceae* family, which have a long history of use in traditional Chinese medicine. Most of these compounds have been isolated in tiny quantities and only 44 out of 529 have been synthesized by chemical methods. In my doctoral studies, the challenging synthesis of highly oxidized DBCODs was tackled, with the goal of devising a general synthetic route to DBCODs as well as deoxygenation strategies allowing for diversification.

In Chapter 2, a simplified system modelling three of the key steps in our planned DBCOD syntheses was developed (Scheme 5.1). Alkylation and aldol couplings were investigated as the first convergent step in the synthesis, for the coupling of a tri-methoxy aryl ketone (±)-**2-28** and tri-methoxy aryl aldehyde **2-14** or the analogous benzyl halide. Aldol coupling proved to be the superior method, affording the desired 1,2-*syn*-1,3-*syn* aldol **2-29** bearing a stereotriad. The second key step accomplished was chelate-controlled methyl addition to set the C8 stereocenter, providing a 1,3-*syn* diol product **2-31**. Third, the C6 oxygen, which was required to direct the stereochemical outcome of the methyl addition, but which was not present in desired product, was removed via photoredox-catalyzed benzylic deoxygenation, providing **2-38**.

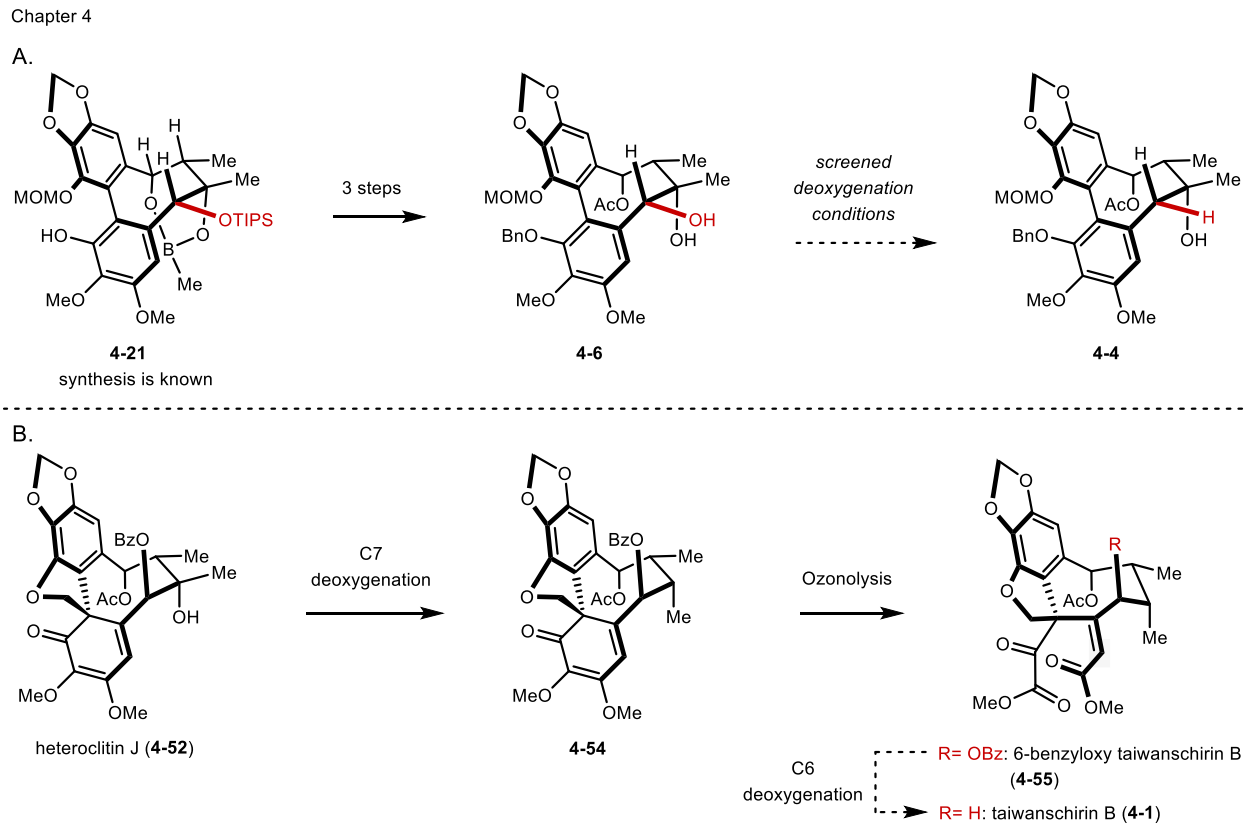
In Chapter 3, stage 3 DBCOD kadsuraol C (**3-3**) was the synthetic target. Functionalized ketone and aldehyde fragments were prepared and then subjected to the key steps of aldol coupling, methyl addition, and benzylic deoxygenation (Scheme 5.1). The effect of conditions and substrate modification on the aldol and methyl additions was investigated and these steps were optimized extensively. The benzylic deoxygenation step was also optimized and brought into a flow setup for scale up. The subsequent functionalization of the substrate was conducted to append aryl borinic ester and aryl halide handles in preparation for the atroposelective Suzuki coupling to form the biaryl axis. The substrate limitations of the Suzuki coupling were explored and the presence of a bulky C6 substituent (such as OTIPS) was found to be crucial to the success of the reaction. This then led to the necessity for the development of a post-cyclization C6 deoxygenation strategy.



Scheme 5.1. Exploration of the key steps in DBCOD synthesis on a model system (Chapter 2) and in efforts towards kadsuraol C (Chapter 3)

In Chapter 4, taiwanschirin B (**4-1**), a stage 3 DBCOD also lacking oxygenation at C6, was targeted. The development of a strategy for the deoxygenation of the C6 alcohol on a cyclic substrate was required for both the syntheses of **4-1** and **3-3**. Another goal of this project was to eventually gain control of oxygenation at all positions around the 8-membered ring, allowing for

access to a great variety of DBCODs. This synthesis was commenced from a known intermediate possessing the DBCOD skeleton (**4-21**) which allowed for ease of access to a substrate (**4-6**) on which C6 deoxygenation conditions could be screened on a cyclic system (Scheme 5.2A). The C6 alcohol proved to act differently from traditional benzylic alcohols due to the lack of conjugation with the neighbouring twisted biaryl, causing it to be recalcitrant to deoxygenation. Therefore, the C6 deoxygenation was pushed to later in the synthesis at a point where it would be α to a π-system with more favorable orbital overlap. In the meantime, the deoxygenation of C7 was accomplished via a Burgess dehydration/ hydrogenation sequence. Heteroclitin J (**4-52**) was successfully converted to **4-55**, which is one C6 deoxygenation away from the target **4-1** (Scheme 5.2B).

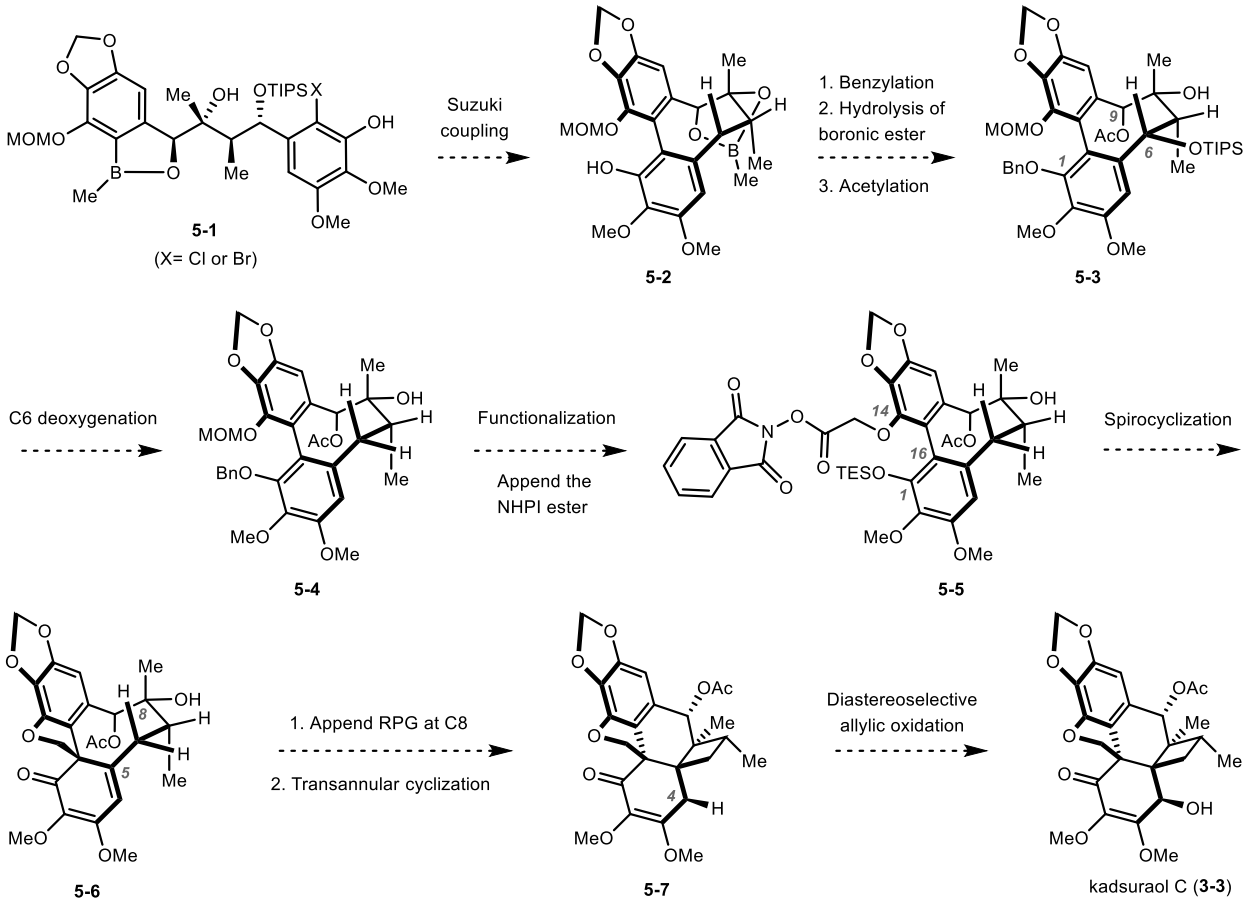


Scheme 5.2. A) C6 deoxygenation screening and B) synthesis of 6-benzyloxy taiwanschirin B (Chapter 4)

5.2. Future directions

5.2.1. Synthesis of kadsuraol C

The presence of a bulky C6 group such as OTIPS was found necessary for the Suzuki coupling forming the biaryl axis to occur. Therefore, a new substrate will be prepared to use as the starting material for the Suzuki coupling: **5-1**. It is expected that **5-1** can be prepared using the same route as substrates **3-71** or **3-101**, but the benzylic deoxygenation step will be skipped and the C6 alcohol will be protected as the triisopropyl silyl ether. Subjecting **5-1** to Suzuki coupling conditions is expected to provide the biaryl **5-2** (Scheme 5.3). Subjecting **5-2** to protection of the C1 phenol with a benzyl group, hydrolysis of the boronic ester, and acetylation at C9 would provide **5-3**. To synthesize kadsuraols A or B, an angeloylation or benzoylation could be performed instead of the acetylation which leads to kadsuraol C. The C6 deoxygenation would then be performed on the cyclic substrate **5-3**. It will likely be necessary to deprotect the silyl group, epimerize the stereocenter and reprotect the C6 alcohol as an activated ester prior to deoxygenation. After the deoxygenation is accomplished, **5-4** will be functionalized in preparation for spirocyclization, including protection of the C1 phenol with TES and appending an NHPI ester off C14.

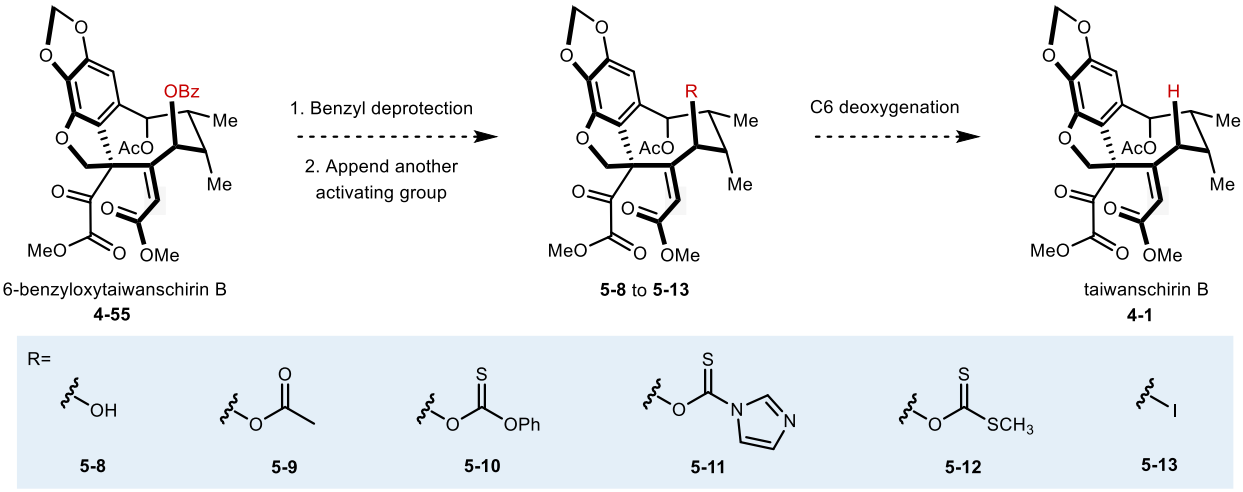


Scheme 5.3. Synthetic plan for the preparation of kadsuraol C

Regioselective *ortho*-spirocyclization methodology previously developed in the group[1,2] would then be applied to **5-5** to afford **5-6**. A radical progenitor (RPG), such as cesium oxalate,[3] would be appended to the C8 alcohol of **5-6** to generate a tertiary radical under photoredox-catalyzed conditions, which could then undergo transannular cyclization onto C5 to form the 6-4 ring system of **5-7**. The conversion of **5-7** to kadsuraol C (**3-3**) would then necessitate a diastereoselective allylic oxidation to install the alcohol at C4.

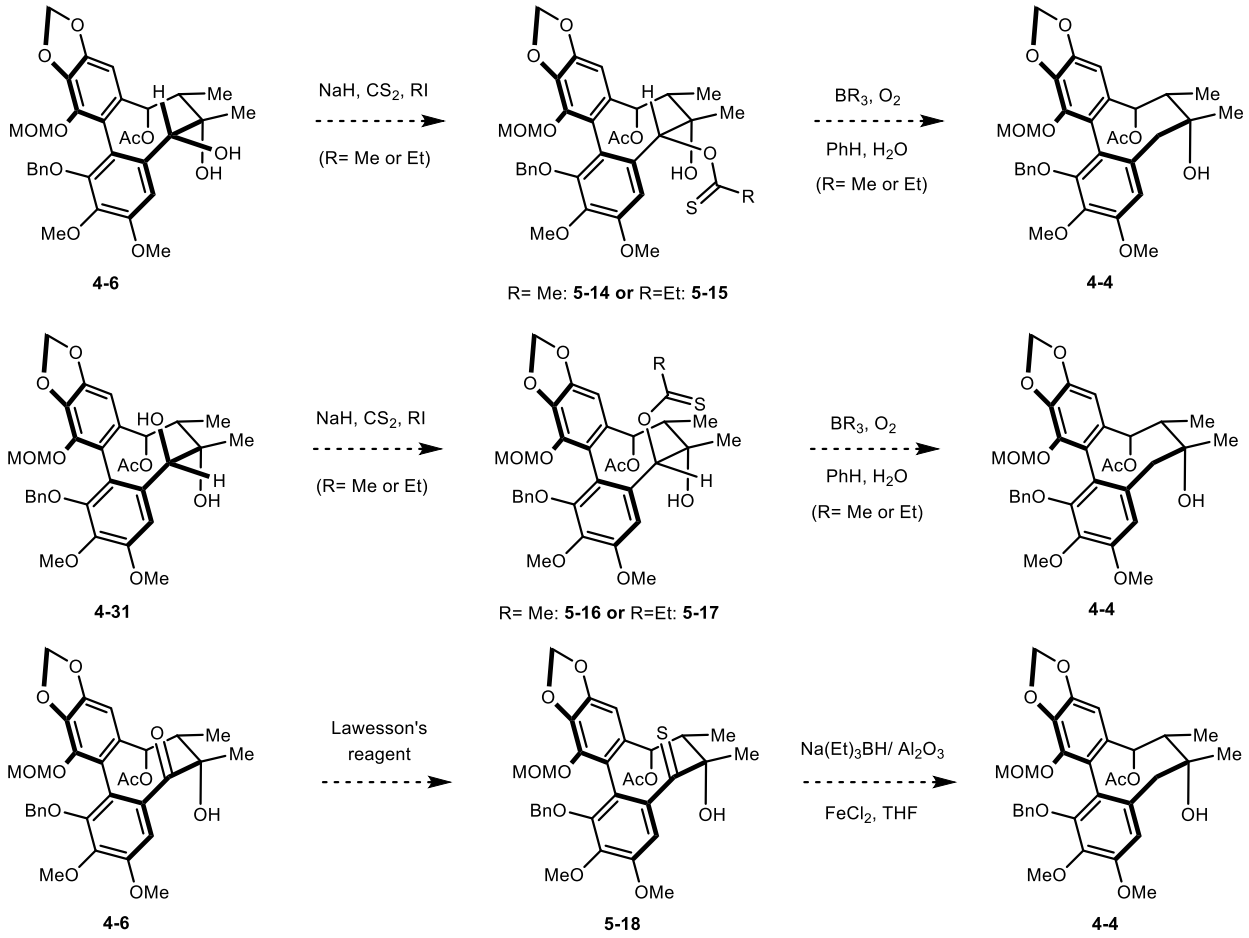
5.2.2. Synthesis of taiwanschirin B

As several methods for the deoxygenation of **4-55** via the C6 benzoyl ester were ineffective, different activating groups at C6 will be investigated next. It is expected that the C6 benzoyl ester can be selectively hydrolyzed to the alcohol (**5-8**) under basic conditions, as it should be more sterically accessible than the C9 acetate (Scheme 5.4). A different activating group (such as an ester, thiocarbamate, or iodide) could then be appended to the C6 alcohol, either via esterification or nucleophilic substitution. It is then anticipated that one of the alternate activating groups will undergo deoxygenation more readily than the benzoate, providing taiwanschirin B. Acetic acid (4.76 in H_2O) and formic acid (3.77 in H_2O) have similar or lower pKas than benzoic acid (4.2 in H_2O), where a lower pKa indicates the conjugate base will be more stable, and thus more easily produced during C-O bond cleavage.[4] Acetate and formate groups are sterically small so it should be feasible to append them to the C6 alcohol despite congestion around this position. Acetylation of alcohol **5-8** would give **5-9** which could be subjected to allylic reduction conditions from Keinan and coworkers,[5] consisting of $Pd(PPh_3)_4$ and diphenylsilane. Formylation of **5-8** would give **5-10** which could be treated with Tsuji's allylic reduction conditions of $Pd_2(dba)_3$, PBu_3, and NH_4CO_2H.[6] Alternatively, a Barton ester could be appended to the C6 alcohol of **5-8**, giving **5-11**, **5-12**, or **5-13**.[7–9] These Barton esters could be subjected to the classic Barton–McCombie deoxygenation conditions employing tributyltin hydride and catalytic AIBN[10] or tin-free conditions employing trialkylboranes (such as BMe_3 or BEt_3) under air[11] or photoredox catalysis.[12] The Garegg-Samuelson reaction[13] to convert an alcohol to an iodide with inversion of stereochemistry had been attempted at the stage of **4-6**, resulting in MOM deprotection (see section 4.4). As substate **5-8** does not bear a MOM group, it would be worthwhile reinvestigating these conditions. If **5-13** can be prepared successfully, it could then be subjected to photoredox-[13] or copper-[14] catalyzed hydrodeiodination conditions.



Scheme 5.4. C6 deoxygenation strategy for the synthesis of taiwanschirin B from **4-55**

It may also be worthwhile to investigate more deoxygenation conditions at an earlier stage in the syntheses (eg. from derivatives of **4-6** and **4-31**, Scheme 5.5). The xanthates of these substrates (**5-14** to **5-17**) could be prepared and subjected to aerobic trialkylborane conditions for deoxygenation to provide **4-4**.[11] Alternatively, the thioketone **5-18** could be prepared from the ketone **4-30** (eg. using Lawesson's reagent[15]) and subjected to desulfurization conditions (eg. using sodium triethylborohydride and iron (II) chloride on alumina[16]) to give **4-4**.



Scheme 5.5. Additional C6 deoxygenation strategies from **4-6, 4-31**, or **4-30**

5.2.3. Selective deoxygenation to access other DBCODs

One of the goals not yet achieved in this work is the development of methodology which can selectively deoxygenate each position of the 8-membered ring, allowing us to access a greater diversity of DBCODs. The C6 deoxygenation methodology which will be developed for use in the syntheses of kadsuraol C and taiwanschirin B could also be utilized in the synthesis of other C6 deoxygenated DBCODs such as longipedlignans C, E, and F and heteroclitin A (Figure 5.1).[17,18] The C7 deoxygenation methodology developed in section 4.4 could be applied to the syntheses of C7 deoxygenated DBCODs such as kadheterin A and epigomisin O.[19,20] Future work will include the development of deoxygenation strategies for other positions around the ring (eg. C9), allowing for access to DBCODs such as epigomisin O, gomisin C, and schirubrisin C.[21,22]

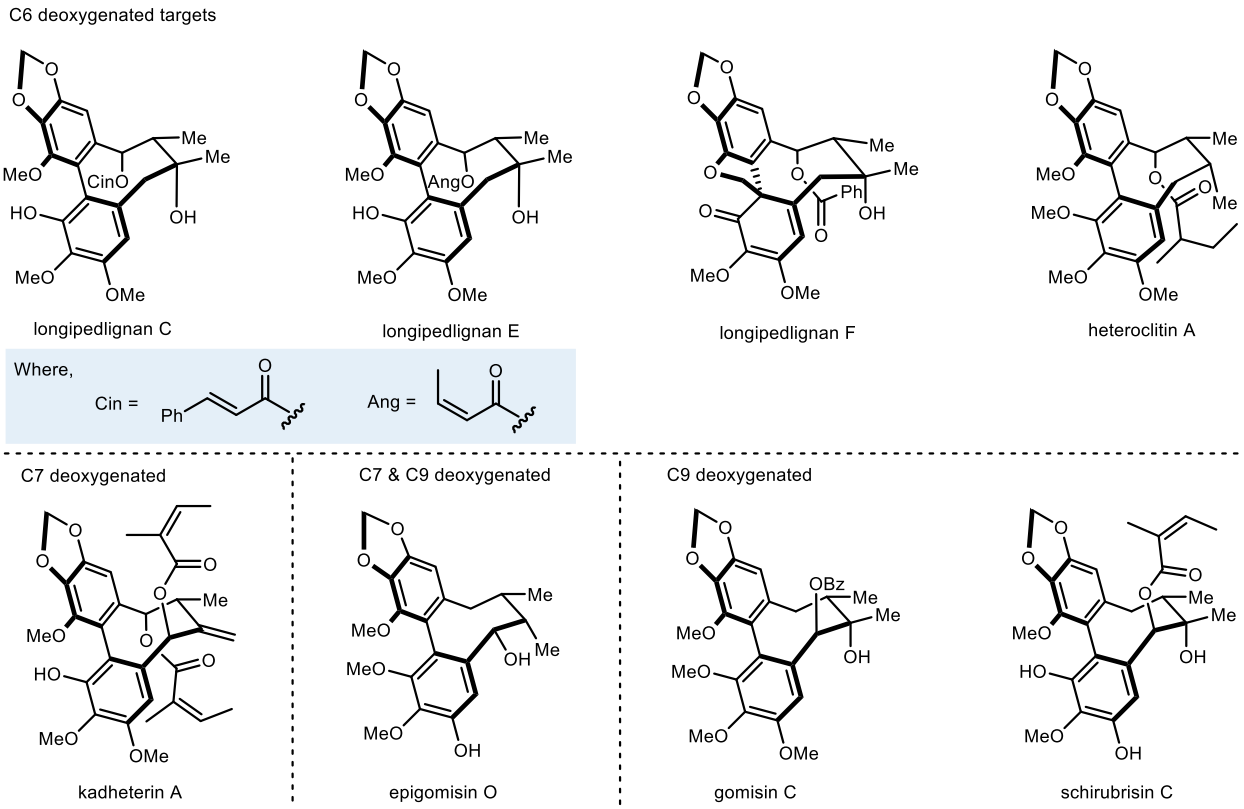


Figure 5.1. Potential future DBCOD targets with deoxygenation at various ring positions

5.3. References

(1) Azpilcueta-Nicolas, C. R.; Meng, D.; Edelmann, S.; Lumb, J. P. Dearomatization of Biaryls through Polarity Mismatched Radical Spirocyclization. *Angew. Chemie - Int. Ed.* **2023**, *62*, e202215422.

(2) Huang, Z.; Lumb, J. P. Mimicking Oxidative Radical Cyclizations of Lignan Biosynthesis Using Redox-Neutral Photocatalysis. *Nat. Chem.* **2021**, *13* (1), 24–32.

(3) Nawrat, C. C.; Jamison, C. R.; Slutskyy, Y.; Macmillan, D. W. C.; Overman, L. E. Oxalates as Activating Groups for Alcohols in Visible Light Photoredox Catalysis: Formation of Quaternary Centers by Redox- Neutral Fragment Coupling. *J. Am. Chem. Soc.* **2015**, *137*, 11270–11273.

(4) Bordwell, F. G. Hans Reich's Collection. Bordwell pKa Table https://organicchemistrydata.org/hansreich/resources/pka/.

(5) Keinan, E.; Greenspoon, N. Highly Chemoselective Allylic Reductions with Silicon Hydrides and Palladium Catalyst. *Isr. J. Chem.* **1984**, *24*, 82–87.

(6) Hubbs, J. L.; Heathcock, C. H. A Second-Generation Synthesis of the C1-C28 Portion of the Altohyrtins (Spongistatins). *J. Am. Chem. Soc.* **2003**, *125* (42), 12836–12843.

(7) Robins, M. J.; Wilson, J. S.; Hansske, F. Nucleic Acid Related Compounds. 42. A General Procedure for the Efficient Deoxygenation of Secondary Alcohols. Regiospecific and Stereoselective Conversion of Ribonucleosides to 2'-Deoxynucleosides. *J. Am. Chem. Soc.* **1983**, *105*, 4059–4065.

(8) Shibatomi, K.; Okimi, T.; Abe, Y.; Narayama, A.; Nakamura, N.; Iwasa, S. Organocatalytic Asymmetric Fluorination of α-Chloroaldehydes Involving Kinetic Resolution. *Beilstein J. Org. Chem.* **2014**, *10*, 323–331.

(9) Singh, V.; Prathap, S.; Porinchu, M. Aromatics to Triquinanes : P -Cresol to (±) - Δ 9(12)-Capnellene. *J. Org. Chem.* **1998**, *63*, 4011–4017.

(10) Barton, D. H. R.; McCombie, S. W. A New Method for the Deoxygenation of Secondary Alcohols. *J. Chem Soc. Perkin Trans. 1* **1975**, 1574–1585.

(11) Spiegel, D. A.; Wiberg, K. B.; Schacherer, L. N.; Medeiros, M. R.; Wood, J. L. Deoxygenation of Alcohols Employing Water as the Hydrogen Atom Source. *J. Am. Chem. Soc.* **2005**, *127*, 12513–12515.

(12) Chenneberg, L.; Baralle, A.; Daniel, M.; Fensterbank, L.; Goddard, J.; Ollivier, C. Visible Light Photocatalytic Reduction of O-Thiocarbamates : Development of a Tin-Free Barton – McCombie Deoxygenation Reaction. *Adv. Synth. Catal.* **2014**, *356*, 2756–2762.

(13) Nguyen, J. D.; Reiß, B.; Dai, C.; Stephenson, C. R. J. Batch to Flow Deoxygenation Using Visible Light Photoredox Catalysis. *Chem. Commun.* **2013**, *49*, 4352–4354.

(14) Dang, H.; Cox, N.; Lalic, G. Copper-Catalyzed Reduction of Alkyl Triflates and Iodides : An Efficient Method for the Deoxygenation of Primary and Secondary Alcohols. *Angew. Chemie - Int. Ed.* **2014**, *53*, 752–756.

(15) El-Barbary, A. A.; Clausen, K.; Lawesson, S.-O. Studies on Organophosphorus

Compounds XX. Syntheses of Thioketones. *Bull. Soc. Chim. Belg.* **1978**, *87* (3), 223–228.

(16) Alper, H.; Ripley, S.; Prince, T. L. Desulfurization of Thiols and Thioketones by Sodium Triethylborohydride and Iron (II) Chloride on Alumina. *J. Org. Chem.* **1983**, *48*, 250–252.

(17) Liu, J.; Pandey, P.; Wang, X.; Qi, X.; Chen, J.; Sun, H.; Zhang, P.; Ding, Y.; Ferreira, D.; Doerksen, R. J.; Hamann, M. T.; Li, S. Hepatoprotective Dibenzocyclooctadiene and Tetrahydrobenzocyclooctabenzofuranone Lignans from Kadsura Longipedunculata. *J. Nat. Prod.* **2018**, *81* (4), 846–857.

(18) Chen, D.-F.; Xu, G.-J.; Yang, X.-W.; Hattori, M.; Tezuka, Y.; Kikuchi, T.; Namba, T. Dibenzocyclooctadiene Lignans from Kadsura Heteroclita. *Phytochemistry* **1992**, *31* (2), 629–632.

(19) Luo, Y. Q.; Liu, M.; Wen, J.; Wang, W. G.; Hu, K.; Li, X. N.; Du, X.; Pu, J. X.; Sun, H. D. Dibenzocyclooctadiene Lignans from Kadsura Heteroclita. *Fitoterapia* **2017**, *119*, 150–157.

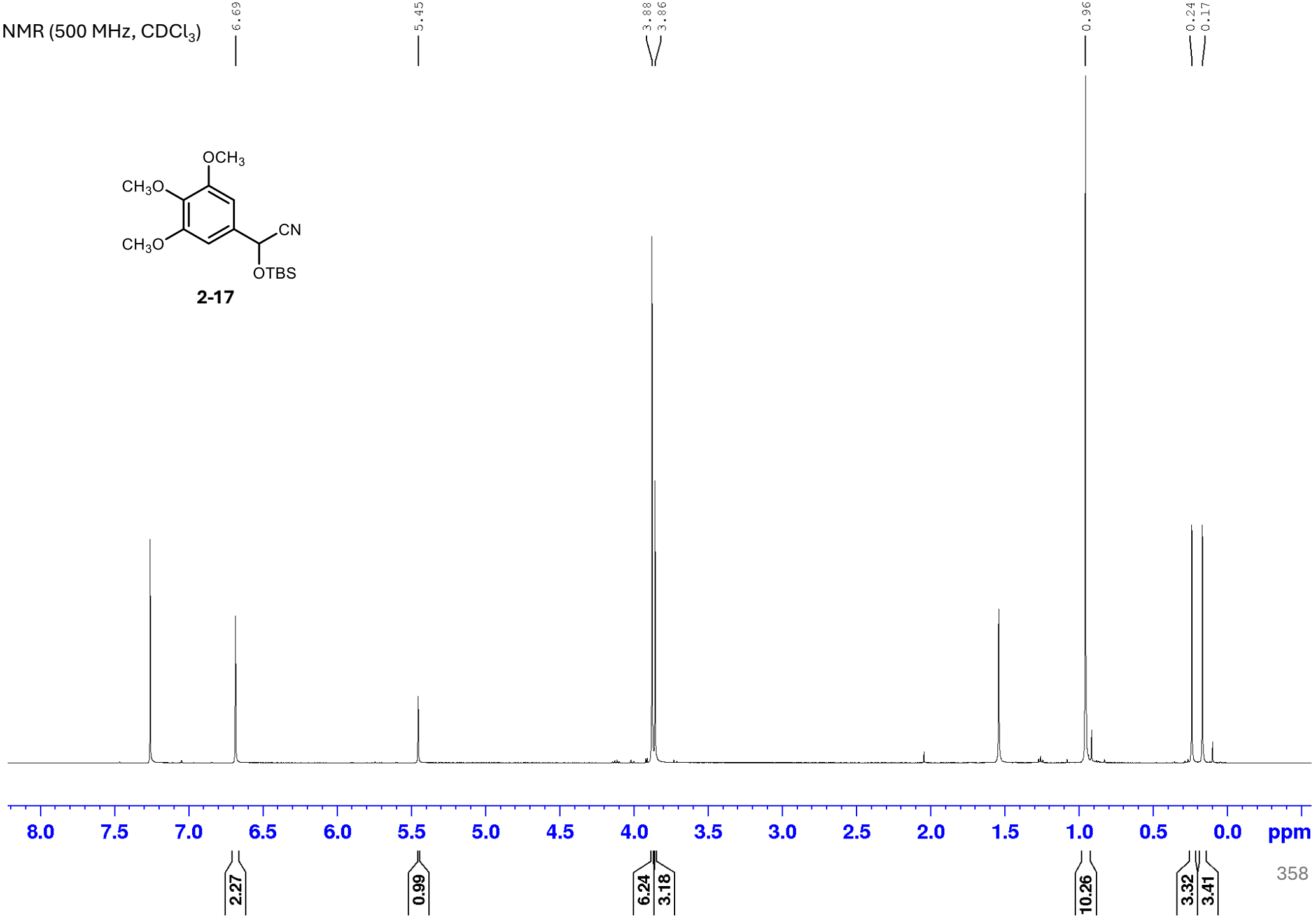
(20) Ikeya, Y.; Taguchi, H.; Yosioka, I.; Kobayashi, H. The Constituents of Schizandra Chinensis BAILL. V. The Structures of Four New Lignans, Gomisin N, Gomisin O, Epigomisin O and Gomisin E, and Transformation of Gomisin N to Deangeloylgomisin B. *Chem. Pharm. Bull.* **1979**, *27* (11), 2695–2709.

(21) Taguchi, H.; Ikeya, Y. The Constituents of Schizandra Chinensis Baill. I. The Structures of Gomisin A,B and C. *Chem. Pharm. Bull.* **1975**, *23* (12), 3296–3298.

(22) Luo, X.; Pu, J. X.; Fan, P.; Shi, Y. M.; Yang, G. Y.; Li, X. N.; Lei, C.; Gao, X. M.; Zhang, H. B.; Xiao, W. L.; Sun, H. D. Four New Dibenzocyclooctadiene Lignans from Schisandra Rubriflora. *Chin. J. Nat. Med.* **2011**, *9* (3), 167–172.

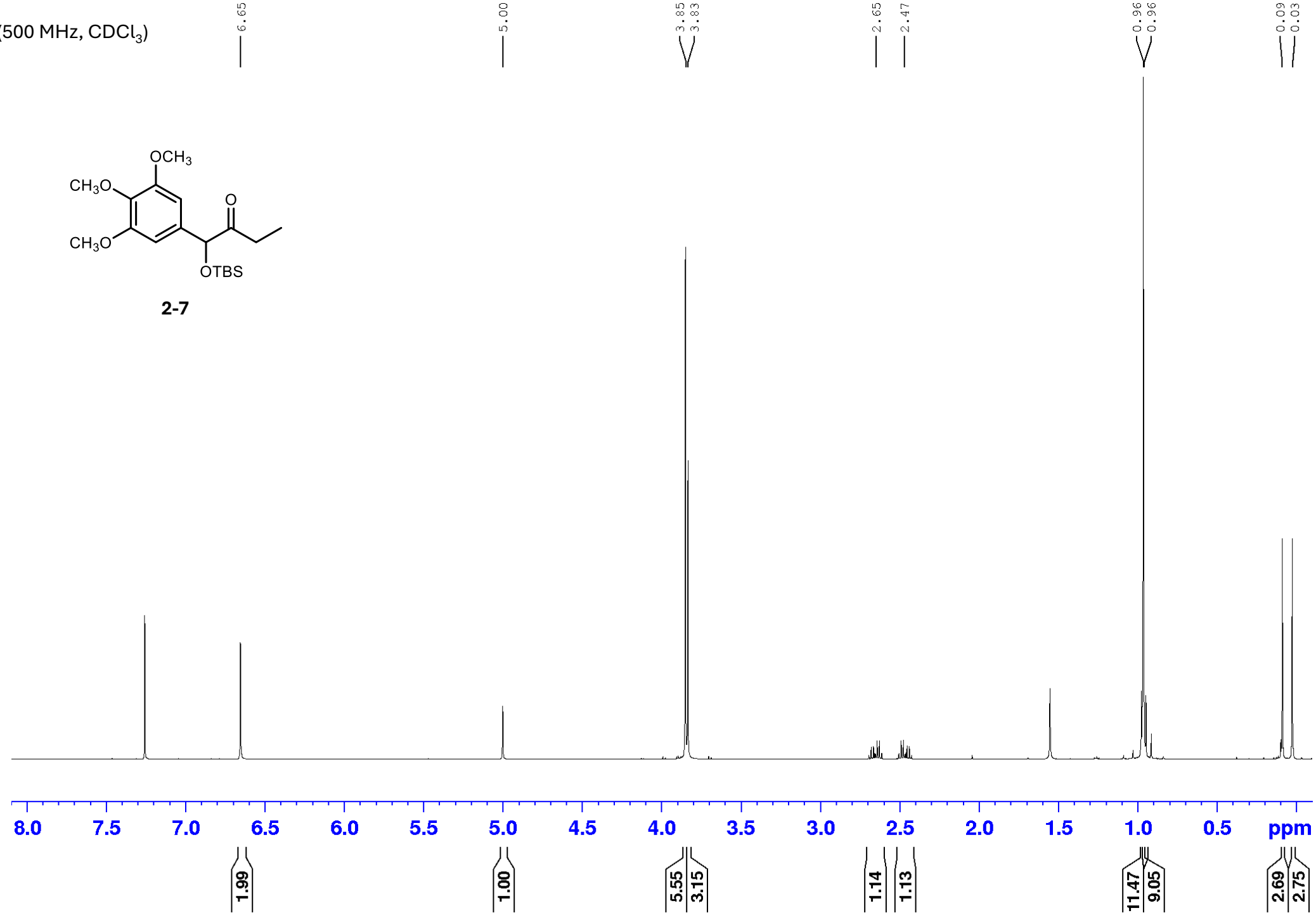
^{1}H NMR (500 MHz, $CDCl_3$)

2-17



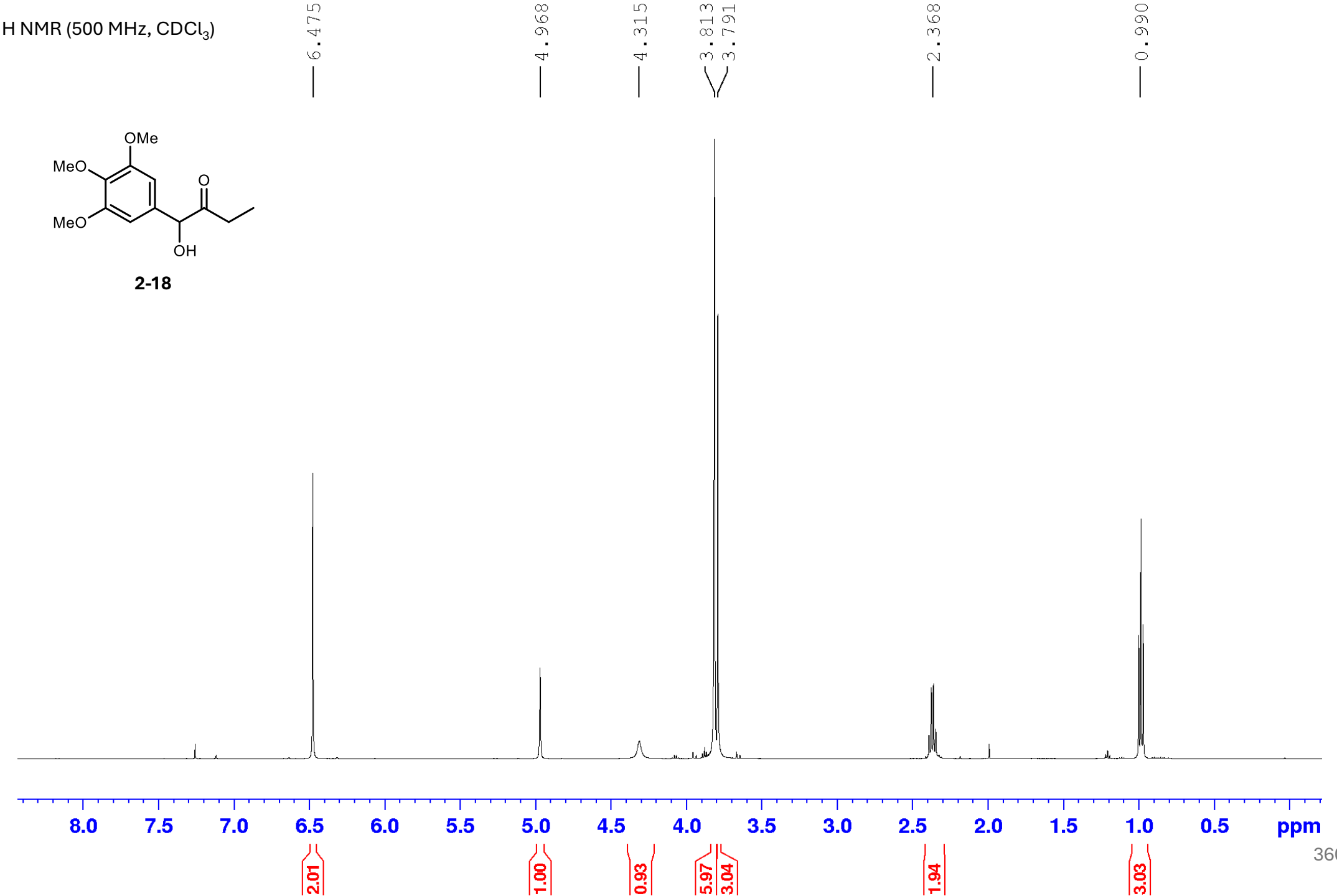
^{1}H NMR (500 MHz, $CDCl_3$)

2-7

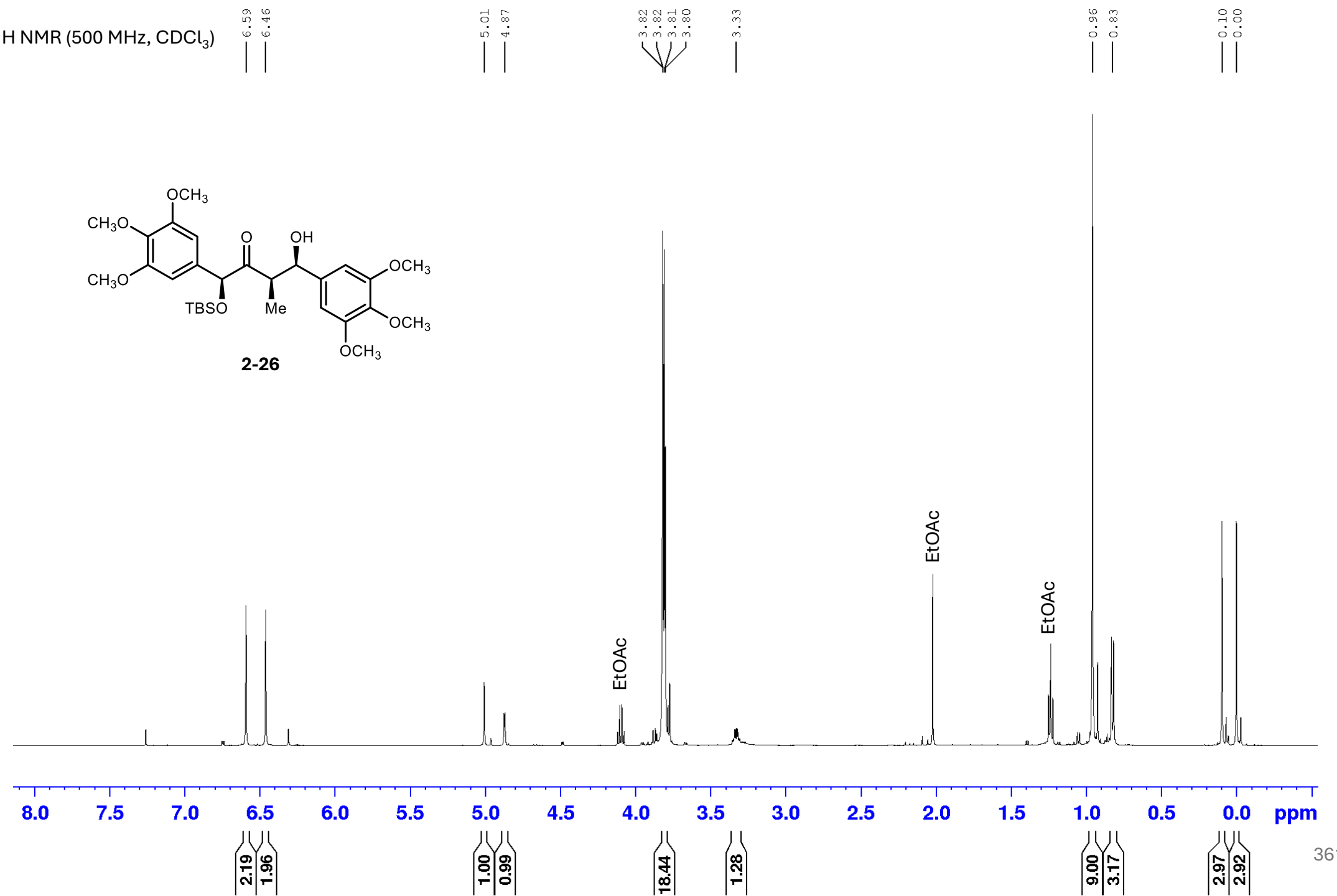


^{1}H NMR (500 MHz, $CDCl_3$)

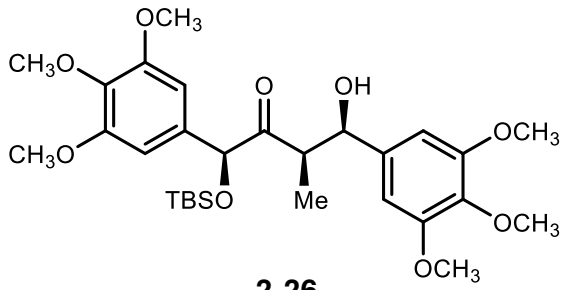
2-18



^{1}H NMR (500 MHz, $CDCl_3$)



^{13}C NMR (125 MHz, $CDCl_3$)



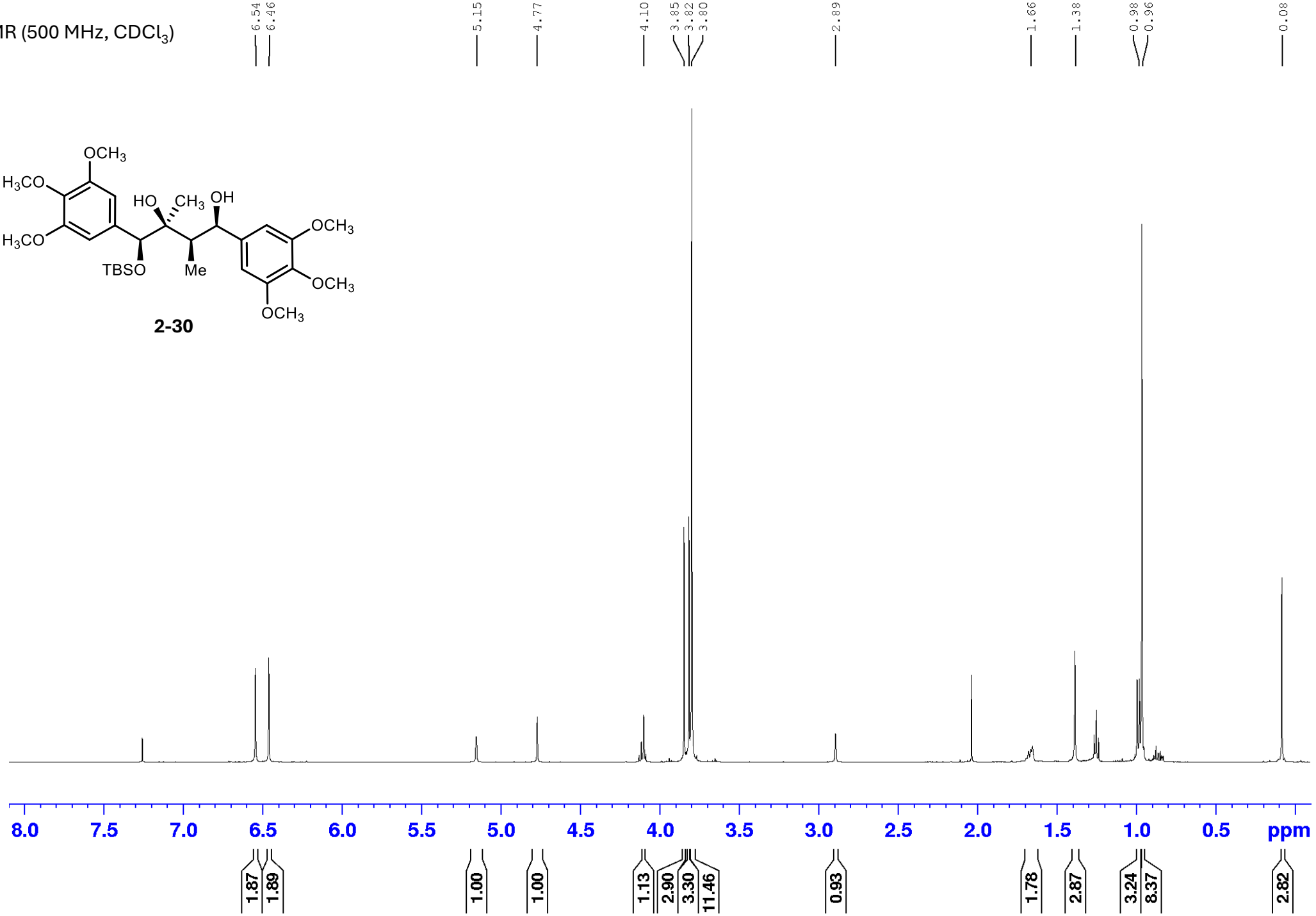
2-26

215.02
153.38
153.06
137.85
137.24
136.91
133.56
103.06
102.77
80.58
72.93
60.88
60.80
56.13
56.00
46.20
25.77
18.27
11.27
-4.86
-5.03

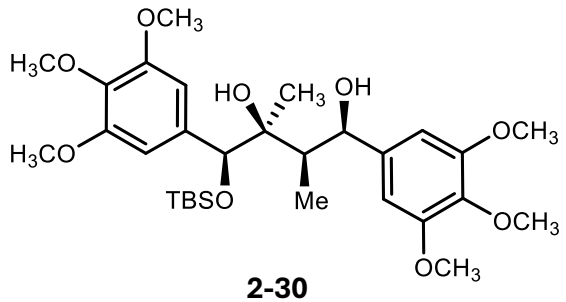
210 200 190 180 170 160 150 140 130 120 110 100 90 80 70 60 50 40 30 20 10 0 ppm

^{1}H NMR (500 MHz, $CDCl_3$)

2-30



^{13}C NMR (125 MHz, $CDCl_3$)



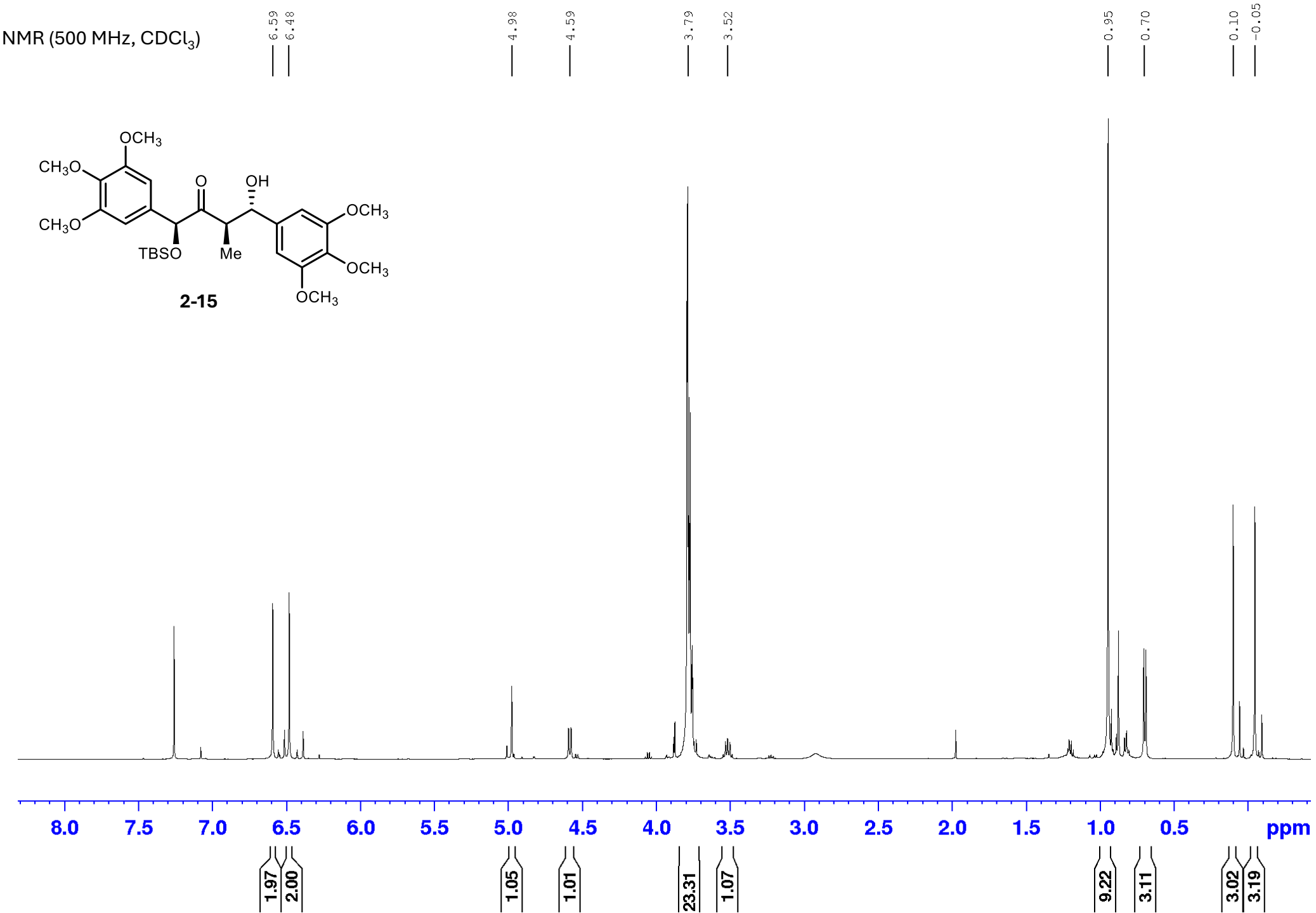
2-30

152.97
152.70
139.36
137.47
136.35
136.04
104.38
102.63
78.76
77.51
72.89
68.16
60.95
60.85
56.12
43.32
38.73
25.86
20.71
18.23
7.03
-4.48
-5.23

210 200 190 180 170 160 150 140 130 120 110 100 90 80 70 60 50 40 30 20 10 0 ppm

^{1}H NMR (500 MHz, $CDCl_3$)

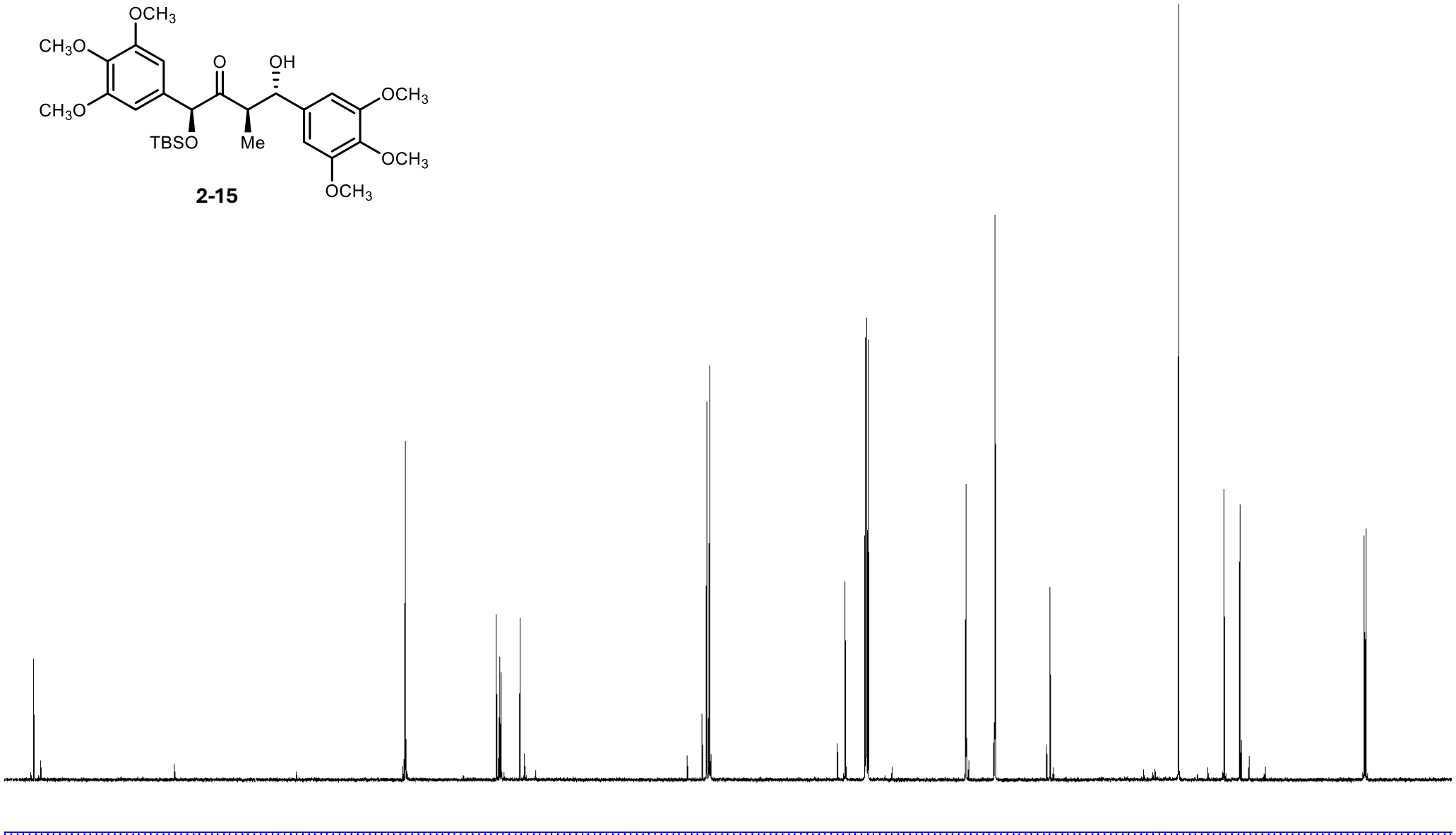
2-15



^{13}C NMR (125 MHz, $CDCl_3$)

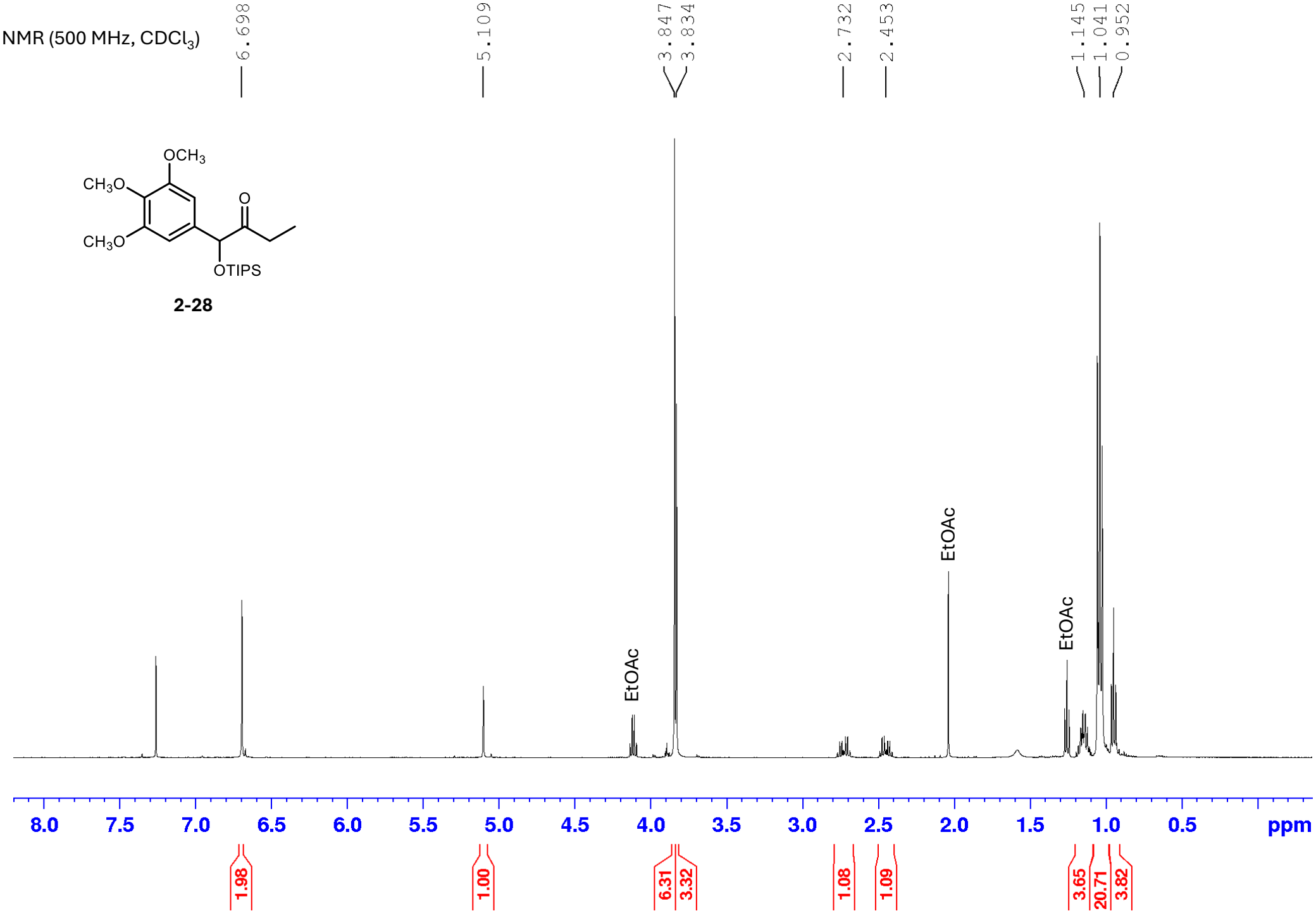
214.26
153.17
153.13
138.14
137.58
137.37
134.26
104.26
103.49
103.20
103.05
80.68
77.34
77.09
60.80
60.74
56.04
55.97
46.92
25.76
18.25
15.68
-4.83
-5.11

2-15

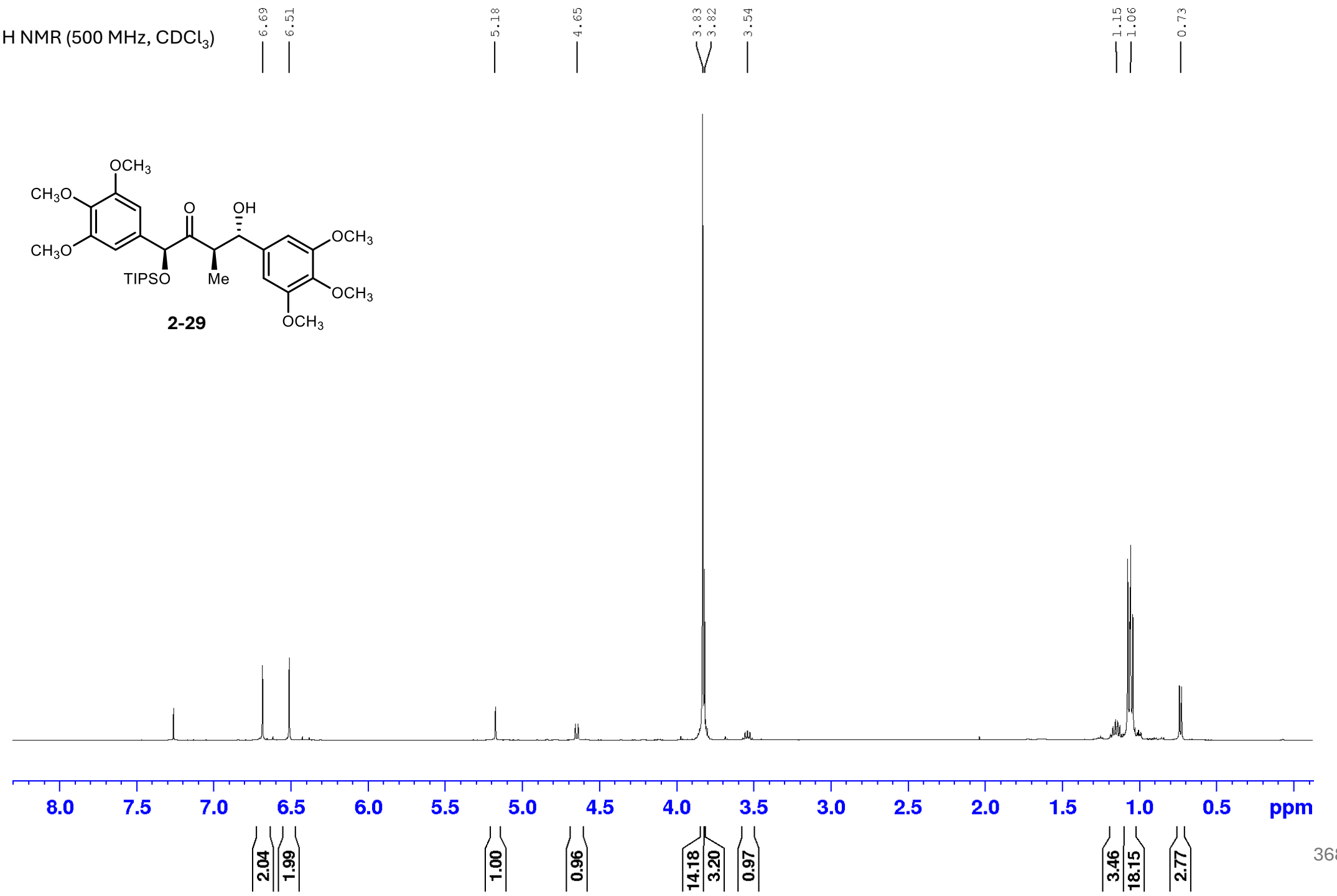


^{1}H NMR (500 MHz, $CDCl_3$)

2-28



^{1}H NMR (500 MHz, $CDCl_3$)

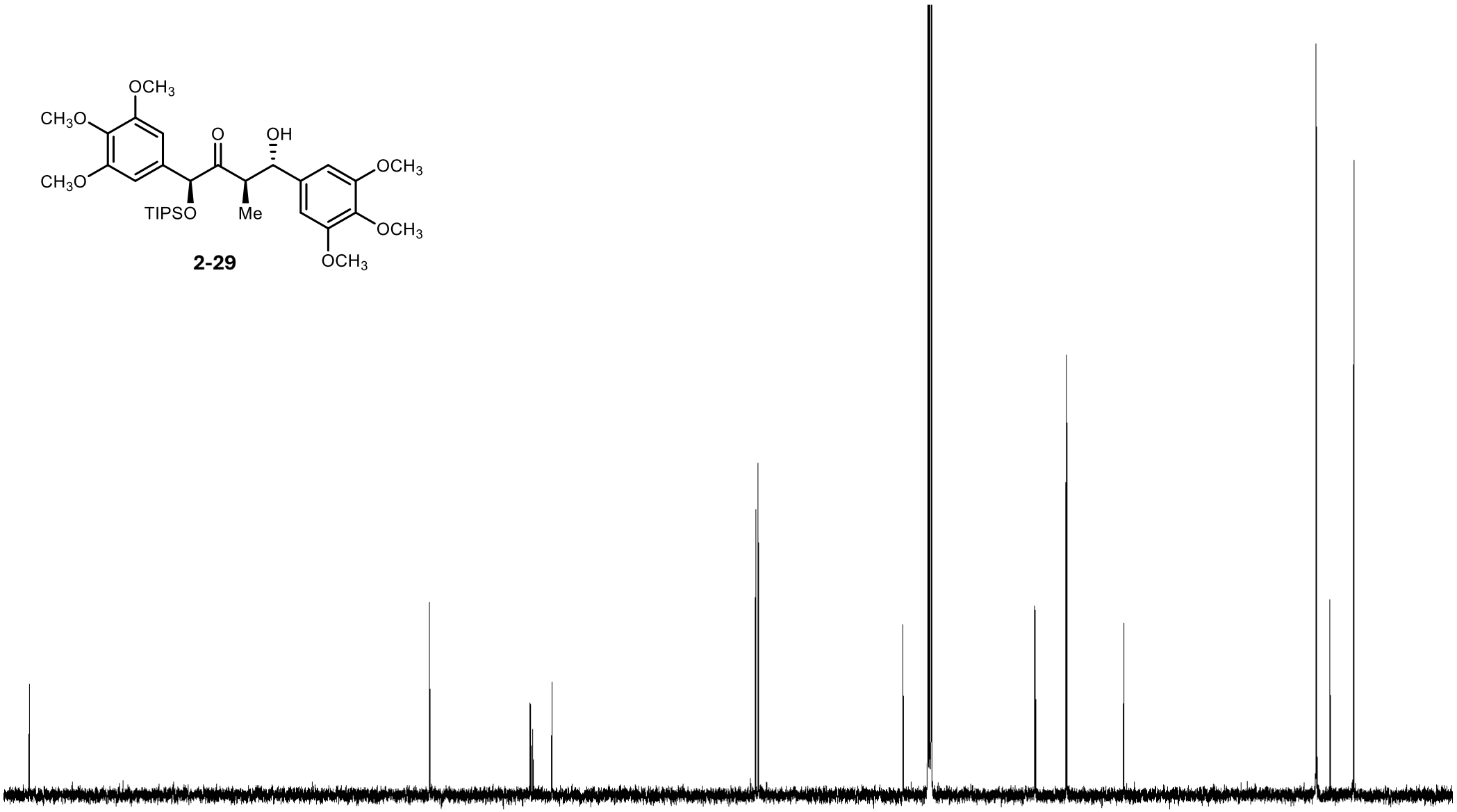


2-29

^{13}C NMR (125 MHz, $CDCl_3$)

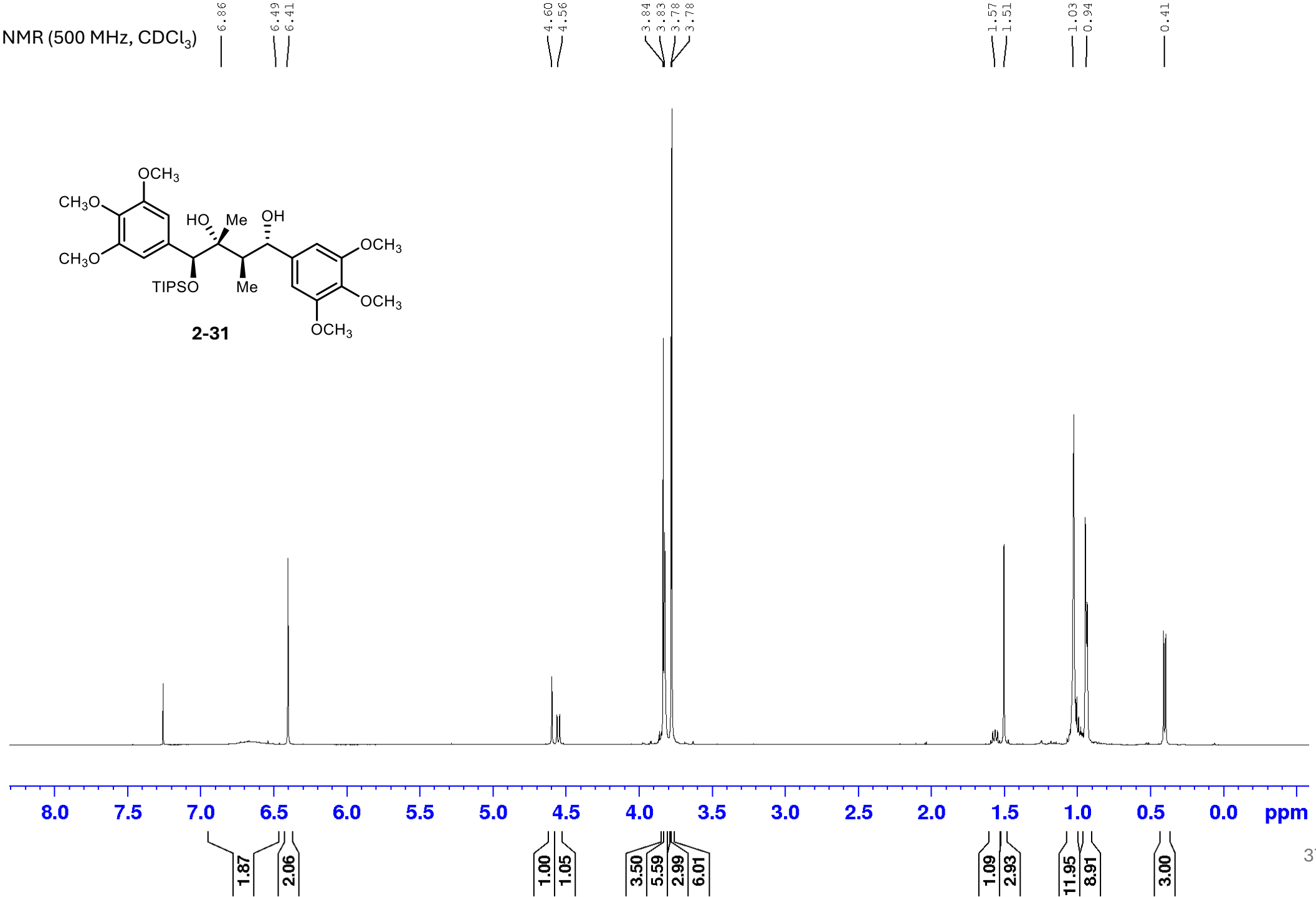
214.34
153.22
153.18
137.84
137.75
137.44
134.54
103.59
103.17
81.09
60.94
60.83
56.16
56.01
47.31
17.99
17.96
15.89
12.31

2-29



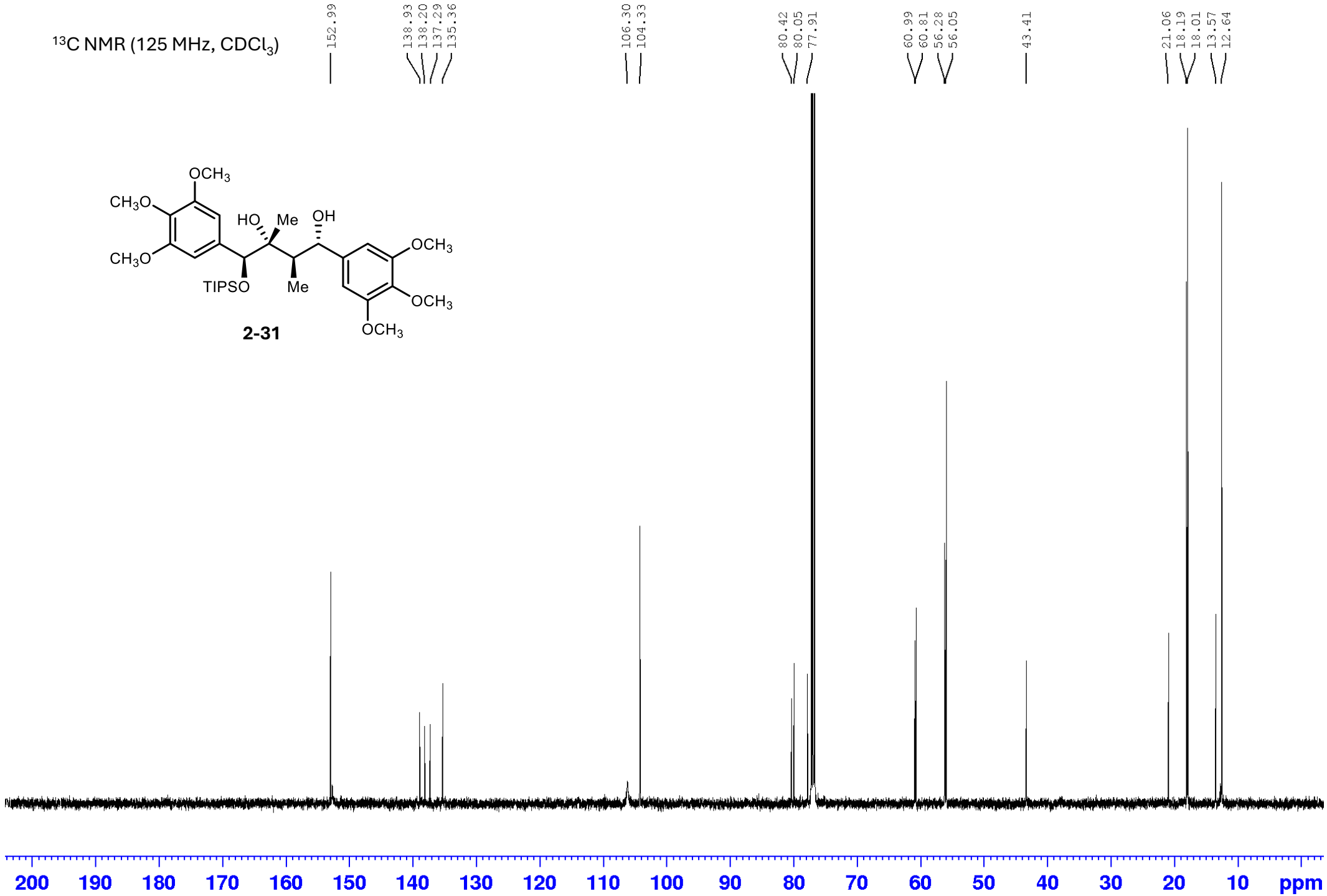
^{1}H NMR (500 MHz, $CDCl_3$)

2-31

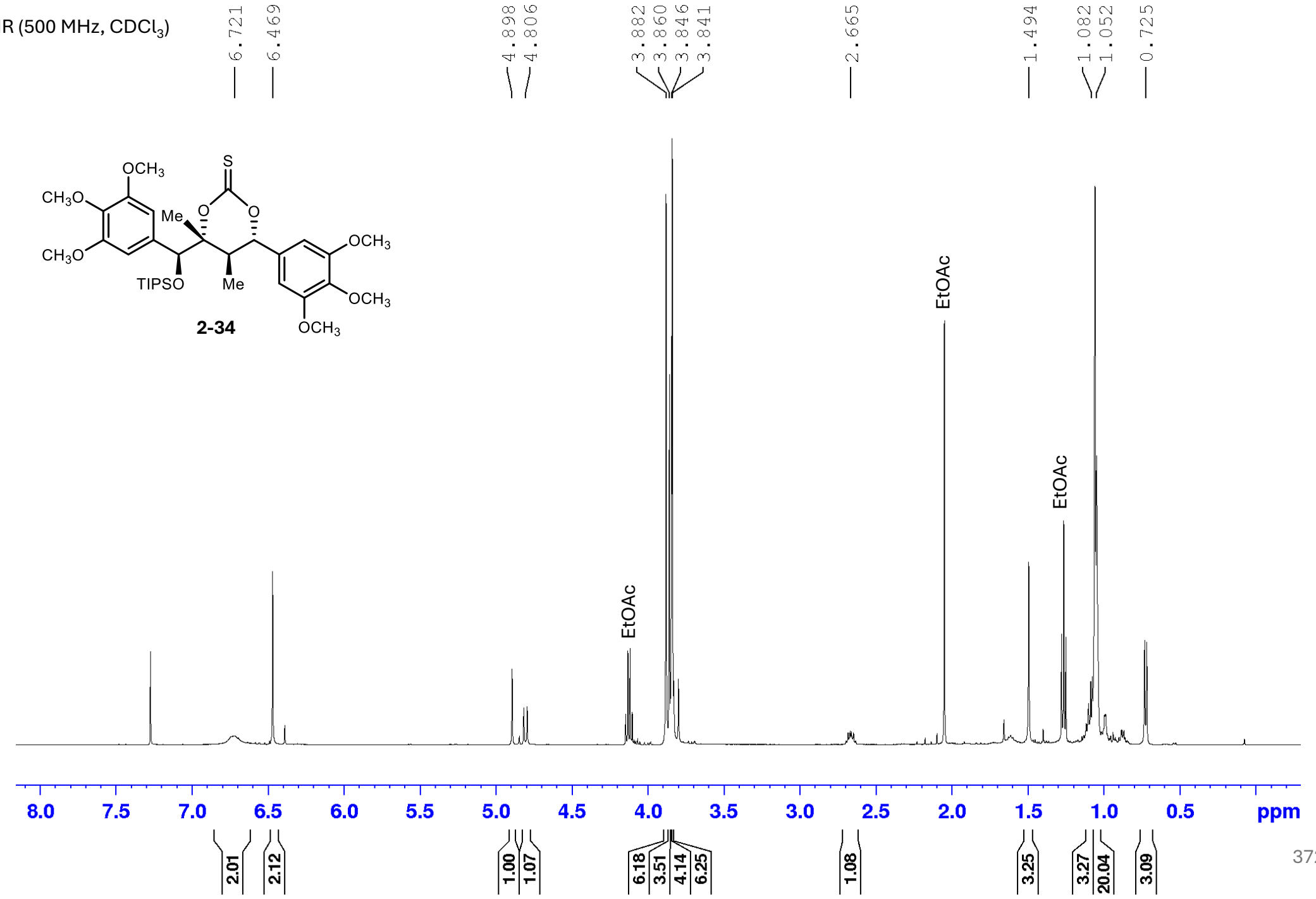


^{13}C NMR (125 MHz, $CDCl_3$)

2-31

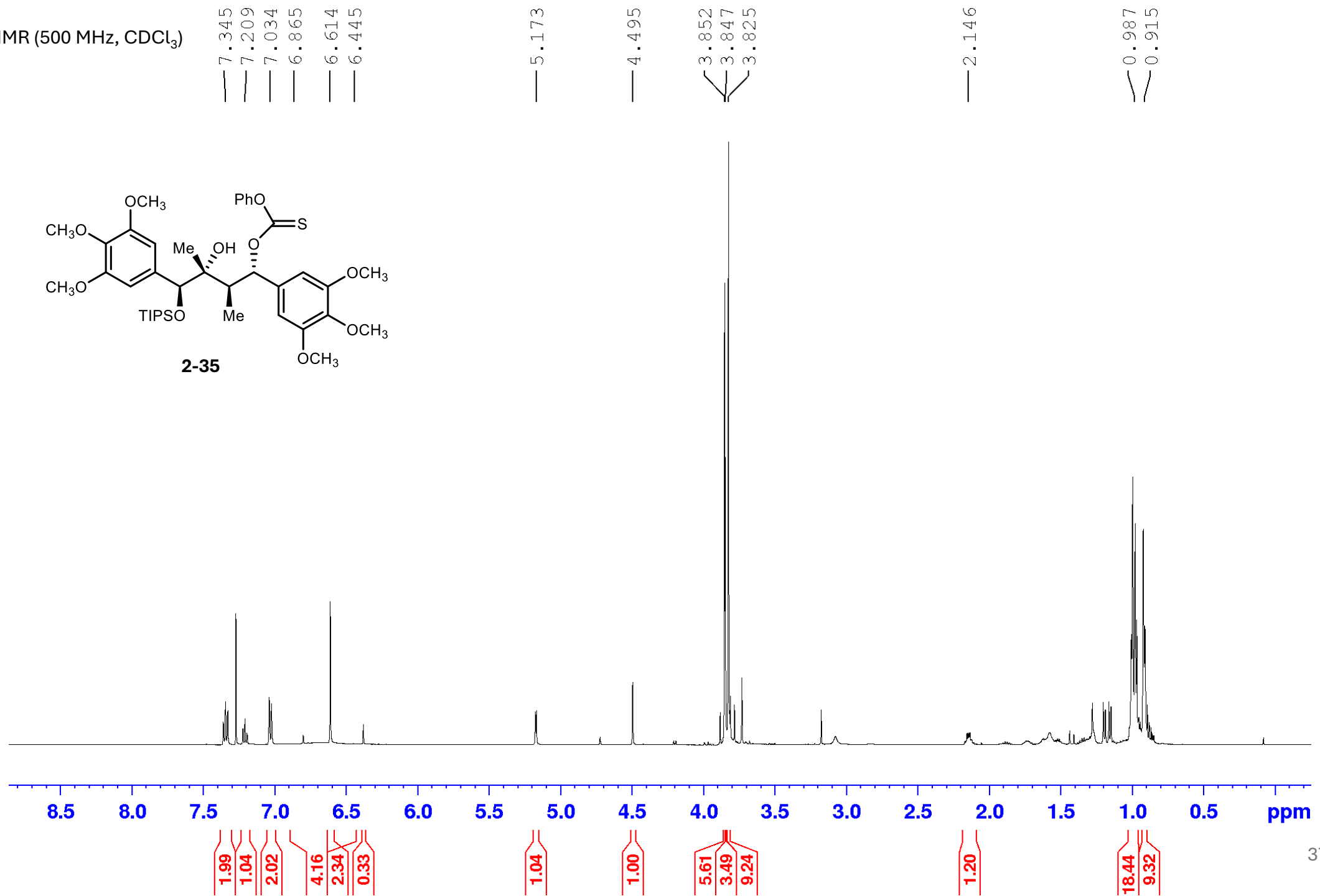


^{1}H NMR (500 MHz, $CDCl_3$)

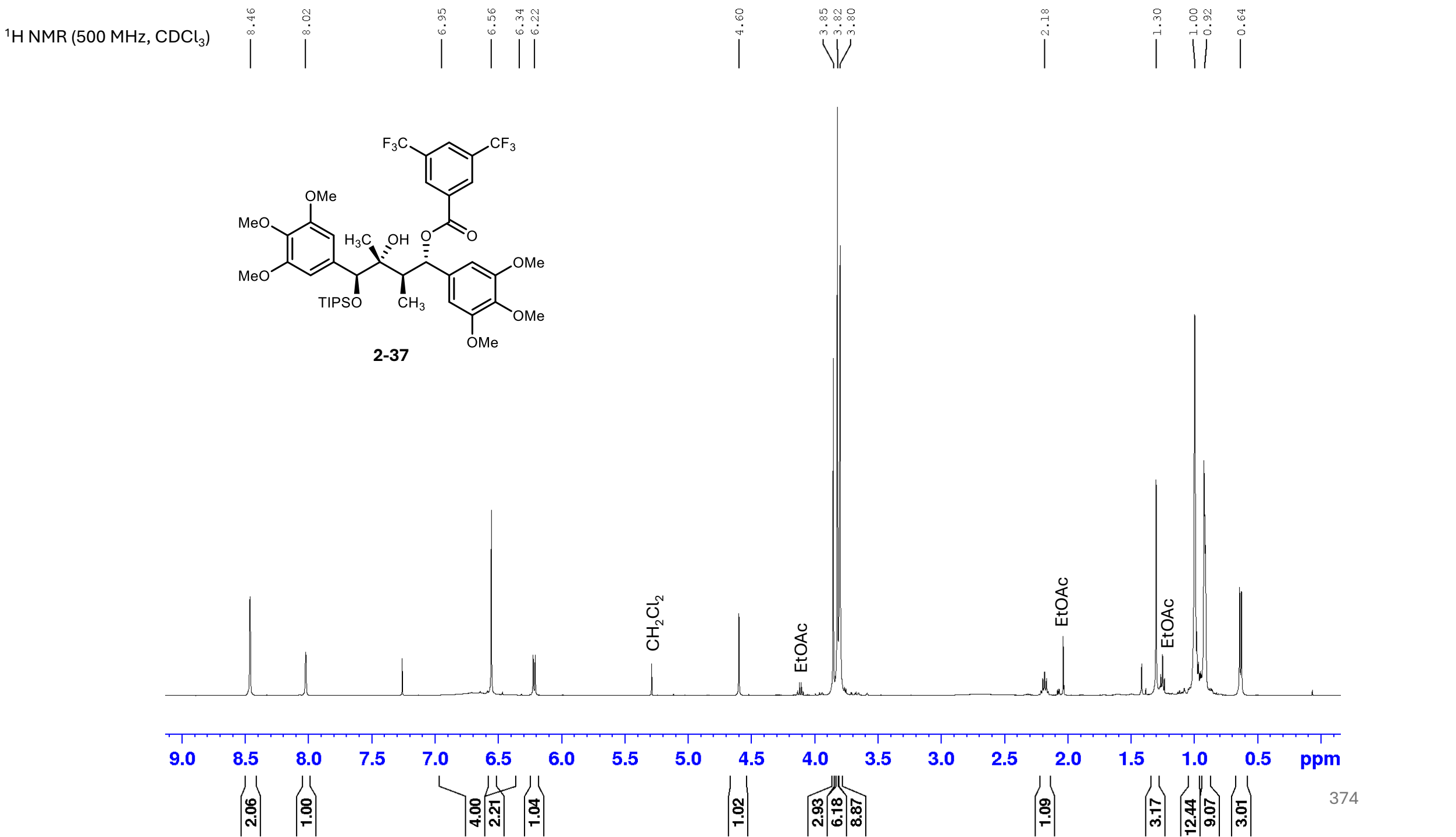


^{1}H NMR (500 MHz, $CDCl_3$)

2-35

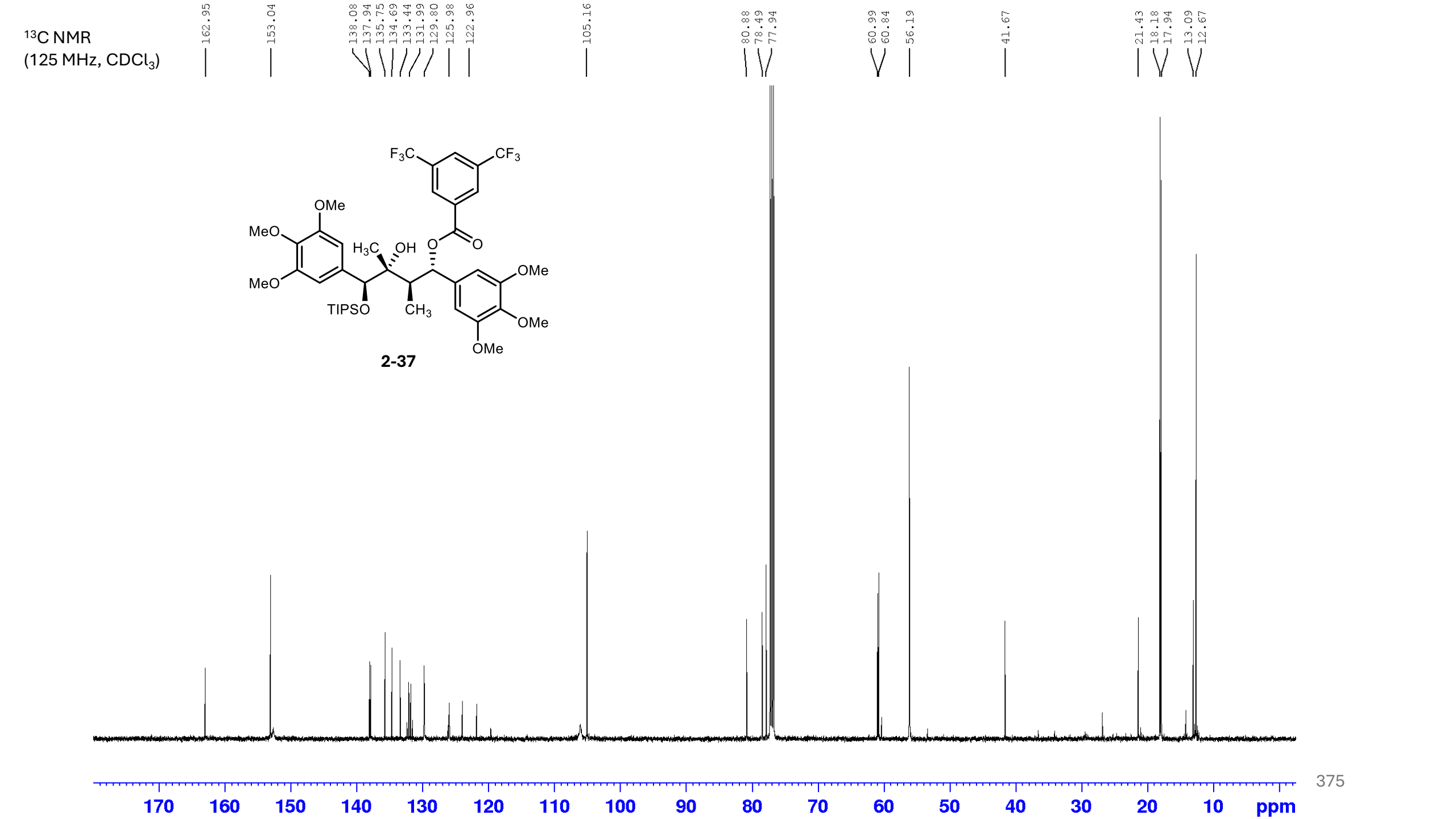


^{1}H NMR (500 MHz, $CDCl_3$)



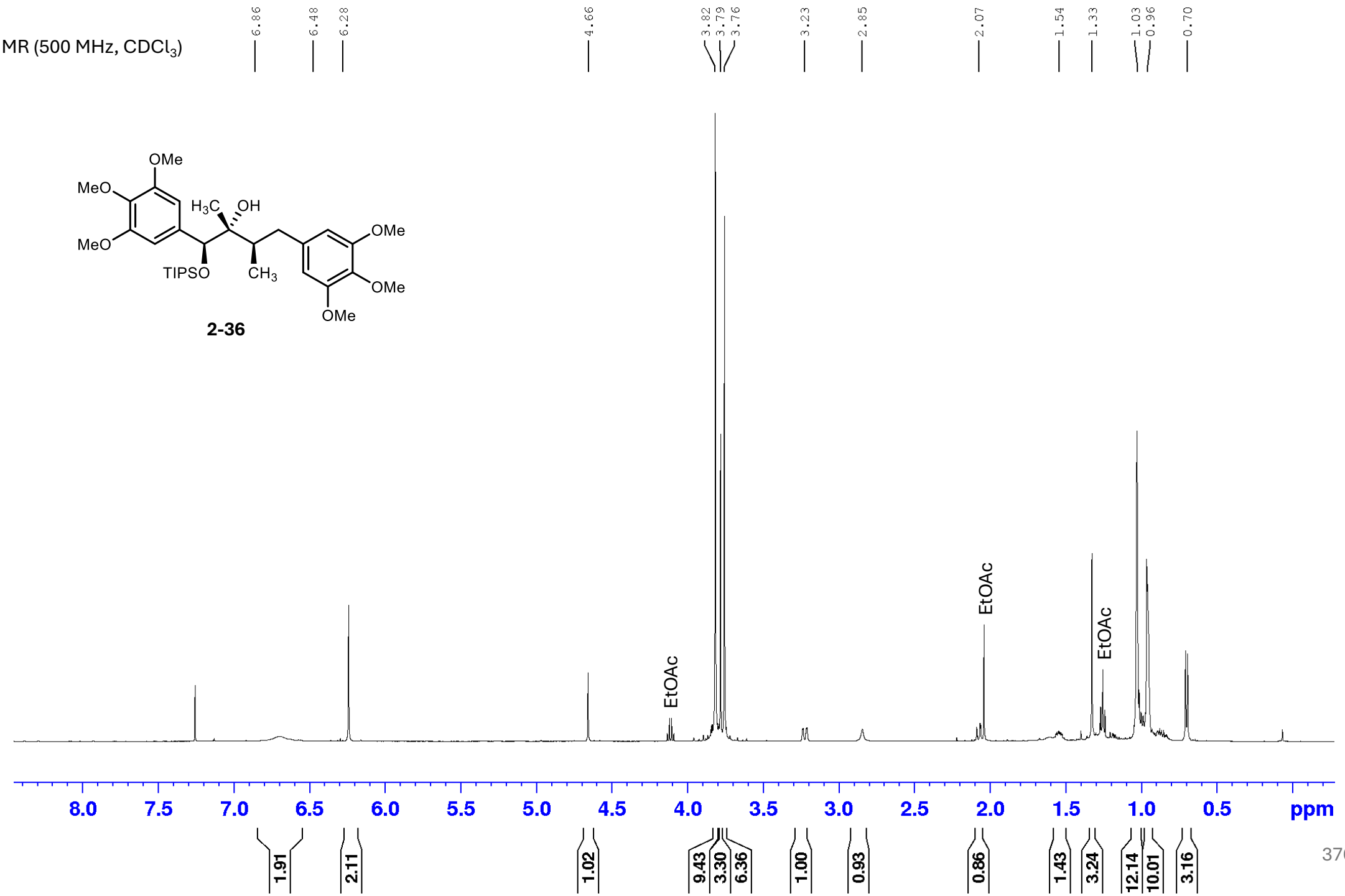
2-37

^{13}C NMR
(125 MHz, $CDCl_3$)

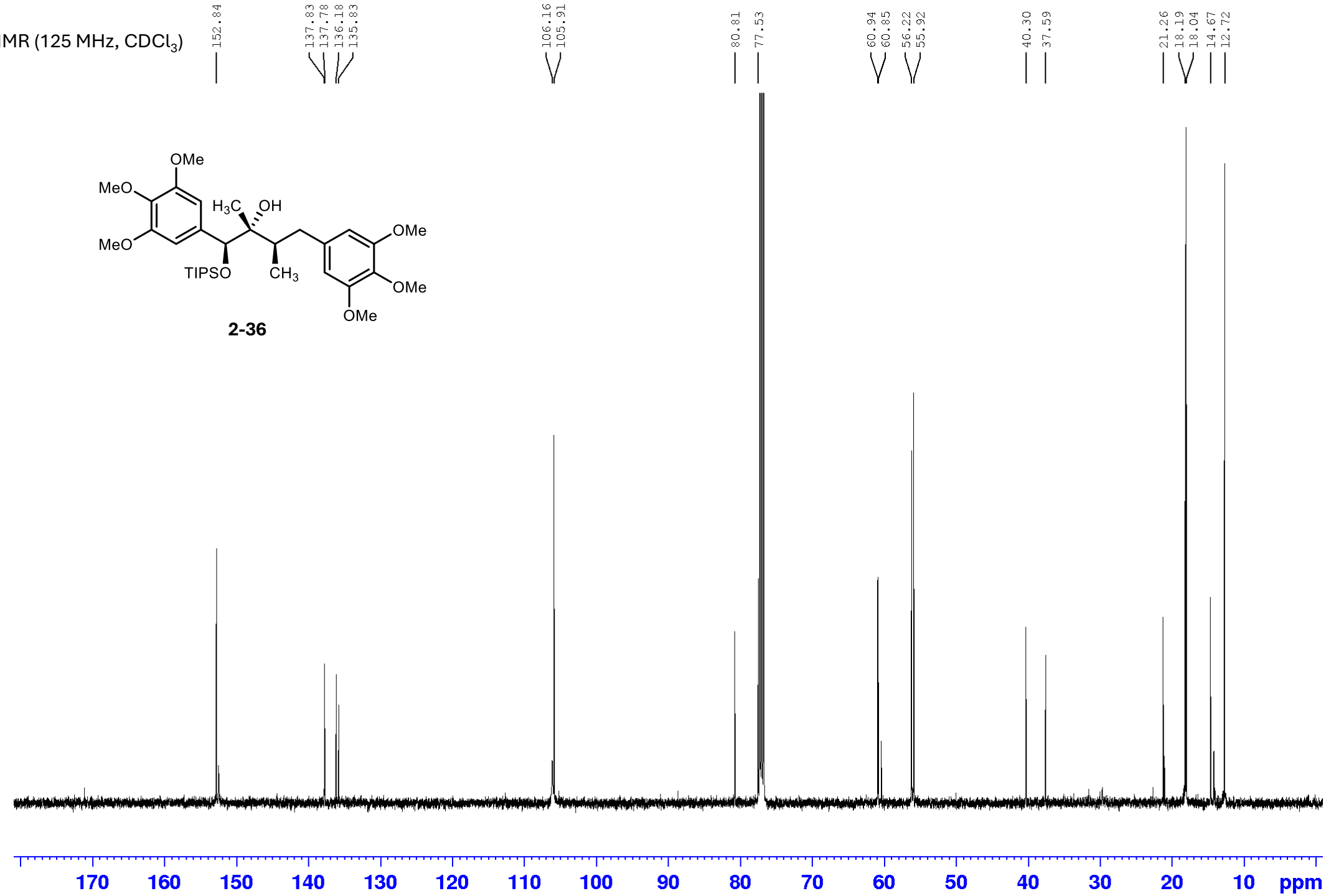


^{1}H NMR (500 MHz, $CDCl_3$)

2-36

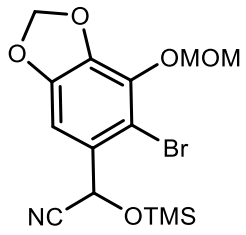


^{13}C NMR (125 MHz, $CDCl_3$)

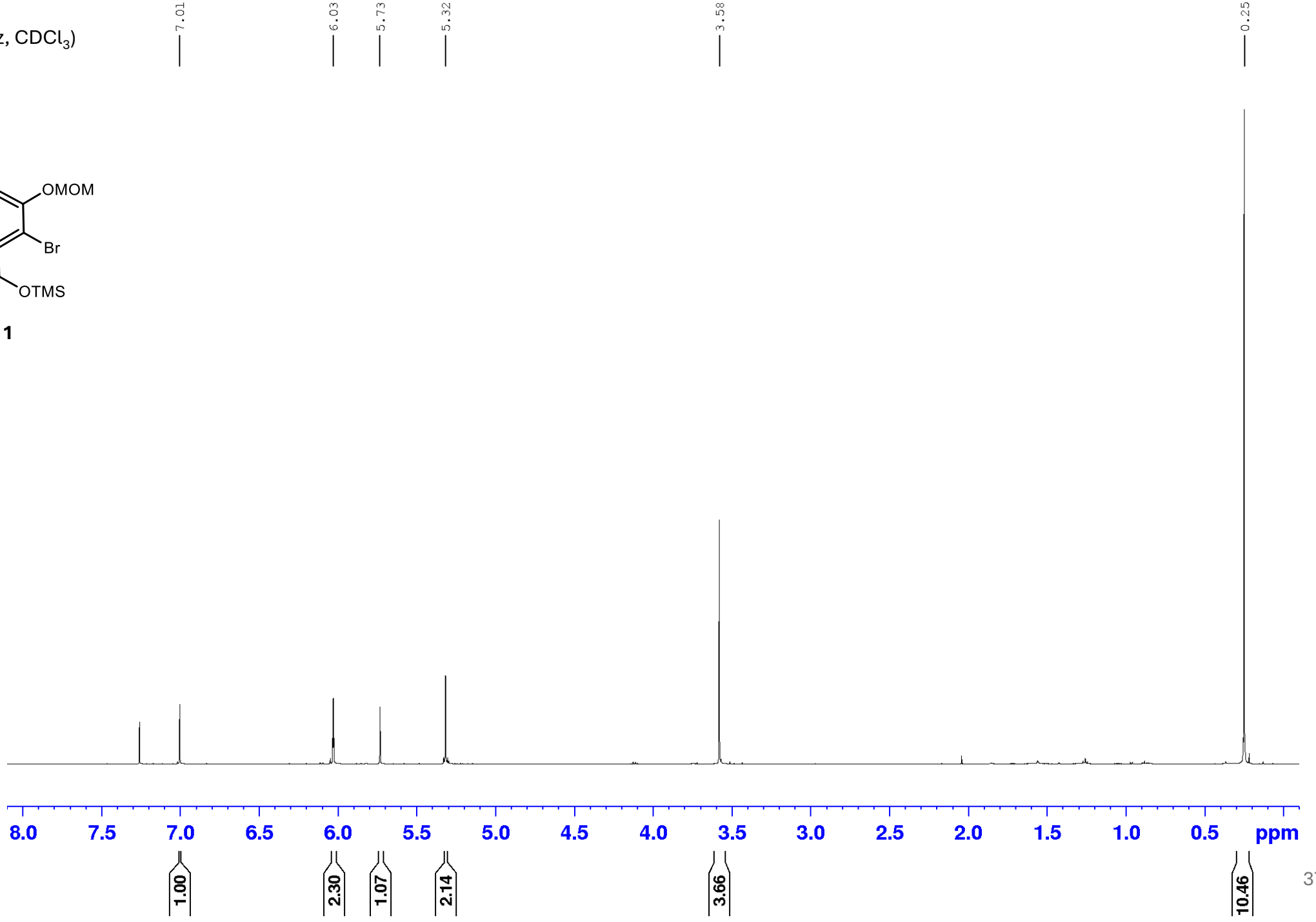


2-36

^{1}H NMR (500 MHz, $CDCl_3$)

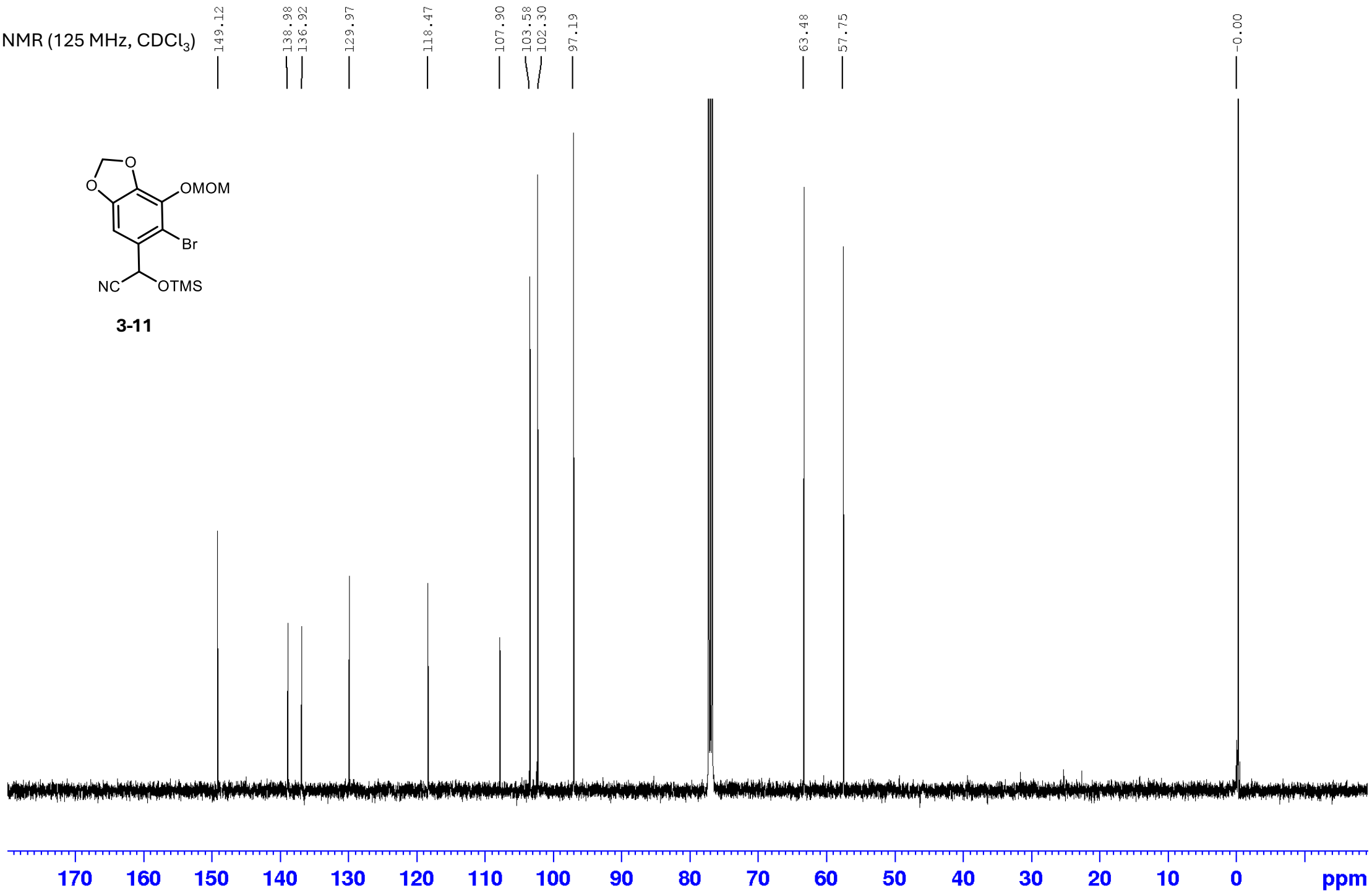


3-11



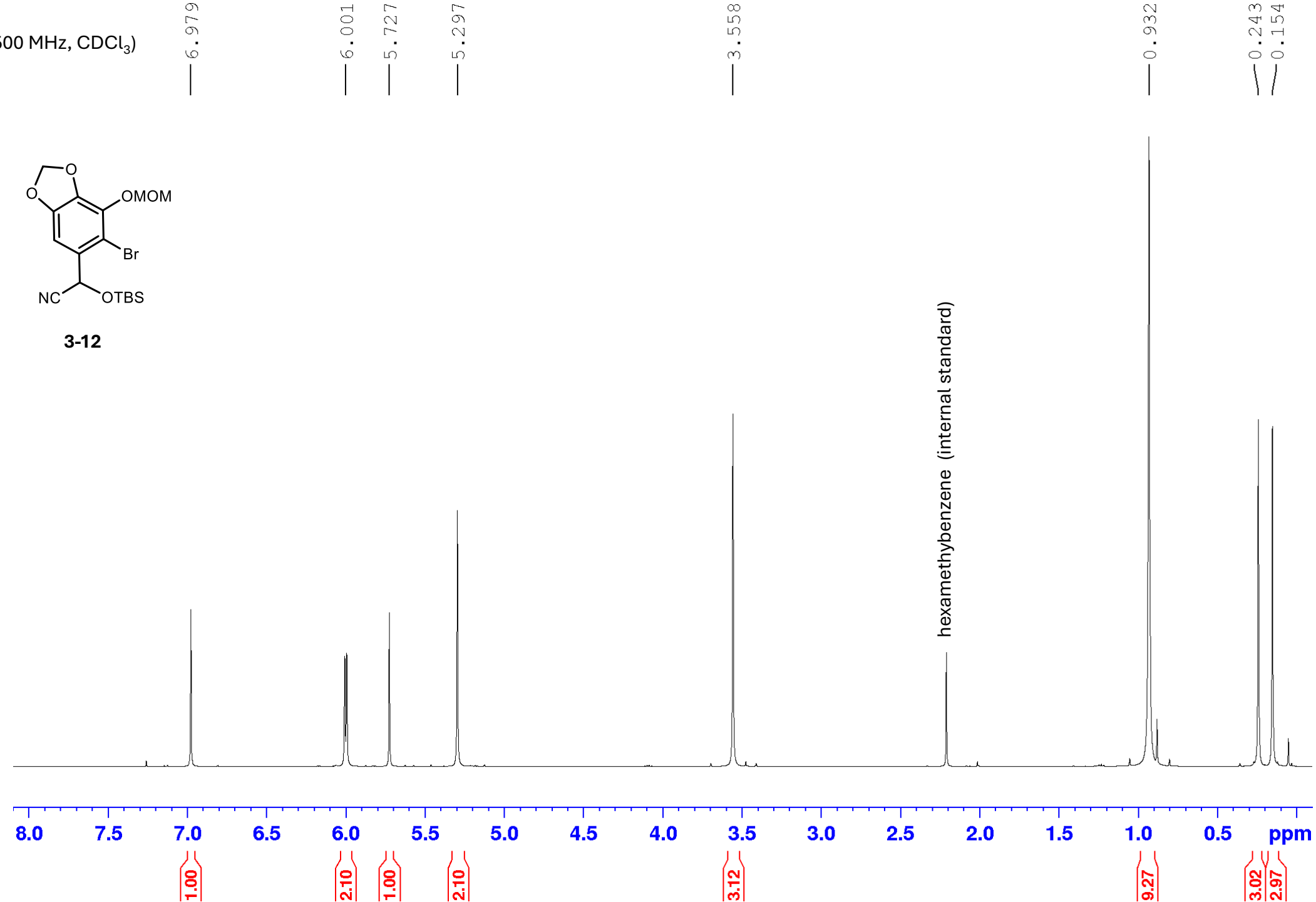
^{13}C NMR (125 MHz, $CDCl_3$)

3-11

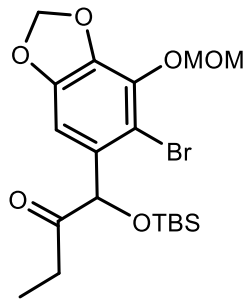


^{1}H NMR (500 MHz, $CDCl_3$)

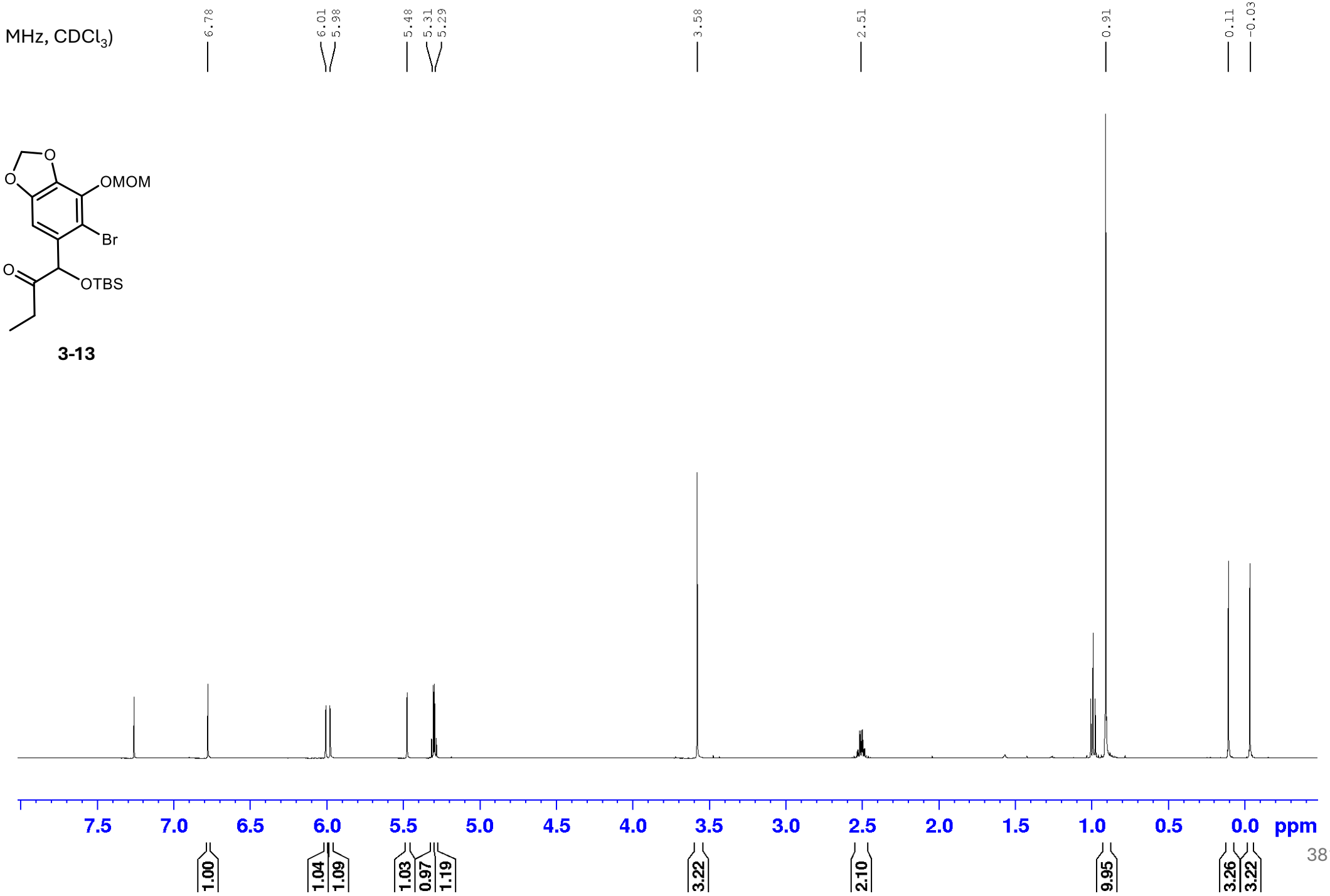
3-12



^{1}H NMR (500 MHz, $CDCl_3$)



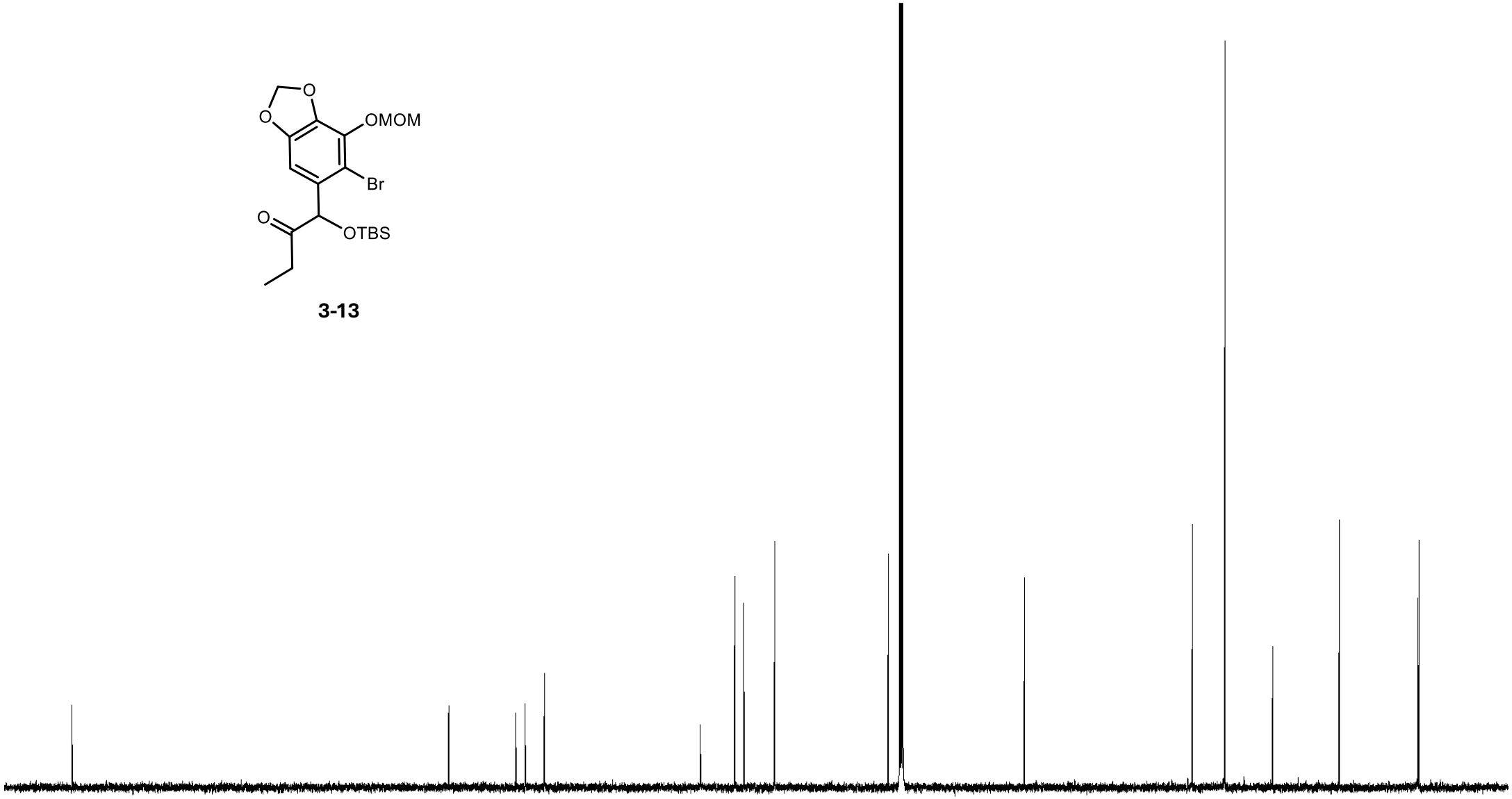
3-13



^{13}C NMR (125 MHz, $CDCl_3$)

208.52
148.76
138.12
136.66
133.61
108.86
103.43
101.98
97.09
79.09
57.47
30.88
25.73
22.66
18.16
14.13
7.53
-4.90
-5.07

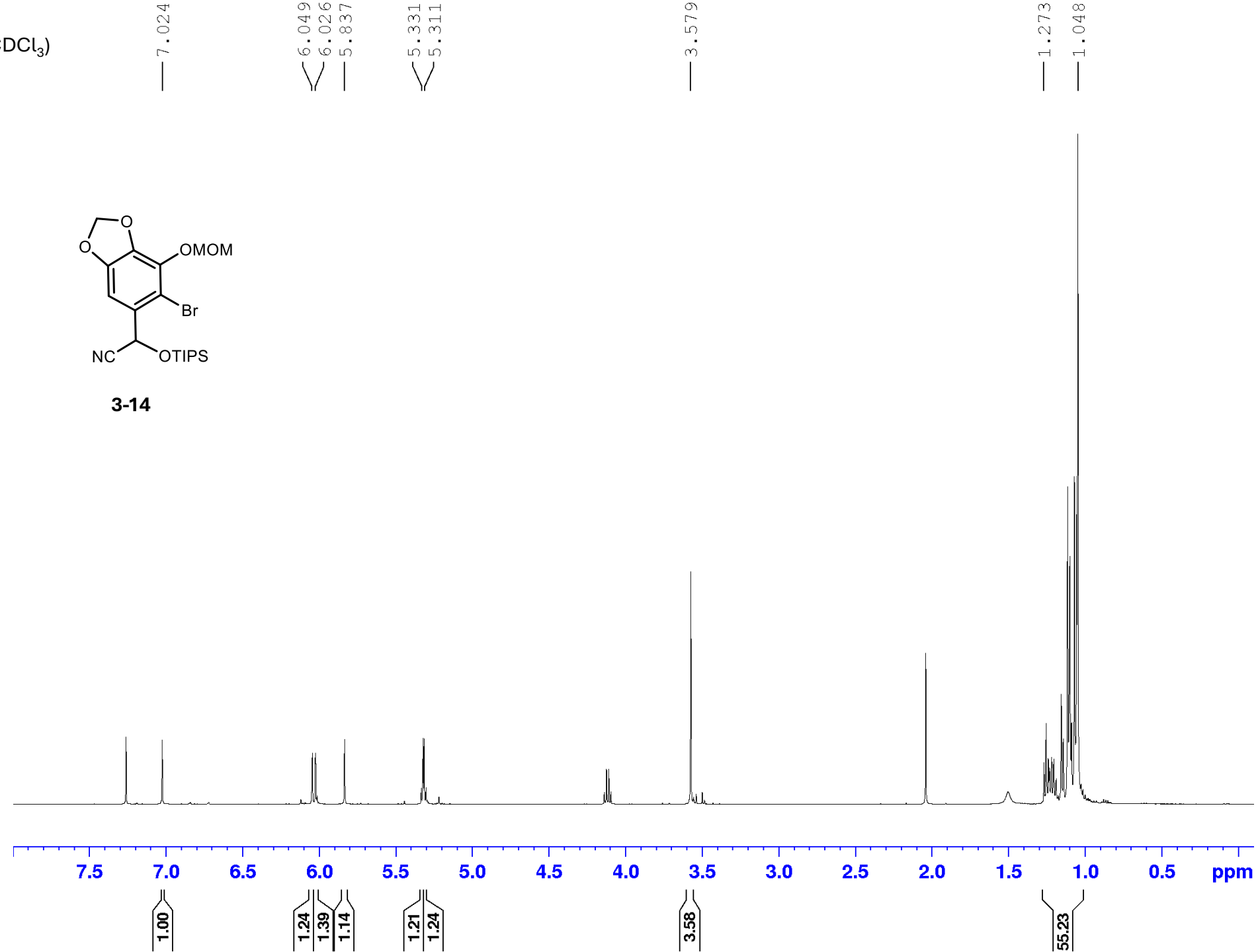
3-13



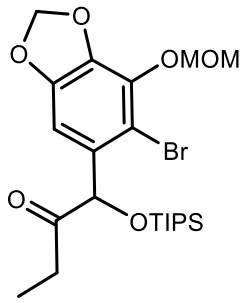
210 200 190 180 170 160 150 140 130 120 110 100 90 80 70 60 50 40 30 20 10 0 ppm

^{1}H NMR (500 MHz, $CDCl_3$)

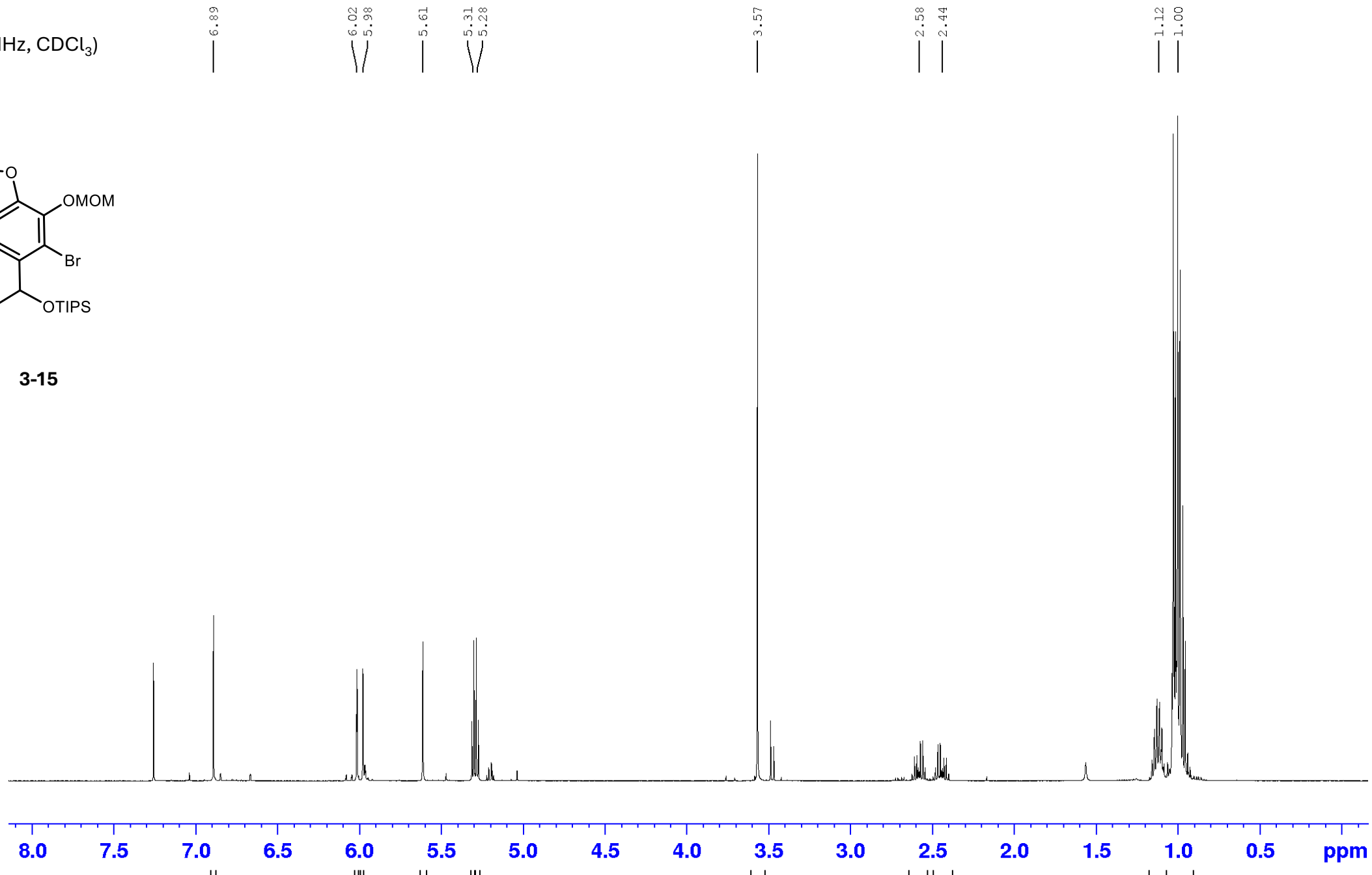
3-14



^{1}H NMR (500 MHz, $CDCl_3$)

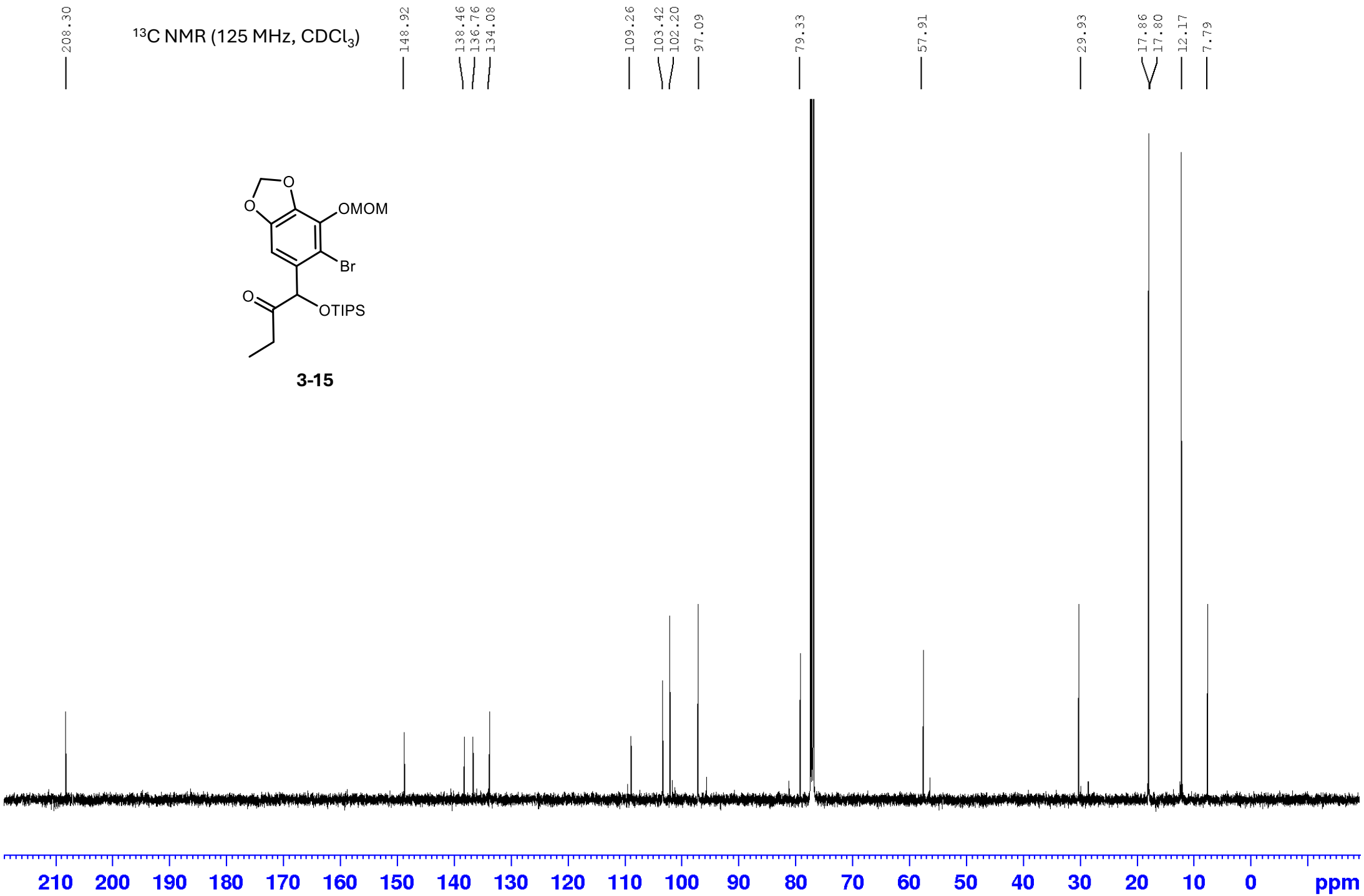


3-15

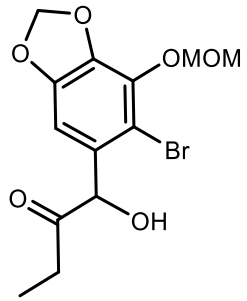


^{13}C NMR (125 MHz, $CDCl_3$)

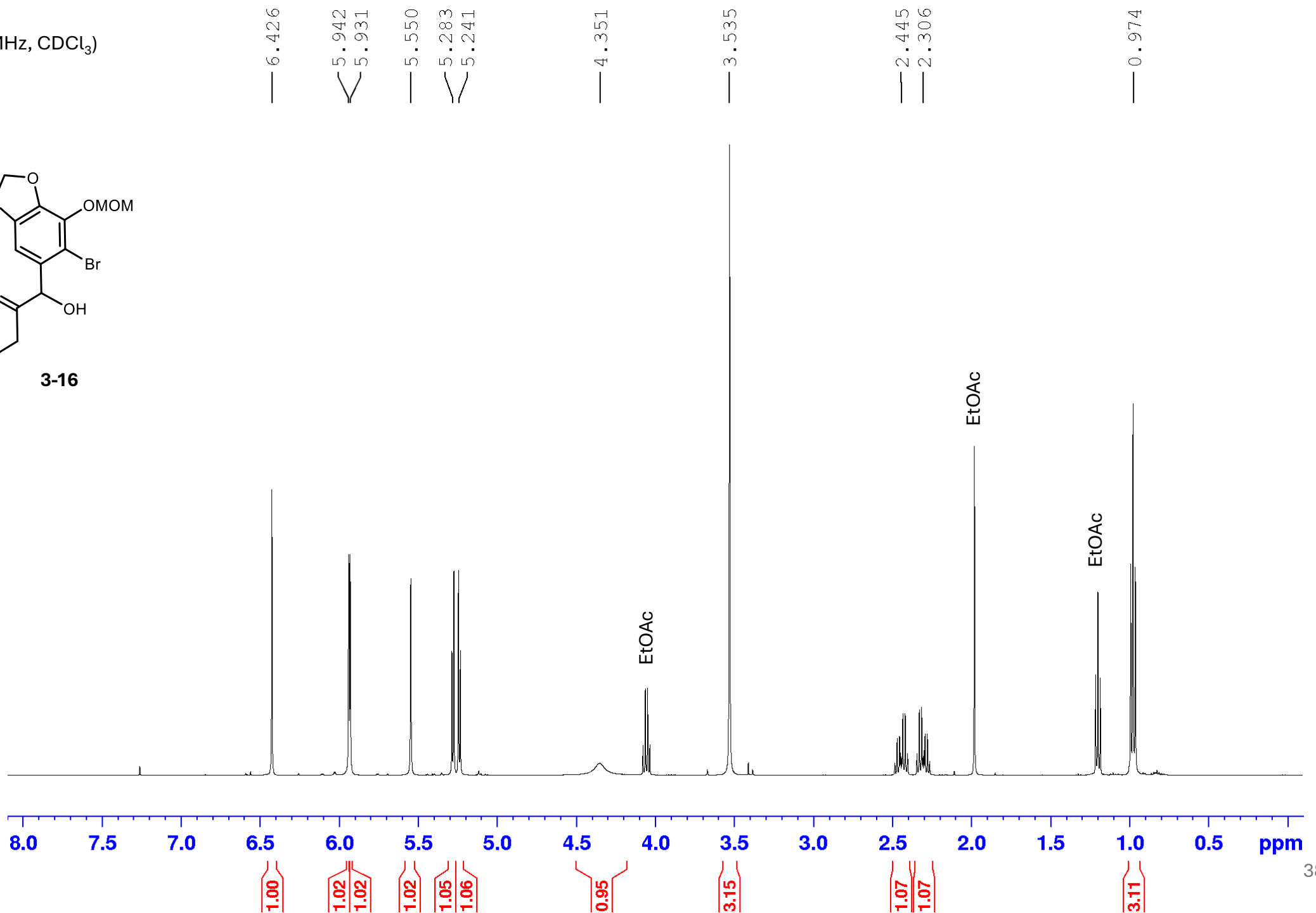
3-15



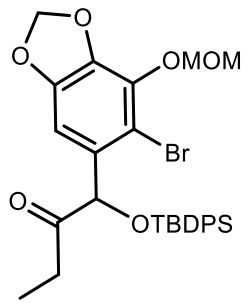
^{1}H NMR (500 MHz, $CDCl_3$)



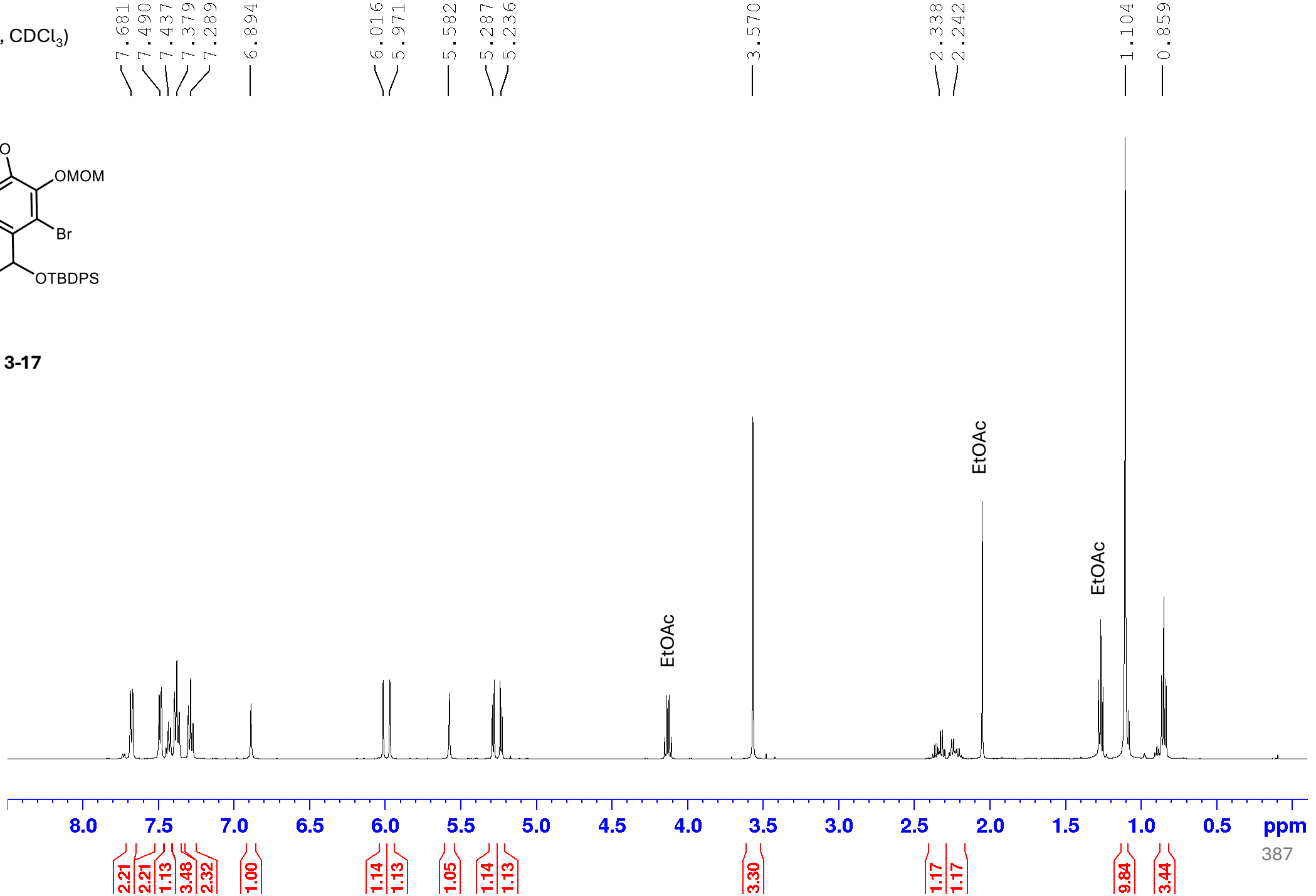
3-16



^{1}H NMR (500 MHz, $CDCl_3$)

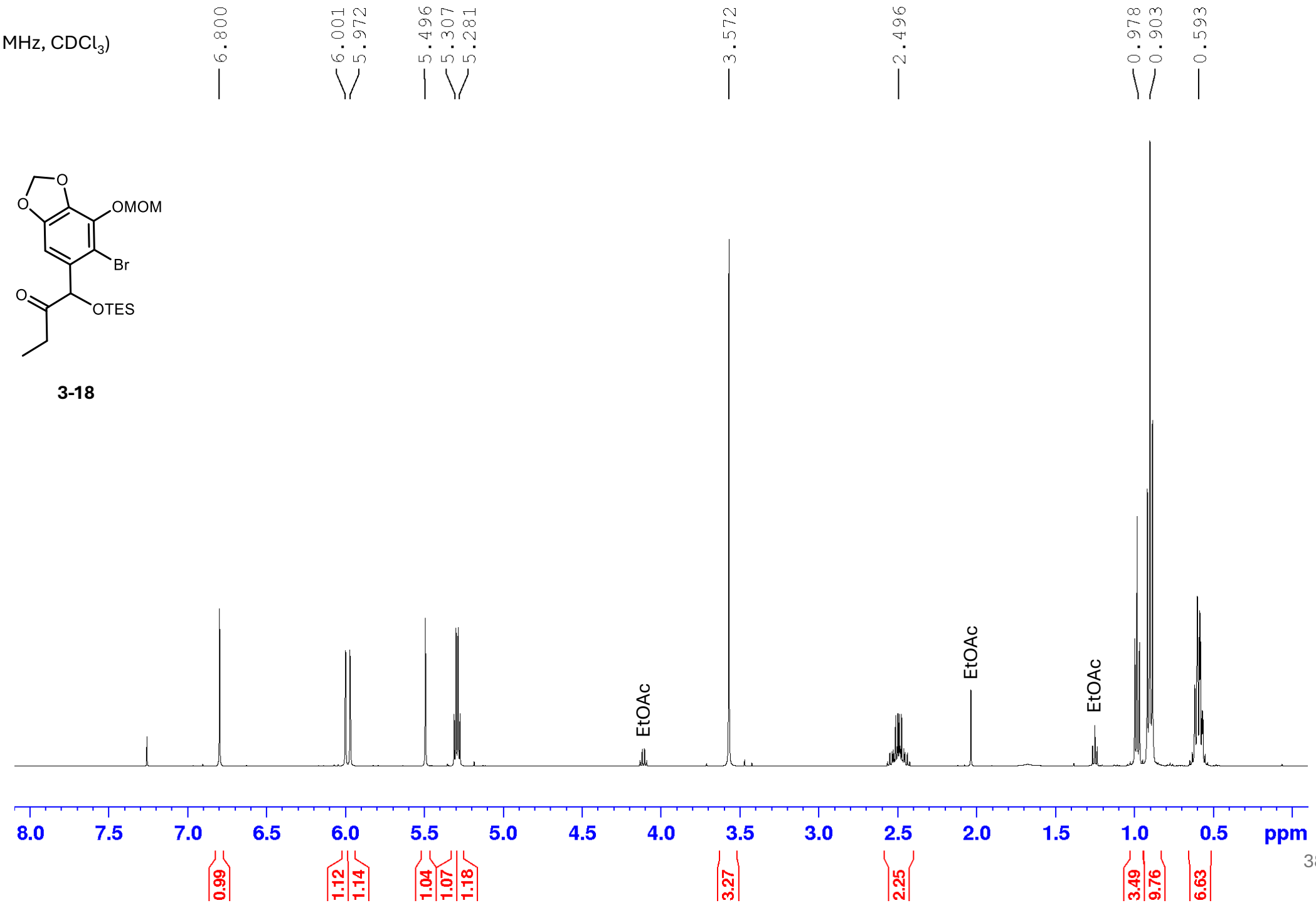


3-17



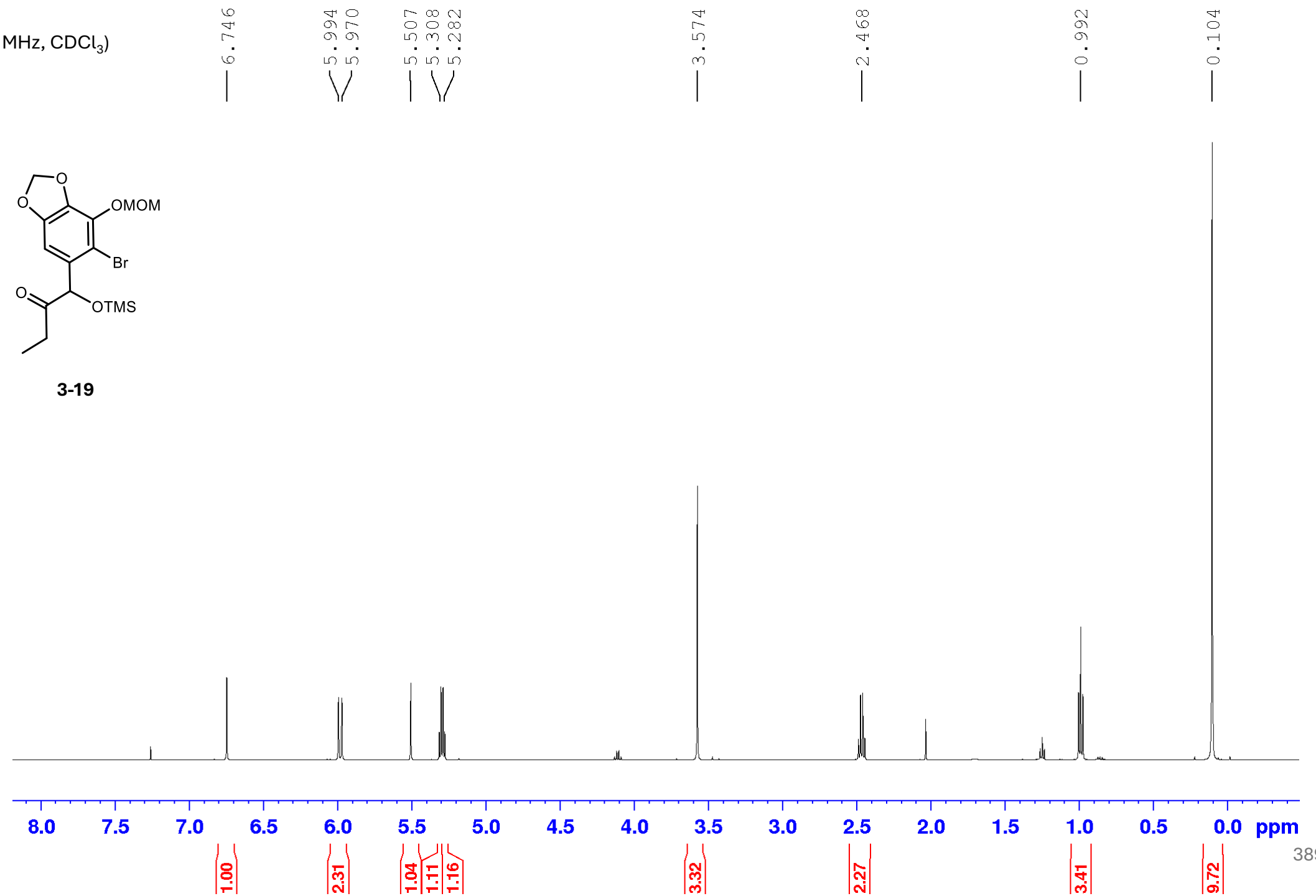
^{1}H NMR (500 MHz, $CDCl_3$)

3-18

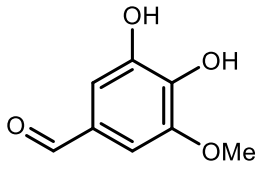


^{1}H NMR (500 MHz, $CDCl_3$)

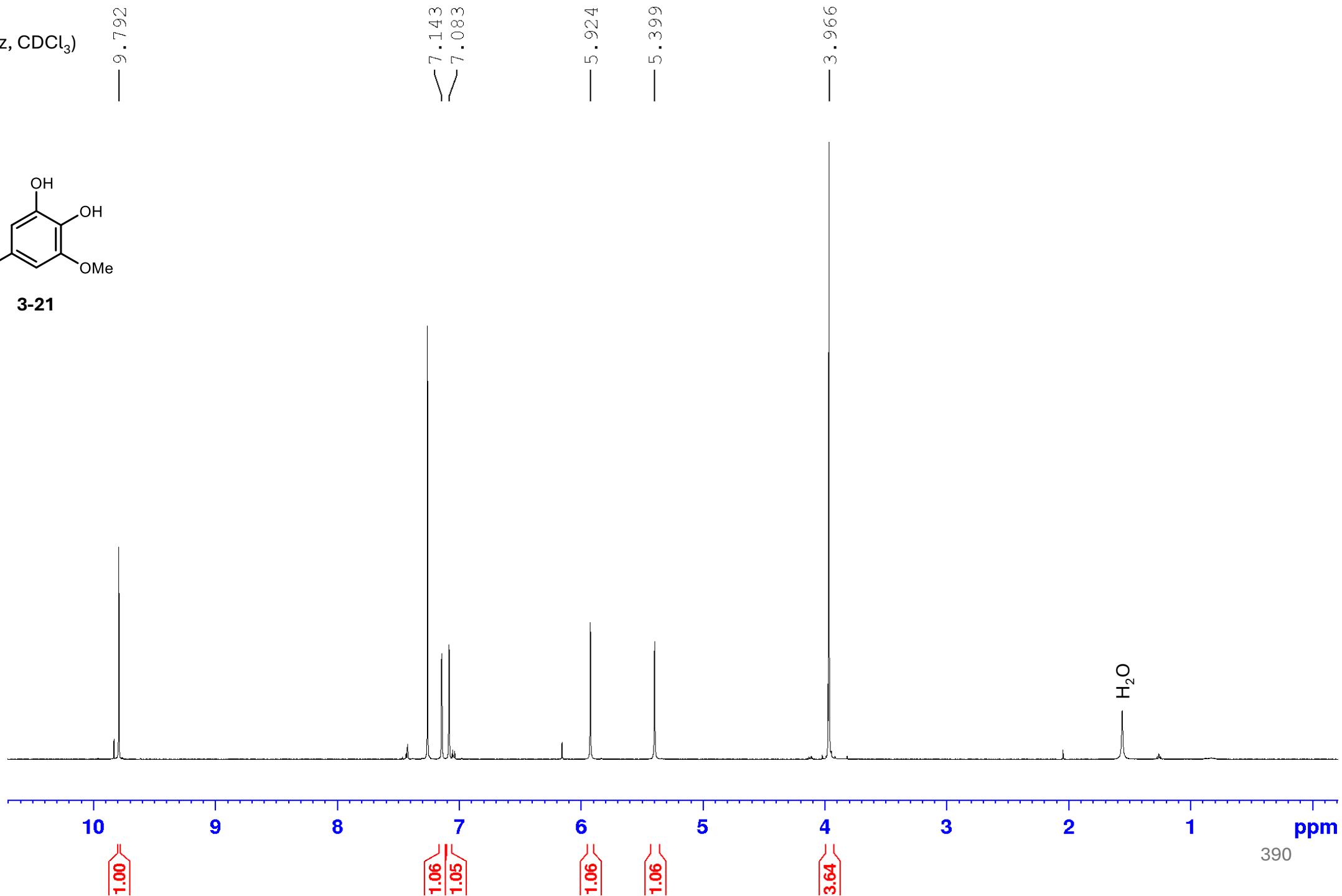
3-19



^{1}H NMR (500 MHz, $CDCl_3$)

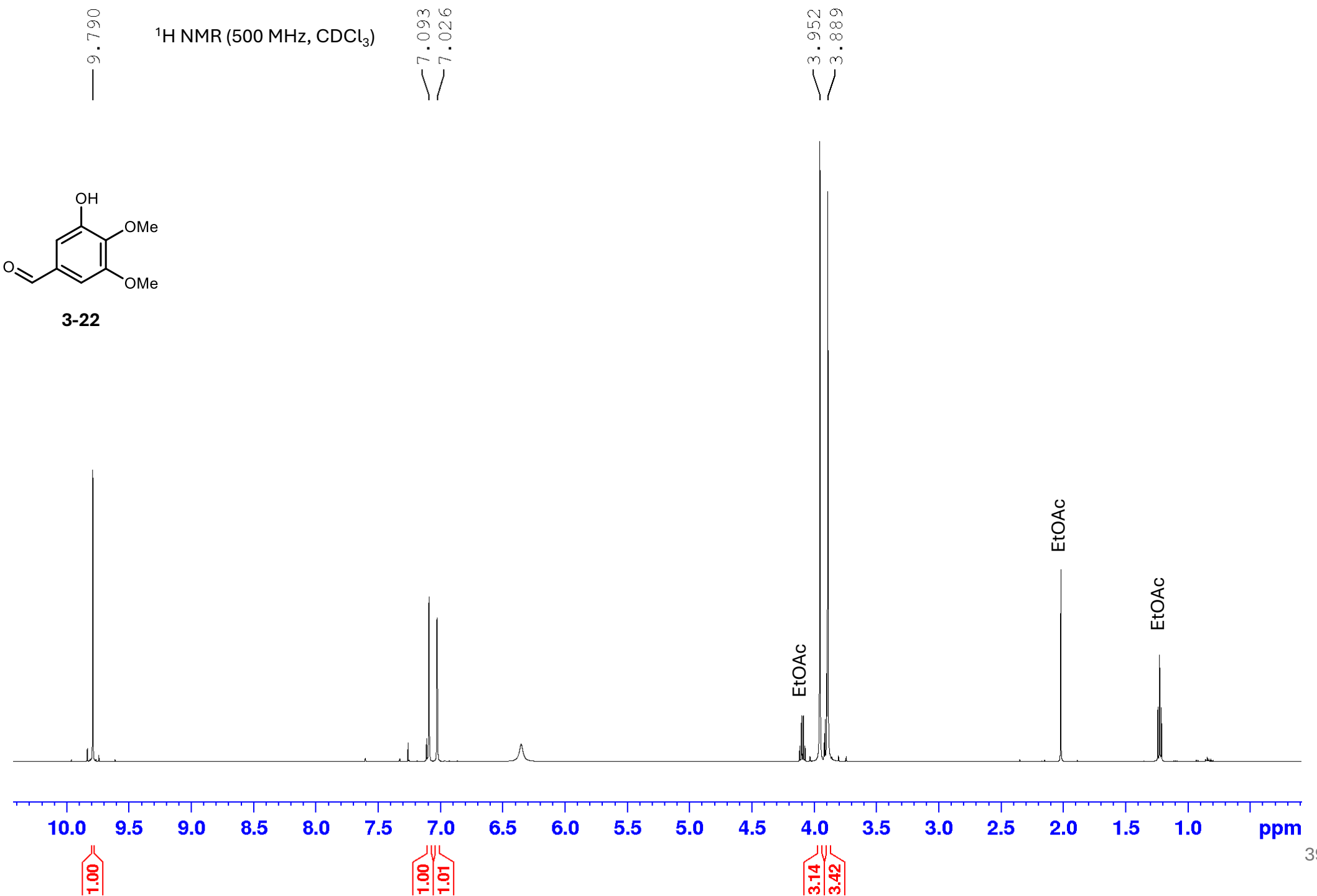


3-21



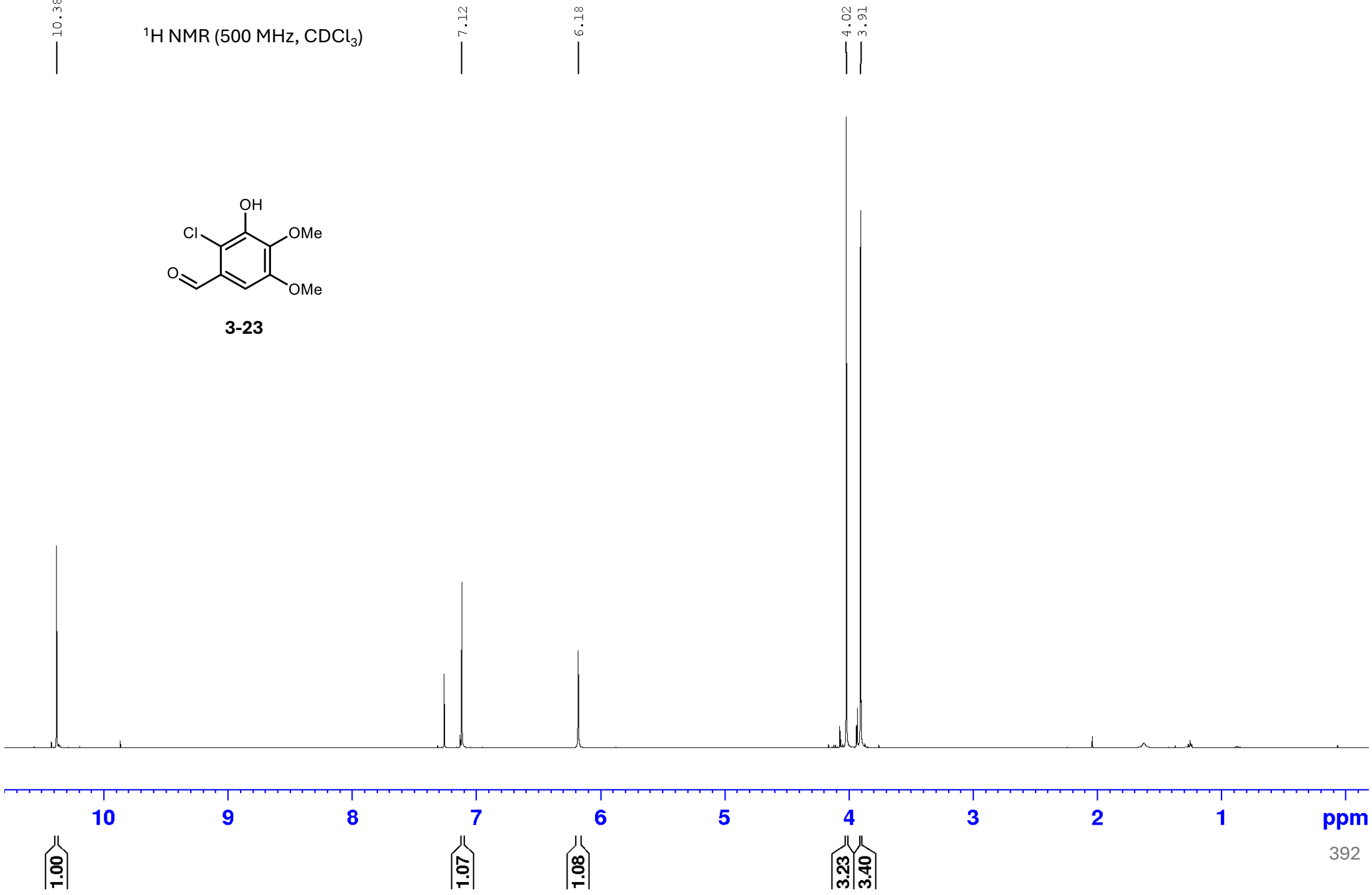
^{1}H NMR (500 MHz, $CDCl_3$)

3-22



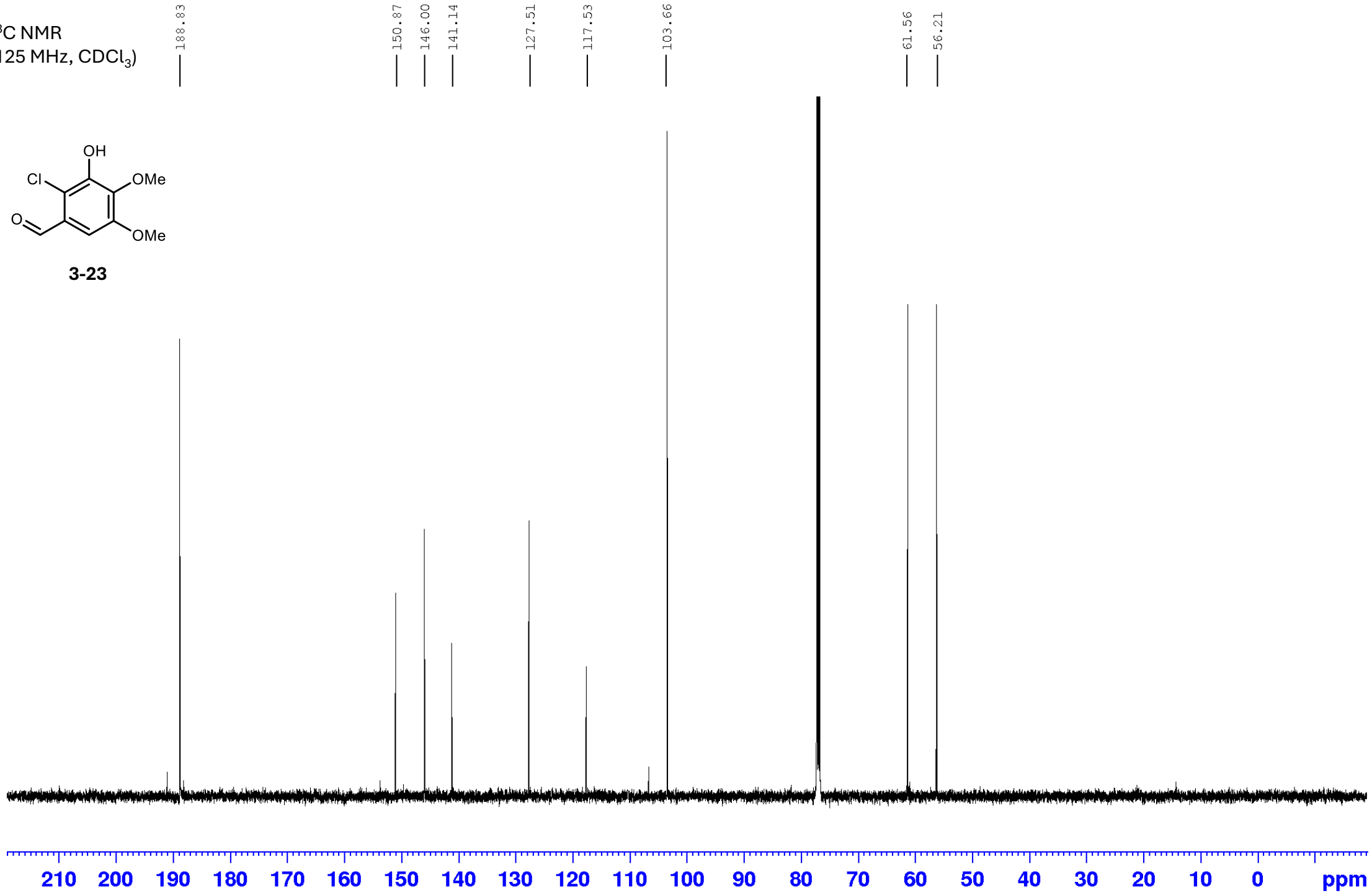
^{1}H NMR (500 MHz, $CDCl_3$)

3-23

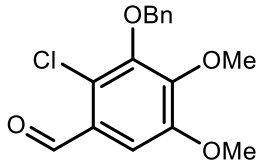


^{13}C NMR
(125 MHz, $CDCl_3$)

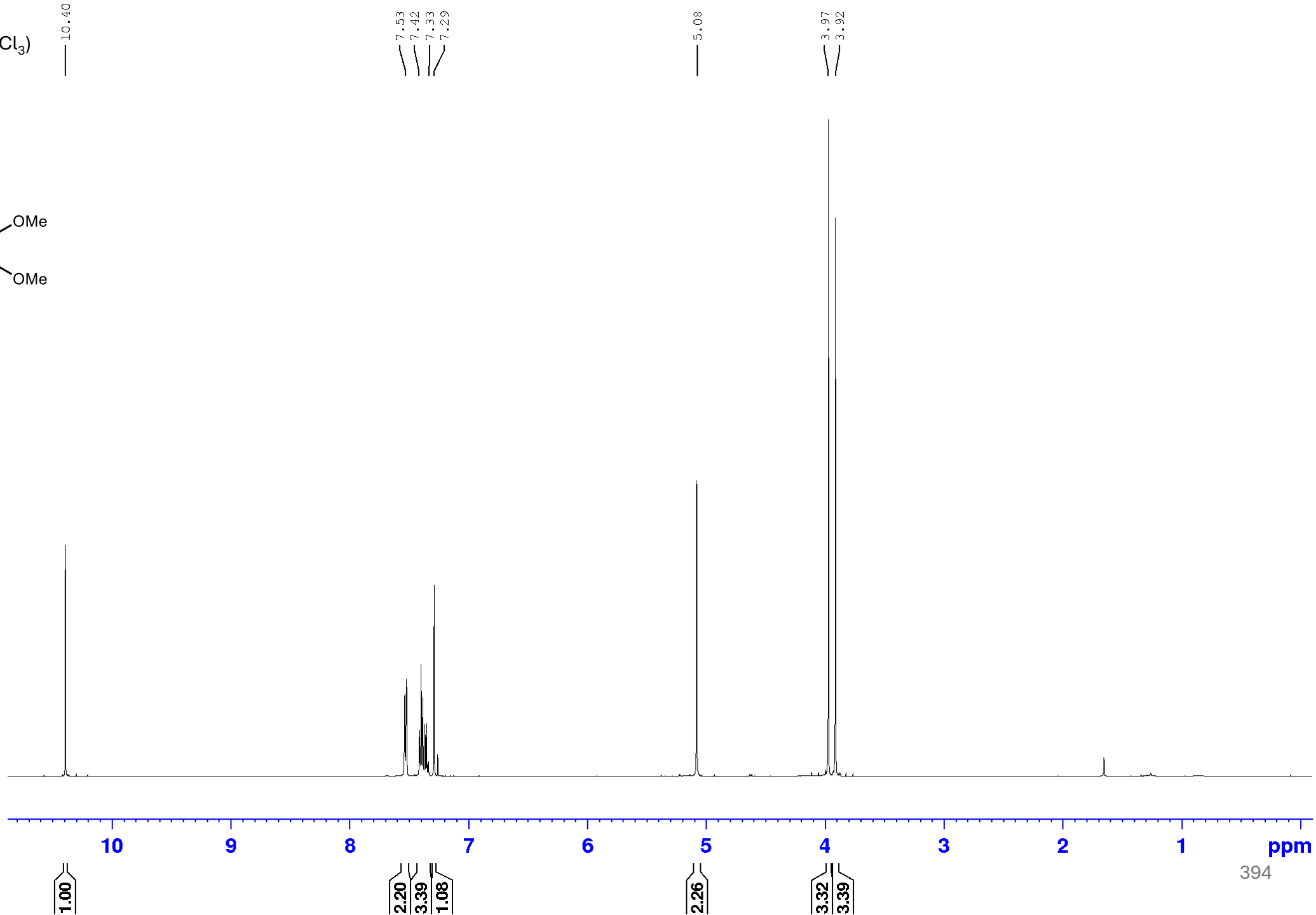
3-23



^{1}H NMR (500 MHz, $CDCl_3$)

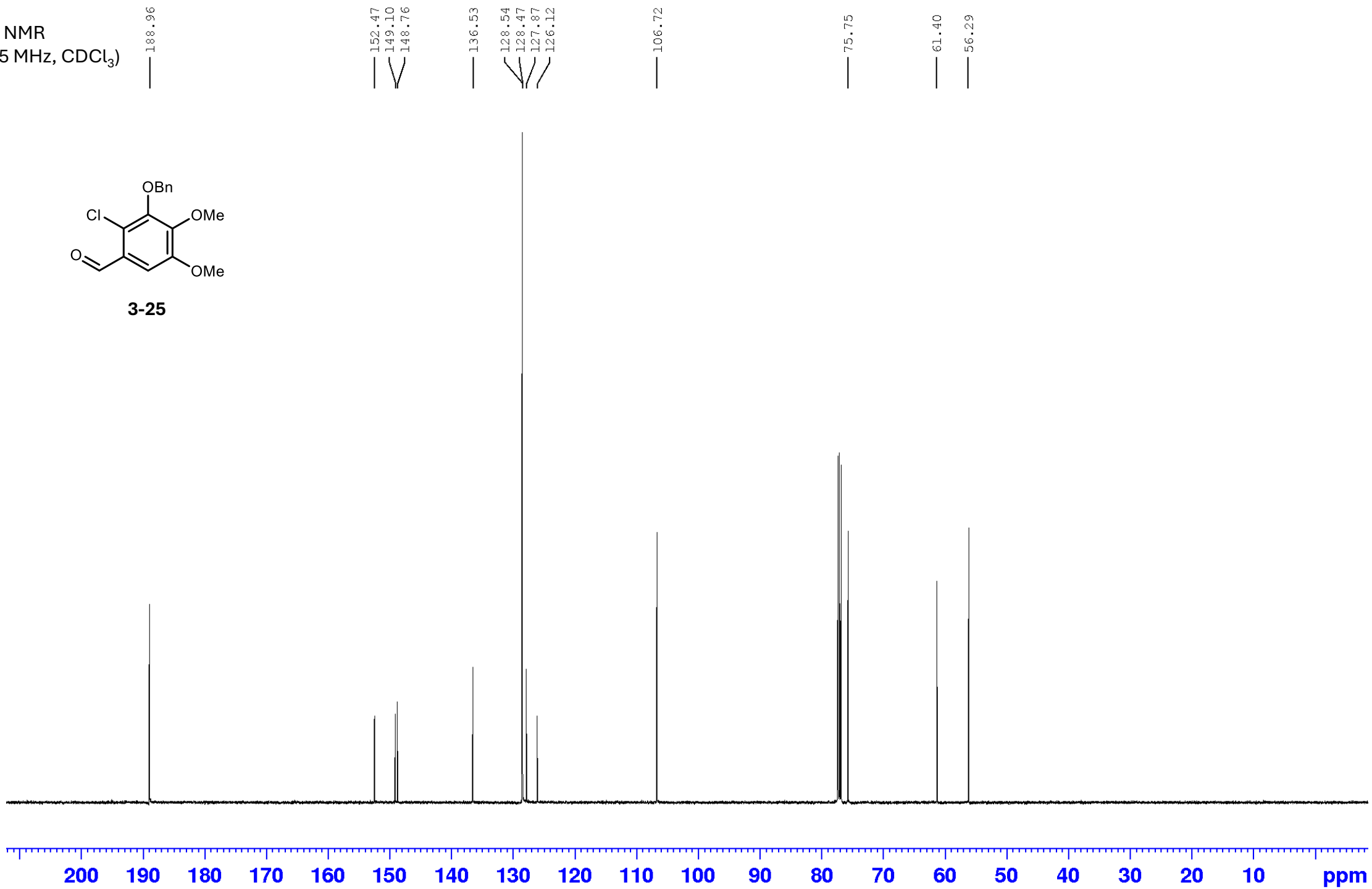


3-25

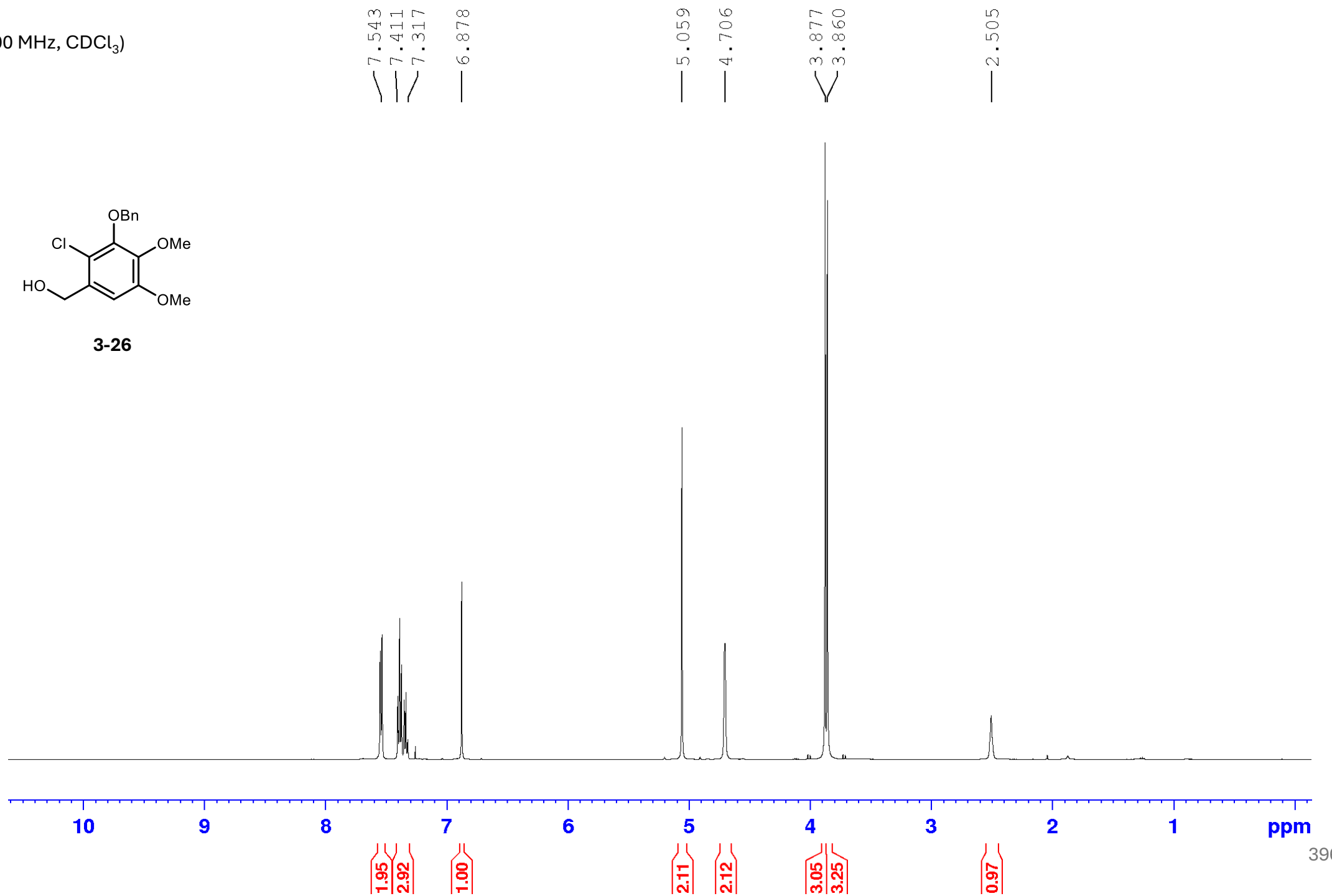


^{13}C NMR
(125 MHz, $CDCl_3$)

3-25



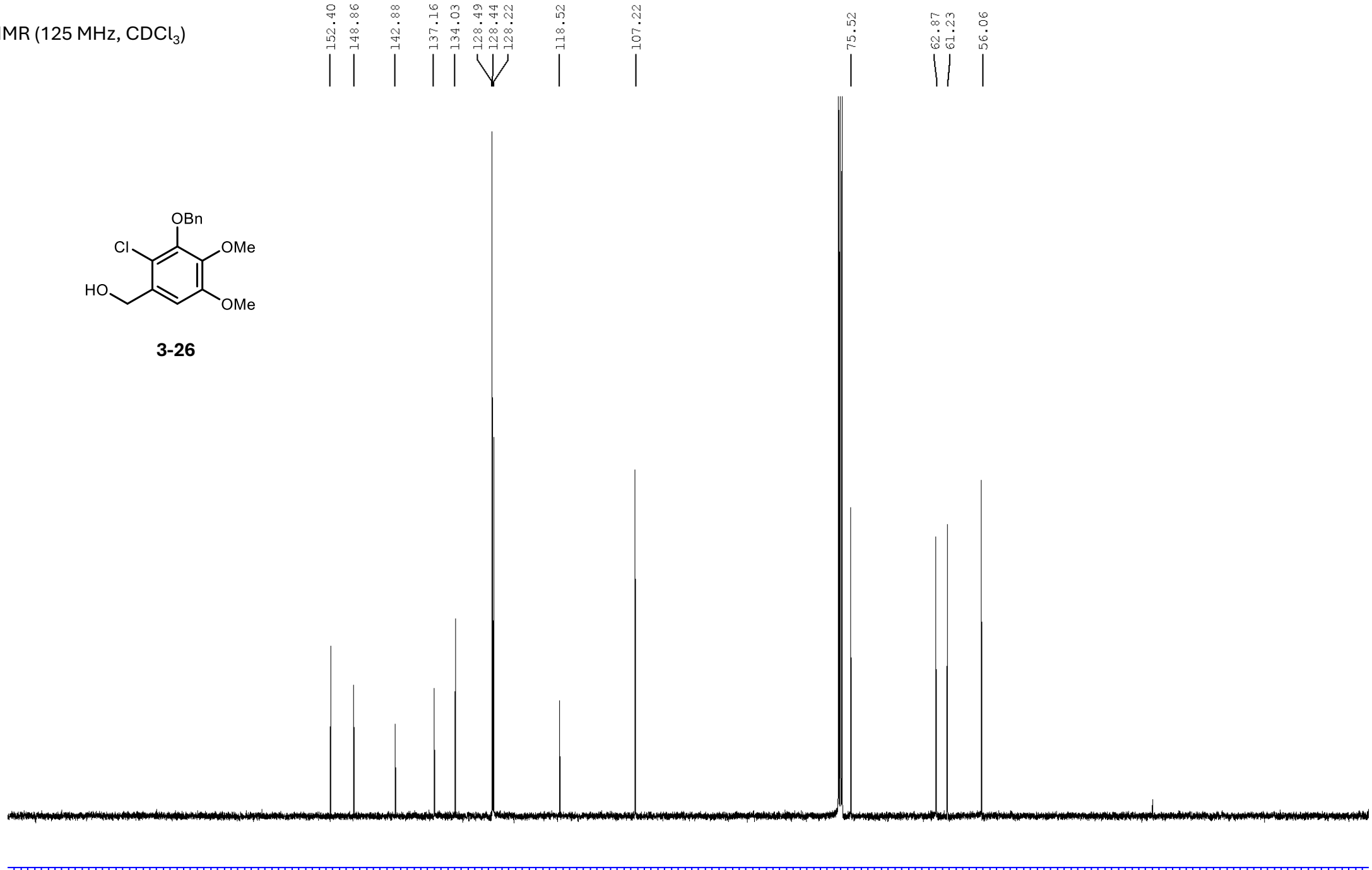
^{1}H NMR (500 MHz, $CDCl_3$)



3-26

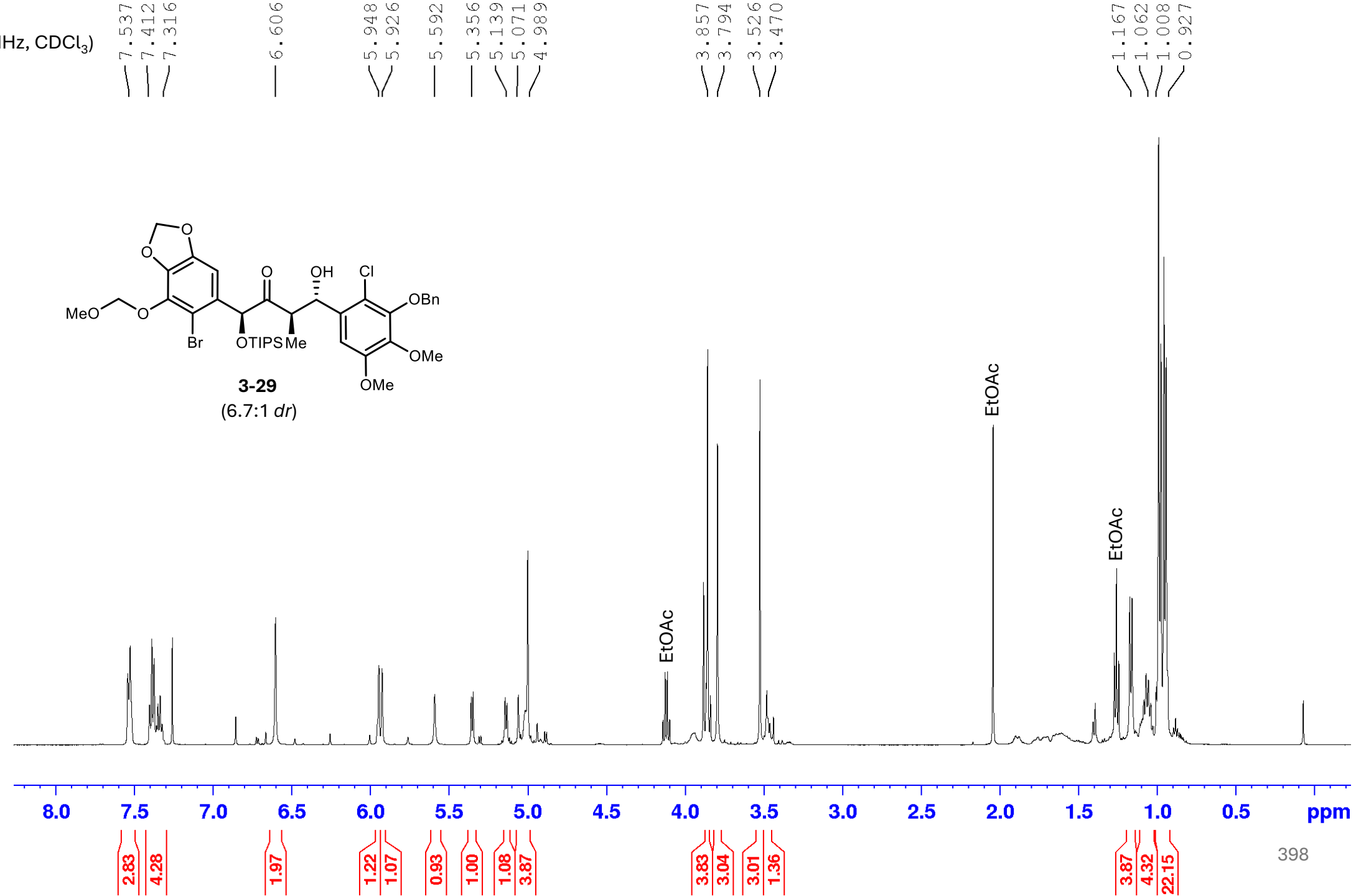
^{13}C NMR (125 MHz, $CDCl_3$)

3-26



^{1}H NMR (500 MHz, $CDCl_3$)

3-29
(6.7:1 *dr*)

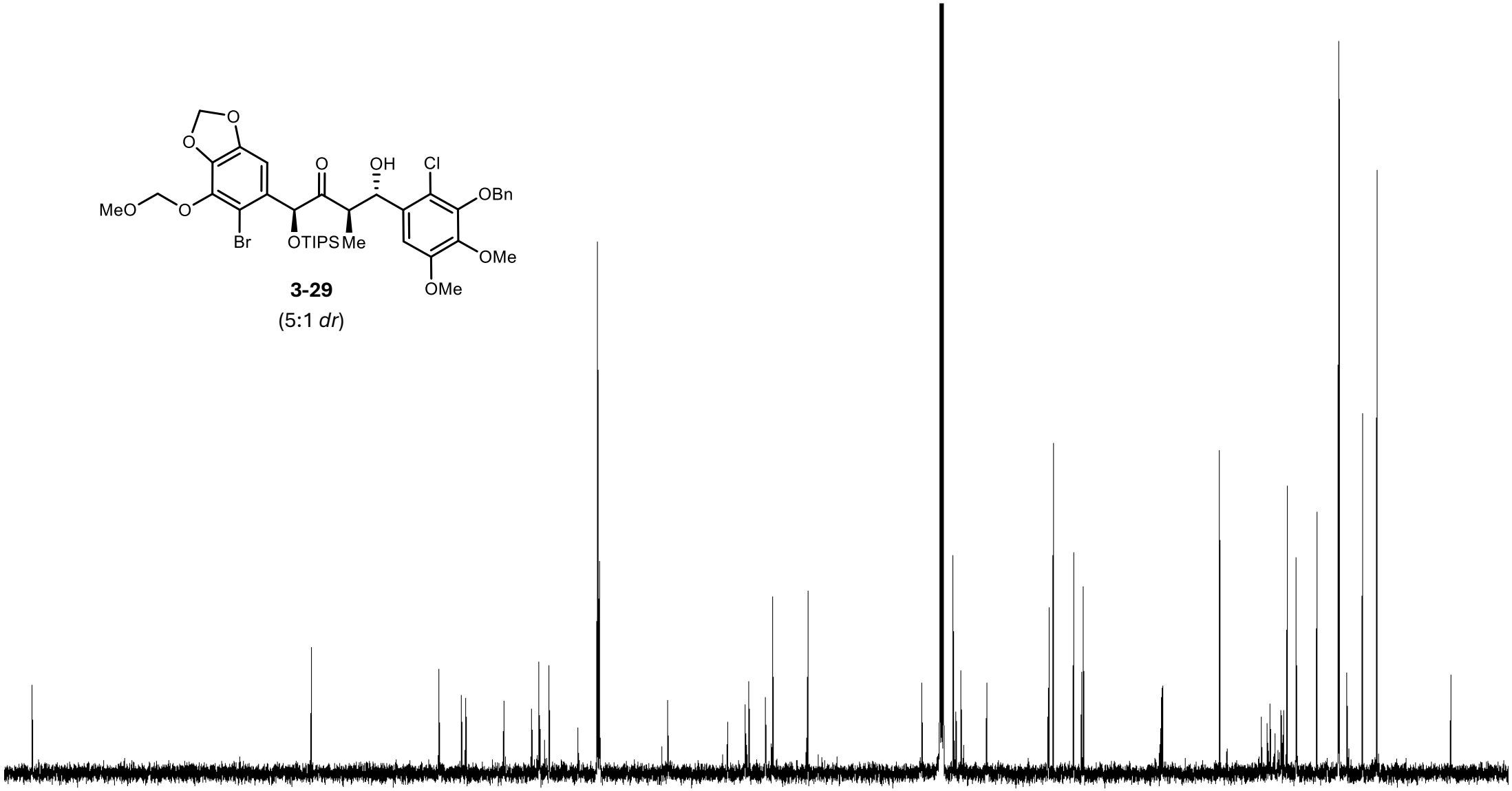


^{13}C NMR (125 MHz, $CDCl_3$)

212.82
152.07
148.73
148.08
142.39
138.28
137.17
135.68
128.41
128.39
128.16
117.93
105.81
102.24
97.01
80.01
75.33
74.15
70.33
61.01
57.33
56.15
55.88
44.08
35.55
25.46
21.05
17.80
17.70
12.08

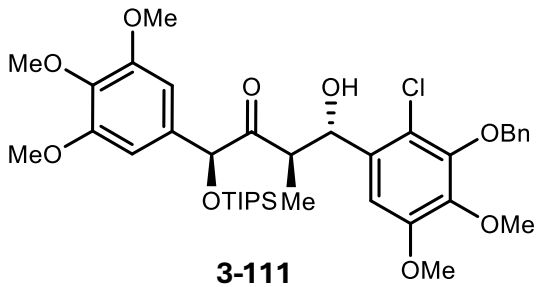
3-29

(5:1 *dr*)



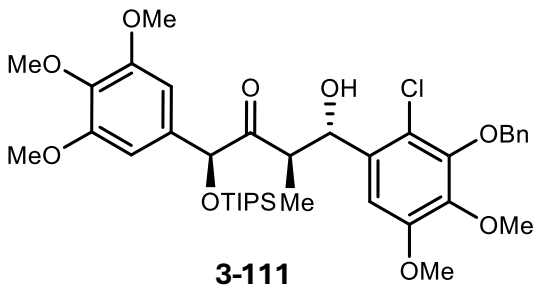
210 200 190 180 170 160 150 140 130 120 110 100 90 80 70 60 50 40 30 20 10 ppm

^{1}H NMR
(500 MHz, $CDCl_3$)



3-111
(4:1 *dr*)

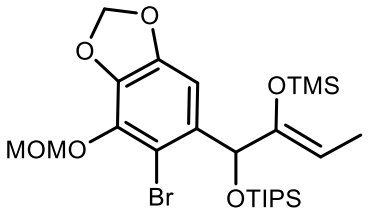
^{13}C NMR (125 MHz, $CDCl_3$)



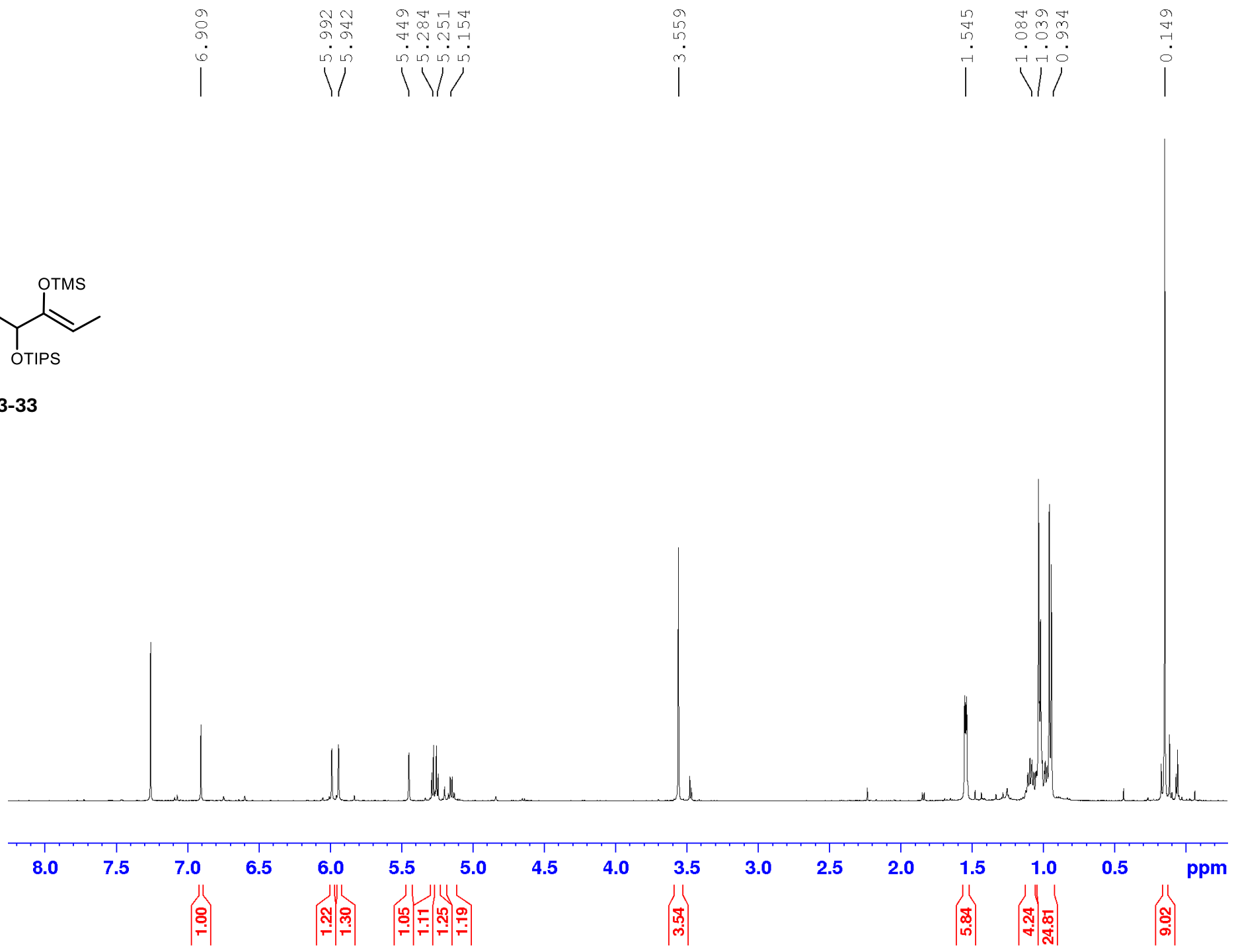
3-111
(4:1 *dr*)

214.75
153.17
152.27
148.36
142.62
137.82
137.17
135.59
134.01
128.37
128.29
128.10
118.82
106.31
103.34
80.81
75.29
73.09
70.15
61.14
60.91
56.11
56.01
45.97
17.97
15.74
12.18

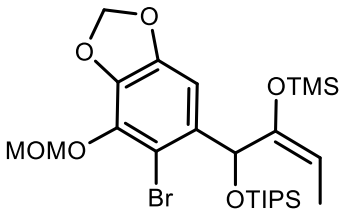
^{1}H NMR (500 MHz, $CDCl_3$)



***Z*-3-33**



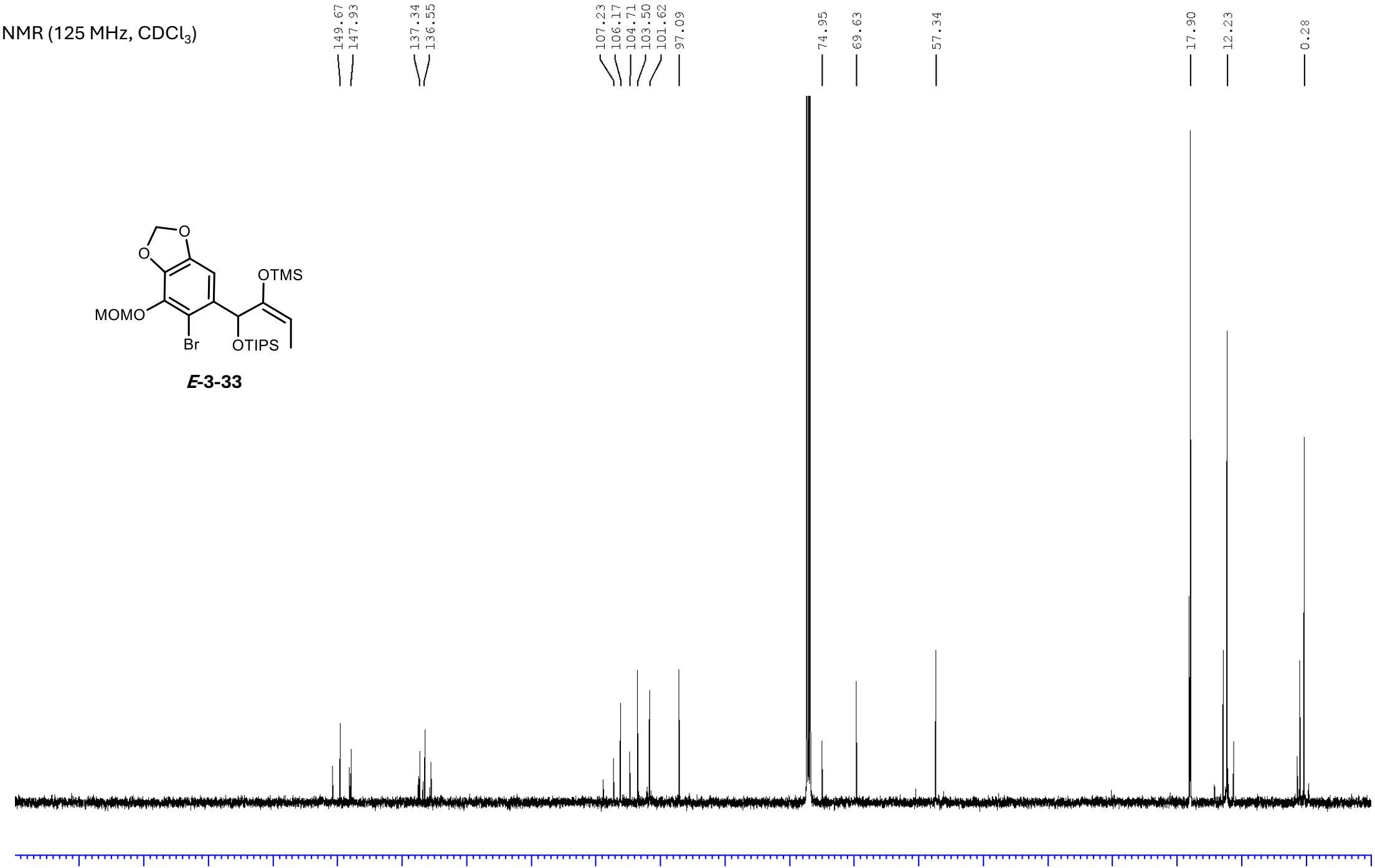
^{1}H NMR (500 MHz, $CDCl_3$)



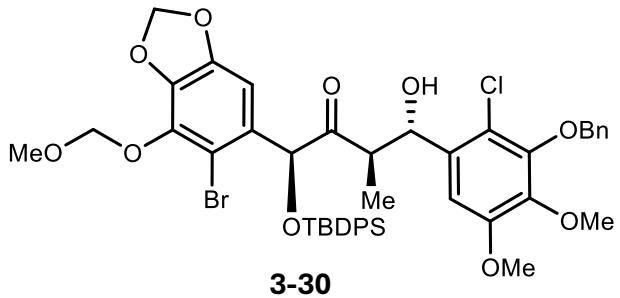
***E*-3-33**

^{13}C NMR (125 MHz, $CDCl_3$)

***E*-3-33**

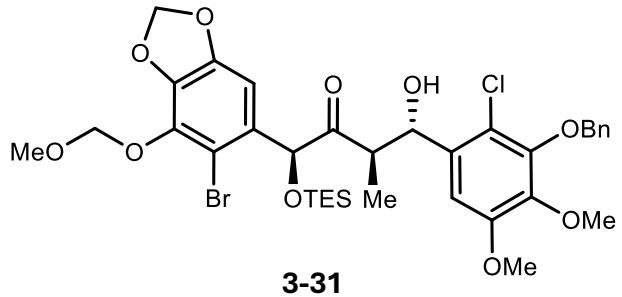


^{1}H NMR (500 MHz, $CDCl_3$)



3-30

^{1}H NMR
(500 MHz, $CDCl_3$)



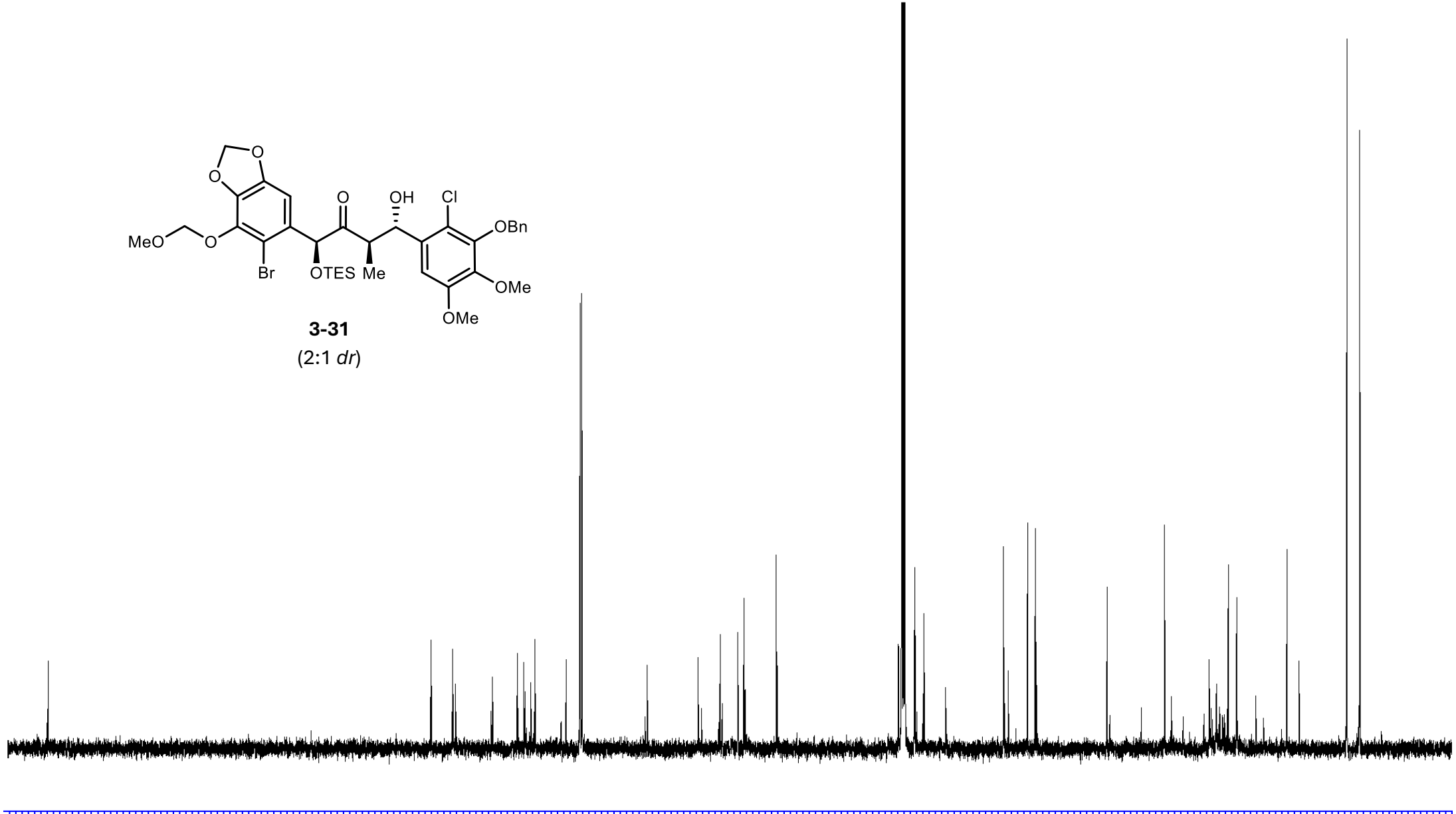
3-31
(2:1 *dr*)

^{13}C NMR (125 MHz, $CDCl_3$)

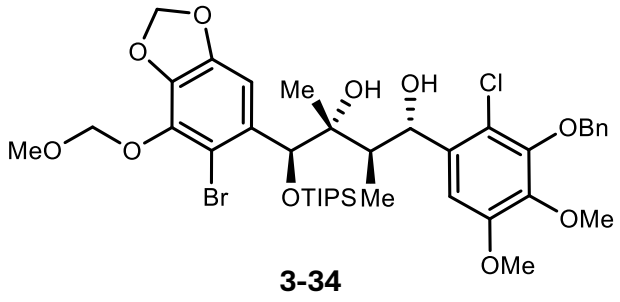
213.00
152.04
148.64
138.39
135.59
128.38
128.12
128.04
106.16
103.35
102.40
97.26
77.85
75.35
75.20
73.77
61.14
57.36
56.13
44.70
35.57
25.47
24.14
16.14
6.58
4.56

3-31

(2:1 *dr*)

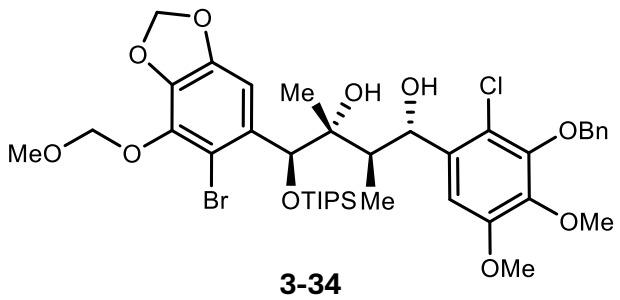


^{1}H NMR (500 MHz, $CDCl_3$)



3-34

^{13}C NMR (125 MHz, $CDCl_3$)

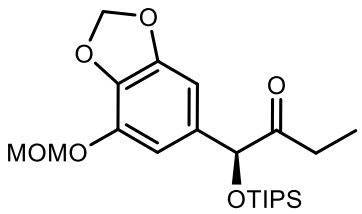


3-34

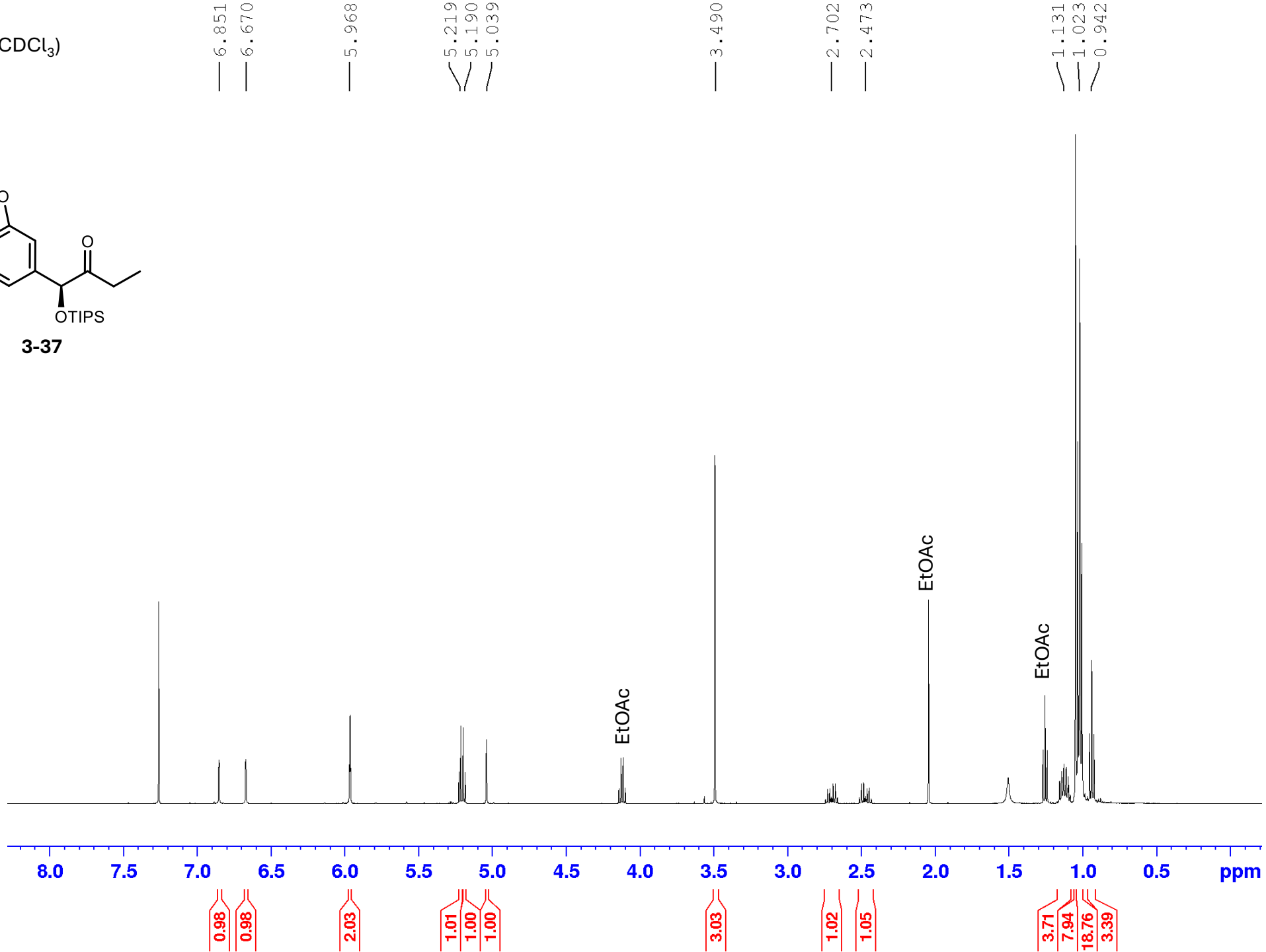
152.46
148.51
147.93
142.61
138.26
137.60
137.12
136.24
134.98
128.47
128.34
128.08
119.51
110.93
106.61
105.71
102.00
97.10
81.18
76.58
75.30
72.63
61.17
57.43
56.16
48.41
27.67
26.96
18.19
17.98
12.83

210 200 190 180 170 160 150 140 130 120 110 100 90 80 70 60 50 40 30 20 10 ppm

^{1}H NMR (500 MHz, $CDCl_3$)

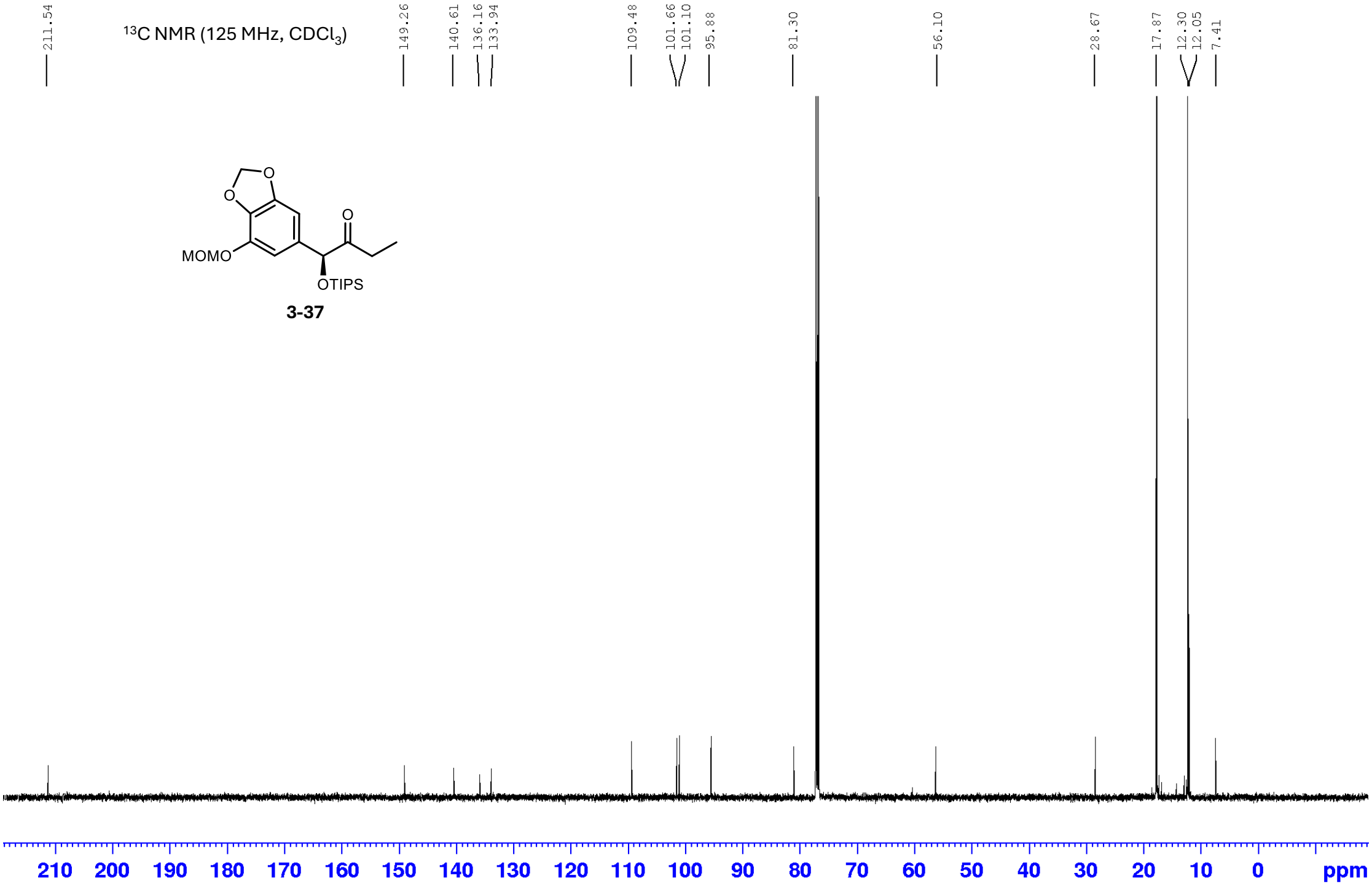


3-37



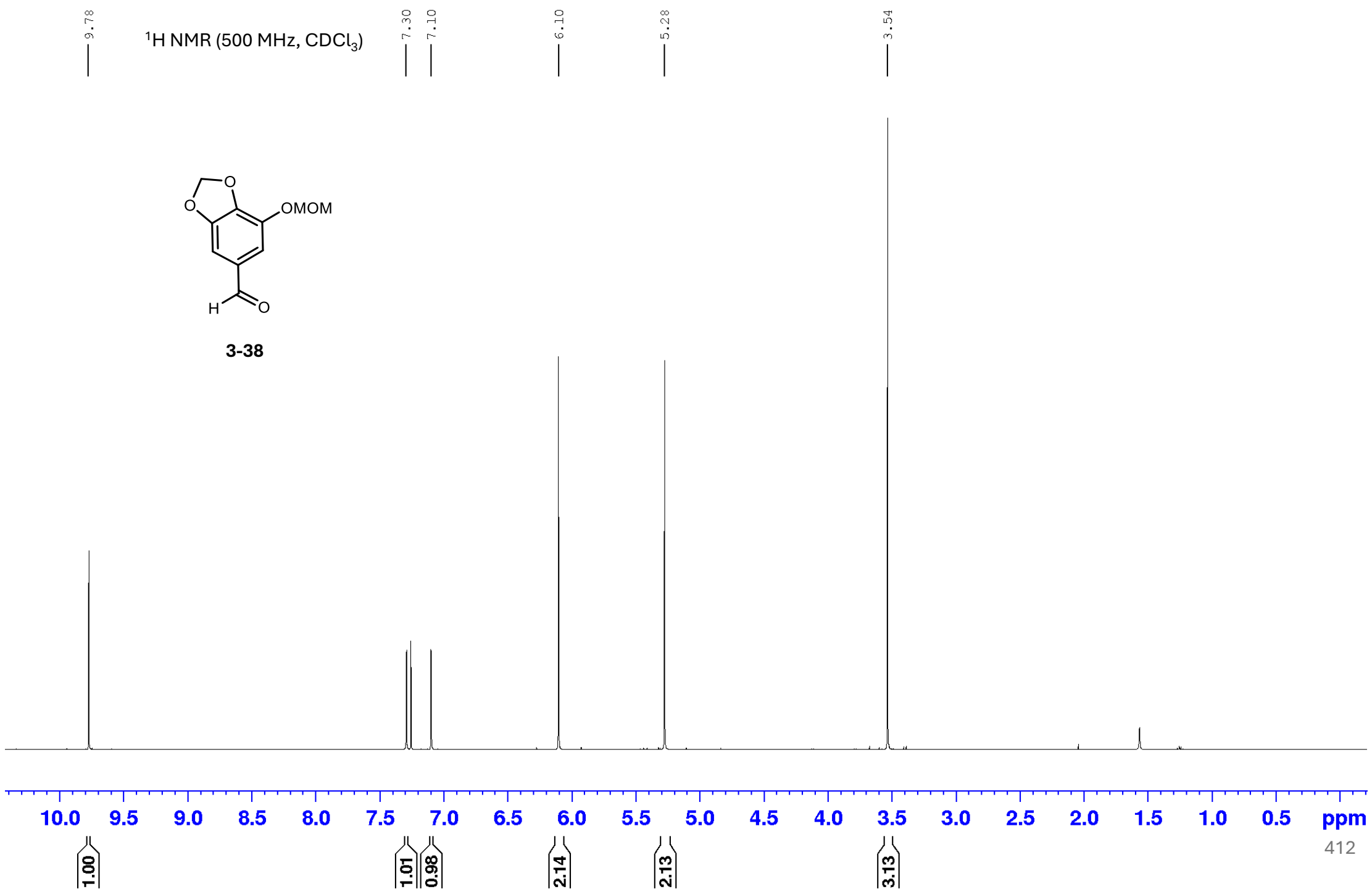
^{13}C NMR (125 MHz, $CDCl_3$)

3-37

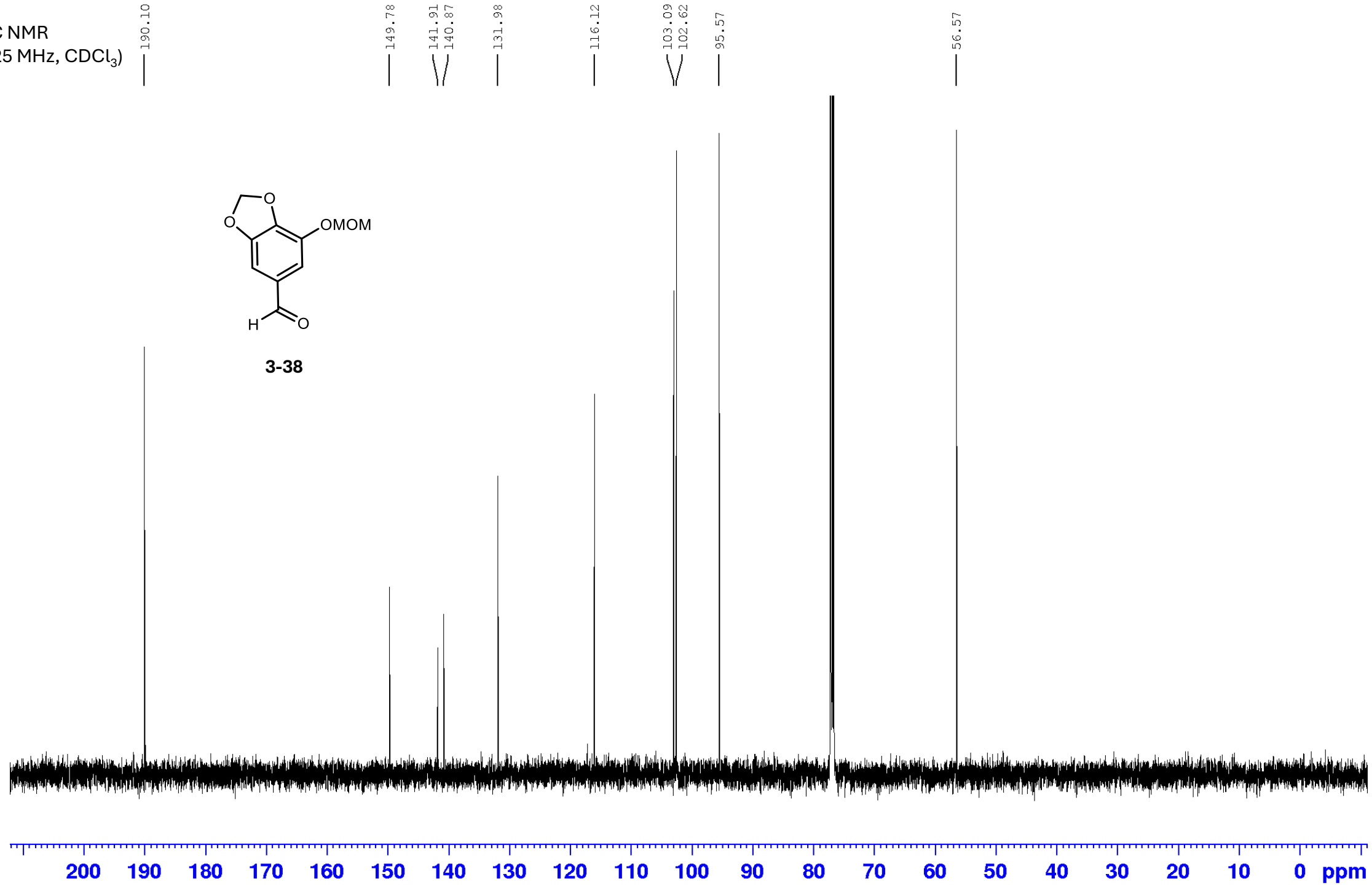


^{1}H NMR (500 MHz, $CDCl_3$)

3-38

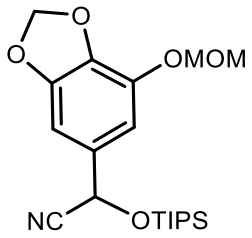


^{13}C NMR
(125 MHz, $CDCl_3$)

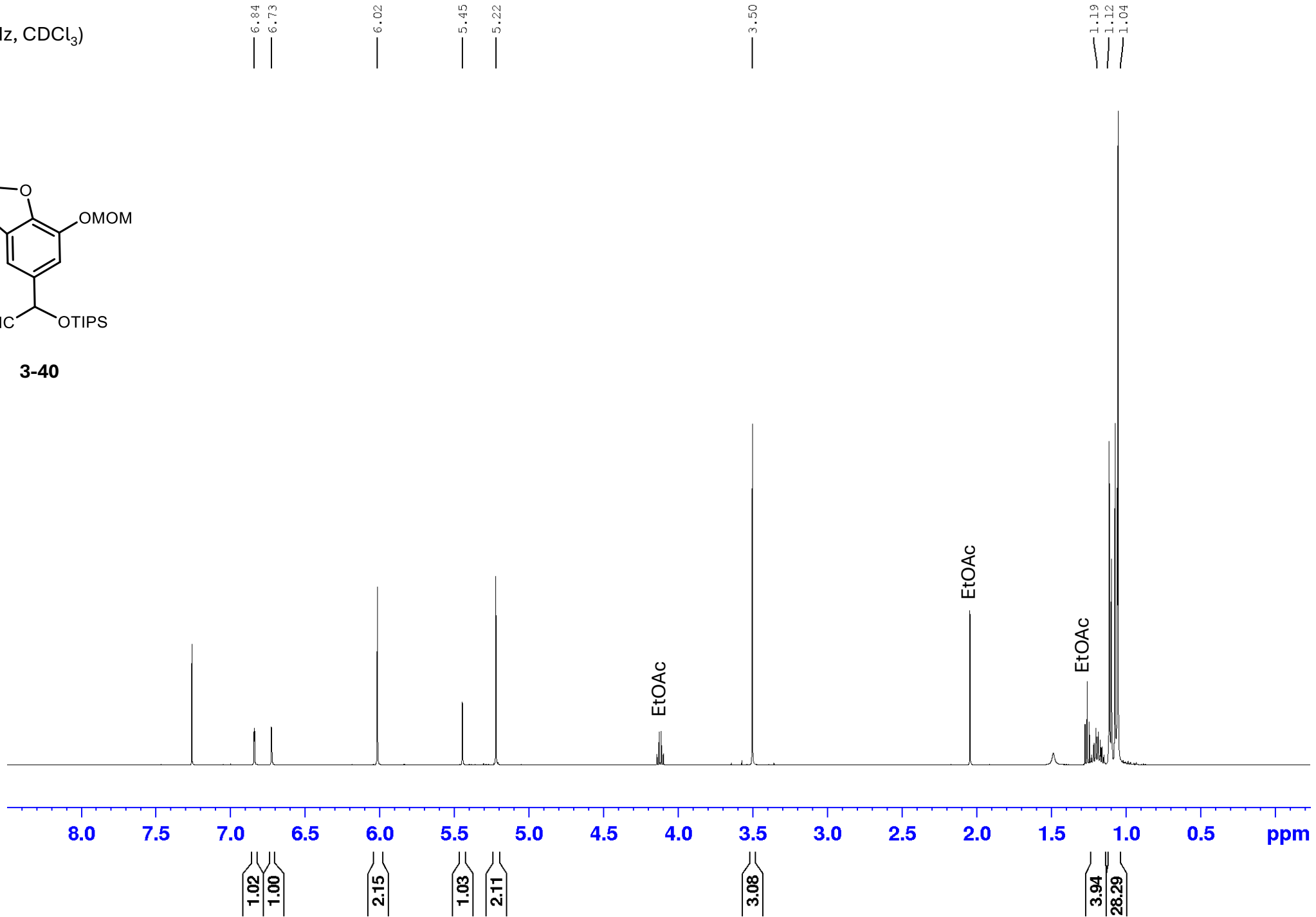


3-38

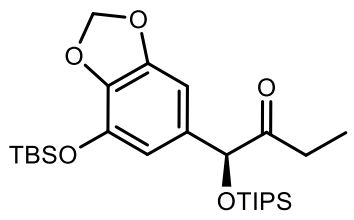
^{1}H NMR (500 MHz, $CDCl_3$)



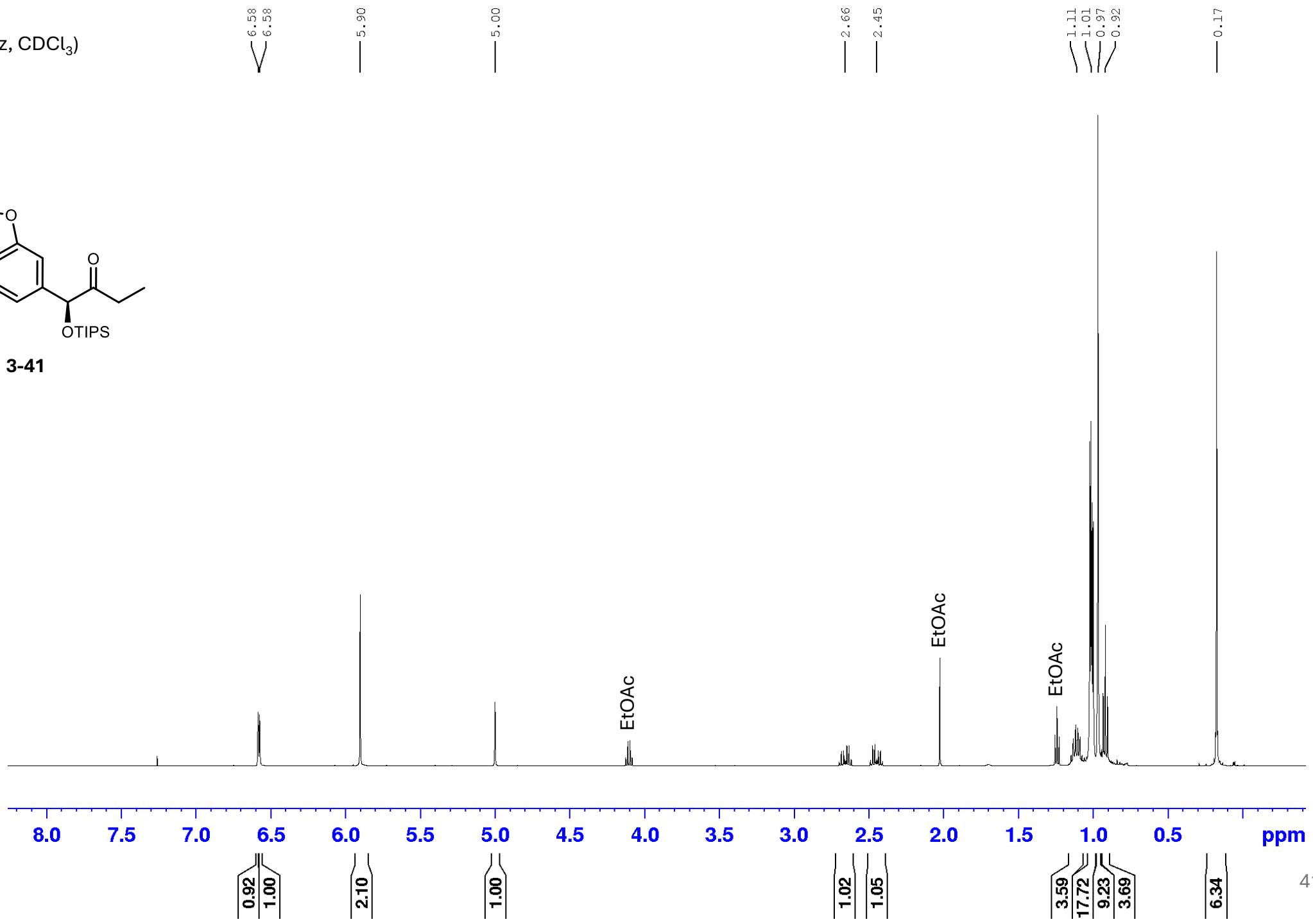
3-40



^{1}H NMR (500 MHz, $CDCl_3$)



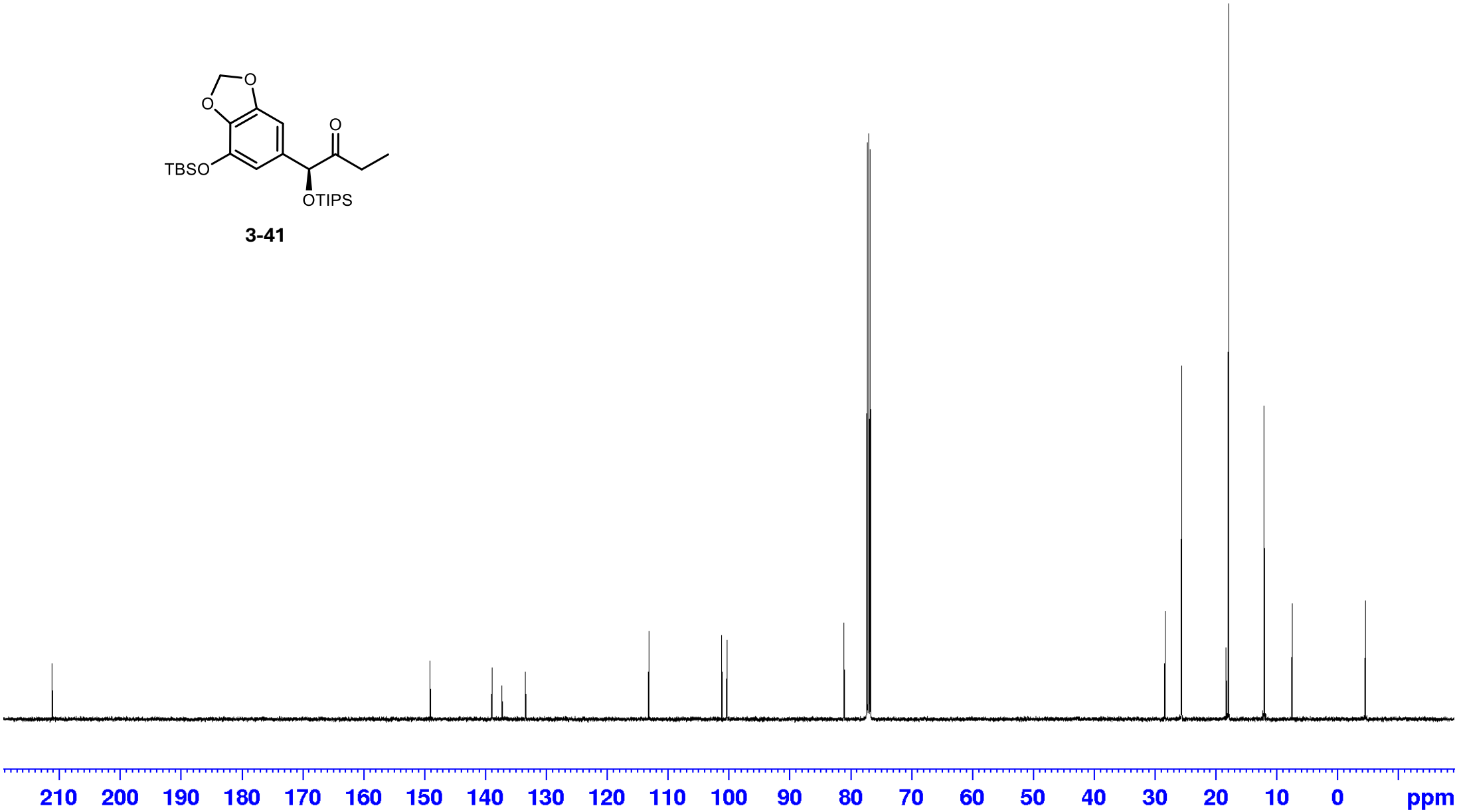
3-41



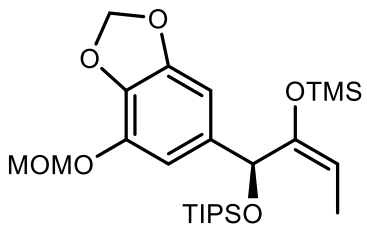
^{13}C NMR (125 MHz, $CDCl_3$)

211.23
149.28
139.26
137.40
133.44
112.95
101.30
100.37
81.13
28.41
25.64
18.31
17.93
12.11
7.45
-4.66

3-41



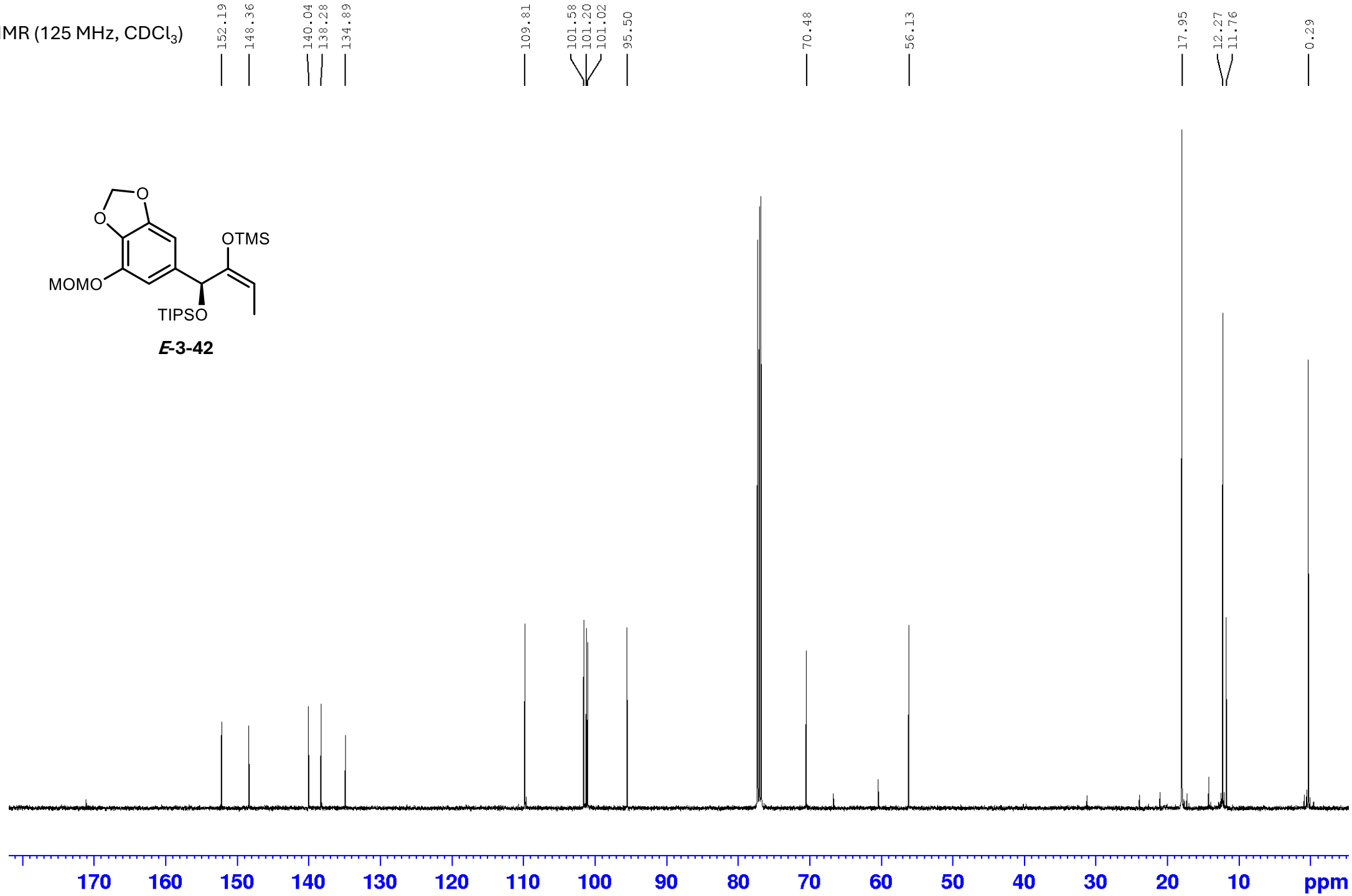
^{1}H NMR (500 MHz, $CDCl_3$)



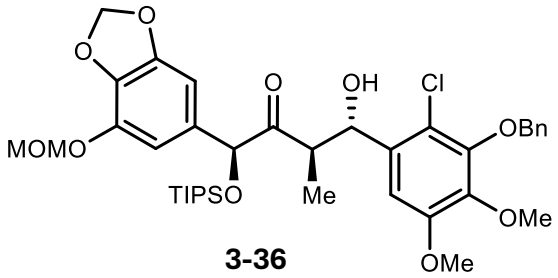
***E*-3-42**

^{13}C NMR (125 MHz, $CDCl_3$)

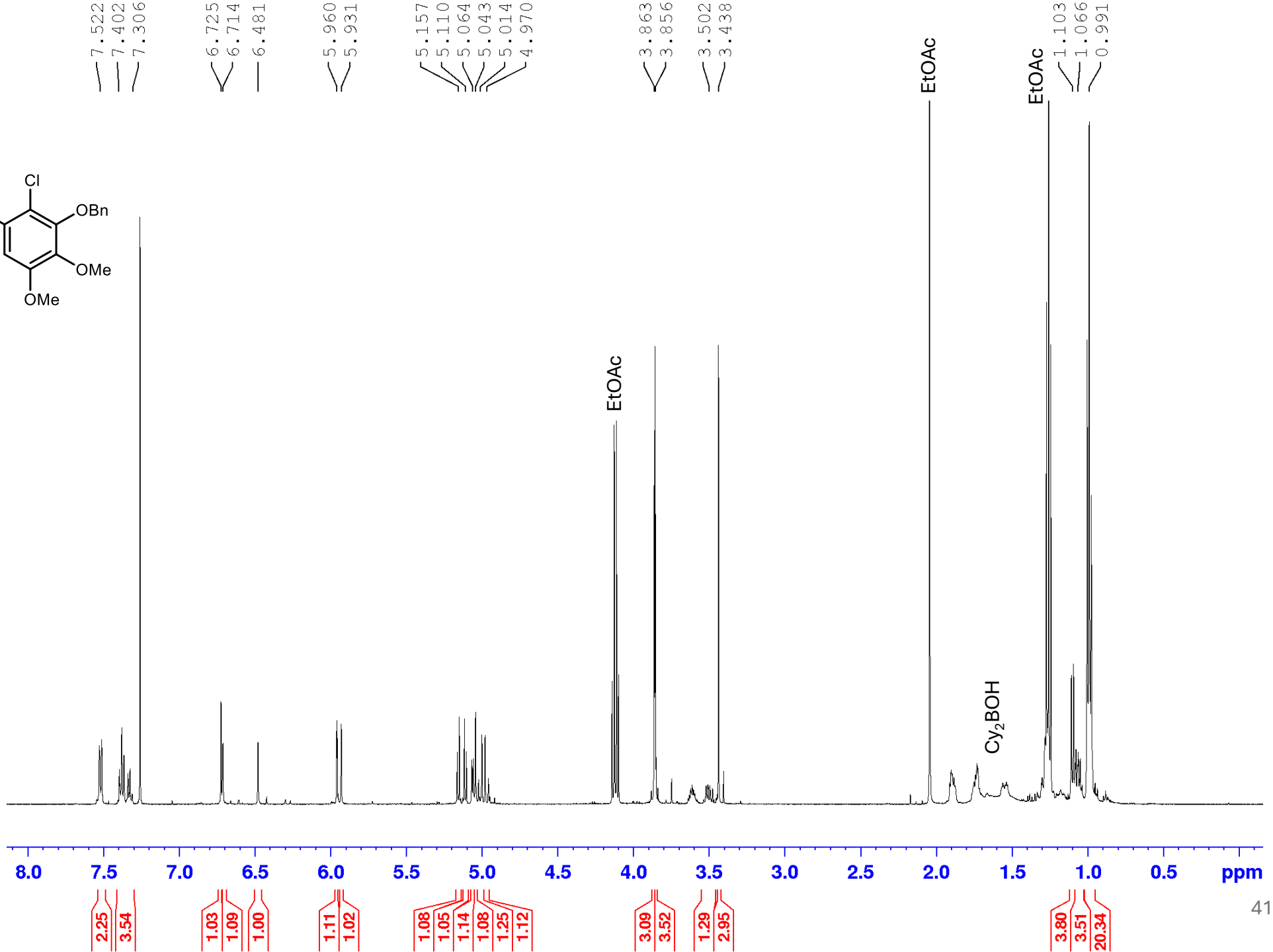
***E*-3-42**



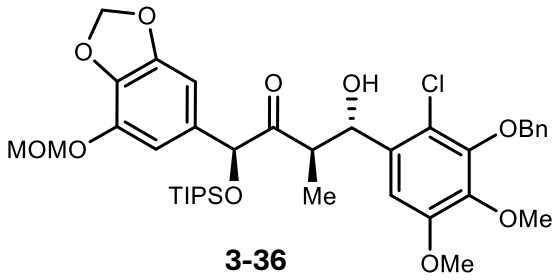
^{1}H NMR (500 MHz, $CDCl_3$)



3-36
(6.4:1 *dr*)



^{13}C NMR (125 MHz, $CDCl_3$)



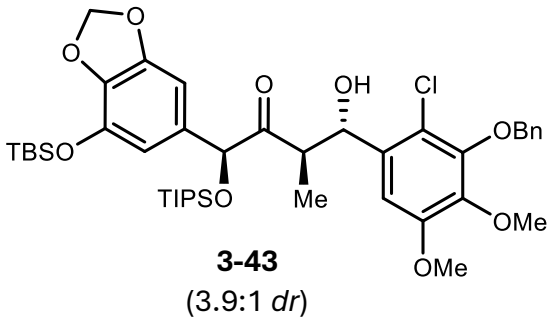
3-36

(4.8:1 *dr*)

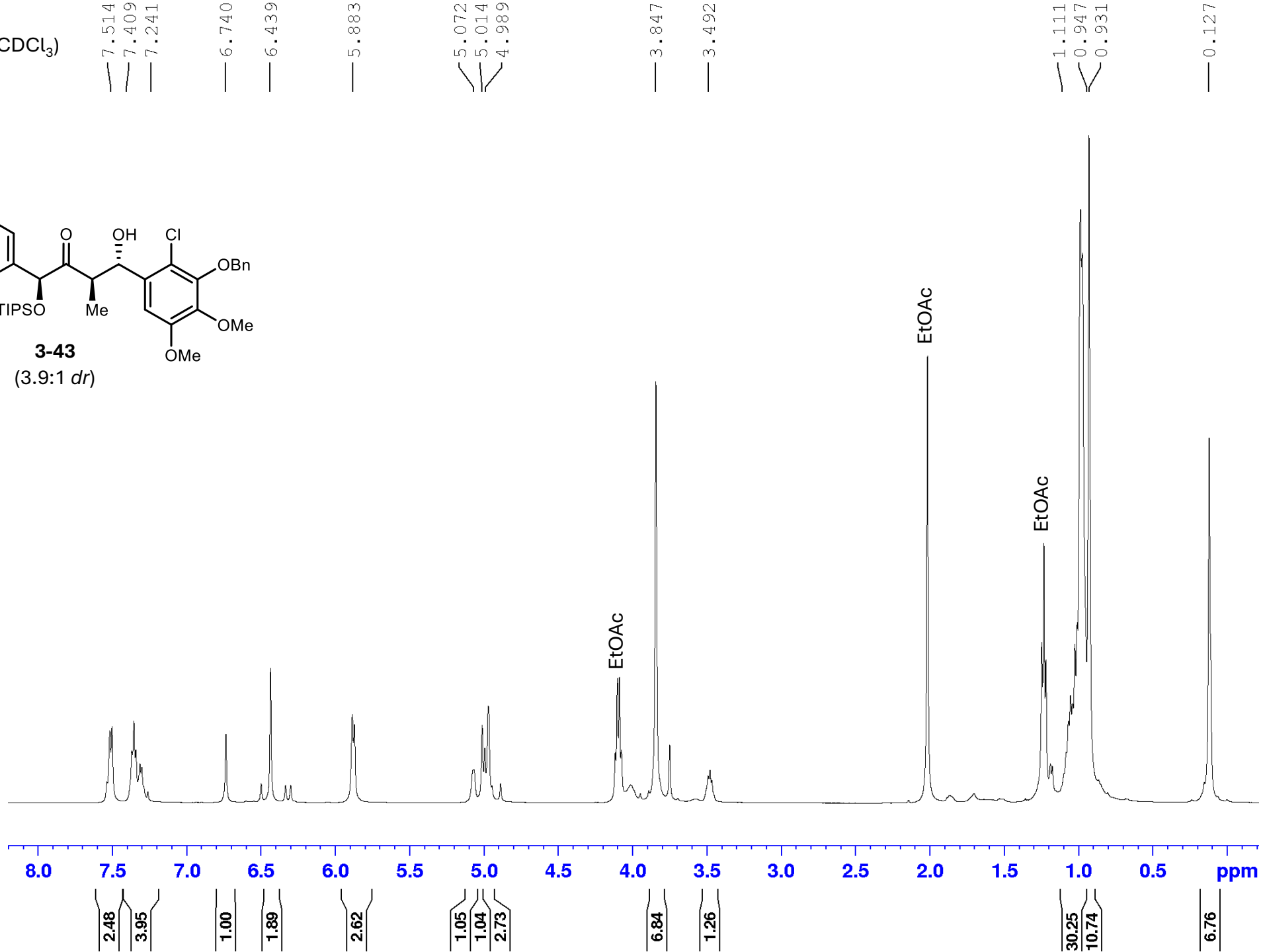
214.25
152.20
149.03
148.22
142.46
140.29
137.27
135.96
135.61
132.32
128.38
128.20
128.05
118.24
110.19
106.07
101.75
101.65
95.47
80.31
75.14
73.43
61.14
56.21
56.03
45.31
17.92
15.98
12.18

210 200 190 180 170 160 150 140 130 120 110 100 90 80 70 60 50 40 30 20 10 ppm

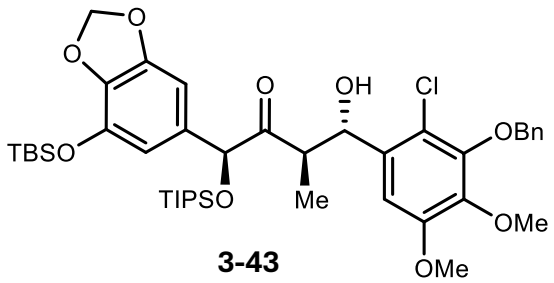
^{1}H NMR (500 MHz, $CDCl_3$)



3-43
(3.9:1 *dr*)



^{13}C NMR (125 MHz, $CDCl_3$)

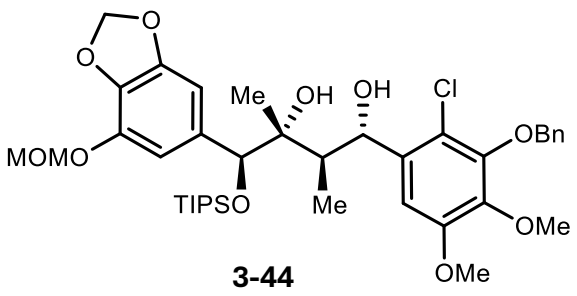


3-43
(2.5:1 *dr*)

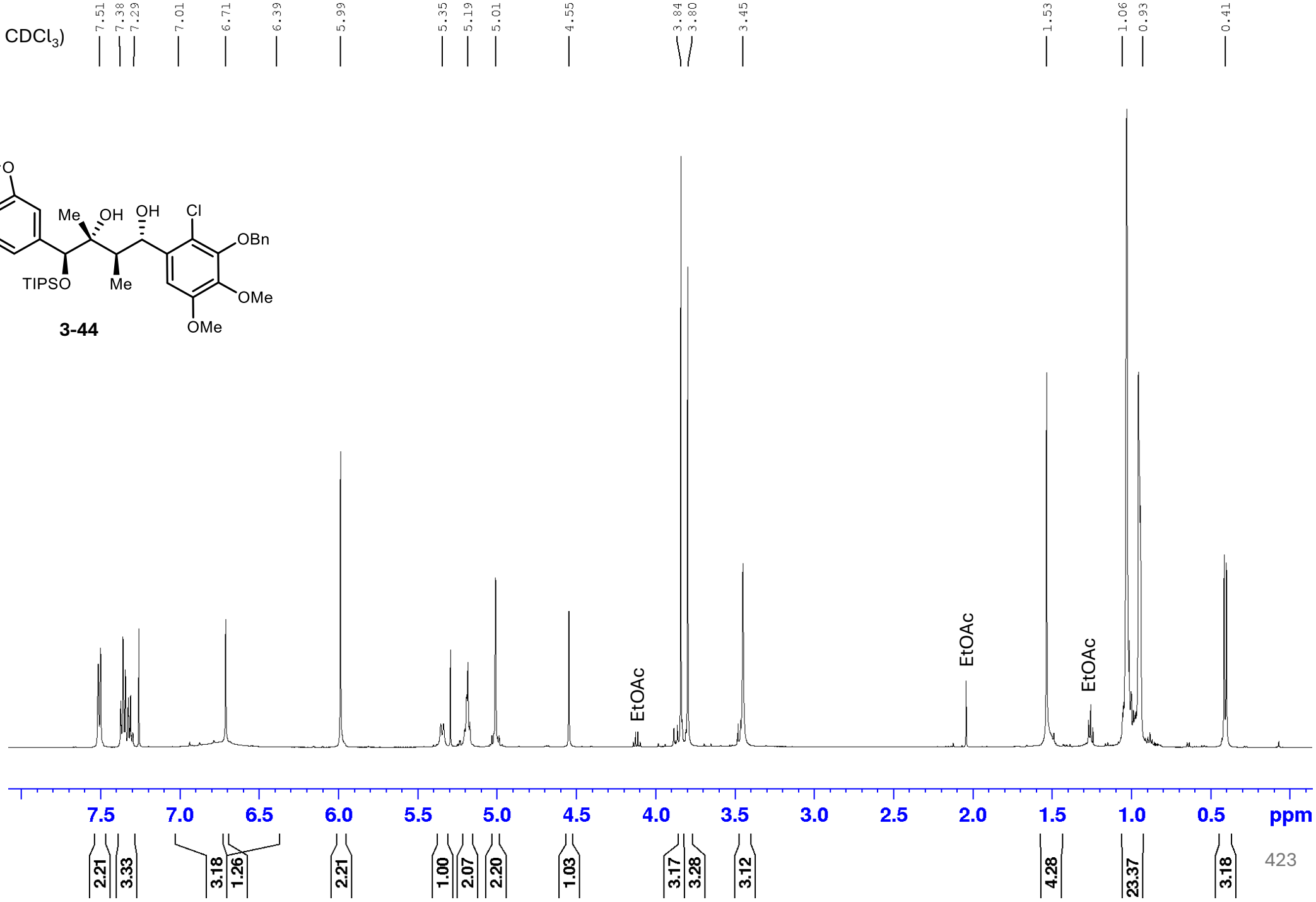
214.25
152.31
149.11
148.34
142.58
138.71
137.55
137.25
135.66
132.04
128.39
128.37
118.48
114.11
106.15
101.36
100.88
80.33
75.25
61.21
56.09
45.52
25.69
17.90
12.12
-4.50

210 200 190 180 170 160 150 140 130 120 110 100 90 80 70 60 50 40 30 20 10 ppm

^{1}H NMR (500 MHz, $CDCl_3$)

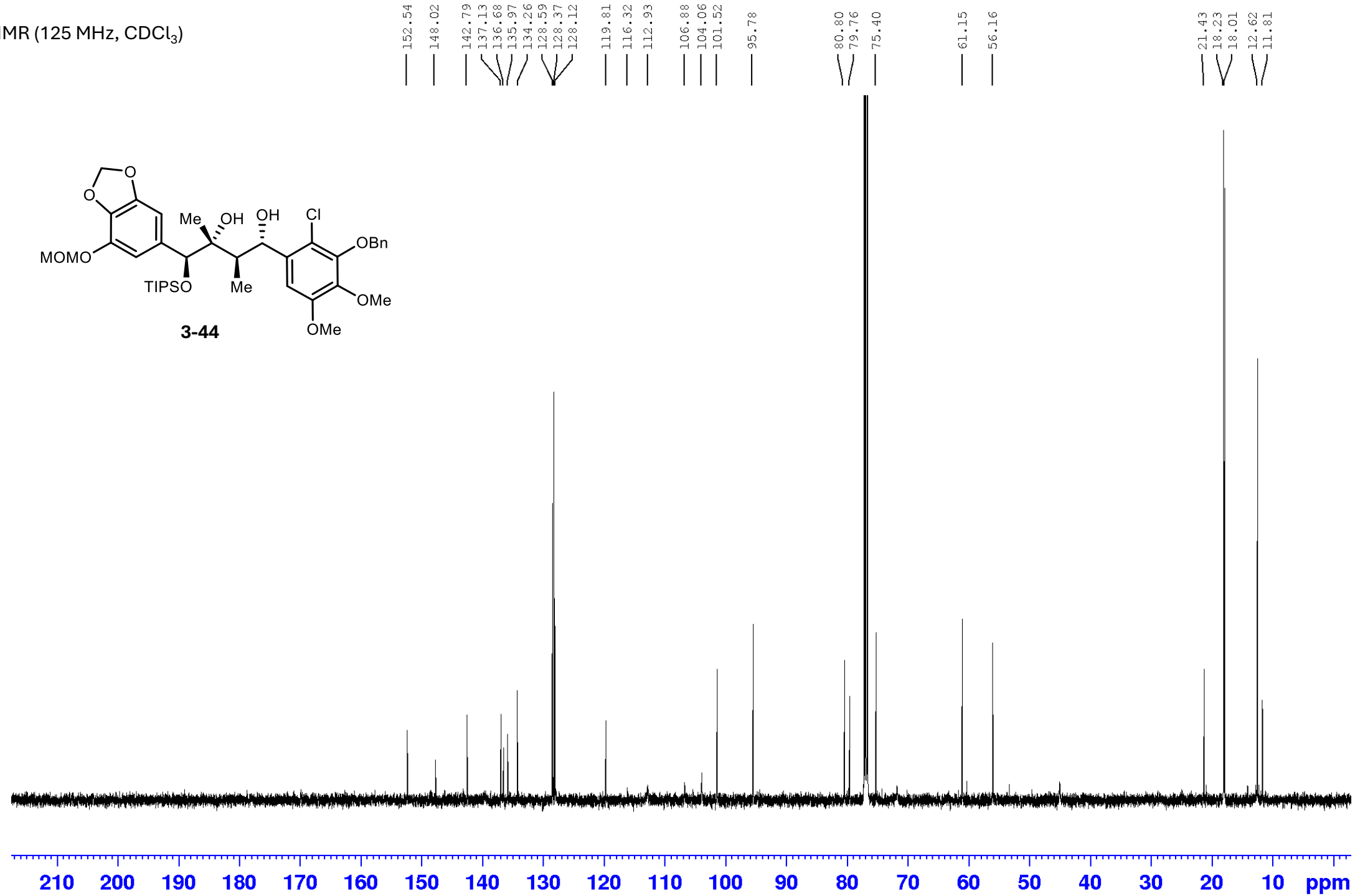


3-44

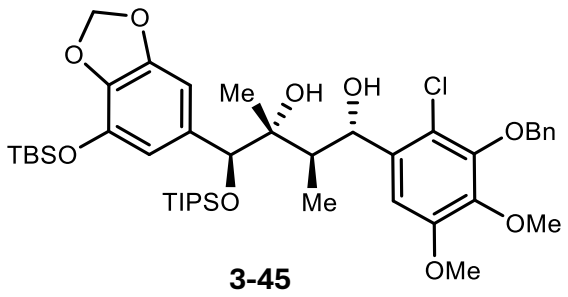


^{13}C NMR (125 MHz, $CDCl_3$)

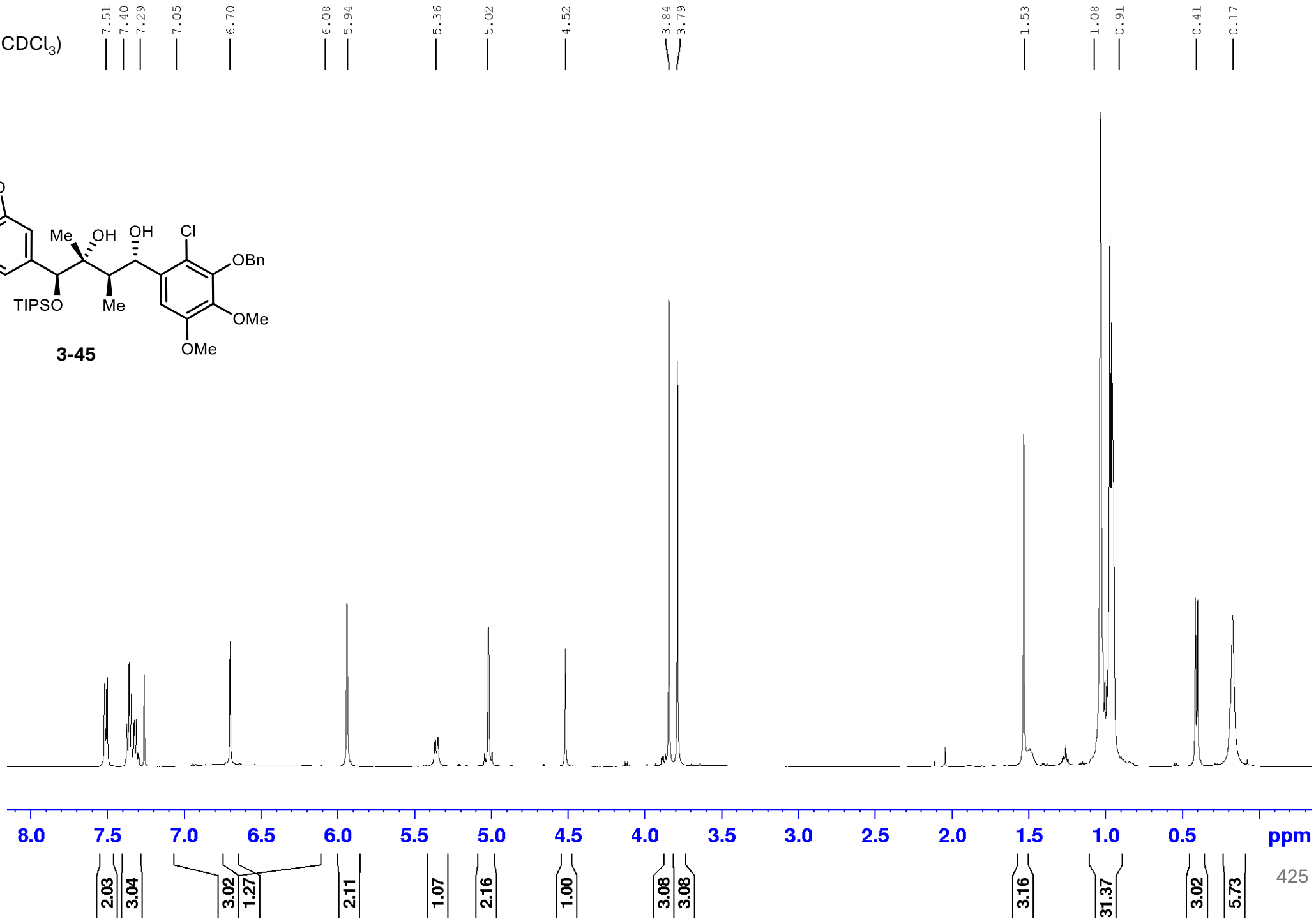
3-44



^{1}H NMR (500 MHz, $CDCl_3$)

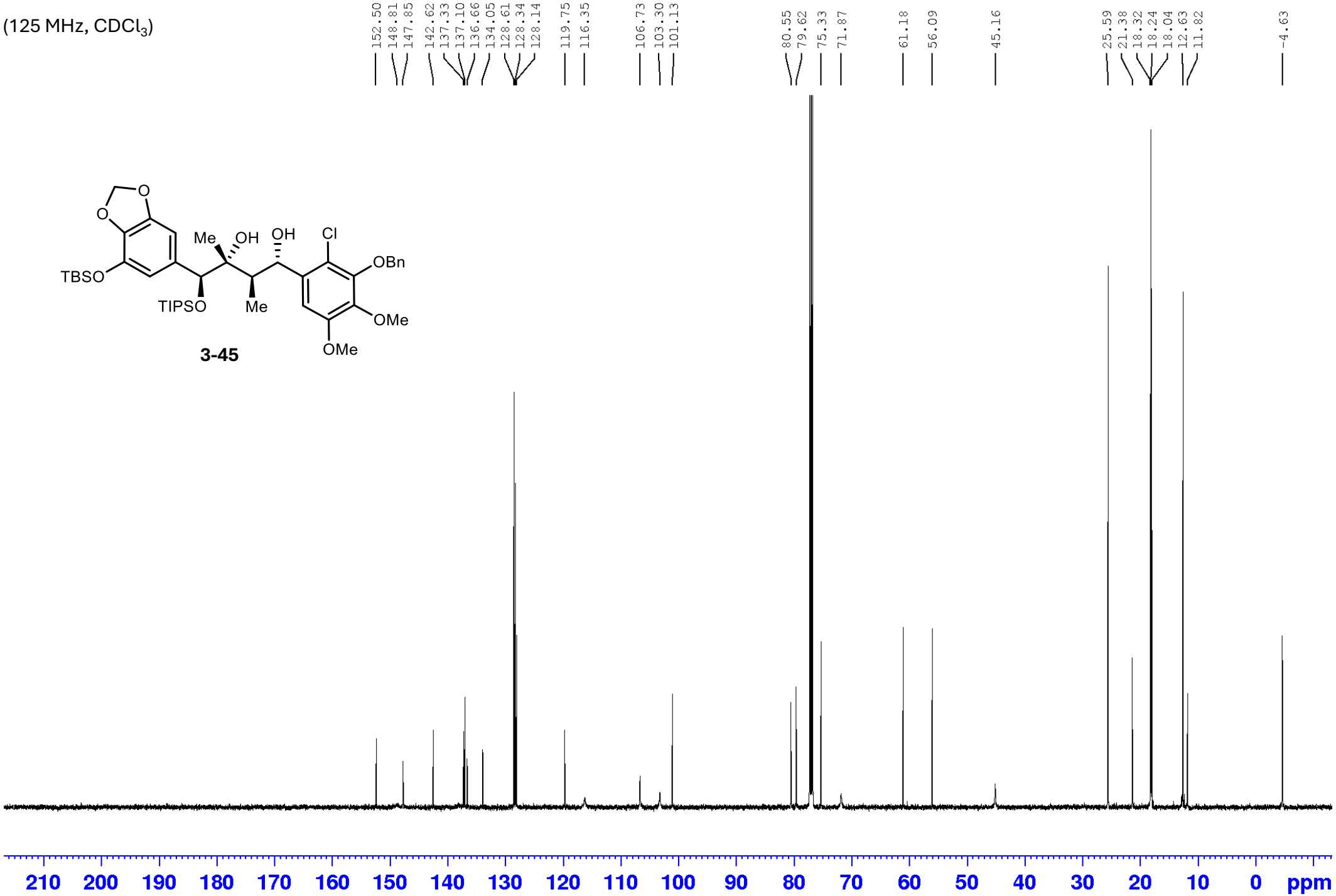


3-45

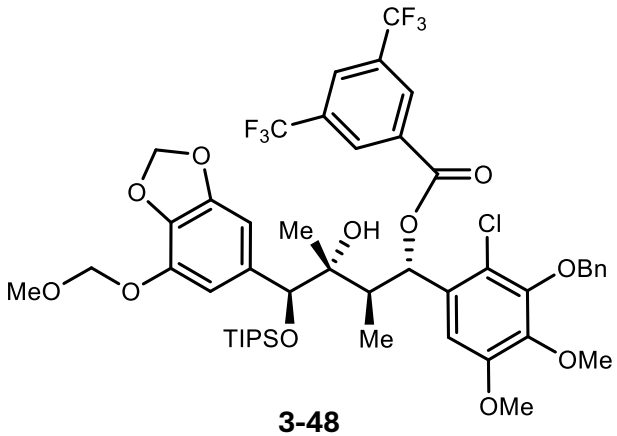


^{13}C NMR (125 MHz, $CDCl_3$)

3-45



^{1}H NMR (500 MHz, $CDCl_3$)

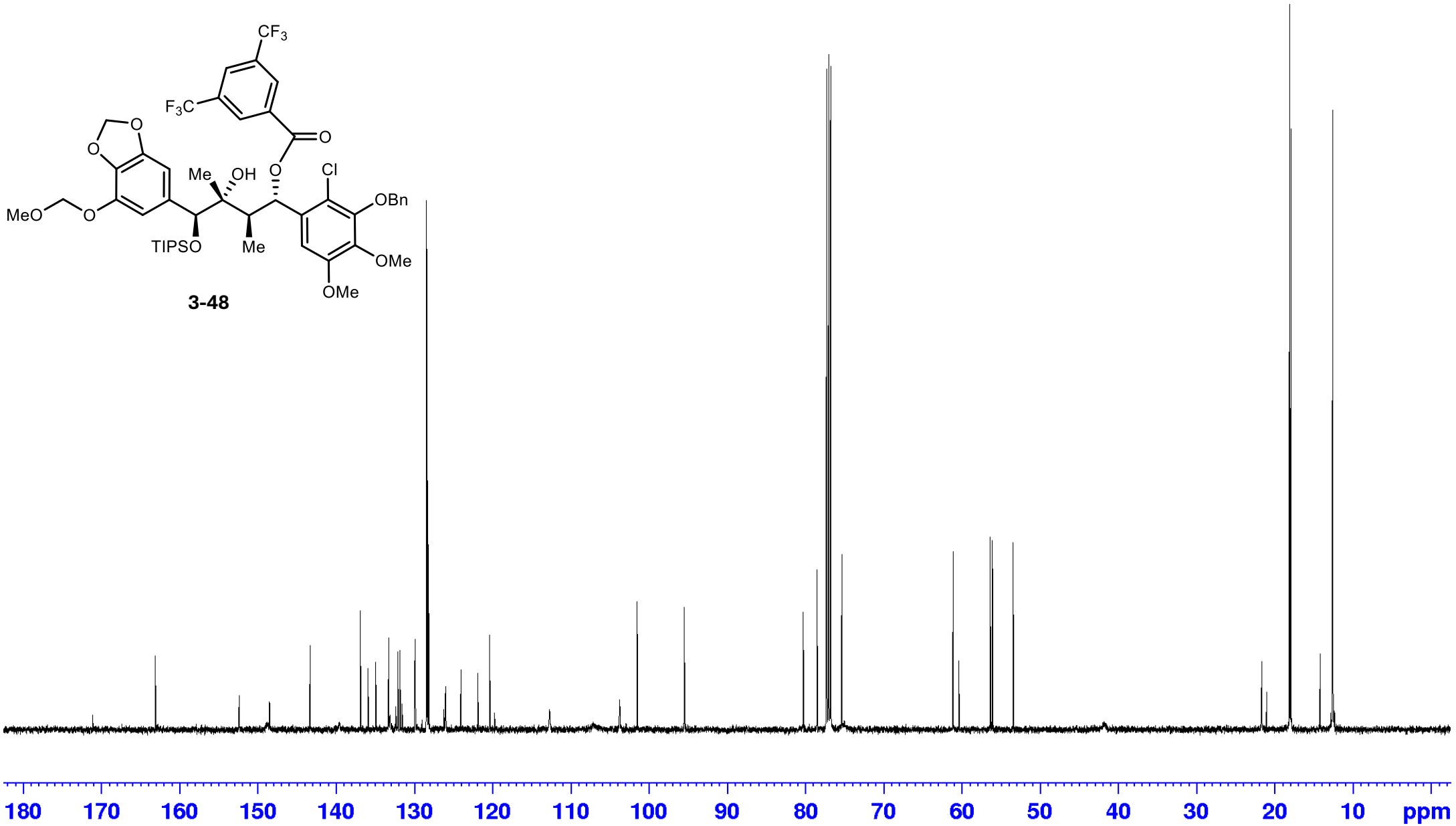


3-48

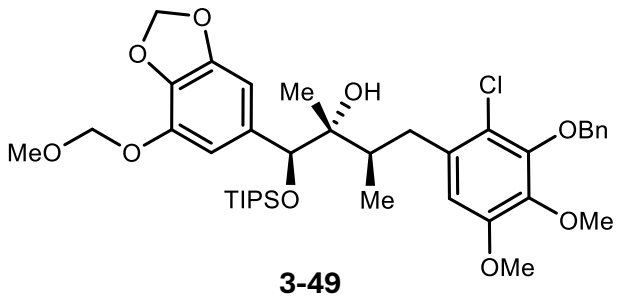
^{13}C NMR
(125 MHz, $CDCl_3$)

163.17
152.44
148.88
148.55
143.35
139.66
136.89
135.95
134.95
133.35
133.14
131.97
129.92
129.08
128.50
128.38
128.17
126.26
125.99
122.98
120.40
119.74
112.80
107.06
103.83
101.53
95.51
80.30
78.51
75.37
61.16
56.38
56.09
53.43
21.68
18.10
17.94
12.60

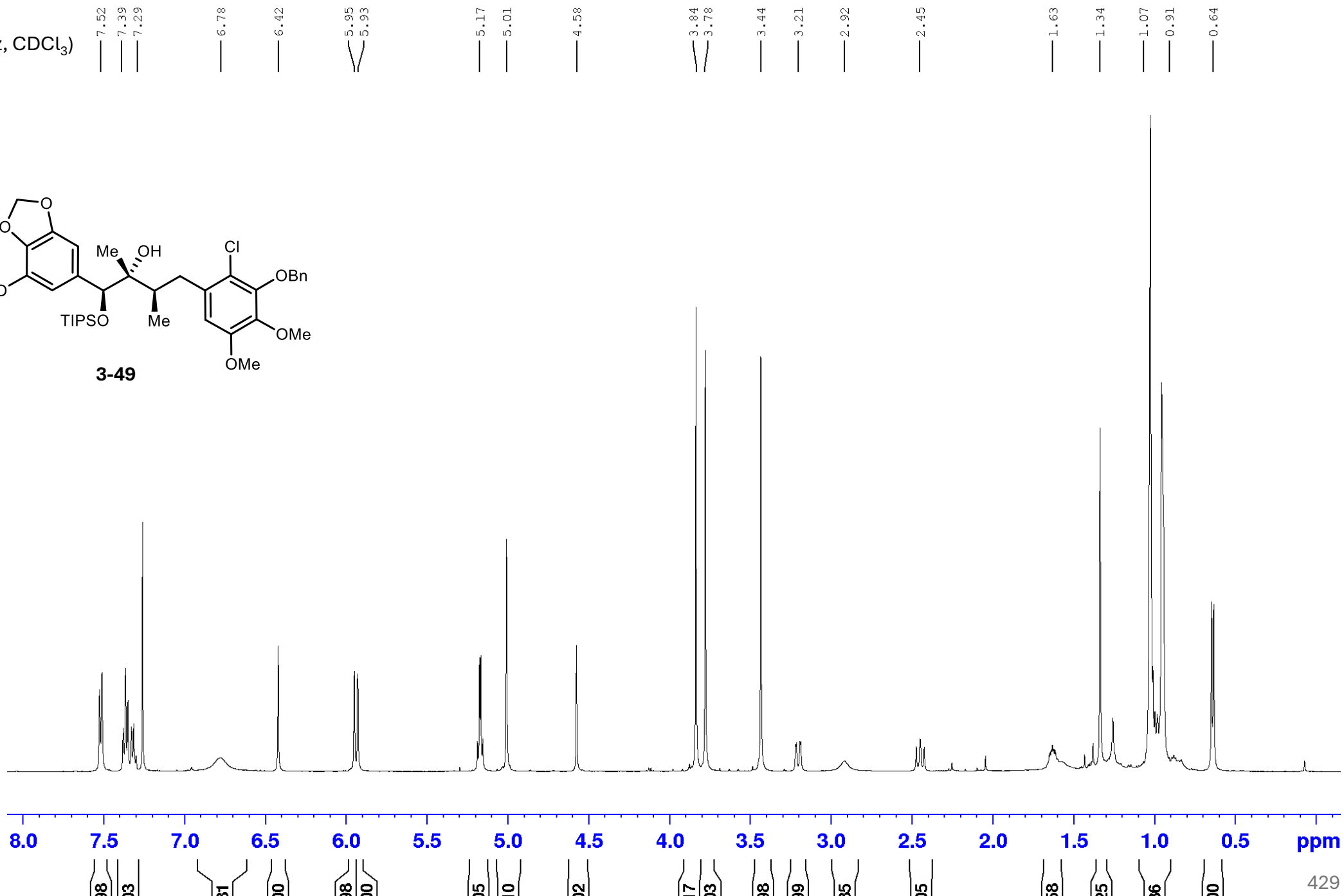
3-48



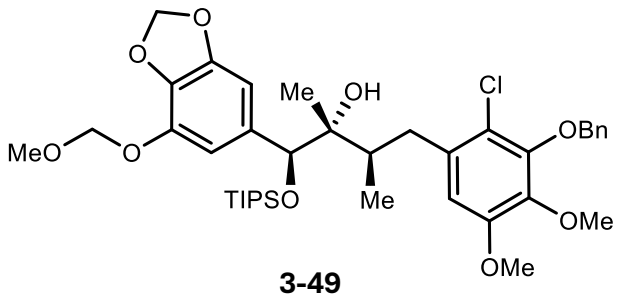
^{1}H NMR (500 MHz, $CDCl_3$)



3-49



^{13}C NMR (125 MHz, $CDCl_3$)

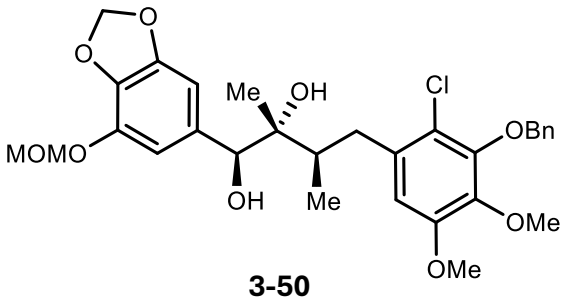


3-49

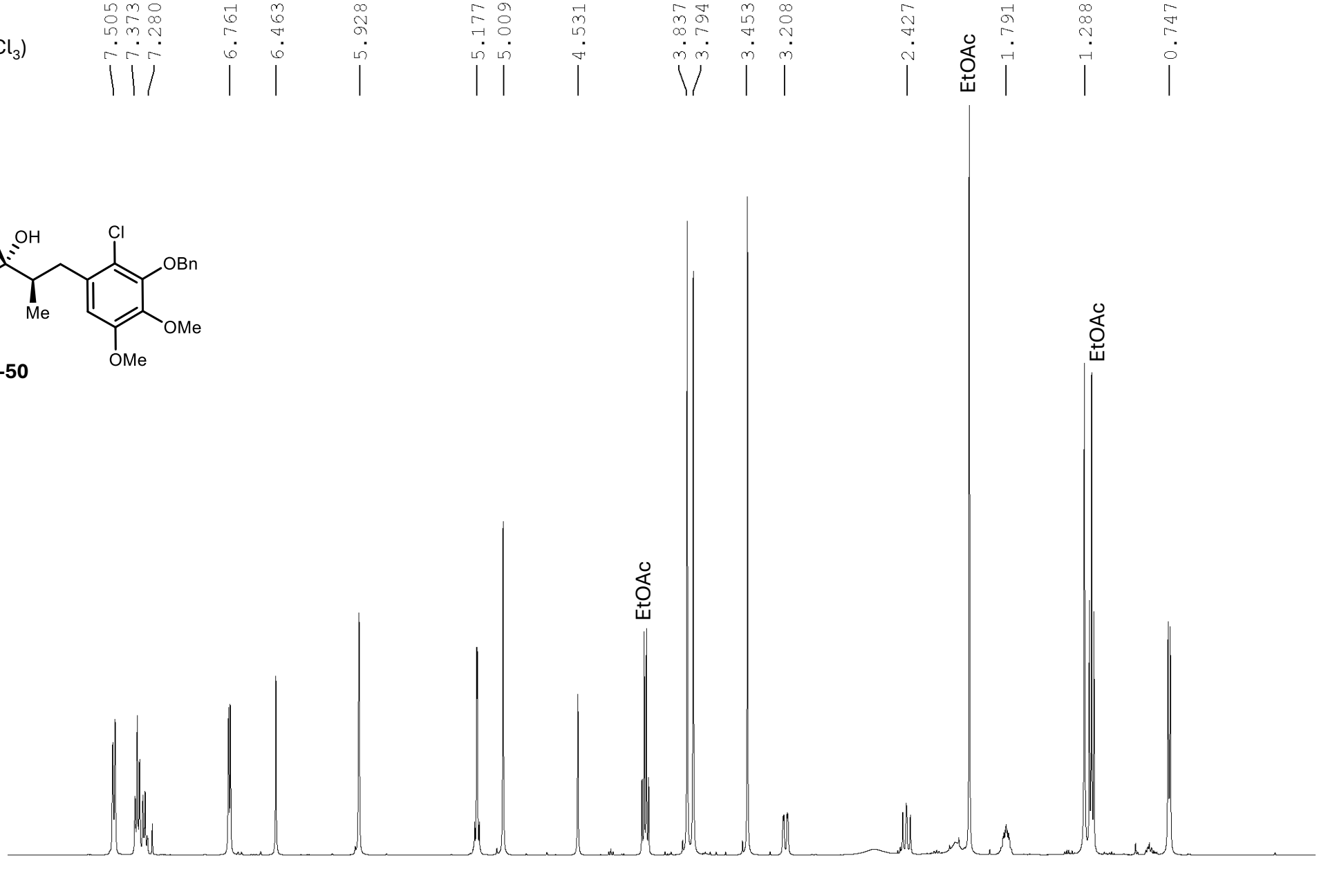
151.53
148.57
141.47
139.60
137.29
135.68
135.35
135.13
128.44
128.34
128.04
120.77
112.81
109.88
104.00
101.34
95.56
80.29
77.84
75.18
61.17
56.14
56.05
39.34
34.55
20.96
18.24
18.02
14.21
12.65

190 180 170 160 150 140 130 120 110 100 90 80 70 60 50 40 30 20 10 ppm

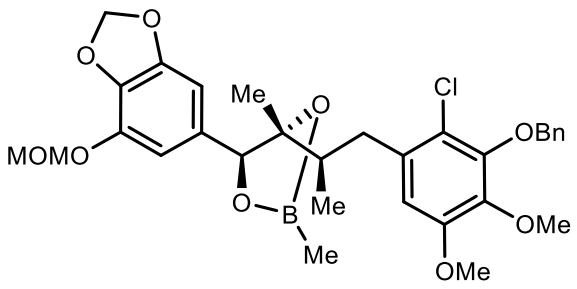
^{1}H NMR (500 MHz, $CDCl_3$)



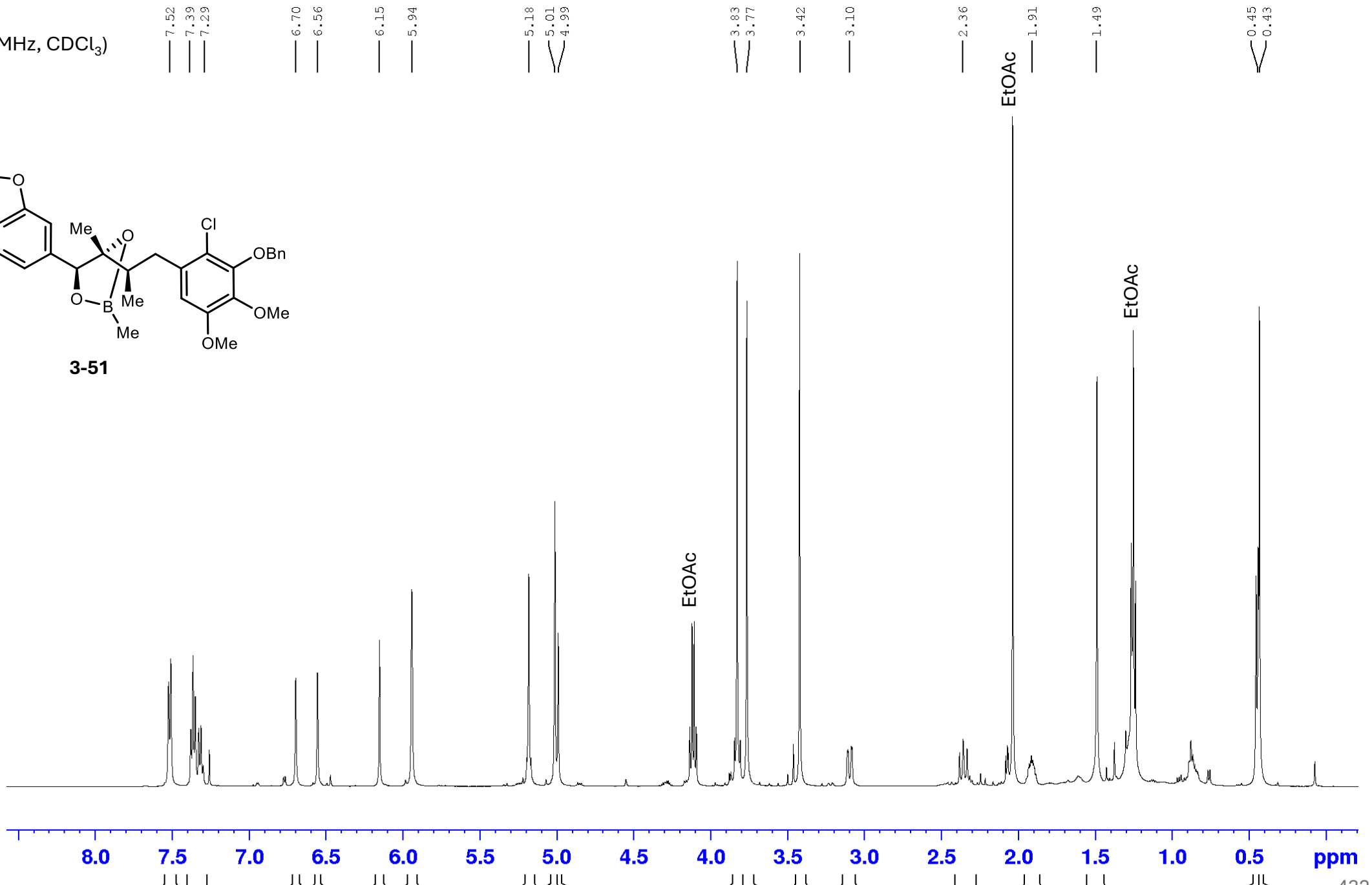
3-50



^{1}H NMR (500 MHz, $CDCl_3$)



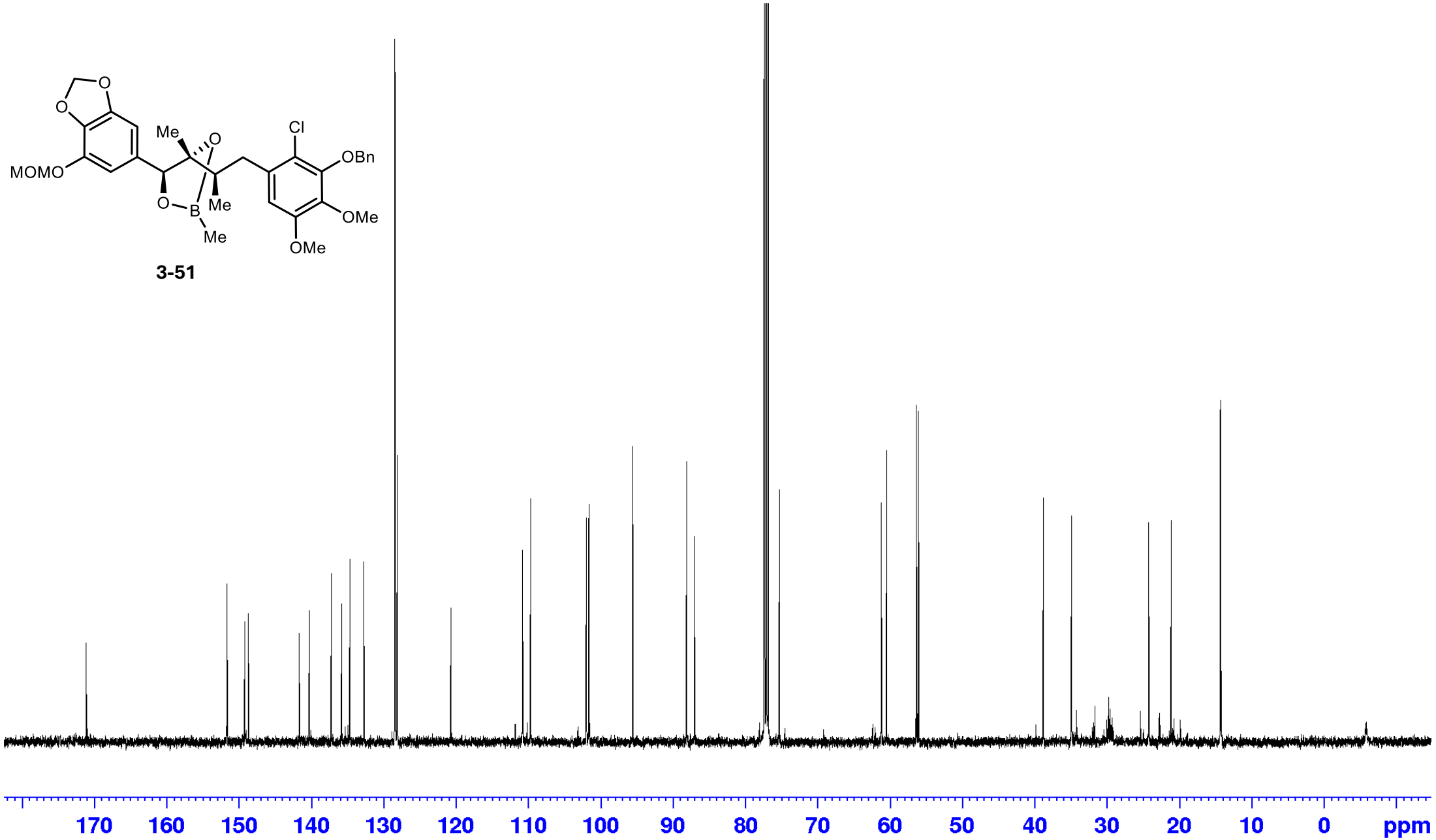
3-51



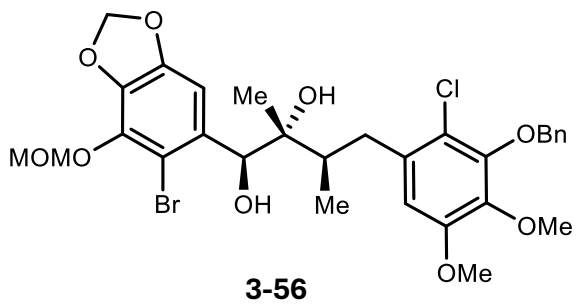
^{13}C NMR (125 MHz, $CDCl_3$)

151.61
149.18
148.74
141.72
140.33
137.28
135.86
134.72
132.79
128.52
128.45
128.17
120.78
110.85
109.73
102.02
101.68
95.60
88.15
87.10
75.33
61.23
56.39
56.06
38.82
34.91
24.23
14.29
-5.75

3-51

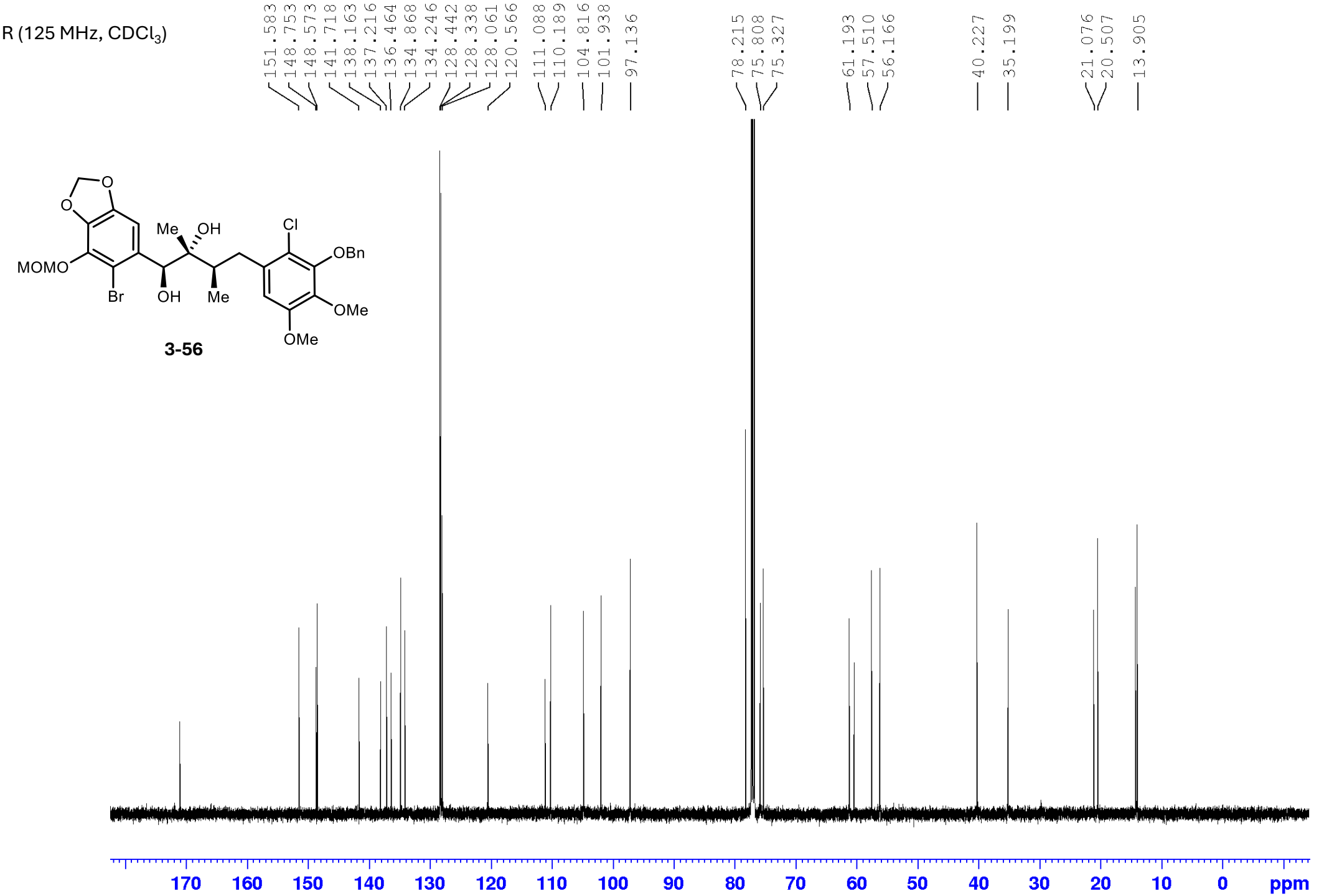


^{1}H NMR (500 MHz, $CDCl_3$)



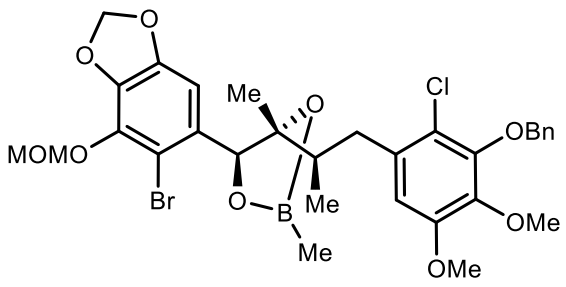
3-56

^{13}C NMR (125 MHz, $CDCl_3$)



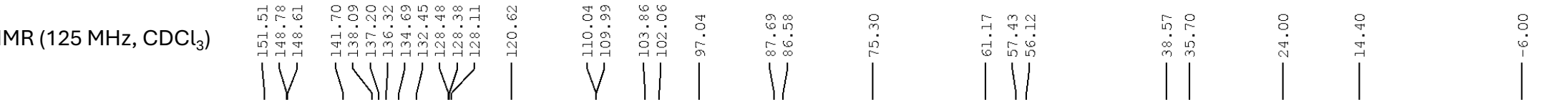
3-56

^{1}H NMR (500 MHz, $CDCl_3$)

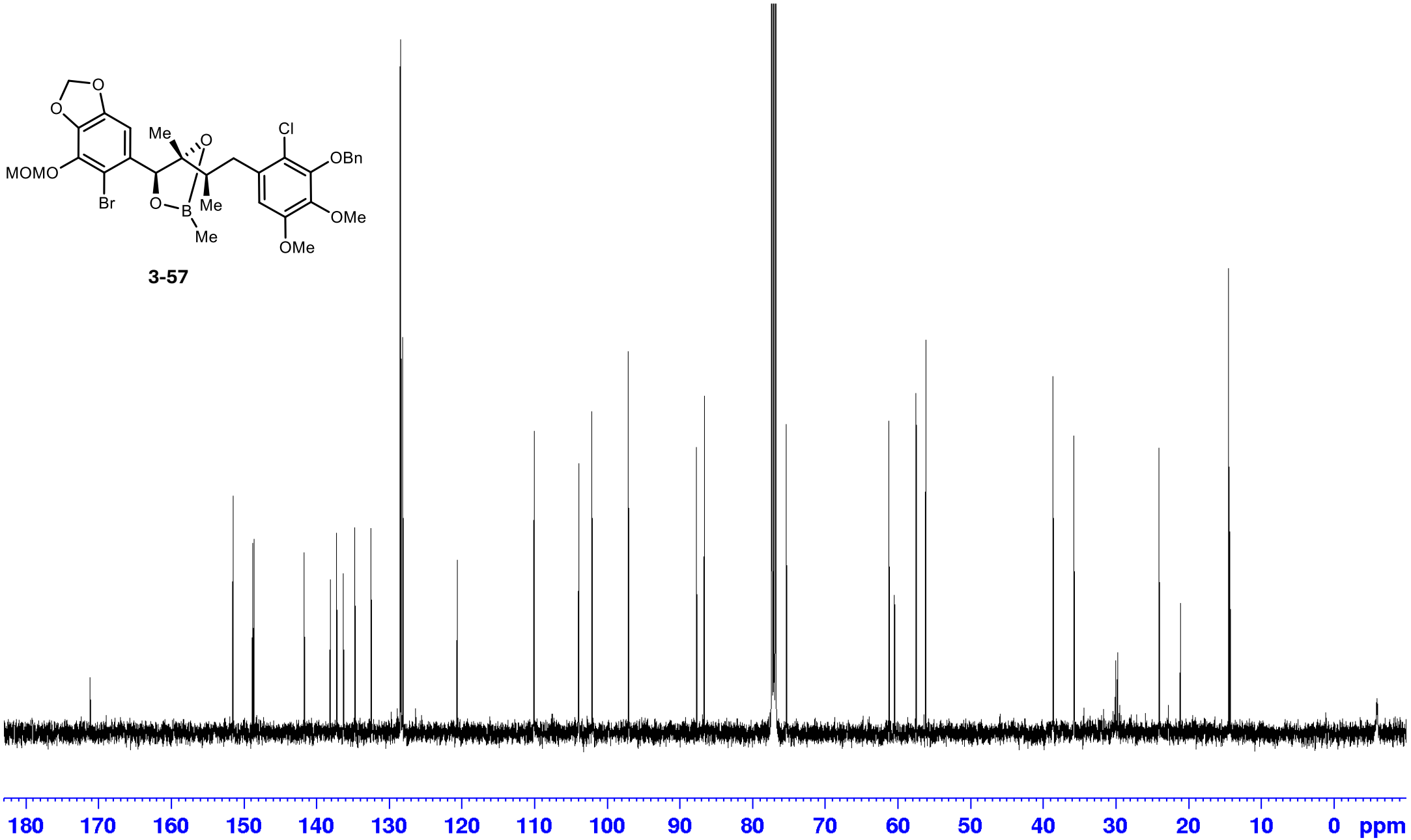


3-57

^{13}C NMR (125 MHz, $CDCl_3$)

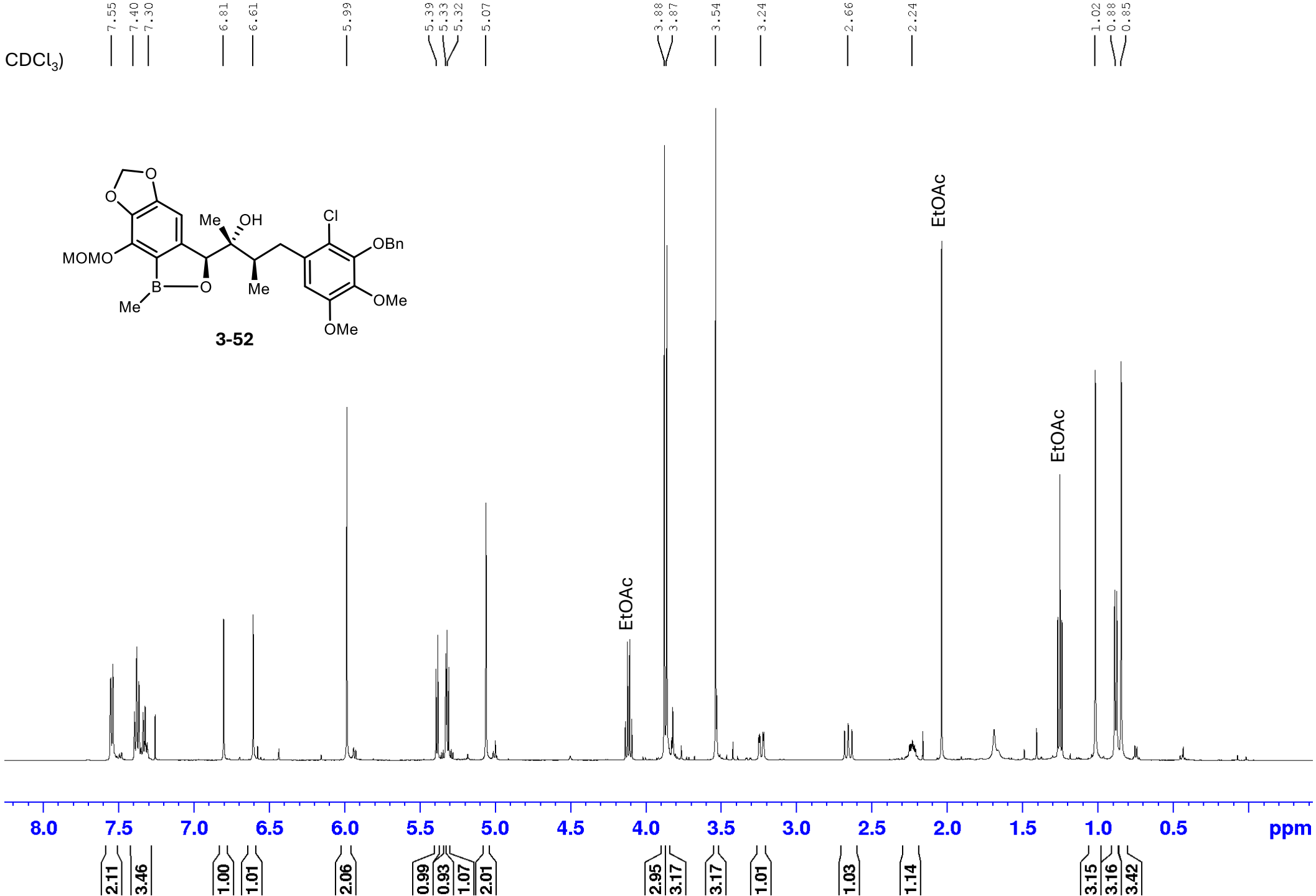


3-57

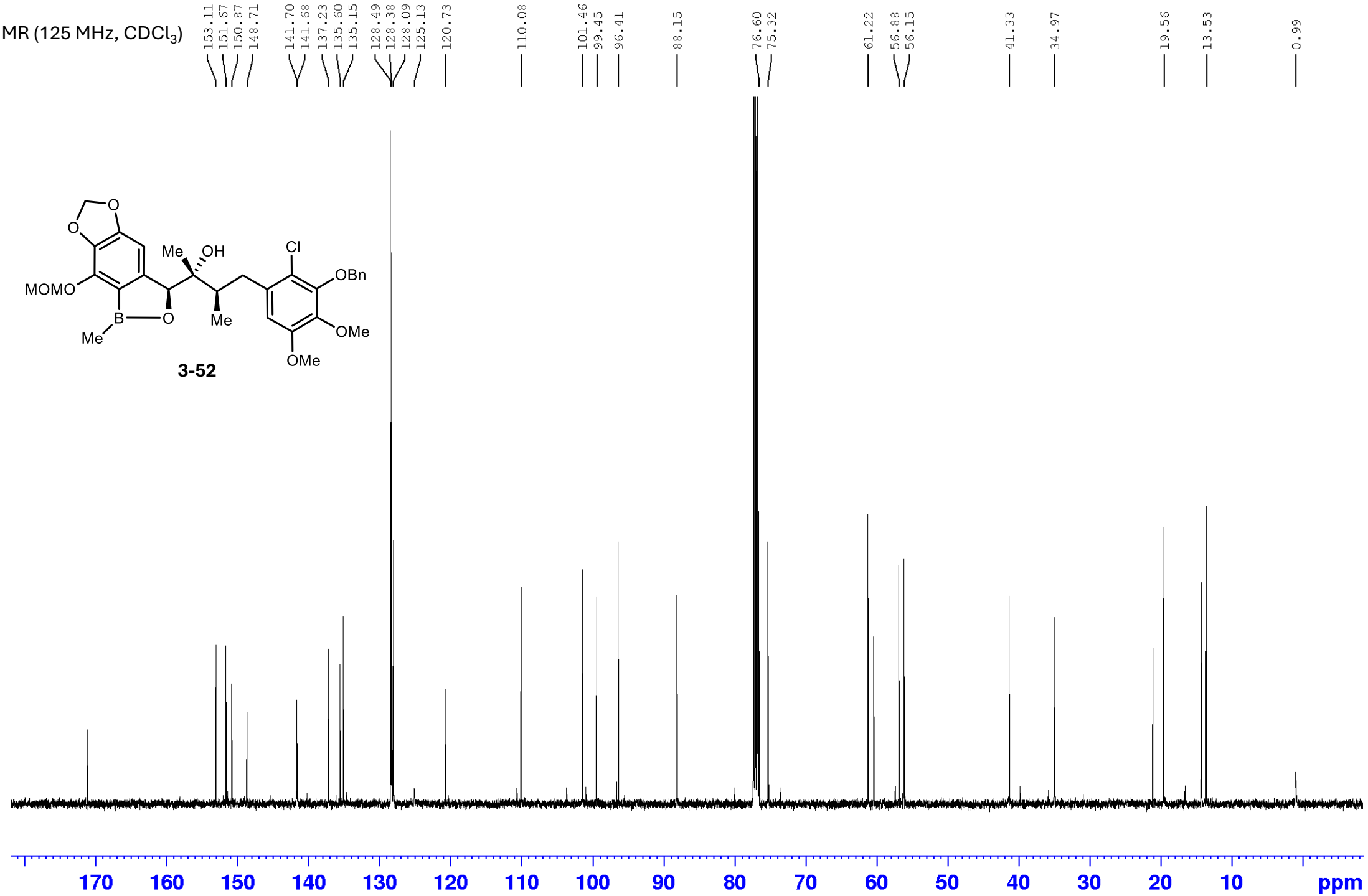


^{1}H NMR
(500 MHz, $CDCl_3$)

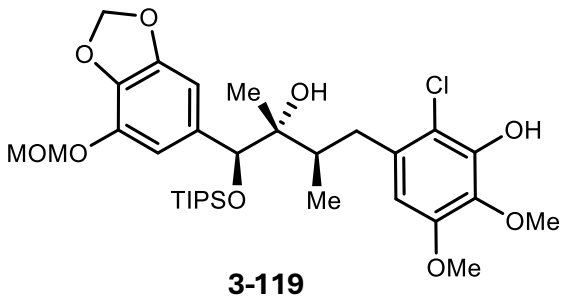
3-52



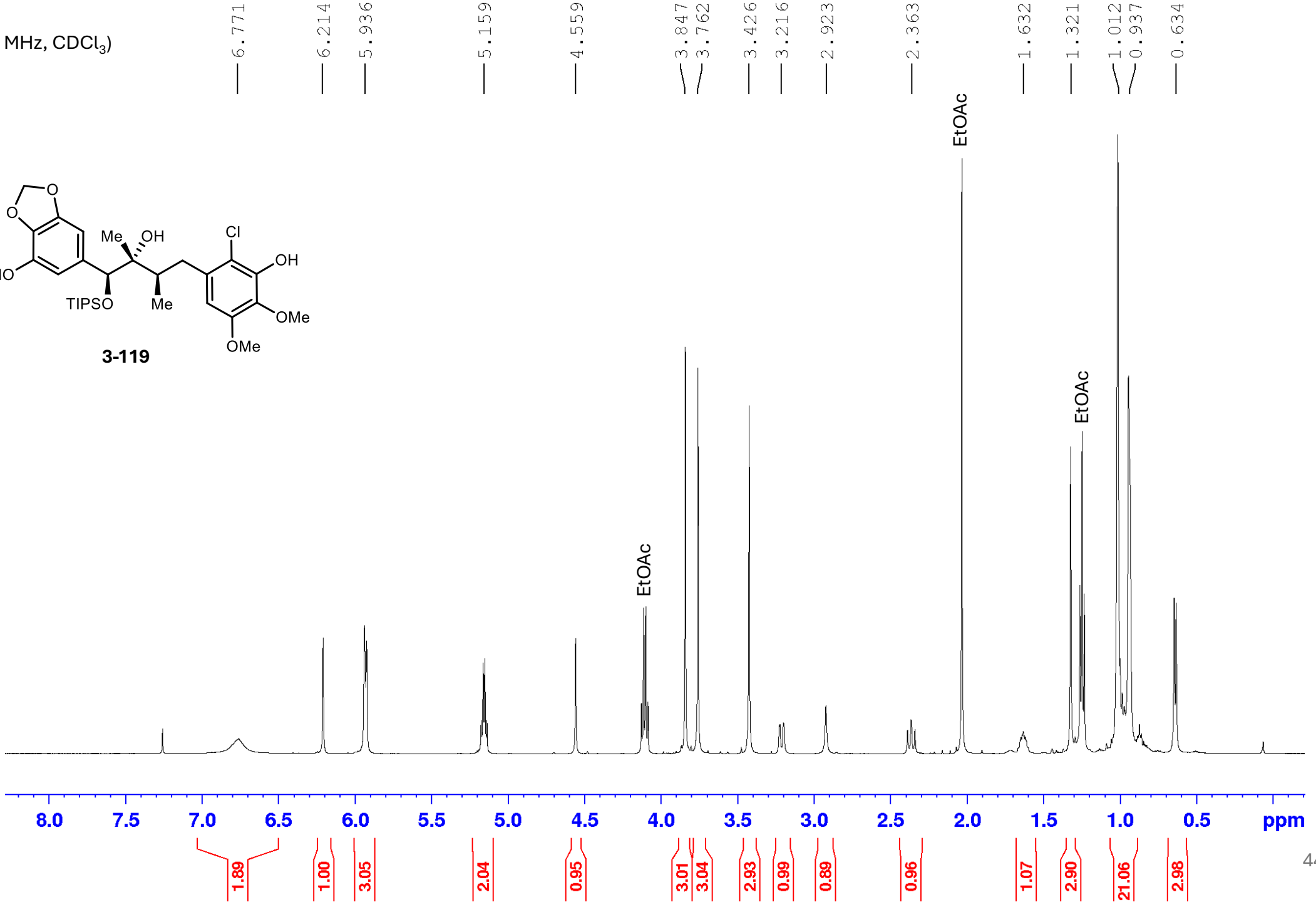
^{13}C NMR (125 MHz, $CDCl_3$)



^{1}H NMR (500 MHz, $CDCl_3$)

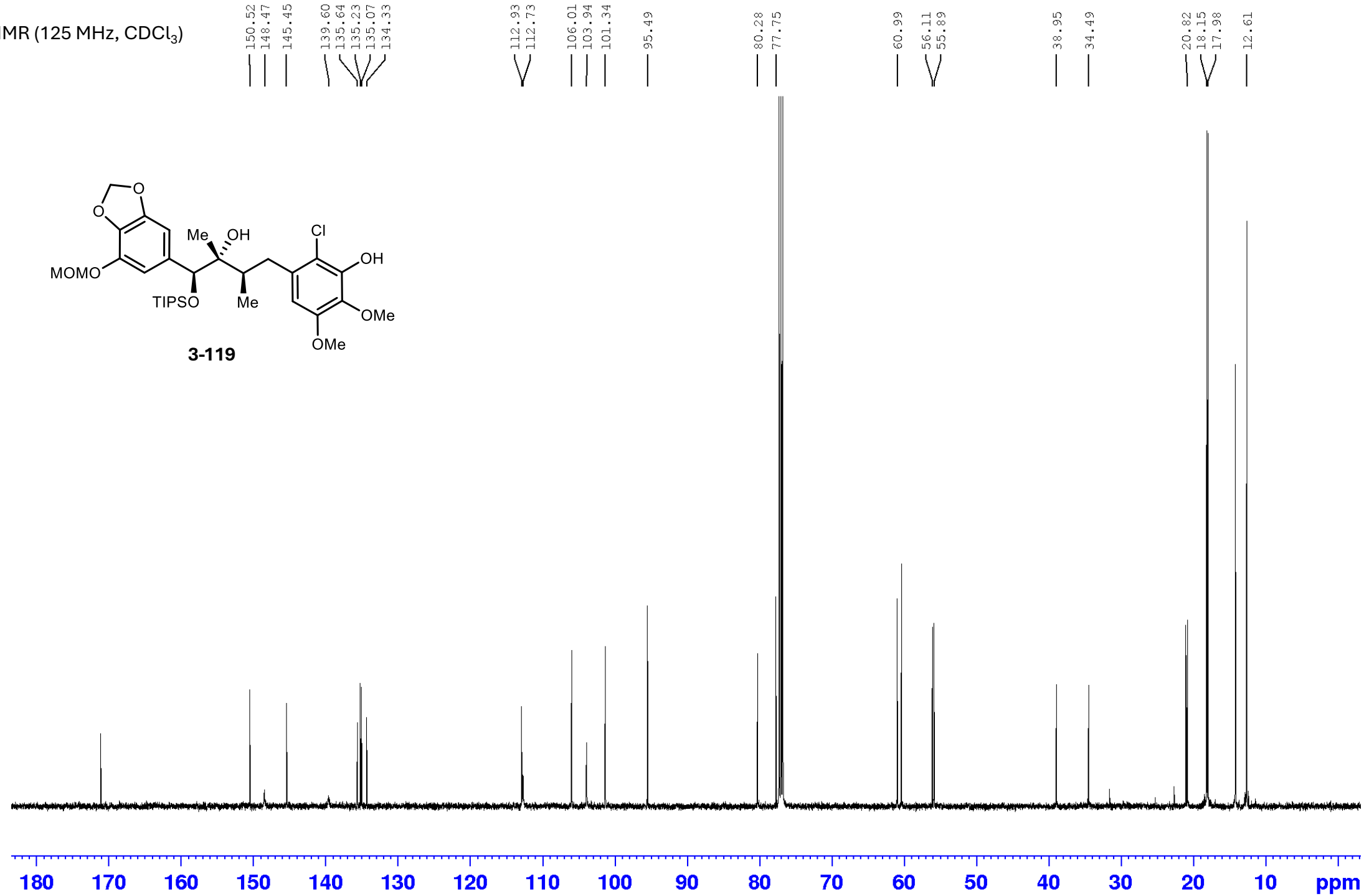


3-119

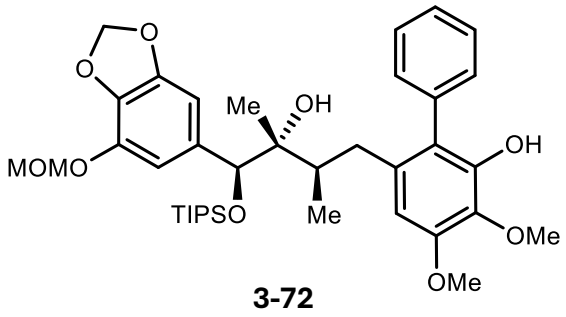


^{13}C NMR (125 MHz, $CDCl_3$)

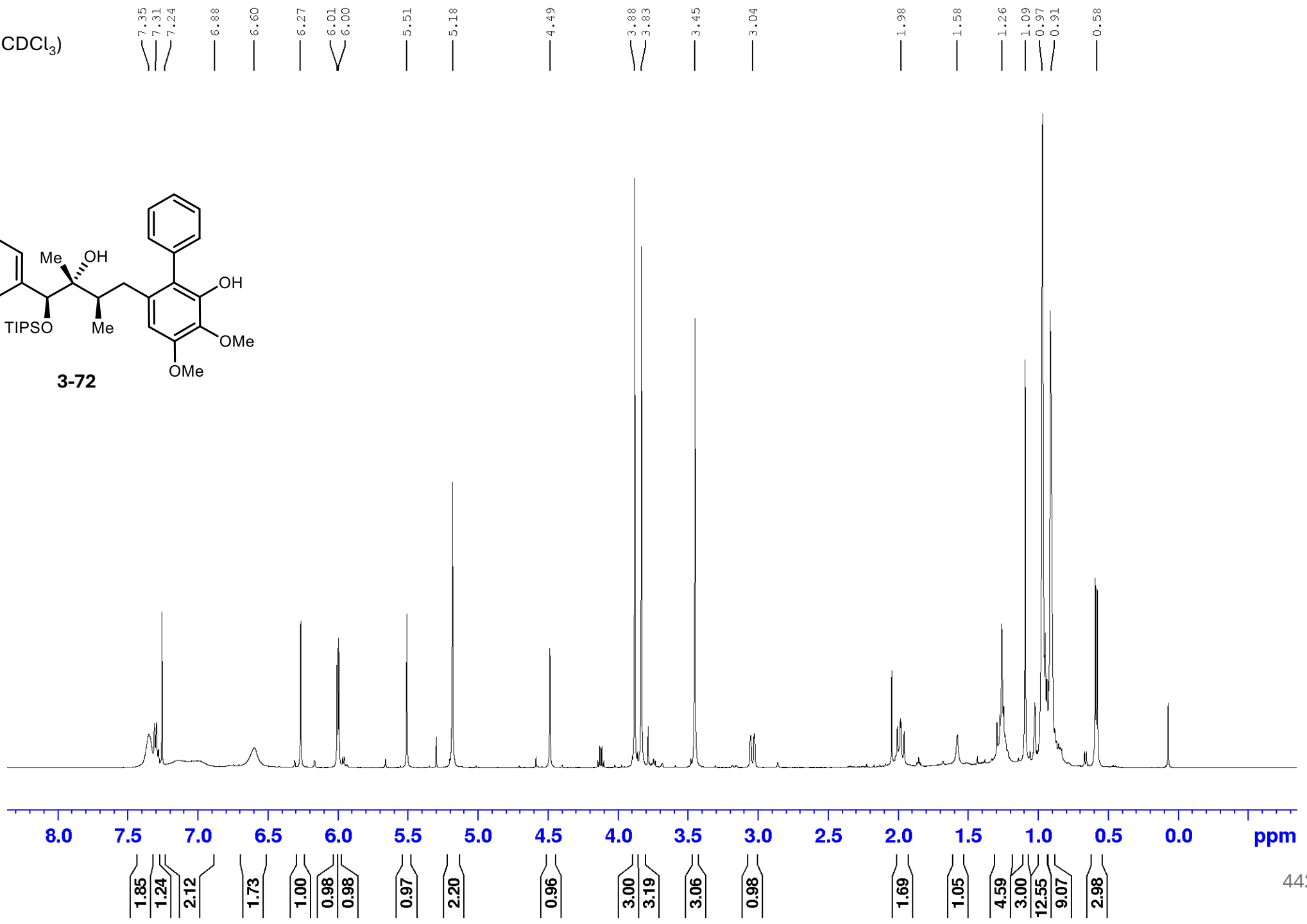
3-119



^{1}H NMR (500 MHz, $CDCl_3$)

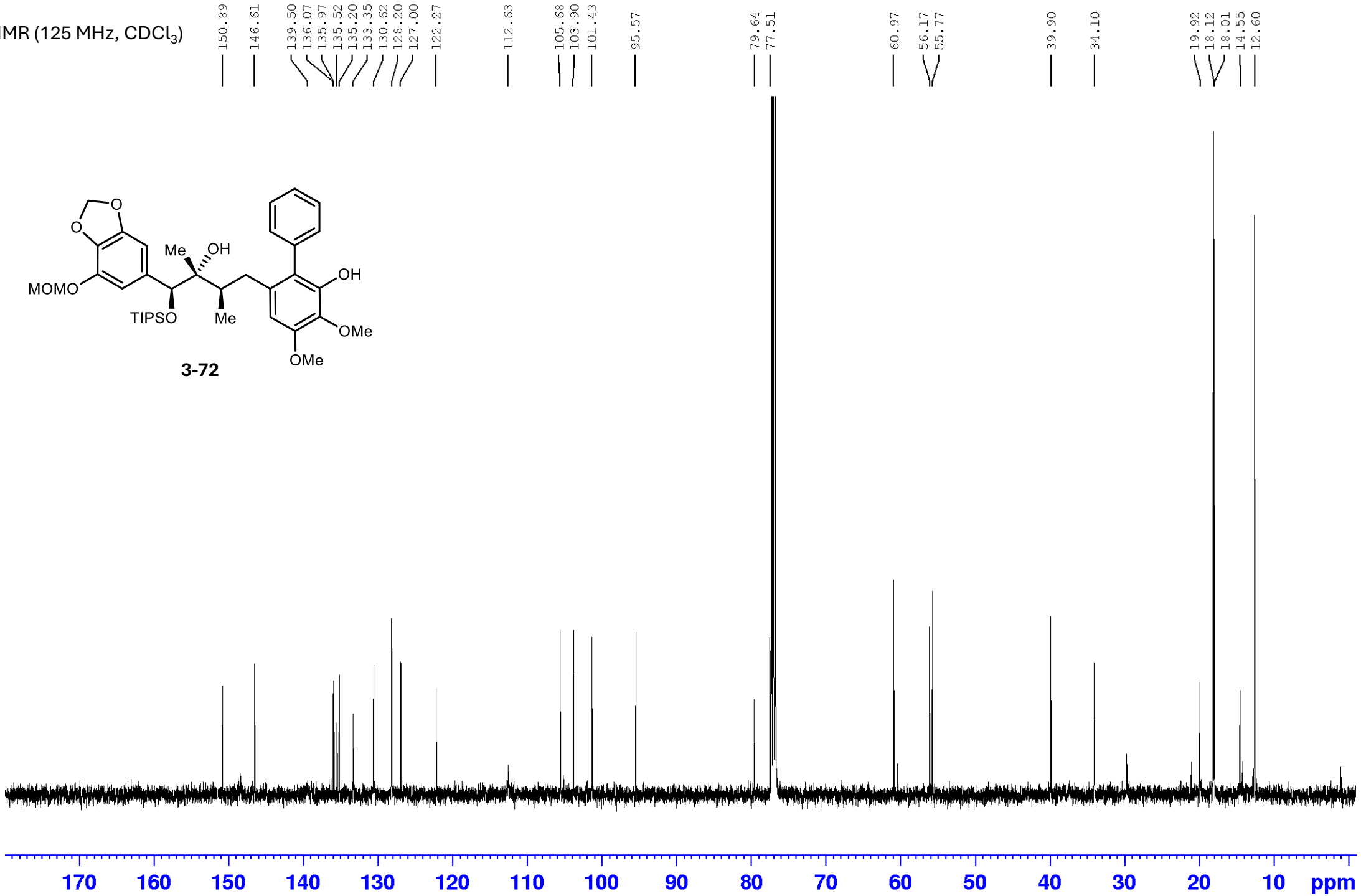


3-72

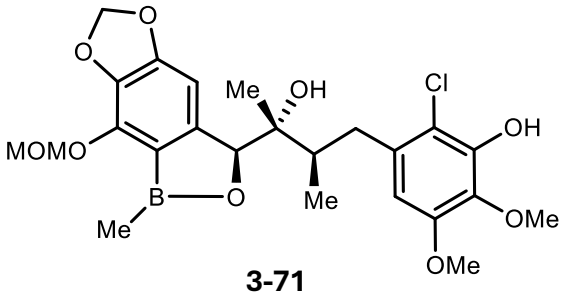


^{13}C NMR (125 MHz, $CDCl_3$)

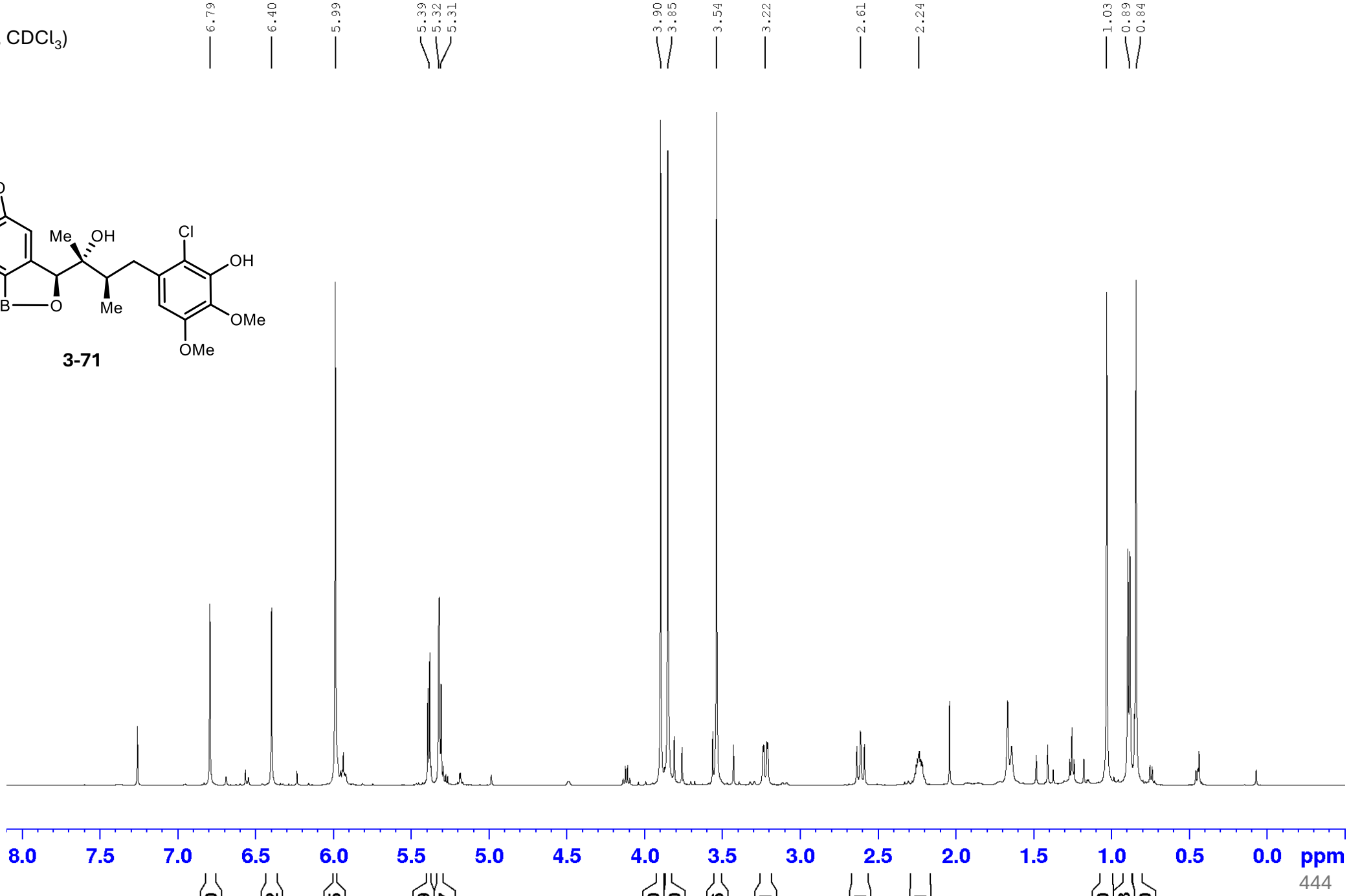
3-72



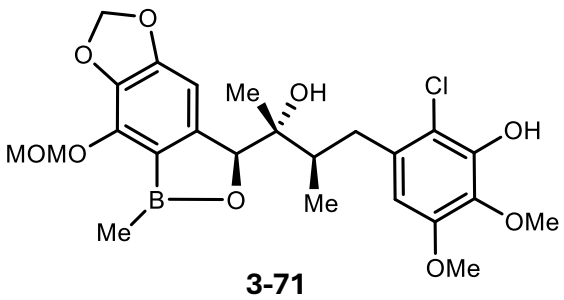
^{1}H NMR (500 MHz, $CDCl_3$)



3-71



^{13}C NMR (125 MHz, $CDCl_3$)

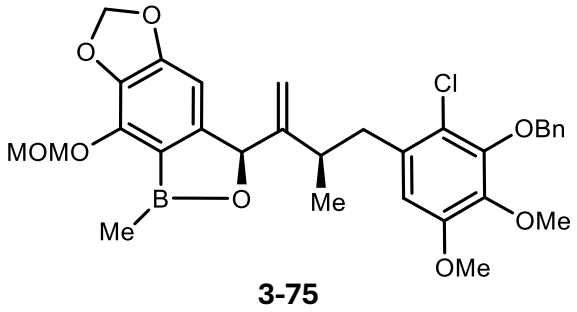


3-71

153.12 150.78 150.67 145.64 141.70 135.62 135.11 134.52 112.91 106.24 101.44 99.39 96.38 88.20 76.61 61.09 56.90 56.02 41.20 34.84 19.58 13.57

170 160 150 140 130 120 110 100 90 80 70 60 50 40 30 20 10 ppm

^{1}H NMR (500 MHz, $CDCl_3$)

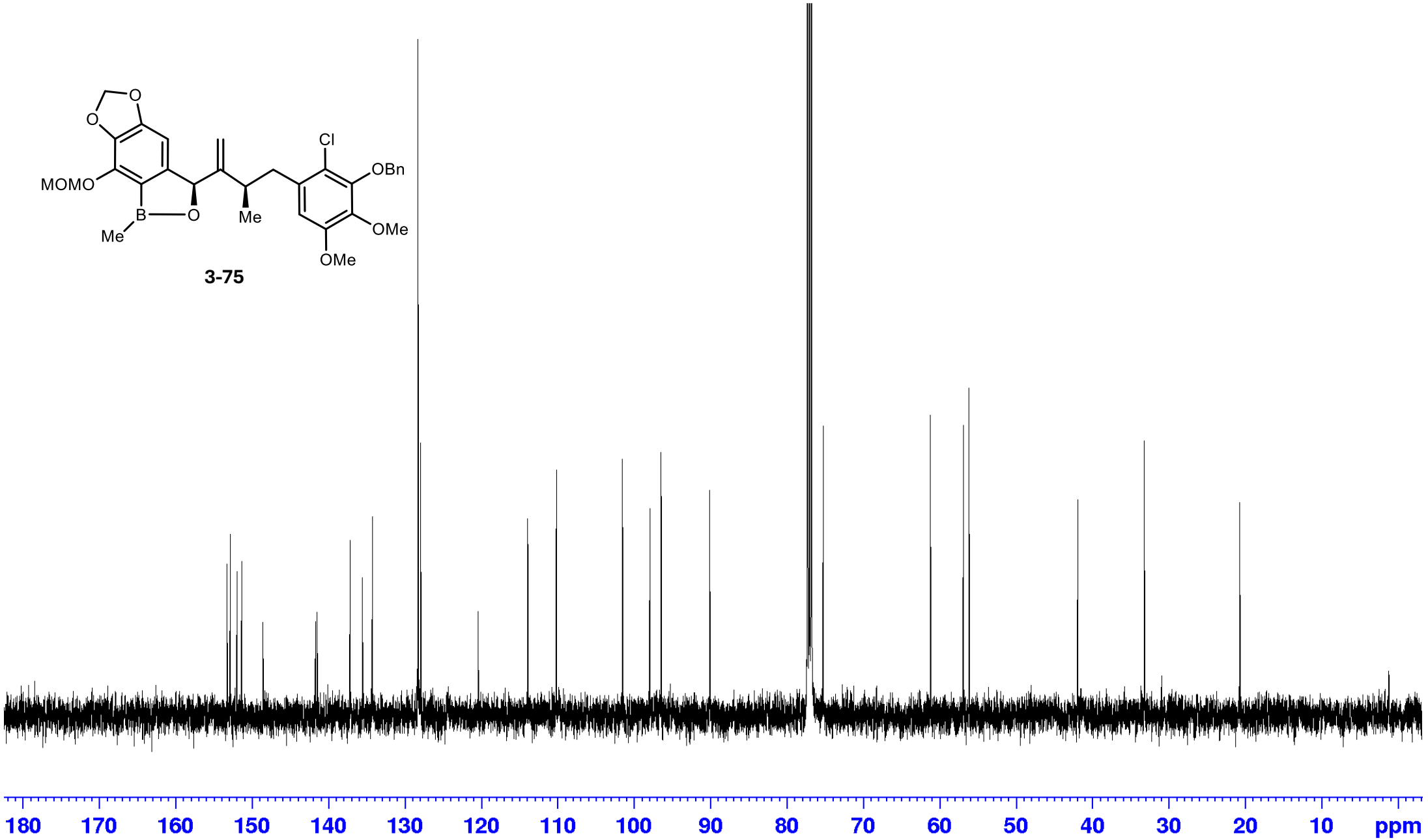


3-75

^{13}C NMR (125 MHz, $CDCl_3$)

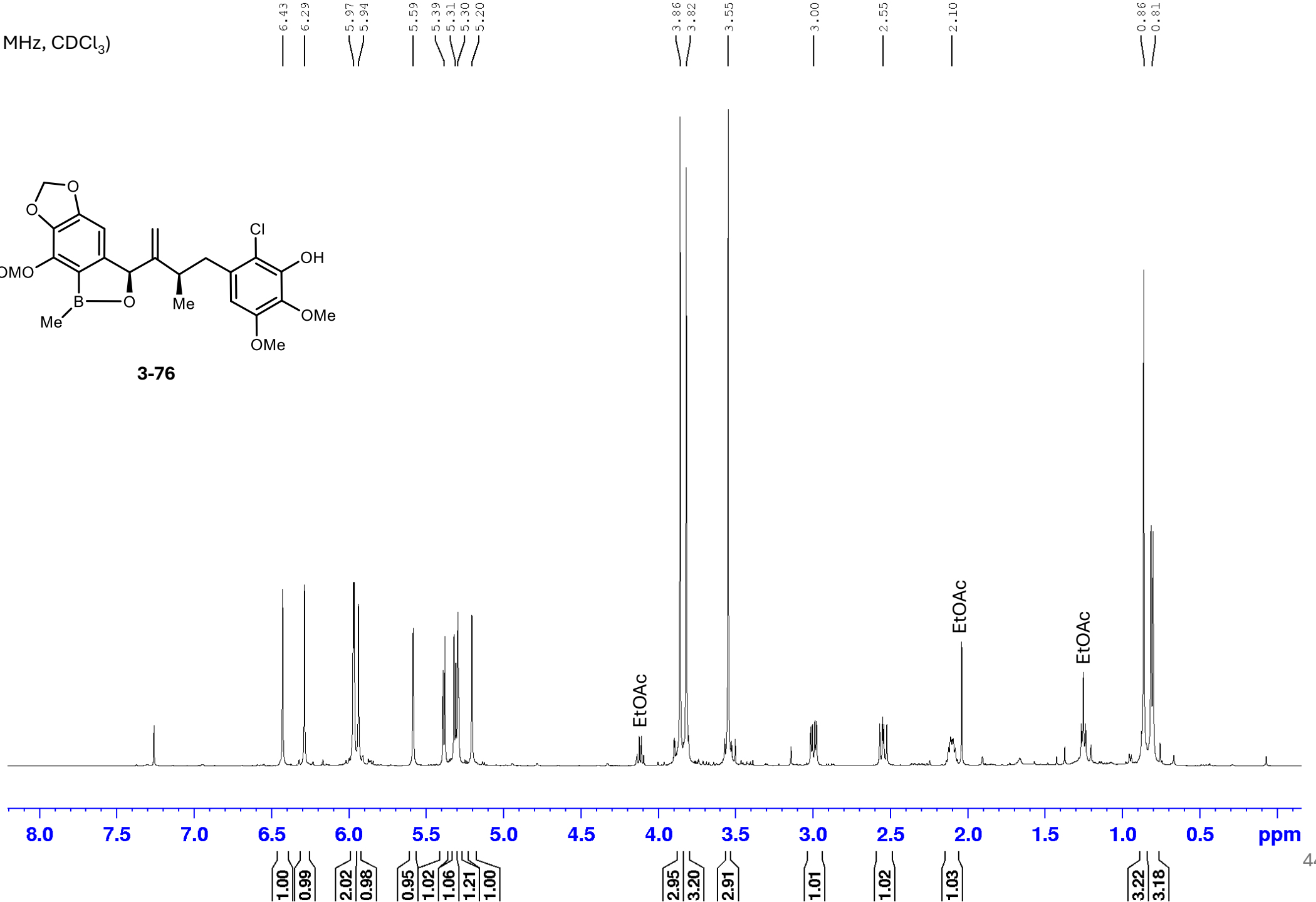
153.35
152.95
152.07
151.46
148.65
141.76
141.57
137.28
135.68
134.33
128.38
128.35
128.04
125.42
120.40
113.92
110.19
101.56
97.91
96.47
90.12
75.22
61.17
56.95
56.20
41.96
33.20
20.71

3-75



^{1}H NMR (500 MHz, $CDCl_3$)

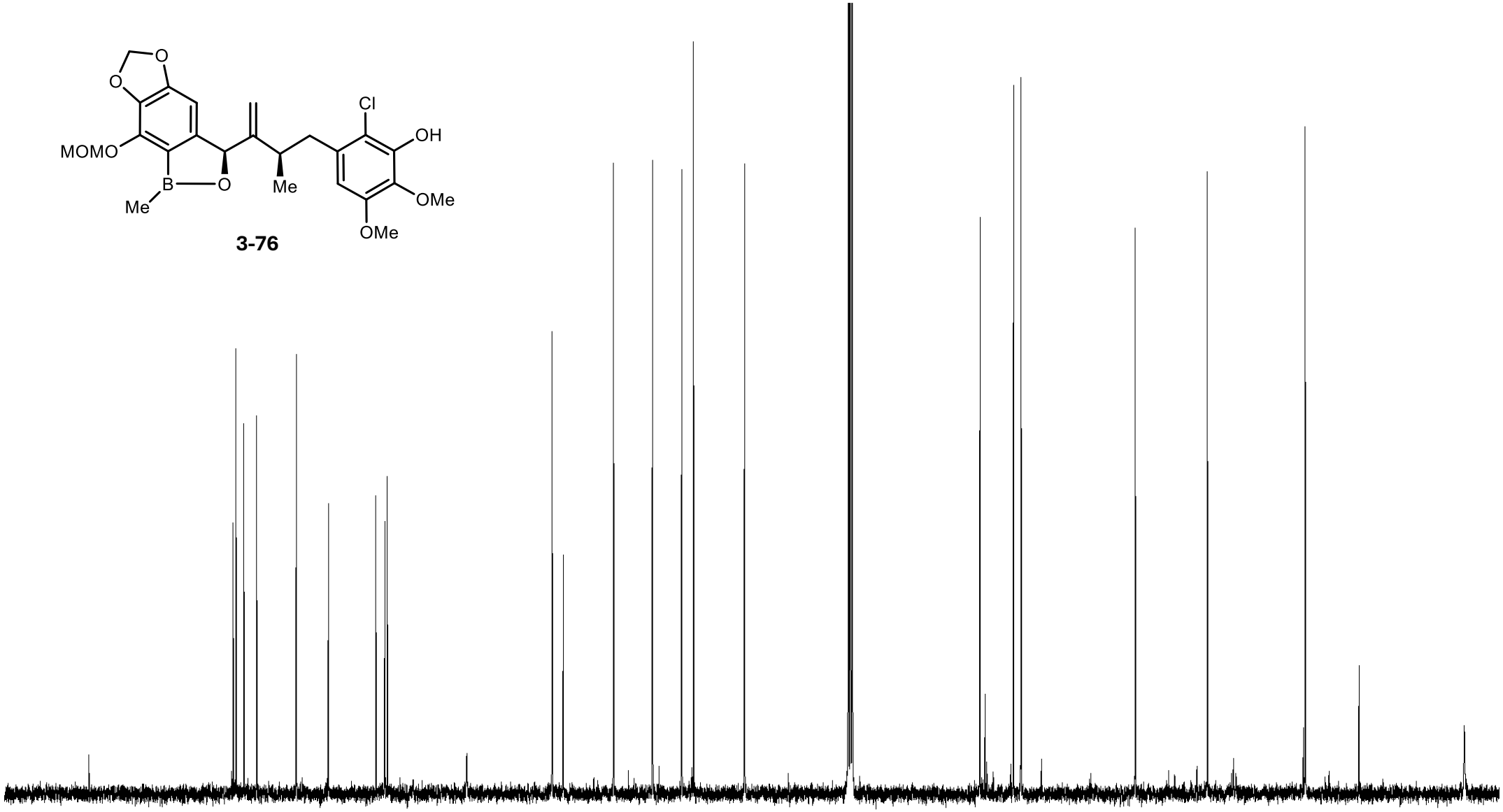
3-76



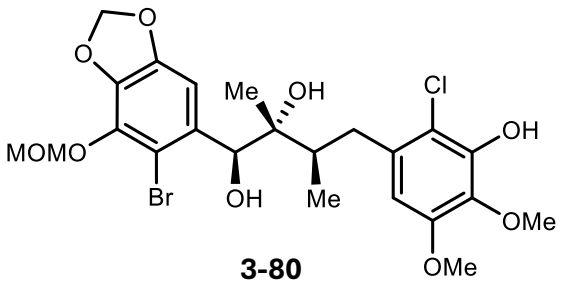
^{13}C NMR (125 MHz, $CDCl_3$)

3-76

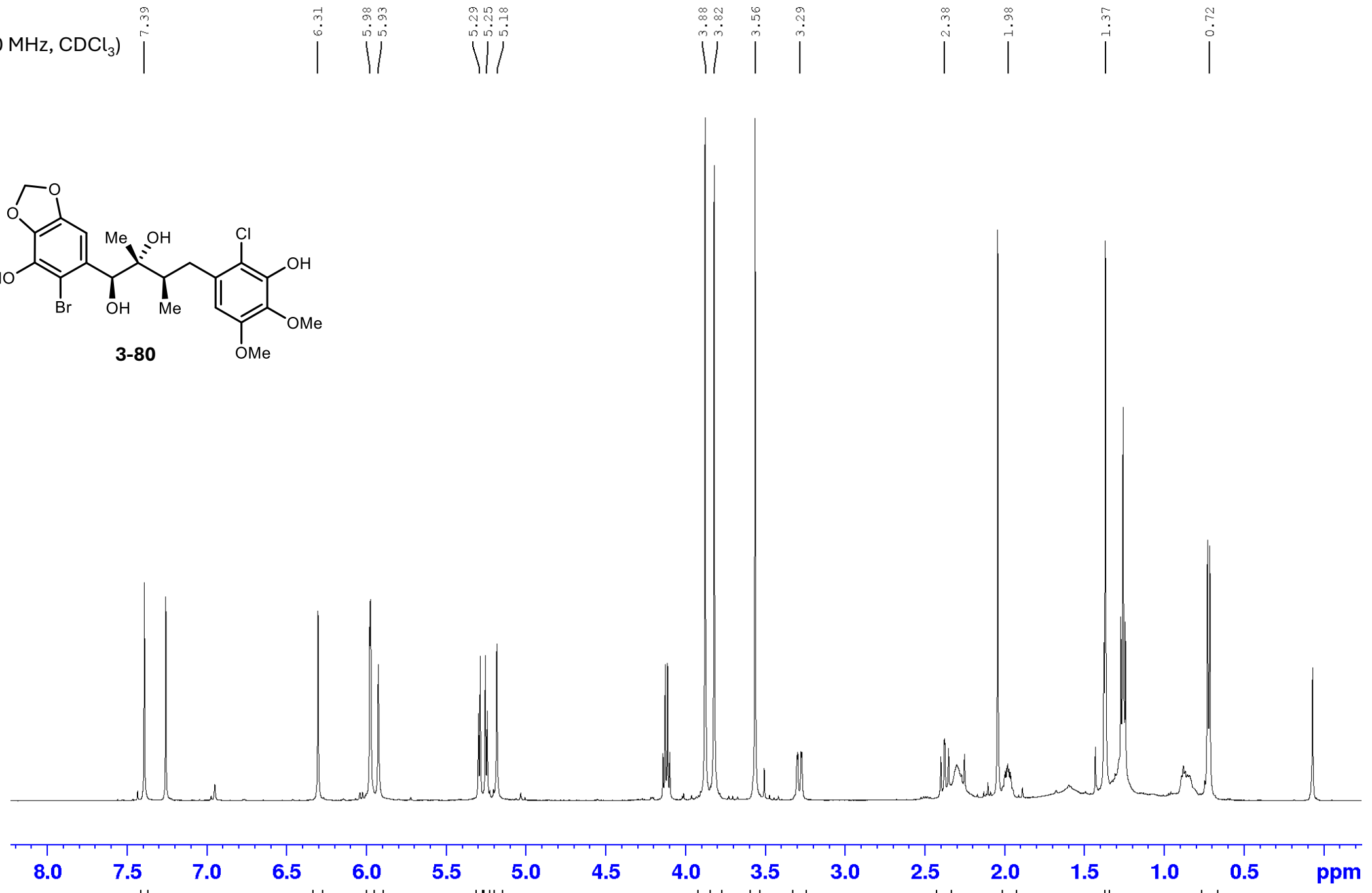
153.32
152.97
152.01
150.44
145.52
141.56
135.68
134.58
134.28
113.93
112.53
106.33
101.49
97.88
96.44
90.11
61.04
56.90
55.97
41.85
32.93
20.84
14.21
1.18



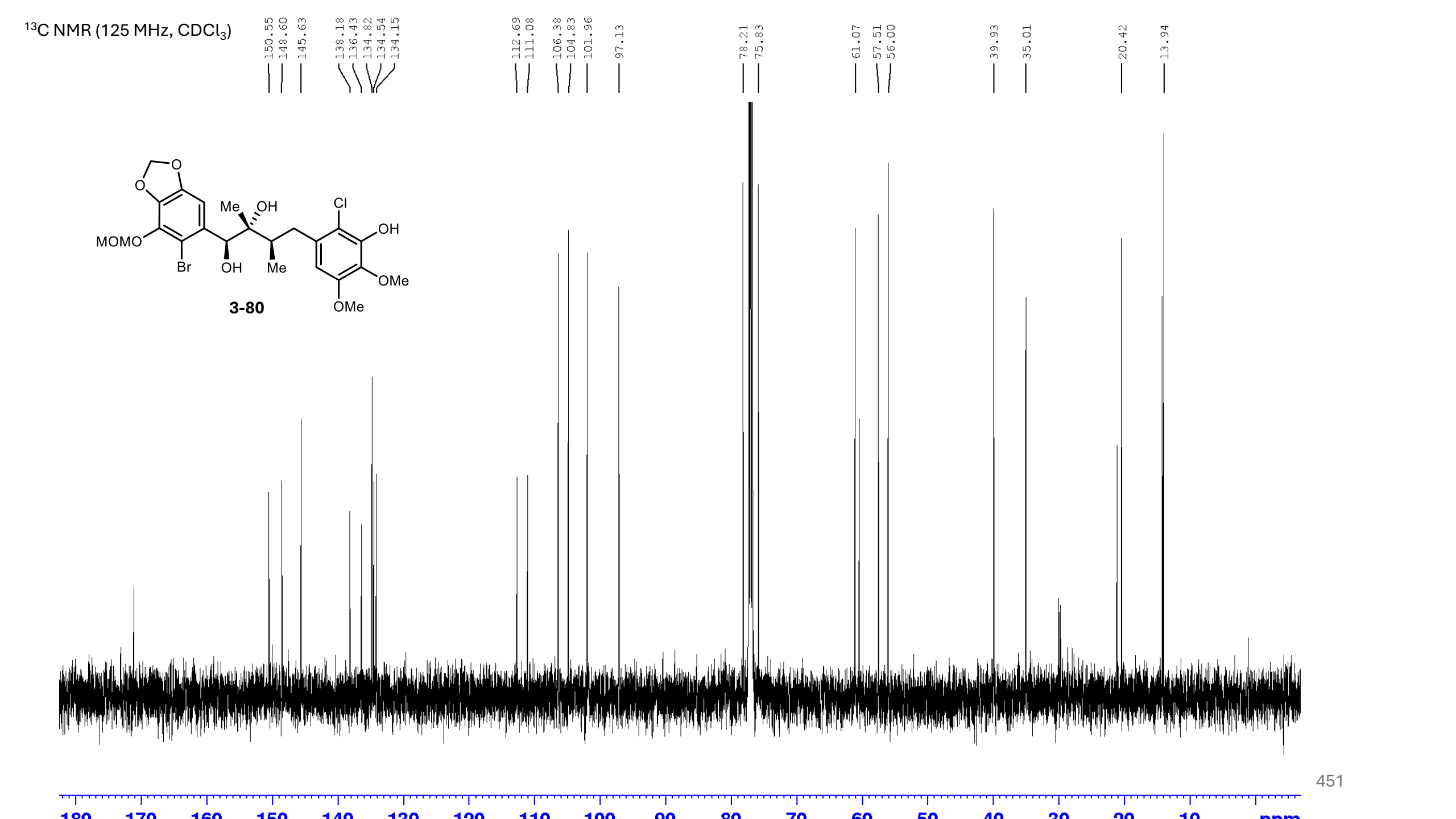
^{1}H NMR (500 MHz, $CDCl_3$)



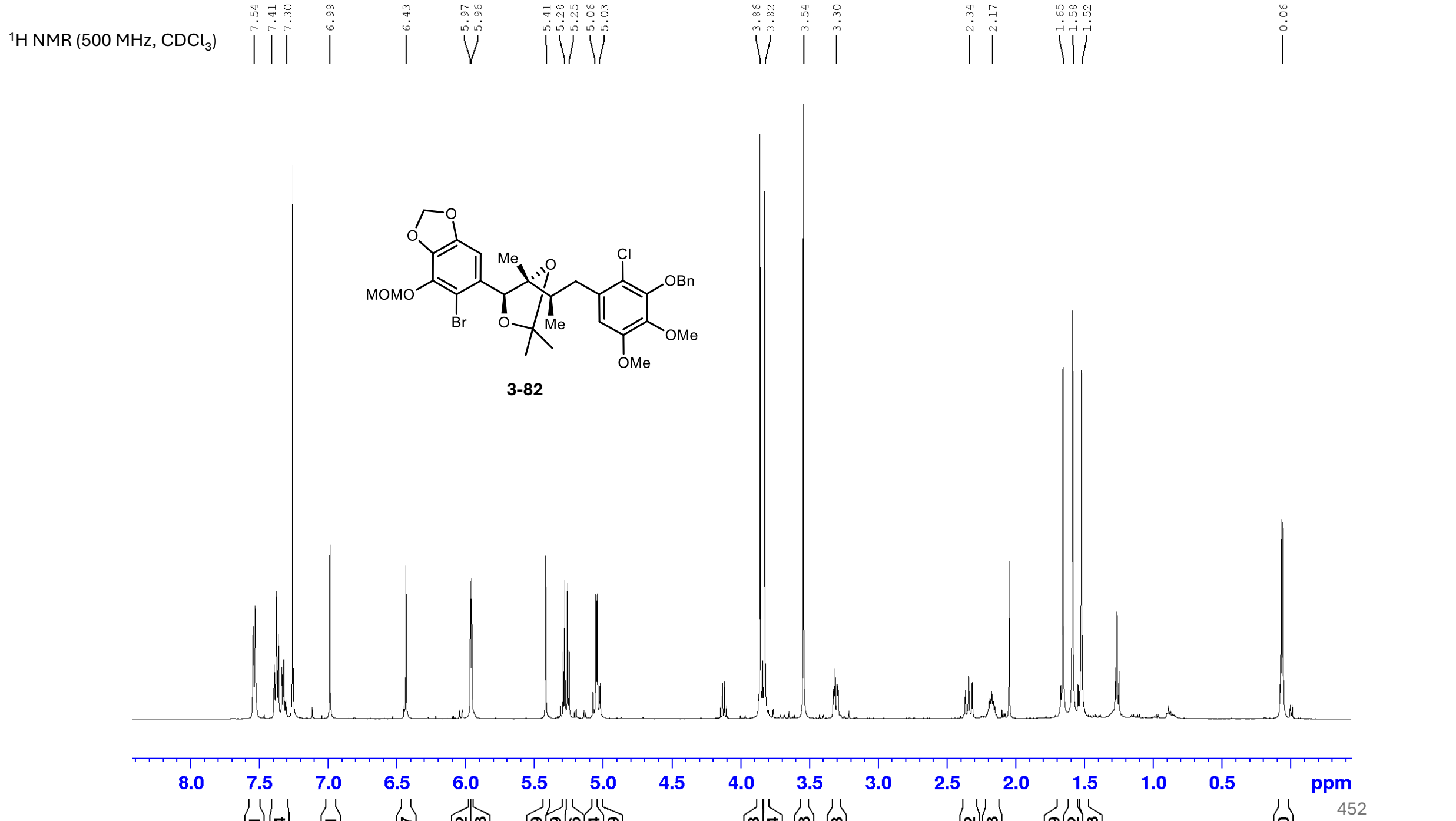
3-80



^{13}C NMR (125 MHz, $CDCl_3$)



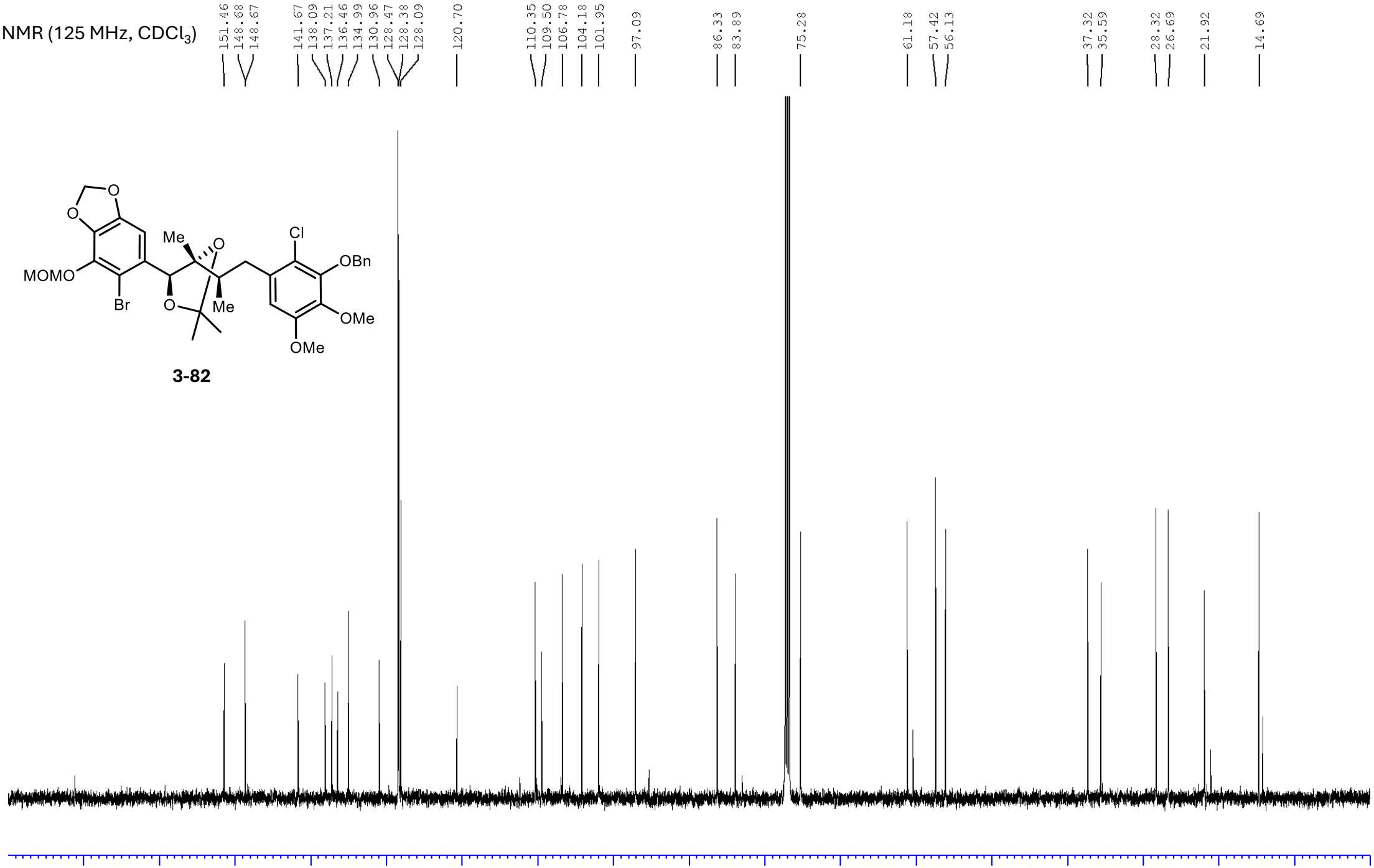
^{1}H NMR (500 MHz, $CDCl_3$)



3-82

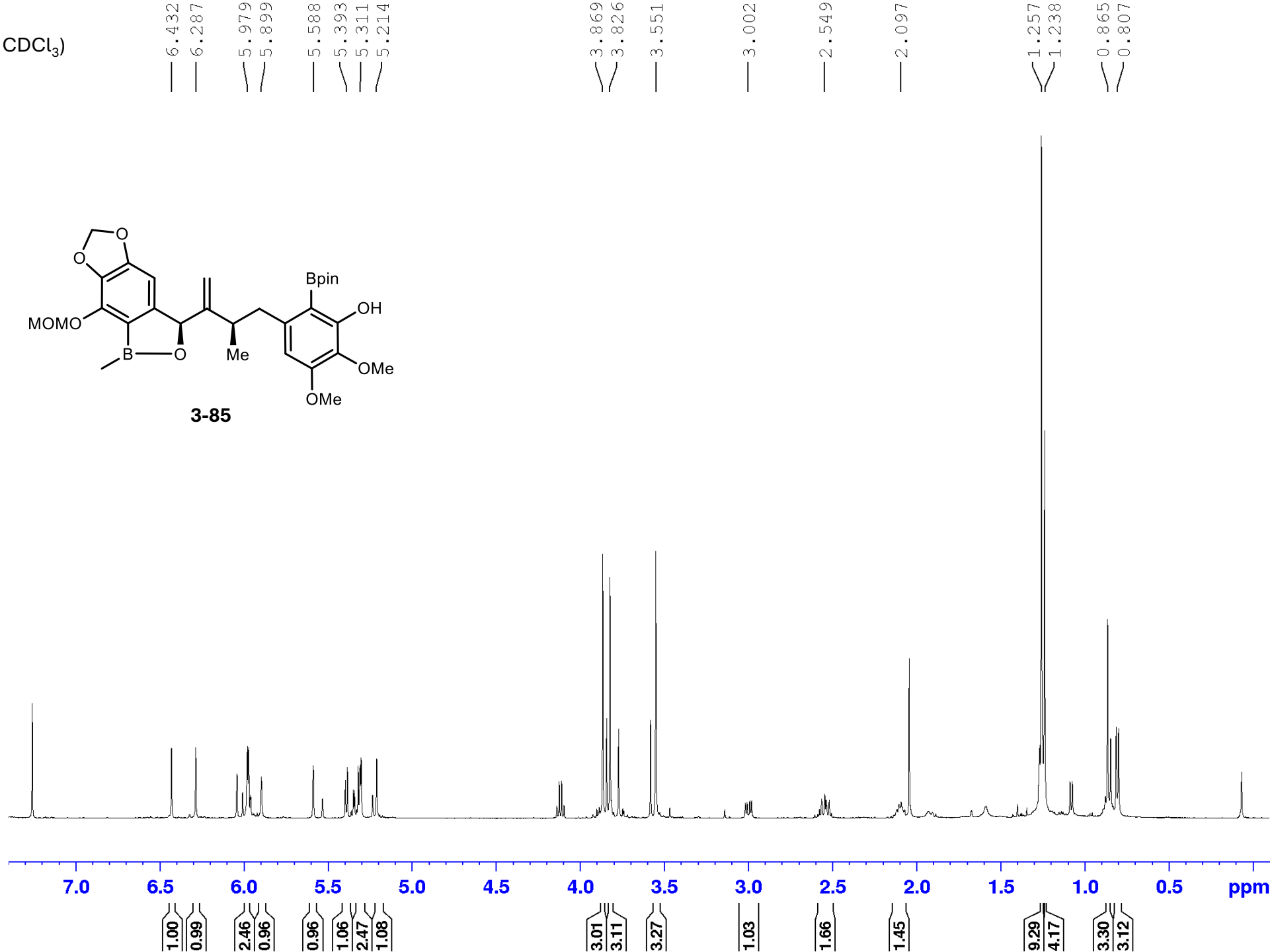
^{13}C NMR (125 MHz, $CDCl_3$)

3-82

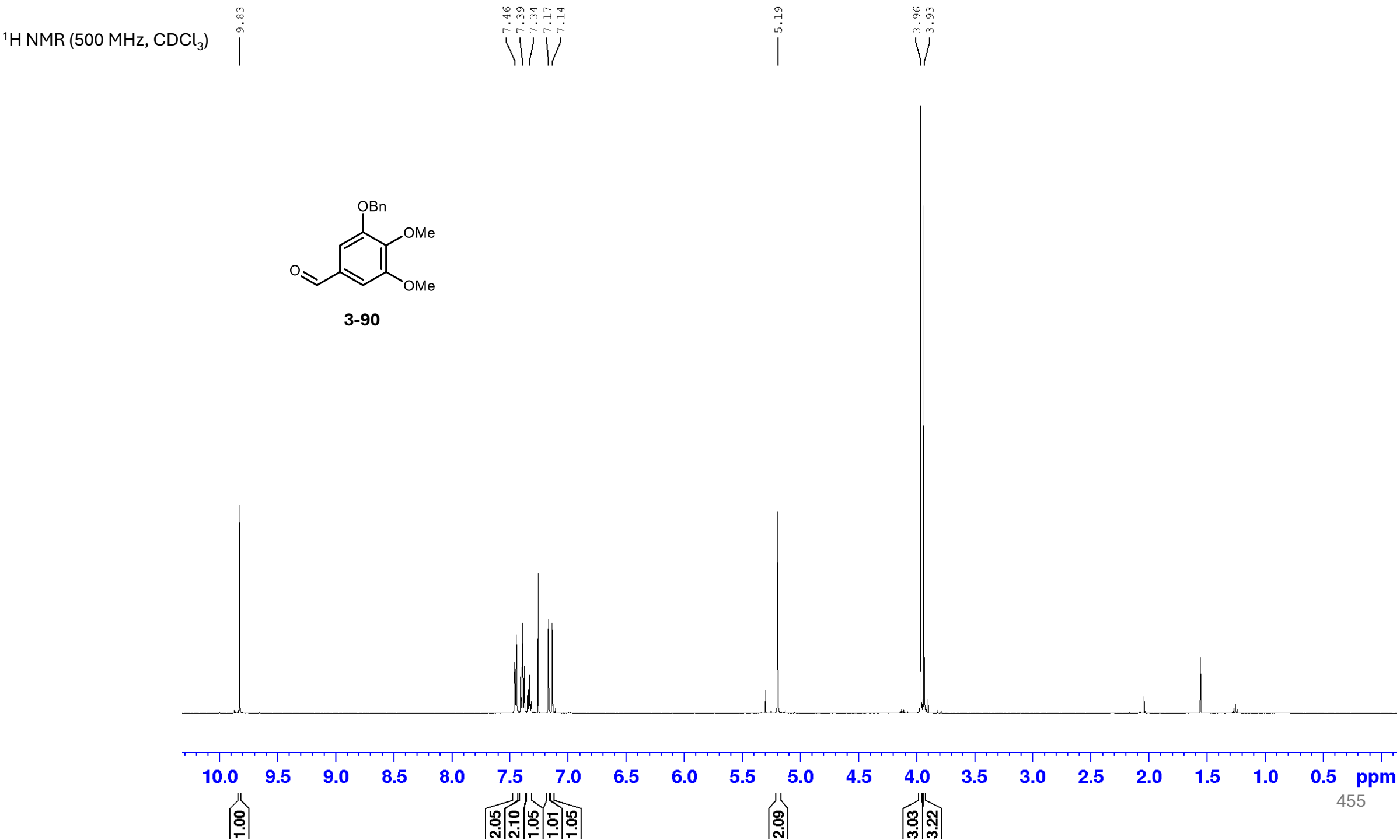


^{1}H NMR (500 MHz, $CDCl_3$)

3-85



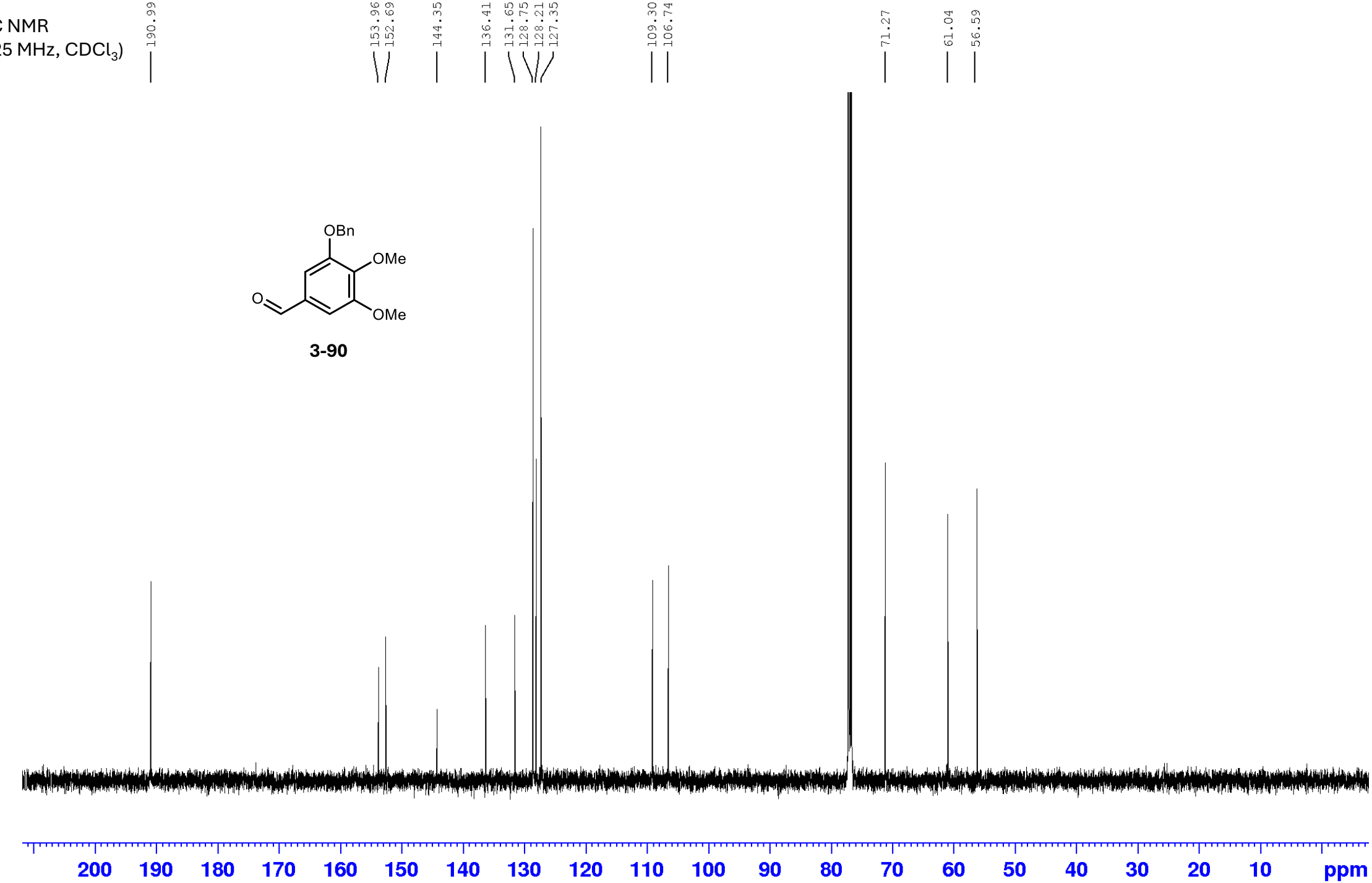
^{1}H NMR (500 MHz, $CDCl_3$)



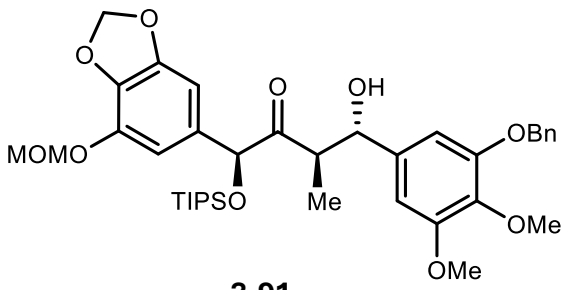
3-90

^{13}C NMR
(125 MHz, $CDCl_3$)

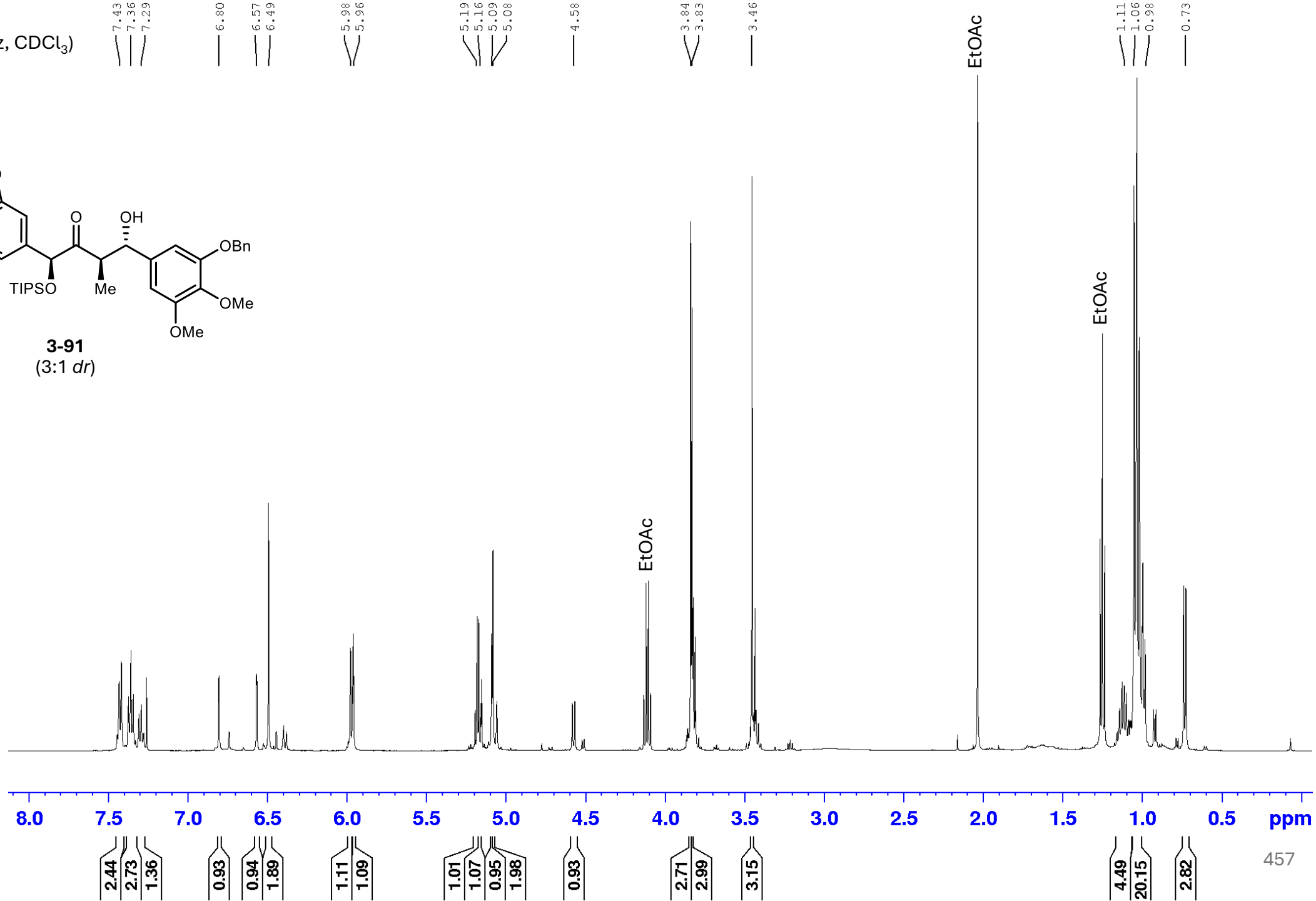
3-90



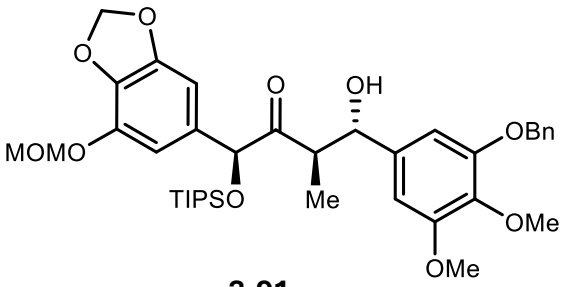
^{1}H NMR (500 MHz, $CDCl_3$)



3-91
(3:1 *dr*)



^{13}C NMR (125 MHz, $CDCl_3$)

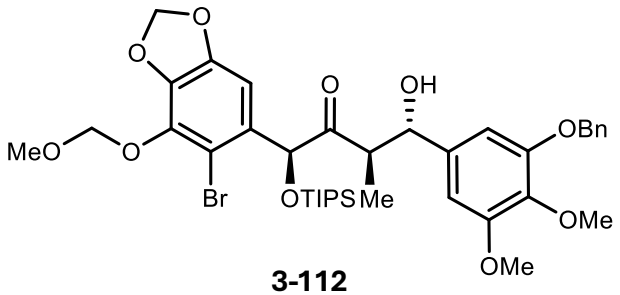


3-91
(3:1 *dr*)

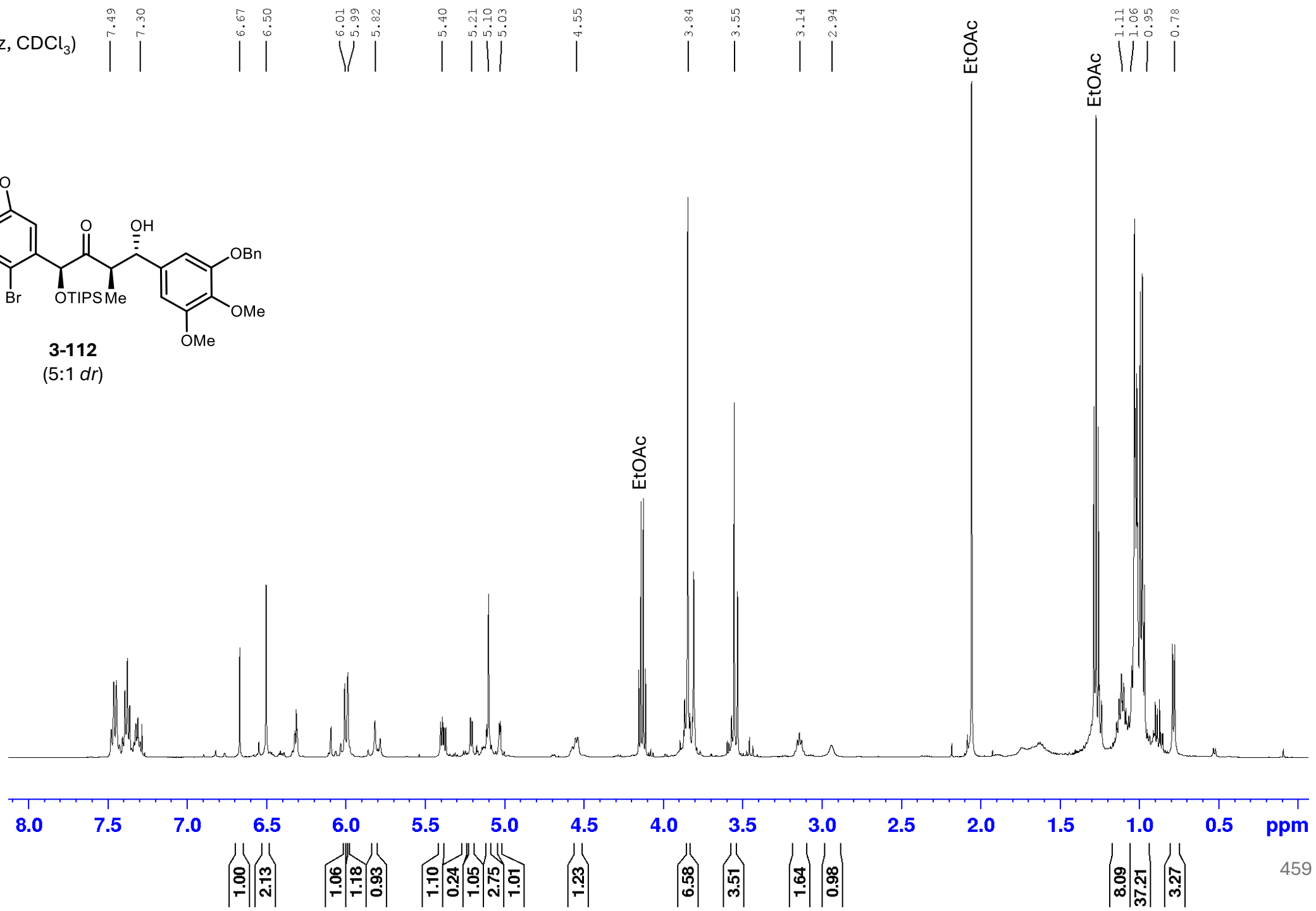
213.67 153.46 152.13 149.23 140.38 138.23 137.73 137.03 136.08 133.31 128.57 128.00 127.37 110.20 105.96 103.69 101.74 101.62 95.54 80.71 76.73 71.00 60.94 56.23 55.93 47.10 17.94 17.91 15.90 12.18

210 200 190 180 170 160 150 140 130 120 110 100 90 80 70 60 50 40 30 20 10 ppm

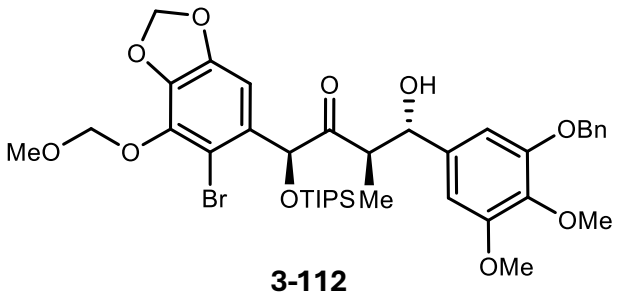
^{1}H NMR (500 MHz, $CDCl_3$)



3-112
(5:1 *dr*)



^{13}C NMR (125 MHz, $CDCl_3$)

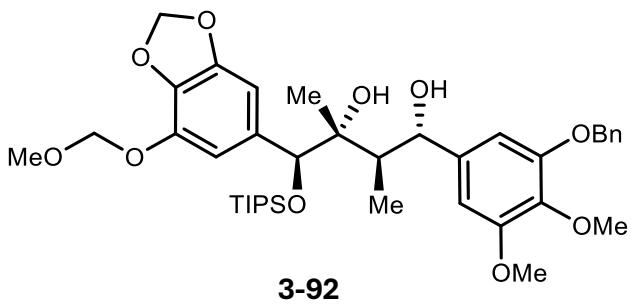


3-112
(5:1 *dr*)

211.58
153.28
152.07
148.86
138.26
138.16
137.95
137.07
136.46
132.31
128.50
127.85
127.35
109.48
105.36
103.29
102.61
102.17
97.02
80.26
77.92
70.88
60.78
57.33
55.99
47.46
17.81
15.67
12.14

210 200 190 180 170 160 150 140 130 120 110 100 90 80 70 60 50 40 30 20 10 ppm

^{1}H NMR
(500 MHz, $CDCl_3$)

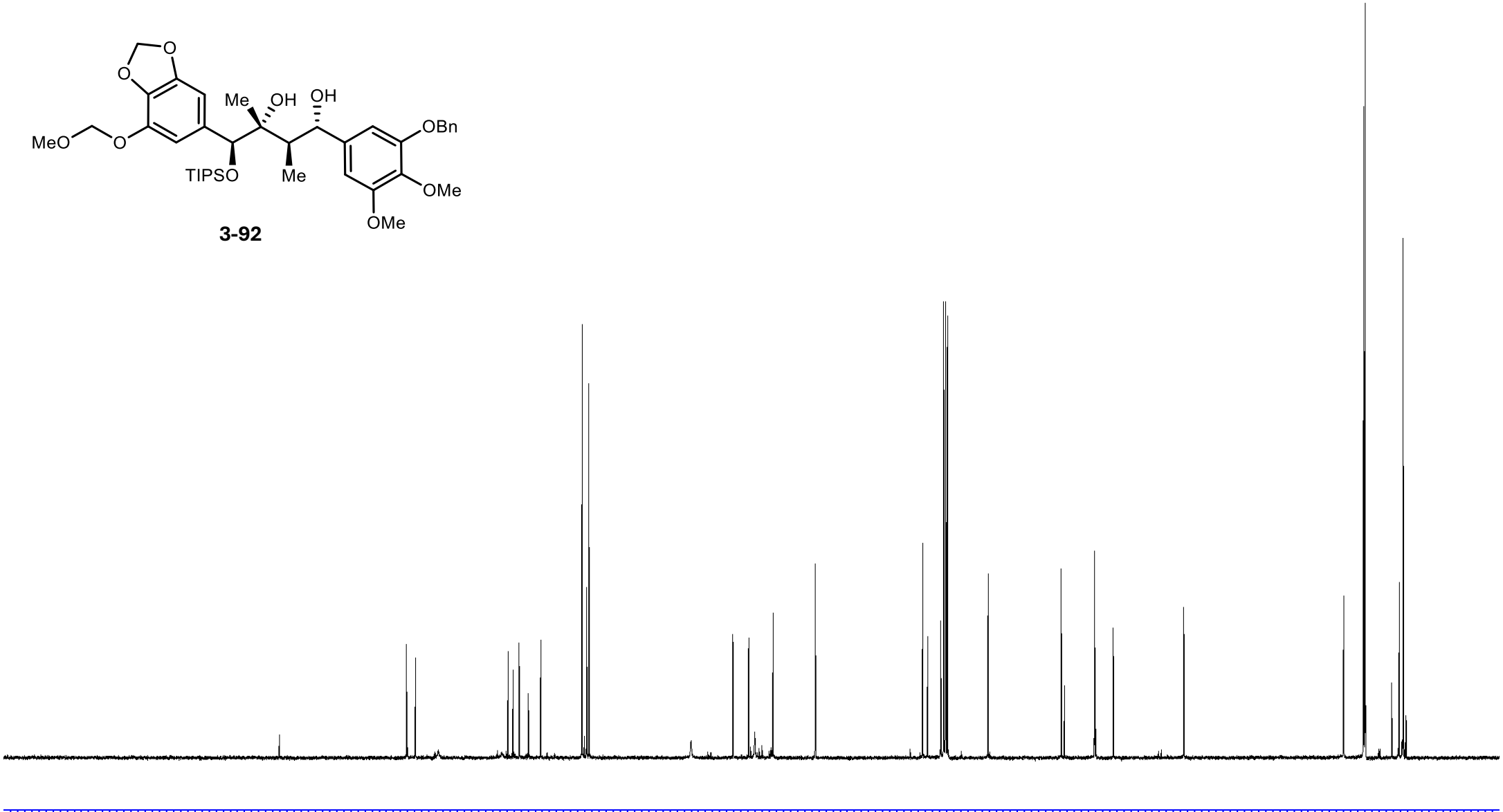


3-92

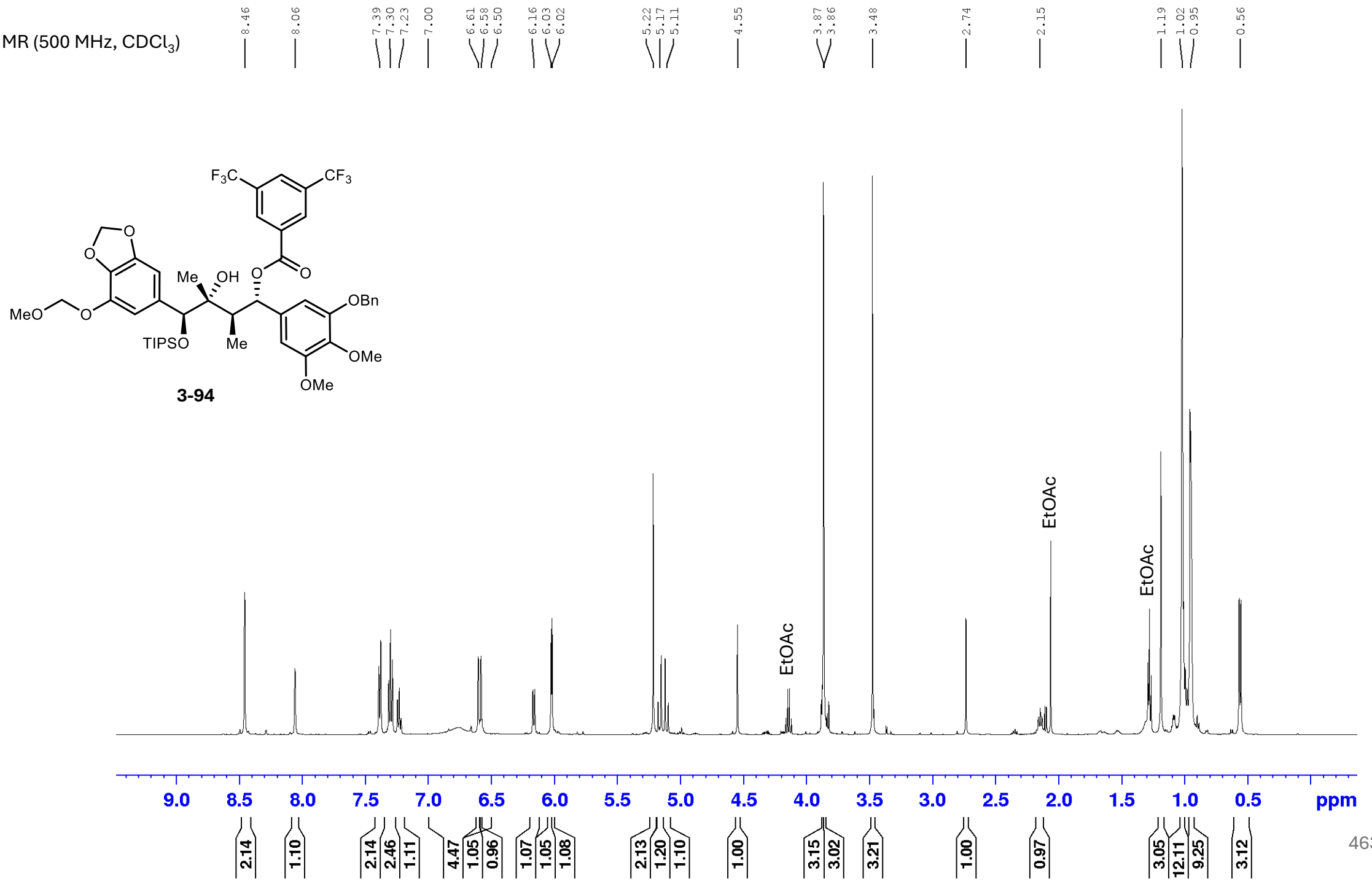
^{13}C NMR (125 MHz, $CDCl_3$)

153.14
151.89
148.70
139.74
138.85
138.15
137.26
135.95
134.24
128.41
127.74
127.43
113.03
107.12
104.90
104.09
101.47
95.52
80.34
79.66
77.79
71.14
60.80
56.13
56.10
53.46
43.51
18.16
17.97
13.16
12.58

3-92



^{1}H NMR (500 MHz, $CDCl_3$)

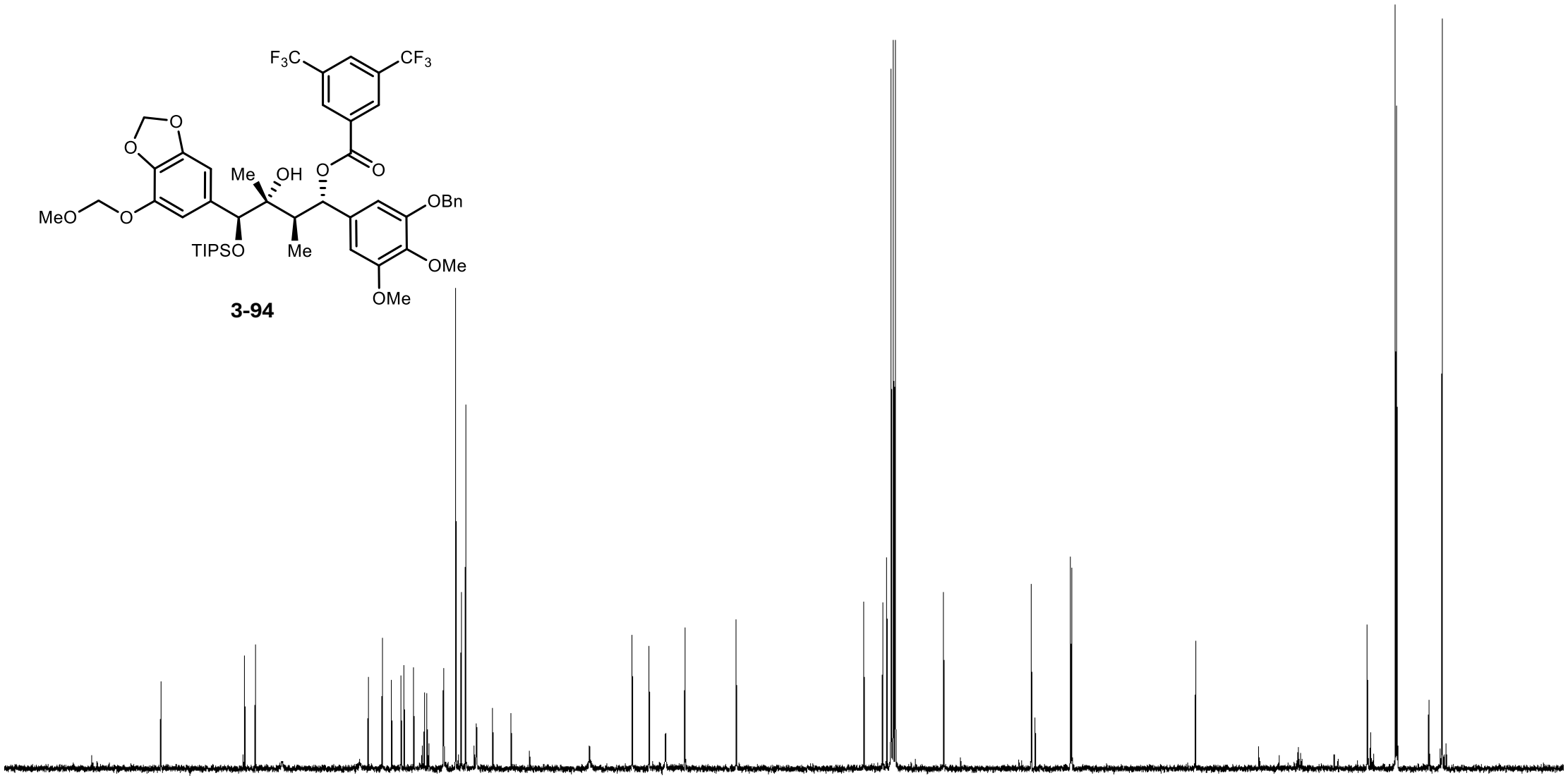


3-94

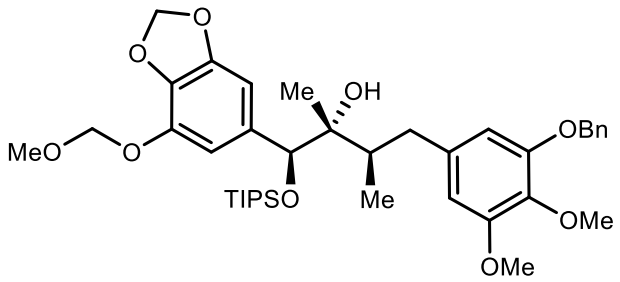
^{13}C NMR
(125 MHz, $CDCl_3$)

162.99
153.20
152.03
148.79
139.69
138.74
137.05
136.08
134.91
134.46
133.36
131.96
129.86
128.43
127.77
127.26
125.97
122.98
119.74
112.72
107.71
105.79
103.83
101.55
80.49
78.29
77.78
71.11
60.88
56.25
56.13
41.56
21.39
18.17
17.94
14.27
12.64

3-94



^{1}H NMR (500 MHz, $CDCl_3$)

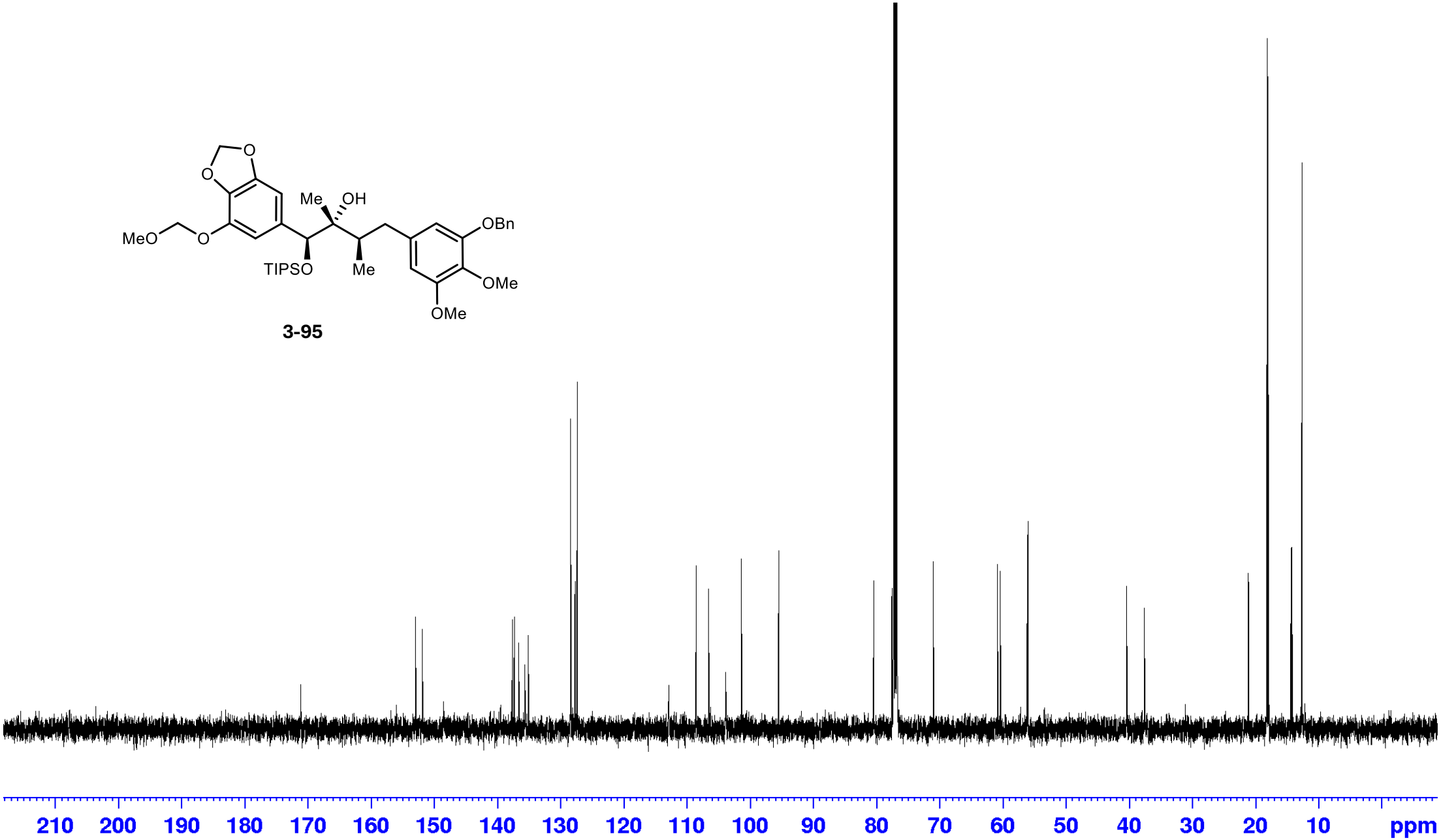


3-95

^{13}C NMR (125 MHz, $CDCl_3$)

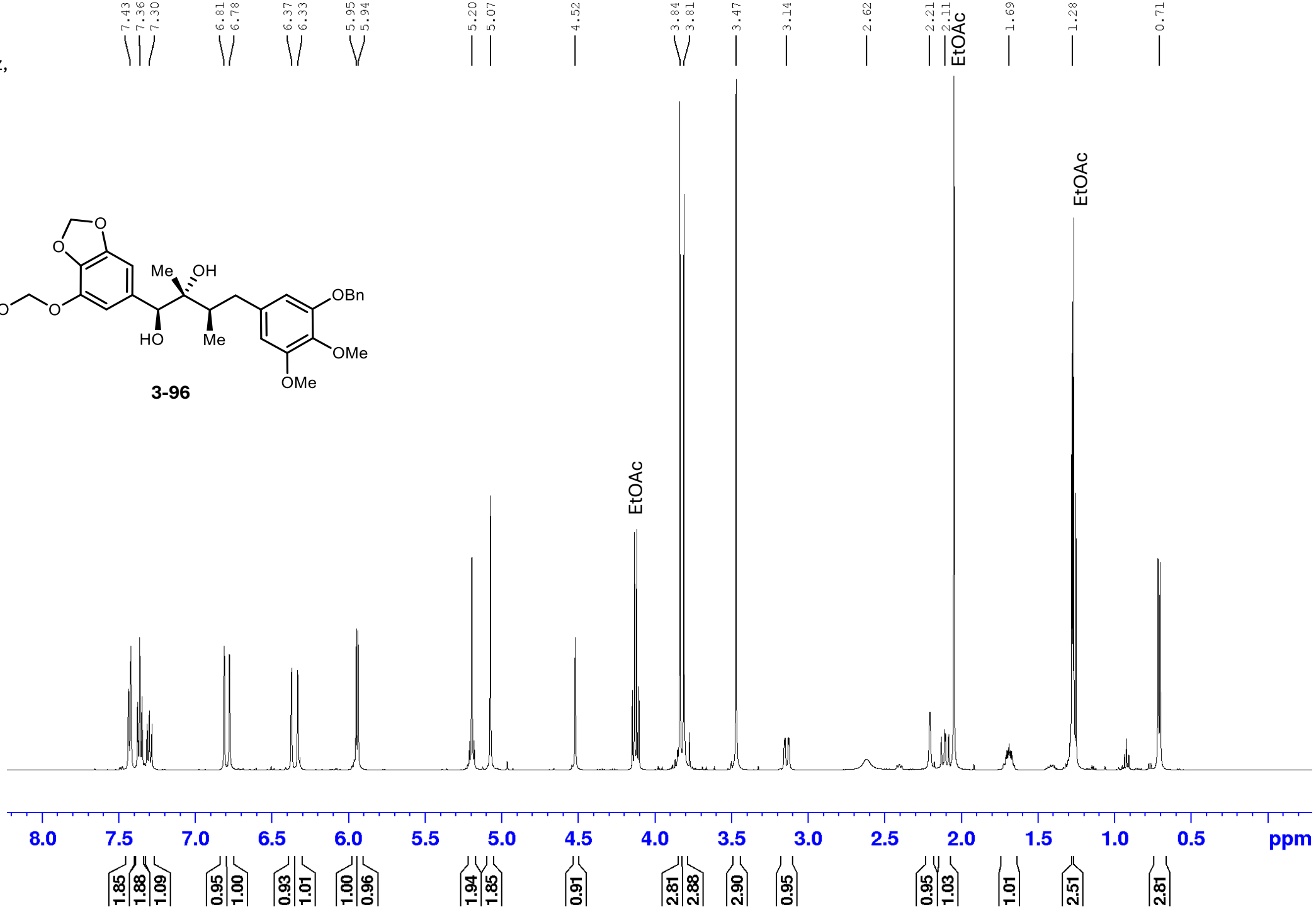
213.75
152.98
151.88
148.58
139.55
137.66
137.36
136.64
135.67
135.15
128.44
127.74
127.38
112.89
108.55
106.59
103.88
101.37
95.51
80.43
77.56
71.02
60.87
56.13
56.03
40.38
37.57
18.16
18.01
14.38
12.65

3-95

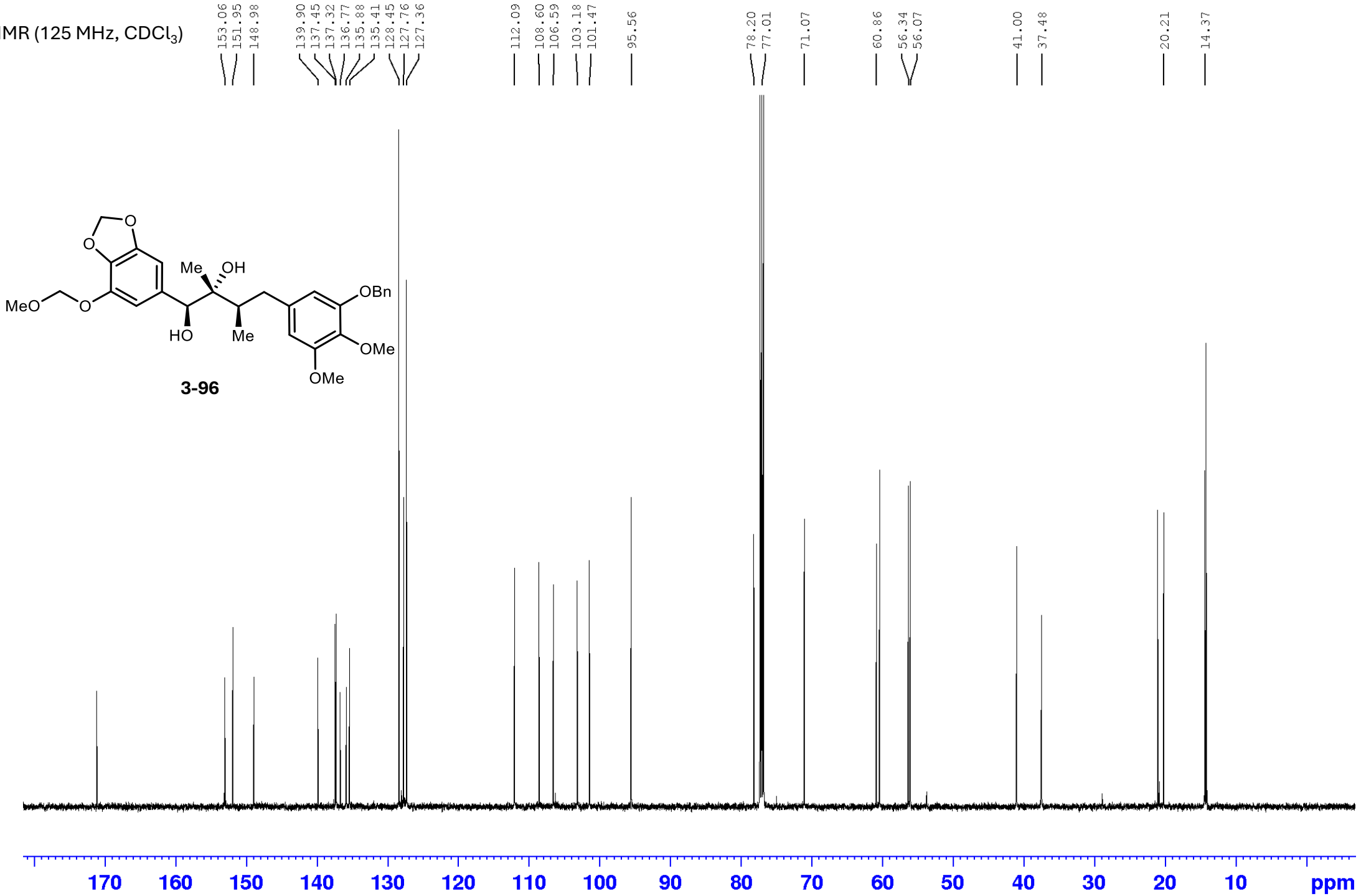


^{1}H NMR
(500 MHz,
$CDCl_3$)

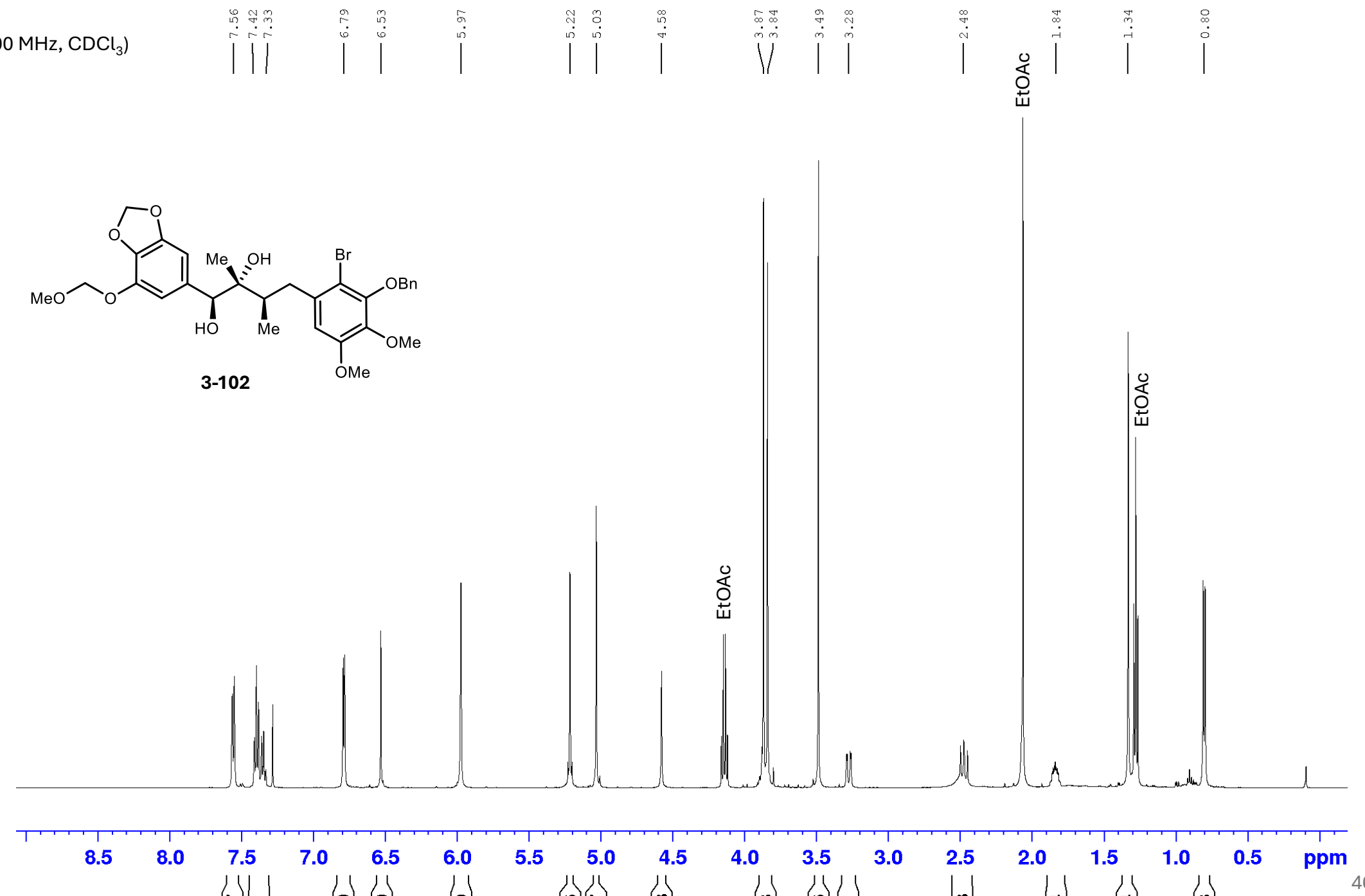
3-96



^{13}C NMR (125 MHz, $CDCl_3$)

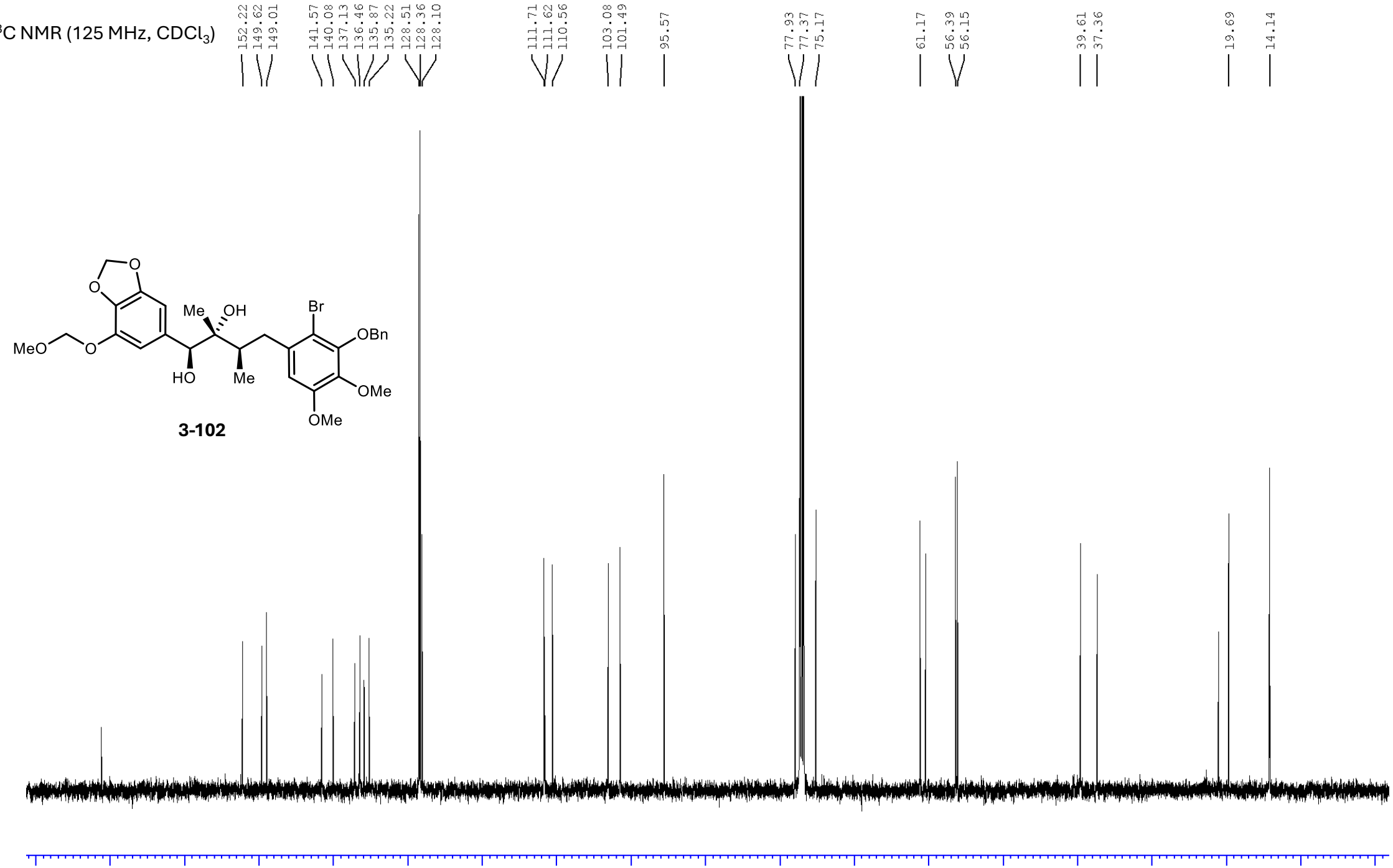


^{1}H NMR (500 MHz, $CDCl_3$)

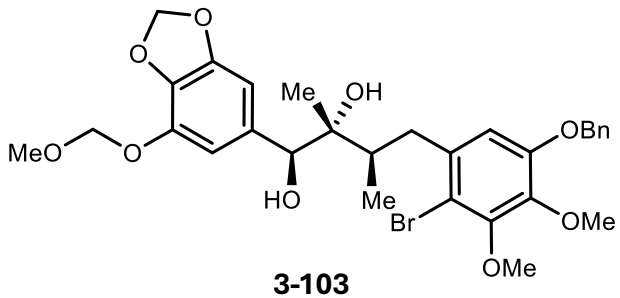


3-102

^{13}C NMR (125 MHz, $CDCl_3$)



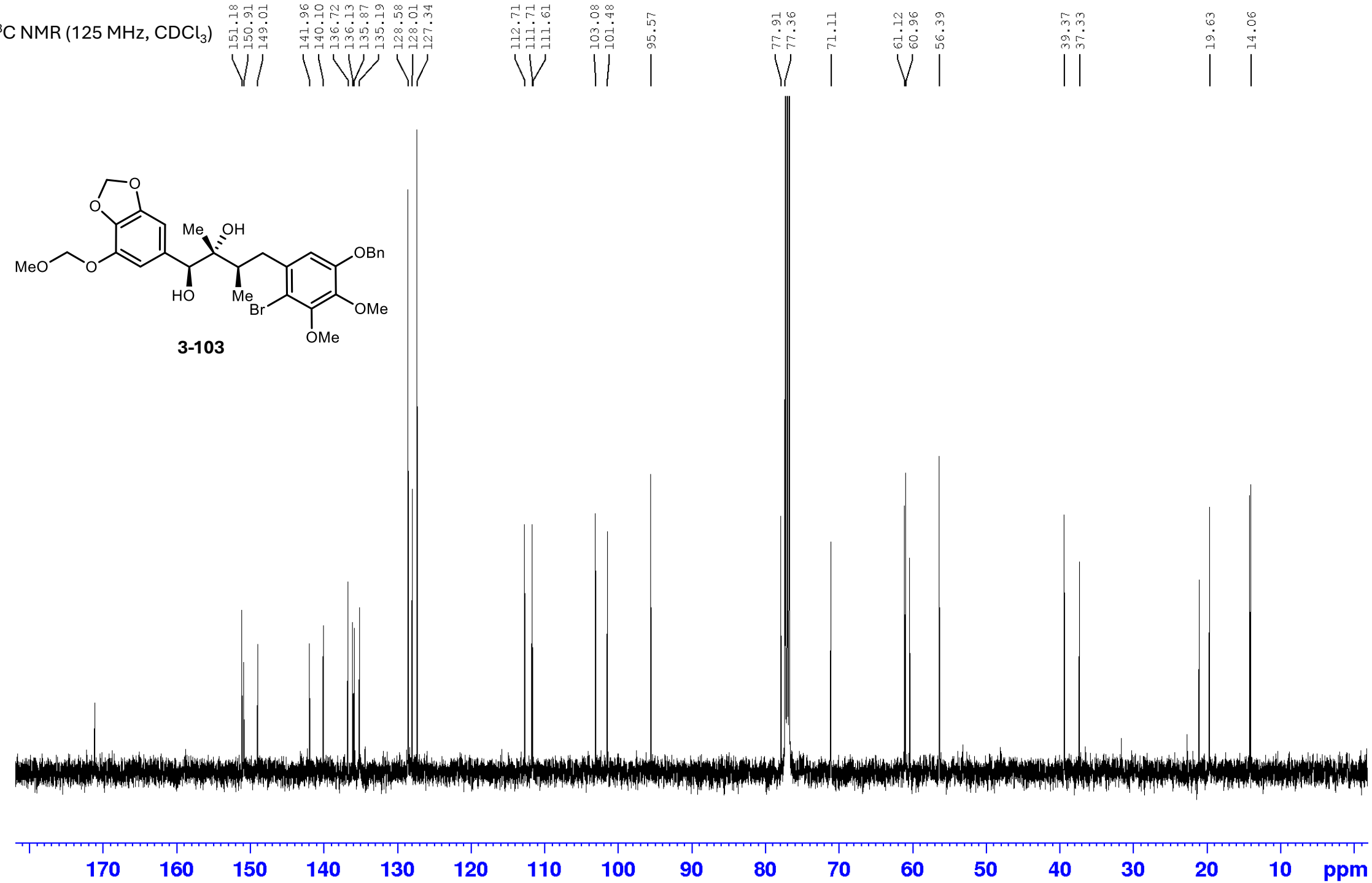
^{1}H NMR (500 MHz, $CDCl_3$)



3-103

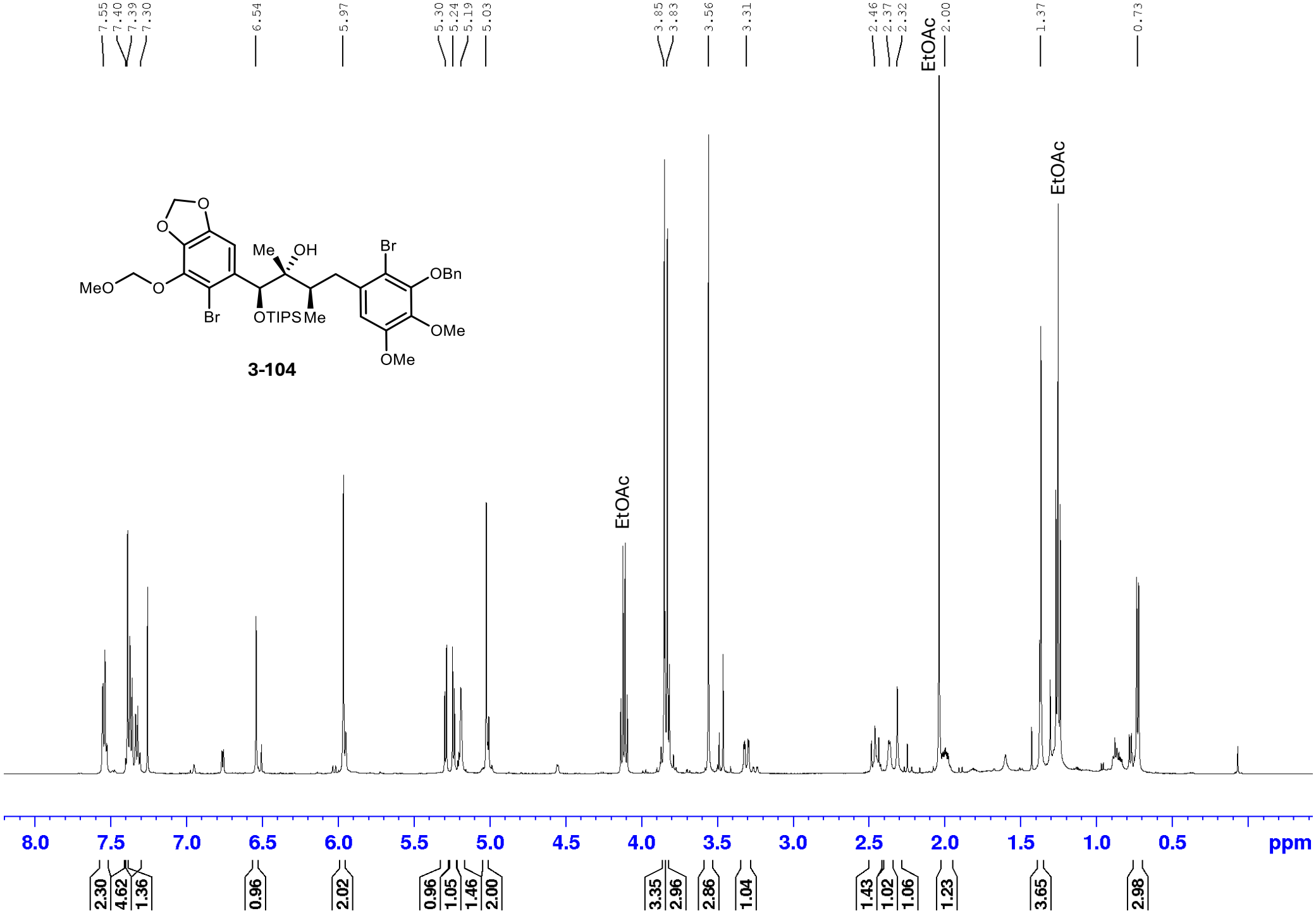
^{13}C NMR (125 MHz, $CDCl_3$)

3-103



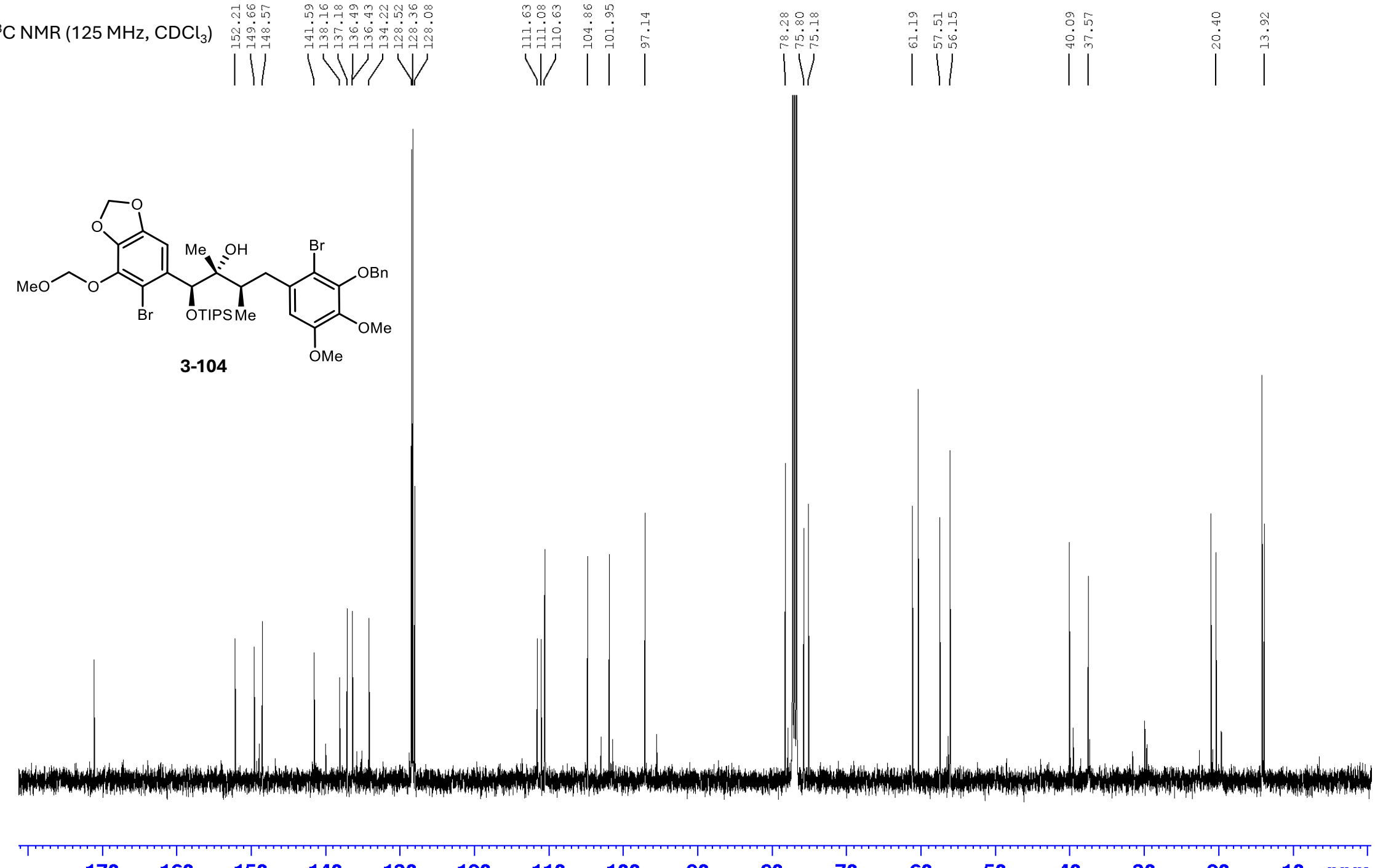
^{1}H NMR
(500 MHz,
$CDCl_3$)

3-104



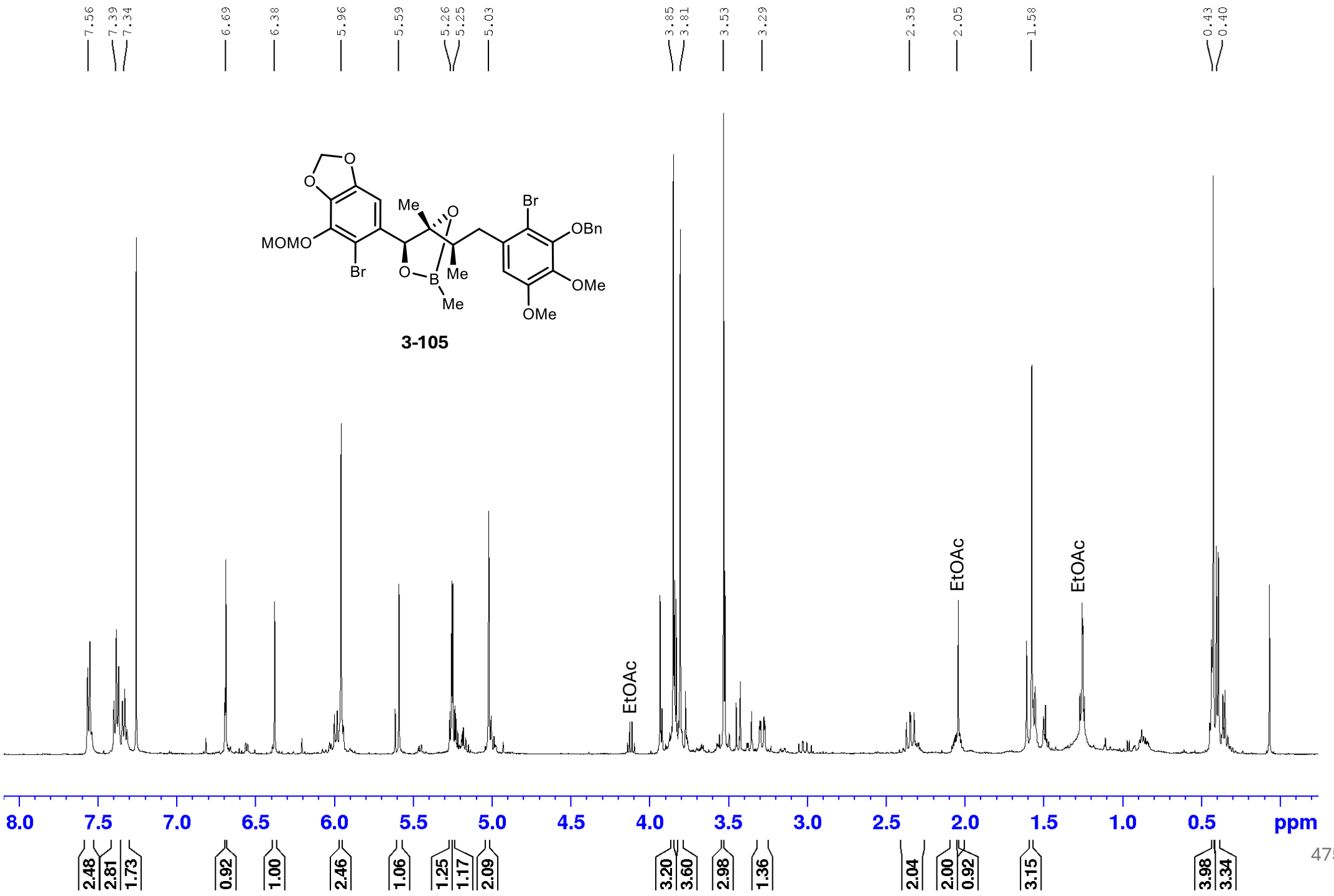
^{13}C NMR (125 MHz, $CDCl_3$)

3-104

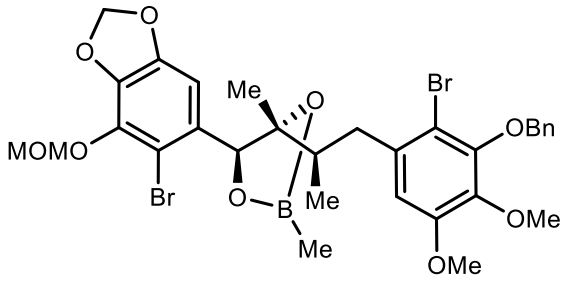


^{1}H NMR
(500 MHz,
$CDCl_3$)

3-105



^{13}C NMR (125 MHz, $CDCl_3$)

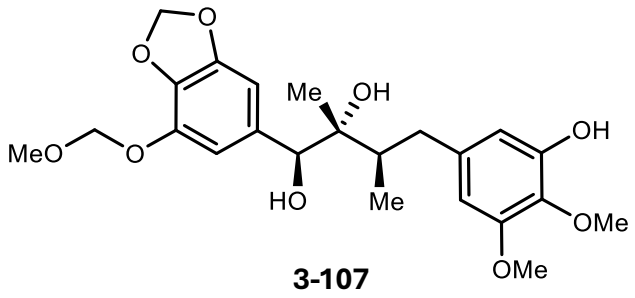


3-105

152.12
149.71
148.61
141.58
138.11
137.17
136.33
132.42
128.56
128.38
128.11
111.64
110.51
109.99
103.93
102.06
97.04
87.66
86.56
75.18
61.17
57.44
56.12
38.37
38.12
29.71
23.92
14.35

170 160 150 140 130 120 110 100 90 80 70 60 50 40 30 20 10 ppm

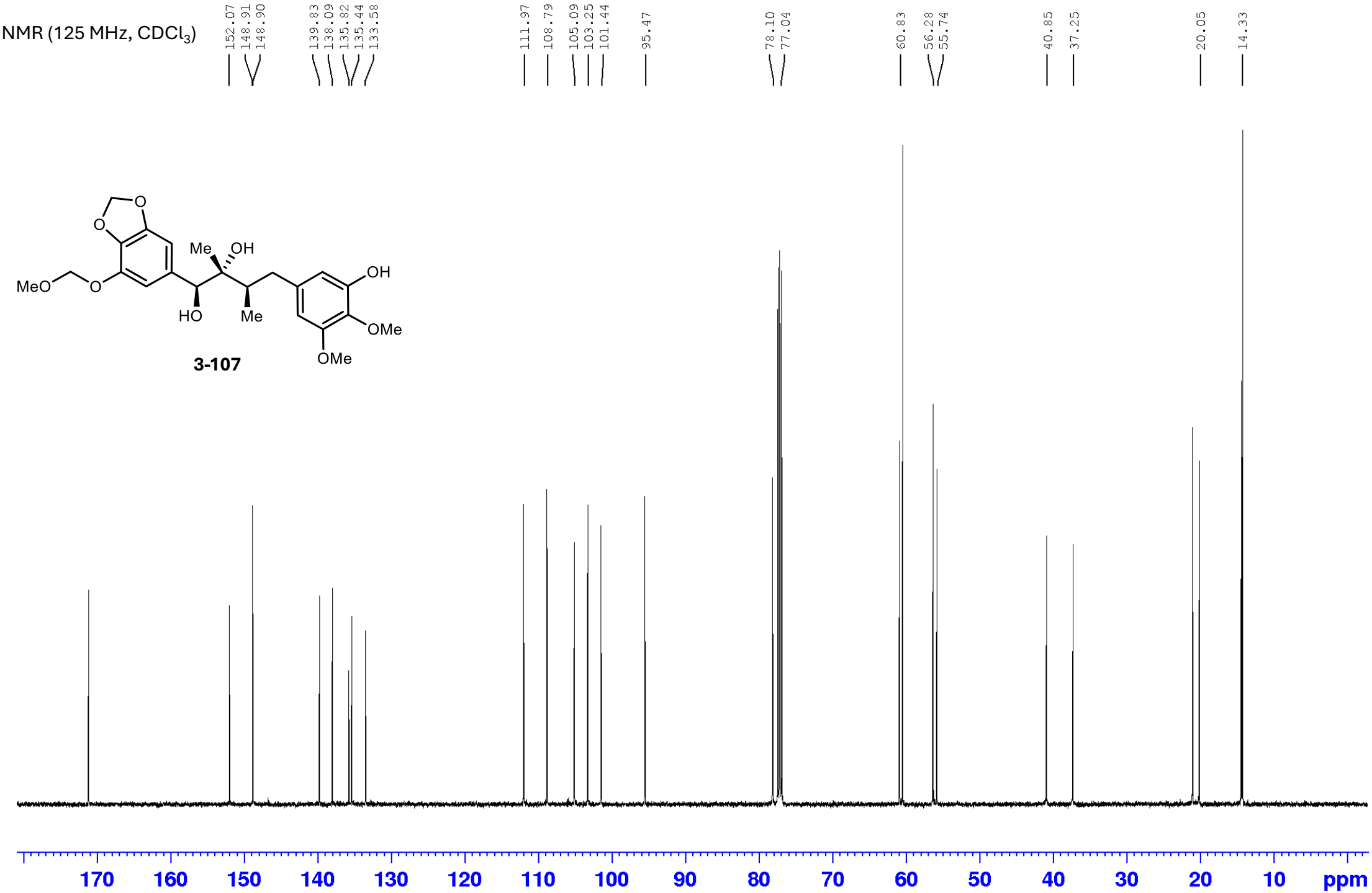
^{1}H NMR (500 MHz, $CDCl_3$)



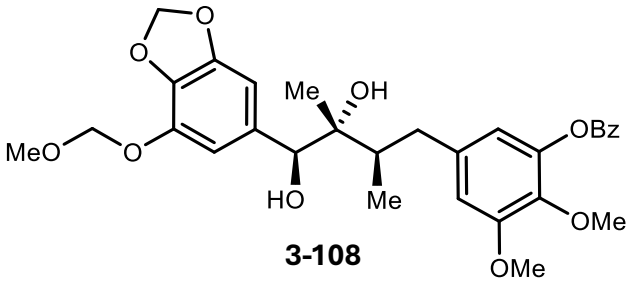
3-107

^{13}C NMR (125 MHz, $CDCl_3$)

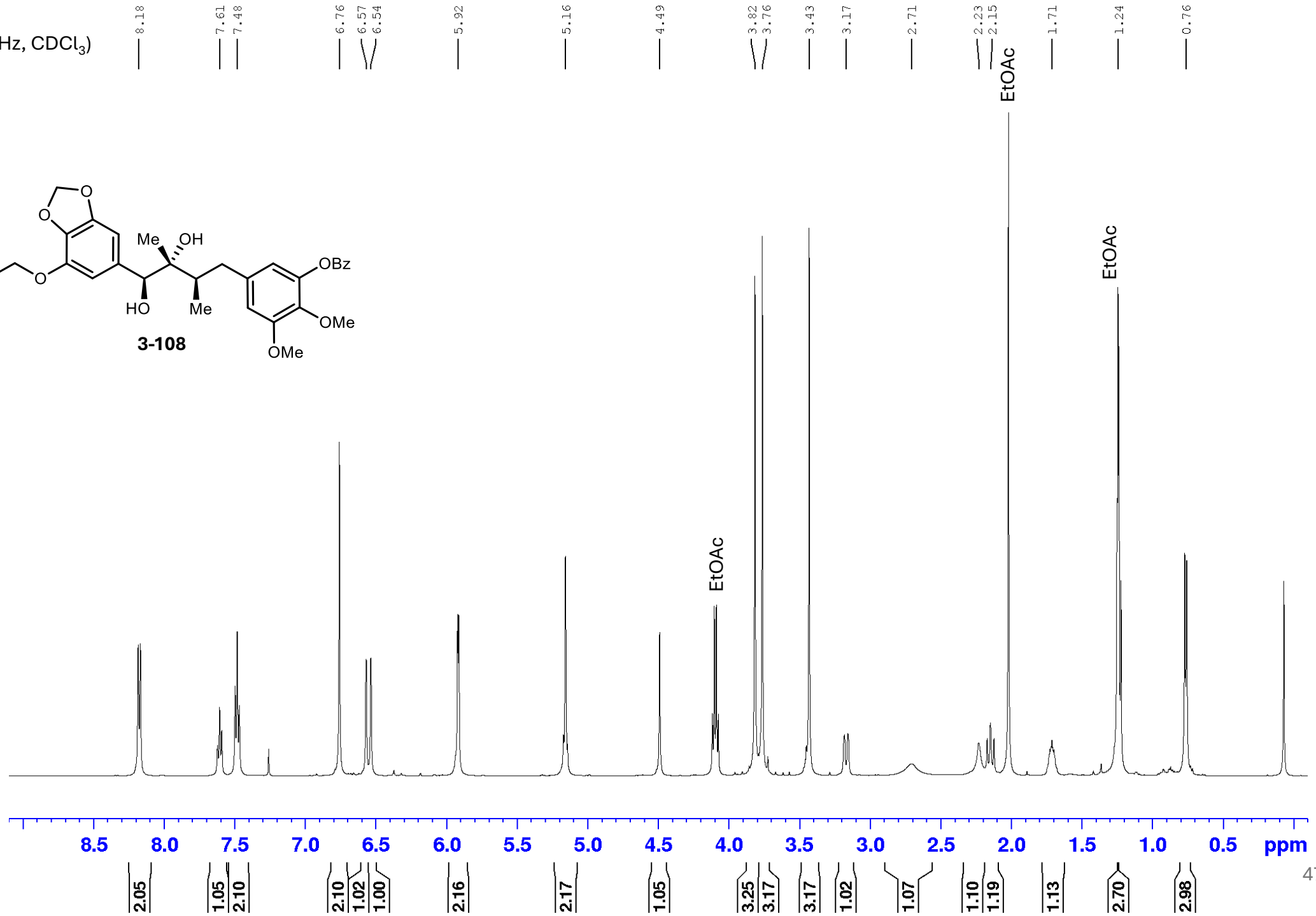
3-107



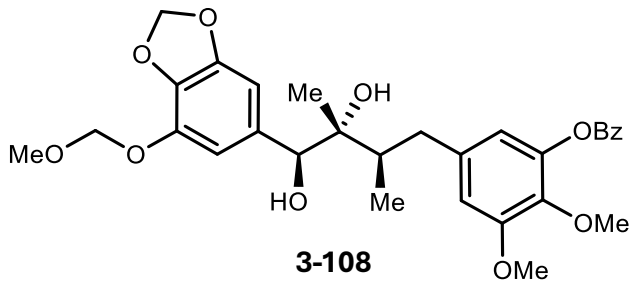
^{1}H NMR (500 MHz, $CDCl_3$)



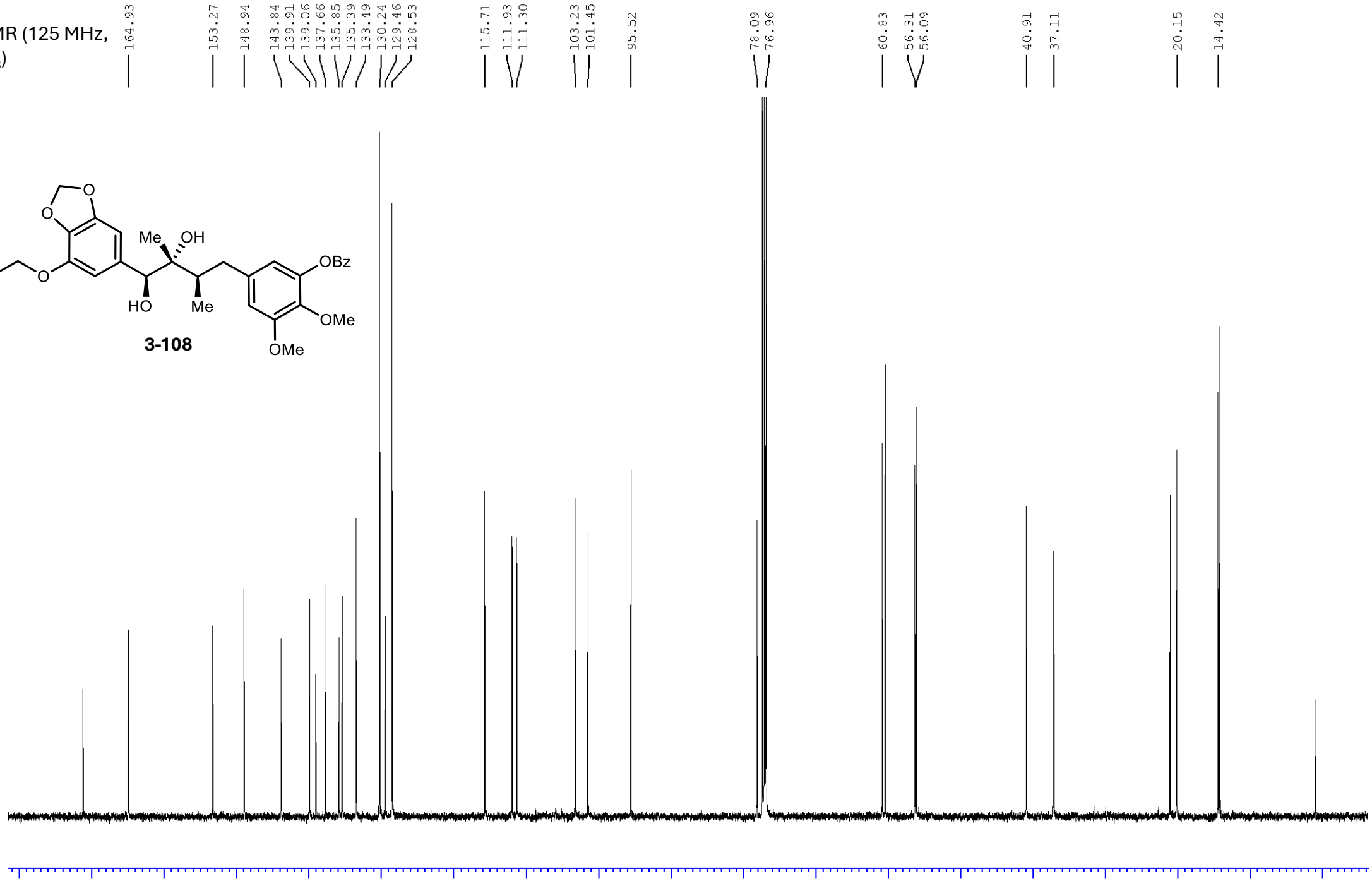
3-108



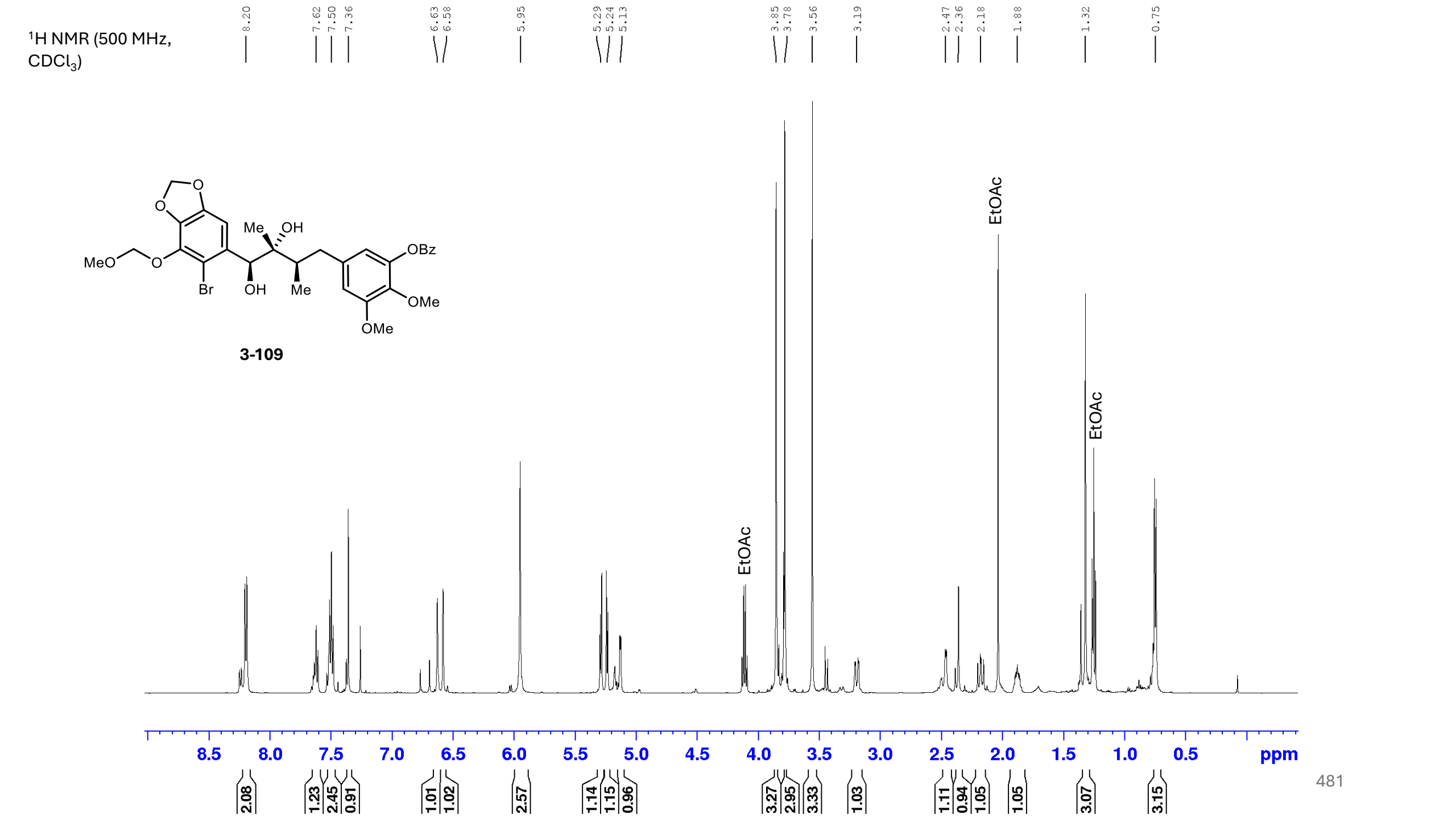
^{13}C NMR (125 MHz, $CDCl_3$)



3-108

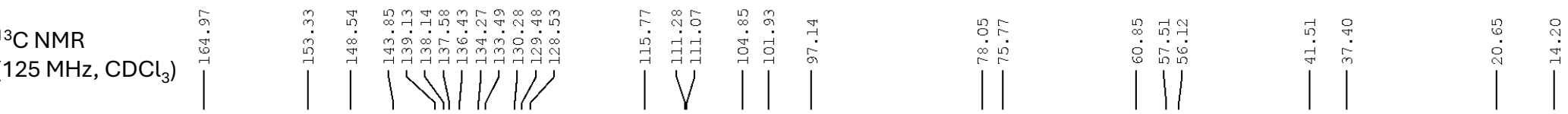


^{1}H NMR (500 MHz, $CDCl_3$)

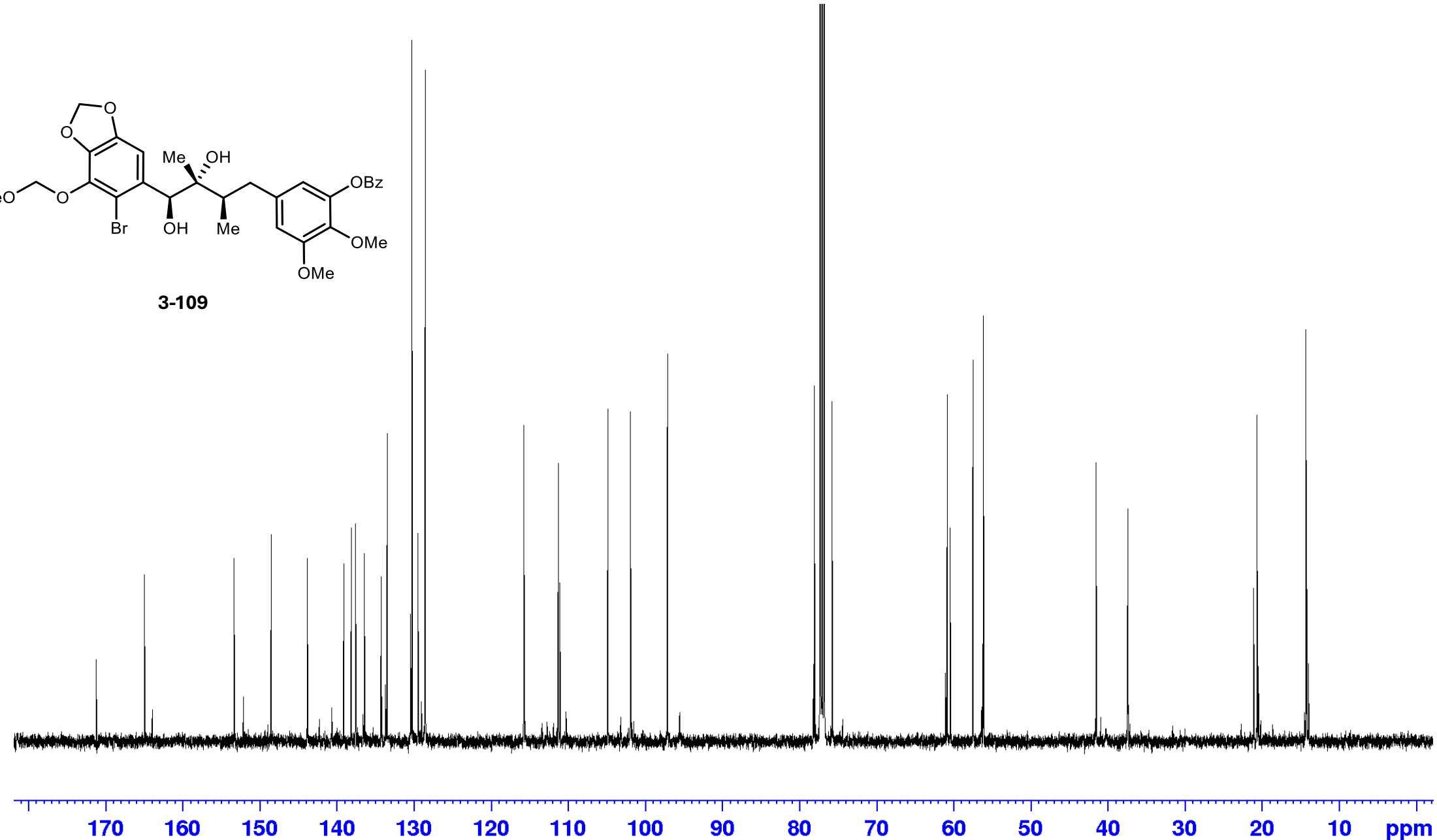


3-109

^{13}C NMR
(125 MHz, $CDCl_3$)

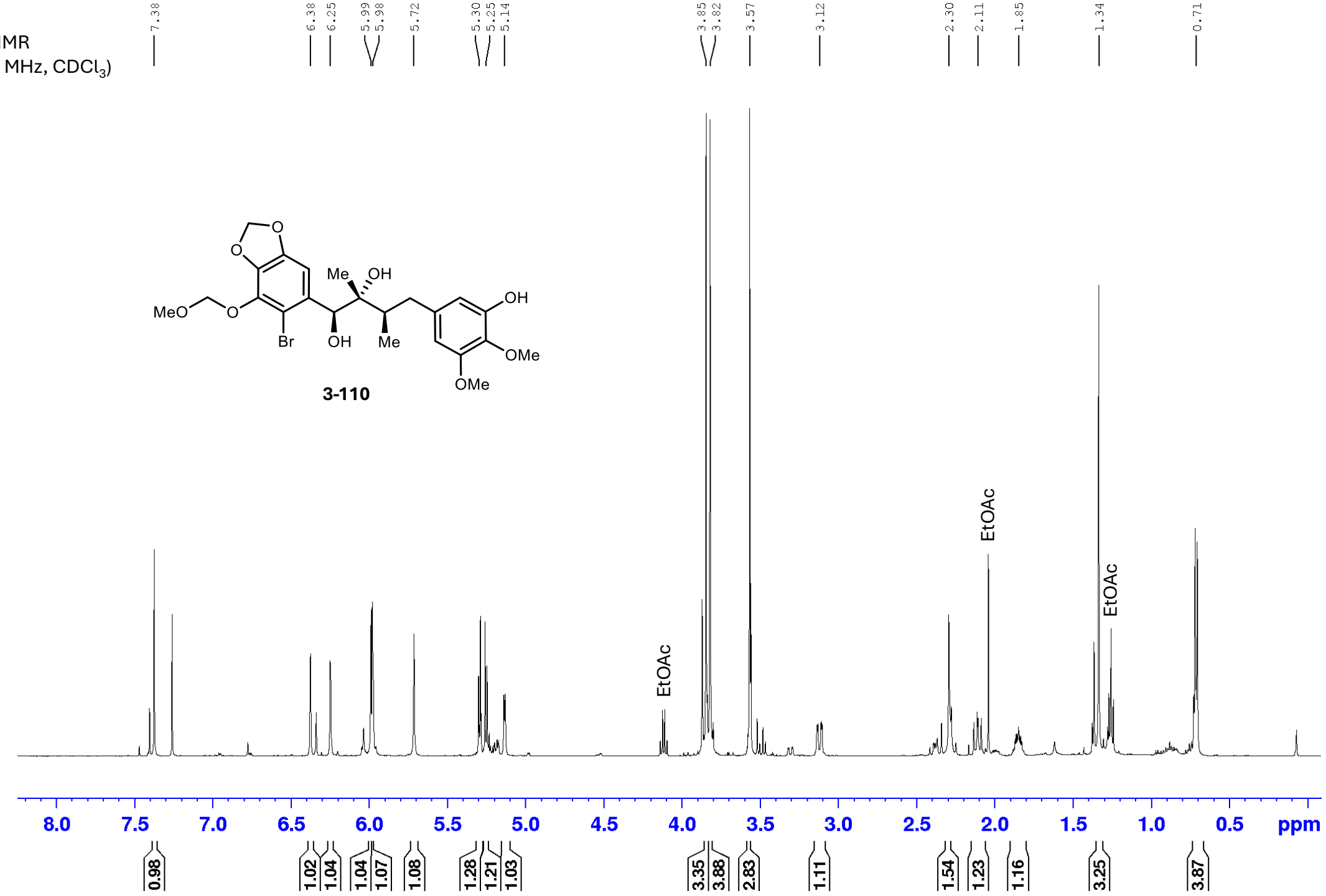


3-109



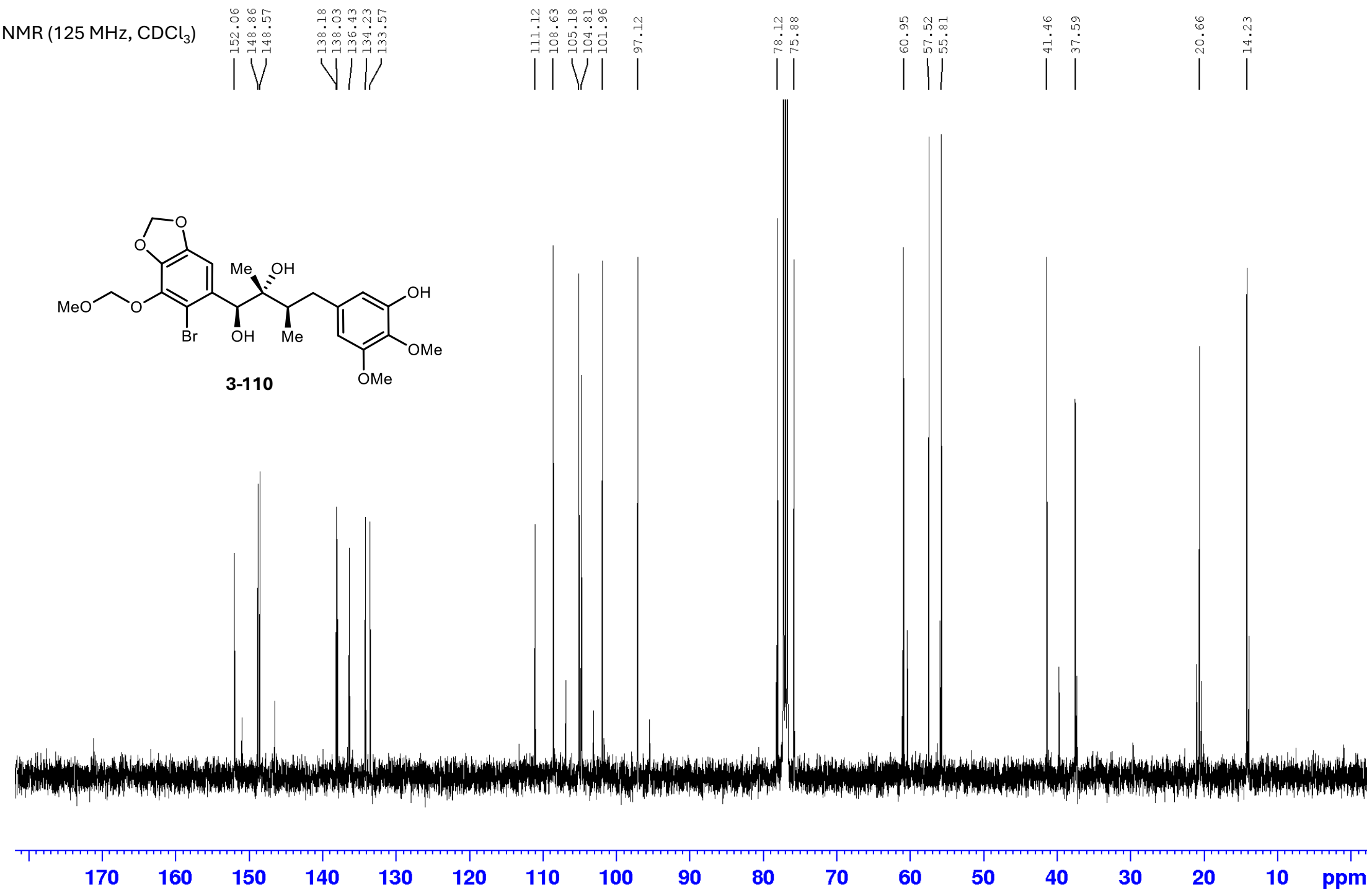
^{1}H NMR
(500 MHz, $CDCl_3$)

3-110

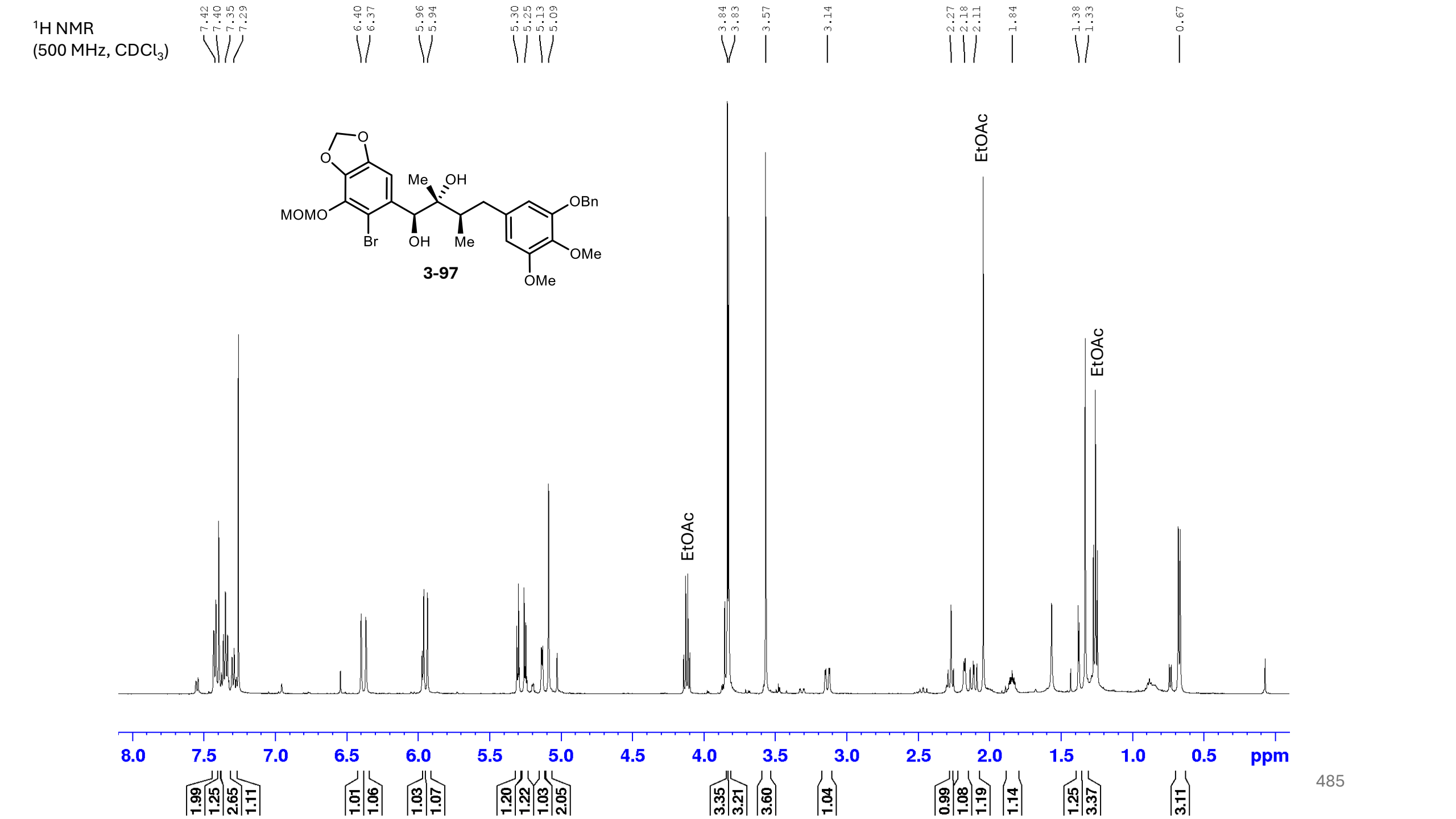


^{13}C NMR (125 MHz, $CDCl_3$)

3-110



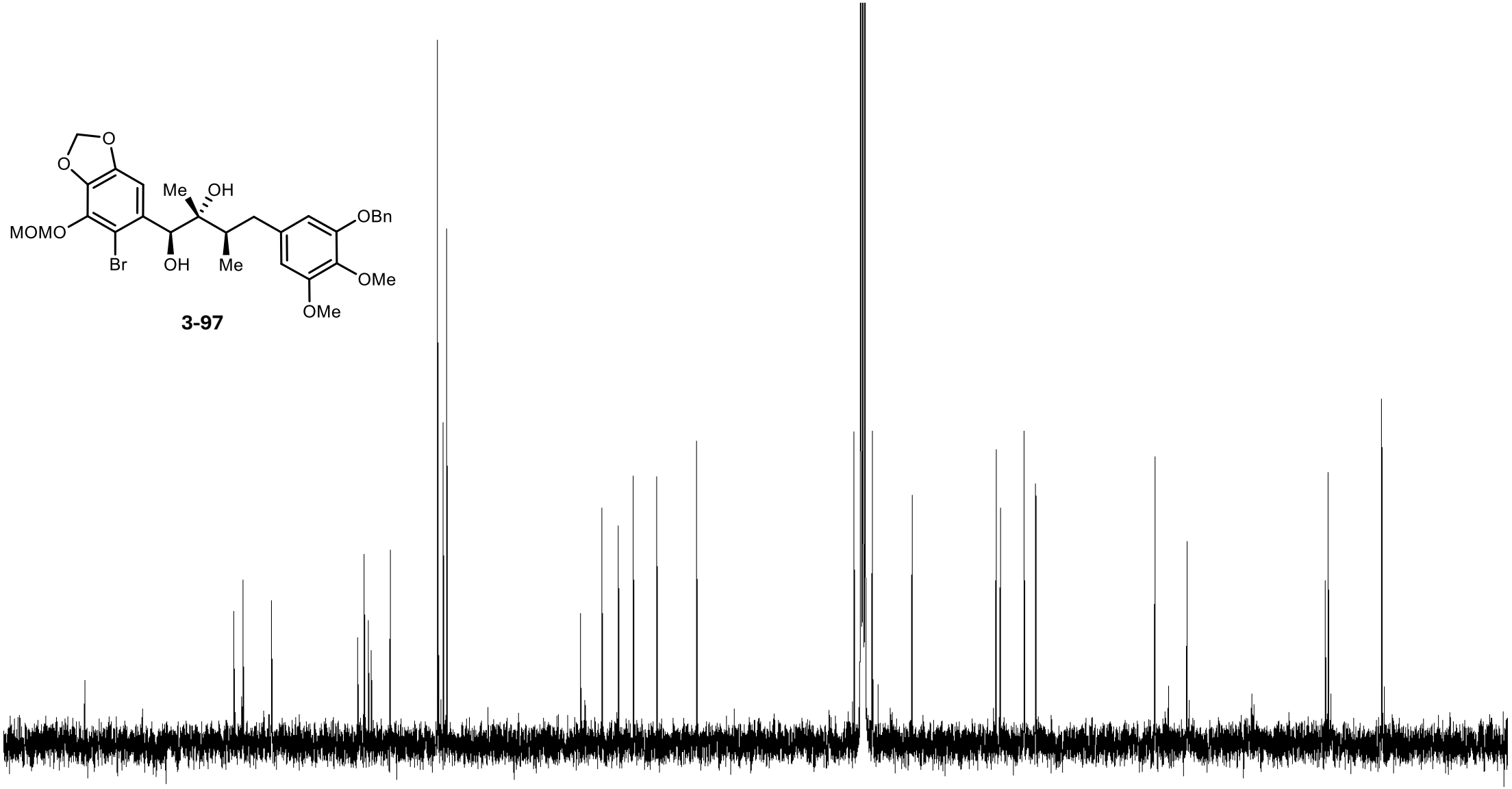
^{1}H NMR
(500 MHz, $CDCl_3$)



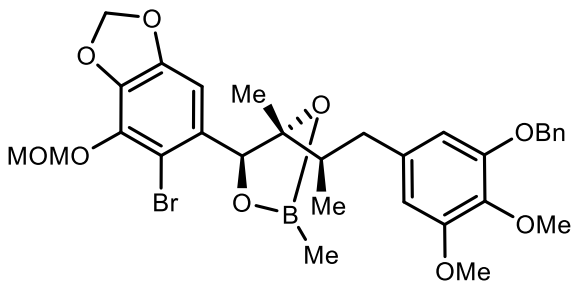
^{13}C NMR (125 MHz, $CDCl_3$)

153.13
152.01
148.55
138.16
137.39
137.34
136.84
136.49
134.20
128.47
127.78
127.36
111.18
108.58
106.59
104.78
101.94
97.13
78.08
75.90
71.09
60.93
57.52
56.11
41.71
37.80
20.72
14.25

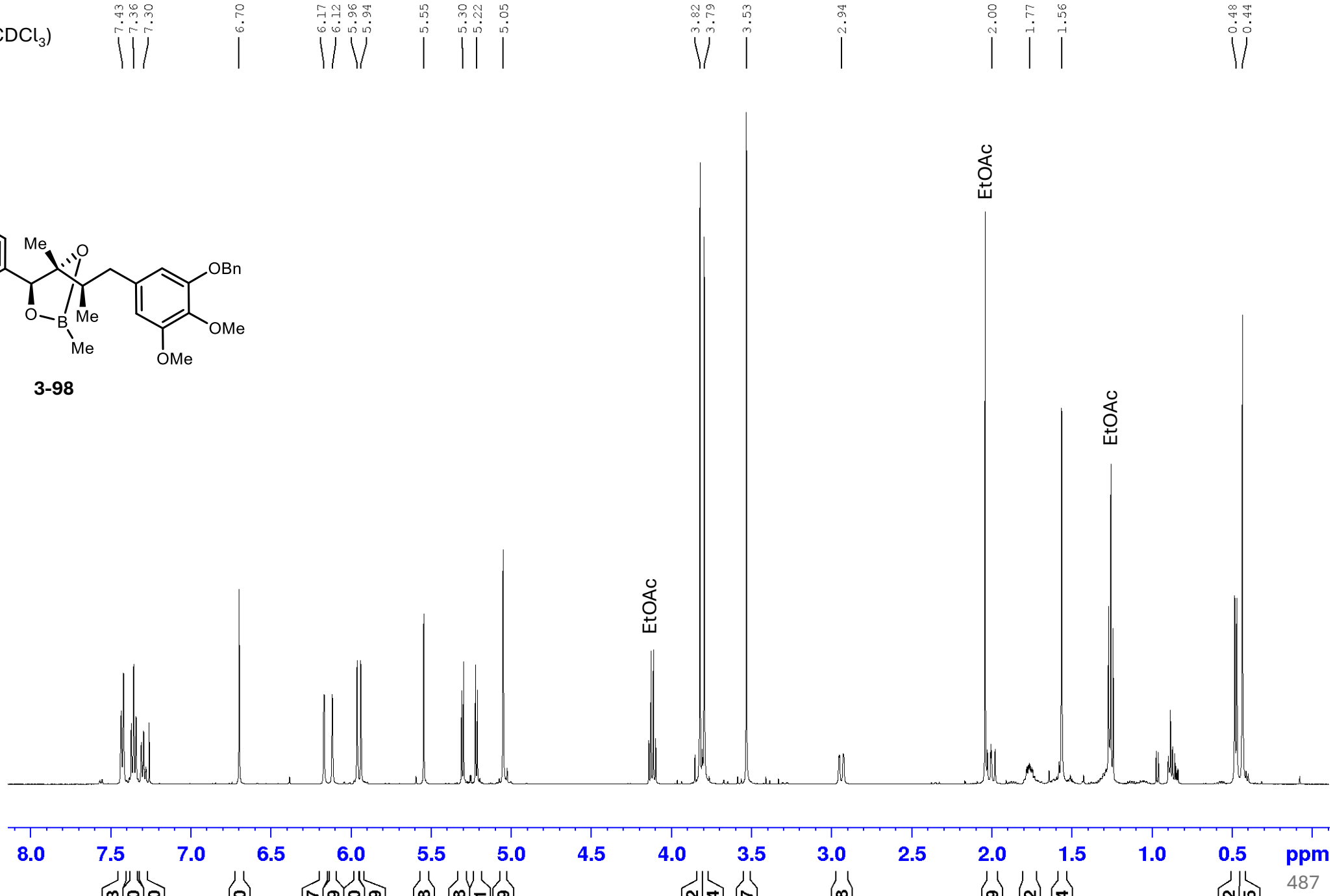
3-97



^{1}H NMR (500 MHz, $CDCl_3$)

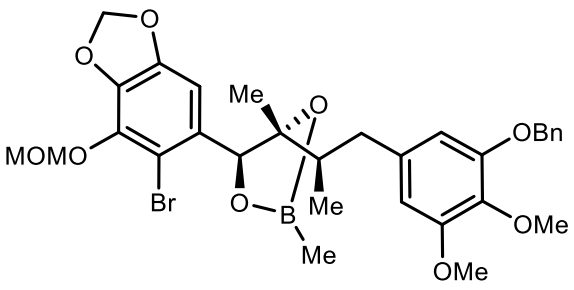


3-98



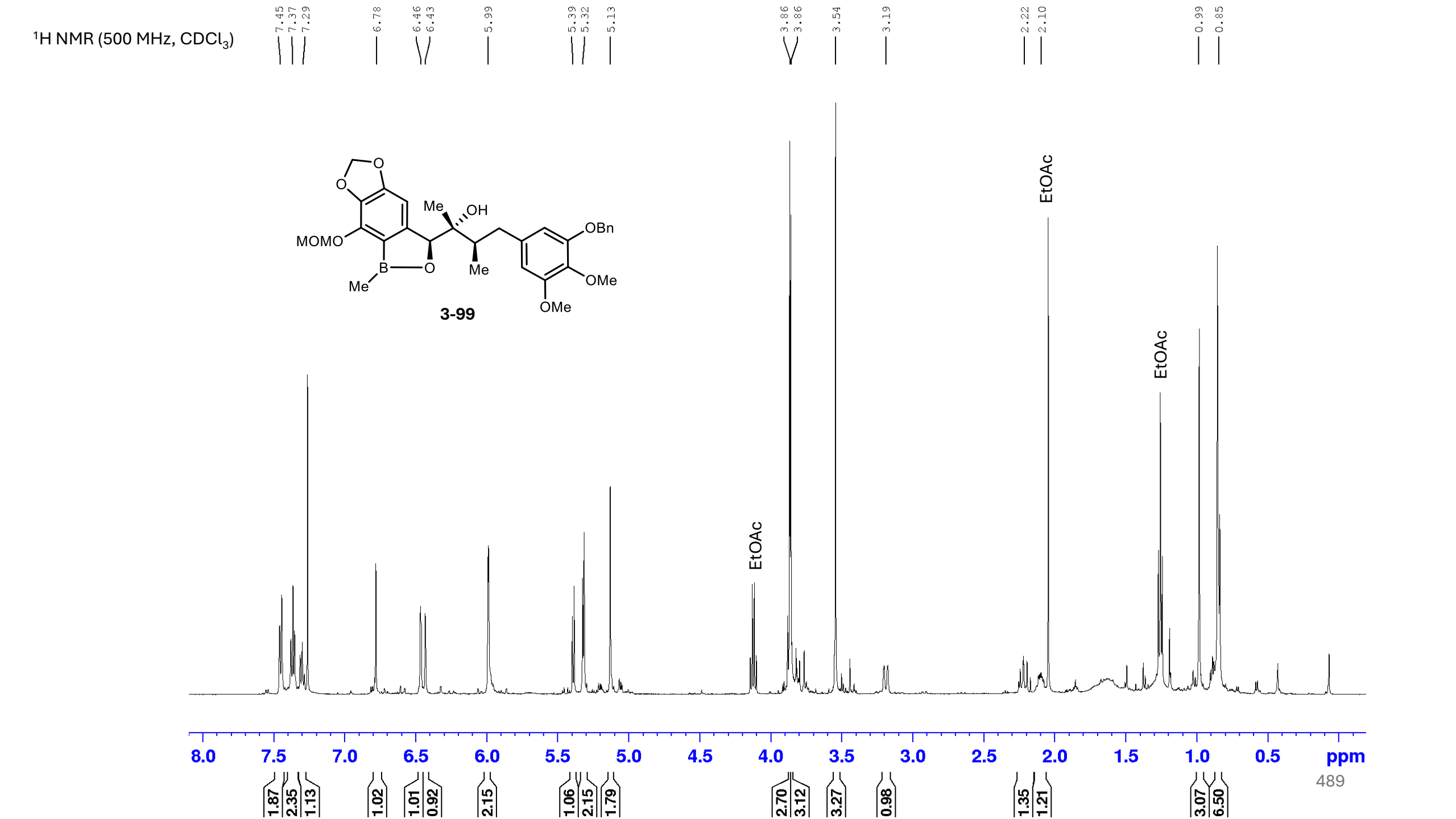
^{13}C NMR (125 MHz, $CDCl_3$)

153.03
151.98
148.59
137.98
137.34
136.96
136.80
136.48
132.81
128.47
127.80
127.36
109.94
108.37
106.45
103.91
102.08
97.06
87.62
86.96
71.05
60.86
57.44
56.04
40.30
38.32
25.51
14.53
-6.03



3-98

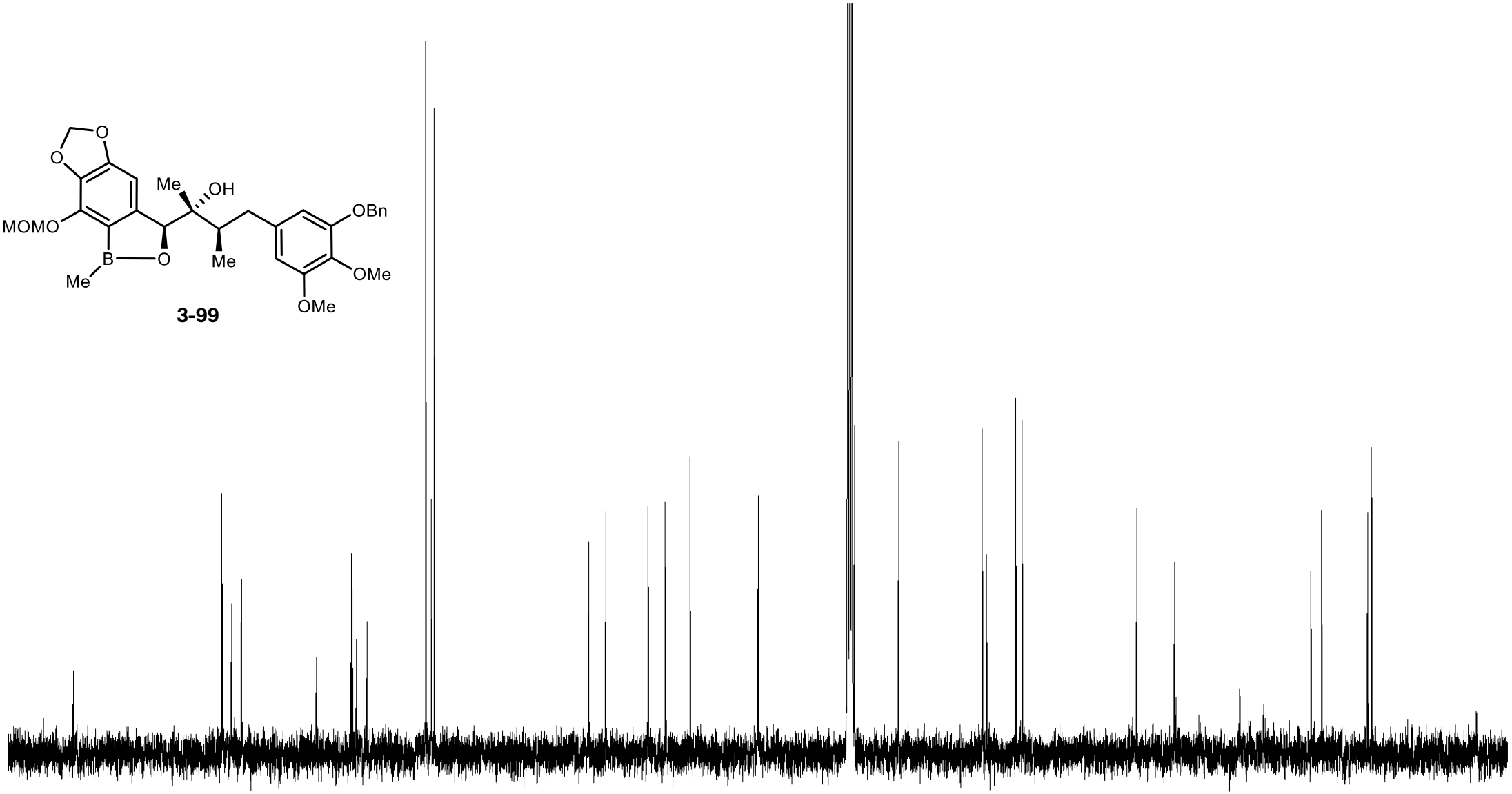
^{1}H NMR (500 MHz, $CDCl_3$)



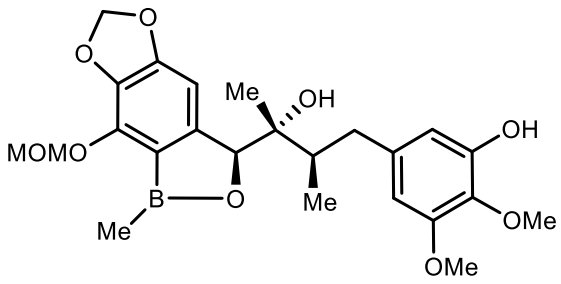
^{13}C NMR (125 MHz, $CDCl_3$)

153.16
152.01
150.81
141.71
137.47
137.36
136.86
135.60
128.48
127.78
127.40
108.71
106.62
101.47
99.38
96.40
88.13
76.44
71.10
60.93
60.41
56.89
56.12
42.22
37.63
21.06
19.79
14.21
13.71

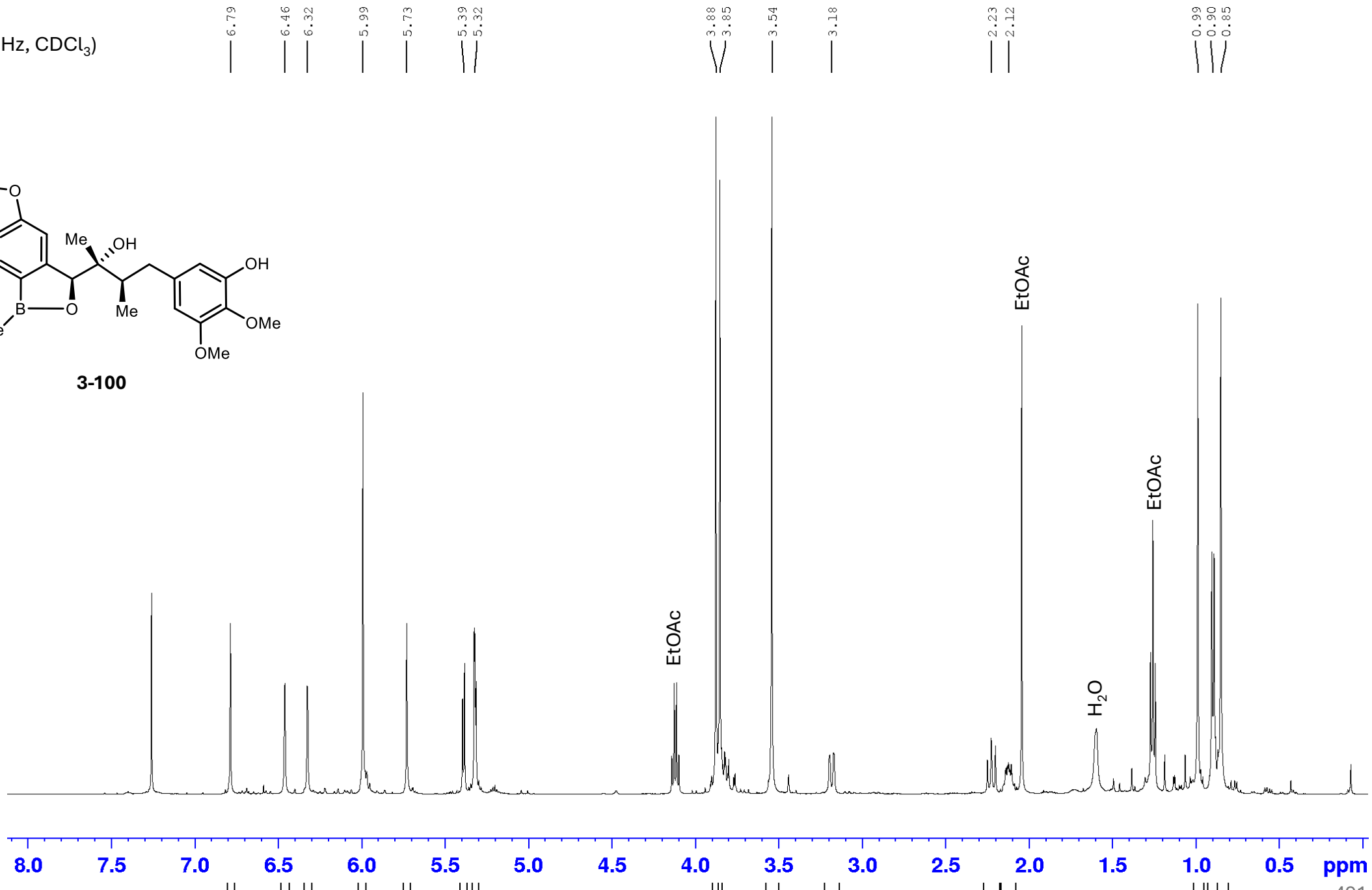
3-99



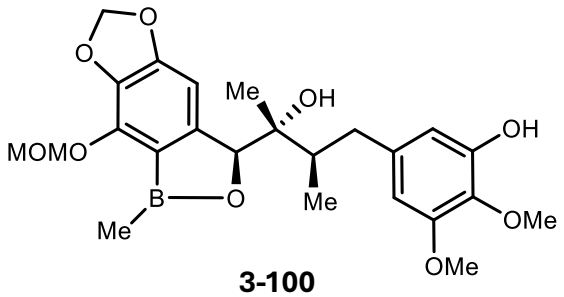
^{1}H NMR (500 MHz, $CDCl_3$)



3-100



^{13}C NMR
(125 MHz, $CDCl_3$)

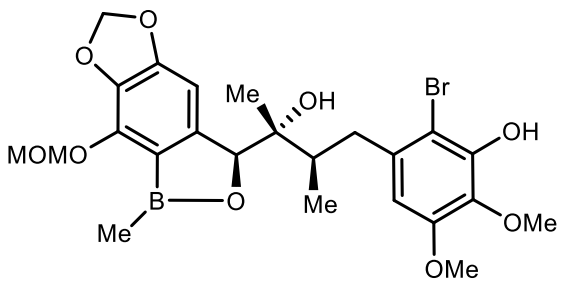


3-100

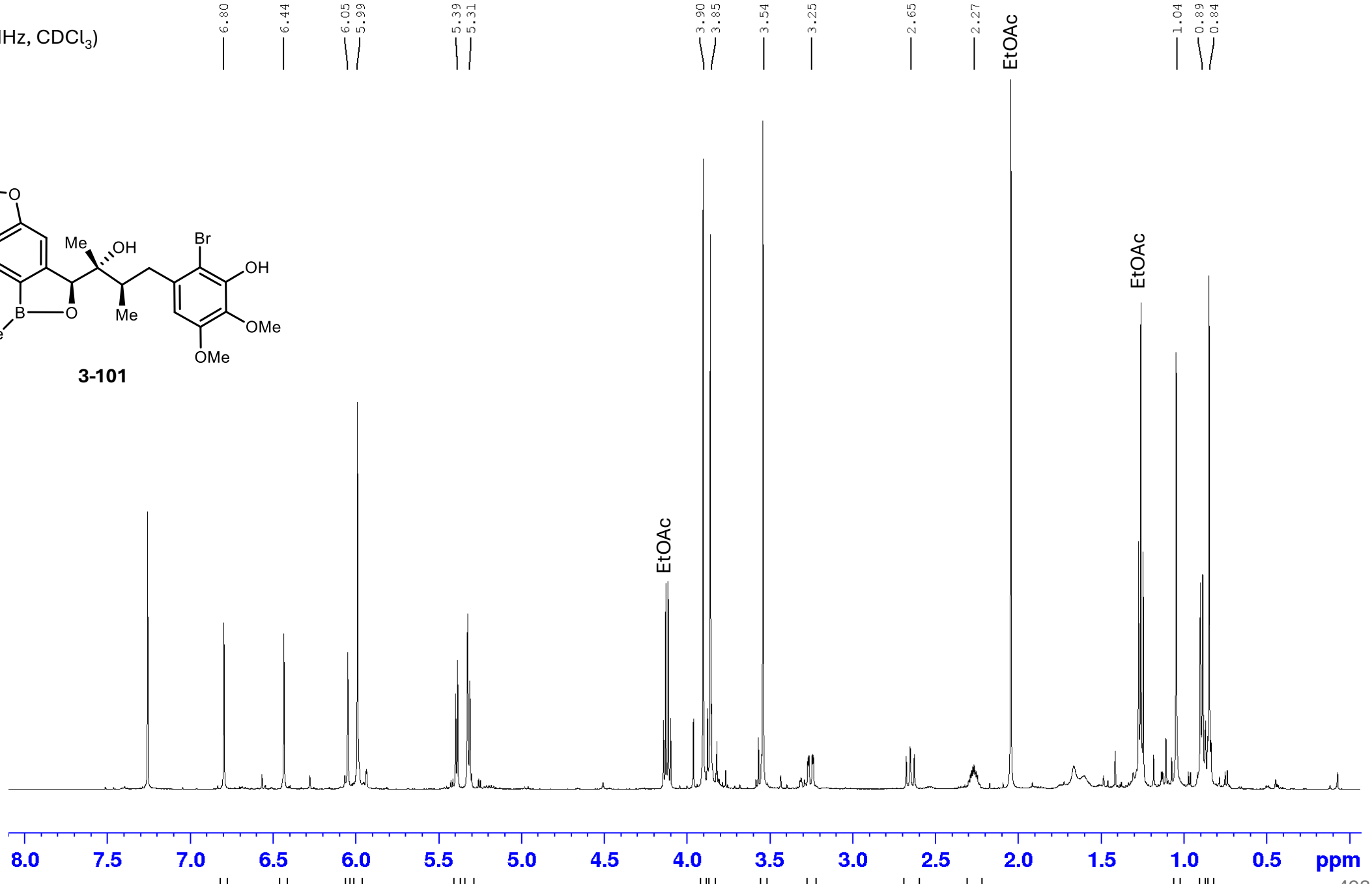
153.13
152.11
150.85
148.89
141.69
138.21
135.60
133.59
108.81
105.13
101.46
99.41
96.40
88.14
76.46
60.97
56.88
55.83
42.14
37.46
19.75
13.73
1.03

170 160 150 140 130 120 110 100 90 80 70 60 50 40 30 20 10 ppm

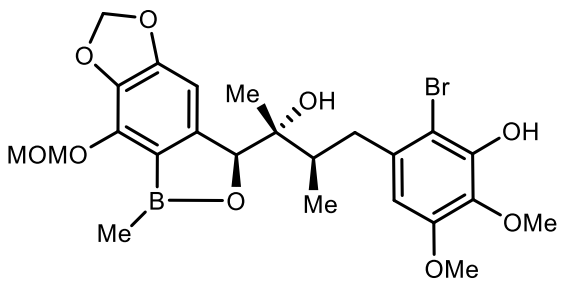
^{1}H NMR (500 MHz, $CDCl_3$)



3-101



^{13}C NMR (125 MHz, $CDCl_3$)



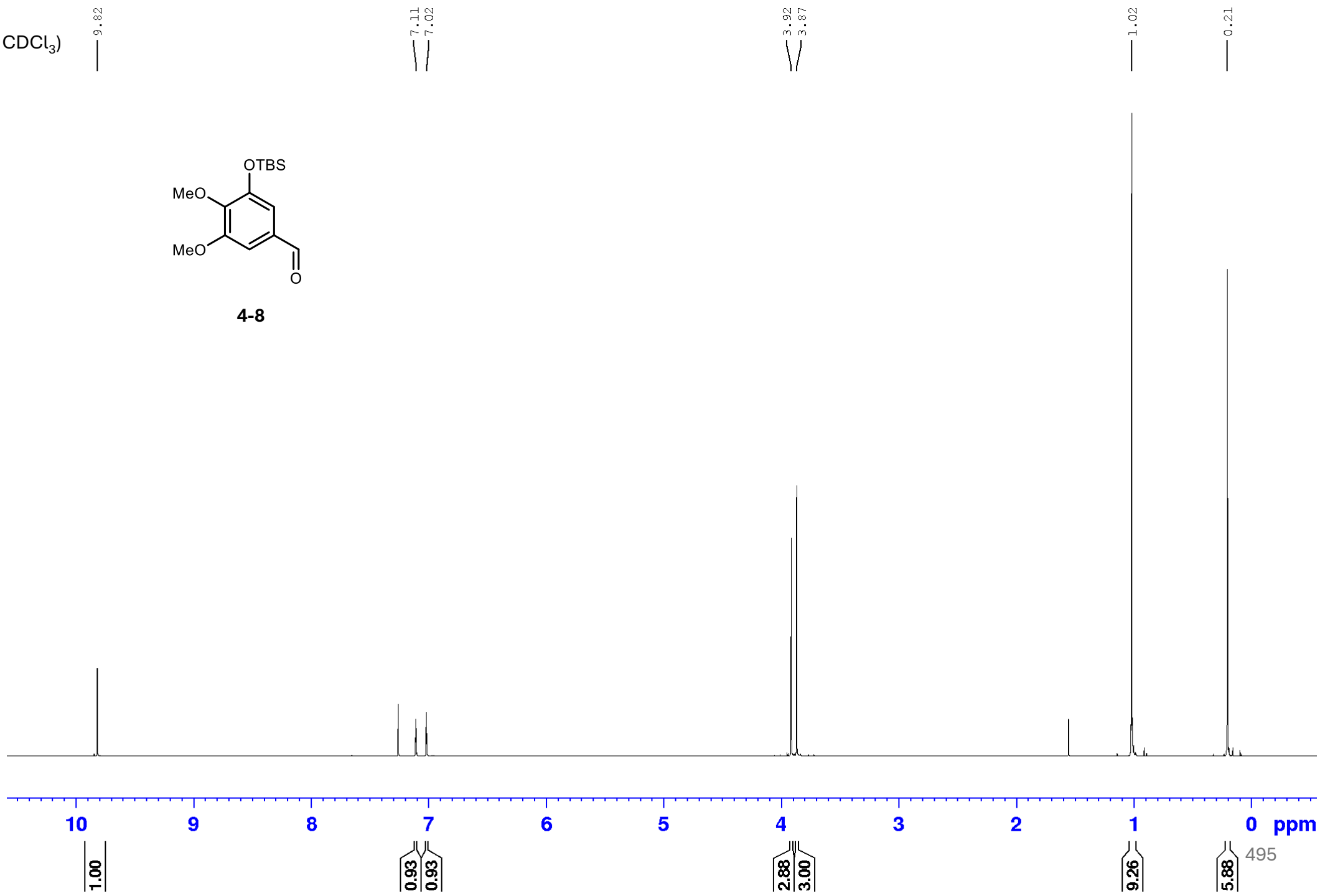
3-101

153.12
151.17
150.77
146.54
141.69
136.71
135.60
134.26
106.66
103.42
101.46
99.43
96.40
88.25
76.64
61.11
56.89
56.00
41.14
37.17
19.55
13.58
1.00

180 170 160 150 140 130 120 110 100 90 80 70 60 50 40 30 20 10 ppm

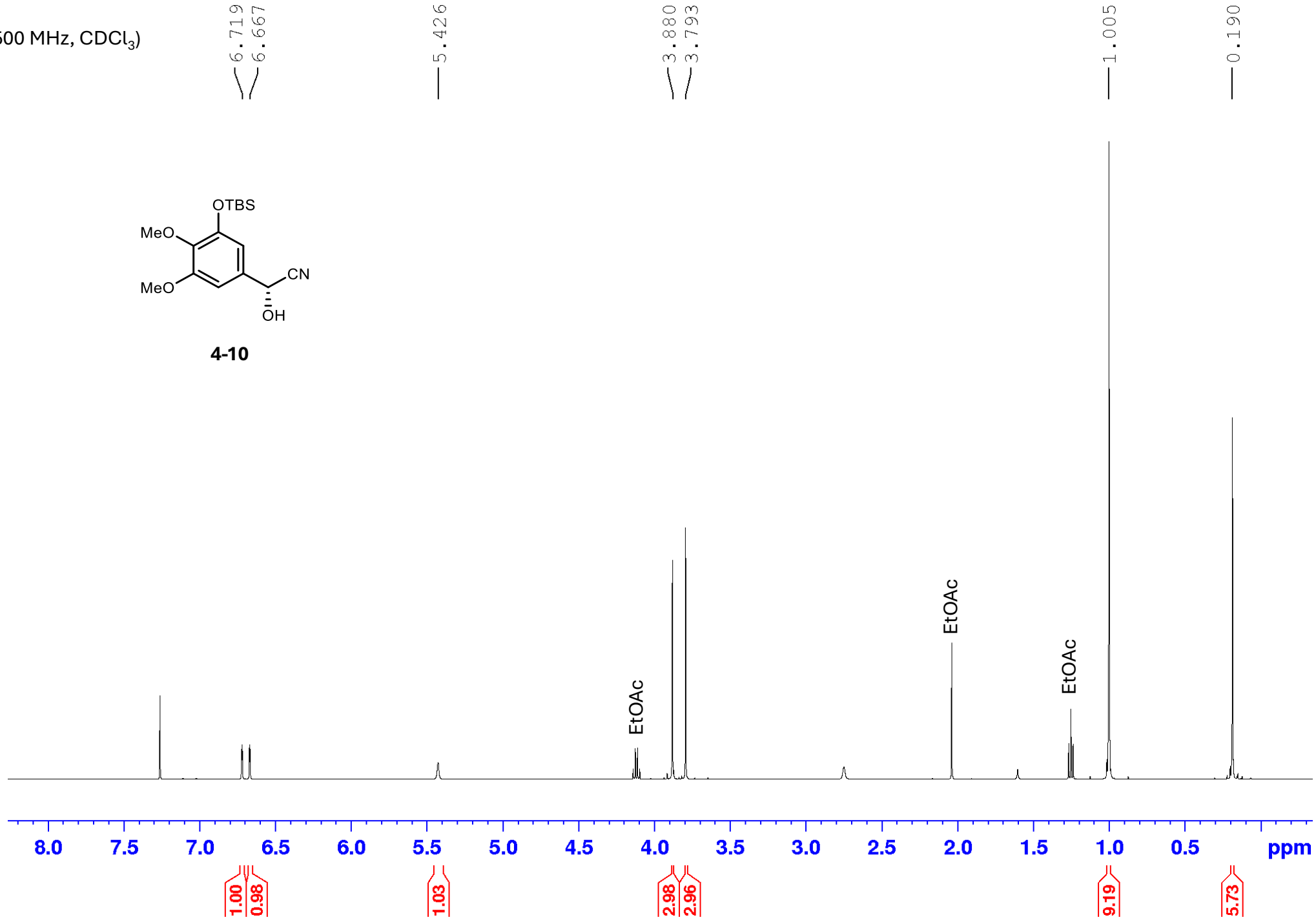
^{1}H NMR (500 MHz, $CDCl_3$)

4-8



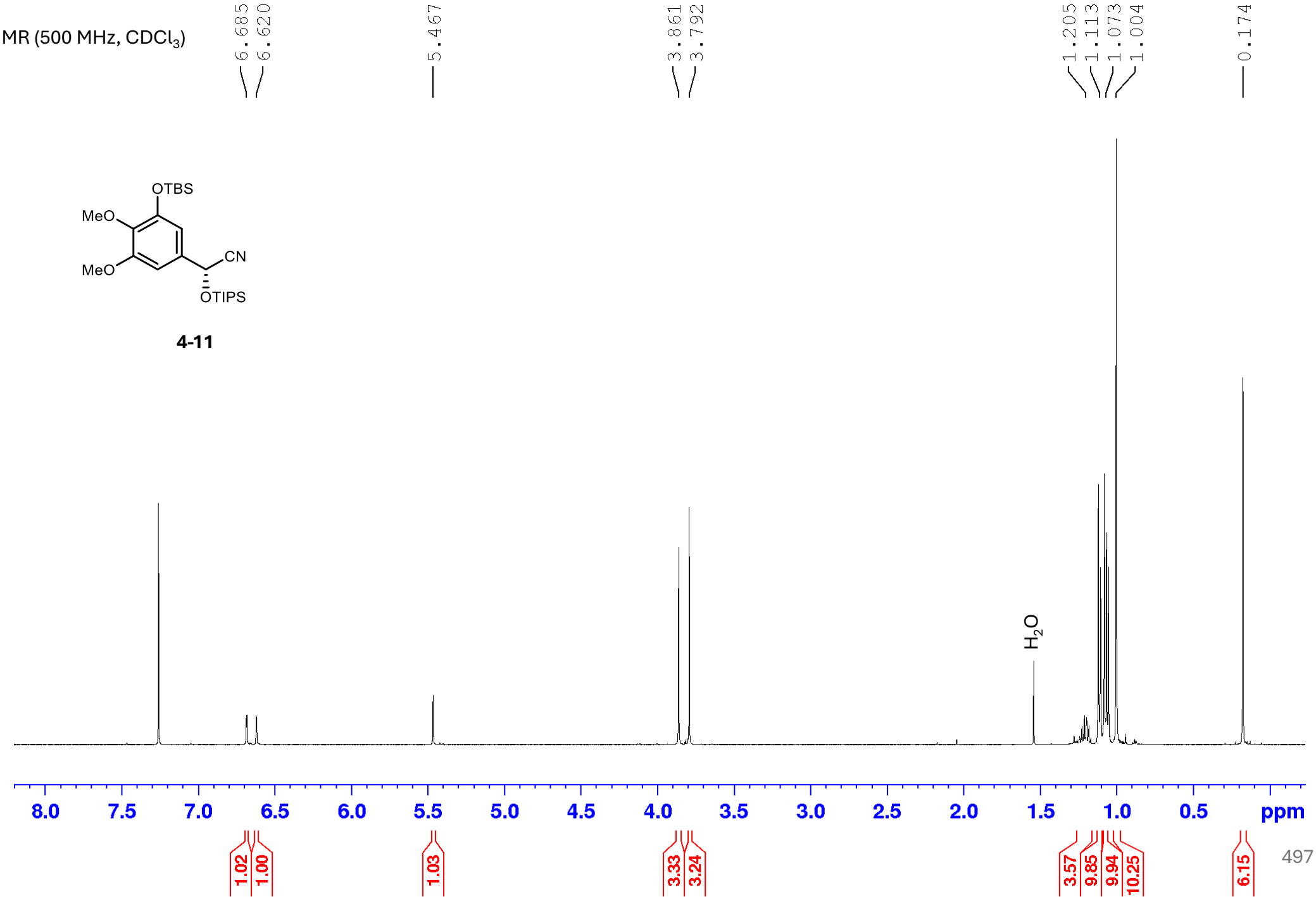
^{1}H NMR (500 MHz, $CDCl_3$)

4-10



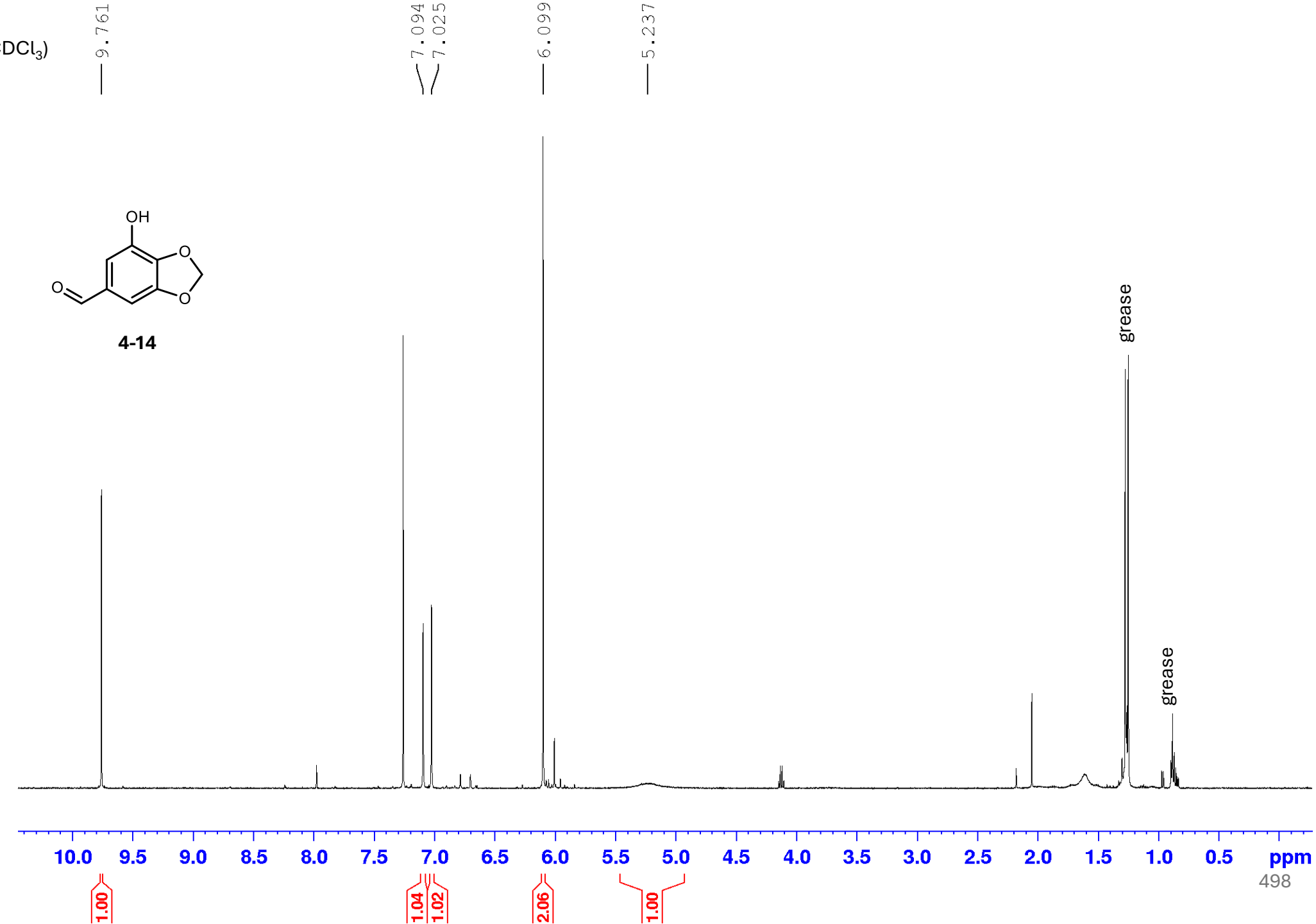
^{1}H NMR (500 MHz, $CDCl_3$)

4-11

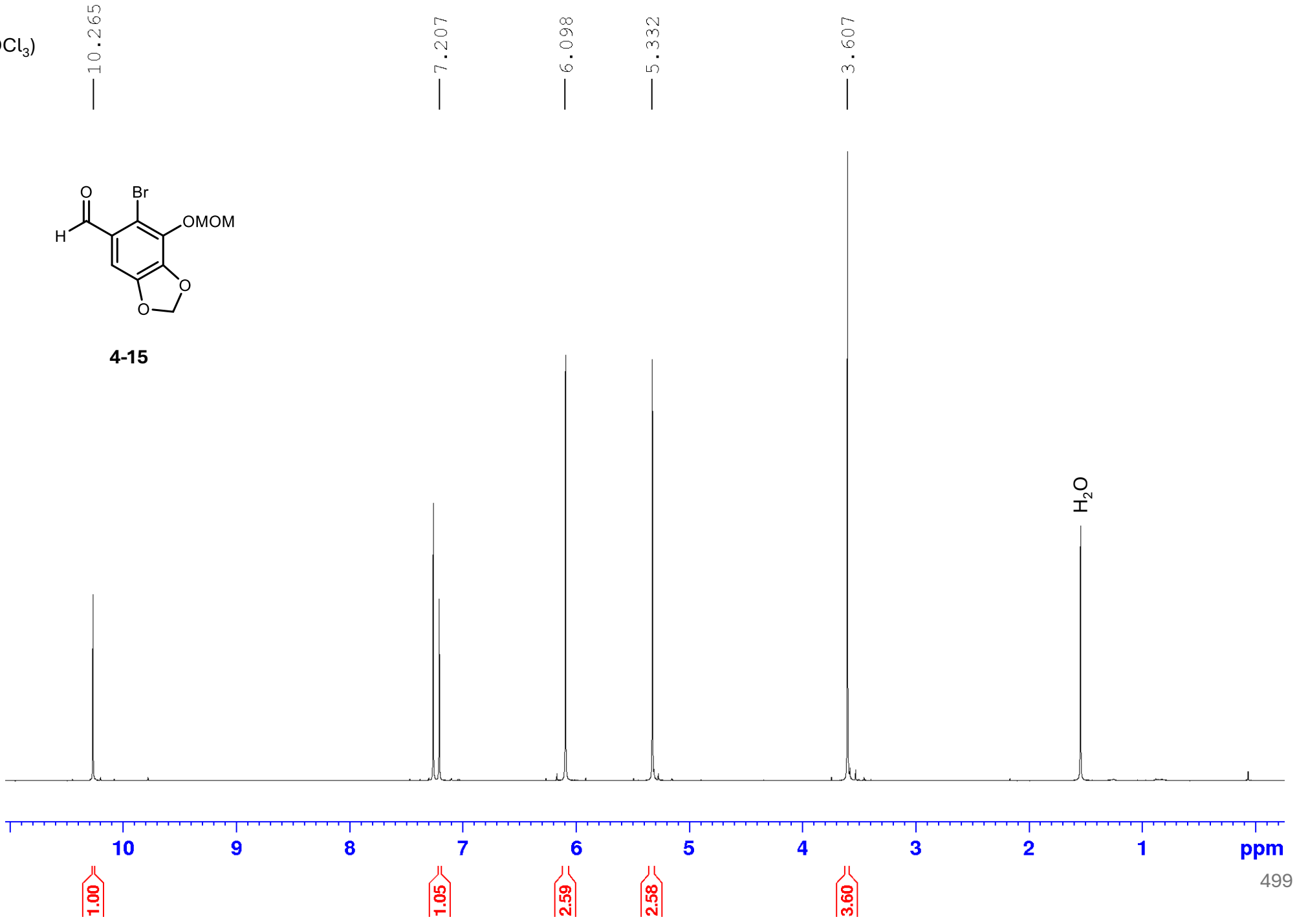


^{1}H NMR (500 MHz, $CDCl_3$)

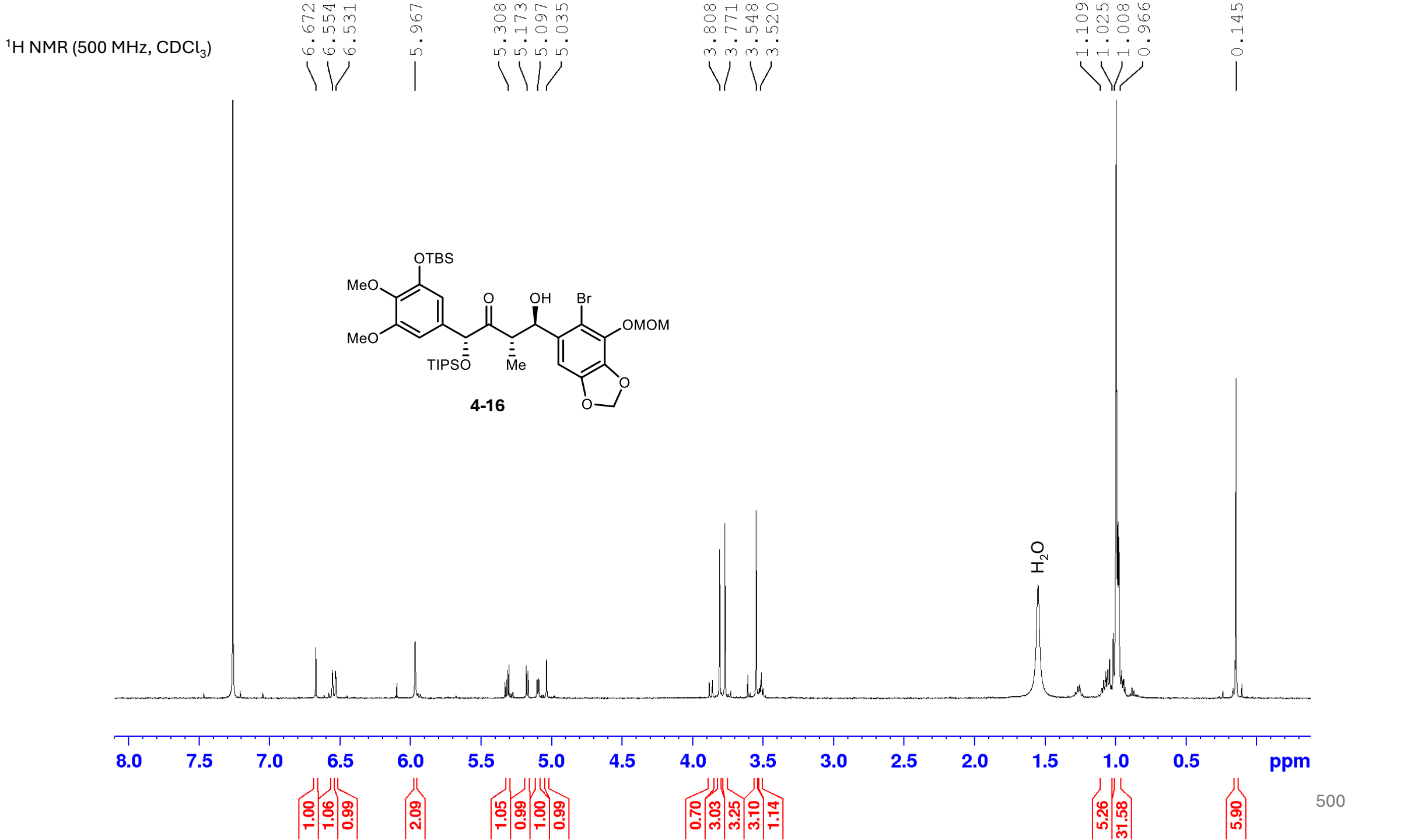
4-14



^{1}H NMR (500 MHz, $CDCl_3$)

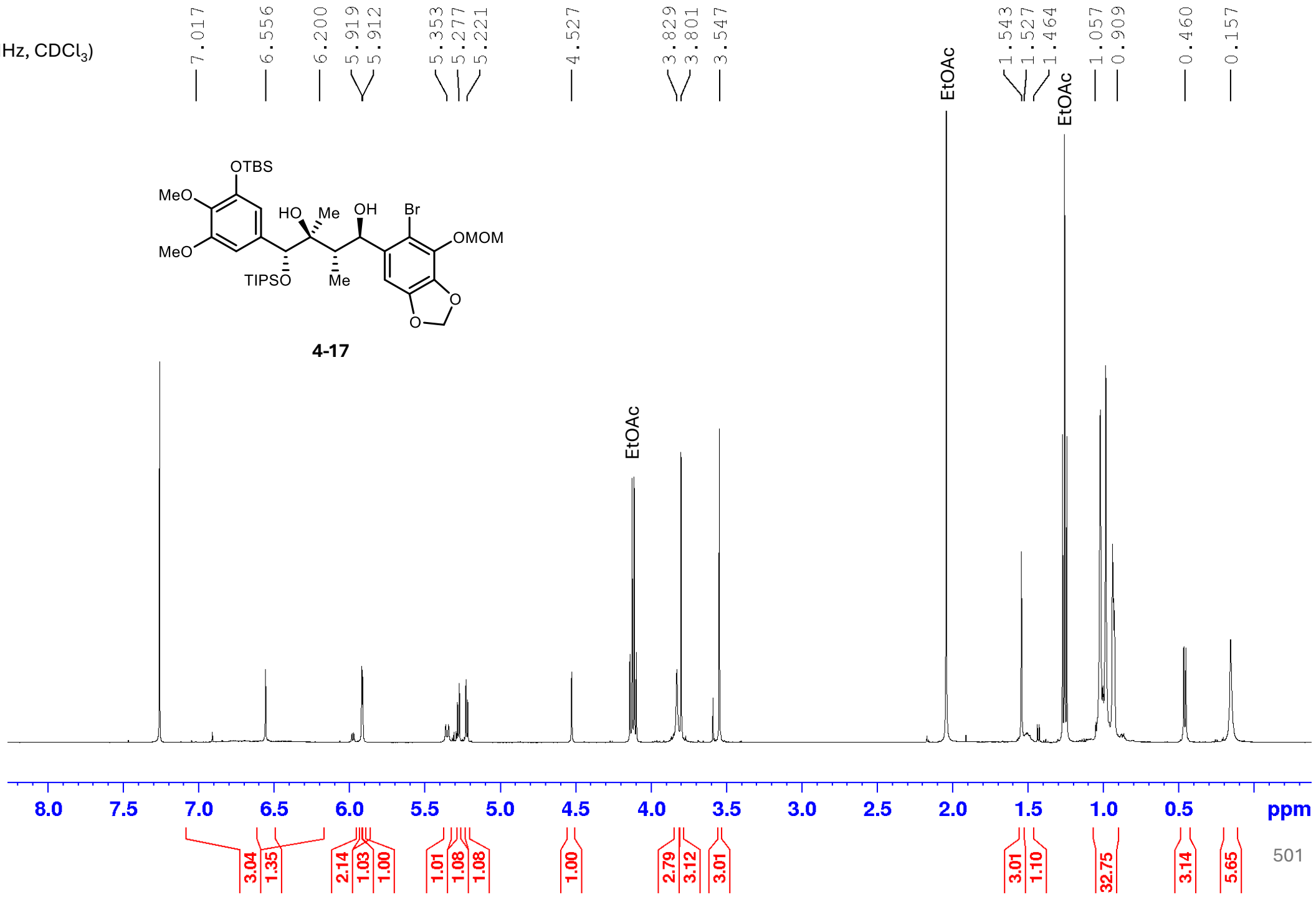


^{1}H NMR (500 MHz, $CDCl_3$)

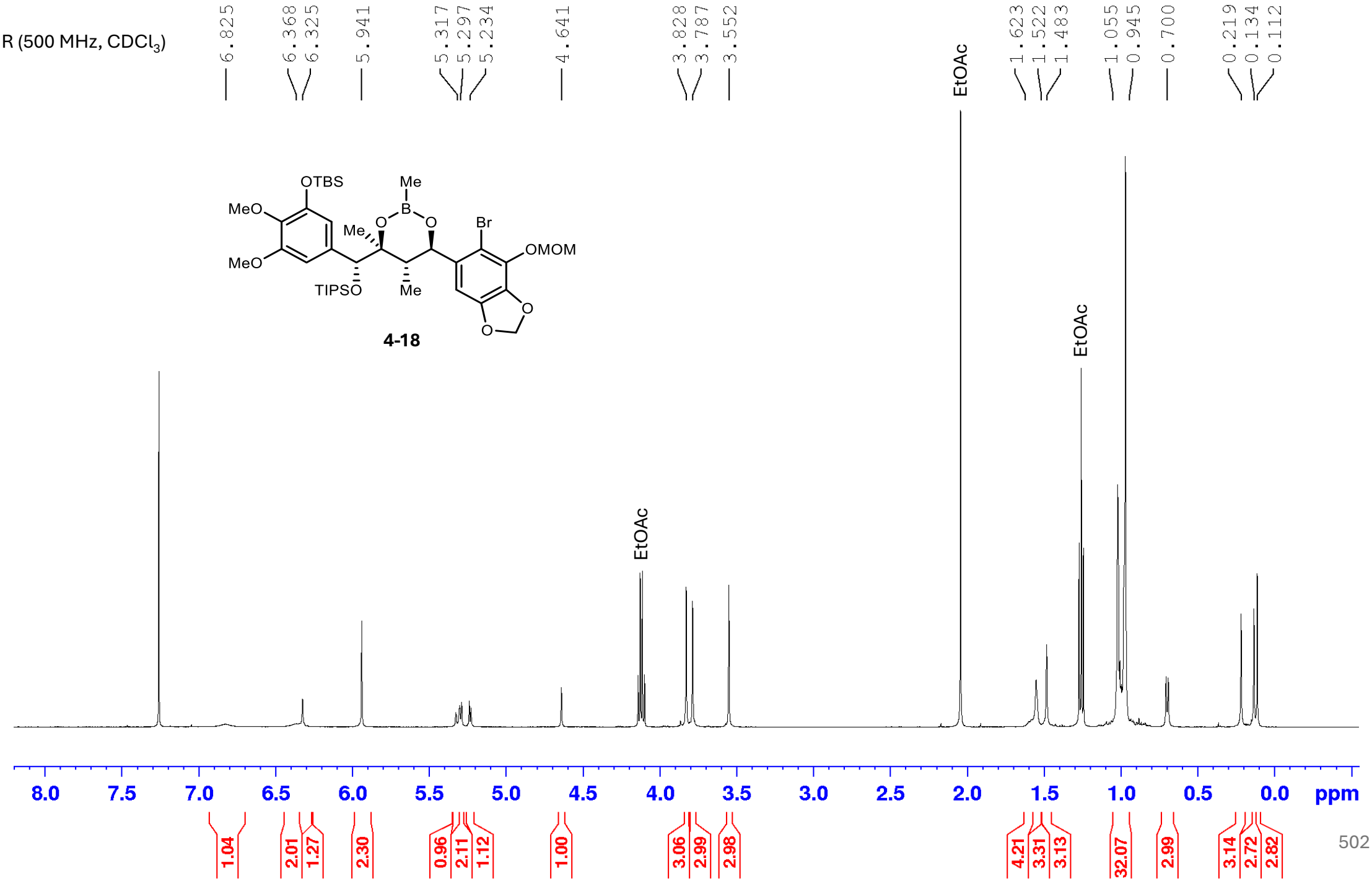


^{1}H NMR (500 MHz, $CDCl_3$)

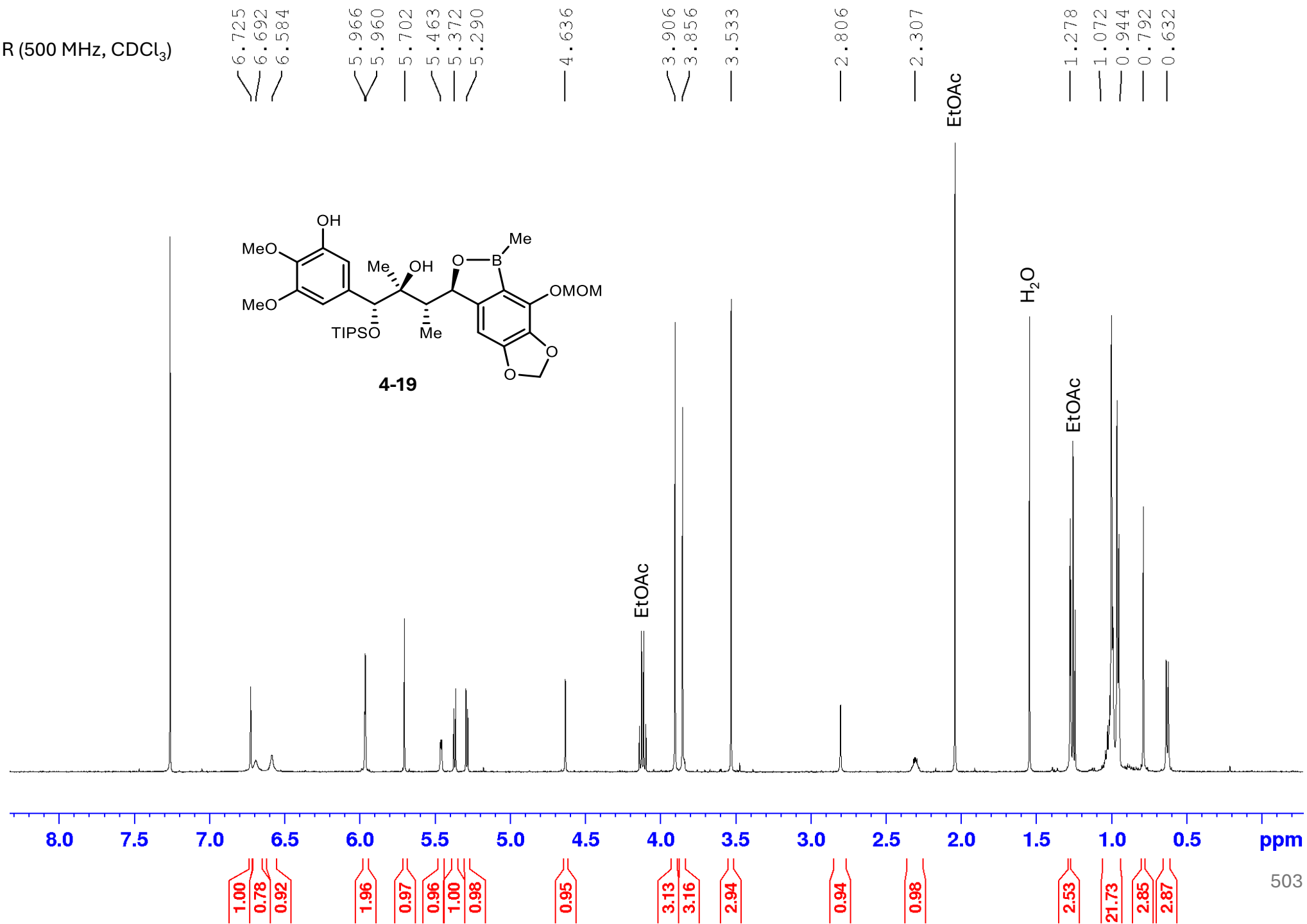
4-17



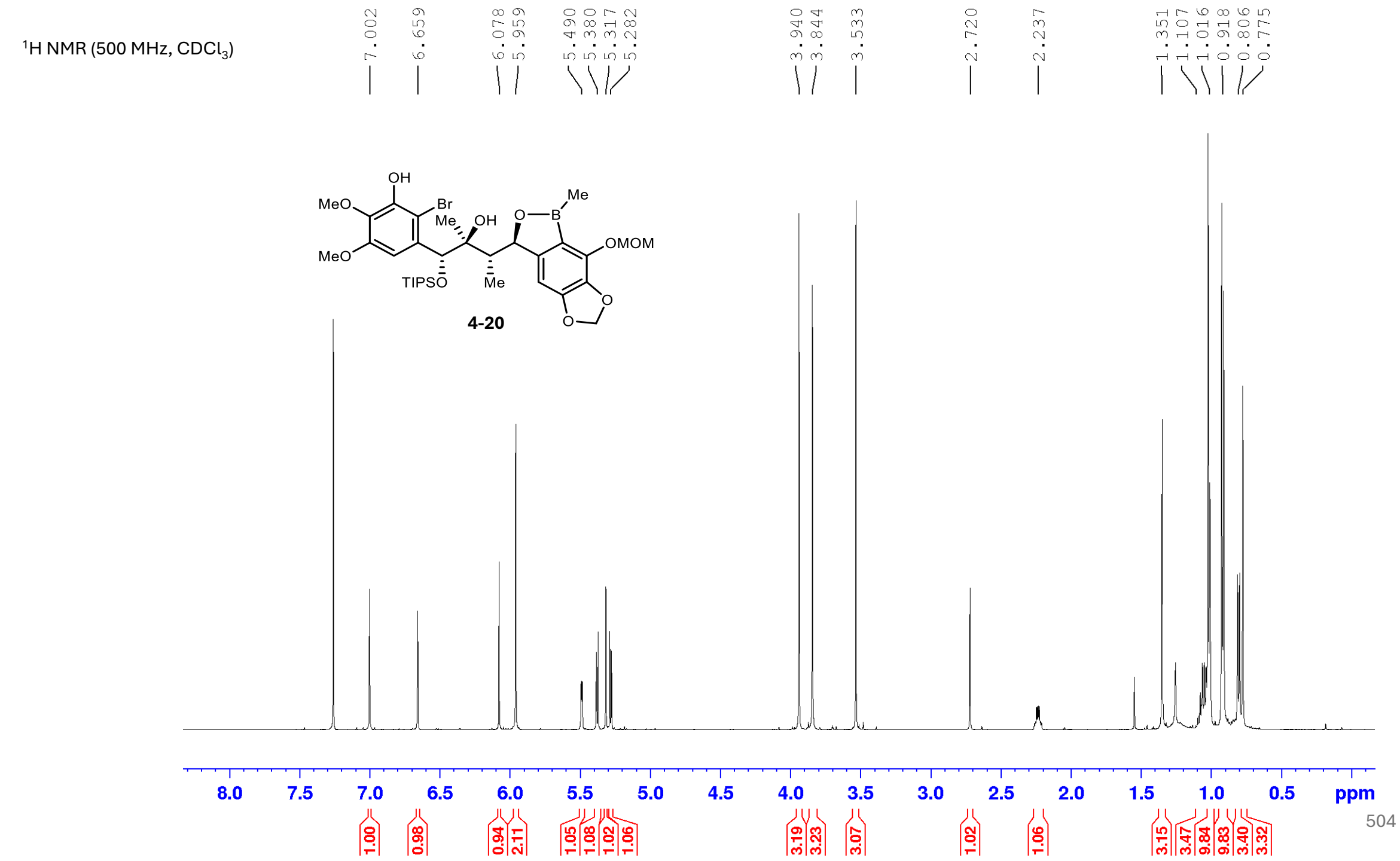
^{1}H NMR (500 MHz, $CDCl_3$)



^{1}H NMR (500 MHz, $CDCl_3$)

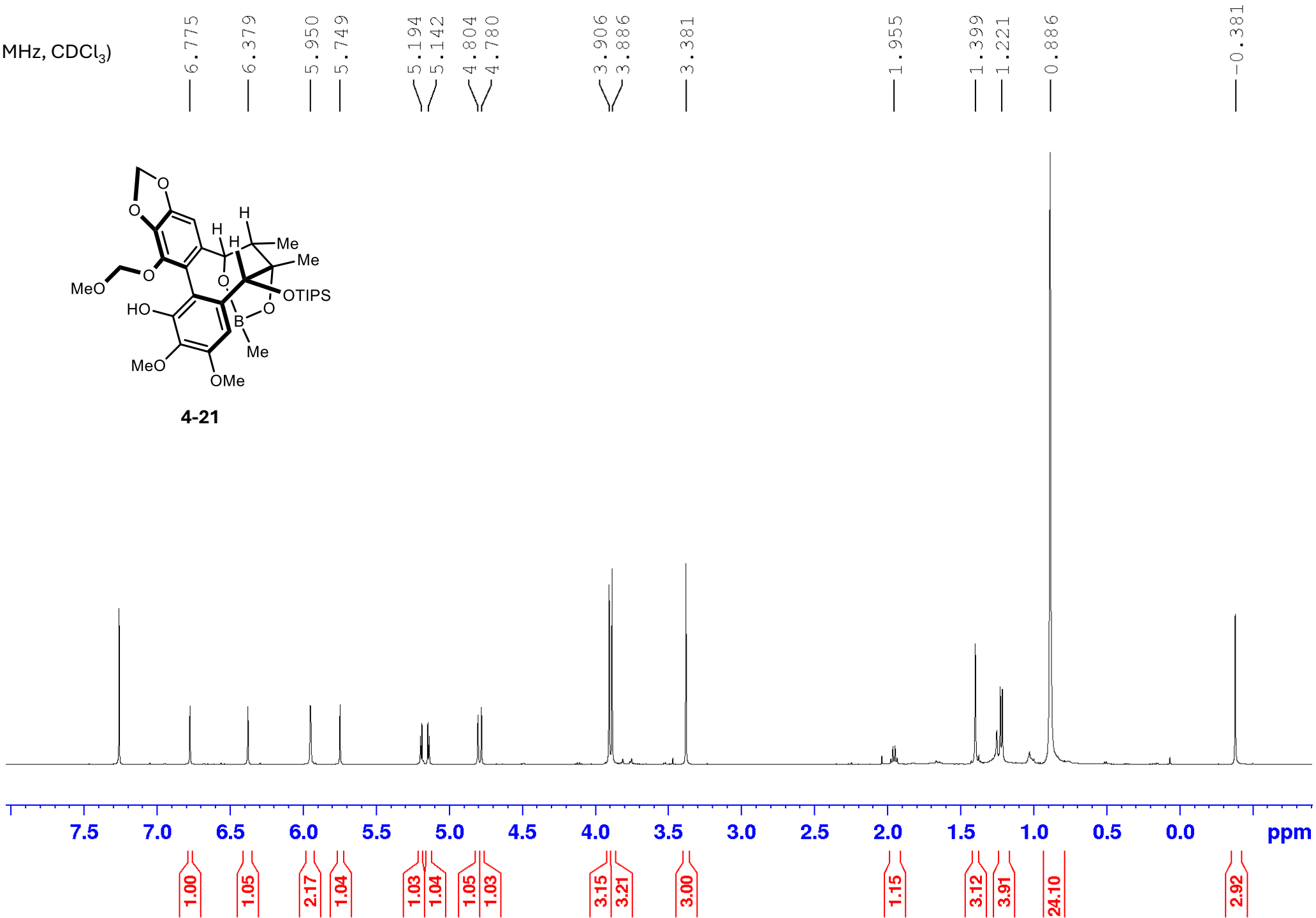


^{1}H NMR (500 MHz, $CDCl_3$)

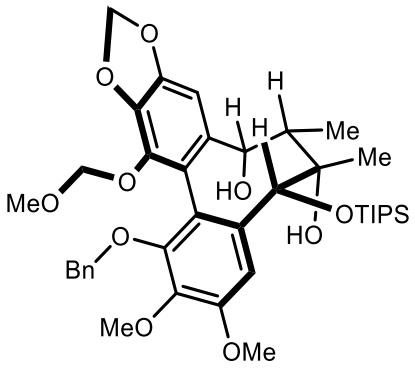


^{1}H NMR (500 MHz, $CDCl_3$)

4-21



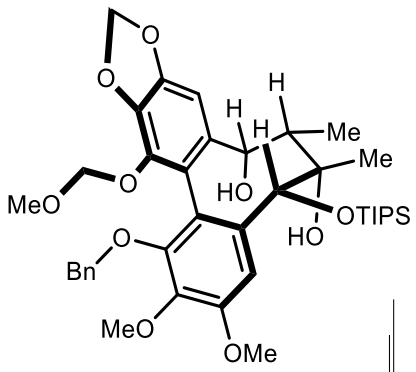
^{1}H NMR (500 MHz, $CDCl_3$)



4-22

^{13}C NMR
(125 MHz,
$CDCl_3$)

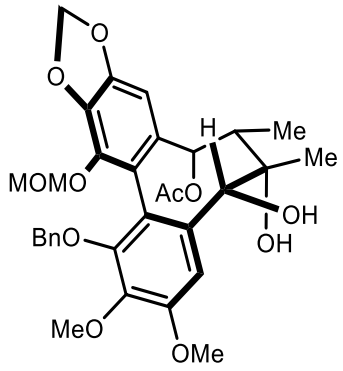
152.27
148.80
148.46
141.28
138.38
138.32
138.30
136.47
135.05
128.51
128.17
127.82
122.11
119.19
109.40
101.98
101.13
96.98
83.48
78.04
76.08
74.12
61.11
57.04
56.02
47.73
25.45
18.24
18.04
17.76
12.62



4-22

150 140 130 120 110 100 90 80 70 60 50 40 30 20 10 ppm

^{1}H NMR (500 MHz, $CDCl_3$)

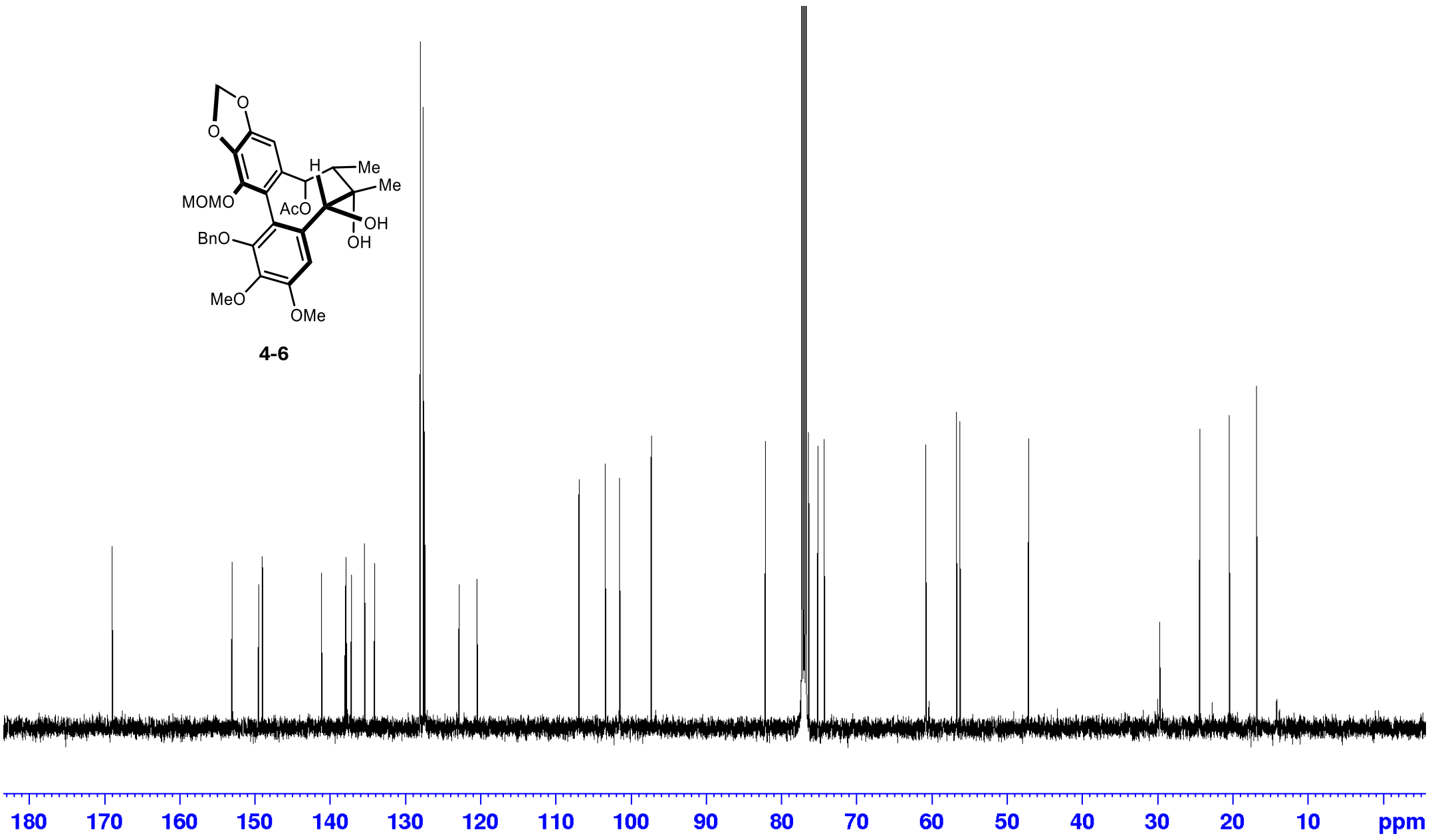


4-6

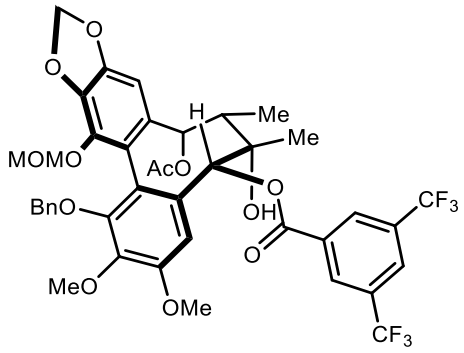
^{13}C NMR
(125 MHz, $CDCl_3$)

169.03
153.02
149.58
149.05
141.19
138.03
137.93
137.24
135.45
134.13
128.05
127.66
127.47
122.92
120.49
106.96
103.45
101.56
97.34
82.17
76.40
75.20
74.34
60.85
56.74
56.29
47.18
29.71
24.40
20.47
16.82

4-6



^{1}H NMR (500 MHz, $CDCl_3$)

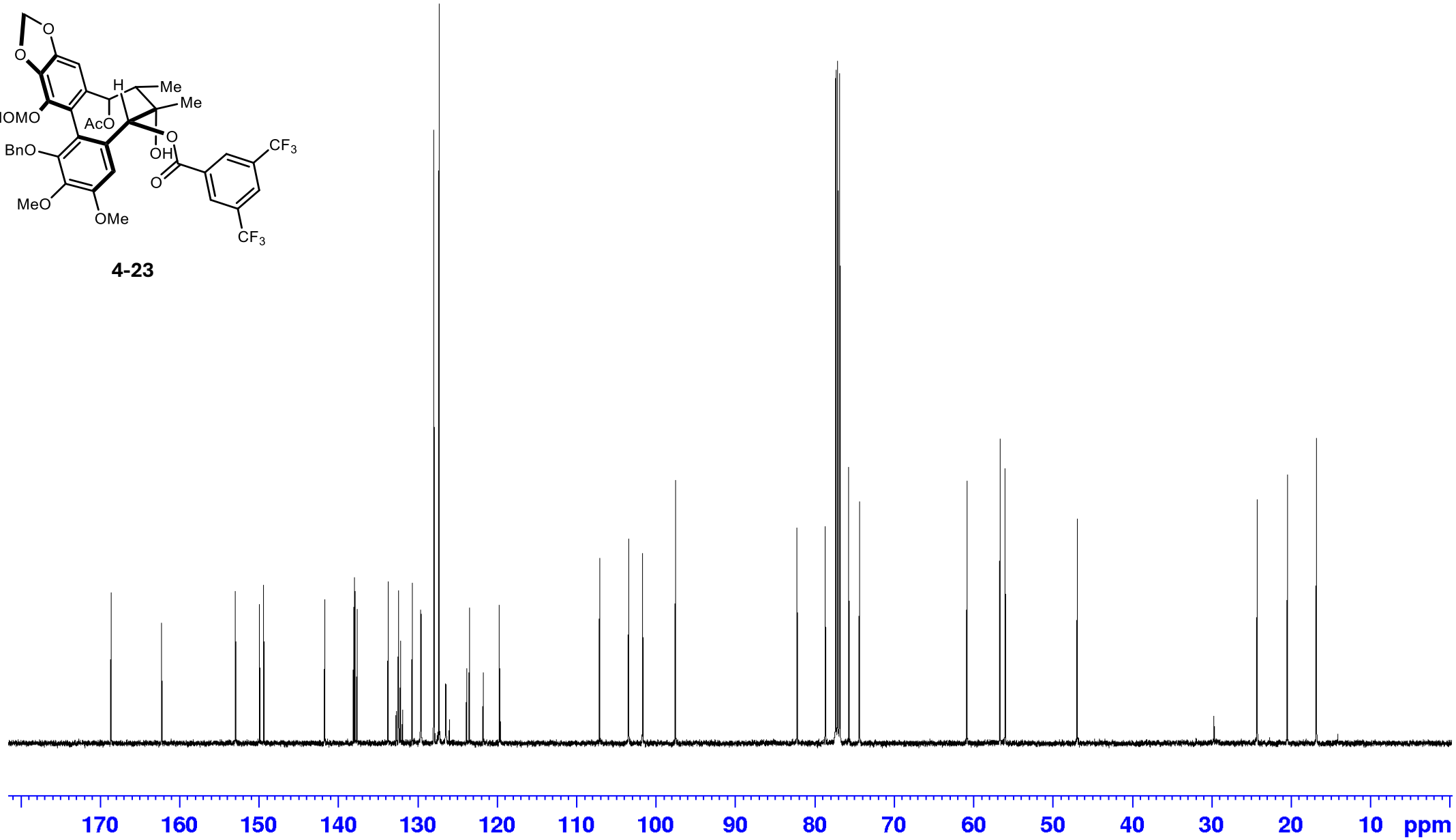


4-23

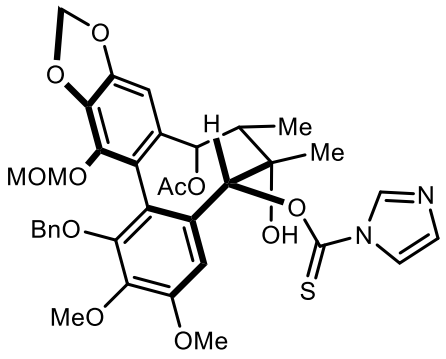
^{13}C NMR
(125 MHz, $CDCl_3$)

168.71
162.33
153.02
149.99
149.46
141.79
138.15
138.00
137.69
133.79
132.46
132.37
130.77
129.68
128.05
127.40
126.54
123.56
122.81
119.70
107.08
103.42
101.65
97.52
82.20
78.65
75.71
74.33
60.78
56.65
55.99
46.91
24.24
20.44
16.77

4-23



^{1}H NMR (500 MHz, $CDCl_3$)

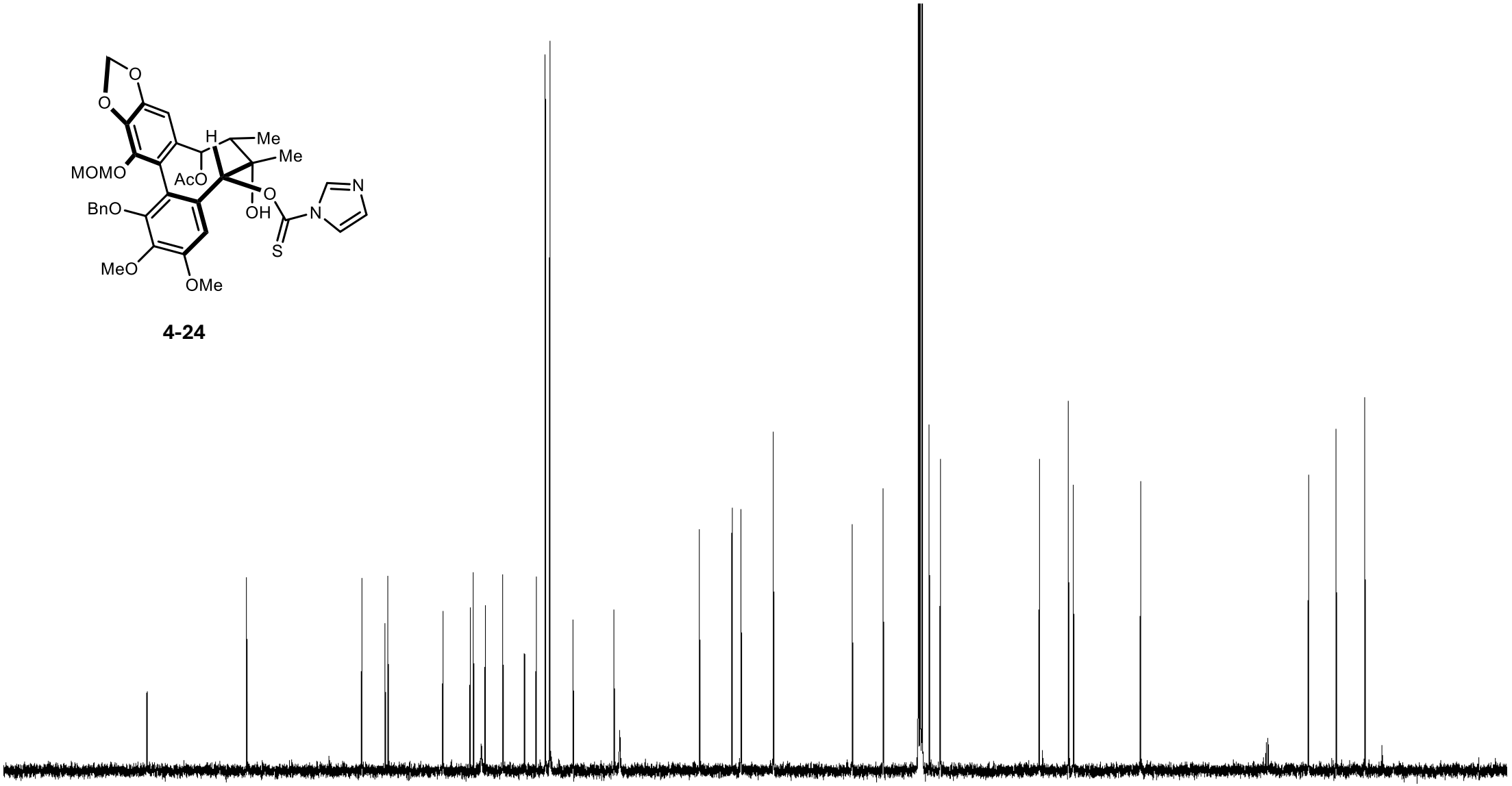


4-24

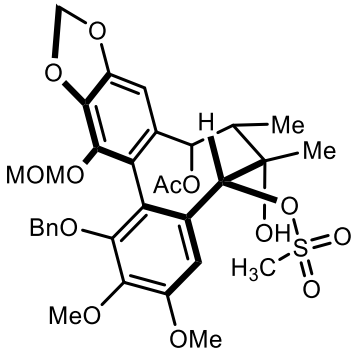
^{13}C NMR
(125 MHz, $CDCl_3$)

182.29
168.72
153.06
149.89
149.49
142.03
138.31
137.86
136.80
136.27
133.86
130.91
129.30
128.08
127.50
127.45
124.30
118.75
117.96
107.10
102.67
101.45
97.03
86.30
82.11
77.26
75.82
74.31
60.83
56.89
56.20
47.06
24.21
20.45
16.54

4-24



^{1}H NMR (500 MHz, $CDCl_3$)

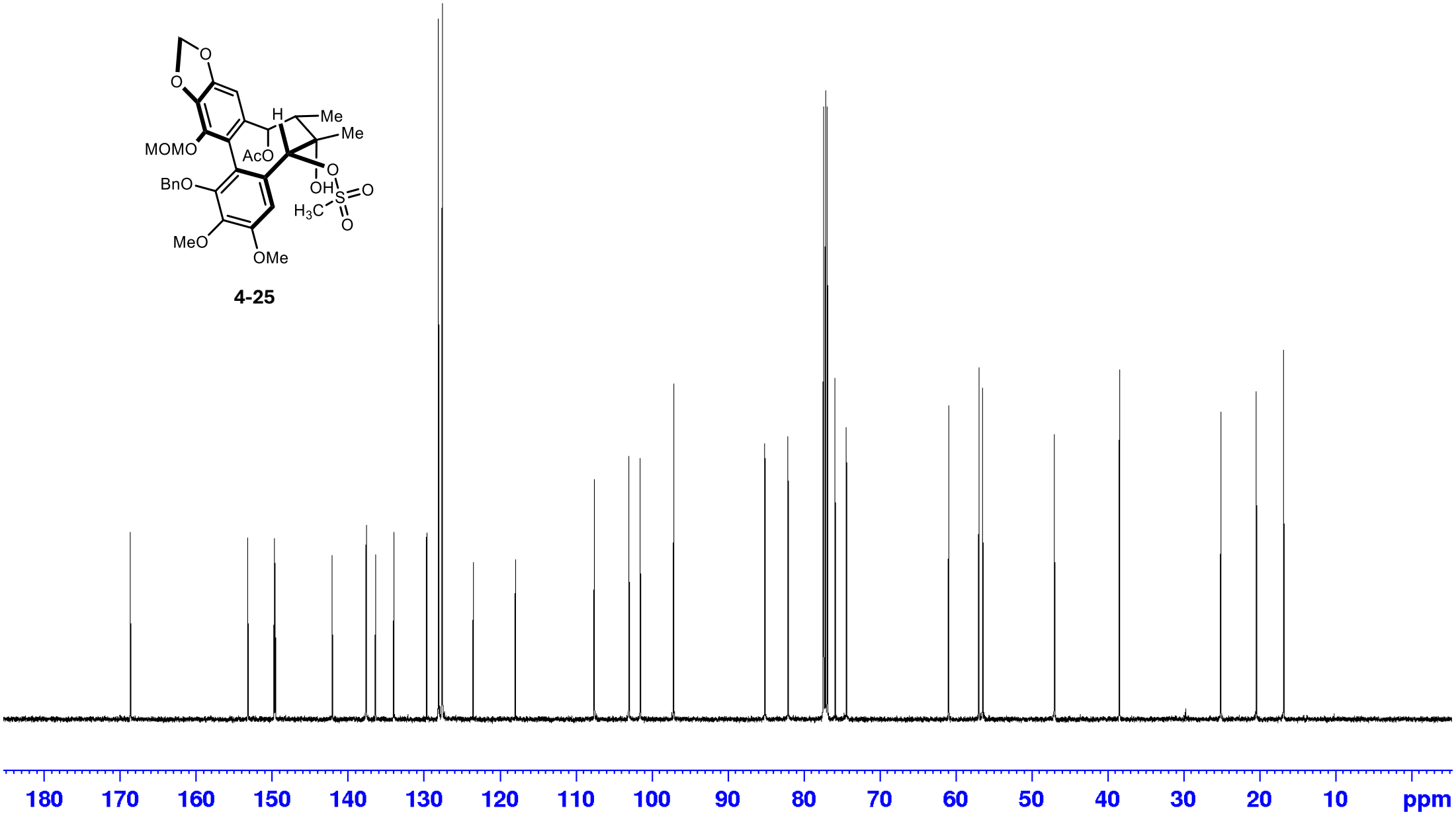


4-25

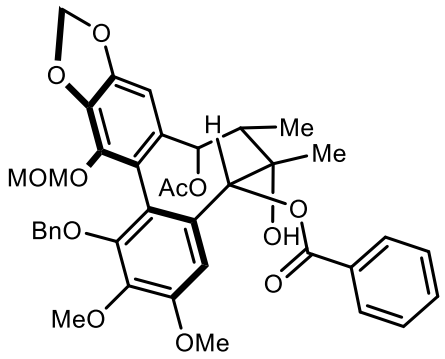
^{13}C NMR
(125 MHz,
$CDCl_3$)

168.69
153.21
149.72
149.62
142.11
137.68
137.61
136.38
133.99
129.66
128.11
127.64
127.59
123.54
117.99
107.59
103.03
101.54
97.12
85.12
82.07
75.87
74.38
60.91
56.94
56.44
46.99
38.44
25.08
20.40
16.80

4-25



^{1}H NMR (500 MHz, $CDCl_3$)

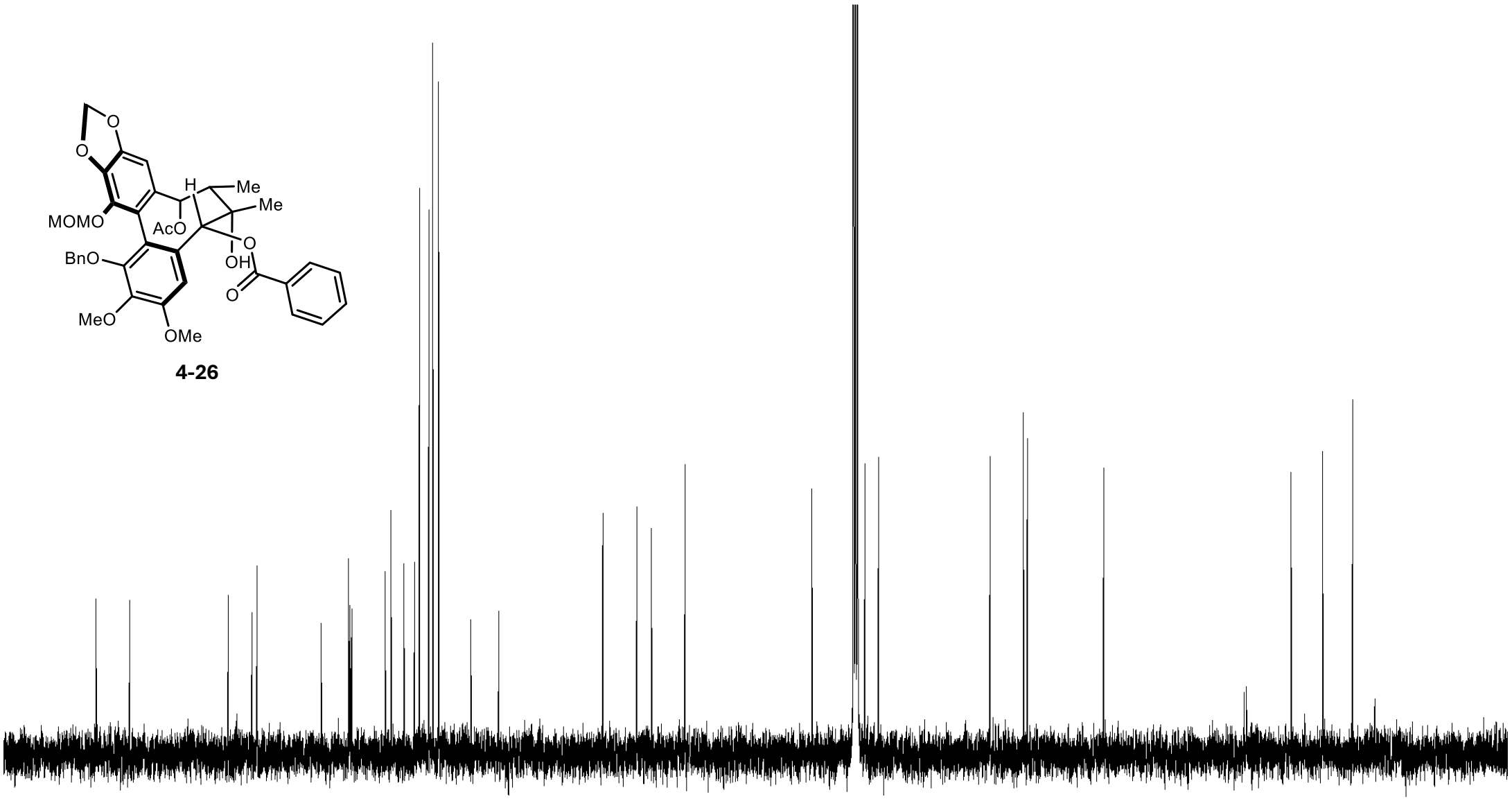


4-26

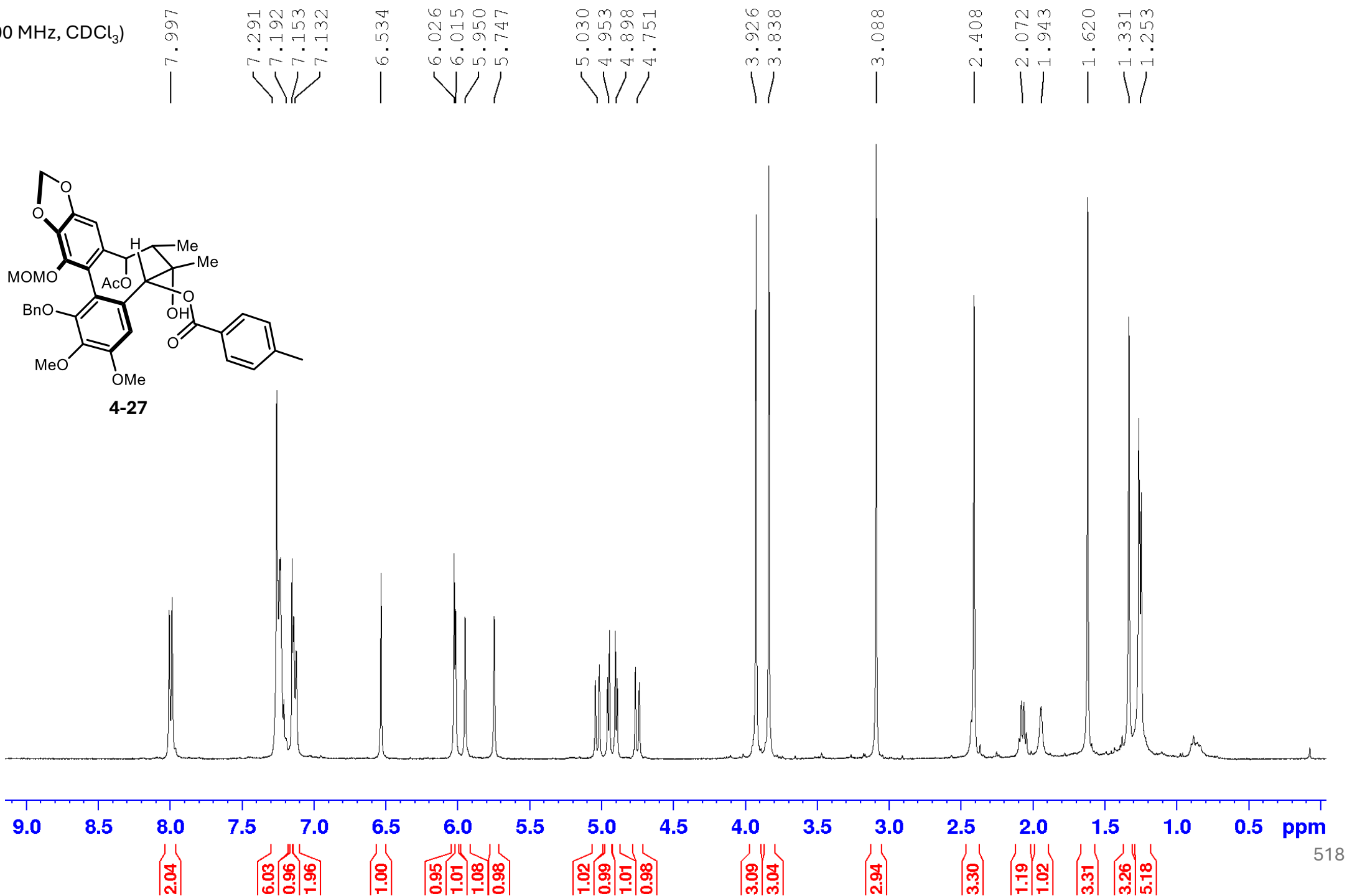
^{13}C NMR
(125 MHz,
$CDCl_3$)

168.81
164.74
152.84
149.90
149.29
141.51
138.19
138.04
137.83
133.77
133.09
131.51
130.23
129.64
128.51
128.02
127.32
127.29
123.42
120.07
107.48
103.37
101.60
97.54
82.28
77.23
75.89
74.25
60.76
56.64
56.17
46.95
24.28
20.48
16.85

4-26



^{1}H NMR (500 MHz, $CDCl_3$)

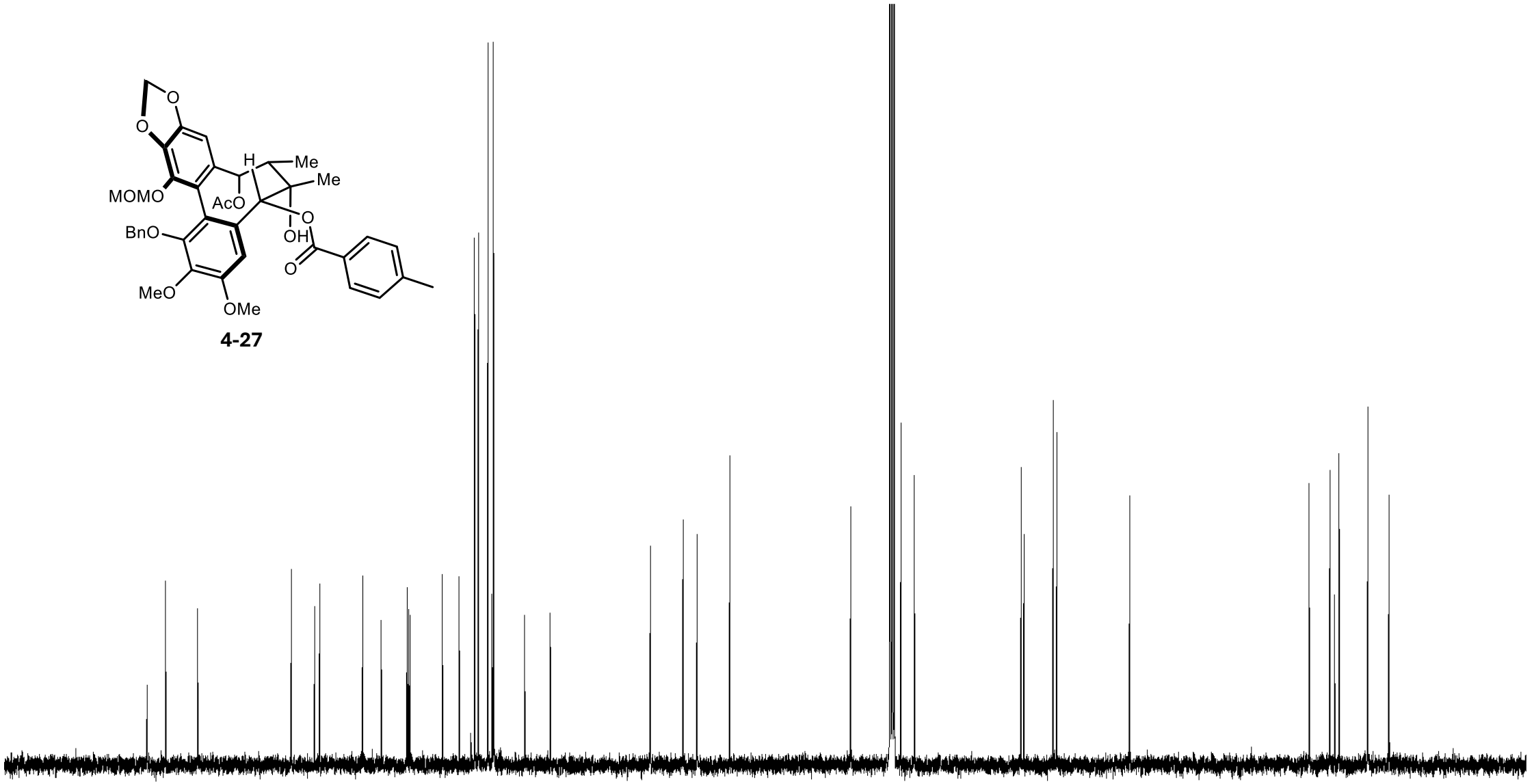


4-27

^{13}C NMR
(125 MHz, $CDCl_3$)

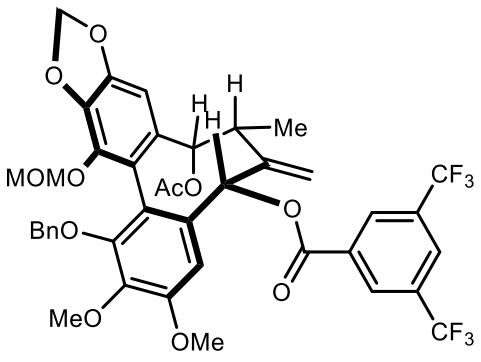
168.82
164.78
152.81
149.88
149.27
143.82
141.46
138.22
138.01
137.84
133.77
131.62
130.15
129.68
129.21
128.01
127.48
127.32
127.27
123.38
120.11
107.49
103.36
101.59
97.54
82.28
75.93
74.25
60.74
56.62
56.15
46.94
24.27
21.67
20.48
16.85

4-27



180 170 160 150 140 130 120 110 100 90 80 70 60 50 40 30 20 10 ppm

^{1}H NMR (500 MHz, $CDCl_3$)

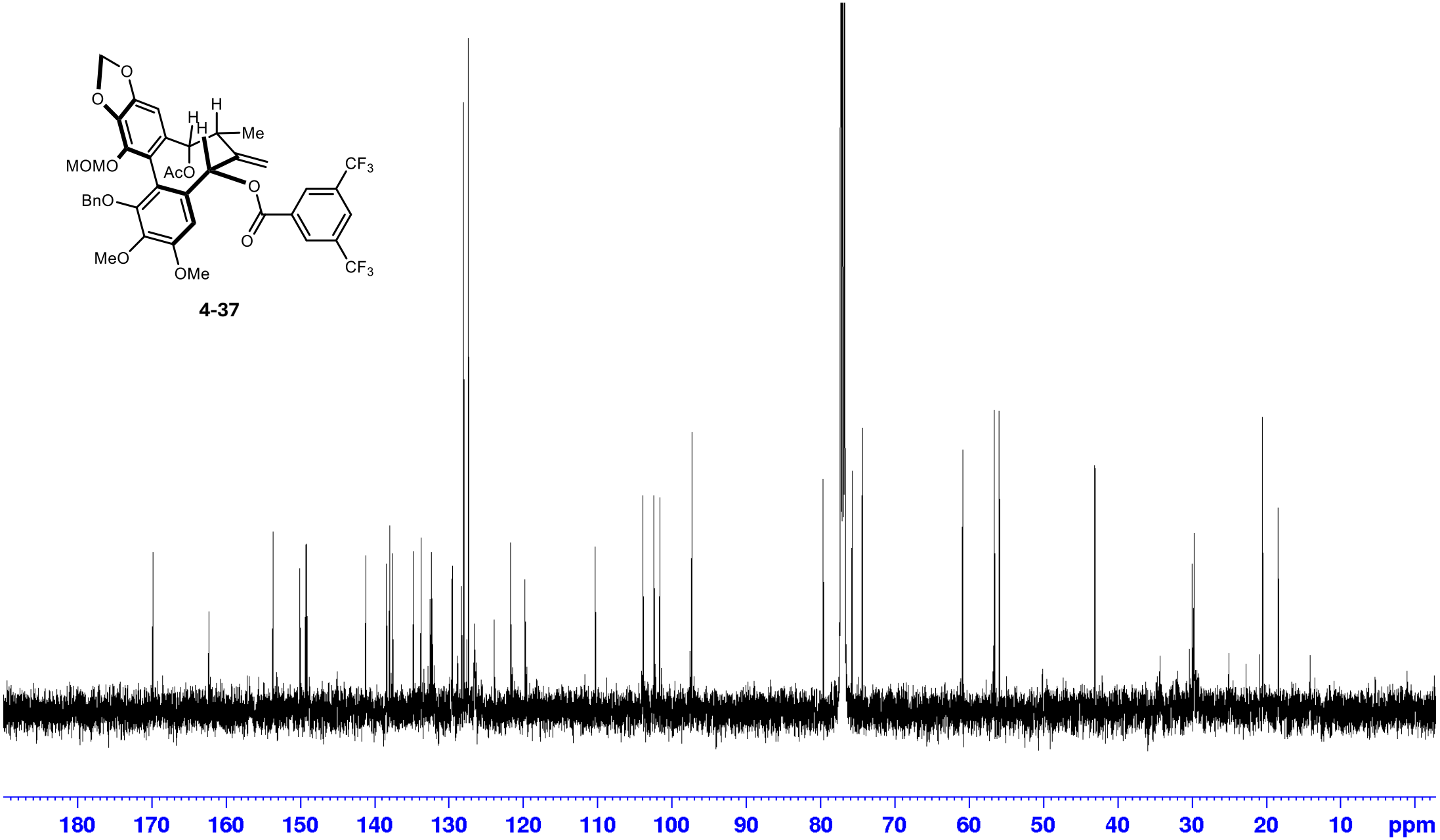


4-37

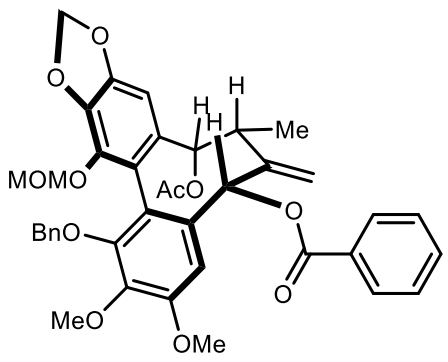
^{13}C NMR
(125 MHz, $CDCl_3$)

169.87
162.33
153.70
150.07
149.26
149.19
141.23
138.41
138.00
137.59
134.79
133.75
132.41
132.39
129.55
128.30
128.07
127.43
127.42
126.58
123.90
122.80
121.72
119.76
110.31
103.91
102.43
101.63
97.31
79.64
75.76
74.38
60.88
56.62
55.94
43.07
20.52
18.39

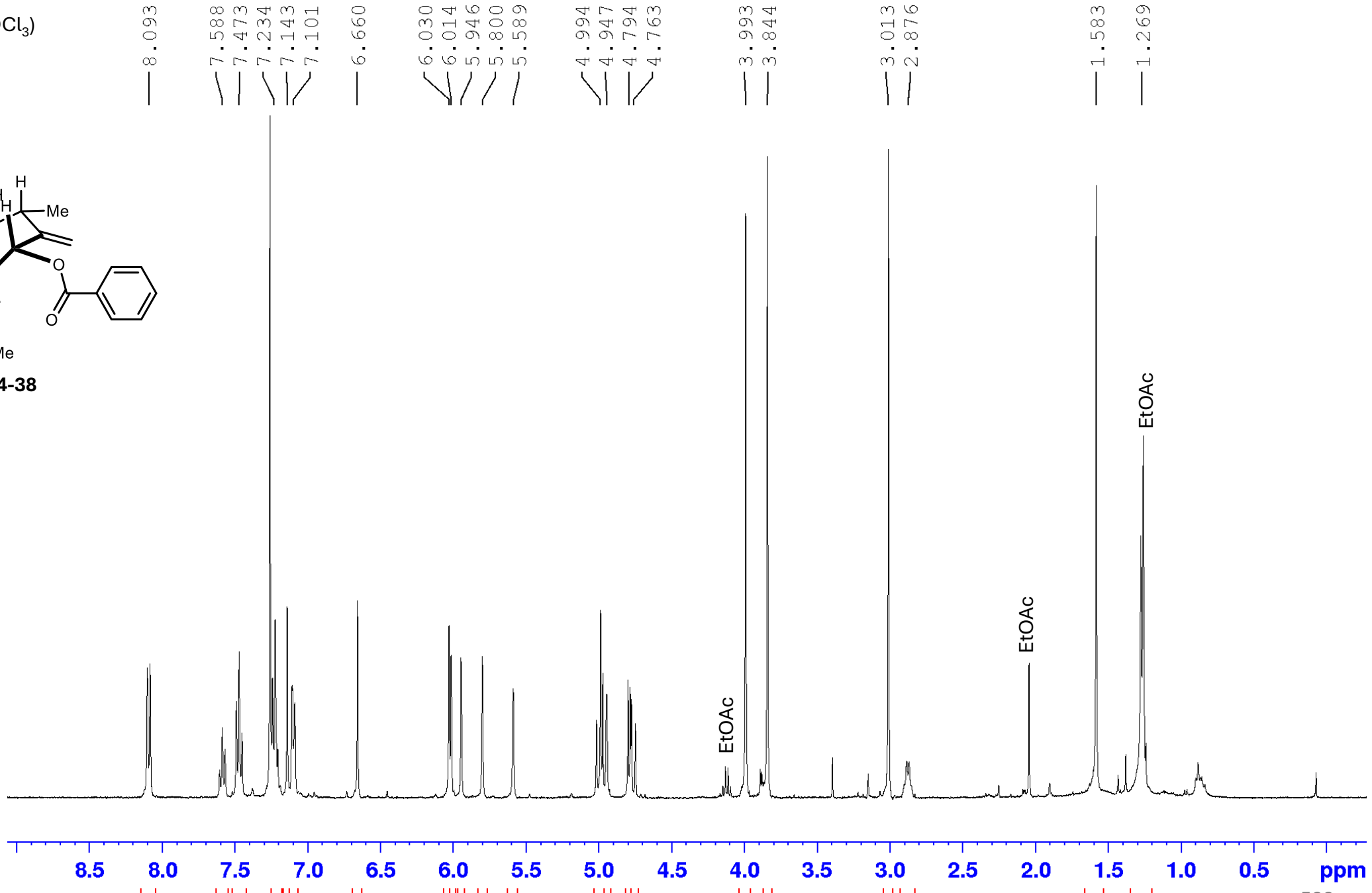
4-37



^{1}H NMR (500 MHz, $CDCl_3$)



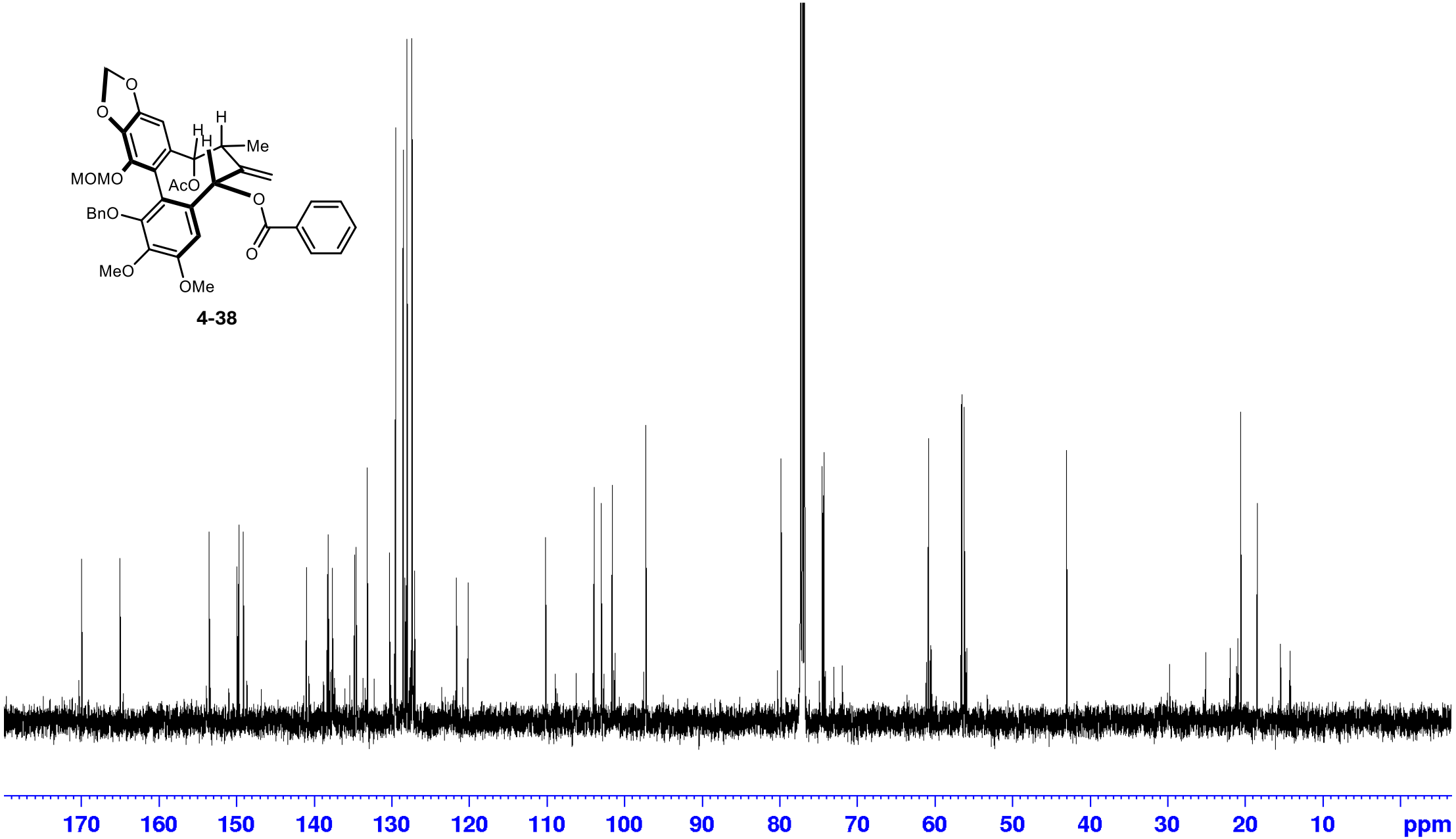
4-38



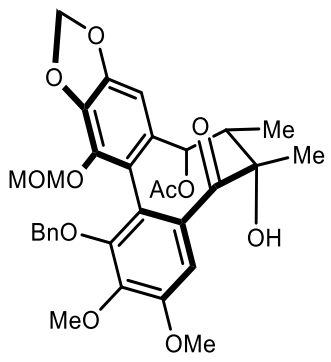
^{13}C NMR (125 MHz, $CDCl_3$)

169.97
165.02
153.57
149.96
149.74
149.12
140.99
138.30
138.18
137.66
134.79
134.60
133.16
130.28
129.52
128.54
128.03
127.39
121.64
120.17
110.16
103.93
102.99
101.59
97.25
79.80
77.25
74.50
74.31
60.84
56.54
56.19
43.01
20.56
18.42

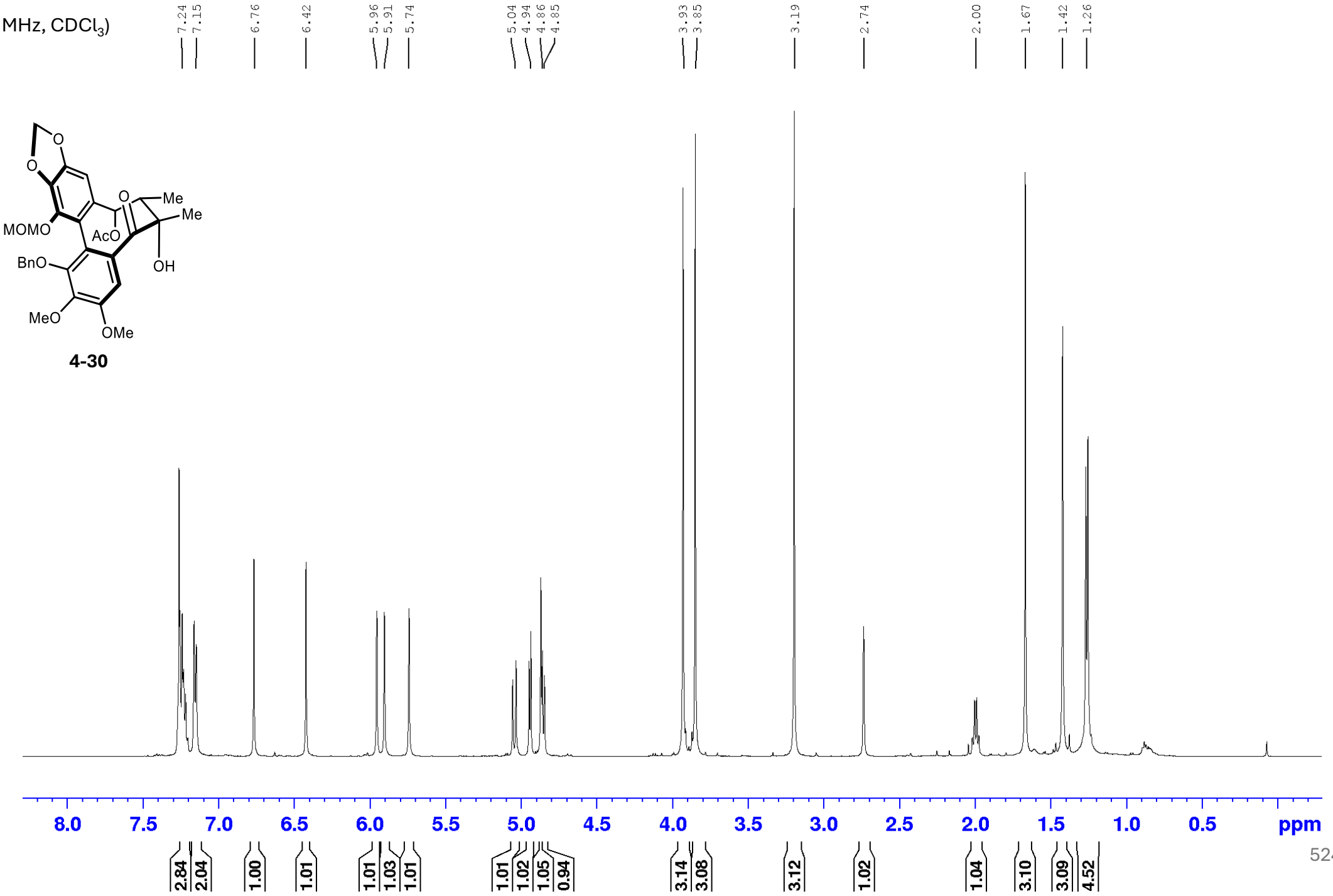
4-38



^{1}H NMR (500 MHz, $CDCl_3$)



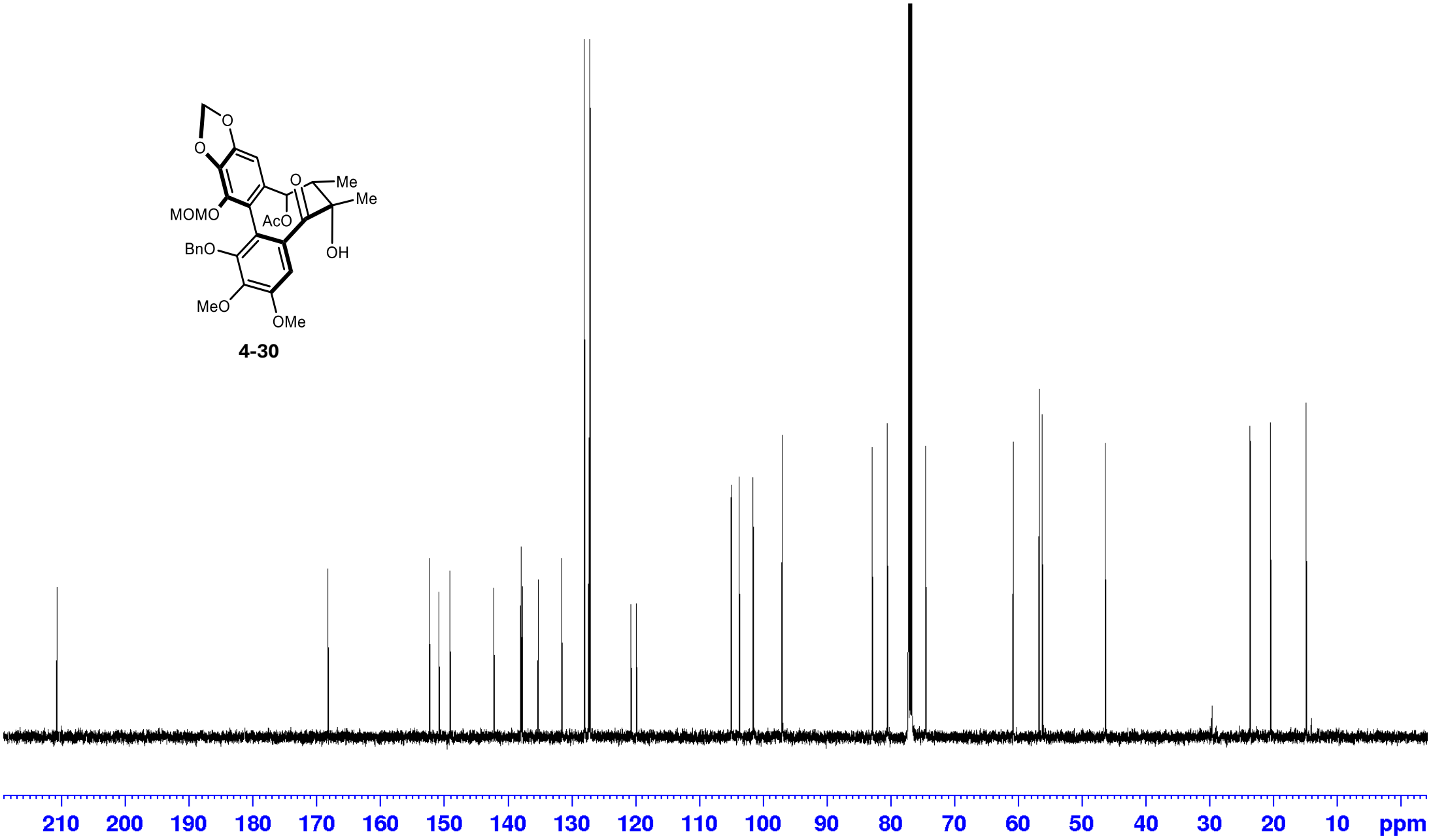
4-30



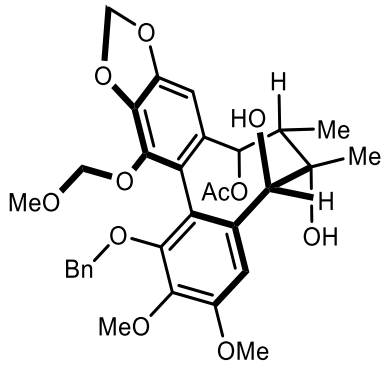
^{13}C NMR
(125 MHz,
$CDCl_3$)

210.69
168.31
152.41
150.90
149.19
142.28
138.13
138.01
137.80
135.35
131.65
128.09
127.39
127.22
120.82
119.96
105.08
103.81
101.64
97.11
82.96
80.59
77.26
74.60
60.85
56.81
56.31
46.43
23.72
20.51
14.94

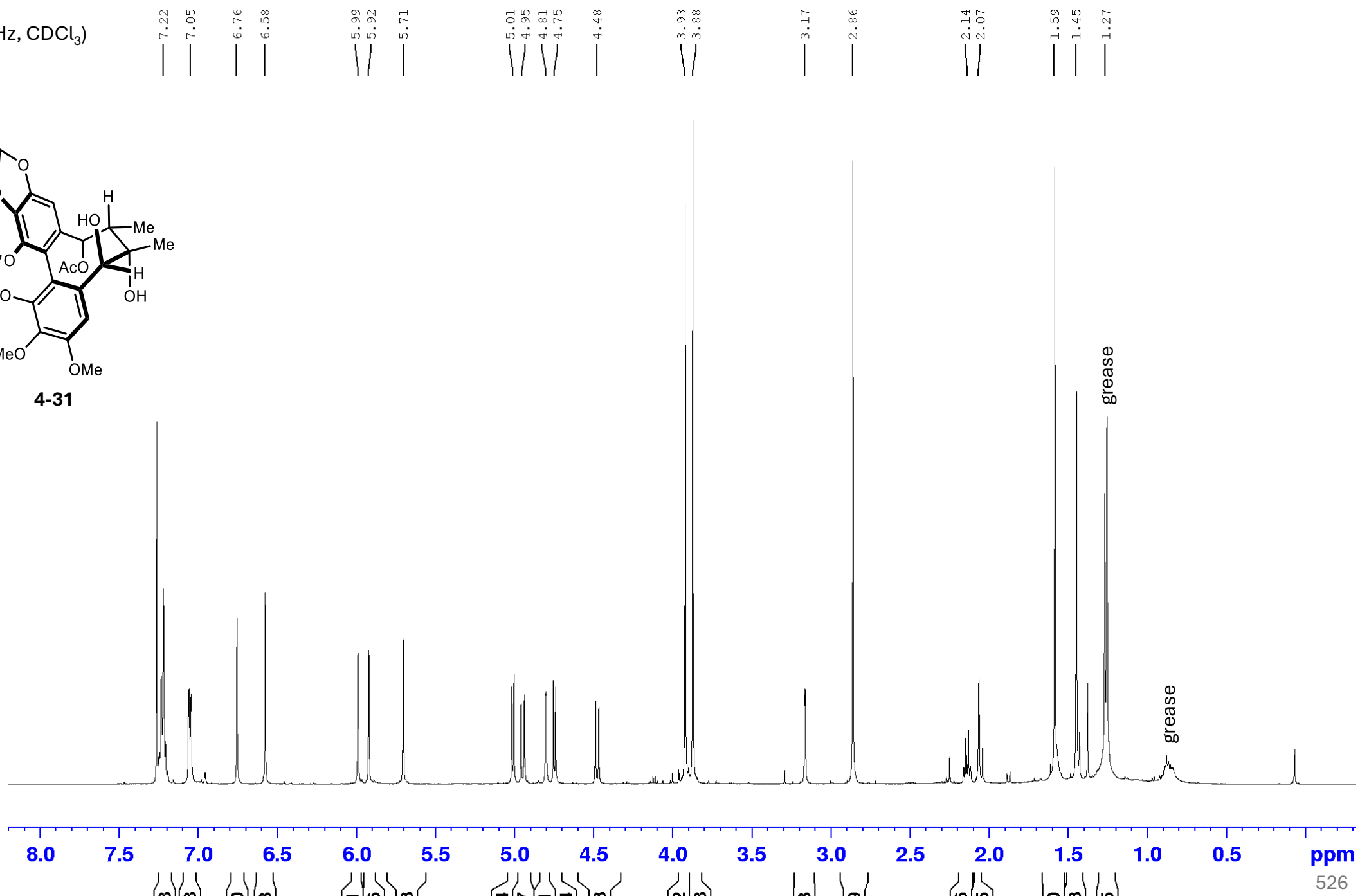
4-30



^{1}H NMR (500 MHz, $CDCl_3$)

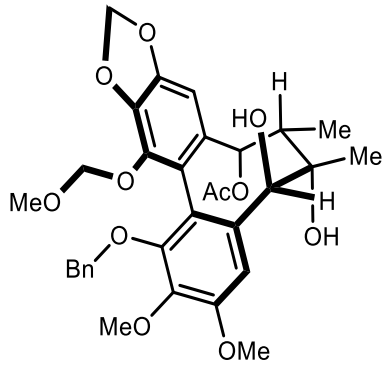


4-31



^{13}C NMR
(125 MHz, $CDCl_3$)

168.79
152.00
150.83
148.83
141.54
138.60
138.05
137.71
134.41
132.91
128.05
127.68
127.47
122.98
122.54
110.62
104.54
101.81
98.51
85.86
83.55
75.15
74.41
61.00
56.49
56.31
41.91
29.06
20.56
17.28

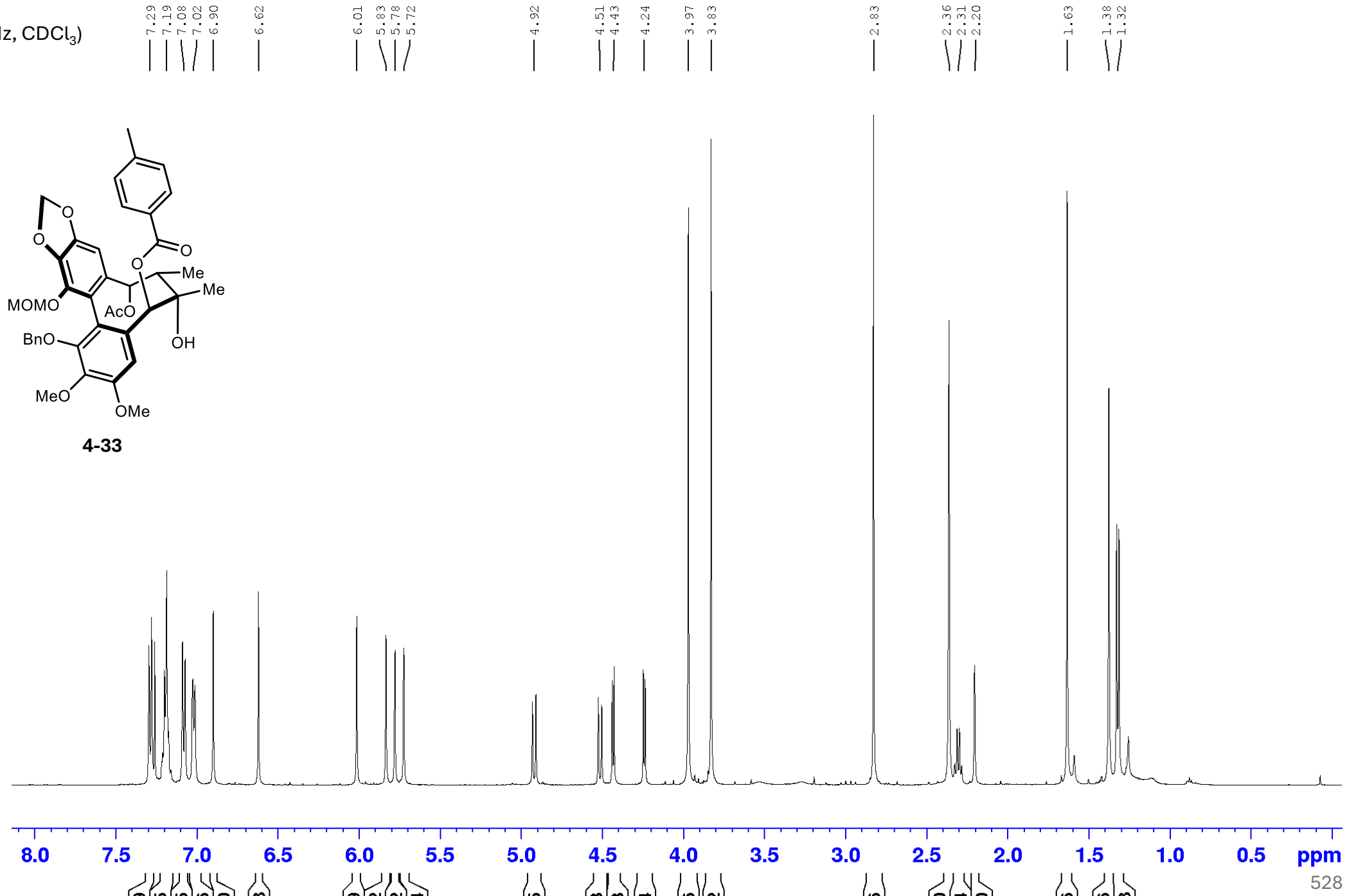


4-31

180 170 160 150 140 130 120 110 100 90 80 70 60 50 40 30 20 10 ppm

^{1}H NMR (500 MHz, $CDCl_3$)

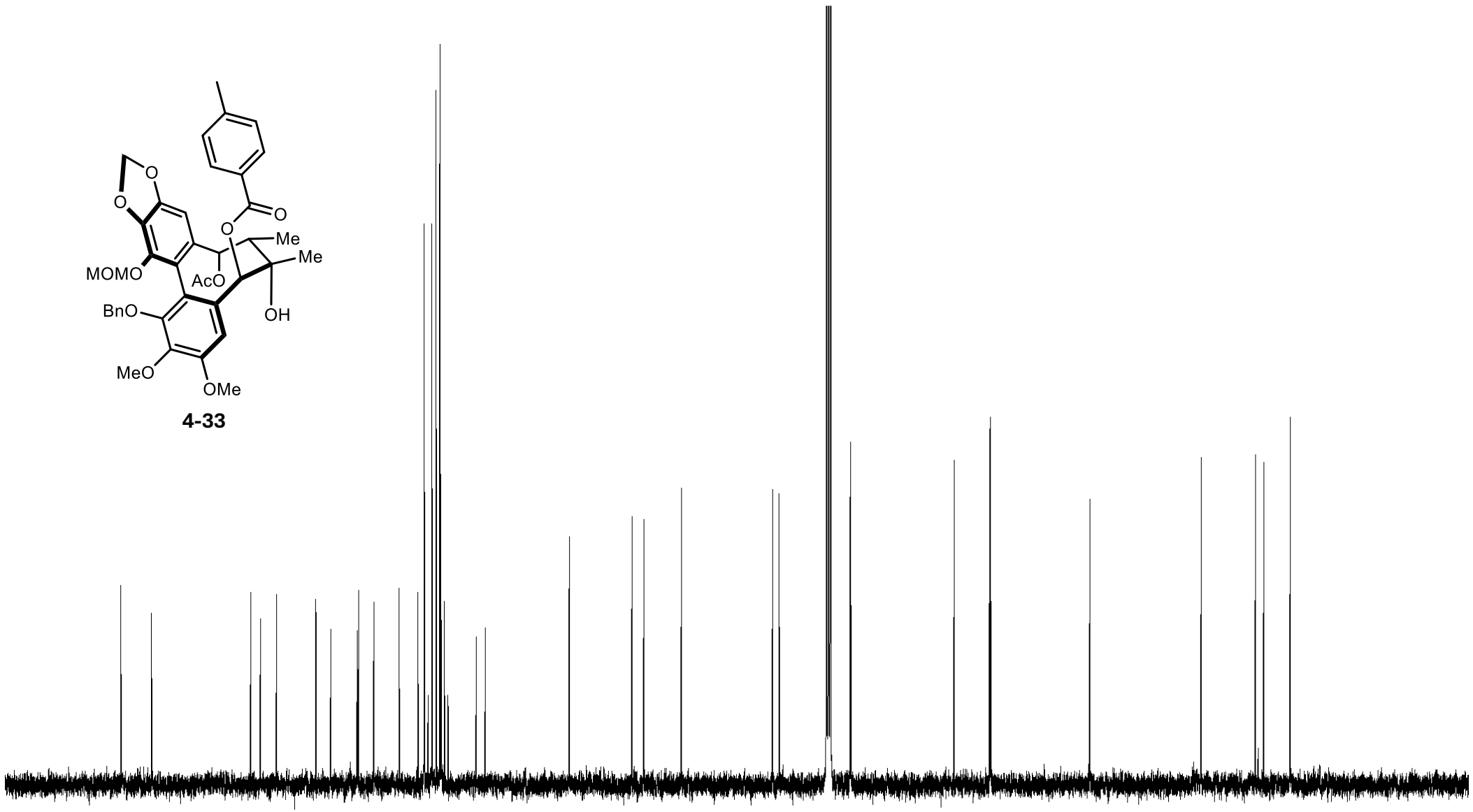
4-33



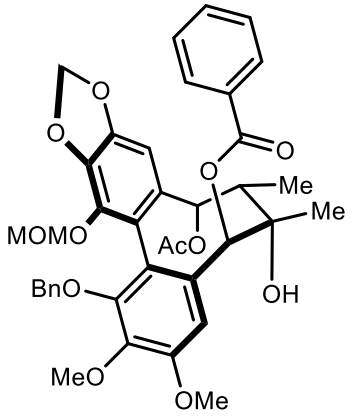
^{13}C NMR
(125 MHz, $CDCl_3$)

168.78
164.80
151.96
150.71
148.61
143.50
141.60
138.16
137.99
136.01
132.71
130.30
129.47
128.48
127.94
127.44
127.30
126.85
122.73
121.55
110.66
102.54
100.99
96.12
84.30
83.45
74.24
74.15
60.76
56.14
56.04
43.17
28.71
21.70
20.61
17.17

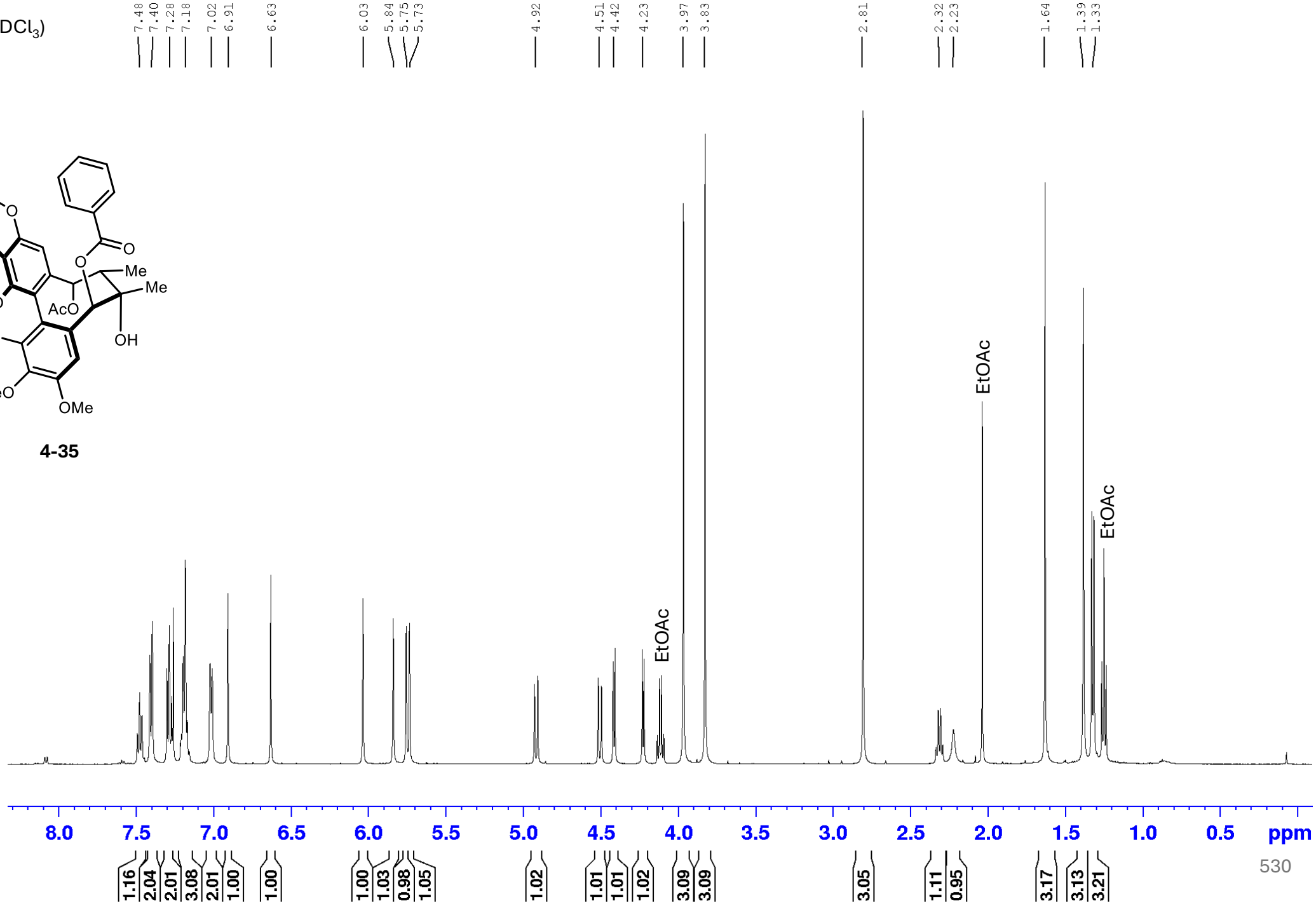
4-33



^{1}H NMR (500 MHz, $CDCl_3$)

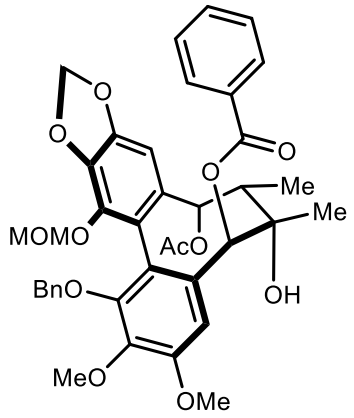


4-35



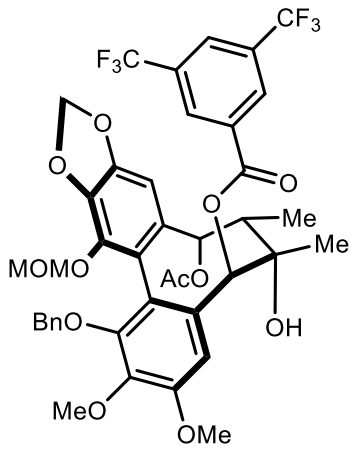
^{13}C NMR
(125 MHz,
$CDCl_3$)

168.78
164.72
151.98
150.71
148.64
141.64
138.20
137.96
136.10
132.86
132.70
130.21
129.55
129.42
127.95
127.77
127.45
127.32
122.74
121.55
110.69
102.60
101.01
96.15
84.45
83.45
74.26
74.15
60.76
56.15
56.01
43.19
28.72
20.61
17.17

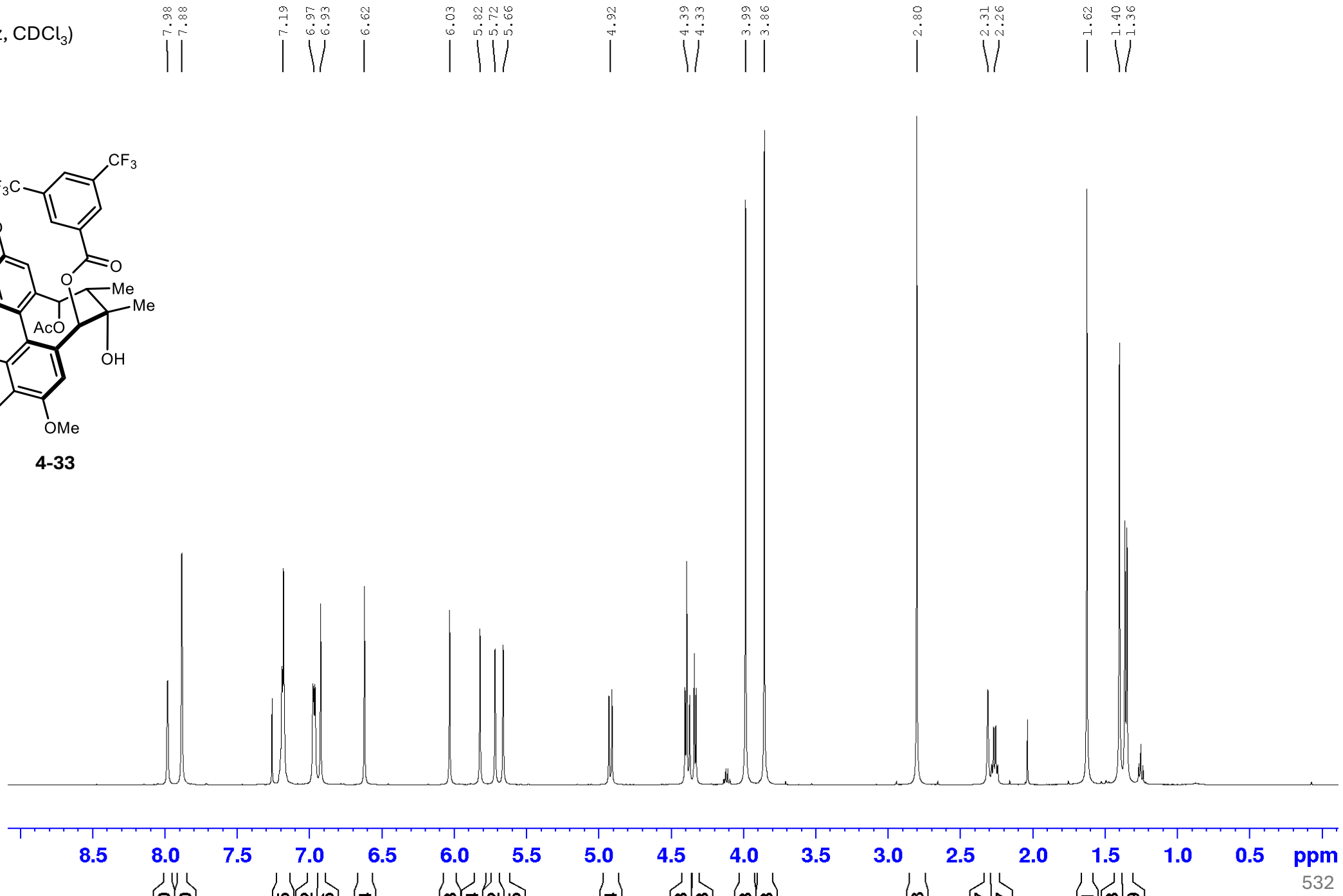


4-35

^{1}H NMR (500 MHz, $CDCl_3$)

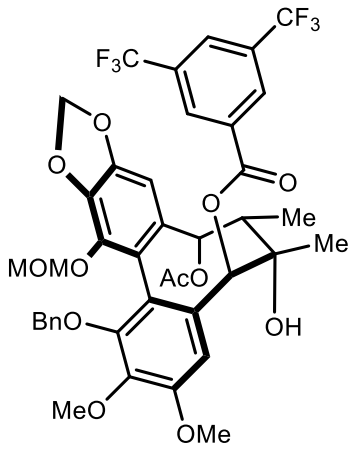


4-33



^{13}C NMR
(125 MHz, $CDCl_3$)

168.63
162.43
152.15
150.60
148.75
141.94
138.15
137.66
136.40
132.61
132.06
131.75
129.50
129.00
127.97
127.62
127.48
126.19
122.79
122.58
121.18
110.78
103.02
101.22
96.60
85.96
83.47
74.32
73.93
60.82
56.21
56.03
43.21
28.84
20.55
17.25

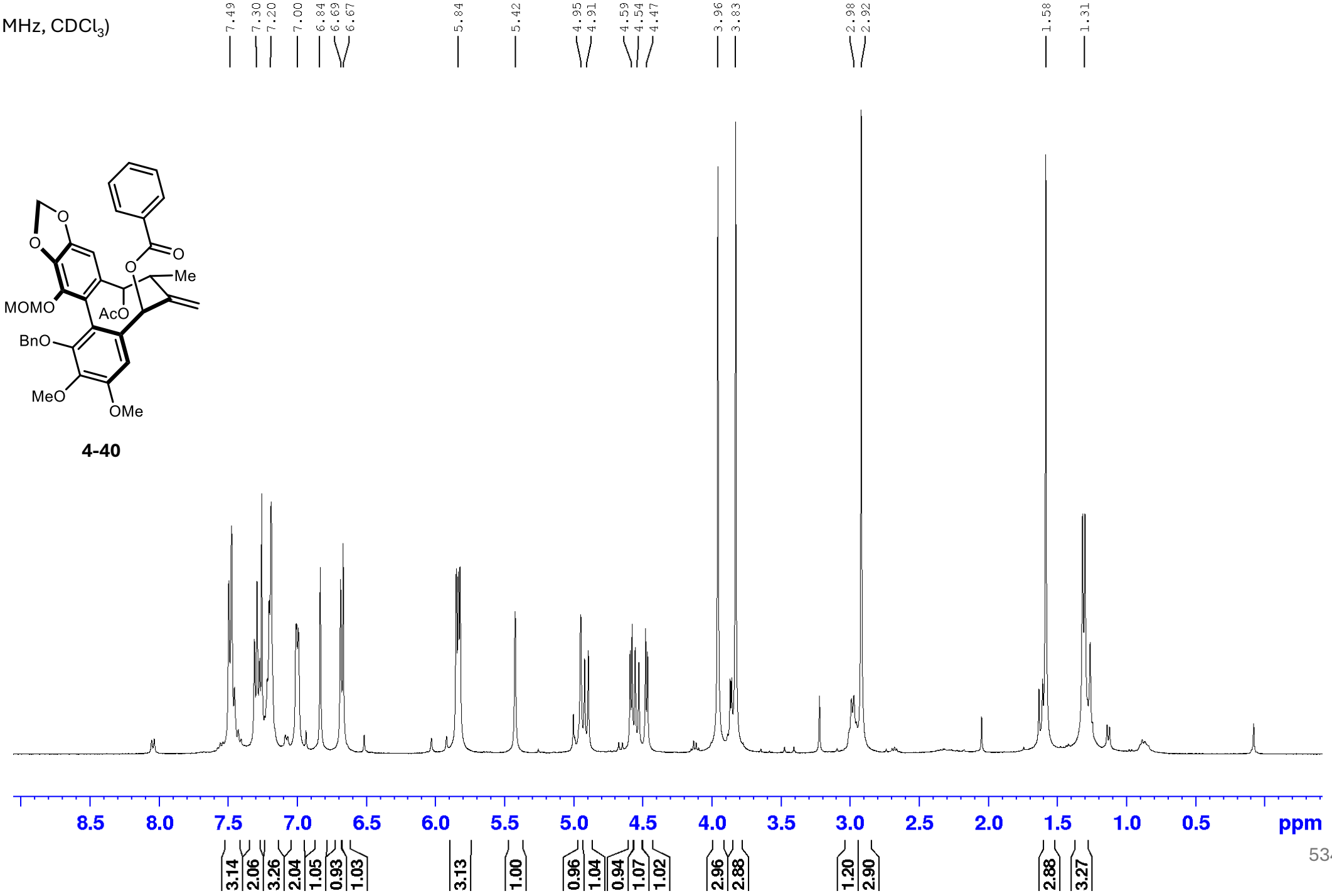


4-33

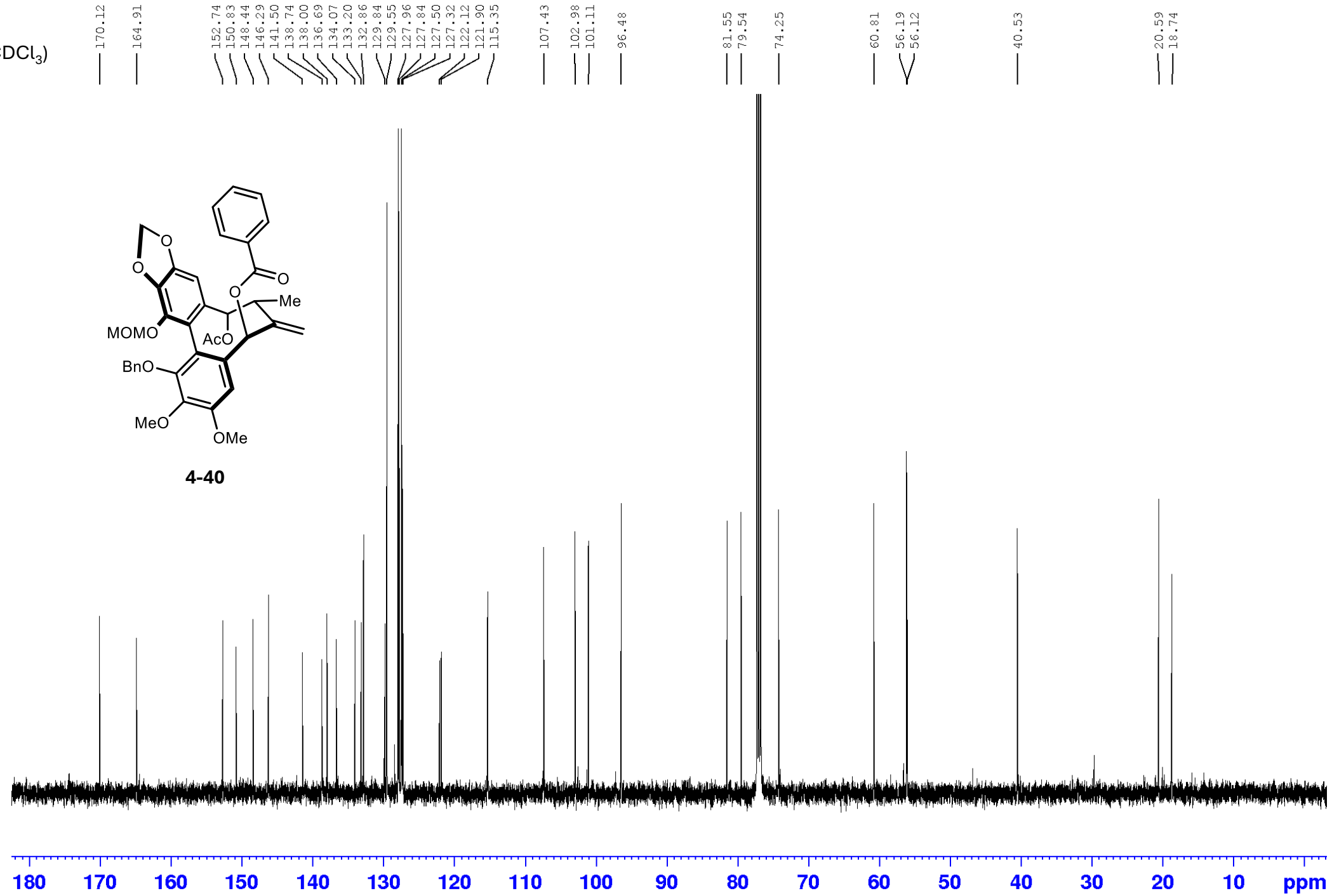
180 170 160 150 140 130 120 110 100 90 80 70 60 50 40 30 20 10 ppm

^{1}H NMR (500 MHz, $CDCl_3$)

4-40

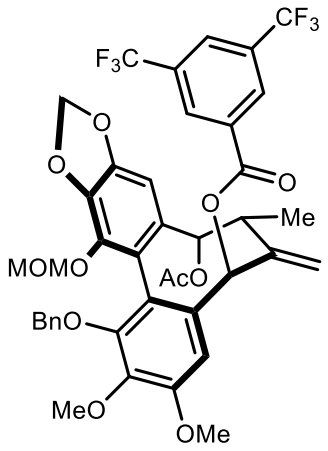


^{13}C NMR
(125 MHz, $CDCl_3$)

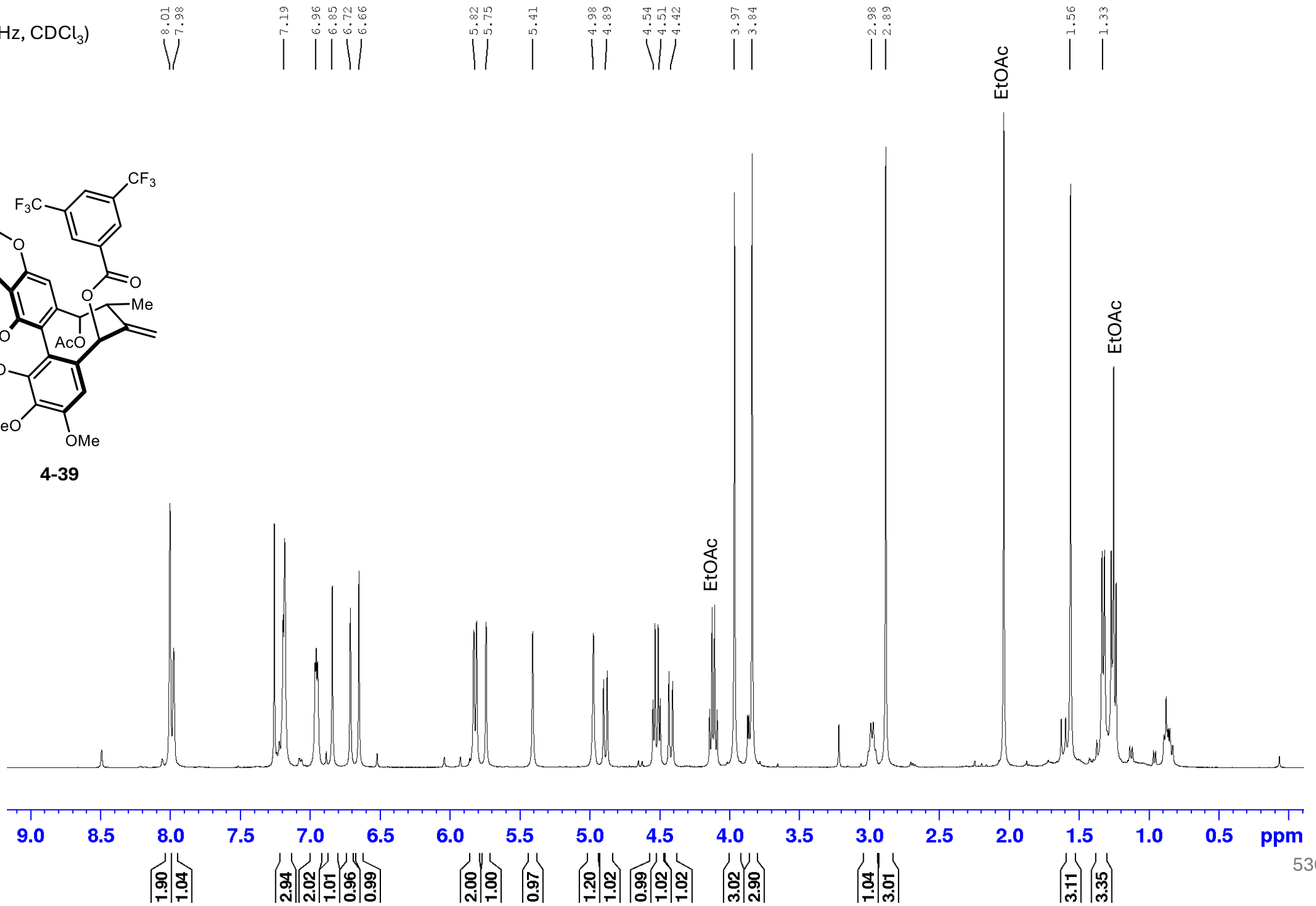


4-40

^{1}H NMR (500 MHz, $CDCl_3$)



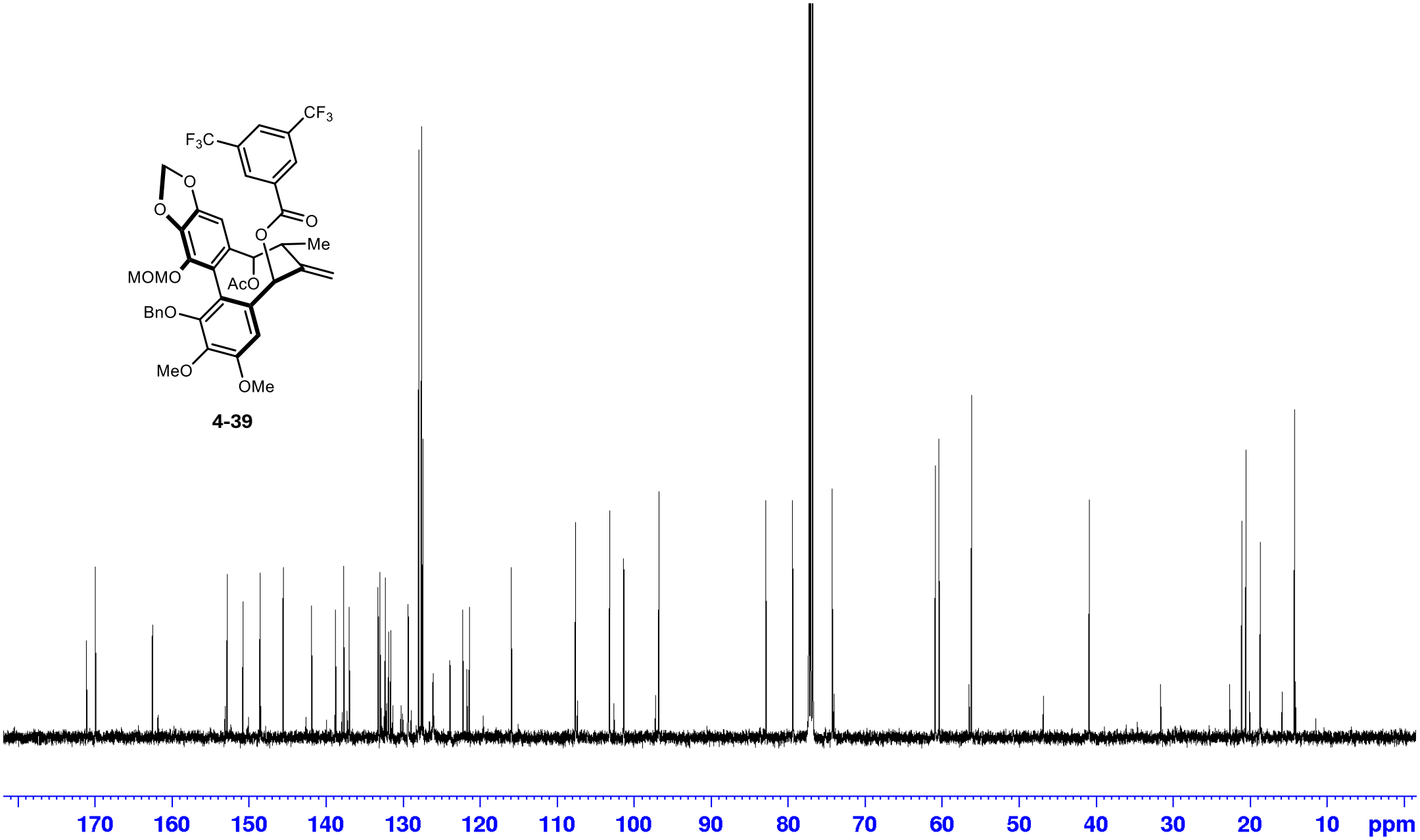
4-39



^{13}C NMR (125 MHz, $CDCl_3$)

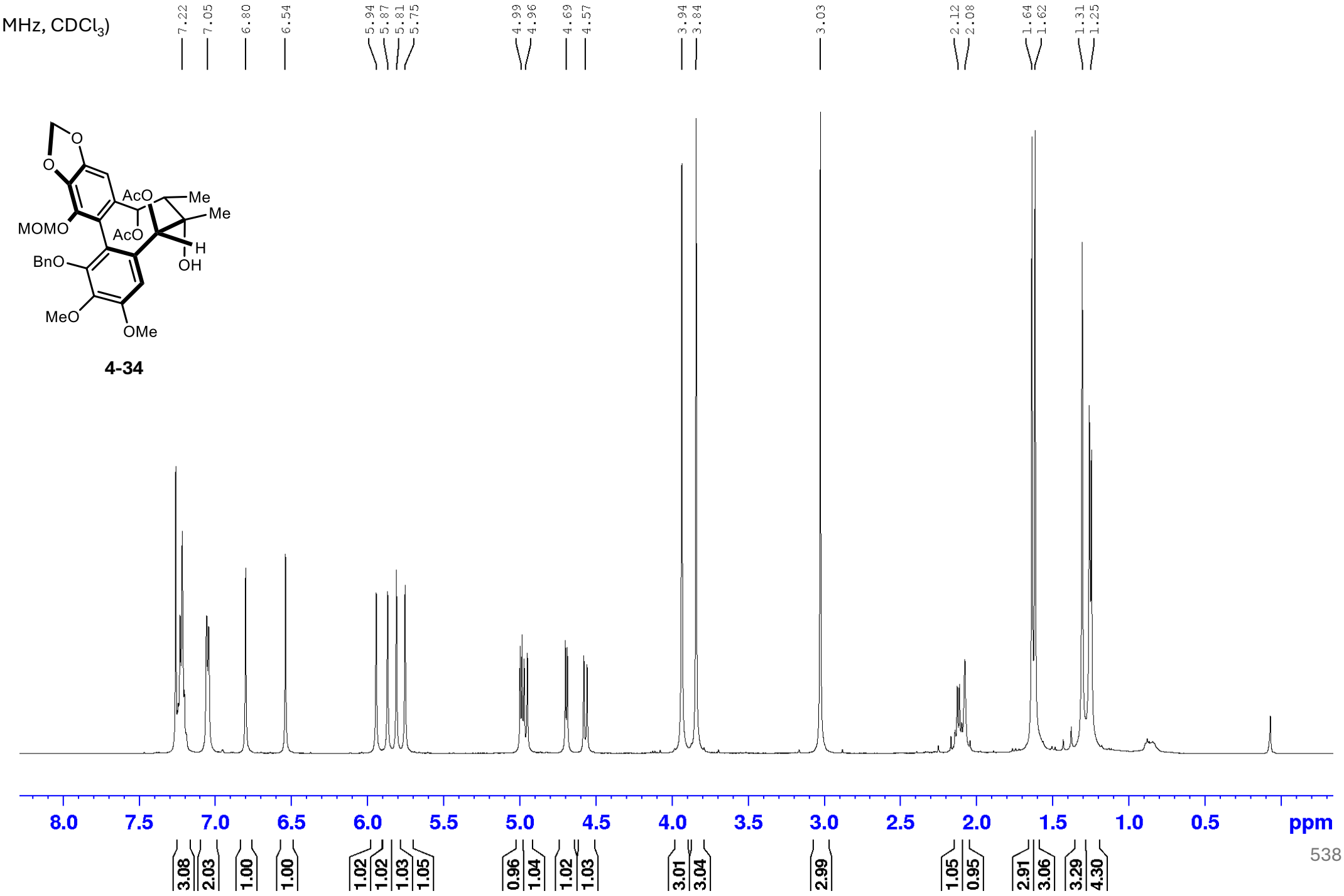
169.97
162.56
152.86
150.78
148.60
145.59
141.86
138.76
137.73
137.00
133.24
133.02
132.32
131.75
129.34
127.97
127.63
127.44
126.11
122.84
122.24
121.40
115.96
107.61
103.18
101.34
96.76
82.87
79.39
74.27
60.86
56.18
56.16
40.86
20.53
18.65

4-39

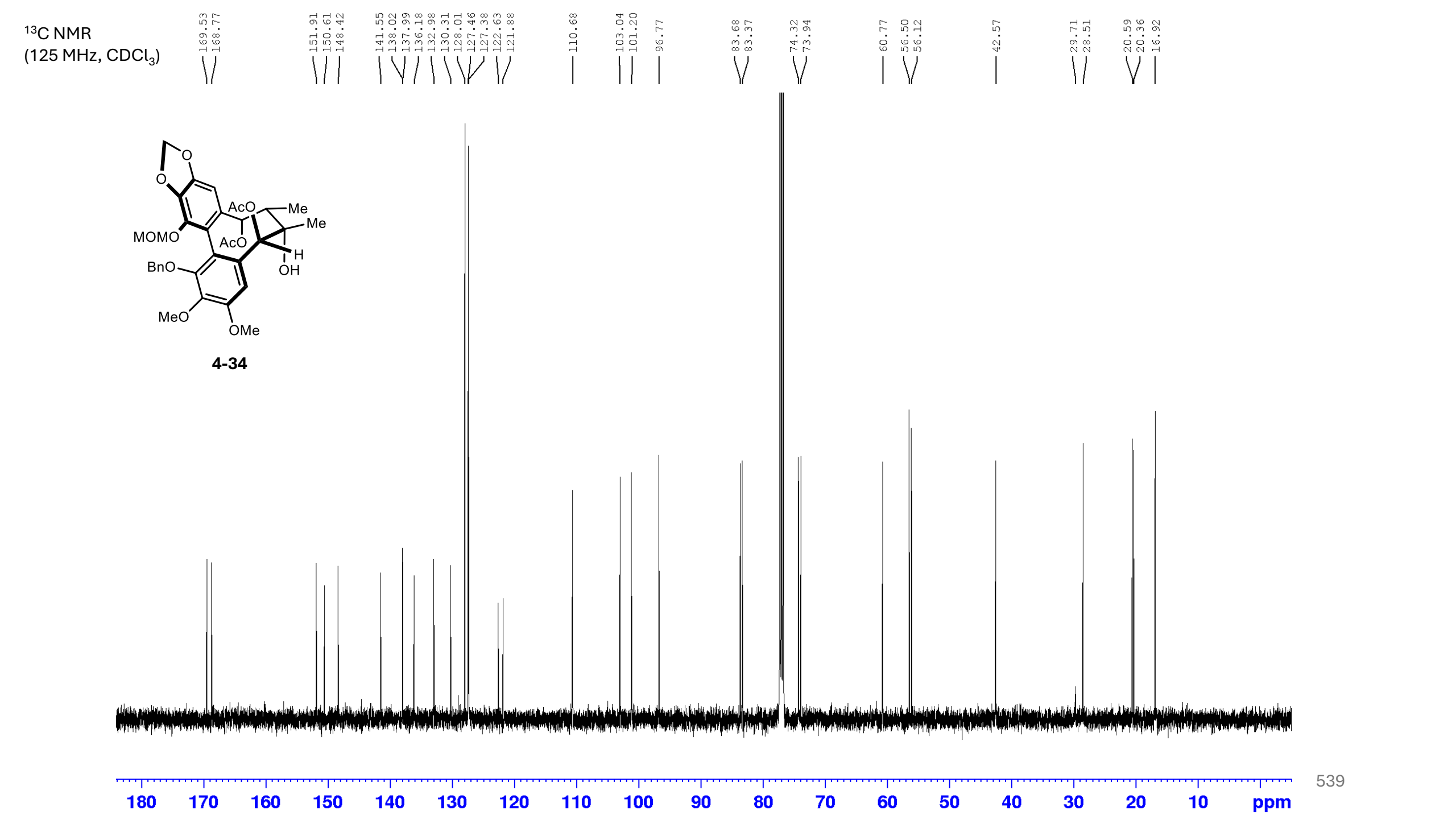


^{1}H NMR (500 MHz, $CDCl_3$)

4-34

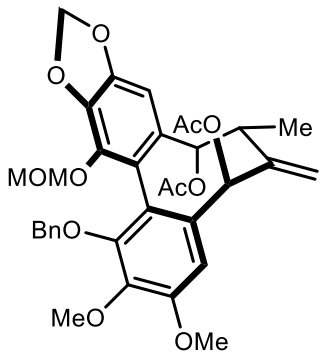


^{13}C NMR
(125 MHz, $CDCl_3$)



4-34

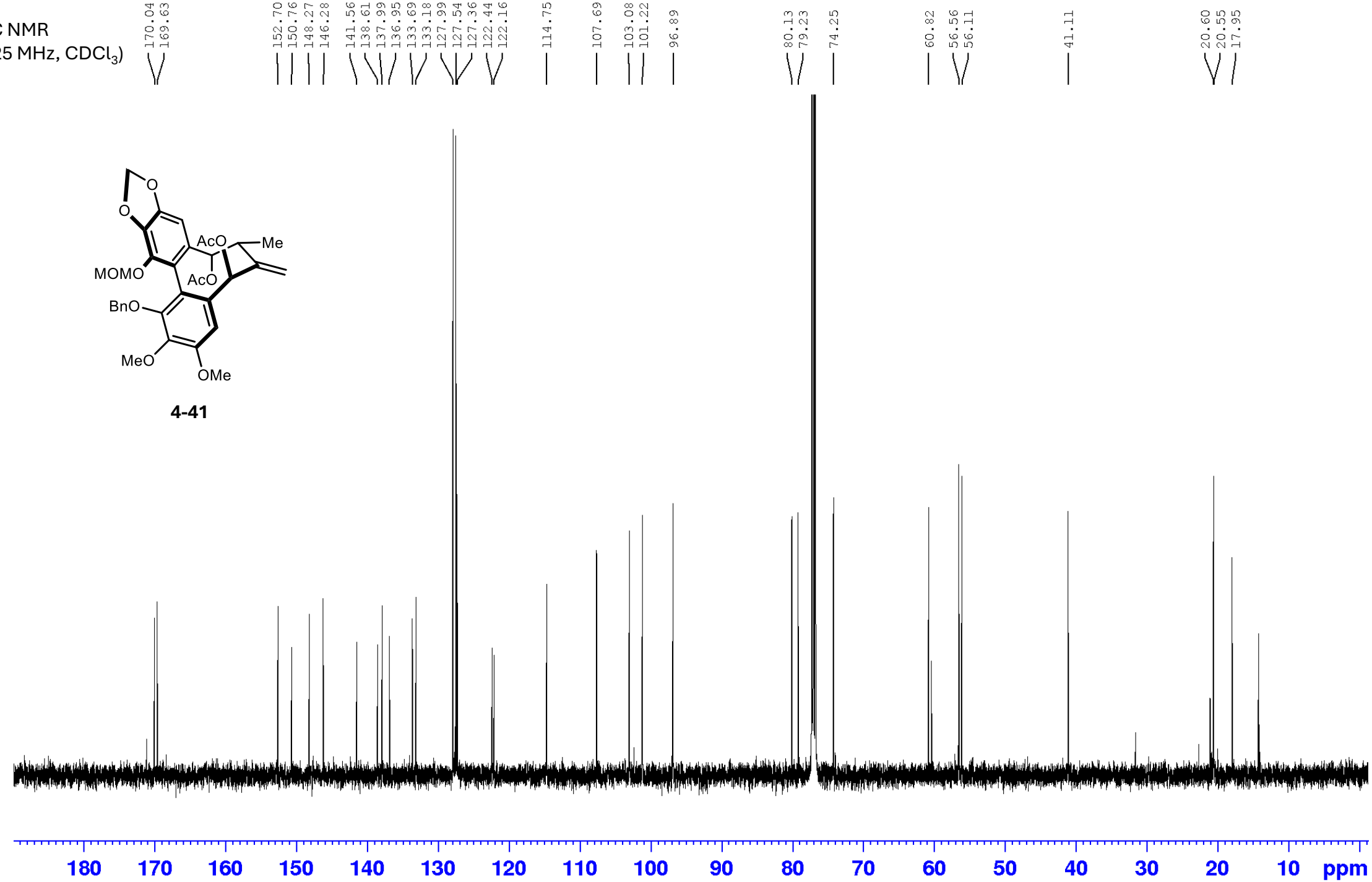
^{1}H NMR (500 MHz, $CDCl_3$)



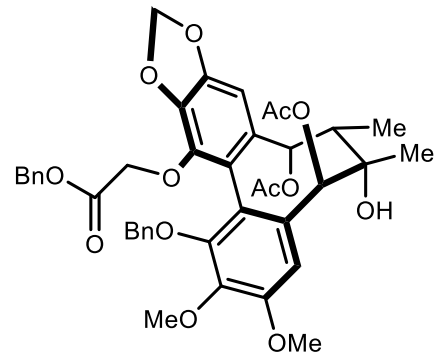
4-41

^{13}C NMR
(125 MHz, $CDCl_3$)

4-41



^{1}H NMR (500 MHz, $CDCl_3$)

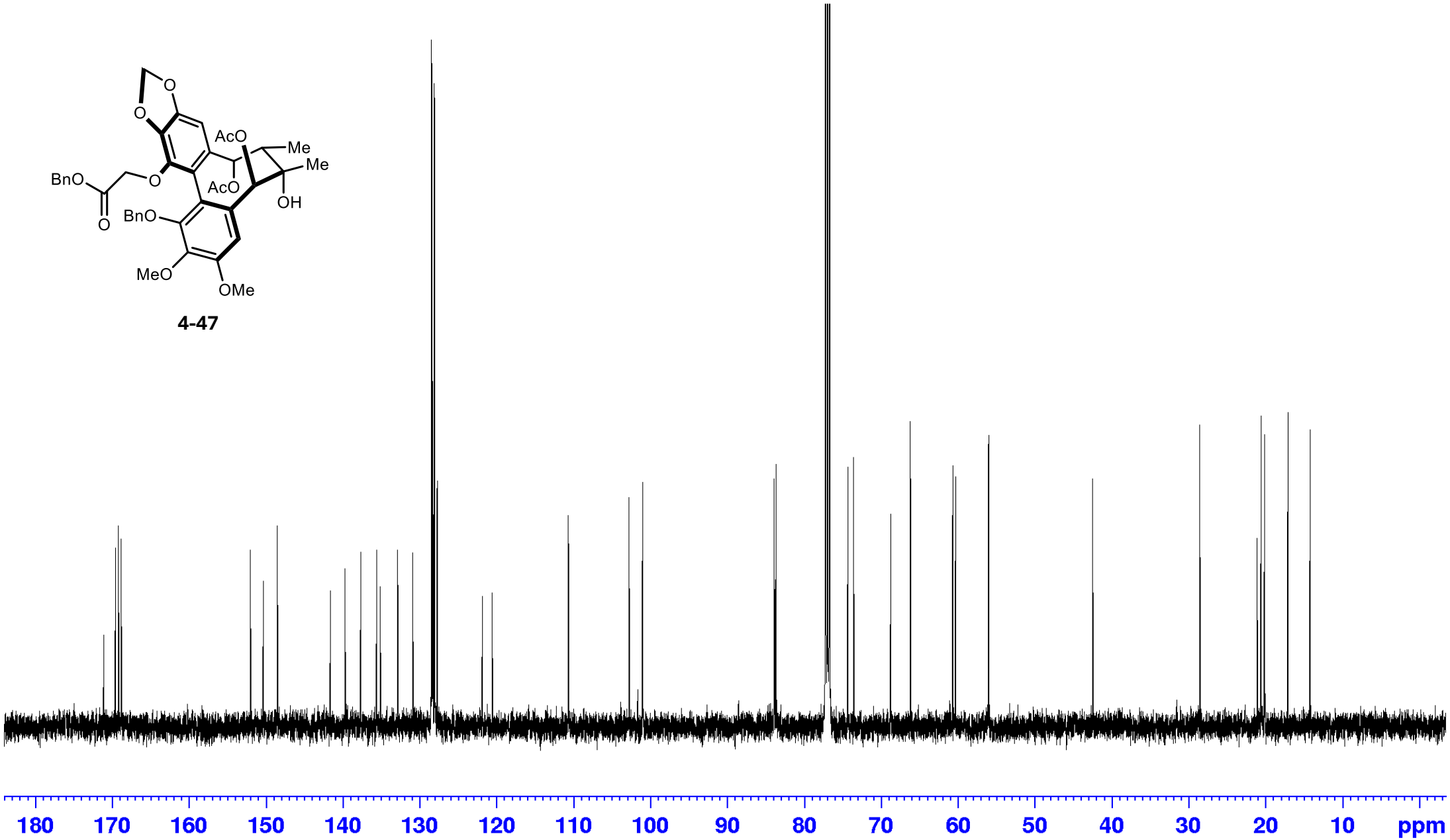


4-47

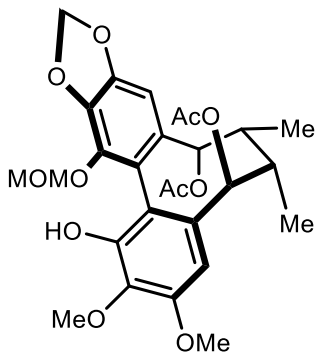
^{13}C NMR
(125 MHz,
$CDCl_3$)

169.65
169.25
168.90
152.03
150.33
148.48
141.62
139.74
137.65
135.57
135.11
132.84
130.91
128.46
128.37
128.26
128.08
128.04
127.71
121.86
120.56
110.74
102.84
101.11
84.00
83.75
74.41
73.64
68.81
66.25
60.77
56.10
42.55
28.53
20.56
20.12
17.09

4-47



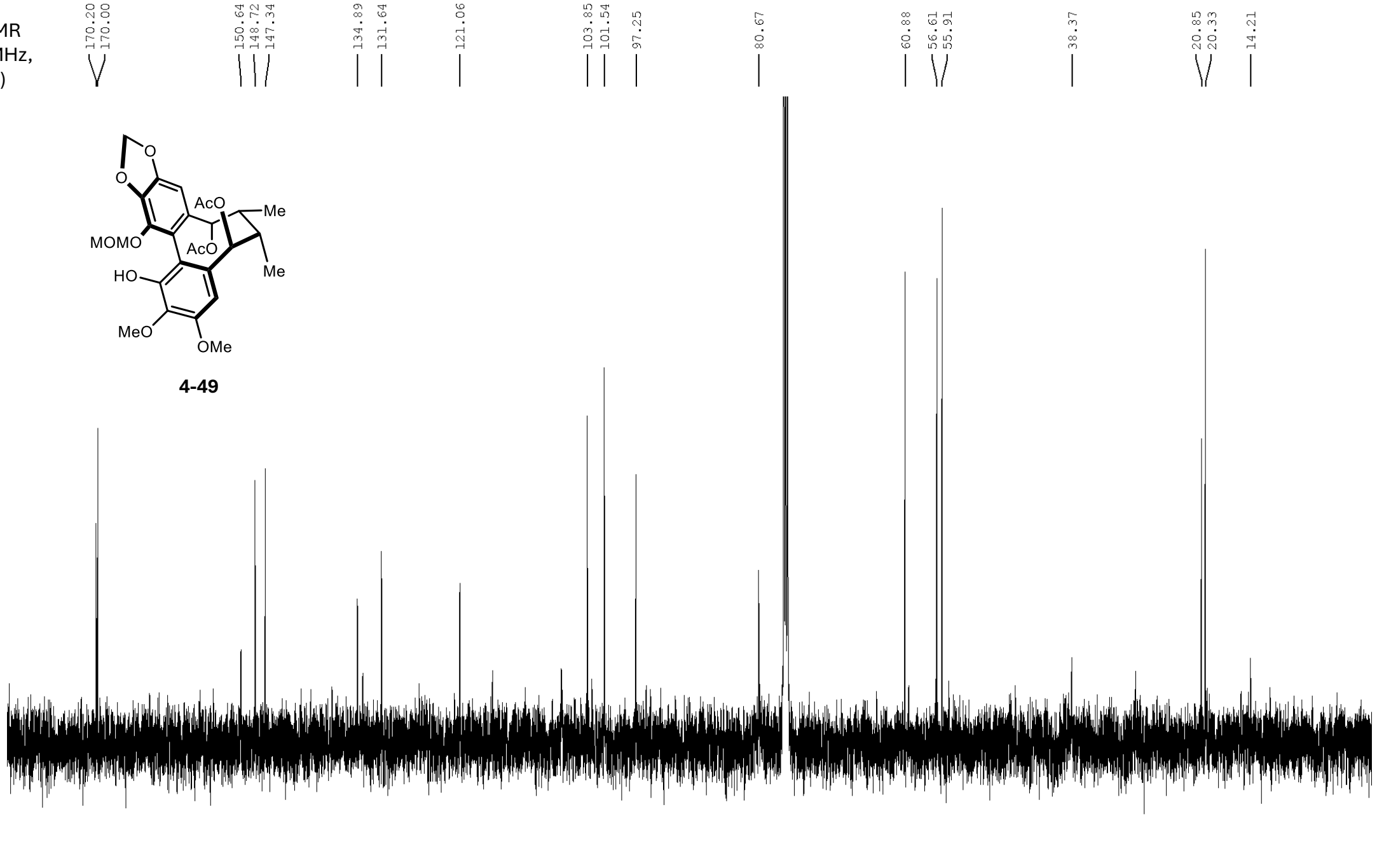
^{1}H NMR (500 MHz, $CDCl_3$)



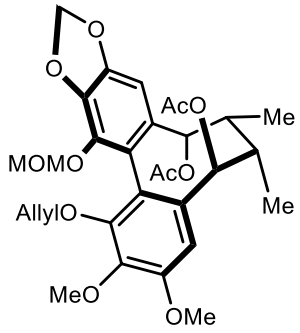
4-49

^{13}C NMR
(125 MHz,
$CDCl_3$)

4-49



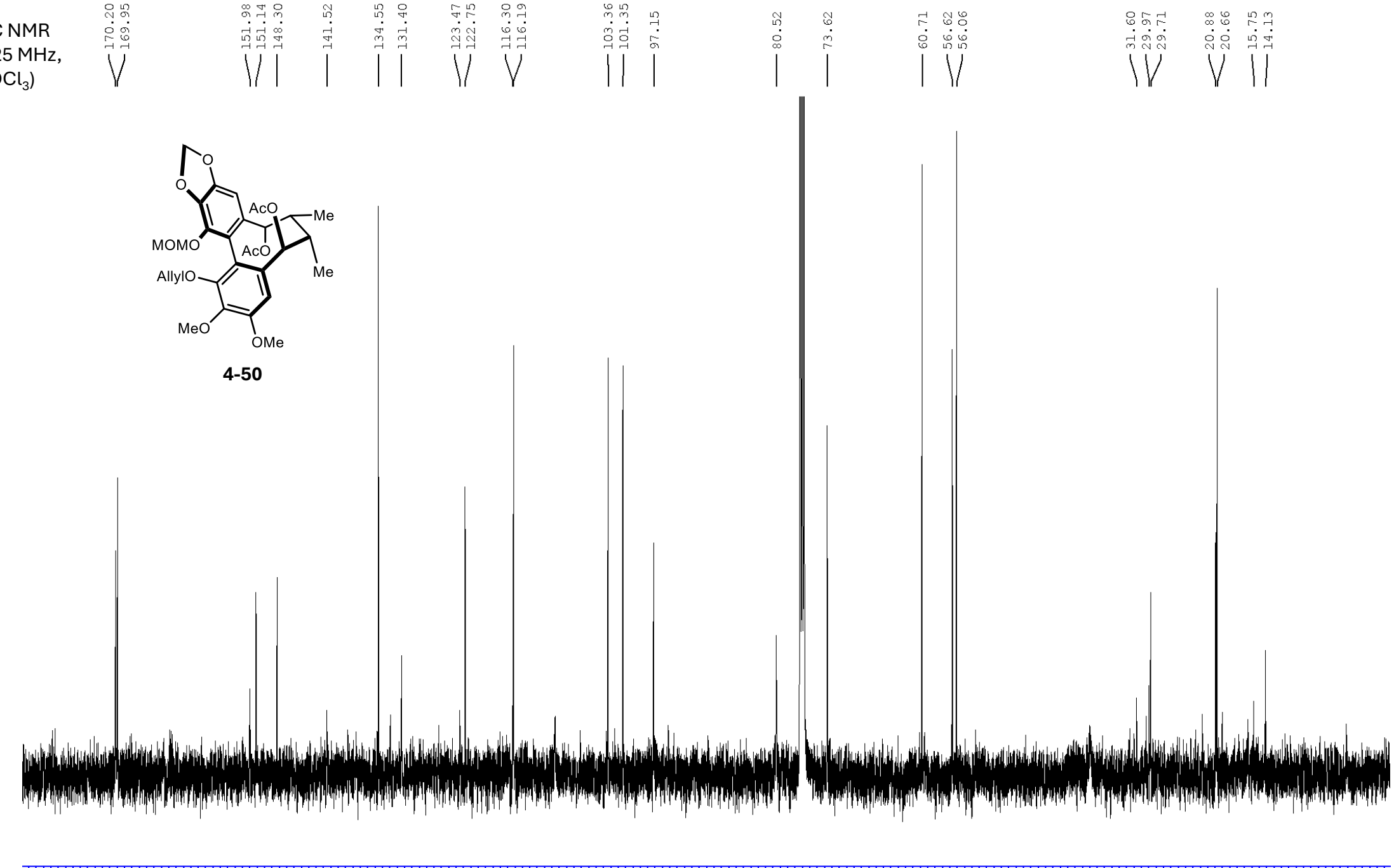
^{1}H NMR (500 MHz, $CDCl_3$)



4-50

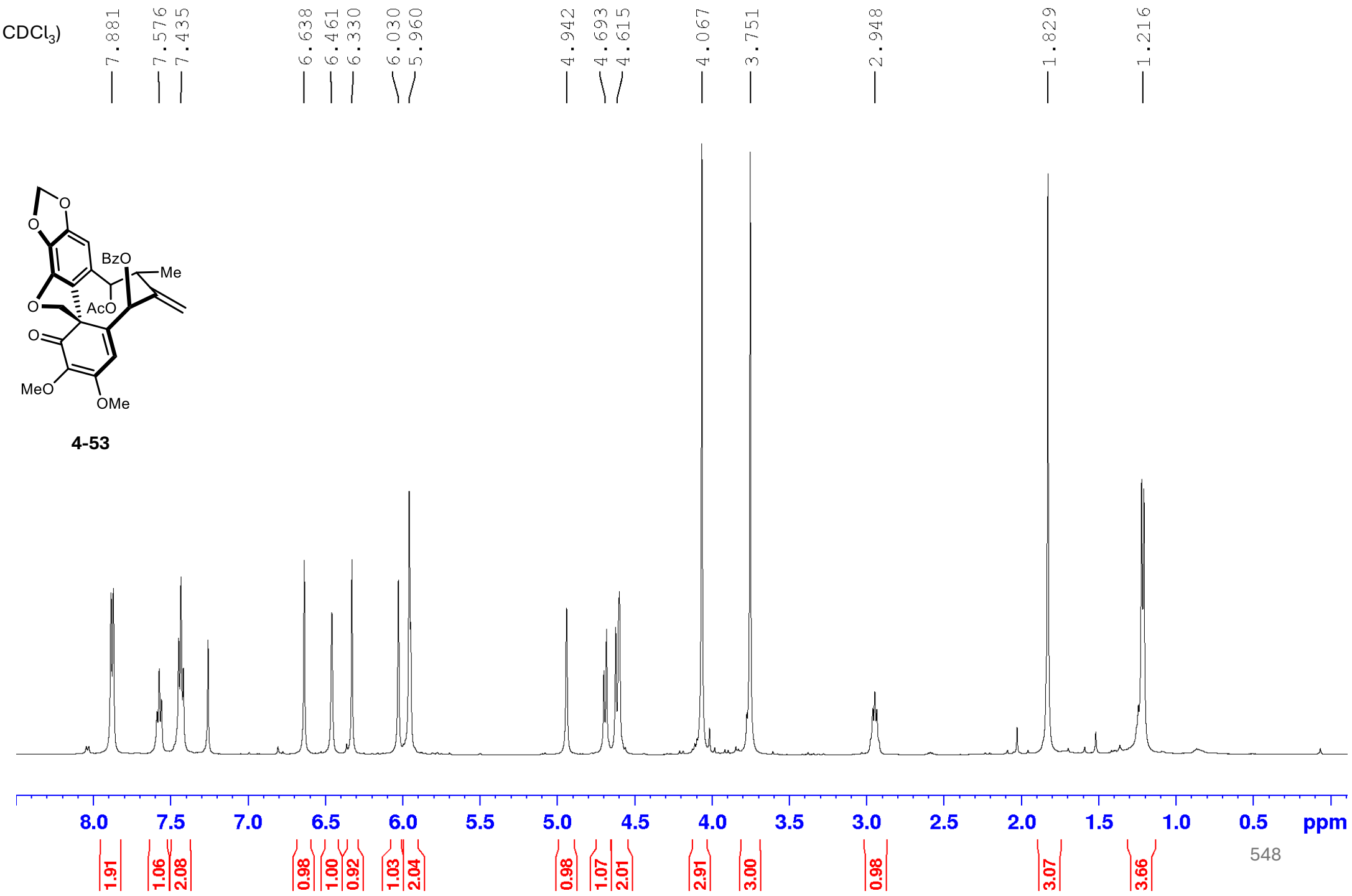
^{13}C NMR (125 MHz, $CDCl_3$)

4-50



^{1}H NMR (500 MHz, $CDCl_3$)

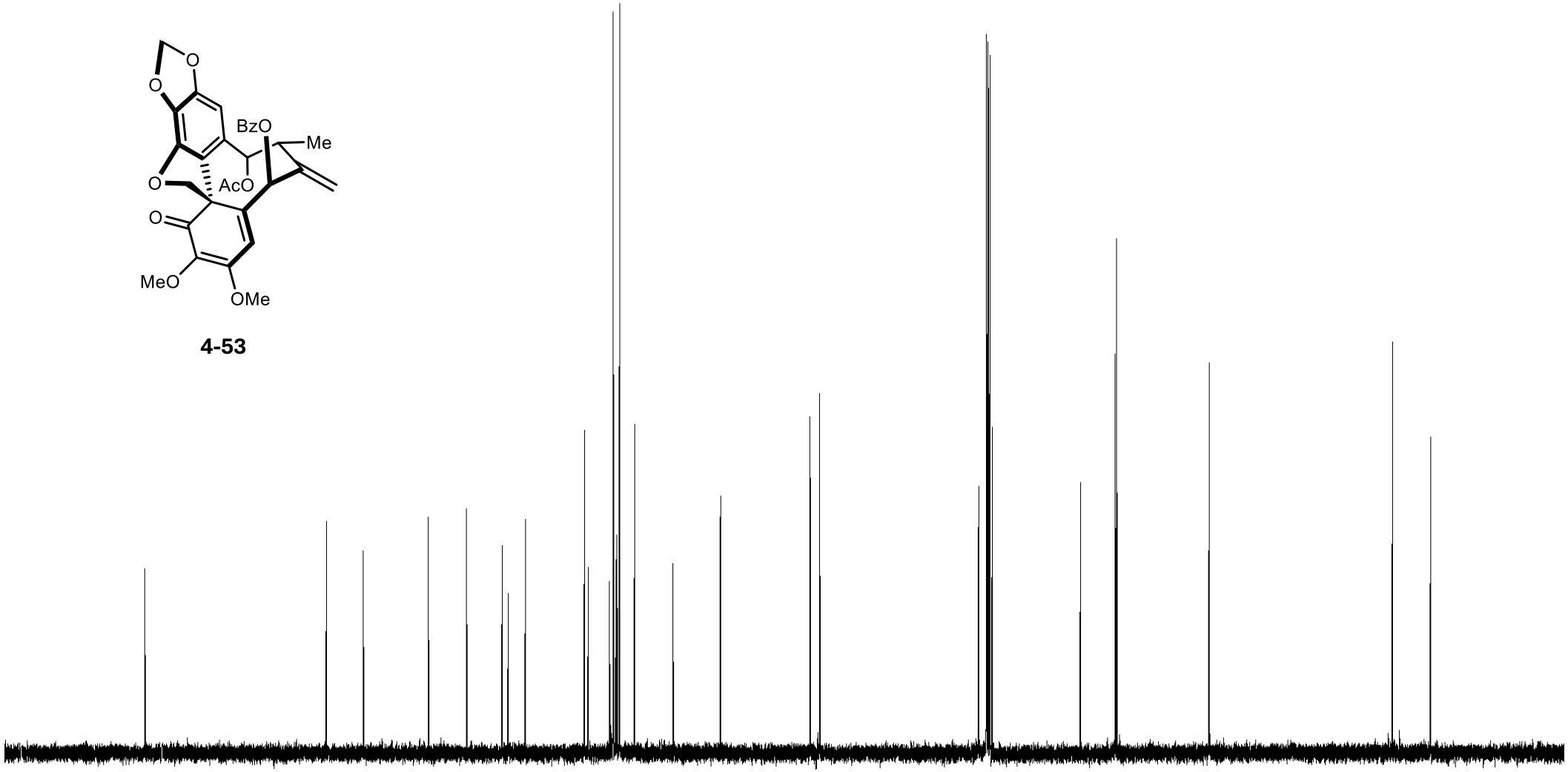
4-53



^{13}C NMR
(125 MHz, $CDCl_3$)

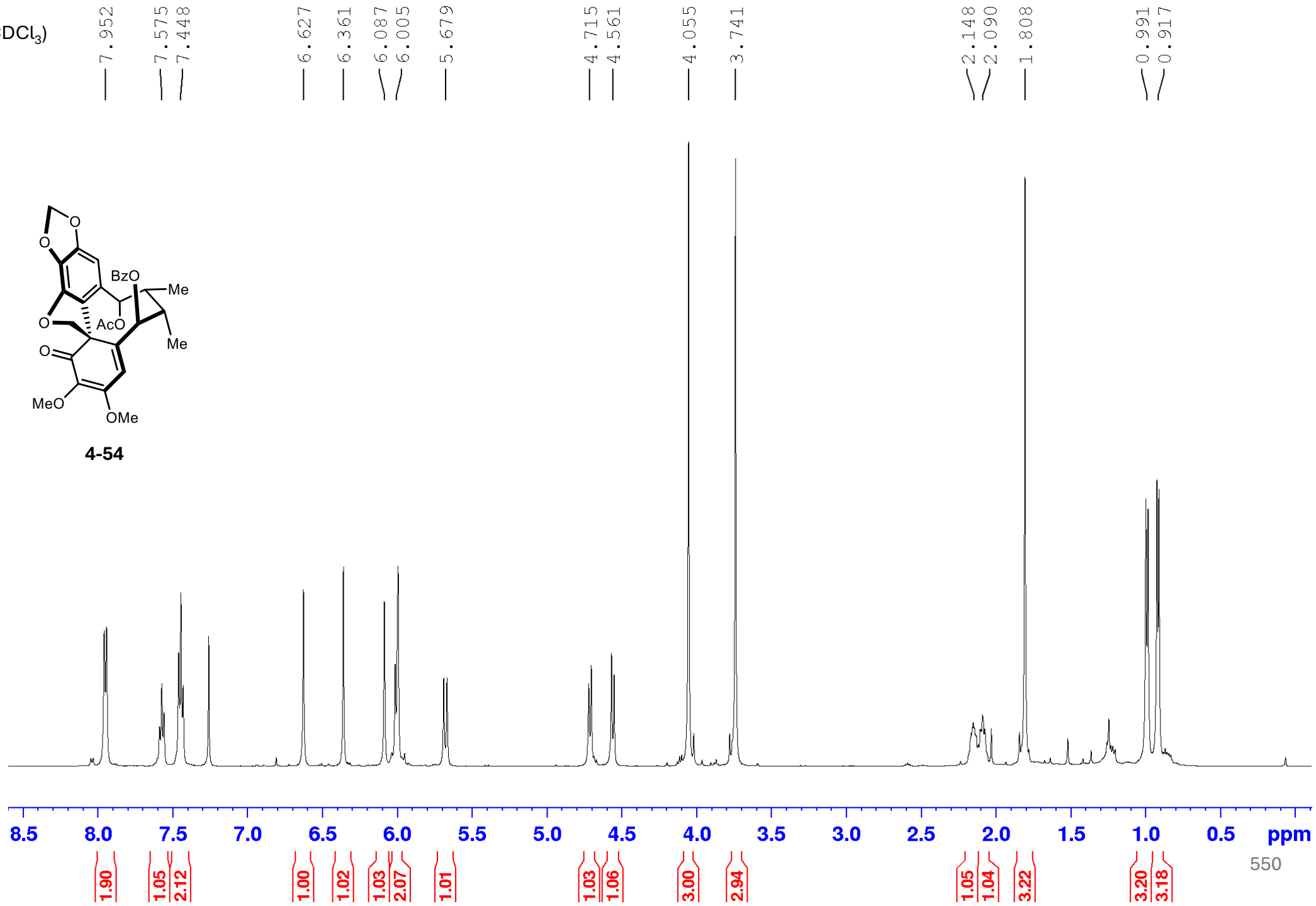
195.244
169.791
164.627
155.528
150.157
145.208
144.350
141.932
133.654
133.124
130.197
129.632
129.229
129.079
128.722
126.637
121.287
114.608
102.034
100.701
78.443
77.314
76.538
64.155
59.275
59.095
46.113
20.418
15.102

4-53



^{1}H NMR (500 MHz, $CDCl_3$)

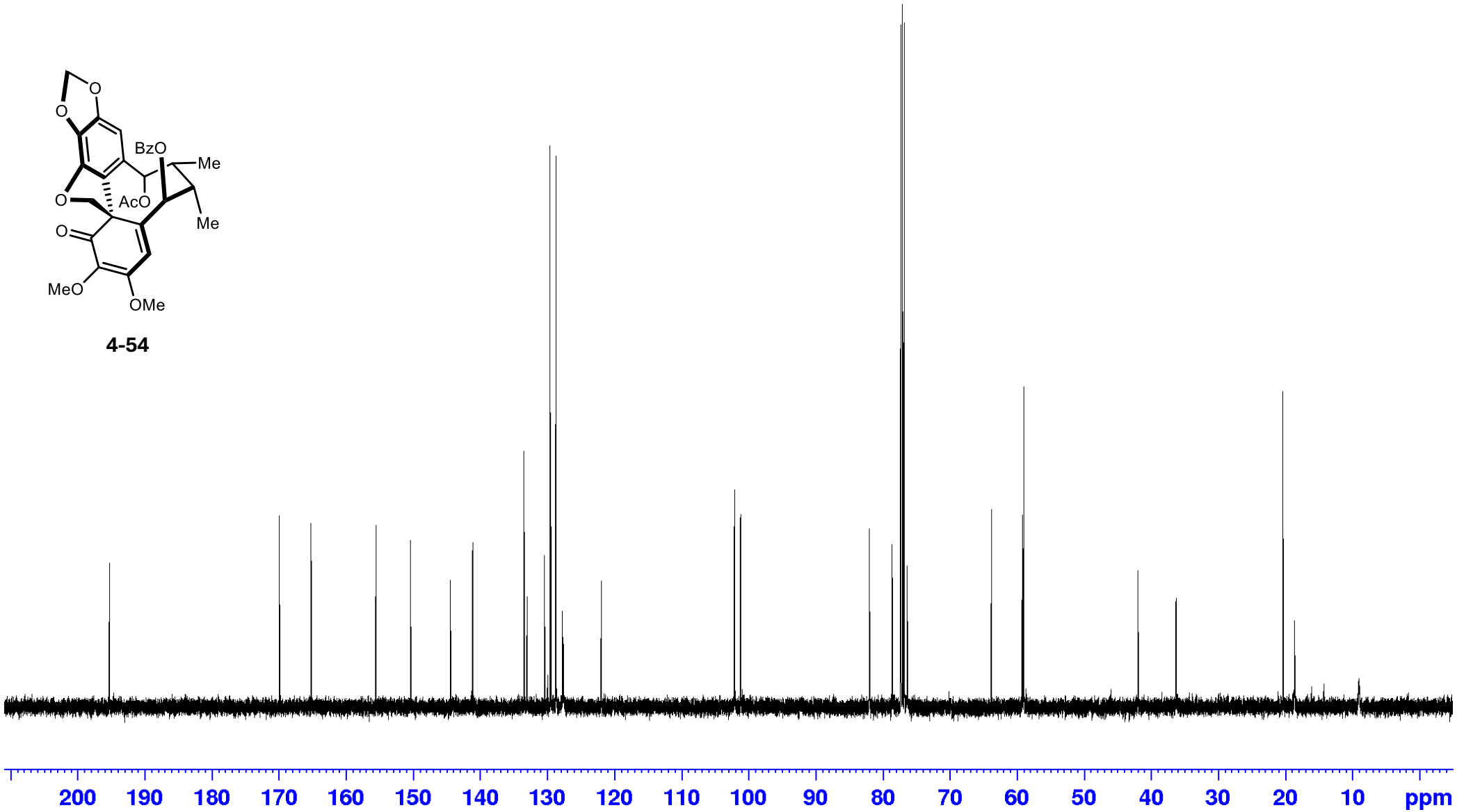
4-54



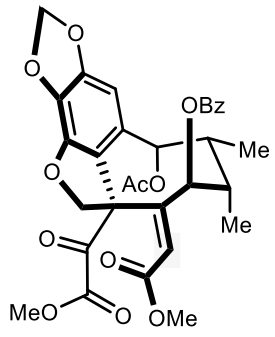
^{13}C NMR
(125 MHz, $CDCl_3$)

195.327
169.954
165.228
155.596
150.420
144.445
141.160
133.488
133.065
130.441
129.618
129.458
128.728
127.797
127.657
121.998
102.140
101.222
82.019
78.598
76.369
63.824
59.201
58.992
41.977
36.295
20.344
18.622
9.022

4-54



^{1}H NMR (500 MHz, $CDCl_3$)



4-55

^{13}C NMR
(125 MHz,
$CDCl_3$)

185.09
170.89
165.81
165.17
161.88
150.65
149.76
145.39
133.18
132.58
130.59
129.51
129.10
128.08
127.84
117.63
102.13
85.19
83.93
80.52
62.43
52.55
51.80
40.14
38.27
20.86
20.41
12.71

4-55

